FEB - FRESENIUS ENVIRONMENTAL BULLETIN
Founded jointly by F. Korte and F. Coulston
Production by PSP - Vimy Str. 1e, 85354 Freising, Germany in
cooperation with PRT-Parlar Research & Technology
Vimy Str 1e, 85354 Freising
Copyright© by PSP and PRT, Vimy Str. 1e, 85354 Freising, Germany
All rights are reserved, especially the right to translate into foreign language or other processes - or convert to a machine language, especially for data processing equipment - without written permission of the publisher. The rights of reproduction by lecture, radio and television transmission, magnetic sound recording or similar means are also reserved.
Printed in Germany-ISSN 1018-4619

FEB-EDITORIAL BOARD

CHIEF EDITOR:
Prof. Dr. Dr. H. Parlar
Parlar Research & Technology-PRT
Vimy Str.1e
85354 Freising, Germany

MANAGING EDITOR:
Dr. P. Parlar
Parlar Research & Technology
PRT, Vimy Str.1e
85354 Freising, Germany

CO-EDITORS:

Environmental Spectroscopy
Prof. Dr. A. Piccolo
Universita di Napoli "Frederico II"
Dipto. Di Scienze Chemica Agrarie
Via Universita 100, 80055 Portici, Italy

Environmental Biology
Prof. Dr. G. Schuurmann
UFZ-Umweltzentrum
Sektion Chemische Ökotoxikologie
Leipzig-Halle GmbH,
Permoserstr.15, 04318
04318 Leipzig, Germany
Prof. Dr. I. Holoubek
Recetox-Tocoen
Kamenice126/3, 62500 Brno, Czech Republic
Prof. Dr. M. Hakki Alma
Igdir Universitesi
76000, Igdir, Turkey

Environmental Analytical Chemistry
Prof. Dr. M. Bahadir
Lehrstuhl für Ökologische Chemie
und Umweltanalytik
TU Braunschweig
Lehrstuhl für Ökologische Chemie
Hagenring 30, 38106 Braunschweig, Germany
Dr. D. Kotzias
Via Germania29
21027 Barza(Va), Italy

Environmental Management
Dr. K. I. Nikolaou
Env.Protection of Thessaloniki
OMPEPT-54636 Thessaloniki
Greece

Environmental Toxicology
Prof. Dr. H. Greim
Senatkommision – DFG / TUM
85350 Freising, Germany

Environmental Proteomic
Dr. A. Fanous
Halal Control GmbH
Kobaltstr. 2-4
D-65428 Rüsselsheim, Germany

Environmental Education
Prof. Dr. C. Bayat
Esenyurt Üniversitesi
34510 Esenyurt, Istanbul, Turkey

Environmental Medicine
Prof. Dr. I. Tumen
Bandirma 17 Eylül Üniversitesi
10200 Bandirma, Turkey

Advisory Board
K. Bester, K. Fischer, R. Kallenborn
DCG. Muir, R. Niessner,W.Vetter,
A. Reichlmayr-Lais, D. Steinberg,
J. P. Lay, J. Burhenne, L. O. Ruzo

Marketing Manager
Cansu Ekici, B. of B.A.
PRT-Research and Technology
Vimy Str 1e
85354 Freising, Germany
E-Mail: parlar@wzw.tum.de
parlar@prt-parlar.de
Phone: +49/8161887988

Fresenius Environmental Bulletin is abstracted/indexed in:
Biology & Environmental Sciences, BIOSIS, CAB International, Cambridge Scientific abstracts, Chemical Abstracts, Current Awareness, Current Contents/Agriculture, CSA Civil Engineering Abstracts, CSA Mechanical & Transportation Engineering, IBIDS database, Information Ventures, NISC, Research Alert, Science Citation Index (SCI), Scisearch, Selected Water Resources Abstracts

CONTENTS

ORIGINAL PAPERS

IMPROVING SWEET CORN × DENT CORN HYBRIDS BASED ON KERNEL COLOR, SIZE AND QUALITY PROPERTIES 2368
Burak Altınel, Fatma Aykut Tonk, Deniz Istipliler, Muzaffer Tosun, Fikret Pazir

LARVICIDAL EFFECT OF *PINUS BRUTIA* TEN. SEED ESSENTIAL OIL TO PINE PROCESSIONARY MOTH (*THAUMETOPOEA WILKINSONI* TAMS.) UNDER LABORATORY CONDITIONS 2375
Gurkan Semiz, Kubra Kocabiyik, Huseyin Cetin

ASSESSMENT OF ESSENTIAL OIL PROPERTIES IN *JUNIPERUS EXCELSA* SUBSP. *EXCELSA* CONES DEPENDING ON SITE FACTORS 2380
Serkan Gulsoy, Gulcan Ozkan, Huseyin Senol, Ahmet Mert

EXPERIMENTAL CONSIDERATION ON HEIGHT AND DISTANCE EFFECTS OF CONSECUTIVE DAMS IN HYDRAULIC FLOW 2390
Mehdi Bensaid, Amir Abbas Kamanbedast, Mohammad Hosein Purmohammadi, Mahmoud Shafai Bajestan, Alireza Masjedi

EVALUATION OF FOSSIL FUEL CONSUMPTION AND ENVIRONMENTAL IMPACTS IN SUGAR BEET PRODUCTION AS A BIOFUEL RAW MATERIAL 2397
Cahit Gungor, H Huseyin Ozturk

INVESTIGATION OF THE EFFECTS OF *DIPLOTAENIA TURCICA* PLANT ROOT EXTRACT ON RAT OVER TISSUE BY HISTOLOGICAL AND STEREOLOGICAL METHODS 2407
Nese Colcimen, Ugur Ozdek, Yeter Deger, Fikret Altindag, Okan Arihan

CHEMICAL COMPOSITION AND ANTIOXIDANT CAPACITIES OF MOSSES GATHERED FROM MOUNT IDA (CANAKKALE, TURKEY) 2413
Ozlem Tonguc Yayintas, Dilek Ozyurt, Birsen Demirata, Yonca Karagul Yuceer, Selehattin Yilmaz

THE DETERMINATION OF CHANGES IN MONTHLY MINERAL CONTENTS OF THORNY SALTWORT (*NOAEA MUCRONATA SUBSP. MUCRONATA*) 2421
Suleyman Temel

STUDY ON ISOLATION AND UTILIZATION OF A CHLOROTHALONIL DEGRADING BACTERIUM, *BACILLUS COAGULANS* BJQ-Z6 2426
Yan Zhao, Chengxiao Zhao, Sichun Tong, Caihua Jin

DETERMINATION OF WATER-YIELD RELATIONSHIP OF COMICE PEAR (*PYRUS COMMUNIS L.*) VARIETY IRRIGATED BY THE IRRIGATION AUTOMATION SYSTEM (IAS) BASED ON PROGRAMMABLE LOGIC CONTROLLER (PLC) 2433
Cafer Gencoglan, Serpil Gencoglan, Yusuf Nikpeyma, Ali Beyhan Ucak

PRESENCE OF CUCURBIT VIRUSES IN ANKARA AND ANTALYA PROVINCE AND MOLECULAR CHARACTERIZATION OF COAT PROTEIN GENE OF *ZUCCHINI YELLOW MOSAIC VIRUS* TURKISH ISOLATES 2442
Serife Topkaya, Cecile Desbiez, Filiz Ertunc

EFFECTS OF SUCROSE AND L-RHAMNOSE ON ANTHOCYANIN AND RELATED GENE EXPRESSION IN ROSE 2450
Yong Zhang, Mengwen Luo, Xuhui Ma, Wei Hou, Haoru Tang

THE RESEARCH OF 17α-ETHINYL ESTRADIOL (EE2) LEVELS IN THE FRESHWATER SOURCES POURED INTO THE NORTHEAST MEDITERRANEAN REGION 2457
Esra Bickici, Meltem Eken

DETERMINATION OF CATALASE ACTIVITY EXPOSED TO ORGANOPHOSPHATE INSECTICIDES AZINPHOS-METHYL AND DIMETHOATE 2464
Hasan Karadag, Fatma Temiz Uzun

ACCUMULATION OF FLUORIDE IN HORSE-CHESTNUT (*AESCULUS HIPPOCASTANUM* L.) LEAVES COLLECTED FROM WEST POMERANIAN DISTRICT OF POLAND 2469
Arkadiusz Telesinski Grzegorz Nowak, Karol Stanislawski, Robert Biczak, Jacek Wrobel, Marek Snieg, Jakub Poblocki, Marek Rynkiewicz

EFFECT OF PRENATAL EXPOSURE TO LEAD ACETATE ON HISTOGENESIS OF THE TESTICULAR TUBULES 2475
Mahmood H Hamash, Ahmed M Khalaf

FUEL CONSUMPTION-DERIVED CARBON DIOXIDE EMISSIONS UNDER TRADITIONAL AND NO-TILLAGE SYSTEMS IN WHEAT PRODUCTION FOR FOOD INDUSTRY 2483
Z Figen Antmen

THE DYNAMIC CHANGES OF PLANT ENDOGENOUS HORMONES IN RESPONSE TO DIFFERENT TEMPERATURES IN SEEDS OF *IDESIA POLYCARPA* MAXIM. FROM XINYANG 2495
Yanmei Wang, Zhen Liu, Fei Li

SYNTHESIS AND RESEARCH OF A NOVEL NEAR INFRARED NMR PROBE TARGETING LIVER CANCER 2506
Ning Guo, Meirong Liu, Zixuan Guo

ASSESSING THE SUSTAINABILITY OF CROP PRODUCTION IN THE GEDIZ BASIN, TURKEY: A WATER, ENERGY, AND FOOD NEXUS APPROACH 2511
Adnan Degirmencioglu, Rabi H Mohtar, Bassel T Daher, Gulden Ozgunaltay-Ertugrul, Omer Ertugrul

CHARACTERISTICS RESEARCH OF SLUDGE MICRO-BUBBLE DRYING AND DERIVED FUEL 2523
Yu Qi, Chi Zhang, Yan Tao, Tianyu Guo, Hongtao Wang, Fang Cao, WeiKe Zhang

AN *IN VITRO* STUDY OF BIOCHEMICAL CHARACTERIZATION AND AMELIORATING EFFECT OF POLYETHYLENE GLYCOL AGAINST CD STRESS IN SUGARCANE 2530
Umair A Khan, Aamir Ali

EFFECTS OF PACLOBUTRAZOL SOAKING ON YIELD AND QUALITY OF THREE VARIETIES *PSEUDOSTELLARIA HETEROPHYLLA* 2539
Hualei Wang, Longjin Li, Zhi Zhao, Hongchang Liu, Chunli Luo, Jinling Li, Fulai Luo, Mingjin Huang, Songshu Chen

THE GENOPROTECTIVE EFFECT OF *CROCUS SATIVUS* L. (SAFFRON) EXTRACT ON DOXORUBICIN-INDUCED GENOTOXICITY IN *DROSOPHILA MELANOGASTER* 2545
Selda Oz, Sukran Cakir-Arica

EFFECT OF APPLICATION OF SHEEP MANURE AND IT'S BIOCHAR ON CARBON EMISSIONS IN SALT AFFECTED CALCAREOUS SOIL IN SANLIURFA REGION SE TURKEY 2553
Erdal Sakin, Ibrahim Halil Yanardag

COMPARISON OF THE EFFECTS OF ZNO NPS, MGO NPS AND IONIC ZINC AND MAGNESIUM ON WHEAT PLANTS 2561
Yifan Ni, Lian Xiao, Fengting Wan, Mengxuan Xu, Lingzhi Qiu, Junfeng Li, Junli Li

SOIL PROPERTIES WERE EVALUATED AS REFLECTING PARAMETERS IN LOW INTENSITY FOREST FIRES IN CANKIRI, TURKEY 2575
Sema Camci Cetin, Aziz Emre Yilmaz, Sabit Ersahin, Ulku Dikmen, Seval Sunal

EGG AND CHICK QUALITY CHARACTERISTICS OF MEAT TYPE JAPANESE QUAIL (*COTURNIX COTURNIX JAPONICA*) LINE BY CANONICAL CORRELATION ANALYSIS 2582
Abdullah Nuri Ozsoy

ESTIMATING SURFACE SOIL LOSSES IN THE MOUNTAINOUS SEMI-ARID WATERSHED USING RUSLE AND GEOSPATIAL TECHNOLOGIES 2589
Mehmet Yavuz, Mustafa Tufekcioglu

ANALYSIS OF ACRYLAMIDE IN MEAT-BASED FOOD PRODUCTS BY USING L-CYSTEINE-CAPPED Mn-DOPED ZnS QUANTUM DOTS AS A ROOM TEMPERATURE PHOSPHORESCENT PROBE 2599
Burak Demirhan, Buket Er Demirhan, Hayriye Eda Satana Kara

STUDY ON CARBON-DIOXIDE EMISSIONS IN CHINA BASED ON STRUCTURAL DECOMPOSITION ANALYSIS 2608
Zhiyuan Ge, Jie Hou

ESTIMATION OF GENETIC PARAMETERS AND GENETIC TREND OF HOLSTEIN FRIESIAN CATTLE POPULATION IN TURKEY 2617
Serdar Genc, M Ihsan Soysal

STUDY ON MEASURES TO IMPROVE WATER QUALITY IN URBAN LAKES: CASING IN LAKE NANHU IN WUHAN 2625
Hao Huang, Fan Wan, Yan Gao, Zhenxing Zhong, Shohrat Annanurov, Xiangguo Zeng

EXPERIMENTAL STUDY THE EFFECT OF SULFATE AND RETENTION TIME ON SOLUBLE AL CONCENTRATION AND SPECIES OF PRECIPITATES DURING NaOH NEUTRALIZATION OF AL-BEARING ACID MINE DRAINAGE 2633
Ruifeng Liang, Gaolei Zhao, Xunchi Pu

DETERMINATION OF ANTIOXIDANT CAPACITIES, CHEMICAL COMPOSITION AND MELISSOPALYNOLOGICAL CHARACTERIZATION OF *VERBASCUM* SPP. AND *EUPHORBIA* SPP. HONEYS 2644
Aslı Ozkok

THE ORIGIN OF THE OAK HONEYDEW HONEY PRODUCED FROM *QUERCUS FRAINETTO* TEN 2650
Aslı Ozkok, Ahmet Ipek, Kadriye Sorkun

NOVEL BIOACTIVITIES OF *CASSIA NEMOPHILA* PODS AGAINST DIABETIC NEPHROPATHY: *IN VITRO* AND *IN VIVO* STUDY 2656
Gauhar Rehman, Saba Arshad, Muhammad Hamayun, Amjad Iqbal, Waqas Ahmad Shams, Anwar Hussain, Khair Zaman, Ayaz Ahmad, Muhib Shah, Sahib Gul

SOME WATERSHED CHARACTERISTICS OF MURAT MOUNTAIN OF TURKEY 2664
Nilufer Yazici, Ismet Celik

SEASONAL CHANGES IN THE FOOD SPECTRUM AND DAY-TIME RHYTHM OF FEEDING IN RED MULLET *MULLUS BARBATUS* (LINNAEUS, 1758) IN THE SOUTHEAST BLACK SEA 2671
Hatice Onay, Goktug Dalgic

EFFECTS OF SOYBEAN OIL SUPPLEMENTATION ON THE GROWTH AND SURVIVAL PERFORMANCE OF RED CLAW CRAYFISH *CHERAX QUADRICARINATUS* IN CULTURE CONDITION 2679
Yavuz Mazlum, Mehmet N Gunduz, Ozlem Guner Gurlek, Metin Yazici

ENDOPHYTIC FUNGI FROM *CARALLUMA ACUTANGULA* CAN SECRETE PLANT GROWTH PROMOTING ENZYMES 2688
Sajid Ali, Sumera Afzal Khan, Muhammad Hamayun, Amjad Iqbal, Abdul Latif Khan, Anwar Hussain, Mohib Shah

EFFECTS OF MELOXICAM ON STRESS AND OXIDATIVE STRESS IN DAIRY COWS UNDERGOING HOOF TRIMMING 2697
Selvinaz Yakan, Vesile Duzguner

ANALYZING THE EFFECTS OF OLIVE LEAVES ON SENSORY AND CHEMICAL PROPERTIES OF REFINED OLIVE OILS USING IMAGE PROCESSING METHODS 2703
Omer Faruk Gamli

ANALYSING THE NATIONAL DATA FOR AGRICULTURAL TECHNOLOGY PENETRATION IN TURKEY 2716
Arif Behic Tekin

RESEARCH ON WATER RESOURCES CARRYING CAPACITY OF CHANGZHOU CITY BASED ON NEURAL NETWORK 2725
Mengyu Liu, Jianyong Zhang, Chenhui Wang, Hui Lu

ANALYSIS OF THREE RELATIONS IN RURAL TOURISM DEVELOPMENT OF CHINA GUIZHOU UNDER THE STRATEGIC BACKGROUND OF RURAL VITALIZATION 2733
Wei Wang

BIOLOGICAL EVALUATION OF 1-(4-(HYDROXY(1-OXO-1,3-DIHYDRO-2H-INDEN-2-YLIDENE)METHYL)PHENYL)-3-PHENYLUREA DERIVATIVES: ANTICHOLINERGICS AND ANTIEPILEPTIC POTENTIALS 2739
Umit Muhammet Kocyigit

A STUDY ON THE EFFECTS OF WOOD VINEGAR ON WEEDS AND CULTIVATED PLANTS IN THE WHEAT AGRO-ECOSYSTEMS 2747
Ibrahim Koc, Ayten Namli, Mehmet Mendes, Suleyman Mesut Pinar, Fatih Cig, Erdal Necip Yardim

TIME-DRIVEN ACTIVITY-BASED COSTING IN THE OPHTHALMOLOGY DEPARTMENT OF STATE HOSPITAL: A CASE STUDY 2754
Pinar Kurt, Metin Saban, Fikret Cankaya, Mehmet Cengiz Annac

THE OPTIMIZATION OF STARCH GELATINIZATION AND QUALITY ATTRIBUTES UNDER HYDROTHERMAL TREATMENT OF PADDY BY RESPONSE SURFACE METHOD 2771
Khurram Yousaf, Adnan Abbas, Xuejin Zhang, Rui Kang, Eisa Belal, Fiaz Ahmad, Kunjie Chen

THE ROLE OF TiO_2 NANOPARTICLES IN DISINFECTION OF GRAM (+) BACTERIA UNDER VISIBLE LIGHT 2780
Merve Ozkaleli Akcetin, Ayca Erdem

BIOLOGICAL ACTIVITY OF FOUR TYPES OF CHITOSAN AGAINST SOME PLANT PATHOGENIC FUNGI 2787
Abdurrahman Onaran, Kader Tokatli, Aslihan Demirdoven, Mustafa Bayram, Yusuf Yanar

EFFECT OF PLANT DENSITY ON GROWTH AND GRAIN YIELD OF SOME HYBRID CORN (ZEA MAYS L.) VARIETIES UNDER MEDITERRANEAN ENVIRONMENT 2795
Omer Konuskan, Cengiz Kilinc

AFLATOXIN M_1 IN TRADITIONAL HOMEMADE YOGHURTS MARKETED IN SOUTHEASTERN TURKEY 2802
Semra Gurbuz, Serap Kilic Altun

PROPERTIES OF COPPER-CONTAMINATED SAND BEFORE AND AFTER STABILIZATION USING ELECTRICAL RESISTIVITY MEASUREMENT 2807
Xiaofeng Liu, Xin Xu, Xiaoqiang Dong, Junboum Park, Jiwei Shen, Shahabaldin Rezania

ASSESSMENT OF AQUIFER RECHARGING USING DAMS IN TERMS OF GEOTECHNICAL CHARACTERIZATION AND HYDROGEOLOGICAL CONDITIONS IN ARID REGIONS 2816
Mustafa Can Canoglu

EVALUATION OF IN VIVO EFFECTS OF *VISCUM ALBUM L.* AND ITS CONSTITUENT *O-COUMARIC ACID* ON BILE ACID SYNTHESIZING CYPS 2825
Tuba Ege, Ayse Mine Gencler Ozkan, Alaattin Sen, Orhan Adali

LAND USE PATTERN CHANGE AND FORECAST ANALYSIS OF ENERGY AND CHEMICAL INDUSTRY BASE IN THE LOESS PLATEAU 2835
Hou Kang, Haihong Li, Shijun Zhao, Juan Wang, Ke Yang, Yue Wang, Doudou Han,Yanan Lu

DETERMINING THE BEST NORMALIZATION TECHNIQUE FOR ESTIMATION USING ARTIFICIAL NEURAL NETWORKS: CASE OF BRUSHTOOTH LIZARDFISH 2842
Levent Sangun

SINTERING CHARACTERISTICS OF CERAMSITE OBTAINED FROM LAKE SEDIMENTS, CLAY, AND LIRIODENDRON 2848
Zhulai Wang, Zuhui Fan, Zizeng Lin, Yali Liu

THE EFFECT OF SOME ROOTSTOCKS ON THE PHYSICAL AND CHEMICAL PROPERTIES OF FRUIT GROWING PROCESS IN ANNA APPLE CULTIVAR 2855
Ali Ikinci, Ibrahim Bolat

RESPONSES OF CHLOROPLASTIC ANTIOXIDANT DEFENSE AND PHOTOSYNTHESIS CHARACTERISTICS OF *HEDYSARUM SCOPARIUM* AND *ATRAPHAXIS BRACTEATA* UNDER DROUGHT STRESS 2864
Xiaoxi Zhang, Hui Liu, Gang Han

ASSESSMENT OF THE WHEATGRASS EFFECTS ON ANTIOXIDANT CAPACITY AND DNA DAMAGE IN RATS WITH EXPERIMENTAL RENAL FAILURE 2876
Leyla Mis, Bahat Comba, Yildiray Basbugan, Semih Yasar, Arzu Comba

A STATISTICAL INVESTIGATION OF THE RELATIONSHIP BETWEEN SPECIES AND ENVIRONMENTAL VARIABLES OF MALACOFAUNA IN FEEDING STREAMS OF SAPANCA LAKE (TURKEY) 2880
Serap Kosal Sahin, Esra Albayrak

AEROSOL BLACK CARBON IN THE NORTHEASTERN QINGHAI-TIBET PLATEAU: DISTRIBUTION, HEALTH RISKS, AND CORRELATION WITH SOIL BLACK CARBON 2889
Xiuyun Min, Jun Wu, Jian Lu, Ronggao Qin, Chunliang Gao, Leiming Li, Xiaoying Guo

RESEARCH ON SOURCES APPOINTMENT OF ABNORMAL CO IN UNDERGROUND MINE 2897
Xinran Hou, Liwen Guo, Fusheng Wang, Yunyun Xu, Xianwei Dong, Dong Gao, Yiming Sun

ADSORPTION ABILITY OF AIR POLLUTANTS BY INDIGENOUS TREE SPECIES IN TA-PIEH MOUNTAINS 2908
Hui Wang, Yao-qing Sun, Miao Zhang, Wen-jing Liu, Le Yang, Xing-wen Zhou

STUDY OF INSECTICIDAL AND BEHAVIORAL EFFECTS AND SOME CHARACTERISTIC OF NATIVE DIATOMACEOUS EARTH AGAINST THE BEAN WEEVIL, *ACANTHOSCELIDES OBTECTUS* (COLEOPTERA: CHRYSOMELIDAE) 2916
Mustafa Alkan, Sait Erturk, Tugba Akdeniz Firat, Emin Ciftci

LEACHING OF SOIL SALINITY BY DRIP IRRIGATION METHOD IN GREENHOUSE CONDITIONS 2923
Abdullah Sayici, Harun Kaman

GENETIC DIVERSITY IN PAKISTANI SOYBEAN GENOTYPES AND NORTH AMERICAN ANCESTRAL LINES USING AGROMORPHOLOGICAL AND RAPD MARKERS 2927
Masood Jan, Mohammad Nisar, Mohammad Ihsan, Farhatullah, Gul Jan, Fatih Hanci

TRAPPING GENDERS OF *CERATITIS CAPITATA* (DIPTERA: TEPHRITIDAE) AND OTHER DIPTERAN WITH VARIOUS ATTRACTANTS ON POMEGRANATE FRUITS IN TURKEY 2937
Nihat Demirel

EFFECTS OF SALINITY STRESS ON THE GROWTH CHARACTERISTICS OF FOUR TURFGRASS SPECIES 2942
Ramazan Keyikoglu, Elcin Aksu, Mehmet Arslan*

ACUTE AND CHRONIC EFFECTS OF PRESSURE ON DYNAMIC THIOL-DISULPHIDE HOMOEOSTASIS IN DIVERS 2949
Ali Erdal Gunes, Hakim Celik, Ozgur Yılmaz, Celal Erbas, Evren Gumus

EVALUATION OF PLANT GROWTH REGULATORS AND CASEIN HYDROLYSATE ADDITION ON SECONDARY PRODUCTS PRODUCTION IN CULTURES OF DATE PALM 2957
Abdullatif A Al-Khateeb, Mohei El-Din Solliman, Hossam S El-Beltagi, Heba Allah A Mohasseb, Solliman A Al-Khateeb

IDENTIFICATION AND EXPRESSION ANALYSIS OF ACID INVERTASES GENE FAMILY IN ROOTS OF METALLICOLOUS AND NON-METALLICOLOUS POPULATIONS OF *RUMEX JAPONICUS* UNDER COPPER STRESS 2968
Yu-Qiao Cao, Zhuang-Zhuang Wei, Jia-Yang Xu, Hui-Fang Shao, Zi-Cheng Xu, Wu-Xing Huang

© by PSP Volume 28 – No. 4/2019 pages 2368-2374 Fresenius Environmental Bulletin

IMPROVING SWEET CORN × DENT CORN HYBRIDS BASED ON KERNEL COLOR, SIZE AND QUALITY PROPERTIES

Burak Altinel[1,*], Fatma Aykut Tonk[2], Deniz Istipliler[2], Muzaffer Tosun[2], Fikret Pazir[1]

[1]Ege University, Faculty of Engineering, Department of Food Engineering, Bornova, Izmir, Turkey
[2]Ege University, Faculty of Agriculture, Department of Field Crops, Bornova, Izmir, Turkey

ABSTRACT

The objective of this study was to determine the most-promising F_1 hybrids with respect to kernel color, size and quality properties using sweet corn and dent corn inbred lines as parents. In this study, the F_1 hybrids were produced using four sweet corn inbred lines as female parents (SC1, SC2, SC3 and SC4) and two dent corn inbred lines as male parents (DC1 and DC2). We observed that kernel size properties and 1000-kernel weight values of F_1 hybrids were similar to those of the male parents. The hybridization of SC1 and SC4 with male parents exhibited a significant increase in L*, a*, b* values in their F_1 hybrids. Total sugar contents of the F_1 hybrids were found to be similar to those of sweet corn inbred lines. The highest sucrose content was found in the SC3 and accordingly in the SC3's hybrids. °Brix values indicated that our F_1 hybrids are at an adequate level from the standpoint of a sweet taste. The findings in the present study led to the conclusion that it is possible to produce new type sweet corn × dent corn hybrids with improved characteristics.

KEYWORDS:
Sweet corn inbred line, Dent corn inbred line, Hybridization, F_1 hybrids, Kernel characteristics.

INTRODUCTION

Maize (*Zea mays* L.), also called corn, is one of the most important cereal grains/crops in the world [1], and it is mainly used in human food and animal feed [2]. Dickerson [3] stated that unlike dent corn (*Zea mays* L. *indentata* Sturt.), sweet corn (*Zea mays* L. *saccharata* Sturt.) is grown primarily for processing and fresh consumption, not feed or flour [4]. Flora and Wiley [5] indicated that the sweetness, texture and aroma characteristics of sweet corn kernels are the most important components in consumer acceptance [6]. Fekonja [7] pointed out that sweet corn is a potential crop for temperate climates; however, it requires additional agronomic improvements [8]. Tracy [9] indicated that sweet corn differs from dent corn because of its genes, which modify the flavor, tenderness, texture, seed viability, and appearance of plants and ears [10]. The recessive allele *Sugary1* (*su1*) is the genetic basis of sweet corn. Sweet corn is differentiated from other corn types by a gene or genes that the alter endosperm starch synthesis [11].

The production of sweet corn globally is increasing because of its high economic value. Therefore, field studies are being performed worldwide to produce high quality sweet corn hybrids. Kumari et al. [12] indicated that certain promising hybrids with high ear weight, high grain yield and high total sugar content can be produced from some sweet corn and dent corn hybridization. Similarly, Özçam [13] reported that promising hybrids with high grain yield could be obtained from sweet corn and dent corn hybridization. However, there are limited studies in the literature related to the producing of promising sweet corn hybrids using sweet corn and dent corn inbred lines as parents.

Against this background, the objective of this study was to determine the most-promising F_1 hybrids with respect to kernel color, size and quality properties using the sweet corn inbred lines as female parents and dent corn inbred lines as male parents. This study was performed in order to screen and identify the best parental inbred lines and hybrids using sweet corn and dent corn inbred lines as parents.

MATERIALS AND METHODS

Plant material and experimental design. The present study was carried out with four sweet corn inbred lines as female parents (SC1, SC2, SC3 and SC4) and two dent corn inbred lines as male parents (DC1 and DC2). Sweet corn inbred lines and dent corn inbred lines were obtained from the breeding programs conducted in the last decade by Department of Field Crops, Faculty of Agriculture, Ege University, İzmir, Turkey. The field experiments were conducted in 2012 and 2013 at the research field of Department of Field Crops, Faculty of Agriculture, Ege University, İzmir, Turkey. The field experiments were set up on clay loam soil.

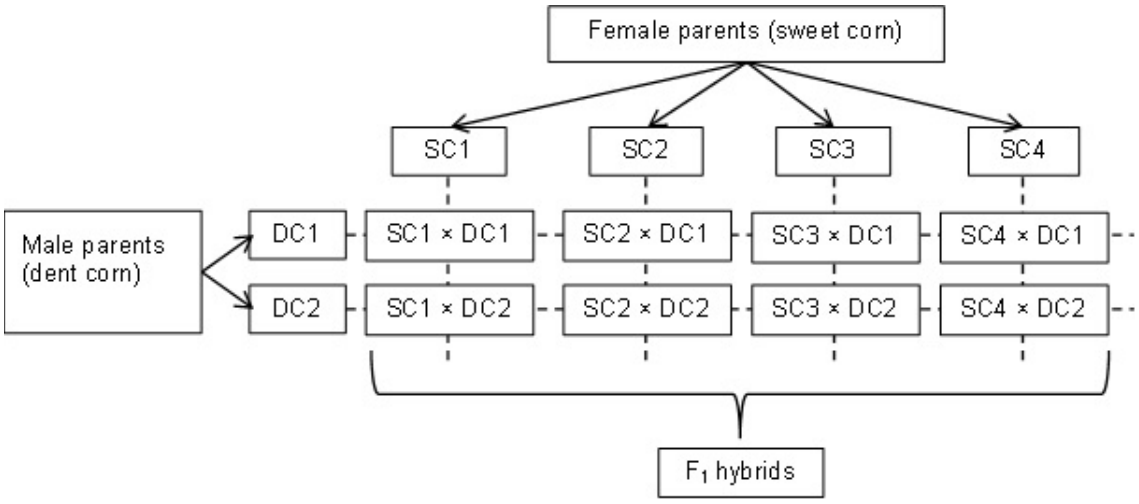

FIGURE 1
F_1 hybrids (sweet corn × dent corn); four sweet corn inbred lines as female parents (SC1, SC2, SC3 and SC4) and two dent corn inbred lines as male parents (DC1 and DC2) were used to produce F_1 hybrids

The characteristics of soil were determined as follows: pH = 7.63, light alkaline, chalky, low salt concentration, moderate nitrogen (N) and phosphorus (P) concentration, and rich in other macronutrients. These characteristics are similar to those of the soil in the study of Furan et al. [14]. Plaza et al. [15] reported that assessment of mineral nitrogen content in soil is assumed to be an indicator of environmental risk due to an excess concentration of nitrogen in soil.

In the present study, hybridization of sweet corn inbred lines and dent corn inbred lines (Fig. 1) were performed in the summer of 2012. Cultivation of F_1 generations was performed in the spring of 2013. The field experiments were arranged in randomized block design with three replications.

Each plot consisted of four rows that were 5 m long. The rows were planted 70 cm apart and 20 cm spaced in the rows. Plot area was 14 m^2 (5 m × 2.8 m). Planting was done by hand and after planting seedling emergence was obtained by sprinkler irrigation. No pesticide was used in the present study. Aksoy et al. [16] pointed out that pesticides cause chromosomal abnormalities and abnormal developments in some plant tissues. In the present study, the experimental area was fertilized at a rate of 30 kg da^{-1} nitrogen (N) and 10 kg da^{-1} phosphorus (P_2O_5). Before planting 10 kg da^{-1} nitrogen and 10 kg da^{-1} phosphorus were used as composed fertilizer (20-20-0). The remaining nitrogen fertilizer was applied as in the form of urea fertilizer during the six-eight leaf growing stage (V6-V8). Therefore, sprinkler irrigation, field management and other cultural practices were made routinely during the trials. The ears were harvested at the late milk stage. Harvesting was made by hand from two rows at the center of each plot (after removing 50 cm up and down sides from each rows) randomly, at the late milk stage.

Laboratory analyses. Kernel analyses of the female parents (SC1, SC2, SC3, SC4), male parents (DC1, DC2) and F_1 hybrids (SC1 × DC1, SC1 × DC2, SC2 × DC1, SC2 × DC2, SC3 × DC1, SC3 × DC2, SC4 × DC1, SC4 × DC2) were carried out in the Cereal Technology Laboratory of Department of Food Engineering, Faculty of Engineering, Ege University, İzmir, Turkey. We froze the ears at – 40 °C immediately after harvesting using a freezer (MDF-U443, Sanyo Electric Co., Ltd., Japan), to prevent conversion of sugar into starch. The measured morphological properties of F_1 hybrids are: kernel length, kernel width, kernel thickness, and 1000-kernel weight. The moisture, starch, total sugar, invert sugar, sucrose, soluble solids (°Brix) content analyses and color (L*, a*, b* values) measurements were performed to determine the characteristics of female parents and F_1 hybrids. The moisture, starch, total sugar, invert sugar, sucrose content analyses were performed to determine the characteristics of the male parents. All chemicals and laboratory reagents used in the laboratory studies were analytical grade.

Before starting laboratory analyses frozen ears of female parents and F_1 hybrids were thawed under the room temperature (25±2 °C) until the temperature of ears reached to the room temperature. After thawing step, the kernels were carefully removed from the ears by hand, and undamaged fresh kernels were chosen for analyses. The length, width and thickness of kernels of F_1 hybrids were measured using a digital caliper (Mitutoyo Corp., Japan). 1000-kernel weight was determined using a digital scale (TP-3002, Denver Instrument, USA). Undamaged fresh kernels obtained from female parents and F_1 hybrids were crashed using a mixer (Omni-Mixer 17220, Ivan Sorvall Inc., USA) for the moisture, starch, total sugar, invert sugar, sucrose, soluble solids (°Brix) content analyses and color (L*, a*, b* values) measurements. Dry kernels obtained

from male parents were milled in a laboratory scale mill (Falling Number AB Type 121, Finland). Moisture content analyses of fresh kernels obtained from female parents and F1 hybrids were conducted according to the method described in Cemeroğlu [17] using a vacuum oven (Wise Ven Fuzzy Control System Vacuum Oven WOV-30, Daihan Scientific Co., Ltd., Korea). Moisture content analyses of dry kernels obtained from male parents were conducted according to ICC Standard Nr. 110/1 [18] using a laboratory scale oven (Typ 2702, Köttermann Systemlabor, Germany). Starch content analyses of samples were conducted according to AOAC Official Method 945.37 [19]. Total sugar and invert sugar content analyses of samples were conducted according to Lane-Eynon Method described in Cemeroğlu [17]. Sucrose content of samples was calculated by using the following formula:

Sucrose content = (Total sugar content – Invert sugar content) × 0.95

Soluble solids (°Brix) content analyses of female parents and F_1 hybrids were conducted at 25±2 °C according to the method described in Cemeroğlu [17] using a digital refractometer (Atago Co. Ltd., Japan). Color (L*, a*, b* values) measurements of female parents and F_1 hybrids were done using a colorimeter (Color Flex, Hunter Lab Inc., USA).

Statistical analysis. The data obtained in the present study were subjected to analysis of variance (ANOVA) using the software of Statistical Package for the Social Sciences–SPSS 15.0 (2006, SPSS Inc., USA). The mean values were compared using the Tukey HSD Post Hoc Test ($P<0.05$).

TABLE 1
Kernel length, width, thickness, and 1000-kernel weight values of F_1 hybrids (sweet corn × dent corn)

F1 hybrids	Kernel length [mm]	Kernel width [mm]	Kernel thickness [mm]	1000-kernel weight [g]
SC1 × DC1	8.56 ± 0.56 ^{e}	7.84 ± 0.35 ^{bc}	4.84 ± 0.48 ^{c}	288.79 ± 14.95 ^{d}
SC1 × DC2	9.14 ± 0.62 ^{d}	8.09 ± 0.62 ^{ab}	5.24 ± 0.62 ^{ab}	314.85 ± 11.01 ^{bc}
SC2 × DC1	10.10 ± 0.47 ^{b}	8.41 ± 0.52 ^{a}	5.28 ± 0.52 ^{ab}	345.76 ± 8.01 ^{a}
SC2 × DC2	10.68 ± 0.69 ^{a}	8.03 ± 0.53 ^{b}	5.55 ± 0.59 ^{a}	335.55 ± 24.01 ^{ab}
SC3 × DC1	8.90 ± 0.79 ^{de}	7.59 ± 0.71 ^{c}	5.16 ± 0.50 ^{abc}	285.84 ± 2.64 ^{d}
SC3 × DC2	9.78 ± 0.71 ^{bc}	8.14 ± 0.55 ^{ab}	5.03 ± 0.55 ^{bc}	310.69 ± 3.51 ^{c}
SC4 × DC1	8.76 ± 0.60 ^{de}	7.90 ± 0.43 ^{bc}	4.96 ± 0.79 ^{bc}	312.51 ± 18.90 ^{c}
SC4 × DC2	9.62 ± 0.82 ^{c}	8.01 ± 0.49 ^{b}	4.89 ± 0.60 ^{bc}	334.11 ± 9.47 ^{ab}

SC1, SC2, SC3, SC4 represent female parents (sweet corn); DC1, DC2 represent male parents (dent corn); ×, denotes hybridization.
Data are expressed as mean values ± standard deviations (n=20 for kernel length, width and thickness; n=8 for 1000-kernel weight).
Mean values within the same column followed by different superscripts are significantly different ($P<0.05$). The letter "a" denotes the highest value.

TABLE 2
Color values (L*, a*, b*) of female parents (sweet corn) and F_1 hybrids (sweet corn × dent corn)

Female parents	L*	a*	b*
SC1	69.5 ± 0.09 ^{D}	3.25 ± 0.03 ^{D}	13.54 ± 0.02 ^{D}
SC2	74.49 ± 0.03 ^{B}	5.03 ± 0.02 ^{C}	16.09 ± 0.02 ^{C}
SC3	82.80 ± 0.11 ^{A}	7.30 ± 0.04 ^{A}	38.69 ± 0.03 ^{A}
SC4	71.30 ± 0.03 ^{C}	5.49 ± 0.04 ^{B}	16.86 ± 0.08 ^{B}
F_1 hybrids			
SC1 × DC1	74.80 ± 0.40 ^{cd}	12.48 ± 0.40 ^{b}	36.73 ± 2.36 ^{cde}
SC1 × DC2	73.83 ± 1.68 ^{d}	11.67 ± 0.20 ^{bc}	35.43 ± 2.76 ^{de}
SC2 × DC1	75.74 ± 0.27 ^{bc}	12.38 ± 0.59 ^{b}	39.66 ± 1.26 ^{b}
SC2 × DC2	73.84 ± 0.57 ^{d}	11.92 ± 0.49 ^{bc}	37.05 ± 1.31 ^{cd}
SC3 × DC1	76.00 ± 1.75 ^{bc}	11.19 ± 0.75 ^{c}	34.43 ± 1.08 ^{e}
SC3 × DC2	70.30 ± 1.14 ^{e}	14.56 ± 0.48 ^{a}	42.67 ± 2.64 ^{a}
SC4 × DC1	77.85 ± 1.12 ^{a}	11.80 ± 0.76 ^{bc}	37.19 ± 1.32 ^{cd}
SC4 × DC2	76.15 ± 1.00 ^{b}	12.30 ± 1.93 ^{b}	38.57 ± 3.45 ^{bc}

SC1, SC2, SC3, SC4 represent female parents (sweet corn); DC1, DC2 represent male parents (dent corn); ×, denotes hybridization.
L*, indicates brightness (0-100 represents dark to light); a*, indicates redness and greenness (a higher positive a* value indicates more red); b*, indicates yellowness and blueness (a higher positive b* value indicates more yellow).
Data are expressed as mean values ± standard deviations (n=4 for female parents; n=16 for F_1 hybrids).
Mean values within the same column followed by different superscripts are significantly different ($P<0.05$). The letter "A" and "a" denote the highest values.

RESULTS AND DISCUSSION

Kernel length, width and thickness, and 1000-kernel weight values of F_1 hybrids are presented in Table 1. Color values (L*, a*, b*) of female parents and F_1 hybrids are presented in Table 2. Moisture, starch, total sugar, invert sugar, sucrose and soluble solids (°Brix) contents of the female, male parents and F_1 hybrids are presented in Table 3.

Özçam [13]; Kumar et al. [20] found a considerable heterosis between sweet corn and dent corn in terms of plant height, ear length, ear diameter, grain number per ear, 100-kernel weight and grain yield. Hallauer et al. [21] reported that kernel length, width and thickness of dent corn are ~9.7 mm, ~8.2 mm and ~5.3 mm, respectively. In the present study, kernel length, width, thickness values of F_1 hybrids were found between 8.56 and 10.68 mm, 7.59 and 8.41 mm, 4.84 and 5.55 mm, respectively (Table 1). These findings indicate that the kernel length, width and thickness of F_1 hybrids are similar to dent corn. We also observed that SC2's hybrids have the highest kernel length, width, thickness and 1000-kernel weight among F_1 hybrids.

As presented in Table 2, the lowest and the highest L*, a*, b* values were measured in SC1 and SC3 parents, respectively. This finding indicates that the color intense of SC3 is higher than other female parents. In the present study, the highest L* values were found in SC4's hybrids. L* values of SC2 × DC1, SC3 × DC1 and SC4 × DC1 were found to be significantly higher than SC2 × DC2, SC3 × DC2 and SC4 × DC2, respectively. The same trend was not observed in a* and b* values among F_1 hybrids. Although not significant, L* value of SC1 × DC1 was found to be slightly higher than SC1 × DC2. The most significant differences in L*, a* and b* values were determined between SC3's hybrids (SC3 × DC1 and SC3 × DC2). This finding indicates that SC3 inbred line is not totally pure line and it needs a couple of generations for inbreeding. The remarkable finding in our study is that the hybridization of SC1 and SC4 with male parents caused a significant increase in L*, a*, b* values in their F_1 hybrids (Table 2).

Singh et al. [22] measured L* value of sweet corn whole meal and dent corn whole meal samples in their study as being similar to each other (measured as 82.3). They found a*: 4.4 and b*: 25.8 for sweet corn whole meal samples, a*: 5.1 and b*: 26.7 for dent corn whole meal samples. In our study, L*, a*, b* values of F_1 hybrids were found to be varied between 70.30 and 77.85, 11.19 and 14.56, 34.43 and 42.67, respectively. These findings indicate that F_1 hybrids of our study have higher color intensity in red and yellow, compared with the data of dent corn and sweet corn obtained by Singh et al. [22].

TABLE 3
Proximate composition of female parents (sweet corn), male parents (dent corn) and F_1 hybrids (sweet corn × dent corn)

Female parents	Moisture [%]	Starch* [%]	Total sugar* [%]	Invert sugar* [%]	Sucrose* [%]	°Brix§
SC1	81.45 ± 0.55 ^{A}	26.48 ± 2.16 ^{B}	6.03 ± 0.14 ^{C}	4.95 ± 0.15 ^{B}	1.03 ± 0.18 ^{C}	11.35 ± 0.15 ^{D}
SC2	75.06 ± 0.35 ^{C}	52.87 ± 1.11 ^{A}	7.27 ± 0.61 ^{B}	5.83 ± 0.24 ^{A}	1.36 ± 0.36^{CB}	16.65 ± 0.15 ^{B}
SC3	79.05 ± 0.95 ^{B}	22.75 ± 0.68 ^{C}	11.45 ± 0.67 ^{A}	2.05 ± 0.24 ^{D}	8.93 ± 0.62 ^{A}	22.83 ± 0.15 ^{A}
SC4	77.71 ± 0.83 ^{B}	50.97 ± 1.81 ^{A}	6.00 ± 0.35 ^{C}	4.02 ± 0.05 ^{C}	1.88 ± 0.29 ^{B}	14.58 ± 0.18 ^{C}
Male parents						
DC1	11.21 ± 0.22 ^{A}	76.88 ± 1.31 ^{A}	0.58 ± 0.01 ^{B}	0.32 ± 0.03 ^{B}	0.25 ± 0.02 ^{B}	nd
DC2	11.25 ± 0.11 ^{A}	75.93 ± 0.49 ^{A}	0.85 ± 0.04 ^{A}	0.51 ± 0.01 ^{A}	0.32 ± 0.03 ^{A}	nd
F_1 hybrids						
SC1 × DC1	40.33 ± 1.32 ^{bc}	35.88 ± 4.24 ^{ab}	10.74 ± 0.98 ^{ab}	6.24 ± 0.12 ^{bc}	4.28 ± 0.94 ^{cd}	15.55 ± 0.78 ^{c}
SC1 × DC2	40.73 ± 0.57 ^{b}	36.54 ± 5.42 ^{ab}	8.08 ± 0.60 ^{c}	6.17 ± 0.14 ^{bc}	1.81 ± 0.51 ^{ef}	17.07 ± 0.13 ^{b}
SC2 × DC1	41.02 ± 0.57 ^{b}	37.76 ± 4.02 ^{ab}	6.68 ± 0.29 ^{c}	4.81 ± 0.35 ^{d}	1.78 ± 0.51 ^{f}	14.97 ± 0.86 ^{cd}
SC2 × DC2	38.69 ± 1.35 ^{cd}	29.72 ± 0.48 ^{c}	10.63 ± 1.87 ^{ab}	4.94 ± 0.72 ^{d}	5.40 ± 1.11^{abc}	14.81 ± 0.59 ^{de}
SC3 × DC1	37.78 ± 2.01 ^{d}	30.72 ± 1.45 ^{c}	11.82 ± 1.57 ^{a}	5.12 ± 0.22 ^{d}	6.36 ± 1.70 ^{a}	14.36 ± 0.59 ^{de}
SC3 × DC2	43.07 ± 1.38 ^{a}	34.30 ± 1.66 ^{bc}	11.98 ± 0.41 ^{a}	5.72 ± 0.51 ^{c}	5.95 ± 0.52 ^{ab}	14.20 ± 0.21 ^{e}
SC4 × DC1	43.53 ± 1.12 ^{a}	39.89 ± 2.68 ^{a}	9.87 ± 0.36 ^{b}	6.55 ± 0.35 ^{ab}	3.15 ± 0.20 ^{de}	18.88 ± 0.09 ^{a}
SC4 × DC2	43.09 ± 0.75 ^{a}	37.07 ± 0.80 ^{ab}	11.84 ±0.66 ^{a}	6.86 ± 0.20 ^{a}	4.74 ± 0.49 ^{bc}	18.95 ± 0.59 ^{a}

SC1, SC2, SC3, SC4 represent female parents (sweet corn); DC1, DC2 represent male parents (dent corn); ×, denotes hybridization.

*, expressed as in dry matter base; §, °Brix at 25±2 °C; nd, not detected.

Data are expressed as mean values ± standard deviations (n=8).

Mean values within the same column followed by different superscripts are significantly different ($P<0.05$). The letter "A" and "a" denote the highest values.

Bilgiç et al. [23] found that the starch contents of dent corn samples used in their study varied between 60 and 78%. Oktem and Oktem [24] reported that sweet corn has 10–11% starch content at its optimum market maturity [7]. Pazır and Kantarcı [25] determined that the starch contents of three sweet corn hybrids (*Sunshine, Merkür, Eltoro*) varied between 20.58 and 20.93%. In our study, starch contents of male parents were found to be higher than female parents and F_1 hybrids (Table 3). SC2 and SC4 have significantly higher starch contents compared with SC1 and SC3. Starch contents of F_1 hybrids were found to vary between 29.72 and 39.89%. The lowest starch contents were found in SC2 × DC2 and SC3 × DC1 among F_1 hybrids. The highest starch content was found in SC4 × DC1.

In a previous study, Bilgiç et al. [23] determined 1–3% total sugar contents in dent corn samples. In the present study, we found that male parents have very low total sugar contents compared with female parents and F_1 hybrids. Total sugar contents of female parents were found to vary between 6.00% (SC4) and 11.45% (SC3). This finding is in agreement with the findings of Tracy [9], who reported that the total sugar content of sweet corn ranged between 4 and 12%. According to Oktem and Oktem [24], sweet corn has 5–6% sugar content at its optimum market maturity [7]. Pereira [26] found a total sugar content of 4.30, 4.60 and 5.20% for the cultivars *Doce Cristal*, *Doce-de-Ouro* and *Superdoce*, respectively [10]. In our study, total sugar contents of F_1 hybrids were found between 6.68 and 11.98%, which are similar to the findings of Pazır and Kantarcı [25], who determined that the total sugar contents of sweet corn hybrids varied between 7.15 and 11.45%. In our study, the lowest total sugar contents were found in SC2 × DC1 and SC1 × DC2 among the F_1 hybrids. The highest total sugar contents were observed in SC3's hybrids and SC4 × DC2. These findings indicate that SC3 can be considered as a good combiner in terms of total sugar content compared with other female parents. Additionally, total sugar contents of F_1 hybrids in our study were found to be in agreement with the data obtained using sweet corn, by Pereira [26]; Tracy [9]; Oktem and Oktem [24]. This finding leads to a conclusion that new type promising hybrids from sweet corn and dent corn were successfully produced in terms of high total sugar content, in the present study.

In our study, the highest invert sugar contents were found in SC4's hybrids, followed by SC1's, SC3's and SC2's hybrids. The invert sugar content of F_1 hybrids varied between 4.81 and 6.86%, which are higher than the data obtained by Pazır and Kantarcı [25], who found 1.55–2.22% invert sugar content in sweet corn hybrids (late planted and harvested as a second crop). This finding indicates that sugar in our F_1 hybrids is in the form of solution.

Kaukis and Davis [27] reported that the primary sugar in sweet corn is sucrose, with lesser amounts of glucose, fructose and maltose, and the sweetness of sweet corn mainly depends on kernel sucrose content [4]. Similarly, Wiley [28] pointed out that sweetness is closely related to the kernel sucrose content of corn [6]. In our study, the sucrose content of F_1 hybrids varied between 1.78 and 6.36%. Sucrose content of SC3 (8.93%) was found to be significantly higher than other female parents (Table 3). Therefore, the highest sucrose content was found in SC3's hybrids, in the present study.

°Brix values of F_1 hybrids in our study were found to be between 14.20 and 18.95. The highest °Brix values were found in SC4's F_1 hybrids, followed by SC1's, SC2's and SC3's hybrids. Tuncay et al. [29] determined 11.03-19.13 and 12.18-20.00 °Brix values in sweet corn hybrids planted during the periods of the main crop and second crop, respectively. Pereira [26] found °Brix values of 17.70, 20.80 and 22.30 for the cultivars *Doce Cristal*, *Doce-de-Ouro* and *Superdoce*, respectively [10]. Pazır and Kantarcı [25] found °Brix values between 20.63-24.18 in three sweet corn hybrids (late planted and harvested as second crop). In our study, °Brix values of F_1 hybrids (planted in the period of second crop) were found to be in agreement with the data obtained by Tuncay et al. [29]. Flora and Wiley [5] pointed out that the significant component of the soluble solids is sugar and a high amount of soluble solids content in the kernel improves the taste of sweet corn, positively. In the present study, °Brix values indicated that F_1 hybrids are at an adequate level from the standpoint of a sweet taste.

CONCLUSION

In this study, the results of kernel length, width, thickness and 1000-kernel weight of F_1 hybrids were found to be similar to those of dent corn samples, as reported by previous studies in the literature. Color values (L*, a*, b*) of F_1 hybrids in the present study were found to be similar to each other. The data recorded for the starch, total sugar, sucrose and soluble solids (°Brix) contents of F_1 hybrids indicated that F_1 hybrids produced in this study had similar properties to sweet corn. The findings in our study lead to the conclusion that it is possible to produce promising sweet corn hybrids that have improved quality characteristics from sweet corn and dent corn inbred lines.

REFERENCES

[1] Zhang, Q., Zhang, L., Evers, J., Van Der Werf, W., Zhang, W. and Duan, L. (2014) Maize yield and quality in response to plant density and application of a novel plant growth regulator. Field Crop Res. 164, 82–89.

[2] Bandeira, C.M., Evangelista, W.P. and Gloria, M.B.A. (2012) Bioactive amines in fresh, canned and dried sweet corn, embryo and endosperm and germinated corn. Food Chem. 131, 1355–1359.

[3] Dickerson, G.W. (2003) Specialty corns. New Mexico State University, Department of Agriculture Cooperating, Guide H-232. Available from: http://aces.nmsu.edu/pubs/_h/H232.pdf. [accessed 01 04 2015].

[4] Farsiani, A., Ghobadi, M.E., and Jalali-Honarmand, S. (2011) The effect of water deficit and sowing date on yield components and seed sugar contents of sweet corn (Zea mays L.). Afr J Agric Res. 26, 5769–5774.

[5] Flora, L.F. and Wiley, R.C. (1974) Sweet corn aroma, chemical components, and relative importance in the overall flavor response. J Food Sci. 39, 770–773.

[6] Wang, A.D., Swiader, J.M. and Juvik, J.A. (1995) Nitrogen and sulfur fertilization influences aromatic flavor components in Shrunken2 sweet corn kernels. J Amer Soc Hort Sci. 120, 771–777.

[7] Fekonja, M., Bavec, F., Grobelnik-Mlakar, S., Turinek, M., Jakop, M. and Bavec, M. (2011) Growth performance of sweet maize under non-typical maize growing conditions. Biological Agriculture and Horticulture. 27, 147–164.

[8] Bavec, F., Bavec, M. and Fekonja, M. (2013) Organic and mineral nitrogen fertilizers in sweet maize (Zea mays L. saccharata Sturt.) production under temperate climate. Zemdirbyste. 100, 243–250.

[9] Tracy, W.F. (1994) Sweet corn. In: Hallauer, A.R. (Ed.) Specialty Types of Maize. CRC Press, Boca Raton, FL, USA, 147–187.

[10] Assunção, A., Brasil, E.M., Oliveira, J.P., Reis, A.J.S., Pereira, A.F., Bueno, L.G. and Ramos, M.R. (2010) Heterosis performance in industrial and yield components of sweet corn. Crop Breed Appl Biot. 10, 183–190.

[11] Tracy, W.F. (2001) Sweet corn. In: Hallauer, A.R. (Ed.) Specialty Corns. CRC Press, Boca Raton, FL, USA, 155–199.

[12] Kumari, J., Gadag, R.N. and Jha, G.K. (2008) Combining ability and heterosis in field vs sweet corn hybrids using line by tester mating design. Indian J Agr Sci. 3, 261–264.

[13] Özçam, S. (2012) Determining performance of crosses inbred dent corn (Zea mays indentata Sturt.) with inbred sweet corn (Zea mays saccharata Sturt.), M.Sc. Thesis. Ege University Graduate School of Natural and Applied Science, İzmir, Turkey (in Turkish).

[14] Furan, M.A., Demir, İ., Yüce, S., Akçalı Can, R.R. and Aykut, F. (2005) Research on Aegean Region Triticale Variety Development Studies and Relationships among Yield and Quality Components in the Developed Variety and Lines. Mediterr Agric Sci. 18, 251–256 (in Turkish).

[15] Plaza, A., Makarewicz, A. and Gasiorowska, B. (2015) Influence of Undersown Catch Crops on Mineral Nitrogen Content Determined in the Soil Profile in Autumn and Spring in Conventional and Organic Farming Systems. Fresen. Environ. Bull. 24, 3315–3319.

[16] Aksoy, Ö., Deveci, A. and Tütünoğlu, B. (2015) Genotoxic Effects of the Fungicide Sportak on *Zea Mays*. Fresen. Environ. Bull. 24, 552–559.

[17] Cemeroğlu, B. (2007) Food analyses. The Journal of Food Technologies Association, No.34, Ankara, Turkey, 535 p (in Turkish).

[18] ICC Standard Nr. 110/1 (2004) Determination of the moisture content of cereals and cereal products (practical method). International Association for Cereal Science and Technology (ICC), Vienna, Austria.

[19] AOAC Official Method 945.37 (1990) Starch in flour, polarization method. Official Methods of Analysis of the Association of Official Analytical Chemists (AOAC). Association of Official Analytical Chemists Inc., Virginia, USA.

[20] Kumar, R., Shahi, J.P. and Srivastava, K. (2013) Estimation of heterosis in field corn and sweet corn at marketable stage. The Bioscan. 8, 1165–1170.

[21] Hallauer, A.R., Russell, W. and Lamkey, K.R. (1988) Corn breeding. In: Sprague, G.F. and Dudley, J.W. (Eds.) Corn and Corn Improvement. Third Edition. ASA-CSSA-SSSA, Madison, Wisconsin, USA, 469–564.

[22] Singh, N., Bedi, R., Garg, R., Garg, M. and Singh, J. (2009) Physico–chemical, thermal and pasting properties of fractions obtained during three successive reduction milling of different corn types. Food Chem. 113, 71–77.

[23] Bilgiç, Ş., Sade, B., Soylu, S., Bilgiçli, N., Cerit, İ., Öz, A., Cengiz, R. and Özkan, İ. (2012) Maize Report. Turkey National Cereal Council (in Turkish).

[24] Oktem, A.G. and Oktem, A. (2005) Effect of nitrogen and intra row spaces on sweet corn (*Zea mays saccharata* Sturt) ear characteristics. Asian J Plant Sci. 4, 361–364.

[25] Pazır, F. and Kantarcı, D. (2012) Optimization of harvesting time by quality criteria of sweet corn. Ege University Scientific Research Project, No. 11-MÜH-019, İzmir, Turkey, 233p. (in Turkish).
[26] Pereira, A.S. (1987) Nutritional composition, taste and quality standards of three sweet-corn cultivars. Hortic Bras. 5, 22–24. (in Portuguese).
[27] Kaukis, K. and Davis, D.W. (1986) Sweet corn breeding. In: Bassett, M.J. (Ed.) Breeding Vegetable Crops. AVI Publishing, Westport, CO, USA, 475–519.
[28] Wiley, R.C. (1985) Sweet corn aroma: Studies of its chemical components and influence on flavor. In: Pattee, H.E. (Ed.) Evaluation of Quality of Fruits and Vegetables. AVI Publishing, Westport, CO, USA, 349–366.
[29] Tuncay, Ö., Bozokalfa, M.K. and Eşiyok, D. (2005) Determination of ear characteristic and technological properties of some sweet corn (Zea mays L. var. saccharata) varieties as main and second crop. The Journal of Agricultural Faculty of Ege University. 42, 47–58. (in Turkish).

Received: **22.04.2017**
Accepted: **02.02.2019**

CORRESPONDING AUTHOR

Burak Altınel
Ege University,
Faculty of Engineering,
Department of Food Engineering,
35100 Bornova, İzmir – Turkey

e-mail: burak.altinel@ege.edu.tr

© by PSP Volume 28 – No. 4/2019 pages 2375-2379 Fresenius Environmental Bulletin

LARVICIDAL EFFECT OF *PINUS BRUTIA* TEN. SEED ESSENTIAL OIL TO PINE PROCESSIONARY MOTH (*THAUMETOPOEA WILKINSONI* TAMS.) UNDER LABORATORY CONDITIONS

Gurkan Semiz[1,*], Kubra Kocabiyik[1], Huseyin Cetin[2]

[1]Pamukkale University, Faculty of Arts & Science, Department of Biology, Denizli, Turkey
[2]Akdeniz University, Faculty of Science, Department of Biology, Antalya, Turkey

ABSTRACT

Thaumetopoea wilkinsoni Tams. is one of the most widespread pest found in the pine forest of Turkey. The objective of this study was to determine larvicidal effects of essential oil obtained from *Pinus brutia* Ten. on the third and fourth instar larvae of *T. wilkinsoni* under laboratory conditions. In the present study, seed essential oil was tested at seven different doses (5 to 1000 ppm) against to this pest. The chemical composition of the oil was determined by GC-MS. The essential oil of *P. brutia* was dominated by monoterpenes. Totally, 14 chemical compounds were identified by GC-MS analysis. β-Pinene (38.15%) and α-pinene (24.99%) were identified as major chemical components followed by trans-β-caryophyllene (15.24 %) and germacrene-D (4.25 %). As a result of analysis, *P. brutia* seed oil showed high larvicidal activity, with LD50 values of 187.88, 122.83 and 68.77 ppm, LD90 values of 608.85, 479.31 and 300.16 ppm at 24, 48 and 72 hours, respectively. The results showed that the activities were dose dependent. Therefore, this essential oil could be useful for to find management strategies against populations of *T. wilkinsoni*. In this study, the larvicidal activity of essential oil from *P. brutia* against *T. wilkinsoni* was evaluated for the first time.

KEYWORDS:
Seed essential oil, Larvicidal activity, *Pinus brutia*, *Thaumetopoea wilkinsoni*, Turkey

INTRODUCTION

Pinus brutia Ten. is a most prominent native forest tree species in Turkey due to both its ecological and economical assets. It has been used in reforestation studies due to its rapid germination and high genetic variation properties. In Turkey, *P. brutia* has the most large natural distribution area and covers 5.4 million ha [1]. As *P. brutia* is a typical light demanding forest tree species, it occurs more at higher elevations on southern places than the northern places. Pine processionary moth (PPM) (*Thaumetopoea wilkinsoni* Tams.) is a major defoliator of the *P. brutia* in Turkey. Natural forests and plantation areas are subject to periodic outbreaks. In mature forests, trees are barely killed, but significant losses bring about in volume and radial growths [2]. It is well known that defoliation may increase tree stress and their susceptibility to secondary pests such as bark beetles and pine weevils, particularly in young trees [3]. Fourth- and fifth-instar larvae can consume all the needles of host trees, so that trees have to be scorched. The average decrease in annual diameter increment for *P. brutia* in damaged areas, compared with healthy trees, can reach about 22% [4]. PPM increased its distribution 6 times between 1938 and 2009 in Turkey [5]. For PPM management, mechanical-physical, chemical, bio-technical and biological methods are widely used. As far as control concerned, the methods mainly based on using by various chemicals [4-8], collecting egg-batches [8] and silky nests [6, 9], plant essential oils [10], pheromone traps [11], parasitoids-predators [6, 12, 13], entomopathogenic fungi/nematodes [14-15], and microbial pathogens [6, 7, 16] in Turkey. Therefore, the aim of this research was to determine the larvicidal activity of seed essential oil (EO) of *P. brutia* against to PPM.

MATERIALS AND METHODS

Study materials and extraction of the EO. Third and fourth instar larvae of PPM were collected from infested *P. brutia* trees in the forest part of Babadag, Denizli, Turkey. *P. brutia* seeds used in the experiments were obtained from the Denizli Forestry Regional Nursery Directorate. PPM larvae and seeds have been transferred to Pamukkale University, Department of Biology, Chemical Ecology Laboratory and then, they were stored under laboratory conditions until experiments were performed. All tests carried out at 20ºC (±2), 60% (±5) relative humidity and 14/10 h light/dark photoperiod in laboratory conditions. Essential oil of the seeds

(500 g) obtained by hydrodistillation for 4 h using a Clevenger-type apparatus with 2000 ml flask. The essential oil collected by decantation was dried over anhydrous sodium sulphate. Obtained essential oil was transferred to a 10 ml volumetric flask and stored in an airtight container prior to analysis at 4°C. The hydrodistillation of *P. brutia* seeds oil in 0.5% (w/w) yield and EO was light colour with a sharp odor.

Chemical analyses. Chemical composition of the EO was analysed by a Hewlett Packard GC type 7820A, MSD 5975; Hewlett Packard, Wilmington, DE, USA. Preparation of EO samples: 15 µl of EO was diluted in 1485 µl of *n*-hexane. A sample of 1 µl was injected under the following conditions: column: HP-5MS (30 m × 0.25 mm, film thickness 0.25 µm, Hewlett Packard); carrier gas helium (1.2 ml/min); the temperature program for terpenes ranged from 50°C to 250°C; the heating rate was 5°C min^{-1}; SCAN technique (mass numbers from m/z 30 to 350 were recorded; signal ions in monitoring; 93, 133, 136, 161, and 204 m/z) was used. The individual peaks were identified by comparison of their retention indices (relative to C8-C25 *n*-alkanes for HP-5MS) as well as by comparing their mass spectra with the Wiley 7 MS library (Wiley, New York, NY, USA) and NIST02 (Gaithersburg, MD, USA) mass spectral database. A series of *n*-alkanes was also injected under same analytical conditions with that of the essential oil for the calculation of Retention Indices (RI). The percentage composition of the samples was computed from the GC peak areas using the normalization method. The component percentages were calculated as mean values from duplicate GC and GC-MS analyses.

Larvicidal assays. For the assays, 1 mL of essential oil from *P. brutia* seeds was dissolved in 100 mL distilled water + Tween 80 (0.3%). Series concentrations ranging from 5 to 1000 ppm of dissolved oil and distilled water+ Tween 80 (0.3%) mixture for control group were prepared. The larval mortality bioassay was carried out according to the test method described by Cetin *et al*. [17] with minor modifications. Field collected larvae nests were opened under fume hood and then larvae transferred into the petri dish with 10 larvae per dish. The larvae were fed on fresh pine needles. Each dose of *P. brutia* seed EO (1 ml per larvae) was topically applied to larvae. Three replicates of each dose and control-Tween 80 (0.3%) were run at a time. Mortality was recorded after an exposure of 24, 48 and 72 hours. Test mortality was determined by observing individuals that were neither moving when prodded with a fine brush nor feeding in the test area Cetin *et al*. (2007).

Data analysis. Percent mortality data were subjected to ANOVA [18] and the means were compared to determine significant differences using Duncan's multiple range tests ($p < 0.05$). Probit analysis of dose-mortality data was conducted to estimate the LD50 and LD90 values and associated 95% confidence limits for each treatment [19].

RESULTS AND DISCUSSION

Chemical composition of the EO. The GC–MS analysis of the EO led to the identification and quantification of a total of 14 major components corresponding to 98.59% of the total oil (Table 1). The main constituents found in the EO were β-pinene (38.15%), α-pinene (24.99%) and trans-β-caryophyllene (15.24%), respectively. The results revealed that monoterpenes in the seed EO were predominant (73.34%), whereas sesquiterpenes were present in lower amounts.

TABLE 1
Composition of the essential oils obtained from seeds *Pinus brutia*

No	Compound name[a]	RI[b]	Content (%)
1	α-Pinene	936	24.99
2	Camphene	950	1.63
3	Sabinene	975	1.39
4	β-Pinene	980	38.15
5	Myrcene	990	2.39
6	3-Carene	1011	1.37
7	Limonene	1032	1.08
8	Trans-β-ocimene	1038	1.54
9	α-Terpinolene acetate	1086	0.80
10	Trans-β-caryophyllene	1420	15.24
11	α-Humulene	1454	1.48
12	Germacrene D	1480	4.25
13	γ-Cadinene	1520	2.11
14	α-Bisabolene	1541	2.17
	Total identified		**98.59**

[a] Compounds listed in order their elution,
[b] RI: retention index measured relative to *n*-alkanes on HP-5MS column.

Larvicidal activity of EO. The larvicidal potential of different doses of seed EO of *P. brutia* against *T. wilkinsoni* is given in Table 2 and 3. Among the seven doses tested, the dosage of 1000 ppm caused 100% larval mortality after 24 h. Larval mortality was not observed throughout the study in the control group. After 24 h, the EO from the seed of *P. brutia* exhibited significant larvicidal activity; the LD50 and LD90 values are 187.88 ppm (Limits; 129.71-266.92 ppm) and 608.85 ppm (Limits; 400.22-1301.57 ppm) respectively. Larval mortality was not observed throughout the study with 5 ppm dose. As we expected, larval mortality rates increased with increasing doses of the EO used. The lowest mortality rate observed as 13.33% with 50 ppm dose at the 24 hours, 6.67% and 10%

TABLE 2
Toxicity of seed essential oils from *Pinus brutia* on *Thaumetopoea wilkinsoni* (Mortality (%) ± SE)

Time (hour)	Test doses (ppm)							
	Control	5	10	50	100	250	500	1000
24	0.0±0.0	0.0±0.0	0.0±0.0	13.3±3.3	23.3±3.3	46.6±3.3	90.0±5.7	100.0±0.0
	$a^{\alpha}A^{\beta}$	aA	aA	aB	aC	aD	aE	aE
48	0.0±0.0	0.0±0.0	6.6±1.1	16.6±1.1	30.0±3.3	66.6±5.8	100.0±0.0	100.0±0.0
	aA	aA	bAB	aB	aC	abD	aE	aE
72	0.0±0.0	0.0±0.0	10.0±0.0	36.6±3.3	56.6±6.6	83.3±8.8	100.0±0.0	100.0±0.0
	aA	aA	bA	bB	bC	bD	aE	aE

$^{\alpha}$: Means within a column followed by the same lower case letter are not significantly different (Duncan's multiple range test, P< 0.05).
$^{\beta}$: Means within a line followed by the same capital letter are not significantly different (Duncan's multiple range test, P< 0.05).

TABLE 3
Larvicidal properties of seed essential oils from *Pinus brutia* against the larvae of *Thaumetopoea wilkinsoni* at 24, 48 and 72 hours

Time (h)	LD50 (ppm)	Limits (ppm)	LD90 (ppm)	Limits (ppm)
24	187.88	129.71-266.92	608.85	400.22-1301.57
48	122.83	50.22-251.16	479.31	237.87-3728.85
72	68.77	46.05-98.39	300.16	195.85-576.94

with 10 ppm dose at the 48 and 72 hours. Some researchers have determined the larvicidal activity of various plant seed oils and extracts against PPM [20, 21]. Cetin *et al*., (2007) reported that the EO from aerial parts of *Origanum onites* showed larvicidal effects against *T. wilkinsoni* larvae. Kanat and Alma (2004) found that steam distilled wood turpentine obtained from *P. brutia* had strong larvicidal activity against *T. wilkinsoni*. Also, Unal and Akkuzu [22] demostrated that *Azadirachta indica* A. Juss extracts showed high larvicidal activity against *T. wilkinsoni*. Up to now, there are no reports on the larvicidal effect of *P. brutia* seed oil against *T. wilkinsoni*. However, some researchers have shown that EOs of *Pinus* sp. and some plant species revealed insecticidal activity against to some pest species [23-26].

PPM is one of the most harmful pest in Mediterranean Basin and it causes serious morphological and physiological losses in *Pinus* forests. After heavily damage by PPM, resistance ability of the damaged tree to drought, pathogens and herbivores may be reduced. Until now, although different methods were used to control this pest, the problem is still unsolved in many part of the Mediterranean Basin where the pest occurs. In this point, *P. brutia* seed EO has significant larvicidal activity against PPM larvae and it might be used for potential larvicides.

The use of plant-derived essential oils is a promising method to control the pests and reduce the negative side-effects of chemical-based insecticides on the environment [27]. Recently, many studies have been conducted to find new plants and plant-derived EOs as a natural and eco-friendly larvicides. In this regard, it is necessary to conduct more detailed research to find active components of this plant EO that are more effective larvicidal activities and less side effect. Using of plant-derived larvicides instead of chemical larvicides reduces the damage would have occurred in the environment.

ACKNOWLEDGEMENTS

The authors are express their gratitude to Scientific Projects Administration Unit of Pamukkale University, Denizli, Turkey for financial support and to the Denizli Forestry Regional Nursery Directorate for providing seed material. All authors read and approved the final version of the manuscript.

REFERENCES

[1] OGM. (2008) Forest Inventory, Main Tree Species http://amenajman.ogm.gov.tr/.
[2] Laurent-Hervouet, N. (1986) Radial growth losses in some species of *Pinus* due to two forest defoliators. I- Case of the pine processionary moth in the Mediterranean area. Annales Forest Science. 43, 239–262. (In French with English abstract).
[3] Kanat, M., Sivrikaya, F., Serez M. (2002) A research on damage of pine processionary moth (*Thaumetopoea pityocampa* Schiff.) on *Pinus brutia* Ten. trees, and the effect of tending activities on the diameter increment of Calabran pine in Kahramanmaras. In: Kanat, M. (ed.) The Proceedings of Pine Processionary Moth Symposium. Kahramanmaras, Turkey, 44–51 (In Turkish with English abstract).

[4] Kanat, M. and Sivrikaya, H. (2004) The effects of chemical control against pine processionary moth, *Thaumetopoea pityocampa* (Schiff.) on diameter increment in *Pinus brutia* (Ten.) trees in Kahramanmaras region. KSU, Journal of Science and Engineering. 7(2), 60-64 (in Turkish with English abstract).

[5] Cebeci, H.H., Oymen, R.T., Acer, S. (2010) Field treatments of Foray 76 B and VBC 60074 against *Thaumetopoea pityocampa* (Den. and Schiff.) in Fethiye-Turkey. African Journal of Agricultural Research. 5(4), 294-297.

[6] Besceli, O. (1969) The biology and control of *Thaumetopoea pityocampa* Schiff.. Forest Research Institute, Technical Bulletin. 35, 65.

[7] Ozkazanc, O. (1986) Studies on the effectiveness of Tarmik-3 (*Bacillus thuringiensis*) on the control of pine processionary caterpillar and determination its more effective dosages. Forest Research Institute, Technical Bulletin. 14.

[8] Ozkazanc, O. (1987) The harmful insects of *Pinus brutia* and their control. Forest Research Institute, Kizilcam. 2, 105-121.

[9] Acatay, A. (1953) Researches on pine processionary moth (*Thaumetopoea pityocampa* Schiff = *Thaumetopoea wilkinsoni* Tams.) and its struggle on the islands. Review of the Faculty of Forestry University of Istanbul. 3, 29-47 (in Turkish).

[10] Kanat, M. and Alma, M.H. (2004) Insecticidal effects of essential oils from various plants against larvae of pine processionary moth (*Thaumetopoea pityocampa* Schiff) (Lepidoptera: Thaumetopoeidae). Pest Management Science. 60, 173–177.

[11] Kucukosmanoglu, A. and Arslangundogdu, Z. (2002) Pheromone trials against pine processionary moth (*Thaumetopoea pityocampa* (Schiff.) in Izmir Forest Directorate. In: Kanat, M. (ed.) The Proceedings of Pine Processionary Moth Symposium. Kahramanmaras, Turkey, 60–66 (In Turkish with English abstract).

[12] Avci, M. (2000) Investigations on structure of egg-batches, parasitism and egg laying habits of *Thaumetopoea pityocampa* (Den. and Schiff) (Lep.: Thaumetopoeidae) in various regions of Turkey. Turkish Journal of Entomology. 24, 167–178 (Turkish, with English abstract).

[13] Kanat, M. and Mol, T. (2008) The effect of *Calosoma sycophanta* L. (Coleoptera: Carabidae) feeding on the pine processionary moth, *Thaumetopoea pityocampa* (Den. and Schiff.) (Lepidoptera:Thaumetopoeidae) in the laboratory. Turkish Journal of Zoology. 32, 367-372.

[14] Er, M.K., Tunaz, H., Gokce, A. (2007) Pathogenicity of entomopathogenic fungi to *Thaumetopoea pityocampa* (Schiff.) (Lepidoptera: Thaumetopoeidae) larvae in laboratory conditions. Journal of Pest Science. 80, 235-239.

[15] Karabörklü, S., Ayvaz, A., Yilmaz, S., Azizoglu, U., Akbulut, M. (2015) Native entomopathogenic nematodes isolated from Turkey and their effectiveness on pine processionary moth, *Thaumetopoea wilkinsoni* Tams. International Journal of Pest Management. 61, 3-8.

[16] Özcankaya, I.M. and Can, P. (2004) Research on improvement of possibilities of mechanical and biological control of pine processionary caterpillar (*Thaumetopoea pityocampa* Den. and Schiff.) (Lep., Thaumetopoeidae)) in young Turkish red pine plantations in Mugla. Ege Forestry Research Institute, Technical Bulletin. 26, 77.

[17] Cetin, H., Erler, F., Yanikoglu, A. (2007) A comparative evaluation of *Origanum onites* essential oil and its four major components as larvicides against the pine processionary moth, *Thaumetopoea wilkinsoni* Tams. Pest Management Science. 63(8), 830-833.

[18] SPSS, (2006) SPSS for Windows Release 15.0 (Computer software), SPSS Inc., Chicago, IL.

[19] Finney, D. J. (1971) Probit Analysis. 3rd Ed. London, Cambridge University Press, Cambridge. Pp. 333.

[20] Kesdek, M., Bayrak, N., Kordali, S., Usanmaz, A., Contuk, G., Ercisli, S. (2013) Larvicidal effects of some essential oils against larvae of the Pine Processionary Moth, *Thaumetopoea pityocampa* (Denis & Schiffermüller) (Lepidoptera: Thaumetopoeidae). Egyptian Journal of Biological Pest Control. 23(2), 201-207.

[21] Kesdek, M., Kordali, S., Coban, K., Usanmaz, A., Ercisli, S. (2014) Larvicidal effect of some plant extracts on the pine processionary moth, *Thaumetopoea pityocampa* (Den. & Schiffermüller) in laboratory conditions. Acta Scientiarum Polonorum, Hortorum Cultus. 13(5), 145-162.

[22] Unal, S. and Akkuzu, E. (2009) Larvaecidal effects of azadirachtin on the pine processionary moth. African Journal of Biotechnology. 8(19), 5128-5131.

[23] Tiberi, R., Niccoli, A., Curini, M., Epifano, F., Marcotullio, M. C., Rosati, O. (1999) The role of themonoterpene in *Pinus* spp. needles, in host selection by the pine processionary caterpillar, *Thaumetopoea pityocampa*. Phytoparasitica. 27, 263–272.

[24] Ulukanlı, Z., Karabörklü, S., Bozok, F., Ates, B., Erdogan, S., Cenet, M., Karaaslan, M.G. (2014) Chemical composition, antimicrobial, insecticidal, phytotoxic and antioxidant activities of Mediterranean *Pinus brutia* and *Pinus pinea* resin essential oils. Chinese Journal of Natural Medicines. 12(12), 901-910.

[25] Çağlar, Ö., Çalmaşur, Ö., Aslan, İ., Kaya, O. (2007) Insecticidal effect of essential oil of *Origanum acutidens* against several stored product pest. Fresen. Environ. Bull. 16, 1395-1400.

[26] Göktürk, T., Kordalı Ş., Çalmaşur, O., Tozlu, G. (2011) Insecticidal effects of essential plant oils against larvae of Great Spruce Bark Beetle, *Dendroctonus micans* (Kuelann) (Coleoptera: Curculionidae: Scolytinae). Fresen. Environ. Bull. 20, 2365-2370.

[27] Bozhüyük, A.U., Kordali, S., Kesdek, M., Altinok, M.A., Varcin, M., Bozhüyük, M.R. (2016) Insecticidal effects of essential oils obtained from six plants against *Callosobruchus maculatus* (F.) (Coleoptera: Bruchidae), a pest of cowpea (*Vigna unguiculata*) (L.). Fresen. Environ. Bull. 25, 2620-2627.

Received: **20.09.2017**
Accepted: **16.12 2018**

CORRESPONDING AUTHOR

Gurkan Semiz
Pamukkale University,
Faculty of Arts & Sciences,
Department of Biology,
Denizli – Turkey

e-mail: gsemiz@pau.edu.tr

© by PSP Volume 28 – No. 4/2019 pages 2380-2389 Fresenius Environmental Bulletin

ASSESSMENT OF ESSENTIAL OIL PROPERTIES IN *JUNIPERUS EXCELSA* SUBSP. *EXCELSA* CONES DEPENDING ON SITE FACTORS

Serkan Gulsoy[1,*], Gulcan Ozkan[2], Huseyin Senol[3], Ahmet Mert[4]

[1]Department of Forest Engineering, Faculty of Forestry, Isparta University of Applied Sciences, 32260 Isparta, Turkey
[2]Department of Food Engineering, Faculty of Engineering, Suleyman Demirel University, 32260 Isparta, Turkey
[3]Department of Soil Science and Plant Nutrition, Faculty of Agriculture Sciences and Technologies, Isparta University of Applied Sciences, 32260, Isparta, Turkey
[4]Department of Wildlife Ecology and Management, Faculty of Forestry, Isparta University of Applied Sciences, 32260 Isparta, Turkey

ABSTRACT

In this study, the relationship between the essential oil amount in the cones of *J. excelsa*, which is an important tree species, and the environmental factors were analyzed. To this end, the ecological site conditions in 40 different sampling areas located in the Lakes Region in the southwest of Turkey (climate, physiographic and edaphic factors) were determined and then the essential oils were isolated from the mature cones collected from each sampling area using Clevenger apparatus. The analysis performed in each sampling area with 3 repetitions revealed that the average essential oil yield of the cones was 3.82±1.08 (%, v/w). During the statistical assessment, first the statistical significance of the difference between the essential oil yields of the sampling areas was determined through one-way analysis of variance and Duncan's multiple range tests. The relationships between the yield of essential oils and site factors were tested by Principal Component Analysis (PCA). The results revealed that the percentage of essential oils in the cones of *J. excelsa* was very high and thus it can be used as a typical essential-oil plant. Furthermore, the statistical analyses showed that the yield of essential oils in the cones varied across the sampling areas in different locations, which might be basically caused by climate and soil properties.

KEYWORDS:
Cone, essential oil, *juniper*, principal component analysis, site factors.

INTRODUCTION

Forests harbor many medicinal and aromatic plant species in their rich floras. Throughout the history, people are known to have used these plant species by traditional methods [1]. Today, these plants in the forests with medicinal and aromatic properties are used in the name of non-wood products with more modern methods and provide significant inputs to the economy of the countries. Across the world, some countries are in a very good position in the export and import of medicinal and aromatic plants, whereas the others are not so actively engaged in this sector [2]. In 2004-2008, the countries that had the best position in this sector with respect to their export potential included primarily People's Republic of China and India [3]. It is not a coincidence that these countries generate high profits from this sector. This is directly related to the fact that they possess so many plant species with potential medicinal and aromatic properties. As a matter of fact, there are 26,092 plant species in China, 4,941 of which have the potential to be used as medicinal and aromatic plants, while India has around 15,000 plant species, 3,000 of which have potential to be used as medicinal and aromatic plants [4].

A general assessment reveals that Turkey is not in the forefront in the export of medicinal and aromatic plants. This is partly related to the fact that some countries have more plant species especially those with medicinal and aromatic properties than Turkey. However, this is not the only reason because it is a fact that Turkey has a very distinctive phytogeographic position in the world and thus considerable amount of plant species. Turkey has 11,707 plant taxa in 1,320 genera of 167 families while nearly one-thirds of them are endemic [5-8]. The studies in the literature demonstrate that nearly 500 of these taxa in Turkey possess medicinal and aromatic properties while minimum 200-350 taxa have export potential; however, only 100-140 of these taxa are exported to other countries [9-12].

According to 2011 data of the International Trade Centre, 3,760 tons of medicinal and aromatic plants on average are exported from Turkey annually, which generates around 13.4 million dollars, and Turkey ranks in the 18th position in the list of medicinal and aromatic plant exporting countries in the world [13]. The data in the period from 2004 to 2008 show that Bulgaria that is neighbour to Turkey exports 9,338 tons of medicinal and aromatic plants on average annually, which generates 21 million

dollars and it ranks in the 11th position in the list [3]. Moreover, Poland that is a central European country exports 15,775 tons, which generates 47.1 million dollars, and it ranks in the 6th position. Another central European country Germany, on the other hand, generates 99.3 million dollars of revenues with the average annual export of 18,076 tons of medicinal and aromatic plants especially after raw material processing and it ranks in the 5th position [3].

In the light of the abovementioned data, the medicinal and aromatic plants possessed by the countries have potential for a very important sector. Some countries such as China and India are inherently lucky in this sector, while some others like Germany, Poland and Bulgaria turn this sector into an advantage with their efforts. For example, although Bulgaria that is neighbour to Turkey has a very low number of plant species (3,650), it generates a very high income from this sector [2, 3]. There is no doubt that it is not a matter of chance for Bulgaria and some other similar countries, which have a very similar ecosystem with Turkey, to use this sector better. The first thing that comes into one's mind about this matter is that these countries concentrate on this sector, carry out research activities, uncover their potential and take their position in the market in advance. Therefore, Turkey and other similar countries that cannot take advantage of this sector despite their superior ecosystem features need to conduct further and more comprehensive research studies in order to determine the potential of medicinal and aromatic plants in their rich floras.

In line with this objective, this study that was conducted in the Lakes Region located in the southwest of Turkey aimed at determining the medicinal and aromatic plant potential by analyzing the yield of essential oils in the cones of *Juniperus excelsa* that is widely distributed in the world and Turkey. Furthermore, the association between the amount of essential oils and the forest habitat factors was also determined and the effect of ecological environmental conditions on this chemical variable was also explored. Therefore, we aimed at finding the information that would allow assessing this issue from a different perspective by elaborating the relationships between the ecology and chemical features of this species.

MATERIALS AND METHODS

Material. *Juniperus excelsa* is one of the juniper taxa of *Cupressaceae* family that is widely distributed primarily in Turkey and all around the world [14]. It is distributed in Albania, Macedonia, Bulgaria, Greece and Greek Island in the west and extends over Turkey to partially Georgia, Azerbaijan and Turkmenistan in the east. Moreover, it is also distribute in Lebanon, Syria and Cyprus in the south, Ukraine and Crimea in the north [15]. The widest distribution area is in Anatolia. *J. excelsa* has two sub-species in Turkey, that are *J. excelsa* subsp. *excelsa* and subsp. *polycarpos* [16]. The research material of the study was the yield of the essential oils in the cones of *J. excelsa* subsp. *excelsa* [17] that is distributed as in pure or mixed stands in the inlands and coastal areas of the Mediterranean Region, inlands of the Aegean, Marmara and Black Sea Regions and in the Eastern Anatolia and Central Anatolia Regions in Turkey.

Study area. The study area is the Lakes Region located at 38° 25' - 36° 06' north latitudes and 29° 30' - 32° 34' east longitudes. There are many lakes in this region formed by the deposition of water in the pits that occurred in time due to the volcanic and tectonic movements. Limestone is the dominant rock type of the mountainous geographical structure that is the extension of the western Taurus range. There are different soil types due to different local climate characteristics and rock types as a result of the highly variable geomorphological formations, while Mediterranean terra-rossa and dark brown forest soil are the most common soil types in the region [18]. Besides, there are usually alluvial and colluvial soils on bottom lands and plain lowlands.

The climate varies significantly across the area depending on the latitude and elevation. According to the long term data, the mean annual precipitation in the region is 600-1300 mm, while the annual temperature is 12-20 °C. It is dry in the summer for about 2-4 months, while the typical Mediterranean climate prevails in the areas open to Mediterranean influence, lowlands and mountain slopes facing the sea, while a transition climate between Mediterranean and continental climate prevails in the high lands that are far from the sea [19]. The region has a very rich species diversity and endemism under the micro climate conditions due to the high geomorphological variability [20,21]. The main forest tree species that are distributed in the region include *P. brutia*, *P. nigra*, *C. libani*, *A. cilicica*, various oak species (*Quercus* sp.) and juniper (*Juniperus* sp.) species.

Data collection. Firstly, in the study, the location of the existing juniper areas in the region was identified using digital maps of stand types and topographic maps. Then, expeditions were organized to these areas, and the appropriate sampling plots were determined taking account of the health status and cone yield of the trees in the natural stands where *J. excelsa* was dominant. In this way, 40 sampling plots were determined and illustrated on a map with a scale of 1/25000 together with the coordinates (Fig. 1).

Starting from July 2013, these sampling plots were visited and ecological site conditions were observed and determined. At that stage, latitude, longitude and elevation (m) measurements were performed using GPS, aspect (°) was determined with a

compass, and the slope (%) was measured using a clinometer. Furthermore, surface stoniness (%) of the land was recorded using T-bar penetration testing [22]. In addition to these, the landform (rocky, stony and flat) and slope position (bottom land, lower slope, medium slope, upper slope, ridge) were identified through field observations [23]. On the other hand, one soil profile was dug between the trees from which cones would be collected and absolute soil depth (cm) was recorded for each profile. Soil samples were taken from the top soil depth layers of the soil profiles (0-5 cm) for various soil analyses. Moreover, the main bedrock formation of each sampling site was determined with the help of the samples collected from the area and the maps obtained from the Directorate General of Mineral Research and Exploration.

After the field studies, Annual Mean Temperature (°C) and Annual Precipitation (mm) were determined through desk studies for each sampling site using the database of climate variables created by Hijmans et al., [24] at global scale and made available at www.worldclim.data.org.

During the desk studies, some index values of the sampling areas were also determined using various formulations. At this stage, first the aspect values of the sampling sites were and converted to Radiation Index (RI) values ranging from 0 to 1 using the following equation [25].

$$RI = \frac{[1-\cos((\pi/180)(Q-30))]}{2} \quad (1)$$

Furthermore, the Heat Index (HI) assessed in the study assuming that it would provide important results was calculated with the following equation [26]:

$$HI = Cos(Radiant((Aspect) - Aspect_{\max})) * (Tan(Radiant(Inclination))) \quad (2)$$

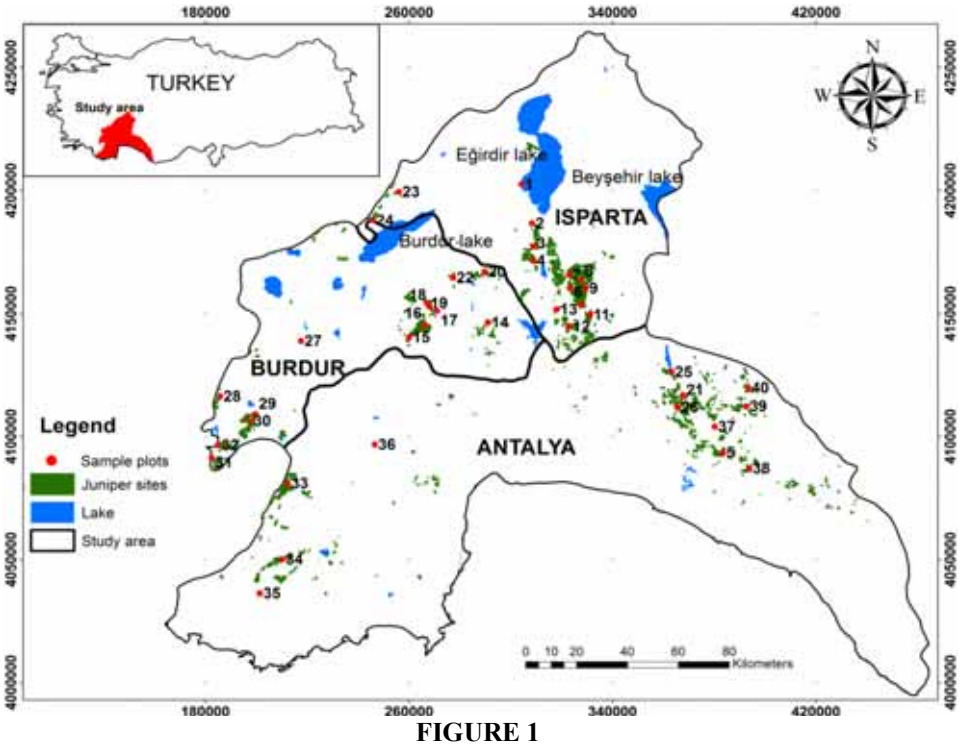

FIGURE 1
Location of *J. excelsa* areas and sampling plots in the Lakes Region

TABLE 1
Environmental variables included in the statistical assessment and the respective codes

	Variable	Code	Variable	Code
Physiographical Factors	Latitude	LTD	Heat index	HTI
	Longitude	LGT	Surface stoniness (%)	SST
	Elevation (m)	ELT	Soil depth (cm)	SDP
	Radiation index	RDI	Slope position	SPT
	Slope (%)	SLP	Landform characteristics	LNC
Climate Variables	Annual Mean Temperature (°C)	AMT	Annual Precipitation (mm)	APR
Soil Variables	Soil reaction (pH)	SPH	Calcium carbonate (%)	CaCO3
	Cation exchange capacity (me/100g)	CEC	Organic matter (%)	OM
	Silt (%)	Silt	Field Capacity (%)	FC
	Sand (%)	Sand	Clay (%)	Clay

After the data about the site conditions were determined by field and desk studies, mature cone samples were collected from each sampling site starting from November 2013. These samples were transported to the laboratory in paper bags without exposure to sunlight on a daily basis.

Laboratory studies. Laboratory studies include the analyses of soil and essential oils. At the first stage, the soil samples collected from the field were air-dried in the laboratory, ground and sieved through 2 mm-screens for the analyses. For the soil samples (three repetitions for each sample), texture was analysed with a hydrometer [27], field capacity (33 kPa) was analysed with pressure plate method, respectively [28]. The pH values of the soils were found using pH meter with glass electrode in a soil-water mixture at a ratio of 1:1 [29]. The lime content of the soils was determined with volumetric method as the equivalents of $CaCO_3$ using Scheibler calcimeter [30]. To determine the amount of organic matter, modified Walkley-Black method was applied [29]. Cation exchange capacity (CEC) was determined by saturating the soils with Na-acetate, then extracting with ammonium acetate and reading the extracted sodium in the atomic absorption spectrophotometer [31].

At the second phase of the laboratory studies, the mature cones collected from the field were air-dried for around 2 months, placed in the drying oven in metal vessels and dried at 35 °C until constant weight. After this procedure, they were ground with an electronic mixer, sieved through 2 mm-screen and the yield of essential oils in (%, v/w) after distillation with Clevenger apparatus was determined [32].

Statistical assessments. The latitude, longitude, elevation (m), slope (%), stone content (%) and average soil depth (cm) recorded from the field and climate, heat index and radiation index included in the study after the desk studies include numerical data. As for the slope position features that were the non-numerical variables, bottom land and lower slop positions were assigned with the code 1, medium slope position with the code 2, upper slope and ridge lands were assigned with the code 3 while as for the landform characteristics, rocky terrain was assigned with 1, stony terrain was assigned with 2 and flat terrain was assigned with 3 so that the variables could be digitized. The variables obtained through all these studies and the codes assigned before the statistical assessments are presented in Table 1.

Following the completion of the field and laboratory studies, all data were recorded in the form of digital values in Microsoft Office Excel. Some descriptive statistics were applied initially to the data available in the digital setting. Then, analysis of variance was applied to the existing data using SPSS 17.0 statistics software and the significance of the difference between the sampling plots was determined. For the multivariate analyses, Past 3 software package was used and the relationships between the yield of essential oils, which were the dependent variables, and all the environmental factors, which were the independent variables, were tested with Principal Component Analysis (PCA) [33].

RESULTS AND DISCUSSION

In this study, the data were obtained from 40 sampling plots in 12 different locations (Eğirdir, Sütçüler, Bucak, Ağlasun, Keçiborlu, Gölhisar, Altınyayla, Elmalı, Kaş, Korkuteli, Akseki and İbradı) in the Lakes district of Turkey. The elevation of these sampling plots ranged from 475 m to 1920 m. It can be suggested that the distribution of species in this elevation range concentrated in the moderately mountainous and highly mountainous areas according to the geomorphological classification proposed by Çepel [34]. In an important study conducted in the region, it was reported that this species was still observed in many areas located at an elevation of 800-1800 m and *J. excelsa* that had a higher ecological tolerance than other species to extreme conditions such as surface stoniness, aspect and dry climate in this elevation range still survived in those areas [35]. In another study conducted on this matter, it was stated that *J. excelsa* trees could grow as high as the tree line in the Mediterranean Region and adapt to summer drought, winter frost, shallow soils and step inclination [36].

As regards the distribution of the study areas by shadow and sunny aspects in percentage, the sampling plots accounted for 57.5 % and 42.5 %, respectively. The results obtained show that this species prefer mainly the shadow and humid aspects. *J. excelsa* is usually resistant to cold and has a high humidity requirement [37]. Indeed, a study conducted on this matter in Ağlasun located in the Lakes Region reported that *J. excelsa* had an increased distribution in the mountainous and moderately mountainous areas especially in north and west aspects at an elevation of 1200 m and above with higher rate of humidity [38].

The inclination (slope) of the sampling plots was around % 10 - % 40, while it can be suggested that the species is distributed mainly in the moderately inclined and steep inclined lands according to the inclination classes proposed by Arbeitskreis [39]. In a study that explored the ecological characteristics of this species, it was stated that the juniper trees had a higher ecological tolerance under the adverse soil conductions on steep inclined lands and they could adapt to these areas [40]. As for the climate characteristics, the mean annual temperature ranged from 9.0 °C to 15.3 °C in the study sites and the mean annual total precipitation ranged from 488.5 mm to 863.9 mm.

As regards the bedrock characteristics, the species is distributed mainly in the rocks of chemical origin such as limestone and dolomite and partly in sedimentary rocks of physical origin such as conglomerate and sandstone. In the previous studies conducted in the region for the ecological characteristics of the species, it was reported that *J. excelsa* concentrated mainly on sedimentary rocks and bedrock of limestone just like our study result [35, 41]. This is considered to be associated with the fact that limestone has a more fissured structure and *J. excelsa* trees uptake water and various minerals from soil at the physiological depth on these rocks using their taproots. More than 90 % of the sampling areas studied were rocky and stony while the surface stoniness was higher than 50 %. As for the overall geological characteristics of the Mediterranean Region, sedimentary rock is known to be the most dominant bedrock type. It was reported that juniper trees that were distributed along the Taurus mountain range continued their distribution on the geomorphological landforms created by the limestone bedrock in this area in the form of mass or after fragmentation especially in areas where they met the adequate light requirement [35]. Therefore, the findings are consistent with the distribution pattern of the species. As for the slope position of the sampling plots that was included in the study, it was observed that the species was distributed in all slope positions from the bottom lands to the ridges and hills.

According to the depth classification proposed by Kantarcı [42], 7 of the soil pits that were dug were very deep (>100 cm), 5 were moderately deep (50-75 cm), 17 were shallow (25-50 cm), and 11 were very shallow (<25 cm). An analysis of the physiochemical results of the soils sampled from the depth layer of 0-5 cm revealed that the pH ranged from 7.1 to 8.5. In another comprehensive study conducted on 3871 soil samples taken from the Lakes Region, it was reported that the pH was 7.0-7.9 in 84.2 % of the samples, while it was 8.0-8.9 in 8.2 % [43]. Such high pH values can be explained by $CaCO_3$ percentages in the mineral soil segment depending on the bedrock type because the soil samples taken from the study sits had 8.2 % $CaCO_3$; therefore, the soils were classified as calcareous [44].

The percentage of organic matter in the sampling plots was found to be 8.9 % while the mean field capacity was 36.3 %. As for the average organic matter amount, the soils in the study area were humic [44]. Since the study area was a forest cover, this leads to high amount of vegetal material on the ground. In general, considering that degradation and decomposition was slow at the elevations where juniper trees were distributed due to the climate conditions, this resulted in high amount of organic matter in the soil especially at the depth of 0-5 cm. As a matter of fact, the field capacity values found in the study were expectedly high, which was consistent with the percentage of organic matter.

The analyses conducted showed that the percentage of clay content in the soil was 4.7-44.2 %, percentage of dust content was 24.4-53.0 %, and the percentage of sand content was 16.5-54.4 %. These values suggest that the soils were loamy. CEC values ranged from 19.5 to 102.9 me/100g, and the mean CEC was 55.9 me/100g. High CEC values found may be associated with high percentage of dust and clay content in the soils and also high percentage of organic matter content [45] because it is a normal consequence that these soils are loamy and thus ideal.

The assessment performed in 40 sampling plots demonstrated that the yield of essential oils in the cones of *J. excelsa* ranged from 1.6-5.8 % v/w in the region while the mean essential oil yield was found to be 3.8 %. Başer [46] classified the plants of Labiatae family with an essential oil yield greater than 2.0 % as plants rich in essential oils. For example, the studies conducted on thyme species as important essential oil plants reported that the essential oil yield of *Origanum vulgare* ssp. *vulgare* was 2.3 % v/w [47], while it was 1.9-3.0 % v/w for *Origanum onites* L. [48,49], and 4.0–4.4 % v/w for *Origanum minutiflorum* O. Schwarz and P. H. Davis [50]. Moreover, the essential oil yield was 0.9 % v/w in *Laurus nobilis* L. that is reported to be an important essential-oil plant [51], and 2.0-2.8 % v/w in *Salvia tomentosa* Mill. [52]. Compared to all these plants, it is possible to say that *J. excelsa* cones have a very high amount of essential oils.

In one of the studies conducted in Turkey on this matter, Topçu et al. [53] distillated juniper cones collected from Isparta and found that the essential oil yield was 3.2 % v/w. Ataş et al., [54] found that the essential oil yield of the cones collected from Antalya was 5.8 % v/w. In another study conducted in recent years, Avcı and Bilir, [55] reported that the yield of the cones of the species increased as they matured and the mean essential oil yield of the mature cones was 2.5 % v/w. Moreover, in another study conducted in Macedonia, Soković et al., [56] found that the essential oil yield of *J. excelsa* cones was 1.2 % v/w, while Shanjani et al., [57] found the essential oil yield of the cones as 2.1 % v/w in another study conducted in Iran. It is understood that the essential oil percentages found in the studies conducted so far vary, while such variations were associated with the genetic characteristics, locality, cone collection methods and timing, drying duration and conditions as well as distillation method [58, 59].

The results of the analysis of variance and Duncan test performed in order to determine the significance of the differences in the essential oil yield between different study sites in the study are presented in Table 2 and Table 3.

Table 2 and Table 3 indicate that the difference between the sampling plots with respect to the yield of essential oils of the cones was statistically significant at $p \leq 0.001$. Table 4 presents Eigenvalues,

TABLE 2
Results of analysis of variance regarding the significance of the difference between the *J. excelsa* cones in the sampling plots

Source of variation	Code	df	Sum of Squares	Mean Square	F
Yield of Essential Oil	YEO	39	135.747	3.481	430.6***

*** significant at p≤0.001 ** significant at p≤0.01 * significant at p≤0.05

TABLE 3
Mean values of the physical and physiochemical characteristics of the *J. excelsa* cones and Duncan's multiple range test results

	YEO		YEO		YEO		YEO
Plots		Plots		Plots		Plots	
	(%,v/w)		(%,v/w)		(%,v/w)		(%,v/w)
p1	3.33±0.12g	p11	3.53±0.12hij	p21	2.40±0.00v	p31	5.53±0.12t
p2	3.33±0.12g	p12	3.60±0.00ij	p22	3.00±0.00ef	p32	4.53±0.12o
p3	3.47±0.12ghi	p13	2.00±0.00b	p23	3.93±0.12kl	p33	3.63±0.06j
p4	4.40±0.00no	p14	2.97±0.06e	p24	5.00±0.00r	p34	4.20±0.00m
p5	1.70±0.00a	p15	4.73±0.12p	p25	4.20±0.00m	p35	5.33±0.12s
p6	4.33±0.12mn	p16	4.33±0.12mn	p26	1.60±0.00a	p36	2.73±0.12d
p7	3.40±0.00gh	p17	3.80±0.00k	p27	4.00±0.10l	p37	4.93±0.12r
p8	4.20±0.00m	p18	4.33±0.12mn	p28	5.33±0.12s	p38	1.73±0.12a
p9	3.53±0.12hij	p19	4.33±0.12mn	p29	5.80±0.00u	p39	4.00±0.00l
p10	3.60±0.00ij	p20	3.13±0.12f	p30	5.80±0.20u	p40	2.93±0.12e

*The values marked with the same letter in the same column are not statistically different (p<0.05).

TABLE 4
Eigenvalues and variance of the first 3 principal components extracted for the soil variables and YEO (%, v/w)

	Eigenvalue	Variance (%)	Cumulative variance (%)	Broken-stick eigenvalue
PC 1	3.503	38.921	38.921	2.829
PC 2	1.982	22.023	60.945	1.829
PC 3	1.286	14.283	75.228	1.329

TABLE 5
Correlations between YEO (%, v/w) and soil variables on PCA-axes

	PC 1	PC 2
SPH	-0.740	-0.106
CaCO3	-0.369	-0.163
OM	0.861	0.317
CEC	0.624	0.378
FC	0.864	0.199
Clay	0.100	***-0.868***
Silt	0.755	-0.239
Sand	-0.550	***0.797***
YEO	-0.245	***0.466***

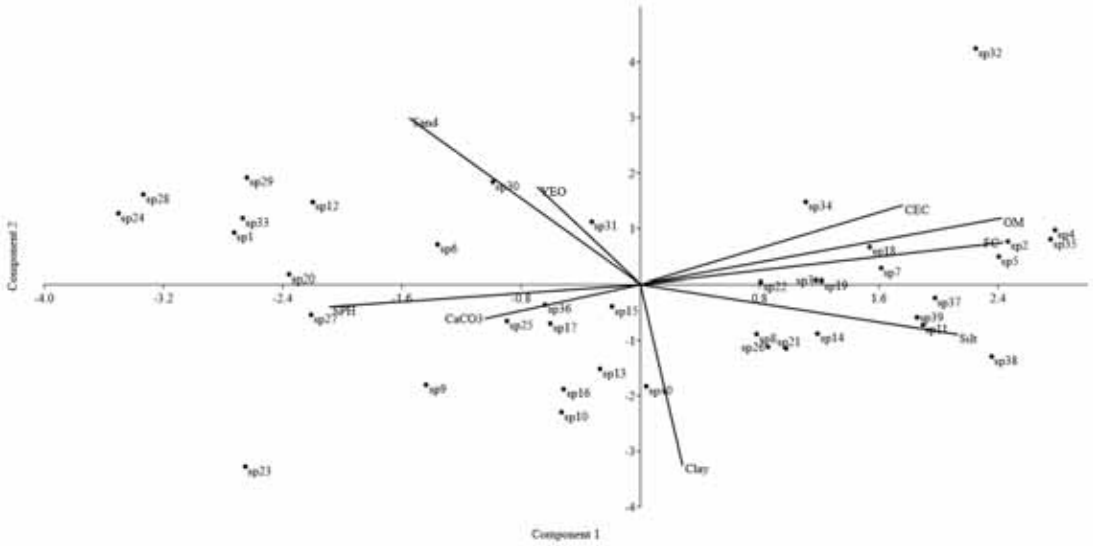

FIGURE 2
PCA–ordination diagram of YEO related to the soil factors in the study area

TABLE 6
Eigenvalues and variance of the first 3 principal components extracted for climatic-physiographic variables and YEO (%, v/w)

	Eigenvalue	Variance (%)	Cumulative variance (%)	Broken-stick eigenvalue
PC 1	3.304	30.036	30.036	3.020
PC 2	2.582	23.470	53.505	2.020
PC 3	1.329	12.083	65.589	1.520

TABLE 7
Correlations between YEO (%, v/w) and climatic-physiographic variables on PCA-axes

	PC 1	PC 2
ELT	0.258	***0.826***
RDI	0.788	-0.385
SLP	-0.705	0.388
HTI	0.842	-0.369
SST	-0.716	-0.087
SDP	0.363	0.276
SPT	-0.498	0.266
LNC	0.597	0.342
APR	-0.200	***-0.532***
AMT	-0.296	***-0.818***
YEO	0.188	***0.492***

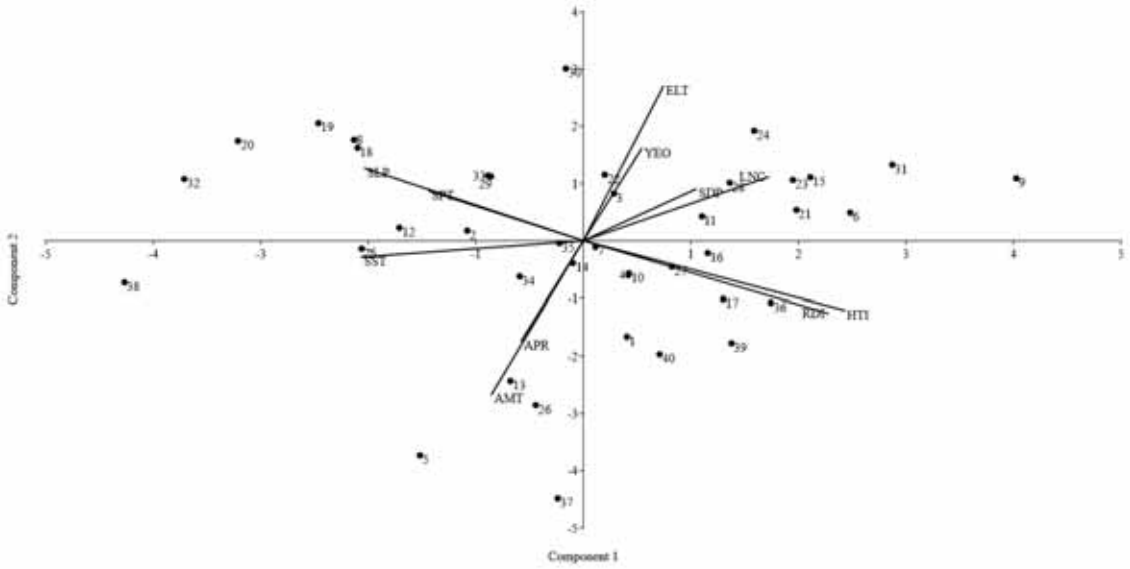

FIGURE 3
PCA–ordination diagram of YEO related to climatic-physiographic variables in the study area

variance (%) and cumulative variance (%) and Broken-stick eigenvalues of the axes as a result of PCA applied to reveal the associations between the difference between the essential oil contents in the sampling areas and the soil factors.

Table 4 indicates that Broken-stick eigenvalues were higher than Eigenvalues on PC 3. Therefore, the associations between the soil variables and yield of essential oil were only analysed for PC 1 and PC 2. Table 5 presents the correlations between these two components and yield of essential oil and soil variables, while Fig. 2 indicates the position of the variables on the ordination axes.

Table 5 and Fig. 2 indicate that the increased sand content of the soils was positively correlated with YEO, whereas the increased clay content was negatively correlated with YEO. This suggests that the soil type in the sampling plots might lead to a statistically significant variation in YEO rates. *J. excelsa* is distributed in the extreme habitats with very shallow soil conditions in rocky and stony landforms [35, 60]. Therefore, the variation in the clay and sand content of the soils in the sampling plots under these conditions affects the water balance in the plant and thus may turn into a stress factor for the plant. It is suggested that this stress factor affecting the plant leads to varying rates of YEO. To clarify further, the increased clay content in *J. excelsa* sites distributed under extreme habitats results in the retention of water in the soil in higher amounts and for a longer time

and thus allows the plant to use that water more. Therefore, the increased clay content in the soil means that the water stress or drought is avoided for the plant to a certain degree and thus YEO decreases. The increased sand content of the soils, however, can be interpreted as totally the opposite of this situation.

Table 6 presents the Eigenvalues, variance (%) and cumulative variance (%) and Broken-stick eigenvalues of the axes found through PCA applied to find the association between the difference in the yield of essential oil between the sampling plots and the physiographical and climate factors.

Table 6 indicates that Broken-stick eigenvalues were higher than Eigenvalues on PC 3; therefore, the relationships between the physiographic-climatic factors and yield of essential oil were interpreted on PC 1 and PC 2. Table 7 presents the correlation coefficients of these two components and yield of essential oil and physiographic-climatic factors, while Fig. 3 presents the position of the variables on the ordination axes.

Table 7 and Fig. 3 indicate that YEO was negatively correlated with the mean annual temperature and mean annual total precipitation, and positively correlated with elevation. The elevation decreased in general from the inlands towards the Mediterranean coast in the lakes region where the study was conducted, while the mean temperature, humidity and precipitation increased. In particular, humidity and precipitation is high in the slopes of the areas close the coast that face the sea. Therefore, *J. excelsa* distributed on the slopes facing the sea in these areas of the region receives more atmospheric humidity and precipitation, which eliminates the water stress and drought partially just like in the relationships with the soil. This is considered to decrease YEO of the plants. To the contrary, *J. excelsa* distributed in the terrestrial areas of the inlands where the mean elevation is higher was found to have higher YEO.

CONCLUSIONS

The results of this study reveal that *J. excelsa* can be directly used as essential-oil plant thanks to the amount of essential oil contained in its cones. On the other hand, it was understood that the amount of essential oil in the plants was influenced by especially the varying drought and water deficiency or water stress parameters of the plant especially due to the climatic factors. Form a different perspective; it can be argued that the essential oil characteristics of the plants can be used as an indicator in the future with a view to observing the changes caused by the changing climatic factors in the ecosystem. However, there is a need for further and more comprehensive studies to explore and clarify this matter.

ACKNOWLEDGEMENTS

We gratefully acknowledge TUBITAK for the financial support of the project (Research Grant No: 112O814).

REFERENCES

[1] Faydaoğlu, E. and Sürücüoğlu, M.S. (2011) History of The Use of Medical and Aromatic Plants and Their Economic Importance. Kastamonu University, Journal of Forestry Faculty. 11, 52-67.

[2] Lange, D. (2006) International trade in medicinal and aromatic plants. In: Bogers, R.J., Craker, L.E., Lange, D. (Eds.) Medicinal and Aromatic Plants: Agricultural, Commercial, Ecological, Legal, Pharmacological and Social Aspects. Springer, Dordrecht, 155–170.

[3] Lubbe, A. and Verpoorte, R. (2011) Cultivation of medicinal and aromatic plants for specialty industrial materials. Industrial Crops and Products. 34, 785– 801.

[4] Schippmann, U., Leaman, J.D. and Cunningham, A.B. (2002) Impact of Cultivation and Gathering of Medicinal Plants on Biodiversity: Global Trends and Issues. Inter Departmental Working Group on Biological Diversity for Food and Agriculture, Rome.

[5] Davis, P.H. (1965) Flora of Turkey and the East Aegean Islands. Vol. 1-9, Edinburgh, Edinburgh University Press.

[6] Davis, P.H., Mill, R.R. and Tan, K. (1988) Flora of Turkey and The East Aegean Islands. Vol. 10, Edinburgh University Press, Edinburgh.

[7] Erik, S. and Tarıkahya, B. (2004) About Flora of Turkey. Kebikeç Resources for Human Sciences Research Journal. 17, 139-163 (In Turkish).

[8] Güner, A., Aslan, S., Ekim, T., Vural, M. and Babac, M.T. (2012) A Checklist of the Flora of Turkey (Vascular Plants). Nezahat Gökyiğit Botanical Garden Publications, Series of Flora I, ISBN: 978- 605-60425-7-7, İstanbul (In Turkish).

[9] Baytop, T. (1999) Therapy with Medicinal Plants in Turkey - Past and Present. Nobel Tıp Kitabevleri, II. Baskı ISBN: 975-420-021-1, İstanbul, 480s.

[10] Ekim, T., Koyuncu, M., Vural, M., Duman, H., Aytaç, Z. and Adıgüzel, N. (2000) Red Data Book of Turkish Plants (Pteridophyta And Spermatophyta). Ankara, 246p.

[11] Özgüven, M., Sekin, S., Gürbüz, B., Şekeroğlu, N., Ayanoğlu, F. and Ekren, S. (2005) Tobacco, Medicinal and Aromatic Plants Production and Trade. 3-7 January 2005, Turkey Agricultural Engineering VI. Technical Congress, Ankara (In Turkish).

[12] Bayramoğlu, M.M., Toksoy, D. and Şen, G. (2009) Medicinal Plant's Trade in Turkey. II. Congress of Socio-Economic Problems in Forestry, 89-98, Isparta.
[13] Akbulut, S. and Bayramoğlu, M.M. (2013) The Trade and Use of Some Medical and Aromatic Herbs in Turkey. Ethno Med. 7, 67-77.
[14] Eliçin, G. (1977) Studies on distribution and important morphological and anatomical characteristics of native Juniper (Juniperus L.) taxa in Turkey. I.U. Publication No: 2327 - 232, İstanbul (In Turkish).
[15] Adams, R.P., Douaihy, B., Dagher-Kharrat, M.D., Farzaliyev, V., Tashev, A.N., Baser, K.H. S. and Christou, A.K. (2014) Geographic variation in the volatile leaf oils of *Juniperus excelsa* and *J. polycarpos*. Phytologia. 96, 96-106.
[16] Yaltırık, F. and Akkemik, Ü. (2011) Natural Gymnospermae in Turkey. Ministry of Environment and Forestry, General Directorate of Forestry. ISBN: 978-605-60143-1-4, Ankara (In Turkish).
[17] Coode, M.J.E. and Cullen J. (1966) *Juniperus* L. In: Davis, P.H. (ed.) Flora of Turkey and the East Aegean Islands (Vol. 1). Edinburgh University Press, Edinburgh, 78–84.
[18] Atalay, İ. (1987) Limits of seed transfer for Cedar (*Cedrus libani* A. Rich.) according to the distribution areas and general ecological properties of near environment. Publications of General Directorate of Forestry, No: 663, Ankara, 167p (In Turkish).
[19] Evliyaoğlu, S. (1996) Tourism Geography of Turkey and Outlines. Dizgi Ofset, Ankara, 72p (In Turkish).
[20] Karaca, S. (2002) Contributions to Flora of Lakes Environments. Suleyman Demirel University. PhD Thesis. Isparta, 86p (In Turkish).
[21] Fakir, H. (2006) Flora of Bozburun Mountain and Its Environs. Turkish Journal of Botany. 30, 149-169 (In Turkish).
[22] Eriksson, C.P. and Holmgren, P. (1996) Estimating stone and boulder content in forest soils evaluating the potential of surface penetration methods. Catena. 28, 121–134.
[23] Zech, W. and Çepel, N. (1972) The relations between the development of some P. brutia stands in South Anatolia and their soil and relief characteristics. İstanbul Matbaası, İstanbul (In Turkish).
[24] Hijmans, R.J., Cameron, S.E., Parra, J.L., Jones, P.G. and Jarvis, A. (2005) Very high resolution interpolated climate surfaces for global land areas. International Journal of Climatology. 25, 1965-1978.
[25] McCune, B. and Keon, D. (2002) Equations for potential annual direct incident radiation and heat load. J. Veg. Sci. 13, 603-606.
[26] Olsson, P.A., Martensson, L.-M. and Hans Henrik, Bruun, H.H. (2009) Acidification of sandy grasslands – consequences for plant diversity. Applied Vegetation Science. 12, 350-361.
[27] Bouyoucos, G.J. (1951) A Recalibration of the hydrometer method for making mechanical analysis of soils. Agronomy Journal. 43, 434–438.
[28] Demiralay, İ. (1993) Soil Physical Analysis. Publication of Atatürk University Faculty of Agriculture, No: 143, Erzurum (In Turkish).
[29] Jackson, M.L. (1958) Soil Chemical Analysis. Prentice-Hall, Inc. Englewood Cliffs, New Jersey, USA, 498p.
[30] Hızalan, E. and Ünal H. (1966) Important chemical analyzes in soils. Publication of Ankara University Faculty of Agriculture No: 278 (In Turkish).
[31] Anonymous (1951) Soil Survey Manual. Soil Survey Staff, USDA, Handbook, 18.
[32] Baydar, H. (2004) Rose oil cultivation and rose oil industry in Turkey. Türk Tarım Dergisi. 160, 54-57 (In Turkish).
[33] Özdamar, K. (2002) Statistical data analysis using softwares-2 (Multivariate Analysis). Kaan Publications, Eskişehir (In Turkish).
[34] Çepel, N. (1995) Forest Ecology (Orman Ekolojisi). Publications of Istanbul University Faculty of Forestry, No: 3886-433, ISBN: 975-404-398-1, Istanbul, 536p (In Turkish).
[35] Özkan, K., Gülsoy, S., Aerts, R. and Muys, B. (2010) Site properties for Crimean juniper (*Juniperus excelsa*) in semi-natural forests of south western Anatolia, Turkey. J. Environ. Biol. 31, 97-100.
[36] Abi-Saleh, B., Nasser, N., Hanna, H., Safi, N., Safi, S. and Tohmé, H. (1996) Examination of the biological diversity of Lebanon: terrestrial flora (Étude de la diversité biologique du Liban: la flore terrestre). Project PNUE/GF/6105, 92-72. Beyrouth, Liban (In French).
[37] Aussenac, G. (2002) Ecology and ecophysiology of circum-Mediterranean firs in the context of climate change, Ann. For. Sci. 59, 823–832.
[38] Fontaine, M., Aerts, R., Özkan, K., Mert, A., Gülsoy, S., Süel, H., Waelkens, M. and Muys, B. (2007) Elevation and exposition rather than soil types determine communities and site suitability in Mediterranean mountain forests of southern Anatolia, Turkey. Forest Ecology and Management. 247, 18-25.
[39] Arbeitskreis, A.K. (1996) Forest Sites. 5th ed. Eching, Germany: IHW-Verlag (In Germany).
[40] Ahmed, M., Naqui, E. and Wang, E.L.M. (1990) Present state of juniper in Roadhmullazi forest of Baluchistan, Pakistan. Pak. J. For. 40, 227-236.

[41] Gülsoy, S. and Özkan, K. (2013) Determination of environmental factors and indicator plant species for site suitability assessment of Crimean juniper in the Acipayam District, Turkey. Sains Malaysiana. 42, 1439–1447.
[42] Kantarcı, M.D. (2000) Soil Science. Publications of Istanbul University Faculty of Forestry, No: 4261-462, ISBN 975 - 505-588-7, İstanbul, 420p (In Turkish).
[43] Ülgen, N. and Yurtsever, N. (1988) Turkey fertilizer Guide (3rd edition). Publications of Soil and Fertilizer Research Institute, No:151/T-59. Ankara, 1-182 (In Turkish).
[44] Petri, H. and Wagner, A. (1978) Forest Sites. Agricultural Publishing Gmbtl., Munster Hiltrup (In German).
[45] Akgül, M. (1994) Land capability classification of Daphan plain. Journal of the Faculty of Agriculture, 25, 14-29.
[46] Başer, K.H.C. (1993) Essential oils of Anatolian Labiatae: A profile. Acta Horticulture. 333, 217–238.
[47] Şahin, F., Güllüce, M., Daferera, D., Sökmen, A., Polissiou, M., Agar, G. and Özer, H. (2004) Biological activities of the essential oils and methanol extract of *Origanum vulgare* ssp. vulgare in the Eastern Anatolia region of Turkey. Food Control. 15, 549–557.
[48] Gönüz, A. and Özgorücü, B. (1999) An investigation on the morphology, anatomy and ecology of *Origanum onites* L. Turkish J. Bot. 23, 19–32.
[49] Yaldiz, G., Sekeroglu, N., Ozguven, M. and Kirpik, M. (2005) Seasonal and diurnal variability of essential oil and its components in *Origanum onites* L. grown in the ecological conditions of Çukurova. Grasas y Aceites. 56, 254–258.
[50] Aslım, B. and Yücel, N. (2008) In vitro antimicrobial activity of essential oil from endemic *Origanum minutiflorum* on ciprofloxacin-resistant Campylobacter spp. Food Chemistry. 107, 602–606.
[51] Başak, S.S. and Candan, F. (2013) Effect of *Laurus nobilis* L. Essential Oil and its Main Components on α-glucosidase and Reactive Oxygen Species Scavenging Activity. Iranian Journal of Pharmaceutical Research. 12, 367-379.
[52] Avcı, A.B. (2013) Essential oil content and composition of *Salvia tomentosa* Mill. from Gölcük, Isparta. Süleyman Demirel Üniversitesi, Fen Bilimleri Enstitüsü Dergisi, 17, 1-4.
[53] Topçu, G., Gören, A.C., Bilsel, G., Bilsel, M., Cakmak, O., Schilling, J. and Kingston, D.G. (2005) Cytotoxic activity and essential oil composition of leaves and berries of *Juniperus excelsa*. Pharmaceutical Biology. 43, 125-128.
[54] Ataş, A.D., Göze, İ., Alim, A. and Akkuş, S. (2012) Chemical composition, antioxidant, antimicrobial and antispasmodic activities of the essential oil of *Juniperus excelsa* subsp. *excelsa*. Journal of Essential Oil Bearing Plants. 15, 476-483.
[55] Avcı, A.B. and Bilir, N. (2014) Variation in Essential Oil Content and Composition of Crimean Juniper (*Juniperus excelsa*) Berries during the Growth Periods. JEOB. 17, 478-485.
[56] Soković, M.D., Ristić, M. and Grubišić, D. (2004) Chemical composition and antifungal activity of the essential oil from *Juniperus excelsa* Berries. Pharmaceutical Biology. 42, 328–331.
[57] Shanjani, P.S., Mirza, M., Calagari, M. and Adams, R.P. (2010) Effects drying and harvest season on the essential oil composition from foliage and berries of *Juniperus excelsa*. Industrial Crops and Products. 32, 83-87.
[58] Vieira, R.F. and Simon, J.E. (2000) Chemical characterization of basil (*Ocimum* spp.) found in the markets and used in traditional medicine in Brazil. Economic botany. 54, 207-216.
[59] Tawatsin, A., Wratten, S.D., Scott, R.R., Thavara, U. and Techadamrongsin, Y. (2001) Repellency of volatile oils from plants against three mosquito vectors. Journal of Vector Ecology. 26, 76-82.
[60] Fisher, M. and Gardner, A.S. (1995) The status and ecology of a *Juniperus excelsa* subsp. *polycarpos* woodland in the northern mountains of Oman. Vegetatio. 119, 33-51.

Received: **05.10.2017**
Accepted: **18.02.2019**

CORRESPONDING AUTHOR

Serkan Gulsoy
Isparta University of Applied Sciences,
Faculty of Forestry
32260 Cunur, Isparta – Turkey

e-mail: srkngulsoy@gmail.com

© by PSP Volume 28 – No. 4/2019 pages 2390-2396 Fresenius Environmental Bulletin

EXPERIMENTAL CONSIDERATION ON HEIGHT AND DISTANCE EFFECTS OF CONSECUTIVE DAMS IN HYDRAULIC FLOW

Mehdi Bensaid[1,2], Amir Abbas Kamanbedast[2,*], Mohammad Hosein Purmohammadi[3], Mahmoud Shafai Bajestan[4], Alireza Masjedi[2]

[1]Department of Water Science and Engineering, Khuzestan Science and Research Branch, Islamic Azad University, Ahvaz, Iran
[2]Department of Water Science and Engineering, Ahvaz Branch, Islamic Azad University, Ahvaz, Iran
[3]Department of Water Science Engineering, Shoushtar Branch, Islamic Azad University, Shoushtar, Iran
[4]Water Engineering Science Faculty, University of Chamran, Ahvaz, Iran

ABSTRACT

Check dams are small structures in order to decrease the slope of waterways, reduce flow rate and inhibiting erosion. Choosing the type of materials, dimensions, distance and height of these different factors, depends on tabs to the quarries, slope and dimensions of waterways, the amount of rainfall and the level of the bed materials in upper watershed. The right choice of materials, dimensions, distance and height tabs play an important role in reducing costs. Therefore, check the flow and scheduling behavior in dealing with obstacles such as check dams correcting mainly "to control the mountainous route in bed, according to the slope of the platform changes, their height and distances as a tracer that is discussed in this article. Considering that the behavior of the flow is a function of the depth of discharge, These tests have achieved on the flume with the length of 12.5 meters in variable slopes, discharges, heights and different intervals for consecutive walls in the lab. As well, the results have been discussed and analyzed for dimension-less ratios of the depth to the height*(y/Hw),* depth to the distance *(y/L),* Froude number and hydraulic factor *(Cd),* that led to the choice of the optimal distance and height of check dams.

KEYWORDS:
Discharge, Flow depth, Check dams, Distance, Bed slope

INTRODUCTION

Considering that most researches have been conducted for flow impact on erosion and sediment control with rough bed transition, history of the present research has direct relation with the above mentioned subject.

Boundary conditions. Because this model has performed in a smooth bed flume, so, the velocity profile is calculated by the Einstein equation as follows, [1]:

$$y = 0 \longrightarrow v = 0 \quad \text{and} \quad y = yn \longrightarrow$$
$$v/u* = 5.75\, log\, (12.27\, R/Ks\, x) \tag{1}$$

yn = Normal depth, $Ks = D65$,
x = Correction coefficient

Movement of sediment materials in the river depends on some factors, based on shields theory, sediment materials movement in the rivers depends on two dimension-less factors, θs Dimension-less Shields No., and Re* Reynolds No. of particles.

According to shields theory, If $Re^* < 5$ it means bed flow is smooth, and sediments movement depends on fluid viscosity; if $5<Re^*<250$ it means that the flow in bed is intermediate, and if $250<Re^*$ the bed flow is rough, and viscosity is not effective on particles movement [1]. Sediment deposition in dam reservoirs causes harmful effects and reduces useful life of dams. So, importance and complication of this matter obliged us to achieve a complete studies on problems. Lack of information and prediction of controlling methods about deposit conditions in dam reservoirs, causes reduction of useful life of dams. To prevent sediment accumulation, the water inputs must be investigated and if possible using appropriate divisions and preventing land erosion in the place of their move by other devices to prevent creation of sediments [2].

To investigate sediment conditions in reservoirs using physical models has become a suitable device for this purpose. This model predicts deposit condition and it's reduction. Regarding data from karun river, since 1968-2014 the distance sections between Karun dam 3 and Abbas pour dam the calibration and validation of the model and the flow behavior for parameters such as depth, bed slope, flow and sediment discharge, height and distance between small dams have been achieved.

Laboratory study of sediment traps have been set up profiles on permeable and non-permeable control dams [3], a sediment trap categories using physical model in a steep flume and impermeable dams made of Plexiglas and permeable dams of the Gabions shows the permeable dams of higher efficiency and less drop trap.

Determination of the coefficient of sediment traps using laboratory flume in times of flood for design flood control dams in order to delay and to estimate the volume of sediment in a laboratory flume slope and the use of two types of sedimentary materials is performed in which the effective factors in the trapping were examined and the and dimensionless effective factors extracted from multiple correlation analysis [6]. Stream sedimentation model in upstream of dams in the mountainous areas is the subject of numerical analysis about the impact of small dams on the rivers [5], that in this article the evolutionary stages of sedimentation in upstream of dams by numerical model based on solve of Saint-venant equations have been investigated. This was a comparison with the results of the laboratory that confirms its compliance with the model took on the sedimentation in dams in the upstream flow. Bed sediment load transfer at the longitudinal gradients steep is the title of a set of experiments at an inclined-large tract has been tested with sand d_{50} = 208μm, and measurements were included, bed shear stress, sediment displacement rates and flow discharge on the steep slope at which positive move in the threshold of the equation Meyer-Peter- Müller modified, as well as on the very steep slope effects of shear stress has been removed [7].

Ghahremani and Kamanbedast [12] explored the variations of flow rate at Karun River and hydrodynamic scour at the bridge pile. They argued that he erosion trend increases rapidly as discharge rate exceeds 300 m3/s. Elyasi and Kamanbedast [10] examined the deviation trend of sediments into ponds based on submerged plates. They stated that submerged plates could reduce the sediment inflow into the basin by up to 30%. Niknam, Kamanbedast and Shahryari [15] simulated sedimentation at Marun Dam, finding out that fine-grained sediments were more progressive than coarse-grained sediments. In fact, sediment aggregates become smaller as they approach the dam wall. Rostami, H. et al., and Rouzegar, J. et al. investigate length of morning glory spillway and labyrinth spillways with physical modelling. [17, 18]. Kamanbedast, A., et al. [13], Estimate the Sediment Transport in Rivers Using CCHE2D Model (Case Study: Karkheh River). Saki, A., et al [19] Designed Rectangular Weir for Flow Regulation at River Fork through a Physical Model. Shirali et al. [21] evaluated the morning glory spillway using physical modelling System; one with a bell shaped opening, another with a modern square shaped opening. The result shows measured pressure at various points on both spillways based on a non-dimensional Froude number. By changing the shape of the cross section, its direct effect on the pressure and cavitation indices.

METHODOLOGY

In order to verify the hypothesis raised in this research, experiments had to be performed, thus a physical model was constructed in the hydraulic laboratory of the Khuzestan Water and Power Training and Higher Education Centre and the necessary experiments implemented. The scaled model included a model of the reservoir, a pump and water conveyance system, and control equipment, in addition to a model of the spillway and discharge tube. A 10 mm glass panel was installed on one side. In order to be able to stabilize the bottom and sides of the reservoir against the pressure of the water, steel rods were used. Fig (1).

FIGURE 1
Longitudinal profile of the laboratory model

Dimensional analysis of Bakingham. Using dimensional analysis method of Bakingham, experimental variations are as follows [20]:

$$f1(y, v, \rho, \mu, g, L, H, Sb, \tau c, Ds, \gamma s) = 0 \quad (2)$$

y = Flow depth, H = Height of small dams, V = Flow velocity, Sb = Bed slope
ρ =Density of water, τc = Critical shear stress, μ= Dynamic viscosity ,Ds= Bed load diameter
g = Gravity acceleration, γs = Particles specific weight, L = Distance between small dams

Which after dimensional analysis, becomes:

$$f2\ [(yg/v^2), (\mu/\rho vy), (H/y), (L/y), (Sb), (gySb/v^2), (DS/y), (y\rho sg/\rho v^2)] = o \quad (3)$$

Which results:

$$\pi 1 = \frac{v^2}{gy}, \pi 2 = \frac{\rho vy}{\mu}, \pi 3 = \frac{y}{H}, \pi 4 = \frac{y}{L}, \pi 5 = Sb, \pi 6 = \frac{v}{u}*, \pi 7 = y/Ds, \pi 8 = v^2/gy\ (1/Gs)$$

And equations governing the flow parameters are as follows:

Froude No., Reynolds No., Dimension-less ratio of depth to dam, Dimension-less ratio of depth to distances of dams, Ratio of flow velocity to shear velocity, Bed slope.

And the experimental functions are as follows:

$$f\ 3 = (Q, y/H, y/L, Fr, Re, v/u) \quad (4)$$

Distorted physical model. In physical models (moving bed), the vertical scale diversion of rivers and canals often is needed to ensure the movement of bed material model. From Peterson equation for the slope ratio results:

$$Sr = yr/Lr \quad (5)$$

And from Manning equation for rough bed modelling simulation results:

$$nr = Rr^{2/3} / Lr^{1/2} \quad (6)$$

Thus, regarding present flume dimensions (W*H*L = 309mm*450mm*12500 mm), using scales for depth, length, width and discharge are as follows:

$dr = dm/dp = 1/50, Lr = Lb/Lp = 1/1250, br = bm/bp = 1/200, Qr = \frac{Qm}{Qp} = br \cdot dr^3/2$

According to the recipe design, implementation and maintenance of flood and sediment control structures (dams retracement) publication 416 Strategic Supervision Department, height, discharge and distance of the small dams for the experiment are as follows:

$Hp1 = 5\,m \rightarrow Hm1 = 0.1\,m$ Where:

$Hp3 = 3\,m \rightarrow Hm3 = 0.06\,m$
$Hp = Prototype\ height$

$Hp2 = 4\,m \rightarrow Hm2 = 0.08\,m\ Hm = Model\ height$

And for applied discharge;

$Qp1 = 1285\,m^3s^{-1} \rightarrow Qm1 = 18\,Ls^{-1}$

$Qp2 = 1070\,m^3s^{-1} \rightarrow Qm2 = 15\,Ls^{-1}$ Where:

$Qp3 = 860\,m^3s^{-1} \rightarrow Qm3 = 12\,Ls^{-1}\ Qp = Prototype\ discharge$

$QP4 = 716\,m^3s^{-1} \rightarrow Qm4 = 10\,Ls^{-1}\ Qm = Model\ discharge$

$Qp5 = 570\,m^3s^{-1} \rightarrow Qm5 = 8\,Ls^{-1}$

As the profiles of overflow weirs can be obtained from rectangular over flow weir of the bottom of the water surface curve, the equation of the model is the same as rectangular overflow discharge equation, so [1]:

$$Q = 2/3\ Cd\ \sqrt{2g}.L.Hd3/2 = C.L.H3/2 \quad (7)$$

The value of C is also variable and based on the shape of diagram according to ratio *Hw/Hd* for over flow spillways. As in the above mentioned diagram is clear, if *Hw/Hd >1.33*, the value of C is almost "fixed and equal to 2.2, which in this case the weir is called long overflow, and *Hv = V0/2g* is ignored and assumes *He = Hd* [1].

Applied intervals (distance between walls) are as follows:

$L1 = 2.5\,m, L2 = 2.6\,m, L3 = 2.7\,m$

Also, applied slopes are as follows [6]:

$S1 = 0.02, S2 = 0.018, S3 = 0.016$

FIGURE 2
Installation of walls and flow formation over the wall

Hydraulic flow test model. First plexiglass walls of Hi1, Hi2 and Hi3 with height of 10 cm, and a length of 2.5 meters distance between them(L1) installed, also the floor slope of S1equal to 0.02, with flow discharge of Q1 equal to 18 l/s was established by electro-pump on it. Along the way the depth and flow rate using the depth gauge and digital tachometers is measured and recorded in the corresponding table. This tests for the walls Hi2 and Hi3 respectively with 8 and 6 cm height in L2 and L3 distances of 2.6 m and 2.7 m in length and the slopes of S2 equal to 0.018 and S3 equal to 0.016 with flow discharge of 15, 12, 10 and8 liters per second is repeated respectively. The depth and the speed of the stream to determine the flow regime and the Froude number was used. The figures no. 2 shows pass mode and formation of the flow in dealing with Hi1 wall. The number of tests related to the hydraulic flow were135 (*3S * 5Q * 3L * 3H = 135*) that eventually caused the ratios of *y/Hw, y/L* and *V* to determine the *Fr no.* and *yd* the overflow depth, also ratio *Hw/He* to determine the values of *Cd*.

In this experiment the different value ratios of "*yi/Hwij* and *yi/Li*" tested for Q1-5 in the slope of the S1-3. Also "i" indicates the number of walls and "j" its height, "*V*" flow rate,"*Fr=V ²/gy*" Froude number, "y" upstream flow depth of dams, "*He*" and "*Cd*" respectively, energy equivalent height of the top of the overflow and hydraulic flow coefficient.

DISCUSSION AND RESULTS

Discussion and analysis of the flow hydraulic tests. At this point the investigation and analysis of the data and information obtained with the use of drawing curves and regression statistical methods such as "Regression" and "Correlation" that lead to determine the descriptive coefficients R^2 and correlation $\sqrt{R^2}$ and comparison of quantitative and qualitative data [7].The target of this part of test is to investigate impact of variations of height *"Hw"* and distance "*L*" on other parameters such as flow depth "y", flow regime "Fr no." and "*Cd*" ,while flow discharge "*Q*" and bed slope "*S*" are changing.

Hydraulic flow tests analysis. Here are comparing changes of depth ratio to height *(y/Hw)*, depth ratio to length *(y/L)*, Froude No., Hydraulic flow coefficient *(Cd)* , with discharges *(Q)* in three slope *(S)* and three intervals *(L)* concluding results of the hydraulic flow tests which performed with consecutive small dams model "figures 6-13".The tests were repeated 135 times, means,*3S*5Q*3H*3L= 135* Tests.

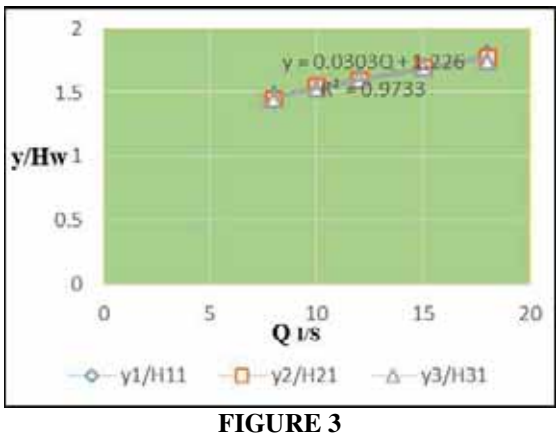

FIGURE 3
Ratio of y/Hw for the consecutive walls (H1j, H2j, H3j)

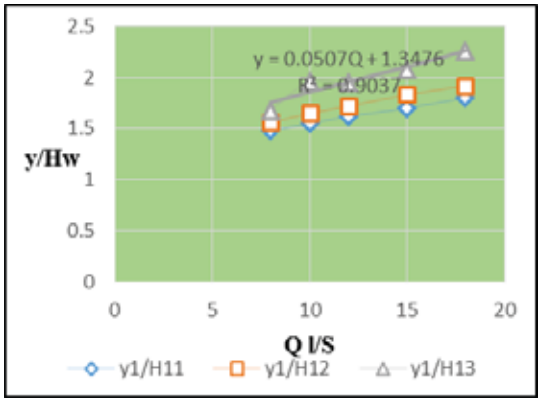

FIGURE 4
Ratio of y/Hw for different height walls comparison (Hi1, Hi2, Hi3)

Results: For the y/Hw graphs:

1) The "figures 3&4", ratio of y/Hw for consecutive and different height walls, shows the consistency and convergence of curves (Uniform Behavior flow) for same height consecutive walls and different phase of corresponding non-elevated walls by changing the flow rate *q1-3*.

2) By reducing the slope "*S"*, the flow varieties is decreased.

3) Because of the relationship between flow *q* and *y /Hw* is direct, the amount of $\sqrt{R^2}$ (Correlation factor) is positive.

Results for the y/L graphs:

1) The "figures 5&6", ratio of y/L for consecutive and different height walls represents the adaptation and integration flow curves in the diagrams below and reduction of different phase, while increasing intervals *L*.

2) Changing the slope "*S*" is not effective on process.

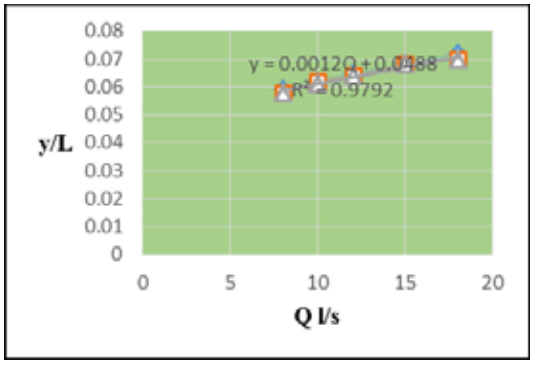

FIGURE 5
Ratio of y/L for the consecutive walls (H1j, H2j, H3j)

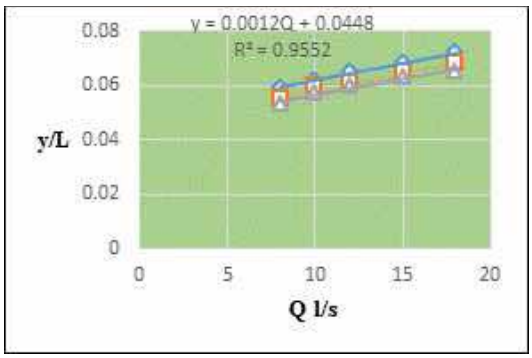

FIGURE 6
Ratio of y/L for different height walls comparison (Hi1, Hi2, Hi3)

Results for the Froude No. graphs:

1) The "figures 7&8" of the froude No. curves of Hi1 and Hi2 walls show more similar; the wall Hi3 shows difference of phase to the others.

2) Slope "*S"* and the distance "*L"* both are not effective the trend.

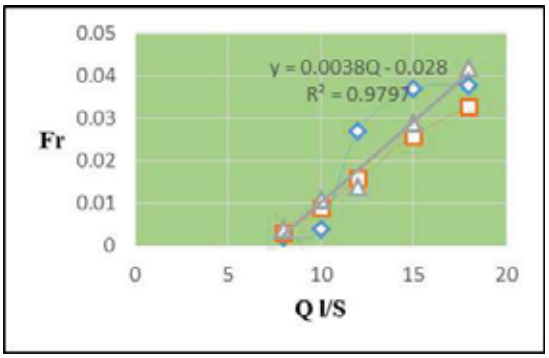

FIGURE 7
Froude No. of the flow for the consecutive walls (H1j, H2j, H3j)

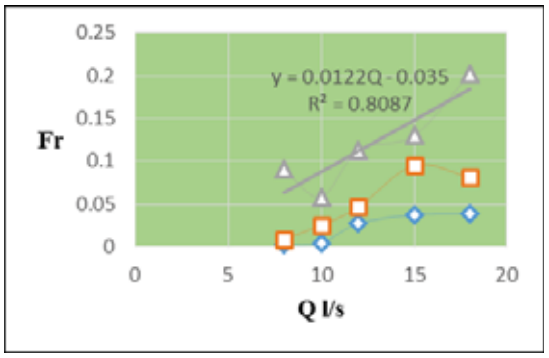

FIGURE 8
Froude No. for different height walls comparison (Hi1, Hi2, Hi3)

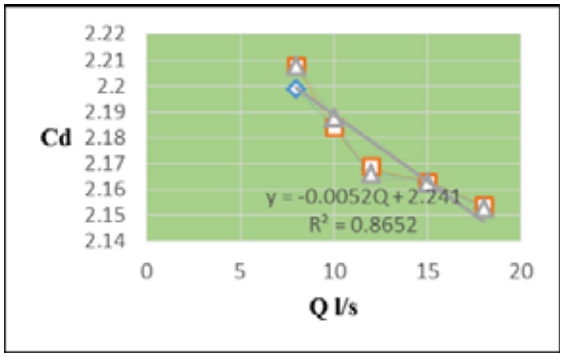

FIGURE 9
Hydraulic coefficient of the flow for the consecutive walls (H1j, H2j, H3j)

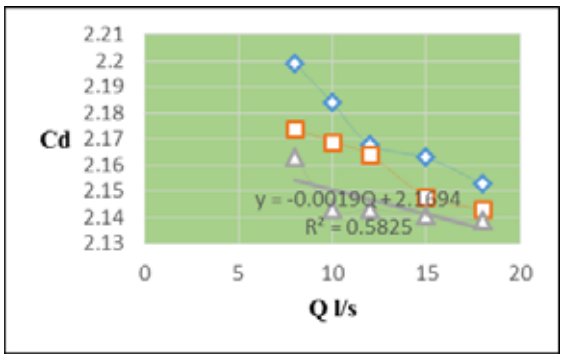

FIGURE 10
Hydraulic coefficient for different height walls comparison (Hi1, Hi2, Hi3)

Results for the Cd hydraulic coefficient:

1) Study of the "figures 9&10", coefficient of Cd for consecutive and different height walls, shows the convergence of curves, volatility and fluctuations in the phase difference at the top and bottom of the downward along.

2) Change the slope of the bed *S* and *L* are not effective on the above process.

Qualitative analysis of current trends in collision with the wall:

1) Reviewing the overall process of the flow, tested in different scenarios, including changes in discharge, height and distances between walls and slopes, with common features, including flow with critical depth, the formation of a hydraulic jump because of the specific energy, passing through the barriers to transfer from one branch to another branch of E-y curve with critical depth yc [3].

2) Froude number is supercritical over the each wall, and subcritical before to reach them [3].

TABLE 1
Correlation Coefficient $\sqrt{R^2}$ for *q1-5*

Hij	*y/Hw*	*y/L*	*Fr*	*Cd*
H1j	0.985	0.997	0.926	0.959
H2j	0.977	0.992	0.997	0.932
H3j	0.96	0.989	0.989	0.93
Hi1	0.999	0.992	0.926	0.959
Hi2	0.997	0.982	0.918	0.984
Hi3	0.95	0.977	0.898	0.762

CONCLUSIONS

1. Regarding correlation coefficient of table 1, and the ratios of "*y/Hw*", the height of the walls is in direct proportion (Positive) to the depth, in other words, increasing the height, increases the depth, as the flow "*q*" increases.

2. Regarding ratios of "*y/L*", the interval of the walls is in divert proportion to the depth, so, increasing the distance, will decrease the depth, as the flow "*q*" increases.

3. Froude number, "*Fr*", is in direct proportion to the flow, and divert proportion to the height of the walls.

4. Hydraulic coefficient, "*Cd*", is in divert proportion to the flow and direct proportion to the height.

5. The length of the walls is considered to form a rectangular overflow as the effective length (W = We), while in the same experiments some part of the length of the overflow has been engaged as effective length, such as slit-check dam models [6].

Notations:

υ = Water viscosity (m²/s), Ds = Bed load diameter (m), V = Flow velocity (m/s)

θs = Dimension- less No. of Shields, L = Distance between check dams (m), y = Flow depth (m)

g = Gravity acceleration (m/s²), Gs = Sediment particles specific weight (2.65), γ = Water specific weight (Kg/m³)

H = Height of check dams (m), Re* = Reynolds No. of particles, μ = Dynamic viscosity (pa.s)

Sb = Bed slope, U* = Mean shear velocity of flow (m/s), τc = Critical shear stress (N/m²)

ρ = Density of water (Kg/m³), γs = Particles specific weight (Kg/m³), τ = Shear stress of the flow (N/m²)

ACKNOWLEDGEMENTS

The present paper is based on PhD dissertation of Mehdi Bensaid, PhD student of aqueous structures of Science and Research Branch of Islamic Azad University of Khuzestan and Ahvaz branch. In addition, the contributions of this university are warmly appreciated. The authors also would like to express their appreciation for the cooperation and assistance extended to Khuzestan Water and Power Organization who made the experiments possible by providing laboratory and models.

REFERENCES

[1] Shfae Bajestan, M. (2015), Sediment transport hydraulic. U. of Chamran publishing, Ahvaz, 1-549.

[2] Publication No. 688 (2011). Vice president of strategic planning and monitoring Guidelines for design, implementation and sediment control structures. River hydraulic roughness coefficient guide. 1-125.

[3] Abrishami, J. (1993), Open channel hydraulics. U. of Ferdowsi publishing, Mashad, 1-501.

[4] Amirjani, R., Kamanbedast, A.A., Heidarnejad, M., Bordbar, A., Masjedi, A. (2017). The effect of specification of cohesive and non- cohesive sedimentation on pressure flashing efficiency in dam reservoirs. Fresen. Environ. Bull. 26, 6674-6679

[5] Campisano, A., Cutore, P., Modica, C. (2013) Modelling sediment deposit evolution upstream of slit-check dams in mountain Streams. (ASCE) World Environmental and Water Resources Congress, 1-12.

[6] Chaploghi A. (2001) Determination of trapping coefficient using flume to control floods and estimate of sediment volume. University of Tarbyat Moddares, Tehran.

[7] Damagaard, J.S, Whitehouse, R., Sulsby, R. (1997) Bed load sediment transport on steep longitudinal slopes. (ASCE) J. of Hydraulic. Eng. 123(12), 1-9.

[8] Dezfoli, M.H.N., Kamanbedast, A.A., Masjedi, A., Heidarnejad, M., Purmohammadi, M.H. (2017) Comparing Methods of Estimating Hydraulic Jumps Stilling Basins' divergent Parameters. Fresen. Environ. Bull. 26, 2231-2236.

[9] Ehdae, B. (1990), General experimental statistics. U. of Chamran publishing, Ahvaz, 1-467.

[10] Elyasi, M. and Kamanbedast, A.A. (2014) The Effect of Angle of Intakes on Diversion sediments in River Bend with CCHE2D Model. Advance in environmental biology. AENSI Journal. 8(22), 180-186.

[11] Guide Publication No. 416 (2007). Vice president of strategic planning and monitoring Guidelines for design, implementation and sediment control structures. 1-92.

[12] Kamanbedast, A.A., Ghahremani, A. (2014) Evaluation of Scour Around Bridge Pile in Flood with Hec-Ras Software. Journal of River Engineering. 2(6), 4p.

[13] Kamanbedast, A.A., Nasrollahpour, R. and Mashal, M. (2013) Estimation of Sediment Transport in Rivers Using CCHE2D Model (Case Study: Karkheh River). Indian Journal of Science and Technology. 6(2). 4112-4115.

[14] Kazemi A., Ebrahimi, A. (2015) Experimental study on trapped sediment profile of permeable & non- permeable check dams. Intl. water engineering conf. Tehran, 1-12.

[15] Niknam, A., Kamanbedast, A. and Shahryari, M. (2015) Determination of sediment distribution in reservoirs with using numerical method (Case study: Maroon Dam). Research Journal of Fisheries and Hydrobiology. 10(9), 85-93.

[16] Recking, A., Frey, P., Belleudy, P., Champagne, J.Y. (2008) Bed load transport flume experiments on steep slopes. (ASCE) J. of Hydraulic Eng. 134(9), 1302-1310.

[17] Rostami, H., Heidarnejad, M., Purmohammadi, M.H., Kamanbedast, A., Bordbr, A. (2016) An Experimental Study into Discharge Coefficient of Labyrinth Weirs with Rectangular-Shaped Plans. Fresen. Environ. Bull. 25, 5138-5144.

[18] Rouzegar, J., Kamanbedast, A.A., Masjedi, A., Heidarnejad, M., Bordbar, A. (2017) The Experimental Investigation of Flow Hydraulics in Zigzag Morning Glory Spillways. Fresen. Environ. Bull. 26, 2389-2396.

[19] Saki, A., Kamanbedast, A.A., Masjedi, A., Heidarnejad, M., Bordbar, A. (2017) A Newly Designed Rectangular Weir for Flow Regulation at River Fork Through A Physical Model (Case Studies of Karkheh/Hufel/Nissan Streams). Fresen. Environ. Bull. 26, 7400-7410.

[20] Shafae Bajestan, M. (2005), Physical & Hydraulic – modelling. U. of Chamran publishing, Ahvaz, 1-268.

[21] Shirali, M., Kamanbedast, A.A., Masjedi, A., Bordbar, A., Heidarnejad, M. (2017). An Experimental Investigation on The Effects of The Shape of The Cross Section in Morning Glory Spillways. 26(11), 6532-6542.
[22] White, R. (2000), Flushing of Sediments from Reservoirs, ICOLD. World Register of Large Dams, HR Wallingford, UK.

Received: **24.10.2017**
Accepted: **16.10.2018**

CORRESPONDING AUTHOR

Amir Abbas Kamanbedast
Department of Water Science and Engineering,
Ahvaz Branch, Islamic Azad University,
Ahvaz – Iran

e-mail:ka57_amir@yahoo.com

© by PSP Volume 28 – No. 4/2019 pages 2397-2406 Fresenius Environmental Bulletin

EVALUATION OF FOSSIL FUEL CONSUMPTION AND ENVIRONMENTAL IMPACTS IN SUGAR BEET PRODUCTION AS A BIOFUEL RAW MATERIAL

Cahit Gungor[1,*], H Huseyin Ozturk[2]

[1]Department of Agricultural Economics, Faculty of Agriculture, University of Cukurova, 01330 Adana, Turkey
[2]Engineering of Agricultural Machinery and Technologies, Faculty of Agriculture, University of Cukurova, 01330 Adana, Turkey

ABSTRACT

Indirect and direct energy consumption for the production of biomass, which will be used as a biofuel raw material, is very important. Therefore in this study, it is aimed to evaluate fossil fuel consumption and its associated carbon dioxide (CO_2) emissions to cultivate sugar beet used as a bioethanol raw material. The total diesel consumption of the tractor with the implements/ machines and harvesting machine was calculated as 1071 L per hectare (ha). The total CO_2 emissions for sugar beet cultivation were calculated as 293.8 kgCO_2 per hectare. It was found that the total fossil fuel (diesel+lubricant oil), energy consumptions and CO_2 emissions for sugar beet cultivation were 107.97 L/ha, 4006.6 MJ/ha and 296.5 kgCO_2/ha, respectively. The specific value of fossil energy consumption related to total fossil fuel was 70.48 MJ per ton tuber. Taking into account the values of specific fuel consumption, 1.9 L fossil fuel was consumed to produce 1 ton sugar beet tuber. Considering the specific value of tuber production, 1 L fossil fuel was consumed to produce 526.57 kg sugar beet tuber. Taking into account the specific value of CO_2 emission, 5.22 CO_2 was released to produce 1 ton sugar beet tuber. For 1 kg ethanol production 0.15 L fossil fuel or 5.72 MJ fossil fuel energy corresponding to this amount of fuel consumption is consumed. As a result, fossil fuel consumption for the production of 1 kg of ethanol from sugar beet molasses results in an emission of 0.42 kgCO_2.

KEYWORDS:
Sugar beet cultivation, fuel consumption, energy use, CO_2 emission.

INTRODUCTION

Decreasing fossil fuel reserves and increasing environmental problems caused by the intensive use of these fuels are increasing the importance of biomass energy in today's world. Greenhouse gas (GHG) emissions resulting from the use of fossil fuels and carbon dioxide (CO_2) accumulation in the atmosphere are one of the main causes of global climate change. For sustainable economic development, these GHG emissions must be at the lowest level. Recently, significant solutions have been developed for the current environmental problems associated with environmental and human health pollutant emissions. In this context, to reduce fossil fuel consumption, the European Commission (EC) has already set the goal of increasing the renewable energy consumption rate from 5% in Europe to 20% by 2020, while OECD countries aim to achieve 15% of total electricity production from biomass energy by 2020 [1]. Similar targets are included in 2023 strategic plans of Turkey.

Comprehensive studies have been performed by several authors regarding to assessment of energy use and the environmental impacts and CO_2 emissions for cultivation processes in different countries of all over the world [2–21]. Regarding environmental sustainability, in recent years it has become of major interest to evaluate cropping systems in terms of energy consumption. The reduction of energy consumption in agriculture became particularly relevant partly because fossil energy is a limited resource to be conserved for future generations [22] and it contributes to greenhouse gas emissions in the atmosphere [23].

One of the key objectives of the biofuels world is to reduce the dependence on food resources while increasing the use of new types of raw materials within advanced biofuels technologies. Particularly in the context of biofuels-food relations, the use of non-food raw materials and the work done in this regard are becoming increasingly important. Biorefinery does not interfere and harm human and animal food sources in accordance with their existence and establishment ethics [24]. As a result, the use of biomass as raw material for biofuels should not create an alternate consumption area for human and animal food. On the other hand, indirect and direct energy consumption for the production of biomass, which will be used as biofuel raw materials, is also very important. Consumption of fossil fuels and other resources and damage to the environment must also be taken into account in biomass production, which will be used as raw ma-

terials for biofuels. This issue was the main basis for this work. Therefore, in this study, it is aimed to evaluate fossil fuel consumption and its associated CO_2 emissions to cultivate sugar beet used as a biofuel raw material.

Sugar beet as a raw material of biofuel. Biofuels also have a significant advantage in terms of CO_2 emissions. As biomass grows, CO_2 used in photosynthesis emits atmospheres as a result of combustion. For this reason, it is assumed that CO_2 emissions are zero when biofuel is in use or burned, in other words, carbon is considered neutral [25, 26]. The most important biofuels that are now widely and commercially used in many countries are biodiesel and bioethanol. Bioethanol is a biofuel that can be produced by fermentation of sugary and starchy plants or by acidic hydrolysis of cellulosic sources. Raw materials include sugar beet, sugar cane, corn, wheat, potatoes; woody plants such as stem, straw, bark; agricultural wastes and residues and molasses which is a by-product of sugar production can be used. Today's production technologies are evaluated for sugars and starchy plants for bioethanol production. The interest in bioethanol has increased since 1970, mainly due to the increase in oil prices and is now increasingly becoming an important environmental effect [27].

In Brazil, the pioneer of bioethanol use, bioethanol was first used in 1931 by blending 5% of the gasoline, and in 1938 the relevant legislation was introduced. In Brazil, which accounts for about 30% of the world bioethanol market, flexible biofuels use bioethanol mixes ranging from 20% to 26% with the use of E85 [28]. Bioethanol in Turkey, is defined as liquid fuel blending component in the scope of the Petroleum Market Law No. 5015. It can be used as gasoline additive according to automotive benzine standard (TS EN 228). With regard to bioethanol produced from domestic sources, which have up to 2% of the volume of gasoline in the relevant legal regulations, the value of the private consumption tax is zero. According to the latest regulations in September 2011, it is mandatory that the content of gasoline supplied as fuel to the market be at least 2% from 2013 and at least 3% from 2014 [24].

Sugar beet production in Turkey. The change of sugar beet cultivation areas and production quantities in the period between the years of 2000–2016 in Turkey are given in Table 1. Sugar beet has been cultivated in 297 739.2 hectares area in the period between the years of 2000–2016 and 16 648 930 tons of product were obtained. The average yield 56 517.14 kg per hectare in Turkey [29].

The main objective of this study to quantify and evaluate CO_2 emissions related to fossil fuel consumption for the sugar beet cultivation in agricultural regions of Turkey. The farms, cultivated sugar beet were surveyed in all agricultural regions of Turkey in 2016. Taking actual farm size as the variable, the total 200 farms was randomly selected by using stratified random sampling. The data were obtained related to energy inputs used for different field operations and yield. The energy related to fuel and lubricant oil consumed by agricultural tractor used with agricultural implements/machinery during cultivating operations was evaluated as a direct energy input. The CO_2 emissions associated with direct fuel and lubricant oil consumptions are estimated according to the Intergovernmental Panel on Climate Change (IPCC) approach. The specific values for fuel consumption, tuber production, energy consumption and CO_2 emission were defined to analyze the relationship between fuel consumption and CO_2 emission for sugar beet cultivation.

MATERIALS AND METHODS

In this study, the farms, cultivated sugar beet, were surveyed in all agricultural regions of Turkey. The data were obtained related to energy inputs used for different field operations and yield. The required sample size has been calculated following equation. The permissible error was defined to be 5 % for 95 % reliability [30].

TABLE 1
Production values of sugar beet cultivation in Turkey [37]

Years	Area sown (ha)	Production (tons)	Yield (kg/ha)
2010	329 166.9	17 942 112	54 510
2011	297 264.8	16 126 489	54 250
2012	280 694.5	14 919 940	53 150
2013	291 328.2	16 488 590	56 600
2014	288 785.1	16 743 045	57 980
2015	274 487.3	16 022 783	58 370
2016	322 447.7	19 592 731	60 760
Mean	**297739.2**	**16 648 930**	**56 517.14**

TABLE 2
Cultivation practices and mechanization implements for sugar beet production

Cultivation practices	Implements	Fuel (diesel) consumption (L/ha)
Soil tillage and seed bed preparation	Disc harrow, plough and roller	41
Sowing	Pneumatic sowing machine	5
Spraying	Sprayer	2
Hoeing	Hoeing machine	2
Fertilizing	Fertilizing machine	2
Harvesting	Harvesting machine	50
Soil preparation	Disc harrow	5

$$n = \left(\sum N_h S_h\right)^2 / \left(N^2 D^2 + \sum N^h S_h^2\right) \quad (1)$$

where; n is the required sample size, N is the number of holdings in target population, N_h is the number of population in h the stratified, S_h is the variance of h the stratified, and D is the precision where (x-X).

Cultivation practices for sugar beet production. In Turkey, sugar beet is generally produced with a four-year rotation system. Pre-plant is harvested a year before so that sugar beet farming is ready for agriculture. Just after the harvest, the soil is prepared with disc harrow and irrigation is applied. As a result of this irrigation, the remaining seeds from weeds and cereal crops are germinated in the field. After reaching the suitable moisture in soil, the tillage process is carried out. In November, 2/3 of the base fertilizer is thrown into the field and the second tillage is made. In the spring, seed bed is prepared by feeding 1/3 of the base fertilization and half of the nitrogen fertilization. It is preferred that the sowing process is done in March. Pneumatic sowing machines are used to achieve a good planting process. In sugar beet production, it is necessary to protect against weeds, diseases and harmfulness during the period from sowing to harvesting. The seeds need to be sprayed in order to provide the necessary protection. Thus, precautions have been taken against diseases and harmful insects. The spraying against disease and pests covers two periods, pre-sowing and post-sowing. The necessary spraying process can be done 3-4 times in case of diseases. 4.5 kg pesticide is used for one hectare (ha) production area. Hoeing is a suitable method for the struggle against weeds. Sugar beet reaches the harvestable age after 6 months from planting. Harvesting is done by hand or by machine. After the harvesting, the remaining beet leaves are mixed with the help of the disc harrow. The amounts of fossil fuel (diesel) consumed per hectare (ha) during the all production processes described here are given in Table 2.

The most important processes affecting yield and quality of sugar beet production are fertilization and irrigation applications. Fertilization should be based on the nutrients and amounts of plant nutrients that sugar beet needs. The best way to do this is to analyze the soil and fertilize it according to your needs. 125 kg of nitrogen, 105 kg of phosphorus and 80 kg of potassium fertilizer are applied per hectare production area. The harvested beets are transported to the sugar factory for processing. Sugar beets can be kept in a storage near the field until they are moved to the factory. Drying or cooling processes are not required during storage. 700 kg of ethanol is produced from the molasses of sugar beet produced in one hectare production area [24].

Cultural practices applied in the conventional system for sugar beet production are given in Table 2. Sugar beet cultivation analyzed in this study corresponds to representative practices in Turkey. Sugar beet is normally grown in crop rotation and under intensive farming. Two power categories of tractors have been used in field operations for sugar beet cultivation. Tractor has two wheels drive and 55 kW power has been used for the light tasks such as secondary tillage, sowing, spraying and fertilizing applications. On the other hand, tractor has four wheels drive and 75 kW power has been used for the heavier tasks such as primary tillage with a plough.

Determination of fuel energy inputs. The energy related to fuel and lubricant oil consumed by agricultural tractor used with agricultural implements/machinery during cultivating operations was evaluated as a direct energy input. In this sense, the calculation methods for the direct energy inputs per hectare are given in following sections.

Energy consumption related to diesel fuel. The fuel energy inputs per hectare related to diesel fuel consumed by agricultural tractor and harvesting machine have been calculated as follows:

$$E_{FC} = M_f \times LHV_f \quad (2)$$

where;

E_{FC} = the fuel energy input per hectare (MJ/ha),
M_f = diesel fuel consumed by tractor or harvesting machine (L/ha) and
LHV_f = the lower heating value of diesel fuel (MJ/L).

TABLE 3
Emission factors and heating values for diesel fuel and lubricant [31]

Fuel type	Lower heating value (GJ/L)	Emission factors (kg CO_2/GJ)
Diesel	0.0371	74.01
Lubricants	0.0382	73.28

The lower heating values depending on fuel types were taken from IPCC, 1996, Volume 2, Section 1 [31]. The lower heating values used in calculations for the diesel fuel and lubricant oil are given in Table 3.

Energy consumption related to lubricant oil. The direct energy inputs related to lubricant oil consumptions were determined taking into account hourly lubricant oil consumption values of agricultural tractor used for cultivation operations and harvesting machine used for harvesting operations in sugar beet production. Therefore, the total energy input related to lubricant oil consumption per unit production area (ha) was determined as follows:

$$E_{TLC} = E_{LC,T} + E_{LC,C} \quad (3)$$

where;

E_{TLC} = the total lubricant oil energy input per hectare (MJ/ha),
$E_{LC,T}$ = energy input for lubricant oil consumed by agricultural tractor (L/ha) and
LHV_f = energy input for lubricant oil consumed by harvesting machine (L/ha).

The energy inputs related to lubricant oil consumed by agricultural tractor and harvesting machine were estimated multiplying the oil consumption with the lower heating value of the lubricant oil.

$$E_{LC} = M_l \times LHV_l \quad (4)$$

where;

E_{LC} = the lubricant oil energy input per hectare (MJ/ha),
M_l = the lubricant oil consumed by tractor or harvesting machine (L/h) and
LHV_l = the lower heating value of lubricant oil (MJ/L).

The hourly lubricant oil consumption of agricultural tractors, depending on the maximum power take off (PTO) for the tractor, has been calculated as follows [32]:

$$M_{l,T} = 0.00059 \times PTO_{\max} + 0.02169 \quad (5)$$

where;

$M_{l,T}$ = the lubricant oil consumed by tractor per hectare (L/h) and
PTO_{max} = the maximum power take off for the tractor (kW).

The maximum PTO for tractor used in cultivation operations was estimated based on the nominal power of tractor (NP) [32].

$$PTO_{\max} = 0.88 \times NP \quad (6)$$

where;

NP = the nominal power of tractor (kW).

The hourly lubricant oil consumption of harvesting machine, depending on the engine power, has been calculated as follows [32]:

$$M_{l,C} = 0.004 \times P_e \quad (7)$$

where;

$M_{l,C}$ = the lubricant oil consumed by harvesting machine per hour (L/h) and
P_e = engine power of harvesting machine (kW).

Calculation methodology for carbon dioxide emissions. The CO_2 default emission factors depending on fuel type based on lower heating values are from IPCC, 1996, Volume 2, Section 1 [31] (Table 3). The methods for calculating CO_2 emissions recommended by the *GHG Protocol - Mobile Guide (03/21/05) v1.3 (Calculating CO2 Emissions from Mobile Sources Guidance to calculation worksheets)* were used in this study. The following equation outlines the recommended approach to calculating CO_2 emissions based on fuel use (assuming data is first obtained in terms of mass or volume).

CO_2 emissions = Fuel used × Heating value × Emission factor

Diesel-based CO_2 emissions = Diesel used × Heating value × Emission factor

Diesel-based CO_2 emissions = L/ha × 0.0371 GJ/L × 74.01 kgCO_2/GJ (8)

Diesel-based CO_2 emissions = kgCO_2/ha

Lubricant oil-based CO_2 emissions = Oil used × Heating value × Emission factor

Lubricant oil-based CO_2 emissions = L/ha × 0.0382 GJ/L × 73.28 kgCO_2/GJ (9)

Lubricant oil-based CO_2 emissions = kgCO_2/ha

The specific fuel consumption. The specific fuel consumption (S_{FC}) and specific seed production (S_{SP}) were defined to analyze the relationship between fuel consumption and sugar beet production. The value of the specific fuel consumption (S_{FC})

indicates the amount of fuel consumed (L) to produce the unit quantity (t) of tuber.

$S_{FC} = FC / GY$ (10)

where S_{FC} is the specific fuel consumption (L/t), FC is fuel consumption (L/ha) and GY is tuber yield (ton/ha).

The specific tuber production. The specific tuber production (S_{SP}) is the ratio of fuel consumption to tuber yield and indicates fuel consumption (L) per kg of tuber.

$S_{SP} = SP / FC$ (11)

where S_{SP} is the specific tuber production (kg/L), SP is tuber production per hectares (kg/ha) and FC is fuel consumption per hectares (L/ha).

The specific energy consumption. The specific energy consumption (S_{EC}) is the ratio of energy consumption to tuber yield and indicates energy consumption (GJ) per ton of sugar beet tuber.

$S_{EC} = EC / FC$ (12)

where S_{SP} is the specific energy consumption (GJ/t), EC is energy consumption per hectares (GJ/ha) and FC is GY is tuber yield (ton/ha).

The specific carbon dioxide emission. The specific CO_2 emission (S_{CO2}) was defined to analyze the relationship between CO_2 emissions and sugar beet production. The S_{CO2} is the ratio of total CO_2 emissions to tuber yield and indicates CO_2 emissions ($kgCO_2$) per ton of sugar beet tuber.

$S_{CO2} = CO_2 / GY$ (13)

where S_{CO2} is the specific CO_2 emission ($kgCO_2$/ton), CO_2 is CO_2 emissions ($kgCO_2$/ha) and GY is tuber yield (ton/ha).

RESULTS AND DISCUSSION

Fuel consumption and carbon dioxide emissions for sugar beet cultivation. The change of diesel fuel consumptions, CO_2 emissions and energy consumptions for sugar beet cultivation is given in Fig. 1 and Fig. 2, respectively. The diesel and related energy consumptions with the agricultural implements and machines for sugar beet cultivation are given in Table 4. The total diesel consumption of the tractor with the implements/machines and harvesting machine was calculated as 1071 L per hectare.

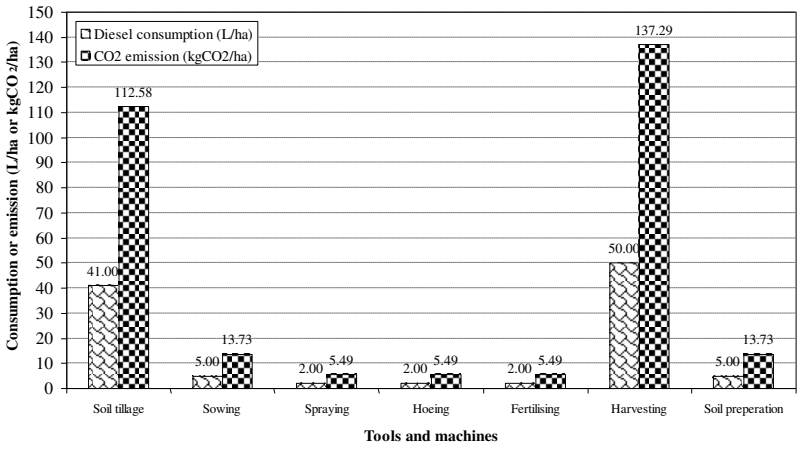

FIGURE 1

The change of diesel consumptions and CO_2 emissions for tools and machines

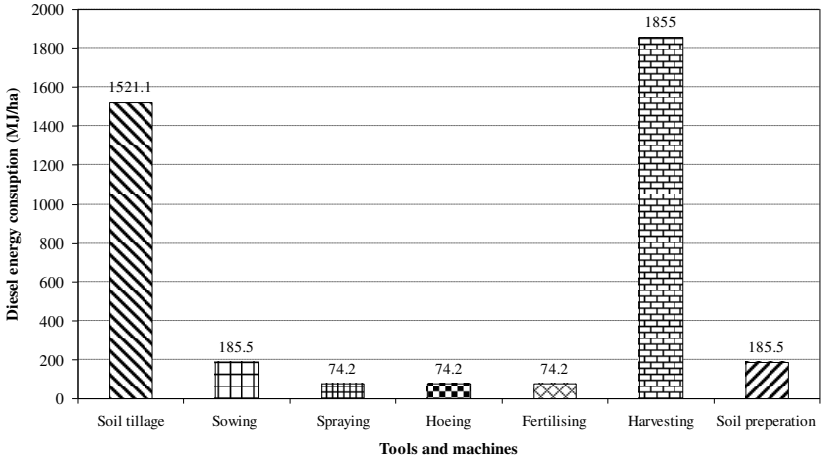

FIGURE 2

The change of diesel energy consumptions for tools and machines

TABLE 4
Diesel consumptions and CO_2 emissions for implements and machines

Tools and machines	Diesel Consumption		Fuel energy (MJ/ha)	CO_2 emission ($kgCO_2$/ha)
	L/ha	%		
Soil tillage and seed bed preparation	41	38.32	1521.1	112.58
Sowing	5	4.67	185.5	13.73
Spraying	2	1.87	74.2	5.49
Hoeing	2	1.87	74.2	5.49
Fertilising	2	1.87	74.2	5.49
Harvesting	50	46.73	1855	137.29
Soil preparation	5	4.67	185.5	13.73
Total	*107*	*100*	*3969.7*	*293.80*

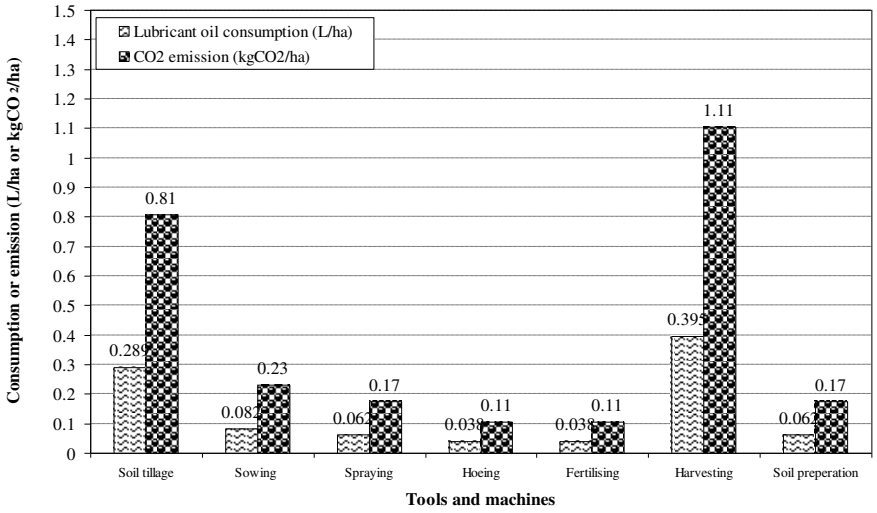

FIGURE 3
The change of oil consumptions and CO_2 emissions for tools and machines

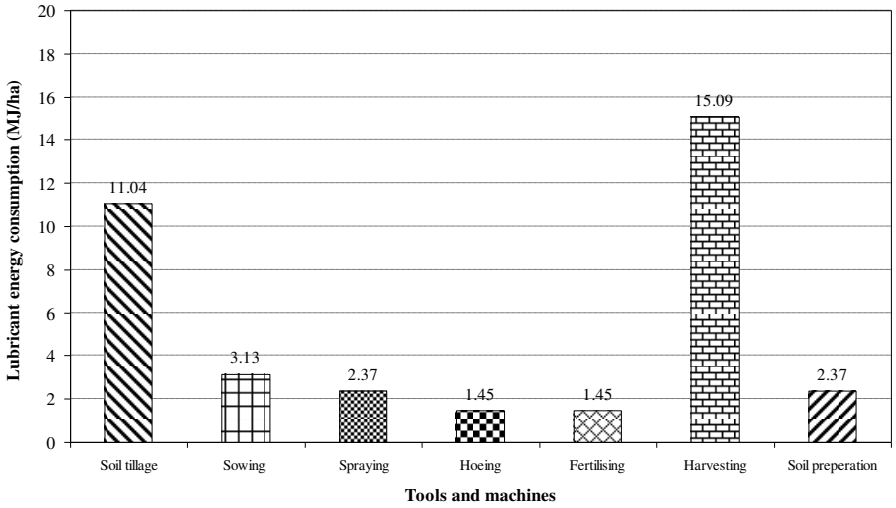

FIGURE 4
The change of lubricant oil energy consumptions for tools and machines

The total diesel consumption for soil tillage and seedbed preparation was 41 L per hectare (Table 4). Fuel consumption with harvesting machine was 50 L per hectare during harvesting. This consumption corresponds to 46.73% of the total fuel consumption for sugar beet cultivation. The 89.6% of the total fuel (96 L/ha) was consumed for soil tillage, seedbed and soil preparation with tillage implements and harvesting with harvester.

The total CO_2 emissions for sugar beet cultivation were calculated as 293.8 $kgCO_2$ per hectare (Fig.1). As it might be expected, CO_2 emissions increased linearly as the amount of fuel consumption increased. The highest CO_2 emission released during harvesting with harvesting machine fol-

lowed tillage operations. The total 137.29 $kgCO_2$ per hectare was released during harvesting with the harvester. In response to amounts of diesel fuel used for per unit area (107 L/ha), the totally 3069.7 MJ fuel energy was consumed per hectare (Fig. 2). Due to fuel consumption is the highest, the maximum fuel energy consumption (1855 MJ/ha) has been realized during harvesting with the harvester. The harvesting with harvesting machine followed by tillage operations (1521.1 MJ/ha).

Lubricant oil consumption and carbon dioxide emissions for sugar beet cultivation. The change of lubricant oil consumptions, CO_2 emissions and energy consumptions for sugar beet cultivation is given in Fig. 3 and Fig. 4, respectively. The lubricant oil and energy consumptions with the agricultural implements and machines for sugar beet cultivation are given in Table 4. The total lubricant oil consumption of the tractor with the implements/machines and combine harvester was 0.97 L per hectare. In response to these amounts of lubricant oil used for per unit area (ha), the totally 36.0 MJ oil energy was consumed per unit area (ha) (Table 5). The total CO_2 emissions related to lubricant oil consumptions were found to be 2.7 $kgCO_2$ per hectare (Fig.3). The 0.395 L lubricant oil was consumed for harvesting operation with harvester. Thus, the highest CO_2 (1.11 $kgCO_2$ per hectare) released for this harvesting operation due to highest oil consumption.

TABLE 5
The lubricant oil consumptions and CO_2 emissions for implements and machines

Tools and machines	Lubricant oil consumption		Fuel energy (MJ/ha)	CO_2 emission ($kgCO_2$/ha)
	L/ha	%		
Soil tillage and seed bed preparation	0.289	29.79	11.04	0.81
Sowing	0.082	8.45	3.13	0.23
Spraying	0.062	6.39	2.37	0.17
Hoeing	0.038	3.92	1.45	0.11
Fertilising	0.038	3.92	1.45	0.11
Harvesting	0.395	40.72	15.09	1.11
Soil preparation	0.062	6.39	2.37	0.17
Total	*0.97*	*100*	*36.90*	*2.70*

TABLE 6
The specific parameters for sugar beet cultivation

Yield (kg/ha)	Diesel + oil consumption (L/ha)	Energy (Diesel+oil) consumption (MJ/ha)	CO_2 emissions ($kgCO_2$/ha)	S_{FC} (L/t)	S_{SP} (kg/L)	S_{EC} (MJ/t)	S_{CO2} ($kgCO_2$/t)
56 852	107.97	4006.6	296.5	1.90	526.57	70.48	5.22

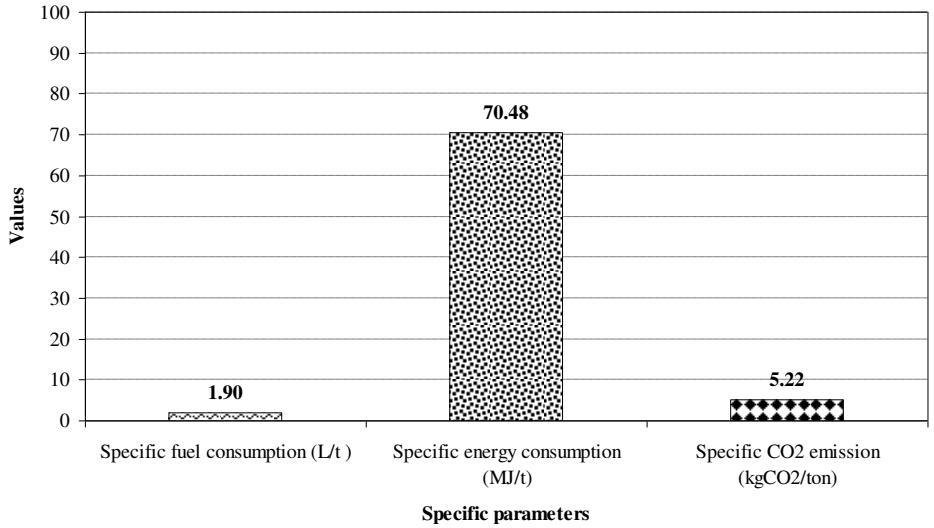

FIGURE 5
The specific parameters for sugar beet cultivation

Specific parameters for sugar beet cultivation. It was found that the total fuel (diesel+lubricant oil), energy consumptions and CO_2 emissions for sugar beet cultivation were 107.97 L/ha, 4006.6 MJ/ha and 296.5 $kgCO_2$/ha, respectively. The specific values of fuel consumption, tuber production and CO_2 emissions were calculated for sugar beet cultivation and given in Table 6 and Fig. 5. Isler [24] indicated that 700 kg of ethanol is produced from the molasses of sugar beet produced in one hectare production area. In this case, for 1 kg ethanol production 0.15 L fossil fuel or 5.72 MJ fossil fuel energy corresponding to this amount of fuel consumption is consumed. As a result, fossil fuel consumption for the production of 1 kg of ethanol from sugar beet molasses results in an emission of 0.42 $kgCO_2$.

The specific fuel consumption. The specific fuel consumption (L/t) defined as the ratio of the total amount fuel (L) consumed in the production process to the total amount of harvested product (t). The specific fuel consumption can be calculated based on dividing fuel consumption (L) by tuber yield (tone=1000 kg). The value of the specific fuel consumption indicates the amount of fuel consumed (L) to produce the unit quantity (t) of tuber product. The specific value of fuel consumption was 1.9 L per ton sugar beet tuber. The lower value of the specific fuel consumption means the energy efficiency of production is higher. Taking into account the values of specific fuel consumption, 1.9 L fossil fuel (diesel+lubricant oil) was consumed to produce 1 ton sugar beet tuber.

The specific tuber production. The average tuber yield was found to be 56 852 kg per hectare for sugar beet cultivation. The specific tuber production (kg/L), as the inverse of the specific fuel consumption value, was defined as the ratio of the total amount of harvested tuber product (kg) to the total amount of fuel (L) used in the cultivation process. The specific value of the tuber production indicates the total amount of harvested product (kg) from the unit production area (ha) corresponds to the unit amount of fuel (L) consumed for the unit production area (ha). The specific tuber production was 526.57 kg/L for sugar beet cultivation (Table 6). The higher value of the specific tuber production means the energy efficiency of production is higher. Considering the specific value of tuber production, 1 L fossil fuel (diesel+lubricant oil) was consumed to produce 526.57 kg sugar beet tuber.

The specific energy consumption. The specific energy consumption (S_{EC}) defined as the ratio of energy consumption (GJ/ha) to the total amount of obtained tuber per hectares (t/ha). The specific value of the energy consumption indicates the amount of energy consumed (L) to produce the unit quantity (t) of tuber product. It was found that the specific value of energy consumption related to total fossil fuel (diesel+lubricant oil) was to be 70.48 MJ per ton tuber (Fig. 5). The lower value of the specific fuel consumption means the energy efficiency of production is higher. Taking into account the specific value of energy consumption, 70.48 MJ fossil fuel energy (diesel+lubricant oil) was consumed to produce 1 ton sugar beet tuber.

The specific carbon dioxide emission. The specific carbon dioxide emission (S_{CO2}) was defined to analyze the relationship between CO_2 emissions and tuber yield. The S_{CO2} is the ratio of total CO_2 emissions to tuber yield and indicates CO_2 emissions ($kgCO_2$) per ton of sugar beet tuber. The specific value of CO_2 emission was calculated as 5.22 $kgCO_2$/t (Fig. 5). The lower value of the specific CO_2 emissions means cultivation system in terms of CO_2 emissions is efficient. Taking into account the specific value of CO_2 emission, 5.22 CO_2 was released to produce 1 ton sugar beet tuber.

CONCLUSIONS

The diesel and lubrication oil consumptions for CO_2 emissions were two of the most significant determinants of the total energy input for sugar beet cultivation. Especially field operations consuming more fuel should be applied based on scientific data to reduce fuel consumption. To reduce fuel consumption in soil tillage practices, unnecessary operations should be avoided in tillage. Consideration should be given to conservative and reduced tillage practices. The land size, production patterns and soil structure should be considered in the selection of agricultural mechanization tools. Agricultural machinery and equipments are required to be renewed at the end of a given study periods. Use of tractors completed economic life cause a lot of environmental pollution as well as economic losses. The precision farming techniques can be used utilized in all stages of plant production until tillage to harvest. For this purpose, decision support system is required. However, sensing, monitoring, control and data transfer systems are necessary for precision farming operations. Agricultural policies should emphasize development of new technologies and alternative energy resources aiming efficient use of energy. other relevant agencies for recommendations to farmers in order to use energy more efficiently.

REFERENCES

[1] Bauen, A.I., Woods, J., Haieles, R. (2004) Bioelectricity Vision: Achieving 15% of Electricity from Biomass in OECD Countries by 2020. Icept and E4tech, 2004.

[2] Abbas, A., Yang, M., Ahmad, R., Yousaf, K., Iqbal, T. (2017) Energy use efficiency in wheat production, a case study of Paunjab Pakistan. Fresen. Environ. Bull. 26, 6773–6779.

[3] Baran, M.F. (2017) Energy and economic analysis of vetch production in Turkey: A case study from thrace region. Fresen. Environ. Bull. 26, 1967–1973.

[4] Baran, M.F., Oguz, H.I., Gokdogan, O. (2017) Determination of energy input-output analysis in organic strawberry production. Fresen. Environ. Bull. 26, 2076–2081.

[5] Gokdogan, O., Erdogan, O., Eralp, O., Zeybek, A. (2016) Energy efficiency analysis of cotton production in Turkey: a case study from Aydin province. Fresen. Environ. Bull. 25, 4959-4964.

[6] Gokdogan, O., Kokten, K., Yilmaz, H.S., Baran, M.F. (2017) Energy usage efficiency of buckwheat production in Turkey. Fresen. Environ. Bull. 26, 2082–2088.

[7] Gunduz, O. (2016) Stochastic Energy (Technical) Efficiency and CO_2 emissions of dried apricot farms in Turkey. Fresen. Environ. Bull. 25, 3548–3556.

[8] Ignjatovic, D., Ignjatovic, N.C., Popovic, M.J. (2017) Potential for energy efficiency and CO_2 emission reduction by refurbishment of housing building stock built before 1919 in Serbia. Fresen. Environ. Bull. 26, 1201–1209.

[9] Kokten, K., Tutar, H., Baran, M.F., Gokdogan, O. (2017) Energy balance of bitter vetch and forage pea production in Turkey. Fresen. Environ. Bull. 26, 2035–2040.

[10] Ucar, K., Saner, G., Engindeniz, S. (2017) The comparative economic analysis of organic and conventional dried apricot production: a case study for Turkey. Fresen. Environ. Bull. 26, 4555–4560.

[11] Yildiz, T., Hazneci, K., Hazneci, E., Ozkaraman, F. (2016) The energy use efficiency determinants of peach production in Samsun province of Turkey. Fresen. Environ. Bull. 25, 4685–4693.

[12] Baran, M.F., Gokdogan, O. (2016) Comparison of energy use efficiency of different tillage methods on the secondary crop corn silage production. Fresen. Environ. Bull. 25, 3808-3814.

[13] Baran, M.F., Polat, R., Gokdogan, O. (2016) Comparison of energy use efficiency of different tillage methods on the secondary crop sunflower production. Fresen. Environ. Bull. 25, 4937-4943.

[14] Bayhan, Y., Celen, I.H., Onler, E. (2017) Determining the energy usage efficiency of different soil tillage methods and no-till method in aftercrop beans production. Fresen. Environ. Bull. 26, 6918–6923.

[15] Kayan, N., Kutlu, I., Ayter, N.G., Adak, M.S. (2017) Effects of different tillage, rotation systems and nitrogen levels on wheat yield in dry farming areas of Central Anatolia (Turkey). Fresen. Environ. Bull. 26, 6346–6355.

[16] Liu, Y.L., Li, Z.L., He, Y.F. (2015) Carbon dioxide and methane emissions from three wetland soils in a subtropical monsoon climate zone. Fresen. Environ. Bull. 24, 2879–2887.

[17] Marakoglu, T., Carman, K. (2015) Long-term effect of reduced tillage on CO_2 emission. Fresen. Environ. Bull. 24, 3220–3228.

[18] Marakoglu, T., Carman, K. (2017) A comparative study on energy efficiency of wheat production under different tillage practices in Middle Anatolia of Turkey. Fresen. Environ. Bull. 26, 3163–3169.

[19] Mujdeci, M., Simsek, S., Uygur, V. (2017) The effects of organic amendments on soil water retention characteristics under conventional tillage system. Fresen. Environ. Bull. 26, 4075-4081.

[20] Taner, A., Arisoy, R.Z., Kaya, Y., Gultekin, I., Partigoc, F. (2015) The effects of various tillage systems on grain yield, quality parameters and energy indices in winter wheat production under the rainfed conditions. Fresen. Environ. Bull. 24, 1463–1473.

[21] Wu, J., Wang, W., Wang, X., Zhu, L., Yang, H., Han, X., Gao, J., Guo, W., Bian, X. (2015) Residue management affects greenhouse gas emissions and soil organic carbon in wheat-rice rotation system. Fresen. Environ. Bull. 24, 2751–2762.

[22] WCED. (1987) World Commission on Environment and Development. Our common future (The Brundtland Report). Oxford University Press, Oxford.

[23] Seguin, B., Arrouays, D., Balesdent, J., Soussana, J.F., Bondeau, A. and Smith, P. (2007) Moderating the impact of agriculture on climate. Agr. Forest. Meteorol. 142(4), 278–287.

[24] Isler, A. (2012) Safflower Oil Ethyl Esther and Life Cycle Assessment. PhD Thesis. Istanbul Technical University Chemical Engineering Dept. Istanbul, Turkey. (In Turkish).

[25] Curran, M.A. (2006) Life cycle assessment: Principles and practice, EPA/600/R-06/060. Scientific Applications International Corporation (SAIC), National Risk Management Research Laboratory, US Environmental Protection Agency, Cincinnati, Ohio.
[26] Kendall, A., Chang, B. (2009) Estimating life cycle greenhouse gas emissions from corn-ethanol: A critical review of current U.S. practices. Journal of Cleaner Production. 17, 1175–1182.
[27] Luque, R., Campelo, J., Clark, J.H. (2011) Handbook of biofuels production: Processes and technologies. Woodhead Publishing, Oxford, Philadelphia.
[28] Ar, F.F. (2011) Bioethanol sector in the world, contribution of the economy to the sector and the situation in our country. Biomass Workshop and Exhibition, Bursa, Turkey,7-8 October, 2011.
[29] TURKSTAT. (2016) Turkish Statistic Foundation. Ankara, Turkey.
[30] Yamane, T. (1967) Elementary Sampling Theory. N.J., USA. Prentice Hall Englewood Cliffs.
[31] IPCC. (1996) The Intergovernmental Panel on Climate Change. Volume 2, Section 1.
[32] Ozturk, H.H. (2010) Energy Management in Plant Production. Hasad Publication. Istanbul, Turkey. (In Turkish).

Received: **21.01.2018**
Accepted: **03.01.2019**

CORRESPONDING AUTHOR

Cahit Gungor
Department of Agricultural Economics
Faculty of Agriculture
University of Cukurova
01330 Adana – Turkey

e-mail: gungorc@cu.edu.tr

© by PSP Volume 28 – No. 4/2019 pages 2407-2412 Fresenius Environmental Bulletin

INVESTIGATION OF THE EFFECTS OF *DIPLOTAENIA TURCICA* PLANT ROOT EXTRACT ON RAT OVER TISSUE BY HISTOLOGICAL AND STEREOLOGICAL METHODS

Nese Colcimen[1,*], Ugur Ozdek[2], Yeter Deger[3], Fikret Altindag[1], Okan Arihan[4]

[1]Van Yuzuncu Yil University, Faculty of Medicine, Department of Histology and Embryology, Van, Turkey
[2]Van Yuzuncu Yil University, Vocational School of Health Services, Van, Turkey
[3]Van Yuzuncu Yil University, Faculty of Veterinary Medicine, Department of Biochemistry, Van, Turkey
[4]Van Yuzuncu Yil University, Faculty of Medicine, Department of Physiology, Van, Turkey

ABSTRACT

Diplotaenia turcica is a plant species which is found in Bitlis-Van-Hakkari region and used in traditional treatments due to its medical and protective activities. Aim of this study is to investigate effects of root extract of *Diplotaenia turcica* plant on rat over tissue with histological and stereological methods. Four groups, with seven rats each, were used in experiments. Experimental groups were as follows; (I): control group, standard food and water was administered, *Diplotaenia turcica* plant root extract groups; (II): 250 mg/kg, (III): 550 mg/kg, (IV): 1000 mg/kg were administered as single dose/day with gastric gauge for 28 days. At the end of the experiments rats were decapitated and right over tissue was obtained. Histologically an increase in over medulla structure and an increase in corpus luteum and Graaf follicle number in cortex in plant administered groups were observed. Total volume comparison showed no difference between groups ($p>0.05$). When follicle numbers were evaluated *Diplotaenia turcica* administered groups showed a significant decrease in Primordial follicle number compared to control ($p<0.05$). No change in Primary follicle number ($p>0.05$) and an increase in Graaf follicle number ($p<0.05$) was observed. These results showed that *Diplotaenia turcica* increases follicular maturation by acting on this process.

KEYWORDS:
Diplotaenia turcica, Ovary, Rat, Stereology

INTRODUCTION

Plants were used in every era of history and by every society for protection of health or regaining it. About a quarter of current drugs are plant originated and deserved active molecules are replicated in laboratory conditions [1]. Search for new molecules from plants continues for many diseases such as epilepsy, cancer and also reproductive disorders. In this aspect plants constitute an important place in both modern medicine and traditional medical treatments. *Diplotaenia turcica* plant was known as *Diplotaenia cachrydifolia* until 2011 but it was declared as a new species in *Umbelliferae (Apiaceae)* family by Pimenov et al. after their work in Bitlis-Van-Hakkari region [2]. Importance of *Diplotaenia turcica* plant comes from its use in herby cheese which is traditional to this region and its use in traditional medicinal purposes. Plant is used as an antidote against bite of venomous animals such as snake and scorpion. In addition root parts of the plant is used for regulation of diabetes and high blood pressure as well as rheumatoid diseases [3,4]. In this study histological and stereological effects of different doses of *Diplotaenia turcica* plant on rat over tissue were investigated.

MATERIALS AND METHODS

Preparation of Plant Root Extract. *Diplotaenia turcica* plant was collected in May-June and taxonomical identification was completed. After collection of roots from their natural environment they were washed with distilled water and cut into small pieces. They were left to dry in a shade and dry ambient. Dried roots were powdered with a grinder. 100 grams of plant root powder were kept in 1000 ml ethyl alcohol (96% purity) for 24 hours and then filtered. Remaining solutes was kept in ethyl alcohol (70% purity) for 24 hours and again filtered. Then both of the filtrate were combined and dried in an evaporator at 70 rpm and 50 °C. Obtained remnant was kept in a water bath at 40 °C until dried totally [5].

Animal and Experimental Procedure. The study was approved by Van Yuzuncu Yil University Local Ethical Committee on Animal Experiments (Approval number: 2016/02). The study was performed on 28 healthy female Wistar albino rats (8 week-old, 200-250 gr of body weight) which were provided from Van Yuzuncu Yil University Experimental Medicine Research and Application Unit

FIGURE 1
General appearance and sizes of Rat Over tissue.

(Van, Turkey). Animals were adjusted to experimental conditions for one week before initiation of administrations. The animals were housed in standard laboratory conditions (22°C ±2 temperature, 40-60 % humidity and a 12 h light/dark cycle) in the cages. They were fed with a standard diet and tap water was provided *ad libitum*. Rats were divided into 4 experimental groups, including 7 rats in each group.

Group 1: Healthy control group, food and water were given *ad libitum* without any administration.

Group 2: 250 mg/kg *Diplotaenia turcica* plant root extract were administered as one dose/day with gastric gauge for 28 days.

Group 3: 550 mg/kg *Diplotaenia turcica* plant root extract were administered as one dose/day with gastric gauge for 28 days.

Group 4: 1000 mg/kg *Diplotaenia turcica* plant root extract were administered as one dose/day with gastric gauge for 28 days. Administration of plants was set to a dosage which does not cause lethality in animals (low, moderate, high) and administration period was to 28 to model normal human menstrual period.

After 28 days of administration, the rats were decapitated under anesthesia with ketamine (75 mg/kg), intraperitoneal (i.p). Abdominal cavity was exposed with a sharp surgical knife, right over tissues were obtained and kept in 10% formaldehyde solution.

Follicle Classification. Ovarian follicles contain a single immature oocyte. Histologically, in the ovarian sections, there were three major types of follicles: primordial, growing primary and mature Graaf [6]. Primordial follicles consist of an oocyte partially or completely encapsulated by squamous (i.e. flattened) pregranulosa cells. Primary Follicles are identified by a single layer of cuboidal granulosa cells around the oocyte [7]. Ultimately, Graaf follicles were the most enlarged follicles, and consisted of cumulus oophorus, corona radiata and a large antrum [6]. We have evaluated both of those 3 follicle groups.

Histological and Stereological Evaluations. Over tissues were fixed with 10% formaldehyde solution for 72 hours then they were embedded within paraffin. Sections of 5 μm thick were obtained and stained with Hematoxylin and Eosin (H&E). Investigations were performed under light microscope. For photographs AxioVision 3,1 Zeiss axioplan 2 imaging (Göttingen, Germany) were used. For determination from stereological analysis, modified method from Cavalieri principle was used (an unbiased counting frame used during the numerical analysis at x40 magnification) [8]. Then total tissue volume rates were calculated via pointed ruler provided in Shetereom 1.5 version software [9, 10]. Volume was estimated using the following formula:

Volume: t x a/p x ΣP

where t is section thickness, a/p is the area of each point on point-counting grid and ΣP is the total number of points hitting the related area [8].

Statistical Analysis. Descriptive statistics for the studied variables (characteristics) were presented as mean, standard deviation, minimum and maximum values. Kruskal-Wallis test was performed to compare groups. Dunn multiple comparison test was used to determine different groups. Statistical significance level was considered as 5% and SPSS (ver: 13) statistical program was used for all statistical computations.

RESULTS

Rat over sizes were measured as 0.5 mm x 2.5 mm x 2 mm (Figure 1). General histological structure of over tissue revealed normal histological appearance in control group. *Diplotaenia turcica* administered groups showed an increase in Graaf follicle and Corpus luteum and a decrease in medulla volume. However vasculogenesis in medulla was

much more augmented in group 2 compared to other groups (Figure 2). When groups are compared for total volume, no difference was observed between groups, whereas *Diplotaenia turcica* administered groups showed a significant decrease in medulla volume ($p<0.038$). In addition an increase in cortex volume was observed but this increase did not reach statistical significance ($p>0.160$) (Table 1). When groups are compared for follicle numbers Primordial follicle number were statistically decreased in *Diplotaenia turcica* administered groups compared to control ($p<0.044$). On the other hand Primary follicle numbers were not changed significantly ($p<0.076$) and Graaf follicle numbers were significantly increased ($p<0.012$) (Table 2).

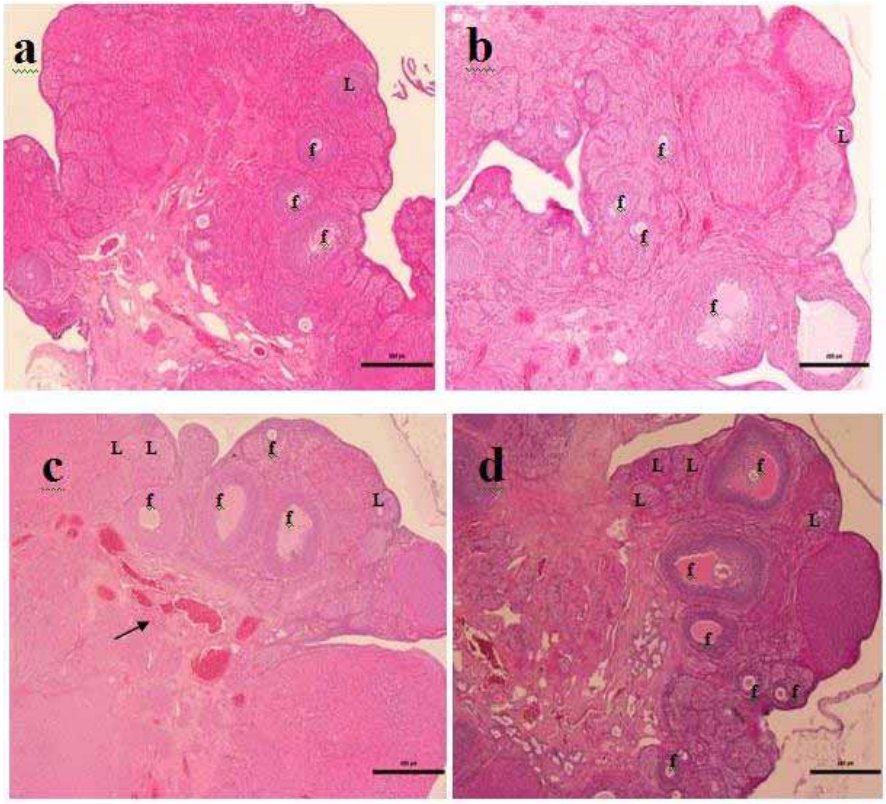

FIGURE 2
a-Over appearance of Control group b-Over appearance of 250 mg/kg *Diplotaenia turcica* administered group c-Over appearance of 550 mg/kg, *Diplotaenia turcica* administered group d-Over appearance of 1000 mg/kg *Diplotaenia turcica* administered group. Arrow, blood vessels (augmented vasculogenesis), f; follicle cells in different phases, L; corpus luteum. Scale bars, 600 µm (H&E).

TABLE 1
Descriptive statistics and comparison results for over volume rates of groups

	Group	Median	Mean	St. Dev.	Min.	Max.	P
T. volume (mm^3)	C	19234 a	18854	2440	14750	22644	.345
	G1	19355 a	19204	3052	16118	24549	
	G2	22731 a	21393	5290	11998	28375	
	G3	19909 a	19772	1190	17918	21016	
Cortex (mm^3)	C	15079 a	14977	1847	11859	17900	.160
	G1	16602 a	16297	2693	13451	20809	
	G2	19510 a	18209	5255	8811	25155	
	G3	17295 a	17118	1172	15321	18316	
Medulla (mm^3)	C	4536 a	3876	1151	2538	5090	**.038**
	G1	2875 b	2906	483	2285	3740	
	G2	3186 ab	3183	302	2736	3755	
	G3	2649 b	2663	131	2509	2856	

C.: Control G1: 250 mg/kg *Diplotaenia turcica* administered G2: 550 mg/kg, *Diplotaenia turcica* administered G3: 1000 mg/kg *Diplotaenia turcica* administered. The different letters (a,b) in the same column indicate differences between the groups ($p<0.05$).

TABLE 2
Descriptive statistics and comparison results for follicle number of groups

	Group	Median	Mean	St. Dev.	Min.	Max.	P
Primordial Fol.	C	18072324 a	16432292	4000816	10008327	21314736	**.044**
	G1	12455022 ab	11494368	4816654	5633099	16979892	
	G2	11144954 b	10684356	3860695	5234746	16782171	
	G3	6888992 b	9026792	5241337	4256317	17957743	
Primary Fol.	C	167285 a	181483	81132	67392	289513	.076
	G1	219695 a	182211	128112	0	373543	
	G2	197274 a	367559	390848	90643	1052104	
	G3	414876 a	471540	285272	85231	864765	
Graaf Fol.	C	77772 b	77399	7674	67392	85891	**.012**
	G1	85004 b	84654	7290	73231	93385	
	G2	197274 a	196495	104857	91651	314471	
	G3	140010 ab	170823	102420	82975	345506	

C.: Control G1: 250 mg/kg *Diplotaenia turcica* administrated G2: 550 mg/kg, *Diplotaenia turcica* administrated G3: 1000 mg/kg *Diplotaenia turcica* administrated. The different letters (a,b) in the same column indicate differences between the groups ($p<0.05$).

DISCUSSION

The incidence of reproductive disorders among women has increased significantly in recent years. Rate of woman between 15-49 years of age applied to clinics for treatment of infertility in United States increased from 9% in 1980 to 15% in 1995. Reason for this increase is thought to be related with factors such as increased labor age, augmented exposure to environmental toxins, nutritional disorders (increased obesity) and increase in sexually transmitted disease. According to Turkey Population and Health Survey, infertility incidence in woman between 15-49 years of age reached 12.2% in Turkey [11]. Infertility is becoming an important public health problem. Fertility rates which are obtained from 2016 population analyses showed that Eastern Anatolia birth rates are high and it is in high rank compared to other regions of Turkey [12]. In this context we aimed to study effect of *Diplotaenia turcica* plant which is an ingredient of widely consumed herby cheese in this region on fertility. Literature search on this subject yield no similar study in this aspect.

Diplotaenia turcica is a member of *Umbelliferae (Apiacea)* family. *Umbelliferae* is a family with some 464 genera according to the generic NOMenclator (GENOM) and are widely distributed across temperate regions, especially in central Asia. In Turkey *Umbelliferae* occupies second largest place in total plant list (450 species in 109 genera). This means that Asiatic Turkey has the highest concentration of species-level *Umbiliferae* diversity in Asia, and probably in the world. Experimental studies conducted on some of the plants belonging to this family reveal some important bioactivities such as antihyperglycemic, hypolipidemic and antioxidant activity [5, 13, 14, 15].

Study on the root extract of *Ligusticum chuanxiong* which is a traditionally used plant from *Umbelliferae (Apiacea)* family yield 2,2-difenil-1-picrylhydrazyl (DAPH) which has a potent antioxidant activity on hydroxyl and superoxide radicals [16]. Stems and roots of *Angelica shikokiana* which is also a member of *Umbelliferae (Apiacea)* family are used for the treatment of cardiovascular and digestive system as well as liver and hyperlipidemia disorders. It is also used as a herbal tea for prevention of anemia, hypertension, diabetes, neuralgia and dermatitis. Root, stem, leaf and seed extract of this plant has potent antioxidant phenolic content which avoids oxidative stress [17].

Diplotaenia turcica is known for its hypoglycemic and blood pressure balancing effects and protective feature against bites of venomous animals such as snake and scorpion. It is also used against diabetes and rheumatoid diseases.

Over total volume assessment showed that, total volume did not change between groups but medulla ratio in over tissue was decreased in *Diplotaenia turcica* administered groups. This finding indicates an increase in over cortex where follicle maturation and emission occurs.

In our study we evaluated primordial, primary and Graaf follicles. We found a decrease in Primordial follicle number whereas no change in primary follicle number and an increase in Graaf follicle number in over tissues of *Diplotaenia turcica* administered groups. Establishment of a primordial follicle pool is critical for female fertility because it represents the total population of oocytes available throughout the reproductive lifetime. Primordial follicle number is a marker of over reserve. On the other hand Graaf follicle number represents number of follicles that can be ovulated and fertilized.

When *Diplotaenia turcica* administered groups were evaluated, it is clear that number of primordial follicle numbers was decreased and Graaf follicle numbers were increased with increasing plant dosage. It is hypothesized that plant pos-

sessed possible estrogenic activity and stimulated gonadotropin release from hypophysis which cause initiation of steroidogenesis and folliculogenesis and therefore stimulated ovarian follicle growth. As a consequence primordial follicle number was decreased and Graaf follicle number was increased. These results indicate an increase in the speed of follicular maturation by the impact of *Diplotaenia turcica*. Another important aspect of this subject is the fact that, many female reproductive disorders derive from disruption of early oocyte development. There are ongoing search for new choices with less side effects for treatment of oocyte growth disorders.

Our results show that *Diplotaenia turcica* plant has an impact on over tissue. However since our study is the first study evaluating effect of plant on the reproductive system, action mechanisms on over tissue and follicle growth stages were not clarified in detail. Further studies on the subject are needed to clarify such mechanisms. Since this plant is an ingredient of herby cheese with different plants, effect of their combination should also be studied. Further research on this subject may both clarify the mechanism of action and also may bring new hope for infertility treatments.

ACKNOWLEDGEMENTS

We thank to Sıddık Keskin for his contribution in statistical analysis.

The authors declare no conflicts of interest.

REFERENCES

[1] Sarışen, O., Çalışkan, D. (2005) Phytotherapy. Attention to medication with plants. STED. 14(8), 182-187. (in Turkish).

[2] Pimenov, M., Kljuykov, E., Degtjareva, G. (2011) Survey of the genus Diplotaenia (Umbelliferae), with description of two new speciesfrom Turkey. BioOne. 41(1), 67-74.

[3] Uce, İ., Tunçtürk, M. (2014) Some wild plants naturally found and widely used in Hakkari. Biological Science Res. J. (Biyoloji Bilim Araş. Derg.) 7(2), 21-25. (in Turkish).

[4] Kaval, I., Behçet, L., Cakilcioglu, U. (2014) Ethnobotanical study on medicinal plants in geçitli and its surrounding (Hakkari-Turkey). J Ethnopharmacol. 155(1), 171-184.

[5] Farkhad, N.K., Farokhi, F., Tukmacki, A. and Band, K.S. (2012) Hydro-alcoholic extract of the root of Prangos ferulacea (L.) Lindl can improve serum glucose and lipids in alloxan-induced diabetic rats. AJP. 2, 179-18.

[6] Altunkaynak, B.Z., Akgül, N., Yahyazadeh, A., Altunkaynak, M.E., Turkmen, A.P., Akgül, H.M., Ünal, B. (2016) Effect of mercury vapor inhalation on tar ovary: Stereology and histopathology. J. Obstet. Gynaecol. Res. 42(4), 410-416.

[7] Rodriguez, H.A., Santambrosio, N., Santamaria, C.G., Munoz-de-Toro, M., Luque, E. (2010). Neonatal exposure to bisphenol A reduces the pool of primordial follicles in the rat ovary. Reproductive Toxicology. 30(4), 550-557.

[8] Gundersen, H.J., Jensen, E.B. (1987) The efficiency of systematic sampling in stereology and its prediction. J Microscopy. 1147, 229-263.

[9] Gundersen, H.J., Bendtsen, T.F., Korbo, L., Marcussen, N., Moller, A., Nielsen, K., Nyengaadr, J.R., Pakkenberg, B., Sorensen, F.B., Vesterby, A. (1988) Some new, simple, efficient stereological methods and their use in pathological research and diagnosis. Apmis. 96, 379-394.

[10] Howard, C.V., Reed, M.G. (1998) Unbiased stereology, three-dimensionel measurements in microscopy. BIOS Scientific Publishers, Oxford. 39-68.

[11] Topcu, H.O., Evliyaoğlu, O., Şahin, Y. (2017) How Basic Infertility Studies Should Be? TJRMS. 1(2), 109-111. (in Turkish).

[12] Turkish Statistics Institution (Türkiye İstatitik Kurumu (TÜİK)). Birth Statistics (Doğum istatistikleri) 2016. http://www.tuik.gov.tr/ Haber Bultenleri. No: 2467 (Access date: 18.05. 2017).

[13] Ahmet, J., Güvenç, A., Küçükboyacı, N., Baldemir, A., Coşkun, M. (2011) Total phenolic contents and antioxidant activities of Prangos Lindl. (Umbelliferae) species growing in Konya province (Turkey). Turk J Biol. 23, 353-360.

[14] Razavi, S.M., Nazemiyeh, H., Zarrini, G., Asna-Asharii, S., Dehghan, G. (2010) Chemical composition and antimicrobial activity of essential oil of Prangos ferulaceae (L.) Lindl from Iran. Nat Prod Res. 24(6), 530-533.

[15] Duran, A., Behçet, L., Öztürk, M. (2015) Diplotaenia bingolensis (Apiaceae), new species from east Anatolia, Turkey. Plant Syst Evol. 301, 467-478.

[16] Liu, J.L., Zheng, S.L., Fan, Q.J., Yuan, J.C., Yang, S.M., Kong, F.L. (2015) Optimisation of high-pressure ultrasonic-assisted extraction and antioxidant capacity of polysaccharides from the rhizome of Ligusticum chuanxiong. Int J Biol Macromol. 76, 80–85.

[17] Mira, A., Tanaka, A., Tateyama, Y., Kondo, R., Shimizu, K. (2013) Comparative biological study of roots, stems, leaves, and seeds of Angelica shikokiana Makino. J Ethnopharmacol. 148, 980–987.

Received: **29.01.2018**
Accepted: **15.02.2019**

CORRESPONDING AUTHOR

Nese Colcimen
Faculty of Medicine,
Department of Histology and Embryology,
Van Yuzuncu Yil University,
Van – Turkey

e-mail: colcimennese@hotmail.com

© by PSP Volume 28 – No. 4/2019 pages 2413-2420 Fresenius Environmental Bulletin

CHEMICAL COMPOSITION AND ANTIOXIDANT CAPACITIES OF MOSSES GATHERED FROM MOUNT IDA (CANAKKALE, TURKEY)

Ozlem Tonguc Yayintas[1,*], Dilek Ozyurt[2], Birsen Demirata[2], Yonca Karagul Yuceer[3], Selehattin Yilmaz[4]

[1]Canakkale Onsekiz Mart University, School of Applied Sciences, Department of Fisheries Technology, Canakkale, Turkey
[2]Istanbul Technical University, Faculty of Science and Letters, Department of Chemistry, Istanbul, Turkey
[3]Canakkale Onsekiz Mart University, Faculty of Engineering, Department of Food Engineering, Canakkale, Turkey
[4]Canakkale Onsekiz Mart University, Faculty of Sciences and Arts, Department of Analytical Chemistry, Canakkale, Turkey

ABSTRACT

Four species of bryophytes were used as material and were gathered from various areas in Mount Ida (Kazdag), Canakkale, Turkey. Volatile compounds were isolated from the moss species with solid phase microextraction (SPME). GC-MS was applied to determine volatiles. The antioxidant capacity of bryophytes was established using CERAC and CUPRAC techniques. Trolox equivalent (TEAC) of aqueous extract of bryophytes was determined at concentrations of 0.0109 (±0.0008)-0.0212 (±0.0009) mmol trolox/g bryophyte and 70% methyl alcohol extract 0.0259 (±0.0013)-0.0058 (±0.0012) mmol trolox/g bryophyte using the CERAC technique and for water extract as 0.0027 (±0.0006)-0.0083 (±0.0012) mmol trolox/g bryophyte and methanol extract 0.0035-0.0095 (±0.0005) mmol trolox/g bryophyte using the CUPRAC technique. The total flavonoid content was analyzed as equivalent mmol catechin/g bryophyte with the $AlCl_3/NaNO_2$ colorimetry technique. The total phenolic content of the species was analyzed with a Folin–Ciocalteu spectrophotometric technique.

KEYWORDS:
Mosses, antioxidant capacity, GC-MS, spectrophotometry, colorimetry

INTRODUCTION

Bryophytes belong to the phylum bryophyte and include three classes; Hepaticopsida (liverworts), Bryopsida (mosses), and Anthocerotea (hornworts). They are small, terrestrial photosynthetic, spore-bearing plants that require a humid environment and can be found all over the world. Bryophytes and liverworts are therapeutically used worldwide [1-3]. Mosses are considered a ***remarkable reservoir*** which offers exciting biologic activity [4]. Some recent results also forecast the valuable effect of bryophytes in AIDS therapy. Evaluating the biological activities of the mosses is a noteworthy contribution to the search for possible sources of medicines [5]. Oxidative stress is well-described as the extreme production of reactive oxygen species (ROS) and the efficiency of the antioxidant defense system [6]. Plants including edible plants and medicinal herbs contain a variety of antioxidants, such as phenolic compounds, nitrogen compounds, vitamins, and terpenoids [7]. *Fissidens* species of Bryophytes produce sugary inferior metabolites. Asakawa et al. [4] reported the properties of bryophytes; for example, their uses in areas of medicine, agriculture and pharmacy. German scientists used bryophytes to cure fungal infections in horses such as *Ceratodon purpureus* and *Bryum argenteum*. There are other medical uses of mosses due to their anti-leukemic properties and use as anticancer agents [8-10]. Indian people living in Kumaon in the Himalaya use some mosses to decrease pus formation [11-12]. Yayintas et al. [13] investigated chemical compounds, antimicrobial, antioxidant and anthocyanin capacities of Turkish mosses.

Phenol content and antioxidant activity of mosses from Yenice forest were determined [14]. The goal of the current study is to examine the antioxidant capacity and volatile components from four studied moss species.

MATERIALS AND METHODS

Chemicals, herbal samples, and instrumentation. Catechin, gallic acid, trolox (6-hydroxy-2,5,7,8-tetramethylchroman- 2-carboxylic acid, abbreviated as TR) and neocuproine were obtained from Sigma–Aldrich Co. (MO, USA). $Ce(SO_4)_2.4H_2O$, Folin-Ciocalteu phenol reagent, sodium carbonate (Na_2CO_3), sodium potassium tartrate ($NaKC_4H_4O_6$), copper(II) chloride dehydrate ($CuCl_2.2H_2O$), copper(II) sulphate ($CuSO_4$), sulphuric acid (H_2SO_4), ammonium acetate (CH_3COONH_4), ethanol (96% wight/weight) (C_2H_5OH), and methyl alcohol (CH_3OH) were obtained from Merck. Sodium nitrite ($NaNO_2$), aluminum chloride ($AlCl_3$), and sodium hydroxide (NaOH) were provided by Riedel. The reagent was

used as analytical reagent mark, and deionized water was used for all the prepared solutions. Polyphenolic substances were prepared daily in absolute 1 mmol L^{-1} C_2H_5OH and 0.040 g $Ce(SO_4)_2.4\ H_2O$ was placed in 100 mL flasks and dissolved with water. Then 17.0 mL of 98.0 % H_2SO_4 was added to the flask and diluted with water [15]. 250 mL 1.0×10^{-2} mol L^{-1} copper chloride stock solution in H_2O was used. 250 mL 7.5×10^{-3} mol L^{-1}ammonium acetate buffer in water (pH 7.0) was used. Neocuproine was prepared daily in 0.0390 g ethanol, and diluted to 25 mL with H_2O [16]. Folin−Ciocalteu's phenol reactive was diluted at 1:2 with distilled water before the experiments. Lowry A solution was prepared with Na_2CO_3 in 0.1 mol L^{-1} NaOH. Lowry B solution was prepared with Cu (II) sulfate in 1.0 % $NaKC_4H_4O_6$. Lowry C solution was prepared by mixing 50 mL of Lowry A and 1 mL of Lowry B [17]. 5% (w/v) $NaNO_3$ and 10% (w/v) NH_4Cl solution were prepared in deionized water. The UV-vis spectra were recorded using Varian model Cary 100 UV−vis spectrophotometry. Solutions were homogenized using a Heidolph Vortex Stirrer (Nuremberg, Germany), Bandelin Sonorex sonicator (Berlin, Germany) and, Biosan PSI-10i orbital shaker (Riga, Latvia).

Plant material. Moss samples were collected from Mount Ida (Kazdaglari), Canakkale in May 2016. Voucher specimens were identified by Dr. Ozlem TONGUC YAYINTAS and deposited in Canakkale Onsekiz Mart University, Vocational School of Applied Sciences, Turkey. We investigated the following species: *Plagiomnium undulatum* (Hedw.) T. Kop., T. 5047; T.5048; *Plagiothecium undulatum* (Hedw.) B.S.G, T. 5049; T.5050; *Neckera complanata* (Hedw.) Hub., T. 5051; T.5052; *Platyhpnidium alopecuroides* (Brid.). A.J.E. Sm., T. 5053; T.5054

Extraction of plant material. 1 g weighed dried moss was placed in a porcelain mortar. The dried plants were extracted with boiling deionized water and mixed in a shaker for 10 min at 450 rpm with sonication. The content was strained through Whatman filter paper and placed into a 50 mL flask. Then it was diluted with deionized H_2O. The aqueous extract of bryophytes was prepared just before measurements to hinder any undesired degradation reactions. 1 g of powdered bryophytes was obtained. These were extracted in flasks with 70 % (v/v) methyl alcohol. Three consecutive batch extractions were completed with the stirrer. Extraction initially was prepared with 20 mL 70% methyl alcohol for 60 min, then with 20 mL 70% methyl alcohol for 45 min, and finally by adding 10 mL 70% methyl alcohol for 15 min. These extracts were strained and placed together in single flasks and diluted by adding 50 mL 70% methyl alcohol at room temperature.

Extraction of volatile compounds by gas chromatography–mass spectrophotometry. Volatile compounds were isolated from moss species with the solid-phase-micro extraction (SPME) technique [18]and identified using GS-MS. 0.4 g of moss was placed in a 40-mL Amber-colored screw-top vial with a hole-cap poly tetrafluoro ethylene/silicon septum (Supelco, Bellefonte, USA), and 0.4 g of NaCl and 10 mL of distilled water were added to the vial. The vial was kept at 40 °C in a water bath for 20 min to equilibrate contents in the tap space. Then, an SPME (2 cm to 50/30 µm DVB/Carboxen/PDMS, Supelco, Bellefonte) needle was inserted into the vial. The SPME fiber was inserted to a depth of 2 cm in the top of the vial. Then, the SPME needle was immediately inserted into a GCMS column. Volatiles were tentatively identified by GC–MS. A Nonpolar HP5 Column (30 m × 0.25 mm i.d. × 0.25-µm film, J and W Scientific) and HP 6890 GC and 7895C mass detector were used for isolation of compounds. This was adjusted from 40 to 230 °C at 10 °C min^{-1} rate, with the initial time 5 and final time 20 min, respectively. Helium gas was selected as a mobilizer at a 1.2 mL·min^{-1} flow rate. The optimum conditions were selected as; capillary direct interface heat, 280 °C; ionization energy, 70 eV; mass range, 35 to 350 amu; and scan rate, 4.45 scans·s^{-1}. The recognition of flavor compounds was made using the comparison of the mass spectra of undetermined volatiles with the NIST Standard and TWRMS Data databases. Flavor substances were analyzed according to their comparative quantity.

CERAC spectrophotometric assay of total antioxidant capacity. 1 mL of 2.0 x 10^{-3} mol L^{-1} Ce(IV) solution and x mL of the bryophyte extract were placed into a tube and diluted with 10 mL H_2O. The mix was allowed to stand for 30 min at room temperature and the absorbance at 320-nm (A_{320} nm) was observed. The antioxidant activity was analyzed and given as mmol trolox equivalent mass of moss [15]. Trolox in the CERAC technique is $\varepsilon = 1.31\times10^4$ L mol^{-1} cm^{-1}. These results are given as mean (±SD) mmol Trolox per gram bryophytes.

CUPRAC spectrophotometric assay of total antioxidant capacity. 1 mL 1.0×10^{-2} mol L^{-1} $CuCl_2$, 1 mL 7.5×10^{-3} mol L^{-1} neocuproine alcoholic solution and 1 mL NH_4Ac buffer solution were placed in a tube and mixed; (x) mL of bryophyte extract followed by (1.1−x) mL of water were added until the total volume was equal to 4.1 mL, and mixed. The absorbance was read against a reactive blank at 450 nm after 30 min [16]. Molar absorption coefficient of Trolox in the CUPRAC technique is $\varepsilon = 1.62\times10^4$ L mol^{-1} cm^{-1}. The results are given as mean (±SD) mmol Trolox per gram dry bryophytes.

$AlCl_3$/ $NaNO_2$ Colorimetric assay of total flavonoid content. Flavonoid compounds were measured with a previously described colorimetric technique [19, 20]. 1.0 mL of the extract or catechin solution was mixed with 2.40 mL of deionized water in a test tube and then 0.20 mL of a 5% (w/v) sodium nitrite solution was added. After 5 min, 0.40 mL of a 10% NH_4Cl solution was added and the mixture was allowed to stand for 20 min before 1.0 mL of 1 M NaOH was added. The absorbance was read at 510 nm with a spectrophotometer. The molar absorption coefficient of catechin for $AlCl_3$/ $NaNO_2$ colorimetric technique is $\varepsilon = 1.14\times10^4$ L mol^{-1} cm^{-1}. The results are given as mean (±SD) mmol catechin per gram dry bryophytes.

Folin-Ciocalteu assay of total phenolic content. Mosses were measured using a spectrophotometric technique for components of phenolic compound with a *Folin–Ciocalteu* spectrophotometric technique [17]. 1.5 mL of deionized water and 0.5 mL of the extract were placed into a tube, then 2.5 mL of Lowry C solution was added, and the mixture was allowed to stand for 10 min. Finally, 0.25 mL of Folin reactive was added, and this was left for 30 min for stability of the observed blue color. The molar absorption coefficient of gallic acid in the *Folin–Ciocalteu* method is $\varepsilon = 5.14\times10^3$ L mol^{-1} cm^{-1}.

Statistical analysis. All the analyses were carried out in triplicate and the results were expressed as mean ± standard deviation (SD). Significant differences between means were calculated by analysis of variance (ANOVA) procedures and correlation test was conducted to determine the correlations among means; $p < 0.05$ was regarded as significant. Statistical analysis was performed using Microsoft office 2010 Excel program.

RESULTS AND DISCUSSION

GC-MS identification of water extracts. The higher abundance values obtained from GC-MS of the water extract samples from four species of mosses are given in Table 1. Gas chromatograms with mass-spectrometric detection of the moss species are given in Figures 1-4.

Optimization of methanol extraction. In our study, we prepared methanol extracts from *Plagiomnium undulatum* using variables of methanol percentages between 30% (v/v, methanol-water) and 100 % (v/v, methanol), and investigated how this affected total antioxidant capacity (TAC) of *Plagiomnium undulatum.* Methanol percentages of 70%(v/v) were obtained as optimum recovery of TAC in this species. Optimization of the percentage of methanol extraction from dry bryophytes as a function of the antioxidant activity is given in Figure 5.

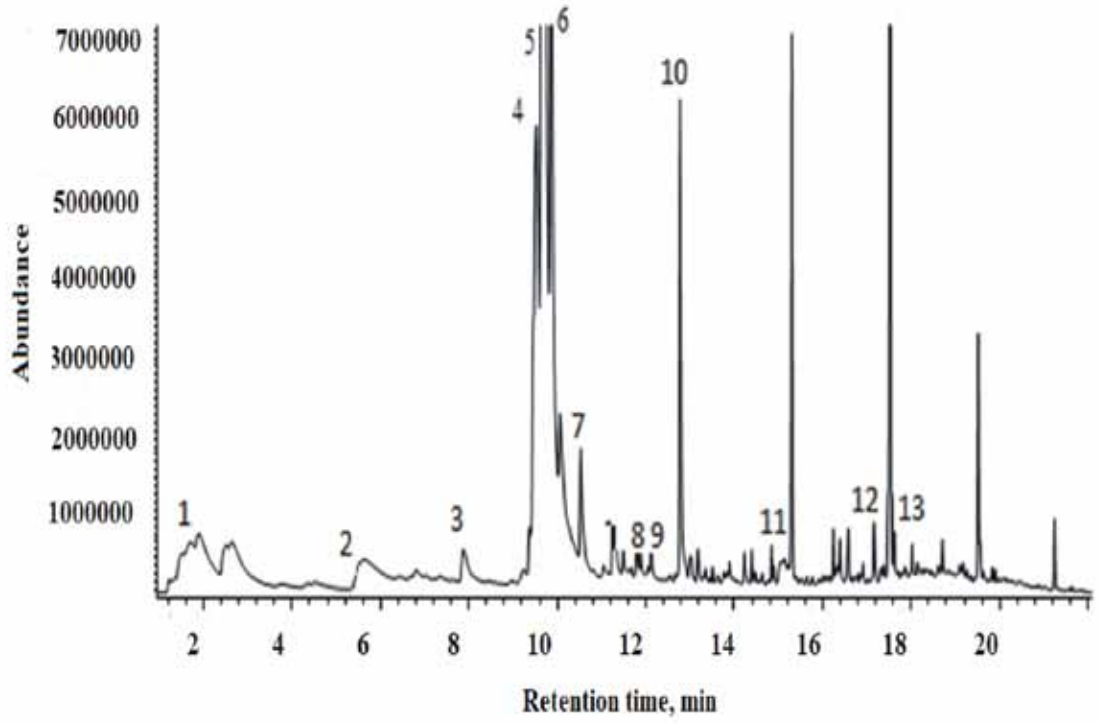

FIGURE 1
Gas chromatogram with mass-spectrometric detection of *Plagiomnium undulatum;*
Numbers refer to the compounds listed in Table 1.

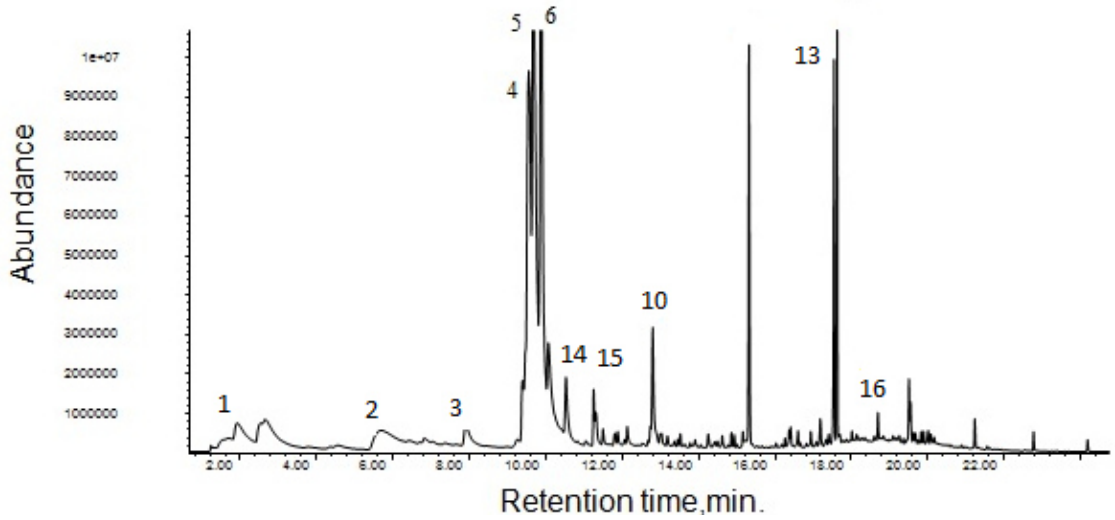

FIGURE 2

Gas chromatogram with mass-spectrometric detection of *Plagiothecium undulatum*;
Numbers refer to the compounds listed in Table 1.

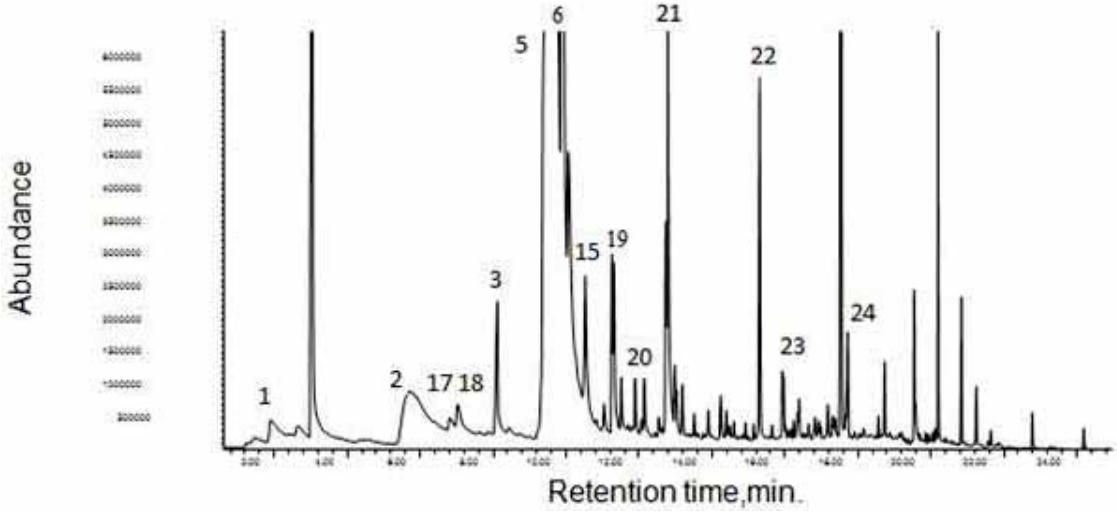

FIGURE 3

Gas chromatogram with mass-spectrometric detection of *Neckera complanata*;
Numbers refer to the compounds listed in Table 1.

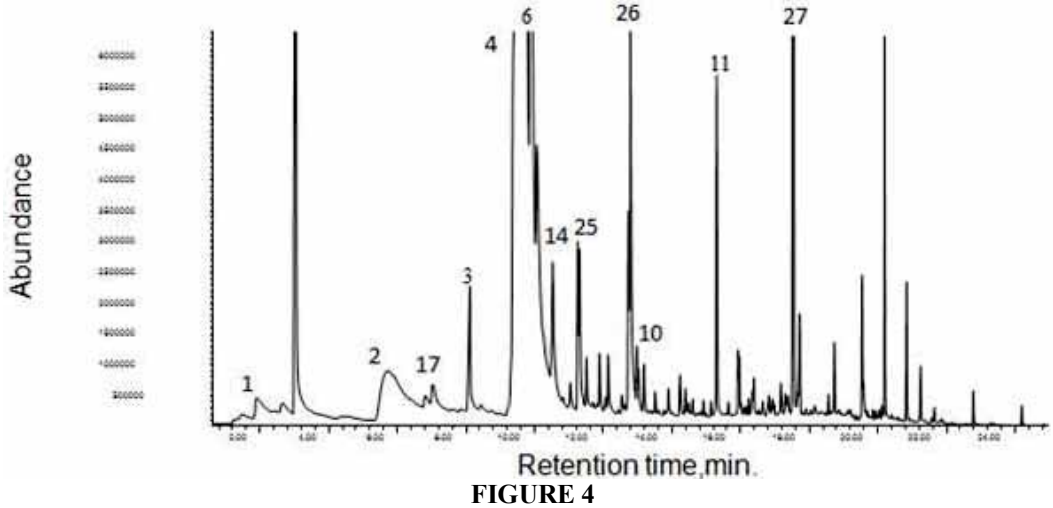

FIGURE 4

Gas chromatogram with mass-spectrometric detection of *Platyhpnidium alopecuroides*;
Numbers refer to the compounds listed in Table 1.

TABLE 1
GC-MS analysis of *Plagiomnium undulatum, Plagiothecium undulatum, Neckera complanata,* and *Platyhpnidium alopecuroides* (water extracts) component.

	Compound number	Retention Time (min)	Identified Substance	Volatiles	Area
Plagiomnium undulatum	1	1.90	chloroform	plant volatile	$1.23x10^8$
	2	5.61	Hexamethyl cyclotrisiloxane	polymeric, oil	$8.91x10^7$
	3	7.87	oxime methoxy phenyl	fungicides	$4.40x10^7$
	4	9.69	3-octanone	flavor and fragrance	$1.49x10^9$
	5	9.86	3 octanol	flavor and fragrance	$3.87x10^8$
	6	10.05	octamethyl cyclotetrasiloxane	organosilicon	$2.28x10^8$
	7	11.66	2 nonanone	fruity odor	$5.06x10^6$
	8	12.05	3 hydroxymandelic, ethyl ester, di TMS	flavor	$6.10x10^6$
	9	12.12	4 hydroxymandelic, ethyl ester, di TMS	flavor	$1.74x10^7$
	10	13.18	naphthalene	ınsecticide – repellent/fumigant	$1.25x10^7$
	11	15.94	butanoic acid butyl ester	sweet fruity flavors	$1.83x10^6$
	12	16.93	geranyl acetone	fruit flavor agent	$5.30x10^6$
	13	17.80	lauric acid methyl ester	fatty, floral, oily, winey odor	$2.69x10^6$
Plagiothecium undulatum	1	1.92	chloroform	plant volatile	$1.32x10^8$
	2	5.69	hexamethyl cyclotrisiloxane	polymeric, oil	$1.38x10^8$
	3	7.89	oxime methoxy phenyl	odor	$5.59x10^7$
	4	9.68	3-octanone	flavor and fragrance	$1.29\ x10^9$
	5	9.87	3 octanol	flavor and fragrance	$6.17x10^8$
	6	10.05	octamethyl cyclotetrasiloxane	organosilicon	$2.92x10^8$
	14	10.52	2-ethyl 1 hexanol	flavor and fragrance	$1.17x10^8$
	15	11.02	E 2 octenal	flavor and fragrance	$2.883x10^5$
	10	13.18	naphtalene	ınsecticide – repellent/fumigant	$1.05x10^7$
	13	17.81	lauric acid methyl ester	fatty, floral, oily, winey odor	$5.64x10^6$
	16	18.71	hexadecane	diesel fuel	$2.03x10^7$
Neckera complanata	1	1.93	chloroform	plant volatile	$4.94x10^7$
	2	5.71	hexamethyl cyclotrisiloxane	polymeric, oil	$2.25x10^8$
	17	6.81	1-hexanol	odor of freshly mown grass	$1.54x10^7$
	18	7.02	1,3,5 octatriene	volatile compounds in food and beverages	$3.74x10^7$
	3	8.12	oxime methoxy phenyl	odor	$8.91x10^7$
	5	9.94	3 octanol	flavor and fragrance	$1.13x10^9$
	6	10.06	octamethyl cyclotetrasiloxane	organosilicon	$4.8\ x10^8$
	15	11.03	E 2 octenal	flavor and fragrance	$2.97x10^7$
	19	11.30	1,3 cyclooctadiene	Toxic, volatile compounds, flammable liquids	$8.96x10^7$
	20	12.13	pristane	Odor, flavor	$3.56x10^7$
	21	12.71	cis 6 nonenol	flavor and fragrance	$7.59x10^7$
	22	15.94	cyclosativene	floral compound	$1.94x10^7$
	23	16.12	alpha cedrene	flavor and fragrance	$2.96x10^6$
	24	17.90	1S cis calamenene	essential oil	$5.04x10^6$
Platyhpnidium alopecuroides	1	1.92	chloroform	Plant volatile	$5.31x10^7$
	2	5.65	hexamethyl cyclotrisiloxane	Polymeric, oil	$1.14x10^8$
	17	6.83	1-hexanol	odor of freshly mown grass	$1.34x10^7$
	3	7.88	oxime methoxy phenyl	odor	$4.35x10^7$
	4	9.65	3-octanone	flavor and fragrance	$3.67x10^8$
	6	10.06	octamethyl cyclotetrasiloxane	organosilicon	$1.48x10^8$
	14	10.52	2 ethylhexanol	flavor and fragrance	$7.40x10^7$
	25	11.25	E 2 octen 1 ol	flavor and fragrance	$4.30x10^6$
	26	13.03	menthol	flavor and fragrance, peppermint oil	$2.58x10^7$
	10	13.17	naphtaline	insecticide – repellent/fumigant	$1.11x10^7$
	11	15.94	butanoic acid butyl ester	sweet fruity flavors	$5.87x10^6$
	27	17.40	beta ionone	volatile oil, fragrance	$1.43x10^7$

Determination of total antioxidant capacity. The analysis was completed 3 times in parallel repetition and the results are calculated as mmol TR/g dry bryophytes and given in Tables 2 and 3. As can be seen from Table 2, the highest amount of antioxidant capacity was found as 0.0212 ±0.0009 and 0.0083 ±0.0012 mmol Trolox/g dry bryophytes for *Plagiomnium undulatum* and the lowest antioxidant capacity was 0.0109 ±0.0008 and 0.0027 ±0.0006 mmol trolox/g dry bryophytes from *Platyhypnidium alopecuroides* after aqueous infusion by CERAC and CUPRAC methods respectively.

Determination of total phenolic content. The analysis was completed 3 times in parallel repetition and the results are given in Table 4. As can be seen from Table 4, the highest phenolic content was obtained as 0.0275 ±0.0011 and 0.0257 ±0.0013 mmol

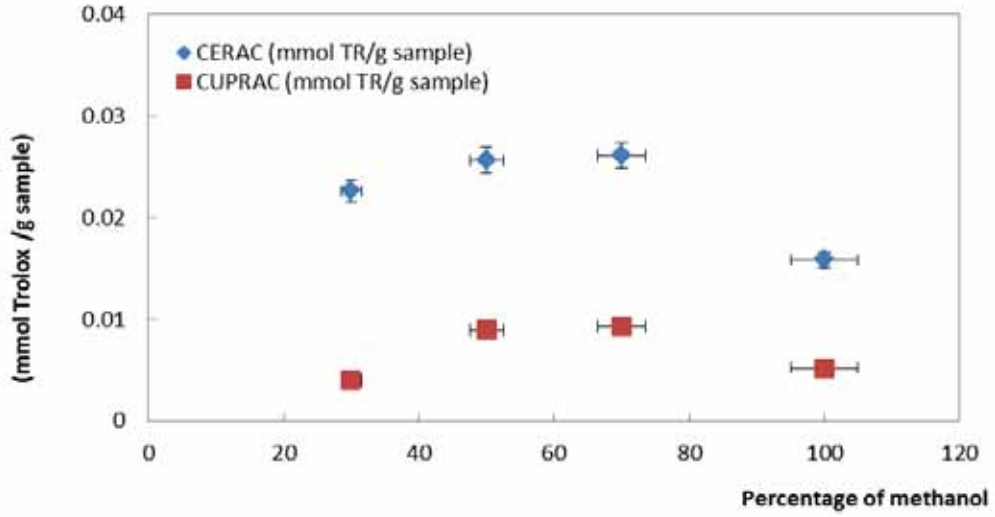

FIGURE 5
Optimization of percentage of methanol extraction of dry bryophytes as a function of to the total antioxidant capacity

TABLE 2
Total antioxidant capacity of aqueous infusion of mosses

Sample	CERAC (mmol trolox/g bryophytes)	CUPRAC (mmol trolox/g bryophytes)
Plagiomnium undulatum	0.0212 ±0.0009	0.0083 ±0.0012
Plagiothecium undulatum	0.0165 ±0.0011	0.0042 ±0.0016
Neckera complanata	0.0122 ±0.0006	0.0038 ±0.0007
Platyhpnidium alopecuroides	0.0109 ±0.0008	0.0027 ±0.0006

TABLE 3
Total antioxidant capacity of 70% (v/v) methanol extraction of mosses

Sample	CERAC (mmol trolox/g bryophytes)	CUPRAC (mmol trolox/g bryophytes)
Plagiomnium undulatum	0.0259 ±0.0013	0.0095 ±0.0005
Plagiothecium undulatum	0.0195 ±0.0008	0.0060 ±0.0011
Neckera complanata	0.0094 ±0.0014	0.0041 ±0.0007
Platyhpnidium alopecuroides	0.0058 ±0.0012	0.0035 ±0.0005

TABLE 4
Total phenolic content of mosses in aqueous infusion and 70% (v/v) methanol extracts.

Sample	Folin- Ciocalteu (mmol gallic acid / g bryophytes)	
	Aqueous infusion	70 % methanol extracts
Plagiomnium undulatum	0.0275 ±0.0011	0.0257 ±0.0013
Plagiothecium undulatum	0.0244 ±0.0014	0.0181 ±0.0005
Neckera complanata	0.0160 ±0.0009	0.0080 ±0.0011
Platyhpnidium alopecuroides	0.0139 ±0.0012	0.0076 ±0.0007

TABLE 5
Total flavonoid content of mosses from aqueous infusion and 70% (v/v) methanol extracts.

Sample	$AlCl_3$/ $NaNO_2$ colorimetric (mmol catechin / g bryophytes)	
	aqueous infusion	70% methanol extracts
Plagiomnium undulatum	0.0034 ±0.0009	0.0020 ±0.0003
Plagiothecium undulatum	0.0027 ±0.0006	0.0017 ±0.0008
Neckera complanata	0.0016 ±0.0005	0.0012 ±0.0006
Platyhpnidium alopecuroides	0.0011 ±0.0003	0.0005 ±0.0004

gallic acid/g bryophytes from *Plagiomnium undulatum* and the lowest phenolic content was 0.0139 ±0.0012 and 0.0076 ±0.0007 mmol gallic acid/g dry bryophytes from *Platyhypnidium alopecuroides* in aqueous infusion and methanol extracts respectively using the Folin-Ciocalteu method.

Determination of total flavonoid content. All analyses were repeated in parallel three times and the results are given in Table 5. As can be seen from Table 5, the highest antioxidant capacity was found as 0.0034 ±0.0009 and 0.0020 ±0.0003 mmol catechin/g bryophytes from *Plagiomnium undulatum* and the lowest capacity was 0.0011±0.0003 and 0.0005 ±0.0004 mmol catechin /g bryophytes from *Platyhypnidium alopecuroides* in aqueous infusion and methanol extracts respectively using the $AlCl_3/NaNO_2$ colorimetric method.

CONCLUSIONS

The importance of mosses has been continuously upgrading because of its effects on microbes are studied but little knowledge exists about secondary metabolites with antioxidant properties of mentioned mosses. These experimental results are proof that *Plagiomnium undulatum* (Hedw.) T.Kop, *Plagiothecium undulatum* (Hedw.) B.S.G, *Neckera complanata* (Hedw.) Hub., and *Platyhpnidium alopecuroides* (Brid.) extracts possess potent antioxidant activity.

All samples showed reducing capacity by CERAC and CUPRAC methods, with the highest performance obtained in *Plagiomnium undulatum* samples. It was observed good correlation between the infusion and methanol extractions results of total antioxidant capacity in the CERAC and CUPRAC methods. This significant proportion of antioxidant activity is caused by phenolic substances within the structure of the mosses as estimated from the GC-MS analysis. According to the study, natural antioxidant compounds should be identified and purified in a more thorough manner on the mosses. These compounds can be used in the pharmaceutical, cosmetic and food industries. Thus new and more effective compounds that enhance cellular defense can be obtained. Total phenolic content shows good positive correlations with total flavonoid content of all samples.

The infusion and methanol extraction of *Plagiomnium undulatum* is indicative of higher phenol content. The reported characteristics give an enhanced functional food property to mosses and contribute to the development of the regional economy, providing an alternative to family income increase.

It is believed that the added value of the project will be creative, natural, innovative and potential to be applied to the industry and especially to the health field. To conclude, here it was demonstrated that the extracts of the investigated mosses have great potential for use in medicine, cosmetics and pharmaceutical applications, as well as for food and agricultural uses.

REFERENCES

[1] Friederich, S., Maier, U.H. and Deus-Neumann, B. (1999) Biosynthesis of cyclic bis(bibenzyls) in *Marchantia polymorpha*. Phytochemistry. 50, 589-598.

[2] Saroya, A.S. (2011) Herbalism, Phytoche-mistry, and Ethnopharmacology. Science Publishers. Punjab, 286-293.

[3] Gokbulut, A., Satılmış. B., Batcıoğlu, K., Cetin, B. and Şarer, E. (2012) Antioxidant activity and luteolin content of *Marchantia polymorpha* L. Turk J. Biol. 36, 381-385.

[4] Asakawa, Y., Ludwiczuk, A. and Nagashima, F. (2013) Phytochemical and biological studies of bryophytes. Phytochemistry. 91, 52–80.

[5] Magtoto, L.M., Alonzo, E.A.M., Lacerna, M.Z.T. and Santiago, J.C. (2016) Total phenol content and antioxidant activity of *Bryum billardieri* Schwaegr. International Journal of Current Pharmaceutical Review and Research. 7, 19-20.

[6] Palma, A., Montoya Mercedes. R., Arteaga Jesús, F. and Rodríguez Mellado Jose, M. (2014) Determination of antioxidant activity of spices and their active principles by differential pulse voltammetry. J. Agric. Food Chem. 62, 582−589.

[7] Lim, C.K., Tiong, W.N. and Loo, J.L. (2014) Antioxidant activity and total phenolic content of different varieties of *Portulaca grandiflora*. International Journal of Phytopharmacy Research Article. 4, 1-5.

[8] Frahm, J.P. (2004) Recent developments of commercial products from bryophytes. Bryologist. 107, 277-283.

[9] Glime, J.M. (2013) Volume 1. Physiological Ecology. E-book sponsored by Michigan Technological University Bryophyte Ecology. Chapter 2.

[10] Dhondiyal, P.B., Pande, N. and Bargali, K. (2013) Antibiotic potential of *Lunularia cruciata* (L.) Dum ex. Lindb (Bryophyta) of Kumaon Himalaya. African Journal of Microbiology Research. 7, 4350-4354.

[11] Pant, G., Tewari, S.D. (1989) Various human uses of bryophytes in the Kumaon region of north-west Himalaya. Bryologist. 92, 120-122.

[12] Kumar, K., Singh, K.K., Asthana, A. and Nath, V. (2000) Ethno therapeutics of bryophyte *Plagiochasma appendiculatum* among the Gaddi tribes of Kangra valley Himachal Pradesh. Pharm. Biol. 38, 353-356.

[13] Yayintas Tonguc, O., Alpaslan, D., Karagul Yuceer, Y., Yilmaz, S. and Sahiner, N. (2017) Chemical composition, antimicrobial, antioxidant and anthocyanin activities of mosses (*Cinclidotus fontinaloides* (Hedw.) P. Beauv. and *Palustriella commutata* (Hedw.) Ochyra) gathered from Turkey. Natural Product Research. 31, 2169–2173.

[14] Aslanbaba, B., Yilmaz, S., Yayintas Tonguc, Ö., Özyurt, D. and Demirata, B. (2017) Total phenol content and antioxidant activity of mosses from Yenice forest (Ida Mountain). Journal of Scientific Perspectives. 1, 1-12.

[15] Ozyurt, D., Demirata, B. and Apak, R. (2007) Determination of total antioxidant capacity by a new spectrophotometric method based on Ce (IV) reducing capacity measurement. Talanta. 71, 1155–1165.

[16] Apak, R., Güçlü, K., Özyürek, M. and Karademir, S.E. (2004) A novel total antioxidant capacity index for dietary polyphenols, vitamins C and E, using their cupric ion reducing capability in the presence of neocuproine: CUPRAC method. J Agric Food Chem. 52, 7970–7981.

[17] Singleton, V.L., Orthofer, R. and Lamuela-Raventos, R.M. (1999) Analysis of total phenols and other oxidation substrates and antioxidants by means of folin-ciocalteu reagent. Methods Enzymol. 299, 152−178.

[18] Pawliszyn, J. (2012) Theory of solid phase microextraction. In: Pawliszyn, J. (Ed.), Handbook of Solid Phase Micro-extraction, Theory and Practice Elsevier Inc, MA, USA, Waltham. 13-59.

[19] Dewanto, V., Wu, X., Adom, K.K. and Liu, R.H. (2002) Thermal processing enhances the nutritional value of tomatoes by increasing total antioxidant activity. Journal of Agricultural and Food Chemistry. 50, 3010–3014.

[20] Sakanaka, S., Tachibana, Y. and Okada, Y. (2005) Preparation and antioxidant properties of extracts of Japanese persimmon leaf tea (kakinoha-cha). Food Chemistry. 89, 569–575.

Received: **08.03.2018**
Accepted: **22.02.2019**

CORRESPONDING AUTHOR

Ozlem Tonguc Yayintas
Canakkale Onsekiz Mart University,
School of Applied Sciences,
Department of Fisheries Technology,
Canakkale – Turkey

e-mail: ozlemyayintas@hotmail.com

© by PSP Volume 28 – No. 4/2019 pages 2421-2425 Fresenius Environmental Bulletin

THE DETERMINATION OF CHANGES IN MONTHLY MINERAL CONTENTS OF THORNY SALTWORT (*NOAEA MUCRONATA SUBSP. MUCRONATA*)

Suleyman Temel*

Igdir University, Faculty of Agriculture, Department of Field Crops, 76000 Igdir, Turkey

ABSTRACT

Determining the changes in mineral content of *Noaea mucronata* plant is significantly important due to the facts that the plant grows in extremely arid and saline areas and appreciably consumed by the grazing sheep. This study was conducted to analyse the mineral content for 7 months during the growing period of *Noaea mucronata* from April to October in 2015 at 3 (three) replication according to the randomized complete block design. *Noaea mucronata* plant grows naturally at the wind erosion sites located in Aralik district, Igdir, in Turkey. P (phosphorus), K (potassium), the contents of Ca (calcium), Mg (magnesium), Na (sodium), Cu (copper), Fe (iron), Zn (zinc) and Mn (manganese) were analysed for approximately 3-5 cm of the stem ends (shoot + leaf) of 5 plants in each of 3 blocks, provided 15 plants in total. We observed a significant change in the mineral content of *Noaea mucronata subsp. mucronata* during the natural growth period. Fe content was the highest element in the summer (July, August and September), Mn content was the highest element in the autumn (September), Mg content was the highest in the spring and autumn (April, August and September), and Cu content was the highest in the spring, summer and autumn (April, July and October) in comparison to the other periods. According to the average of seven months, the contents of P, K, Ca, Mg, Na, Cu, Fe, Zn and Mn were 0.49%, 1.04%, 2.50%, 0.47%, 0.15%, 2.00 ppm, 211.95 ppm, 36.60 ppm and 39.90 ppm, respectively. Research results revealed that the contents of P, K, Ca, Na and Zn were high during the spring period (April, May and June).

KEYWORDS:
Noaea mucronata, macro and micro mineral content, growth stage

INTRODUCTION

Minerals are important structural and nutritional elements for animal tissues and organs, and also play roles in the body homeostasis, balancing the osmotic pressure and acid-base equilibrium. Furthermore, they take part in many metabolic actions together with some other enzymes, vitamins and hormones Minerals are essential matters in animal production and the animal requirements of some important minerals must be met by the addition of mineral feed stuffs and premixtures [1]. The number of these essential minerals was determined to be around 24 macro and micro minerals to maintain the animal productivity and health [2-3].

The mineral requirements of plants can be obtained from the soil. The amount of mineral elements in plants is greatly influenced by the species and varieties of plants, plant development stages, soil structure and environmental factors. Therefore, a good quality of roughage is critical in farm animal nutrition since they are a good source ofnot only proteins and carbohydrates, but also a good source of minerals [4].

Some plants used as roughage have a high level of resistance to extreme climatic and soil conditions, and they grow easily in the areas where several cultivated plants cannot. In terms of nutrient content, they can provide sufficient amount of minerals and vitamins for the grazing [5, 6, 7, 8, 9, 10].

Despite the fact that a low feed value of *Noaea mucronata* was reported by previous studies, the grazing sheep preferably consumed the vegetative parts of *Noaea mucronata* in the areas where it is dormant and other plant species are not prevalent [11, 12]. It has been reported that the sheep and goat prefer shoots and leaf of *Noaea mucronata* [12, 13], and it can ideally be an alternative forage in extremely arid and saline for the grazing animals.

In this study, we examined, by the development periods, the macro and micro nutrient contents of the species of *Noaea mucronata*, which may grow in saline and sandy areas that have extreme climatic and soil conditions.

MATERIALS AND METHODS

The research area was located in the eastern Turkey, Aralik district, Igdir province. The region has hot and dry summer and cold winter, which is quite different from the remaining of Eastern Anatolia Region. The study area is known as the second largest erosion area in Turkey (13.542 ha), and has

an average annual precipitation of 256.0 mm, a relative humidity in the ratio of 51.6% and an average temperature of 12.4^0 C [14] (Anonymous, 2015). Soils at the study site have loamy structures which are indicate low ratios of lime (0.41%), organic materials (0.45%) and phosphor (1.52 ppm) [7].

By imitating grazing habits of animals, an approximately 3-5 cm of shoot + leaf part was obtained from the stems end parts of plants for 7 months from the beginning of late April until the end of October, and used to determine the mineral contents of plant samples. The research was established in a protected area, and it was conducted in a completely randomized block design with three replicates. Each block contained 5 randomized *Noaea mucronata* plants, and 15 plants were available in 3 blocks in total. Approximately, 1.5 kg sample materials were collected manually (from 5 plants) for each replication in total, and they were placed into the paper bags. The samples, which were collected from the land, were dried in open air at first, and then, using a drying oven, the temperature set 70^o C until their weights were stabilized. The dried samples were ground through a laboratory mill using a sieve diameter of 1 mm.

The ground plant samples were placed into the microwave wet decomposition unit resistant to 40 bars (speedwave MWS-2 Berghof productts+ Instruments Harresstr.1. 72800 Enien Gernmany) in 3 different steps (1st Step: 5 minutes by using 75% of microwave power under 145 ^{o}C, 2nd Step: 10 minutes by using 90% of microwave power under 180 ^{o}C, 3rd Step: 10 minutes by using 40% of microwave power under 100 ^{o}C) by using nitric acid – hydrogen peroxide (2:3). The amounts of N, P, K, Ca, Mg, Na, Cu, Fe, Zn and Mn were determined by reading an ICP-OES spectrophotometer (Inductively Couple Plasma spectrophotometer) (Perkin - Elmer, Optima 2100 DV, ICP/OES, Shelton, CT 06484-4794, USA) [15].

Data was subjected to an analysis of variance and a Duncan' multiple comparison test for the plant mineral contents in seven months by using a statistical package program [16].

RESULTS AND DISCUSSION

The macro and micro mineral contents of *Noaea mucronata* plant from April to October are provided in Table 1.

P, K, Ca, Mg, Na, Cu, Fe, Zn and Mn contents of *Noaea mucronata* plant by a period of 7 months as average, including the period from April to October, were in the ratios of 0.49%, 1.04%, 2.50%, 0.47%, 0.15%, 2.00 ppm, 211.95 ppm, 36.60 ppm and 39.90 ppm respectively. Significant changes were observed in macro and micro mineral contents (except for Na) by months (Table 1).

P, K, Ca and Zn contents of the plant were significantly high in the first periods of plants development (April, May and June), but decreasing was observed in the following periods of development.

P content ranged from 0.24% and 1.07% in the plant samples. The highest P content of *Noaea mucronata* plant was in April (1.07%), and thereafter it drastically reduced to around 0.24-0.27% just after the period of maturation starting from the month of August. Plant P levels were reported to be greatly changed at different climate conditions [17-18], different locations [5-18] and different plant organs [5]. As a result, the feeds must include the P as the nutrition of ruminants. The P is used in the development of the bone structure of animals, and it is also available in the structure of critical compounds, such as phosphorprotein, phospholipid and nucleic acid. P deficiency is an important problem in farm animals may cause to a decreased production and reproduction efficiency [1-19]. It suggests that the P content in the feeds of animals must be in a range of 0.12% to 0.52% for a optimum development and growth [20]. We determined that the amount of P in the studied plants during the summer and autumn (July, August, September and October) period is in the range of the recommended levels of [20], but the P levels of *Noaea mucronata* during the months of April, May and June have exceeded these levels. Nevertheless, the grazing

TABLE 1
Mineral contents of *Noaea mucronata* during the growing periods

Months	P (%)	K (%)	Ca (%)	Mg (%)	Na (%)	Cu (ppm)	Fe (ppm)	Zn (ppm)	Mn (ppm)
April	1.07 a	1.22 b	2.88 a	0.51 a	0.15	2.03 abc	166.46 cd	54.70 a	33.13 de
May	0.65 b	1.54 a	2.88 a	0.46 bc	0.16	1.76 bc	142.06 d	46.16 a	34.90 d
June	0.57 b	1.48 ab	2.33 b	0.41 c	0.16	2.10 abc	188.30 cd	48.83 a	35.56 d
July	0.33 c	0.88 c	2.45 b	0.45 bc	0.14	2.43 a	273.40 a	33.90 b	27.96 e
August	0.24 c	0.73 c	2.28 b	0.48 ab	0.15	1.93 bc	240.33 ab	25.63 c	47.90 b
September	0.25 c	0.72 c	2.38 b	0.53 a	0.16	1.63 c	257.00 ab	22.90 c	58.56 a
October	0.27 c	0.69 c	2.32 b	0.43 bc	0.14	2.13 ab	216.06 bc	24.10 c	41.30 c
Average	0.49	1.04	2.50	0.47	0.15	2.00	211.95	36.60	39.90
F value and significant	103.37**	14.18**	4.71**	6.091**	1.16^{öd}	3.30*	9.63**	24.72**	31.67**

$^{a, b, c, d \text{ and } e}$ Different letters in the same column indicate significant differences in the mineral contents between the growing periods. *F values are significant at 5% probability level, **F values are very significant at 1% probability level, ns: no significant.

period in the region for sheep starts from April till October during which the animals may not be needed any additional P supplements due to the fact that the levels of P in *Noaea mucronata* optimally meets the P requirements of animals.

We found that the K content reached its highest level around 1.22%, 1.54% and 1.48% in April, May and June, respectively. However, there was constant decrease in K content to 0.88%, 0.73%, 0.72% in July, August, September and October, respectively. It was evident that the K content drastically dropped as the plant gets mature. In previous studies, it was determined that the K content may be altered by the different climates [17-18-21], different growing locations [5-18-21], different organs of the plants [5] and different plant species [22]. The K is critical for osmotic regulation of body fluids and acid base equilibrium. In addition, the K affects the activity of muscles and carbohydrate metabolism [1-19]. It suggests that the K content in the animal feed must be around 0.6%, and the maximum tolerable Mg content of the animals is about 3.0% [20]. According to the research findings, no K deficiency may be observed in the animals consuming the plants of *Noaea mucronata*. We observed that *Noaea mucronata* had Mg content higher than the levels suggested for animals by [20] overall the growing periods of *Noaea mucronata* develops, but it was below the maximum tolerable level.

The highest Ca content *Noaea mucronata* was obtained in April and May (2.88%), but its level significantly ($P<0.05$) decreased as the plant gets maturated. It was determined that the Ca content can be influenced by climates [17-18-21], locations where the plant grows [5-18-21], various organs of the plants [5] and plant species [22]. The Ca is a mineral that is necessary in the formation of the skeletal and dental structure of animals. In the case of Ca deficiency, bone formation is weakened and metabolic disorders are increased [1-19]. It is reported that a 15 gr of Ca per kg feed is sufficiently enough for farm animals [1]. It suggests that the Ca content of the animal feeds at different stages of growth and development can be ranged from 0.15% to 1.18% range [20]. It was determined that *Noaea mucronata* had Ca content higher than the recommended levels by [20] during the entire growing periods of *Noaea mucronata*. Therefore, during grazing periods, farms animals in the region may not need an additional Ca supplement.

The highest Mg content, 0.51%, 0.48% and 0.53% was obtained in April, August and September, respectively, while there was a little decrease in Mg content in May and June. The results of previous studies revealed that the Mg content changed by different climates [17-18-21], different locations [5-18-21], different organs of the plant [5] and different plant species [22]. The Mg plays a critical role in bone and teeth formation, has metabolic benefits in the activities of several enzymes for carbohydrate and lipid metabolisms [1-19]. The Mg content in animal feeds were set around 0.12% to 0.20%) by [20], and these levels were well provided by the studied plants during the growing periods for grazing animals.

The Na content *Noaea mucronata* were in the range of 0.14% to 0.16% from April to October, and non-critical changes were observed over the growing periods. However, in the previous researches, it was determined that the Na content changes by climates [17-21], locations where the plant grows [5-21], and various organs of the plant [5]. Na facilitates to preserve osmotic pressure of body fluids and to ensure acid base equilibrium. In case of the Na deficiency in the feeds, the animals may reduce the utilizations from the nutrients of animal feeds and thereby the reduced animal production is inevitable [1-19]. It suggested 0.06% and 0.08% Na content of animal feeds for different stages of animals [20], which can be more than met by the Na content of *Noaea mucronata* grew in any period in the region.

The highest Cu contents were observed during July, October, June and April and, their values were 2.43 ppm, 2.13 ppm, 2.10 ppm and 2.03 ppm, respectively. We determined that the Cu contents were high in all growing periods, but low during the transition periods. The plant Cu levels were previously reported to be greatly influent by several factors: climates [18-23-24-25] and locations [18-23-25]. The copper mineral is necessary for bone and haemoglobin formation, development of connective tissues, keratinisation and tissue pigmentation. In case of its deficiency in the feeds, the animals may experience poor appetite, anaemia, easy fracture of bones and disorders in reproduction efficiency [1-19]. It suggests that the amount of Cu requirement in the animals must be 10 ppm, and the maximum tolerable Cu in the feeds is around 100 ppm [20]. It was observed that *Noaea mucronata* had a Cu content lower than these levels.

When the plant gets mature, there is an increase in its Fe content. In this study, the highest Fe contents were observed in July, September and August as 273.40 ppm, 257.00 ppm and 240.33 ppm, respectively. According to previous studies, the Fe content changes by climates [18-23-24-25], locations where the plant grows [18-23-25] and plant species [22]. The iron is available in the structure of several organs in the body, and it also plays a great role in realization of several biochemical reactions. In case of iron deficiency in the feeding, the amount of oxygen available in the tissues may decrease due to the decrease in the amount of haemoglobin, preventing several metabolic and biochemical reactions to occur [1-19]. It suggests that the amount of Fe content that the animals must obtain from the feeds is 50 ppm, and that the maximum tolerable Fe content in the feeds is around 1.000 ppm [20]. In this study, the *Noaea mucronata*

had Fe content higher than the suggested levels by [20], but it was below the maximum tolerable level.

The Zn content of the studied plant was 54.70, 48.83 and 46.16 ppm in April, June and May, respectively. It markedly decreased in the summer and autumn. It is well known that the Zn content changes by climates [18-23-24-25], locations where the plant grows [18-23-25] and plant species [22]. The zinc plays a critical role in the protein, nucleic acid and carbohydrate metabolism, formation of feathers and bones, and production and storage of hormones. In case there is a zinc deficiency in animal feeds, the utilization of feed nutrients and thereby animal growth rates are worsened [1-19]. It suggests that the Zn requirement for the development and growth of the animals is 30 ppm, and that the maximum tolerable Zn content in the feeds is 500 ppm [20]. The *Noaea mucronata* had the Zn content higher than the levels suggested by [20] in April, May, June and July when *Noaea mucronata* develops, but that it was below the maximum tolerable level. The lower Zn contents suggested by [20] were obtained in the other months (August, September and October).

The Mn content of the plant in September was around 58.56 ppm, in comparison to the other periods. The Mn content of the plant was in its lowest level in the summer (July). In previous studies, it was determined that the Mn content changes by climates [18-23-25], locations where the plant grows [18-23-25] and plant species [22]. The Manganese plays a critical role in activation of several enzymes, in the growth and reproductive efficiency of animals, and in the formation of bones and teeth. The manganese deficiency in feeds mostly makes an effect on poultry and it may also cause reproductive efficiency disorders in bovines [1-19]. It suggests that the Mn content that must be available in the feeds for the development and growth of the animals is 20 ppm, and that the maximum tolerable Mn content in the feeds is 1.000 ppm [20]. It was observed that *Noaea mucronata* had Mn content higher than the ratio suggested by [20] in any of the months when *Noaea mucronata* develops, but that it was below the maximum tolerable level.

CONCLUSION

We measured the changes in the mineral contents of *Noaea mucronata* from April to October for 7 months. The critical changes were observed in the macro and micro mineral (except for Na) contents of *Noaea mucronata* during the growing periods of *Noaea mucronata*. The averaged P, K, Ca, Mg, Na, Cu, Fe, Zn and Mn contents were determined as 0.24% - 1.07%, 0.69% - 1.54%, 2.32% - 2.88%, 0.41% - 0.53%, 0.14% - 0.16%, 1.63 - 2.43 ppm, 142 - 273 ppm, 22.90 - 54.70 ppm and 27.96-58.56 ppm, respectively. We recommended that the levels of P, K, Ca, Zn, Na, Mg, Fe and Mn analysed for the studied plant can meet the requirements of grazing sheep in the region, but the level of Cu not.

REFERENCES

[1] Kutlu, H.R., Gorgulu, M. and Celik, L.B. (2005) General Animal Feeding Lecture Notes, ZM-208. Çukurova University, Faculty of Agriculture, Department of Animal Science, Feeds and Animal Feeding, Adana, 69-84.

[2] McCaughan, C.J. (1992) Treatment of mineral disorders in cattle. Veterinary Clinics of North America: Food Animal Practice. 8(1), 107-145.

[3] McDowell, L.R. (1992) Minerals in Animals and Human Nutrition. Academic Press, New York.

[4] Egritas, O. and Asci, O.O. (2015) Determination of some mineral matter contents in common vetch-cereals mixtures. Academic Journal of Agriculture. 4(1), 13-18.

[5] Ahmad, K., Ashraf, M., Khan, Z.I. and Valeem, E.E. (2008) Evaluation of Macro-Mineral Concentrations of Forages in Relation to ruminants Requirements: A Case study in Soone valley, Punjab, Pakistan. Pakistan Journal of Botany. 40(1), 295-299.

[6] Ghazanfar, S., Latif, A., Mirza, I.H. and Nadeem, M.A. (2011) Macro-Minerals Concentrations of Major Fodder Tree Leaves and Shrubs of District Chakwal, Pakistan. Pakistan Journal of Nutrition. 10(5), 480-484.

[7] Oktay, G. and Temel, S. (2015) Determination of Annual Fodder Value of Ebu Cehil (Calligonum Polygonoides L. Ssp. Comosum (L'Hér.)) Shrub. Journal of Agricultural Faculty of Gaziosmanpasa University. 32(1), 30-36.

[8] Tan, M. and Temel, S. (2012) Alternative Feed Crops. Ataturk University Agricultural Faculty Course Publications, Erzurum. No: 246, 195-207.

[9] Temel, S., Sürmen, M. and Tan, M. (2015) Effects of Growth Stages on the Nutritive Value of Specific Halophyte Species in Saline Grasslands. The Journal of Animal and Plant Sciences. 25(5), 1419-1428.

[10] Temel, S. (2015) Determination of Fodder Quality Parameters in Vegetative and Seed Maturity Stages of Salsola tragus L. and Noaea mucronata (Forssk.) Asch. & Schweinf. International Journal of Agriculture and Wildlife Science (IJAWS). 1(1), 23-30.

[11] Al-Eisawi, D.M. (1998) Wild Flowers of Jordan and Neighboring Countries. Al Rai Jordan Press Foundation, 296p.

[12] Al-Oudat, M., Khatib Salkini, A. and Tiedeman, J. (2005) Major native plant species in the Knanasser area, Syria (Al-Hass and Shbeith mountains). ICARDA Aleppo, Syria, 147p.
[13] Meybodi, N.B. and Arzani, H. (2005) An Investigation of Range Plants' Palatability and Goat Behavior in Posht-kooh Rangelands, Yazd Province. Iranian Journal of Natural Resources. 58(4), 909-919.
[14] Anonymous (2015) Igdir Meteorology Provincial Directorate Data.
[15] Mertens, D. (2005) AOAC Official Method 922.02. In: Horwitz, W., Latimer, G.W. (Eds.) Plants Preparation of Laboratuary Sample. Official Methods of Analysis, 18th ed. AOAC-International Suite Gaitherburg, Maryland USA, 1-2.
[16] SPSS (1991) Statistical Package For The Social Sciences (SPSS/PC+). Chicago, IL.
[17] Espinoza, J.E., McDowell, L.R., Wilkinson, N.S., Conrad, J.H. and Martin, F.G. (1991) Forage and soil mineral concentrations over a three-year period in a warm climate region of central Florida. I. Macrominerals. Livestock Research for Rural Development, Florida Agricultural Experiment Station Journal Series No. R-01101, 3(1).
[18] Gokkus, A., Parlak, A.Ö. and Baytekin, H. (2013) Change of Mineral Composition of Herbaceous Species at the Mediterranean Shrublands. Journal of Tekirdag Agricultural Faculty. 10(1), 1-10.
[19] McDonald, P., Edwards, R.A., Greenhalgh, J.F.D., Morgan, C.A., Sinclair, L.A. and Wilkinson, R.G. (2011) Animal Nutrition. 7th Edition, Pearson Books, Chapter 6, 112-137.
[20] NRC. (2000) Nutrient Requirements of Beef Cattle. 7th Edition. National Academy Press, Washington, D.C.
[21] Khan, Z.I., Hussain, A., Ashraf, M., Valeem, E.E. and Akhtar, M.S. (2004a) Seasonal Variation in Soil and Forage Mineral Concentrations in Semiarid Region of Pakistan. Pakistan Journal of Botany. 36(3), 635-640.
[22] Acar, Z., Ayan, I., Asci, O., Basaran, U. and Mut, H. (2009) Biodiversity in Morphological Properties and Nutritional Values of Forage Grass Species. Journal of Environmental Biology. 30(4), 583-589.
[23] Khan, Z.I., Hussain, A., Ashraf, M., Valeem, E.E. and Akhtar, M.S. (2004b) Soil and Forage Mineral (Trace Elements) Status of a Grazing Pasture in The Semiarid Region of Pakistan. Pakistan Journal of Botany. 36(4), 851-856.
[24] Khan, Z.I., Hussain, A., Ashraf, M. and McDowell, R. (2006) Mineral Status of Soils and Forages in Southwestern Punjab-Pakistan: Micro-minerals. Asian-Australasian Journal of Animal Sciences. 19(8), 1139-1147.
[25] Kumagai, H., Kato, K., Ishida, N., Katsumata, M., Jachja, J., Yano, H. and Kawashima, R. (1989) A Study on Nutritional Status of trace Minerals in Cattle in Indonesia. Asian-Australasian Journal of Animal Sciences. 2(3), 279-280.

Received: **13.03.2018**
Accepted: **20.02.2019**

CORRESPONDING AUTHOR

Suleyman Temel
Iğdır University,
Faculty of Agriculture,
Department of Field Crops,
76000 Igdir – Turkey

e-mail: stemel33@hotmail.com

© by PSP Volume 28 – No. 4/2019 pages 2426-2432 Fresenius Environmental Bulletin

STUDY ON ISOLATION AND UTILIZATION OF A CHLOROTHALONIL DEGRADING BACTERIUM, *BACILLUS COAGULANS* BJQ-Z6

Yan Zhao[1,*], Chengxiao Zhao[2], Sichun Tong[3], Caihua Jin[4]

[1]Shanghai Institute of Quality Inspection and Technical Research, Shanghai 200233, China
[2]College of Science, Nanjing Forestry University, Nanjing 210037, China
[3]Collaborative Innovation Center of Sustainable Forestry in Southern China of Jiangsu Province, (Nanjing Forestry University), Nanjing 210037, China
[4]Pudong Agrotechnology Extension Center, Shanghai 201201, China

ABSTRACT

A strain BJQ-Z6 capable of highly degrading chlorothalonil was isolated from soil. The strain BJQ-Z6 was identified as *Bacillus coagulans* based on 16S rRNA and analysis of morphology, physiological and biochemical characters. The optimal pH value and temperature were 7.0 and 45-50°C. The 7d degradation rate of 100 mg/L chlorothalonil by strain BJQ-Z6 could reach about 98.9% in mineral salt medium. The combined applications of the strain BJQ-Z6 and the strain BJQ-Z1 was considered an effective means for rapidly degrading chlorothalonil. The degradation rate of chlorothalonil (100mg/L) by the strain BJQ-Z6 and the strain BJQ-Z1 could reach about 99.5% in 6d. In addition, the strain BJQ-Z6 showed a high tolerance to chlorothalonil. It was believed that the strain BJQ-Z6 could be used for control of chlorothalonil (or hydroxychlorothalonil) pollution.

KEYWORDS:
Chlorothalonil, biodegradation, *Bacillus coagulans*

INTRODUCTION

Chlorothalonil is a contact fungicide from the chloronitrile group, and it is often used to control fungal pathogens in various fruit and vegetable crops, as well as in tree farming practices [1]. The chlorothalonil residue may bring some trouble to soil organism, aquatic systems and public health [2-4]. Previous research results showed that long-term use of chlorothalonil could cause a decrease in soil microbial population and soil enzyme activity [5-7]. For human, chlorothalonil could cause dermatitis, severe eye and skin irritation, and gastrointestinal discomfort, it has been classified as probable human carcinogen by U.S. Environmental Protection Agency [8, 9]. Chlorothalonil is considered to be moderately persistent in soil, and the half-life of chlorothalonil in field situations can even reach 6 months (U.S. EPA). Therefore, more attention must be paid to the degradation of chlorothalonil, and the microbial degradation is usually considered the most important way of chlorothalonil degradation [10-12]. In addition, chlorothalonil is easily converted to its more toxic and persistent 4-hydroxy metabolite and cause greater harm [13, 14]. 4-hydroxy-2,5,6- trichloroisophthalonitrile (hydroxychlorothalonil) is considered the most important primary metabolite resulting from chlorothalonil degradation [15-17]. Therefore, in the process of biodegradation of organic pollutants, not only need to focus on the parent pollutants, but also must pay attention to intermediate metabolites [18].

At present, several soil microorganisms capable of co-metabolizing low concentrations of chlorothalonil at the presence of other carbon sources were isolated [19-21]. However, there were only a few studies on the isolation of pure culture capable of degrading high concentrations of chlorothalonil without providing other carbon sources. In this study, *Bacillus coagulans* BJQ-Z6, a strain that could degrade chlorothalonil and hydroxychlorothalonil was isolated. Its degradation potential and the application for environment protection were studied.

MATERIALS AND METHODS

Chemicals and Media. Chemicals: chlorothalonil (99.5%) was purchased from Sigma-Aldrich Company. All other chemicals used were of analytical grade and commercially available.

Culture media: (1). Mineral salt medium: $MgSO_4 \cdot 7H_2O$ 0.2 g, $(NH_4)_2SO_4$ 0.1 g, K_2HPO_4 0.1g, $CaSO_4$ 0.05 g, $FeSO_4 \cdot 7H_2O$ 0.01 g, water 1.0 L, pH 7.0. (2). Isolation medium: mineral salt medium containing chlorothalonil (100 mg/L) was used to isolate chlorothalonil degrading bacteria. (3). Enrichment medium: peptone 8.0 g, yeast extract powder 5.5 g, beef extract powder 3.5 g, sodium chloride 5 g, water 1.0 L, pH7.0.

Isolation and identification of chlorothalonil degrading bacteria. The soil sample was collected from cropland in SHANGHAI City, China, in which chlorothalonil has been used for more than 8 years. 6.0 g soil sample was placed in 100ml isolation medium for shaking culture at 35°C (120 rpm). The concentration of the residual chlorothalonil was determined every 24h [22, 23]. 6ml culture solution with 3d degradation rate >75% was transferred to enrichment medium containing same concentration of chlorothalonil, and continuously transferred for more than 5 times. After the degradation effect was verified again, the above enrichment medium was coated on mineral salt culture plate containing chlorothalonil for inverted culture at 35°C. The eugonic bacterial colonies were selected and repeatedly streaked on the culture plate to obtain the pure culture. The new isolates were identified by using 16SrRNA sequence analysis.

Effect of temperature on the growth of strain BJQ-Z6. Inoculums of chlorothalonil degrading bacteria were prepared in advance [24]. 4% strain BJQ-Z6 inoculum was incubated in mineral salt culture medium containing 100mg/L chlorothalonil under the different temperature. OD_{600} was determined every 12h after the shaking culture.

Effects of pH on the growth of strain BJQ-Z6. pH of mineral salt culture medium (containing 100mg/L chlorothalonil) was adjusted to 6.0, 6.5, 7.0, 7.5 and 8.0. Then they were inoculated with 4% inoculum respectively. The shaking culture was performed at 45°C. OD_{600} was taken regularly.

Tolerance of the strain BJQ-Z6 on chlorothalonil. The concentration of chlorothalonil in mineral salt medium was adjusted respectively to 50mg/L, 100mg/L, 200mg/L, 400 mg/L and 800 mg/L. Then the strain BJQ-Z6 was inoculated respectively for shaking cultivation at 45°C. OD_{600} was determined regularly, so as to evaluate the tolerance of strain BJQ- Z6 on chlorothalonil.

Degradation of chlorothalonil by strain BJQ-Z6. 4% strain BJQ-Z6 inoculum was inoculated in mineral salt culture medium containing 100mg/L chlorothalonil, and then place it in the shaker (120rpm, 45°C). The concentration of chlorothalonil and 4-hydroxy-2,5,6-trichloroisophthalonitrile (hydroxychlorothalonil) were determined every 24h [22, 23].

Degradation of hydroxychlorothalonil by strain BJQ-Z6. The mineral salt culture medium containing 50mg/L hydroxychlorothalonil was inoculated with 4% strain BJQ-Z6 inoculum, and then place it in the shaker (120rpm, 45°C). The concentration of hydroxychlorothalonil was determined regularly.

Degradation of chlorothalonil by combining strain BJQ-Z6 and strain BJQ-Z1. The strain BJQ-Z1 was a chlorothalonil degrading bacterium deposited in our laboratory. It was identified as *Bacillus pumilus* according to 16S analytical method (GenBank accession number MH113276). The strain BJQ-Z1 could effectively convert chlorothalonil to hydroxychlorothalonil at a faster rate, but it degrades hydroxychlorothalonil slower than strain BJQ-Z6. Therefore, it is speculated that the combined applications of the strain BJQ-Z6 and the strain BJQ-Z1 may have a higher degraded efficiency.

4% strain BJQ-Z6 inoculum and 4% strain BJQ-Z1 inoculum were inoculated simultaneously in mineral salt culture medium containing 100mg/L chlorothalonil, and then incubate in incubator. The concentration of chlorothalonil and hydroxychlorothalonil were determined every 24h.

RESULTS AND DISCUSSION

Identification and characterization of chlorothalonil degrading bacteria. A strain capable of using chlorothalonil as the sole carbon sources and energy source was isolated from soil, named BJQ-Z6. It was G^+, facultative anaerobic, motile, straight bacillus, 0.6-1.0×2.0-4.0 um in size. There was oval spores in the terminal of thallus. It forms smooth, opalescent and opaque colonies on the nutrient broth plate. It was positive in tests for amylolysis, catalase, V.P. test, glucose fermentation, but the indole test was negative [25]. The strain BJQ-Z6 was identified as *Bacillus coagulans* according to 16S sequence analysis (The 16S analysis of strain BJQ-Z6 was commissioned to Shanghai SANGON company, GenBank accession number MH074883).

Effects of temperature and pH on the strain BJQ-Z6 growth. The strain BJQ-Z6 has the highest growth level at 45-50°C, higher or lower temperatures will affect its growth (Fig. 1). The experimental results show that strain BJQ-Z6 was suitable for growth at higher temperatures and had a strong chlorothalonil degrading ability. The degradation rate of chlorothalonil (initial concentration was 100mg/L) was about 77% after 3 days of incubation, and could reach more than 91% after 5d at 45°C (Fig. 4). In general, the temperature on the one hand could affect the growth of microorganisms and enzyme activity, on the other hand the temperature could also directly affect the degradation rate of organic compounds. The increase of the temperature would cause the acceleration of enzymatic degradation reaction, but the excessively high temperature would lead to the inactivation of degrading enzymes and other enzymes [26-28]. Based on the above factors, 45-50°C was considered as the optimum temperature of the strain BJQ-Z6 for growth and degrading chlorothalonil.

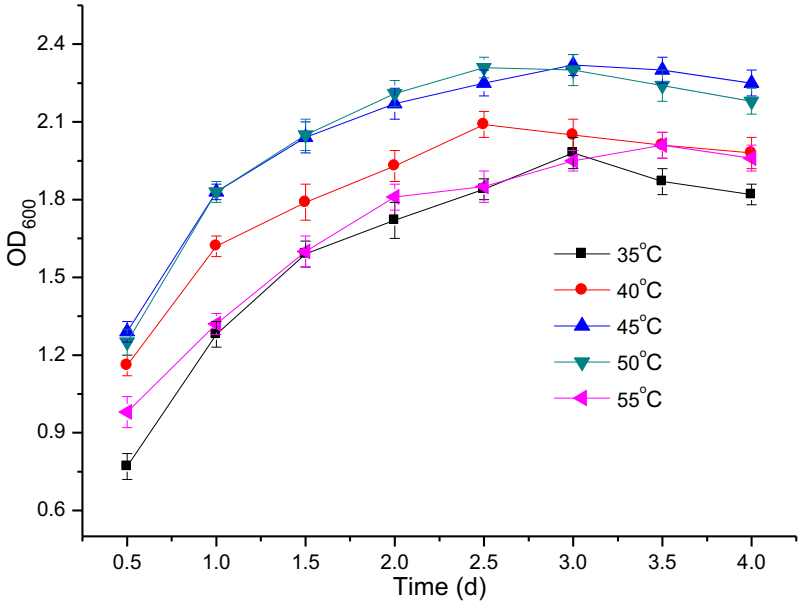

FIGURE 1
Effect of temperature on the growth of strain BJQ-Z6

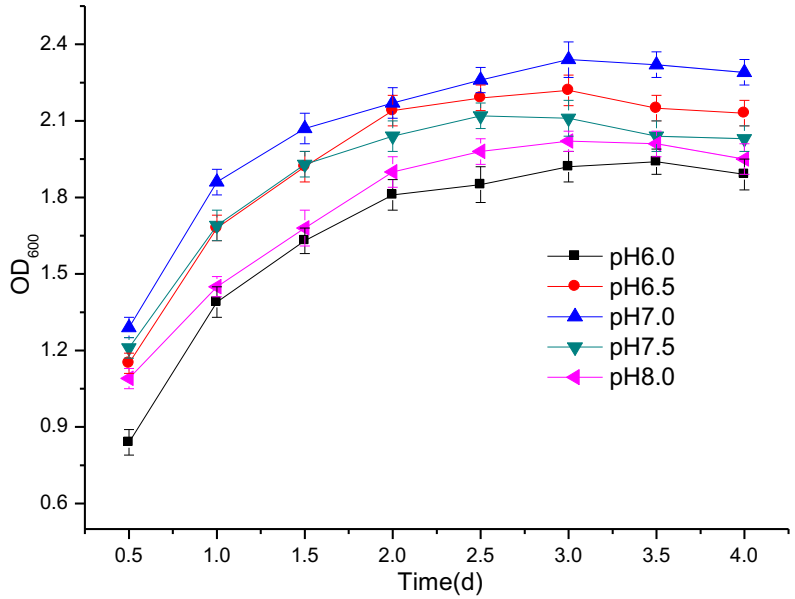

FIGURE 2
Effect of pH on the growth of strain BJQ-Z6

The growth status and degradation ability of microorganism were usually affected by environment pH. The experimental results showed that the growth state of strain BJQ-Z6 at pH 7.0 was better than that under other pH conditions (Fig.2), and the optimum pH of the strain BJQ-Z6 was pH7.0. Generally, pH could not only cause the change of the degrading ability through influencing microbial growth, but also could directly influence the activities of relevant degrading enzymes.

Tolerance of the strain BJQ-Z6 on chlorothalonil. OD_{600} did not change significantly ($P>0.05$) when the concentration of chlorothalonil was increased from 50mg/L to 200mg/L. But OD_{600} would decrease significantly if the concentration of chlorothalonil increased to 400mg/L or 800mg/L (Fig.3). The results showed that the growth of the strain BJQ-Z6 had been inhibited by 400mg/L chlorothalonil, but it was still growing. Therefore, it was preliminarily considered that the strain BJQ-Z6 could tolerate at least 800mg/L chlorothalonil under the experimental conditions. Although the strain BJQ-Z6 would be significantly inhibited by 800mg/L triclopyr, it still could effectively degrade chlorothalonil (because chlorothalonil was used as the sole carbon source in the study). According to the existing results, it was inferred that the strain BJQ-Z6 had a strong degradation ability to chlorothalonil, which could be used in a wider range of

chlorothalonil concentration. In addition, it was possible that the strain BJQ-Z6 was used in the bioremediation of chlorothalonil pollution. The degradation ability of the strain BJQ-Z6 might be closely related with the long-term use of chlorothalonil in cropland soil. Generally, soil microorganism that continuously encounter the artificially synthesized compound might be induced the ability to degrade the compound [29, 30].

Degradation of chlorothalonil and hydroxychlorothalonil by the strain BJQ-Z6. The results in Fig.4 showed that the chlorothalonil could be rapidly degraded by the strain BJQ-Z6. The degradation rate of chlorothalonil (100mg/L) by the strain BJQ-Z6 could reach about 98.9% in 7d. Degradation of chlorothalonil under the experimental conditions was fitted to the first order decay model ($C=C_0 \cdot e^{-kt}$), "t" was the degradation time, "k" was the degradation rate constant, "C_0" was initial concentration. $C=100e^{-0.3905t}$, $R^2=0.9295$, half life=1.77d. At the same time, it was found that the concentration of hydroxychlorothalonil rises first and then falls in the degradation process of chlorothalonil. In addition, hydroxychlorothalonil could be degraded by the strain BJQ-Z6 (Fig. 5). These results suggested that the strain BJQ-Z6 could completely degrade chlorothalonil, and hydroxychlorothalonil was an important intermediate metabolite of chlorothalonil. It was believed that the strain BJQ-Z6 could be used for control of chlorothalonil (or hydroxychlorothalonil) pollution.

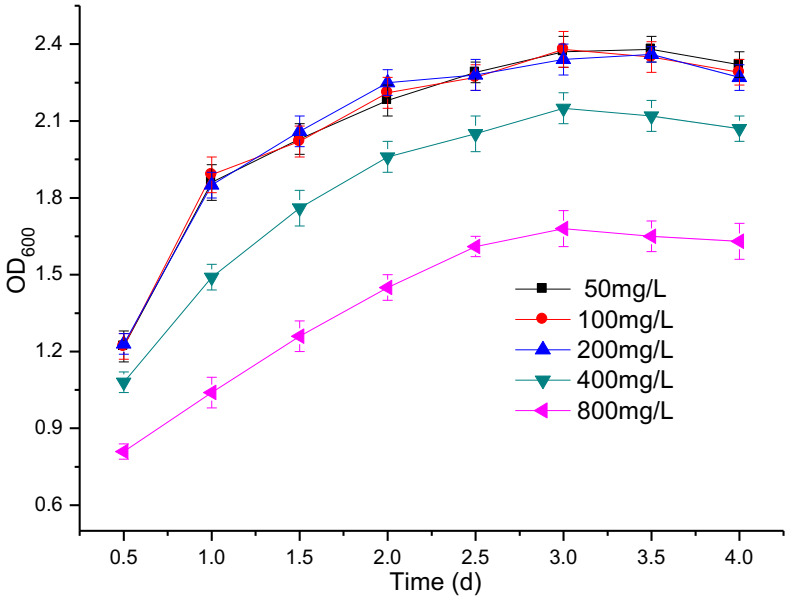

FIGURE 3
Effect of concentration of chlorothalonil on the growth of strain BJQ-Z6

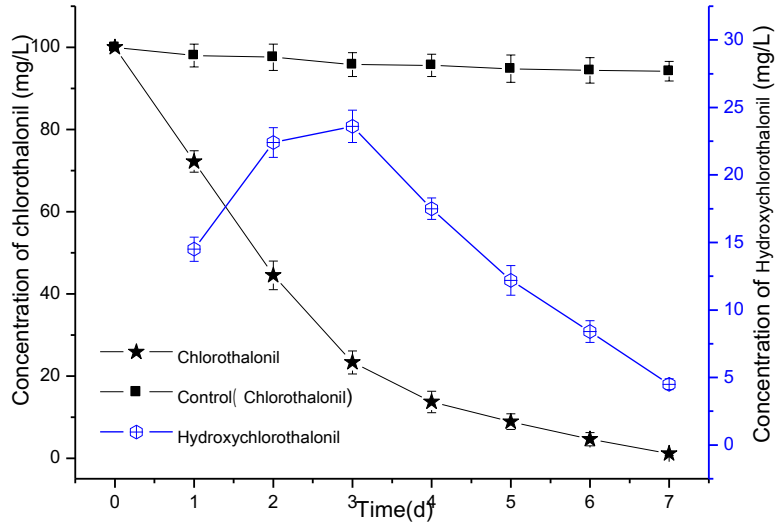

FIGURE 4
The curve on degradation of chlorothalonil by the strain BJQ-Z6 and the concentration of hydroxychlorothalonil

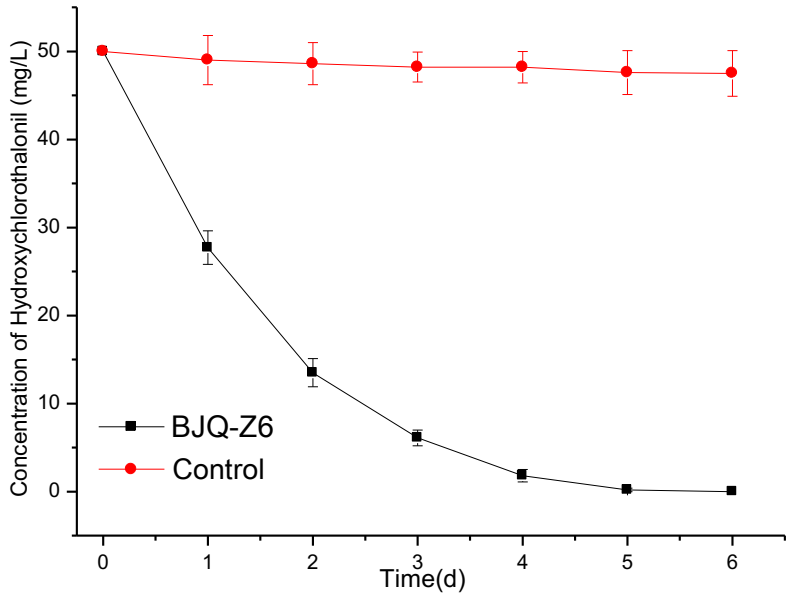

FIGURE 5
The curve on degradation of hydroxychlorothalonil by the strain BJQ-Z6

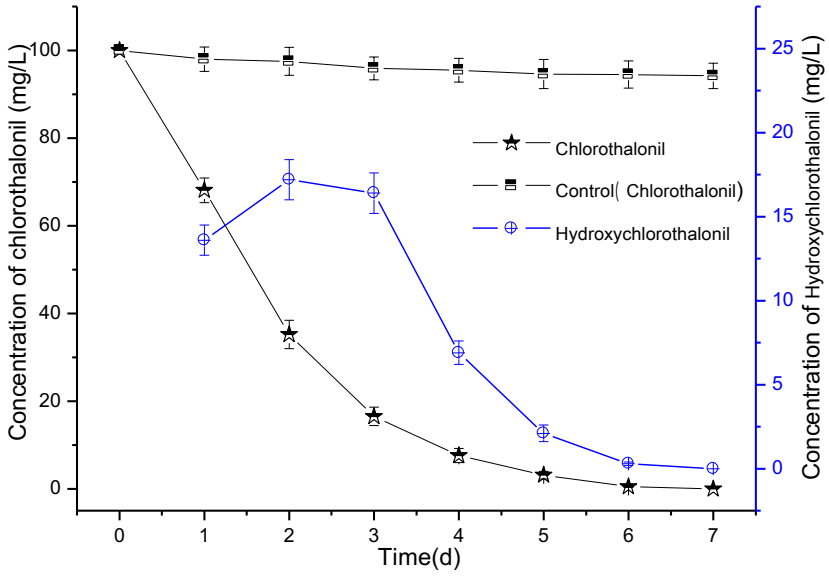

FIGURE 6
The curve on chlorothalonil degradation by the strain BJQ-Z6 and the strain BJQ-Z1

Degradation of chlorothalonil by the strain BJQ-Z6 and BJQ-Z1. The results in Fig. 6 showed that the chlorothalonil could be rapidly degraded by the strain BJQ-Z6 and the strain BJQ-Z1. The degradation rate of chlorothalonil (100mg/L) by the strain BJQ-Z6 and the strain BJQ-Z1 could reach about 99.5% in 6d. It can be indicated by comparing the data in Fig. 4 and Fig. 6 that the degradation rate of chlorothalonil when the two strains were combined was higher than when the strain BJQ-Z6 alone was used. In addition, the concentration of hydroxychlorothalonil shown in Fig. 6 was significantly lower than that in Fig. 4. It indicates that the combined application of the strain BJQ-Z6 and the strain BJQ-Z1 will help to reduce the accumulation of intermediate (hydroxychlorothalonil), and effectively increase the biodegradation rate of chlorothalonil.

CONCLUSION

In this study, *Bacillus coagulans* BJQ-Z6 was isolated from soil, which could degrade chlorothalonil. The optimal pH value and temperature of strain BJQ-Z6 were 7.0 and 45-50°C. The strain BJQ-Z6 also had high tolerance to chlorothalonil. It could tolerate at least 800mg/L chlorothalonil under the experimental conditions. The degradation rate of chlorothalonil (100mg/L) by the strain BJQ-Z6 could reach about 98.9% in 7d. The experimental results

suggested that the strain BJQ-Z6 could completely degrade chlorothalonil, and hydroxychlorothalonil was an intermediate metabolite of chlorothalonil biodegradation. The combined applications of the strain BJQ-Z6 and the strain BJQ-Z1 was considered an effective means for rapidly degrading chlorothalonil. The degradation rate of chlorothalonil(100mg/L) by the strain BJQ-Z6 and the strain BJQ-Z1 could reach about 99.5% in 6d. It was believed that the strain BJQ-Z6 could be used for control of chlorothalonil (or hydroxychlorothalonil) pollution.

ACKNOWLEDGEMENTS

This study was funded by the Natural Science Fundation of Jiangsu Provincial Universities (No. 17KJB610004) and China Postdoctoral Science Foundation (No.2017M611827).

REFERENCES

[1] Canadian Council of Ministers of the Environment. (1999) Canadian water quality guidelines for the protection of aquatic life: Chlorothalonil. In Canadian Environmental Quality Guidelines, 1999. Canadian Council of Ministers of the Environment, Winnipeg, MB, Canada.

[2] White, P.M.J., Potter, T.L. (2010) Metolachlor and chlorothalonil dissipation in gypsum-amended soil. Journal of Environmental Science and Health. Part. B Pesticides Food Contaminants and Agricultural Wastes. 45(7), 729-738.

[3] Liang, B., Rong, L., Dong, J., Sun, J., Qiu, J., Zhao, Y. (2010). Hydrolytic dechlorination of chlorothalonil by ochrobactrum, sp. ctn-11 isolated from a chlorothalonil-contaminated soil. Current Microbiology. 61(3), 226-233.

[4] Zhu, J., Zhao Y., Ruan H. (2017). Isolation and utilization of a chlorothalonil degrading bacterium, *Pseudomonas fluorescens* BJQ-11. Fresen. Environ. Bull. 26, 4108-4112.

[5] Zhang, M., Teng, Y., Xu, Z., Wang, J., Christie, P., Luo, Y. (2016) Cumulative effects of repeated chlorothalonil application on soil microbial activity and community in contrasting soils. Journal of Soils and Sediments. 16(6), 1754-1763.

[6] Tu, C.M. (1993) Effect of fungicides, captafol and chlorothalonil, on microbial and enzymatic activities in mineral soil. Journal of Environmental Science and Health. Part. B. Pesticides Food Contaminants and Agricultural Wastes. 28(1), 67-80.

[7] Yu, Y.L., Shan, M., Fang, H., Wang, X., Chu, X.Q. (2006) Responses of soil microorganisms and enzymes to repeated applications of chlorothalonil. Journal of Agricultural and Food Chemistry. 54(26), 10070-10075.

[8] Draper, A., Cullinan, P., Campbell, C., Jones, M., Newman, T.A. (2003) Occupational asthma from fungicides fluazinam and chlorothalonil. Occupational and Environmental Medicine. 60(1), 76-77.

[9] U.S. Environmental Protection Agency (1999) R.E.D. facts. Prevention, pesticides and toxic substances (4508C) Chlorothalonil. EPA-738-F-99-008.

[10] Tohru, M., Koichi, F., Arata, K. (1998) Bacterial and fungal contributions to chlorothalonil degradation in soil. Soil Science and Plant Nutrition. 44(3), 297-304.

[11] Shi, X.Z., Guo, R.J., Takagi, K., Miao, Z.Q., Li, S.D. (2011) Chlorothalonil degradation by ochrobactrum lupini strain tp-d1 and identification of its metabolites. World Journal of Microbiology and Biotechnology. 27(8), 1755-1764.

[12] Regitano, J.B., Tornisielo, V.L., Lavorenti, A., Pacovsky, R.S. (2001) Transformation pathways of ^{14}C-chlorothalonil in tropical soils. Archives of Environmental Contamination and Toxicology. 40(3), 295-302.

[13] Wu, X., Yin, Y., Wang, S., Yu, Y. (2014) Accumulation of chlorothalonil and its metabolite, 4-hydroxychlorothalonil, in soil after repeated applications and its effects on soil microbial activities under greenhouse conditions. Environmental Science and Pollution Research. 21(5), 3452-3459.

[14] Kazos, E.A., Nanos, C.G., Stalikas, C.D., Konidari, C.N. (2008) Simultaneous determination of chlorothalonil and its metabolite 4-hydroxychlorothalonil in greenhouse air: dissipation process of chlorothalonil. Chemosphere. 72(10), 1413-1419.

[15] Liu, X., Gou, Z., Hu, Q., Wang, J. (2016). Hydrolytic dehalogenation of the chlorothalonil isomer o-tetrachlorophthalonitrile by pseudochrobactrum, sp. bsq-1. International Biodeterioration and Biodegradation. 107, 42-47.

[16] Katayama, A., Ukai, T., Nomura, K., Kuwatsuka, S. (2014) Formation of a methylthiolated metabolite from the fungicide chlorothalonil by soil bacteria. Bioscience Biotechnology and Biochemistry. 56(9), 1520-1521.

[17] Chaves, A., Shea, D., Danehower, D. (2008) Analysis of chlorothalonil and degradation products in soil and water by GC/MS and LC/MS. Chemosphere. 71(4), 629-638.

[18] Zhu, J., Dai, L., Yang, N., Li, X., Zhao, Y. (2017) Study on biodegradation mechanism of triclopyr butoxyethyl ester and utilization of a triclopyr butoxyethyl ester degrading bacterium, *Bacillus coagulans* Tbe-9. Fresen. Environ. Bull. 26, 7561-7567.
[19] Gu, X.M., Wei, C.J., Jia, L.F. (2012) Isolation, identification and degradative characters of chlorothalonil-degrading bacteria bjq2. Journal of Agro-Environment Science. 31(2), 306-311.
[20] Zhang, M.Y., Teng, Y., Zhu, Y., Christie, P. (2014) Isolation and characterization of chlorothalonil-degrading bacterial strain h4 and its potential for remediation of contaminated soil. Pedosphere. 24(6), 799-807.
[21] Zhang, Y., Lu, J., Wu, L., Chang, A. (2007) Simultaneous removal of chlorothalonil and nitrate by bacillus cereus strain ns1. Science of the Total Environment. 382(2-3), 383-387.
[22] Negeri, B.O., Foster, G.D., Khan, S.U. (2000) Determination of chlorothalonil residues in coffee. Toxicological and Environmental Chemistry. 77(1-2), 41-47.
[23] Van Doorn, C., Vink, M., Van der Poll, J.M. (1995) Gas chromatographic determination of chlorothalonil and its metabolite 4-hydroxy-2,5,6-trichloroisophtalonitrile (HTI) in water. Chromatographia, 40(7), 458-462.
[24] Zhu, J., Zhao, Y., Ruan, H. (2017) Isolation and characterization of a triclopyr degrading bacterium, *Bacillus mycoides* TR-9. Fresen. Environ. Bull. 26, 3639-3643.
[25] Zhu, J., Zhao, Y., Xie, K., Li, X., Chen, Yi. (2018) Study on biodegradation of chlorpyrifos and utilization of a chlorpyrifos degrading bacterium, *Bacillus amyloliquefaciens* CZ-5. Fresen. Environ. Bull. 27, 1196-1201.
[26] Tamura, K. (2001) Microbial pesticide degradations and evolutionary analysis of degrading enzymes. Journal of Pesticide Science. 26(3), 309-317.
[27] Zhu, J., Zhao, Y., Li, X., Chen, W. (2018) Effects of chlorimuron-ethyl on soil microorganisms and enzyme activities under moderate salt stress. Fresen. Environ. Bull. 27, 2358-2365.
[28] Rouchaud, J., Roucourt, P., Vanachter, A. (2008) Hydrolytic biodegradation of chloropthalonil in the soil and in cabbage crops. Toxicological and Environmental Chemistry. 17(1), 59-68.
[29] Petric, I., Karpouzas, D. G., Bru, D., Udikovic-Kolic, N., Kandeler, E. (2016) Nicosulfuron application in agricultural soils drives the selection towards ns-tolerant microorganisms harboring various levels of sensitivity to nicosulfuron. Environmental Science and Pollution Research. 23(5), 1-14.
[30] Felsot, A., Maddox, J.V., Bruce, W. (1981) Enhanced microbial degradation of carbofuran in soils with histories of furadan use. Bulletin of Environmental Contamination and Toxicology. 26(1), 781-788.

Received: **27.03.2018**
Accepted: **22.02.2019**

CORRESPONDING AUTHOR

Yan Zhao
Shanghai Institute of Quality Inspection
and Technical Research,
Shanghai 200233 – China

e-mail: sqi_zhaoyan@qq.com

© by PSP Volume 28 – No. 4/2019 pages 2433-2441 Fresenius Environmental Bulletin

DETERMINATION OF WATER-YIELD RELATIONSHIP OF COMICE PEAR (*PYRUS COMMUNIS L.*) VARIETY IRRIGATED BY THE IRRIGATION AUTOMATION SYSTEM (IAS) BASED ON PROGRAMMABLE LOGIC CONTROLLER (PLC)

Cafer Gencoglan[1,*], Serpil Gencoglan[1], Yusuf Nikpeyma[2], Ali Beyhan Ucak[3]

[1]Department of Biosystem, Faculty of Agriculture, University of Kahramanmaras Sutcu Imam, Kahramanmaras, Turkey
[2]Department of Horticulture, Faculty of Agriculture, University of Kahramanmaras Sutcu Imam, Kahramanmaras, Turkey
[3]Department of Biosystem, Faculty of Agriculture, University of Siirt, Siirt, Turkey

ABSTRACT

The aims of this study are to determine water-yield relationships of Comice Pear (*Pyrus communis* L.) variety irrigated by irrigation automation system (IAS) based on Programmable Logic Controller (PLC).

Irrigation treatments consisted of five different irrigation levels as 120% (I_{120}), 100% (I_{100}), 80% (I_{80}), 60% (I_{60}) and 40% (I_{40}) of the pan evaporation and were carried out in 3 replications according to the design of random blocks. Irrigations were applied to parcels by IAS based PLC when the total amount of water evaporated from Class A Pan was equal to or greater than 35 mm. Soil moisture was measured by sensor (MAS-1) running with dielectric constant of soil in layers of 30 cm at depth of 90 cm of soil profile.

Total evaporation of 1104 mm was measured from the Class A Pan by the IAS during the irrigation season. The IAS irrigated Comice pear variety 27 times during irrigation season. The irrigation interval ranged from 3 to 12 days. The amount of water given to the irrigation treatments of I_{120}, I_{100}, I_{80}, I_{60} and I_{40} in each irrigation were 40-62, 33-52, 26-42, 20-31 and 13-21 mm, respectively. The amounts of evapotranspiration (ET) in irrigation treatments were found to be 1287, 1046, 869, 669 and 527 mm, respectively. Under these conditions, the mean fruit yields from irrigation treatments were 15.3, 12.5, 12.6, 11.3 and 9.8 ton per hectare, respectively. Relationships between fruit yield (ton ha^{-1}) and net irrigation water (Inw, mm) and evapotranspiration (ET, mm) were found as Fy = 0.0062Inw + 7.0091 (R^2 = 0.91**) and Fy = 0.0065ET + 6.552 (R^2 = 0.92**), respectively. The yield response factor (ky) was 0.60. As the amount of the applied irrigation water decreased, pear yield also decreased but IWUE and WUE increased. However, there was no statistically difference among the yields of the irrigation treatments. Irrigation scheduling based on a 0.4 and 0.6 crop-pan coefficients and their treatments are recommended to the pear producers experiencing water shortage. Under abundant water conditions, I_{120}, I_{100} and I_{80} crop-pan coefficients and treatments are also suggested. The pear producers should not consider that the shoot length of Comice Pear take as irrigation timing criteria. In addition, the result of study also showed that IAS could be used to control drip irrigation system, Class A Pan, irrigation scheduling, and to calculated ET and to measure soil moisture.

KEYWORDS:
Irrigation automation, PLC, Comice Pear

INTRODUCTION

Water management is a key issue for agricultural crops, which are grown under dry and semi dry climatic conditions. Water scarcity has occurred in many Turkey regions, as in other regions of the world, especially in the last two decades due to drought and increasing competition for water. Furthermore, there is a growing community expectation that agricultural sector will utilize water efficiently to achieve production and environmental goals. As a result of these expectations, irrigators need to adopt efficient water management strategies.

Crop water production functions, which are relationships between crop yield and water, are used by planners to estimate the economic consequences of decisions relating to alternative water distribution. The functions yield important clues in the interpretation of irrigation system capacities, irrigation scheduling and water use efficiency [1]. The functions are not only used for water requirements of plants, plant growth models, water use efficiencies, irrigation programs, water deliveries, but also for planning, operating and economic analysis of irrigation systems [2]. Moreover, the way to economically irrigate a plant depends on the knowledge of the relationship between yield and

water [3]. Although the functions have been widely used for management purposes in water deficient areas as a guideline for irrigation, they do not account for the effects of timing of water application [4]. They can be determined both applying different amount of irrigation water and at non sensitive plant growth stages, doing deficit irrigation.

Many studies on pear trees irrigation have been conducted, some of these are related to irrigation scheduling [5, 6] irrigation methods [7, 8, 9], crop coefficient (kc) [10, 11], deficit irrigation [12, 13, 14] regulated deficit irrigation (RDI) [15, 16, 17, 18, 19], partial root zone drying (PRD) [20, 8, 21, 22, 23] and saline water use [24, 25]. The studies related to pear irrigation conducted so far show that there is a need of crop water production function of pear and also this kind of studies will contribute irrigation science.

The aims of this study are to determine of water yield relationships of Comice Pear (*Pyrus communis* L.) variety irrigated by irrigation automation system (IAS) based on Programmable Logic Controller (PLC).

MATERIALS AND METHODS

In 2015, a field experiment was conducted at the garden of Agricultural Faculty, University of Kahramanmaras Sutcu Imam (37º32′08″ N and 36º54′59″ E and altitude 700 m above sea level), in Kahramanmaras, Turkey. The experimental garden consisted of a 15-year-old drip-irrigated orchard of 'Comice' pear grafted on quince C (*Cydonia oblonga* Mill) rootstock spaced 0.6 × 4.5 m apart. The experimental garden lies within an area of 20 000 ha with intensive cropping supported by irrigation. This has a Mediterranean climate with cool, rainy winters and hot, dry summers prevailing in the experimental area. Long-term average rainfall in the area is 728 mm. The 2015 growing season temperatures were typical of the long term means at Kahramanmaras. However, rainfall was 58.9 mm for the 2015 growing season (June–October), which was less than the long term mean of 63.6 mm.

Soil type was a brown-alluvial with the soil profile deeper than 1 m. Some physical and chemical properties of the experimental soil were given in Table 1.

Irrigation water quality is classified as C_2S_1, with pH 7.26, and an average electrical conductivity of 410 μS m^{-1}, and sodium absorption rate (SAR) of 0.01. The quality of irrigation water is suitable in terms of toxicity and osmotic potential for pear trees [26].

Irrigation treatments consisted of five different irrigation levels as 120% (I_{120}), 100% (I_{100}), 80% (I_{80}), 60% (I_{60}) and 40% (I_{40}) of the pan evaporation. Accordingly, five crop-pan coefficients (Kcp1=1.2, Kcp2=1.0, Kcp3=0.8, Kcp4=0.6 and Kcp5=0.4) were identified for scheduling requirements. Experiment was carried out as the design of random blocks with 3 replications. Each of the 15 individual plots was 10 m long, containing 14-15 plants. When the total amount of water evaporated from Class A Pan was equal to or greater than 35 mm, the pear plots were irrigated [27]. Irrigation started in June and ended in October.

An irrigation automation system (IAS) based PLC was developed. IAS had three parts, the first of them was electrical panel, the second was software and the third was drip irrigation system and Class A Pan. In the panel, there were PLC with ethernet, 3 digital output module, 1 digital input module, 2 analog input module, inverter, touch panel, 3 power supply with different outputs, 7 switcher, 3G/4G modem, USB modem and 23 relay. A program was written for IAS to control the water tank, Class A Pan, the drip irrigation system, fertilizer tank and pluviometer, and to measure soil moisture, and to calculate volume of irrigation water and ET. In programming the IAS, CODESYS-ST language was used, and 16 digital inputs (DI), 23 digital outputs, 21 analog inputs (AI) and 1 analog output were utilized in the program. For IAS, SD card module was selected to save data into SD card related to soil moisture, water level in Class A Pan, irrigation water, deep percolation, ET and rainfall.

Following standards given by Doorenbos and Pruitt [28] a screened Class A Pan was located a place next to the experimental garden surrounding by vegetation but no shadowing. In order to control water level and the excess water caused by precipitation in the Pan, a solenoid valve (Ø1/2"), pressure transducer (50 mBar) and motopump were connected to the Pan (Figure 1). In addition, a pluviometer was placed next to the Pan to measure rainfall. The irrigation scheduling was prepared according to the A class evaporation method. The daily evaporation rate was determined from class A Pan by taking the difference of daily water levels measured by IAS using pressure transducer.

TABLE 1
Some physical and chemical properties of experimental soil

Soil depth (cm)	Texture	Field capacity (g g^{-1})	Wilting point (g g^{-1})	Bulk density (gr cm^{-3})	pH	Soil salinity ECe (dS m^{-1})	$CaCO_3$ (%)	Organic matter(%)
0-30	CL	35.04	22.39	1.38	7.61	0.022	9.29	0.88
30-60	CL	35.99	24.17	1.36	7.76	0.018	7.96	1.76
60-90	C	41.19	20.43	1.50	7.80	0.019	9.29	2.67

FIGURE 1
Class A Pan and water depth measurement system.
1:Slatted Platform, 2: Pressure transducer, 3: Motopump, 4: Solenoid valve, 5: Raingage, 6: Class A pan

Experimental plots were irrigated by drip irrigation method. For this purpose, two drip lateral (∅16 mm) were located to the distance of 35.5 cm from both side of three row on irrigation plots (I_{120}, I_{100}, I_{80}, I_{60} and I_{40}), with inline dripper flow rate of 4 L h^{-1}, operating pressure of 1 atm, dripper distance of 71 cm. Main and manifold pipe were ∅32 mm. On the head of lateral, digital water meters (1 pulse is equal to 1 L) and solenoid valves (∅1/2"), and on dead end, plugs were mounted to each of the two laterals in the irrigation plots. The drip irrigation control unit had a water tank (7 ton), a motopump (2.2 kW), a hydrocyclone, a sand-gravel filter, a fertilizer tank and a disk filter. A pressure transducer (250 mBar) was used to control water level in the water tank. The fertilizer tank was also controlled by two solenoid valves (∅1/2") and one electromotor rotary actuators (∅2") [29, 30].

The irrigation amount to be applied to the treatments was calculated by IAS's the program using Eq. 1 [31].

$$V=Ep*Kcp*L*W \quad (1)$$

Where; V: Amount of irrigation water to be applied to the treatments (mm), Ep: Amount of Class A Pan evaporation (mm) (taken as Ep being equal to or greater than 35 mm depending on Pan evaporation). Kcp: Crop-pan coefficients (Kcp1=1.2, Kcp2=1.0, Kcp3=0.8, Kcp4=0.6 and Kcp5=0.4), L: Irrigation plots length (10 m). W: Wetted area width (1.42 m). Infiltration rate of experimental soils was measured as 6.4 mm h^{-1} and dripper flow rate was chosen as 4 L h^{-1}. Dripper distance was calculated as 0.71 m from Papazafirou [32] method. If one lateral is located on pear tree rows of experimental plots, it cannot be reached minimum percent of wetted area being 30% for semi arid regions. For this reason, each of pear tree rows had two laterals in order to obtain a value of wetted area greater than the minimum wetted area percentage. Under these conditions, width and percentage of wetted area were 1.42 m and 31.6%. IAS applied the calculated irrigation water to the plots through digital water meter.

In order to be able to measure correctly soil moisture in the layers of 30 cm in pear rooting depth of 90 cm, the calibration equations were developed for soil moisture sensors (MAS-1) using by PLC before irrigation season. At block II, the three sensors were placed in depth of 15, 45 and 75 cm each treatment. The effective rooting of the pear tree was taken as 60 cm. For the plots, soil moisture was determined by the sensors' output substituted in calibration equation in the layers of 30 cm in the soil profile of 90 cm. The soil moisture sensors have input power 12-32 VDC and output 4-20 mA, which were developed in the reading standards for PLC, and runs according to dielectric constant of soil.

Evapotranspiration (ET) was calculated by IAS's program with the water balance equation (Eq. (2)) [33, 34, 35, 36].

$$ET = I + P + Dp \pm R_{off} \pm \Delta s \quad (2)$$

Where; ET is evapotranspiration (mm), I is the amount of irrigation water applied (mm), P is precipitation (mm), Δs is soil water content change (mm) in the 60 cm soil profile, Dp is deep percolation from pear effecting rooting depth (mm), and Rf is amount of runoff (mm). Since the amount of irrigation water was controlled, run off was assumed to be zero. In the depth of 60-90 cm soil layer, soil moisture content was measured using the sensors' calibration equations just before irrigation and one day after irrigation. Deep percolation from the effective rooting depth (0-60 cm) was determined subtracting the latter measurements from the former ones [37].

Water-use efficiency (WUE) and irrigation water-use efficiency (IWUE) values were calculated from the fruit yield divided by seasonal ET and total seasonal irrigation water, respectively [38, 39, 40].

Regression analysis was used to determine crop water production function for fruit yield versus I and ET [41, 42]. In addition, the fruit yield response factor (ky) was determined to quantify the relative yield reduction response to water supply (1-Ya/Ym) and relative evapotranspiration deficit (1-ETa/ETm) using the Steward Model [43, 44] (Eq. (3)):

$$\left(1-\frac{Ya}{Ym}\right)=ky\left(1-\frac{ETa}{ETm}\right) \quad (3)$$

Where; Ya is the actual harvested fruit yield (t ha^{-1}), Ym is the maximum harvested fruit yield obtained from treatment I_{120} (t ha^{-1}), ky is the yield response factor, ETa is the actual evapotranspiration (mm) and ETm is the maximum evapotranspiration (mm) associated with no plant water stress.

Shoot lengths were measured four times during the irrigation season on the tree marked branch of the pear three for each treatment.

Analysis of variance (ANOVA) was performed on fruit yields of the irrigation treatments [42].

RESULTS AND DISCUSSION

Irrigation Automation System (IAS). IAS successfully executed irrigation program, and controlled Class A Pan, water tank, all digital water meters, solenoid valves, fertilizer tank, and measured soil moisture content, and calculated irrigation water amount and ET. The other results of IAS were given below.

Soil Water Content, Irrigation Water and Evapotranspiration. To read soil moisture in the layers of 0-30, 30-60 and 60-90 cm, calibration equations were determined for experimental area soils using PLC and soil moisture sensors. These were

$Pv_{(0-30)}$=0.0035DD-24.16 (R^2=0.789), $Pv_{(30-60)}$=0.0037DD-22.13 (R^2=0.857) and $Pv_{(60-90)}$=0.0034DD-21.81 (R^2=0.802) (DD: Digital data of sensors, Pv: Volume basis soil moisture content). Soil moisture sensors, which run with dielectric constant of soil, are affected from bulk density, texture, soil chemical properties, roots, stones and noise. Calibration equations were also developed to be able to read correctly soil moisture content by Gencoglan [45] for neutron probe, Demirel [46] for FDR sensors, Gercek [47] for tensiometer and Varble and Chávez [48] for CS616/625, TDT and 5TE.

Soil moisture content (in depth units, mm) in layers of 30 cm in effective pear rooting of 60 cm was determined using soil moisture sensor just before irrigation during the irrigation season (Figure 2). As seen in Figure 2, soil moisture content changed between field capacity (291.3 mm) and wilting point (191.3 mm) in the pear effective rooting depth. In I_{120}, I_{100}, I_{80}, I_{60} and I_{40} irrigation treatments, soil moisture content ranged from 232.9 to 255.8, 220.6 to 253.6, 235 to 247.6, 230 to 248.9 and 198.0 to 227.9, respectively.

In the treatments, the measured soil moisture changed depending on the applied irrigation water amount, and in the effective rooting depth, the measured soil moisture decreased as the irrigation water amount declined [49]. Generally, the highest soil moisture was measured in I_{120} and the lowest in I_{40}. At the start of irrigation season, the soil moisture contents of the irrigation treatments were close to each other but to the end of the season, differences increased and was the lowest in the I_{40}.

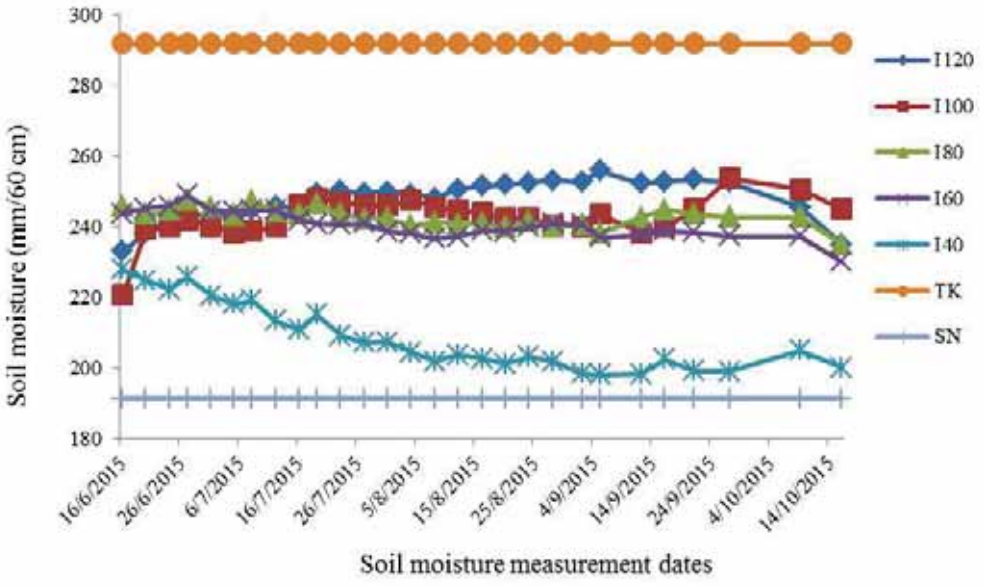

FIGURE 2
Soil moisture content in the irrigation treatments

Irrigation of Comice dwarf pear started on 16.06.2015 and with the start of leaves to turn yellow and ended on 09.10.2015. IAS measured totally evaporation of 1104 mm from Class A Pan during the irrigation period. In the first irrigation, amount of 52 mm irrigation water was applied to refill available water to the field capacity in the effective rooting depth of 60 cm. When total evaporation from Class A Pan was equal to or greater than 35 mm, IAS calculated amount of irrigation to be applied to I_{120}, I_{100}, I_{80}, I_{60} and I_{40} irrigation treatments. It started irrigations at 10:10 am and irrigated 27 times Comice dwarf pear. Irrigation interval changed between 3-12 days depending on climatic conditions [50]. In the second half of June, and July and August irrigation interval was 3-4 days, in September 3-6 days and in October increased to 12 days. In each irrigation, amount of water applied to I_{120}, I_{100}, I_{80}, I_{60} and I_{40} irrigation treatments varied between 62-40, 52-33, 42-26, 31-20 and 21-13 mm, respectively, and the irrigation treatments were applied totally 1314, 1104, 894, 683 and 473 mm water, respectively, depending on Kcp (Table 2). I_{120} and I_{40} treatment were received the highest water with 1314 mm and the lowest with 473, respectively.

Deep percolation (Dp) observed from effective pear rooting of 60 cm in I_{120}, I_{100}, I_{80} and I_{60} irrigation treatments, except I_{40}. These were calculated as 52, 76, 53 and 55, respectively. Net irrigation waters (Inw) for irrigation treatments were calculated as subtracting Dp from I and given in Table 2.

Kang et al. [20] applied irrigation water of 291, 223 and 141 mm to the pear trees using continuously surface irrigations and fixed partial root zone drying (FPRD) and alternative partial root zone drying (APRD), respectively. In another pear irrigation study, Kang et al. [10] applied irrigation water of 735, 682 and 522 mm using same irrigation techniques. In the former study by Kang at al. [20] the applied irrigation water was close to I_{40} treatment, which was applied the least water but in the latter study by Kang at al. [10] were close to I_{60}, which had the second lowest irrigation water. Differences in irrigation water, it may be from irrigation scheduling, irrigation techniques and climatic conditions.

Water consumption (ET) of pear, determined in the irrigation treatments, varied between 527 and 1287 mm (Table 2). Reduction in water use under deficit treatments varied between 19 and 114% according to full irrigation treatment (I_{120}). The lowest water use observed in I_{40} and the highest was in I_{120}.

Fruit Yield and Water Use Efficiencies. Results of the variance analysis indicated that the effect of different irrigation water levels on pear fruit yield harvested from the irrigation treatments was determined not to be statistically significant ($P>0.05$). In the irrigation treatments, the highest fruit yield was obtained from I_{120} plots, averaging 15.3 t ha^{-1}, followed by fruit yields for the I_{80}, I_{100}, I_{60} and I_{40} plots. Minimum yield was harvested from the I_{40} treatment, averaging 9.8 t ha^{-1} (Table 2). Even though irrigation amounts related to crop-pan coefficients did not significantly affect pear yield, increasing irrigation amounts did yield more. Although the number of fruits is the highest in I_{40} irrigation treatment (averaging 20 fruit per tree) than the other treatment's (averaging I_{120}=19, I_{100}=16, I_{80}=17 and I_{60}=15), the yield per hectare is low due to the water stress reducing the fruit weight. A similar result was determined by Marsal et al. [18] in pear trees. In their study, application different amount of water by drip irrigation to pear tree, no differences were found statistically among the yield, and fruit number and size. In another study by Marsal et al. [17], it was reported that water stress decreased the fruit size. O'Connell and Goodwin [22] notified that the high water deficit contributed to water savings, but significantly reduced the yield.

IWUE and WUE were calculated for irrigation treatments. The highest IWUE and WUE were found for the I_{40} treatment (0.4 Kcp) with 2.1 kg m^{-3} and 1.9 kg m^{-3}, respectively, and were lowest in treatments I_{100} and I_{120} (0.4 and 1.2 Kcp) with 1.2 kg m^{-3} and 1.2 kg m^{-3}, respectively (Table 2). As seen in Table 2 there was an increasing trend in IWUE and WUE with decreasing applied irrigation water. Kang et al. [20] found that PRD technique increased the water use efficiency in pear tree. Zhao et al. [8] obtained the highest water use efficiency with 3.02 kg m^{-3} in drip irrigated pear at 32% wetting rate.

TABLE 2
Irrigation water, evapotranspiration, fruit yield and water use efficiency

Irrigation Treatments	*I (mm)*	*Dp (mm)*	*Inw (mm)*	*ET (mm)*	*Yield (ton ha^{-1})*	*IWUE (kg m^{-3})*	*WUE (kg m^{-3})*
I_{120}	1314	52	1262	1287	15.3	1.2	1.2
I_{100}	1104	76	1028	1046	12.5	1.2	1.2
I_{80}	894	53	841	869	12.6	1.5	1.5
I_{60}	683	55	628	669	11.3	1.8	1.7
I_{40}	473	0	473	527	9.8	2.1	1.9

Net irrigation water (Inw).

As mentioned above, since there is no statistically difference among the five irrigation treatments and if irrigation water is scarce, I_{40} and I_{60} irrigation treatments can be recommended to the pear producers, and also, both irrigation treatments' Kcp could be taken into account in the irrigation scheduling. On the other hand, if it is abundant and labor is cheap, the I_{120}, I_{100} and I_{80} irrigation treatments can be suggested to them, and theirs Kcp could be considered in the scheduling.

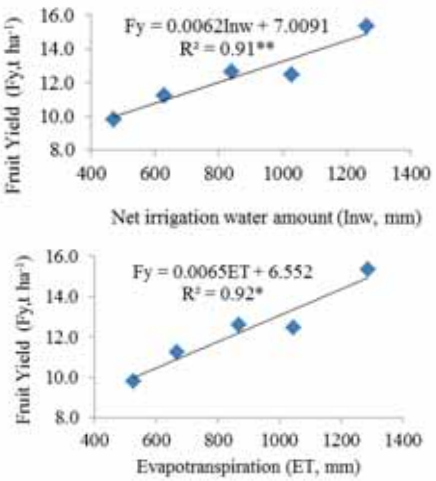

FIGURE 3
Relationships between irrigation water and evapotranspiration versus pear yield

Water-Yield Relationship. Significant linear relationships were established between the applied net irrigation water (Inw, mm) and evapotranspiration (ET, mm) versus pear yield for the irrigation treatments ($P < 0.01$) (Figure 3). The relationships' were Fy = 0.0062Inw + 7.0091(R^2 = 0.91**) and Fy = 0.0065ET + 6.552 (R^2 = 0.92**, respectively. The equations' slope and intercept were close to each other since deep percolation, resulted from irrigations, considered. In parallel with increased Inw and ET, an increase in the yield was observed as well. From the equations', an 100 mm increase in Inw or ET, about 0.6 kg increase in pear fruit yield was resulted. Similar linear results were found by a number of researchers. For example, Kırac [51] and Kırac [52] determined linear relationships in "Mondial Gala" and "Red Chief" study, respectively and Senyigit [40].

Slope of the relationships between relative pear fruit yield reduction and relative evapotranspiration deficit, termed ‘‘yield response factor (ky)’’ by Doorenbos and Kassam [44], was found to be 0.6 for Comice pear variety (Figure 4). If ky is greater than 1, it is reported that such plants are sensitive to irrigation water and that ky <1 is not sensitive [44]. According to these results, Comice pear is generally not sensitive to irrigation water. A 1% decrease in ET caused a 0.6% decrease in yield. Doorenbos and Kassam [44] indicated that plants had different ky values. In this context, it is not possible to compare pear's ky values with the value of the other trees.

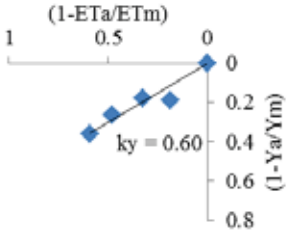

FIGURE 4
The relationship between relative yield decrease and relative evapotranspiration deficit for Comice Pear

Shoot Length. The average shoot lengths measured in irrigation treatments were given in Figure 5. As seen in Figure 5, there was not much change in the slope of the shoot elongation lines during irrigation season. These measurements showed that the amount of irrigation water applied at different levels had no effect on the shoot length. In other words, there was no the shoot extension in the treatments in the irrigation season. Shoot extension occurs during the second and fourth growth stages [53]. These two growth stages are outside the irrigation season. For this reason, shoot extension cannot be considered as criteria of irrigation timing for Comice Pear. Zhao et al. [8] determined that in pear trees aged 24 years old, the shoot length significantly was reduced by drip irrigation method.

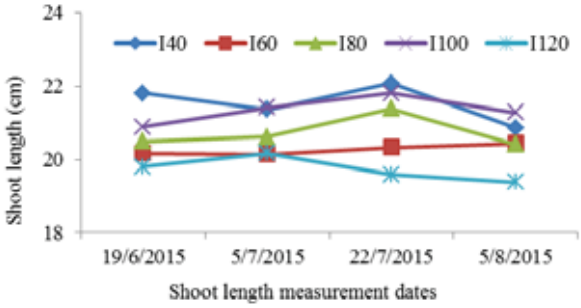

FIGURE 5
Shoot length measurements in the irrigation treatments

CONCLUSIONS

The irrigation frequency changed between 3-12 days depending on climatic conditions. In the irrigation treatments, linear relationships were established between the total applied net irrigation water and evapotranspiration versus pear yield, and yield decreased with the increasing water deficit and conversely, values of IWUE and WUE increased. Irrigation scheduling based on a 0.4 and 0.6 crop-pan coefficients and their treatments are recommended to the pear producers experiencing water shortage. Under abundant water conditions, I_{120}, I_{100} and I_{80} crop-pan coefficients and treatments are also suggested. The pear producers should not consider that the shoot length of Comice Pear take as irrigation timing criteria. In addition, the result of study also showed that IAS could be used to control drip irrigation system, Class A Pan, irrigation scheduling, and to calculated ET and to measure soil moisture.

ACKNOWLEDGEMENTS

The research was funded by the Scientific and Technological Research Council of Turkey (TUBITAK), TUBITAK Project No:213O097.

REFERENCES

[1] Sammis, T.W. (1981) Yield of Alfalfa and Cotton as Influenced by Irrigation. J. Agron. 73, 323-329.

[2] Howell, T.A., Musick, J.T. (1984) Relationship of Dry matter production of field crops to water consumption. Proc. Int. Con. on Crop Water Requirements, Paris. 11-14. September 1984.

[3] Barrett, J.W.H., Skogerboe, G.V. (1978) Effect of irrigation regime on maize yields. J. Irrig. Drain. Div. Am. Soc. Civ. Eng. 104,179-193.

[4] Zhang, H., Oweis, T. (1999) Water–yield relations and optimal irrigation scheduling of wheat in the Mediterranean region. Agric. Water Manage. 38, 195-211.

[5] Fernández, J.E., Cuevas, M.V. (2010) Irrigation scheduling from stem diameter variations: a review. Agric. For. Meteorol. 150, 135-151.

[6] Han, L.X., Wang, Y.K., Li, X.B., Zhang, P. (2012) Improved irrigation scheduling for pear-jujube trees based on trunk diameter sensing data. Arf. J. Biotechnol. 11, 1597-1606.

[7] Chen, C., Roseberg, R.J., Sugar, D., Selker, J.S. (2001) Effect of micro sprinkler irrigation on pear fruit growth and post harvest quality. Hort. Technology, 11, 56-61.

[8] Zhao, Z., Wang, W., Wu, Y., Huang, X. (2012) Yield and water use efficiency of pear trees under drip irrigation with different surface wetted percentages, Int. J. Agric. Biol. 14, 887-893.

[9] Zhi, Z., Xingfa, H., Yang, W., Wei, W. (2011) Response of fragrant pear growth to different micro-irrigation conditions. In 8th International Micro Irrigation Congress. 21 October 2011, Tehran, Iran, 138-146.

[10] Kang, S., Hu, X., Du, T., Zhang, J., Jerie, P. (2003) Transpiration coefficient and ratio of transpiration to evapotranspiration of pear tree (*Pyrus* communis) under alternative partial-root-zone drying conditions. Hydrol Process. 17, 1165–1176.

[11] Girona, J., Marsal, J., Mata, M., Del Campo, J. (2003) Pear crop coefficients obtained in a large weighing lysimeter. In: Snyder R.L. (Eds.) IV International Symposium on Irrigation of Horticultural Crops, 664, 277-281.

[12] Ramos, D.E., Weinbaum, S.A., Shackel, K.A., Schwankl, L.J., Mitcham, E.J., Mitchell, F.G., McGourty, G. (1993) Influence of Tree Water Status and Canopy Position on Fruit Size and Quality of Bartlett Pears. In: Sugar D., (Eds.), VI International Symposium on Pear Growing. 3, 192-200.

[13] Costa, J.M., Ortuño, M.F., Chaves, M.M. (2007) Deficit irrigation as a strategy to save water: physiology and potential application to horticulture. J. Integr. Plant Biol. 49, 1421-1434.

[14] Wang, Y., Travers, S., Bertelsen, M.G., Thorup-Kristensen, K., Petersen, K.K., Liu, F. (2014) Effect of root pruning and irrigation regimes on pear tree: growth, yield and yield components. Sci. Hortic. 41, 34-43.

[15] Zhao, Z., Wang, W., Wu, Y., Xu, M., Huang, X., Ma, Y., Ren, D. (2015) Leaf physiological responses of mature pear trees to regulated deficit irrigation in field conditions under desert climate. Sci. Hortic. 187, 122-130.

[16] Fereres, E., Soriano, M.A. (2006) Deficit Irrigation for Reducing Agricultural Water Use. J. Exp. Bot. 58, 147-159.

[17] Marsal, J., Rapoport, H.F., Manrique, T., Girona, J. (2000) Pear fruit growth under regulated deficit irrigation in container-grown trees. Sci. Hortic. 85, 243-259.

[18] Marsal, J., Mata, M., Arbonés, A., Rufat, J., Girona, J. (2002) Regulated deficit irrigation and rectification of irrigation scheduling in young pear trees: an evaluation based on vegetative and productive response. Eur. J. Agron. 17, 111–122.

[19] Cui, N., Du, T., Kang, S., Li, F., Zhang, J., Wang, M., Li, Z. (2008) Regulated deficit irrigation improved fruit quality and water use efficiency of pear-jujube trees. Agric. Water Manage. 95, 489-497.
[20] Kang, S., Hu, X., Goodwin, I., Jerie, P. (2002) Soil water distribution, water use, and yield response to partial root zone drying under shallow ground water table condition in a pear orchard. Sci. Hortic. 92, 277-291.
[21] Gong, D., Kang, S., Zhang, J. (2005) Responses of canopy transpiration and canopy conductance of peach (Prunus persica) trees to alternate partial root zone drip irrigation. Hydrol Process. 19, 2575-2590.
[22] O'Connell, M.G., Goodwin, I. (2007) Water stress and reduced fruit size in micro-irrigated pear trees under deficit partial rootzone drying. Aust. J. Agric. Res. 58, 670-679.
[23] Abrisqueta, J.M., Mounzer, O., Alvarez, S., Conejero, W., García-Orellana, Y., Tapia, L. M., Ruiz-Sánchez, M. C. (2008) Root dynamics of peach trees submitted to partial rootzone drying and continuous deficit irrigation. Agric. Water Manage. 95, 959-967.
[24] Oron, G., DeMalach, Y., Gillerman, L., David, I., Lurie, S. (2002) SW-soil and water: effect of water salinity and irrigation technology on yield and quality of pears. Biosyst Eng. 81, 237-247.
[25] Okubo, M., Furukawa, Y., Sakuratani, T. (2000) Growth, flowering and leaf properties of pear cultivars grafted on two Asian pear rootstock seedlings under NaCl irrigation. Sci. Hortic. 85, 91-101.
[26] Kanber, R., Unlu, M. (2010) Water and soil salinity in agriculture. C.U., Faculty of Agriculture, Publication No: 281, Book Publication No: A-87, Adana (In Turkish).
[27] Gencoglan, C., Gencoglan, S. (2016a) Measuring the water head in the pan evaporation using the pressure transducer and the programmable logic controller (PLC). Uludag Uni., Agric. Faculty Journal, 30, 35-43 (In Turkish).
[28] Doorenbos, J. Pruitt, W.O. (1977) Crop Water Requirements. Irrigation and Drainage Paper, 24.
[29] Gencoglan, C., Gencoglan, S., Ucak, A.B. (2015) Development of a system for measuring soil hydraulic conductivity using a programmable logic control (PLC) and a pressure transducer. International Congress on Soil and Water Resources. 1-3 September 2015 Kahramanmaras (In Turkish).
[30] Gencoglan, C., Gencoglan, S. (2016b) Development of irrigation automation system (IAS) using by programmable logic controller (PLC) and its application on irrigation scheduling created using Class A Pan. In: Kovacevic, D. (Eds.) VII. International Scientific Agriculture Symposium, Agrosym 2016, 6-9 October 2016, Jahorina, Bosnia and Herzegovina. Proceedings, 1823-1828.
[31] Gencoglan, C., Altunbey, H., Gencoglan, S. (2006) Response of green bean (P. Vulgaris L.) to subsurface drip irrigation and partial root-zone-drying irrigation. Agric. Water Manage. 84, 274-280.
[32] Papazafirou, Z.G. (1980) A Compact Procedure for Trickle Irrigation System Design. ICID Bulletin. 29(1), 28-36.
[33] Garrity, P.D., Watts, D.G., Sullivan, C.Y., Gilley, J. R. (1982) Moisture deficits and grain sorghum performance: evapotranspiration–yield relationships. Agron. J. 74, 815–820.
[34] James, D.W., Hanks, R.J., Jurinak, J.J. (1982) Modern irrigation soils. John Wiley and Sons, New York.
[35] Beyce, O., Madanoglu, K., Ayla, C. (1972) Water statistics for some irrigated crops grown in Turkey. Central Soil Water Research Institute Publications, General Publication No: 15, Technical Publication No: 12 (In Turkish).
[36] Howell, T.A., Musick, J.T., Tolk, J.A. (1986) Canopy Temperature of irrigated winter wheat. Trans The ASAE, 29, 1692-1698.
[37] Kırda, C. (1999) With water budget method, plant water consumption studies. In: Kanber, R., Steduto, P. (Eds.) The Methodology used in determination of plant water consumption: Review and Evaluation, Adana, Turkey. 85-103 (In Turkish).
[38] Tanner, C.B., Sinclair, T.R. (1983) Efficient water use in crop production: research or research? In: Taylor, H.M., Jordan, W.R., Sinclair, T.R. (Eds.) Limitations to Efficient Water Use in Crop Production. ASA, Madison, WI, 1–27.
[39] Howell, T.A., Cuenca, R.H., Solomon, K.H. (1990) Crop yield response. In: Hoffman, G.J., Howell, T.A., Solomon, K.H. (Eds.), Management of Farm Irrigation Systems. ASAE, St. Joseph, MI.
[40] Senyigit, U., Kadayifci, A., Uysal, F.O. (2018) Response of 'Jersey Mac' apple trees grafted on M9 rootstock to deficit irrigation under transition zone in west Anatolia. Fresen. Environ. Bull. 27, 2567-2573.
[41] Yurtsever, N. (1984) Experimental statistical methods. Ministry of Agriculture, Forestry, General Directorate of Rural Affairs Publications, Ankara (In Turkish).

[42] Bek, Y., Efe, E. (1987) Research and Experimental Methods I. C.U. Faculty of Agriculture, Publication No. 71. Adana (In Turkish).
[43] Stegman, B.A., Hanks, R.J., Musick, J.T., Watts, D.G. (1981) Irrigation water management-adequate or limited water irrigation. In: Challenges at the 80's, Proceeding of the ASAE Second National Irrigation Symposium, University of Nebraska, Pub. ASAE, St. Joseph, MI, 20–23 October 1980, 154–165.
[44] Doorenbos, J. Kassam, A.H. (1979) Yield response to water. FAO Irrigation and Drainage Paper, Roma, Italy.
[45] Gencoglan, C. (1996) Determining the water production function, root distribution and crop water stress index of maize and validation of CERES maize crop growth model under Cukurova. PhD Thesis. Cukurova University, Graduate School of Natural and Applied Sciences, Adana (In Turkish).
[46] Demirel, K., Camoglu, G., Akcal, A. (2018) Effects of water stress on four varieties of Gladiolus. Fresen. Environ. Bull. 27, 9300-9307.
[47] Gercek, S. (1991) A study on the calibration curves of neutronmeter, tensiometer and nylon blocks used in the determination of soil moisture content under Harran Plain conditions. M.Sc. Thesis. Cukurova University, Graduate School of Natural and Applied Sciences, Adana (In Turkish).
[48] Varble, J.L., Chávez, J.L. (2011) Performance evaluation and calibration of soil water content and potential sensors for agricultural soils in eastern Colorado. Agric. Water Manage. 101, 93–106.
[49] Ucak, A.B., Gencoglan, C., Bagdatli, M.C., Turan, N., Arslan, H., Inal, B. (2016) Determination of water-efficiency relationships and silage quality characteristics of the maize species for silage (Zea Mays L.) The First Product Grown Under Semi-Arid Climate Conditions, Fresen. Environ. Bull. 25, 6053-6068.
[50] Allen, R.G., Pereira, I.S., Raes, D., Smith, M. (1998) Crop Evapotranspiration (Guidelines for Computing Crop Water Requirements). FAO Irrigation and Drainage Paper No. 56. Rome, Italy.
[51] Kırac, A.M. (2007) Effect of deficit irrigation and partial root drying irrigation techniques on some development parameters of dwarf apple. Ms. Sc. Thesis. Kahramanmaras Sutcu Imam University, Graduate School of Natural and Applied Sciences, Kahramanmaras (In Turkish).
[52] Kırac, A.M. (2016) Effects of the deficit and partial root drying irrigation techniques on 'red chief' apple trees grafted on MM 106 rootstock. PhD Thesis. Kahramanmaras Sutcu Imam University, Graduate School of Natural and Applied Sciences, Kahramanmaras (InTurkish).
[53] Rendell McGuckian Consulting Group. (2017) Guidelines for Irrigation Management for Apple & Pear Growers http://apal.org.au/wp-content/uploads /2013/04/Apple_pear_ guidelines_ Irrigation_ Management.pdf

Received: **04.05.2018**
Accepted: **22.02.2019**

CORRESPONDING AUTHOR

Cafer Gencoglan
University of Kahramanmaras Sutcu İmam,
Faculty of Agriculture,
Department of Biosystem Engineering,
46060 Kahramanmaras – Turkey

e-mail: gencoglan@ksu.edu.tr

© by PSP Volume 28 – No. 4/2019 pages 2442-2449 Fresenius Environmental Bulletin

PRESENCE OF CUCURBIT VIRUSES IN ANKARA AND ANTALYA PROVINCE AND MOLECULAR CHARACTERIZATION OF COAT PROTEIN GENE OF *ZUCCHINI YELLOW MOSAIC VIRUS* TURKISH ISOLATES

Serife Topkaya[1,*], Cecile Desbiez[2], Filiz Ertunc[3]

[1]Gaziosmanpasa Universty, Faculty of Agriculture, Department of Plant Protection, 60000 Tokat, Turkey
[2]INRA, UR407 Pathologie Végétale, Domaine Saint Maurice, F-84143 Montfavet, France
[3]Ankara University, Faculty of Agriculture, Department of Plant Protection, 061100 Ankara, Turkey

ABSTRACT

Cucurbits are widely grown vegetables in different provinces of Turkey. However their production is restricted by pests and pathogens including different plant viruses, among which *Zucchini yellow mosaic virus* (ZYMV) is particularly damaging. Infections by this virus during the early stages of plant development causes deformation of fruits and significant yield losses. During 2009-2014, 221 cucurbits samples were collected from fields and greenhouses from different provinces of Turkey. Serological testing was performed by double antibody sandwich enzyme-linked immunosorbent assay (DAS-ELISA) for presence of *Watermelon mosaic virus* (WMV), ZYMV, *Cucumber mosaic virus* (CMV), *Papaya ring spot virus* (PRSV), *cucumber green mottle mosaic virus* (CGMMV) and *Squash mosaic virus* (SqMV). For molecular analaysis of ZYMV, full-length CP nucleotide sequences were obtained for 45 ZYMV isolates and compared with sequences from worldwide isolates available in databases. The CP coding regions of Turkish ZYMV were 837 nt long and encoded 279 amino acids (aa). Forty two isolates from different regions were classified in the molecular subgroup A1, the most frequent in the Mediterranean Basin, Europe and Africa. Three isolates collected from Antalya region were classified in subgroup A4 and showed 99 % sequence identity with isolates from the same subgroup that have emerged recently in France.

KEYWORDS:
Coat protein, Cucurbit viruses, Molecular variability, *Zucchini yellow mosaic virus*

INTRODUCTION

Vegetable production has a great economic importance in Turkey. According to the FAO (2014), vegetable cultivated area is 808.000 hectares with a production of 28.448.118 tons [1]. The southern part of Turkey, especially Antalya province, is the main and most intensive vegetable-growing area. However cucurbit production is restricted by different plant virus infections. *Zucchini yellow mosaic virus* (ZYMV) is one of the most economically important viruses of cucurbit crops worldwide, including in Turkey [2, 3, 4]. ZYMV was first isolated from a zucchini squash plant in Northern Italy in 1973 [2, 5] and was later reported as a major cucurbit virus in the world. The virus causes very severe mosaic, mottling, deformations on leaves and fruits of the infected cucurbit plants [2, 6] and affects the yield and quality of the crops: infected plants are reduced in-size and their fruits are often deformed and unmarketable. One of the main features of ZYMV is the great biological variability among strains whereby differences in host range as well as symptoms severity can be expected [7].

ZYMV is a member of the genus *Potyvirus* in the family *Potyviridae.* It has a positive sense-single stranded RNA of about 9.5 kb [8]. So far, more than 500 ZYMV sequences are available in GenBank, mostly CP-coding regions. Three major molecular groups of ZYMV have been defined in the World, namely Group A, Group B, and Group C. Group C contains isolates from Vietnam and China, Group B was observed in Reunion Island and in Australia, whereas Group A is present worldwide [7,9]. Within Group A, three clusters (clusters 1–3) were originally defined [10], and three others, namely clusters 4–6, containing mostly isolates from China and Korea, were distinguished later when the number of sequences available increased [9]. In the Mediterranean Basin, cluster A1 was observed in France since 1979, as well as in Spain, Portugal, Tunisia, Turkey, Israel, Syria, and Jordan [7, 10]; cluster A2 was observed in Italy since 1973 [10],Tunisia [11], Jordan and France since 1979; cluster A3 was detected in Spain and South-eastern France. In addition to these three clusters, surveys have revealed the presence of clusters 4 and 5 insouth-eastern France since 2004, probably in relation to recent

introductions, and their current emergence in that area [7].

In Turkey, Turkish ZYMV isolates cluster A1 was reported from Adana and Mersin provinces [10, 12, 13]. Whether other clusters are also present in Turkey remains unknown. The aim of this research was thus to characterize the molecular variability of ZYMV Turkish isolates and investigate the presence of emerging strains.

MATERIALS AND METHODS

Collection of virus isolates. During the years 2010-2014, a total of 221 samples were collected from cucurbit plants (squash, pumpkin, cucumber, melon and watermelon) from Ankara (Nallıhan, Beypazarı, Cubuk, Sereflikochisar, Gölbası, Kazan, Ayaş, Ankara University (AUZF) and Antalya (Kumluca, Demre, Elmalı, Serik, Aksu) provinces of Turkey. Surveys were conducted in Ankara province at open fields during the summer seasons in 2010-2014 and the samples from Demre, Kumluca, Aksu, Serik districts were collected from greenhouse- grown cucurbits in winter in 2011-2012. Antalya-Elmalı samples were collected from open fields in 2010-2014 summer time.

Samples were collected from plants showing severe systemic mosaics, vein banding, stunting, blister, and deformations on fruits and leafs of infected plants. Major simptoms of melon were mottling, leaf deformation and samples collected from greenhouses in Demre, Aksu, Serik and Kumluca districts showed mosaic, stunting and yellowing symptoms on leaf and mottling on fruit, blistering of leaf and mottling on fruits on squash.

DAS-ELISA test. All collected samples were tested by double antibody sandwich enzyme-linked immunosorbent assay (DAS-ELISA) [14] for the presence of ZYMV and other viruses: *Cucumber mosaic virus* (CMV, *Cucumovirus*), *Watermelon mosaic virus* (WMV, *Potyvirus*), *Papaya ringspot virus* (PRSV, *Potyvirus*), *Cucumber green mottle mosaic virus* (CGMMV, *Tobamovirus*) and *Squash mosaic virus* (SqMV, *Comovirus*). The test was applied according to manufacturer's instructions (Loewe Biochemica GmbH-GERMANY). Absorbance values were measured at 405 nm using an ELISA reader. The examples used as a positive control were provided from antisera manufacturer's and healthy cucurbit plants were used as negative control. All samples were tested in duplicates. The samples with absorbance value two to three times higher than the negative control were considered to be infected.

Molecular characterization of ZYMV isolates. RNA extraction and RT-PCR amplification. Total RNAs were extracted from samples of ZYMV-infected plants modified the protocol described by Astruc et al. [15]. Forty-five samples were selected from different hosts and geo-graphic locations. Thirty–three samples were cho-sen from collected samples during the surveys and nine ZYMV isolates added from Konya, Karaman and Aksaray, collected in 2009-2010, were supplied by Dr. Serkan Yesil (Selcuk University, Agricultural Faculty, Plant Protection Department). Three samples collected from only one field in Burdur province for moleculer analysis in 2014.

Total RNA extraction was made according to Astruct et al. [15]. For the complementary DNA synthesis (cDNA), a mix of 2 µl total RNA, 1µl random hexamer primer (5'-d(NNNNNN)-3'N = G, A, T or C)(10µ) and 8 µl distilled water were heated at 65°C for 5 min then stored on ice for 3 min before being added to the reverse transcription mix: 4µl MMLV buffer (5X), 0,2 mM dNTP (25 mM), 0,25 µl RNAse inhibitor (10u/µl), 0,25 µl MMLV (Reverse transcriptase- (Thermo Fisher Scientific)(20-20u/µl) and distilled water in a final volume of 20µl. The mix was incubated for 5 minute at 25 ºC, 1 h at 37 ºC and 10 minute at 72 ºC in a Biometra T1 Thermocycler.

PCR reactions were carried out in a volume of 25 µl containing 2,5 µl of cDNA, 10 pmol each primer ZYCP-F 5'-AGAGGCTATYTGCGCTGC-3' and ZYCP-R 5'- TAAAGCTTCCGACAGG-ACTAC-3' [16] 10 mm dNTPs, 1,5mM $MgCl_2$ and 2,5u Taq DNA polymerase (Promega). The primer pair amplifies a nucleotide segment of 1260 bp including partial NIb gene, full CP gene and 3′-NCR. PCR conditions are a first denaturation at 94°C for 5 min, followed by 35 cycles of 94°C for 30 sec, 55°C for 45sec and 72°C for 30 sec, and a final elongation step at 72°C for 7 [16]. The PCR products were visualized by electrophoresis on 1,2% agarose gel and investigated by gel imaging system of Sygene (UK), before being sent for direct sequencing with forward and reverse primers to GENOKS company (Turkey).

Sequence comparisons and phylogenetic analysis. The sequences obtained with forward and reverse primers were assembled with CAP3 software [17]. Complete CP-coding sequences of ZYMV isolates were compared to those of reference isolates belonging to the main ZYMV molecular groups as defined by Lecoq and Desbiez [7]. CP nucleotide sequences were aligned with those of reference isolates (Table 2) with ClustalW included in MEGA 6 [18]. Pairwise distances between isolates (p-distances) were calculated with MEGA 6. CP nucleotide sequences were submitted to GenBank (Table 1).

Host, isolate name, georaphical origin, year of collected samples and accession number of ZYMV isolates are shown in the Table 1.

TABLE 1
List and accession numbers of GenBank ZYMV isolates selected for molecular study

Number	Isolate name	Host	Year collected	Geographical origin	Acsession number
Seq1	KZN1	*Cucurbita sp*.	2010	Ankara-Kazan	KP872538
Seq2	KZ1	*Cucurbita sp*.	2010	Ankara-Kazan	KP872539
Seq3	AKS2-5	C. moschata	2010	Aksaray	KP872540
Seq4	AKS5-7	*Cucurbita pepo L*	2009	Aksaray	KP872541
Seq5 q5	AKS6-2	*Cucurbita pepo L*	2009	Aksaray	KP872542
Seq6	ER6-8	*Cucurbita pepo L*	2009	Konya-Ereğli	KP872543
Seq7	YUN8-4	*Cucurbita pepo L*	2010	Konya-Yunak	KP872544
Seq8	A3-1	*Cucurbita pepo L*	2010	Konya	KP872545
Seq9	KAR12-4	*Cucurbita pepo L*	2010	Karaman	KP872546
Seq10	KAR15-1	*C. moschata*	2010	Karaman	KP872547
Seq11	AS1	*Cucurbita sp.*	2012	Antalya-Aksu	KP872548
Seq12	AS5	*Cucurbita sp.*	2012	Antalya-Aksu	KP872549
Seq13	AS6	*Cucurbita sp.*	2012	Antalya-Aksu	KP872550
Seq14	AS8	*Cucurbita sp.*	2012	Antalya-Aksu	KP872551
Seq15	AS11	*Cucurbita sp.*	2012	Antalya-Aksu	KP872552
Seq16	BE5	*Cucurbita sp.*	2014	Ankara-Beypazarı	KP872553
Seq17	BE6	*Cucurbita sp.*	2014	Ankara-Beypazarı	KP872554
Seq18	BE7	*C. moschata*	2014	Ankara-Beypazarı	KP872555
Seq19	BE10	*Cucurbita sp.*	2014	Ankara-Beypazarı	KP872556
Seq20	BE13 m	*Cucurbita sp.*	2014	Ankara-Beypazarı	KP872557
Seq21	BE15	*Cucurbita sp.*	2014	Ankara-Beypazarı	KP872558
Seq22	BE18	*Cucurbita sp.*	2014	Ankara-Beypazarı	KP872559
Seq23	BE22 m	*Cucurbita sp.*	2014	Ankara-Beypazarı	KP872560
Seq24	BE26 m	*Cucurbita sp.*	2014	Ankara-Beypazarı	KP872561
Seq25	BE27 m	*Cucurbita sp.*	2014	Ankara-Beypazarı	KP872562
Seq26	BRD1	*C. moschata*	2014	Burdur	KP872563
Seq27	BRD2	*C. moschata*	2014	Burdur	KP872564
Seq28	BRD4	*C. moschata*	2014	Burdur	KP872565
Seq29	C5	*C. moschata*	2011	Ankara- Çubuk	KP872566
Seq30	C11	*C. moschata*	2011	Ankara- Çubuk	KP872567
Seq31	C13	*C. moschata*	2011	Ankara- Çubuk	KP872568
Seq32	C17	*Cucumis melo L.*	2011	Ankara- Çubuk	KP872569
Seq33	H1M m	*Cucumber*	2012	Antalya- Demre	KP872570
Seq34	D14	*Cucumber*	2014	Antalya- Demre	KP872571
Seq35	AYS7	*Cucurbita sp.*	2013	Ankara-Ayaş	KP872572
Seq36	G1 m	*Cucurbita sp.*	2011	Ankara-Gölpazarı	KP872573
Seq37	G2	*Cucurbita sp.*	2011	Ankara-Gölpazarı	KP872574
Seq38	G3	*Cucurbita sp.*	2011	Ankara-Gölpazarı	KP872575
Seq39	K3 m	*Cucurbita sp.*	2012	Antalya-Kumluca	KP872576
Seq40	K17	*Cucurbita sp.*	2012	Antalya-Kumluca	KP872577
Seq41	E-7	*Cucumis melo L.*	2012	Antalya-Elmalı	KP872578
Seq42	Y23	*Cucurbita sp.*	2012	Antalya-Elmalı	KP872579
Seq43	Y4	*Cucumis melo L.*	2012	Antalya-Elmalı	KP872580
Seq44	S5	*Cucurbita sp.*	2012	Ankara-Şereflikoçhisar	KP872581
45	Y21 m	*Cucurbita sp.*	2012	Antalya- Elmalı	MG214089

m: Fruit samples

TABLE 2
Accession number of reference isolates

Referance name	Acsession number	Group	Country
ZYMV KUCHYNA	DQ124239	A1	Slovakia
ZYMV-NAT	EF062582	A1	Israel
ZYMV-FARS	JN183062	A1	Iran
ZYMV- H	KF976712	A1	Czech Republic
ZYMV-ADANA	JF317296	A1	Turkey
VE10-160	JX310115	A1	Venezuela
VE10-129	JX310103	A1	Venezuela
ZYMV –AHLAT	JF317297	A1	Turkey
TN TNV CUCU 2	KJ866939	A1	India
ZYMV-Iraq	JQ026020.1	A1	Iraq
ZYMV-California	L31350	A2	California
ZYMV_PA_2006	JQ716413	A2	USA
MAL	HM005308	A2	Mali
Florida	D13914.1	A3	USA
ZYMV C-16	DQ645729.1	A3	Spain
ZYMV-Liaocheng	EF122498	A4	China
ZYMV-CO5-205	JN861008	A4	France
ZYMV-Shangyu	AF513550	A4	China
ZYMV-CH99/116	AY611021	A4	China
ZYMV-KR-PE	AY278999	A5	Korea
ZYMV-KR-PS	AY279000	A5	Korea
ZYM-KR-PA	AY278998	A5	Korea
ZYMV-RDA	AB369279	A5	South Korea
TW-TN3	AF127929	A6	Taiwan
Strain A	AJ429071	A6	Korea

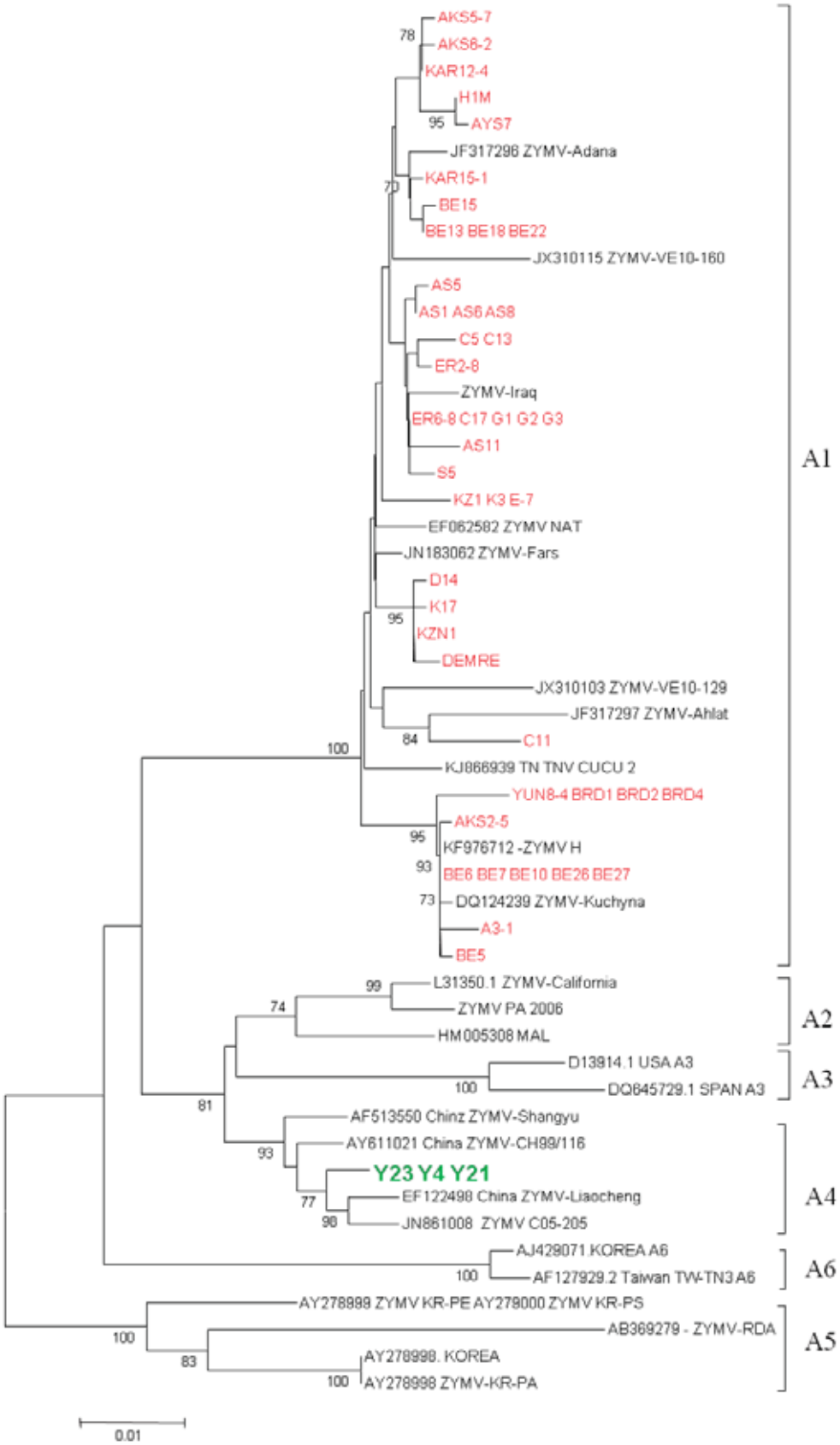

FIGURE 1
Neighbor-joining tree obtained from CP-coding region (837 nt)of the 45 Turkish ZYMV isolates from this study and 15 ZYMV sequences from worldwide origins belonging to molecular group A. Bootstrap support (1000 bootstraps) above 70% are indicated for each node. The scale bar represents a genetic distance of 0.01.

RESULTS

Presence of cucurbit viruses. A total of 217 samples were collected in Ankara (117 samples) and Antalya (100 samples) province and samples tested with DAS-ELISA for presence cucurbit viruses. According to ELISA results, 38% of the 217 samples collected between 2010 and 2014 were infected with ZYMV. Most samples were also infected with other viruses: 46% WMV, 15 % CMV, 9% PRSV, 8% CGMMV, 3% SqMV. In Antalya province, the collected samples were infected with WMV (39%), ZYMV (27%), CMV (17%), CGMMV (%2). SqMV and PRSV were not detected in samples from the Antalya province. The most occurence virus was WMV (39) %followed by ZYMV (27%) and CMV (17%).

In Ankara province, 117 samples were tested and 96 were found to be infected with the investigated viruses (82%). All tested viruses were detected in single or in mixed infection in Ankara province. All viruses were detected with different percentages on collected samples: the collected samples were infected with WMV (53%), ZYMV (50%), CMV (14%), SqMV (5%), PRSV (15%), CGMMV (15%). The most infection rate of WMV was determined in AUZF followed by Cubuk and Beypazari districts. WMV was the most prevalent virus detected in samples (46%) followed by ZYMV in 82 samples (38%). The most prevalent viruses in Antalya and Ankara provinces are WMV and ZYMV.

Molecular diversity and phylogenetic analysis. RT-PCR amplification of 45 isolates from different Turkish provinces yielded a fragment of 1260 nt, encompassing part of the Nib coding region, the coat protein and part of the 3' non coding region. The CP coding regions of all Turkish ZYMV isolates were 837 nt long and encoded 279 amino acids (aa) (GenBank accessions KP872538- KP872581; Table 1). When ZYMV CP aminoacid sequences were analysed, the highly conserved amino acid triplet Asp-Ala-Gly (DAG), essential for aphid transmission [19] was found at the N-terminal part of the coat protein of all Turkish isolates.

Sequence comparisons among the 45 isolates revealed the presence of two clusters of sequences. The first cluster contained CP sequences from 42 isolates from Ankara, Burdur, Aksaray and Konya provinces that shared 98-99% identity between each other, as well as 99% identity with isolates from Iran, Iraq, Venezuela and Germany.Three isolates (Y4, Y21 and Y23) collected from Elmalı-Antalya region in 2011 shared 96% identity between each other, as well as 99 % identity with ZYMV C05-205 isolate from France and ZYMV-Liaocheng and ZYMV-Shangyu from China (Figure 1).

According to phylogenetic tree, the isolates collected from different province clustered same subcluster. For example two isolates (D14 and DEMRE) from Antalya and one isolates (KZN) from Ankara province clustered same subcluster. The H1M isolate from Antalya clustered with ZYMV-Ahlat isolates from Adana province. Also three isolates collected from different region (KZ1 from Ankara-Kazan, K3 from Antalya-Kumluca and E-7 from Antalya-Elmalı) (Table 1) share same nucleotide sequences. On the other hand, the C11 and C13 isolates collected the same field from Ankara province but they are clustered different subcluster in the phylogenetic tree (Figure 1). Isolates collected in the same field were not always more closely related than isolates from different areas of Turkey.

DISCUSSIONS

ZYMV is one of the most destructive viruses of cucurbit crops worldwide. We aimed to estimate the prevalence of ZYMV in Ankara and Antalya province of Turkey and differentiate ZYMV isolates by DAS-ELISA and sequence analysis of CP coding region. For these reasons, the surveys were conducted for detection of some major viruses, ZYMV, WMV, CMV, PRSV, SqMV, and CGMMV in cucurbit plantations (squash, cucumber, melon and watermelon fields) in Antalya and Ankara provinces by using DAS-ELISA method. All of the samples in this study were infected by at least one virus. DAS-ELISA results showed that ZYMV and WMV are prevalent in Turkey, as reported before [20,21,22,23,24,25]. WMV was the most widespread virus followed by ZYMV, CMV, SqMV, PRSV and CGMMV. The five viruses were detected with different prevalences on collected samples from Ankara provinces and WMV, ZYMV and CMV were detected in Antalya province. Our results, the most prevalent virus is WMV in collected sample from open fields but ZYMV was predominant in greenhouse cultivation areas (data not shown). ZYMV was the most widespread virus in Thrace region, as observed before [26], Konya and Karaman province [25,27] WMV infection was the most common virus (53.9%) in Samsun province [28].

In Turkey ZYMV was first isolated from diseased squash from the Adana province by Yılmaz and Davis [3]. After that ZYMV has been reported from other regions: CMV, ZYMV and WMV have been reported in the Black Sea region [29], CMV and ZYMV in Gaziantep province [28], CMV, ZYMV, PRSV, SqMV and WMV in Thrace region [26], CMV, ZYMV and WMV in Samsun [21], ZYMV and CMV in Hatay province [30]. In recent years, ZYMV, CMV, WMV, PRSV, SqMV and CGMMV (*Cucumber green mottle mosaic Tobamovirus*) were detected in Ankara and ZYMV, CMV and WMV in Antalya [31], CMV in lakes

region [32], ZYMV, CMV, WMV, PRSV and SqMV were reported in Konya province on seed-pumpkins [27].

Although there are numerous serological and biological studies about the presence of ZYMV, there have been few molecular studies in Turkey. Ozer et al. [12] studied two severe Turkish isolates of ZYMV from squash and muskmelon [ZYMV-Adana (Ad) and ZYMV-Ahlat (Ah), respectively]. Comparison with the nucleotide sequences of 23 isolates from different geographical regions worldwide revealed both isolates belonged to molecular cluster A1, the most common molecular cluster of ZYMV worldwide, including isolates from Europe, Africa, the Middle East, the Indian subcontinent and South America. In another study, Kamberoğlu et al. [13] reported that 3 Turkish ZYMV isolates from Adana and Mersin provinces of Cukurova region (ZYMV-TR3, ZYMV-TR15 and ZYMV-TR17) also belonged to subcluster A1.

On the other hand, in our study, molecular diversity of Turkish isolates of ZYMV was determined from Antalya, Burdur, Ankara, Konya and Aksaray provinces. Sequence analyses based on CP sequences revealed that most of the sequenced isolates (42/45) are closely related molecularly and belong to subcluster A1. Sequence analysis of ZYMV isolates showed that the presence of one major group of strains, and a few highly divergent isolates related to same geographic origins.

Three of the Turkish isolates did not fit to subcluster A1, but belonged to subcluster A4 containing isolates from China as well as from Poland and South-eastern France. Lecoq and Desbiez [7] reported the presence of clusters 4 and 5 in south-eastern France since 2004, probably in relation to recent introductions, and their current emergence in that area [33].

To our knowledge this is the first report about of presence of molecular group (A4) of ZYMV in Turkey. But due to the scarcity of molecular information on ZYMV in Turkey, we do not know if: this group has been present in the country for a long time. Kamberoglu et al. [13] reported the presence of an isolate of “emerging” type of WMV in Turkey. The situation may be similar between ZYMV and WMV, with recent introduction of isolates belonging to divergent molecular subgroups. However the reasons for this almost simultaneous emergence of new molecular groups of the two viruses, similar to what was observed in France in the 2000’, remains incompletely understood province [34]. Further surveys are required to explain the genetic diversity of ZYMV and to determine if group A4 is now emerging in Turkey.

ACKNOWLEDGEMENTS

This research was funded by Ankara University Scientific Research Projects Division (BAP) coded 12B4347002. We are grateful for Dr. Serkan Yeşil for providing us some ZYMV isolates of Konya, Karaman and Aksaray.

This research did not involve any human participants and/or animals. The authors declare that they have no conflict of interest.

REFERENCES

[1] Yanmaz, R., Duman, I., Yaralp, F., Demir, K., Sarıkamıs G., Sari, N., Balkaya, A., Kaymak, C., Akan, S., Ozalp, R. (2015) New Opportunities and Changes in Vegetable Production. Turkey Agricultural Engineering 8. Technical Congress Proceedings. 1, 579-605. (in Turkish)

[2] Desbiez, C., Lecoq, H. (1997) Zucchini yellow mosaic virus. Plant Pathology. 46, 809–29

[3] Yılmaz, M.A., Davis, R.F. (1984) Identification of viruses infecting vegetable crops along the Mediterranean Sea coast in Turkey. J. Turkish Pytopathology. 14, 1- 18.

[4] Ertunc, F. (1992) Studies on viral pathogens of pumpkin in Ankara Province. Ankara University Agriculture Faculty Publications. No, 1252. (in Turkish)

[5] Lisa, V., Boccardo, G., D’Agostino, G., Dellavalle, G., d’Aquilio, M. (1981) Characterization of a potyvirus that causes Zucchini yellow mosaic. Phytopathology. 71, 667–672.

[6] Sevik, M.A., (2017) The Infection Process and Symptom Expression of Zucchini Yellow Mosaic Virus Isolates from Squashes in Cucurbit Crops. Fresen. Environ. Bull. 26, 5372-5376

[7] Lecoq, H., Desbiez, C. (2012) Viruses of cucurbit crops in the mediterranean region: an ever-changing picture. Advances in Virus Research. 84, 67-126.

[8] Gal-On, A. (2007) Zucchini yellow mosaic virus: insect transmission and pathogenicity – the tails of two proteins. Mol. Plant Pathol. 8, 139–150.

[9] Coutts, B.A., Kehoe, M.A., Webster, C.G., Wylie, S.J., Jones, A.L. (2011) Zucchini yellow mosaic virus: Biological properties, detection procedures and comparison of coat protein gene sequences. Arch. Virol. 156, 2119–2131.

[10] Desbiez, C., Wipf-Scheibel, C., Lecoq, H. (2002) Biological and serological variability, evolution and molecular epidemiology of Zucchini yellow mosaic virus (ZYMV, Potyvirus) with special reference to Caribbean islands. Virus Res. 85, 5- 16

[11] Yakoubi, S., Desbiez, C., Fakhfakh, H., Wipf-Scheibel, C., Fabre, F., Pitrat, M., Marrakchi, M., Lecoq, H. (2008) Molecular, biological and serological variability of Zucchini yellow mosaic virus in Tunisia. Plant Pathol. 57,1146–1154.

[12] Ozer, M., Sipahioğlu, H.M., Usta, M., Fidan, H. (2012) Cloning and sequencing of coat protein gene of Zucchini yellow mosaic virus isolated from squash and muskmelon in Turkey. Turkish Journal of Biology. 36, 423-429.

[13] Kamberoglu, M.A., Caliskan A.F., Desbiez, C. (2016) Current Status of Some Cucurbit Viruses in Cukurova Region (Adana and Mersin Provinces) of Turkey and Molecular Characterization of Zucchini Yellow Mosaic Virus Isolates. Romanian Biotechnological Letters. 21, 11709-11719

[14] [Clark, M.F., Adams, A.N. (1977) Characteristics of the Microplate Method of Enzyme-Linked Immunosorbent Assay for the Detection of Plant Viruses. Journal of General Virology. 34(3), 475-83

[15] Astruc, N., Marcos, J.F., Macquaıre, G., Candresse, T., Pallás, V. (1996) Studies on the diagnosis of hop stunt viroid in fruit trees: identification of new hosts and application of a nucleic acid extraction procedure based on non-organic solvents. European Journal of Plant Pathology. 102, 837-846.

[16] Ali, M.C., Maoka, T., Natsuaki, K.T. (2009) Biological and molecular characterization of two Zucchini yellow mosaic virus isolates from Syria. Bulletin OEPP/EPPO Bulletin. 39, 99–104.

[17] Huang, X., Madan, A. (1999) CAP3: A DNA sequence assembly program. Genome Res. 9, 868-877

[18] Tamura, K., Stecher, G., Peterson, D., Filipski, A., Kumar, S. (2013) MEGA6: molecular evolutionary genetics analysis version 6.0. Molecular biology and evolution. 30(12), 2725-2729.

[19] Atreya, C.D., Atreya, P.L., Thornbury, D.W., Pirone T.P. (1992). Site-directed mutations in the potyvirus HC-Progene affect helper component activity, virus accumulation, and symptom expression in infected tobaccoplants. Virology. 191, 106-111.

[20] Yılmaz, M.A., Abak, K., Lecoq, H., Baloglu, S., Sarı, N., Kesici, S., Ozaslan, M., Güldür, M. (1994) Control of Zucchini Yellow Mosaic Virus (ZYMV) in Cucurbits by ZYMV-WK Strain. 9th Congress of Mediterranean Phytopathological Union-Kuşadası-Aydın-Türkiye, 353-35.

[21] Sevik, M.A., Arlı-Sökmen, M. (2003) Viruses infecting cucurbits in Samsun, Turkey. Plant Disease. 87(4), 341-344.

[22] Dag, D.S. (2005) Identification of Cucurbit Viruses By DAS-ELISA Assays in Gaziantep. Institute of Natural and Applied Sciences of Gaziantep University. Gaziantep

[23] Karamanlı, A. (2007) Survey of *Cucumber Mosaic Virus* (CMV) and *Zucchini Yellow Mosaic Virus* (ZYMV) in Turkish Republic of Northern Cyprus in Cucurbits Growth Field. Master thesis. Institute of Natural and Applied Sciences Of Çukurova University, Adana

[24] Yardimci, N., Korkmaz, S. (2004). Studies on Spread and Identification of Zucchini Yellow Mosaic Virus Disease in the North-West Mediterranean Region of Turkey by Biological Indexing and Double-stranded RNA Analysis. Plant Pathology Journal. 3, 1-4.

[25] Yeşil, S., Ertunc F. (2013) Virus diseases of cucurbits in Karaman province. International Journal of Ecosystems and Ecology Science (IJEES). 3(2), 235-240.

[26] Koklu, G., Yılmaz, O. (2006) Occurrence of cucurbit viruses on field-grown melon and watermelon in the Thrace region of Turkey. Phytoprotection. 87, 123-130

[27] Yesil, S., Ertunc, F. (2012) Virus diseases of cucurbits in Konya province. Proceedings of the Xth EUCARPIA Meeting on Genetics and Breeding of Cucurbitaceae. 791-796

[28] Ozaslan, M., Aytekin, T., Bas, B., Kılıc, I.H., Afacan, I.D., Dag, D.S. (2006) Virus diseases of cucurbits in Gaziatep-Turkey. Plant Pathology Journal. 5, 24-27

[29] Citir, A., Kutluk, N.D., Saglam, N., Ilbagi, H. (1998) Diagnoses of Virus Diseases with Simptomatolojic and Biological Methods in Cucumber and Zucchini Plants in Amasya,Corum, Samsun and Tokat provinces. Turkey VIII. Phytopathology Congress 331-335.(in Turkish)

[30] Sertkaya, G., Sertkaya, E., Yetişir, H., Kaya, K. (2010) Incidence and transmission of Zucchini Yellow Mosaic Potyvirus (ZYMV) in cucurbits in Hatay Province of Turkey. Cucurbitaceae. 2010, 216-218.

[31] Topkaya, S., Ertunc, F. (2012) Current status of virus infections in cucurbit plantations in Ankara and Antalya provinces. Proceedings of the Xth EUCARPIA Meeting on Genetics and Breeding of Cucurbitaceae. 759-762

[32] Yardimci, N., Çulal Kılıç, H., Kor, A. (2015) Identification of Cucumber Mosaic Virus (CMV) on Squash (Cucurbita Pepo L.) Cultivars in Lakes Region of Turkey. Fresen. Environ. Bull. 24, 417 - 421

[33] Lecoq, H., Wipf-Scheibel, C., Chandeysson, C., Le Van, A., Fabre, F., Desbiez, C. (2009) Molecular epidemiology of Zucchini yellow mosaic virus in France: An historical overview. Virus Res. 141, 190–200.

[34] Lecoq, H., Wipf-Scheibel, C., Nozeran, K, Millot, P., Desbiez, C. (2014) Comparative molecular epidemiology provides new insights into Zucchini yellow mosaic virus occurrence in France. Virus Research. 186, 135-143

Received: **12.05.2018**
Accepted: **14.02.2019**

CORRESPONDING AUTHOR

Serife Topkaya
Gaziosmanpasa University,
Faculty of Agriculture,
Department of Plant Protection,
60240 Tokat – Turkey

e-mail: serife.topkaya@gop.edu.tr

© by PSP Volume 28 – No. 4/2019 pages 2450-2456 Fresenius Environmental Bulletin

EFFECTS OF SUCROSE AND L-RHAMNOSE ON ANTHOCYANIN AND RELATED GENE EXPRESSION IN ROSE

Yong Zhang, Mengwen Luo, Xuhui Ma, Wei Hou, Haoru Tang*

College of Horticulture, Sichuan Agricultural University, Chengdu, Sichuan, 611130, China

ABSTRACT

Sugar plays a key role in the anthocyanin biosynthesis in plants. In this experiment, roses 'Wonderland' were selected as the materials, and the change at different florescence of petal color, anthocyanin content and the expression of anthocyanin synthesis pathway genes and transcription factors under spraying sucrose and L-rhamnose on roses were investigated to explore how sugar works. The results showed that both sugar treatments induced the expression of MYB10 and regulated the expression of anthocyanin synthesis genes such as CHS, CHI, DFR, UFGT and PAL, changed the color of petals to a certain degree and eventually increased the accumulation of anthocyanin in petals, and the sucrose effect was better than that of L-rhamnose. And sugar treatment may also lead to the peak of anthocyanin synthesis early in petals by premature MYB10 expression. This study provides a theoretical basis for the different color cultivation of the rose industry.

KEYWORDS:
Rose, Sugar treatment, Color, Anthocyanin, Gene expression

INTRODUCTION

Color is one of the most important ornamental characters of the rose, therefore, the study on the relationship between color and anthocyanin and its regulation mechanism can provide a theoretical basis for breeding of flower colors modification.

Anthocyanins are one of the most important pigment groups in floral organs which are a kind of secondary metabolites in plants and the products of phenylalanine metabolic pathway. They are transported to the vacuole after synthesis in cytoplasm and endoplasmic reticulum, showing red and purple.

Anthocyanin biosynthesis is the result of both intrinsic and exogenous factors: the enzyme encoded by the gene determines the type of anthocyanin synthesis, and environmental factors not only affect the rate of anthocyanin biosynthesis, but also their accumulation and stability effect. Previous studies have shown that biosynthesis of anthocyanins requires the co-expression of at least 15 structural genes. These genes can be divided into two categories: one is the early biosynthesis genes expressed in the early stage of anthocyanin biosynthesis, including PAL, CHS, CHI, F3H; the other is the late biosynthetic genes expressed in the later stages of the anthocyanin biosynthesis pathway, including DFR, ANS, and UFGT. The expression of early and late biosynthetic genes of anthocyanins is controlled by different regulatory genes. CHS and DFR belong to two different types of biosynthetic genes, and their regulation is also different [1]. Studies have shown that MYB10 in the MYB transcription factor family in Rosaceae is related to anthocyanin levels [2]. It was found in apple that MYB10 overexpression increased the level of anthocyanin and MYB10 was inhibited by MYB1[3].

The function of sugar in anthocyanin synthesis is multiple. Firstly, it is a precursor of anthocyanin glycosyl and is also a component of the structure of anthocyanin glycosides. What's more, it involved in carbohydrate metabolism is the energy source for the synthesis of anthocyanins. And sugar as an osmoregulator affects flower growth and anthocyanin synthesis by regulating the osmotic potential of cells [4]. Meanwhile, sugar acts as a signal molecule in flower growth and anthocyanin synthesis and regulates the expression of anthocyanidin synthase gene through specific signal transduction pathway, which affects flower development and coloration. Studies have shown that sucrose can promote CHS, ANS gene expression in carrot hypocotyls and anthocyanin accumulation [5]. In corn roots, sucrose on the accumulation of anthocyanin has contributed [6]. However, previous studies did not find its mechanism of action.

In this study, we plan to determine the changes of anthocyanin content, the expression of CHS, PAL, DFR, UFGT, ANS and transcription factor MYB10, MYB1 under the control of sucrose and L-rhamnose during rose 'Wonderland' blooming to investigate the effect of sugar treatment on anthocyanin and its mechanism of action.

FIGURE 1
Different stage of 'Wonderland' blossom
(S1: Bud stage, S2: Early bloom stage, S3: Bloom stage, S4: Decay stage)

TABLE 1
The sequence of related genes in the anthocyanin synthesis pathway of 'Wonderland'

Primer name	Primers (5'→3')	Amplified products
ANS F	AGGAGAAGTATGCCAATG	175
ANS R	GCCACAATATAATCGGAAG	
CHI F	GTTCCATACCAGCAGTTG	85
CHI R	CACGCAATCATCACTCTC	
CHS F	ACAGACTGGAACTCACTT	108
CHS R	CCTTGTGGCTTCTAACTT	
DFR F	AAGCAACTGGAGTGATGT	159
DFR R	AATGGACCGATTACGAGAG	
MYB1 F	GCCTCCAACAACAACAAC	82
MYB1 R	CCTCTCCAATCTCCTTTCC	
MYB10 F	ACAGGCAAGTTCATCTCA	198
MYB10 R	GGCTCTTTATGTTCGGTATT	
UFGT F	GATGATGACGAGGAGGAG	78
UFGT R	GCTGATGTATGCTACTGATG	
16SRNA F	AGGATCCGCGTCAAGGGTGGAGGCC	126
16SRNA R	GTCCTTGATTTCCTTCTTGCTCTGC	
PAL F	GCCTACATTGACGATCCT	104
PAL R	GCATTCTTCTCATTCTCACC	

MATERIALS AND METHODS

Plant materials and treatment. Rose species 'Wonderland', planted in Sichuan Agricultural University (29° 97' N, 102° 97' E). Twenty plants with the same growth environment and consistent growth were selected and randomly divided into three groups: CK, S and L, of which CK was treated with water, and S and L were sucrose and L-rhamnose respectively. The optimum concentrations of sucrose and L-rhamnose were obtained from pre-experiment, which were 140 g•L^{-1} and 80 mg•L^{-1}. The 'Wonderland' petals of the treated plants were taken during the bud, early bloom, bloom and decay stage (as shown in Fig.1), and the petals were quickly frozen by liquid nitrogen and stored in an ultra-low temperature refrigerator for use.

Determination of anthocyanin content. Weigh petal 1.000g, ground into powder under liquid nitrogen, 1% concentrated hydrochloric acid in methanol for 24 hours, the extract was centrifuged 8000 r / min 2 min, the supernatant was used Mapada's UV1100 UV-Vis photometer Absorbance at 530 nm and 657 nm was measured using the formula ΔA = A530-1/4 A657, expressed in units of ΔA • L^{-1}.

Measurements of petal color. The CIELAB color system is extensively used to evaluate petal color. Flower color was measured with a color meter (CR-10, Konica Inc., Osaka, Japan). The color meter was calibrated with a white standard calibration plate before use. Color was measured in the middle of each petal (three replicates per flower) to ensure equal measurement conditions. Values L*, a*, b* and chroma (C*) were measured to describe the color of the flowers.

Determination of gene expression. Total RNA was extracted by CTAB method. Take 4 μl of RNA and run on a 1% agarose gel to measure RNA quality. First-strand cDNA was synthesized using TaKaRa PrimeScript ™ RT reagent Kit with gDNA Eraser (Perfect Real Time) Reverse Transcription Kit. The gene sequences were found in NCBI. The gene accession numbers are: ANS (AB239787); CHI (AY04321); CHS (AB038246); DFR (AB490072); UFGT (AB292797); PAL (AB542949); MYB1 (EU082130); MYB10 (EU155164). Primers were designed based on the sequences found.

Amplification was performed with SYBR® Premix Ex Taq II using a CFX 96 Touch Quantitative PCR machine. The amplification procedure is as follows: Step 1: 95 °C for 30 min, Step 2: (95 °C for

5 s, 60 °C for 30 s) × 40 cycles, Step 3: Melt Curve. The original qRT-PCR results were collated, and the relative quantitative data were analyzed by 2-ΔΔCt method. The water-treated samples of the bud stage were used as a blank control, and the relative quantification results of the target genes of each sample were calculated by the $2^{-\Delta\Delta Ct}$ method.

RESULTS

Effect on the anthocyanin content. The changes in anthocyanin content in the petals under the control of sucrose and L-rhamnose were shown in Fig.2. The content of anthocyanin in CK group showed the trend of first ascending and then descending, reaching the highest at the bloom stage. The anthocyanins in the petals under the sucrose and L-rhamnose treatment showed a gradual decrease with the opening of 'Wonderland'. On the whole, the content of anthocyanin in petals increased significantly after treatment, and the effect of sucrose treatment was better than that of L-rhamnose.

Effect on the flower color indices. The color differences were shown in Fig.3. During the development of the flowers, the L* value after treatment was significantly higher than that of the control group. a* and C* reached the maximum value in the early bloom stage, and the treated effect was also significantly greater than that of the control group. b* and a*/b* are both negative values. The value after treatment in b* is higher than that of the control group, while the value after treatment in a*/b* is lower than the control group. For H°, the change during each time stage is not obvious, and the change between the two treatments is also not obvious. In general, the color of the treated petal had a more obvious change, and the effect after sucrose treatment was more pronounced than that of L-rhamnose.

Effect on the genes expression. As shown in Fig 4, in sucrose treatment, CHS, CHI and DFR had the highest relative expression at the bud stage, except for the decrease of CHS expression at the bloom stage, CHS, CHI, and DFR were almost not expressed relative to the CK group in the following three stage. In L-rhamnose treatment, the expression of CHS and CHI were inhibited during bloom and decay stage but the expression of DFR changed little in each stage. In addition, the relative expression of UFGT in S and L groups at the same time during early bloom stage showed a significant increase while in bloom and decay stage significantly reduced. The relative expression level of MYB1 in the S and L groups was higher than that in the CK group. MYB10 showed a trend of first increasing and then decreasing in early bloom stage to bloom stage in S group, down-regulation in bloom stage to decay stage. However, there was no significant difference in the MYB10 in the L group compared with the CK group.

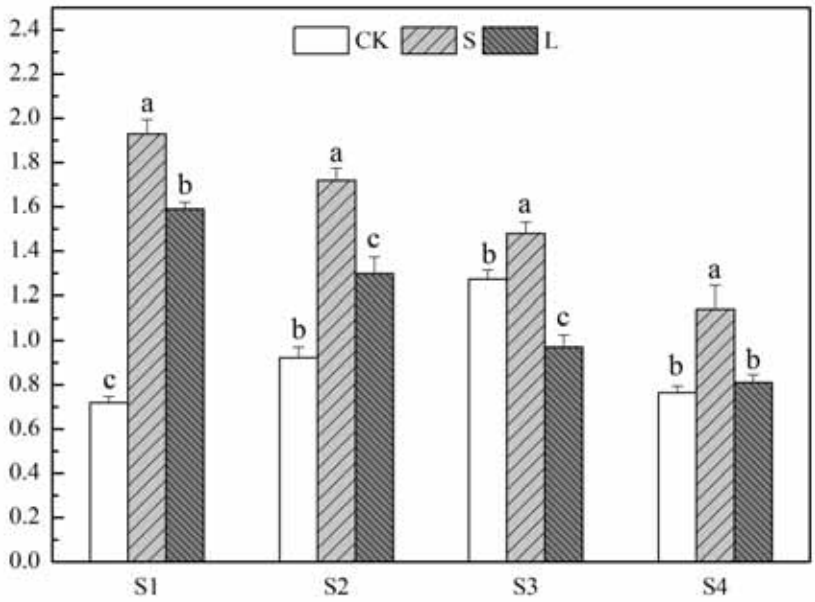

FIGURE 2
Anthocyanin content under different treatments in different stages
(S1: Bud stage; S2: Early bloom stage; S3Bloom stage; S4: Decay stage; CK: Control treatment; S: Sucrose treatment; L: L-rhamnose treatment: the same below).
Different letters (a-d) in columns denote statistically significant differences among cultivars by Duncan's multiple range test at $P < 0.05$.

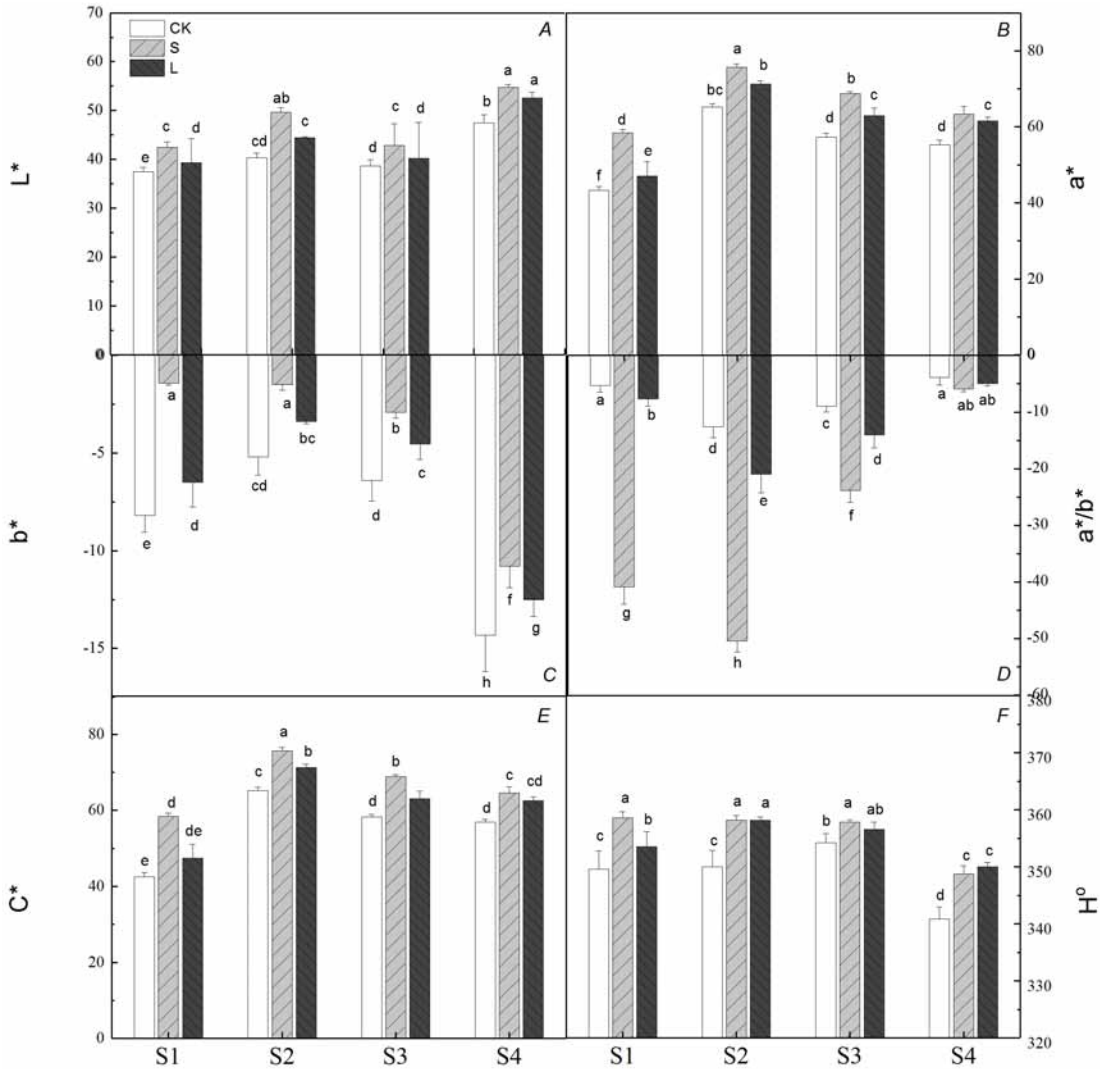

FIGURE 3

The colorimetric parameters of petals under different treatments at different stages.

Different letters (a–d) in columns denote statistically significant differences among cultivars by Duncan's multiple range test at $P < 0.05$.

The above results showed that the expression of CHS, CHI and DFR both increased significantly during the bud stage after sucrose treatment, and significantly higher than in the CK group during the bud stage, indicating that sucrose treatment significantly induced the expressions of CHS, CHI and DFR at the bud stage. In contrast, the expression levels of CHS, CHI and DFR after L-rhamnose treatment were not significantly different from those of CK group and the expression of CHS decreased at the bloom stage. Compared with the change of anthocyanin content, anthocyanin content was maintained at a high level when the expression of CHS, CHI and DFR gene was induced in S group indicating that the increase of the expression of these genes may promote the synthesis of anthocyanin. In the L group, the expression of CHI and UFGT was inhibited in the decay stage. Compared with the CK group whose anthocyanin content was lower than that of the CK group in the decay stage, it was speculated that the content of anthocyanin was also influenced by UFGT.

DISCUSSION

In this study, anthocyanin in 'Wonderland' petals treated with sucrose showed a significant improvement over the control and L-rhamnose treatments. And from the results, we can speculate that both sugar treatments may make the anthocyanin accumulation peak from bloom stage to early bloom stage. As for color, in the uniform color space, different values represent different colors and brightness. After the two sugars treatments, the redness and brightness were more obvious than the control group, and the effect of sucrose was better than the rhamnose treatment. From the results we know both sugar treatments can change the color of petals and increase the ornamental value of flowers.

And the trend of anthocyanin content in the petals of 'Wonderland' was basically the same as that of CHS, CHI, DFR, UFGT and PAL, which was consistent with that sucrose promoted the accumulation

of anthocyanin content and the expression of CHS and DFR genes in gerbera [7]. In the present study, CHS, CHI and PAL are upstream genes in the anthocyanin biosynthesis pathway that regulate chalcone synthase, 4-hydroxychalcone isomerase and phenylalanine lyase; DFR and UFGT is a downstream gene in the anthocyanin biosynthesis pathway that regulates flavonol-4-reductase and flavonoid 3,5- glycosyltransferase. The trend of their development in the process of rose "Wonderland" was in accordance with that of anthocyanin. It was speculated that sucrose treatment could induce the expression of CHS, CHI, DFR, UFGT and PAL in the rose to promote the accumulation of anthocyanin. L-rhamnose treatment also induced the expression of related genes, but the effect was not as obvious as sucrose treatment.

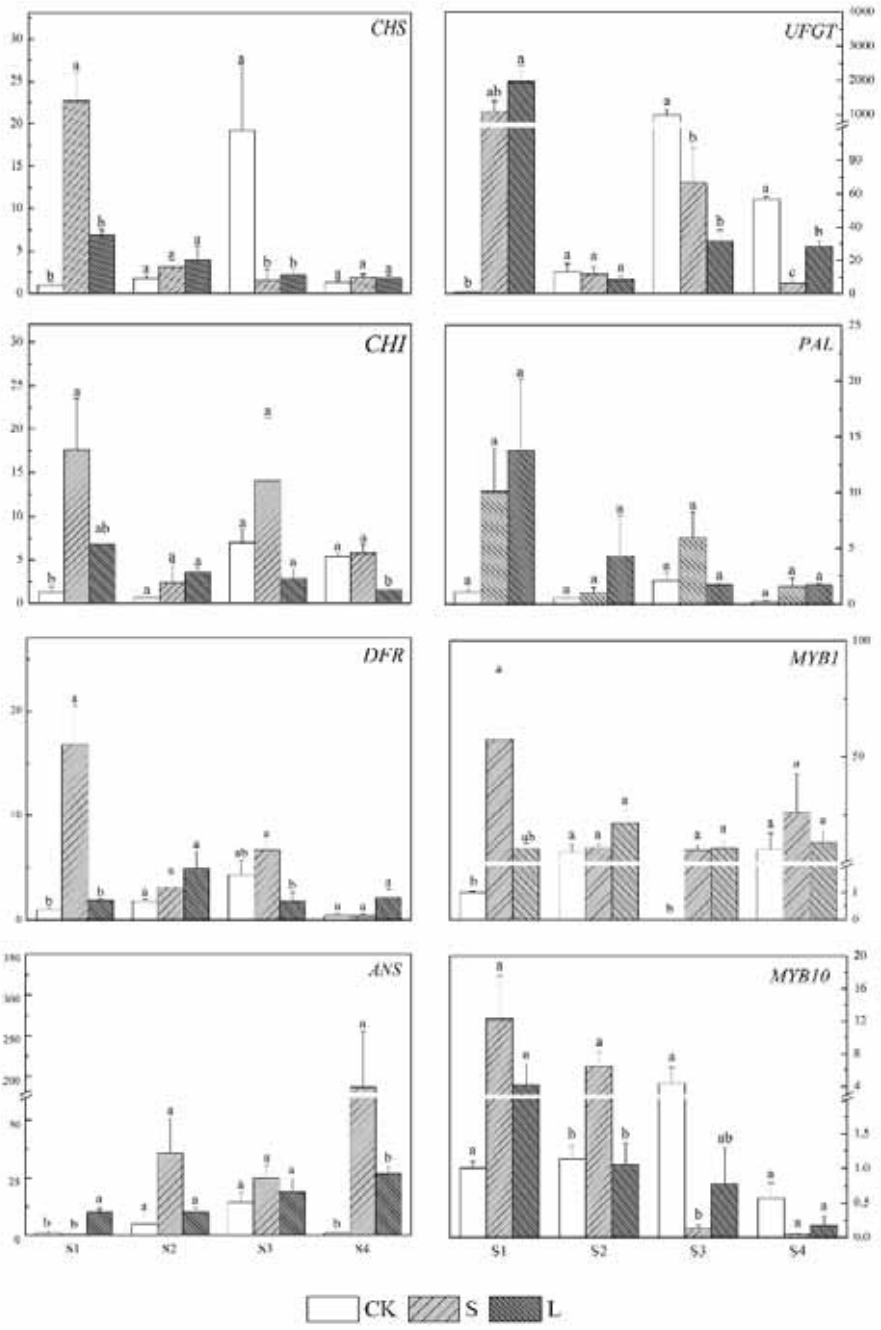

FIGURE 4
Relative expression levels of anthocyanin biosynthesis-related genes in different treatments at different Stages.

Different letters (a–d) in columns denote statistically significant differences among cultivars by Duncan's multiple range test at $P < 0.05$.

Previous studies have shown that the synthesis of anthocyanins in many plants is regulated by the MYB transcription factor family, for example, three anthocyanin synthesis-related transcription factors MdMYB10, MdMYBA and MdMYB1found in apple [2, 8-9]. Currently, only the MYB10 transcription factor is found in the rose associated with transcription of the anthocyanin synthesis gene in the petal. In this experiment, the expression of MYB10 in different stages of rose petals was determined and found that MYB10 expression was the highest at bloom stage in control treatment, and was consistent with that of CHS, CHI, DFR, UFGT and PAL. After two sugar treatments, the expression level of MYB10 gene was the highest at bud stage, which was also consistent with the trend of CHS, CHI, DFR, UFGT and PAL. Therefore, we speculate from the results that the expression of CHS, CHI, DFR, UFGT and PAL may be regulated by MYB10. MYB10 may regulate anthocyanin accumulation in rose petals by inducing the expression of CHS, CHI, DFR, UFGT and PAL. MYB1 was found to be likely to inhibit MYB10 expression in strawberry [10]. However, in this experiment, we did not find a clear correlation between MYB1 and MYB10 and the expression of anthocyanin pathway genes, suggesting that MYB1 is no important in the synthesis of anthocyanins.

CONCLUSION

It can be speculated that sugar treatment can induce the expression of MYB10 to regulate the expression of anthocyanin biosynthesis genes such as CHS, CHI, DFR, UFGT and PAL, and eventually increase the accumulation of anthocyanin in petals. Both two sugar treatments may have advanced the peak of anthocyanin synthesis in rose petals by premature MYB10 expression and sucrose treatment effect better than L-rhamnose.

ACKNOWLEDGEMENTS

The project is supported by the Sichuan Provincial Department of Education project, No. 15ZB0002.

The authors declare no conflict of interest.

REFERENCES

[1] Zhang, L., Li, W.H., Jiang, S.M., Zhu, G.F., Wang, B.Q., Li, H.Q. (2008) Progress of Molecular Basis of Biosynthesis and Transcriptional Regulation of Anthocyanins. Acta Horticulturae Sinica. 35, 909-916 (in Chinese).

[2] Wang, K.L., Bolitho, K., Grafton, K., Kortstee, A., Karunairetnam, S., McGhie, T.K., Espley, R.V., Hellens, R.P., Allan, A.C. (2010) An R2R3 MYB transcription factor associated with regulation of the anthocyanin biosynthetic pathway in Rosaceae. BMC Plant Biology. 10(50).

[3] Chagné, D., Wang, K.L., Espley, R.V., Volz, R.K., How, N.M., Rouse, S., Brendolise, C., Carlisle, C.M., Kumar, S., Silva, N.D., Micheletti, D., McGhie, T., Crowhurst, R.N., Storey, R.D., Velasco, R., Hellens, R.P., Gardiner, S.E., Allan, A.C. (2006) An Ancient Duplication of Apple MYB Transcription Factors Is Responsible for Novel Red Fruit-Flesh Phenotypes. Plant Physiology. 161, 225-239.

[4] Solfanelli, C., Poggi, A., Loreti, E., Alpi, A., Perata, P. (2006) Sucrose-Specific Induction of the Anthocyanin Biosynthetic Pathway in Arabidopsis. Plant Physiology. 140, 637.

[5] Hara, M., Oki, K., Hoshino, K., Kuboi, T. (2003) Enhancement of anthocyanin biosynthesis by sugar in radish (Raphanus sativus) hypocotyl. Plant Science. 165, 259-265.

[6] Meng, X.C., Zhang, Y.J., Wang, X.J. (2014) Effects of Light, GA_3 and Sucrose on Anthocyanin Accumulation in Roots of Zea Mays. Journal of South China Normal University. (04), 25-28 (in Chinese).

[7] Meng, X.C., Peng, J.Z., Wang, X.J. (2007) Anthocyanin Accumulation and CHS, DFR Gene Expression Regulated by Light and Sugar in Gerbera hybrida Ray Floret. Acta Horticulturae Sinica. (01), 227-230 (in Chinese).

[8] Telias, A., Wang, K.L., Stevenson, D.E., Cooney, J.C., Hellens, R.P., Allan, A.C., Hoover, E.E., Bradeen, J.M. (2011) Apple skin patterning is associated with differential expression of MYB10. BMC Plant Biology. 11(93).

[9] Espley, R.V., Hellens, R.P., Putterill, J., Stevenson, D.E., Amma, S.K., Allan, A.C. (2007) Red colouration in apple fruit is due to the activity of the MYB transcription factor, MdMYB10. The Plant Journal. 49, 414–427.

[10] Wang, K.L., McGhie, T.K., Wang, M., Liu, Y.H., Warren, B., Storey, R., Espleyl, R.V., Allan, A.C. (2014) Engineering the anthocyanin regulatory complex of strawberry (Fragaria vesca). Frontiers in Plant Science. 5, 651.

Received: **13.05.2018**
Accepted: **12.02.2019**

CORRESPONDING AUTHOR

Haoru Tang
College of Horticulture,
Sichuan Agricultural University,
Chengdu, Sichuan, 611130 – China

e-mail: htang@sicau.edu.cn

© by PSP Volume 28 – No. 4/2019 pages 2457-2463 Fresenius Environmental Bulletin

THE RESEARCH OF 17α-ETHINYL ESTRADIOL (EE2) LEVELS IN THE FRESHWATER SOURCES POURED INTO THE NORTHEAST MEDITERRANEAN REGION

Esra Bickici, Meltem Eken*

Iskenderun Technical University, Marine Sciences and Technology Faculty, 31200, Iskenderun, Hatay, Turkey

ABSTRACT

Rivers are ecosystems affected first by environmental pollution. Pollutants originating from domestic, industrial and agricultural activities are firstly involved in rivers. At times when the human population was low, waste materials that had been mixed into rivers could be diluted in a short distance and disintegrated from natural routes. However, with the excessive population growth and industrialization that accompanied development, domestic and industrial wastes also multiplied and the rivers became unable to clean themselves.In the Northeastern Mediterranean, where the freshwater is exposed to a wide variety of different wastewater, it is inevitable for the settlement centers in the vicinity to leave the Iskenderun Gulf, which is a commercially important region, irreversibly polluted.In this study, accumulation levels of 17α-ethinylestradiol (EE2) hormones were investigated in the chemicals that disturbed the endocrine system that caused the pollution of some freshwater sources pouring into İskenderun Bay and started to worry scientists in the last decade.In our country, 17 alpha-ethinylestradiol (EE2) hormone levels were found to be high in all freshwater resources covered by the study, according to the Regulation on the Monitoring of Surface Waters and Underground Waters in which the Water Framework Directive was implemented at the national level.

KEYWORDS:
Iskenderun Bay, 17 alpha-ethinylestradiol (EE2), freshwater pollution, endocrine disruptors

INTRODUCTION

Endocrine disruption has become of increasing concern during the past decade. Compounds involved in these mechanisms may interfere with the normal endocrine function of both wildlife and humans. Adverse effects due to endocrine disruptors include decreased sperm count, development of hormonally sensitive carcinomas (female breast cancers, testicular and prostate cancers) in humans.

Chemicals (EDC), which result from the use of humans and disrupt the endocrine system, have effects similar to those of endogenous hormones in vertebrates and interact with the endocrine system. EDC has been detected in industrial wastes and livestock feed wastes. It has been observed that the fish living in the water polluted with these wastes have defects in the reproductive systems. 17α-ethinylestradiol (EE2) is a very strong synthetic estrogen and is used as a birth control tablet all over the world. The 17α-ethinylestradiol (EE2) hormone imitates the natural estrogen in fish, increasing the concentration of the nearby vitellogenin and causing males to become females. Jobling et al. [1] found that antiandrogens and estrogenic synthetic hormones cause gonadal disturbances and malnourishment of men in 51 cases taken in the UK. As a result, it is safe to say that the chemicals that disrupt the endocrine system can lead to irreversible damage to the ecosystem.

The past several years have seen a steady drumbeat of news reports, blog posts, and scientific studies which have raised concerns about the presence of estrogenic compounds (natural estrogens and synthetic chemicals that mimic natural estrogen) in waterways and drinking water, and the potential harm to human health or aquatic life.

The impact on wildlife exposed to estrogens has largely focused on aquatic organisms such as fish. The protein vitellogenin, whose production is stimulated upon exposure to estrogen in male and female organisms, serves as a good marker to indicate environmental exposure of estrogens in non-mammalian vertebrates. Several studies document that steroidal estrogens led to vitellogenin production at concentrations as low as 1 ng/L, some refer to this condition as the emasculation of male fish [2]. The demasculization of fish can lead to an altered sex ratio within a population and sex reversals [3, 4].Research shows that EE2 depress the growth of tilapia (*Oreochromis niloticus*) larvae, which is likely relevant for other fish species [5, 6]. Altered fish size has shown to change the timing of fecundity, the sex ratio of the population and the survival rate in young fish, thus the changed growth may cause large disturbances for the species and consequently the ecosystem [5, 7].

Estrogens can be introduced to the environment through municipal and agricultural activities as both point and nonpoint sources. These compounds reach the rivers, estuaries, and coastlines either through the discharge of effluents coming from sewage treatment plants — or directly from sewage that deliver their content into waterways. EE2 is a semisynthetic derivate from the natural hormone estradiol (E2) [8]. EE2 is excreted from urine and feces from individuals taking medications containing EE2 [9]. For this reason, hormones are expected to be present primarily in wastewater from households, which are transported through the sewer system to the wastewater treatment plant (WWTP).

The Mediterranean, covering an area of 2.5 million km² with the world's largest inland sea, From the Gibraltar Strait to the Atlantic Ocean; The Suez Canal is also separated from the Red Sea. For this reason, it is extremely important both for our country's economy and world ecology. Iskenderun Bay, which is one of the most important fishing areas of the region and which is located on the Mediterranean coast of our country and also contains rich fish species, is one of the areas under the threat of intensive pollution due to settlement areas, industrial establishments and the sea traffic. Iskenderun Bay is one of the regions where the terrestrial entrances are most concentrated in the northeastern Mediterranean. The Gulf is exposed to intensive environmental impacts due to industrial enterprises, residential units, river discharges and ship traffic. In addition, cage fishery studies have been carried out in the bay recently. All these activities increase the concentration of nutrient salts in the water, creating suitable environments for phytoplankton increases [10,11]. However, it is under heavy pollution due to intensive marine traffic with the factories that it houses around the bay and intensive domestic tourism in the summertime. The Gulf is also open to all kinds of wastes of Eastern Mediterranean countries with its current systems [12].

The treatment of urban wastewater and operation of waterworks are critical steps to minimize the environmental burden imposed by natural and synthetic micro-pollutants and protect humans and the environment from these pollutants' adverse effects. But first of all, it is necessary to establish the problem of determining the environmental pollution burden. Although there are many studies on the pollution of the Gulf of Iskenderun, there is very little work on the resources spilled into the Gulf. This situation not only points out that this research is necessary as the Northeast Mediterranean has many settlements in vicinity and is a crucial trading area, but also because İskenderun Bay is approaching to an immutable level of pollution due to the discharges of different wastewater contents.

80 countries, including 40% of the world's population, are already suffering from water shortages. For this reason, it is vital to prevent the pollution of river resources by means of precautions to be taken without disturbing the quality of life by means of well-assessed water resources and conscious water and wastewater management. The abandonment of the Iskenderun Bay, which is exposed to wastewater discharges with very different contents, is becoming more and more alarming in terms of both our country's economy and world ecology.

MATERIALS AND METHODS

The samples were made seasonally between May 2014 and April 2015. A total of 75 water samples were run in 3 replications. The 17α-ethinylestradiol (EE2) hormone in water samples taken from 7 different discharge points (Ceyhan River, Demirtaş Stream, Deliçay, Payas Stream, Akçay Stream, Feyazan Channel and Arsuz Stream) poured into Iskenderun Bay (Figure 1), after applied with the appropriate extraction method, using ethinylestradiol (EE2) EIA kit read on Elisa Reader (BİO-TEK ELx800) (Figure 2). In this study, wastewater samples taken from 7 different discharge points (Ceyhan River, Demirtaş Stream, Deliçay, Payas Stream, Akçay Stream, Feyazan Channel and Arsuz Stream) poured into Iskenderun Bay were investigated.

RESULTS AND DISCUSSION

According to the Duncan test results in Table 1, seasonal differences in 17α ethinylestradiol hormone averages were found statistically significant in water samples taken from Akçay Stream, Arsuz Stream, Ceyhan River, Demirtaş Stream, Feyezan Channel and Payas Stream ($p < 0,05$).According to t-test results for Deliçay Stream, the difference between spring and winter averages was statistically significant ($p < 0.05$). 17α-Ethinylestradiol hormone levels were found to be 1,986 ± 0,216 µg / l in the Ceyhan River and 1,502 ± 0,335 µg / l in the lowest Deliçay Stream. According to the Duncan test results in Table 1, the differences in the annual averages of 17α-ethinylestradiol hormone levels of all freshwater sources were statistically insignificant ($p > 0.05$).

When the reports in Table 2 were examined, 17 α -ethinylestradiol (EE2) hormone levels were found to be higher in this study than all other studies. The Water Framework Directive (WFD) 2000/60 / EC, which is a framework directive on the quality of the European Union, provides an integrated approach to environmental protection and management with the objective of protecting the quality of surface water resources and improving the condition of aquatic

FIGURE 1
Sampling Stations

FIGURE 2
Elisa Reader (BİO-TEK ELx800)

TABLE 1
17α Ethinylestradiol (EE2) hormone findings (µg/l)

Months	January	April	July	October	
REGIONS (EE2) (µg/l)	$\overline{X} \pm S\ \overline{x}$ (min.-maks.)	$\overline{X} \pm S\ \overline{x}$ (min.-maks.)	$\overline{X} \pm S\ \overline{x}$ (min.-maks.)	$\overline{X} \pm S\ \overline{x}$ (min.-maks.)	Annual average
AkcayStream	1,703±0,003[a] (1,700-1,710)	1,986±0,003[c] (1,980-1,990)	-	1,957±0,003[b] (1,950-1,960)	1,885±0,091
Arsuz Stream	1,740±0,002[c] (1,740-1,742)	1,708±0,006[b] (1,700-1,720)	0,993±0,002[a] (0,990-1,000)	2,761±0,004[d] (2,760-2,770)	1,806±0,364
CeyhanRiver	1,596±0,005[a] (1,590-1,600)	1,645±0,003[b] (1,640-1,650)	2,487±0,004[d] (2,480-2,490)	2,196±0,003[c] (2,190-2,200)	1,986±0,216
DeliçayStream	1,831±0,003[a] (1,830-1,840)	1,161±0,003[b] (1,160-1,170)	-	-	1,502±0,335
DemirtaşStream	1,520±0,003[b] (1,516-1,525)	1,281±0,004[a] (1,270-1,290)	1,799±0,004[c] (1,790-1,810)	1,940±0,003[d] (1,930-1,950)	1,640±0,146
Feyezan Channel	0,660±0,005[a] (0,651-0,668)	1,899±0,004[c] (1,890-1,910)	1,209±0,003[b] (1,203-1,215)	2,840±0,004[d] (2,830-2,850)	1,659±0,470
Payas Stream	1,799±0,004[b] (1,790-1,810)	1,559±0,004[a] (1,550-1,570)	1,869±0,005[c] (1,860-1,880)	1,952±0,004[d] (1,950-1,960)	1,801±0,084

The averages symbolized by the letters a, b, c and d are statistically different (p <0,05); There is a difference between the averages marked with different letters for each line (p <0.05). $\overline{X} \pm S\ \overline{x}$: Arithmetic mean ± Standard error

TABLE 2
Studies on 17 alpha-ethinylestradiol (EE2) hormones

RESEARCH AREA	EE2 CONCENTRATION	REFERENCE
TURKEY/ Büyükçekmece Basin (surface waters)	11,7-14,0 ng/L (min-max)	[13]
GERMANY, CANADA and BRAZIL (wastewater treatment)	0,001 µg/L (max.)	[14]
ROME (river waters and wastewater treatment)	0,003 ng/L (max.)	[15]
HOLLAND (rivers and wastewaters)	0,1-0,3 ng/L (min-max)	[16]
ITALY (Tiber River)	0,4 ng/L (max.)	[17]
SPAIN (wastewater)	3,0 ng/L (max.)	[18]
TOKYO (river waters)	1,0 ng/L (max.)	[19]
AMERİCA (wastewater)	73 ng/L (max.)	[20]
SPAIN (wastewater)	4,3-51 ng/L (min.-max.)	[21]
SPAIN (surface water)	10-280 ng/L (min.-max.)	[22]
TAIWAN (drinking water treatment plant)	7,53-27,4 ng/L (min.-max.)	[23]
SOUTH KOREA and ASIA (river waters)	4,3- 28,6 ng/L (min.-max.)	[24]
CHINA (river waters)	0,28-2,67 ng/L (min.-max.)	[25]
CHINA/TIANJIN (river waters)	0,4-24,4 ng/L (min.-max.)	[26]
HONG KONG (rivers)	0,33 ng/L (max.)	[27]
VENEDIC LAGOON	0,8-34 ng/L (min.-max.)	[28]
CHINA (Yangtze riveri)	0,11-53,4 ng/L (min.-max.)	[29]
FRANCE (river water)	1,4 ng/L (max.)	[30]
CHINA(Taihu lake)	6,03-10,2 ng/L (min.-max.)	[31]
CHINA (river water)	0,52- 101,9 ng/L(min-max)	[32]
CHINA (Licun river)	7-24 ng/L (min.-max)	[33]
SOUTH KOREA (wastewater)	1,3 ng/L (max.)	[34]
AUSTRIA (rivers, canals)	0,33 ng/L (max.)	[35]
POLAND (surface water)	3,2-6,47 ng/L	[36]
TURKEY (Akçay Stream)	1,89 µg/L (ort.)	This study
TURKEY (Arsuz Stream)	1,81 µg/L (ort.)	This study
TURKEY (Ceyhan River)	1,99 µg/L (ort.)	This study
TURKEY (Deliçay Stream)	1,50 µg/L (ort.)	This study
TURKEY (Demirtaş Stream)	1,64 µg/L (ort.)	This study
TURKEY (Feyezan Channel)	1,66 µg/L (ort.)	This study
TURKEY (Payas Stream)	1,80 µg/L (ort.)	This study

ecosystems. One of these approaches is the identification and implementation of environmental quality standards for hazardous substances that pose a risk to water resources. "Regulation on the Monitoring of Surface Waters and Underground Waters" regulates the implementation principles of the Water Framework Directive at the national level in our country. The 17 α -ethinylestradiol (EE2) hormone is located within the 117 point source pollutants identified specifically for Turkey. The annual average value of 17 α -ethinylestradiol hormones was determined as 0.5 µg / L and the maximum permissible concentration was 0.9 µg / L, based on the environmental quality standards calculated in the project work carried out by the Ministry of Forestry and Water Affairs and recommended by experts.

In Turkey, 17 alpha-ethinylestradiol (EE2) hormone levels were determined to be high in all the freshwater resources covered by the study, according to the Regulation on the Monitoring of Surface Waters and Underground Waters in which the Water Framework Directive was implemented at the national level. 17α-ethinylestradiol (EE2) is a very strong synthetic estrogen and is used as a birth control tablet all over the world. The freshwater resources studied in the scope of the study are more exposed to domestic wastewater than they are close to settlement areas. Human medicines such as contraceptive tablets containing 17α-ethinylestradiol (EE2) reach the sewage through urea and feces and then to the wastewater treatment plant. Since these medicines reaching the treatment plant cannot be remedied by conventional treatment methods, they cause environmental problems in the receiving environment. Birth control pills are widely used for medical treatment as well as for protection from pregnancy. These include regulation of menstruation, reduction of menstrual cramps, decrease in premenstrual syndrome, decrease in menstrual migraine, decrease in the incidence of overt tumor and cysts, and decrease in endometrium cancer risk.

Considering that birth control pills are used both for pregnancy protection and for medical treatment purposes, and most patients are also buying these drugs without prescription and considering that these drugs cannot be removed from wastewater by conventional treatment methods, it is considered probable that the 17α-ethinylestradiol (EE2) hormone level in freshwater sources is high.

CONCLUSION

The presence of estrogenic chemicals in the stable environment constitutes a problem in terms of public health and ecosystem structure.The EE2 hormone is a compound that reaches the environment from the wastewater treatment plants without being completely destroyed.There is limited information on the use of many chemicals suspected of being endocrine disruptive, chemical, transport, quantities, decay, transformation and ultimate fate of the end-effector.The main reason for this lack of information is the insufficient analytical methods of measuring the trace amounts of such chemicals in the environment until recent years.This inadequacy is not only due to the fact that the chemicals cannot be quantitatively measured at low concentrations but also due to the fact that the metabolites and their metabolites cannot be identified by existing analytical methods [37,38]. Most of the scientific studies so far have focused on the effects of endocrine disrupting chemicals on the reproductive systems of vertebrate mammals.With this study, it is determined how much the accumulation levels of hormones are in the aquatic environment and it is important to be preliminary information for future studies.

ACKNOWLEDGEMENTS

The authors gratefully acknowledge thefinancial support of Mustafa Kemal University (BAP 2013/8981).

REFERENCES

[1] Jobling, S., Williams, R., Johnson, A., Taylor, A., Gross-Sorokin, M.Y., Nolan, M., Tyler, C.R., Van Aerle, R., Santos, E. and Bright, G.C. (2006) Predicted exposures to steroid estrogens in UK Rivers correlate with widespread sexual disruption in wild fish populations. Environ. Health Perspectives. 114, 32-39.

[2] Irwin, LK., Gray, SL., Oberdorster, E. (2001) Vitellogenin induction in painted turtle, Chrysemyspicta, as a biomarker of exposure to environmental levels of estradiol. Aquat Toxicol. 55, 49-60.

[3] Hutchinson, T.H., Pounds, N.A., Hempel, M. and Williams, T.D. (1999) Impact of natural and synthetic steroids on the survival, development, and reproduction of marine copepods (Tisbebattagliai). Sci. Total Environ. 233, 167-179.

[4] Lai, K.M., Scrimshaw, M.D. and Lester, J.N. (2002) The effects of natural and synthetic steroid estrogens in relation to their environmental occurrence. Crit. Rev. Toxicol. 32, 113-132.

[5] Shved, N., Berishvili, G., D'Cotta, H., Baroiller, J-F., Segner, H., Eppler, E., Reinecke, M. (2007) Ethinylestradiol differentially interferes with IGF-I in liver and extrahepatic sites during development of male and female bony fish. Journal of Endocrinology. 195, 513–523.

[6] Shved, N., Berishvili, G., Baroiller, J-F., Segner, H., Reinecke, M. (2008) Environmentally relevant concentrations of 17alpha-ethinylestradiol (EE2) interfere with the growth hormone (GH)/insulinlike growth factor (IGF)-I system in developing bony fish. Toxicological Sciences. 106, 93–102.

[7] Paull, G.C., Lange, A., Henshaw, A.C., Tyler, C.R. (2008) Ontogeny of Sexual Development in the Roach (Rutilusrutilus) and Its Interrelationships with Growth and Age. Journal of Morphology. 269, 884–895.

[8] Aris, A.Z., Shamsuddin, A.S. and Praveena, S.M. (2014) Occurrence of 17alpha-ethynylestradiol (EE2) in the environment and effect on exposed biota: a review. Environment International. 69, 104-109.

[9] Hannah, R., D'Aco, V.J., Anderson, PD., Buzby, M.E., Caldwell, D.J., Cunningham, V.L. (2009) Exposure assessment of 17α- ethinyl estradiol in surface waters of the United States and Europe. Environ Toxicol Chem. 28, 2725–2732.

[10] Polat, S., Olgunoğlu, M., Akiz, A., Koray, T. (2006) Potentially Harmful Phytoplankton Species Distributed in Northeastern Mediterranean Coastal Waters (Iskenderun Bay). E.U. Journal of Fisheries and Aquatic Sciences. 23(1-2), 169–172. (In Turkish)

[11] Başusta, N. (1997) Pelagic and Demersal Fishes in İskenderun Bay. Ç.U. Science. Enst, Department of Aquaculture Adana. (In Turkish)

[12] Avşar, D. (1999) Physico-Chemical Properties of the Eastern Mediterranean Regarding the Distribution of a New Skifomedüz *(Rhopilemano-madica).* TUBITAK T Journal of Zoology. 23(2), 605-616. (In Turkish)

[13] Aydın, E., Talinli, İ. (2013) Analysis, occurrence and fate of commonly used pharmaceutical and hormones in the Buyukcekmece Watershed, Turkey. Chemosphere. 90(6), 2004–12.

[14] Ternes, T.A., Stumpf, M., Mueller, J., Haberer, K., Wilken, R.D., Servos., M. (1999) Behavior and occurrence of estrogens in municipal sewage treatment plants. I. investigations in Germany, Canada and Brazil. Sci Total Environ. 225, 81-90.

[15] Baronti, C., Curini, R., D'ascenzo, G., Corcia, A.D., Gentili, A., Samperi R. (2000) Monitoring Natural and Synthetic Estrogens at Activated Sludge Sewage Treatment Plants and in a Receiving River Water. Environmental Science and Technology. 34, 5059-5066.

[16] Belfroid, A.C., Van der Horst, A., Vethaak, A.D., Schafer, A.J., Rijs, G.B., Wegener, J. and Cofino, W.P. (1999) Analysis and occurrence of estrogenic hormones and their glucuronides in surface water and waste water in The Netherlands. Sci. Total Environ. 225, 101-8.

[17] Lagana, A., Bacaloni, A., De Leva, I., Faberi, A., Fago, G., Marino, A. (2004) Analytical methodologies for determining the occurrence of endocrine disrupting chemicals in sewage treatment plants and natural waters. Analytica Chimica Acta. 501, 79–88.

[18] Carpinteiro, J., Quintana, J.B., Rodriguez, I., Carro, A.M., Lorenzo, R.A., Cela, R. (2004) Applicability of solid-phase microextraction followed by onfibersilylation for the determination of estrogens in water samples by gas chromatography–tandem mass spectrometry. Journal of Chromatography A. 1056, 179–185.

[19] Kawaguchi, M., Ishii, Y., Sakui, N., Okanouchi, N., Ito, R., Inoue, K., Saito, K., Nakazawa, H. (2004) Stir bar sorptive extraction with in situ derivatization and thermal desorption–gas chromatography–mass spectrometry in the multi-shot mode for determination of estrogens in river water samples. Journal of Chromatography A. 1049, 1–8.

[20] Kolpin, D.W., Furlong, E.T., Meyer, M.T., Thurman, E.M., Zaugg, S.D., Barber, L.B., Buxton, H.T. (2002) Pharmaceuticals, hormones, and other organic wastewater contaminants in U.S. streams 1999–2000: a national reconnaissance. Environ. Sci. Technol. 36(6), 1202–1211.

[21] Azzouz, A., Ballesteros, E. (2013) Influence of seasonal climate differences on the pharmaceutical, hormone and personal care product removal efficiency of a drinking water treatment plant. Chemosphere. 93, 2046-2054.

[22] Camacho-Munoz, D., Martin, J., Santos, J.L., Aparicio, I., Alonso, E. (2010) Occurrence, temporal evolution and risk assessment of pharmaceutically active compounds in Doñana Park (Spain). Journal of Hazardous Materials. 183, 602-608.

[23] Chen, C.Y., Wen, T.Y., Wang, G.S., Cheng, H.W., Lin, Y.H., Lie, G.W. (2007) Determining estrogenic steroids in Taipei waters and removal in drinking water treatment using high–flow solid phase extraction and liquid chromatography/tandem mass spectrometry. Science of the Total Environment. 378, 352-365.

[24] Duong, C., Ra, J.S., Cho, J., Kim, S.D. (2009) Estrogenic chemicals and estrogenicity in river waters of South Korea and seven Asian countries. Chemosphere. 78(3), 286-93.

[25] Jiang, W., Yan, Y., Ma, M., Wang, D., Luo, Q., Wang, Z., Satyanarayanan, S.K. (2012) Assessment of source water contamination by estrogenic disrupting compounds in China. Journal of Environmental Sciences. 24, 320-328.

[26] Lei, B., Huang, S., Zhou, Y., Wang, D., Wang, Z. (2009) Levels of six estrogens in water and sediment from three rivers in Tianjin area, China. Chemosphere. 76, 36-42.

[27] Li, W.C. (2014) Occurrence, sources, and fate of pharmaceuticals in aquatic environment and soil. Environmental Pollution. 187, 193-201.

[28] Pojana, G., Gomiero, A., Jonkers, N., Marcomini, A. (2007) Natural and synthetic endocrine disrupting compounds (EDCs) in water, sediment and biota of a coastal lagoon. Environ Int. 33, 929–36.

[29] Shi, J., Liu, X., Chen, Q., Zhang, H. (2014) Spatial and seasonal distributions of estrogens and bisphenol A in the Yangtze River Estuary and the adjacent East China Sea. Chemosphere. 111, 336-343.

[30] Vulliet, E., Cren-Olive, C. (2011) Screening of pharmaceuticals and hormones at the regional scale, in surface and groundwaters intended to human consumption. Environmental Pollution. 159, 2929-2934.

[31] Yan, Z., Lu, G., Liu, J., Jin, S. (2012) An integrated assessment of estrogenic contamination and feminization risk in fish in Taihu Lake, China. Ecotoxicology and Environmental Safety. 84, 334-340.

[32] Yuan, X., Li, T., Zhou, L., Zhao, X. (2014) Characteristics and Risk Assessment of Estrogenic Compounds in Rivers of Southern Jiangsu Province, China. IER Procedia. 9, 176-184.

[33] Zhou, X., Lian, Z., Wang, J., Tan, L., Zhao, Z. (2011) Distribution of estrogens along Licun River in Quingdao, China. Procedia Environmental Sciences. 10, 1876-1880.

[34] Kim, S.D., Cho, J., Kim, I.S., Vanderford, B.J., Snyder, S.A. (2007) Occurrence and removal of pharmaceuticals and endocrine disruptors in South Korean surface,drinking, and waste waters. Water Res. 41, 1013-1021.

[35] Hohenblum, P., Gans, O., Moche, W., Scharf, S., Lorbeer, G. (2004) Monitoring ofselected estrogenic hormones and industrial chemicals in groundwaters and surface waters in Austria. Sci. Total Environ. 333, 185-193.

[36] Grzegorz, C., Wieslaw, K. (2012) Comparing Methods of 17α-ethinylestradiol (EE2) Determination in Surface Water. Department of Microbiology, Instituteof Biology, Jan Kochanowski University in Kielce, Świętokrzyska, Kielce, Poland.15, 25-406.

[37] Daughton, C.G., Ternes, T.A. (1999) Pharmaceuticals and Personal Care Products in The Environment: Agents of Subtle Change? Environmental Health Perspectives. 107(6), 907-938.

[38] Roefer, P., Synder, S., Zegers, R.E., Rexing, D.J. and Fronk, J.L. (2000) Endocrine-Disrupting Chemicals in Asource Water. Journal of AWWA. 92(8), 52-58.

Received: **17.05.2018**
Accepted: **20.02.2019**

CORRESPONDING AUTHOR

Meltem Eken
Iskenderun Technical University
Marine Sciences and Technology Faculty,
31200 Iskenderun, Hatay – Turkey

e-mail: duralmeltem@yahoo.com

© by PSP Volume 28 – No. 4/2019 pages 2464-2468 Fresenius Environmental Bulletin

DETERMINATION OF CATALASE ACTIVITY EXPOSED TO ORGANOPHOSPHATE INSECTICIDES AZINPHOS-METHYL AND DIMETHOATE

Hasan Karadag*, Fatma Temiz Uzun

Adiyaman University, Science and Letters Faculty, Chemistry Department, 02040, Adiyaman, Turkey

ABSTRACT

In this investigation, the effects of azinphos-methyl and dimethoate on bovine liver catalase were searched. The catalase enzyme activity values were measured by the interaction of the catalase with azinphos-methyl and dimethoate prepared at concentrations of from 0 to 500 mg / L. The catalase enzyme activity sharply decreased while azinphos-methyl concentration increased. An irreversible inhibition was determined in the catalase activity which interacts with azinphos-methyl. However, following dimethoate application, the catalase activity showed a decline at concentrations of 25, 50 and 100 mg / L of dimethoate and an elevation at concentrations of 250 and 500 mg / L of dimethoate. The catalase behaved differently according to varying concentrations of dimethoate with inhibitions at low concentrations and activations at high concentrations.

KEYWORDS:
Catalase, Azinphos-methyl, Dimethoate, Organophosphate, Insecticide

INTRODUCTION

Azinphos-methyl, [(O,O-dimethyl-S-((4-oxo-1,2,3-benzotriazin-3(4H)-yl)methyl) phosphordithioate, (AZM)] used in various parts of the world to protect food products from pest is an organophosphate insecticide. AZM exhibits toxicity by inhibiting the enzyme acetylcholinesterase. Acetylcholinesterase hydrolyzes acetylcholine. Inhibition of acetylcholinesterase lead to smooth muscle contractions, glandular secretions, skeletal muscle twitching and at higher dose, paralysis [1-3].

Dimethoate [O, O-dimethyl-S (N-methylcarbomethyl) phosphorodithioate, (DM)] is a systemic organophosphate insecticide. Like other organophosphates, DM is also an acetylcholinesterase inhibitor in the brain or blood compartment. Acetylcholinesterase inhibitions were shown at animals by oral, dermal or inhalation exposures of DM [4]. DM is used in agriculture to keep safe tree fruits such as apples and pears and tobacco from aphids and leaf rodents [5]. The widespread use of DM can cause adverse health effects due to retention at soil, product and water [6].

Catalase (EC 1.11.1.6.) (CAT) contains four subunit or tetramer, each subunit contain 1 Fe-protoheme IX part (4 heme groups per tetramer) [7-8]. CAT is exist in living organisms. Hydrogen peroxide is oxidant agent. CAT catalysis the convertion of hydrogen peroxide to water and oxygen [9].

AZM and DM organophosphate pesticides are widely used in agricultural applications. Pesticides have the advantage of eliminating harmful organisms. But, on the other hand, they have residual problems. They cause oxidative stress in living organisms. For this reason, we examined the effect of AZM and DM organophosphate pesticides on bovine liver catalase.

MATERIALS AND METHODS

Chemicals. Azinphos-methyl ($C_{10}H_{12}N_3O_3PS_2$) (45333) (Fig.1.a), dimethoate ($C_5H_{12}NO_3PS_2$) (45449) (Fig.1.b), catalase from bovine liver (C40) were bought from Sigma-Aldrich. Other chemicals used were analytical grade.

Protein determination. The protein was determined spectrophotometrically at 750 nm according to the method of Lowry et al. (1951) [10]. Bovine serum albumin was used as standard for the measurement of CAT protein concentration. For measurement of protein concentration, four solutions were prepared: 1. Solution (A): 0.5 g $CuSO_4$. 5 H_2O and 1 g sodium citrate dihydrate were dissolved at distilled water and completed to 100 mL by distilled water; 2. Solution (B): 20 g Na_2CO_3 and 4 g NaOH were dissolved at distilled water and completed to 1000 mL by distilled water; 3. Solution (C): 2 mL solution A was added to 100 mL solution B; 4. Solution (D): 15 mL Folin-Ciocalteu was added to 15 mL distilled water. After that, 2.5 mL solution C was added to 0.5 mL of CAT solution, shaked, waited for 10 minutes at room temperature, mixed with 0.25 mL solution D, shaked, waited for 30 minutes and read at 750 nm for determination of CAT concentration.

CAT activitiy. CAT activity was determined by the method of Lartillot et al. (1988) [11] which is worked by Bergmeyer (1974) previously [12], CAT activity was measured spectrophotometrically at 240 nm using a specific absorption coefficient as 0.040 cm^2 /µmol H_2O_2. For this purpose, 2.5 mL substrate solution as 10 mmol / L of H_2O_2 in 50 mmol / L pH = 7.5 phosphate buffer [13] and 20 µL of CAT solution were mixed at room temperature for 2 min and the reaction was terminated by adding 0.5 mL of 1 mol / L HCl. CAT activity was calculated as µmol H_2O_2 convertion / mg protein / min or (U / mg).

Effect of insecticides on enzyme activity. Preparation of 5000 mg / L AZM in 2 mL absolute ethyl alcohol and 5000 mg / L DM in 2 mL absolute ethyl alcohol were used. Because of low solubility of AZM and DM in water, AZM and DM were dissolved in absolute ethyl alcohol. After that, arrangement of 25, 50, 100, 250 and 500 mg / L AZM and DM with ethyl alcohol plus 700 µL CAT solution about 0.5 mg protein / mL were done [14]. At control or 0 ppm, 300 µL absolute ethyl alcohol and 700 µL CAT solution were used. Solution volume of enzyme and ethyl alcohol and organophosphate insecticide was 1 mL. The preparation was waited at room temperature for half hour. After that, activities of CAT were measured.

Value analysis. The values are shown as mean ± standard deviation. For the statistical analyses, one-way analysis of variance (ANOVA) was used, followed by the Student Newman-Keul's test using the SPSS version 22 statistical software (SPSS Inc., Chicago, IL, USA). Differences were considered as significant if $p < 0.05$.

RESULTS

Effect of azinphos-methyl on CAT activity. Different AZM concentrations interacted with CAT solutions, after that activities of CAT and standard deviation were determined and shown in Table 1. The activity-concentration graph is illustrated in Fig.2. When analzed Table 1 and Fig.2 it has been observed that the AZM concentration increases while CAT enzyme activity sharply decreases. An irreversible inhibition was observed in the CAT activity which interacts with AZM. With compared to the control activity, there are statistical differences between all CAT activities which interacted with the AZM ($p < 0.05$, $n = 3$). The percent reductions of catalase enzyme activity at 25, 50, 100, 250 and 500 mg / L of AZM were 78.8; 73.7; 75.0; 81.4 and 72.2 respectively.

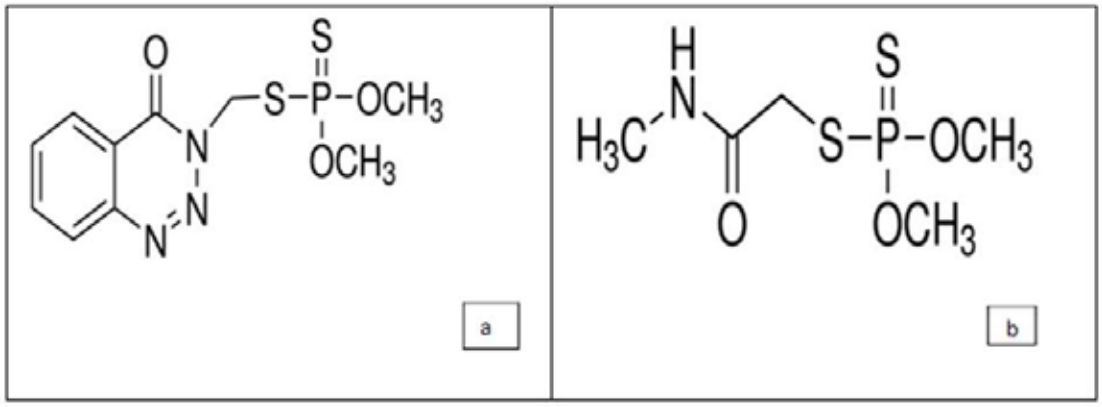

FIGURE 1
Structures of azinphos-methyl (a) and dimethoate (b)

TABLE 1
Influence of azinphos-methyl and dimethoate insecticide concentrations on catalase activity

Insecticide Concentration (mg / L)	CAT activity ± standart deviation (U / mg) at AZM	CAT activity ± standart deviation (U / mg) at DM
0	5393 ± 69[a]	1673 ± 7[a]
25	1141 ± 34[bd]	989 ± 14[b]
50	1417 ± 91[c]	1327 ± 41[c]
100	1348 ± 226[bc]	1097 ± 35[d]
250	1003 ± 34[d]	1747 ± 24[e]
500	1498 ± 140[c]	1749 ± 12[e]

Values are shown as mean ± standard deviation. At the table "a, b, c, d and e" letters are used for differences of activity levels. There are statistical differences between values which are indicated with different letters ($p < 0.05$, $n = 3$)

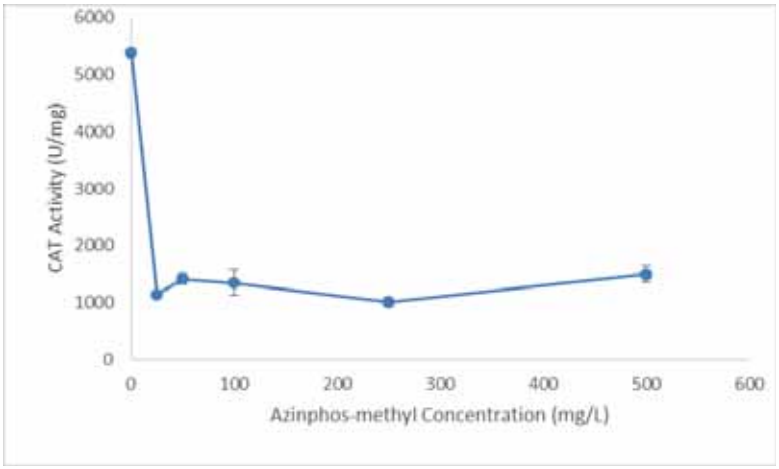

FIGURE 2
Influence of azinphos-methyl concentrations on catalase activity

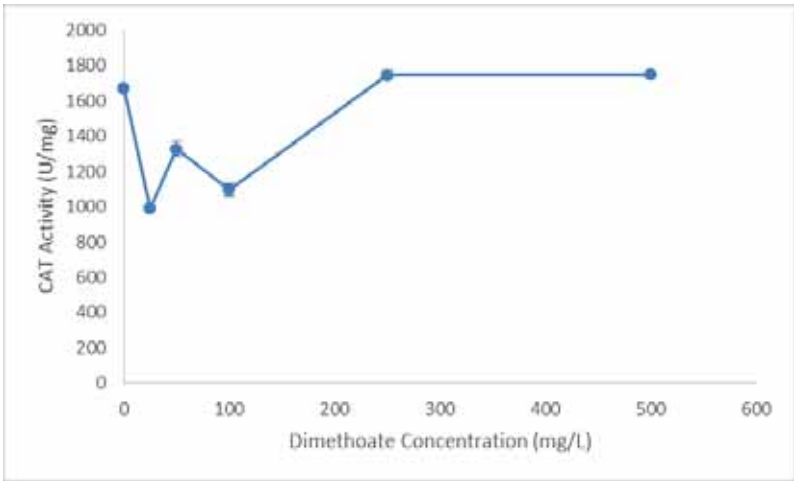

FIGURE 3
Influence of dimethoate concentrations on catalase activity

Effect of dimethoate on CAT activity. Different DM concentrations interacted with CAT solutions, after that activities of CAT and standard deviation were determined and shown in Table 1. The activity-concentration graph is illustrated in Fig.3. When compared to the control group, the decreases and increases in CAT enzyme activity were statistically significant at all tested interaction concentrations of the DM ($p < 0.05$, $n = 3$). When analzed Table 1 and Fig.3 it has been observed that catalase enzyme activity decreased at 25, 50 and 100 mg / L of DM concentrations and catalase enzyme activity increased at 250 and 500 mg / L of DM concentrations. The percent reductions of catalase enzyme activity at 25, 50, 100 mg / L of DM were 40.9; 20.7; 34.4 respectively, the percent increases of catalase enzyme activity at 250 and 500 mg / L of DM were 4.4 and 4.5 respectively.

DISCUSSION AND CONCLUSIONS

Margoliash and Schejter (1962) demonstrated irreversible inhibition of catalase by 3-amino-1,2,4-triazole [15]. AZM inhibited CAT enzyme as irreversible. AZM includes similar group as 1,2,3-benzotriazin. A similar work was conducted by Aksoy et al. (2004). They studied inhibition of catalase from human erythrocyte with azide. They found that catalase inhibited by azide as noncompetitive [16]. Ferrari et al. (2007) exposed to juvenile rainbow trout *(Oncorhynchus mykiss)* to sublethal concentrations of AZM (2.5 and 5 µg / L). They indicated that in liver and/or kidney, CAT activities continuously decreased [17].

DM poisoning causes cellular damage and oxidative stress. This leads to lipid peroxidation and free radical formation [18]. Hydrogen peroxide is a form of reactive oxygen species (ROS). When hydrogen peroxide occurs, CAT turns hydrogen peroxide into water and oxygen. Increases at CAT activity might be response to production of hydrogen peroxide or ROS [19]. Catalase activity de-

creased at low insecticide concentrations such as under 25, 50 and 100 mg / L concentrations of DM. Beside this, catalase enzyme activity increased at high insecticide concentrations such as under 250 and 500 mg / L concentrations of DM. There are similar results like our findings. For example, at low DM concentration, Saafi et al. (2011) found reduced catalase activities [20]. Saafi et al. (2011), exposed DM (20 mg /kg / day) to male adult Wistar albino rats. At rat liver, catalase activity was reduced significantly by DM. Pretreatment of date palm fruite extract restored the liver damage and ameliorated catalase activities. At high DM concentration, Amara et al. (2011) found increased catalase activities [21]. Amara et al. (2011) treated adult Wistar rats to DM (0.2 g / L of drinking water), DM + selenium (0,5 mg kg^{-1} of diet), DM + vitamin E (100 mg / kg of diet) or DM + selenium + vitamin E for 30 days. They observed an inrease at catalase activities in the cerebral cortex of rats. They found neurotoxicity reduction by natural antioxidants like selenium and vitamin E. Application of selenium and/or vitamin E through the diet ameliorated the catalase activities.

Catalase was inhibited by AZM as irreversible. AZM has 1,2,3 - benzotriazin. Benzotriazin contains three nitrogen and unpaired electrons. Our suggestion is that this group can serve electrons to tie Fe-protoheme IX part and it inhibits catalase enzyme.

DM leads to free radical formation. Because of that, at low DM concentrations catalase activity decreased. But at high DM concentrations, catalase enzyme activity increased. This is might be due to production of hydrogen peroxide or ROS.

ACKNOWLEDGEMENTS

This study was supported by the Adiyaman University Scientific Research Projects Unit, Project Number: FEFYL / 2017 - 0005.

REFERENCES

[1] Loewy, R.M., Monza, L.B., Kiers, V.E., Savini, M.C. (2011) Pesticide distribution in an agricultural environment in Argentina. J. Environ. Sci. Health B. 46, 662–670.

[2] USEPA (United States Environmental Protection Agency) (2006) Interim registration eligibility decision for azinphos-methyl. Case no. 0235. https://archive.epa.gov/pesticides/reregistration/web/pdf/azinphosmethyl_ired.pdf (accessed Apr 2018).

[3] Cacciatore, L.C., Nemirovsky, S.I., Guerrero, N.R.V., Cochón, A.C. (2015) Azinphos-methyl and chlorpyrifos, alone or in a binary mixture, produce oxidative stress and lipid peroxidation in the freshwater gastropod planorbarius corneus. Aquat. Toxicol. 167, 12–19.

[4] USEPA (United States Environmental Protection Agency) (2006) Interim registration eligibility decision for dimethoate. Case no. 0088. https://nepis.epa.gov/Exe/ZyPDF.cgi/P10049N4.PDF?Dockey=P10049N4.PDF (accessed Apr 2018).

[5] Hayes, W.J. and Laws, E.R. (1991). Handbook of Pesticide Toxicology. Vol. 3. Classes of Pesticides. Academic Press, New York, pp 1471-1526.

[6] IPCS/WHO (International Programme on Chemical Safety/ World Health Organization) (1996) Principles and methods for assessing direct immunotoxicity associated with exposure to chemicals. Environ. Health Crit., 180, Geneva, Switzerland.

[7] Bergmeyer, H.U. (1983). Methods of enzymatic analysis. Vol. 3, Third Edition; VCH, Weinheim, West Germany, pp 165.

[8] Bergmeyer H. U. (1983). Methods of enzymatic analysis. Vol. 3, Third Edition, VCH, Weinheim, West Germany, pp 273.

[9] Chelikani, P., Fita, I., Loewen, P.C. (2004) Diversity of structures and properties among catalases. Cell. Mol. Life Sci. 61(2), 192–208.

[10] Lowry, O.H., Rosebrough, N.J., Farr, A.L., Randall, R.J. (1951) Protein measurement with the folin phenol reagent. J. Biol. Chem. 193, 265–275.

[11] Lartillot, S., Kadziora, P., Athios, A. (1988) Purification and characterization of new fungal catalase. Prep. Biochem. 18(3), 241–246.

[12] Bergmeyer, H.U. (1974). Methods of enzymatic analysis. Vol. 1, 2nd ed, Academic press, New York, USA, 438-439.

[13] Tukel, S.S., Alptekin, O. (2004) Immobilization and kinetics of catalase onto magnesium silicate. Process Biochem. 39, 2149–2155.

[14] Karadag, H., Bilgin, R. (2010) Effect of cyprodinil and fludioxonil pesticides on human superoxide dismutase. Asian J. Chem. 22(10), 8147-8154.

[15] Margoliash, E., Schejter, A. (1962) Kinetics of the irreversible inhibition of catalase by 3-amino-1,2,4-triazole in the presence of hydrogen peroxide and catalase-hydrogen peroxide complex I hydrogen donors. J. Biol. Chem. 237(7), 2359-2363.

[16] Aksoy, Y., Balk, M., Ogus, I.H., Ozer, N. (2004) The mechanism of inhibition of human erythrocyte catalase by azide. Turk J. Biol. 28, 65-70.

[17] Ferrari, A., Venturino, A., Pechén de D'Angelo, A.M. (2007) Effects of carbaryl and azinphos methyl on juvenile rainbow trout (*Oncorhynchus mykiss*) detoxifying enzymes. Pestic. Biochem. Phys. 88, 134–142.
[18] Amara, I.B., Soudani, N., Troudi, A., Bouaziz, H., Boudawara, T., Zeghal, N. (2011) Antioxidant effect of vitamin e and selenium on hepatotoxicity induced by dimethoate in female adult rats. Ecotox. Environ. Safe. 74, 811–819.
[19] Ritola, O., Livingstone, D.R., Peters, L.D., Lindstrom-Seppa, P. (2002) Antioxidant processes are affected in juvenile rainbow trout (*Oncorhynchus mykiss*) exposed to ozone and oxygen-supersaturated water. Aquaculture. 210, 1–19.
[20] Saafi, E.B., Louedi, M., Elfeki, A., Zakhama, A., Najjar, M.F., Hammami, M., Achour, L. (2011) Protective effect of date palm fruit extract (*Phoenix Dactylifera L.)* on dimethoate induced-oxidative stress in rat liver. Exp. Toxicol. Pathol. 63, 433–441.
[21] Amara, I.B., Soudani, N., Hakim, A., Troudi, A., Zeghal, K.M., Boudawara, T., Zeghal, N. (2011) Selenium and vitamin e, natural antioxidants, protect rat cerebral cortex against dimethoate-induced neurotoxicity. Pestic. Biochem. Phys. 101, 165–174.

Received: **18.06.2018**
Accepted: **22.02.2019**

CORRESPONDING AUTHOR

Hasan Karadag
Adiyaman University,
Science and Letters Faculty,
Chemistry Department,
02040, Adiyaman – Turkey

e-mail: hkaradag@adiyaman.edu.tr

© by PSP Volume 28 – No. 4/2019 pages 2469-2474 Fresenius Environmental Bulletin

ACCUMULATION OF FLUORIDE IN HORSE-CHESTNUT (*AESCULUS HIPPOCASTANUM* L.) LEAVES COLLECTED FROM WEST POMERANIAN DISTRICT OF POLAND

Arkadiusz Telesinski[1,*], Grzegorz Nowak[2], Karol Stanislawski[2], Robert Biczak[3], Jacek Wrobel[1], Marek Snieg[4], Jakub Poblocki[5], Marek Rynkiewicz[4]

[1]Department of Plant Physiology and Biochemistry, West Pomeranian University of Technology in Szczecin, 17 Słowackiego Str., 71-434, Szczecin, Poland
[2]Department of Meteorology and Landscape Architecture, West Pomeranian University of Technology in Szczecin, 3 Papieża Pawła VI Str., Szczecin, Poland
[3]Department Biochemistry and Ecotoxicology, Jan Długosz University in Częstochowa, 13/15 Armii Krajowej Av., Częstochowa, Poland
[4]Department of Construction and Use of Technical Device, West Pomeranian University of Technology in Szczecin, 1 Papieża Pawła VI Str., Szczecin, Poland
[5]Clinic of Endocrinology, Metabolic Diseases and Internal Diseases, Pomeranian Medical University in Szczecin, 1 Unii Lubelskiej Str., Szczecin, Poland

ABSTRACT

Since the finding that fluoride is a bioelement, research on its biological role, its applicability in practice, and its toxicity has intensified. Fluoride is characterized by a narrow safety margin. The entire ecosystems located within the range of fluoride emitters are highly susceptible, especially plants, to fluoride toxicity. The West Pomeranian District in Poland is an area with chemical plants that emit significant amounts of fluoride into the atmosphere. Literature regarding the use of various plant species as bioindicators of fluoride in air is currently available. However, to the best of our knowledge, there is no information regarding the accumulation of fluorides in horse chestnut leaves. Therefore, in this study, we aimed to assess the fluoride content in horse chestnut leaves according to the distance from the emitter and the year of collection of leaves. Horse chestnut leaves were collected in the first week of July from 2013 to 2016 from the 12 measurement points located in the West Pomeranian District, Poland. The fluoride content was determined potentiometrically. According to the results, fluoride content in horse chestnut leaves ranged from 6.89 mg/kg DW to 22.88 mg/kg DW. The median value of fluoride content decreased as the distance from the emission source increased. However, the year of sampling did not significantly affect the fluoride content in horse chestnut leaves. Thus, these results indicate the potential application of horse chestnut leaves as a bioindicator of air pollution with fluorides.

KEYWORDS:
Horse chestnut, fluoride, bioindication, distance from emitter

INTRODUCTION

The concentrations of many chemical elements in the atmosphere have been changed due to the anthropogenic activities [1]. Environmental pollution with fluoride is currently one of the most important problems to be dealt because of its hazardous effect on our ecosystems [2]. The principal anthropogenic sources of fluoride include aluminum smelters; fertilizer factories; and industrial activities such as brick, tile, pottery and cement works, ceramic industries, and glass manufacturers [3]. Owing to the regulation imposed by the government, most fluoride emitters have recently equipped their premises with effective filters to remove fluorides prior to disposal [2]. However, fluoride emission into the atmosphere continues to be a problem [4,5]. In the air, fluorides are present in the gaseous or in particulate form (principally as hydrogen fluoride – HF and silicon tetrafluoride – SiF_4). Both forms are deposited on the surface of leaves, but gaseous fluoride is also absorbed through stomata and is extremely phytotoxic [6]. Śnioszek et al. [5] noted that fluorides accumulate in plants mostly from air via absorption through leaves. Fluoride uptake via root system is not found to be significant in the air-polluted areas [7].

According to Petrova et al. [1], *Aesculus hippocastanum* L. is one of the most studied plants with respect to air pollution with heavy metals because it is large and has compound leaves, is easy to recognize and sample, and is widely cultivated on streets and parks as an ornamental tree. However, there is no mention of this species in the literature regarding its sensitivity to the presence of fluorides in the air [8-11].

In West Pomeranian District of Poland, two fertilizer plants are located. In our previous studies, we have shown that these plants cause increased runoff of fluoride into the soil, sand, grass, and

vegetables [12–15].

Therefore, in this study, we aimed to assess the fluoride content in horse chestnut leaves according to the distance from the emitter and the year of collection of leaves.

MATERIALS AND METHODS

Horse chestnut leaves were collected in the first week of July from 2013 to 2016 from 12 measuring points located in the West Pomeranian District, Poland. Four of the measurement points were located within the city of Szczecin at a distance of 15-17 km from the main emitter of fluorides in this area. The remaining measurement points were located in the area of the West Pomeranian District in towns differently distant from the emitter. In each location, there were clusters or avenues of chestnut trees; we collected 13 leaves from different trees of this species at each point. Table 1 shows the location of sampling sites. A pooled sample was made from the collected leaves from a given year, which was then dried and ground.

TABLE 1
Location of sampling sites

Place	Distance from emitter of fluoride compounds (km)	Direction
Szczecin, Piłsudskiego Str.	16.40	S
Szczecin, Sowackiego Str.	15.00	S
Szczecin, Jarowita Str.	16.81	S
Szczecin, Narutowicza Str.	17.03	S
Krzymów	67.52	SW
Gryfino	36.58	SW
Czachowo	62.13	NE
Buk	15.52	SW
Batowo	64.48	SE
Krajnik Dolny	63.00	SW
Cieszyno	98.46	E
Konie	64.98	E

Fluoride content was determined based on the method described by Eyde [16]. Briefly, the dried and ground samples were fused in nickel crucibles with sodium hydroxide. Then, water, diluted hydrochloric acid, and citrate buffer were added to the melt. For the potentiometric method, fluoride concentration was determined in the presence of TISAB III buffer with an Orion Research ion-selective electrode. The fluoride content was expressed in mg/kg DW.

The results were statistically analyzed using one-way analysis of variance, which was performed independently for each year of the study. Homogeneous groups were compared with Tukey honest significant difference (HSD) post-hoc comparisons (p<0.05). The median, first, and third quadrilles of fluoride content in horse chestnut leaves were also calculated depending on the distance from the emitter and the year of the study. To determine whether distance of the emitter and year of analysis influenced on the fluoride content in horse chestnut leaves, there was a 3D surface matched for the experiment data, by means of the method of the smallest squares with the distance weighing. This technique depicts the tendency of changes in fluoride content according to both distance of the emitter and the year of analysis. Software Statistica v. 13.1 (Statsoft, Inc., Krakow, Poland) was used for statistical analyzes.

RESULTS AND DISCUSSION

Fluoride content in horse chestnut leaves was found to vary depending on the year of research. In 2013-2014, the highest fluoride content was recorded in the city of Szczecin on Słowackiego Street and in Buk, located at the smallest distance from the emitter (15-17 km). This content varied in the following ranges in individual years of research: in 2013, it was 22.83-22.88 mg/kg DW and in 2014, it was 21.09-21.84 mg/kg DW. In 2015, we did not find any significant differences in the fluoride content in horse chestnut leaves collected from Szczecin on Słowackiego and Piłsudskiego Streets and in Buk: 19.63-20.43 mg/kg DW. In 2016, however, we found statistically highest concentrations of fluorides in horse chestnut leaves collected from Buk than that of other areas - 20.47 mg/kg DW (Table 2). Lowest concentration of fluorides in horse chestnut leaves was found in Cieszyn, that is, the village furthest away from the emitter than that of other areas (from 6.89 mg/kg DW in 2013 to 9.57 mg/kg DW in 2015).

Comparison of the median value of fluoride content in horse chestnut leaves depending on the distance from the emitter was performed. The median value of fluoride content in leaves collected at a distance of 15-17 km and 36.6–67.5 km from the emitter was found to be around 18.51-20.79 mg/kg DW and 11.95 mg/kg DW to 15.07 mg/kg DW, respectively. In contrast, the median value of fluoride content in horse chestnut leaves collected at the point furthest away from the emitter was found to be around 8.07 mg/kg DW (Figure 1). This phenomenon of decreasing content of fluoride in horse chestnut leaves depending on the increasing distance from the emitter has been confirmed by other authors, who have investigating the accumulation of fluorides in various plant species [4, 6, 12, 14, 17-21]. Gaseous fluoride is absorbed through stomata of the leaves and is transported via transpiration into the principal sites of accumulation at the tip and leaf margins, where they can cause physiological, biochemical, and structural damage, and even cell death, depending on the concentration in the

cell sap [22]. In addition to the direct uptake through stomata, plants can incorporate fluoride from contaminated soils [23]. However, in highly polluted areas, direct absorption of airborne fluorides by the plant foliage normally masks any uptake via soil [20]. A previous study did not show the relationship between fluoride content in soil and distance from the emitter [13].

In Szczecin, the median value of fluoride content in horse chestnut leaves ranged from 17.11 mg/kg DW to 21.09 mg/kg DW (Figure 2). The lowest value was recorded in the leaves collected from Jarowita Street than that of other areas, whereas the highest value was recorded in the leaves collected from Słowackiego Street than that of other areas. However, the median values of fluoride content in horse chestnut leaves depending on the year of research showed that the values were similar for each year (range: from 14.47 mg/kg DW to 16.41 mg/kg DW) (Figure 3).

TABLE 2
Fluoride content in horse chestnut leaves collected in sampling sites

Place	Year			
	2013	2014	2015	2016
Szczecin, Piłsudskiego Str.	18.67±0.36b	16.48±0.19b	19.63±0.53a	18.69±1.13b
Szczecin, Słowackiego Str.	22.83±0.93a	21.84±0.41a	20.43±0.31a	18.92±0.84b
Szczecin, Jarowita Str.	18.07±0.07b	16.80±0.34b	14.70±0.19bc	17.44±0.40c
Szczecin, Narutowicza Str.	18.33±0.12b	20.96±0.37a	14.59±0.07bc	18.12±0.10bc
Krzymów	11.13±0.31d	13.37±0.17c	13.49±0.36cd	13.86±0.24e
Gryfino	14.58±0.45c	16.30±0.29b	15.27±0.28b	14.99±0.13d
Czachowo	14.88±0.29c	17.06±0.28b	14.13±0.28c	15.37±0.53d
Buk	22.88±0.25a	21.09±0.55a	20.13±0.36a	20.47±0.58a
Batowo	12.69±0.18d	13.19±0.26c	12.70±0.42de	14.41±0.40de
Krajnik Dolny	12.34±0.32d	13.04±0.46c	13.52±0.23cd	12.54±0.28f
Cieszyno	6.89±0.44e	8.34±0.47d	9.57±0.56f	7.99±0.33h
Konie	12.34±0.13d	12.09±0.17c	11.61±0.48e	10.95±0.72g

The same letters for an enzyme in columns are assigned to the same homogeneous groups (HSD Tukey test)

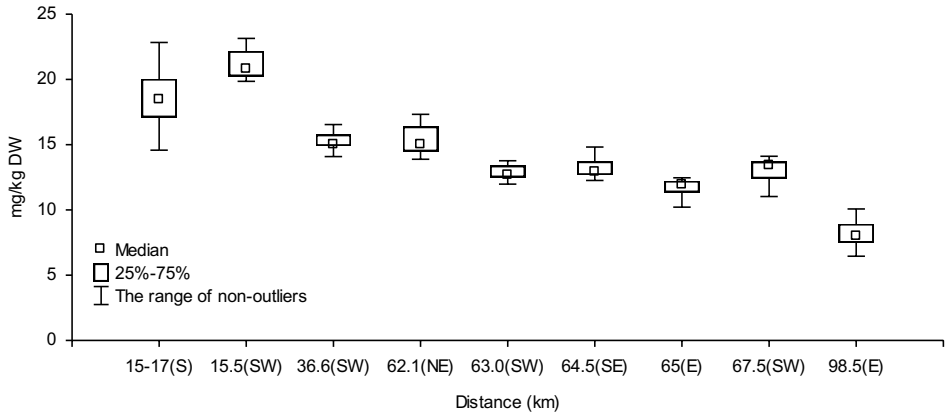

FIGURE 1
Median values of fluoride content in horse chestnut leaves depending on distance of emitter

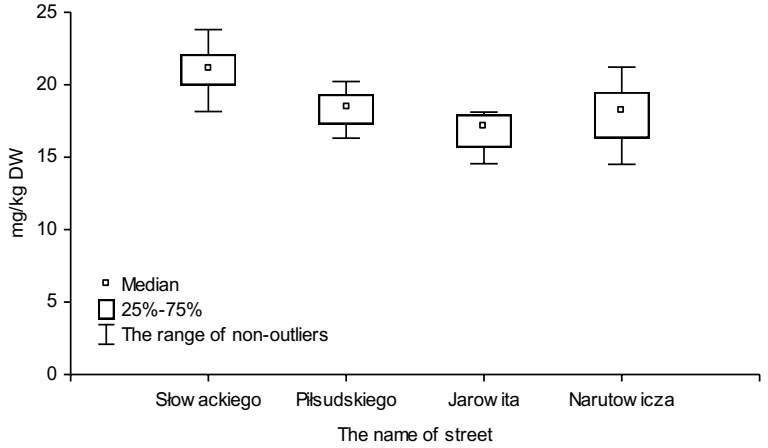

FIGURE 2
Median values of fluoride content in horse chestnut leaves collected in Szczecin

FIGURE 3
Median values of fluoride content in horse chestnut leaves depending on year

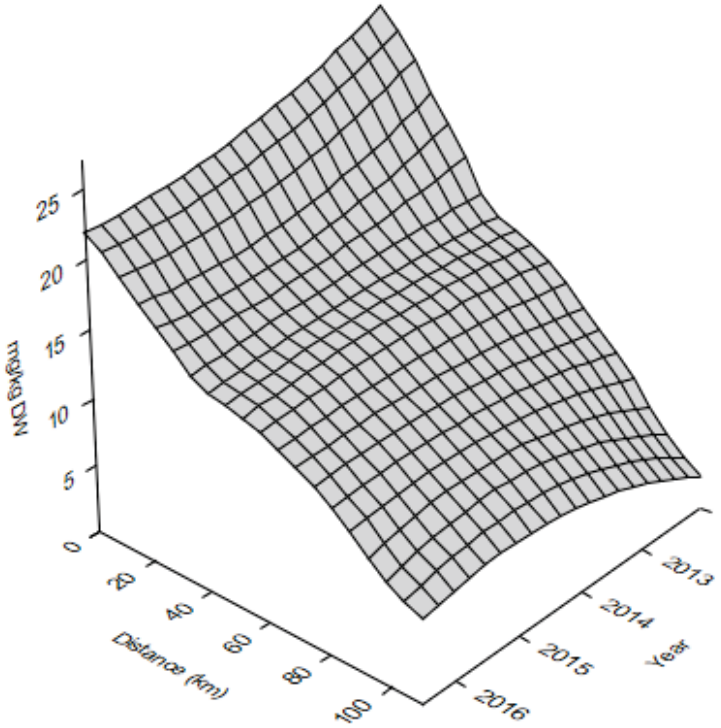

FIGURE 4
The 3D diagram of relationship between fluoride content in horse chestnut leaves and year and distance form emmiter

The 3D diagram of fluoride content in horse chestnut leaves indicates a clear correlation between the decreases in fluoride content with increasing distance from the emitter, regardless of the year of sample collection (Figure 4). As already mentioned, the decrease in the content of fluorides in the leaves of various plant species along with the increase in the distance from the emission sources has been confirmed by many authors [14, 17-21]. In addition, Kłódka et al. [12] state that the fluoride content is always higher in the aboveground parts of plants than underground parts. This is due to the fact that in areas under the influence of the emission, fluorides primarily accumulate in the leaves [6]. However, Divan et al. [24] found that the presence of fluorides in the leaves does not always reflect the atmospheric pollution, because plants can take it from soil through the root system. Therefore, the action of fluoride on a plant should be considered from two points of view: as the effect of fluorides contained in dust and industrial gases on the plant and as the effect of fluoride during its collection absorption by the root system [25]. However, according to the literature, plants accumulate fluorides in their tissues primarily from the air [26].

CONCLUSION

The fluoride content in horse chestnut leaves collected in 2013-2106 in the West Pomeranian District (Poland) ranged from 6.89 mg/kg DW to 22.88 mg/kg DW. It changed both depending on the year of the study and the date of research. The median values of fluoride content decreased as the distance from the emission source increased. However, the year of samples collection did not significantly affect the fluoride content in horse chestnut leaves. These results indicate the potential use of horse chestnut leaves in the bioindication of fluoride content in the air.

REFERENCES

[1] Petrova, S., Yurukova, L., Velcheva, I. (2012) Horse chestnut (*Aesculus hippocastanum* L.) as a biomonitor of air pollution in the town of Plovdiv (Bulgaria). Journal of Bioscience and Biotechnology. 1(3), 241-247.

[2] Walna, B., Kurzyca, I., Bednorz, E., Kolendowicz, L. (2013) Fluoride pollution of atmospheric precipitation and its relationship with air circulation and weather patterns (Wielkopolski National Park, Poland). Environmental Monitoring and Assessment. 185(7), 5497-5514.

[3] Cape, J.N., Fowler, D., Davison, A. (2003) Ecological effects of sulfur dioxide, fluorides, and minor air pollutants: recent trends and research needs. Environment International. 29, 201-211.

[4] Franzaring, J., Hrenn, H., Schumm, C., Klumpp, A., Fangmeier, A. (2006) Environmental monitoring of fluoride emissions using precipitation, dust, plant and soil samples. Environmental Pollution. 144, 158-165.

[5] Śnioszek, M., Telesiński, A., Smolik, B., Zakrzewska, H. (2018) Effect of fluoride and bentonite on biochemical aspects of oxidative stress in *Pisum sativum* L. Journal of Ecological Engineering. 19(2), 164-171.

[6] Kinnunen, H., Holopainen, T., Räisänen, M.L., Kärenlampi, L. (2003) Fluoride in birch leaves, ground vegetation, litter and humus in the surroundings of a fertilizer plant and apatite mine in Siilinjärvi, eastern Finland. Boreal Environment Research. 8, 185-192.

[7] Jha, S.K., Nayak, A.K., Sharma, Y.K. (2008) Response of spinach (*Spinacea oleracea*) to the added fluoride in an alkaline soil. Food and Chemical Toxicology. 46(9), 2968-2971.

[8] Weinstein, L.H., Davison, A.W. (2003) Native plant species suitable as bioindicators and biomonitors for airbone fluoride. Environmental Pollution. 125, 3-11.

[9] Telesiński, A., Śnioszek, M. (2009) Bioindicators of environmental pollution with fluorine. Bromatologia i Chemia Toksykologiczna. 42(4), 1148-1154 (in Polish).

[10] Rodriguez, J.H., Wannaz, E.D., Pignata, M.L., Fangmeier, A., Franzaring, J. (2012) Fluoride biomonitoring around a large aluminium smelter using foliage from different tree species. Clean – Soil Air Water. 40(12), 1315–1319.

[11] Proskura N. (2015) Bioindication and biomonitoring of air pollution. Life Science Journal. 12(8), 65-67.

[12] Kłódka, D., Musik, D., Wójcik, K., Telesiński, A. (2008) Fluorine content in selected vegetables grown within the area affected by emission of that element from the ,,Police" Chemical Plant. Bromatologia i Chemia Toksykologiczna. 41(4), 964-969 (in Polish).

[13] Telesiński, A., Smolik, B., Grabczyńska, E. (2010) Formation of adenylate energy charge (AEC) versus in fluorine content in forest soil in the area affected by emission from Police Chemical Plant. Journal of Elementology. 15(2), 355-362.

[14] Krzywy, E., Ciubak, J., Możdżer, E., Telesiński, A. (2013) Impact of emitters from Fosfan Company Ltd. on the fluorine content in soil and grasses. Przemysł Chemiczny. 92(8), 1461–1463 (in Polish).

[15] Telesiński, A., Czałczyńska-Podolska, M., Węgrzynowski, Ł., Biczak, R., Telesińska, N. (2017) Changes of fluoride content in the sand from sandboxes located on children playgrounds in Police (West Pomerania, Poland). Journal of Ecological Engineering. 18(5), 168-172.

[16] Eyde, B. (1982) Determination of fluoride in plant material with ione-selective electrode. Fresenius' Zeitschrift für Analytische Chemie. 311, 19-22.

[17] Jha, S.K., Nayak, A.K., Sharma, Y.K., Mishra, V.K., Sharma, D.K. (2008) Fluoride accumulation in soil and vegetation in the vicinity of brick fields. Bulletin of Environmental Contamination and Toxicology. 80(4), 369-373.

[18] Koblar, A., Tavčar, G., Ponikvar-Svet, M. (2011) Effects of airborne fluoride on soil and vegetation. Journal of Fluorine Chemistry. 132(10), 755-759.

[19] Hong, B.D., Joo, R.N., Lee, K.S., Lee, D.S., Rhie, J.H., Min, S., Song, S.G., Chun, D.Y. (2016) Fluoride in soil and plant. Korean Journal of Agricultural Science. 43(4), 522-536.

[20] Baunthiyal, M., Ranghar, S. (2015) Accumulation of fluoride by plants: potential for phytoremediation. Clean. Soil, Air, Water. 43(1), 127-132.

[21] Singh, G., Kumari, B., Kriti, S.G., Kumar, N., Mallick, S. (2018) Fluoride distribution and contamination in the water, soil and plants continuum and its remedial technologies, an Indian perspective – a review. Environmental Pollution. 239, 95-108.
[22] Jain, A., Mohapatra, A.K., Yunus, G.Y., Tiwari, R., Parakh, A., Verma, S. (2017) Estimating concentration of fluoride in edible leaves locally grown around Raipur, Chhattisgarh. Journal of Indian Association of Public Health Dentistry. 15(2), 177-180.
[23] Mezghani, I., Elloumi, N., Abdallah, F.B., Chaieb, M., Boukhris, M. (2005) Fluoride accumulation by vegetation in the vicinity of a phosphate fertilizer plant in Tunisia. Fluoride. 38(1), 69-75.
[24] Divan Jr, A.M., Oliva, M.A., Ferreira, F.A. (2008) Dispersal pattern of airbone emission from an aluminium smelter in Ouro Preto, Brazil, as expressed by foliar fluoride accumulation in eight plant species. Ecological Indicators. 8, 454-461.
[25] Telesiński, A., Śnioszek, M., Smolik, B., Malinowska, K., Mikiciuk, M., Cichocka, J., Zakrzewska, H. (2011) Fluoride uptake in hydroponic culture by different clones of basket willow, *Salix viminalis* L. Fluoride. 44(4), 255-259.
[26] Horntvedt, R. (1997) Accumulation of airborne fluorides in forest trees and vegetation. Forest Pathology. 27(2), 73-82.

Received: **23.06.2018**
Accepted: **21.01.2019**

CORRESPONDING AUTHOR

Arkadiusz Telesinski
Department of Plant Physiology and Biochemistry,
West Pomeranian University of
Technology in Szczecin,
17 Słowackiego Str., 71-434,
Szczecin – Poland

e-mail: arkadiusz.telesinski@zut.edu.pl

© by PSP Volume 28 – No. 4/2019 pages 2475-2482 Fresenius Environmental Bulletin

EFFECT OF PRENATAL EXPOSURE TO LEAD ACETATE ON HISTOGENESIS OF THE TESTICULAR TUBULES

Mahmood H Hamash, Ahmed M Khalaf*

Faculty of Pharmacy and Medical Sciences, Al-Ahliyya Amman University, Amman, 19328, Jordan

ABSTRACT

Histological changes in developing Testis in normal and in those embryos exposed to Lead Acetate, by a single intraperitoneal injection at 10 day of pregnancy, were compared. Seminiferous tubules during prenatal life appear solid only acquire lumen after birth. The toxic effect of Lead Acetate caused reduction in number of Germ cells (Gonocytes) and disorganization of tubular structure with degenerative changes occasionally. The differences were minimized by time as seen in postnatal ages.

KEYWORDS:
Lead acetate, Swiss mice, Testis, Seminiferous tubules, Embryo, Gonocytes.

INTRODUCTION

The toxicity of Lead on Mammals including human has been reported frequently in various studies [1, 2]. Systems of the body are affected by Lead and other heavy metals, mainly by increase in free radicals [3], and due to interference with enzymes activities particularly those dealing with free radicals. It was found that Lead toxicity has a great effect on reproductive organs especially the testes and ovaries in the adult [4, 5], in addition to liver [6] and kidneys [7].

Mogra et al. [8] studied the general effect of maternal Lead Acetate exposure on general development of mice and reported that administering Lead Acetate before the 8th day of gestation leads to failure of implantation. Giving the Lead Acetate at 8th day leads to reduction in number of pregnancy, while administering Lead Acetate on day 10 of pregnancy does not lead to gross abnormalities, but may alter the histological structure and functional parameters.

A study by Garu et al. [9] exposing pregnant mice to Lead acetate in drinking water for the whole period of pregnancy and studying developing testes 7 day after birth showed some histological changes, particularly changes in developing Spermatogonia and alteration in distribution of seminiferous tubules.

In the study reported in this article we followed Mogra et al. [8], in taking a single intraperitoneal injection on the 10th day of pregnancy and studying histological changes in developing Testis in 3 developmental stages: 16 day of gestation, 1 day after birth, and 2 weeks old neonates.

MATERIALS AND METHODS

Female Swiss albino mice of 8-12 weeks of age and weighing 40-60 grams, were used in this study. The animals were kept under condition of 25 °C and 12 h light and dark cycle. Food and water were available ad-libitum. Animals were handled and treated in accordance with National Health Institute of Health Guide for the Care and Use of Laboratory Animals.

For obtaining pregnancy 3-4 females and one male were mixed at the end of the day. Females were checked next morning for vaginal plug. In case that occurs, this is considered as day 0 of gestation. Pregnant animals were divided into 3 main groups, each with a control and experimental subgroups, as following:

Group I-A. Pregnant mice receive i. p. injection of distilled water. Pregnant mice were scarified at the 16th day of gestation. Uteri were removed and put in Hank's balance solution, and embryos were examined under dissecting microscope to check for presence of Testes. Testes can be recognized during dissection of the embryo to be rostral to position of urinary bladder. Testes were removed together with surrounding tissues and fixed in 10% formalin.

Group I-B. This is the experimental group were the pregnant mice receive a single i.p. injection of 0.3 ml of 0.6% of lead acetate in distilled water, on day 10th of gestation. Pregnant animals were sacrificed at the 16th day of gestation. Uteri were removed and immersed in Hank's balance solution. Embryos were removed and dissected and Testes were removed with some surrounding tissue and fixed in 10% formalin

Group II-A. Pregnant mice receive i.p. injection of distilled water. New born or one day old neonates, whose mothers were given i.p. injection

of distilled water, were scarified and examined. Males were dissected to confirm the presence of Testes. Testes can be recognized during dissection of the embryo to be in a position infero-lateral to urinary bladder. Testes were removed together with surrounding tissues and fixed in 10% formalin

Group II-B. The pregnant mice receive a single i.p. injection of 0.3 ml of 0.6% of lead acetate in distilled water, on day 10th of gestation. Newborns at day 1 after birth were dissected under stereomicroscope. Testes were removed with some surrounding tissue and fixed in 10% formalin

Group III-A. Pregnant mice receive i.p. injection of distilled water at day 10 of pregnancy. Male neonates of 2 weeks' old were dissected under stereo microscope from scrotum and fixed in 10% formalin. Testes were removed together with surrounding tissues and fixed in 10% formalin.

Group III-B. This is the experimental group; 2weeks old male neonates, whose mothers have received a single i.p. injection of .3 ml of .6% of lead acetate in distilled water, on day 10th of gestation, were dissected under stereo microscope. Testes were removed together with surrounding tissues and fixed in 10% formalin.

Tissues were processed for light microscopy according to Bancroft [10]. After fixation, dehydration by graded alcohol, cleared by Xylene and embedded paraffin. Blocks were sectioned at 5 um thickness and stained with hematoxylin-eosin stain and examined by Nikon-Eclipse light microscope.

RESULTS

Group I-A. This is a control group. Embryos of 16 days of gestational age were extracted. The Testes are still in lumbar region of the abdomen, at a level superior to upper level of urinary bladder. The testes are of small sizes, almost spherical in shape. Tubules-cords are slightly curved. There is no lumen. The center is filled with loosely arranged large cells, each with a large rounded dark nucleus. These represent the Gonocytes. The periphery is made of more closely packed cells that form a continuous layer. The cells in this layer are of variable sizes: small, triangular, and elongated. Basal lamina is present outside the peripheral layer, with elongated peritubular (myoid) cells, forming an envelope around the tubule. Inter-tubular spaces contain abundant interstitial tissue and small blood vessels. Some large cells, represent pre-cells of Leydig were sometimes recognized (Figure 1, A&B).

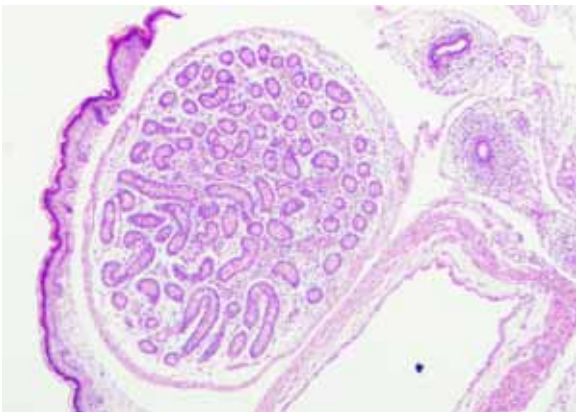

A

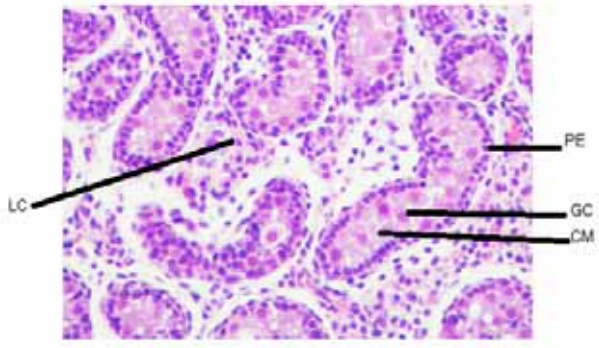

B

FIGURE 1

Sections in testis of 1 day newborn. (A) section through the whole testis(X40). (B) Appearance of sectioned semineferous tubules-cords (X200): PE: Peripheral Epithelium, GC: Gonocytes., CM: Central Matrix., LC: Leydig cells.

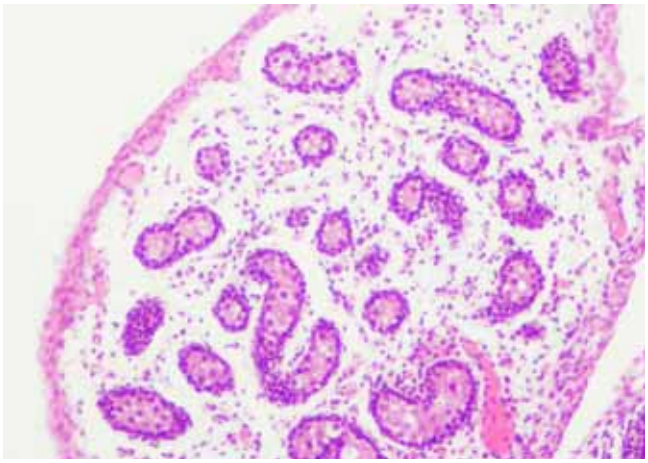

A

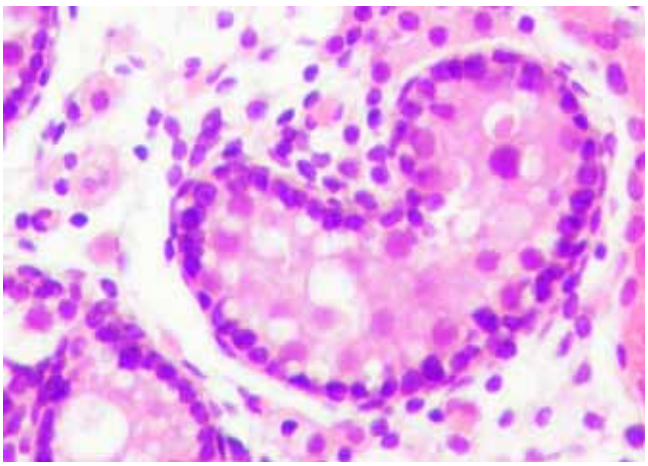

B

FIGURE 2

(A): Section in the testis (B): A section of tubule of experimental group, showing reduction in number of Gonocytes in the center and vacuolization of the central matrix (X400).

Group I-B. In embryos of this experimental group, the testes appear in normal position. Sections of the Testis show scattered tubules-cords, most of them are curved, in deeper position they are mostly straight. The parts of tubules close to the capsule are coiled or appear in the shape of question mark but of reverse direction. The peripheral epithelial layer is intact, but most of the cells are small in size with few scattered large cells with rounded nuclei (Gonocytes). In some tubules there are signs of degenerating Gonocytes. The center of the tubule shows shrinking matrix and few scattered Gonocytes (large cells with large rounded nuclei). The shrinkage of central matrix gives the impression of appearance of lumen. Basal lamina is mostly indistinctive and there are fewer elongated peritubular cells. There are wider spaces between the tubule-cords, containing loose connective tissue and mesenchymal cells (Figure 2: A& B).

Group II-A. This group concerns control (normal) new born, of 1 day of age, in which case the mother has not been exposed to Lead Acetate. The Testes have descended to a level at inferolateral positions of the urinary bladder.

In section the tubules appear curved forming, in subcapsular region a figure of question mark, and more straight in deeper position. The peripheral cellular layer of the tubule is epithelial like, and cells are close to each other as a continuous layer with sometimes distinct basal lamina, around which there are elongated cells representing the Myoid cells. The cells in the peripheral layer are of variable sizes: small and large globular or triangular and large elongated. The latter represent the pre-Sertoli cells. In the center of the tubule there is a large number of large eosinophilic cells with rounded large nuclei (Gonocytes). These cells are embedded in a matrix (the central matrix). Some similar large cells are also seen in between the cells of the peripheral epithelium. Interstitial tissue is not condensed and contains few scattered large cells and small blood vessels (Figure 3: A, B &C).

Group II-A. This group concerns control (normal) new born, of 1 day of age, in which case the mother has not been exposed to Lead Acetate. The Testes have descended to a level at inferolateral positions of the urinary bladder.

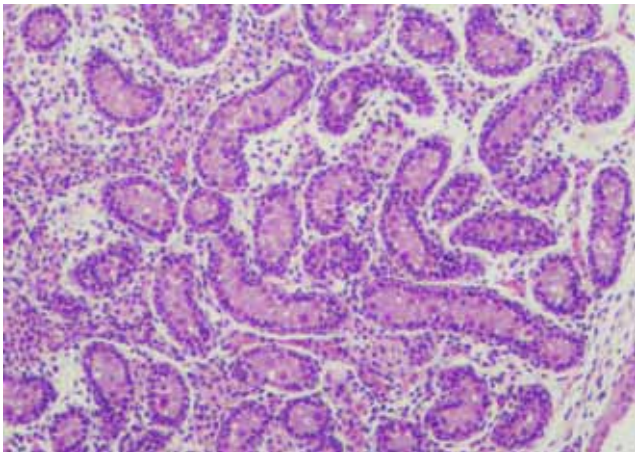

A

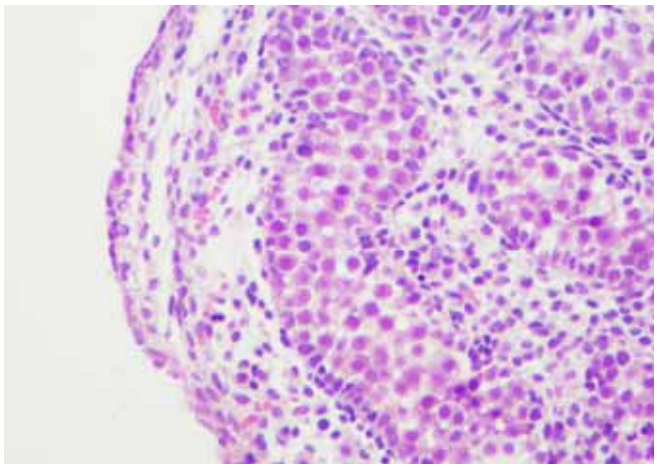

B

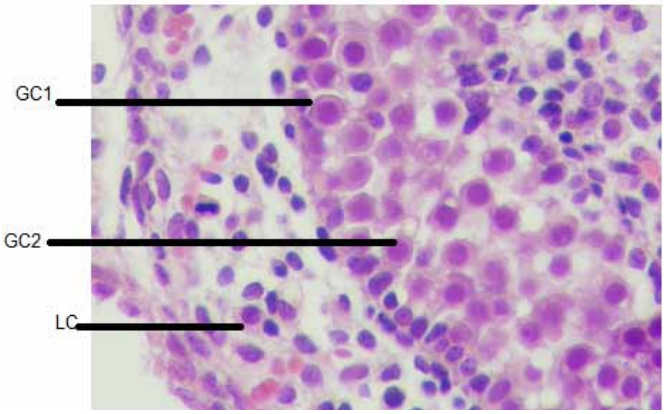

C

FIGURE 3

(A) General arrangement of tubule in control newborn Testis. (X100) (B) A tubule-cord (X200). (C): magnified view of the tubule in (B) showing: GC1: Gonocyte insinuating in the peripheral epithelium. GC2: Gonocyte., LC: Leydig cell. Notice the large number of Gonocytes in the center. (X400)

In section the tubules appear curved forming, in subcapsular region a figure of question mark, and more straight in deeper position. The peripheral cellular layer of the tubule is epithelial like, and cells are close to each other as a continuous layer with sometimes distinct basal lamina, around which there are elongated cells representing the Myoid cells. The cells in the peripheral layer are of variable sizes: small and large globular or triangular and large elongated. The latter represent the pre-Sertoli cells. In the center of the tubule there is a large number of large eosinophilic cells with rounded large nuclei (Gonocytes). These cells are embedded in a matrix (the central matrix). Some similar large cells are also seen in between the cells of the peripheral epithelium. Interstitial tissue is not condensed and contains few scattered large cells and small blood vessels (Figure 3: A, B &C).

Group II-B. In this group, the mother was exposed to Lead Acetate at the 10th day of gestation. The tubules are less organized compared to control. The peripheral cell layer is irregular or interrupted. The basal lamina is not distinctive in all areas. Gonocytes in the center are scanty and some show degenerative changes. The number of Gonocyte seen in-between the peripheral cells is less than what has been seen in the control. There is shrinking in the central matrix with irregular spaces. In some areas cellular degeneration involves a whole tubule or groups of tubules. Inter tubular spaces contain interstitial tissue and blood vessels. In some regions there signs of hemorrhage in these spaces (Figure: 4).

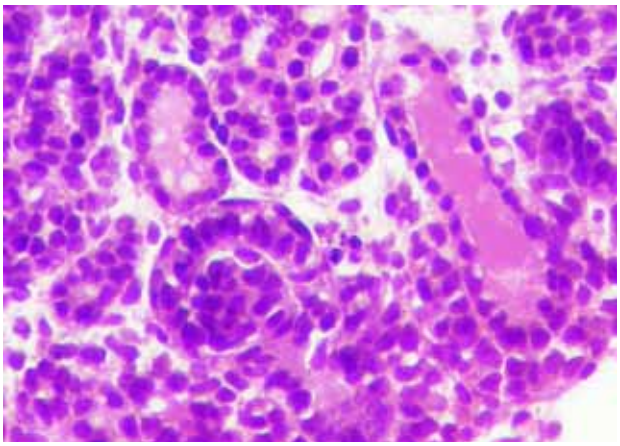

FIGURE 4
A section in the Testis of experimental newborn: reduction in number of Goncytes (X200).

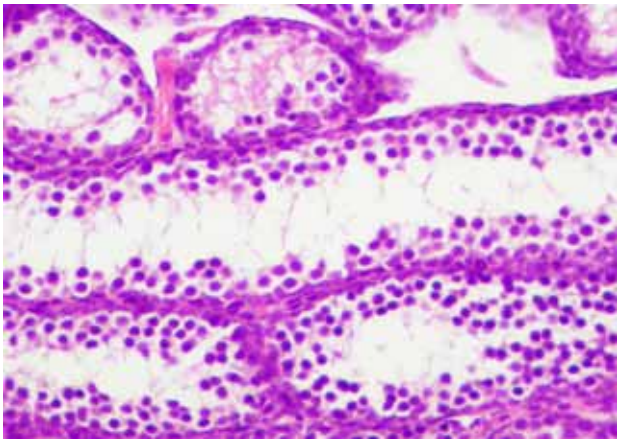

A

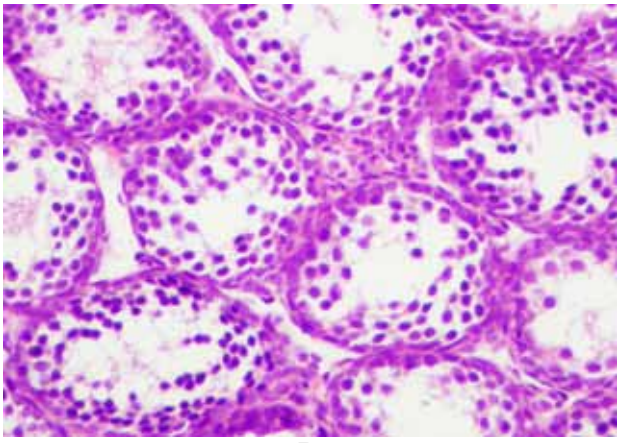

B

FIGURE 5
Seminiferous tubules in control 2weeks old mice; (A) tubules sectioned longitudinally(X200); (B) cross section of tubules(X200). The wall contains several layers of cells. Interstitial spaces are reduced.

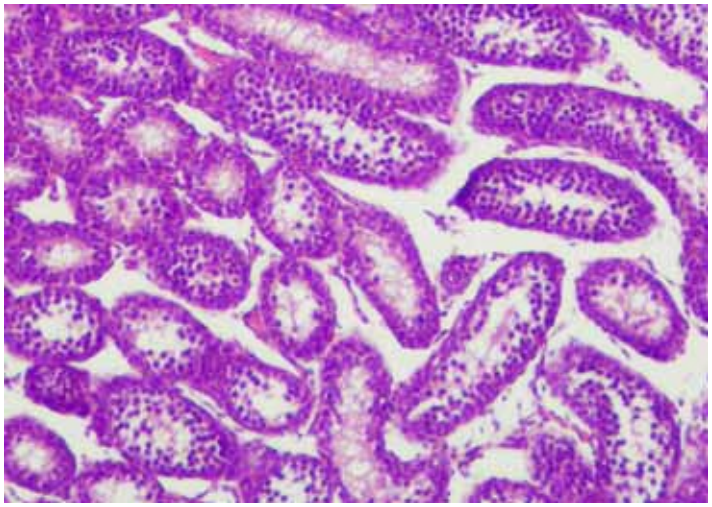

A

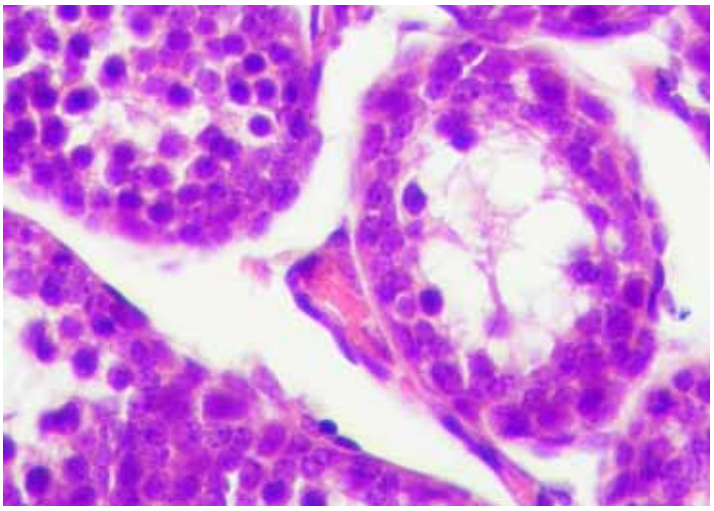

B

FIGURE 6
Tubules of Testis of experimental 2weeks old mice (A): Oblique sections X100; (B): Crossed sectioned tubules X400.

Group III-A. This is a control group in which new born at age of 2weeks after birth. The Testis have descended down into a position, just under the abdominal wall inferior to position of the urinary bladder. Seminferous tubules are curved with elongated deeper side. There are 3 important features in this stage: (1) there is obvious continuous lumen. (2) The wall of the tubule is continuous and multilayered, with various types of cells: Spermatogonia, Sertoli cells, and to deeper side there secondary generations of spermatogonia. Usually there are 2-4 layers of cells in the wall. The lumen contains no Gonocytes or matrix. The basal lamina is distinctive with outer layer of Myoid cells. (3) The tubules are enlarged and of large number. The inter- tubular spaces are reduced very much and interstitial tissue is condensed. Interstitial cells of Leydig could be recognized by their large size and eosinophilic cytoplasm (Figure 5: A&B).

Group III-B. In experimental group of 2 weeks of age of young mice, the seminiferous tubules are intact and of normal shape, with obvious lumen. The wall consists of multilayers of cells. The basal layer is compact and surrounded by thin Myoid cells. There are more loose rounded cells toward the luminal side. Interstitial tissue is scanty (Figure 6: A&B).

DISCUSSION

The toxic effects of Lead compounds on reproduction were extensively studied by various authors [11]. In male, the effect on adult testis and sperm quality was a subject for a number of studies [12]. These studies were extended into the effect of exposure during embryonic life on the reproductive parameters in postnatal animals [13]. The studying of the effect of exposure of the pregnant mother to Lead Acetate on development of the Testis was following variety of methods of administration, length of period of exposure, and the dose used.

Most studies followed the method of administering the Lead Acetate with drinking water for the whole length of pregnancy and studying changes in postnatal period [9]. The study of Mogra et al. [8] showed that exposing the pregnant mice in early stages leads to failure of implantation and pregnancy. Administering the Lead Acetate from day 10 of pregnancy leads to no gross morphological abnormalities, but may causes histological and functional changes in the testis.

Garu et al. [9] studied the histological alterations in seminiferous tubule of young mice, that had exposed to lead Acetate during the whole embryonic period, through the drinking water of the pregnant mothers. They demonstrated specific changes in seminiferous tubules of postnatal animals. In the study reported here the mother was exposed to single i.p. injection of Lead acetate solution at the 10^{th} day of the pregnancy that is at the period of organogenesis [14]. This period was considered as the critical period and sensitive in development of the organs [15]. The period of studying the results extends from the embryonic stage, where the testis has developed and started to descend caudally, and tubule-cords are solid and lack the lumen, having only one layer of peripheral epithelium, to newborn stage and the two weeks of postnatal age where the Testis has descended down in the inferior part of pelvic region, close to abdominal wall and skin.

Results in group I-A, which is the embryonic stage of 16-17 day of pregnancy showed the tubule-cords without lumen, and having peripheral layer of epithelium. The cells in this layer are mostly pre-Sertoli cells. In the center there are large rounded cells with large rounded nuclei in a matrix. These are the primordial germ cells that are going to give rise to pre-spermatogonia (Gonocytes). These cells tending to insinuate themselves in between the cells of the peripheral layer.

In group I-B, there appear variable degrees of alterations that include the reduction in number of Gonocytes seen in the center of the tubule. This indicates that germ cells are most sensitive to the effect of Lead Acetate toxicity. This is also what was concluded from studies on adult Testis [16, 17]. Germ cells are sensitive to increase in ROS [3]. Free radicles increase the chance of DNA damage [18].

Results of group II-A, that is of control newborn show the development and growth of seminiferous tubules. Tubules are still without lumen. The center contains large number of Gonocytes. A number of these cells invaded the peripheral epithelium. Leydig cells in the interstitial tissue can be recognized as large polyhedral with esinophilic cytoplasm. That indicates these cells are functioning at this stage and secreting Testosterone.

In the experimental group of this stage (group II-B), the seminiferous tubules show some disorganization and sometimes signs of degeneration. There is less number of Gonocytes in the center, this is apparent from comparing figure 4 with figure3, and fewer cells of the Gonocyte present in the epithelial wall.

After birth, normal changes in histology of seminiferous tubule is characterized by presence of the lumen, multi layered epithelial wall that is consisting of insinuated Gonocytes which become smaller to form Spermatogonia and Sertoli cells. Usually no Gonocytes are left in the lumen. In experimental group III-B, the seminiferous tubules acquire lumen like in the normal development, but still some Gonocytes fail to insinuate themselves between the cells of the peripheral epithelium, as some of these cells remain to the luminal side away from the peripheral epithelium.

CONCLUSION

The study includes description of histological changes in the Testis during development from the period of prenatal stage of 16 day of pregnancy to 2 weeks of postnatal life. The effect of a single dose of Lead Acetate injected intraperitoneally during the critical period of organogenesis, produces alteration in specific histological features, especially the germ cells and to some extent other types of cells. These changes may lead to important functional disorders.

ACKNOWLEDGEMENTS

The authors wish to thank Dean, faculty of Pharmacy and Medical Sciences and Dean, Graduate studies and Scientific Research, Al Ahliyya Amman University, Jordan for providing necessary facilities. This project was funded by Deanship of Graduate studies and Scientific Research- Al Ahliyya Amman University, Jordan, (Grant number 1/10/2014/2015). The authors would like to thank Prof. Dr. Ashok K. Shakya for his suggestions and for reviewing the manuscript; Mrs. Afnan Mahdawi, Mr. Ali Dhmor (Biolab), and Mr. Mohammed Dahbor for their technical assistance.

The authors declare no conflict of interest.

REFERENCES

[1] Izimove, I.F. (1998) Problems of Lead effect on Organism. Med. Labor and Hygiene. Ecology. 2, 1-4.

[2] Tuormaa, T.E. (1995) The Adverse Effect of Lead. Journal of Orthomolecular Medicine. 10, 149-164.

[3] Aitken, R.J., Clarkson, J.S. and Fishel, S. (1989) Generation of Reactive Oxygen Species, Lipid Peroxidation and Human Sperm function. Biology of Reproduction. 41, 183-197.
[4] Haouas, Z., Zisi, I., Sallem, A., Bhauri, R. Ajina, T., Zaouali, M. and Mehdi, M. (2015) Reproductive toxicity of Lead Acetate in Adult Male Rats. Journal of Cytology and Histology. 6, 293-308.
[5] Subina, O.S. and Dudenkova, N.A. (2014) Modification of Morphological structures of Ovaries and the Early Cycles of Albino Rats Under the Effect of Lead Acetate. Global Veterinaria. 12, 449-454.
[6] Omotoso, B.R., Abiodun, A. and Ijomone, O.M. (2015) Lead-Induced Damage on Hepatocytes and Hepatic reticular fibers in Rats. Journal of Biosciences and Medicines. 3, 27-35.
[7] Jabeen, R., Tahir, M. and Waqas, S. (2010) Teratogenic Effect of Lead Acetate on Kidney. Journal of Ayub Medical College Abbottabad. 22, 76-79.
[8] Mogra, S., Sharma, R. and Qureshi, N. (2009) Effects of Maternal Lead Acetate Exposure on Prenatal development of Swiss Albino Mice. Asian Journal of Environmental Science. 4, 216-220.
[9] Garu, U., Sharma, R. and Barber, I. (2011) Effect of Lead Toxicity on Developing Testis of Mice. International Journal of Pharmaceutical Sciences and Research. 2, 2403-2407.
[10] Bancroft, J.D. (2008) Theory and Practice of Histological Technique. 6th ed. Churchill Livingstone.
[11] Chowdhury, A.R. (2009) Recent Advances in Heavy Metals Induced Effect on Male Reproductive Function. Journal of Medical Sciences. 2, 37-42.
[12] El-Sayeda, Y.S., El-Neweshy, M.S. (2010) Impact of Lead Toxicity on Male Rat Reproduction at Hormonal and Histopathological levels. Toxicological and Environmental Chemistry. 92, 765-774.
[13] Corpas, I., Castillo, M., Marquina, D. and Benito, M.J. (2002) Lead intoxication in Gestational and Lactation periods Alter the Development of Male Reproductive Organs. Ectotoxicol. Ecotoxicology and Environmental Safety. 53, 259-266.
[14] Theiller, K. (1989) The House Mouse: Atlas of Embryonic Development. Springer-Verlag, Berlin.
[15] Wilson, J.G. (1973) Environment and Birth Defects. Academic Press. New York.
[16] Acharya, U.R., Acharya, S. and Mishra, M. (2003) Lead Acetate Induced Cytotoxicity in Male Germinal of Swiss Mice. Industrial Health. 41, 291-294.
[17] Adhikari, N., Inha, N., Narayan, R. and Saxena, D.K. (2001) Lead –Induced Cell Death in Testis of Young Rats. Journal of Applied Toxicology. 21, 275-277.
[18] Al-Omar, M.A., Abbas, A.K., Al-Obaidy, S.A. (2000) Combined Effect of Exposure to Lead and Chlordane on Testicular tissue of Swiss Mice. Toxicology Letters. 10, 1-8.

Received: **08.07.2018**
Accepted: **21.12.2018**

CORRESPONDING AUTHOR

Ahmed M Khalaf
Faculty of Pharmacy and Medical Sciences,
Al-Ahliyya Amman University,
Amman 19328 – Jordan

e-mail: amk47had@yahoo.com

© by PSP Volume 28 – No. 4/2019 pages 2483-2494 Fresenius Environmental Bulletin

FUEL CONSUMPTION-DERIVED CARBON DIOXIDE EMISSIONS UNDER TRADITIONAL AND NO-TILLAGE SYSTEMS IN WHEAT PRODUCTION FOR FOOD INDUSTRY

Z Figen Antmen*

Cukurova University, Faculty of Engineering, Department of Industrial Engineering, 01330 Saricam, Adana, Turkey

ABSTRACT

In this experimental study, effects of the traditional and no-tillage systems on grain yield, energy consumption and carbon dioxide (CO_2) emissions were compared in winter wheat production in Southeastern Anatolia region of Turkey. The CO_2 emissions associated with direct fuel and lubricant oil consumptions have estimated according to the Intergovernmental Panel on Climate Change (IPCC) approach. The fuel consumptions per hectare were determined as 50.96 L and 13.1 L under traditional and no-tillage systems, respectively. The use of traditional system released 145.57 kgCO_2 per hectare, while the no-tillage system released only 37.42 kgCO_2 per hectare. Under traditional tillage system the plowing (79.3 kgCO_2/ha) had a great influence on total CO_2 emissions, accounting for 54.5 % of total CO_2 emissions. The grain yield (6017 kg/ha) under no-tillage system was 796 kg per hectare lower than that of traditional tillage system. The specific fuel consumptions (SFC) were 7.78 L/t and 2.26 L/t under traditional and no-tillage systems, respectively. While 1 liter fuel was consumed to produce 441.83 kg grain under traditional tillage system, 128.6 kg grain was obtained per L fossil fuel consumed under the no-tillage system. Compared to traditional tillage system, 5.52 L less fossil fuel in the other word 204 MJ less fossil energy was consumed to produce per ton of grain wheat. Under no-tillage system to produce per ton grain wheat 243.6% less CO_2 was released during tillage and sowing practices compared to traditional tillage system.

KEYWORDS:
Wheat, Tillage, Energy consumption, CO_2 emissions

INTRODUCTION

The agricultural sector is already a large contributor to global energy use and greenhouse gas (GHG) emissions, and the environmental impact of agriculture is likely to increase as our population grows to nine billion and requires more protein and calories [1]. Agriculture is responsible for 9% of greenhouse gas emissions for 2014. Greenhouse gas emissions from agriculture come from livestock such as cows, agricultural soils, and rice production. While CO_2 emissions come from a variety of natural sources, human-related emissions are responsible for the increase that has occurred in the atmosphere since the industrial revolution. Agricultural land use and land cover changes, account for about 20 percent of annual global emissions of carbon dioxide (CO_2) covers. A significant portion of CO_2 emissions due to agricultural activity can be reduced by conservation agriculture [2].

Tillage is a technological operation which requires considerable working time input and ample fuel consumption [3]. Traditional deep ploughing is the least efficient and most energy-intensive tillage method [4]. The use of reduced tillage technologies or no-tillage practically does not alter or ever so often even improves soil chemical and physical properties and crop yields are often similar to those obtained using traditional tillage technologies. Calculations of energy balance of the different technologies showed that reduced tillage technologies are often superior not only in terms of lower working time input and fuel consumption but also in terms of being more environmentally-sustainable, i.e. they produce lower greenhouse gas emissions [5]. With reduced energy input intensity one can cut down on crop production costs and contribute to sustainable agricultural development. A well balanced management of energy input intensity is one of the top priorities of contemporary energy policy, since energy is a critical factor of socio-economic development of any country [6], which enables safeguarding of energy security, economic competitiveness and environmental protection [7].

Filipović et al., [8], evaluated five different tillage systems and their influence on fuel consumption, labor requirement and yield of maize and winter wheat production. The compared tillage systems were: 1. traditional tillage system (CT), 2. reduced tillage system (RT), 3. conservation tillage system I (CP), 4. conservation tillage system II (CM), 5. no-tillage system (NT). The crop rotation was maize (*Zea mays* L.) – winter wheat (*Triticum*

aestivum L.) – maize – winter wheat. Comparing the fuel consumption to CT system, RT system consumed 6.8% less, CP system 12.1% less, CM system 27.4%less, while NT system consumed even 82.7% less fuel. The labor requirement showed that RT system saved 7.6%, while CP system required 21.8% less, CM system 38.6% less labor, respectively. NT system saved 81.7% of labor in comparison to CT system. The highest yield of maize in the first experimental year was achieved under CT system and the lowest under RT system. In all others experimental years the highest yield of winter wheat and maize was achieved under CM system, while the lowest under RT system.

Plow used high energy as compared to cultivator and no-tillage, for the farmers who cannot afford much inputs energy cost, cultivator can be recommended to grow maize crop successfully on the basis of energy input-output. Further studies are also recommended for the researchers to carry out such similar studies in maize crop. Memon et al., [9], compared plow with cultivator and zero tillage in order to seed bed preparation for maize cultivation. The results showed that the highest maize grain yield (4380 kg/ha) was in plow as compared to (3972 kg/ha) in cultivator, while the lowest yield was in (3136 kg/ha) zero tillage. The maximum energy input was observed with plow (12387 MJ/ha) followed by cultivator (11383 MJ/ha) and the lowest energy input was found in zero tillage (11301 MJ/ha). Shamabadi [10] evaluated traditional tillage (CT), tow reduced tillage (RT1and RT2) and direct seeding (NT) for sunflower production. The highest energy consumption (12.3 GJ/ha) and carbon emissions (248 kg C-eq/ha and 155 kg C-eq/t) were related to the traditional method. The least energy input (9.12 GJ/ha) and carbon emission (183.3 kg C-eq/ha and 118.6 kg C-eq/t), were related to NT method. In conservation tillage, input energy and fuel consumption per hectare were 30% and 90% lower than traditional method, respectively, but there was no reduction in yield and energy output.

Lately, the comprehensive studies have been performed on energy use and environmental assessment in different cultivation methods and crop management systems for wheat and other agricultural products [11–54]. Even though a lot of work is done with concerning the mechanization applications on seed yield and quality characteristics of crops and effects of tillage systems on soil properties and plant developments, the studies concerning the assessment of traditional and conservation tillage systems in terms of fuel consumption-derived CO_2 emissions are limited. Therefore, the main objectives of the present study were to investigate the fuel consumption with the adoption of no-tillage and the effect in crop yield and to evaluate CO_2 emissions for winter wheat cultivation.

MATERIALS AND METHODS

Tillage and Cultivation Processes. The experiment was carried out on production plots of 210 m^2 (25 m ×8.40 m) in Koruklu Talat Demiroren Research Station belong to GAP Agricultural Research Station in Sanlıurfa province of Turkey (36° 42′ N and 38° 58′ E, altitude 410 m). The experiment was carried out in a randomized block trial design with two subjects and three replications. The traditional and no-tillage systems, given in Table 1, have been tested for winter wheat production in the present study. The soil texture of the experimental parcels is clay and soil characteristics of the parcels given in Table 2.

TABLE 1
Tillage methods and equipments used in the experiment

Cultivation system	Process equipments
No-tillage system	Sowing machine into stubble
Traditional system	Moldboard plow + disc harrow + scrubber + sowing machine

TABLE 2
Soil characteristics of experimental area

Parcels	Depth (cm)	Lime (%)	P_2O_5 (kg/da)	K_2O (kg/da)	Organic matter (%)	Volumetric mass (g/cm^3)	Texture	Moisture (%)	Porosity (%)
Parcels of no-tillage	0 –15	24.3	1.31	75.9	1.81	1.37	Clay	6.05	48.30
	15 –30	24.8	1.40	67.8	1.89	1.40	Clay	7.08	47.17
Parcels of traditional method	0 –15	24.3	1.73	63	1.41	1.36	Clay	6.65	48.68
	15 –30	24.3	1.48	77.7	1.53	1.32	Clay	8.54	50.19

The traditional method of preparing the seedbed is based on plough and rotary harrow. However, the main disadvantage of this method is represented by excessive field traffic, high energy cost, time limits during soil preparation, and bad weather in the spring. Under the traditional system, after the soil tillage with the moldboard plow is done, the cut pieces are disassembled with disc harrow. Later, after the scrubber was passed, the sowing was done and the water was given. In the no-tillage system, the sowing was carried out with the sowing machine with stubble. In the sowing of wheat, the rows were arranged to be 14 cm apart. In wheat cultivation, the planting standard is set at 25 kg/da. In fertilizing process, 6 kg/da P_2O_5 and 18 kg/da nitrogenous fertilizer were given in all parcels. After the first irrigation, herbicide was applied for weed control in all parcels. In the wheat development period, water was applied 3 times in total and the irrigation was completed. The tillage implements were operated with the four-wheel drive tractors with the engine power of 75 kW whereas planting and cultivation operations were performed with a tractor of 50 kW. The ears of wheat plant were harvested during the period of harvesting. Yields were calculated according to the moisture value of 14%.

The effective field capacity of each implement was determined in the operation conditions. The task times for the tillage systems were measured by using a chronometer in order to obtain management data of farm machineries used in seedbed preparation. Fuel energy input for each application was calculated based on the fuel consumption in the operation conditions. At the beginning of each operation, the fuel tank of the tractor was filled fully, and then refilled fully at the end of each operation to determine fuel consumption. The fuel energy input was estimated multiplying the total fuel consumption with diesel fuel energy equivalent. The lubricant consumption of the tractor was calculated depending on its power as follows [24]:

$$OC = 0.004 \times P_t \quad (1)$$

where; OC is the oil consumption of the tractor in L per hour and P_t is the power of the tractor in kW.

Calculation of Fuel and Lubricant Oil Consumption. The tillage implements were operated with the four-wheel drive tractors with the engine power of 75 kW whereas planting and cultivation operations were performed with a tractor of 50 kW. The effective field capacity of each implement was determined in the operation conditions. The task times for the tillage systems were measured by using a chronometer in order to obtain management data of farm machineries used in seedbed preparation. Fuel energy input for each application was calculated based on the fuel consumption in the operation conditions. At the beginning of each operation, the fuel tank of the tractor was filled fully, and then refilled fully at the end of each operation to determine fuel consumption. The fuel energy input was estimated multiplying the total fuel consumption with diesel fuel energy equivalent.

The energy input related to lubricant oil (EI_o) which occurs due to the consumption of engine oil in wheat cultivation was determined by considering of consumed oil by the engine of tractor per hour, during the process of wheat cultivation. The oil consumption of the tractor engine per hour was determined by depending on the highest power take off (PTO) shaft power of the tractor, which can be formulated as follows [24]:

$$OCT = 0.00059 \times HSP_{max} + 0.02169 \quad (2)$$

where; OCT is the oil consumption of the farm tractor per hour (L/h) and HSP_{max} is the maximum PTO shaft power of the tractor (kW).

The maximum PTO shaft power (HSP_{max}) of the agricultural tractor that was used for the cultivation process of rapeseed was considered as 88% of its rated power (RPT, kW) and determined as follows [23]:

$$HSP_{max} = 0.88 \times RPT \quad (3)$$

The oil energy amount that consumed per unit area in wheat cultivation process was calculated depending on the amount of oil that consumed by engine of the tractor per hour during the cultivation process, the lower calorific value of consumed oil and work efficiency of the tractor per area, which is defined as:

$$EI_o = m_o \times LHV_o \times t_t \quad (4)$$

where; m_o is oil consumption of tractor engine per hour (L/h), LHV_o is the lower calorific value of oil (MJ/L) and t_t is working time of the tractor per cultivated area (h/ha).

During cultivation operations in the field, the lower calorific value of engine oil (SAE 40) was taken into account as 38.2 MJ/kg [55].

Calculation Methodology Used for Carbon Dioxide Emissions. Fuel consumption data were obtained from direct measurements of diesel fuel used. The lubricant consumption of the tractor was calculated based on equation (1). The CO_2 default emission factors depending on fuel type based on lower heating values are from IPCC, 1996, Volume 2, Section 1 [49].

The methods for calculating CO_2 emissions recommended by the *GHG Protocol - Mobile Guide (03/21/05) v1.3 (Calculating CO_2 Emissions from Mobile Sources Guidance to calculation worksheets)* were used in this study. The following equation outlines the recommended approach to calculating CO_2 emissions based on fuel use (assuming data is first obtained in terms of mass or volume).

CO_2 emissions = Fuel used x Heating value x Emission factor

Diesel-based CO_2 emissions = Diesel used x Heating value x Emission factor

Diesel-based CO_2 emissions = L/ha x 0.0371 GJ/L x 74.01 $kgCO_2$/GJ

Diesel-based CO_2 emissions = $kgCO_2$/ha

Lubricant oil-based CO_2 emissions= Oil used x Heating value x Emission factor

Lubricant oil-based CO_2 emissions=L/ha x 0.0382 GJ/L x 73.28 $kgCO_2$/GJ

Lubricant oil-based CO_2 emissions = $kgCO_2$/ha

Calculation Methodology Used for the Specific Parameters. The Specific Fuel Consumption. The specific fuel consumption (SFC) and specific grain production (SGP) were defined to analyze the relationship between fuel consumption and grain production. The value of the specific fuel consumption (SFC) indicates the amount of fuel consumed (L) to produce the unit quantity (t) of grain product.

$$SFC = FC / GP \quad (5)$$

where; *SFC* is the specific fuel consumption (L/t), *FC* is fuel consumption (L/ha) and *GP* is production (t/ha).

The Specific Energy Consumption. The specific energy consumption (*SEC*) is the ratio of energy consumption per hectare (MJ/ha) to grain yield (t/ha) and indicates energy consumption (MJ) per ton of wheat.

$$SEC = EC / GP \quad (6)$$

where; *SEC* is the specific energy consumption (MJ/t), *EC* is energy consumption per hectares (MJ/ha) and *GP* is grain production (t/ha).

The Specific Carbon Dioxide Emission. The specific carbon dioxide emission (SCO_2) was defined to analyze the relationship between CO_2 emissions and wheat production. The SCO_2 is the ratio of total CO_2 emissions per hectare ($kgCO_2$/ha) to grain yield (ton/ha) and indicates CO_2 emissions ($kgCO_2$) per ton of grain.

$$SCO_2 = CO_2 / GP \quad (7)$$

where; SCO_2 is the specific carbon dioxide emission ($kgCO_2$/t), CO_2 is the total CO_2 emission per hectare ($kgCO_2$/ha) and *GP* is grain production (t/ha).

The Specific Grain Production. The three different specific grain productions (SGP) were defined based on fuel and energy consumptions and CO_2 emissions per hectare. The specific grain production based on fuel consumption (SGP_F) is the ratio of grain yield per hectare (kg/ha) to fuel (diesel and lubricant oil) consumption (L/ha). The SGP_F is the inverse of the SFC and indicates fuel consumption (L) per kg of grain.

$$SGP_F = GP / FC \quad (8)$$

where; SGP_F is the specific grain production based on fuel consumption (kg/L), *GP* is grain production per hectares (kg/ha) and *FC* is fuel consumption (L/ha).

The specific grain production based on energy consumption (SGP_E) is the ratio of grain yield (kg/ha) to energy consumption per hectare (MJ/ha). The SGP_E is the inverse of the SEC and indicates grain production (kg) per MegaJoule (MJ) of energy consumption.

$$SGP_E = GP / EC \quad (9)$$

where; SGP_E is the specific grain production based on energy consumption (kg/MJ), *GP* is grain production per hectare (kg/ha) and *EC* is energy consumption (MJ/ha).

The specific grain production based on CO_2 emission (SGP_{CO2}) is the ratio of grain production (kg/ha) to CO_2 emission per hectare ($kgCO_2$/ha). The SGP_{CO2} is inverse of the SCO_2 and indicates grain production (kg) per kg of CO_2 emission.

$$SGP_{CO2} = GP / CO_2 \quad (10)$$

where; SGP_{CO2} is the specific grain production based on energy consumption (kg/MJ), *GP* is grain production (kg/ha) and CO_2 is the total CO_2 emission per hectare ($kgCO_2$/ha).

RESULTS AND DISCUSSION

Fuel Consumption and Carbon Dioxide Emission. Fuel consumption values according to replications for the cultivation methods applied in wheat production are given in Table 3. The fuel consumption per hectare was determined as 50.96 L for the traditional system and 13.1 L for the no-tillage system. The *t*-test was applied to evaluate the relationship between fuel consumption and cultivation systems used in wheat production, and the results are given in Table 4. When examined the data on Table 4, different cultivation systems' effects on fuel consumption values is statistically excessively important ($p<0.001$). As a result of the statistical analysis made, there was a difference in the level of 0.001 importance among the cultivation systems. According to the mean fuel consumption values, the traditional tillage system consumes more 37.86 L fuel per hectare than no-tillage system. *t*-values on Table 3 show negative relation between the fuel consumption and the cultivation systems. Filipovic et al., [8] found that the fuel consumptions in wheat cultivation were to be 49.52±12.05 L/ha and 5.91±1.33 L/ha for the traditional tillage and no-tillage systems, respectively. In the present study, the fuel consumption value (50.96 L/ha) determined for the traditional system is approximately similar to their result (49.52±12.05 L/ha). On the other hand, Köller [56] reported that the fuel consumption was to be 13.40 L per hectare under the no-tillage system. The fuel

consumption value (13.1 L/ha) determined for the no-tillage system in the present study for wheat cultivation is very convenient to him result (13.4 L/ha).

The change of the total fuel consumption (diesel and lubricant oil) and related CO_2 emission for the cultivation systems is given in Fig. 1. Lubricant oil consumptions per hectare were 0.5184 L and 2.0184 L for the no-tillage and the traditional systems, respectively (Table 4). In this case, the total fuel consumption (diesel + oil) per hectare was determined as 13.62 L for the no-tillage system and 52.98 L for the traditional system. Thus, the total fuel consumption for the traditional system was about 39.36 L (289 %) higher per hectare than that of the no-tillage system.

The use of the traditional system released 145.57 $kgCO_2$ per hectare, while the no-tillage system released only 37.42 $kgCO_2$ per hectare (Fig. 1). If the traditional system is used for winter wheat production, 108.15 $kgCO_2$ higher per hectare was released compared to the no-tillage system. Filipovic et al., [8] found that the traditional tillage (136.18 $kgCO_2$/ha) released 120.4 $kgCO_2$ higher per hectare compared to the no-tillage (15.78 $kgCO_2$/ha) for winter wheat production in Croatia conditions. They have reported that the use of the reduced tillage and the no-tillage systems saved 35.3–42.9% and 87.8–88.1%, respectively, thus reducing part of the CO_2 emission for maize (*Zea mays* L.), wheat (*Triticum aestivum* L.), soybean (*Glycine max* L.) and barley (*Hordeum sativum* L.) production in Croatia conditions. Koga et al., [57] reported that the total CO_2 emissions from fuel consumptions were to be 826.2 $kgCO_2$ and 701.5 $kgCO_2$ per hectare under traditional and the reduced tillage systems, respectively, for winter wheat (*Triticum aestivum* L.) production in Japan conditions. They have reported that under reduced tillage systems in which soil preparation in early spring was reduced and plowing after harvesting was omitted, 47.5 L/ha of diesel oil equivalent to 125.4 kg CO_2/ha could be saved, regardless of crop species. Consequently, total CO_2 emissions could be reduced by 15–29%, respectively, in winter wheat production.

TABLE 3
***t*-test results for fuel consumption according to cultivation methods**

Cultivation methods	Fuel consumption (L/ha) Mean	Standard deviation	*t*-value	*p*-value
No-tillage	13.10	0.56	-96.487	0.000**
Traditional tillage	50.96	0.38		

TABLE 4
Diesel and lubricant oil consumptions and crop yields for cultivation systems

Cultivation system	No-tillage	Traditional system			
Equipments	Sowing machine	Plow	Disc harrow	Scrubber	Sowing machine
Fuel consumption (L/ha)	13.1	27.76	8.1	7.2	7.9
	13.1		50.96		
Oil consumption (L/ha)	0.5184	1.0992	0.3208	0.2848	0.3128
	0.5184		2.0184		
Grain yield (kg/ha)	6017		6813		

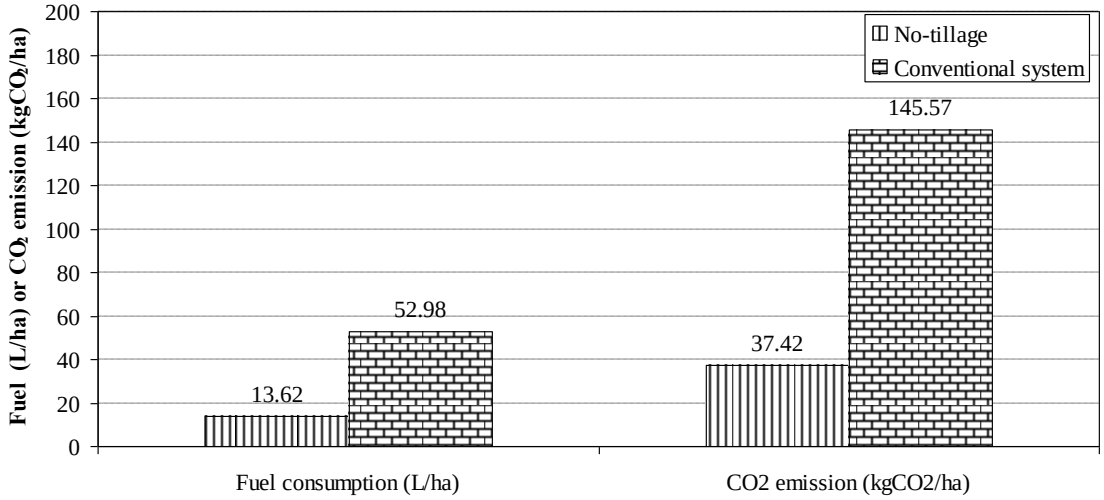

FIGURE 1
Fuel consumption and related CO_2 emission for the cultivation systems

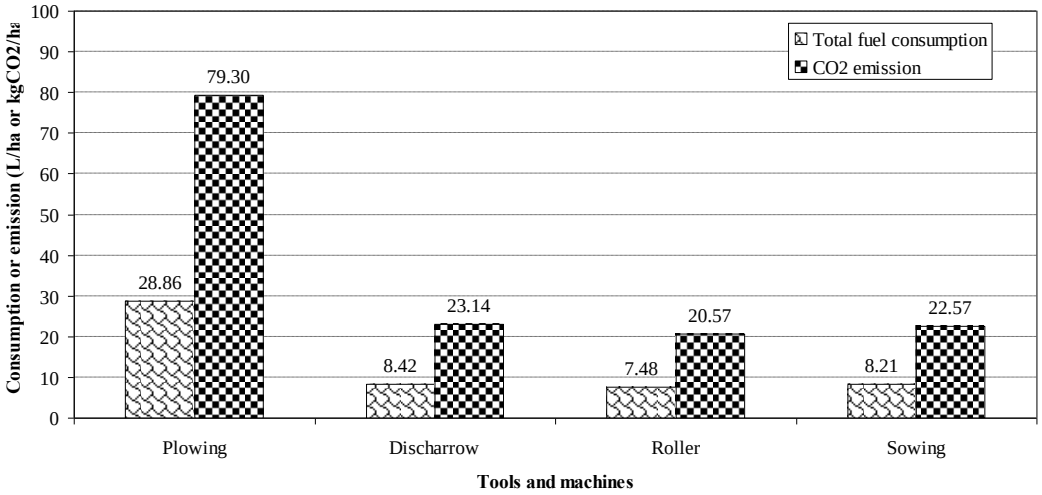

FIGURE 2
Fuel consumptions and related CO_2 emissions for the traditional system

Figure 2 shows the total fuel (diesel and lubricant oil) consumptions and related CO_2 emissions according to agricultural equipments for the traditional system. The traditional tillage system is based on a high intensity of soil engagement and inversion of the soil with plough. The almost 54.5% of the total fuel consumption (28.86 L/ha) was accounted to the ploughing under the traditional tillage system for winter wheat production. Since the plough was the most fuel consuming tillage implement, under the traditional tillage system the plowing (79.3 $kgCO_2$/ha) had a great influence on total CO_2 emissions, accounting for 54.5 % of total CO_2 emissions. Filipovic et al., [8] found that the fuel consumption with the ploughing was to be 28.16 ±6.53 L/ha for wheat cultivation. In the present study, the fuel consumption value (28.86 L/ha) determined for soil tillage with the plough is very close to their result (28.16 ±6.53 L/ha) for wheat cultivation. However, Koga et al., [57] found that the fuel consumption value was to be 29.8 L/ha for soil tillage with the plough under the traditional tillage system in winter wheat production.

Bowers [58] has reported that the average fuel consumption under the ploughing is to be 17.49 ±2.06 L/ha, the chisel ploughing 10.20±1.50 L/ha, while the no-till planter requires 4.02 ±1.03 L/ha. Comparing these data to other sources, wide variations can be expected due to soil types, field conditions, working depths, etc. On the other hand, Köller [56] reported that the fuel consumption under the ploughing was 49.40 L/ha and under the chisel ploughing 31.30 L/ha. The average fuel consumption depends on soil texture, tillage system and differences within stubble crops (winter wheat, barley) and row crops (maize, soybean). For this reason, significant differences in fuel consumption have reported under traditional tillage and no-tillage systems.

The fuel consumptions under the traditional tillage system were 8.42 L/ha and 8.21 L/ha with the disc harrow and seeding practices, respectively. Koga et al., [57] found that the fuel consumptions values for seedbed preparation with rotary harrow in winter wheat production were to be 41.3 L/ha and 20.7 L/ha under the traditional and reduced tillage systems, respectively. They reported that the fuel consumptions for sowing and basal fertilization with drill seeder were to be 6.7 L/ha under the traditional and reduced tillage systems. On the other hand, Filipovic et al., [8] found that the fuel consumption with the disc harrow and planter for wheat cultivation were to be 6.38±3.30 L/ha and 3.34±0.88 L/ha, respectively.

Figure 3 shows the total energy consumptions related to diesel and lubricant oil consumptions with the agricultural equipments under the traditional and no-tillage systems for winter wheat production. Under the traditional system, 2473.5 MJ of fossil fuel (diesel+lubricant oil) energy was consumed per hectare, while the total energy consumption was 505.81 MJ/ha under the no-tillage system. The total energy consumption under the no-tillage system was 1967.7 MJ per hectare lower than that of the traditional tillage system. Compared to the no-tillage system, it is clear that about 5 times more energy per hectare was consumed under the traditional system.

Grain Yield. The *t*-test was applied to evaluate the relationship between grain yield and cultivation systems used in wheat production, and the results are given in Table 5. Different tillage systems affect the yield parameters. *t*-test results show that tillage systems effects on yield values is statistically important ($p<0.05$). The traditional cultivation system affected mean yield values positively. No-tillage system reduced the wheat yield values more than 796 kg per hectare according to the traditional tillage system.

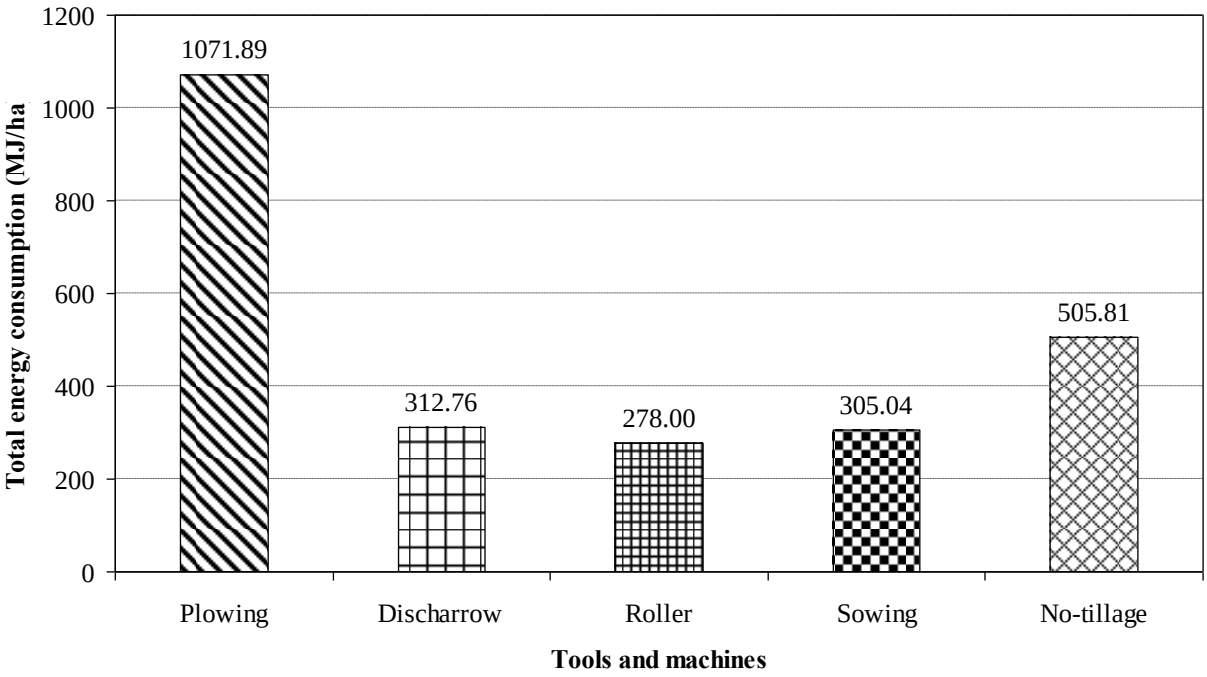

FIGURE 3
The energy consumptions under the traditional system

TABLE 5
***t*-test results for grain yield according to the cultivation systems**

Cultivation methods	Grain yield (kg/ha) Mean	Standard deviation	*t*-value	*p*-value
No-tillage	6016.67	356.42	-3.753	0.020*
Traditional tillage	6813.33	90.18		

Figure 4 shows of change of the specific fuel and energy consumptions and CO_2 emissions under the traditional and no-tillage systems. The specific fuel consumption (SFC; L/t) was defined as the ratio of the total amount fuel (L) consumed under tillage system to the total amount of harvested grain (t). The value of the SFC indicates the amount of fuel consumed (L) to produce the unit quantity (t) of grain product. The value of the specific energy consumption (SEC) indicates the amount of energy consumed (MJ) to produce the unit quantity (t) of grain product. The lower values of the SFC and the SEC mean the energy efficiency of production is higher. The values of the SFC were 7.78 L/t and 2.26 L/t under the traditional and no-tillage systems, respectively (Figure 4). Taking into account the SFC and SEC values, while 7.78 L fossil fuel (diesel+lubricant) or 288.81 MJ fossil energy was consumed to produce 1 ton grain wheat under the traditional tillage system, only 2.26 L fossil fuel or 84.06 MJ fossil energy was consumed per ton wheat production under the no-tillage system. Compared to the traditional tillage system, 5.52 L less fossil fuel in the other word 204 MJ less fossil energy was consumed to produce per ton of wheat. The value of the specific energy CO2 emission (SCO_2) indicates the amount of CO_2 released ($kgCO_2$) to produce the unit quantity (t) of grain product. The lower value of the SCO_2 means the environmental sustainability of production is higher. If the traditional tillage system is used for winter wheat production, 15.15 kg higher CO_2 was released per ton grain compared to the no-tillage system. Under the no-tillage system to produce per ton grain 243.6% less CO_2 was released during the tillage and sowing practices compared to the traditional tillage system.

Figure 5 shows of change of the specific grain productions under the traditional and no-tillage systems. The specific grain production based on fuel consumption (SGP_F; kg/L) is the inverse of the SFC and was defined as the ratio of the total amount of harvested grain product (kg) to the total amount of fossil fuel (L) consumed for seed bed preparation and sowing practice. The SGP_F indicates the amount of grain (kg) produced per litre (L) fossil fuel consumed under the applied system. The higher value of the SGP_F means the efficiency of fuel use in production system is higher. The SGP_F in winter wheat production were 128.60 kg/L and 441.83 kg/L under the traditional tillage and the no-tillage systems, respectively (Figure 5). Consid-

ering the values of SGP_F for winter wheat production, while 1 L fuel was consumed to produce 441.83 kg grain under the traditional tillage system, 128.6 kg grain was obtained per L fossil fuel consumed under the no-tillage system. This means that 313.23 kg more grain are obtained per L of fossil fuel consumed under the no-tillage system compared to the traditional tillage system.

The specific grain production based on energy consumption (SGP_E; kg/MJ) is the inverse of the SEC and was defined as the ratio of the total amount of harvested grain product (kg) to the total amount of fossil energy (MJ) consumed for seed bed preparation and sowing practice. The SGP_E indicates the amount of grain (kg) produced per megaJoule (MJ) fossil energy consumed under the applied system. The higher value of the SGP_E means the efficiency of energy use in production system is higher. The SGP_E in winter wheat production were 3.47 kg/MJ and 11.90 kg/MJ under the traditional tillage and the no-tillage systems, respectively (Fig.5). This means that 8.43 kg more grain are obtained per MJ of fossil energy consumed under the no-tillage system compared to the traditional tillage system.

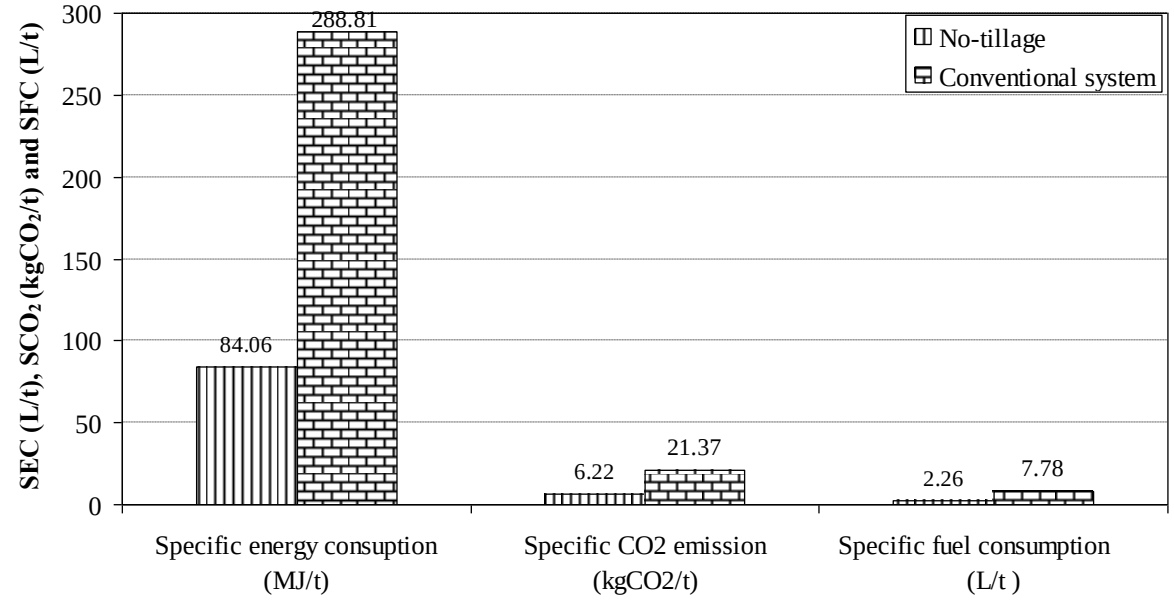

FIGURE 4

The specific fuel and energy consumptions and CO_2 emissions under the traditional and no-tillage systems

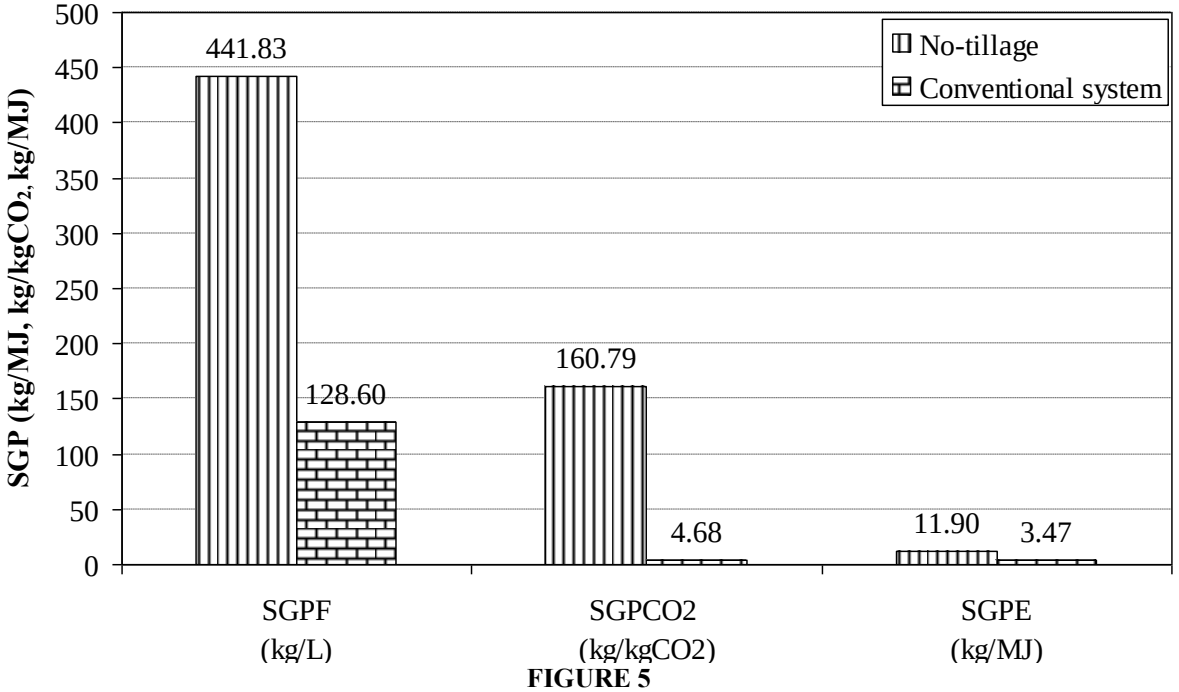

FIGURE 5

The specific grain productions under the traditional and no-tillage systems

Similarly, the specific grain production based on CO_2 emission (SGP_{CO2}; kg/kgCO_2) is the inverse of the SCO_2 and was defined as the ratio of the total amount of harvested grain product (kg) to the total amount of CO_2 (kg) released for seed bed preparation and sowing practice. The SGP_{CO2} indicates the amount of grain (kg) produced per kg CO_2 released under the applied system. The higher value of the SGP_{CO2} means the efficiency of environmental sustainability in production system is higher. The SGP_{CO2} in winter wheat production were 4.68 kg/kgCO_2 and 160.79 kg/kgCO_2 under the traditional tillage and the no-tillage systems, respectively (Fig.5). This means that 156.11 kg more grain are obtained per kg CO_2 released under the no-tillage system compared to the traditional tillage system.

CONCLUSION

The values of fossil fuel consumption show that significant energy savings could be obtained with the no-tillage system. Similarly, the values of total CO_2 emissions show that the significant CO_2 emissions savings could be achieved with the no-tillage system. Taking into account the significant environmental advantages that can be obtained with the adoption of a reduced tillage system; the no-tillage system appears the best method for the substitution of the moldboard plow for wheat production. Therefore, to reduce CO_2 emissions in agricultural production, it will be necessary to apply new technologies which reduce fuel consumption significantly. The results of this study can be used by policy makers and other relevant agencies for recommendations to farmers in order to use energy more efficiently. Proper management of resources and their application at the right time can improve the efficiency of the farmers in the use of farm inputs.

REFERENCES

[1] Gustavo, G., Camargo, T., Matthew, R., Richard, T.L. (2013) Energy use and greenhouse gas emissions from crop production using the farm energy analysis tool. BioScience. 63(4), 263–173.

[2] IPCC (2010) Climate Change: Impacts, Adaptation and Vulnerability. Contribution of Working Group II to the Fourth Assessment Report of the Intergovernmental Panel on Climate Change. Cambridge University Press, Cambridge, UK, 976p.

[3] Sarauskis, E., Vaiciukevicius, E., Romaneckas, K., Sakalauskas, A., Baranauskaite, R. (2009) Economic and energetic evaluation of sustainable tillage and cereal sowing technologies in Lithuania. Rural Development. 4(1), 280–285.

[4] Sarauskis, E., Buragiene, S., Romaneckas, K., Sakalauskas, A., Jasinskas, A., Vaiciukevicius, E., Karayel, D. (2012) Working time, fuel consumption and economic analysis of different tillage and sowing systems in Lithuania. Engineering for Rural Development. 11, 52–59.

[5] Castoldi, N., Bechini, L. (2010) Integrated sustainability assessment of cropping systems with agro-ecological and economic indicators in Northern Italy. European Journal of Agronomy. 32(1), 59–72.

[6] Sarauskis, E., Masilionyte, L., Kriauciuniene, Z., Romaneckas, K., Buragiene, S. (2013) Evaluation of energy and environmental aspects of reduced tillage systems applied in maize cultivation. World Academy of Science, Engineering and Technology, International Journal of Biological, Biomolecular, Agricultural, Food and Biotechnological Engineering. 7(10), 13–20.

[7] Ang, B.W., Mu, A.R., Zhou, P. (2010) Accounting frameworks for tracking energy efficiency trends. Energy Economics. 32, 1209-1219.

[8] Filipovic, D., Silvio, K., Zlatko, G.O., Robert, Z., Djuro, B. (2006) The possibility of fuel saving and reduction of CO2 emission in the soil tillage in Croatia. Agriculture Ecosystem and Environment. 115(1-4), 290–294.

[9] Memon, S.Q., Dayo, R.A., Jarwar, G. (2015) Energy requirement and energy efficiency for production of maize crop. European Academic Research. II(11), 14609–14614.

[10] Shamabadi, Z. (2015) Conservation tillage can reduce energy consumption and carbon emissions in the production of rainfed sunflower. Research on Crop Ecophysiology. 10/2(1), 51–63.

[11] Meisterling, K., Samaras, C., Schweizer, V. (2009) Decisions to reduce greenhouse gases from agriculture and product transport: LCA case study of organic and conventional wheat. Journal of Cleaner Production. 17(2), 222–230.

[12] Biswas, W.K., Graham, J., Kelly, K., John, M.B. (2010) Global warming contributions from wheat, sheep meat and wool production in Victoria, Australia–a life cycle assessment. Journal of Cleaner Production. 18(14), 1386-1392.

[13] Pishgar-Komleh, S.H., Ghahderijani, M., Sefeedpari, P. (2012) Energy consumption and CO2 emissions analysis of potato production based on different farm size levels in Iran. Journal of Cleaner production. 33, 183–191.

[14] Zhang, M.Y., Wang, F.J., Chen, F., Malemela, M.P., Zhang, H.L. (2013) Comparison of three tillage systems in the wheat-maize system on carbon sequestration in the North China Plain. Journal of Cleaner Production. 54, 101–107.
[15] Cui, Z.L., Wu, L., Ye, Y.L., Ma, W.Q., Chen, X.P., Zhang, F.S. (2014) Trade-offs between high yields and greenhouse gas emissions in irrigation wheat cropland in China. Biogeosciences. 11, 2287–2294.
[16] Alam, M.K., Biswas, W.K., Bell, R.W. (2016) Greenhouse gas implications of novel and conventional rice production technologies in the Eastern-Gangetic plains. Journal of Cleaner Production. 112, 3977–3987.
[17] Ali, S.A., Tedone, L., De Mastro, G. (2015) Optimization of the environmental performance of rainfed durum wheat by adjusting the management practices. Journal of Cleaner Production. 87, 105–118.
[18] Bacenetti, J., Fusi, A., Negri, M., Fiala, M. (2015) Impact of cropping system and soil tillage on environmental performance of cereal silage productions. Journal of Cleaner Production. 86, 49–59.
[19] Houshyar, E., Dalgaard, T., Tarazkar, M.H., Jørgensen, U. (2015) Energy input for tomato production what economy says, and what is good for the environment. Journal of Cleaner Production. 89, 99–109.
[20] Yan, M., Cheng, K., Luo, T., Yan, Y., Pan, G., Rees, R.M. (2015) Carbon footprint of grain crop production in China–based on farm survey data. Journal of Cleaner Production. 104, 130–138.
[21] Cardozo, N.P., de Oliveira Bordonal, R., La Scala Jr, N. (2016) Greenhouse gas emission estimate in sugarcane irrigation in Brazil: is it possible to reduce it, and still increase crop yield. Journal of Cleaner Production. 112, 3988–3997.
[22] Nunes, F.A., Seferin, M., Maciel, V.G., Flôres, S.H., Ayub, M.A.Z. (2016) Life cycle greenhouse gas emissions from rice production systems in Brazil: A comparison between minimal tillage and organic farming. Journal of Cleaner Production. 139, 799–809.
[23] Ozturk, H.H. (2016) Energy use for wheat cultivation in Southeast Anatolia Region of Turkey. Agricultural Mechanization in Asia, Africa and Latin America. 47(3), 47–53.
[24] Ozturk, H.H. (2018) An assessment of carbon dioxide emissions related to fuel consumption for sunflower cultivation. Fresen. Environ. Bull. 27, 710–719.
[25] Wang, Z.B., Zhang, H.L., Lu, X.H., Wang, M., Chu, Q.Q., Wen, X.Y., Chen, F. (2016) Lowering carbon footprint of winter wheat by improving management practices in North China Plain. Journal of Cleaner Production. 112, 149–157.
[26] Ali, S.A., Tedone, L., Verdini, L., De Mastro, G. (2017) Effect of different crop management systems on rainfed durum wheat greenhouse gas emissions and carbon footprint under Mediterranean conditions. Journal of Cleaner Production. 140, 608–621.
[27] Alimagham, S.M., Soltani, A., Zeinali, E., Kazemi, H. (2017) Energy flow analysis and estimation of greenhouse gases (GHG) emissions in different scenarios of soybean production (Case study: Gorgan region, Iran). Journal of Cleaner Production. 149, 621–628.
[28] Chiriacò, M.V., Grossi, G., Castaldi, S., Valentini, R. (2017) The contribution to climate change of the organic versus conventional wheat farming: A case study on the carbon footprint of wholemeal bread production in Italy. Journal of Cleaner Production. 153, 309–319.
[29] Fantin, V., Righi, S., Rondini, I., Masoni, P. (2017) Environmental assessment of wheat and maize production in an Italian farmers' cooperative. Journal of Cleaner Production. 140, 631–643.
[30] He, G., Cui, Z., Ying, H., Zheng, H., Wang, Z., Zhang, F. (2017) Managing the trade-offs among yield increase, water resources inputs and greenhouse gas emissions in irrigated wheat production systems. Journal of Cleaner Production. 164, 567–574.
[31] Kamali, F. P., Meuwissen, M.P., de Boer, I.J., van Middelaar, C.E., Moreira, A., Lansink, A.G.O. (2017) Evaluation of the environmental, economic, and social performance of soybean farming systems in southern Brazil. Journal of Cleaner Production. 142, 385–394.
[32] Lovarelli, D., Bacenetti, J., Fiala, M. (2017) Effect of local conditions and machinery characteristics on the environmental impacts of primary soil tillage. Journal of Cleaner Production. 140, 479–491.
[33] Lu, X., Liao, Y. (2017) Effect of tillage practices on net carbon flux and economic parameters from farmland on the Loess Plateau in China. Journal of Cleaner Production. 162, 1617–1624.
[34] Nabavi-Pelesaraei, A., Rafiee, S., Mohtasebi, S.S., Hosseinzadeh-Bandbafha, H., Chau, K.W. (2017) Energy consumption enhancement and environmental life cycle assessment in paddy production using optimization techniques. Journal of Cleaner Production. 162, 571–586.

[35] Parajuli, R., Kristensen, I.S., Knudsen, M.T., Mogensen, L., Corona, A., Birkved, M., Pena, N., Graversgaard, M., Dalgaard, T. (2017) Environmental life cycle assessments of producing maize, grass-clover, ryegrass and winter wheat straw for biorefinery. Journal of Cleaner Production. 142, 3859–3871.

[36] Wang, Z.B., Chen, J., Mao, S.C., Han, Y.C., Chen, F., Zhang, L.F., Li, Y.B., Li, C.D. (2017) Comparison of greenhouse gas emissions of chemical fertilizer types in China's crop production. Journal of Cleaner Production. 141, 1267–1274.

[37] Yang, Y., Li, Y., Zhang, S., Chen, F., Hou, H., Ma, J. (2017) Monitoring the impact of fugitive CO2 emissions on wheat growth in CCS-EOR areas using satellite and field data. Journal of Cleaner Production. 151, 34–42.

[38] Fan, J., McConkey, B.G., Janzen, H.H., Miller, P.R. (2018) Emergy and energy analysis as an integrative indicator of sustainability: A case study in semi-arid Canadian farmlands. Journal of Cleaner Production. 172, 428–437.

[39] Forleo, M.B., Palmieri, N., Suardi, A., Coaloa, D., Pari, L. (2018) The eco-efficiency of rapeseed and sunflower cultivation in Italy. Joining environmental and economic assessment. Journal of Cleaner Production. 172, 3138–3153.

[40] Houshyar, E., Wu, X.F., Chen, G.Q. (2018) Sustainability of wheat and maize production in the warm climate of southwestern Iran: An emergy analysis. Journal of Cleaner Production. 172, 2246–2255.

[41] Goglio, P., Smith, W.N., Grant, B.B., Desjardins, R.L., Gao, X., Hanis, K., Burgess, P.J. (2018) A comparison of methods to quantify greenhouse gas emissions of cropping systems in LCA. Journal of Cleaner Production. 172, 4010–4017.

[42] Maraseni, T.N., Deo, R.C., Qu, J., Gentle, P., Neupane, P.R. (2018) An international comparison of rice consumption behaviours and greenhouse gas emissions from rice production. Journal of Cleaner Production. 172, 2288–2300.

[43] Noya, I., González-García, S., Bacenetti, J., Fiala, M., Moreira, M.T. (2018) Environmental impacts of the cultivation-phase associated with agricultural crops for feed production. Journal of Cleaner Production. 172, 3721-3733.

[44] Squalli, J., Adamkiewicz, G. (2018) Organic farming and greenhouse gas emissions: A longitudinal US state-level study. Journal of Cleaner Production. 192, 30–42.

[45] Taki, M., Rohani, A., Soheili-Fard, F., Abdeshahi, A. (2018) Assessment of energy consumption and modeling of output energy for wheat production by neural network (MLP and RBF) and Gaussian process regression (GPR) models. Journal of Cleaner Production. 172, 3028–3041.

[46] Tedone, L., Ali, S.A., Verdini, L., De Mastro, G. (2018) Nitrogen management strategy for optimizing agronomic and environmental performance of rainfed durum wheat under Mediterranean climate. Journal of Cleaner Production. 172, 2058–2074.

[47] Todorović, M., Mehmeti, A., Cantore, V. (2018) Impact of different water and nitrogen inputs on the eco-efficiency of durum wheat cultivation in Mediterranean environments. Journal of Cleaner Production. 183, 1276-1288.

[48] Yadav, G.S., Das, A., Lal, R., Babu, S., Meena, R.S., Saha, P., Singh, R., Datta, M. (2018) Energy budget and carbon footprint in a no-till and mulch based rice–mustard cropping system. Journal of Cleaner Production. 191, 144-157.

[49] Abbas, A., Yang, M., Yousaf, K., Khan, K.A., Iqbal, T., Hassan, S.H. (2018) Comparative analysis of energy use efficiency in food grain production systems of Pakistan. Fresen. Environ. Bull. 27, 1053–1059.

[50] Sowinski, J., Wojciechowski, W. (2018) Nitrogen efficiency of winter wheat on different tillage methods for whole crop silage. Fresen. Environ. Bull. 27, 230–235.

[51] Sowinski, J., Wojciechowski, W. (2018) Effect of winter wheat tillage methods on nitrogen fertilizer efficiency. Fresen. Environ. Bull. 27, 6727–6733.

[52] Marakoglu, T., Carman, K. (2017) A comparative study on energy efficiency of wheat production under different tillage practices in Middle Anatolia of Turkey. Fresen. Environ. Bull. 26, 3163–3169.

[53] Baran, M.F., Gokdogan, O. (2016) Comparison of energy use efficiency of different tillage methods on the secondary crop corn silage production. Fresen. Environ. Bull. 25, 3808-3814.

[54] Taner., Arısoy, R.Z., Kaya, Y., Gültekin, İ., Partigöç, F. (2015) The effects of various tillage systems on grain yield, quality parameters and energy indices in winter wheat production under the rainfed conditions. Fresen. Environ. Bull. 24, 1463–1473.

[55] IPCC (1996) Calculating CO2 emissions from mobile sources guidance to calculation worksheets. GHG Protocol - Mobile Guide (03/21/05) v1.3.

[56] Köller, K. (1986) Production of Cereals Under Labor. Swiss Journal of Agriculture. 28, 30-39.
[57] Koga, N., Tsuruta, H., Tsuji, H., Nakano, H. (2003) Fuel consumption derived CO2 emissions under conventional and reduced tillage cropping systems in northern Japan. Agric. Ecosyst. Environ. 99, 213–221.
[58] Bowers, W. (1992) Agricultural field equipment. In: Fluck, R.C. (Ed.) Energy in World Agriculture. Energy in Farm Production, Elsevier, Amsterdam, 6, 117.

Received: **11.07.2018**
Accepted: **25.11.2018**

CORRESPONDING AUTHOR

Z Figen Antmen
Cukurova University
Faculty of Engineering
Dept. of Industrial Engineering
01330 Sarcam, Adana – Turkey

e-mail: zfantmen@hotmail.com

© by PSP Volume 28 – No. 4/2019 pages 2495-2505 Fresenius Environmental Bulletin

THE DYNAMIC CHANGES OF PLANT ENDOGENOUS HORMONES IN RESPONSE TO DIFFERENT TEMPERATURES IN SEEDS OF *IDESIA POLYCARPA* MAXIM. FROM XINYANG

Yanmei Wang, Zhen Liu*, Fei Li

College of Forestry, Henan Agricultural University, Zhengzhou, 450002 China

ABSTRACT

This paper discussed the changes of endogenous hormones in the process of dormancy release of *I. polycarpa* Maxim. seeds treated at low temperatures, and laid a foundation for further exploring it's dormancy release mechanism. The dynamic changes of endogenous hormones at low temperatures were determined by high performance liquid chromatography (HPLC). The results showed that: (1) The germination rate was highest after treatment for 60 d at 5°C. (2) The Indole acetic acid (IAA) content showed "decrease-rise-decrease" at 5°C and 12°C, and "decrease-rise" at 10 °C and 15°C. The IAA content was significant differences ($p<0.01$) between 60 d and 20d, 40d. (3) The content of GA_3 (Gibberellin A_3) showed "decrease-rise" at 5 °C and 10 °C, and "decrease-rise-decrease" at 12 °C and 15 °C. The changes of GA_3 content were consistent at different temperatures from 0d to 40d, but was extremely significant between 40d and 60d. (4) Except for 12 °C, the ZR (trans-Zeatin-riboside) content was significantly ($p<0.01$) different between 60d and 0d, 20d and 40d. (5) Overall, the ABA (abscisic acid) content showed a downward trend. The ABA content of the untreated seeds was significantly different from which were treated at 5°C, 10°C, 12°C, and 15°C treatment for 20d, 40d and 60d($p<0.01$). (6) The germination rate was significantly and negatively correlated with the ABA content, but it was positively correlated with the following hormone ratios: GA_3/ABA, ZR/ABA, (IAA+GA_3)/ABA, (IAA+ZR)/ABA, (GA_3+ZR)/ABA, and (IAA+GA_3+ZR)/ABA. It is concluded that all the low temperatures had effects on the dormancy release of the seeds. However, the seeds from Xinyang tended to the dormancy characteristics of the warm-temperate plants, and the lower temperature was conducive to dormancy release. The endogenous hormonal responses in the seeds of *I. polycarpa* Maxim. in Xinyang were sensitive and varied. The content of ABA and the ratio of GA_3/ABA may be the key factors for the release dormancy.

KEYWORDS:
Idesia polycarpa Maxim, dormancy release, low temperature treatments, the germination rate, endogenous hormone

INTRODUCTION

Idesia polycarpa Maxim. is a deciduous tree of the genus *Idescia* of the family Flacourtiaceae. It is native to tropical or subtropical. It's oil content is high and is called a "beautiful tree depot". However, the natural germination rate is generally low, and natural regeneration is difficult, resulting in a decrease in natural populations and limiting their development succession. Several studies have reported the methods to improve the germination rate, for example, removing the waxy outer layer of seeds [1], soaking and adding plant growth regulators [2], immersing in alkaline and straw ash water [3], dewaxing [4], and low-temperature and wet sand treatment [5]. Although the germination rate of seeds can be improved via the above methods, the result is not ideal. Wang [6] found that the seed of *I. polycarpa* Maxim. possesses dormancy character.

Many factors affect seed dormancy [7], and plant hormone is the most important endogenous factor regulating seed dormancy, and is directly involved in seed dormancy release [8-10]. ABA, IAA, GA_3 and ZR (trans-Zeatin-riboside) have major roles in the regulation of dormancy release of the seed. Changes in hormone content, as well as interactions between different hormones, have a great influence on seed dormancy and germination.

Different provenances of *I. polycarpa* Maxim. seeds have different dormancy release effects by different low temperature treatments [11]. However, there is a lack of works on endogenous changes of *I. polycarpa* Maxim. seeds. Therefore, the aim of this study was to investigate the changes in endogenous hormone content in seeds of *I. polycarpa* Maxim. from Xinyang, which is located in the transition zone from the northern subtropic to the warm temperate. In the process of the dormancy release at low temperatures treatments, the dynamic changes

of plant endogenous hormones were explored, and the relationship between the endogenous hormone and the seed germination rate were analyzed. The results provided an important information for the mechanism of dormancy release of the seed of *I. polycarpa* Maxim. and the theoretical basis and technical support for breeding.

MATERIALS AND METHODS

Materials. The seeds of *I. polycarpa* Maxim. were collected from Xinyang Kikungshan (114°5'E, 31°50'N) of Henan Province, which belongs to the transition zone from the northern subtropic to the warm temperate, with an average annual temperature of 12 °C, an extremely highest temperature of 39.6 °C, and an extremely lowest temperature of -17 °C. The ≥10℃ accumulated temperature is 4800 ℃. Frost-free period average is 250 d. Average rainfall is 1300 mm annually, and average sunshine is 2100 h annually.

Methods. The wet seeds of *I. polycarpa* Maxim**.** were put in artificial climate chambers (LRH-250-GSI) at low temperatures (5 ℃, 10 ℃, 12 ℃, 15 ℃) for 60d. 0d treatment was the control (CK). In the low-temperature treatment process, the dynamic changes of endogenous hormones were measured every 20 days by To test the seeds germination rate, the seeds were sampled at 0 d, 20 d, 40 d, and 60 d, then placed in Petri dishes (100 seeds per dish) and kept at variable temperature (15°C/ 25°C, 12 h each). The number of germinated seeds was counted every 5d. Each treatment was replicated three times.

Data processing. Excel, Origin and SPSS were used to process and analyze the data.

RESULTS

Effect of low-temperature on the seed germination rate of I. polycarpa Maxim. from Xinyang.Based on the results showed in Table 1, the germination rate of untreated seeds was 38.3%. The germination rate treated at low temperatures increased over time, indicating that the four kinds of temperatures can effectively release dormancy. The germination rate reached the maximum after 60 d treatment at all 4 low temperatures while the germination rate was the highest (94.67%) at 5 °C. The germination rate did not show significant difference between the 5 °C and 10 °C after 60 d ($p>0.05$), but the difference was significant between 5 °C and 12 °C, as well as 5 °C and 15 °C ($p<0.01$). The results indicated that the dormancy release of seeds from Xinyang was not completely dependent on the range of the low temperature. However, the dormancy characteristic was partial to the plant seeds in the warm temperate, and lower temperature was conducive to dormancy release.

Effect of low-temperature on the changes of the IAA content of *I. polycarpa* Maxim. Seeds. In the process of dormancy release (Fig.1), the IAA content showed "decrease-rise-decrease" trend at 5°C, and 12°C, but "decrease-rise" trend at10°C and 15°C. At low temperatures, the difference of the IAA content was significant ($p<0.01$) between 60 d and 0d, 20d, 40d, but it was not significant between 60 d and 0 d（$p>0.05$）.

Effect of low-temperature on the changes of the GA_3 content of *I. polycarpa* Maxim. Seeds. The GA_3 content showed "decrease-rise" trend at 5 °C and 10 °C, and "decrease-rise-decrease" at 12 °C and 15 °C. From 0d to 40 d, the changes of the GA_3 content at low temperatures were consistent (Fig.2). The difference of the GA_3 content between 40d and 60d was extremely significant at low temperatures ($p<0.01$).

Effect of low-temperature on the changes of the ZR content of *I. polycarpa* Maxim. Seeds. The ZR content was "rise" at 5 °C, "decrease-rise" at 12 ºC, and "rise-decrease" at 10 °C, and15 °C(Fig.3). Except for 12 °C, the difference of the ZR content was significant ($p<0.01$) between 60 d and 0 d, 60 d and 20 d, 60 d and 40 d.

TABLE 1
The difference of the seed germination rate of *I. polycarpa* Maxim. at 15/25 ℃ after low-temperature treatments

Treatment days (d)	Pre-chilling temperature (℃) and GR			
	5	10	12	15
0 d	38.3±0.4gH	38.3±0.4gH	38.3±0.4gH	38.3±0.4gH
20 d	79.3±0.2eF	71.7±0.8fG	72.0±1.3fG	68.7±1.1fG
40 d	90.0±0.6bBC	86.0±0.5cdCD	88.7±0.3bcBCD	83.3±2.7dDE
60 d	94.7±1.1aA	92.0±1.2abAB	89.3±0.8bcBC	89.0±1.6bcBC

Note: Different lowercase letters in the same column indicating significant difference ($p<0.05$), different capital letters indicate extremely significant difference ($p<0.01$). The same is true forTab.2-Tab.5 below. GR stands for the germination rate in Tab. 1-5.

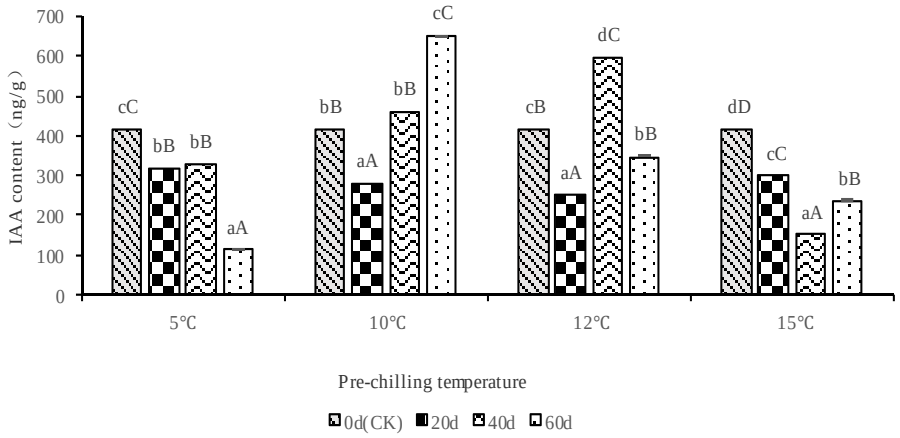

FIGURE 1
The changes of the IAA content of *I. polycarpa* Maxim. seeds from Xinyang at low temperatures

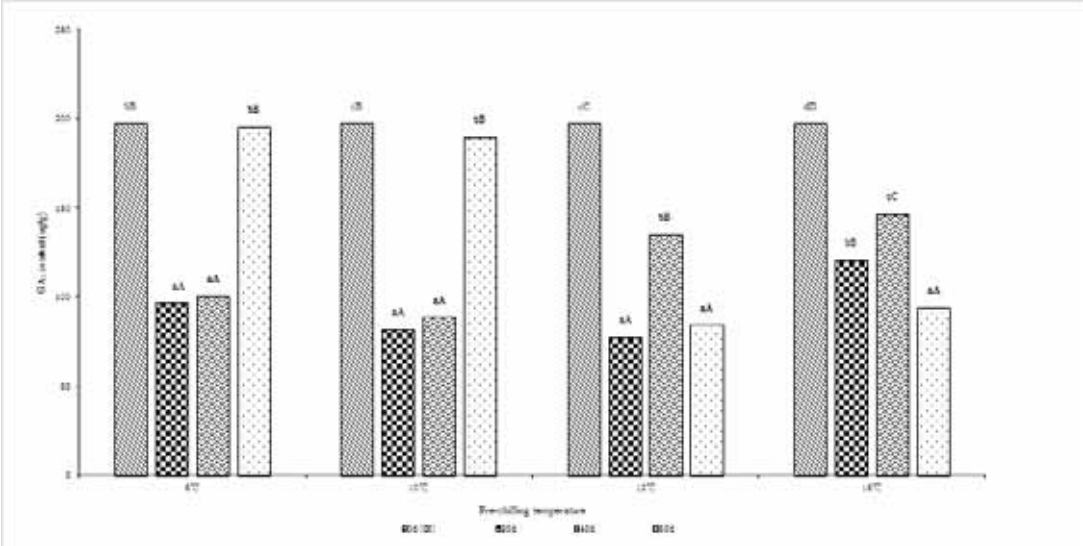

FIGURE 2
The changes of GA_3 content of *I. polycarpa* Maxim. seeds from Xinyang at low temperatures

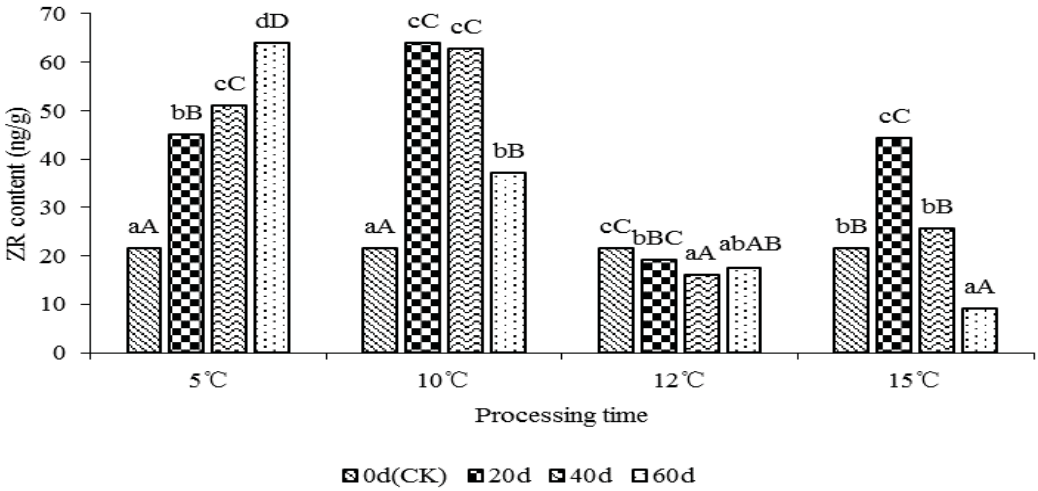

FIGURE 3
The changes of the ZR content of *I. polycarpa* Maxim. seeds from Xinyang at low temperatures

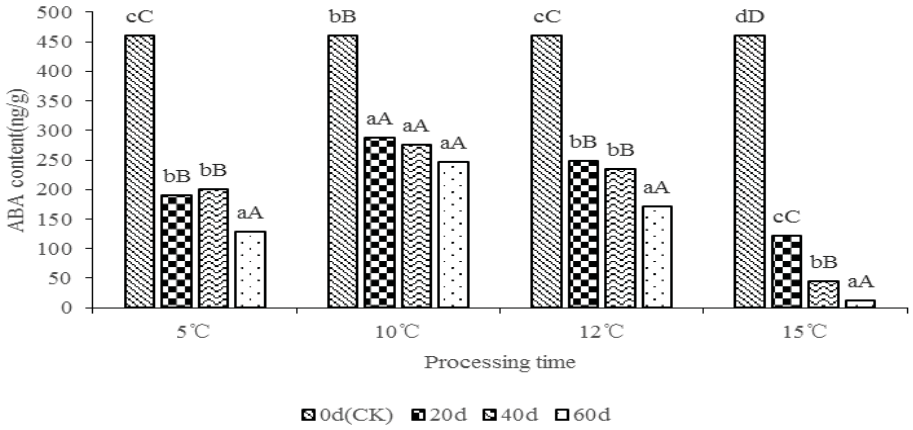

FIGURE 4
The changes of the ABA content of *I. polycarpa* Maxim. seeds from Xinyang at low temperatures

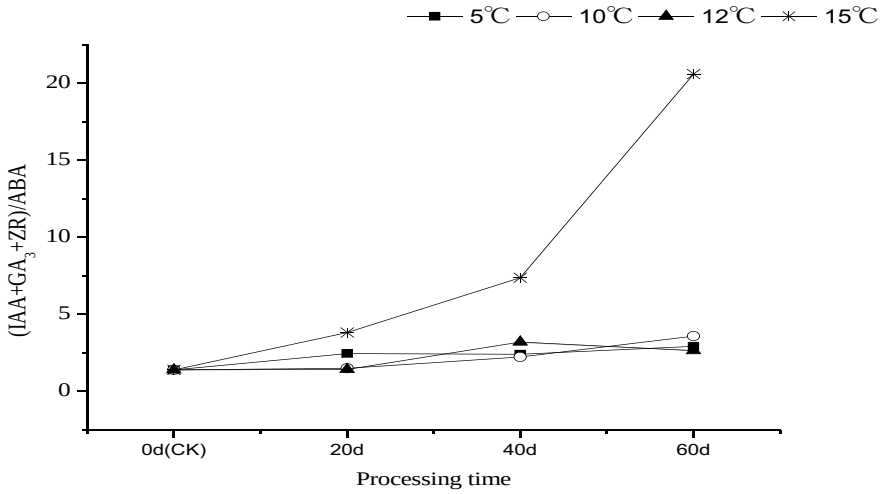

FIGURE 5
The ratio changes of (IAA+GA_3+ZR)/ABA of *I. polycarpa* Maxim. seeds from Xinyang at low temperatures

Effect of low-temperature on the changes of the ABA content of *I. polycarpa* Maxim. Seeds. The ABA content decreased at low temperatures. It decreased rapidly at the first 20 d, then decreased slightly in the next 40 d(Fig.4). The ABA content of untreated seeds was significantly different from the seeds treated at 5 °C, 10 °C, 12 °C, and 15 °C ($p<0.01$), indicating that different low-temperature treatments had a great influence on the ABA content.

Effect of low-temperature on the changes of (IAA+GA3+ZR)/ABA of *I. polycarpa* Maxim. Seeds. The ratio of (IAA+GA_3+ZR)/ABA gradually increased over time (Fig.5). The difference of the ratio was not significant between 5 ℃, 10 ℃, and12 ℃ ($p>0.05$), but was significant ($p < 0.01$) between 15 ℃ and 5 ℃, 10 ℃, and12 ℃.

The changes of the ratios were almost consistent with GA_3/(ABA+IAA), ZR/(ABA+IAA), (GA_3+ZR)/(ABA+IAA), and the trends of the ratio were almost the same as (IAA+ZR)/ABA, (GA_3+ZR)/ABA, (IAA+GA_3)/ABA, ZR/ABA, IAA/ABA and GA_3/ABA(Fig.6).

The correlation between endogenous hormone and the seed germination rate at 5℃. The germination rate was positively correlated with the IAA and ABA content, but it was correlated with the ZR content. The germination rate was positively correlated with the following ratios: GA_3/ABA, ZR/ABA, (IAA+GA_3)/ABA, (IAA+GA_3+ZR)/ABA, (IAA+ZR)/ABA, (GA_3+ZR)/ABA, ZR/(ABA+IAA), GA_3/ (ABA+IAA) and (GA_3+ZR)/(ABA+IAA) (Tab.2).

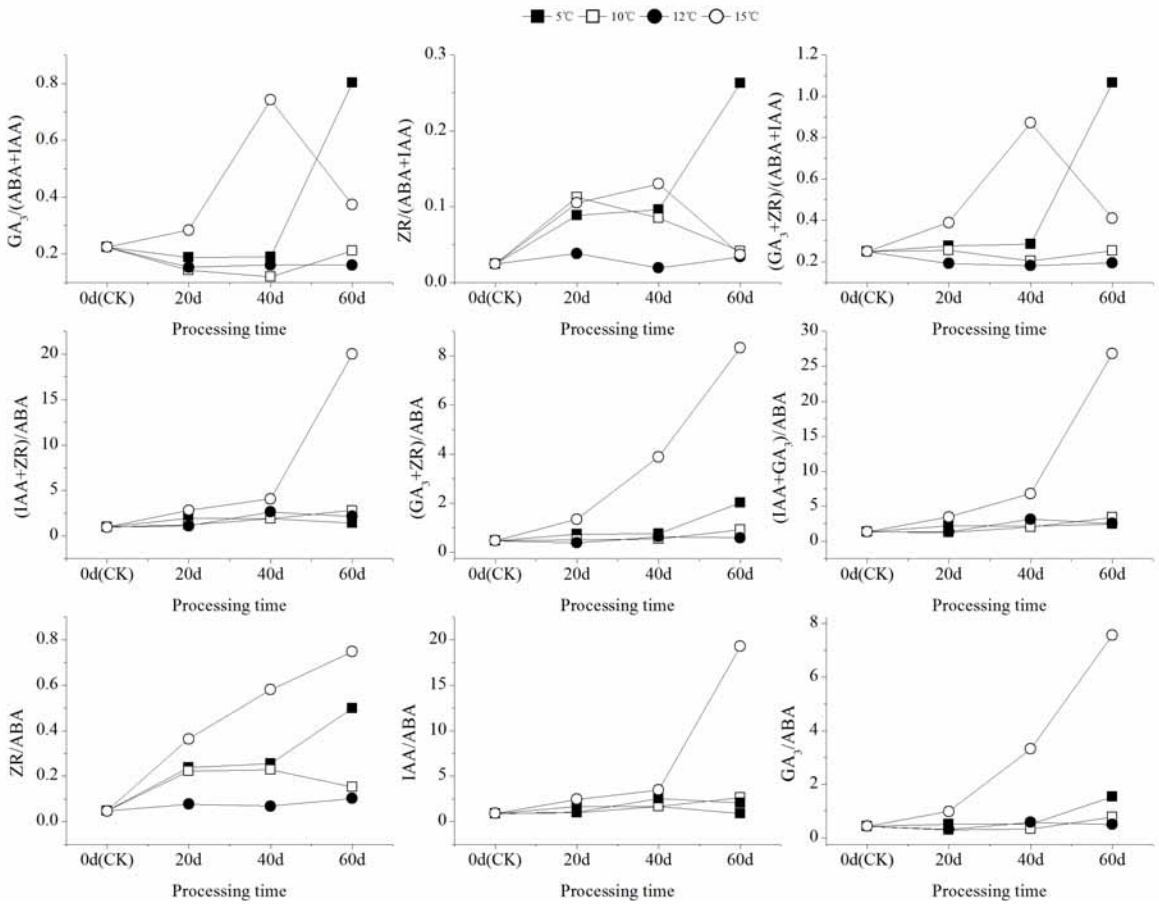

FIGURE 6
The changes of the 9 endogenous hormone ratios of *I. polycarpa* Maxim. seeds from Xinyang at low temperatures

TABLE 2
The correlation between endogenous hormone content and the germination rate of *I. polycarpa* Maxim. at 5℃

	IAA	ABA	GA_3	ZR	GR
IAA	1				
ABA	.784**	1			
GA_3	-.254	.401	1		
ZR	-.891**	-.962**	.180	1	
GR	-.793**	-.971**	.338	.983**	1

Note: * * significant correlation at 0.01 level (bilateral) * significant correlation at 0.05 level (bilateral) the same below (Tab.6-Tab.17)

TABLE 3
The correlation between the ratio of endogenous hormone and the germination rate of *I. polycarpa* Maxim. at 5 ℃

	IAA/ ABA	GA_3/ ABA	ZR/ ABA	(IAA+GA_3)/ ABA	(IAA+ZR)/ ABA	(GA_3+ZR)/ ABA	(IAA+GA_3+ZR)/ ABA	GR
IAA/ABA	1							
GA_3/ABA	-.527	1						
ZR/ABA	-.094	.894**	1					
(IAA+GA_3)/ABA	.351	.611*	.897**	1				
(IAA+ZR)/ABA	.917**	-.146	.310	.694*	1			
(GA_3+ZR)/ABA	-.423	.993**	.941**	.700*	-.028	1		
(IAA+GA_3+ZR)/ ABA	.231	.705*	.946**	.992**	.599*	.784**	1	
GR	.315	.612*	.896**	.968**	.659*	.701*	.968**	1

TABLE 4
The correlation between the ratios of endogenous hormone and the germination rate of *I. polycarpa* Maxim. at 5 ℃

	GA_3/(ABA+IAA)	ZR/(ABA+IAA)	(GA_3+ZR)/(ABA+IAA)	GR
GA_3/(ABA+IAA)	1			
ZR/(ABA+IAA)	.930**	1		
(GA_3+ZR)/(ABA+IAA)	.996**	.961**	1	
GR	.587*	.839**	.660*	1

TABLE 5
The correlation between endogenous hormone content and the germination rate of *I. polycarpa* Maxim. at 10℃

	IAA	ABA	GA_3	ZR	GR
IAA	1				
ABA	-.327	1			
GA_3	.603*	.466	1		
ZR	.401	-.682*	.965**	1	
GR	-.549	-.962**	.293	.528	1

TABLE 6
The correlation between the ratio of endogenous hormone and the germination rate of *I. polycarpa* Maxim. from Xinyang at 10℃

	IAA/ ABA	GA_3/ ABA	ZR/ ABA	(IAA+GA_3)/ ABA	(IAA+ZR)/ ABA	(GA_3+ZR)/ ABA	(IAA+GA_3+ZR)/ ABA	GR
IAA/ABA	1							
GA_3/ABA	.826**	1						
ZR/ABA	.175	-.348	1					
(IAA+GA_3)/ABA	.992**	.890**	.064	1				
(IAA+ZR)/ABA	.995**	.772**	.273	.976**	1			
(GA_3+ZR)/ABA	.952**	.925**	.035	.975**	.933**	1		
(IAA+GA_3+ZR)/ABA	.998**	.853**	.147	.997**	.990**	.969**	1	
GR	.401	.826**	.700*	.757**	.878**	.710**	.809**	1

TABLE 7
The correlation between the ratios of endogenous hormone and the germination rate of *I. polycarpa* Maxim. at 10 ℃

	GA_3/(IAA+ABA)	ZR/(GA_3+ABA)	(GA_3+ZR)/(IAA+ABA)	GR
GA_3/(IAA+ABA)	1			
ZR/(GA_3+ABA)	-.888**	1		
(GA_3+ZR)/(IAA+ABA)	.639*	-.213	1	
GR	.404	.330	.306	1

The correlation between the endogenous hormone and the seed germination rate at 10℃. The ABA content was negatively correlated with the germination rate (Tab.5). The germination rate was positively correlated with the following hormone ratios: GA_3/ABA, ZR/ABA, (IAA+GA_3)/ABA, (IAA+ZR)/ABA, GA_3+ZR)/ABA and (IAA+GA_3+ZR)/ABA (Tab.6, Tab.7).

The correlation between the endogenous hormone and the seed germination rate at 12℃. At 12℃, the ABA content were negatively correlated with the germination rate, but they were positively correlated with GA_3 and ZR content (Tab.8). The germination rate was positively correlated with the following ratios: GA_3/ABA, ZR/ABA, (IAA+GA_3)/ABA, (IAA+ZR)/ABA, (GA_3+ZR)/ABA, (IAA+GA_3+ZR)/ABA, GA_3/(ABA+IAA) and (GA_3+ZR)/(ABA+IAA) (Tab.9 and Tab.10).

The correlation between the endogenous hormone and the seed germination rate at 15℃. As shown, the ABA and IAA content were negatively correlated with the germination rate at 15℃ (Tab.11), but they were positive correlated with the GA_3 content. The germination rate was positively correlated the following ratios: GA_3/ABA, ZR/ABA, (IAA+GA_3)/ABA, (IAA+ZR)/ABA, (GA_3+ZR)/ABA, (IAA+GA_3+ZR)/ABA, GA_3/(ABA+IAA) and (GA_3+ZR)/(ABA+IAA) (Tab.12 and Tab.13).

TABLE 8
The correlation between the endogenous hormone content and the germination rate of *I. polycarpa* Maxim. from Xinyang at 12℃

	IAA	ABA	GA_3	ZR	GR
IAA	1				
ABA	.081	1			
GA_3	.505	.887**	1		
ZR	-.457	.845**	.534	1	
GR	-.212	-.957**	.718**	.959**	1

TABLE 9
The correlation between the ratios of endogenous hormone and the germination rate of *I. polycarpa* Maxim. from Xinyang at 12 ℃

	IAA/ ABA	GA_3/ ABA	ZR/ ABA	(IAA+GA_3)/ ABA	(IAA+ZR)/ ABA	(GA_3+ZR)/ ABA	(IAA+GA_3+ ZR)/ ABA	GR
IAA/ABA	1							
GA_3/ABA	.871**	1						
ZR/ABA	.443	.084	1					
(IAA+GA_3)/ABA	.998**	.899**	.405	1				
(IAA+ZR)/ABA	1.000**	.862**	.466	.997**	1			
(GA_3+ZR)/ABA	.928**	.980**	.282	.947**	.924**	1		
(IAA+GA_3+ZR)/ABA	.999**	.892**	.427	1.000**	.998**	.944**	1	
GR	.487	.846**	.794**	.813**	.857**	.629*	.825**	1

TABLE 10
The correlation between the ratios of endogenous hormone and the germination rate of *I. polycarpa* Maxim. from Xinyang at 12 ℃

	GA_3/(ABA+IAA)	ZR/(ABA+IAA)	(GA_3+ZR)/(ABA+IAA)	GR
GA_3/(ABA+IAA)	1			
ZR/(ABA+IAA)	-.406	1		
(GA_3+ZR)/(ABA+IAA)	.967**	-.159	1	
GR	.875**	.075	.924**	1

TABLE 11
The correlation between the endogenous hormone content and the germination rate of *I. polycarpa* Maxim. seed from Xinyang at 15℃

	IAA	ABA	GA_3	ZR	GR
IAA	1				
ABA	.894**	1			
GA_3	.580*	.882**	1		
ZR	.108	.056	.083	1	
GR	-.897**	-.977**	.856**	.265	1

TABLE 12
The correlation between the ratios of endogenous hormone and the germination rate of *I. polycarpa* Maxim. from Xinyang at 15 ℃

	IAA/ ABA	GA_3/ ABA	ZR/ ABA	(IAA+GA_3)/ ABA	(IAA+ZR)/ ABA	(GA_3+ZR)/ABA	(IAA+GA_3+ZR)/ ABA	GR
IAA/ABA	1							
GA_3/ABA	.958**	1						
ZR/ABA	.773**	.888**	1					
(IAA+GA_3)/ABA	.997**	.978**	.812**	1				
(IAA+ZR)/ABA	1.000**	.963**	.787**	.998**	1			
(GA_3+ZR)/ABA	.951**	.999**	.905**	.972**	.957**	1		
(IAA+GA_3+ZR)/ ABA	.996**	.980**	.820**	1.000**	.997**	.975**	1	
GR	.396	.825**	.993**	.738**	.711**	.847**	.748**	1

TABLE 13
The correlation between the ratios of endogenous hormone and the germination rate of *I. polycarpa* Maxim. from Xinyang at 15℃

	GA_3/(IAA+ABA)	ZR/(IAA+ABA)	(GA_3+ZR)/(IAA+ABA)	GR
GA_3/(IAA+ABA)	1			
ZR/(IAA+ABA)	.704*	1		
(GA_3+ZR)/(IAA+ABA)	.991**	.793**	1	
GR	.609*	.401	.599*	1

Effect of IAA on seeds dormancy release. The previous study indicates that seed germination can be promoted by IAA. The increasing IAA content helps increase germination rate [12]. However, some studies also show that an elevated IAA content can contribute to seed dormancy [13]. Whether IAA promotes or inhibits dormancy depends on the IAA concentration and the type of seed [14]. Sprouting in the ear of wheat was effectively inhibited by applying IAA solution to *Triticum aestivum* L. at the mature stage [15]. *Medicago truncatula,* germination was promoted by IAA at a low concentration and inhibited by IAA at a high concentration. The sensitivity to IAA vary from plant species to plant species [16]. Under high salt conditions, exogenous IAA regulates germination of *Arabidopsis* seeds, and the inhibitory effect becomes stronger with increasing IAA concentrations [17]. The large amount of IAA produced by transgenic *Arabidopsis* iaaM-OX strongly inhibit the germination of its seeds [18]. These studies indicate that auxin plays an important role in regulating seed germination, and mainly has an inhibitory effect [19]. In addition to ABA, IAA is one of the most important hormones in seed dormancy. Both induce and maintain seed dormancy [20]. In this study, the germination rate was negatively correlated with the IAA content at 5℃ and 15℃, indicating that a higher IAA content might inhibit the germination of seeds during the dormancy release process of *I. polycarpa* Maxim.

Effect of ZR on seeds dormancy release. ZR is an important form of cytokinin (CTK) transport in xylem. CTK can promote cell division, counteract the material that inhibits germination and regulates the material and energy metabolism in the process of seed development. Yang [21] concluded that CTK mainly promotes the release of dormancy and subsequent germination by improving the biosynthesis of ETH. The ZR content in *I. polycarpa* Maxim. seeds was very low, and the change of the ZR content varied markedly depending on temperature. At 5℃, 10℃ and 12℃, the germination rate was positively correlated with the ZR content. The ZR content was increased in the low temperature treatment, and therefore promoting dormancy release.

Effect of ABA on seeds dormancy release. The seed dormancy and node germination are controlled by ABA [22]. It has been reported that whether seeds remain dormant or germinate depends on their sensitivity to ABA, rather than their ABA content [23]. Changes in ABA signals can release seed dormancy to some extent [24]. Thus, the content and function of ABA, as well as tissue sensitivity to ABA, affect seed dormancy and germination [25]. Under different temperature treatments, the ABA content in the seeds of *I. polycarpa* Maxim. was significantly negatively correlated with the germination rate, indicating that the reduction of ABA would help to relieve dormancy of *I. polycarpa* Maxim seeds. These results are similar to those for *Tilia amurensis Rupr* [26], *Cyclocarya paliurus* [27] and *Taxus chinensis* (Pilger) Rehd [28], *Taxus yunnanensis* [29].

Effect of GA3 on seeds dormancy release. Gibberellin is one of growth hormones with the function of releasing dormancy, which is conducive to activating the activity of enzymes related to metabolism in seeds, therefore seeds can germinate successfully. This study indicated that GA_3 could promote seed germination but it was not significantly correlated with the germination rate at 5℃ and 10℃. However, the GA_3 content was positively correlated with the germination rate at 12℃ and 15℃, indicating that GA_3 can promote the seed dormancy [30].

Effect of dynamic balance on seeds dormancy release. Early genetic studies show that ABA and GA_3 inhibit each other's synthesis [31]. ABA and GA_3 play decisive roles in the process of seed dormancy and germination [32-33]. Whether seed dormancy or germination depends on the relative content of ABA and GA_3 [7]. At 5℃, the GA_3 content showed a “decrease-rise-decrease” trend, and the germination rate was positively correlated with the GA_3/ABA ratio, indicating that the seed germination rate of *I. polycarpa* Maxim. was affected by the co-operative actions of GA_3 and ABA [34].

Similar to auxin, ABA has the effect of inhibiting germination. When seeds germinating, ABA was shown to inhibit hypocotyl elongation via enhancement of the auxin signal [35]. Auxin interacts with ABA in the regulation of seed germination and

other developmental processes [36]. Auxin was found to promote bud dormancy of *Marchantia polymorpha* L. [37]; Under drought conditions, however, plants reduced the growth of lateral roots to resist drought, and ABA and auxin were antagonistic to each other [38], indicating that the relationship between auxin and ABA is not always fixed. Their relationship may change in different physiological processes. At different low temperatures, endogenous hormones in the seeds of *I. polycarpa* Maxim. played important and differential synergistic effects.

CONCLUSION

Treatments at 5°C-15°C all had effects on the dormancy release of *I. polycarpa* Maxim. seeds from the transition zone from the northern subtropical to the warm temperate. However, the dormancy characteristics of *I. polycarpa* Maxim. seeds from Xinyang were favored to the dormancy characteristics of the warm-temperate plants, and the lower temperature was conducive to dormancy release. The endogenous hormones in the seeds of *I. polycarpa* Maxim. from Xinyang were sensitive to different temperature treatments. The decrease in ABA content at different temperatures facilitated the dormancy release, while the dormancy release of *I. polycarpa* Maxim. was dynamically balanced by hormones such as GA_3/ABA. However，there are differences in the synergy effects at different temperatures.

ACKNOWLEDGEMENTS

The authors wish to express their sincere thanks to the personnel of Henan Agricultural University for their kind assistance in the experiments. This research was supported by Henan Provincial Department of Science and Technology Research Project (182102110070).

REFERENCES

[1] Zhu, Z.Y., Ji, Y.H., Shen, D.F., Liang, Z.H. (2001) A preliminary study on growing seedlings of *Idesia polycarpa* Maxim. Journal of Jiangsu Forestry Science and Technology. 28, 6-8.

[2] Li, S.X., Lan, S.R., Wu, S.S., Xu, J.Y., Zhai, J.W., Peng, D.H. (2015) Effects of soaking time and plant growth regulators on germination of *Idesia polycarpa* Maxim seeds. Seed. 34, 8-12.

[3] Wang, L.Y., Tao, C.F. (2002) The cultivation techniques of *Idesia polycarpa* Maxim. Practical forestry technology. (9), 19-20.

[4] Zhou, J.B., Jiang, Y., Zhao, Z.R., Cai, M., Fu, S.L., Fu, S.L. (2015) Improvement of seed germination of *Idesia polycarpa* by dewaxing and low temperature treatment in moist sand. Journal of Anhui Agricultural University. 42, 159-164.

[5] Tang, X.S., Ye, Y., An X.L., Tang, L. (2013) Effect of Different Storage Methods on Seeds Germination of *Idesia polycarpa*. Seed. 12, 16-20.

[6] Wang, Y.M., Wang, H.Y., Dai, L., Li, F., Liu, Z. (2015) Effect of Different Low Temperature Treatments on Breaking *Idesia polycarpa* Seed Dormancy among 12 Provenances. Journal of Shandong Agricultural University. 4, 51-56.

[7] Yu, M., Xu, H., Zhang, H., Zu, Y. (2016) Regulation of plant hormones on seed dormancy and germination. Plant Physiology Communications. 52, 599-606.

[8] Chen, Q.L., Guo, Y.H., Jiang, Y., Tu, P. (2016) Mechanism of fluridone-induced seed germination of cistanche tubulosa. Pakistan Journal of Botany. 48, 971-976.

[9] Pawlowski, T.A., Staszak, A.M. (2016) Analysis of the embryo proteome of sycamore (*Acer pseudoplatanus* L.) seeds reveals a distinct class of proteins regulating dormancy release. Journal of Plant Hysiology. 195, 9-22.

[10] Álvarez-Flórez, F., López-Cristoffanini, C., Jáuregui, O., Melgarejo, L.M., López-Carbonell, M. (2017) Changes in ABA, IAA and JA levels during calyx, fruit and leaves development in cape gooseberry plants (*Physalis peruviana* L.). Plant Physiology and Biochemistry. 115, 174-182.

[11] Wang, Y.M., Wang, H.Y., Dai, L., Li, F., Liu, Z. (2015) Effect of Different Low Temperature Treatments on Breaking Idesia polycarpa Seed Dormancy among 12 Provenances. Journal of Shandong Agricultural University. 46(1), 51-56.

[12] Li, B.Z., Wu, Y., Tian, R.H., Suo, L.D., Li, X. (1998) Changes of Endogenous Plant hormones in the Seeds of *Carategus Pinnatifida* during dormancy and Post-Maturation. Plant physiology communications. 34, 254-256.

[13] Zhao, Y.H., Yang, S.L., Liu, H.Q. (2001) Dynamics of endogenous hormone in American ginseng seed during morphological afterripening period and their regulation to embryo development. Chinese Traditional and Herbal Drugs. 32(2), 159-162.

[14] Gao, W.Y., Li, Z.L., Xiao, P.G. (1996) The changes of hormone in the process of breaking dormancy in Firtillalria thunbergii Miq seed. Chinese Traditional and Herbal Drugs. 27(4), 231-232.

[15] Ramaih, S., Guedira, M., Paulsen, G.M. (2003) Relationship of indoleacetic acid and tryptophan to dormancy and preharvest sprouting of wheat. Funct Plant Biol. 30, 939-945.
[16] Liu, J.L. (2010) Effects of 7 plant growth regulators on seed germination of Medicago truncatula. Agric Res Arid Areas. 28(2), 113-117.
[17] Park, J., Kim, Y.S., Kim, S.G., Jung, J.H., Woo, J.C., Park, C.M. (2011) Integration of auxin and salt signals by the NAC transcription factor NTM2 during seed germination in *Arabidopsis*. Plant Physiol. 56, 537-549.
[18] Cheng, Y.F., Dai, X.H., Zhao, Y.D. (2006) Auxin biosynthesis by the YUCCA flavin monooxygenases controls the formation of floral organs and vascular tissues in Arabidopsis. Genes Development. 20, 1790-1799.
[19] Li, Z.H., Zhang, J., Liu, Y.L., Zhao, J.h., Fu, J.J., Ren, X.L., Wang, G.Y., Wang, J.H. (2016) Exogenous auxin regulates multi-metabolic network and embryo development, controlling seed secondary dormancy and germination in *Nicotiana tabacum* L. BMC Plant Biology. 16, 41.
[20] Liu, X.D., Zhang, H., Zhao, Y., Feng, Z. Y., Li, Q., Yang, H. Q., Luan, S., Li, J.M., He, Z.H. (2013) Auxin controls seed dormancy through stimulation of abscisic acid signaling by inducing ARF-mediated ABI3 activation in *Arabidopsis*. Proceeding of the national academy of sciences. 110, 15485-15490.
[21] Yang, R.C., Zhang, H.J., Wang, Q., Guo, Y.D. (2012) Regulatory Mechanism of plant hormones on seed dormancy and germination (review). Acta Agrestia Sinica. 20, 1-9.
[22] Albertos, P., Romero-Puertas, M.C., Tatematsu, K. Albertos, P., Romero-Puertas, María C., Tatematsu, K., Mateos, I., Sánchez-Vicente, Inmaculada, Nambara, E., Lorenzo, O. (2015) S-nitrosylation triggers ABI5 degradation to promote seed germination and seedling growth. Nature Communications. 6, 8669.
[23] Leonkloosterziel, K.M., Bunt, G.A.V.D., Zeevaart, J., Koornneef, M. (1996) Arabidopsis mutants with a reduced seed dormancy. Plant Physiol. 110, 233-240.
[24] Feurtado, J.A., Yang, J., Ambrose, S.J., Cutler, A.J., Abrams, S.R., Kermode A.R. (2007) Disrupting abscisic acid homeostasis in western white pine (Pinus monticola Dougl. Ex D. Don) seeds induces dormancy termination and changes in abscisic acid catabolites. Journal of Plant Growth Regulation. 26, 46-54.
[25] Gianinetti, A., Vernieri, P. (2007) On the role of abscisic acid in seed dormancy of red rice. Journal of Experimental Botany. 58, 3449-3462.
[26] Yang, L.X., Wang, H.N., Zhang, L. (2012) Changes of hormone content in *Tilia amurensis* seeds during cold stratification. Economic forest researches. 30, 15-18.
[27] Yang, W.X., Fang, S.Z. (2008) Dynamic changes of endogenous hormones in Cyclocarya paliurus seed during stratification. Journal of Nanjing forestry university (Natural sciences edition). 32, 85-88.
[28] Zhang, Y.J. (2007) Studies on seed dormancy mechanism of *Taxus chinensis var.* mairei. Nanjing: Nanjing forestry university. 6.
[29] Bian, F., Su, J.R., Liu, W.D., Li, S. (2018) Dormancy release and germination of *Taxus yunnanensis* seeds during wet sand storage. Scientific Reports. 8, 3205.
[30] Wei, L.Z., Cheng, J.H., Li, L., Wu, J. (2012) Regulation of plant height by gibberellins biosynthesis and signal transduction. Chinese Journal of Biotechnology. 28, 144-153.
[31] Eiji, N., Masanori, O., Kiyoshi, T., Ryoichi, Y., Mitsunori, S., Yuji, K. (2010) Abscisic acid and the control of seed dormancy and germination. Seed Science Research. 20(2), 55-67.
[32] Shu, K., Liu, X. D., Xie, Q., He, Z.H. (2015) Two faces of one seed: hormonal regulation of dormancy and germination. Molecular Plant. 9(1), 34-45.
[33] Dekkers, B.J.W., He, H., Hanson, J., Willems, L.A.J., Jamar, D.C.L., Cueff, G., Rajjou L., Hilhorst H.W., Bentsink L. (2016) The Arabidopsis delay of germination 1 gene affects abscisic acid insensitive 5 expression and genetically interacts with ABI3 during Arabidopsis seed development. The Plant Journal. 85(4), 451-465.
[34] Pu, M., Sun, Y.Y., Gao, C.J., Li, K. (2016) Relationship between Endogenous Hormone Content and Embryo Growth and the Seed Germination of Paris polyphylla var. Yunnansensis. Forest Research. 29, 268-273.
[35] González-Guzmán, M., Apostolova, N., Bellés, J.M., Barrero, J.M., Rodríguez, P.L. (2002) The short-chain alcohol dehydrogenase ABA2 catalyzes the conversion of xanthoxin to abscisic aldehyde. Plant Cell. 14, 1833-1846.
[36] Shuai, H.w., Meng Y.J., Luo X.F., Chen, F., Qi Y., Yang, W.Y., Shu K. (2016) The roles of auxin in seed dormancy and germination. Hereditas. 38, 314-322.
[37] Eklund, D.M., Ishizaki, K., Floressandoval, E., Kikuchi, S., Takebayashi, Y., Tsukamoto, S., Hirakawa, Y., Nonomura M., Kato H., Kouno, M., Bhalerao R. P., Lagercrantz U., Kasahara, H., Takayuki, Kohchi, T., Bowman J.L. (2015) Auxin produced by the indole-3-pyruvic acid pathway regulates development and gemmae dormancy in the liverwort Marchantia polymorpha. The Plant Cell. 27, 1650-1669.
[38] Seo, P.J., Xiang, F.N., Qiao, M., Park, J.Y., Park, C.M. (2009) The MYB96 transcription factor mediates abscisic acid signaling during drought stress response in *Arabidopsis*. Plant physiology. 151(1), 275-289.

Received: **23.07.2018**
Accepted: **27.11.2018**

CORRESPONDING AUTHOR

Zhen Liu
College of Forestry,
Henan Agricultural University,
Zhengzhou, 450002 – China

e-mail: liuzh20@163.com

© by PSP Volume 28 – No. 4/2019 pages 2506-2510 Fresenius Environmental Bulletin

SYNTHESIS AND RESEARCH OF A NOVEL NEAR INFRARED NMR PROBE TARGETING LIVER CANCER

Ning Guo*, Meirong Liu, Zixuan Guo

College of life science and technology, Xi'an Electronic and Science University, Xi'an, China

ABSTRACT

At current phase, the incidence situation of liver cancer is not optimistic. In terms of liver cancer treatment, the first choice is the surgical treatment. But in the practical clinical operations, how to make accurate identification on the tumor margin is a problem very difficult to be solved by the medical circle. In recent years, the near-infrared fluorescence imaging technique is in relevantly frequent development, which creates a chance and possibility for the further settlement of the problem. On the basis of this clinical problem, a kind of new liver cancer targeting near-infrared nanoprobe of high sensitivity and high specificity can, combined with near-infrared fluorescence imaging technique, achieve the accurate identification of liver cancer and tumor margin, so as to provide the solution for this difficult problem.

KEYWORDS:
Nanoprobe, Liver cancer, Near-infrared fluorescence imaging, Targeting, Specificity, Sensitivity

INTRODUCTION

Internationally, the liver cancer attacks severer increasingly and now has become the cancer with fatality rate ranked at the second place. World Health Organization clearly pointed out relevant data in the World Cancer Report 2014 [1] published in 2014, and just in 2012, newly-increased people with liver cancer in China takes more than 50% worldwide, while the people died from liver cancer also occupies more than a half of that worldwide. Assuming that, keeping the current situation to develop, it is expected that, within 2015-2030, the people died from liver cancer in China will be more than ten million, so that the emergent actions shall be taken to improve the treatment effect.

Experimental. Near-infrared nanoprobe. At present, the method at first choice for treatment of liver cancer clinically is the surgical operation, for the reason that the operation can directly excise the targeted focus. However, for the judgment on the tumor location, the physicians mainly make based on their own experience and pathological section [2], while the invasiveness and heterogenicity of liver cancer are relatively significant, which proceed along with peripheral vessels and tissues of human body upon infiltration, thus even increasing the judgment difficult on tumor margin. Therefore, it is hard to thoroughly excise through operation, causing the easy relapse and metastasis after operation, together with extremely poor prognosis, as well as relapse rate in five years after operation more than 70%. Moreover, frequently, it is easy to excise some non-tumor tissues in the surgical operation. As one of most important organs in human body, the liver functions are very complex, and the excision of normal liver cell easily affects the postoperative metabolism, immunization and other functions of the patients, causing the survival rate in 5 years below 40%.

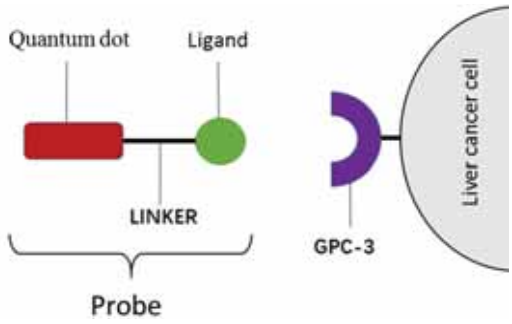

FIGURE 1
Probe structure

Hence, in the practical clinical operation, how to make accurate identification on tumor margin is the problem hard to be solved by the medical circle [3]. While in application of surgical operation for excision of tumor, its key problem is how to identify the tumor margin. As for it, Chinese government has approved the use of near-infrared fluorescence dye – indocyanine green (ICG), mainly for imaging in the liver cancer operation and the biopsy of tumor sentinel node [4]. However, as such indocyanine green cannot form the active targeting, how to improve its imaging clinically is also an important problem urgently to be solved. We try to synthesize a kind of new probe to improve the imaging specificity with combination of near-infrared fluorescence imaging technique, to raise a solution for this problem.

The probe consists of three part: ligand identifying target in cancer cell, quantum dot able to be motivated by near-infrared fluorescence, and linker connecting above two.

Ligand. Data show that, prepare 48 cell blocks (30 of liver cancer and 18 of liver metastatic cancer) through liver FNA (fine needle aspiration) and label with glypican-3 (GPC-3). GPC-3 of about 97% patients with HCC can be immune to its expression. Through studies, it can be found that, the sensitivity obtained from diagnosis on HCC with GPC-3 is about 96.7%, and specificity can be up to 100% [5]. Another experience proves that, positive rate of GPC-3 in liver cancer tissue is roughly equal to 88.3%, while that of normal liver tissue is usually only 16.7% [6]. This series of experiences prove that, GPC-3 can be taken as the new target of liver cancer diagnosis.

Zhu et al, in the study, separated the polypeptide containing twelve amino acids out and signified by TJ12P1 [7], and found that the affinity of corresponding GPC3 antibody can be 280.4±33.51 nM. It is worth noting that, TJ12P1 is of high specificity to GPC3 antibody, but does not fuse with normal liver cell, so that the polypeptide can be used for distinguishing the liver cancer tissue of the patients and the normal adult liver tissue, which shows the great imaging potential [8-13].

Quantum dot. (1) Synthesis and study of quantum dot. On account of gradually quicken development of current imaging technique and nanotechnology, one current research hotspot is the application of molecular imaging probe in the biomedical field, including a typical nanotechnology: quantum dot. In 2010, for the first time, the scientist has published the paper and pointed out that, Ag_2S QDs near-infrared fluorescence has an excellent emission property, and in China, some relevant researchers also work out a kind of nanoprobe successfully with AG_2S QDs, that is, Ag_2S QDs-Iodinate Oil@DSPE-PEG2000-FA. Such probe is of good biocompatibility, which can successfully obtain good tumor targeting through its use in the tumor-bearing mice, and also is a kind of new approach for targeted diagnosis and accurate judgment and identification on the tumor margin. Featured by good fluorescence imaging capacity, low toxicity, high tumor intake and deep tumor penetrability, CuIns quantum dots show the strong near-infrared (NIR) emission with 730 nm as center and have the bright fluorescence and wide excitation spectrum. On account of its unique specificity, increasing attentions from the domestic circle are paid to it in recent years.

Temperature / Intensity / Time	200	210	220	230	240
10min	53.46	57.90	103.7	195.2	222.1
15min	62.28	47.32	108.0	203.0	273.9
20min	108.8	305.3	451.2	553.3	270.1
25min	169.4	454.0	772.1	803.7	291.1
30min	209.5	579.0	1133	435.0	137.0
35min	216.9	1190	580.1	——	——

Temperature / Wavelength / Time	200	210	220	230	240
10min	593.0	598.0	597.0	606.0	622.0
15min	598.0	598.0	613.0	611.0	628.0
20min	602.0	615.0	622.0	628.0	674.0
25min	610.0	626.0	627.0	633.0	709.0
30min	613.0	633.0	628.0	637.0	714.0
35min	618.0	636.0	650.0	——	——

FIGURE 2
Table I (Left) Table II (Right)

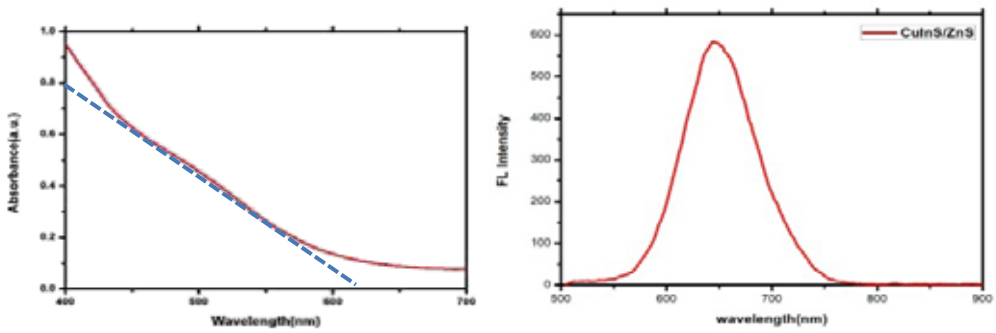

FIGURE 3
Ultraviolet absorption spectrum (Left); Fluorescence emission spectrum (Right)

FIGURE 4
Color change of different quantum dots under ultraviolet light

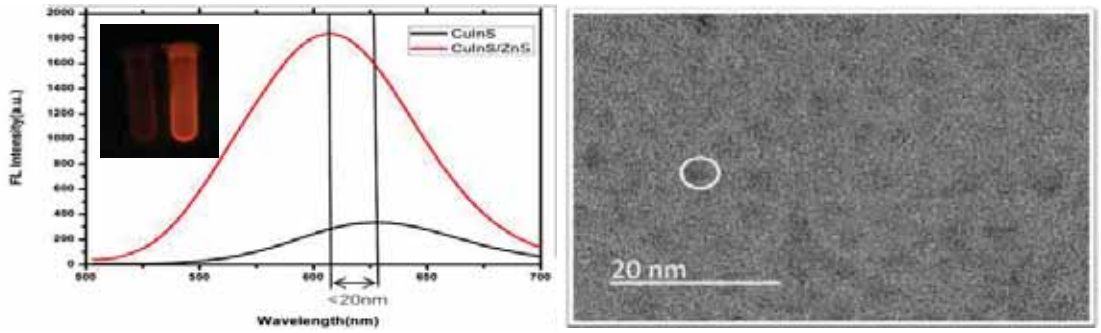

FIGURE 5
Comparison of fluorescence intensities of quantum dot before and after ZnS cladding (Left); Electronic microscopy of signal source of quantum dot (Right)

We synthesize CuInS quantum dots with thermal synthesis method, and there is tiny swelling (Left, Figure 3) at 460 nm around in its ultraviolet absorption, showing the possible fluorescence emission which is proved by subsequent experiences. Measure the fluorescence emission at 460 nm and 600-800 nm strong fluorescence emission peak (Right, Figure 3) can be obtained. Meanwhile, during the experience, the emission peak of quantum dot and synthesis heating time are in close relation (Figure 2). According to the Table 1, it can be obtained: Fluorescence intensity increases at first and then decreases following the increase of heating temperature, and increases at first and then decreases following the extension of heating time. From the Table 2, it can be seen: Fluorescence wavelength shows a positive correlation with the heating temperature, and such increase amplitude may increase with the increase of heating time.

As the high fluorescence intensity cannot be obtained at high penetrability (long wavelength), we apply ZnS cladding to modify CuInS quantum dot and finally obtain CuInS/ZnS quantum dot, and Figure 5 Left is the contrast diagram of fluorescence intensities of quantum dot before and after cladding. It is found that, fluorescence intensity of quantum dot after ZnS cladding improves to a great extent, together with a blue shit less than 20nm which is the normal situation. Right figure in Figure 5 shows the scanning diagram of quantum dot under the electronic microscope. Through the analysis on this diagram, it can be found that, the radius of the quantum dot is roughly equal to 6nm, in roughly consistence with our expectation, which also show in even distribution, but without large-scale condensation.

(2) Experimental steps. Synthesis of CuInS/ZnS quantum point. Make CuI (0.2 mmol) and zinc stearate ($Zn(SA)_2$) (0.1 mmol), under the magnetic stirring, and mix $In(Ac)_3$ (0.2 mmol) and OA (0.1 mmol) with 8.0 mL ODE and 1.0 mL DDT in four-neck flask. Under argon protection and magnetic stirring, heat the solution to 100℃ and degas for 30min. Later, further heat it to the specific reaction temperature (210-290℃) under argon atmosphere. After 60min, cool the reaction solution to 150℃, and successively inject 2 mL sulfur precursor (0.1 M, in ODE/oleylamine, v / v 10/1) and 3mL zinc stearate solution (0.1 M, in ODE). After reaction for 60min with temperature increased to 220℃, cool down to the room temperature, add the cyclohexane in prepared CuInS/ZnS QD, add the ethanol until it turns to turbid, and collect through centrifugation (8000 rpm, 20 min). Implement more than two times of purification with hexane/ethanol (1/3) cosolvent through centrifugation, and disperse ZCIS quantum dots obtained finally to the cyclohexane.

RESULTS AND DISCUSSION

Probe synthesis. As the synthesis of CuInS/ZnS quantum point is supported by high-temperature oil phase system, to drive the following extensive application of the quantum dot in biomedical field, relevant hydrophily modification shall be made on it, with some steps facilitating its functionalization. Exactly because of the existence of above problems, we consider to synthesize the hydrophilic quantum dot polyethylene glycol 1000 vitamin E succinate carboxylic group (tpgs) after

modification, and then apply it in the fluorescence living imaging. Its principle is use the interaction between the hydrophobicity and Van Der Waals force, and interaction (instead of replacement of hydrophobic ligand) between the hydrophobic wake of amphiphilic ligand and the hydrophobic ligand on nanocrystal, and the nanocrystal micelles. Therefore, the carboxyl on the particle surface makes it have good water solubility, change small in fluorescence intensity and keep relatively stable in PBS solution within 24 h.

To connect TJ12P1 polypeptide to the quantum dot surface, the most direct method usually is to connect the amidogen with polypeptide-linked N segment to the carboxylation surface of quantum dot through the carboxyamino reaction. Carboxyl end on EDC/NHS activated quantum dot is used by us, so that NH_2- in the guanidine can have a neutralization reaction with carboxyl, that is, the carboxyl loses a hydrogen ion, and accordingly, NH_2- gets a hydrogen ion. This is mainly because that the carbonyl in carboxyl induces the electron to be absorbed and OH oxygen electronegativity in carboxyl to be weakened, to decrease the binding capacity on H, so as to achieve the connection of quantum dot and polypeptide.

Experimental steps. Preparation of hydrophilic CuInS/ZnS quantum dot: Mix the hydrophobic nanoparticles (namely, CuInS/ZnS) (25 nmol) and modified tpgs (50nmol) in $CHCL_3$ (5 mL). Mix the solution under the room temperature and put overnight. Stir the obtained mixture for 10min. After the solution evaporation, disperse these nanocrystals into the water again. Filter the nanocrystal solution through 0.22-μmMCE injecting filter (Fisher Scientific). Wash the excess tpgs with rotary filter (Millipore, 10K NMWL, 10000×g, 10 min) for multiple times, and then disperse the nanocrystals in the water again for further study.

Connection of quantum dot with polypeptide. Dissolve CuInS/ZnS quantum dot (0.20 nmol) into 2-(N-morpholino) ethyl sulfonic acid buffer solution (MES buffer solution, 0.1 M, 150 μL, pH = 6.0). Add EDC (5.0 mg/mL, 50 μL) and Sulfo-NHS (5.0 mg/mL, 50 μL) water solution into the quantum buffer solution, and apply the mild oscillation incubation under room temperature for 1h. Take phosphate-buffered saline (PBS buffer solution, pH=7.4) as the elution buffer solution. Concentrate the QD solution collected through the rotary filter (10K NMWL, Millpore, 10000×g, 10 min) to 50μL, and dissolve in the PBS buffer solution (250 μL, pH 7.4) again. Take TJ12P1 polypeptide into QD solution, and incubate under room temperature for 2h. Transfer the mixture to the rotary filter (100K NMWL, Millpore, 10000×g, 10 min) and concentrate to 50μL. And then add into the PBS buffer solution (200 μL, pH 7.4) and mix again. Repeat the washing step for 2 times to thoroughly eliminate the free ligand. Finally, disperse the purified QD (0.15 nmol) to PBS buffer solution (45 0μL, pH 7.4) again.

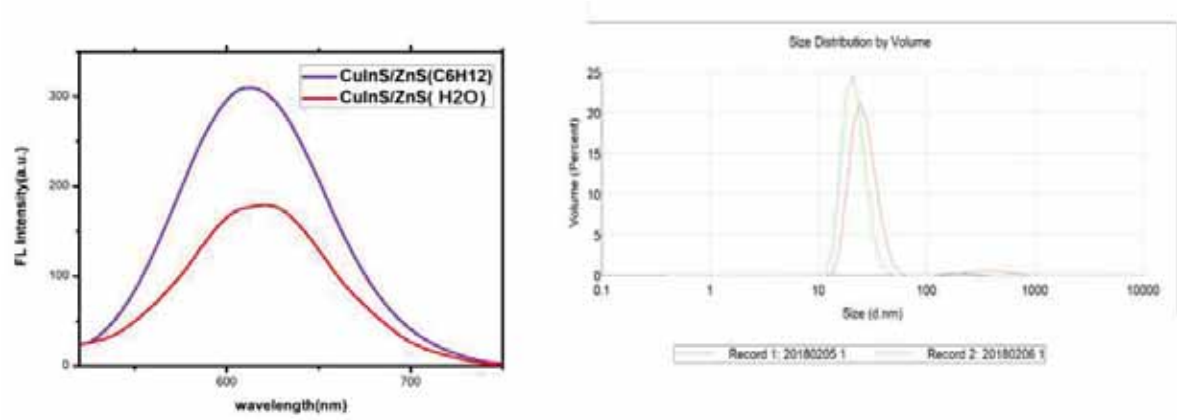

FIGURE 6
Comparison of fluorescence intensities of aqueous-phase quantum dot (Left); Stability of aqueous-phase quantum dot in PBS within 24h (Right)

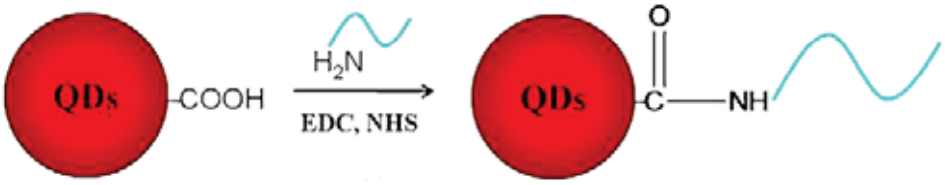

FIGURE 7
Probe synthesis

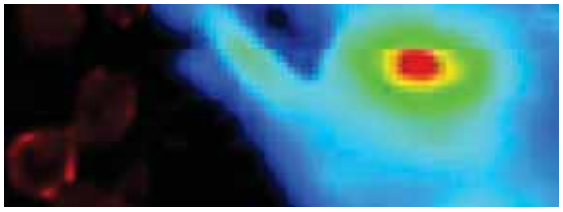

FIGURE 8
Cell experiment (Left); Mice experiment (Right)

Probe performance and its performance study. Two obvious advantages of CuInS quantum dot are: 1: There is fluorescence emission under near-infrared condition; 2. There is no heavy metal element. Therefore, in the application in fluorescence living imaging of biomedicine, the advantages of quantum dot are widely accepted. And then, we also verify that the use of near-infrared nanoprobe obtained through this method can be effectively applied in the study of fluorescence living imaging. Subsequent physicochemical, cell and mice experience results show that, the probe maintain the advantages including high fluorescence yield (7%, small particle diameter (20 nm around)), high sensitivity, high specificity and low toxicity, to provide certain solution for settlement of difficult identification of tumor margin in human operation.

CONCLUSION

In recent years, the near-infrared fluorescence imaging technique is in relevantly frequent development, which creates a chance and possibility for the further settlement of the problem. On the basis of this clinical problem, a kind of new liver cancer targeting near-infrared nanoprobe of high sensitivity and high specificity can, combined with near-infrared fluorescence imaging technique, achieve the accurate identification of liver cancer and tumor margin, so as to provide the solution for this difficult problem.

REFERENCES

[1] Lee, H., Akers, W., Bhushan, K. (2011) Near-infrared pH-activatable Fluorescent Probes for Imaging Primary and Metastatic Breast Tumors. Bioconjugate Chemistry. 22, 777-784.

[2] Arbab, A.S., Wei, L., Frank, J.A. (2006) Cellular magnetic resonance imaging: current status and future prospects. Expert Review of Medical Devices. 3, 427-439.

[3] Cui, S., Yin, D., Chen, Y. (2013) In vivo targeted deep-tissue photodynamic therapy based on near-infrared light triggered upconversion nanoconstruct. Acs Nano. 7, 676-688.

[4] Guillouzo, A., Guguenguillouzo, C. (2008) Evolving concepts in liver tissue modeling and implications for toxicology. Expert Opin Drug Metab Toxicol. 4, 1279-1294.

[5] Battiston, A.A., Bitter, J.H., Groot, F.M.F.D. (2003) Evolution of Fe species during the synthesis of over-exchanged Fe/ZSM5 obtained by chemical vapor deposition of $FeCl_3$. Journal of Catalysis. 213, 251-271.

[6] Jin, Q., Feng, L., Zhang, S.J. (2017) Real-time tracking the synthesis and degradation of albumin in complex biological systems with a near-infrared fluorescent probe. Analytical Chemistry. 89, 9884–9891.

[7] Amly, W., Karaman, R. (2016) Recent updates in utilizing prodrugs in drug delivery (2013-2015). Expert Opinion on Drug Delivery. 13, 571-591.

[8] Mizrahi, D.M., Ziv-Polat, O., Perlstein, B. (2011) Synthesis, fluorescence and biodistribution of a bone-targeted near-infrared conjugate. European Journal of Medicinal Chemistry. 46, 5175-5183.

[9] Lee, H., Akers, W., Bhushan, K. (2011) Near-infrared pH-activatable Fluorescent Probes for Imaging Primary and Metastatic Breast Tumors. Bioconjugate Chemistry. 22, 777-784.

[10] Law, B., Curino, A., Bugge, T.H. (2004) Design, synthesis, and characterization of urokinase plasminogen-activator-sensitive near-infrared reporter. Chemistry and Biology. 11, 99-106.

[11] Pomper, M.G., Lee, J.S. (2005) Small animal imaging in drug development. Current Pharmaceutical Design. 11, 3247-3272.

[12] Wang, D., Tan, J., Kang, H. (2011) Synthesis, self-assembly and drug release behaviors of pH-responsive copolymers ethyl cellulose-graft -PDEAEMA through ATRP. Carbohydrate Polymers. 84, 195-202.

[13] Condron, C.L., Kauzlarich, S.M., Ikeda, T. (2008) Synthesis, structure, and high-temperature thermoelectric properties of boron-doped Ba8Al14Si31 clathrate I phases. Inorganic Chemistry. 47, 8204-8212.

Received: **26.08.2018**
Accepted: **29.01.2019**

CORRESPONDING AUTHOR

Ning Guo
College of life science and technology,
Xi'an Electronic and Science University
Xi'an – China

e-mail: 484803751@qq.com

© by PSP Volume 28 – No. 4/2019 pages 2511-2522 Fresenius Environmental Bulletin

ASSESSING THE SUSTAINABILITY OF CROP PRODUCTION IN THE GEDIZ BASIN, TURKEY: A WATER, ENERGY, AND FOOD NEXUS APPROACH

Adnan Degirmencioglu[1,*], Rabi H Mohtar[2,3], Bassel T Daher[2], Gulden Ozgunaltay-Ertugrul[4], Omer Ertugrul[4]

[1]Ege University, Faculty of Agriculture, Department of Agricultural Engineering and Technology, Bornova, Izmir, Turkey
[2]Texas A&M University, Department of Biological and Agricultural Engineering, College Station-Texas, 77843, USA
[3]Faculty of Agriculture and Food Sciences, American University of Beirut, Beirut 1107 2020, Lebanon
[4]KirsehirAhi Evran University, Faculty of Agriculture, Department of Biosystems Engineering, Kirsehir, 40100, Turkey

ABSTRACT

This study assesses the sustainability of crop production system in Gediz Basin, Turkey and develops forward-looking scenarios for optimal utilization and sustainable allocation of its resources using the water, energy, and food (WEF) Nexus holistic systems approach. Gediz basin data for the year 2014 are used to analyze the current situation and to develop future scenarios, including climate change, urbanization, changes in water sources, and technological developments in the field of agricultural production. The study results indicate that reduction in land availability as a consequence of urbanization and increased water scarcity due to climate change are inevitable. Moreover, sustainably maintaining current levels of agricultural production requires that serious consideration be given to the selection of drought resistant varieties and new farming practices, such as direct planting to reduce energy use and drip irrigation systems to save water.

KEYWORDS:
Crop production, water requirement, fuel consumption, climate change, land use, agricultural technologies

INTRODUCTION

Globally, agriculture accounts for about 70% of water use [1]. Agriculture is also an important input for energy production. With water and energy as inputs, it is possible to manufacture bio-energy products or to recycle energy through biomass [2, 3]. Thus, water, energy, and food resource systems are tightly interconnected and interdependent [4]. As it is increasingly apparent through sudden changes in weather patterns, rainfall amounts, and temperature increases, climate change will continue to affect agricultural production levels, bringing forward risks that cannot be overlooked: increased environmental awareness in agricultural operations necessitates the use of machinery and technologies with more intricate applications [5].

With growing pressures to produce food for growing populations globally, there is a need for better understanding and quantifying its interlinkages with water and energy systems [6, 7, 8, 9]. Water assets vary around the world, even within regions of a given country [10]. With regard to quality, water can be categorized into three categories: blue, green, and grey. As a result of this classification, a map of water assets of 50 countries around the world was drawn and virtual water flow maps were created between countries. As sources of irrigation, blue and green water have an important role in agriculture. Blue water is defined as the rivers, lakes, underground, and aquifer water. Green water is accepted as rainfall water stored in the soil. Grey water is defined as water that is somewhat polluted, i.e. waste water, but which can be brought to utilizable standards by processing [11]. Through food trade, virtual water gets imported and exported: the export of water and the physical utilization of water resources by the exporting country saves water for the importing country [12]. In this sense, on a global scale, Japan has 134 Gm^3/year (80% green, 9% blue, and 12% grey water). Mexico and Italy follow at 83 and 54 Gm^3/year, respectively, as water saving countries [13].

Turkey, United States of America, India, Australia, Uzbekistan, and China, make up 49% of the virtual global blue water export [13]. It has been stated that these countries are, albeit partially, distressed when it comes to water [14, 15, 16]. In light of this information, the sustainability and efficiency of using limited water resources in the face of such copious amounts of virtual water exports can be questioned [13]. Moving from a global context to the national level, countries need to identify policies, which would ensure the optimal use of existing natural resources as it plans for meeting food demands of its future populations [17]. Accordingly, it is also needed to understand the regional and transboundary impact of such policies [18, 19].

The main objectives of this study were to determine the sustainability of the current agricultural system in the Gediz Basin, Turkey; and develop sustainable allocation and forward-looking scenarios for optimal utilization of its resources using the WEF Nexus holistic system approach.

MATERIALS AND METHODS

Gediz Basin. The Turkish Ministry of Food, Agriculture, and Livestock identifies thirty distinct basins, with lists of crops and cropping patterns for each, based on soil and climate conditions, among others. The Gediz basin includes 26 towns as depicted in Figure 1.

The Gediz Basin covers 1.922 % of the total area of Turkey and is part of the Aegean region and Mediterranean rainfall regimes, which are characterized by hot dry summers and cool winters. The average annual rainfall is about 500 mm, with extremes of 300 mm and 850 mm having occurred in the past. The total agricultural land in the basin is about 1774 km^2.

Data. The basin produces a variety of field crops, vegetables, and fruits; the list of crops and the production and yield for each crop, fertilizer needs, and financial values are provided from the database of the Turkish Statistical Institute [20] and tabulated in Table 1 for only top fifteen crops in terms of the land that they are grown and water consumption.

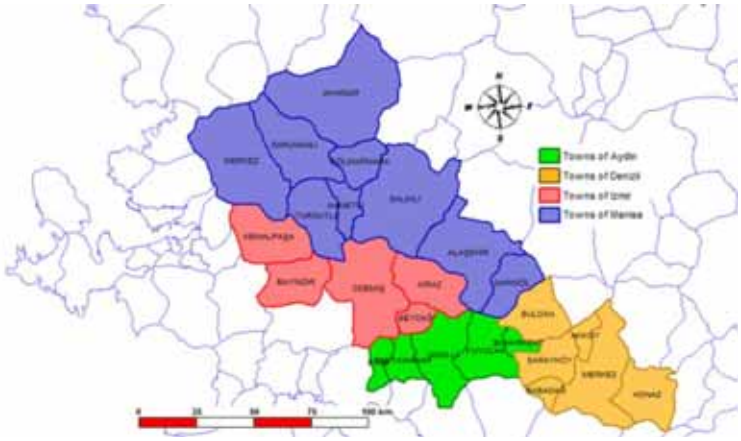

FIGURE 1
Gediz basin and its boundaries along with towns within the basin

TABLE 1
Data for the top fifteen crops grown in the basin [20]

Field crop	Area grown (ha)	Production (Tons)	Yield (Tons/ha)	Seasonal water req. (m^3/ha)	Irrigation req. (m^3/ha)	Nitrogen req. (kg/ha)	Phosphorus req. (kg/ha)	Potassium req. (kg/ha)	Gasoline consumption (L/ha)	Financial value (TL/ton)
Barley	31057.4	85380.0	2.75	4709.1	419.3	90	40	0	47.8	620
Clover	13100.0	745587.0	56.92	10143.8	7293.1	132.1	75	75	43	520
Corn	42049.2	444066.8	10.56	2530	1794.9	272.7	166.6	0	159.1	620
Corn for silage	43709.4	2325906.0	53.21	2530	1794.9	272.7	166.6	0	131	280
Cotton	13134.7	73967.0	5.63	7140	6492.7	185.4	125	0	222.0	1470
Potato	9652.8	353071.0	36.58	7647.3	7000	187.6	78	30	315.1	1160
Tobacco	14318.8	9671.0	0.68	2354.7	1707.4	76.8	30	0	70.4	11750
Vetch	11057.6	151566.0	13.71	4836.1	2312.9	50	50	0	76.7	450
Wheat	86989.2	301762.0	3.47	4836.1	1182.9	120	40	0	65.6	740
Tomato	14643.1	975484.0	66.62	4028.5	2849.5	136.1	73.1	37.7	180.46	450
Cherry	18392.1	72513.0	3.94	2094.4	1084.5	187.5	180.2	166.1	267.93	3530
Fig	20827.0	91688.0	4.40	6250	0	41.5	55.4	55.4	141.3	2580
Olive	126956.3	311187.0	2.45	8928.4	0	90	72	50.93	50.93	2560
Raisins	58593.2	1041554.0	17.78	6584.5	5396	172.85	153	90	171.07	1540
Table grape	25376.5	499661.0	19.69	6584.5	5396	55.8	51.5	41.6	225.55	1540

TABLE 2
Energy consumption for different sources of water

Energy need for water (kWh/m^3)	
Groundwater	0.4068
Surface water by GDSHW	0.209
Groundwater by Solar Energy Solar	0.406

TABLE 3
Carbon emissions of different sources

Carbon emissions of different sources	
Diesel gasoline*	0.002357 tons CO_2/L or 778 g CO_2/kWh
N, P and K fertilizers**	0.0026 tons/ kg
Hydroelectric power***	24 g CO_2/kWh
Solar panel toproof***	32 CO_2/kWh

* and *** [25, 26]; **: [24]

This study also uses data provided by recent studies [21] which include the water requirements for all crops grown in a basin neighbouring the Gediz basin, which has the climatic and soil conditions. The study includes seasonal water requirements along with the irrigation amounts for crops, vegetables, and fruits using two different methods: Penman-Monteith and Blaney-Criddle. Fuel consumption is the only energy input considered, which reflects the reality of the main energy source for agriculture in Turkey. Data for tractor use or time (hr/ha)spent using tractors and fuel consumption for each crop, vegetable and fruit, are determined and tabulated along with the tractor use for farming operations [22, 23].

Water in the basin is provided from two sources; it is either pumped from deep wells, or drawn from the General Directorate of State Hydraulic Works (GDSHW). GDSHW delivers surface water to farmers through concrete channels, mostly by flow of gravity. The energy consumption for different sources of water in the basin was calculated for per cubic meter (Table2). Carbon emission values are given in Table3 [24, 25, 26].

Water-Energy-Food (WEF) Nexus Concept and Methodology. Water, energy, and food are inextricably linked to one another which require a methodology for studying the tradeoffs between decisions made within the three resource systems. Water is the most important input for agricultural crop production, but is also needed to produce energy. On the other hand, energy is required for many agricultural operations in the field, including the transport of agricultural goods, and pumping ground and surface water. The lack or intensive use of any of these sources triggers decline in the others and may jeopardize their security. Hence, a certain balance among the three should be insured to maintain the security level of each [4, 27, 28]. Consequently, to improve our understanding of the three interconnected resources, there is a need to quantify their interlinkages through data-driven and quantitative modeling approaches [28, 29]. Much research in recent years has focused on modelling based on WEF Nexus Concept. Most of them focused on management of a single resource such as water resources, energy systems or planning of agricultural production, or two resources such as water-energy nexus [30, 31, 32, 33, 34, 35]. There are also some studies focused on modeling of resource allocation on water, energy and food resources [36, 37, 38, 39, 40, 41].

WEF Nexus based modeling can increase consistency of decision-making that put forth sustainable resource allocation policies. In previous studies, WEF Nexus Tool 2.0 has been developed as a common platform to evaluate scenarios that aim to identify strategies for sustainable resource allocation [36, 39]. The tool provides ability to create variable scenarios under different conditions of water, energy and food resources. Although the analyses of resources produce outputs as requirements-consumptions of resources and Carbon emissions at the national level, basin level scenarios are needed to be created to obtain region specific interactions of resources.

Scenarios are created to represent different variations of water and energy inputs for products grown in the basin and are able to calculate the following outputs for each scenario;

- Water requirements
- Land requirements
- Energy requirements
- Carbon emissions
- Financial costs

For this purpose, a master excel sheet was modified for each scenario by including possible changes in land size resulting from urbanization, water requirements affected by climate change projections, expected changes in water portfolios for agriculture (surface or ground water) and technologies for pumping water from underground sources. The WEF Nexus block diagram, with the input-output entities calculated for the development

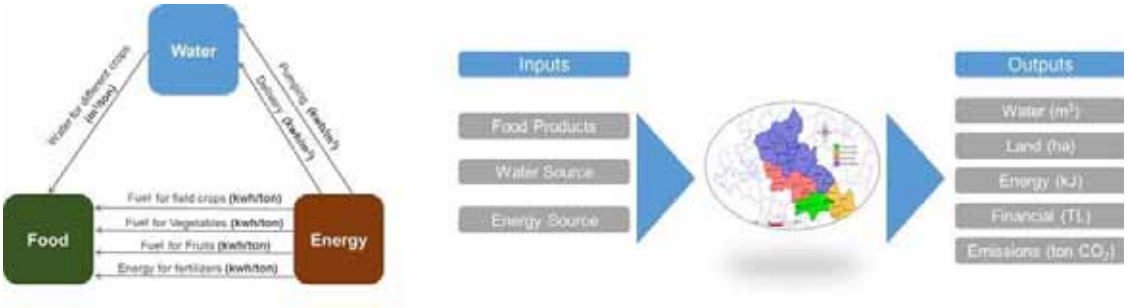

FIGURE 2
WEF Nexus block diagram (left) and Input-output entities considered for the development of different scenarios in the Gediz Basin

of different scenarios in the Gediz Basin are depicted in Figure 2.

Water (W). Water requirement is a result of crop production [42]: each crop requires a certain amount of water, consisting of blue (provided by irrigation) or green water (available water in the soil) [43].

$$Wi = Li * (W_s - 10*W_a) \quad (1)$$

where;

Wi= amount of total water needed for a specific crop (m^3)

Li= Land allocated to the certain crop (ha)

W_s= Seasonal water requirement for the crop (m^3/ha)

W_a= Water available to the crop (mm)

The total amount of water (Wi) needed to grow all crops in the basin is fulfilled from different sources: surface, underground, or desalinated. In this study, only surface and groundwater sources are considered. The formulation of total amount of water based on the water source equals the amount needed for plant growth is formulated as below.

$$W = \Sigma Wi = SW + GW \quad (2)$$

where,

SW= Surface water (m^3)

GW= Ground water (m^3)

Land (L). Land is the total area in ha and the sum of the land allocated to grow specific crops, vegetables and fruits in the basin.

$$L = \sum [\, DOM_i \text{ (ton) X Li(ha/ton)} \,] \quad (3)$$

where,

L = Total land needed to grow locally produced food products.

DOMi= Production (tons)

L_i = Land required to growth a unit amount of crop (ha/ton)

Energy (E). Energy needed in the basin is for farming operations in the field, transportation, fertilizer use, and pumping water from different sources [4, 44]. It is calculated as following;

$$E = E_1 + E_2 \quad (4)$$

E= Total domestic energy needed for the scenario (kJ)

E_1 = Energy needed for either pumping or treating water for irrigation (kJ)

E_2 = Energy needed for tillage, harvest, fertilizer production, and local transport (kJ)

Depending on the choice of water supply source, whether conventional or non-conventional, respective energy costs can be calculated (E_1). Whether surface or ground water pumping, treated, waste, or desalinated water, each would have its respective energy footprint depending on the domestically available plants and their efficiencies. Depending on the amount of water needed for the growth of the created food self-sufficiency scenario and sources of water identified to secure those needs, respective energy values can be calculated.

$$E_1 = E_{GWe} + E_{GWs} + E_{SW} \quad (5)$$

E_{GW} = Total energy needed for pumping water from deep well pumps using electricity (kJ)

$$E_{GWe} \text{ (kJ)} = S_{GWE} \text{ (kJ/m}^3\text{)} \times [\alpha_w \times W \text{ (m}^3\text{)}] \quad (6)$$

E_{GWs} = Total energy needed for pumping water from deep well pumps using solar energy (kJ)

$$E_{GWs} \text{ (kJ)} = S_{GWS} \text{ (kJ/m}^3\text{)} \times [\gamma_w \times W \text{ (m}^3\text{)}] \quad (7)$$

$E_{SW.}$ = Total energy needed for pumping surface water (kJ)

$$E_{SW} \text{ (kJ)} = S_{SW} \text{ (kJ/m}^3\text{)} \ [\delta_w \times W \text{ (m}^3\text{)}] \quad (8)$$

where,

S_{GWE}, S_{GWS} and S_{SW} are specific energy requirements in kJ per unit volume of water in m^3 and, α_w, γ_w and δ_w are the coefficients in decimals

The second part of "energy costs" (E_2) is calculated as the sum of the energy needed for tillage, fertilizer production, harvesting and local transport. This calculation is made for each crop separately.

$$E_2 = E_{farming} + E_{transport} + E_{fert.} \quad (9)$$

where,

$E_{farming}$(kJ)=Total energy needed for farming operations

$E_{farming}$(kJ)= Total energy needed for local transport and

$$E_{fert.\ T} \text{ (kJ)} = \sum [E_{fert.\ (i)} \text{ (kJ/kg)} \times FERT._{(i)} \text{ (kg/ton)} \times DOM_i\text{(ton)}] \quad (10)$$

where,

$E_{fert.\ T}$ (kJ)=Total energy needed for producing the required amount of fertilizer
$E_{fert.(i)}$ (kJ/kg) = Energy required for producing a kg of fertilizer (depends on type of fertilizer)
$FERT._{(i)}$ (kg/ton) = Amount of fertilizer applied per ton of product (i) produced.

The total energy needed for farming is the sum of the energy requirements for all crops in the region and is calculated by finding the fuel consumption to grow a given crop, for example cotton, starting with soil tillage and ending with harvest and transportation. Field operations vary from one crop to another as each crop, vegetable and fruit has its own characteristics that alter farming operations. Vegetable and fruit production in Turkey generally, and in the Gediz Basin specifically, are mostly labor dependent; the farming operations for field crops are mostly mechanized. Fruits and vegetables are more labor dependent and harvested by pickers or other special harvesters. In this study, farming operations such as tillage by plough, harrowing (seedbed preparation equipment), planting or transplanting, spraying, fertilizer distribution, hoeing and irrigation operations, and harvesting for each crop, vegetable and fruit are considered. In this respect, there are different ways to calculate the fuel consumed by tractors, which is based on the yearly use of tractors for farming or transport operations, as in the equation below.

$$Q_{avg} = 0.223 \cdot P_{pto} \quad (11)$$

where $O_{avg}$is: average diesel fuel consumption and $P_{pto}$is: rated pto power

This equation is valid for tractors such as those used in the Gediz basin, which run between 700 and 1000 hours per year. The rated Power take-off (P_{pto}) is a factor of tractor power and usually assumed to be 80% of tractor power, considering losses in transmission systems, etc.

Calculation of fuel consumption uses equation (11), the time spent for growing a specific crop must be known, so that the multiplication of time spent in total per unit area will result in total fuel consumption per unit land in liters.

$$C_g = Q_{avg} \cdot T_{farming} \cdot L \quad (12)$$

where,
C_g= Diesel fuel consumption for a specific crop (L)
$T_{farming}$= Time spent per unit of land for farming operations for a specific crop (h/ha)
L= Land allocated to specific crop (ha)

While the machinery parks of the farms in towns of the Gediz basin are similar, average tractor power varies from one town to another. However, differences are not great: tractor power distribution data obtained from the Turkish Statistical Institute for the year 2014 were used to calculate the fuel consumption. The rated Pto power was matched with the crops grown in each town and fuel consumption for each crop at a specific town was calculated. The time spent (hours) per hectare for each crop was obtained from a study conducted in Turkey [45]. The data, in terms of time spent per hectare using tractors, were updated in accordance with the many technological developments that have occurred, such as the use of new equipment or machinery in farming operations in the region, since the study was published.

Carbon footprint (C). Each of the mentioned energies consumed, as noted above, have their respective carbon footprints. Whether for energy consumed to secure water for irrigation or for other production and transportation practices, carbon is emitted into the atmosphere [39]. The carbon emission calculations based on the activities are formulated as in the following:

$$C = C_1 + C_2 \quad (13)$$

$$C_1 = C_{GWe} + C_{GWs} + C_{SW} \quad (14)$$

$$C_2 = C_{farming} + C_{transport} + C_{fert} \quad (15)$$

As parallel to energy consumption, carbon emissions are quantified as the following,

$$C_1 = C_{GWe} + C_{GWs} + C_{SW} = E_{GW}(kJ) \times (\text{ton } CO_2/kJ) + E_{GWs}(kJ) \times (\text{ton } CO_2/kJ) + E_{SW}(kJ) \times (\text{ton } CO_2/kJ) \quad (16)$$

$$C_{2\ =}\ E_{till.\ T}(kJ) \times (\text{ton } CO_2/kJ) + E_{transport}(kJ) \times (\text{ton } CO_2/kJ) + E_{fert.}(kJ) \times (\text{ton } CO_2/kJ) \quad (17)$$

Financial Value. $LFV(TL) = \Sigma [\ Prod_i\ (ton) \times Pri_i\ (TL/ton)\ ]$ (18)
$Prod_i$ (ton) = Total production of a product (i) locally.
Pri_i (TL/ton) = Selling market price of product (i).
LFV(TL) = Total value of production of locally produced product

Sustainability Index. The sustainability of a scenario to be developed in this study will be defined by calculating its "sustainability index" as follows:

$$\text{Water Index} = WI = Wi / Wa \quad (19)$$

$$\text{Land Index} = LI = Li / La \quad (20)$$

$$\text{Local Energy Index} = EI = Ei / Ea \quad (21)$$

$$\text{Local Carbon Index} = CI = Ci / Ca \quad (22)$$

$$\text{Financial Index} = FI = Fi / Fa \quad (23)$$

$$\text{Energy IMP Index} = EIMP\ I = E\ IMPi / E\ IMPa \quad (24)$$

$$\text{Carbon IMP Index} = CIMP\ I = C\ IMPi / C\ IMPa \quad (25)$$

Wi = The total water needed for scenario i
Li = The total land area needed for scenario i
Ei = The total local energy needed for scenario i
Ci = The total local carbon emitted by scenario i
Fi = The total finances for scenario I = Flocal + Fimport (local and import)
E IMPi=The total local energy needed for scenario i
C IMPi=The total local carbon emitted by scenario i
Wa = Total max acceptable water extracted and produced by available water resources for agricultural production

La = Max acceptable/arable local land use
Ea = Max acceptable energy use = a cap could be put on max energy generation and use for agricultural production. It is influenced by current capacities, and decision of upgrade.
Ca = Max acceptable carbon emissions = a cap put by a government to cut carbon emitted
Fa = Max acceptable limits for expenditures to supply food locally and through imports
E IMPa= Max energy consumed through transporting imported food products
C IMPa = Max carbon emitted through transporting imported food products

Therefore, the scenario with the lowest score would be most sustainable, as defined by the decision maker.

Scenario i: S.I. $i = [WI_i(100-I_W) + LI_i(100-I_L) + EI_i (100-I_E) + CI_i (100-I_C) + FI_i (100-I_F) + EIMP\ I_i (100-I_{EIMP}) + CIMP\ I_i (100-I_{CIMP})] /100$ (26)

$$I_W + I_L + I_E + I_C + I_F + I_{EIMP} + I_{CIMP} = 100 \quad (27)$$

I_W = Importance factor assigned for the water assessment parameter
I_L = Importance factor assigned for the land assessment parameter
I_E = Importance factor assigned for the energy assessment parameter
I_C = Importance factor assigned for the carbon assessment parameter
I_F = Importance factor assigned for the financial assessment parameter
I_{EIMP} = Importance factor assigned for 'energy for global transport' assessment parameter
I_{CIMP} = Importance factor assigned for 'carbon emissions due to global transport' assessment parameter

Crop related phenomena include land, water, and fertilizer needs; energy used for farming operations, transport and pumping water (from surface or groundwater sources); and carbon emissions, as obtained for the food production. Hence, the effect of each crop on sources, energy, and carbon emission is investigated separately and using a special analysis called "parameter relative sensitivity analysis." The parameter relative sensitivity analysis determines the effect of changing each input parameter on different outputs and for this purpose, using the equation:

$$S_r = \left(\frac{O - O_b}{P_{b\pm\Delta} - P_b} \right) \frac{P_b}{O_b} \quad (28)$$

In this equation, S_r is the relative sensitivity value, O the new output, O_b the output of base scenario, P the new parameter value, and P_b the base parameter value in base scenario. "b" is the base average value and Δ represents the change in parameter value from base [46].

Development of Future Scenarios. Future scenarios using the WEF Nexus concept were created and then divided into two parts: near future (present to the year 2020), and long term (years 2030, 2040 and 2050).

In the last two decades, the region survived one drought and one rainy year: these were considered the extremes and are assumed to happen in the region in the future. The normal year data, in terms of seasonal water and irrigation requirements, were correlated to the data of extreme years, as shown in Figure 3. For these scenarios, the water requirement data of normal year were replaced based on the regression models as shown in the Figures.

In the long term scenarios, urbanization, climate change, and technological developments were considered. The trend in urbanization was calculated based on the data released by the Turkish Statistical Institute and the total land used for agriculture data from 2000 thru 2014. It was found that the land area for agriculture, as a general trend, decreases annually in the basin. The changes in local costs are depicted for near future and long term scenarios. As seen from the Figure, local costs go down as a natural result of reduction in land. This also means that self-sufficiency in each crop declines and the export of some crops from the basin will be jeopardized (Figure 4).

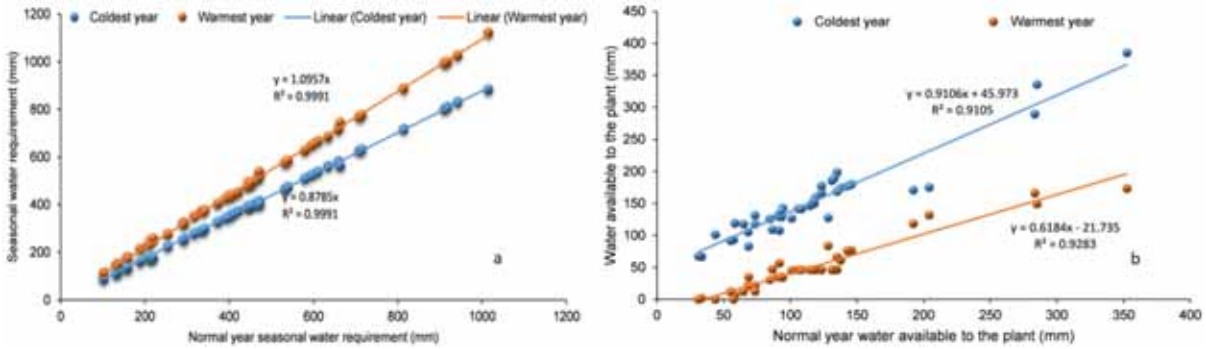

FIGURE 3
Relationship between normal year seasonal water requirement with the coldest and hottest year (a) Relationship between normal year water available to the plant and with the coldest and hottest year (b)

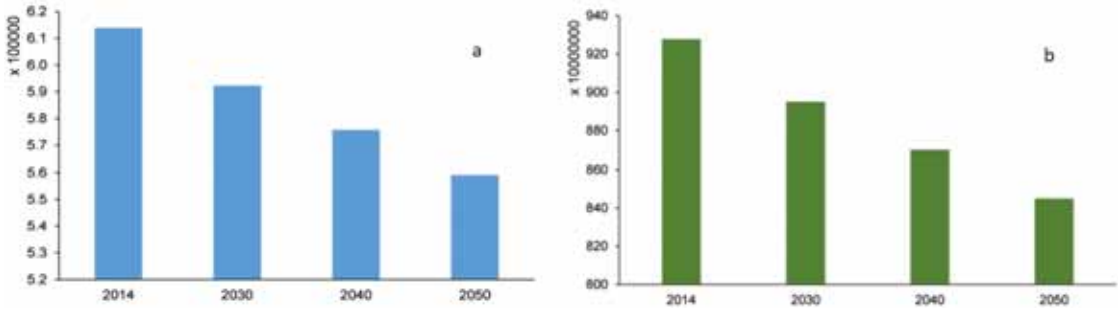

FIGURE 4
Changes in land size (ha) (a) and changes in the cost of production (TL) (b) in the long term scenarios

TABLE 4
Codes and Explanations of the Scenarios

Scenario code	Explanation
NFNSSE0	This is the based scenario that included only normal years. The ratio of surface and groundwater was 43 and 57%, respectively. No solar energy was considered in this scenario.
NFNSSE5	This scenario is the same as above, except the solar energy. It was considered that 5% of the total is pumped using solar energy
NFHSSE0	The hottest season was considered, hence the water requirement data was set along with the irrigation requirement for each crops. No solar energy was considered.
NFHSSE5	This is the same as scenario except the solar energy use. The level of solar energy to pump groundwater was set to 5%.
NFCSSE0 and NFCSSE5	The coldest season included a different set of data than the normal and hot season and was created without and with 5% solar energy, as was the case in the above scenarios.
UCSSE0	Solar energy use was not assumed in this scenario while the ratio of surface and groundwater was 43 and 57%, respectively. Rainy year data were used in terms of the seasonal water requirement and for irrigation purposes. The land size was reduced 3.52 % as compared to year 2014 which was 613917.20 ha
UCSSE5	Same as the above scenario except 5% of the water was assumed to be pumped from underground by using solar energy panels
UCSSW53SE0	In this scenario, the ratio of the surface water was increased to 53%, cold season data were considered along with no use of solar energy
UCSSW53SE5	The same as above scenario except the solar energy use in irrigation water was assumed to be 5%
UHSSE0	Same as scenario UCSSE0 except hottest year seasonal water requirement data were considered
UHSSE5	Same as above except the solar energy use for pumping water was considered at 5% level of the water used for irrigation
UHSSSW53SE0	Same as scenario 2030UCSSW53SE0except the surface water ratio was increased to 53%
UHSSSW53SE5	Same as above except 5% solar energy use was assigned

The four digit numbers in front of the scenario codes in figures refer to the year, NF refers to Near Future

This reduction was calculated to be 3.52, 6.22 and 8.92 % of the base year (2014), for the years 2030, 2040 and 2050, respectively. As in the near future scenarios, extreme precipitation years were considered since it is assumed that climate change in the long term will be between these two extremes. In some scenarios, the surface water use ratio increased to 53%, since the General Directorate of Hydraulics Works plans to put forward some new projects in the region that will increase the use of surface water. The increase from 43 to 53% was calculated based on the declared numbers of the institute. Beyond that, urbanization, climate change, and solar energy use rates were assumed to increase over the long term. This was added into scenarios as different percentages: 5% in 2030, 10% in 2040, and 15% in 2050. Including the near future scenarios, a total of 45 scenarios were developed in the study. Detailed information for each scenario is given in Table 4.

RESULTS AND DISCUSSION

As of 2014, the total land used for plant production in the basin is calculated to be 613917.2 ha, and the total water requirement is 1337.5 hm^3. For the WEF Nexus study, crops were divided into two groups to allow crops that govern the land and water needs to be easily analyzed and discussed separately. After sorting the data, the top 15 crops, accounting for 86.3 % of the land use and 79.4% of total water, were separated from the other 80 crops, vegetables, and fruits and then used for further analysis using WEF Nexus concept. The relative sensitivity analysis in this study was carried out only for the year 2014 and for the top 15 crops, by

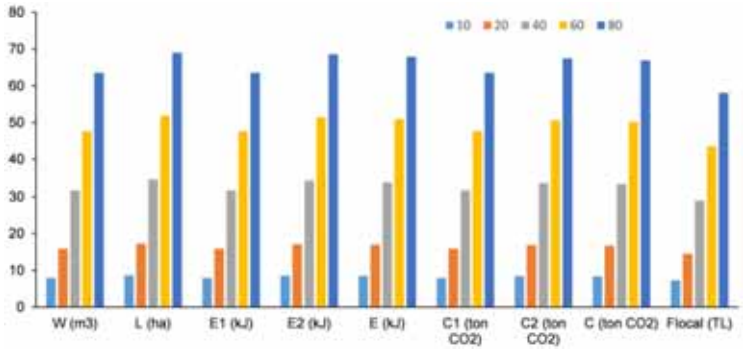

FIGURE 5
Percent changes in water, land, energy, carbon emission and local cost as a result of increasing self-sufficiency in the top 15 crops from 10 thru 80 %

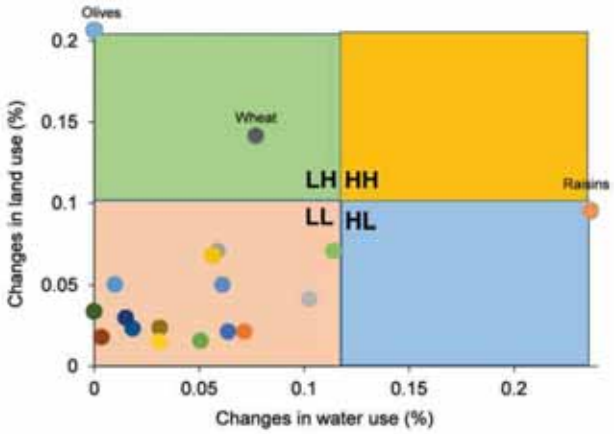

FIGURE 6
Percent changes in water use and land as a result of 20 increase in self-sufficiency of top fifteen crops, average of 22 field crops, 38 vegetables and 20 fruits

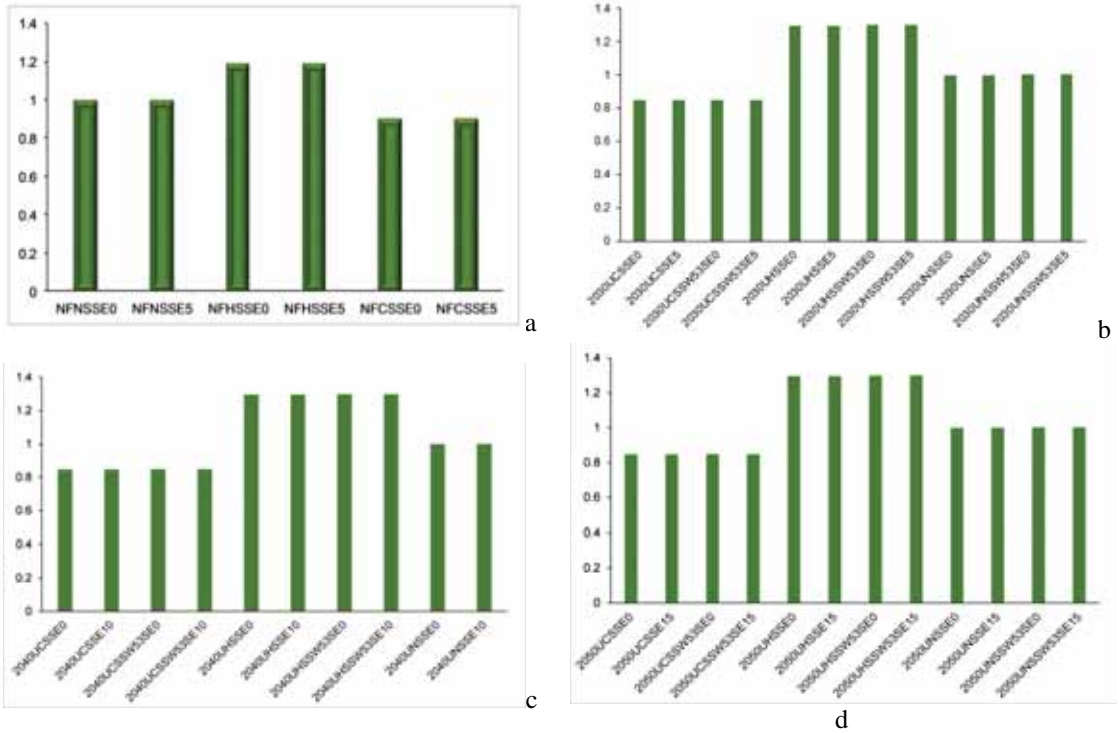

FIGURE 7
Sustainability index comparison for the near future (a), 2030 (b), 2040 (c) and 2050 (d) scenarios

increasing the self-sufficiency from 10 to 80%. The total changes can be seen in Figure 5.

The results are valuable in terms of crop management in the basin. If any change occurs in the future, changes in need for sources can readily be obtained. Another schematic view of the top 15 crops and the average of the other vegetables and fruits (total of 18 data) can be seen in Figure 6, which is divided into four equal areas by considering the ranges of the X and Y axis. As seen from the Figure, most of the crops accumulate in the regions of low land and water values, while some extreme crops such as raisins, wheat, and olives are out of the accumulated region.

The comparison of all near future scenarios can only be made from the point of the sustainability index, which requires importance factors that should be assumed for the evaluations. The sustainability index values were calculated for the long term scenarios; the results are given in Figures 7 for near future scenarios (a) and the years 2030 (b), 2040 (c) and 2050 (d). The calculations were achieved separately for each year, and normal season water requirements data was assumed to be the base scenario. Figure was drawn based on the importance factor of 0.3 for water and land while the energy parameter was assumed to be 0.2. The carbon and financial assessment parameters were also kept at the same level (0.1). The lowest sustainability indexes are obtained for the coldest seasons, making more sustainable and favorable scenarios. Normal season scenarios follow this scenario, while the hot season scenario is less favorable: the sustainability indexes are higher than the other scenarios. These reductions in the land of the basin, as stated in above, would be 3.52%, 6.22% and 8.92% for 2030, 2040 and 2050, respectively. Based on the linear relationship between land use and food production in this study, it can be expected that the self-sufficiency of each crop will decrease at the same rate as the land reduces, assuming the land reductions will be equally distributed in all crops in the basin.

On the other hand, the population growth in both the basin, and in Turkey as a whole, will enlarge the gap in a country's ability to feed its people and may result in a reduction in self-sufficiencies such that Turkey may become a food importing country. The results tabulated in the Tables above for these scenarios are discussed below. The trend for each year is the same as other years, and a rainy year is always a favorable year in terms of water need. The increased precipitation in such a year not only reduces the evapotranspiration from the plants, but also reduces irrigation needs and saving significant amounts of water. Increasing the surface water use in all long term scenarios did not change the sustainability index. This trend is the same when solar energy use was increased in the basin. Even though the sustainability index does not change, increased surface water use in the basin will help significantly increase ground water levels. The studies conducted in the region indicate that the groundwater pumping depth increases year by year [47, 48].

A comparison among near future and long term scenarios should be considered, along with the changes in self-sufficiency values. For example, the same scenarios in 2030, 2040 and 2050 seem to reveal similar sustainability index values. However, even though the sustainability index values are similar, self-sufficiency declines if the time period is extended from 2030 to 2050. Hence, it could be said that changes in urbanization, along with climate change (drought seasons), make each scenario less sustainable as compared to the sustainability of 2014. A decrease in self-sufficiency by years can be avoided by growing drought resistant crop varieties and changing farming practices, such as direct seeding application, known as zero tillage. This application will significantly reduce fuel consumption, which in turn reduces carbon emission. Precision farming practices, such as variable rate fertilizer distribution, can also help to reduce the fertilizer input costs in agricultural production and cause less pollution in groundwater sources from consequent reduction in chemical drainage. There is an opportunity to reduce water use significantly in agricultural production by employing drip irrigation for many crop products in the region. It is believed that this will help save significant amounts of water in the basin.

Another issue with the basin is land fragmentation, an unsolved phenomenon for the entire country [23]. The number of parcels owned by one farmer ranges between 4 and 25, while the average land size is about 0.75 ha [22]. This situation is considered to be an important obstacle as it reduces efficiency in farming applications. Based on the linear relationship in the WEF Nexus study, it could be expected that the self-sufficiency of each crop will decrease at the same rates that land area is reduced, assuming the land reductions are equally distributed across all crops in the basin. On the other hand, the population growth in both the basin and Turkey may enlarge the gap for the country to feed its own people and result in reduced self-sufficiency.

CONCLUSIONS

The following can be concluded from the study:

1. The source of energy for crop production in the basin is petroleum, used for farming operations, transport, pumping surface water and fertilizer production. Solar energy seems to be an appropriate source, especially for pumping

groundwater. It is expected to become widespread not only in the basin, but nationwide.

2. The crop pattern in the region is an effective parameter for land allocation and water demand. Olive, wheat, and raisin production are considered the governing crops in the basin. Future changes in crop patterns may cause a shift toward increased water need and/or land allocations. Hence, the management in the basin requires acknowledgement of linkages between natural resources and quantification of these linkages.

3. Self-sufficiency and sustainability in the basin are likely to worsen in the long term, compared to the year 2014.

4. The reduction in available land for agriculture, as a consequence of urbanization and water scarcity due to climate change, is inevitable. In order to maintain sustainability at the current level, varieties resistant to drought should be selected and some new farming practices (direct planting and drip irrigation systems) should be seriously considered and adopted.

5. Environmentally friendly applications in agriculture are believed to reduce energy inputs, and result in less pollution. These applications could be described as the implementation of precision farming in agricultural operations along with the use of solar energy to reduce carbon emissions.

6. The WEF Nexus concept is well suited to study the basins in Turkey. Applying the concept to the other basins is of importance and the entire country profile can be obtained and then WEF Nexus concept, including importing materials from other countries (virtual water), applied and nationwide WEF study will be conducted.

7. Adding crop yields that reflect the use of different amounts of water during their growth is expected to bring non-linearity to the WEF Nexus concept: many crops respond to water used in a non-linear way. Excessive water use and water at certain levels can result in the same yield, but with differences in the amounts of water saved. The reflection of this issue in WEF Nexus work will also make other parameters non-linear. It is believed that this issue is worth studying.

ACKNOWLEDGEMENTS

This research article has been produced from a project titled “Strategic Planning of Natural Resources: Dynamic Modelling of Water, Energy and Food (WEF) Nexus for the Gediz Basin –Turkey”. The project was carried out with the scholarship award granted by the Scientific and Technological Research Council of Turkey.

REFERENCES

[1] FAO (2016) Water withdrawal by sector, around (2010) http://www.fao.org/nr/water/aquastat/Tables/WorldData-Withdrawal_eng.pdf. Last accessed: 04/20/2018

[2] Rosegrant, M.W., Ringler, C. and Zhu, T. (2009)Water for Agriculture: Maintaining Food Security under Growing Scarcity. Annual Review of Environment and Resources. 34, 205-222.

[3] Yang, H., Zhou, Y., Liu, J. (2009) Land and water requirements of biofuel and implications for food supply and the environment in China. Energy Policy. 37(5), 1876-1885.

[4] Mohtar, R.H., Daher, B. (2012) Water, Energy and Food: The ultimate Nexus.Encylopedia of Agricultural, Food, and Biological Engineering, Second ed. Taylor and Francis.

[5] Mohtar, R.H. (2011) An Integrated Sustainability Index for Effective Water Policy. In: Waughray, D. (ed.) Water security: the water-food-energy-climate nexus World Economic Forum Water Initiative. Island Press. Washington, Covelo, London.

[6] Bazilian, M., Rogner, H., Howells, M., Hermann, S., Arent, D., Gielen, D., Steduto, P.,Mueller, A., Komor, P., Tol, R.S.J., Yumkella, K.K. (2011) Considering the energy, water and food nexus: Towards an integrated modeling approach. Energy Policy.39(12), 7896-7906.

[7] Daher, B., WEF Nexus Research Group, and Texas A&M University (2017) IWRA Sustainability in the Water-Energy-Food Nexus: Bridging Science and Policy Making. Policy Briefing Water International. Available from:http://agrilife.org/wefnexus/files/2015/01/IWRA.pdf

[8] FAO (2014)Walking the Nexus Talk: Assessing the Water-Energy-Food Nexus. Retrieved from http://www.fao.org/3/a-i3959e.pdf. Last accessed: 04/20/2018.

[9] Flammini, A., Puri, M., Pluschke, L., Dubois, O. (2014) Walking the Nexus Talk: Assessing the Water-Energy-Food Nexus in the Context of the Sustainable Energy for All Initiative. Environment and Natural Resources Working Paper No. 58 – FAO, Rome, ISSN 2226-6062. Retrieved from: http://www.fao.org/3/a-i3959e.pdf , Last accessed: 01/21/2018.

[10] Mekonnen, M.M., Hoekstra, A.Y. (2011a) The green, blue and grey water footprint of crops and derived crop products. Hydrology and Earth System Sciences Discussions. 8, 763-809.

[11] Hoekstra, A.Y. and Chapagain, A.K. (2008) Globalization of water: Sharing the planet's freshwater resources. Blackwell Publishing, Oxford, UK.
[12] Lee, S.H., Mohtar, R.H., Choi, J.Y., Yoo, S.H. (2016) Analysis of the characteristics of the global virtual water tradenetwork using degree and eigenvector centrality, with a focus onfood and feed crops. Hydrology and Earth System Science. 20, 4223-4235.
[13] Mekonnen, M.M. and Hoekstra, A.Y. (2011b) National water footprint accounts: the green, blue and grey water footprint of production and consumption. Value of Water Research Report Series No. 50, UNESCO-IHE, Delft, the Netherlands.
[14] Alcamo, J., Henrichs, T. (2002) Critical regions: A model-based estimation of world water resources sensitive to global changes. Aquatic Sciences. 64(4), 352-362.
[15] Alcamo, J., Döll, P., Henrichs, T., Kaspar, F., Lehner, B., Rösch, T., Siebert, S. (2003) Global estimates of water withdrawals and availability under current and future "business-as-usual" conditions. Hydrological Sciences Journal. 48(3), 339-348.
[16] Smakhtin, V., Revenga, C., Döll, P. (2004) A pilot global assessment of environmental water requirements and scarcity Water International. 29(3), 307-317.
[17] Ringler, C., Bhaduri, A. and Lawford, R. (2013)The nexus across water, energy, land and food (WELF): potential for improved resource use efficiency? Current Opinion in Environmental Sustainability. 5, 617–624.
[18] Mohtar, R.H. (2016) The importance of the Water-Energy-Food Nexus in the implementation of The Sustainable Development Goals (SDGs).Policy Brief.PB-16/30.OCP Policy Center, Morocco.
[19] Daher, B., Mohtar, R.H., Pistikopoulos, E.N., Portney, K.E., Kaiser, R., Saad, W. (2018)Developing Socio-Techno-Economic-Political (STEP) Solutions for Addressing Resource Nexus Hotspots. Sustainability. 10(512).
[20] TurkStat, (2014)Turkish Statistical Institute. Crop Production Statistics. www.tuik.gov.trLast accessed: 04/20/2017.
[21] Canli, S. (2014) Agricultural irrigation requirement on Menemen plain and possible effects of irrigation water in terms of plant, soil and irrigation systems. MSc Thesis. Ataturk University, Institute of Natural and Applied Sciences, Erzurum. (in Turkish).
[22] Özgünaltay-Ertuğrul, G. (2013) Values and Key Relations on Tractor Use as in the Example of Gediz Basin. PhD. Dissertation.Ege University, Institute of Natural and Applied Sciences, Bornova-Izmir, Turkey. (in Turkish).
[23] Evcim, H. Ü., Değirmencioğlu, A., Özgünaltay Ertuğrul, G., Aygün, İ., (2012) Advancements and transitions in technologies for sustainable agricultural production. Economic and Environmental Studies. 12(4), 459-466.
[24] Wood S. and Cowie, A., (2004) A Review of Greenhouse Gas Emission Factorsfor Fertiliser Production.IEA Bioenergy – Task 38.http://task38.org/publications/GHG_Emission_Fertilizer_Production_July2004.pdf.
[25] Sovacool, B.K., (2008) Valuing the greenhouse gas emissions from nuclear power: A critical survey.Energy Policy. 36(2008) 2940– 2953.
[26] Schlömer S., Bruckner, T., Fulton, L., Hertwich, E., McKinnon, A., Perczyk, D., Roy, J., Schaeffer, R., Sims, R., Smith, P. and Wiser, R. (2014) Annex III: Technology-specific cost and performance parameters. In: Edenhofer, O., Pichs-Madruga, R., Sokona, Y., Farahani, E., Kadner, S., Seyboth, K., Adler, A., Baum, I., Brunner, S., Eickemeier, P., Kriemann, B., Savolainen, J., Schlömer, S., von Stechow, C., Zwickel, T. and Minx, J.C. (eds.) Climate Change 2014: Mitigation of Climate Change. Contribution of Working Group III to the Fifth Assessment Report of the Intergovernmental Panel on Climate Change Cambridge University Press/ Cambridge, United Kingdom and New York, NY, USA.
[27] Ferroukhi, R., Nagpal, D., Lopez-Peña, A., Hodges, T., Mohtar, R.H., Daher, B., Mohtar, S.,Keulertz, M. (2015)Renewable Energy in the Water, Energy and Food Nexus. International Renewable Energy Agency, Abu Dhabi, United Arab Emirates.
[28] Leck, H., Conway, D., Bradshaw, M., Rees, J., (2015)Tracing The Water–Energy–Food Nexus: Description, Theory and Practice. Geography Compass. 9/8(2015), 445–460.
[29] Granit, J., Fogde, M., Holger Hoff, S.E.I., Joyce, J. (2013) Unpacking the water-energy-food nexus: Tools for assessment and cooperation along a continuum. Cooperation for a Water Wise World, 45p.
[30] Rosegrant, M.W., Ringler, C., McKinney D.C., Cai, X., Keller, A. and Donoso, G. (2000) Integrated economic–hydrologic water modelling at the basin scale: the Maipo river basin. Agricultural Economics. 24(2000) 33–46.
[31] Hightower, M., Pierce, S.A. (2008) The energy challenge. Nature. 452, 285–286.
[32] Li, G.C., Huang, G.H., Lin, Q.G., Zhang, X.D., Tan, Q., Chen, Y.M. (2011) Development of a GHG-mitigation oriented inexact dynamic model for regional energy system management. Energy. 36, 3388–3398.

[33] Hu, Q., Huang, G., Cai, Y., Huang, Y. (2011) Feasibility-based inexact fuzzy programming for electric power generation systems planning under dual uncertainties.Appl. Energy. 88, 4642–4654.
[34] Bernardi, A., Giarola, S. and Bezzo, F. (2012)Optimizing the economics and the carbon and water footprints of bioethanol supply chains. Biofuels, Bioprod. Bioref. 6, 656–672.
[35] Zhang, X., Vesselinov, V.V., (2016). Energy-water nexus: Balancing the tradeoffs between two-level decision makers. Appl. Energy. 183, 77–87.
[36] Mohtar, R. H., Daher, B. (2014) A Platform for Trade-off Analysis and Resource Allocation: The Water-Energy-Food Nexus Tool and its Application to Qatar's Food Security [part of the 'Valuing Vital Resources in the Gulf' Series], Chatham House.http://agrilife.org/wefnexus/files/2015/01/20141216WaterEnergyFoodNexusQatarMohtarDaher.pdf.
[37] Walker, R.V., Beck, M.B., Hall, J.W., Dawson, R.J., Heidrich, O. (2014) The energy-water-food nexus: Strategic analysis of technologies for transforming the urban metabolism. Journal of Environmental Management. 141(2014) 104-115.
[38] Biggs, E.M., Bruce, E., Boruff, B., Duncan, J.M.A., Horsley, J., Pauli, N., McNeill, K., Neef, A., vanOgtrop, F., Curnow, J., Haworth, B., Duce, S., Imanari, Y. (2015) Sustainable development and the water–energy–food nexus: A perspective on livelihoods. Environmental Science and Policy. 54(2015) 389–397.
[39] Daher, B., Mohtar, R.H. (2015) Water–energy–food (WEF) Nexus Tool 2.0: guiding integrative resource planning and decision-making. Water International. 40(5-6), 748-771.
[40] Rasul, G., Sharma, B. (2016) The nexus approach to water-energy-food security: an option for adaptation to climate change. Clim. Policy.16, 682-702.
[41] Karan, E., Asadi, S., Mohtar, R., Baawain, M. (2018)Towards the optimization of sustainable food-energy-water systems: A stochastic approach. Journal of Cleaner Production. 171(2018), 662-674.
[42] Zhang, X. and Vesselinov V.V. (2017)Integrated modeling approach for optimal management of water, energy and food security nexus. Advances in Water Resources. 101(2017), 1–10.
[43] Siebert, S., Döll, P. (2010)Quantifying blue and green virtual water contents in global crop production as well as potential production losses without irrigation. Journal of Hydrology. 384(3-4), 198–217.
[44] Garcia, D.J., You, F. (2016)The water-energy-food nexus and process systems engineering: A new focus. Computers and Chemical Engineering. 91, 49–67.
[45] Koral, A. I, Altun, A. (1998) A guide for the production inputs of the crops grown in Turkey. T.C. Basbakanlik, Koy Hizmetleri Genel Mudurlugu, APK Dairesi Baskanligi, Toprakve Su Kaynaklari Arastirma Sube Mudurlugu Yayin no:104, Rehber no: 16, Ankara, 360p. (in Turkish).
[46] Daher, T.B. (2012)Water, energy and food nexus: A basis for strategic planning of natural resources. MSc. Thesis. Purdue University, West Lafayette, IN, 200p.
[47] Simsek, C., Filiz, S. (2005) Hydrogeology and vulnerability of Aquifer of the Torbali plain and vicinity.DEU Muhendislik Fakultesi, Fen veMuhendislikDergisi. 7(2), 21-37. (in Turkish).
[48] Simsek, C., Demirkiran, Z., Cetiner, L., Gunduz, O., Ocal, G. (2009) Three dimensional interactive hydrogeological model of the Kemalpasa Plain. DEU Muhendislik Fakultesi, Fen ve Muhendislik Dergisi. 11(31), 10-21. (in Turkish).

Received: **28.8.2018**
Accepted: **18.02.2019**

CORRESPONDING AUTHOR

Adnan Degirmencioglu
Ege University,
Faculty of Agriculture,
Department of Agricultural Engineering
and Technology
Bornova, Izmir – Turkey

e-mail: adnan.degirmencioglu@ege.edu.tr

© by PSP Volume 28 – No. 4/2019 pages 2523-2529 Fresenius Environmental Bulletin

CHARACTERISTICS RESEARCH OF SLUDGE MICRO-BUBBLE DRYING AND DERIVED FUEL

Yu Qi, Chi Zhang*, Yan Tao, Tianyu Guo, Hongtao Wang, Fang Cao, WeiKe Zhang

College of Environmental Science and Engineering, Taiyuan University of Technology, Taiyuan, 030024, China

ABSTRACT

At present, incineration method is one of important means of sludge "four-disposal principles (reduction, stabilization, harmlessness and resource), which is rarely applied in sludge landfill. However, the existing problem is high water content of sludge resulting in high drying cost and unsatisfactory burning effect. In this study, a foaming agent (sodium lauryl sulfate, SDS) was employed for micro-bubble drying of the sludge and pulverized coal was added as the combustion-supporting material, further researching change of water content and heat value in the process of sludge foaming. The properties of sludge-derived fuel were analyzed by X-ray diffraction and thermogravimetric techniques. The results show that suitable introduction of foaming agent (SDS) improves the formation of micro-bubble structure of sludge, enhances the water evaporation area in interior of the sludge and facilitates the contact between pulverized coal and sludge particles as well as greatly promotes the heat of combustion for sludge drying and mixture of coal and sludge. Moreover, when SDS/sludge ($g \cdot g^{-1}$) is 0.25, water content of dewatered sludge is decreased from 77.9% to 55.1% and low heat value of the sludge-derived fuel increases by about 47%. In addition, the result also shows that the weight loss ratio is positively correlated with the low heat value of the fuel, that is to say, the adding of SDS improves the low heat value, thereby, promoting the reducing quantity of the fuel in a certain control range of temperature.

KEYWORDS:
Sludge drying, Micro-bubble excitation, Thermogravimetric analysis, Drying mechanism

INTRODUCTION

According to statistics, till to the end of the year 2015, it is estimated that 3830 urban sewage treatment plants have been built in China with a sewage treatment capacity of 1.62 million m^3/d and associated sludge exceeding 30 million tons in every year (80% water content). According to relevant statistical data by the end of year 2014, innocuously disposed sludge is about 56% by some methods, such as, building materials, incineration, compost and sanitary landfill. Incineration is the most thorough reduction technique in many methods for disposition of sludge. This technique has the advantages of making sludge volume reduce less than 10% of the original sludge and obtaining the stable inert slag for incineration products, thereby, achieving the resourceful use of building materials. Therefore, the technique truly realizes the stabilization, harmlessness and resourcefulness in sludge treatment and disposal.

The pyrolysis reaction of sludge is very complex due to high water content, low heat value and a large number of heat-degradable organic components [1]. If a certain amount of sludge is mixed into coal, it will improve the pyrolysis characteristics of coal and catalytic the pyrolysis process of coal [2]. However, water content of sludge cannot reach below 60% by traditional concentration and dewatering technology due to the high water content and the low percentage of solid content [3], which directly affects the sludge drying and burning difficulty. Therefore, it is necessary to introduce a variety of sludge drying techniques to achieve more deep dehydration. Presently, the commonly used technologies for sludge drying including traditional sludge drying, heat drying, microwave drying and solar drying [4-7]. However, to the best of our knowledge, there are few studies on the use of chemical drying method and synthesized sludge-derived fuel by addition of pulverized coal. More importantly, sludge drying can remove water by evaporation and diffusion processes, and the two processes are continuous and alternate [8]. Based on above all, in this paper, through adding of foaming agent (sodium lauryl sulfate, SDS), stabilizing agent (acrylic acid) and drying agent (metal compound), pulverized coal and sludge particles can sufficient contact, and further the change rule of heat value was also researched. Moreover, the structure characteristics and drying mechanism were analyzed by X-ray diffraction and thermogravimetric techniques.

TABLE 1
Physical and chemical properties of the sludge

Water content/%	pH	Ash/%	Volatiles %	High heat value Cal/g	Low heat value Cal/g	Organic matter content/%
77.9	7.6	60.59	34.83	1613	106.6	49.7

TABLE 2
Physical and chemical properties of the pulverized coal

Coal samples	Water content/%	Ash	Volatiles	High heat value Cal/g	Low heat value Cal/g
Anthracite	1.9	32.61	10.16	5147	4918
coking coal	1.4	44.28	12.61	4281	4084
Bituminous	1.2	28.17	9.52	6216	6024

MATERIALS AND METHODS

Materials. The sludge samples utilized in this study were thick, which were collected from dehydrated sludge of sewage treatment plant in Hexi, Taiyuan. Sodium lauryl sulfate was purchased from Zhedong Chemical Plant in Shangyu City. Acrylic acid was obtained by Tianjin Zhiyuan Chemical Reagent Co., Ltd. The pulverized coals used (anthracite, bituminous, coking coal) were collected from Liliu Coking Co., Ltd in Lvliang, Shanxi. Calcium oxide, magnesium oxide, calcium sulfate, iron sulfate (used as drying agent) were purchased from Sinopharm Chemical Reagent Co., Ltd. Physical and chemical properties of the sludge and pulverized coal are shown in Table 1 and Table 2, respectively.

Pre-treatment of the sludge. The dewatered sludge was firstly stirred by high-speed agitator and the rotate speed is 240 r/min, thus the viscous sludge was violently cut, which realized liquefaction of sludge and increase of fluidity. At the same time, by means of the high-speed agitation, the sludge particles and the stirring cutter can collided and rubbed each other at a high speed, thus breaking up the sludge capillary water and squeezing out the molecular water closely wrapped by sludge fibers. Before the stirring, the addition of potassium sodium tartrate (accounts for 1.2-1.6% of sludge quality) to the sludge further improves fluidity of the sludge.

Micro-bubble excitation treatment. Different contents of SDS powder were added to the tested sludge, and then quickly stirred (180 r/min) to produce appropriate amount of micro-bubble in the sludge colloids and build a mixture of micro-bubble sludge. In addition, acrylic acid was added as a foam stabilizer in the process of micro-bubble formation.

Sludge conditioning. The obtained sludge was putted into the mixed agitator, and then add sludge drying agent and quicklime, where the adding quantity of the sludge drying agent and quicklime respectively were 5-20% and 1-5% relative to the sludge. The mixture were stirred fully for 5-15 min and the semi-finished sludge was obtained. In here, the sludge drying agent was mixed by the following mass ratio: MgO: $CaSO_4$: $Fe_2(SO_4)_3$ = 3-5: 2-5: 1-3.

The adding of pulverized coal. The above obtained semi-finished sludge was putted into the low-speed agitator, subsequently the sludge with 30-50% of heat value supplement (pulverized coal) was also introduced. Then they were stirred for 10-20 min.

Characterization of samples. The structures of as-synthesized samples were characterized on a DX-2700 bench top X-ray diffractometer (Dandong fangyuan Instrument Co., Ltd.) using Cu-Kα radiation (40kV, 30mA). The scanning rate was 4° min^{-1} with a step of 0.06°. The thermogravimetric analysis (TGA-DSC) was performed on NETZSCH, STA 449F3 using Pt crucible in static air atmosphere. The reaction process was carried out in the range of 33-813 ℃ with a heating rate of 10 °C/min.

RESULTS AND DISCUSSION

Mechanism Analysis of micro-bubble drying. The main objective of sludge conditioning is to improve solid-liquid separation of sludge. In this study, a certain amount of SDS powder was added before introducing the conditioner to the tested sludge. It can be observed that the mixture continuously produced the micro-bubbles with a diameter of less than 1mm and was accompanied by a certain amount of water precipitation with increasing the SDS powder contents. When the mass ratio of SDS and sludge was 0.25, the micro-bubble structure of mixture remained stable in the process of resting 20 to 30 min, that is to say, only a few micro-bubble structure were broken. The water content of sludge solid decreased from 77.9% to ca. 55.1%. After that, the water content gradually becomed flat and then increased slowly. The detailed procedure is shown in Fig. 1.

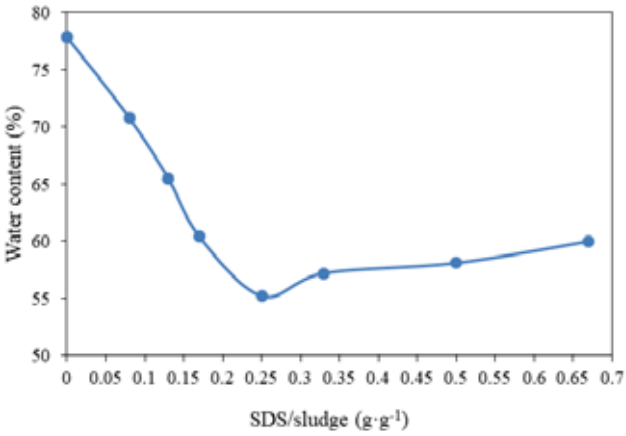

FIGURE 1
Water content of the sludge in different proportions of SDS/ sludge

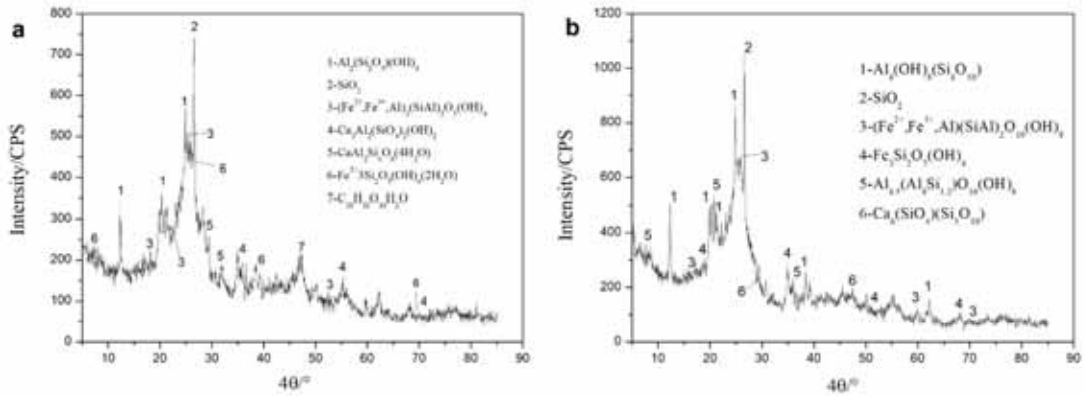

FIGURE 2
XRD patterns of the as-synthesized samples: (a) SDS/sludge(g·g^{-1})=0.1, (b) SDS/sludge(g·g^{-1})=0.25

Relevant studies have shown that SDS is a commonly used ionic detergent, which can disintegrate the cell membrane and bind the hydrophobic part of the membrane protein and further separate it from the membrane. In addition, high concentration of SDS can also damage the non-covalent bonds of the protein, such as, the ionic bond and hydrogen bond. Moreover, surfactant can not only make large molecules such as proteins and DNA on the surface of the sludge separate from the sludge particles, but also make these substances dissolve in water easily and reduce the interstitial water between the sludge particles, resulting in faster sedimentation rate of the sludge and reduced volume of dewatered sludge. Also, the combination of surfactant and Mg^{2+} can effectively remove the water in sludge [9-10]. Furthermore, the addition of quicklime also can effectively improve the drying rate of sludge. When mass ratio of CaO and wet sludge was 10 g/kg, drying time of the sludge can be shortened by ca. 18.2%. However, as mass of quicklime was increased (exceeding 20 g/kg), the drying rate changed slowly [11].

According to mentioned above, sludge drying is carried out alternately by evaporation and diffusion, therefore, the introduction of SDS and foam stabilizer in high-speed stirring can adequately contact with water in the sludge, which effectively enhances the pore number and evaporation area in the sludge resulting in water rapidly evaporated in the process of diffusion and precipitation. In addition, the drying agent can also make the sludge rapidly produce solid-liquid separation phenomenon and form stable flocculated structure.

Component analysis of sludge in microbubble drying. To analysis the effect of SDS contents on the sludge, the X-ray diffraction was performed and the results are shown in Fig. 2. It can be observed that the main substance in the two mixtures is SiO_2 attributed to extensive existence in nature and relatively stable properties. From Fig. 2a, the sample exists hydrate, namely, coordination crystal water, which is transformed into water molecule and precipitate with the increase of SDS content (Fig. 2b). Moreover, existence of aluminum salt (kaolinite) is related to the addition of aluminum-containing flocculant (introduced to sludge before dehydration and fully mixed with sludge) in the dehydration process of the sludge. The long-train structure of surfactant can promote the formation of excellent adsorption bridging function

between sludge floc, therefore, the adding of SDS improved the settling property of the sludge [12]. In addition, the added quicklime can easily absorb the bound water and presents alkalinity. Subsequently, the hydroxyl silicates reduced the adsorption hydration energy. Thus, the dissolution reaction can be ignored and a relatively stable solid precipitation was formed [13], which further promoted the solid-liquid separation.

Analysis of the sludge-derived fuel (SDF) in micro-bubble excitation. The influence of SDF on heat value. Herein, two sets of tests were designed. The selected sludge samples were from the product after pretreatment (water content is ca. 35%).

(1) The relationship between SDS content and heat value of SDF was researched in the first set of experiment. And the dosage of each component is shown in Table 3.

TABLE 3
The dosage of each component

Samples	Anthracite (g)	Sludge (g)	SDS (g)
SDF1	50	15	0
SDF2	50	15	1.5
SDF3	50	15	3
SDF4	50	15	3.75
SDF5	50	15	5
SDF6	50	15	7.5
SDF7	50	15	10
SDF8	50	15	15

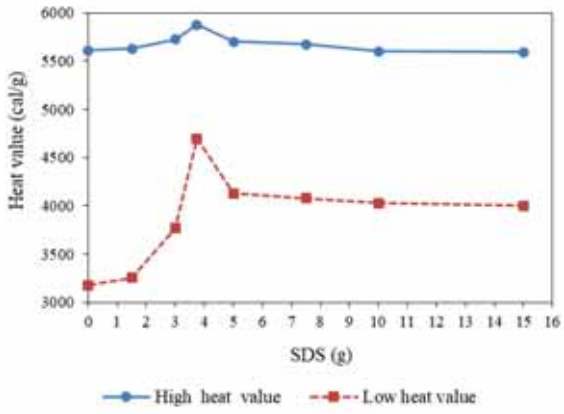

FIGURE 3
Heat values of the SDF in different dosages of SDS.

The different between high heat value and low heat value is that water in fuel combustion products is liquid or gas, that is to say, liquid water and vaporous water are high and low heat value, respectively. The low heat value is equal to the condensation heat of water vapor deducted from the high heat value. The high and low heat values of the tested samples were measured by coal assay and shown in Fig. 3. It can be observed that maximum difference of high heat value between the samples is 283 cal/g and each value is greater than that of pure anthracite. However, the change of low heat value is more obvious which presents high before low and tends to be flat with the addition of SDS. Furthermore, sample 4 shows the maximum high and low heat value. Compared with the low heat value, it is about 47% higher than that of the mixture of coal and sludge without adding of the SDS.

According to the mentioned above, the adding of SDS can make bound water of the sludge convert water molecule which is separated from the sludge by evaporation. In addition, hydroxyl silicates (kaolinite) of mixture will occur decomposition reaction in high temperature due to the existence of SiO_2 and Al_2O_3, and external hydroxyl (constitution water) and internal hydroxyl (interlayer water) are removed gradually, further transformed into $Al_2O_3 \cdot SiO_2$ [14-17]. The water in the two parts forms steam, which has a certain influence on high heat value, and further verifying that SDS has an excellent dehydrating effect on the sludge.

For low heat value, the micro-bubble structure constructed by the SDS on the mixture changes the original chaotic state of sludge, thereby, increasing the internal surface area and the contact amount of oxygen. The micro-bubble structure is beneficial to fully contact between the coal powder and sludge particles in stirring, then forming a uniform mixed fuel, which will have a positive effect on the improvement of low heat value. The introduction of excessive SDS content results in the insufficient dissolution, and the amount of micro-bubble and low heat value gradually decrease.

(2) The changes of the low heat value for the same SDS content and different coal sources were investigated in the second set of experiment. And content of each component is shown in Table 4. The obtained heat value of each mixture by coal assay is also presented in Fig. 4.

From Table 4, the heat values decrease in the order of different coal resources (bituminous > anthracite > coking coal), which is consistent with that of sludge-derived fuel. More importantly, heat value of the sludge-derived fuel is far larger than that of the pure sludge (Fig. 4). It indicates that the mixture can promote each other in the process of pyrolysis. The heat value of coal determines heat value of the derived fuel under the same mass for each component.

TABLE 4
Content of the main components for different SDF

Samples	Coal (g)	Sludge (g)	SDS (g)
SDF1	Anthracite 50	15	3.75
SDF2	Coking coal	15	3.75
SDF3	Bituminous 50	15	3.75

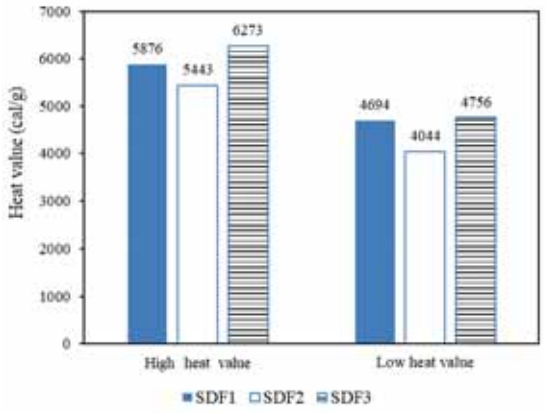

FIGURE 4
Comparison of heat value of SDF for different coal sources

Thermogravimetric analysis of the derived fuel. Heating rate is one of the main influence factors for biomass pyrolysis characteristics, and it has important influence on yield and characteristics of product. When the rate was in the range of 10-40 °C/ min, it can be considered that heating rate had litter effect on the pyrolysis characteristics of sludge [18]. The TG-DTG-DSC curves of the four fuels were explored in the heating rate of 10 °C/min under air atmosphere (Fig. 5, 6). It can be found from TG-DTG that combustion process of the tested sludge is mainly divided into four stages, and the weight loss ratio for each stage decreases in the sequence: 2 > 3 > 1 > 4. The temperature range in the first stage is 35-200 °C, corresponding to the precipitation process of the free water and the combined water in the sludge. The second stage in the range of 200-380 °C is attributed to the precipitation and combustion of volatile (organic matter), and the weight loss ratio is about 30%, which is the main control stage in the combustion process. Furthermore, the maximum combustion rate occurs at around 280 °C. The temperature of 380-590 °C is related to carbonization of unburned organic matter and combustion of fixed carbon. The last stage in the temperature of more than 590 °C is mainly due to the precipitation and decomposition of inorganic salts [19-20].

For other three fuels, the combustion process is approximately the same, and the weight loss ratio is the largest for combustion of pure coal, namely, the reducing quantity is optimal. Compared to without adding SDS fuel (SDF2), the introduction of the SDS (SDF1) increases rapidly the weight loss ratio and rate of the fuel in the range of 200-250 ℃. The reason is that the combustion reaction releases CO and CO_2 as increasing the temperature due to the melting point of SDS (ca. 200 ℃) leading to decrease of the mass. Moreover, the weight loss rate of SDF1 is higher than that of SDF2 in the range of 450-690 ℃ (Fig. 5b), and the weight loss ratio is also accord with the same rule in the range of 550-650 ℃ (Fig. 5a).

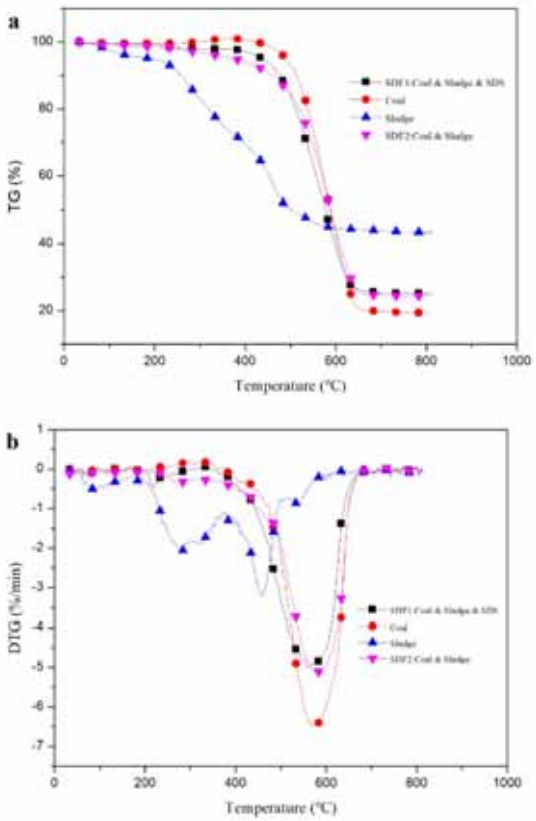

FIGURE 5
TG and DTG curves of the four fuels

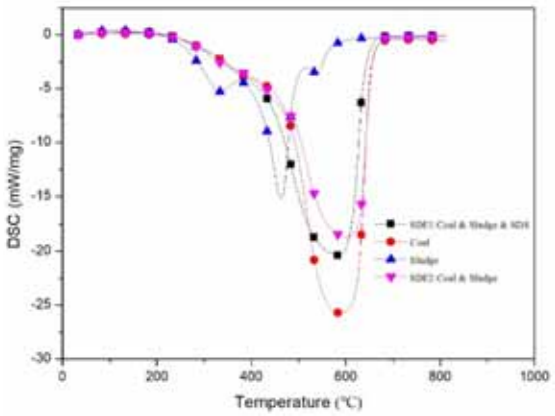

FIGURE 6
DSC curves of the four fuels

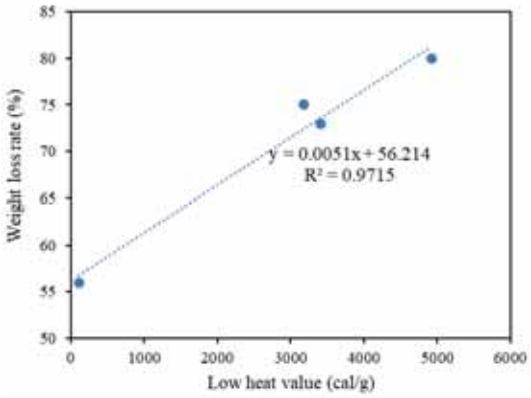

FIGURE 7
The relation curve of weight loss ratio and low heat value

From Fig.6, DSC curve of sludge pyrolysis exists two exothermic peaks, and the peak area of the second peak is higher than that of the first peak. Namely, heat release of the third stage is larger than that of the second stage. The exothermic peaks for other three fuels appear at ca. 590 ℃ and the exothermic peak of SDF1 is higher than that of SDF2, which is consistent with the sequence of their weight loss ratio and low heat value. In addition, the low heat value of fuel is positively correlated with its weight loss ratio (the fitting index is 0.9715) (Fig. 7).

CONCLUSION

This work focuses on the two difficult problems for sludge incineration: high water content and low heat value. The method of adding SDS to sludge was used to analyze the change of the sludge water content and the composition as well as combustion characteristics of the derived fuel mixed with coal. The results are as follows:

(1) The micro-bubble structure was formed by the addition of SDS, which is beneficial to evaporation of water and contact between pulverized coal and sludge particles as well as the contact amount of oxygen. It has positive effect on sludge drying and combustion heat value of mixture.

(2) When the mass ratio ($g \cdot g^{-1}$) of SDS and sludge is 0.25, water content of the sludge decreases from 77.9% to 55% and subsequently tends to be flat.

(3) Dosage of SDS has a certain influence on SDF component. That is to say, when the adding amount of SDS is too little, there are more hydrates existing in the SDF. And the water molecules in the hydrate are easy to detach from the SDF under heating conditions and reduce the heat value of the SDF.

(4) When the amount of coal remains unchanged and SDS/sludge（$g \cdot g^{-1}$）is 0.25，the low heat value of the SDF can increase by about 47%.

(5) The low heat value of fuel is positively correlated with its weight loss ratio, namely, the adding of SDS enhances the low heat value of sludge-derived fuel and promotes the reducing quantity of fuel in a certain control range of temperature.

ACKNOWLEDGEMENTS

This project was supported by Scientific and Technological Innovation Programs of Higher Education Institutions in Shanxi. (No.2017125).

REFERENCES

[1] Wang, X.T., Li, Q., Mu, X.J., Xu, B., Lan, W.J., Liu. C.M. (2014) Experimental Study of Pyrolytic Characteristics of Sewage Sludge and Coal. Power System Engineering. 4(1-2), 10.

[2] Arenillas, A., Rubiera, F., Pevida, C., Pis, J.J. (2001) A comparison of different methods for predicting coal devolatilisation kinetics. Journal of Analytical and Applied Pyrolysis. 58(2), 685-701.

[3] Shao, L.M., He, P.J. (2000) Technology and application analysis of thermal drying treatment for municipal sewage sludge. Shanghai: Shanghai Science and Educational Literature Press. 268.

[4] Ni, C.L., Zhang, F.M., Guo, R.G., Liu, M., Huang. F., Liu. F.X. (2010) An Introduction to Sludge Drying Technology. Drying Technology and Equipment. 2, 74-78.

[5] Mehrdadi, N., Joshi, S., Nasrabadi, T., Hoveidi, H. (2007) Application of Solar Energy for Drying of Sludge from Pharmaceutical Industrial Waste Water and Probable Reuse. International Journal of Environmental Research. 1(1), 42-48.

[6] Zhang, G.M., Wu, M.S., Zhang, W.H., Zhang, X.H. (2003) Study of Ultrasonic Treatment of Sludge. Urban Environment and Urban Ecology. 12(6), 258-259.

[7] Menéndez, J., Inguanz, M., Pis, J.J. (2002) Microwave-induced pyrolysis of sewage sludge. Water Research. 36,3261-3264.

[8] Deng, W.Y., Li, X.D., Yan, J.H., Wang, F., Chi, Y., Cen, K. (2011) Moisture distribution in sludges based on different testing methods. Journal of Environmental Sciences-China. 23(5), 875-880.

[9] Zhai, Z.H., Wang, X.Z., Ding, M.X. (2011) Cell Biology. Fourth Edition. Beijing: Higher Education Press, 61.

[10] Chen, Y.G., Yang, H.Z., Wu, G.B., Gu, G.W. (2000) Surfactant Improving Activated Sludge Dewaterability and Its Mechanism. Environmental Science. 21(5), 97-100.
[11] Wang, Z., Ma, X.Q., Peng, X.W., Liao, Y.F., Xu, Z.B., Hu, S.H. (2016) Microscopic study on CaO improving dryness of dyeing sludge based on directional random walk method. Renewable Energy Resources. 34(3), 462-468.
[12] Lu, W., Zhang, D.F., Hu, K.L., Wang, P.P. (2008) Effect and mechanism of cationic surfactants on sludge dewaterability. Environmental Chemistry. 27(4), 444 -448.
[13] Wu, H.H., Liu, P.H., Zhang, Q.Y., He, G.P. (2005) Mechanisms of Adsorption of Heavy Metal Ions on Kaolinite and Their Solution as a Function of pH. Geological Journal of China Universities. 11(1), 85-91.
[14] Zhang, Y.Y., Yang, F.L., Cheng, F.Q. (2015) Study on Kaolinite Dehydroxylation Characteristic and Kinetics in coal gangue. Coal Conversion. 38(3), 78-81.
[15] Ptáček, P., Šoukal, F., Opravil, T., Havlica, J., Brandštetr, J. (2011) The kinetic analysis of the thermal decomposition of kaolinite by DTG technique. Powder Technology. 208(1), 20-25.
[16] Ptáček, P., Šoukal, F., Opravil, T., Nosková, M., Havlica, J., Brandštetr, J. (2010) The non-isothermal kinetics analysis of the thermal decomposition of kaolinite by Effluent Gas Analysis technique. Powder Technology. 203(2), 272-276.
[17] Ptáček, P., Kubátová, D., Havlica, J. (2010) Isothermal kinetic analysis of the thermal decomposition of kaolinite: The thermogravimetric study. Thermochimica Acta. 501(1), 24-29.
[18] Chang, F.M., Wang, Q.B., Wang, K.J. (2015) Thermogravimetric characteristics and kinetic analysis of co-pyrolysis of sewage sludge and coal. Chinese Journal of Environmental Engineering. 5, 2412-2418.
[19] Liu, J.Y., Fu, J.W., Sun, S.Y. (2016) Co-combustion of various sources of sludge and its combustion performance. Acta Scientiae Circumstantiae. 36(3), 940-952.
[20] Xiong, S.J., Zhang, B.P., Yu, D.K. (2011) Study on pyrolysis kinetics of dried and wet sewage sludge. Journal of Huazhong University of Science and Technology. 2, 124-128.

Received: **03.09.2018**
Accepted: **24.02.2019**

CORRESPONDING AUTHOR

Chi Zhang
College of Environmental Science and Engineering,
Taiyuan University of Technology,
Taiyuan, 030024 – China

e-mail: allstep@163.com

© by PSP Volume 28 – No. 4/2019 pages 2530-2538 Fresenius Environmental Bulletin

AN *IN VITRO* STUDY OF BIOCHEMICAL CHARACTERIZATION AND AMELIORATING EFFECT OF POLYETHYLENE GLYCOL AGAINST CD STRESS IN SUGARCANE

Umair A Khan*, Aamir Ali

Department of Botany, University of Sargodha, Sargodha, Pakistan

ABSTRACT

Polyethylene glycol is considered as an important antioxidant which plays important role in defence mechanisms of plants. The ameliorating role of PEG against Cd stress under *in vitro* conditions was studied in callus cultures of Saccharum sp. (cvs. HSF 240). Callus induction and proliferation was carried out on MS medium supported with 2, 4-D and NAA either alone or in combination with BAP and Kinetin. Cd stress (0.1-0.5 mM) was applied to well proliferated calli. By increasing the concentration of Cd stress, average weight of callus was decreased and complete necrosis occurred at 0.5 mM after 30 days of Cd stress. Specific activities of catalases, peroxidises, PAL, total soluble protein contents and total amino acid contents were maximum at 0.4 mM of Cd. Well proliferated calli were pre-treated with 1% PEG for 24 hours to combat the effect of Cd stress. PEG minimize the effect of Cd stress on average callus weight, specific activities of catalases, peroxidises, PAL, total amino acid contents, total soluble protein contents. At higher concentration of Cd stress (0.4mM), PEG failed to show ameliorating effect.

KEYWORDS:
Polyethylene glycol, Cadmium, Sugarcane callus, *in vitro* cultures, abiotic stress

INTRODUCTION

Heavy metal stress has created major environmental issues because of their adverse biological impact on environment and life. Once entered in the soil, they deteriorate the quality of soil [1]. Different metals up to certain limit play a crucial part in plant growth and development but after that they become lethal and intrude with morphological, physiological and biochemical processes of plant that may result in stunted growth, changes in structure, reduced accumulation of dry matter and also disturb the level of antioxidants [2]. The way heavy metals effect plant growth depends upon certain factors like environmental conditions, pH and plant species [3]. Essential or nonessential metal ions in high quantity directly affect metal-sensitive enzymatic system that leads to death of plant [4]. Among various heavy metals, Cd has been reported to have intense and incessant effects on plant [5]. Due to water soluble ability, its uptake through plants root system is quite easy. Cadmium affects the plant metabolism by the production of reactive oxygen species (ROS) [6] that results in oxidative stress [7] which ultimately leads to genetic, physiological or biochemical disorders [8]. Cd has been reported to have acute and persistent effects on sugarcane crop [5]. About 2% decrease in sugarcane yield each year due to Cd stress has been reported [9] in Pakistan. To solve the problem of Cd stress that effect yield, use of different ameliorators in last few years have emerged as an option. Among different ameliorants, Polyethylene glycol (PEG) has been reported to minimize the effects of heavy metal stress. Field experiments need a complete crop cycle and two year data, however *in vitro* techniques provide an alternative option of study in minimum possible time. In present study *in vitro* grown cells of sugarcane variety HSF-240 were pre-treated with PEG and then brought under different concentrations of Cd stress.

MATERIALS AND METHODS

Plant Material. The explants of sugarcane variety, HSF-240 were obtained from Botanical Garden, Department of Botany, University of Sargodha. Explants were washed with running tap water and were then surface sterilized with 75 % ethanol for 5 minutes to avoid contamination as new whorl of leaves are well wrapped inside old leaves and are naturally sterilized therefore any further treatment for sterilization was not required.

Callus Induction. Explants were inoculated on MS [10] medium supplemented with varying concentration of auxins and cytokinins either alone or in combination with each other for callus induction. Cultures were kept in growth room at 16 h

light (from fluorescent light tubes) with light intensity of 2000-3000 lux and 8 h dark period.

Cadmium stress treatment and PEG pre-treatment. In present investigation, in first set of experiment *in vitro* grown calli were subjected to different concentrations of Cd stress ranging from 0.1-0.5mM while in other set of experiment *in vitro* grown cells were pre-treated with PEG and then brought under same concentration of Cd stress. Data was compared to check the effect of PEG and then biochemical investigation of these treatments was carried out.

Biochemical Analysis. Quantitative analysis for total soluble proteins contents [11], total amino acid contents [12], specific activity of PAL [13], catalases and peroxidises [14] were studied both for PEG treated and untreated calli under Cd stress.

RESULTS AND DISCUSSION

Callus induction. For callus induction, MS medium was supplemented with different concentrations of 2, 4-D and NAA either alone or in combination with BAP and kinetin. Data was collected after 55 days of inoculation. When 2, 4-D was used alone at lower concentration i.e. 5 µM in MS medium, 54% callus induction was obtained after 55 days of callus induction with an average callus weight of 0.25 g. By increase in concentration of 2, 4-D, rate of callus induction was increased. Best results were obtained at 15 µM of 2, 4-D where 86% cultures exhibited callus induction with an average callus weight of 0.98 g per culture vial (Fig. 1, 2). Data presented in table 1 shows that further increase in concentration of 2, 4-D in MS medium became toxic and the rate of callus induction was decreased i.e. at 20 µM the rate of callus induction was 68% with average callus weight of 0.55 g. Minimum result of callus induction was recorded when 2, 4-D was used in combination with BAP (5 µM 2, 4-D+10 µM BAP) i.e. 0.22gm after 55 days of inoculation. Demonstration of importance of 2, 4-D was carried out and it was reported that 2, 4-D proved to be best to induce callus induction from newly formed leaves but at higher concentration i.e. 3.5 mg/l [15].

Ameliorating effect of PEG on callus growth under Cd stress. Data presented in table 2 shows that in control, average weight of 70 days old callus was 1.23 g. After 15 days of treatment with 0.1, 0.2, 0.3, 0.4 and 0.5 mM Cd, weight of callus (70 days old) was decreased to 1.10gm, 0.80gm, 0.45gm, 0.25gm and 0.11gm respectively. However in cultures pre-treated with PEG the weight of callus was 7.27%, 5% and 2.22% higher as compared to cultures without pre-treatment under 0.1, 0.2 and 0.3mM Cd stress. At 0.4 and 0.5mM Cd stress, PEG failed to combat the stress of Cd.

TABLE 1
Effect of different hormones on callus growth and proliferation

Sr. No	Medium composition	Conc. (µM)	No. of test tubes showing callus proliferation	%age of callus proliferation	Callus age (Days)	Fresh weight of callus (g)
01	MS + 2,4- D	5 µM 2,4- D	5.4±0.8^{e}	54	55	0.25±0.09^{ef}
		10 µM 2,4- D	7.4±0.489^{bc}	74	55	0.57±0.12^{cd}
		15 µM 2,4- D	8.6±0.8^{a}	86	55	0.98±0.20^{a}
		20 µM 2,4- D	6.8±0.74^{cd}	68	55	0.79 ±0.08^{b}
02	MS + 2, 4-D + BAP	5 µM 2, 4-D + 5 µM BAP	5.8±0.74^{de}	58	55	0.42±0.04^{de}
		10 µM 2, 4-D+5 µM BAP	6.8±0.74^{cd}	68	55	0.54±0.14^{cd}
		15 µM 2, 4-D+5 µM BAP	8.2±0.4^{ab}	82	55	0.77±0.20^{b}
		20 µM 2, 4-D+5 µM BAP	6.2±0.4^{cd}	62	55	0.63±0.11^{bc}
		5 µM 2, 4-D+10 µM BAP	5.4±0.8^{e}	54	55	0.22±0.04^{f}
		10 µM 2, 4-D+10 µM BAP	7.2±0.74^{c}	72	55	0.42±0.08^{de}
		15 µM 2, 4-D+10 µM BAP	8.2±0.74^{ab}	82	55	0.67±0.14^{bc}
		20 µM 2, 4-D+10 µM BAP	6.8±0.5^{cd}	68	55	0.55 ±0.07^{cd}
03	MS+NAA+ Kinetin	5 µM NAA+5 µM BAP	5.2±0.74^{e}	52	55	0.32±0.10^{ef}
		10 µM NAA+5 µM BAP	6.8±0.74^{cd}	68	55	0.36±0.12^{ef}
		15 µM NAA+5 µM BAP	5.4±0.48^{e}	54	55	0.40±0.05^{def}
		20 µM NAA+5 µM BAP	5.2±0.4^{e}	52	55	0.30±0.09^{ef}
		5 µM NAA+10 µM BAP	5.4±0.48^{e}	54	55	0.24±0.06^{ef}
		10 µM NAA+10 µM BAP	6.6±0.48^{cd}	66	55	0.30±0.10^{ef}
		15 µM NAA+10 µM BAP	5.2±0.4^{e}	52	55	0.35±0.07^{ef}
		20 µM NAA+10 µM BAP	5±0.63^{e}	50	55	0.26±0.06^{ef}
LSD (0.05)			**0.916**			**0.157**

Mean followed by different letters in the same column differ significantly at P=0.05 according to Duncan's new multiple range tests.

TABLE 2
Effect of pretreatment of Polyethylene Glycol (PEG) on callus growth and proliferation

Cd. conc. (mM)	No. of test tubes inoculated	Fresh weights of 70 days old callus cultures (g) under Cd stress			Fresh weights of 85 days old callus cultures (g) under Cd stress		
		Without pretreatment of PEG	After pretreatment of PEG	% increase/ decrease	Without pretreatment of PEG	After pretreatment of PEG	% increase/ decrease
Control	10	1.23 ± 0.28^{a}	1.242±0.55^{a}	0.81	1.25 ± 0.55^{a}	1.25±0.44^{a}	00
0.1	10	1.10 ± 0.27^{a}	1.18±0.50^{a}	7.27	1.08 ± 0.58^{a}	1.14±0.29^{ab}	5.5
0.2	10	0.80 ± 0.25^{ab}	0.84±0.30^{ab}	5	0.77 ± 0.43^{ab}	0.81±0.31^{b}	5.5
0.3	10	0.45 ± 0.10^{bc}	0.46±0.22^{bc}	2.22	0.41 ± 0.23^{bc}	0.39±0.25^{c}	-4.8
0.4	10	0.25±0.05^{bc}	0.24±0.06^{c}	-4	0.22± 0.06^{bc}	0.21±0.07^{c}	-4.5
0.5	00	0.11 ± 0.02^{c}	0.10±0.03^{c}	-9.09	---	---	00
LSD		**0.566**	**0.505**		**0.561**	**0.403**	

Mean followed by different letters in the same column differ significantly at P=0.05 according to Duncan's new multiple range tests.

TABLE 3
Effect of pretreatment of Polyethylene Glycol (PEG) on total amino acid contents of callus cultures

Cd Conc. (mM)	Total amino acid contents of 70 days old callus cultures (mg/g callus) under Cd stress			Total amino acid contents of 85 days old callus cultures (mg/g callus) under Cd stress		
	Without pretreatment of PEG	After pretreatment of PEG	% increase/ decrease after pretreatment	Without pretreatment of PEG	After pretreatment of PEG	% increase/decrease after pretreatment
Control	21.20±0.78^{e}	22.59±0.52^{c}	5.65	27.25±0.66^{e}	24.98±0.70^{d}	3.65
0.1	30.25±0.83^{d}	35.02±0.54^{b}	15.76	33.83±0.95^{c}	36.48±0.40^{b}	7.83
0.2	36.43±0.92^{b}	37.18±0.51^{a}	2.05	43.53±0.74^{a}	45.38±0.43^{a}	4.24
0.3	40.94±0.84^{a}	42.23±0.88^{a}	3.15	36.49±0.96^{b}	36.82±0.58^{b}	0.90
0.4	33.51±0.83^{c}	34.55±0.84^{b}	3.10	30.7±0.70^{d}	30.84±0.99^{c}	0.45
0.5	20.07±0.51^{e}	22.40±0.80^{c}	11.60	00	---	---
LSD	**2.46**	**2.38**		**2.29**	**2.719**	

Mean followed by different letters in the same column differ significantly at P=0.05 according to Duncan's new multiple range tests.

When the duration of Cd stress under *in vitro* conditions was prolonged to 30 days, it was noticed that after 0.1, 0.2, 0.3, 0.4 mM stress of Cd, the weight of the callus (85 days old) was 1.08 gm, 0.77 gm, 0.41 gm and 0.22 gm respectively (Fig. 3, 4). Complete necrosis occurred at 0.5mM stress of Cd (Fig. 5). Pre-treatment of calli with PEG before 30 days of Cd stress resulted in better response of callus growth i.e. calli pre-treated with PEG when brought to 0.1 and 0.2mM stress of Cd resulted in 5.5% increase in callus weight as compared to untreated calli under Cd stress while at 0.3 and 0.4mM concentration of Cd, pre-treatment of PEG failed to show any better response on growth (Fig. 6, 7).

The reduced growth can be explained by the fact that much of the available energy for cell or tissue metabolism could have been used against stress [16]. Stress/ toxicity generated by Cd disturbs the physiological processes of plant which result in the production of reactive oxygen species [17]. High concentration of Cd became toxic leading to reduction of growth and necrosis of cells/ tissues (Fig. 05). A group of scientists also figured out that at higher stress of Cd under *in vitro* conditions, rate of callus growth and proliferation is drastically affected leading to its necrosis [18]. Raza et al. (2013) reported that high level of Cd directly affects morphological attributes and growth pattern.

To combat the effect of Cd stress, certain osmoticums like salicylic acid (SA), ethylene (ET), Polyethylene glycol etc. have been reported to be used [19]. These play an important role in cell by reprogramming the genetic machinery that results in adequate defence reactions and an increase in plant tolerance to minimize the biological damage caused by the stress [20]. Such osmoticums are widely utilized by cell in their metabolism for synthesis of certain proteins. These proteins activate biological defence mechanism [21] by facilitating cell division and expansion [22]. In present study, pre-treatment of Polyethylene glycol resulted in less necrosis and increased growth of callus (Table 2). Successful demonstration regarding ameliorating effect of PEG against heavy metal stress in tomato has also been reported [23].

Effect of PEG pre-treatment on total amino acid contents. Data presented in table 3 reflects the effect of Cd stress on total amino acid contents of sugarcane calli. In control total amino acid contents were 21.20 mg/g of callus. As a result of 15 days of Cd stress (0.1mM, 0.2mM, 0.3mM, 0.4mM and

0.5mM concentration) total amino acid contents were 30.25, 36.43, 40.94, 33.51 and 20.01 mg/g of callus after 15 days of stress. A slight increase in the total amino acid contents after Cd stress was recorded when calli were pre-treated with PEG i.e. 15.76%, 2.05%, 3.15%, 3.10% and 11.60% higher total amino acid contents after 0.1, 0.2, 0.3, 0.4 and 0.5mM stress of Cd.

After prolonged stress of 30 days, total amino acid contents were 33.83, 43.53, 36.49, 30.7 mg/g of callus at 0.1mM, 0.2mM, 0.3mM and 0.4mM of Cd stress. In this case pre-treatment of PEG resulted in an increase in total amino acid contents i.e. an increase of 7.83%, 4.24%, 0.90% and 0.45% over calli without pre-treatment after 0.1, 0.2, 0.3 and 0.4mM stress of Cd.

In present study, pre-treatment of PEG resulted in an increase of total amino acid contents (Table 3). PEG enhances the uptake of nitrate ions [24] which are converted in to nitrite with the help of nitrate reductase. Many other enzymes convert nitrite into ammonium ion. Ammonium ion is then incorporated into α-ketoglutarate which forms glutamate or glutamine. Nitrate reductase performs important role as it catalyzes the first step in the amino acid synthetic metabolic pathway by up taking nitrate ions. Therefore, the pre-treatment of PEG in present study might be the reason which enhanced the uptake of nitrate ions that result in increase of total amino acid contents.

Effect of PEG pre-treatment on total soluble protein contents. It is obvious from table 4 that in control, total soluble protein contents were 1.01 mg/g of tissue. After 15 days (70 days old calli) of Cd stress i.e. 0.1mM, 0.2mM, 0.3mM, 0.4mM and 0.5mM concentration, total soluble protein contents were 0.177, 0.143, 0.142, 0.140 and 0.153 mg/g of tissue. Pre-treatment of PEG resulted an increase of 3.38%, 9.79%, 0.70%, 2.14% and 5.88% of total soluble protein respectively.

In case of 30 days stress i.e. 85 days old calli, similar trend of decrease in total soluble protein contents was recorded as was after 15 days of Cd stress i.e. 0.25, 0.17, 0.17 and 0.16 mg/g of tissue after 0.1mM, 0.2mM, 0.3mM and 0.4mM of Cd stress. Pre-treatment of PEG ameliorated effect of Cd stress but upto certain limit i.e. at 0.1, 0.2 and 0.3mM stress of Cd, 6.8%, 70.58% and 29.41% increase in total soluble proteins contents was recorded as compared to untreated calli. At higher concentration of Cd i.e. 0.4mM, pre-treatment of PEG failed to ameliorate the effects of Cd.

As far as total soluble protein contents in present study are concerned, they were found to be increased after PEG treatment (Table 4). Pre-treatment of PEG itself can also be a possible reason of increase in total soluble protein content. PEG is a polymeric osmoticum which is relatively non-toxic and can be a source of osmotic stress [25]. Stressors can increase the total soluble protein contents by enhancement in the production of stress related proteins [26]. The introduction of such proteins (generally referred to as stress proteins) could have resulted in an increase in the overall quantity of soluble protein contents in the plant tissue exposed to stress [27].

Effect of PEG pre-treatment on specific activity of phenylalanine ammonium lyase (PAL). Data presented in Table 5 depicts the effects of 15 days stress of Cd for the specific activity of PAL. In control, specific activity of PAL was 0.035 units/mg of proteins. Specific activity of PAL was 0.043, 0.056, 0.065, 0.070 and 0.065 units/mg of proteins after 0.1mM, 0.2mM, 0.3mM, 0.4mM and 0.5mM stress of Cd. Pre-treatment of PEG resulted in minimizing the stress of Cd i.e. an increase of 18.60%, 23.21%, 13.84%, 15.71% and 7.69% in specific activity of PAL was recorded after 0.1, 0.2, 0.3, 0.4 and 0.5mM Cd stress.

TABLE 4
Effect of pretreatment of Polyethylene Glycol (PEG) on total soluble proteins contents

Cd Conc. (mM	Total soluble protein contents of 70 days old callus cultures (mg/g callus) under Cd stress			Total soluble protein contents of 85 days old callus cultures (mg/g callus) under Cd stress		
	Without pre-treatment of PEG	After pretreatment of PEG	% increase/ decrease after treatment	Without pretreatment of PEG	After pretreatment of PEG	% increase/ decrease after treatment
Control	1.01±0.023^{a}	0.93±0.36^{a}	-4.34	0.69±0.19^{a}	0.034±0.096^{a}	-16.21
0.1	0.177±0.004^{b}	0.183±0.037^{b}	3.38	0.25±0.04^{b}	0.267±0.04^{ab}	6.8
0.2	0.143±0.022^{b}	0.157±0.080^{b}	9.79	0.17±0.014^{b}	0.29±0.16^{ab}	70.58
0.3	0.142±0.027^{b}	0.143±0.06^{b}	0.70	0.17±0.013^{b}	0.22±0.10^{ab}	29.41
0.4	0.140±0.062^{b}	0.143±0.024^{b}	2.14	0.16±0.069^{b}	0.12±0.05^{ab}	-27.27
0.5	0.153±0.028^{b}	0.162±0.030^{b}	5.88	00	00	
LSD	**0.10**	**0.480**		**0.26**	**0.299**	

Mean followed by different letters in the same column differ significantly at P=0.05 according to Duncan's new multiple range tests.

TABLE 5
Effect of pretreatment of Polyethylene Glycol (PEG) on specific activity of Phenylalanine ammonium lyase of callus

Cd Conc. (mM)	Specific activity of PAL of 70 days old callus cultures (units/mg of protein) under Cd stress			Specific activity of PAL of 85 days old callus cultures (units/mg of protein) under Cd stress		
	Without pretreatment of PEG	After pretreatment with PEG	% increase/ decrease	Without pretreatment of PEG	After pretreatment with PEG	% increase/ decrease
Control	0.035±0.01^{c}	0.047±0.004^{b}	34.28	0.039±0.008^{b}	0.039±0.005^{d}	00
0.1	0.043±0.007^{bc}	0.051±0.004^{b}	18.60	0.048±0.005^{b}	0.051±0.005^{c}	6.25
0.2	0.056±0.01^{abc}	0.069±0.01^{a}	23.21	0.096±0.133^{a}	0.10±0.027^{b}	4.16
0.3	0.065±0.006^{abc}	0.074±0.005^{ab}	13.84	0.097±0.012^{a}	0.099±0.003^{ab}	2.06
0.4	0.070±0.19^{a}	0.081±0.010^{ab}	15.71	0.065±0.010^{ab}	0.087±0.003^{a}	33.84
0.5	0.065±0.11^{ab}	0.070±0.007^{ab}	7.69	00	00	00
LSD	**0.028**	**0.039**		**0.033**	**0.012**	

Mean followed by different letters in the same column differ significantly at P=0.05 according to Duncan's new multiple range tests

TABLE 6
Effect of pretreatment of Polyethylene Glycol (PEG) on specific activity of peroxidases of callus cultures

Cd Conc. (mM)	Specific activity of peroxidases of 70 days old callus cultures (units/mg of protein) under Cd stress			Specific activity of peroxidases of 70 days old callus cultures (units/mg of protein) under Cd stress		
	Without pretreatment of PEG	After pretreatment of PEG	% increase/ decrease	Without pretreatment of PEG	After pretreatment of PEG	% increase/ decrease
Control	0.5 ±0.242^{b}	0.4±0.19^{b}	-20	0.069 ±0.044^{ab}	0.071±0.014^{b}	2.89
0.1	0.983 ±0.282^{ab}	1.04±0.07^{ab}	5.79	0.99 ±0.346^{ab}	1.09±0.15^{ab}	10.10
0.2	1.413 ±0.288^{ab}	1.423±0.40^{ab}	0.70	1.43 ±0.405^{ab}	1.77±0.14^{a}	23.77
0.3	1.566 ±0.251^{ab}	1.676±0.18^{a}	7.02	1.91 ±0.8^{a}	2.05±0.45^{a}	7.32
0.4	1.826 ±0.036^{a}	1.863±0.53^{a}	2.02	1.93±0.52^{a}	1.7±0.74^{a}	-11.91
0.5	1.9±0.575^{a}	1.826±0.55^{a}	-4.73	00	00	00
LSD	**1.089**	**1.145**		**1.396**	**1.125**	

Mean followed by different letters in the same column differ significantly at P=0.05 according to Duncan's new multiple range test

As far as the specific activity of PAL after 30 days of Cd stress is concerned, it was increased gradually up to 0.3mM concentration. At 0.4mM of Cd stress, PAL activity was again decreased to 0.065 units/mg of protein. Pre-treatment of PEG resulted in an increase of 6.25%, 4.16%, 2.06% and 33.84% in specific activity of PAL after 0.1, 0.2, 0.3 and 0.4mM Cd stress.

In present investigation, the specific activity of PAL was also found to be increased by pre-treatment of PEG (Table 5). Phenylalanine ammonia-lyase plays a key role in phenylpropanoid metabolism which produces secondary metabolites that strengthens the defence of plants. As a result of PAL activity, cinnamic acid is produced in phenylpropanoid pathway which provides entry point for synthesis of certain valuable phenolic compounds that strengthen the defence system of plant [28]. Osmoticums like PEG is capable of increasing expression of stress related gene and inducing systemic acquired resistance (SAR) in plant against different type of stresses that stimulate phenolic production in plants [29]. In present study, pre-treatment of PEG might have activated the gene expression related to the specific activity of PAL, enhancing phenolic metabolism to produce antioxidant phenolics and lignin precursors for the purpose to reduce toxic effect of Cd.

Effect of PEG pre-treatment on specific activity of peroxidases. As far as the specific activity of peroxidase after 15 days of Cd stress is concerned, in control it was 0.5 units/mg of proteins while after 0.1mM, 0.2mM, 0.3mM, 0.4mM and 0.5mM stress of Cd, the specific activity of peroxidases was found to be 0.98, 1.41, 1.56, 1.82 and 1.91 units/mg of protein. When calli were pre-treated with PEG and were then brought under 0.1, 0.2, 0.3 and 0.4mM stress of Cd, an increase of 5.79%, 0.70%, 7.02% and 2.02% in specific activity of peroxidises was recorded. At higher concentration of Cd stress i.e. 0.5mM concentration, pre-treatment of PEG failed to suppress the effect of Cd stress (Table 6).

When the stress of Cd was increased to 30 days (85 days old callus), specific activity of peroxidases was recorded as 0.99, 1.43, 1.91 and 1.93 units/mg of proteins after 0.1, 0.2, 0.3 and 0.4mM stress of Cd. Pre-treatment of PEG resulted in better response as compared to calli without its pre-treatment. As a result of PEG pre-treatment, the specific activity of peroxidases of Cd treated calli was 10.10%, 23.77%, 7.32% higher as compared to untreated calli at 0.1mM, 0.2mM and 0.3mM concentration respectively. However at higher concentration of Cd i.e. 0.4mM concentration, pre-treatment of PEG did not affect the specific activity of peroxidises.

Increase in the specific activity of peroxidises was also recorded after pre-treatment of PEG, however at higher concentration, PEG failed to show ameliorating effect i.e. 0.4 and 0.5mM Cd stress (Table 6). Peroxidases (POD) are enzymes that usually oxidize phenolic compounds (defence proteins) which play a crucial role against environmental stresses [30]. Being hydrogen peroxide (H_2O_2) scavengers, peroxidase utilize phenolic compounds to produce phenoxyl radicals by using H_2O_2 as electron donors [31]. Peroxidase participates in lignin biosynthesis and might built up a physical barrier against heavy metals toxicity and other stresses. Increase in specific activity of peroxidases in any kind of stress is often linked with regular incorporation of phenolic compounds within the cell [32]. In present study, due to regular incorporation of phenolics in the cell, it can be suggested that the activity of peroxidases increased to oxidize the phenolic compounds, rendering the toxic effect of Cd stress.

Effect of PEG pre-treatment on specific activity of catalases. It is quite evident from table 7 that in 70 days old calli, the specific activity of catalases was 4.94 units/ml of enzymes in control. After treatment with 0.1, 0.2, 0.3, 0.4 and 0.5mM stress of Cd, the activity of catalases was 5.26, 7.57, 7.90, 7.86 and 7.96 mg/g tissue. However when calli were pre-treated with PEG before bringing under Cd stress, the specific activity of catalases was 7.93, 9.13, 8.5, 8.2 and 8.1 units/mg of proteins which was 50.76%, 20.60%, 7.59%, 4.32% and 1.75% higher as compared calli without pretreatment of PEG.

When Cd stress (0.1-0.5) was prolonged to 30 days under *in vitro* conditions, specific activity of catalases was recorded 4.7, 4.26, 5.2 and 4.16 mg/g tissue at 0.1mM, 0.2mM, 0.3mM and 0.4mM stress of Cd. However after 30 days of pre-treatment with PEG, specific activity of catalases of Cd treated calli was 3.13%, 10.55% and 4.20% higher at 0.1mM, 0.2mM and 0.3mM concentration of Cd while in case of 0.4mM stress, PEG failed to overcome the effect of Cd stress.

Prevention of oxidative damage to cells during stress has been suggested as one of the mechanisms of stress tolerance which can be attributed to enhanced catalase activity [33]. Possible reason of enhanced catalase activity of Cd treated calli in the present study (Table 7) could be the pretreatment of PEG which resulted in the inhibition of several reactive oxygen species [34] by the activation of antioxidant enzymes. Therefore greater catalase activities in calli pre-treated with PEG can be correlated with the ability of this enzyme to detoxify the damaging effects of hydrogen peroxide produced under Cd stress. Keeping this in view, it can be suggested that pre-treatment of PEG trigger few biochemical changes leading to combat heavy metal stress.

TABLE 7
Effect of pretreatment of Polyethylene Glycol (PEG) on specific activity of catalases of callus

Cd Conc. (mM)	Specific activity of catalases of 70 days old callus cultures (units/mg of protein) under Cd stress			Specific activity of catalases of 85 days old callus cultures (units/mg of protein) under Cd stress		
	Without pretreatment of PEG	After pre-treatment of PEG	% increase/ decrease	Without pretreat-ment of PEG	After pre-treatment of PEG	% increase/ decrease
Control	4.94±0.43^{a}	6.46±0.65^{b}	30.76	4.56±0.40^{c}	4.73±0.43^{b}	3.72
0.1	5.26±1.38^{a}	7.93±0.37^{ab}	50.76	5.10±1.003^{bc}	5.26±0.52^{ab}	3.13
0.2	7.57±0.43^{a}	9.13±0.40^{a}	20.60	6.63±0.29^{bc}	7.33±1.50^{ab}	10.55
0.3	7.90±1.14^{a}	8.5±1.11^{ab}	7.59	7.13±0.49^{ab}	7.43±0.67^{ab}	4.20
0.4	7.86±0.82^{a}	8.2±0.67^{ab}	4.32	8.9±1.01^{a}	7.93±1.39^{a}	-10.89
0.5	7.96±0.51^{a}	8.1±0.41^{ab}	1.75	00	00	00
LSD	**2.74**	**2.031**		**2.00**	**2.851**	

Mean followed by different letters in the same column differ significantly at P=0.05 according to Duncan's new multiple range tests.

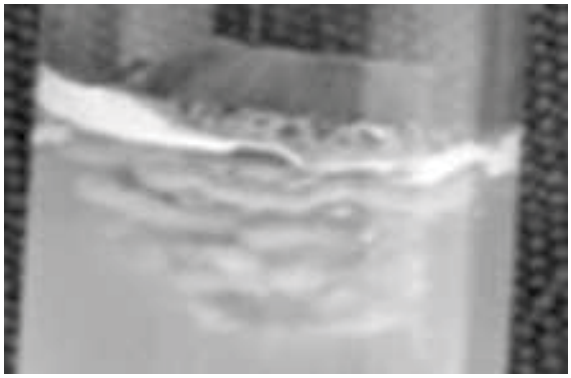

FIGURE 1
Callus formation after 25 days of inoculation on MS medium containing 15 µM 2, 4- D (4X)

FIGURE 2
Callus proliferation after 55 days of inoculation on MS medium containing 15 µM 2, 4-D (3X)

FIGURE 3
Callus proliferation on MS medium supplemented with 0.3mM stress of Cd after 30 days of subculture (4X)

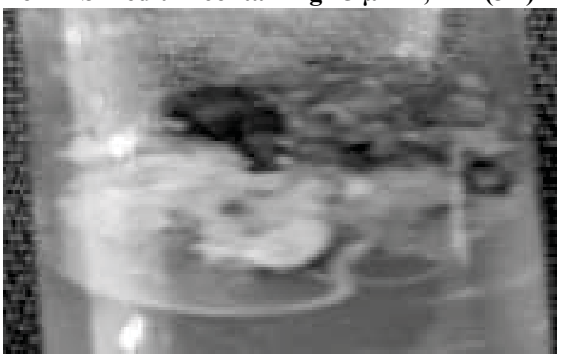

FIGURE 4
Callus proliferation on MS medium supplemented with 0.4 mM stress of Cd after 30 days of subculture (4X)

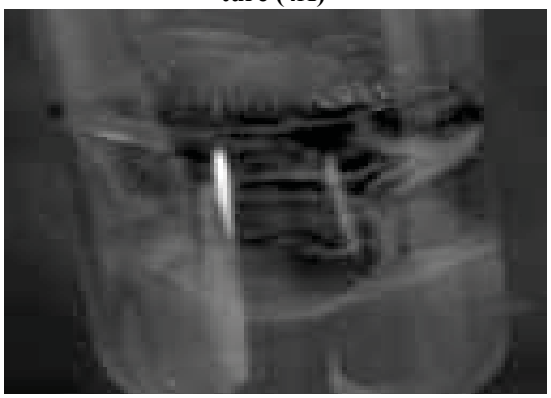

FIGURE 5
Necrosis of callus at 0.5 mM of Cd stress after 30 days of subculture

FIGURE 6
Proliferation of callus pretreated with PEG after 0.3mM stress of Cd (4X)

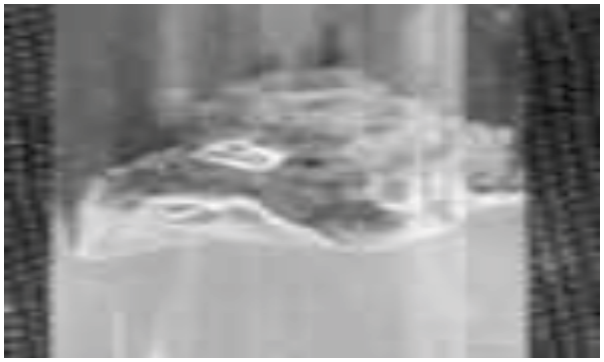

FIGURE 7
Proliferation of callus pretreated with PEG after 0.4mM stress of Cd 4X

REFERENCES

[1] Alloway, B.J. (1995) Heavy Metals in Soils. Blackie Academic and Professional, Glasgow.

[2] Nasim, S.A. and Dhir, B. (2010) Heavy metals alter the potency of medicinal plants. Rev. Environmental Contamination and Toxicology. 203, 139–149.

[3] Cheng, S. (2003) Effects of heavy metals on plants and resistance mechanisms. Environmental Science and Pollution Research. 10(4), 256–264.

[4] John, R. Ahmad, P. Gadgil, K. and Sharma, S. (2008) Effect of cadmium and lead on growth, biochemical parameters and uptake in Lemna polyrrhiza L. Plant Soil and Environment. 54(6), 262–270.

[5] Raza, S.H., Fahad, S. and Maleeha, T. (2013) Screening of Cadmium Tolerance in Sugarcane Using Antioxidative Enzymes as a Selection Criteria. Pakistan Journal of Life and Social Sciences. 34(2), 456-468

[6] Grant, A. and Sheppard, S. (2008) Fertilizer Impacts on Cadmium Availability in Agricultural Soils and Crops. Human. Economics and Risk Assessment. 14(2), 210-228.

[7] Shekhawat, G.S. Prasad, M. Verma, K. and Sharma, A. (2008) Changes in growth, lipid peroxidation and antioxidant system in seedlings of Brassica juncea (L.) czern. under cadmium stress. Biochemistry and Cell Architecture. 8(3), 145-149.

[8] Azevedo, H., Pinto, G. Santos, C. (2005) Cd effects in sunflower: nutritional imbalances in plants and calluses. Journal of Plant Nutrition. 28, 2221-2231.

[9] Qureshi, R.H. (1993) Alternative Strategies for Tackling the Soil Salinity Problem. M.phil Thesis. Department of Soil Science, University of Agriculture, Faisalabad.

[10] Murashige, T. and Skoog, F. (1962) A revised medium for rapid growth and bioassays with tobacco tissue cultures. Physiology of Plants. 15(3), 473-497.

[11] Racusen, D. and Johnston, D.B. (1961) Estimation of protein in cellular material. Nature. 191(4787), 492-493.

[12] Hamilton P.B., and Van-Slyke, D.D. (1943) Amino acids determination with ninhydrin. Journal of Biology and Chemistry. 15(6), 231–233.

[13] Pendharker, M.B. and Nair, P.M. (1975) Induction of phenylalanine ammonia-lyase (PAL) in gamma-irradiated potatoes. Radiation Biology. 15(2), 185-188.

[14] Beers, R. Sizer, I. (1952) A spectrophotometric method for measuring the breakdown of hydrogen peroxidase by catalase. Journal of Biology and Chemistry. 195, 133-140.

[15] Hoque, M.E. Mansfield, J.W. (2004) Effect of genotype and explant age on callus Induction and subsequent plant regeneration from root-derived callus of Indica rice genotypes. Plant Cell Tissue and Organ Culture. 78(3), 217-223.

[16] Iqbal, S.M. and Srivastava, P.S. (2000) *In vitro* micropropagation of *Silybum marianum* L. from various explants and silybin content. Journal of Plant Biochemistry and Biotechnolgy. 9(2), 81–87.

[17] Ali, A., Shagufta, N., Fayyaz A.S. and Javed, I. (2008) Rapid clonal multiplication of sugarcane through callogenesis and organogenesis. Pakistan Journal of Botany. 40(1), 123-138.

[18] Gandonou, C. Errabii., T. Abrini., J. Idaomar, M. and Senhaji, S.N. (2006) Selection of callus cultures of sugarcane (Saccharum sp.) tolerant to NaCl and their response to salt stress. Plant Cell, Tissue and Organ Culture. 87(1), 9-16.

[19] Schützendübel, A. and Polle, A. (2002) Plant responses to abiotic stresses: heavy metal induced oxidative stress and protection by mycorrhization. Journal of Experimental Botany. 53, 1351-1365.

[20] Gandonou, C. Abrini, J. Idaomar, M. and Skali-Senhaji, N. (2005) Effects of NaCl on growth and ion and proline accumulation in sugarcane (Saccharum sp.) callus culture. Belgian Journal of Botany. 138(3), 173-180.

[21] Spoel, S.H. and Dong, X. (2008) Making sense of hormone crosstalk during plant immune responses. Cell Host Microbe. 3(6), 348–351.

[22] Fujita, Y., Ukena, E.H. Iefuji., Giga-Hama, Y. and Takegawa, K. (2006) Homocysteine accumulation causes a defect in purine biosynthesis: further characterization of Schizosaccharomyces pombe methionine autotrophs. Microbiolog. 152(2), 397-404.

[23] Arrigoni, O., Arrigoni-Liso, R. and Calabrese, G. (1977) Ascorbic acid requirement for biosynthesis of hydroxyproline-containing proteins in plants. FEBS Letters. 82(1), 135-138.

[24] Munns, R. (2002) Comparative physiology of salt and water stress. Plant Cell and Environment. 25(2), 239-250.

[25] Chen, S.Y., Xiao, S. Zhang, M.X. Chen, T. Wang, H.C. and Li-Zhe, A. (2005) Antisense and RNA expression for a chloroplastic superoxide dismutase gene in transgenic plants. Botany Bulletin Academics Sinica. 46, 175-182.

[26] Aslam, M., Travis, R.L. and Huffaker, R.C. (1992) Comparative kinetics and reciproca1 inhibition of nitrate and nitrite uptake in roots of uninduced and induced barley (Hordeum vulgare L.) seedlings. Plant Physiology. 99(3), 1124-1133.

[27] Chazen, O. and Neumann, P.M. (1994) Hydraulic signals from the roots and rapid cell wall hardening in growing maize leaves, are primary responses to PEG induced water deficits. Plant Physiology. 104(4), 1385-1392.
[28] Dal-Corso, G. Farinati, S. Maistri, S. and Furini, A. (2008) How plants cope with cadmium: Staking all on metabolism and gene expression. Journal of Integrated Plant Biology. 50(10), 1268-1280.
[29] Ashraf, M. and O'Leary, J.W. (1999) Changes in soluble proteins in spring wheat stressed with sodium chloride. Biology of Plant. 42(1), 113-117.
[30] Hahlbrock, K. and Scheel, D. (1989). Physiology and molecular biology of phenylpropanoid metabolism. Annual Review of Plant Physiology and Plant Molecular Biology. 40(1), 347-369.
[31] Wang, J, Sun, P.P. Chen, C.L. Wang, Y. Fu, X.Z. and Liu, J. H. (2011) An arginine decarboxylase gene PtADC from *Poncirus trifoliata* confers abiotic stress tolerance and promotes primary root growth in *Arabidopsis*. Journal of Experimental Botany. 62(1), 2899–2914.
[32] Flohe, L. and Ursini F. (2008) Peroxidase: a term of many meanings. Antioxidants and redox signaling. Journal of Biotechnology. 10(9), 1485–1490.
[33] Michalak (2006) Phenolic compounds and their antioxidant activity in plants growing under heavy metal stress. Poland Journal of Environmental Studies. 15(4), 523-530.
[34] Asadi, A, Nejad, R. Soltani, N. Najafi, F. and Rad, A. (2011) Physiological variability in cyanobacterium Phormidium sp. Kutzing ISC31 (Oscillatoriales) as response to varied microwave intensities. African Journal of Agricultural Research. 6(7), 1673-1681.
[35] Cheeseman, J.M. (2007) Mechanism of salinity tolerance in plants. Plant Physiology. 87(6), 547-550.
[36] Padh, H. (1990) Cellular function of ascorbic acid. Biochemistry and Cell Biology. 68(10), 1166–73.

Received: **12.09.2018**
Accepted: **21.02.2019**

CORRESPONDING AUTHOR

Umair A Khan
Department of Botany,
University of Sargodha,
Sargodha – Pakistan

e-mail: malickomair888@gmail.com

© by PSP Volume 28 – No. 4/2019 pages 2539-2544 Fresenius Environmental Bulletin

EFFECTS OF PACLOBUTRAZOL SOAKING ON YIELD AND QUALITY OF THREE VARIETIES *PSEUDOSTELLARIA HETEROPHYLLA*

Hualei Wang*, Longjin Li, Zhi Zhao, Hongchang Liu, Chunli Luo, Jinling Li, Fulai Luo, Mingjin Huang, Songshu Chen

College of agriculture, Guizhou University, Guizhou Key Laboratory of Propagation and Cultivation on Medicinal Plants, Guizhou, China

ABSTRACT

Field experiments were conducted to study the influence of different concentrations of paclobutrazol on the agronomic traits, yield and quality of three varieties *P.heterophylla*. The main results of the test showed that soaking seeds with different concentrations of paclobutrazol promoted the number of roots and the length of the whole plant, and inhibited the diameter of the stem. The 20 mg/L treatment had the largest increase in root number and whole plant length, which were 39.27% and 20.30%, respectively. The diameter of the stem decreased by 9.79% in 2 mg/L treatment. All the 13 agronomy traits showed low concentration inhibition. The effects of soaking seeds with paclobutrazol on the yield and yield components of three *P.heterophylla* varieties were different. Three *P.heterophylla* varieties had the highest yield of Qian *P.heterophylla* No.1, followed by Fengkang No.1. Compared with the control, soaking seeds with different concentrations of paclobutrazol promoted the number of roots and the length of the whole plant, and inhibited the diameter of the stem. The 20 mg/L treatment had the largest increase in root number and whole plant length, which were 39.27% and 20.30%, respectively. Soaking seeds with paclobutrazol improves the quality of three *P.heterophylla* varieties. Compared with the control, soaking seeds with different concentrations of paclobutrazol mainly increased the quality of *P.heterophylla* by increasing the content of *P.heterophylla* extract and total saponins; the contents of extracts of 0.2mg/L, 2mg/L and 20mg/L treatments increased 8.53% and 5.14 %, 5.71% respectively, the total saponin content increased 10.79%, 20.38%, 15.58%, respectively.

KEYWORDS:
Pseudostellaria heterophylla, seeding rate, paclobutrazol, agronomic traits, yield, quality

INTRODUCTION

Pseudostellaria heterophylla is sweet, slightly bitter, spleen and lung meridian, and has the functions of replenishing qi, strengthening spleen, promoting fluid and moistening lung. It mainly treats spleen deficiency, body fatigue, loss of appetite, weakness after illness, thirsty from sweat, dry lung and cough [1]. *Pseudostellaria heterophylla* contains polysaccharides, saponins, cyclic peptides, essential oils, phospholipids, fatty acids, sterols, trace elements and amino acids [2].

Paclobutrazol, also known as chloroprazole, is a highly effective plant growth retardant, whose physiological function of Paclobutrazol is mainly to hinder the biosynthesis of gibberellin and accelerate the decomposition of auxin in vivo, thus delaying and inhibiting plant growth. The previous research showed that Paclobutrazol increased the growth of *Pseudostellaria heterophylla* root enlargement [3]; The dry matter, protein, starch and saponin contents of yam tubers treated with Paclobutrazol were increased by 7.02%, 3.71%, 4.87% and 0.009% respectively, while the soluble sugar content was slightly decreased by 0.37% [4, 5].

As a common Chinese medicinal material, *Pseudostellaria heterophylla* has a large market demand, and the wild *Pseudostellaria heterophylla* resources are limited. Through this study, we can select the best varieties of *Pseudostellaria heterophylla* and the combination of seed soaking concentration of Paclobutrazol to provide scientific and technical support for the stable, high-yield, high-quality and efficient planting of *Pseudostellaria heterophylla* in the cultivation technology. In terms of theoretical value, the effect of Seed Soaking with Paclobutrazol on yield and quality of three varieties of *Pseudostellaria heterophylla* was clarified to provide scientific theoretical basis for rational and effective utilization of Paclobutrazol in cultivation of *Pseudostellaria heterophylla*.

MATERIALS AND METHODS

Experimental Position. The basic fertility of the soil plough layer in the experimental plot was determined by referring to "Agrochemical Analysis of Soil" edited by Bao Shidan [6]. The results showed that the available nitrogen was 114.44 mg/kg, the available phosphorus was 55.41 mg/kg, the available potassium was 123.92 mg/kg, the organic matter content was 33.44 g/kg, and the pH was 4.89.

Experimental Materials. Three varieties were selected for this research, Feng Kang No. 1, main cultivar and Qian *Pseudostellaria heterophylla* No.1.

Main Reagents. 15% Paclobutrazol Wettable Powder (Sichuan Guoguang Agricultural and Chemical Co., Ltd.), Ethanol, Concentrated Sulfuric Acid, Steamed Phenol, Concentrated Sulfuric Acid, Chloroform, n-Butanol, Glacial Acetic Acid, Vanillin Aldehyde, Deionized Water for Experimental Water.

Main instruments. electronic balance with precision of 0.01g and 0.0001g, Petri dish, electrothermal blast drying box (101-1AB, Tianjin Tester Instruments Co., Ltd.), porcelain crucible, vacuum silica gel dryer, muffle furnace (x-12-10, Tianjin Tester Instruments Co., Ltd.), enzyme labeling instrument (Thermo Multiskan FC), etc.

Experimental Design. (1) Experiment design of soaking seed with Paclobutrazol. In the experiment of two factors (A) and concentration of Paclobutrazol (C), factor A was determined by three levels: Fengkang No. 1, Main variety A2 and Qian *Pseudostellaria heterophylla* A3. The three levels of factor C were 0.2mg/L as C1, 2mg/L as C2 and 20 mg/L as C3. The seeding amount of each variety was 525kg/hm^2, and no Paclobutrazol was used as control C. A total of 12 levels of combinations, 3 replicates, completely randomized design, the plot area 10m^2. In 2017, the experiment was carried out at Liupanshui Walnut Flat Experimental station.

Composition determination. Eighteen agronomic characters, yield and three yield components were determined, i.e. root weight per unit area, root number per unit area and root weight per block, were determined. The content of water, ash, extract, polysaccharide and total saponin in *Pseudostellaria heterophylla* were determined.

Experimental Methods. Field planting management. *Pseudostellaria heterophylla* was planted on ridges with a width of 0.85 m and a thickness of 7 cm. N 185 kg/hm^2, P_2O_5 260 kg/hm 2 and K_2O 100 kg/hm^2 were applied as base fertilizer. Paclobutrazol soaking test, the root of *Pseudostellaria heterophylla* was soaked in different concentrations of Paclobutrazol solution for 1 hour, drying the surface water of *Pseudostellaria heterophylla* and then sowing.

Determination of agronomic characters of Radix pseudo ginseng. The agronomic characters of *Pseudostellaria heterophylla* were observed in June 2017, the root diameter and stem diameter were measured with digital vernier calipers, and the root weight, total biomass, underground biomass and aboveground biomass of *Pseudostellaria heterophylla* were weighed with an electronic balance with a precision of 0.01g after low temperature drying.

Yield and yield components of Radix pseudo ginseng. In July 2017, we harvested 1 m^2 *Pseudostellaria heterophylla* tuber roots, removed impurities, washed, marked, dried the root surface moisture, weighed fresh weight, baked at 55 C to constant weight, weighed, calculated drying rate, converted into hectare yield; measured the root weight per unit area, root number per unit area, single root weight.

Determination of quality index of Radix pseudo ginseng. According to the Chinese Pharmacopoeia (2015 Edition), the contents of water, ash and extract of *Pseudostellaria heterophylla* were determined. The content of polysaccharides in Radix heterophylla was determined by phenol sulfuric acid method [7]. The content of total saponins in *Pseudostellaria heterophylla* was determined by vanillin-glacial acetic acid and sulfuric acid method [8].

Data statistical analysis. The experimental data were sorted out by Excel table and analyzed by DPS. The agronomic characters, yield and quality of different factors, different levels and combinations of *Pseudostellaria heterophylla* were analyzed and compared by Duncan's new complex range method.

RESULTS AND DISCUSSION

Effects of soaking seeds with Paclobutrazol on Agronomic Traits of 3 varieties of *Pseudostellaria heterophylla*. Table 1 showed that different concentrations of Paclobutrazol have certain effects on agronomic traits of *Pseudostellaria heterophylla*, and different concentrations of Paclobutrazol have different effects on agronomic traits of *Pseudostellaria heterophylla*. Compared with the control, the number of seed roots increased with the increase of seed soaking concentration. The number of seed roots increased by 6.43%, 26.67% and 39.27% in 0.2 mg/L treatment, 2 mg/L treatment and 20 mg/L treatment respectively. The plant height increased by 20.30% in the treatment of 20mg/L, and the diameter of stem decreased by 9.79% in the treatment of 2mg/L. Soaking seeds with Paclobutrazol inhibited most of the agronomic traits of *Pseudostellaria*

heterophylla at low concentrations. With the increase of the concentration of paclobutrazol, the inhibiting effect was weakened or the phenomena of high concentration promoted. The number of sub roots increased by 20mg/L was the largest, followed by 2mg/L processing, and the number of sub roots in 0.2mg/L processing was not significant.

From Table 2, it can be seen that seed soaking with Paclobutrazol has certain effects on the agronomic characters of *Pseudostellaria heterophylla*, and has certain regularity. The effect of Seed Soaking with Paclobutrazol on Agronomic Traits of *Pseudostellaria heterophylla* was inhibited at low concentration, weakened with the increase of concentration, or promoted at high concentration. The treatments of 0.2mg/L, 2mg/L and 20mg/L reduced the leaf number of Fengkang No. 1 by 20.50%, 12.95% and 5.61%, respectively. The leaf number of main cultivars decreased by 12.46%, increased by 8.27%, increased by 37.01%, decreased by 61.67%, 48.13%, 26.51%, and increased by 35.73%, 15.81% and 9.65% respectively. The number of underground stem nodes decreased by 30.04%, 36.50%, 12.22%, 11.36%, 1.59%, 2.27% and 5.76%, 19.60% and 27.95% respectively.

Effects of soaking seeds with Paclobutrazol on Yield and yield components of 3 varieties of *Pseudostellaria heterophylla.* The results showed that the effect of 0.2mg/L treatment on reducing single root weight is greater than that of 2mg/L treatment and 20mg/L treatment, and the effect of 2mg/L treatment is similar to that of 20mg/L treatment. Soaking seeds with different concentrations of Paclobutrazol had no significant difference in yield, root weight per unit area and root number per unit area. 0.2mg/L treatment, 2mg/L treatment and 20mg/L treatment decreased the yield and root weight per unit area of *Pseudostellaria heterophyll*a by 44.76%, 34.51% and 39.66% respectively. The root number per unit area of *Pseudostellaria heterophylla* was reduced by 573/m^2, 505/m^2 and 555/m^2, 32.32%, 28.48% and 31.30% respectively. The single root weight of *Pseudostellaria heterophylla* was reduced by 0.0166g/a, 0.0079g/a and 0.0115g/a, 16.12%, 7.67% and 11.17% respectively (Table 3).

Table 4 shows that the yield, root weight per unit area and root number per unit area of the main cultivars treated with 2mg/L and 20mg/L were significantly higher than those of the control. The yield of 2mg/L treatment was increased by 124.22% and the root number per unit area increased by 115.33%. The yield of 20mg/L treatment and the increase of root area per unit area were 19.05%, and the root number per unit area increased by 15.62%. Feng Kang No.1 and Qian No.1 Radix pseudo ginseng were inhibited by Paclobutrazol.

TABLE 1
Multiple comparisons of agronomic characters of different Paclobutrazol concentrations in *Pseudostellaria heterophylla*

Agronomic traits	Paclobutrazol concentration			
	C0	C1	C2	C3
Number of branches of main stem	1.47±0.63b	1.18±0.68b	1.52±1.09b	1.94±1.34a
First order branching number	5.11±3.08a	3.58±1.80b	4.85±2.65a	5.00±2.94a
Number of leaves	73.87±37.71a	48.40±20.13b	62.97±29.14a	72.19±28.50a
Number of underground stem nodes	3..22±0.82a	2.20±0.99b	2.27±0.84b	2.48±0.81b
Number of aerial stem nodes	4.67±0.95ab	3.95±1.26c	4.24±1.09bc	4.77±1.12a
Number of subroots	11.51±6.54b	12.25±8.04b	14.58±9.63ab	16.03±10.39a
Number of enlarged roots	8.29±5.13a	5.65±4.95b	6.82±4.22ab	8.23±5.18a
Whole plant length (cm)	21.58±4.46b	22.32±4.95b	22.45±4.04b	25.96±5.79a
Length of underground stem (cm)	5.98±2.01ab	4.94±1.66c	5.25±1.89bc	6.20±1.80a
Stem length (cm)	6.27±1.35b	5.57±1.66c	6.63±1.65ab	7.04±1.63a
Leave length (cm)	4.78±0.87a	4.67±1.12a	4.56±1.20a	4.72±0.88a
Leave width (cm)	2.76±0.75ab	2.42±0.64c	2.47±0.55bc	2.85±0.82a
Diameter of expanded root (mm)	3.84±1.43a	2.56±1.42b	3.62±0.81a	3.66±0.97a
Stem diameter (mm)	2.35±0.45a	2.12±0.71b	2.07±0.64b	2.13±0.74b
Swelling weight of roots (g)	0.79±0.62ab	0.51±0.42c	0.62±0.41bc	0.92±0.84a
Total biomass (g)	3.15±1.67ab	2.11±1.20c	2.76±1.70bc	3.73±1.98a
Underground biomass (g)	1.15±0.72ab	0.81±0.49c	0.96±0.49bc	1.32±0.91a
Aboveground biomass (g)	2.00±1.16ab	1.30±0.88c	1.79±1.41bc	2.41±1.32a

Note: Different letter represent significant difference of two treatments.

TABLE 2
Multiple comparison of Paclobutrazol seed soaking concentration and combinations of *Pseudostellaria heterophylla* varieties on the agronomic traits

Level combination	First order branching number	Number of leaves	Number of underground stem nodes	Number of aerial stem nodes	Number of subroots	Number of enlarged roots
A1C0	3.73±2.58c	61.87±27.72bcde	3.47±0.64a	4.73±0.96ab	8.20±4.44cd	6.33±4.30cdef
A1C1	4.07±2.19bc	49.20±23.06e	3.27±0.46ab	4.80±1.52ab	16.33±7.13ab	10.13±3.74ab
A1C2	4.64±2.47bc	53.86±22.47de	2.79±0.80bc	4.29±0.83ab	13.00±10.25bcd	8.00±3.53abcde
A1C3	3.03±1.57c	58.40±16.62bcde	2.50±1.18cde	4.80±1.40ab	8.50±8.57cd	4.40±5.34efg
A2C0	3.80±2.27c	55.60±28.60cde	3.47±0.99a	4.87±1.25ab	11.67±5.85bcd	6.87±3.40bcdef
A2C1	3.20±1.61c	48.67±18.62e	1.33±0.49g	3.13±0.52c	6.27±4.65d	1.27±1.22g
A2C2	4.10±3.14bc	60.20±30.04bcde	1.80±0.79fg	4.10±1.60b	9.40±5.64cd	3.90±3.07fg
A2C3	4.45±2.07bc	76.18±34.32bcd	2.55±0.52cd	5.18±0.98a	17.64±9.96ab	10.27±3.98ab
A3C0	7.80±2.54a	104.13±37.27a	2.73±0.59bc	4.40±0.51ab	14.67±7.61bc	11.67±5.84a
A3C1	3.40±1.35c	46.80±19.62e	1.90±0.57efg	3.90±0.74bc	15.10±8.44bc	5.50±4.09def
A3C2	6.00±2.18ab	80.22±32.73bc	2.00±0.50def	4.33±0.87ab	22.78±7.12a	8.22±5.02abcd
A3C3	7.30±3.50a	81.60±28.17b	2.40±0.70cdef	4.30±0.82ab	21.80±8.55a	9.80±4.37abc
Level combination	Underground stem length (cm)	Leaf length (cm)	Leaf width (cm)	Enlarged seed root diameter (mm)	Stem diameter (mm)	Whole plant length (cm)
A1C0	6.86±1.93a	4.35±0.86cde	2.67±0.99ab	4.12±1.51ab	2.49±0.43ab	20.07±3.31de
A1C1	5.51±1.44abcd	5.11±1.04abc	2.76±0.63ab	2.57±0.53c	2.39±0.48abc	23.75±3.79bcd
A1C2	6.08±1.83abc	4.38±0.97cde	2.53±0.50bcd	3.32±0.90bc	2.46±0.46abc	22.29±2.68bcd
A1C3	4.94±1.34cde	4.25±0.64de	2.50±0.51bcd	3.81±1.18b	1.39±0.30d	30.10±5.20a
A2C0	5.53±1.51abcd	4.91±0.87bcd	2.97±0.71ab	2.50±0.56c	2.08±0.45c	23.48±5.62bcd
A2C1	3.65±1.28e	3.83±0.96e	1.97±0.48d	1.68±1.37d	1.43±0.44d	24.53±4.91bc
A2C2	4.15±1.68de	3.63±0.62e	2.01±0.35cd	4.04±0.75ab	1.28±0.29d	24.80±5.10bc
A2C3	6.98±2.11a	5.13±0.92abc	2.90±0.52ab	3.45±0.97b	2.24±0.62bc	25.67±4.29b
A3C0	5.54±2.34abcd	5.10±0.74abc	2.64±0.47ab	4.89±0.81a	2.46±0.38abc	21.20±3.67cd
A3C1	6.02±1.25abc	5.28±0.60ab	2.57±0.49abc	3.87±1.50b	2.77±0.40a	16.91±1.50e
A3C2	5.18±1.71bcd	5.87±0.88a	2.90±0.43ab	3.63±0.52b	2.32±0.28bc	20.09±3.34de
A3C3	6.60±1.18ab	4.75±0.88bcd	3.16±1.20a	3.75±0.78b	2.76±0.49a	22.14±5.37bcd

Note: Different letter represent significant difference of two treatments.

TABLE 3
Multiple comparisons of yield and yield components of *Pseudostellaria heterophylla* in different seed soaking concentrations of Paclobutrazol

Paclobutrazol concentration	Yeils (kg/hm^2)	Root tuber weight (g/m^2)	Number of root tubers ($/m^2$)	Single root tuber weight (g)
C0	1844.97±1221.12aA	184.50±122.11aA	1773±1200aA	0.1030±0.0151aA
C1	1019.17±493.67bB	101.92±49.37bB	1200±601bB	0.0864±0.0050cC
C2	1208.19±415.96bB	120.82±41.59bB	1268±425bB	0.0951±0.0056bB
C3	1113.33±436.78bB	111.33±43.68bB	1218±487bB	0.0915±0.0034bBC

Note: Different letter represent significant difference of two treatments.

TABLE 4
Multiplicate comparison table of seed soaking concentration of Paclobutrazol and yield and yield components of *Pseudostellaria heterophylla* at various Levels

Level combination	Yield (kg/hm^2)	Root tuber weight (g/m^2)	Number of root tubers ($/m^2$)	Single root tuber weight (g)
A1C0	1598.17±85.73bB	159.82±8.57bB	1350±82bcdBCDE	0.1188±0.0125aA
A1C1	1082.38±89.77bcdBCDE	108.24±8.98bcdBCDE	1313±65bcdBCDE	0.0823±0.0028dC
A1C2	905.39±121.40cdeBCDE	90.54±12.14cdeBCDE	979±178cdeBCDE	0.0930±0.0044bcBC
A1C3	1044.01±89.44bcdBCDE	104.40±8.94bcdBCDE	1167±94bcdBCDE	0.0895±0.0005cdBC
A2C0	614.52±36.66deDE	61.45±3.67deDE	698±67deDE	0.0884±0.0071cdBC
A2C1	456.09±133.02eE	45.61±13.30eE	503±164eE	0.0915±0.0045cdBC
A2C2	1377.86±533.69bcBCD	137.79±53.37bcBCD	1503±566bcBCD	0.0913±0.0045cdBC
A2C3	731.60±114.30deCDE	73.16±11.43deCDE	807±141deCDE	0.0909±0.0018cdBC
A3C0	3322.22±565.75aA	332.22±56.58aA	3272±613aA	0.1018±0.0023bB
A3C1	1519.03±304.53bBC	151.90±30.45bBC	1782±395bB	0.0855±0.0024cdC
A3C2	1341.33±430.39bcBCD	134.13±43.04bcBCD	1322±399bcdBCDE	0.1011±0.0020bB
A3C3	1564.39±459.44bB	156.44±45.95bB	1682±583bBC	0.0942±0.0051bcBC

Note: Different letter represent significant difference of two treatments.

TABLE 5
Effect of soaking seed concentration of Paclobutrazol on quality of *Pseudostellaria heterophylla*

Paclobutrazol concentration	moisture content (%)	ash content (%)	Net content of extract (%)	Net content of Polysaccharides (%)	Total saponin content (%)
C0	5.31±0.32dC	3.64±0.29a	43.96±1.90bB	10.20±0.57a	4.17±0.49bB
C1	6.94±1.05bAB	3.44±0.39a	47.71±2.06aA	9.54±1.97a	4.62±1.12aAB
C2	6.72±0.40cB	3.35±0.23a	46.22±2.21aA	9.72±1.27a	5.02±0.99aA
C3	7.21±0.57aA	3.39±0.64a	46.47±1.69aA	10.52±1.25a	4.82±0.79aA

Note: Different letter represent significant difference of two treatments.

TABLE 6
Comparison of the quality of Radix pseudo ginseng by combination of Soaking with Paclobutrazol and various levels of *Pseudostellaria heterophylla* combination

Level combination	moisture content (%)	ash content (%)	Net content of extract (%)	Net content of Polysaccharides (%)	Total saponin content (%)
A1C0	5.14±0.18fE	3.71±0.12abAB	43.01±2.09eC	9.82±0.07abAB	3.84±0.28efDE
A1C1	5.88±0.10eD	3.18±0.52bABC	45.63±1.19bcdeABC	10.20±0.84aAB	3.44±0.90fE
A1C2	7.14±0.36bB	3.32±0.11bABC	47.28±0.60abcAB	8.74±1.44abAB	3.90±0.39efDE
A1C3	7.05±0.06bcB	3.56±0.33abAB	45.40±1.81cdeABC	10.36±2.21aAB	4.11±0.49defCDE
A2C0	5.16±0.34fE	3.50±0.22abAB	45.74±0.74bcdeABC	10.03±0.61abAB	4.76±0.28cdBCD
A2C1	6.71±0.11cdBC	3.63±0.32abAB	48.94±1.21aA	7.79±2.73bB	4.67±0.05cdeBCD
A2C2	6.40±0.25dC	3.56±0.19abAB	47.55±2.21abcAB	9.84±1.04abAB	5.10±0.30bcABC
A2C3	7.90±0.18aA	3.97±0.03aA	46.37±0.80abcdABC	10.09±0.33abAB	5.49±0.51abcAB
A3C0	5.63±0.22eDE	3.71±0.47abAB	43.14±1.54eC	10.75±0.48aAB	3.91±0.10efDE
A3C1	8.24±0.16aA	3.51±0.25abAB	48.57±2.08abA	10.64±0.51aAB	5.76±0.40abAB
A3C2	6.62±0.04dBC	3.17±0.21bBC	43.83±1.19deBC	10.58±0.83aAB	6.07±0.36aA
A3C3	6.68±0.29cdBC	2.64±0.42cC	47.64±1.95abcAB	11.10±0.67aA	4.86±0.73cdBCD

Note: Different letter represent significant difference of two treatments.

Effect of soaking seeds with Paclobutrazol on the quality of 3 varieties of *Pseudostellaria heterophylla.* Table 5 shows that Paclobutrazol treatment at different concentrations increased water content, extract content and total saponin content of *Pseudostellaria heterophylla* in varying degrees, and water content increased by 30.70%, 26.55% and 35.78% in 0.2 mg/L treatment, 2 mg/L treatment and 20 mg/L treatment, the content of extract increased by 8.53%, 5.14%, 5.71%, the total saponin content increased by 10.79%, 20.38%, 15.58%. To sum up, Paclobutrazol can improve the quality of *Pseudostellaria heterophylla* by increasing the content of extracts and total saponins of *Pseudostellaria heterophylla*.

According to Table 6, the quality of Paclobutrazol treatment of three varieties was higher than that of the control. Among them, the contents of extracts of three treatments of main variety, 2 mg/L treatment of Fengkang 1, 0.2 mg/L treatment and 20 mg/L treatment of Qian Paclobutrazol No.1 were 48.94%, 47.55%, 46.37%, 47.28%, 48.57%, 47.64% more than control. The contents of total saponins were the highest in the 20 mg/L treatment of main cultivar, 0.2 mg/L treatment and 2 mg/L of Qian Paclobutrazol No.1, which were 5.49%, 5.76% and 6.07% respectively. The comprehensive analysis showed that the quality of 20 mg/L treatment of Qian Paclobutrazol No.1 was the best, followed by 20 mg/L treatment of main cultivar and 0.2 mg/L treatment of Qian Paclobutrazol No.1.

CONCLUSIONS

Soaking seeds with Paclobutrazol had certain effects on the agronomic characters, yield and quality of the three varieties. Soaking seeds with Paclobutrazol could improve the quality of the three varieties in the range of 0.2-20 mg/L. Soaking seeds with 2 mg/L and 20 mg/L Paclobutrazol solution could improve the yield and quality of the main varieties.

After soaking seed with Paclobutrazol, shortening the number of stem nodes and the number of underground stem nodes increased the number of roots of *Pseudostellaria heterophylla*. Soaking seeds with Paclobutrazol promoted the whole plant length and reduced stem diameter of *Pseudostellaria heterophylla*.

ACKNOWLEDGEMENTS

This research was supported by Construction Program of Biology First-class Discipline in Guizhou (GNYL［2017］009) and Guizhou Province medical plant breeding and planting talent base (Guizhou Ren Ling FA [2013] No.15).

REFERENCES

[1] Liu, X., Zhang, X., Wu, Y., Lin, F. (2013) Effects of Pseudostellaria heterophylla (Miq.) Pax on the activities of CYP450 enzymes in rats using a cocktail approach. Lat Am J Pharm. 32(6), 931-935.
[2] Yu, Y., Qin, M., Yu, G. (2003) Advances in studies on chemical constituents, pharmacological effects and quality evaluation of *Pseudostellaria heterophylla*. Chinese Wild Plant Resources. 4(1-3), 7.
[3] Chen, X. (2009) Study on mechanism and regulation of root swelling of ginseng Ficus. Fujian Agriculture and Forestry University.
[4] Chen, X., Shi, C., Wang, Z., Zhang, L., Zhang, X. (2012) Effect of Paclobutrazol on Starch Accumulation and Related Enzyme Activity of Storage Root in Edible Sweet Potato cv. Beijing 553. Scientia Agricultura Sinica. 45(1), 192-198.
[5] Gong, M., Luo, H., Yuan, H., Wei, S., Yang, X., and He, L. (2015) Effects of Exogenous Gibberellin and Paclobutrazol on Tuber Expansion and Bulbil formation of Chinese Yam. Acta Horticulturae Sinica. 42(06), 1175-1184.
[6] Bao, S.D. (2000) Soil Agro-chemistrical Analysis. Beijing: China Agriculture Press. 56-58, 81-83, 106-108.
[7] Zhong, F., Peng, G., Li, G. (1997) Effect of Content of Polysaeeharide on the Quality of Taizishen (*Pseudostellaria heterophylla*) in Shan Dong. Chinese Traditional and Herbal Drugs. 28(7), 428-430.
[8] Chen, Y., Liu, Z., Cai, X., Jin, S. (2014) Determination of total saponins in *Pseudostellaria heterophylla*. Strait Pharmaceutical Journal. 26(6), 77-78.

Received: **17.09.2018**
Accepted: **18.02.2019**

CORRESPONDING AUTHOR

Hualei Wang
College of agriculture,
Guizhou University,
Guizhou Key Laboratory of Propagation and Cultivation on Medicinal Plants
Guizhou – China

e-mail: gzuwhl@126.com

© by PSP Volume 28 – No. 4/2019 pages 2545-2552 Fresenius Environmental Bulletin

THE GENOPROTECTIVE EFFECT OF *CROCUS SATIVUS* L. (SAFFRON) EXTRACT ON DOXORUBICIN-INDUCED GENOTOXICITY IN *DROSOPHILA MELANOGASTER*

Selda Oz*, Sukran Cakir Arica

Department of Biology, Faculty of Science and Art, Kirikkale University, Kirikkale, Turkey

ABSTRACT

Crocus sativus L. (saffron) is a medicinal plant that has been used for the prevention and treatment of various diseases since ancient times. Saffron also has a distinctive aroma and is used as a food coloring, in addition to its therapeutic effects. In this study the genotoxic and antigenotoxic impacts of saffron were evaluated using the somatic mutation and recombination test (SMART). Doxorubicin, a chemotherapeutic drug, was used as a genotoxic agent to evaluate the antigenotoxic activity of saffron. Transheterozygous larvae obtained from a standard cross between flare (flr^3) and multiple wing hair (*mwh*) mutant strains of *Drosophila melanogaster* were treated with the test materials. Saffron extract was applied at three different concentrations (1,5 and 10 mg/mL) to evaluate any genotoxic effect. In the antigenotoxic assessment, each dose of the saffron extract was co-administered with doxorubicin (0.125 mg/mL). The data obtained from our study indicated that the ethanol extract of saffron did not show any genotoxic effect but instead exerted a powerful protective effect against the genotoxic effect of doxorubicin that was dose dependent.

KEYWORDS:
Antigenotoxicity, doxorubicin, *Drosophila melanogaster*, mutation, saffron, SMART assay

INTRODUCTION

The therapeutic effects of plants were discovered in ancient times and they have been used in the treatment of various diseases since then. Although there are advanced modern medical techniques, nowadays people tend to choose herbal treatment methods more frequently. Herbal medicine has many advantages compared to modern medicine, such as being cheaper, being easier to administer and resulting in fewer side effects [1]. According to World Health Organization (WHO) data, 80% of the world's population use herbal remedies [2]. People use herbal healing methods in combination with conventional treatment methods to help recover from various illnesses [3-5]. Though plants are effective in the prevention or treatment of many diseases, the simultaneous application of plants and drugs may reduce or increase the efficacy of drugs, or they may cause serious side effects [6].

Crocus sativus L. (saffron) is a plant belonging to the Iris family (Iridaceae) with a strong aroma and coloring properties. It is a perennial, bulbous plant with a blue–purple flower. The stigmas and styles of its flower are used as a spice [7]. This therapeutic plant has been used in alternative medicine since ancient times because of a wide range of curative properties including anti-inflammatory, sedative, cardioprotective, diaphoretic, aphrodisiac, diuretic, stomachic, antiseptic, expectorant, decongestant, antispasmodic and pain relief effects [8]. According to the phytochemical analysis, saffron contains anthocyanin, carotenoid (crocin, crocetin, α-carotene, β-carotene, lycopene and zeaxanthin), monoterpene aldehyde (safranal, picrocrocin), isophorone, and flavonoid (kaempferol, taxifolin and naringenin) compounds [9-11]. Saffron and/or its components have many beneficial effects on health, including antigenotoxic, anticarcinogenic, antioxidative, anti-inflammatory, immunoprotective, antihyperglycemic, antiischemic, antihypertensive, antidepressant, neuroprotective and anti-obesity properties [12-24].

Doxorubicin, a chemotherapeutic drug, is commonly used to treat various types of cancer including lymphoma, myeloma, sarcoma and carcinoma [25]. The active mechanism of doxorubicin affects normal cells as well as cancerous cells [26]. Doxorubicin causes genotoxicity and cytotoxicity in cells by mechanisms including intercalating into DNA base pairs, generating free radicals, inhibiting topoisomerase II activity and stopping DNA and RNA synthesis. It binds to DNA by entering between base pairs. This causes structural degradation of genetic material and inhibition of RNA synthesis. Reactive oxygen species (ROS) generated as a result of doxorubicin-induced redox reactions, cause genotoxicity via damage to cellular DNA and other macromolecules in the cell, and this can cause serious side effects like cardiotoxicity and can impact the immune system [27-31]. The progress of these side effects

depends on repeated doses of large amounts of doxorubicin, limiting its use.

In view of this, the somatic mutation and recombination test (SMART) was used to investigate the antigenotoxic effect of saffron on any genotoxicity caused by doxorubicin. SMART is an *in vivo* genotoxicity assay allowing the detection of mutational or recombinational changes occurring in the imaginal discs of *Drosophila melanogaster* [32]. This assay has been used to observe the mutagenic and recombinogenic effects of a wide variety of agents such as food dyes, insecticides, nanoparticles, plant compounds, UV light, and drugs [33-38].

MATERIALS AND METHODS

Test materials. Saffron samples were obtained from local producers in Safranbolu in March 2014. The samples were ground in a porcelain mortar and extracted with ethanol (w/v; 1:10) on a horizontal shaker (125 rpm) at room temperature for 24 hours. Then, the extractions were filtered, and ethanol was removed using a rotary evaporator (Buchi Rotavapor R-210). Lyophilized extracts were stored in dark bottles at +4°C until used. An 0.125 mg/mL amount of doxorubicin (Santa Cruz Biotechnology Inc., CA, USA) was used as a positive control. The dose of the doxorubicin was determined according to a previous study [39]. Distilled water was used as a negative control. Doxorubicin and the lyophilized saffron extract were dissolved in distilled water just before treatment. Formula 4-24® (Instant *Drosophila* medium, Carolina Biological Supply Cooperation, Burlington, NC, USA) was used as the medium for all treatments in the study.

Strains and crosses. The marker *flare-3 (flr^3)* and *multiple wing hairs (mwh*) strains of *Drosophila melanogaster* were used in the experiments. Lindsley and Zimm [40] gave detailed information about these strains in their work. Third instar transheterozygous larvae were obtained from a standard (ST) cross between virgin *flr^3 (flr^3/In (3LR), TM3 BdS)* females and *mwh (mwh/mwh)* males. Two different types of progeny can be produced from a standard cross: marked transheterozygous (MH) and balancer-heterozygous (BH) types. MH (*mwh+/+flr^3*) individuals have phenotypically normal wings. In the MH genotype, spots occur due to somatic recombination or mutation, and both single spots (*flr^3* or *mwh*), or twin spots (*flr^3* and *mwh*), can be observed on the wings. Deletions, point mutations, chromosome aberrations or recombination between *flr^3* and *mwh* genes can produce single spots, while recombination between the *flr^3* gene and the centromere of chromosome 3 generate twin spots [32]. BH flies (*mwh*/*TM3 BdS*) have phenotypically serrated wings. In the BH genotype, recombination is suppressed by the *TM3* balancer chromosome, so spots occur only due to mutation and only *mwh* single spots can be observed on the wings. In this study MH wings were subjected to evaluation.

Treatments. In treatments, the procedure described by Graf et al. [32] was followed, with 1 to 3-day-old virgin *flr^3* females mated with *mwh* males. Eggs derived from this cross were collected over an 8 hour period in vials containing instant *Drosophila* medium. Afterwards the third instar (72 ± 4 hours) transheterozygous larvae were collected by washing out the medium with tap water. Larvae were placed in vials containing instant medium (1.5 g) hydrated with test solution (5 mL). One hundred larvae were treated in each experimental group and three replications were performed. Saffron extract was separately applied as three different doses to evaluate its genotoxic effect. Each dose of the extract was applied in combination with doxorubicin to evaluate antigenotoxic activity. Larvae were treated with distilled water in the negative control group and with doxorubicin in the positive control group. Fly stocks were maintained, and experiments were conducted at 25 ± 1°C and 40 to 60% humidity. Emerging individuals carrying the MH genotype with phenotypically wild-type wings were selected from each application group and collected in vials contain 70% ethanol then stored at +4°C until the wings were permanently mounted.

Microscopic analyses. The wings of individuals were picked up using forceps then fixed on slides with Entellan (Merck) and analyzed for different types of mutant clones under a light microscope with 10×40 magnification. Forty pairs of wings were examined in each application group and mutant clones were scored as single small, single large and twin spots, as previously described [32].

Statistical analysis. In each experimental group, the frequencies of each of the type of mutant spots were compared pair-wise (negative control versus saffron extract; positive control (doxorubicin) versus doxorubicin plus saffron extract), and then analyzed using the conditional binomial test at a 5% significance level [41]. The data obtained was evaluated using a multiple decision procedure and the results were determined to be negative, positive or inconclusive [42]. In co-treatments, the inhibition percentage (IP) was computed by the following formula:

IP = [(doxorubicin alone-saffron extract plus doxorubicin)/doxorubicin alone] ×100] [43].

RESULTS

In this study the genotoxic and antigenotoxic effects of saffron extract were determined with the

TABLE 1
Genotoxicity test results obtained in marked trans-heterozygous (MH) progeny treated separately with doxorubicin and saffron extract.

Treatment (mg/mL)	N	Small single spots (1-2 cells) (*m*=2)			Large single spots (>2 cells) (*m*=5)			Twin spots (*m*=5)			Total *mwh* spots (*m*=2)			Total spots (*m*=2)			F
		No	Fr	D	No	Fr	D	No	Fr	D	No	Fr	D	No	Fr	D	
Dw	80	7	0.09		3	0.04		1	0.01		11	0.14		11	0.14		0.56
Dxr																	
0.125	80	122	1.53	+	52	0.65	+	19	0.24	+	183	2.29	+	193	2.41	+	9.38
SE																	
1	80	7	0.09	i	4	0.05	i	1	0.01	i	11	0.14	i	12	0.15	i	0.56
5	80	9	0.11	i	6	0.08	i	0	0.00	i	13	0.16	i	15	0.19	i	0.67
10	80	6	0.08	i	4	0.05	i	0	0.00	i	9	0.11	-	10	0.13	i	0.46

N: Number of wings, F: Frequency of clone formation per 10^5 cells, Dw: distilled water, Dxr: doxorubicin, SE: saffron extract, No: number, Fr: frequency, D: statictical diagnosis according to Frei and Würgler (1988); +: positive, -: negative, i: inconclusive, m: multiplication factor; probability levels α=β= 0.05.

TABLE 2
Antigenotoxicity test results obtained in marked trans-heterozygous (MH) progeny after co-treatment with doxorubicin and saffron extract.

Treatment (mg/mL)		N	Small single spots (1-2 cells) (*m*=2)			Large single spots (>2 cells) (*m*=5)			Twin spots (*m*=5)			Total *mwh* spots (*m*=2)			Total spots (*m*=2)			F	I%
			No	Fr	D	No	Fr	D	No	Fr	D	No	Fr	D	No	Fr	D		
Dw		80	7	0.09		3	0.04		1	0.01		11	0.14		11	0.14		0.56	
Dxr																			
0.125		80	122	1.53	+	52	0.65	+	19	0.24	+	183	2.29	+	193	2.41	+	9.38	
Dxr	SE																		
0.125	1	80	15	0.19	-	27	0.34	-	1	0.01	-	23	0.29	-	43	0.54	-	1.18	77.59
0.125	5	80	10	0.13	-	8	0.10	-	2	0.03	-	16	0.20	-	20	0.25	-	0.82	89.63
0.125	10	80	9	0.11	-	7	0.09	-	2	0.03	-	14	0.18		18	0.23	-	0.72	90.46

N: Number of wings, F: Frequency of clone formation per 10^5 cells, Dw: distilled water, Dxr: doxorubicin, SE: saffron extract, No: number, Fr: frequency, D: statictical diagnosis according to Frei and Würgler (1988); +: positive, -: negative, i: inconclusive, m: multiplication factor; probability levels α=β= 0.05.

SMART assay using an ST cross. The genotoxicity test results are summarized in Table 1.

The saffron extract was applied at three different concentrations (1, 5 and 10 mg/mL) to evaluate its genotoxic effect. It was observed that the mutant spot numbers were the same or exhibited very little difference between the saffron-treated groups and the negative control group. Statistical analysis revealed that the differences between the results were insignificant (Table 1). The genotoxicity assay showed that the saffron extract did not exhibit any toxic effects at the doses used.

The positive control doxorubicin was applied at 0.125 mg/mL and showed a powerful genotoxic effect, as expected. It was observed that the frequencies of all mutant spots in the doxorubicin-treated group were significantly higher than in the negative control group (Table 1). It was seen that the small single spot type was the most frequently induced mutant clone after the doxorubicin treatment.

In co-treatments, 1, 5 and 10 mg/mL doses of saffron extract were applied in combination with 0.125 mg/mL of doxorubicin and the antigenotoxic potential of the saffron extract was evaluated. Antigenotoxicity studies showed that the saffron extract modified the genotoxic effect of the doxorubicin. The simultaneous application of saffron extract and doxorubicin produced antigenotoxic effects by inhibiting the mutant clone formation at all the tested dose levels. The calculated inhibition percentages were 77.59 %, 89.63 % and 90.46 % at 1, 5 and 10 mg/mL doses, respectively (Table 2). These results indicated that the saffron treatment showed a powerful protective effect against the genotoxic effect of doxorubicin, and that its protective effect was increased depending on the dose.

DISCUSSION

Cancer is one of the most common diseases in the world. WHO estimated that global cancer rates could reach 15 million by 2020. Chemotherapy, radiotherapy and surgical methods applied in modern cancer therapy may not always produce effective results, and cancer cells may develop resistance to these treatment methods over time [2]. Chemotherapy is one of the basic methods in cancer treatment, but chemotherapy drugs can affect normal cells as well as cancerous cells and cause serious side effects [44]. In recent years, a number of studies have been conducted to reduce or prevent the side effects of these drugs using herbs and herbal components as an adjuvant in patients and animals. These studies

demonstrated that clinical use of herbal medicines can be efficient at chemoprevention to counter the adverse effects of chemotherapeutic agents [45-48]. It is thought that medicinal plants are effective in the treatment and prevention of cancer by enhancing the body's resistance to diseases by supporting the immune system, preventing or reducing the side effects of modern treatment methods, and providing nutritional and physiological support as well as containing anticancer compounds [49].

Doxorubicin is a highly effective and commonly used chemotherapeutic agent in the treatment of multiple cancer types [25]. It is known that elevated levels of ROS are generated as a result of using doxorubicin [50]. ROS are byproducts of normal metabolic activities in aerobic organisms and necessary for the regulation of cellular functions, the formation of cellular responses to infectious agents, the regulation of cell-signaling pathways, and physiological and biosynthetic processes. While ROS are necessary and useful in organisms at low amounts, they have harmfull effects at high concentrations [51-53].

Antioxidants are substances that can destroy ROS and remove their harmful effects [54]. Excess levels of ROS are neutralized by non-enzymatic (carotenoid, flavonoid, glutathione and thiol) or enzymatic (superoxide dismutase, catalase and glutathione peroxidase) antioxidants and are kept at low levels in the cell [52]. When ROS are accumulated or the amount of antioxidants decreases in the cell, oxidative stress is produced when the balance between ROS and antioxidants is disrupted. Oxidative stress may lead to diabetes, aging, arteriosclerosis, neurodegenerative diseases and cancer by inducing abnormalities in the structure and function of macromolecules such as DNA, RNA and lipids [54-56].

Doxorubicin is highly effective against a wide range of cancers, but clinical use of this drug is limited by increased doxorubicin-induced ROS generation. Therefore some studies have been conducted on lowering the doxorubicin-induced ROS level with various herbs or herbal compounds. In these studies, it has been experimentally demonstrated that doxorubicin-induced genotoxicity can be reduced by dietary intake of antioxidants and antioxidant-rich plants [39, 57, 58].

In this study, the effect of administering the saffron extract orally to combat doxorubicin-induced genotoxicity was tested on the *Drosophila melanogaster*. According to our results, the saffron extract alone did not show any genotoxic effect, and it provided protection against the genotoxicity of doxorubicin at the doses tested. The results of our study corroborate previous findings demonstrating the antigenotoxic effects of saffron. It has been shown that the ingestion of aqueous saffron extract inhibited genotoxicity of some anti-tumor drugs (mitomycin C, cisplatin and cyclophosphamide) and urethan in mice [59]. Saffron, and its component crocin, also inhibited methyl methanesulfonate (MMS)-induced DNA damage in mice [12]. Sadeghnia et al. [15] reported that safranal had a protective effect against quinolinic acid (QA)-mediated excitotoxicity in rats. Lipid peroxidation and DNA damage induced by QA were significantly reduced, and the changes in hippocampal thiol redox and antioxidant status were prevented by administering safranal. It was suggested that safranal may be used in the prevention and treatment of neurodegenerative disorders.

In our study, we found that saffron extract showed a strong dose-dependent antigenotoxic effect against the genotoxicity of doxorubicin. On the basis of data obtained from previous studies, it can be suggested that saffron may cause an antigenotoxic effect on doxorubicin-induced genotoxicity by eliminating ROS. Premkumar et al. [13] detected that saffron causes an increase in enzymatic (catalase, glutathione peroxidase, glutathione S-transferase and superoxide dismutase) and non-enzymatic (glutathione) antioxidant levels, and a reduction in lipid peroxidation in Swiss albino mice treated with genotoxic agents. Makhlouf et al. [60] showed that saffron provided a strong protection against electrolysis-induced free radicals in the organs (liver, kidneys, lung and heart) of a hamster. It was indicated that saffron decreased the lipid peroxidation level induced by superoxide dismutase, and the activity was dose dependent. In another study, saffron extract and its compounds –safranal and crocin – showed high radical scavenging activity against DPPH radicals [14] It was also shown that saffron enhanced survival rates by reducing H_2O_2-induced oxidative stress in bacteria and yeast [9].

Experimental studies showed that dietary phytochemicals can play an effective role in preventing diseases caused by ROS [61, 62]. Antioxidants play an important role in the formation of anticancer activities in medicinal plants [63]. Antioxidant intake from diet or supplements has been shown to reduce the risk of developing cancer [64,65]. It has been reported that the relationship between nutrition and mortality can reach up to 70% in colorectal cancer [66].

Previously, *in vivo* and *in vitro* anticancer properties have been detected in saffron, and its promising effects in cancer treatment have been noted. It has been shown that saffron has a selective cytotoxic effect on cancer cells and exerts its anticarcinogenic effect by different mechanisms, such as inducing apoptosis, preventing cell proliferation, inhibiting angiogenesis, and blocking the gene expression and synthesis of proteins [67-70].

Saffron has anticarcinogenic, antigenotoxic, antioxidant and immunoprotective effects, and it has many more beneficial effects for health. Moreover, studies have demonstrated that the toxic effect of saffron on living organisms is quiet low. It has been reported that oral intake of saffron extract at concentrations from 0.1 to 5 g/kg is non-toxic in mice. In

another study, the LD_{50} value of saffron to be administered orally in mice was calculated to be 20.7 gr/kg [71]. Modaghegh et al. [72] reported that oral intake of saffron tablets in the range from 200 to 400 mg/day causes insignificant biochemical and hematological parameter changes in healthy adults.

In addition to its therapeutic effects, saffron has traditionally been used as a spice in certain national cuisines because of its coloring and aromatic qualities [7, 49]. Saffron has powerful coloring effects. Crocetin and crocin carotenoids are the main compounds responsible for the color of the saffron [73], and it can color 100.000 times its own weight of liquids [74]. It can be suggested that saffron can be added as a food coloring agent to ready-to-eat foods. Dietary intake of saffron can provide prevention against genotoxic and carcinogenic agents, and support the immune system.

CONCLUSIONS

Doxorubicin is a chemotherapeutic agent that has genotoxic effects on normal cells as well as cancer cells. Saffron is a medicinal plant with an antigenotoxic effect. It is also a promising cancer chemopreventative agent due to its strong and selective toxic effect on cancer cells.

The detoxification systems that are naturally present in organisms deactivate genotoxic agents through various mechanisms; however, these systems may be deficient when organisms are frequently exposed to these agents over a long period of time. In addition to detoxification systems, antigenotoxic substances, taken in through nutrition, can prevent the harmful effects of genotoxins.

Based on the results of this study, saffron extract can strongly counter the genotoxic effect of doxorubicin on the healthy cells of *Drosophila.* In conclusion, saffron extract can be used as adjuvant against doxorubicin-induced genotoxicity. Co-administering saffron with doxorubicin can provide a protective effect for normal cells. We can also suggest that saffron can be used as a food additive because of its strong aromatic and coloring qualities. Saffron can provide antigenotoxic, antioxidant and anticarcinogenic protection against possible genotoxins that people are exposed to in their daily life, so it can be possible to prevent or delay genotoxin-induced diseases.

ACKNOWLEDGEMENTS

This work was supported by the Coordination Unit for Kırıkkale University Scientific Research Projects (Project number: 2012/010).

REFERENCES

[1] Murray, M.T. (2013) Botanical Medicine-A Modern Perspective. In: Pizzorno, J.E. and Murray, M.T. (eds.) Textbook of Natural Medicine. 4 Edition. Elsevier, St. Louis, USA, 255-260.

[2] Safarzadeh, E., Shotorbani, S.S. and Baradaran, B. (2014) Herbal medicine as inducers of apoptosis in cancer treatment. Advanced Pharmaceutical Bulletin. 4(Suppl 1), 421-427.

[3] Leach, M.J., Lauche, R., Zhang, A.L., Cramer, H., Adams, J., Langhorst, J. and Dobos, G. (2017) Characteristics of herbal medicine users among internal medicine patients: A cross-sectional analysis. Journal of Herbal Medicine. 10, 59-63.

[4] Naja, F., Mousa, D., Alameddine, M., Shoaib, H., Itani, L. and Mourad, Y. (2014) Prevalence and correlates of complementary and alternative medicine use among diabetic patients in Beirut, Lebanon: a cross-sectional study. BMC Complementary and Alternative Medicine. 14(1), 185.

[5] Yeong, S.W. and Choong, Y.C. (2017) Knowledge and characteristics of herbal supplement usage among community pharmacy customers in a Malaysian population. Complementary Therapies in Medicine. 35, 92-108.

[6] Fugh-Berman, A. (2000) Herb-drug interactions. The Lancet. 355(9198), 134-138.

[7] Javadi, B., Sahebkar, A. and Emami, A. (2013) A Survey on Saffron in Major Islamic Traditional Medicine Books. Iranian Journal of Basic Medical Sciences. 16(1), 1-11.

[8] Hosseinzadeh, H. and Nassiri-Asl, M. (2013) Avicenna's (Ibn Sina) the Canon of Medicine and Saffron (Crocus sativus): A Review. Phytotherapy Research. 27(4), 475-483.

[9] Baba, S.A., Malik, A.H., Wani, Z.A., Mohiuddin, T., Shah, Z., Abbas, N. and Ashraf, N. (2015) Phytochemical analysis and antioxidant activity of different tissue types of *Crocus sativus* and oxidative stress alleviating potential of saffron extract in plants, bacteria, and yeast. South African Journal of Botany. 99, 80-87.

[10] Goli, A.H., Mokhtari, F. and Rahimmalek, M. (2012) Phenolic Compounds and Antioxidant Activity from Saffron (Crocus sativus L.) Petal Sayed. Journal of Agricultural Science. 4(10), 175-181.

[11] Tuberoso, C.I., Rosa, A., Montoro, P., Fenu, M.A. and Pizza, C. (2016) Antioxidant activity, cytotoxic activity and metabolic profiling of juices obtained from saffron (Crocus sativus L.) floral by-products. Food Chemistry. 199, 18-27.

[12] Hosseinzadeh, H., Abootorabi, A. and Sadeghnia, H.R. (2008) Protective effect of Crocus sativus stigma extract and crocin (trans-crocin 4) on methyl methanesulfonate-induced DNA damage in mice organs. DNA and Cell Biology. 27(12), 657-664.

[13] Premkumar, K., Abraham, S.K., Santhiya, S.T. and Ramesh, A. (2003) Protective effects of saffron (Crocus sativus Linn.) on genotoxins-induced oxidative stress in Swiss albino mice. Phytotherapy Research. 17(6), 614-617.

[14] Assimopoulou, A.N., Sinakos, Z. and Papageorgiou, V.P. (2005) Radical scavenging activity of *Crocus sativus* L. extract and its bioactive constituents. Phytotherapy Research. 19(11), 997-1000.

[15] Sadeghnia, H.R., Kamkar, M., Assadpour, E., Boroushaki, M.T. and Ghorbani, A. (2013) Protective effect of safranal, a constituent of crocus sativus, on quinolinic acid-induced oxidative damage in rat hippocampus. Iranian Journal of Basic Medical Sciences. 16(1), 73-82.

[16] Hosseinzadeh, H. and Younesi, H.M. (2002) Antinociceptive and anti-inflammatory effects of Crocus sativus L. stigma and petal extracts in mice. BMC Pharmacology. 2(1), 7.

[17] Boskabady, M.H. and Farkhondeh, T. (2016) Antiinflammatory, Antioxidant, and Immunomodulatory Effects of *Crocus sativus* L. and its Main Constituents. Phytotherapy Research. 30(7), 1072-1094.

[18] Fatehi, M., Rashidabady, T. and Fatehi-Hassanabad, Z. (2003) Effects of Crocus sativus petals' extract on rat blood pressure and on responses induced by electrical field stimulation in the rat isolated vas deferens and guinea-pig ileum. Journal of Ethnopharmacology. 84(2-3), 199-203.

[19] Zheng, Y.Q., Liu, J.X., Wang, J.N. and Xu, L. (2007) Effects of crocin on reperfusion-induced oxidative/nitrative injury to cerebral microvessels after global cerebral ischemia. Brain Research. 1138, 86-94.

[20] Akhondzadeh, S., Fallah-Pour, H., Afkham, K., Jamshidi, A.H. and Khalighi-Cigaroudi, F. (2004) Comparison of *Crocus sativus* L. and imipramine in the treatment of mild to moderate depression: A pilot double-blind randomized trial [ISRCTN45683816]. BMC Complementary and Alternative Medicine. 4(1), 12.

[21] Rao, S.V., Muralidhara, Yenisetti, S.C. and Rajini, P.S. (2016) Evidence of neuroprotective effects of saffron and crocin in a Drosophila model of parkinsonism. Neurotoxicology. 52, 230-242.

[22] Mashmoul, M., Azlan, A., Yusof, B.N.M., Khaza'ai, H., Mohtarrudin, N. and Boroushaki, M.T. (2014) Effects of saffron extract and crocin on anthropometrical, nutritional and lipid profile parameters of rats fed a high fat diet. Journal of Functional Foods. 8, 180-187.

[23] Malaekeh-Nikouei, B., Mousavi, S.H., Shahsavand, S., Mehri, S., Nassirli, H. and Moallem, S.A. (2013) Assessment of cytotoxic properties of safranal and nanoliposomal safranal in various cancer cell lines. Phytotherapy Research. 27(12), 1868-1873.

[24] Tanaka, T., Mori, T., Yuan, C.S., Soed, S., Tung, N.H. and Shoyama, Y. (2015) The Function of Saffron and its Constituent in Gastroenterological Tissues. Global Journal of Gastroenterology and Hepatology. 3, 31-38.

[25] Malla, S., Prasad Niraula, N., Singh, B., Liou, K. and Sohng, J.K. (2010) Limitations in doxorubicin production from Streptomyces peucetius. Microbiological Research. 165(5), 427-435.

[26] Antunes, L.M.G., de Barros E Lima Bueno, R., da Luz Dias, F. and de Lourdes Pieres Bianchi, M. (2007) Acetylsalicylic acid exhibits anticlastogenic effects on cultured human lymphocytes exposed to doxorubicin. Mutation Research/Genetic Toxicology and Environmental Mutagenesis. 626(1), 155-161.

[27] Thorn, C.F., Oshiro, C., Marsh, S., Hernandez-Boussard, T., McLeod, H., Klein, T.E., and Altman, R. B. (2011) Doxorubicin pathways: pharmacodynamics and adverse effects. Pharmacogenetics and Genomics. 21(7), 440-446.

[28] Meredith, A.M., and Dass, C.R. (2016) Increasing role of the cancer chemotherapeutic doxorubicin in cellular metabolism. Journal of Pharmacy and Pharmacology. 68(6), 729-741.

[29] Tacar, O., Sriamornsak, P. and Dass, C.R. (2013) Doxorubicin: an update on anticancer molecular action, toxicity and novel drug delivery systems. Journal of Pharmacy and Pharmacology. 65(2), 157-170.

[30] Yang, F., Teves, S.S., Kemp, C.J. and Henikoff, S. (2014) Doxorubicin, DNA torsion, and chromatin dynamics. Biochimica et Biophysica Acta. 1845(1), 84-89.

[31] Octavia, Y., Tocchetti, C. G., Gabrielson, K. L., Janssens, S., Crijns, H. J., and Moens, A. L. (2012) Doxorubicin-induced cardiomyopathy: from molecular mechanisms to therapeutic strategies. Journal of Molecular and Cellular Cardiology. 52(6), 1213-1225.

[32] Graf, U., Würgler, F.E., Katz, A.J., Frei, H., Juon, H., Hall, C.B. and Kale, P.G. (1984) Somatic mutation and recombination test in Drosophila melanogaster. Environmental Mutagenesis. 6(2), 153-188.

[33] Sarikaya, R., Selvi, M. and Erkoc, F. (2012) Evaluation of potential genotoxicity of five food dyes using the somatic mutation and recombination test. Chemosphere. 88(8), 974-979.
[34] Cakir, S. and Sarikaya, R. (2005) Genotoxicity testing of some organophosphate insecticides in the *Drosophila* wing spot test. Food and Chemical Toxicology. 43(3), 443- 450.
[35] Carmona, E.R., Escobar, B., Vales, G. and Marcos, R. (2015) Genotoxic testing of titanium dioxide anatase nanoparticles using the wing-spot est and the comet assay in Drosophila. Mutation Research/Genetic Toxicology and Environmental Mutagenesis. 778, 12-21.
[36] Costa, W.F., Oliveira, A.B.D. and Nepomuceno, J.C. (2010) Genotoxicity of lapachol evaluated by wing spot test of *Drosophila melanogaster*. Genetics and Molecular Biology. 33(3), 558-563.
[37] Kaya, B., Kocaoğlu, S. and Demir, E. (2006) Analysis of UV-Stimulated Recombination in the Drosophila SMART Assay. Environmental and Molecular Mutagenesis. 47(5), 357-361.
[38] Lopes, J.C., Machado, N.M., Saturnino, R.S. and Nepomuceno, J.C., (2015) Recombinogenic activity of Pantoprazole((R)) in somatic cells of Drosophila melanogaster. Genetics and Molecular Biology. 38(1), 101-106.
[39] Dias, C.D., Araujo, B.C., Dutra, E.S. and Nepomuceno, J.C. (2009) Protective effects of beta-carotene against the genotoxicity of doxorubicin in somatic cells of *Drosophila melanogaster*. Genetics and Molecular Research. 8(4), 1367-1375.
[40] Lindsley, D.L. and Zimm, G.G. (1992) The Genome of Drosophila Melanogaster. Academic Press, San Diego, USA.
[41] Kastenbaum, M.A. and Bowman, K.O. (1970) Tables for determining the statistical significance of mutation frequencies. Mutation Research. 9, 527-549.
[42] Frei, H. and Würgler, F.E. (1988) Statistical methods to decide whether mutagenicity test data from Drosophila assays indicate a positive, negative, or inconclusive result. Mutation Research. 203(4), 297-308.
[43] Abraham, S.K. (1994) Antigenotoxicity of coffee in the Drosophila assay for somatic mutation and recombination. Mutagenesis. 9(4), 383-386.
[44] Hosseini, A., Mousavi, S.H., Ghanbari, A., Shandiz, F.H., Raziee, H.R., Rad, M.P. and Mousavi, S.H. (2015) Effect of saffron on liver metastases in patients suffering from cancers with liver metastases: A randomized, double blind, placebo-controlled clinical trial. Avicenna Journal of Phytomedicine. 5(5), 434-440.
[45] Danwilai, K., Konmun, J., Sripanidkulchai, B.O. and Subongkot, S. (2017) Antioxidant activity of ginger extract as a daily supplement in cancer patients receiving adjuvant chemotherapy: A pilot study. Cancer Management and Research. 9, 11-18.
[46] Gou, H., Gu, L.Y., Shang, B.Z., Xiong, Y. and Wang, C. (2016) Protective effect of Bu-Zhong-Yi-Qi decoction, the water extract of Chinese traditional herbal medicine, on 5-fluorouracil-induced intestinal mucositis in mice. Human and Experimental Toxicology. 35(12), 1243-1251.
[47] Habibi, E., Shokrzadeh, M., Chabra, A., Naghshvar, F., Keshavarz-Maleki, R. and Ahmadi, A. (2015) Protective effects of *Origanum vulgare* ethanol extract against cyclophosphamide-induced liver toxicity in mice. Pharmaceutical Biology. 53(1), 10-15.
[48] Lam, W., Bussom, S., Guan, F., Jiang, Z., Zhang, W., Gullen, E.A., Liu, S.H. and Cheng, Y.C. (2010) The four-herb Chinese medicine PHY906 reduces chemotherapy-induced gastrointestinal toxicity. Science Translational Medicine. 2(45), 45ra59.
[49] Bolhassani, A., Khavari, A. and Bathaie, S.Z. (2014) Saffron and natural carotenoids: Biochemical activities and anti-tumor effects. Biochimica et Biophysica Acta. 1845(1), 20-30.
[50] Shabalala, S., Louw, J., Muller, C. and Johnson, R. (2017) Polyphenols, autophagy and doxorubicin-induced cardiotoxicity. Life Sciences. 180, 160-170.
[51] Thannickal, V.J. and Fanburg, B.L. (2000) Reactive oxygen species in cell signaling. American Journal of Physiology-Lung Cellular and Molecular Physiology. 279(6), L1005-L1028.
[52] Valko, M., Rhodes, C.J., Moncol, J., Izakovic, M. and Mazur, M. (2006) Free radicals, metals and antioxidants in oxidative stress-induced cancer. Chemico-Biological Interactions. 160(1), 1-40.
[53] Brieger, K., Schiavone, S., Miller, F.J. and Krause, K. (2012) Reactive oxygen species: from health to disease. Swiss Medical Weekly. 142, w13659.
[54] Birben, E., Sahiner, U.M., Sackesen, C., Erzurum, S. and Kalayci, O. (2012) Oxidative stress and antioxidant defense. World Allergy Organization Journal. 5(1), 9-19.
[55] Dai, D.F., Chiao, Y.A., Marcinek, D.J., Szeto, H.H., and Rabinovitch, P.S. (2014) Mitochondrial oxidative stress in aging and healthspan. Longevity and Healthspan. 3(1), 6.
[56] Ray, P.D., Huang, B.W. and Tsuji, Y. (2012) Reactive oxygen species (ROS) homeostasis and redox regulation in cellular signaling. Cellular Signalling. 24(5), 981-990.

[57] Abidli, N., Ghaly, I.S., Hassanane, M.M., Ahmed, E.S. and Khalil, W.K.B. (2015) Myrtus species prevents reproductive toxicity induced by doxorubicin in male mice. Asian Journal of Pharmaceutical and Clinical Research. 8(3), 169-175.

[58] Öz, S. and Çakır Arıca, S. (2016) Evaluation of antigenotoxic effect of Myrtus communis L. (myrtle) fruit extract. In: International Conference on Natural Science and Engineering (ICNASE'16), Kilis 7 Aralık University, Kilis, 2753-2760.

[59] Premkumar, K., Thirunavukkarasu, C., Abraham, S.K., Santhiya, S.T. and Ramesh, A. (2006) Protective effect of saffron (Crocus sativus L.) aqueous extract against genetic damage induced by anti-tumor agents in mice. Human and Experimental Toxicology. 25(2), 79-84.

[60] Makhlouf, H., Saksouk, M., Habib, J. and Chahine, R. (2011) Determination of antioxidant activity of saffron taken from the flower of Crocus sativus grown in Lebanon. African Journal of Biotechnology. 10(41), 8093-8100.

[61] Borek, C. (2004) Dietary antioxidants and human cancer. Integrative Cancer Therapies. 3(4), 333-341.

[62] Lobo, V., Patil, A., Phatak, A. and Chandra, N. (2010) Free radicals, antioxidants and functional foods: Impact on human health. Pharmacognosy Reviews. 4(8), 118.

[63] Agarwal, N., Majee, C. and Chakraborthy, G.S. (2012) Natural herbs as anticancer drugs. International Journal of PharmTech Research. 4(3), 1142-1153.

[64] Pantavos, A., Ruiter, R., Feskens, E.F., De Keyser, C.E., Hofman, A., Stricker, B.H., Franco, O.H. and Kiefte-De Jong, J.C. (2015) Total dietary antioxidant capacity, individual antioxidant intake and breast cancer risk: The Rotterdam study. International Journal of Cancer. 136(9), 2178-2186.

[65] Rossi, M., Tavani, A., Ciociola, V., Ferraroni, M., Parpinel, M., Serafini, M., Bellocco, R., Zucchetto, A., Montella, M., Serraino, D., Lagiou, P. and La Vecchia, C. (2016) Dietary total antioxidant capacity in relation to endometrial cancer risk: a case-control study in Italy. Cancer Causes and Control. 27(3), 425-431.

[66] Anand, P., Kunnumakara, A.B., Sundaram, C., Harikumar, K.B., Tharakan, S.T., Lai, O.S., Sung, B. and Aggarwal, B.B. (2008) Cancer is a preventable disease that requires major lifestyle changes. Pharmaceutical Research. 25(9), 2097-2116.

[67] Bathaie, S.Z., Miri, H., Mohagheghi, M.A., Mokhtari-Dizaji, M., Shahbazfar, A.A. and Hasanzadeh, H. (2013) Saffron aqueous extract inhibits the chemically-induced gastric cancer progression in the wistar albino rat. Iranian Journal of Basic Medical Sciences. 16(1), 27-38.

[68] Trujillo-Jiménez, F., García-López, P., García-Carrancá, A. and Abdullaev, F.I. (2004) Effect of saffron on the viability of normal and malignant human cells in vitro. Acta Horticulturae. 650, 463-469.

[69] Magesh, V., Bhavani, K.D., Senthilnathan, P., Rajendran, P. and Sakthisekaran, D. (2009) In vivo protective effect of crocetin on benzo(a)pyrene-induced lung cancer in swiss albino mice. Phytotherapy Research. 23(4), 533-539.

[70] Mousavi, M., Baharara, J. and Shahrokhabadi, K. (2014) The Synergic Effects of Crocus Sativus L. and Low Frequency Electromagnetic Field on VEGFR2 Gene Expression in Human Breast Cancer Cells. Avicenna Journal of Medical Biotechnology. 6(2), 123-127.

[71] Abdullaev, F.I. (2002) Cancer chemopreventive and tumoricidal properties of saffron (Crocus sativus L.). Experimental Biology and Medicine. 227(1), 20-25.

[72] Modaghegh, M.H., Shahabian, M., Esmaeili, H.A., Rajbai, O. and Hosseinzadeh, H. (2008) Safety evaluation of saffron (Crocus sativus) tablets in healthy volunteers. Phytomedicine. 15(12), 1032-1037.

[73] Bathaie, S.Z., Farajzade, A. and Hoshyar, R. (2014) A review of the chemistry and uses of crocins and crocetin, the carotenoid natural dyes in saffron, with particular emphasis on applications as colorants including their use as biological stains. Biotechnic and Histochemistry. 89(6), 401-411.

[74] Ünaldı, Ü. (2007) A Plant Exposed to Danger: Saffron (Crocus Sativus). Fırat University Journal of Social Science. 17(2), 53-67. (article in Turkish with an abstract in English).

Received: **20.09.2018**
Accepted: **20.02.2019**

CORRESPONDING AUTHOR

Selda Oz
Department of Biology
Faculty of Science and Art,
Kırıkkale University
Kırıkkale – Turkey

e-mail: seldaoz@kku.edu.tr

© by PSP Volume 28 – No. 4/2019 pages 2553-2560 Fresenius Environmental Bulletin

EFFECT OF APPLICATION OF SHEEP MANURE AND ITS BIOCHAR ON CARBON EMISSIONS IN SALT AFFECTED CALCAREOUS SOIL IN SANLIURFA REGION SE TURKEY

Erdal Sakin*, Ibrahim Halil Yanardag

Department of Soil Science and Plant Nutrition, Agriculture Faculty of Harran University, Osmanbey Campus, Sanliurfa, Turkey

ABSTRACT

The terrestrial carbon (C) cycle is a very important part of the global C cycle. Researches have been carried out aimed at reduction of the increasing C emissions and soil salinity that result from intense human activity, in recent years. Organic matter that has been transformed into biochar is more resistant to decomposition and disintegration activity of microorganisms. Therefore, source of organic matter is becoming important in terms of reduction of C emission. The effects of application of sheep manure (SM) and sheep manure biochar (SMBC) on the C dynamics of the calcareous soils with different soil salinity level has been examined in this study. For this aim, soil samples were taken from the Harran Plain and measured by applying different salt concentrations (EC=0, 4, 8, 12 and 16 dS m^{-1}) in laboratory conditions. At the end of the study, amount of CO_2-C flux from the soils was compared with the control group, a reduction was observed in both treatments (SM and SMBC), the greatest reduction being observed in SMBC. While reductions of 15.62% (EC=4 dS m^{-1}), 19.5% (EC=8 dS m^{-1}), 40.15% (EC=12 dS m^{-1}) and 48.43% (EC=16 dS m^{-1}) were observed in samples with SM, the corresponding reductions in samples with SMBC were observed as 21.76%, 52.94%, 58.82% and 67.64% respectively at the end of the first month of the study. As a result, CO_2 efflux was decreased in line with increasing EC values. However, this situation is considered not to be dependent only on the increase in amount of saline in the soil, but at the same time to be related to the biochar added to the soil. When comparing the effect of SM and SMBC treatments to carbon - storage of soil, SMBC resulted in lower carbon emissions. Since SM undergoes a normal process and is mineralized, more CO_2 is released. Therefore, in cases where organic waste is added to soil, converting this to biochar first will be of great importance both for the soil and for atmospheric CO_2.

KEYWORDS:
Biochar, soil salinity, C emission, SE Turkey

INTRODUCTION

Salinity is one of the most effective limiting factors in global food safety. According to the latest data, approximately 1128 million hectares (Mha) of areas are affected by salinity on a global scale [1]. In the past, when the effects of salinity on the physical and chemical properties of soil were examined, the losses occurring in soils, the carbon emissions, the structure of soils and the plant health aspects were not properly studied [2]. Due to the low biomass production capacity of agricultural areas affected by salinization, the reduction in biomass access to soil results in inadequate accumulation of organic matter [3]. For this reason, the effect of salinity on carbon dynamics of soils affected by salinity are two - sided, namely in the form of (i) the effect of carbon losses in high and sloping areas where especially secondary salinization is observed, (ii) the effect of increased sodicity and sodic soils on carbon dynamics [4].

Animal manure treatments improve the physical, chemical and biological soil properties [5-7] that improve the sustainability and ensure the aeration of degraded soils. Application of organic matter (such as green manures, compost, and food processing wastes, etc.) can both ameliorate and increase the C stocks and fertility of saline soils. These effects vary depending on the amount of carbon present in the soil as well as on the type and amount of material applied [8]. Gong et al. [9] determined that organic amendments are widely used in agricultural ecosystems due to their positive roles in reducing climate change by way of bonding carbon to the soil and in increasing soil fertility. Li et al. [9] stated that the general response of CO_2 emissions in the soil to organic amendments remains unclear and is made up of a complex process.

Biochar is a C-rich organic material produced during slow exothermic thermal decomposition of biomass at temperatures ≤700 °C under zero or low oxygen conditions which described as black gold for agricultural cultivation. Biochar could remain between 100-1000 years in the soil, is formed from persistent carbon [3], storing carbon in the soil and thereby reducing global greenhouse gases [10]. Since biochar either reduces the uptake of Na^+ or facilitates its removal from plant, and can be re-

duced the negative effects of salinization in terms of plant and soil [11].

Malik and Azam [12] determined that while soil salinity increases, the amount of CO_2 cumulatively reduced in their 90-day incubation studies. They stated that at low salinity (0.5 dS m^{-1}) had no effect on CO_2 emissions. However, when the amount of soil CO_2 is compared with the control at 2 dS m^{-1} salinity level, an output about twice as much as the control soil has been detected.

Most of the studies conducted on the organic carbon dynamics of soils have been made using salt-free and problem-free soils. Although the arid and semi-arid areas affected by salinity in Turkey are large, there is little information regarding levels of carbon emissions of soils affected by salinity. For this reason, there is a great need for work to be done on this subject in our country.

The aim of this study is to observe the effect on carbon dynamics of applying sheep manure (SM) and sheep manure biochar (SMBC) to calcareous soils at different salt concentrations and to compare the effect of organic matter source on the CO_2 emission with different soil salinity concentration.

MATERIALS AND METHODS

The study area is located at (37°10"17'N and 39°00"14'E and altitude 490 m) Harran Plain, 1 km west of Gulveren village, which is situated 20 km east of Şanlıurfa (South East Turkey). The soil samples were taken at depths of 0-5 cm on the. The soils are classified as Calcic Vertisol (IUSS, 2007) with AC horizon, clayey and calcareous soils formed from the parent material of limestone. The soils are slightly alkaline, with low salinity, and low organic carbon content (Table 1). In the region, summers are dry and hot, while the winters are mild with low precipitation. In some years the rainfall is insufficient for agricultural production. The mean annual rainfall is 448.11 mm, while a highest mean annual temperature of 41.12 °C has been seen in July and a lowest of 2.41 °C has been observed in February. A highest mean annual relative humidity of 92.32% and a lowest of 33.29% have been recorded.

The soil samples collected from the site were dried in air, ground and passed through a 2-mm sieved in a laboratory condition. Soil organic C (SOC) was determined by potassium dichromate oxidation and calcium carbonate equivalent (CaCO3), pH values, cation exchangeable capacity (CEC), electrical conductivity (EC, Crisol-31 EC meter, GLP Inc.) were determined by Method of Anne [13], described by Duchaufour [14], Bernard Calcimeter Method; as described Duchaufour [14]; Peech [15]; Chapman [16]; Bower and Wilcox [17], respectively. Exchangeable cations (Sodium, Potassium, Calcium and Magnesium Equivalent) are taken as an index of comparable quantity of these cations extracted with NaCl solution [18] and measured by AAS (AAnalyst-800 AAS, Perkin Elmer Precisely). To determine the water content of the soil samples, an 800 g soil sample was placed in 9.6 L plant pots with holes in the bottom and sealed with filters, saturated, and covered with plastic, after which it was left for 72 hours and its soil water content was determined. Next, 500 g of soil was placed in 2 L plastic containers and sheep manure (SM) and sheep manure biochar (SMBC) were added at a rate of 5 g C kg and mixed. Throughout the study, the soil samples were kept at 50% soil water content with different EC values (EC= 0 dS m^{-1}, EC= 4 dS m^{-1}, EC= 8 dS m^{-1}, EC= 12 dS m^{-1} and EC= 16 dS m^{-1}). To prepare the saline solution, NaCl salt was used. The soil samples were incubated under laboratory conditions at a constant heat of 24.0±2.0 °C over a 14-week period. The samples were changed once a week. At sample-changing times, all samples were aired for 30 minutes.

The CO_2 emitted from the soil samples was measured with the soda-lime method [19] in the following way:

$$E_{CO2} = (SLad-SLin)*WC / (A*t)$$

Here, E_{CO2} is the total amount of CO_2 emitted during incubation (g CO_2 m^{-2} day^{-1}); SLad is the CO_2-adsorbed amount of soda lime (g), SLin is the amount of soda lime at the initial (g); A is the area (m^2); t is the incubation time (time spent in the field); and WC is the water correction coefficient (1.69).

TABLE 1
Some physicochemical properties of soil in the test area

Soil Reaction (pH 1:2.5)	7.30
Electrical Conductivity (µscm^{-1})	72.6
Calcareousness ($CaCO_3$ %)	30.6
Organic Carbon (%)	0.74
Exchangeable cation (cmol kg^{-1})	
Calcium	31.0
Potassium	1.08
Magnesium	3.00
Sodium	2.09
Cation Exchange Capacity (CEC, cmol kg^{-1})	37.2
Soil fractions (%)	
Sand	15.0
Silt	40.0
Clay	45.0

RESULTS AND DISCUSSIONS

In line with the increased EC values in both treatments, a decrease in the amount of CO_2-C emitted from the soil was observed when compared with the control group. It was shown that this decrease was greater in soils treated with SMBC. -

The results showed that CO_2–C emissions in soils treated with SM was decreased compared with the control group (0.95 g CO_2-C kg^{-1}) while EC values increased. This decrease was 0.85 (EC=4 dS m^{-1}), 0.55 (EC=8 dS m^{-1}), 0.51 (EC=12 dS m^{-1}) and 0.48 g CO_2-C kg^{-1} (EC=16 dS m^{-1}) (Fig. 2a). When the amount of CO_2-C emitted in soils treated with SMBC was compared with the control group (0.32 g CO_2-C kg^{-1}), however, a decrease was observed with 0.23, 0.21, 0.20 and 0.14 g CO_2-C kg^{-1} according to the corresponding EC values, respectively (Fig. 1b).

The amount of CO_2-C from SM and SMBC was decreased as EC values increased at the end of one month of the study. When the result compared with the control groups, this decrease was 15.62% (EC=4 dS m^{-1}), 19.5% (EC=8 dS m^{-1}), 40.15% (EC=12 dS m^{-1}) and 48.43% (EC=16 dS m^{-1}) for SM, whereas it was 21.76%, 52.94%, 58.82% and 67.64% respectively in SMBC. In the final week of the study, EC application did not show a significant difference within the SM and control group ($P>0.05$). Artiola et al. [20] stated that the reduction was 40% in the end of first month for their incubation study. It has been noted in previous studies that biochar applications slow down the decomposition time of organic carbon and have a positive effect on the storage of carbon in the soil due to it resistant to decomposition [21].

Organic matter that has been transformed into biochar is more resistant to decomposition and disintegration activity of microorganisms. Since farm manure that is not subjected to any kind of thermal procedure in decompose and disintegrate process over a long period, it could have a higher level of easily biodegradable carbon, and this may result in a higher CO_2 efflux [22].

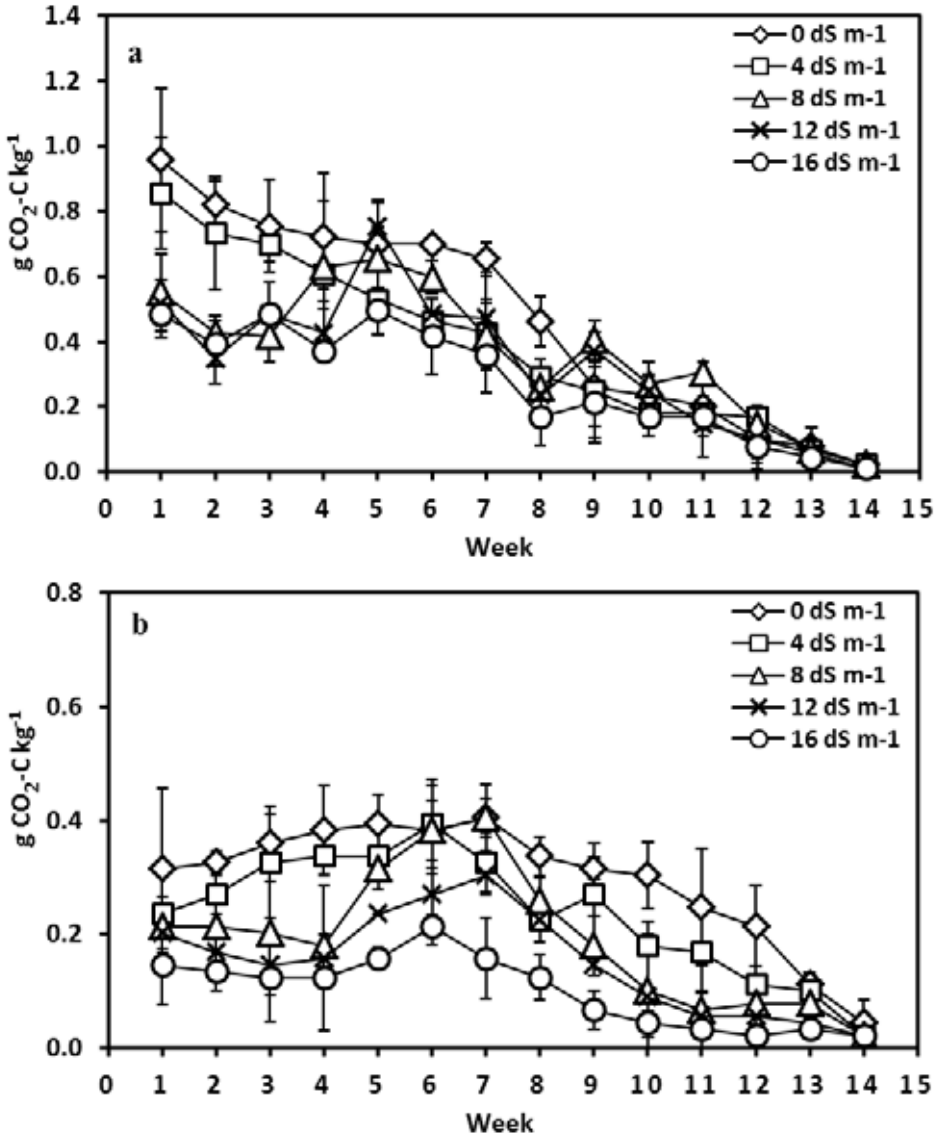

FIGURE 1
Evaluation of CO_2 emissions with application of a. Manure and b. Biochar

In the study conducted by Yanardağ et al. [22] on Entisol, Alfisol and Mollisol soils treated with farm manure, pig slurry and biochar, it was determined that CO_2 emissions were higher in soils treated with farm manure. However, the lowest CO_2 emissions were obtained with BC applications. At the same time, they stated that there were higher rates of labile carbon in farm manure and pig slurry, and that because of this CO_2 emissions for these treatments were high. In addition, Woolf et al. [23] stated that when biochar was added to soil over a long period, the soil could store more carbon compared to other organic waste and that therefore, this would be beneficial for reducing global climate change. The findings obtained and views put forward in the studies carried out on this subject are such as to support the findings of our study.

Examining the effect of salt on the carbon dynamics of soil, it was revealed that compared with the control group, the amount of CO_2-C treated with SM and SMBC was lower (Fig. 1a, b). The lowest emissions were observed in samples treated with SMBC. Also, our study was observed that when soil salinity was increased, the amount of CO_2–C emitted from soil decreased.

As a results, soils treated with SMBC has low CO_2-C emissions, due to high salt adsorption capacity of BC, together with decomposition of organic matter, ensure enhancement of the soil structure by combining the cations with the clay minerals in the soil. In addition, soil organic compounds are directly affected by these enhancements. Sodium, which has a high adsorption capacity of soil solution, results in the withdrawal of other elements from the affected area by adsorption to the clay surface [23, 24]. Thomas et al. [11] stated that since biochar either reduces the uptake of Na^+ in plants or facilitates its distribution, moreover may be reduce the negative effects of salinization. Akhtar et al. [26] reported that salinity stress of plants was limited with biochar application.

In this study, CO_2–C emissions were more rapid during the first weeks, then decreasing and stabilizing. On a weekly basis, the highest efflux was measured in the first week (Fig. 2a, b). It is considered that in the first weeks, since the air-dry soil was brought to 50% field capacity, the biodegradable carbon in the manure was easily degraded by microorganisms, resulting in higher emissions. Then, in next weeks, with the reduction in labile C, the slow degradation by the more recalcitrant form of carbon that remained resulted in lower emissions.

The CO_2–C emission of soil was 0.31 g CO_2-C kg^{-1} with SMBC application, and it decreased in 67.05% when compared the control groups with BC applications at EC = 0 level, and it was ranged 0.95 g CO_2-C kg^{-1} for SM in the first week of the study. The comparison of cumulative values showed a decrease of 42.56% at the fourth week, while the decrease had become 62.16% at the final week (14th week) of the study. Setia et al. [27], following 49-day incubation in salt-free soil, found that cumulative CO_2-C emissions of soils treated with wheat residue were significantly higher compared to the control group. Artiola et al. [20] studied CO_2–C emissions of alkaline soils (silty sandy texture) with 2% and 4% of biochar application over 4 months. At the end of the first month of the study, a 40% of CO_2–C emissions reduction was recorded. Again, at the end of the fourth month, it was determined that the cumulative CO_2–C emissions ratio was 31% lower in BC application when compared control group. Also, they reported that biochar reduced the bulk density of the soil, and increased soil-water content.

The amount of CO_2 emitted from the soils was decreased with increasing salt concentrations in both treatments. However, this reduction was higher in SMBC (Fig 2a, b). Accordingly, in the first week of the study, CO_2-C emissions was ranged between 0.24 g CO_2-C kg^{-1} (25%), 0.21 g CO_2-C kg^{-1} (33.25%), 0.20 g CO_2-C kg^{-1} (35.71%) and 0.14 g CO_2-C kg^{-1} (53.57%) in the 4, 8, 12 and 16 dS m^{-1} of EC levels respectively. The cumulative reductions were 20%, 34.78%, 48.64% and 66.03% respectively at corresponding EC levels at the end of the study.

The series of decreases was observed with SMBC application at 4th week, which 15.44%, 44.63%, 51.22% and 61.78% at the 4, 8, 12 and 16 dS m^{-1} of EC levels respectively. It was revealed that with SMBC application, high range of recalcitrant C remains in the soil for longer and results in lower CO_2 emissions when compared with normal animal manure. Moreover, with increased EC values, CO_2 emission was decreased and this decrease was lower in SMBC when compared with other applications. The CO_2–C emission was higher at EC=0 dSm^{-1} level in both treatments. It is considered that this situation is normal for healthy soils, since living conditions in this soil are ideal for soil creatures. However, this situation disappears in saline soils when salinity level increases. Since salty soils are saturated with water, activity of organisms decreases and so CO_2–C is reduced[28-30].

Seti et al. [27] determined that cumulative CO_2-C values was decreased of 51% in the silty-loamy soils and 56% in the sandy-loamy soils at EC= 5 dS m^{-1} level. In the further stage of the experiment, while reductions was 31%, 21% and 15% at EC= 6.0, 7.0 and 8.0 dS m^{-1} respectively in sandy-loamy soils, there were decreases of 42%, 38% and 27% at the corresponding salinity levels in silty-loamy soils. Cumulative CO_2-C efflux increased sharply over time in control group soils [27]. Salinity decreases C mineralization due to its different negative effects on microorganisms in the soil. The negative effect of salinity on soil respiration was understood in previously conducted studies [31].

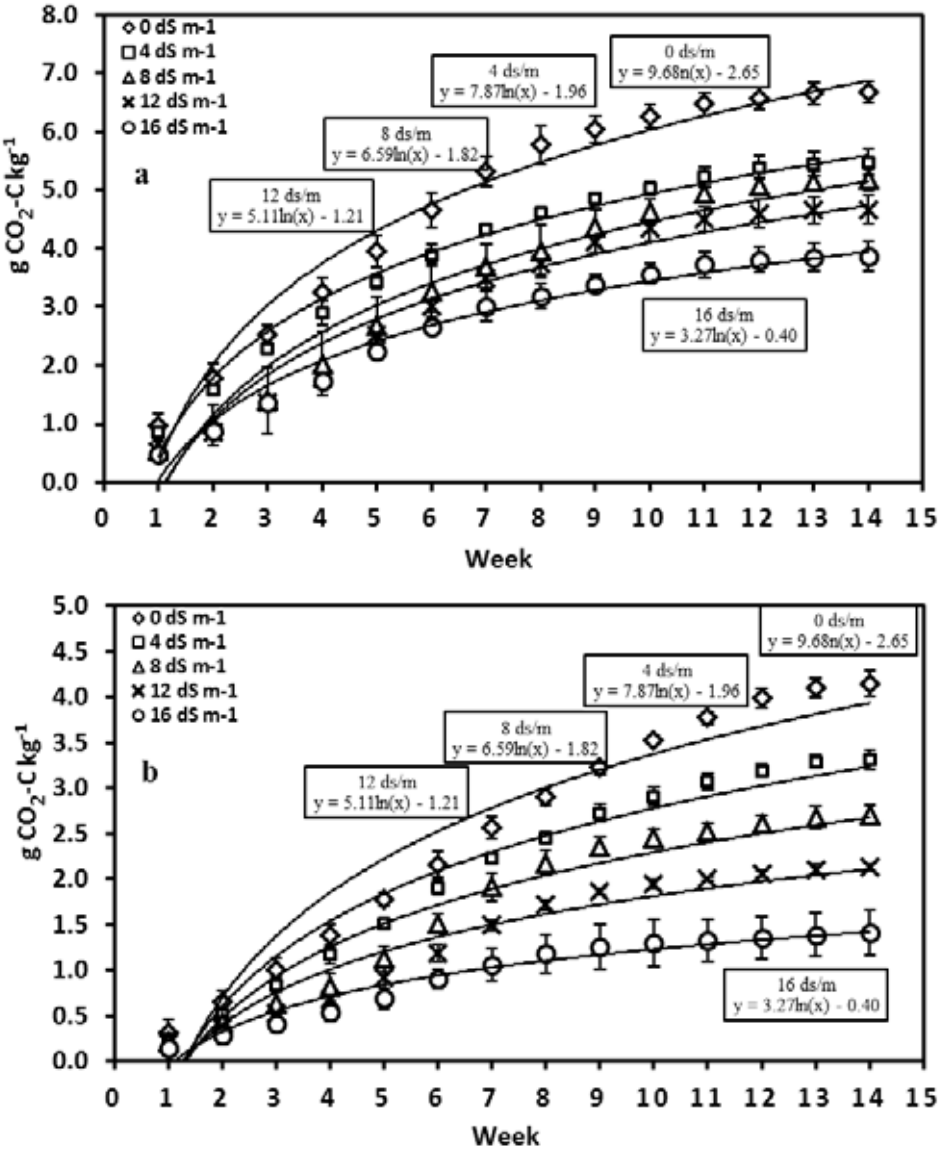

FIGURE 2
Cumulative CO_2-C emissions with application of a. Manure and b. Biochar

TABLE 2
Repeated measures analysis of variance (ANOVA) for CO_2 emissions

Source of Variation	Soil Salinity				
	0 dS m^{-1}	4 dS m^{-1}	8 dS m^{-1}	12 dS m^{-1}	16 dS m^{-1}
Treatment [a]	78.8*	56.9*	170.7*	218.3*	169.2*
Time [a]	28.6*	20.8*	34.8*	39.0*	20.3*
Treatment X Time [a]	10.3*	7.1*	8.3*	10.6*	6.1*

[a] Significant at: *P<0.001

The results of variance analysis (ANOVA) that was made in relation to the effects of salinity, time, treatment and treatment-time interaction on carbon emissions are given in Table 2. In the study, the all salinity levels were statistically significantly interacted with treatment, time and treatment-time interaction based on carbon emissions of soil (P<0.001). For treatment groups at 8, 12 and 16 dS m^{-1} salinity levels, carbon emissions were found to be higher relation than those of the control group. With regard to time, however, at 8 and 12 dS m^{-1} salinity levels, carbon emissions were found to be higher relation than those of the control group. Repeated ANOVA shows that soil CO_2-C emissions reacted significantly to sheep manure and its biochar according to time factors and different rates of soil salinity. Besides these, interactions between incubation period and soil salinity were found to be significant (p<0.001) (Table 2).

TABLE 3
Linear regression analysis (Y=mX+b) of CO_2-C emissions and soil salinity.

Y[a]	X	b	m	β[b]	r^2	F[c]
CO_2-C	0 dS m^{-1}	0.492	43.15	0.99	0.99	1862*
	4 dS m^{-1}	0.595	23.78	0.98	0.98	565*
	8 dS m^{-1}	0.686	16.85	0.96	0.96	283*
	12 dS m^{-1}	0.886	18.20	0.96	0.97	331*
	16 dS m^{-1}	1.372	14.48	0.95	0.95	210*

[a] CO_2 respiration
[b] Standardized Coefficient
[c] *P<0.001*

Regression analysis results showing the relationship between carbon emissions and salinity are given in Table 3. The linear relationship (Y=mX+b) between salinity levels and carbon emission was found to be highly significant (r^2=0.95-0.99; P<0.001). The regression equation coefficient (b) increases according to salinity level, whereas the regression coefficient (m) decreases. A linear model was obtained between carbon emissions and salt concentrations. Analysis results show correlations with carbon emissions of r^2=0.99 in the 0 dS m^{-1} control group, r^2=0.98 in 4 dS m^{-1} salinized soil, r^2=0.96 in 8 dS m^{-1} salinized soil, r^2=0.97 in 12 dS m^{-1} salinized soil and r^2=0.95 in 16 dS m^{-1} salinized soil. The carbon emissions can be estimated with regression coefficients determined for different salinity levels given in Table 3.

CONCLUSIONS

Examination of the effects of SM and SMBC applied to soil on carbon storage reveals that SMBC results in fewer C emissions. As SM undergoes a normal process and is mineralized, more CO_2-C is emitted due to its high labile C content. It was observed in this study that in the short term, since biochar disintegrates slowly in the soil, is more resistant to decomposition, and remains in the soil for a long period, it provides carbon storage in the soil. It was revealed that biochar reduces degradation-disintegration of OC in the soil and has a powerful effect on storage of carbon in the soil.

Organic sources are added to soil is very important in terms of soil and for atmospheric CO_2-C sequestration. It is argued that biochar produced for use as a soil enhancer has the potential to balance CO_2 emissions and is a strategy for reducing climate change. The potential for biochar to reduce climate change, and its long-term complex effect on carbon storage because it is a highly stable material, have been revealed to a large extent. Therefore, use of more recalcitrant carbon such like biochar could help long terms C cycle.

As a result, CO_2–C emissions decreased in line with increased EC values. It is considered that this situation depends only on the increased amount of salt in the soil, however, this study observed that biochar addition to the soil could help decreasing negative affect of salinity and with this founding biochar has two side soil improvement one of increase long term C sequestration and the other decrease negative affect of salinity in terms of plant and soil system.

The majority of studies about organic carbon dynamics of soils have been made on salt-free and problem-free soils. Although in many country, large areas affected by salinity in arid or semi-arid such as Turkey, there is little information regarding levels of CO_2-C emissions of soils affected by salinity. Therefore, there is a great need for further research on a wider scale on this matter in our country.

REFERENCES

[1] Wicke, B., Smeets, E., Dornburg, V., Vashev, B., Gaiser, T., Turkenburg, W. and Faaij, A. (2011) The global technical and economic potential of bioenergy from salt-affected soils. Energy Environ. Sci. 4, 2669–2681.
[2] Jeffery, S., Verheijen, F.G.A., Van Der Velde, M. and Bastos, A.C. (2011) A quantitative review of the effects of biochar application to soils on crop productivity using meta-analysis. Agric. Ecosyst. Environ. 144, 175–187.
[3] Cheng, C.H., Lehmann, J., Thies, J.E. and Burton, S.D. (2008) Stability of black carbon in soils across a climatic gradient. J. Geophys. Res. 113, 20-27.
[4] Wong, V.N.L., Greene, R.S.B., Murphy, B.W, and Dalal, R.S. (2004) Mann Carbon Dynamics in Salt-Affected Soils. In: Regolith 2004, (Roach, I.C. ed). CRC LEME, 407-410,
[5] Boysan-Canal, S., Bozkurt, M.A. and Kipcak, S. (2018) The effects of organic amentmnets on cadium uptake of spinach (spinacia oleracea L.) and plant growth under cadmium toxicity. Fresen. Environ. Bull. 27, 3174-3179.
[6] Belliturk, K., Hinisli, N., Adiloglu, A. (2017) The effect of vermicompost, sheep manure, and cow manure on nutrition content of curly lettuce (Lactuva Sativa var.). Fresen. Environ. Bull. 26, 116-1120.

[7] Sakin, E., Celik, A., Dogan, Z., Yalcin, H. and Seyrek, A. (2018) Comparing carbon pools and some soil quality parameters of soils in organic and conventional agriculture land. Fresen. Environ. Bull. 27, 7536-7544.
[8] Mapanda, F., Wuta, M., Nyamangara, J. and Rees, R.M. (2011) Effects of organic and mineral fertilizer nitrogen on greenhouse gas emissions and plant-captured carbon under maize cropping in Zimbabwe. Plant Soil. 343, 67-81.
[9] Li, L.J., You, M.Y., Shi, H.A., Ding, X., Qiao, Y.F., Han, X.Z. (2013) Soil CO_2 emissions from a cultivated Mollisol: Effects of organic amendments, soil temperature, and moisture. Eur. J. Soil Biol. 55, 83-90.
[10] Chowdhury, M.A., De Neergaard, A. and Jensen, L.S. (2014) Potential of aeration fow rate and bio-char addition to reduce greenhouse gas and ammonia emissions during manure composting. Chemosphere. 97, 16–25.
[11] Thomas, S.C., Frye, S., Gale, N., Garmon, M., Launchbury, R., Machado, N., Melamed, S., Murray, J., Petroff, A. and Winsborough, C. (2013) Biochar mitigates negative effects of salt additions on two herbaceous plant species. J. Environ. Manage. 129, 62–68.
[12] Malik, K.A. and Azam, F.E. (1979) Effect of Salinity on carbon and nitrogen transformations in soil. Pak. J. Bot. 11, 113-122.
[13] Anne, P. (1945) Carbone organique (total) du sol et de l'humus. Ann. Agron. 15, 161-172.
[14] Duchaufour, P.H. (1970) Precis de Pedologie. Masson. Paris, 481,
[15] Peech, M. (1965) Hidrogen-ion activity. Methods of Soil Analysis. American Society of Agronomy. 2, 914-916.
[16] Chapman, H.D. (1965) Cation Exchange Capacity. Methods of Soil Analysis. American Society of Agronomy. 2, 891-900.
[17] Bower, C.A. and Wilcox, L.V. (1965) Soluble salts. Methods of Soils Analysis. American Society of Agronomy. 2, 933-940.
[18] Pratt, P.F. (1965) Potassium. In: Black, C.A. (eds.) Medhods of soil analaysis. Part 2 ASA, Madison, USA, 1023-1031
[19] Edwards, N.T. (1982) The use of soda-lime measuring respirasyon rates in terrestrial systems. Pedobiologia. 23, 321-330.
[20] Artiola, J.F., Rasmussen, C. and Freitas, F. (2012) Effects of a biochar-amended alkaline soil on the growth of Romaine lettuce and bermudagrass. Soil Sci. 177, 561-570.
[21] Weiwei L., Weixin, D., Junhua, Z., Yi. L., Jiafa, L., Nanthi. B. and Zubin, X. (2014) Biochar suppressed the decomposition of organic carbon in a cultivated sandy loam soil: A negative priming effect. Soil Biol. Biochem. 76, 12-21.
[22] Yanardag, I.H., Zornoza. R., Faz. C., Buyukkilic Yanardag, A., Mermut, A. (2015) Evaluation of carbon and nitrogen dynamics in different soil types amended with pig slurry, pig manure and its biochar by chemical and thermogravimetric analysis. Biol. Fertil. Soils. 51, 183–196.
[23] Woolf, D. and Lehmann, J. (2012) Modelling the long-term response to positive and negative priming of soil organic carbon by black carbon. Biogeochem. 111, 83–95.
[24] Qadir, M. and Schubert, S. (2002) Degradation processes and nutrient constraints in sodic soils. Land Degrad. Dev. 13, 275–294.
[25] Ozdemir, S., Dede, O.H. and Koseoglu, G. (2004) Recycling of msw compost and sewage sludge as growıng substrate for ornamental potted plants. Fresen. Environ. Bull. 13, 30-33.
[26] Akhtar, S.S., Anders, M.N. and Liu, F. (2015) Biochar mitigates Salinity Stress in potato. J. Agro. Crop Sci. 201, 368–378.
[27] Setia, R., Marschner, P., Baldock, F. and Chittleborough, D. (2010) Is CO_2 evolution in saline soils affected by an osmotic effect and calcium carbonate? Biol. Fertil. Soils. 46, 781–792.
[28] Oren, A. and Steinberger, Y. (2008) Coping with artifacts induced by $CaCO_3$–CO_2–H_2O equilibria in substrate utilization profiling of calcareous soils. Soil Biol. Biochem. 40, 2569–2577.
[29] Sakin, E. and Yanardag, I.H. (2017) Effect of the different land uses on soil organic carbon and carbon emissions in Harran Plain SE Turkey. In: Arapgirlioglu, H., Atik, A., Elliot, RE., Turgeon, E. (eds.) Researches on science and Art in 21st century Turkey. Volume 1. Gece Kitaplıgı Yayınevi, Ankara, 135-143.
[30] Sakin, E. and Seyrek, A. (2017) The effect of application of boiochar and different salt concentrations to soil on CO_2 emissions. In: Arapgirlioglu, H., Atik, A., Elliot, RE., Turgeon, E. (eds.) Researches on science and Art in 21st century Turkey. Volume 1. Gece Kitaplıgı Yayınevi, Ankara, 83-88.
[31] Rietz, D.N, and Haynes, R.J. (2003) Effects of irrigation-induced salinity and sodicity on soil microbial activity. Soil Biol. Biochem. 35, 845–854.

Received: **26.09.2018**
Accepted: **29.01.2019**

CORRESPONDING AUTHOR

Erdal Sakin
Department of Soil Science and Plant Nutrition,
Agriculture Faculty of Harran University,
Osmanbey Campus,
Sanliurfa – Turkey

e-mail: esakin@harran.edu.tr

© by PSP Volume 28 – No. 4/2019 pages 2561-2574 Fresenius Environmental Bulletin

COMPARISON OF THE EFFECTS OF ZNO NPS, MGO NPS AND IONIC ZINC AND MAGNESIUM ON WHEAT PLANTS

Yifan Ni, Lian Xiao, Fengting Wan, Mengxuan Xu, Lingzhi Qiu, Junfeng Li, Junli Li*

School of Chemistry, Chemical Engineering and Life Sciences, Wuhan University of Technology, Wuhan 430070, China

ABSTRACT

Due to special properties, ZnO and MgO nanoparticles (NPs) have wide applications in various fields and can be easily dispersed into air and soil. Plants contacts soil directly and are also an important source of food. Hence, studies on phototoxicity of ZnO NPs and MgO NPs to plants are needed. In this study, wheat plants were exposed to ZnO NPs, MgO NPs and ionic Zn, Mg at concentration of 50 and 200 mg/L dissolved in water. Growth parameters, Zn and Mg accumulation, total protein, soluble sugar and antioxidant system were determined after 4 days of treatment. Results showed that ionic Zn and Mg reduced the shoot and root length and also lead to increments of total proteins, soluble sugars and antioxidant enzyme activity. 200 mg/L Mg^{2+} increased chlorophyll contents by 29%. 200 mg/L Mg^{2+} and ZnO NPs also increased root activity. In other words, Zn and Mg oxide nanoparticles exhibited less physiology toxicity than ionic Zn and Mg of the same concentration.

KEYWORDS:
ZnO nanoparticles; MgO nanoparticles; Ionic Zn; Ionic Mg; Phytotoxicity.

INTRODUCTION

Zinc (Zn) and magnesium (Mg) are essential micronutrients for plants. They usually exist as a part or a cofactor of enzymes [1]. Zinc is involved in plant structure and function [2]. Zinc is required for the activity of dehydrogenases, aldolases, isomerases, transphosphorylases, RNA and DNA polymerases, and is also involved in the synthesis of tryptophan, cell division, maintenance of membrane structure and photosynthesis, and acts as a regulatory cofactor in protein synthesis [3]. Mg is a contributor to ATPase, RNA polymerase, protein kinase, and other enzymes [4] and stabilizes the structure of DNA and RNA [5]. In plants, Mg is essential in synthetic of chlorophyll [6]. Zinc also plays a crucial role in metabolization of auxin. Nearly 1/3 of the world's population suffered from zinc deficiency [7] ,which mostly results in inadequate dietary intake of Zn [8]. Inorganic (ZnO, ZnSO4) and chelated sources of Zn (Zn-EDTA, glycine-chelated Biomin Zn) are the most commonly used zinc fertilizer [9]. Foliar Zn application alone or with soil application is the common way of fertilizing [10], for which Zn could mobile in phloem [9]. However, high level of zinc, as heavy metal particles, could lead to soil pollution and toxicity to plant cells [11]. Mg_2SO_4 and $Mg(NO_3)_2$ are commonly used Mg fertilizer. Soil and water pollution could also result in high concentration of Mg.

Nanoparticles (NPs) are nanosized particles (smaller than 100 nm) that could be manufactured by a coprecipitation method, a vapor deposition process and a Sol-gel method. Due to their size and diverse morphology, NPs can be easily dispersed into the environment, where they interact with both biotic and abiotic components [12]. Researches have find that certain NPs could lead to damages to some human cells and heart [13, 14]. Methods are found to reduce the NPs, but the majority of NPs are in the environment at present[15].On the other hand, the unique physical, chemical, magnetic and optical characteristics also lead to wide applications of NPs in medicine, agriculture, chemistry, environment and food industries [16-19]. However, the impact of nanoparticles on environment and human is an elusive problem now and needs further study.

ZnO NPs are one of the most widely used nanoscale metal oxides with photocatalyzing and photo-oxidizing abilities. ZnO NPs are also added in sunscreens and sun care products owing to their excellent UV absorption and reflective properties [20]. ZnO NPs are also used as pesticides and fungicides, because of their antibacterial activity with various particle sizes [21] and ability to kill fungi.

Similarly, MgO NPs can also be applied as antimicrobial agents [22] and cancer treatment agents [23] owing to their antimicrobial activity. ZnO and MgO NPs, owning to their surface effect, may be the alternative of their bulk counterpart as a new type of fertilizer [24]. Since ZnO and MgO NPs have such wide range of applications in many aspects, these nanoparticles can be easily released into the environment through precipitation, irriga-

tion, and sludge disposal[25]. Furthermore, we should evaluate whether they are safe before we apply them to agriculture, cosmetics and other industries. Researches on the potential toxicity of these NPs in ecology are need. In some experiments, high level of NPs does present phytotoxicity on plants [26]. Other studies found that ZnO NPs and MgO NPs showed their toxicity by inducing reactive oxygen species (ROS) activities [27, 28].

Wheat is one of the most important grain crops and provides nutrition and energy to many of the world population, especially in the developing countries [29]. China produced most wheat in the world every year [30]. And Wheat and its products are the important source of Zn supplied in foods in China [31]. In order to evaluate safety of MgO and ZnO NPs, wheat plants were exposed to Mg^{2+}, Zn^{2+}, MgO and ZnO NPs at 50 and 200 mg/L respectively. Fresh and dry biomass, root and shoot length and chlorophyll content were measured to evaluate plant growth. Total soluble proteins and soluble sugars were measured to evaluate the activity of plant cells. Total soluble protein is involved in many intracellular reactions. The soluble sugar is main substance to provide energy. Root activity was measured to evaluate the vitality of roots. Besides, we measured ROS indexes to find out whether MgO and ZnO NPs activate the antioxidant system of wheat. SOD, CAT and POD are three key enzymes in plant antioxidant defense system. MDA is an indicator of lipid peroxidation of plant cells. APX and anthocyanin are also substances to scavenge some oxides. Besides, we determined Zn and Mg accumulation in wheat roots and leaves. In our study, we compared these indexes between ionic Zn, Mg and nanosized ZnO, MgO, and between low and high levels of ZnO, MgO NPs. We find that generally ZnO and MgO NPs shows less toxicity than their bulk counterpart, but NPs at high concentration still have phytotoxicity to some extent.

MATERIALS AND METHODS

Experiment design. Wheat plants were treated by 50, 200 mg/L ZnO NPs, MgO NPs, Zn^{2+} and Mg^{2+} using hydroponics. We also used ionic Zn and Mg for comparison. The Zn or Mg content of Zn^{2+} and Mg^{2+} group was equivalent to Zn or Mg content of ZnO NPs and MgO NPs groups. It is noteworthy that the concentration of Zn^{2+} and Mg^{2+} was not actually 50 or 200 mg/L. In this study, the concentration of Zn^{2+} and Mg^{2+} was described as 50 and 200 mg/L for convenience.

Characterization of nanoparticles. The ZnO NPs and MgO used in our study were bought from Macklin Inc. (Shanghai, China). Mean diameters of ZnO NPs and MgO NPs are both 100 nm. The NPs were characterized by TEM. Fig. S1 shows the TEM images of ZnO NPs and MgO NPs.

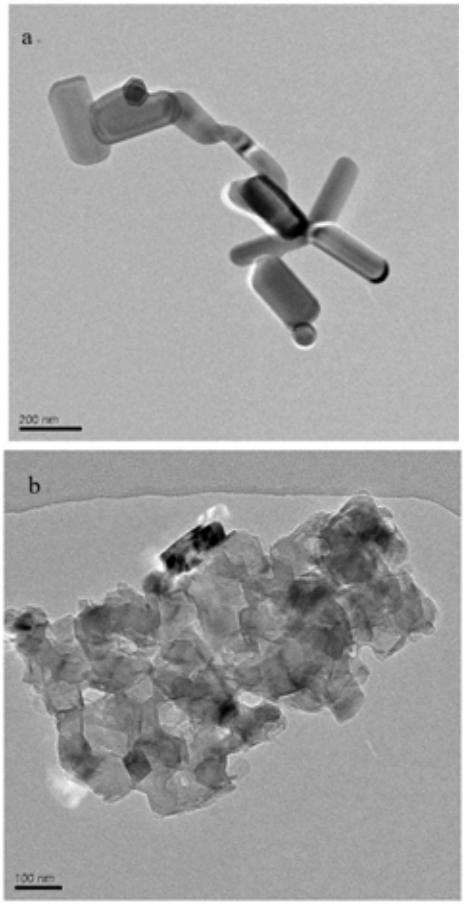

FIGURE S1
TEM images of ZnO NPs (a) and MgO NPs (b).

Preparation of particle suspension. ZnO NPs and MgO NPs (50, 200 mg/L) were suspended in deionized water and sonicated (Ultrasonic Cleanser KQ2200B, 100 W, 40 kHz, Kun Shan Ultrasonic Instruments Co., Ltd., China) for 36 hours. Solutions of Zn^{2+} and Mg^{2+} were prepared from $ZnSO_4 \cdot 7H_2O$ and $MgSO_4 \cdot 7H_2O$ also in deionized water.

Plant growth and treatments. Wheat seeds were soaked in deionized water for 4 h, and then wrapped by wet gauze and put in an incubator in the dark at 30ºC for 24 h. After germination, seeds were dispersed on a clean plate in the same condition for another 24 h. And then seedlings were put on a filter paper for 3 days in a growth chamber at 28/18ºC with a 16/8 light/dark photoperiod; the light intensity was 2000 lx. Then, plants were allocated in boxes filled with 2.5 L deionized water. After growing for 2 days, deionized water was changed to 1/4 Hoagland nutrient solution and grew for 2 days before treatment. There was a vent board in each box to pump air into the container for 30

min every 3 h. After 2 days, 1/4 Hoagland nutrient solution was replaced by NPs suspensions (n-ZnO/MgO) and controls (DW, $ZnSO_4 \cdot 7H_2O$, and $MgSO_4 \cdot 7H_2O$) with 1/4 Hoagland nutrient solution for 4 days before experiment.

Preparation of enzyme extraction. Plant roots were washed in 130 mg/L EDTA-Na_2 before ground to wash down metal particles attached to root surface. 0.3 g root and 0.3 g leave tissues were ground separately in pH7.8 phosphate buffered solution (PBS) followed by centrifugation at 4000 r/min for 10 min. Enzyme extraction was the supernatant and added PBS (pH7.8) to 10 mL. Each sample was replicated three times for statistical significance.

Protein and soluble sugar contents. The protein content was determined by a Bradford method [32]. 100 mg Coomassie Brilliant Blue G-250 was dissolved in 50 mL of 95% ethanol and 100 mL of 85% (w/v) H_3PO_4, and then was added to 1000 mL with deionized water. 0.5 mL of enzyme extraction, and 0.5 mL of PBS (pH 7.8) were added to 5 mL of Coomassie Brilliant Blue G-250 solution prepared before. After 5 min of staining, absorbance of the supernatant was measured at 595 nm by a UV-752N spectrophotometer (Shanghai Precision Scientific Instrument Co., Ltd, China). The sugar content was measured by using the anthrone method [33]. 0.2 mL of enzyme extraction was added to 5 mL anthrone solution (0.2g anthrone dissolved in 100 mL of 98% sulfuric acid) in a tube. The mixture was heated at 100ºC in water bath for 15 min and then the absorbance was measured at 630 nm.

Antioxidant system activities. Superoxide dismutase (SOD) was analyzed using the nitro blue tetrazolium (NBT) method [34]. 3.5 mL of PBS (pH 7.8), 0.5 mL of 100 mM EDTA-Na_2, 0.5 mL of 130 mM methionine, 0.2 mL distilled water, 0.3 mL of enzyme extraction, 0.5 mL of 750 mM NBT, and 0.5 mL of 20 mM lactochrome were added to a glass tube. Then, samples were exposed to the light for 20 min. The reference solution prepared in deionized water rather than enzyme extraction was put in dark. The absorbance was measured at 560 nm. Peroxidase (POD) was determined by a guaiacol method. POD reaction mixture was prepared by the following procedures. 28 mL guaiacol was heated and dissolved in 50 mL of 100 mM PBS (pH 7.8), and after completely dissolving and cooling to ambient temperature, 19 mL of 30% H_2O_2 was added. The reaction system contained 0.1mL of enzyme extraction, 0.9 mL of 100 mM PBS (pH 7.8), and 3 mL of POD reaction mixture. The mixture was mixed by hand and the absorbance at every 30 s was measured at 470 nm for 270 s [35]. Catalase (CAT) was determined as described by Aebi [36]. A volume of 0.4 mL of enzyme extraction, 2.0 mL deionized water, 0.6 mL of 0.1% H_2O_2 and 3.0 mL 100 mM PBS (pH 7.8) were added to a tube with a lid and mixed by hand. The absorbance was measured at 240 nm every 30 s for 270 s. Malondialdehyde (MDA) was measured by Thiobarbituric Acid (TBA) method. A volume of 1mL enzyme extraction and 2.0 mL of 0.6% thiobarbituric acid (TBA) were added to a centrifuge tube and boiled at 100ºC in water bath for 15 min. After fast cooling to ambient temperature, the mixture was centrifuged at 4000 rpm for 10 min. The absorbance was measured at 450, 532 and 600 nm [37]. Ascorbate peroxidase (APX) was determined as described by Saruyama and Tanida [38]. The APX reaction mixture was prepared by adding 7.445 mg EDTA-Na_2 into 50 mL of PBS (pH7.0). The reaction mixture contained 2.4 mL APX reaction mixture, 0.6mL of enzyme extraction, 2.4 mL deionized water, 2 µL 30% H_2O_2 and 20 µL ASA. The absorbance was measured at 290 nm every 10 s for 90 s.

Chlorophyll contents. To determined Chlorophyll content, 100 mg fresh leaves were added into 9 mL 95% ethanol until leaves were completely bleached. Then the light absorption of the supernatant was measured at 649 and 665 nm [39]. The chlorophyll content can be calculated by the formula:

$Chla = 13.95A_{665} - 6.8A_{649}$; $Chlb = 24.96A_{649} - 7.32A_{665}$; total chlorophyll = Chla + Chlb (1)

Anthocyanin contents. 50 mg samples were ground in 1:1 (v/v) HCl in methanol and added the same solution to 10 ml then stood for 30 min. The absorbance of the supernatant was measured at 530 and 657 nm by spectrophotometer. The final anthocyanin concentration was determined by the formula,

Anthocyanin concentration = (A530−1/4 A657)/M (2)

Root activity. Root activity was determined by the reported method [40] 150 mg roots were cut and soaked in 1.5 ml 0.4% 2,3,5-Triphenyl-2H-tetrazolium chloride (TTC) solution and 1.5ml PH 6.89 PBS in the dark at 37 ºC for 2 h. Then 2 ml 1 mol/L H_2SO_4 was added to stop the reaction. Took out all the supernatant with burettes and then added 6 ml methanol. The samples were put in an incubator in the dark at 37 ºC for 7 h before the supernatant was examined light absorption at 485 nm.

Zn and Mg contents. Wheat plants were collected and washed in 130mg/L EDTA-Na_2 to remove metal particles attached to the root surface.

Then fresh wheat plants were dried at 60 ºC with a dry oven for 48 h. 100 mg dried root and shoot tissues were digested in 3 mL HNO_3 in boiling water bath for 2 h. 0.5 mL of 30 % H_2O_2 was added and tissues were digested at 100 ºC for 0.5 h. Zn and Mg concentrations were determined by Avanta M atomic absorption spectrophotometer (GBC, Australia).

Statistical analysis. All data were expressed as mean ± standard errors (SE) with three replications. Data were analyzed using the SPSS statistic 22 software. The data were performed with one-way ANOVA followed by Duncan' s multiple comparison tests ($p \leq 0.05$). Bar graphs in this article were made by the Origin 75 software.

RESULTS

Effects of metal ions and NPs on the plant growth. To compare the effects of NPs on the wheat growth, the wheat plants were treated with Mg^{2+}, MgO NPs, Zn^{2+} and ZnO NPs after 4 days of treatment. Fig. S2 displayed the dry and fresh biomass of wheat plants with these different treatments. No significant changes of the dry biomass were observed at all treatments (Fig. S2a and b). Fresh weight showed no apparent differences after Mg^{2+} and MgO NPs treatments (Fig. S2c). However, the fresh biomass was significantly reduced under 200 mg/L ZnO NP exposure compared to the control group (Fig. S2d).

Fig. 1 showed the shoot and root length of wheat plants. The photos of plant growth (Fig. S3, S4) are available in Supplementary Material. Treatment results showed that Mg^{2+} and MgO NPs did not obviously alter the root length of wheat (Fig. 1a) and Zn^{2+} (50 or 200 mg/L) and ZnO NPs (50 mg/L) reduced the root length by 32.1%, 41.2% and 17.5% respectively (Fig. 1b). 200 mg/L ZnO NPs significantly reduced the root length by 45.9% compared to the control (Fig. 1b). Compared to the control, Mg^{2+} at 200 mg/L reduced the shoot length by 33.9% while the other Mg group showed no significant changes. ZnO NPs at 50 mg/L increased the shoot length, while Zn^{2+} at 50 mg/L and ZnO

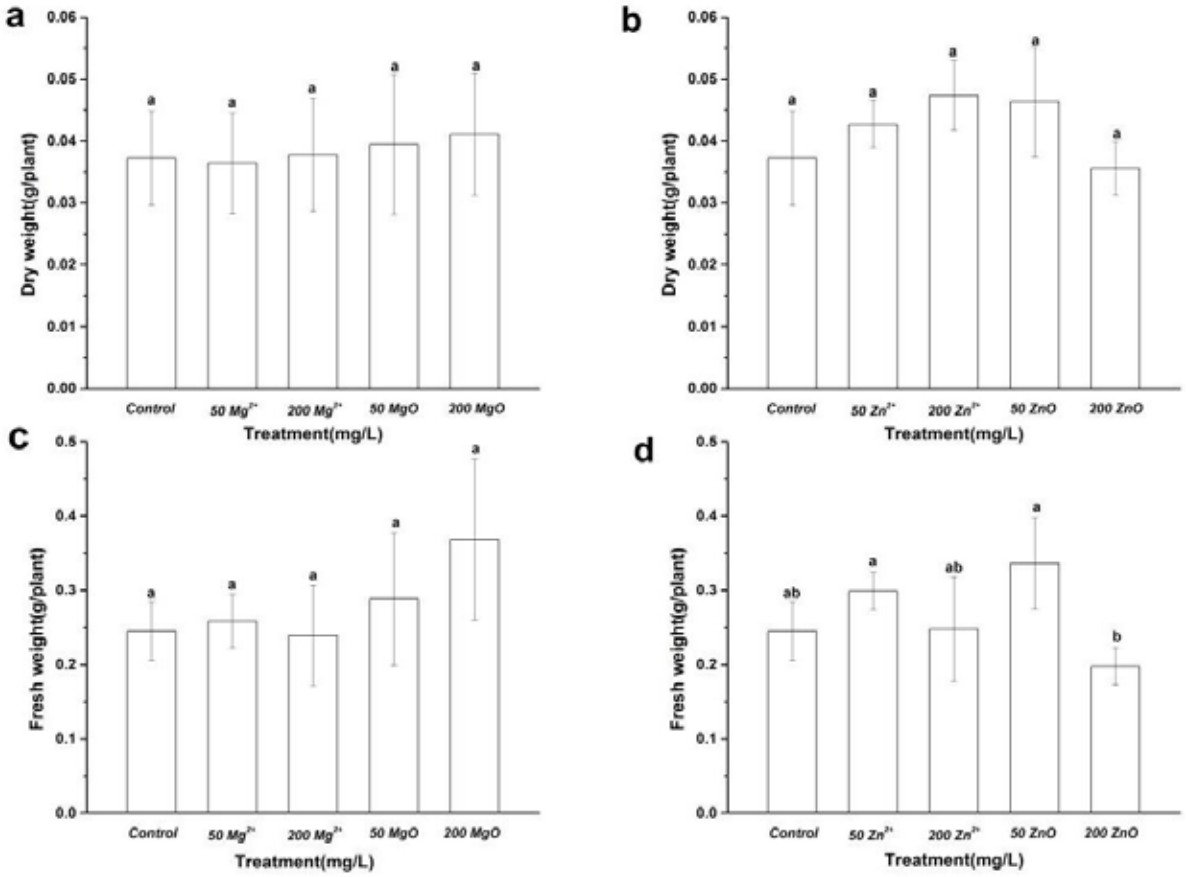

FIGURE S2

Dry weight of wheat plants treated with 50 and 200 mg/L of (a) Mg2+, MgO NPs and (b) Zn2+, ZnO NPs for 4 days. Fresh weight of wheat plants treated with 50 and 200 mg/L of (c) Mg2+, MgO NPs and (d) Zn2+, ZnO NPs after 4 days of treatment. Values represent the mean value ± standard deviation of 3 replications. Letters represent statistically significant differences between the treatments compared to the control group at $p \leq 0.05$ levels.

NPs at 200 mg/L imposed reduction at the shoot length statistically (Fig. 1d). 200 mg/L ZnO NPs reduced fresh biomass, the root and shoot length. Compared to the shoot length after treatment with 50 mg/L Mg^{2+}, Zn^{2+}, MgO and ZnO NPs, it could be easily found that ionic Mg and Zn imposed significant reduction while their nanosized counterpart did not.

Zn and Mg uptake. Generally, the content of Mg and Zn in roots is higher than the content in shoots. Treatment with 200 mg/L MgO NPs showed the highest Mg concentration in both roots and shoots. Mg and Zn contents in roots were increased as the concentration of treatments increased. Meanwhile, even exposed to the same concentration of treatments, Mg and Zn content in roots treated with Mg^{2+} and Zn^{2+} were lower compared with treatment with MgO and ZnO NPs. In shoots, the content of Mg increased in the order of 0 (control), Mg^{2+}, 50 mg/L MgO NPs and 200 mg/L MgO NPs. There was no significant difference between 50 and 200 mg/L Mg^{2+}. Opposite to Mg, Zn content in shoots treated with ZnO NPs was higher compared with Zn^{2+} treatment. No significant diversity was observed between low and high concentrations of ionic Zn and ZnO NPs. The Mg and Zn content in roots treated with 200 mg/L metal ions were higher than that with 50 mg/L, while there was no difference in shoots.

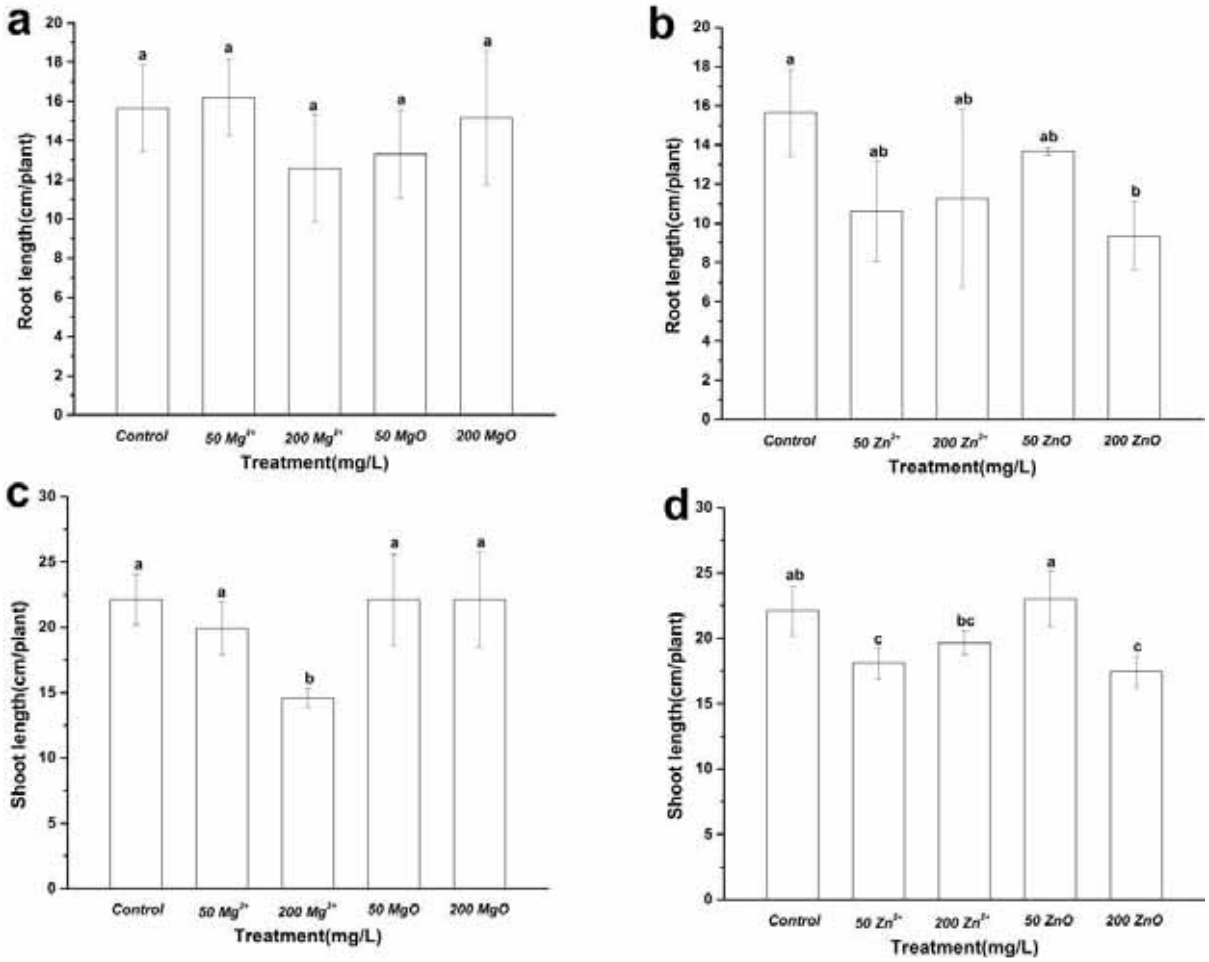

FIGURE 1

Root length of wheat plants treated with 50 and 200 mg/L of (a) Mg^{2+}, MgO NPs and (b) Zn^{2+}, ZnO NPs for 4 days. Shoot length of wheat plants treated with 50 and 200 mg/L of (c) Mg^{2+}, MgO NPs and (d) Zn^{2+}, ZnO NPs after 4 days of treatment. Values represent the mean value ± standard deviation of 3 replications. Letters represent statistically significant differences between the treatments compared to the control group at $p \leq 0.05$ level

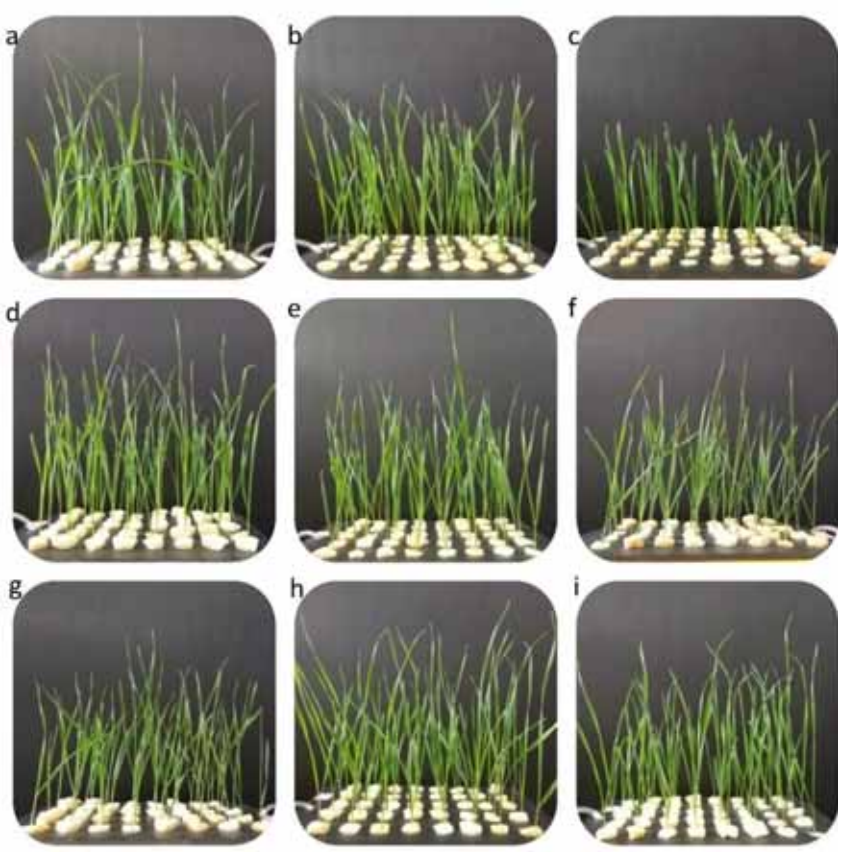

FIGURE S3
Photos of leaves of wheat plants after 4 days treated with (a) 0(control), (b) 50mg/L Mg^{2+}, (c) 200mg/L Mg^{2+}, (d) 50mg/L MgO NPs, (e) 200mg/L MgO NPs, (f) 50mg/L Zn^{2+}, (g) 200mg/L Zn^{2+}, (h) 50mg/L ZnO NPs, (i) 200mg/L ZnO NPs.

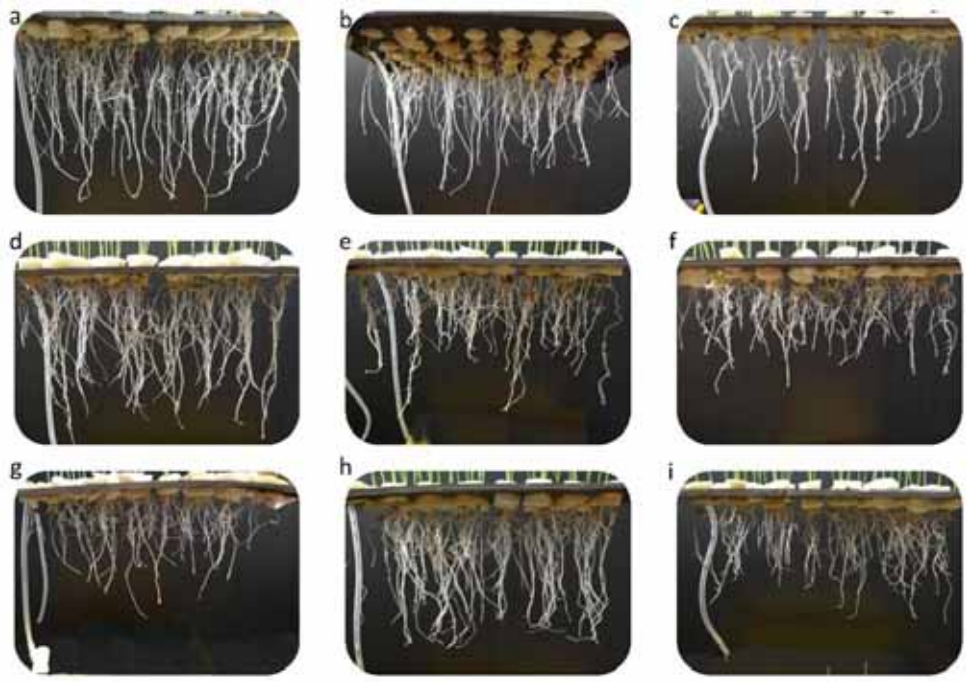

FIGURE S4
Photos of roots of wheat plants after 4 days treated with (a) 0(control), (b) 50mg/L Mg^{2+}, (c) 200mg/L Mg^{2+}, (d) 50mg/L MgO NPs, (e) 200mg/L MgO NPs, (f) 50mg/L Zn^{2+}, (g) 200mg/L Zn^{2+}, (h) 50mg/L ZnO NPs, (i) 200mg/L ZnO NPs.

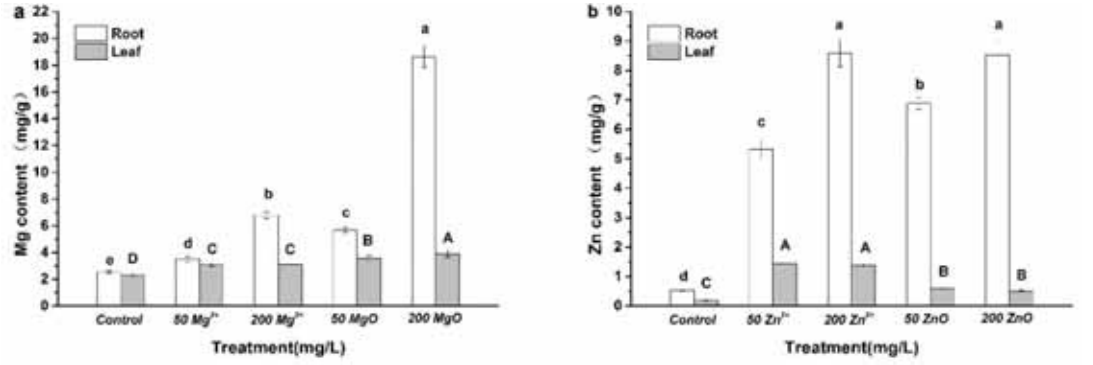

FIGURE 2

Zn and Mg contents of roots and leaves of wheat plants treated with 50 and 200 mg/L of (a) Mg^{2+}, MgO NPs and (b) Zn^{2+}, ZnO NPs for 4 days. Values represent the mean value ± standard deviation of 3 replications. Letters represent statistically significant differences between the treatments compared to the control group at $p \leq 0.05$ levels.

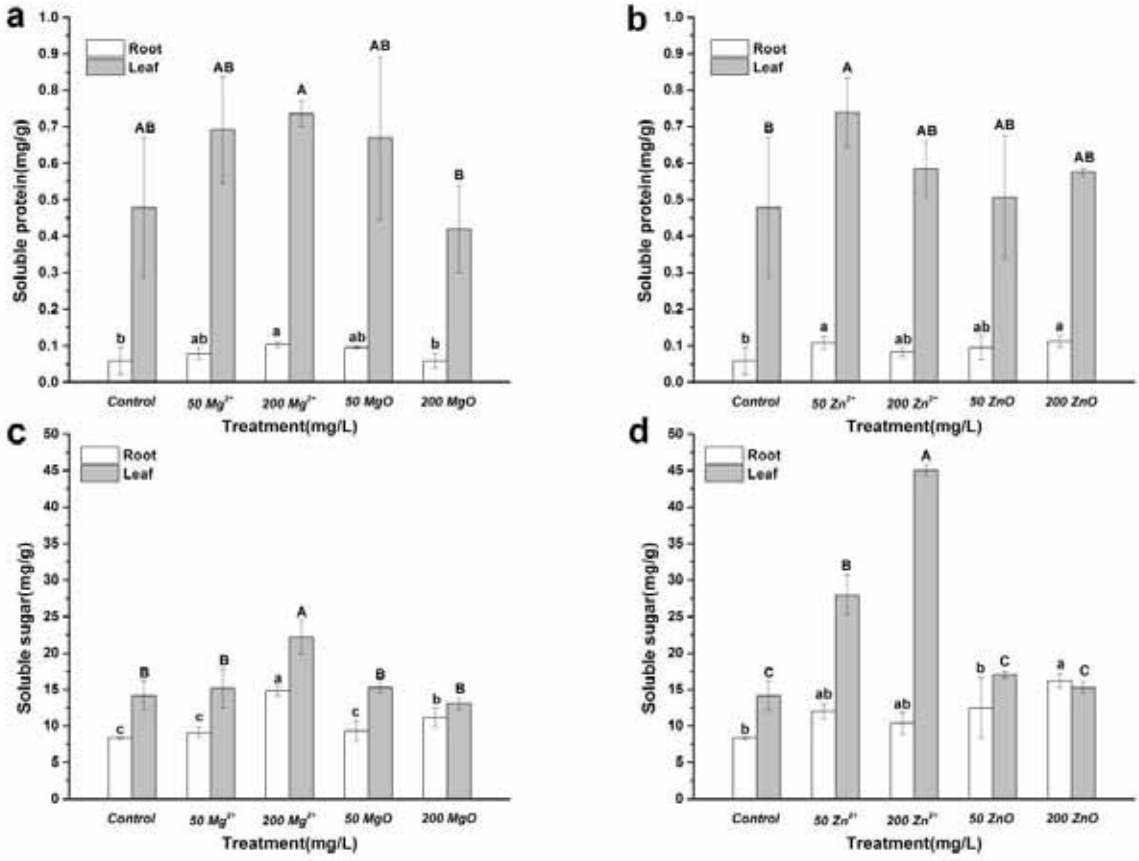

FIGURE 3

Protein contents of roots and leaves of wheat plants treated with (a) Mg^{2+}, MgO NPs and (b) Zn^{2+}, ZnO NPs for 4 days. Soluble sugar contents of roots and leaves of wheat plants treated with (c) Mg^{2+}, MgO NPs and (d) Zn^{2+}, ZnO NPs for 4 days. Values represent the mean value ± standard deviation of 3 replications. Letters represent statistically significant differences between the treatments compared to the control group at $p \leq 0.05$ levels.

Effects of metal ions and NPs on protein and sugar contents. Treatment with Mg^{2+} at 200 mg/L and Zn^{2+} at 50 mg/L caused a statistical increase in total protein contents in both the root and leaf (Fig. 3a and b). 200 mg/L ZnO NPs also increased protein contents in roots. 200 mg/L MgO and 50 or 200 mg/L ZnO NPs increased soluble sugar contents in roots, while no apparent changes were found in plants treated with 200 mg/L Mg^{2+}. In accordance with protein contents, the soluble sugar contents in roots and shoots were at a high level at 200 mg/L Mg^{2+} (Fig. 3c). In shoots, sugar contents were increased after treatment with 50 and 200 mg/L Zn^{2+}(Fig. 3d).

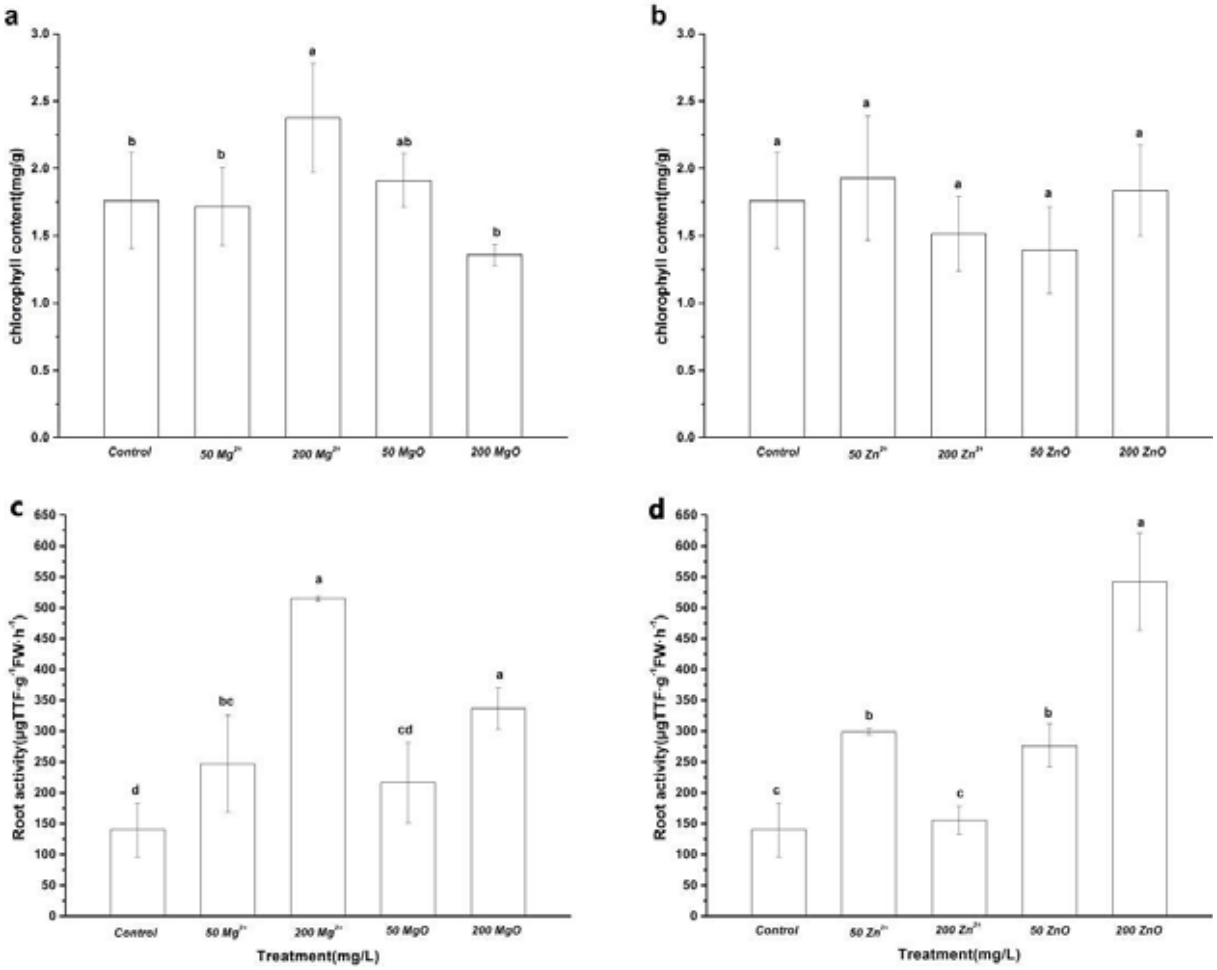

FIGURE 4

Chlorophyll contents of leaves of wheat plants treated with (a) Mg^{2+}, MgO NPs and (b) Zn^{2+}, ZnO NPs for 4 days. Root activity of wheat plants treated with (c) Mg^{2+}, MgO NPs and (d) Zn^{2+}, ZnO NPs for 4 days. Values represent the mean value ± standard deviation of 3 replications. Letters represent statistically significant differences between the treatments compared to the control group at $p \leq 0.05$ levels

Effects of metal ions and NPs on Chlorophyll contents and root activity. Mg^{2+} at 200 mg/L imposed a significant increase in Chlorophyll contents in leaves of wheat plants (Fig. 4a). However, chlorophyll contents did not have significant differences between ionic Zn and ZnO NPs treatments (Fig. 4b). An increase in root activity was observed in almost all treatments (Fig. 4). Root activity of plants after treatments of 200 mg/L Mg^{2+} was higher than that of MgO NPs, while in Zn treatments, 200 mg/L ZnO NPs group owned the highest root activity. Notably, root activity of 200mg/L MgO and ZnO NPs is higher than it of 50 mg/L MgO and ZnO NPs.

Effects of metal ions and NPs on Antioxidant system activities. 200 mg/L Mg^{2+} increased SOD in leaves, while 50 and 200 mg/L Zn^{2+} also increased SOD activity in roots and leaves (Fig. 5a and b). Meanwhile, plants exposed to MgO and ZnO NPs had lower SOD activity than ionic treatments. In leaves, SOD activity under MgO and ZnO NPs was even lower than the control. There was no significant change of CAT activity in leaves. 200 mg/L Mg^{2+} NPs increased CAT activity in roots by 149.8% (Fig. 5b and c). A slight increase in CAT activity after Zn^{2+} treatment was also observed, while 50 mg/L ZnO NPs reduced CAT activity in roots. NPs also showed less toxicity to CAT activity. To our surprise, CAT activity in roots at 200 mg/L ZnO NPs increased. The high level of ZnO NPs may stimulate synthesis of H_2O_2 and activate CAT. An increase in POD activity was observed in both roots and leaves after 200 mg/L Zn^{2+} and Mg^{2+} treatment (Fig. 5e-f). However, MgO and ZnO NPs at 50 mg/L slightly reduced POD activity in roots. POD activity after MgO and ZnO NP treatment was lower than that after Mg^{2+} and Zn^{2+} treatment, which is consistent with SOD and CAT activity. These confirm the former conclusion that MgO and ZnO NPs are less toxicity than ionic Mg and Zn.

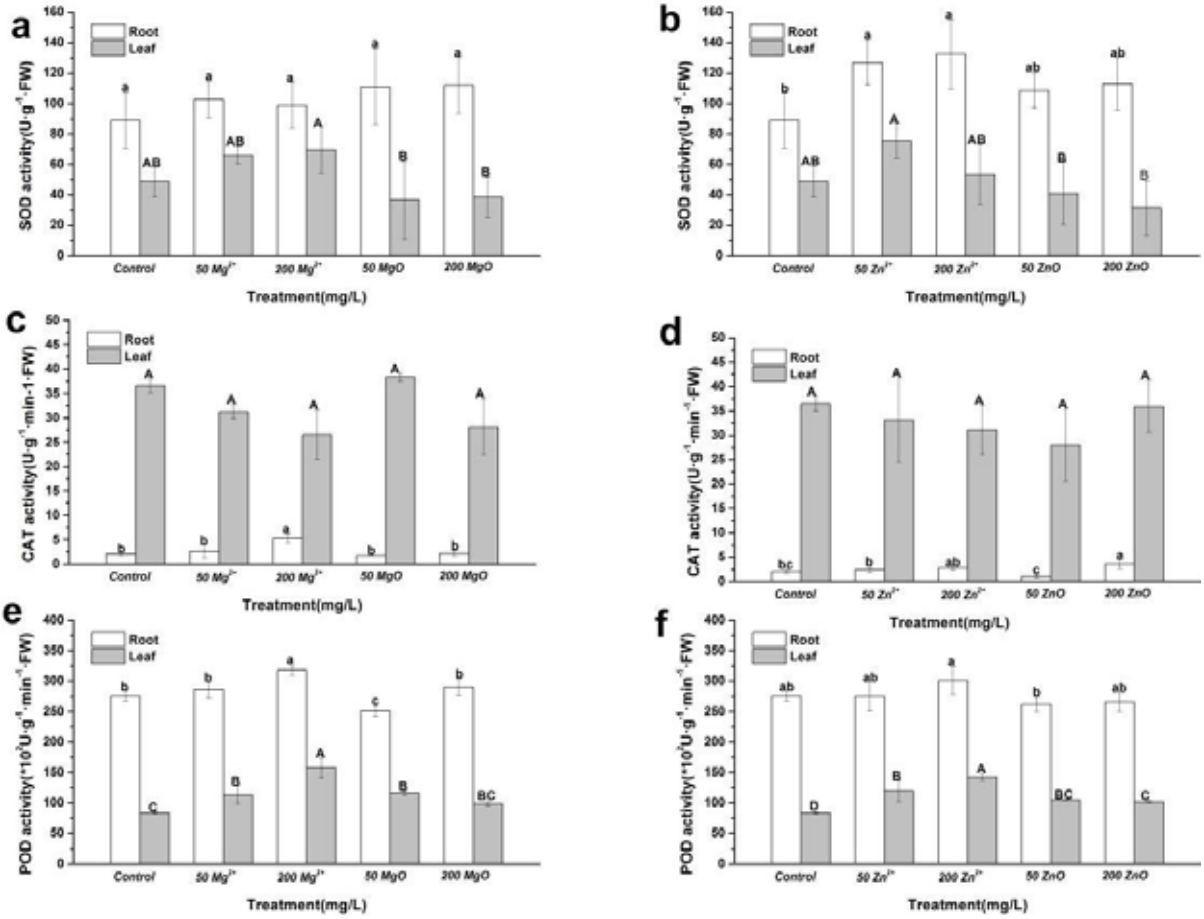

FIGURE 5

Activity of CAT of leaves and roots of wheat plants treated with (a) Mg^{2+}, MgO NPs and (b) Zn^{2+}, ZnO NPs for 4 days. SOD of leaves and roots of wheat plants treated with (c) Mg^{2+}, MgO NPs and (d) Zn^{2+}, ZnO NPs for 4 days. POD of leaves and roots of wheat plants treated with (e) Mg^{2+}, MgO NPs and (f) Zn^{2+}, ZnO NPs for 4 days. Values represent the mean value ± standard deviation of 3 replications. Letters represent statistically significant differences between the treatments compared to the control group at $p \leq 0.05$ levels.

The MDA content was significantly increased in roots at 50 mg/L MgO NPs and 50, 200 mg/L ZnO NPs (Fig. 6a-b). ZnO NPs at the lower concentration imposed a significant decrease in MDA contents of roots, while an increase was observed in plants exposed to higher concentration of ZnO NPs (Fig. 6b). In roots, there was an increase in APX activity in wheat plants at 50 mg/L Mg^{2+} and Zn^{2+} (Fig. 6c-d). However, increasing was not observed in 200 mg/L Mg^{2+} and Zn^{2+}. Significant increment of APX activity in leaves was also observed in plants treated with 200 mg/L MgO NPs (Fig. 6c). No significant impact on anthocyanin contents in leaves were presented at all treatments. There was a significant decline of 78.7%, 76.7%, 84.3%, and 72.1% in anthocyanin contents in roots of wheat plants exposed to 50, 200 mg/L MgO NPs and 50, 200 mg/L ZnO NPs.

DISCUSSION

In this study, we compared the physiology effects of ZnO NPs, MgO NPs, ionic Zn and Mg at 50 and 200 mg/L on wheat plants growing in water. Plant growth, protein and sugar content, antioxidant enzyme activity and other parameters were investigated. 200 mg/L ZnO NP significantly reduced the fresh weight of wheat plants. It has been reported that nanoparticles show phytotoxicity as the concentration increases [26]. Mg^{2+} and MgO NPs did not alter root length of wheat plants. Root length was only reduced by 200 mg/L ZnO NPs. It could be inferred that ZnO NPs imposed negative effects on roots and might hinder the absorption of water. Similar results of root elongation reduction were observed in *Arabidopsis thaliana* [41]. Extensive vacuolation, loss of nuclear organization, ruptured plasma membrane, and shrinkage of the protoplast were observed in Allium root cells

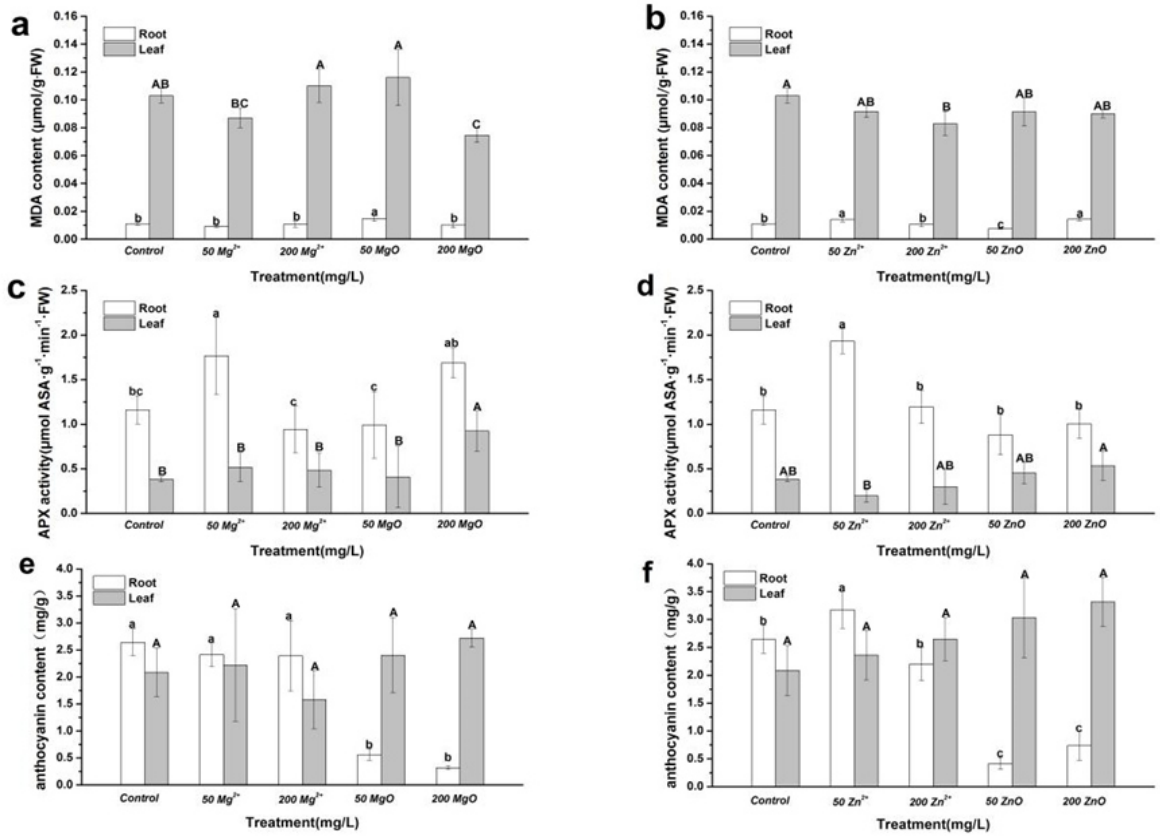

FIGURE 6

MDA contents of leaves and roots of wheat plants treated with (a) Mg^{2+}, MgO NPs and (b) Zn^{2+}, ZnO NPs for 4 days. APX activity of leaves and roots of wheat plants treated with (c) Mg^{2+}, MgO NPs and (d) Zn^{2+}, ZnO NPs for 4 days. anthocyanin contents of leaves and roots of wheat plants treated with (e) Mg^{2+}, MgO NPs and (f) Zn^{2+}, ZnO NPs for 4 days. Values represent the mean value ± standard deviation of 3 replications. Letters represent statistically significant differences between the treatments compared to the control group at $p \leq 0.05$ level.

exposed to ZnO NPs [26]. As for shoot length, only 200 mg/L Mg^{2+} of Mg treatments imposed reduction at the shoot length, while Zn^{2+} at 50 mg/L and ZnO NPs at 200 mg/L reduced the shoot length. The simultaneous reduction of fresh biomass, the root and shoot length caused by 200 mg/L ZnO NPs showed the phytotoxicity of high concentration of ZnO NPs. They could be transported to leaves by vessels like their bulk counterpart. However, how they function in plants, are still unclear, which might be converted to ionic Zn in cells or exist as NPs. Some publications indicated that NPs could be up taken and transported to aerial parts of plants [42]. 50 mg/L Mg^{2+}, Zn^{2+} showed significantly reduction of shoot length while MgO and ZnO NPs did not. Ionic treatments showed higher toxicity than the NPs, which might be owing to the fact that ionic Zn and Mg are totally soluble for plants but NPs exist as molecules [43].

Zn and Mg content of roots and leaves revealed the uptake and translocation in wheat plants. Higher Zn and Mg contents of roots than leaves may be because mineral elements including Mg and Zn are up taken by roots and transported to the aerial part of plants. We also observed higher Mg and Zn content in roots treated with MgO and ZnO NPs than that with Mg^{2+} and Zn^{2+}. This might be explained by the high specific surface area, and unusual surface properties of NPs, which makes NPs attach to the surface of roots [26]. ZnO NPs aggregating was observed with soil clay mineral under electron microprobe [44]. The absorption and aggregation elevated the concentration of NPs around roots. The content of Mg in leaves was higher with Mg^{2+} treatments than MgO NPs treatments, which was opposite to Zn treatments. The uptake of nutrition elements is influenced by various factors, such as the ability of plants to uptake elements and competition between elements. We could infer that partial MgO NPs were transported to shoots as the molecule. The study indicated that NPs could be absorbed and translocated to aerial part of plants [45].

The soluble protein is an important substance involved in plant growth activity. Most of crucial enzymes, such as antioxidant enzymes and metabolic enzymes, are soluble proteins. Sugar is the major substance that supplies energy in cells, which

is also involved in cell structure, signal transduction and stress resistance [46-48]. 200 mg/L Mg^{2+} increased protein and sugar contents in both roots and shoots. Sugar contents in shoots were increased after treatment with 50 and 200 mg/L Zn^{2+}. Ions showed more toxicity than NPs. This may be due to the fact that ions are totally soluble while NPs exist mainly as molecules.

Chlorophyll contents reflect leave growth status of in plant [49]. 200 mg/L Mg^{2+} significantly increased the chlorophyll contents in leaves of wheat plants while no changes were observed in Zn treatments. Mg^{2+} is an essential component of chlorophyll, and therefore, high concentration of Mg^{2+} may promote the synthesis of chlorophyll [6]. Dehydrogenase activity is an indicator of root vitality and reflects physiological condition of plant tissues [50]. Almost all treatments imposed increasing in root activity. However, root activity of MgO and ZnO NPs at 200mg/L is higher than it at 50 mg/L, which was consistent with the Mg and Zn content in roots. The high level of NPs increased root activity of wheat plants. Moreover, plants exposed to 200 mg/L ZnO NPs had relatively shorter root lengths [51]. This may be because the high level of NPs activated the defendant system in roots and induced stress reactions, therefore, the root activity was increased to eliminate the stress. By comparison of the effect of ZnO NPs and soluble zinc ($ZnCl_2$) at the same concentration, much lower toxicity of soluble zinc was observed [41]. This suggested that the toxicity of NPs cannot be simply explained by releasing of ions, and the NPs themselves contributed to the toxicity.

SOD, CAT, POD are three crucial enzymes of plant antioxidant defense system. SOD can convert O^{2-} to H_2O_2 and constitutes the first line of defense against ROS [52]. CAT can prevent the accumulation of toxic levels of H2O2 [53], while POD can scavenge other peroxides [26].These enzymes were activated to scavenge the peroxides and relieve the damages when plants are in adversity. SOD activity in roots was increased by 50, 200 mg/L Zn^{2+} treatments. Also, 200 mg/L Mg^{2+} increased SOD in leaves, while the same increasing was not observed in MgO or ZnO NPs treatments. 200 mg/L Mg^{2+} NPs also increased CAT activity in roots. Therefore, MgO and ZnO NPs induced less free radicals than Mg^{2+} and Zn^{2+}. NPs exhibited less physiological toxicity than equivalent ions, which is concurred with previous explanation that ionic particles were easier for plants to take in than NPs, which shows more toxicity than NPs [51].

POD activity was increased by nearly all treatments, which indicated that NPs owned toxicity to some extent. However, POD activity of ions treatments was higher than NPs treatments. Study on alfalfa plants observed similar results that ionic Zn decreased plant size, produced yellow leaves, implied lower cell activity and higher H_2O_2 accumulation while ZnO NPs did not show these effects [43].

Our results indicate that ionic Mg and Zn increase SOD, POD, CAT activity and MgO and ZnO NPs slightly increase or even reduce activity of these antioxidant enzymes. Changes of antioxidant defense system illustrate that Zn or Mg particles interacted with cellular components that lead to oxidative damages to plant cells. However, further study is needed to figure out the specific mechanism of the reactions.

MDA content is an indicator to lipid peroxidation of plant cells [54]. 50 mg/L MgO NPs and 50, 200 mg/L ZnO NPs increased MDA content in roots of wheat plants, which mean the existence of lipid peroxidation in root cells. Surprisingly, reduction in MDA contents of leaves was observed. Zinc is involved in membrane structure, which may be why Zn shows lower toxicity than Mg even at the same concentration [55, 56]. APX is one of the important antioxidant enzymes in eliminating ROS, and especially is the crucial enzyme cleaning hydrogen peroxide in chloroplast [55]. The increase in APX activity in roots of wheat plants was observed in 50 mg/L Mg^{2+} and Zn^{2+}, not in 200 mg/L. Lower contents of ionic Mg and Zn induce the antioxidant responses of plant roots. But high concentration of Mg^{2+} and Zn^{2+} may damage the regulation of the antioxidant reactions, which lead to the phenomenon. High level of MgO NPs also increased APX activity in leaves. As stated before, high level of NPs show more toxicity in plants. Leaves do not contact the solution directly, which might be the reason why only high levels of NPs rise APX activity in leaves. Anthocyanin content can also eliminate ROS produced by plant cells [57]. We observed sharp decreasing of anthocyanin contents in roots exposed to MgO and ZnO NPs. The decreasing of anthocyanin contents in roots represented that NPs may affect the synthesis of anthocyanin contents, which required further studies.

In this study, we compared the physiology effects of ZnO NPs, MgO NPs, ionic Zn and Mg at 50 and 200 $mg.L^{-1}$ on wheat plants growing in water. Results showed that the high level of ZnO NPs imposed negative effects on wheat plants growth by reducing fresh biomass, shoot and root lengths. Besides, protein contents, sugar contents, CAT activity, MDA and APX were increased by 200$mg.L^{-1}$ ZnO NPs. The high level of ZnO NPs presented phytotoxicity to wheat plants, but MgO NPs did not. NP efficiency is related to species and concentration. However, generally ZnO and ZnO NPs have lower toxicity than Zn^{2+} and Mg^{2+} since Zn^{2+} and Mg^{2+} cause increments on protein and sugar contents, SOD, CAT and POD. We find that

Zn, Mg ionic and ZnO and MgO NPs changes morphology and biochemistry of wheat plants by activating the antioxidant system. As stated before, ZnO and MgO NPs are also less toxicity than Zn^{2+} and Mg^{2+} in the perspective of antioxidant system. Antioxidant enzymes like SOD, CAT and POD were upregulated under stress, while contents of other antioxidants like MDA, APX and antioxidant also changed to eliminate the effects that ROS brought to wheat plants. However, which kind of NPs and the concentration of them are things that need to be considered. Further research is needed to elucidate the mechanism of Zn and Mg oxide nanoparticles translocating and affecting the physiology of wheat plants.

ACKNOWLEDGEMENTS

This work was supported by the Fundamental Research Funds for the Central Universities (WUT2017IB006; WUT2018IB021; WUT2018 IB023)

REFERENCES

[1] Tanoi, K., Kobayashi, N.I., Saito, T., Iwata, N., Hirose, A., Ohmae, Y., Ren, I., Suzuki, H. and Nakanishi, T.M. (2013) Application of 28 Mg to the kinetic study of Mg uptake by rice plants. Journal of Radioanalytical and Nuclear Chemistry. 296(2), 749-51.

[2] Broadley, M.R., White, P.J., Hammond, J.P., Zelko, I. and Lux, A. (2007) Zinc in plants. New Phytologist. 173(4), 677–702.

[3] Davarpanah, S., Tehranifar, A., Davarynejad, G., Abadía, J. and Khorasani, R. (2016) Effects of foliar applications of zinc and boron nanofertilizers on pomegranate (Punica granatum cv. Ardestani) fruit yield and quality. Scientia Horticulturae. 210, 57-64.

[4] Tanoi, K., Kobayashi, N. I., Saito, T., Iwata, N., Kamada, R., Ren, I., Suzuki, H., Hirose, A., Ohmae, Y. and Sugita, R. (2014) Effects of magnesium deficiency on magnesium uptake activity of rice root, evaluated using 28 Mg as a tracer. Plant and Soil. 384(1-2), 69-77.

[5] Staiger, M., Pietak, A., Huadmai, J. and Dias, G. (2006) Magnesium and its alloys as orthopedic biomaterials: A review. Biomaterials. 27(9), 1728-34.

[6] Terpstra, W., Lambers, J.W.J. (1983) Interactions between cholorophyllase, chlorophyll a, plant lipids and Mg 2+. Biochimica et Biophysica Acta (BBA) - Protein Structure and Molecular Enzymology. 746(1–2), 23-31.

[7] Stein, A.J. (2010) Global impacts of human malnutrition. Plant and Soil. 335(1-2), 133-54.

[8] Zhang, Y.Q., Sun, Y.X., Ye, Y.L., Karim, M.R., Xue, Y.F., Yan, P., Meng, Q.F., Cui, Z. L., Cakmak, I. and Zhang, F.S. (2012) Zinc biofortification of wheat through fertilizer applications in different locations of China. Field Crops Research. 125(1), 1-7.

[9] Haslett, B.S., Reid, R.J., Rengel, Z. (2001) Zinc Mobility in Wheat: Uptake and Distribution of Zinc Applied to Leaves or Roots. Annals of Botany. 87(3), 379-86.

[10] Cakmak, I. (2008) Enrichment of cereal grains with zinc: Agronomic or genetic biofortification? Plant and Soil. 302(1-2), 1-17.

[11] White, C.L. (1993) Zinc in Soils and Plants Springer Netherlands.

[12] Marusenko, Y., Shipp, J., Hamilton, G. A., Morgan, J. L. L., Keebaugh, M., Hill, H., Dutta, A., Zhuo, X., Upadhyay, N., Hutchings, J. (2013) Bioavailability of nanoparticulate hematite to Arabidopsis thaliana. Environmental Pollution. 174(5),150-6.

[13] Demir, E., Turna, F., Burgucu, D., Kiliç, Z., Burunkaya, E., Kesmez, Ö., Yeşil, Z., Akarsu, M. and Kaya, B. (2013) Genotoxicity of different nano-sizes and ions of silica nanoparticles. Fresen. Environ. Bull. 22, 2901-9.

[14] Ballı, E., Çömelekoğlu, Ü., Yalın, S., Battal, D., Ocakoğlu, K., Söğüt, F., Yaman, S., Türkseven, Ç.H., Eroğlu, P. and Karagül, İ. (2016) Toxic effects of silica nanoparticles on heart: Electrophysiological, biochemical, histological and genotoxic study. Fresen. Environ. Bull. 25, 370-2.

[15] Zhang, J., Xin, S., Li, F. (2013) Removal of SiO2 nanoparticles from aqueous phase by using polymer aluminum chloride (PAC). Fresen. Environ. Bull. 22, 890-4.

[16] O'Carroll, D., Sleep, B., Krol, M., Boparai, H. and Kocur, C. (2013) Nanoscale zero valent iron and bimetallic particles for contaminated site remediation. Advances in Water Resources. 51(1), 104-22.

[17] Noubactep, C., Car, S., Crane, R. (2012) Nanoscale Metallic Iron for Environmental Remediation: Prospects and Limitations. Water Air and Soil Pollution. 223(3), 1363-82.

[18] Klaine, S.J., Alvarez, P.J.J., Batley, G.E., Fernandes, T.F., Handy, R.D., Lyon, D.Y., Mahendra, S., Mclaughlin, M.J. and Lead, J.R. (2008) Nanomaterials in the environment: Behavior, fate, bioavailability, and effects. Environmental Toxicology and Chemistry. 27(9), 1825.

[19] Nowack, B., Bucheli, T.D. (2007) Occurrence, behavior and effects of nanoparticles in the environment. Environmental Pollution. 150(1), 5-22.
[20] Serpone, N., Dondi, D., Albini, A. (2007) Inorganic and organic UV filters: Their role and efficacy in sunscreens and suncare products. Inorganica Chimica Acta. 360(3), 794-802.
[21] Padmavathy, N., Vijayaraghavan, R. (2008) Enhanced bioactivity of ZnO nanoparticles—an antimicrobial study. Sci Technol Adv Mater. 9(3), 035004.
[22] Perelshtein, I., Applerot, G., Perkas, N., Grinblat, J., Hulla, E., Wehrschuetzsigl, E., Hasmann, A., Guebitz, G. and Gedanken, A. (2010) Ultrasound Radiation as a "Throwing Stones" Technique for the Production of Antibacterial Nanocomposite Textiles. Acs Appl Mater Interfaces. 2(7), 1999-2004.
[23] Krishnamoorthy, K., Moon, J.Y., Hyun, H.B., Cho, S.K. and Kim, S.J. (2012) Mechanistic investigation on the toxicity of MgO nanoparticles toward cancer cells. Journal of Materials Chemistry. 22(47), 24610-7.
[24] Nair, P.M., Chung, I.M. (2017) Regulation of morphological, molecular and nutrient status in Arabidopsis thaliana seedlings in response to ZnO nanoparticles and Zn ion exposure. Science of the Total Environment. 575(187).
[25] Gottschalk, F., Sonderer, T., Scholz, R.W. and Nowack, B. (2009) Modeled environmental concen-trations of engineered nanomaterials (TiO(2), ZnO, Ag, CNT, Fullerenes) for different regions. Environmental Science and Technology. 43(24), 9216-22.
[26] Ghosh, M., Jana, A., Sinha, S., Jothiramajayam, M., Nag, A., Chakraborty, A., Mukherjee, A. and Mukherjee, A. (2016) Effects of ZnO nanoparticles in plants: Cytotoxicity, genotoxicity, deregulation of antioxidant defenses, and cell-cycle arrest. Mutation Research/genetic Toxicology and Environmental Mutagenesis. 807(25-32).
[27] Yu, H. L., Ng, A. M. C., Xu, X., Shen, Z., Gethings, L. A., Wong, M. T., Chan, C. M. N., Guo, M. Y., Ng, Y. H., Djuri, A. B. (2014) Mechanisms of Antibacterial Activity of MgO: Non-ROS Mediated Toxicity of MgO Nanoparticles Towards Escherichia coli. Small. 10(6), 1171–83.
[28] Krishnamoorthy, K., Manivannan, G., Sang, J. K., Jeyasubramanian, K. and Premanathan, M. (2012) Antibacterial activity of MgO nanoparticles based on lipid peroxidation by oxygen vacancy. Journal of Nanoparticle Research. 14(9), 1-10.
[29] Cakmak, I., Pfeiffer, W.H., McClafferty, B. (2010) Biofortification of durum wheat with zinc and iron. Cereal Chemistry. 87(1), 10-20.
[30] Liu, S.X., Mo, X.G., Lin, Z.H., Xu, Y.Q., Ji, J.J., Wen, G., Richey, J., Green, T.R., Yu, Q.A. and Ma, L.W. (2010) Crop yield responses to climate change in the Huang-Huai-Hai Plain of China. Agricultural Water Management. 97(8), 1195-209.
[31] Ma, G., Jin, Y., Li, Y., Zhai, F., Kok, F.J., Jacobsen, E. and Yang, X. (2008) Iron and zinc deficiencies in China: what is a feasible and cost-effective strategy? Public Health Nutrition. 11(6), 632-8.
[32] Kruger, N.J. (1994) The Bradford method for protein quantitation. Methods in Molecular Biology. 32(32), 9.
[33] Ludwig, T.G., Goldberg, H.J.V. (1956) The anthrone method for the determination of carbohydrates in foods and in oral rinsing. Journal of Dental Research. 35(1), 90-4.
[34] Wang, Y., Ying, Y., Chen, J. and Wang, X. (2004) Transgenic Arabidopsis overexpressing Mn-SOD enhanced salt-tolerance. Plant Science. 167(4), 671-7.
[35] Castillo, F.J., Penel, C., Greppin, H. (1984) Peroxidase Release Induced by Ozone in Sedum album Leaves: Involvement of Ca. Plant Physiology. 74(4), 846-51.
[36] Aebi, H. (1983) Catalase in vitro. Methods in Enzymology. 105(105), 121-6.
[37] Heath, R.L., Packer, L. (1968) Photoperoxidation in isolated chloroplasts. I. Kinetics and stoichiometry of fatty acid peroxidation. Archives of Biochemistry and Biophysics. 125(1), 189.
[38] Saruyama, H., Tanida, M. (1995) Effect of chilling on activated oxygen-scavenging enzymes in low temperature-sensitive and -tolerant cultivars of rice (Oryza sativa L.) Plant Science. 109(2), 105-13.
[39] Lichtenthaler, H.K. (1987) [34] Chlorophylls and carotenoids: Pigments of photosynthetic biomembranes. Methods in Enzymology. 148C(1), 350-82.
[40] Lindstr, M.A., Nystr, M.C. (1987) Seasonal variation in root hardiness of container-grown Scots pine, No. Canadian Journal of Forest Research. 17(8), 787-93.
[41] Lee, C.W., Mahendra, S., Zodrow, K., Li, D., Tsai, Y.C., Braam, J. and Alvarez, P.J. (2010) Developmental phytotoxicity of metal oxide nanoparticles to Arabidopsis thaliana. Environmental Toxicology and Chemistry. 29(3), 669-75.

[42] Zhao, L., Sun, Y., Hernandezviezcas, J. A., Hong, J., Majumdar, S., Niu, G., Duartegardea, M., Peraltavidea, J.R. and Gardeatorresdey, J. L. (2015) Monitoring the Environmental Effects of CeO2 and ZnO Nanoparticles Through the Life Cycle of Corn (Zea mays) Plants and in Situ μ-XRF Mapping of Nutrients in Kernels. Environmental Science and Technology. 49(5), 2921-8.

[43] Bandyopadhyay, S., Plascenciavilla, G., Mukherjee, A., Rico, C.M., Joséyacamán, M., Peraltavidea, J.R. and Gardeatorresdey, J.L. (2015) Comparative phytotoxicity of ZnO NPs, bulk ZnO, and ionic zinc onto the alfalfa plants symbiotically associated with Sinorhizobium meliloti in soil. Science of the Total Environment. 515–516, 60-9.

[44] Zhao, L., Peralta-Videa, J. R., Ren, M., Varela-Ramirez, A., Li, C., Hernandez-Viezcas, J.A., Aguilera, R.J. and Gardea-Torresdey, J.L. (2012) Transport of Zn in a sandy loam soil treated with ZnO NPs and uptake by corn plants: Electron microprobe and confocal microscopy studies. Chemical Engineering Journal. 184(2), 1-8.

[45] Dietz, K.J., Herth, S. (2011) Plant nanotoxicology. Trends in Plant Science. 16(11), 582-9.

[46] Koch, K. (2004) Sucrose metabolism: regulatory mechanisms and pivotal roles in sugar sensing and plant development. Current Opinion in Plant Biology. 7(3), 235-46.

[47] Levitz, S.M. (2004) Interactions of Toll-like receptors with fungi. Microbes and Infection. 6(15), 1351-5.

[48] Zaragoza, O., Rodrigues, M.L., De, J.M., Frases, S., Dadachova, E. and Casadevall, A. (2009) The capsule of the fungal pathogen Cryptococcus neoformans. Advances in Applied Microbiology. 68(1), 133.

[49] Ma, C., Chhikara, S., Minocha, R., Long, S., Musante, C., White, J.C., Xing, B. and Dhankher, O.P. (2015) Reduced Silver Nanoparticle Phytotoxicity in Crambe abyssinica with Enhanced Glutathione Production by Overexpressing Bacterial γ-Glutamylcysteine Synthase. Environmental Science and Technology. 49(16), 10117.

[50] Clemensson-Lindell, A. (1994) Triphenyltetrazolium chloride as an indicator of fine-root vitality and environmental stress in coniferous forest stands: Applications and limitations. Plant and Soil. 159(2), 297-300.

[51] Liu, Z., Wang, T., Wang, W. (2016) Effects of CuO NPs on ROS, Antioxidant Enzyme Activity and Root Activity of the Alfalfa Seedlings. Asian Journal of Ecotoxicology. 11(5), 117-124.

[52] Alscher, R.G., Erturk, N., Heath, L.S. (2002) Role of superoxide dismutases (SODs) in controlling oxidative stress in plants. Journal of Experimental Botany. 53(372), 1331.

[53] Panda, S.K., Choudhury, S. (2005) Chromium stress in plants. Brazilian Journal of Plant Physiology. 17(17), 95-102.

[54] Tsikas, D. (2016) Assessment of lipid peroxidation by measuring malondialdehyde (MDA) and relatives in biological samples: Analytical and biological challenges. Analytical Biochemistry. 524(13).

[55] Sato, Y., Murakami, T., Funatsuki, H., Matsuba, S., Saruyama, H. and Tanida, M. (2001) Heat shock-mediated APX gene expression and protection against chilling injury in rice seedlings. Journal of Experimental Botany. 52(354), 145.

[56] Cakmak, I. (2000) Possible roles of zinc in protecting plant cells from damage by reactive oxygen species. New Phytologist. 146(2), 185-205.

[57] Prior, R.L. Cao, G., Martin, A., Sofic, E., McEwen, J., O'Brien, C., Lischner, N., Ehlenfeldt, M., Willy Kalt, W., Gerard Krewer, G., Mainland, C.M. (1998) Antioxidant Capacity As Influenced by Total Phenolic and Anthocyanin Content, Maturity, and Variety of Vaccinium Species. Journal of Agricultural and Food Chemistry. 46(7), 2686-93.

Received: **27.09.2018**
Accepted: **19.02.2019**

CORRESPONDING AUTHOR

Junli Li
School of Chemistry,
Chemical Engineering and Life Sciences,
Wuhan University of Technology,
Wuhan 430070 – P.R. China

e-mail: lijunli0424@sina.com

© by PSP Volume 28 – No. 4/2019 pages 2575-2581 Fresenius Environmental Bulletin

SOIL PROPERTIES WERE EVALUATED AS REFLECTING PARAMETERS IN LOW INTENSITY FOREST FIRES IN CANKIRI, TURKEY

Sema Camci Cetin[1,*], Aziz Emre Yilmaz[2], Sabit Ersahin[1], Ulku Dikmen[1], Seval Sunal[1]

[1] Department of Soil Science and Ecology, Forest Faculty, Cankiri Karatekin University, Cankiri, Turkey
[2] Sabanozu Forestry Administration, Cankiri, Turkey

ABSTRACT

Forest fires change many features in forest ecosystems such as soil properties. This study investigated the effects of forest fire on soil physical (clay, sand, silt, bulk density, field capacity, wilting point and plant available water) and soil chemical (organic matter, $CaCO_3$, pH, EC and agregat stability index) parameters in newly fired ecocsystem, Cankiri, Turkey. Sand and bulk density being soil physical parameters showed best description in order to negative effect of forest fires and were significantly important ($P<0.05$ and $P<0.01$, respectively). In all soil chemical parameters, only EC parameters was significantly important ($P<0.05$) for reflecting forest fire. Severity of fire can be classified as low and high intensity. In this study, having low intensity fire in research area decreased the negative effects of forest fire.

KEYWORDS:
Forest fires, soil properties, low intensity fire

INTRODUCTION

Forest ecosystems globally cover more than 4.1 billion hectares [1]. It is estimated that between 530 and $555x10^6$ ha are globally influenced by fire every year [2]. Based on annual fire budgets, annually burned $10\text{-}15x10^6$ ha of boreal and temperate forest, $20\text{-}40x10^6$ ha of tropical and subtropical savannas, woodlands and open forests are lost [3]. Fire is absolutely the main disturbance in Mediterranean basin [4-6]. Fire also is critically significant disturbance in Turkey [7]. In Turkey, 15 million ha of forestlands were burned between 1937 and 2004 [7].

Forest fires are basically environmental issues which can be recognized as a global phenomenon [2,8]. It is clear that fires influence more land area than any other natural disturbance [9]. Fire affects whole ecosystem including flora, fauna, atmosphere and soil [10]. Also forest fires influence vegetation [11] and combustion causes limitation or destroy forest floor [12]. Actually, soil and vegetation are long-termly affected by forest fires [13]. That is why forest fires can be recognized as an important disturbance in forest ecosystems due to affecting the vegetation, soil and nutrient cycles [11].

Fires affect soil and vegetation by different regime components which are fire frequency, size, intensity, seasonality, type and severity [14]. Another researcher included fuel loading (i.e. live and dead materials), fire climate, slope, topography, soil texture and moisture, soil organic content, and time since last burned and area burned [15]. Fires are natural phenomenon that they regulate ecosystem productivity and diversity by increasing mineralization of nutrients in organic matter, promoting fast growing early successional species [16-18].

Two types of fires can be classified into: (i) prescribed (controlled) fires and (ii) wildfires [19]. Both fires have similar features about their effects. The effects can be direct and indirect. Direct effects show the following features: "(i) loss of vegetation, (ii)combustion of the organic horizon, (iii) increasing soil heating, (iv) loss of elements (nitrogen and carbon to the atmosphere), (v) deposition of charcoal and ash" [15, 20].

Forest fires affect many physical, chemical, mineralogical and biological soil properties [13, 19, 21-23]. Indirect effect of fire can be summarized as (i) "altered soil moisture and pH, (ii) along with increased erosion and (iii) physical and chemical effects of charchoal deposition" [15, 24-26]. Also, fire may influence soil nutrient status via nutrient addition (direct effect) and changing soil environment (indirect effect) [27]. Fire can affect many soil properties such as minimize or destroy soil structure and soil organic matter and decreased porosity which changes result increased hydrophobicity (water repellency) [21]. Similar results were found by DeBano et al. [17].

It is clear that differentiation of aboveground structure can directly influence belowground systems by different symptoms. Those are followed: (i) changing nutrient inputs (affecting soil and litter, micro- and macro-flora and fauna), (ii) elevating soil temperature due to increased soil heating, and (iii) changing evapotranspiration rates [15]. During forest fires large amount of CO_2 are released to the atmosphere [2]. For that reason forest fires concern

as a global warming parameter because of emmission of CO_2 [28]. About 95 % of fires are originated from human induced fires in Mediterranean basin [28]. Basically, forest fires can affect changes in soil quality, especially in the surface horizon [29]. After fire, rehabilitation of soil quality takes too long time [29].

The objectives of this study were summarized as: (i) to determine the effects of wildfire on soil physical parameters, (ii) to determine the effects of wildfire on soil chemical paramaters, (iii) to evaluate whether soil parameters is more informative in all other parameters.

MATERIAL AND METHODS

Study Area. The study area was located in Çankırı, Turkey (40º 49'03"N; 32º43'24"E). Research area was chosen to define surface fire-effects on soil properties in scots pine and black pine stands which is located in the borders of Ilgaz, Çankırı, Turkey. Annual average temperature is 11.1ºC and annual precipitation ranges 400 to 500 mm. Fire area was burned in October, 2012. Ten months after fire, soil samples were taken.

Soil Sampling and Soil analyses. Soil samples were collected from burned and unburned sites from 0-20 cm depth. Totally 70 samples were taken in both sites. Soil samples which were used for physical and chemical analysis, were air dried, ground to 2 mm, placed in plastic bags and securely stored.

Soil texture (sand, silt and clay %) was analyzed by hydrometer method as described by Gee and Bauder [30]. Soil bulk density was determined by method described by Blake and Hartge [31]. Field capacity and wilting point were analyzed using methods of Cassel and Nielson [32]. Aggregation index was determined by method described by Kemper and Rosenau [33]. pH and Electrical conductivity were measured 1:2.5 soil: water suspension by methods of U.S. Salinity Laboratory Staff [34]. Soil organic matter was analyzed using Walkey-Black method [35]. $CaCO_3$ content was determined by Scheibler calcimetre using method of Çağlar [36]. Soil analyses were repeated by twice.

Statistical analyses. Statistical analyses were evaluated by Excel Program including explanatory statistics, correlation and t-test in both burned and unburned samples.

RESULTS AND DISCUSSION

Some physical and chemical properties of soil samples are given in Table 1. Clay and silt content, bulk density, plant available water, pH, aggregate stability index decreased in burned sites whereas sand content, field capacity, wilting point, organic matter, $CaCO_3$ content, EC increased in burned sites.

TABLE 1
Some properties in burned and unburned sites in research areas.

Soil properties	Burned	Unburned
Clay (%)	28.00	29.70
Sand (%)	54.03	51.56
Silt (%)	17.97	18.75
Bulk density (g.cm^{-3})	1.31	1.43
Field capacity (%)	32.54	30.57
Wilting point	15.38	15.36
Plant available water	17.16	15.21
Organic matter (%)	8.07	7.40
$CaCO_3$ (%)	2.70	2.28
pH	6.68	6.79
EC (dS cm^{-1})	0.06	0.04
Aggregate stability index	2.26	2.35

Explanatory statistical analyses are given in Table 2 and 3 respectively in burned and unburned results. t-test results are given in Table 4.

TABLE 2
Explanatory statistical analyses in burned sites.

Soil properties	Sample number	Arithmetical mean	Standard variation	Maximum	Minimum	Skewness	Kurtosis	Variation coefficient
Clay (%)	35	28.00	4.83	37.70	18.95	0.40	-0.46	17.26
Sand (%)	35	54.03	6.52	68.20	42.30	0.14	-0.67	12.06
Silt (%)	35	17.97	2.87	22.50	11.25	-0.64	-0.20	15.98
Bulk density (g.cm^{-3})	35	1.31	0.21	1.70	1.00	0.20	-1.07	16.06
Field capacity (%)	35	32.54	17.65	90.49	12.19	1.59	2.73	54.25
Wilting point (%)	35	15.38	7.93	43.87	3.82	2.27	2.27	51.57
Plant available water	35	17.16	16.60	79.59	0.75	2.11	5.53	96.76
Organic matter (%)	35	8.07	2.24	11.61	3.59	-0.43	-1.00	27.74
$CaCO_3$ (%)	35	2.70	2.00	13.46	0.87	4.78	26.31	74.04
pH	35	6.68	0.45	7.70	5.80	0.16	0.21	6.68
EC (ds.cm^{-1})	35	0.06	0.04	0.17	0.01	1.33	1.89	58.21
Aggregate stability index	35	2.26	1.88	7.15	0.29	0.69	-0.45	83.13

TABLE 3
Explanatory statistical analyses in unburned sites.

Soil properties	Sample number	Arithmetical mean	Standard variation	Maximum	Minimum	Skewness	Kurtosis	Variation coefficient
Clay (%)	35	29.70	4.51	43.00	21.80	0.68	0.94	15.20
Sand (%)	35	51.56	6.32	65.70	40.00	0.07	-0.61	12.27
Silt (%)	35	18.75	3.11	25.00	12.50	-0.07	-0.28	16.60
Bulk density($g.cm^{-3}$)	35	1.43	0.23	1.75	1.00	-0.39	-1.13	16.40
Field capacity (%)	35	30.57	13.46	61.12	16.02	1.34	0.84	44.03
Wilting point (%)	35	15.36	6.32	33.59	6.16	0.98	1.23	41.15
Plant available	35	15.21	12.19	47.95	0.16	1.21	0.78	80.14
water	35	7.40	2.79	12.71	2.06	-0.04	-1.00	37.72
Organic matter (%)	35	2.28	1.18	7.27	0.35	2.10	8.37	52.00
$CaCO_3$ (%)	35	6.79	0.32	7.40	6.30	0.34	-0.93	4.68
pH	35	0.04	0.02	0.15	0.01	2.28	8.59	55.24
EC ($ds.cm^{-1}$)	35	2.35	2.03	6.46	0.38	0.65	-1.08	86.35
Aggregate stability index								

TABLE 4
t-test and P-value in burned and unburned areas.

Soil properties	Burned (mean)	Unburned (mean)	t-test	P-value
Clay (%)	28.00	29.70	-1.85	0.072
Sand (%)	54.03	51.56	2.29	0.028*
Silt (%)	17.97	18.75	-1.5	0.142
Bulk density ($g.cm^{-3}$)	1.31	1.43	-2.9	0.005**
Field capacity (%)	32.54	30.57	0.547	0.588
Wilting point (%)	15.38	15.36	0.017	0.987
Plant available water	17.16	15.21	0.541	0.592
Organic matter (%)	8.07	7.40	1.202	0.238
$CaCO_3$ (%)	2.70	2.28	0.980	0.334
pH	6.68	6.79	-1.27	0.212
EC ($ds.cm^{-1}$)	0.06	0.04	2.4	0.022*
Aggregate stability index	2.26	2.35	-0.174	0.853

Sand and EC content were found significantly ($P<0.05$) increased in burned sites. However, bulk density was found significantly ($P<0.01$) decreased in burned sites compared to unburned sites.

DISCUSSION

Fires absolutely cause physical, chemical and biological changes in soil properties and diverse effects to environment [15, 37, 38, 39-43]. However, Berber et al. [44] found that surface fires have limited effect on soil properties. Infect, forest fires influence both vegetation and soil [13]. Forest fires destroy forest flora and change soil properties which affect runoff and erosion [45]. In this study, soil properties were influenced by fire and the most effective parameters were sand ($P<0.05$), bulk density ($P<0.01$) and EC ($P<0.05$). There is a differentiation in all other properties but this difference is not statistically significant.

Forest fire changes soils by several features: (i) loss or reduction of soil structure, (ii) loss or reduction of soil organic matter, (iii) lowered porosity and (iv) increased pH [19,23]. In this study, soil organic matter content show close results and not significantly important. Actually soil organic matter is combusted by fires as a result of reducing the depth of or eliminating surface organic horizons [46]. It can be explain not come out loss of soil organic matter by forest fire intensity. Compare to slightly or moderately burned soil, in severely burned soil showed the most noticeable soil parameters as soil colour and texture [47]. Generally, soil colour changes via forest fire. Redder hue can be seen after fires due to Fe-oxides transformation and complete removal of organic matter [19, 47]. This appearance was not observed in the research area in this study.

Soil texture also changes dramatically after forest fires. Generally the most sensitive textural fraction is clay [48]. Ulery and Graham [47] indicated that less clay content was found in reddened soil layers in burned soil compared to unburned soils. Also, blackened layers and sand-size aggregates formed in surface soil in forest fires [13]. Besides blackened layers and sand-size aggregations, coarser textures appeared after forest fires because of a greater proportion of sand [13]. When soil temperature reaches about 400°C, clay hydration and clay lattice structure start to collapse [48]. Actually, sand were found statistically important change in this study. Clay showed some differentiation but not significantly important.

In this study, EC parameter showed significantly increase in burned sites compared to unburned sites. Hernandez et al. [49] found that 9 months after fire higher EC values were found in burned soils compared to unburned soils. These similar results were found and supported.

Chemical properties such as soil pH also affects due to burning of soil. Tufekcioglu et al. [50] found soil pH was significantly higher level in burned soils than unburned soils. Similar results were found by many scientists [38, 47, 51-53]. Many scientists indicated that soil pH is generally higher levels in burned soils due to forest fires [18, 50, 54]. Certini [19] underlined that significant increase occurs only at higher temperatures (400-500ºC). After forest fires, ash formation may increase soil pH due to high pH of ash [55,56]. Soil pH especially rise in 0-10 cm soil layer whereas no significant increase in 10-30 cm soil layer [57].

Because of organic acids denaturation, soil heating causes "inexorably" increase in soil pH [19]. Ulery et al. [47] indicated that after burning, topsoil pH could increase almost three units. However, in this study there is decrease in soil pH but not significantly important.

Due to forest fires, bulk density of forest soils significantly increased [18,19]. Bulk density increases with ash depth [58]. However, in this study, bulk density was found significantly ($P<0.01$) decreased in burned sites compared to unburned sites.

Because of destroy of forest vegetation cover after forest fire, it could be observed in increase of runoff and soil erosion rates [59-61]. Another words we can say "forest fire destroy the vegetation cover and alter soil properties that influence runoff and erosion" [45].

The time is generally needed to pass for forest fire adverse effect. Kutiel and Naveh [62] found that almost 14 months required negligible effect in between burned and unburned soils. Choromanska and Deluca [63] indicated that decline of C and N mineralization after fire did not recover after 9 months of a study period. Similarly, Ekinci et al. [64] negative effects after fire on soils could be continued after 8 years. They underlined another study recovery of soil quality is very slow after fire [29]. Kavdir et al. [29] concluded that forest fires can change soil quality basically in the surface horizon. After 12 years, soil quality was recovered by itself in fire location [29]. In this study soil samples were taken about ten months later after fire.

The impacts of forest fires on soil quality depends on the fire severities and the type of fire [15]. Similarly, entire effects depend on several factor such as intensity and duration of the fire, soil type, soil moisture content, precipitation events and history of post fire duration and intensity [60, 61]. Certini [19] suggested that fire severity consists of intensity and duration. Duration can be defined as "the length of time burning occurs at a particular point" [62]. Intensity of fire can be high or low. In moderately and low intensity fires, the temperatures will be reached to 400ºC and 500ºC. Whereas in high intensity fires, the temperatures will be reached to 675ºC [15].

Generally, high severity fires cause significant changes depending on soil type which has different trends [68]. In general, low intensity fires do not produce important alterations in aggregate stability with some exceptional cases [68]. After having low intensity fires, litter and soil organic matter are combusted and final result which is higher nutrient storage in plant tissues [13]. In contrast, high intensity fires following steps occur. These are (i) complete loss of soil organic matter, (ii) volatilization of N, P, S, K and (iii) kill of microbes [13]. Moreover, some organic compounds are formed by intense forest fire and these compounds with property of hydrophobic which results into high water repellent soils [13].

To summarize all information about fire severity, our results showed less negative effects on soil parameters because of having low intensity fire.

CONCLUSION

Every year many forest areas are affected by forest fires. Selecting refractive soil parameters after forest fire should be good in order to evaluate effects of forest fires. Sand and bulk density as soil physical parameters were more informative parameters for evaluating fire effect and were significantly important ($P<0.05$ and P0.01, respectively). Only EC parameters was significantly important ($P<0.05$) in soil chemical parameters for reflecting forest fire. Having low intensity fire in research area decreased the negative effects of forest fire.

ACKNOWLEDGEMENT

Financial support for his study was partly provided by Cankiri Karatekin University Research Fund (Project number:2013/08). The authors thank colleague Dr. Melda Dölarslan for helpful correction to edit the English on final draft of this paper.

REFERENCES

[1] Dixon, R.K., Wisniewski, J. (1995) Global forest systems: an uncertain response to atmospheric pollutants and global climate change. Water Air Soil Pollut. 85, 101-110.

[2] Gonzalez-Perez, J.A., Gonzalez-Vila, F.J., Almendros, G., and Knicker, H. (2004) The effect of fire on soil organic matter- a review. Environment International. 30(6), 855-870.

[3] Goldammer, J.P. (1995) Biomass burning and the atmosphere. Paper presented at forests and Global Climate Change: Forests and Global Carbon Cycle.

[4] Trabaud, L. (1984) Man and fire: impacts on Mediterranean vegetation. In: Castri, F., Goodall, D.W., Spetch, R.L. (eds.) Mediterranean type shrublands. Ecosystems of the World. Vol. 11. Amsterdam. Elsevier. 523-537.
[5] Naveh, Z. (1990) Fire in Mediterranean-A landscape ecological perspective. In: Goldamner, J.G., Jenkins, M.J. (eds.) Fire in ecosystems dynamics: Mediterranean and Northern perspective. The Hague. SPB Academic Publishing. 1-20.
[6] Barbero, M., Loisel, R. and Quezel, P. (1998) Pines of the Mediterranean Basin, Pinus. In: Richardson, D.M. editor. Ecology and biogeography of Pinus Cambridge Univ. Press. 153-170.
[7] Yildiz O, Esen D, Sarginci M, Toprak B. (2010) Effects of forest fire on soil nutrients in Turkish pine (Pinus brutia, Ten.) ecosystems. Journal of Environmental Biology. 31, 11–13.
[8] Bowman, D.M.J.S., Balch, J.K., Artaxo, P., Bond, W.J., Carlson, J.M., Cochrane, M.A., D'Antonio, C.M., DeFries, R.S., Doyle, J.C., Harrison, S.P., Johnston, F.H., Keeley, J.E., Krawchuk, M.A., Kull, C.A., Marston, J.B., Moritz, M.A., Prentice, I.C., Roos, C.I., Scott, A.C., Swetnam, T.W., van der Werf, G.R., and Pyne, S.J. (2009) Fire in the Earth System, Science. 324, 481–484.
[9] Lavorel, S., Flannigan, M.D., Lambin, E.F., Scholes, M.C. (2006) Vulnerability of land systems to fire: interactions among humans, climate, the atmosphere, and ecosystems. Mitigation and Adaptation Strategies for Global Change. 12, 33–53.
[10] Doerr, S., Cerdà, A. (2005) Fire effects on soil system functioning: new insights and future challenges. International Journal of Wildland Fire Preface. International Journal of Wildland Fire. 14, 339–342.
[11] Schmidt, M.W.I., Skjemstad, J.O., Gehrt, E., Kogel-Knabner, I. (1999) Charred organic carbon in German chernozemic soils. Eurasian Journal of Soil Science. 50, 351–365.
[12] Simard, D.G., Fyles, J.W., Pare, D., and Nguyen, T. (2001) Impact of clear-cut harvesting and wildfire on soil nutrient status in the Quebec boreal forest. Can. J. Soil. Sci. 81, 229–237.
[13] Verma, S. and Jayakumar, S. (2012) Impact of Forest Fire on Physical, Chemical and Biological Properties of Soil: A. Proceedings of the International Academy of Ecology and Environmental Sciences. 2(3), 168–176.
[14] Flannigan M.D., Stocks B.J., Wotton B.M. (2000) Climate change and forest fires. The Science of the Total Environment. 262, 221–229.
[15] Neary, D.G., Klopatek, C.C., DeBano, L.F., Ffolliott, P. (1999) Fire effects on belowground sustainability: a review and synthesis. Forest Ecology and Management 122, 51–71.
[16] Busse, M.D., Cochran, P.H., and Barrett, J.W. (1996) Changes in ponderosa pine site productivity following removal of understory vegetation. Soil Sci. Soc. Am. J. 60. 1614–1621.
[17] DeBano, L.F, Neary, D.G., Ffolliott, P.F. (1998) Fire's effects on ecosystems. John Wiley and Sons: New York.
[18] Boerner, R.E.C., Hart, S., Huang, J. (2009) Impacts of Fire and Fire Surrogate treatments. Ecological Applications. 19(2), 338–358.
[19] Certini, G. (2005) Effect of fire on properties of soil. A renew. Oecologica. 143, 1-10.
[20] Pietikainen, J., Fritze, H. (1993) Microbial biomass and activity in the humus layer following burning: short-term effects of 2 different fires. Canadian Journal of Forest Research. 23, 1275–1285.
[21] Pantomi, S., Voncir, N., Babaji, G., and Mustapha, S. (2010) Effect of burning on soil chemical properties in the dry sub-humid savanna zone of Nigeria. Researcher. 2, 78–83.
[22] Kutiel, P. and Inbar, M. (1993) Fire impacts on soil nutrients and soil erosion in a Mediterranean Pine Forest Plantation. Catena. 20, 129-139.
[23] DeBano, L.F. (1998) The effect of forest fire on soil properties. Symposium on Management and Productivity of Western –Montane Forest Soil. Boise, ID. USA. 151-156.
[24] Amaranthus, M.P. and Trappe, J.M. (1993) Effects of erosion on ecto and VA-mycorrhizal inoculum potential of soil following forest fire in southwest Oregon. Plant Soil. 150, 41–49.
[25] Acea, M.J. and Carballas, T. (1999) Microbial fluctuations after soil heating and organic amendment. Bioresour. Technol. 67, 65–71.
[26] Hart, S.C., DeLuca, T.H., Newman, G.S., MacKenzie, M.D. and Boyle, S.I. (2005) Post-fire vegetative dynamics as drivers of microbial community structure and function in forest soils. For. Ecol. Manage. 220, 166–184.
[27] Marion, G., Moreno, J., Oechel, W. (1991) Fire severity, ash deposition, and clipping effects on soil nutrients in chaparral. Soil Science Society of America journal. 55(1), 235-249.
[28] FAO, 2007. Fire Management-Global Assessment (2006) FAO Forestry Paper, 151. Available at: http://www.fao.org/docrep/009/a0969e /a0969e00.htm.
[29] Kavdir, Y., Ekinci, H., Yüksel, O., and Mermut, A.R. (2005) Soil aggregate stability and 13C CP/MAS-NMR assessment of organic matter in soils influenced by forest wildfires in Canakkale, Turkey. Geoderma. 129, 219–229.

[30] Gee, G.W., Bauder, J.W. (1986) Particle-size Analysis. In: Page A.L. (ed.) Methods of soil analysis, Part I, Physical and mineralogical methods. 2nd Edition. Madison: American Society of Agronomy and Agronomy Monograph. 9, 383- 411.
[31] Blake G.R., Hartge, K.H. (1986) Bulk Density. In: Klute, A(ed.) Methods of Soil Analysis, Part I. Madison: American Society of Agronomy Monograph. 9, 363–375.
[32] Cassel, D.K. and Nielsen, D.R. (1986) Field capacity and available water capacity. In: A. Klute, (Ed.), Methods of Soil Analysis, Part 1, 2nd ed. ASA and SSSA, Madison, WI. 901–926.
[33] Kemper, W.D. and R.C. Rosenau (1986) Aggregate stability and size distribution. pp. 425-442. In: Klute, A. (ed/) Methods of Soil Analysis. Part 1: Physical and Mineralogical Methods. No. 9, Agronomy. ASA. SSSA, Madison, WI.
[34] US Salinity Laboratory Staff (1954) Diagnosis and improvement of saline and alkali soils. US Department of Agriculture Handbook 60, Washington, D.C.
[35] Nelson, D.W., and Sommers, L.E. (1982) Total carbon, organic carbon and organic matter. In: Page, A.L. (ed.). Methods of soil analysis. Part 2. 2nd ed. Argon. Monogr. 9. ASA. Madison, WI. 539-579.
[36] Çağlar, K.Ö. (1958) Earth Science. Ankara University Faculty of Agriculture Publications. No: 10, Ankara.
[37] Mataix-Solera, J. and Guerrero, C. (2007) Effects of forest fires on edaphic properties. In: Mataix-Solera, J. (Ed.) Forest Fires, Soils and Water Erosion. Caja Mediterráneo-CEMACAM Font Roja-Alcoi, Alicante, 5-40.
[38] Úbeda, X. and Outeiro, L. (2009) Physical and chemical effects off ire on soil. In: Cerdà, A., Robichaud, P.R. (Eds.) Fire Effects on Soils and Restoration Strategies. Science Publishers, Enfield, NH, 105-133.
[39] Jakubus, M., Kaczmarek, Z., Michalik, J., Grzelak, M. (2010) The effect of different tree plantings and soil preparation methods on contents of selected heavy metals in post-fire soils. Fresen. Environ. Bull. 19, 312-317.
[40] Kaynas, B.Y. (2017) The Long-Term Changes of Main Surface-Dwelling Arthropod Groups with Time Since Fire in Pinus Brutia Forests Of Southwestern Anatolia. Fresen. Environ. Bull. 26, 426-431.
[41] Ratknic, T., Ratknic, M., Cirkovic-Mitrovic, T., Brasanac-Bosanac, L. (2018) The impact of climate factors on the wildfire occurrence in Serbia. Fresen. Environ. Bull. 27, 4014-4022.
[42] Tufekcioglu, M., Saglam, B., Tufekcioglu, A. (2017) Effects of fire intensity and slope on surface soil erosion following a prescribed fire in old Pinus nigra stands. Fresen. Environ. Bull. 26, 7227-7234.
[43] Varol, T. and Ertugrul, M. (2015) Climate change and forest fire trend in the Aegean and Mediterranean regions of Turkey. Fresen. Environ. Bull. 24, 3436-3444.
[44] Berber, A.S., Tavşanoğlu, Ç., Turgay, O.C. (2015) Effects of surface fire on soil properties in a mixed chestnut-beech-pine forest in Turkey. FLAMMA. 6 (2), 78-80.
[45] Fox, D.M., Darboux, F. and Carrega, P. (2007) Effects of fire-induced water repellency on aggregate stability, splash erosion, and saturated hydraulic conductivity for different size fractions. Hydrological Processes. 21(17), 2377-2384.
[46] Neff, J.C., Harden, J.W. and Gleixner, G. (2005) Fire effects on soil organic matter content, composition, and nutrients in boreal interior Alaska. Canadian Journal of Forest Research. 35(9), 2178-2187.
[47] Ulery, A.I., and Graham, R.C. (1993) Forest fire effects on soil colour and texture. Soil Science Society of America Journal. 57(1), 135-140.
[48] Neary, D.G., Ryan, K.C., DeBano, L.F. (2008) Wildland fire in ecosystems: effects of fire on soil and water. USDA Forest Service, Rocky Mountain Research Station, General Technical Report RMRS-GTR-42-vol. 4.
[49] Hernández, T., García, C., Reinhardt, I. (1997) Short-term effect of wildfire on the chemical, biochemical and microbiological properties of Mediterranean pine forest soils. Biol Fertil Soil. 25, 109–116.
[50] Tufekcioglu, A., Kucuk, M., and Bilgili, E. (2010) Soil properties and root biomass responses to prescribed burning in young corsican (Pinus nigra Arn) stands. Journal of Environmental Biology. 31, 369-373.
[51] Altun, L., Bilgili, E., Saglam, B., Kucuk, O., Yilmaz, M. and Tufekcioglu, A. (2004) Soil organic matter, soil pH and soil nutrient dynamics in forest stands after fire. In: Proceedings Book of International Soil Congress (ISC) on "Natural Resource Management for Sustainable Development". June 7-10, 2004, Erzurum/Turkey. 67-73.
[52] Mitros, C., Mcintyre, S. and Moscato-Goodpaster, B. (2002) Annual burning affects soil pH and total nitrogen content in the cero oak woodlands. Tillers, 3, 29-32.
[53] Neal, J., Wright, L. and Bollen, W.B. (1965) Burning Douglas – Fir slash; physical, chemical and microbial effects in the soil. Forest Research Laboratory, Research Paper No. 1 Oregon State University Corvallis-USA.

[54] Aref, I.M., Atta, H.A. and Ghamade, A.R. (2011) Effect of forest fires on three diversity and some soil properties. International Journal of Agriculture and Biology. 13, 659-664.
[55] Molina, M., Fuentes, R., Calderón, R. (2007) Impact of forest fire ash on surface charge characteristics of Andisols. Soil Science. 172(10), 820-834.
[56] Schafer, J.L., Mack, M.C. (2010) Short-term effects of fire on soil and plant nutrients. Plant Soil. 334, 433-447.
[57] Sha, L.Q., Deng, J.W., Xie, K.Y. and Meng, Y. (1998) Study on the Change of Soil Nutrient Before and After Burning Secondary Forest in Xishuangbanna. Acta Phytoecologia Sinica. 22(6), 513-517.
[58] Cerdà, A. and Doerr, S.H. (2008) The effect of ash and needle cover on surface runoff and erosion in the immediate post-fire period. Catena. 74(3), 256–263.
[59] Prosser, I.P. and Williams, L. (1998) The effect of wildfire on runoff and erosion in native Eucalyptus forest. Hydrological Processes. 12(1998), 251-265.
[60] Johansen, M.P., Hakonson, T.E., Breshears, D.D. (2001) Post-fire runoff and erosion from rainfall simulation: contrasting forests with shrublands and grasslands. Hydrological Processes. 15, 2953-2965.
[61] Wohlgemuth, P.M., Hubbert, K.R., Robichaud, P.R. (2001) The effects of log erosion barriers on post-fire hydrologic response and sediment yielding small forested watersheds, southern California. Hydrological Processes. 15, 3053–3066.
[62] Kutiel, P., and Naveh, Z. (1987) Soil properties Beneath Pinus halepensis and Quercus calliprinos trees on burned and unburned mixed forest on Mt. Carmel. Israel Forest Ecology and Management. 20, 11-24.
[63] Choromanska, U., DeLuca, T.H. (2002) Microbial activity and nitrogen mineralization in forest mineral soils following heating: evaluation of post-fire effects. Soil Biol Biochem. 34, 263–271.
[64] Ekinci, H., Kavdir, Y., Yuksel, O, Yiğni, Y., Cetin, S.C., Altay, H. (2008) Fire induced changes in soil characteristics in Keşan, Turkey. Proceedings of the International Meeting on Soil Fertility, Land Management, and Agroclimatology. 73-82.
[65] Chandler, C., Cheney, P., Thomas, P., Trabaud, L., and Williams, D. (1983) Forest fire bahavior and effects. Fire in intensity. Vol. I. New York, Wiley.
[66] Pyne, S.J., Andrews, P.L., Laven, R.D. (1996) Introduction to Wildland Fire: Second Edition. John Wiley and Sons. Inc. New York, USA. 1-769.
[67] Mataix-Solera, J., Guerrero, C., García-Orenes, F., Bárcenas, G.M., Torres, M.P. (2009) Forest fire effects on soil microbiology. In: Cerdà, A., Robichaud, P. (Eds.) Fire Effects on Soils and Restoration Strategies, Science Publishers, Inc., Enfield, New Hampshire USA. 133-175.
[68] Mataix-Solera, J., Cerdà, A., Arcenegui, V., Jordán, A., Zavala, L.M. (2011) Fire effects on soil aggregation: a review. Earth-Science Reviews. 109, 44-60.

Received: **04.10.2018**
Accepted: **17.02.2019**

CORRESPONDING AUTHOR

Sema Camci Cetin
Department of Soil Science and Ecology,
Forest Faculty,
Cankiri Karatekin University,
Cankiri – Turkey

e-mail: semacamcicetin@hotmail.com

© by PSP Volume 28 – No. 4/2019 pages 2582-2588 Fresenius Environmental Bulletin

EGG AND CHICK QUALITY CHARACTERISTICS OF MEAT TYPE JAPANESE QUAIL (*COTURNIX COTURNIX JAPONICA*) LINE BY CANONICAL CORRELATION ANALYSIS

Abdullah Nuri Ozsoy*

Isparta University of Applied Sciences, Faculty of Agricultural Sciences and Technologies, Department of Animal Sciences, 32260, Isparta, Turkey

ABSTRACT

Canonical correlation analysis is a multivariate analysis technique used to determine the relationships between two data sets with more than one variable. The use of canonical correlation analysis in biological studies about revealing the relations of quantitative characteristics can provide additional information to the investigator. In this study, total of 146 meat type female quails were used. 13 eggs were collected from each of 15-week-old and pedigree-raised quails. Four of these eggs were used for egg quality characteristics, 5 for chick quality characteristics analysis and 4 for egg protein analysis. The egg quality characteristics that are discussed in the research are; egg weight (EW), shape index (SI), shell weight (SW), albumen weight (AW), yolk weight (YW), albumen density (AD), yolk density (YD), and egg crude protein (CP) content. Chick quality features are; hatching weight (HW), daily chick weight (CW) and chick length (CL). As a result of the research, high canonical correlations (0.907) between egg quality characteristics and chick quality characteristics were determined. When egg quality characteristics are supposed as independent variables (X) and chick quality characteristics dependent variables (Y), 82.30% of the total variation in the Y variable set can be explained by the X variable set. This suggests that egg quality characteristics are likely to be determinants of chick quality characteristics. In the formation of the canonical variables in the egg quality traits set, the albumen weight had the highest contribution as the original values whereas in chick quality traits set, chick weight had the highest additive value.

KEYWORDS:
Canonical correlation, quail, egg quality, chick quality

INTRODUCTION

The egg quality characteristics are of factors determining the hatching performance and the quality of the chicks in breeding flocks and also the future yield performance of the flock [1-4]. Environmental and genetic factors affecting egg quality traits in poultry have been elucidated in many researches [5-13]. The relationship between egg and chick is mostly explained by genetic and phenotypic correlations between the physical properties of the egg and the chick weight [11, 14-16]. Despite these measurements, which do not harm the embryo developing in the egg, are biologically friendly ways of determining the coherence between the egg and the chick, the information revealed from these relationships are rather limited. Thus, advanced statistical approaches can help to extract more detailed information in such researches.

In statistical methods, Pearson correlation coefficients are commonly used as a statistical tool to delineate the linear relationship among the properties. In cases where the prerequisite of normal distribution is not met, methods such as Spearman rank or Kendal-Tau correlations may be used. Multiple correlation coefficients are efficient tool to scale the relationships between the characteristics and multiple independent variables with a dependent variable. However, if there are multiple-dependent and -independent variables in any case, canonical correlation analysis can be preferred to explore the relations. The canonical correlation analysis, which is a multivariate analysis technique, has been used by various researchers for revealing additional information in the analysis of biological properties [17-20]. Therefore, in this study, egg and chick quality traits of meat type Japanese quail (*Coturnix coturnix japonica*) line were investigated by using canonical correlation analysis.

MATERIALS AND METHODS

The material of the study was obtained from the population of Japanese quail in the poultry breeding unit of the Faculty of Agricultural Sciences and Technologies at Isparta University of Applied Sciences. A total of 146 female and male quails were randomly selected from this population at the age of 4 weeks. These quails were placed on individual compartment cages according to 1:1 sex ratio.

Thirteen fertilized eggs from these families in individual cages were taken at the age of 15 weeks. Four of these eggs were used for egg quality characteristics, 4 for egg protein analysis and 5 of them were hatched for determining the chick quality characteristics.

The quails had been fed with a ration containing 3100 kcal / kg metabolic energy and 24% crude protein during the entire experimental period. Adlibitum feeding and unlimited water were provided in the study.

According to the canonical correlation analysis, two sets of variables were formed. In one of these variable sets there comprised the egg quality characteristics (X) and the other consisted of the chick quality characteristics (Y). The egg quality characteristics set (X) had the following variables: egg weight (EW), shape index (SI), shell weight (SW), albumin weight (AW), yolk weight (YW) albumin density (AD), yolk density (YD) and egg crude protein content (HP) whereas the set of chick quality characteristics (Y) were: hatching weight (HW), daily chick weight (CW) and length (CH).

Egg weight, egg shell weight, albumin weight, yolk weight, hatching weight and daily chick weight characteristics were accurately determined with a balance having 0.01 g precision. The egg width and height were carefully measured by means of a digital calliper at 0.01 mm precision.

The following equation was used to determine the shape index (SI):

SI (%) = (*(egg width (mm)/egg length (mm)) x 100*

Daily chick weight and length (CH) measurements were made 24 hours after hatching.

Density analysis. The eggs were broken and the albumin and yolk were separately weighed. At the end of this process, each of albumin and yolk was placed in separate containers and mixed until homogenized. Then analytical amount of samples were taken to determine the density by using the digital refractometer device (0.1% precision, 0-85% Brix measurement range, Hanna HI96801) which quantifies the amount of solids dissolved in liquids.

Protein analysis. Homogenised 4 eggs obtained from each of the individual female quail were frozen at -20°C in polypropylene containers until the analysis. The samples were thawed and re-homogenized by a mixer just before the analysis. Scopes of 1.000 g aliquot was taken and put on the ashless filter paper. The samples were then digested with concentrated H_2SO_4 along with catalyser mixture as described in the conventional Kjeldahl method [21]. Then the ammonium concentration of the digests was steam distilled and the distillates were titrated by absolutely 0.1 equivalent/L HCl standard solution. Triplicates of the control without any sample were also carried out. The amount of crude protein (CP) was quantified from the equation given below:

CP (%) = (0.1 * 0.014 * 6.25 * (Vs-Vc) * 100) / sample weight (g)

where 0.014 is a constant related to molecular weight of nitrogen, 6.25 is conversion factor of nitrogen to CP, Vs volume of HCl standard solution in mL, and Vc volume of standard solution used for the control in mL.

Statistical analysis. The canonical correlation analysis used the CANCORR procedure of the SAS computer program to identify and measure canonical relationships between egg and chick quality feature sets [22]. Both between-group and within-group Pearson correlation coefficients of the entire data-set are calculated in the first step of the canonical correlation analysis. Then, the linear combinations of variable sets are defined as follows [23, 24]:

$U_n = a_{n1}X_1 + a_{n2}X_2 + \cdots + a_{np}X_p$

$V_n = b_{n1}Y_1 + b_{n2}Y_2 + \cdots + b_{nq}X_q$

where a_{np} and b_{nq} are canonical coefficients, U_n and V_n are the n^{th} pair of canonical variants. The canonical correlations between the canonical variable pair are finally calculated by using the formula given below:

$r_n = cov(U_n, V_n)/\sqrt{var(U_n) * var(V_n)}$

The correlations calculated as above are called canonical weights or canonical structure [25].

By dividing the sum of squares of canonical weights by the number of variables (p and q) in the sets, the explained variance of that set U_x^2 *ve* V_y^2 can be obtained [19] as given below:

$U_{x_i}^2 = \sum_{j=1}^{p} a_{ij}^2 / p$

and

$U_{y_i}^2 = \sum_{j=1}^{q} b_{ij}^2 / q$

RESULTS AND DISCUSSION

The descriptive statistics regarding the egg and chick quality traits were given in Table 1.

The correlation matrices among the original variables of the data-set were shown in Table 2. The correlation between the egg quality and chick quality variable groups are high, the largest one was 0.86 between hatching weight and egg weight. There are comparatively larger within-set correlations as high as 0.94 between egg weight and yolk weight, and 0.84 between hatching weight and chick weight parameters.

The correlation coefficients between the EW, SI, AW and YW variables included in the egg quality trait set were in accordance with the reported significance levels in the literature [10, 26-28]. In the study, the correlations between AD and YD variables and other egg characteristics from egg quality characteristics were generally markedly different, the way of the relation is opposite in this study, and incompatible with the values reported by Zita et al. [29].

As Table 3 shows, three canonical correlations are 0.907, 0.523 and 0.321. The first two of these canonical correlations are significant (p≤0.05) whereas r_3 canonical coefficient (0.321) was not found to be significant (p>0.05). Therefore, these two canonical correlation coefficients have revealed that chick quality traits sets were largely functioned by eggs quality features.

The canonical coefficients and standardized canonical coefficients for the first canonical correlation was considered to be very determinant, therefore only these data were presented in Table 4. Because variables cannot be measured in the same units, it is a better way to interpret standardized coefficients instead of raw coefficients [22].

TABLE 1
Descriptive statistics of variables

Sets	Traits	n	$\bar{X} \pm St_{dev}$	Min.	Max.	CV (%)
Egg quality traits set (X)	Egg weight (g)	584	12.6 ± 1.16	9.23	15.4	9.19
	Shape index (%)	584	78.3 ± 4.47	65.9	127.0	5.71
	Shell weight (g)	584	1.41 ± 0.15	1.03	2.21	10.4
	Albumen weight (g)	584	6.80 ± 0.79	1.14	8.91	11.6
	Yolk weight (g)	584	3.82 ± 0.46	2.56	4.95	11.9
	Albumen density (%)	584	16.3 ± 0.72	14.3	18.7	4.41
	Yolk density (%)	584	50.1 ± 1.50	42.5	53.8	2.99
	Crude protein (%)	143	11.3 ± 1.71	6.87	13.7	15.1
Chick quality traits set (Y)	Hatching weight (g)	730	9.50±0.88	6.50	11.8	9.29
	Daily chick weight (g)	730	11.1±1.09	6.95	13.9	9.82
	Chick length (g)	730	11.9±0.44	10.4	14.1	3.73

TABLE 2
Correlations among the original variables

Traits	Egg quality traits set (X)								Chick quality traits set (Y)		
	EW	SI	SW	AW	YW	AD	YD	CP	HW	CW	CL
EW	1										
SI	-0.34**	1									
SW	0.65**	-0.21*	1								
AW	0.79**	-0.27**	0.46**	1							
YW	0.94**	-0.32**	0.53**	0.58**	1						
AD	0.08	-0.04	0.04	0.09	0.05	1					
YD	0.29**	0.02	0.11	0.02	0.39**	0.05	1				
CP	0.05	-0.09	-0.04	0.004	0.08	0.17	0.23*	1			
HW	0.86**	-0.24**	0.49**	0.82**	0.67**	-0.04	0.38**	0.04	1		
CW	0.73**	-0.19*	0.45**	0.66**	0.67**	0.06	0.27**	0.07	0.84**	1	
CL	0.52**	-0.20*	0.37**	0.49**	0.47**	0.09	0.09	-0.04	0.59**	0.79**	1

* and ** donate significant correlations at p≤0.05 and p≤0.01, respectively.

TABLE 3
Canonical correlations and multivariate statistics

Canonical variable pairs	Canonical correlation	Adjusted canonical correlation ($r_n \pm s_{\bar{x}}$)	Squared canonical correlation (R^2)	Likelihood ratio	F Value	Pr > F
r_1	0.907	0.897±0.02	0.8230	0.1153	9.92	<0.0001
r_2	0.523	0.462±0.08	0.2739	0.6513	2.56	0.0025
r_3	0.321	0.255±0.10	0.1030	0.8970	1.46	0.2051

Multivariate statistics and F approximations

Statistic	Value	F Value	Pr > F
Wilks' Lambda	0.115	9.92	<0.0001
Pillai's Trace	1.200	6.22	<0.0001
Hotelling-Lawley Trace	5.140	15.62	<0.0001
Roy's Greatest Root	4.648	44.16	<0.0001

TABLE 4
Coefficients of the first canonical variable pair

Raw canonical for the egg traits		
Parameters	Raw canonical coef.	Standardized canonical coef.
EW	0.201	0.1769
SI	-0.016	-0.0464
SW	1.126	0.1302
AW	1.002	0.5994
YW	0.618	0.1968
AD	0.170	0.1002
YD	-0.005	-0.0043
CP	-0.027	-0.0463
Raw canonical for the chick traits		
HW	1.346	1.0676
CW	-0.198	-0.1604
CL	0.352	0.1134

The standardized coefficients are the coefficient which shows the amount of change in the canonical variable for each unit of change in the standard deviation of the original variable [17]. In this case, the equation of U_1 and V_1 canonical variables will be as follows:

$$U_1 = 0.177\,EW - 0.046SI + 0.130SW + 0.599AW + 0.197YW + 0.100AD - 0.0043YD - 0.046CP$$

$$V_1 = 1.068HW - 0.160CW + 0.113CL$$

The canonical coefficients of SI, YD and HP in the first canonical equation (U_1) for egg properties-set variables are negatively marked and low value. In contrast, EW, SW, AW, YW and AD canonical coefficients were found to be positive. In these variables, it can be said that the suppressor variable was AW. Variables other than CW were positive when the first canonical variable equation (V_1) was created for the chick quality feature set. It can be said that the suppressor variable for this set was HW.

The values of canonical loads between the raw variables in the canonical variables are given in Table 5.

TABLE 5
Correlations between variable sets and their canonical variables

X Variable set		Y Variable set	
Traits	U_1	Traits	V_1
EW	0.988	HW	0.997
SI	-0.301	CW	0.799
SW	0.525	CL	0.562
YW	0.956		
AW	0.714		
YD	0.308		
AD	0.008		
CP	0.031		

The highest correlation between the canonical variable U_1 and its related the X variable set was determined between EW, YW and AW properties. The relationships between the canonical variable V_1 and the raw data-set in the group of Y variables which it was derived were found to be high (0.997, 0.799 and 0.562).

In some cases, it may be a more accurate approach to examine the correlations between the canonical variable and the original (raw) variables in its own set [30]. This analysis, which constitutes a procedure of canonical correlation analysis, is called the canonical structure analysis. The canonical structure analysis is readily obtainable for X and Y sets. However, since Y variable set is a function of X variable set, only canonical structure analysis of Y variable set was examined here. The canonical structure analysis results were presented in Table 6.

The first canonical variable in Y variable set explained a very large part of the variance in this set (77.51%). The cumulative rates of three canonical variables can explain all of the 100% variance. On the other hand, 63.79% of the variance in the Y variable set can be explained by the variables in the X variable set or egg variable set. The cumulative rates of three canonical variables were 69.36%. In this case, it can be said that the variance of the quality characteristics of the chicks that formed the Y variable set was largely explained by the egg quality characteristics set. In order to determine the predictive power of the canonical variables of a set of variables by the original values of the variables in the other set, the squared multiple correlations are used [31, 17]. Therefore, as the chick characteristics were a result of the egg, the predictive power of the X set canonical variables (U_1 and U_2) and the variation of the original values in the Y set were shown in Table 7.

Accordingly, the canonical variables (U_1 and U_2) obtained from the X set explained 81.79% of the variance in HW from the variables in the Y set. This is a fairly high value. However, a decrease in the explained variance of one-day chick weight (CW) was

TABLE 6
Canonical redundancy analysis

Canonical variable number	Proportion	Cumulative proportion	Canonical R^2	Proportion	Cumulative proportion
V_1	0.1406	0.1406	0.8229	0.1157	0.1157
V_1	0.0545	0.1951	0.2739	0.0149	0.1307
V_1	0.0656	0.2607	0.1030	0.0068	0.1374
Raw Variance of the Y explained by their own canonical Variables				The opposite canonical variables	
V_1	0.7751	0.7751	0.8229	0.6379	0.6379
V_2	0.1902	0.9653	0.2739	0.0521	0.6900
V_3	0.0347	1.000	0.1030	0.0036	0.6936

TABLE 7
Squared multiple correlations of canonical variables

Variables	U_1	U_2
HW	0.8179	0.8180
CW	0.5247	0.6147
CP	0.2602	0.3884

somehow apparent as the X-set canonical variables have been revealed. This showed that the effect of the egg properties on chick weight continues to decrease with time. As a matter of fact, the correlation coefficients [32-34] between egg weight and chick weekly weights revealed this situation. Egg quality characteristics in X set canonical variables explained 26.02% of the variation of chick length trait. This value was lower than the value obtained from HW and CW properties.

CONCLUSIONS

Results of this study indicated that by using canonical correlation analysis tool it was possible to determine the chick quality traits from the egg quality traits to great extent (82.3%). SW, YW and AW properties in egg quality feature set can able to explain the variance in the Y variables set at considerably acceptable rates. This can be treated as an indication that egg quality characteristics are of operational factors on chick quality characteristics. In the formation of canonical variables in the egg quality feature set, the original values of the egg white weight had the highest contribution whereas in chick quality feature set, chick weight had the highest contribution. Despite the canonical variables obtained from the chick quality feature set explained whole variance in the raw variable set, the V_1 canonical variable obtained from this set explained only 77.51% of the variance in the original variables.

REFERENCES

[1] Altan, Ö., Oğuz, İ. and Akbaş, Y. (1998) Effects of selection for high body weight and age of hen on egg characteristics in Japanese quail (*Coturnix coturnix japonica*). Turkish Journal of Veterinary and Animal Science. 22, 467-473 (in Turkish).

[2] Iqbal, J., Khan, S.H., Mukhtar, N., Ahmed, T. and Pasha, R.A. (2016) Effects of egg size (weight) and age on hatching performance and chick quality of broiler breeder. Journal of Applied Animal Research. 44(1), 54-64.

[3] Ulmer-Franco, A.M., Fasenko, G.M. and O'Dea Christopher, E.E. (2010) Hatching egg characteristics, chick quality, and broiler performance at 2 breeder flock ages and from 3 egg weights. Poultry Science. 89, 2735-2742.

[4] Taskın, A., Karadauvut, U., Cayan, H., Genc, S. and Coskun, I. (2015) Determination of small variation effects of egg weight and shape index on fertility and hatching rates in Japanese quail (*Coturnix coturnix japonica*). Journal of Selçuk University Natural and Applied Science. 4(2), 73-83.

[5] Scott, T.A. and Silversides, F.G. (2000) The effect of storage and strain of hen on egg quality. Poultry Science. 79, 1725-1729.

[6] Zhang, L.C., Ning, Z.H., Xu, G.Y., Hou, Z.C. and Yang N. (2005) Heritabilities and genetic and phenotypic correlations of egg quality traits in brown-egg dwarf layers. Poultry Science. 84, 1209-1213.

[7] Daikwo, S.I., Dim, N.I. and Momoh, O.M. (2013) Inheritance of egg quality traits in the Japanese quail. International Journal of Poultry Science. 12(3), 153-156.

[8] Chimezie, V.O., Fayeye, T.R., Ayorinde, K.L. and Adebunmi, A. (2017) Phenotypic correlations between egg quality traits in three varieties of Japanese quail. Agrosearch. 17(1), 44-53.
[9] Narinc, D., Aygun, A., Karaman, E. and Aksoy, T. (2015) Egg shell quality in Japanese quail: characteristics, heritabilities and genetic and phenotypic relationships. Animal. 9(7), 1091-1096.
[10] Sato, K., Ida, N. and Ino, T. (1989) Genetic parameters of egg characteristics in Japanese quail. Jikken Dobutsu. 38(1), 55-59.
[11] Silva, L.P., Ribeiro, J.C., Crispim, A.C., Silva, F.G., Bonafé, C.M., Silva, F.F. and Torres, R.A. (2013) Genetic parameters of body weight and egg traits in meat-type quail. Livestock Science. 153, 27–32.
[12] Karabayir, A., Ogutcu, M. and Arifoglu, N. (2018) Influence of disinfectant added to drinking water on quail growth performance and egg quality. Fresen. Environ. Bull. 27, 3051-3058.
[13] Dogan, S.C., Baylan, M., Erdogan, Z., Akpinar, G.C., Kucukgul, A. and Duzguner, V. (2016) Performance, egg quality and serum parameters of Japanese quails fed diet supplemented with *Spirulina platensis*. Fresen. Environ. Bull. 25, 5857-5862.
[14] Saatci, M., Omed, H. and Ap Dewi, I. (2006) Genetic parameters from univariate and bivariate analyses of egg and weight traits in Japanese quail. Poultry Science. 85, 185-190.
[15] Sefton, A.E. and Siegel, P.B. (1974) Body weight relationships of newly hatched Japanese quail. Poultry Science. 53(3), 1254–1256.
[16] Lotfi, E., Zerehdaran, S. and Raoufi, Z. (2012) Genetic properties of egg quality traits and their correlations with performance traits in Japanese quail. British Poultry Science. 53, 585-591.
[17] Keskin, S. and Özsoy, A.N. (2004) Canonical correlation analysis and its an application. Journal of Agricultural Sciences. 10(1), 57-71 (in Turkish).
[18] Takma, Ç., Gevrekçi, Y., Özsoy, A.N. and Çevik, M. (2017) Canonical correlation analysis on egg production traits of quails. Süleyman Demirel University Journal of the Faculty of Agriculture. 12(1), 92-99.
[19] Ribeiro, J.C., Silva, L.P., Caetano, G.C., Crispim, A.C., Pacheco, R.O. and Torres, R.A. (2016) Canonical correlation analysis applied to production and reproduction traits of meat type quails. Ciência Rural. 47(7), 1289-1294.
[20] Keskin, I. and Dag, B. (2009) Investigation of relationship amongst milk and wool yield traits of Awassi sheep by using canonical correlation analysis. Journal of Animal and Veterinary. 8(3), 464-468.
[21] AOAC - Association of Official Analytical Chemists. (1990) Official methods of analysis. 15th ed. Washington D.C., 1078p.
[22] SAS Institute Inc, (2002) SAS/STAT user's guide. Version 9.1, Cary, North Carolina, USA.
[23] Kendall, M.G. (1980) Multivariate analysis. Charles Griffin and Company, LTD, London. 210p.
[24] Johnson, R.A. and Wichern, D.W. (2002) Applied multivariate statistical analysis. Prentice-Hall, Inc., Upper Saddle, New Jersey, 792p.
[25] Özdamar, K. (2013) Statistical data analysis with package programmes. Volume 2. Nisan Kitabevi, Eskişehir, Turkey, 474p (in Turkish).
[26] Sari, M., Tilki, M. and Saatci, M. (2016) Genetic parameters of egg quality traits in long-term pedigree recorded Japanese quail. Poultry Science. 951, 743–1749.
[27] Alkan, S., Karabag, K., Galic, A. and Balcioglu, M.S. (2008) Effects of genotype and egg weight on hatchability traits and hatching weight in Japanese quail. South African Journal of Animal Science. 38(3), 231-237.
[28] Narinc, D., Aygun, A., Karaman, E. and Aksoy, T. (2015) Egg shell quality in Japanese quail: characteristics, heritabilities and genetic and phenotypic relationships. Animal. 9(7), 1091-1096.
[29] Zita, L., Ledvinka, Z. and Klesalová, L. (2013) The effect of the age of Japanese quails on certain egg quality traits and their relationships. Veterinarski Arhiv. 83(2), 223-232.
[30] Sharma, S. (1996) Applied multivariate techniques. John Wiley and Sons, Inc., New York, USA, 493p.
[31] Çankaya, S. (2005) Canonical correlation analysis and its application on animal science. PhD Thesis. Cukurova University Institute of Natural and Applied Sciences, Adana (in Turkish).
[32] Sarı, M., Saatci, M. and Tilki, M. (2010) Estimation of genetic parameters for live weights characteristics using REML procedures in Japanese quails (*Coturnix coturnix japonica*). Journal of the Faculty of Veterinary Medicine. 16(5), 729-733 (in Turkish).
[33] Sezer, M., Berberoglu, E. and Ulutas, Z. (2006) Genetic association between sexual maturity and weekly live-weights in laying-type Japanese quail. South African Journal of Animal Science. 36(2), 142-148.
[34] Resende, R.O., Martins, E.N., Georg, P.C., Paiva, E., Conti, A.C.M., Santos, A.I., Sakaguti, E.S. and Murakami, A.E. (2005) Variance components for body weight in Japanese quails *(Coturnix japonica)*. Brazilian Journal of Poultry Science. 7(1), 23-25.

Received: **10.10.2018**
Accepted: **18.02.2019**

CORRESPONDING AUTHOR

Abdullah Nuri Ozsoy
Isparta University of Applied Sciences,
Faculty of Agricultural Sciences and Technologies,
Department of Animal Sciences,
32260, Isparta – Turkey

e-mail: abdullahozsoy@yahoo.com

© by PSP Volume 28 – No. 4/2019 pages 2589-2598 Fresenius Environmental Bulletin

ESTIMATING SURFACE SOIL LOSSES IN THE MOUNTAINOUS SEMI-ARID WATERSHED USING RUSLE AND GEOSPATIAL TECHNOLOGIES

Mehmet Yavuz*, Mustafa Tufekcioglu

Faculty of Forestry, Department of Forest Engineering, Artvin Coruh University, Artvin, 08100, Turkey

ABSTRACT

Integrating Revised Universal Soil Loss Equation (RUSLE) model and geospatial technologies to estimate surface soil erosion losses has gained popularity among the researchers across the world. Yet, assessing the soil erosion risk for arid and semi-arid continental mountainous watersheds requires more challenges to cope with. The purpose of this study is to assess potential surface soil erosion risk areas for Uzundere sub-watershed in Erzurum, Turkey using RUSLE model and 50 cm pan-sharpened WorldView-2 imagery within GIS and remote sensing framework. The sub-factors of RUSLE were estimated using meteorological data for rainfall erosivity (R-factor), 5-m DEM for slope length and steepness (LS-factor), NDVI for land cover and crop management (C-factor), and soil samples collected in 35 sampling plots (20x20 m) for soil erodibility (K-factor). It was found that 25.38 tons of soil per hectare was washed away from the Uzundere sub-watershed each year. It was also categorized that of the total study area 44.5% was under very low (0-5 t ha^{-1} yr^{-1}), 10.3% low (5-10), 13.6% moderate (10-20), 17.2% high (20-50), and 14.5% very high (> 50) risk category. It can be concluded that despite the low average annual rainfall (585 mm yr^{-1}), a very steep topography and high slope length with a few vegetation cover were the main contributors of the high surface soil losses from the study area.

KEYWORDS:
Sheet and rill erosion, RUSLE and GIS, WorldView-2

INTRODUCTION

One of the most crucial environmental issues in the world is soil erosion that adversely affects the natural resources, agricultural productions, biodiversity, and many other ecosystem services through topsoil loss or by reducing soil fertility [1]. High amounts of sedimentation generated by the surface soil erosion generally reduce the quality of water resources and associated aquatic life by increasing the activity of the toxic algal blooms [2]. These environmental changes may play significant role on the integrity of the landscape ecology, and prevent the socioeconomic and agricultural development in many countries over the long term [3]. One of the main driving factors for these environmental changes is alteration of natural land-uses to agricultural practices such as land cultivation in steep areas, improper soil tillage, and excessive grazing over the last century. Extensive agricultural practices, for instance, have been performed by ancient human settler in Mesopotamia and Anatolia for centuries. As a result, 80% of the Turkey's fertile agriculture areas are exposed to severe erosion today [4]. According to the report by the Turkey's National Action Program for Combating Desertification, about one billion tons of soil is washed away from terrestrial areas to rivers and seas each year [5]. Particularly fragile ecosystems such as arid and semi-arid areas, mountain passes, and transition zones are more susceptible to erosion processes due to high climatic heterogeneity, harsh and rugged topography, and loose geologic formation [6, 7].

Coruh River basin as being the particular one (21100 km^2), located in the transition zone between Eastern Black Sea and Northeastern Anatolia, is one of the most erosion-prone regions in Turkey. Average 5.8 million m^3 of soil is transported from the basin to Black Sea in each year via water-induced erosion annually. In addition to surface soil loss by the water runoff in a basin, natural disasters such as flood, landslide, and avalanche that are also contributing vast amount of soils into the river system during winter time [8]. Coruh River, 426 km long and average annual flow of 6.3 billion m^3 yr^{-1}, as the fastest flowing river in Turkey has also important hydropower potential that providing a contribution of 3.67% to total runoff of Turkey [9, 10, 11]. In order to use this high hydropower potential, 16 dams and 162 regulators were planned along the river and its tributaries. Muratlı, Borçka, Deriner, Artvin, Arkun, and Gullubag dams and hydropower plants have completed and started producing electricity, but a few are still in construction progress as of 2018. These dams and regulators will produce

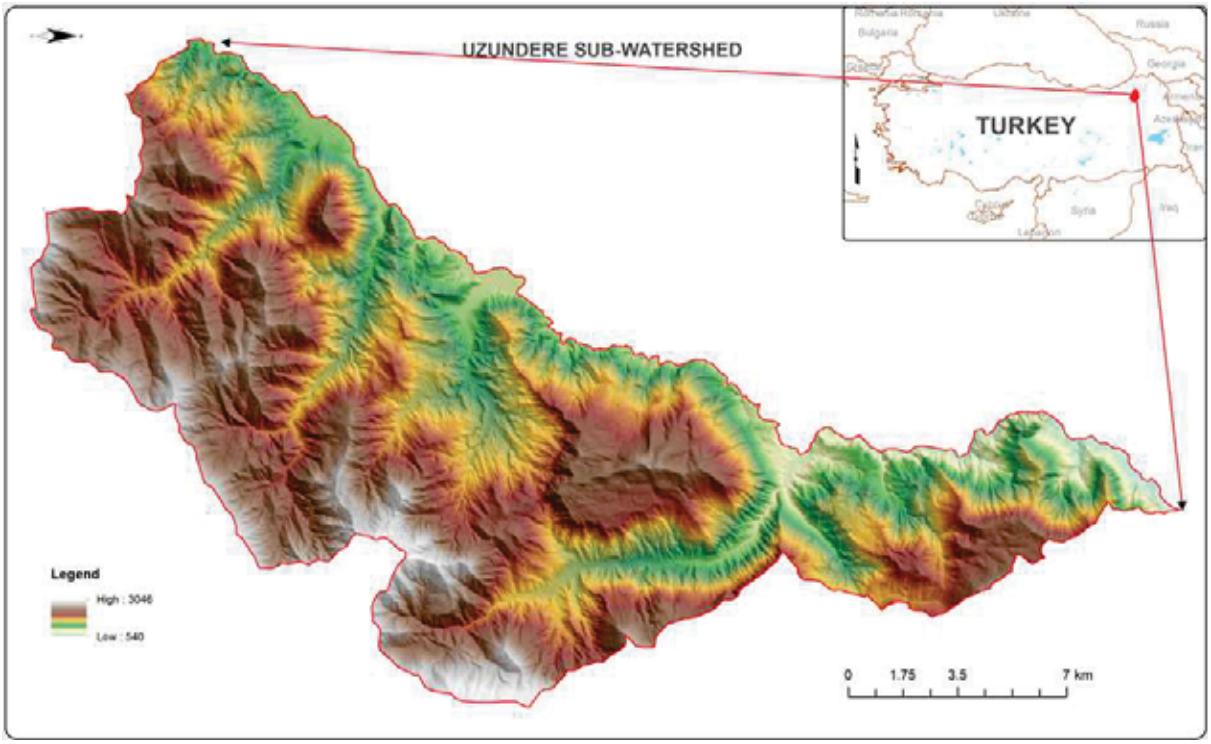

FIGURE 1
Location of Uzundere sub-watershed in Erzurum, Turkey.

9.56% of Turkey's total hydropower energy of 163 billion KWh as of 2015. Due to the ongoing intensive erosion process in the basin, there is severe risk of quick deposition into the dam reservoirs. Indeed, soil and other deposited material fill up the reservoirs restrict the economic lifespan of these dams.

In order to extent lifespan of these dams and to improve livelihood of the villagers, the Coruh River Watershed Rehabilitation Project has been initiated by the Ministry of Forestry and Water Affairs with the collaboration of Japan International Cooperation Agency (JICA) in 2012. The purpose of the seven-year program is not only for protecting top soil and water resources, but also for taking actions to prevent natural disasters such as avalanches, landslides, flooding and most importantly enhancing the welfare of local population affected by land degradation and dam constructions in the basin. The project, at the first stage, focuses 12 pilot sub-watersheds including Uzundere sub-watershed that is considered to have the roughest terrain and to be the most sparsely vegetated one in the region.

Accurate prediction of surface (sheet and rill) soil loss by a spatial modelling within Uzundere sub-watersheds is crucial due to selecting suitable location for the appropriate erosion control practices. Although many studies have been carried out to predict surface soil losses using Universal Soil Loss Equation (USLE) within Geographic Information System (GIS) and Remote Sensing (RS) framework in Turkey, most of them used coarse cartographic materials or satellite images with low spatial resolution [4, 7, 12]. Among the others the most commonly used model for the surface soil erosion is the Revised Universal Soil Loss Equation (RUSLE ver. 2.0) [13], due to its practical application and modest data requirements [14, 15]. RUSLE can be used to estimate soil losses for each alternative management case along with a topography, soil type and precipitation data. Moreover, it can easily be combined with GIS, RS and geostatistics techniques [16, 17]. Thus, advanced analysis of individual erosion factors such as rainfall, soil type, slope, vegetation cover and erosion control practices can be successfully performed by dividing the area into small cells [18]. In this way, soil loss in a given area can be estimated and soil loss maps with erosion risk categorization can be produced.

The main objective of this study is to estimate potential surface soil losses of the Uzundere sub-watershed within Coruh River basin in Erzurum, Turkey with the spatial assessment of the high erosion risk areas using RUSLE methodology and a 50 cm pan-sharpened WorldView-2 imagery.

MATERIALS AND METHODS

Study area. Uzundere sub-watershed is the study area within the Coruh watershed located in Erzurum Province, Turkey. It stretches from north latitudes 40°26'36" to 40°46'44" and east longitudes of 41°30'46" to 41°46'29" and covers an area of 31114 ha (Fig. 1). The region has mountainous terrain that ranges from 540 m to 3046 m with a mean elevation of 1678 m above the mean sea level and very steep

slopes that range from 0% to 578% (mean slope: 58%). The climate is continental (semi-arid) climate with 8.3 °C average temperature [19]. Average annual precipitation is about 537 mm per year. Almost 40% of the area is occupied by grassland followed by degraded (37%) and productive (18%) forest and agricultural land use (5%). Dominant tree species of the productive forests is scots pine *(Pinus sylvestris* L.*).* The degraded forest species include juniper *(Juniperus sp.)*, sumac *(Rhus coriaria)* and other bushy vegetation. The dominant bedrock type is limestone [20]. Soil type in the forested areas of the region is brown forest soil, generally shallow and has a texture of sandy loam which is well drained with moderate permeability. Therefore, productive vegetation cover with greater than 10% crown closure presents a very small proportion in the area.

Datasets and image preprocessing. The digital forest inventory maps used for estimating vegetation cover in this study were provided by the Turkish General Directorate of Forestry. The 5-m Digital Elevation Model (DEM) data, used for estimating Slope Length and Steepness (LS) Factor, obtained from the Turkish Mapping Agency (General Command of Mapping). WorldView-2 satellite data at a spatial resolution of 50 cm (pan-sharpened) acquired in June 2011 were used in this study for calculating Normalized Difference Vegetation Index (NDVI) values and estimating C-factor values of Uzundere sub-watershed. The geometrical adjustments and topographical corrections were applied to the WorldView-2 satellite imagery and digital aerial imagery in ERDAS Imagine software using the 5-m DEM data.

Model structure. GIS based and remote sensing supported RUSLE method was used for this study to estimate annual soil loss for each pixel in Uzundere sub-watershed. The RUSLE equation is expressed as [13];

$$A = R \; x \; K \; x \; LS \; x \; C \; x \; P \quad (1)$$

where A is the mean soil loss (t ha^{-1} yr^{-1}), R is the rainfall-runoff erosivity factor (MJ mm ha^{-1} h^{-1} yr^{-1}), K is the soil erodibility factor (t.h MJ^{-1} mm^{-1}), LS is the slope length-steepness factor (dimensionless), C is the land cover and crop management factor (dimensionless) and P is the support practices factor (dimensionless). The following sub-sections describe the generation of the RUSLE factors R, K, LS, C and P maps.

Rainfall-runoff erosivity (R) factor. R-factor is the potential erosivity effect of a specific rainfall's kinetic energy and its intensity on soil. The available monthly and yearly rainfall data of 42 years (1970-2011) collected from Tortum meteorology station that is located in the study area at 1572 m elevation were used for calculating R-factor using the following widely used equation as expressed in [21]:

$$R = \sum_{k=1}^{12} 1.735 \text{ x } 10^{(1.5\, log10(Pi^2/P) - 0.08188)} \quad (2)$$

where P_i (mm) is the average monthly precipitation and P (mm) is the average annual total precipitation. The average annual total precipitation for the Tortum Weather Station was 476 mm yr^{-1}. This calculated R-factor value is only valid for the location of the Tortum Weather Station located at the elevation of 1572 m. Because of that, the new R-factor values need to be calculated for the entire sub-watershed. Eq.3 by [22] was used to calculate these new R-factor values and then were interpolated to all sub-watershed using a spatial model in the Spatial Analyst extension tool in ArcGIS 10.2.

$$R_{new}=R_{station}(P_{new}/P_{station})^{1,75} \quad (3)$$

where R_{new} is the new calculated R-factor value for given cell, $R_{station}$ is the calculated mean R-factor value of meteorology station, P_{new} is the calculated new annual precipitation value for given cell and $P_{station}$ is the recorded annual precipitation value of meteorology station.

Soil erodibility (K) factor. K-factor is the resistance of the soil against runoff and degradation depending upon its natural attributes. It is calculated with 4 parameters; texture, structure, organic matter (OM), and permeability. For this purpose, 35 soil core samples were randomly taken in the depth of 0-15 cm from the study area [23]. The soil core samples from 0-15 cm depth were used to calculate texture, structure, organic matter (OM), and permeability of the sampling plots. The percent of OM content was determined by using [24]'s wet burning method. The percent sand, silt and clay rates in these samples were analyzed at the soil laboratory using [25]'s hydrometer method. Afterwards the K-factor was calculated using [26] and [27];

$$K = 0.0293\left(0.65 - D_G + 0.24{D_G}^2\right)exp\left[-0.0021\left(\frac{OM}{f_{clay}}\right) - 0.00037\left(\frac{OM}{f_{clay}}\right)^2 - 4.02f_{clay} + 1.72{f_{clay}}^2\right] \quad (4)$$

$$D_G = -3.5f_{clay} - 2.0f_{silt} - 0.5f_{sand} \quad (5)$$

where OM is the organic matter content in percent, f_{clay} is the clay, f_{silt} is the silt and f_{sand} is the sand content in friction. Then, large soil group maps for the study area obtained from the General Directorate of Rural Services was updated according to the lab results of these soil samples.

Slope length and steepness (LS) factor. According to the [13]; the topography contributes to soil erosion with two factors: slope length (L) and slope steepness (S). The LS-factor is obtained by multiplying the L-factor and S-factor. The amount of

soil loss increases when the slope steepness and length increases [21]. Combined LS factor was calculated for the study area by using 5 m resolution Digital Elevation Model (DEM) with the following equation [28];

$$LS = [(Flow_accumulation \times cell_size) / 22.13]^{0.4} \times [sinslope / 0.0896]^{1.3} \quad (6)$$

where *LS* is the combined slope length and steepness factor, *flow accumulation* is the accumulated upslope contributing area for a given cell, *cell size* is the size of a pixel (for this study 50 cm), and *sin slope* is the slope degree value in sin and *0.0896* is the conversion factor. With this equation, the LS-factor map was produced in ArcGIS 10.2 software using Spatial Analyst Tool.

Land cover and crop management (C) factor. C-factor represents the effects of land uses and land cover types on soil loss in RUSLE equation and plays an effective protection role against erosion. The C-factor calculation is based on the soil-loss-ratio (SLR) and the only factor that can be changed over time but it is difficult to identify these changes with the SLR method. Therefore, many researchers have developed C-factor estimating methods using Normalized Difference Vegetation Index (NDVI) [29-31]. These methods use different regression models to correlate between NDVI values of imagery and C-factor values measured in the field. The details of these methods can be seen in a recent study by Vatandaslar and Yavuz [32]. Based on these, NDVI map of Uzundere sub-watershed was produced using a 50-cm-resolution WorldView-2 satellite image acquired in July 2011. Finally, the following regression model was used for mapping C-factor values pixel-by-pixel;

$$C\text{-}Factor = 1/(1.0525 + 1.6760 \times 348004079118.509^{NDVI}) \quad (7)$$

Support practices (P) factor. P-factor represents the erosion rate with a specific conservation practice (terraces, vegetation cover, etc.) to the corresponding erosion rate with up and down slope tillage [13]. Because there was no conservation practices in the study area, P-factor values were assigned to 1 for all pixels.

Sediment Delivery Ratio (SDR) and Sediment Yield (SY). Sediment Yield was calculated using the Sediment Delivery Ratio equation which was adopted from Boyce [33] as shown in Eq. 8 and 9 below:

$$SDR = 0.5656 \times A^{-0.11} \quad (8)$$

where A is the area of study site in km^2. Using the SDR value from Equation (8), SY value was calculated using the following formula by [21]:

$$SY = SDR \times SE \quad (9)$$

where, SY=sediment yield (ton ha^{-1} yr^{-1}), SDR= sediment delivery ratio, and SE= annual potential soil loss (A) (ton ha^{-1} yr^{-1}). Each pixel of annual potential soil loss map was multiplied with SDR in order to obtain the SY map of Uzundere sub-watershed.

RESULTS AND DISCUSSION

Rainfall and runoff erosivity (R) factor. The R-factor values for the years between 1970 and 2011 in the study area were found to be in the range of 0.00 - 1312 MJ.mm ha^{-1} hr^{-1} yr^{-1} with an average value of 359.76 MJ.mm ha^{-1} hr^{-1} yr^{-1} (Table 1). Generally, north and southeast sections of the sub-watershed had the higher R-factor values than those of the other sections (Fig. 2A). The ranges of high R-factors values at these specific areas of the watershed were due to great increase in elevation (Fig. 1). However, despite low precipitation and low average R-factor value from the entire sub-watershed, field observations showed that soil erosion by the rain effects in flush occurred after every heavy storm can substantially increase the amount of surface soil losses. As a result, the stream and gully beds were filled of sediments and in some cases opened a new scour for bank erosion potential. Similar conclusions reached by the other studies; Bayramin et al. [6] indicated that climatic characteristics of the semi-arid regions with extreme rainfall events and hardly succeeding vegetative season together with the high topographic inclination increased the potential risk of erosion. Study by Tufekcioglu [34] carried out in the neighboring Oltu sub-watershed within the Coruh River basin revealed that rill and interrill erosion were the dominant pathways of sediment transport that usually takes play during a single storm event in this semi-arid watershed.

TABLE 1
Descriptive statistics of RUSLE factors results for Uzundere sub-watershed in metric SI units.

Soil Erosion Factors	min	max	mean	st dev	var. of coef.
Rainfall Erosivity (R) (MJ.mm ha^{-1} hr^{-1} yr^{-1})	0.00	1312.12	359.76	241.52	0.67
Slope Length and Steepness (LS)	0.00	8290.90	16.23	24.39	1.50
Soil Erodibility (K) (ton.hr MJ^{-1} mm^{-1})	0.02	0.26	0.13	0.02	0.17
Land Cover and Crop Management (C)	0.00	1.00	0.35	0.28	0.78
Conservation Practices (P)	1.00	1.00	1.00	-	0.00
Annual Soil Loss (A) (ton ha^{-1} yr^{-1})	0.00	4442.84	25.38	56.08	2.21

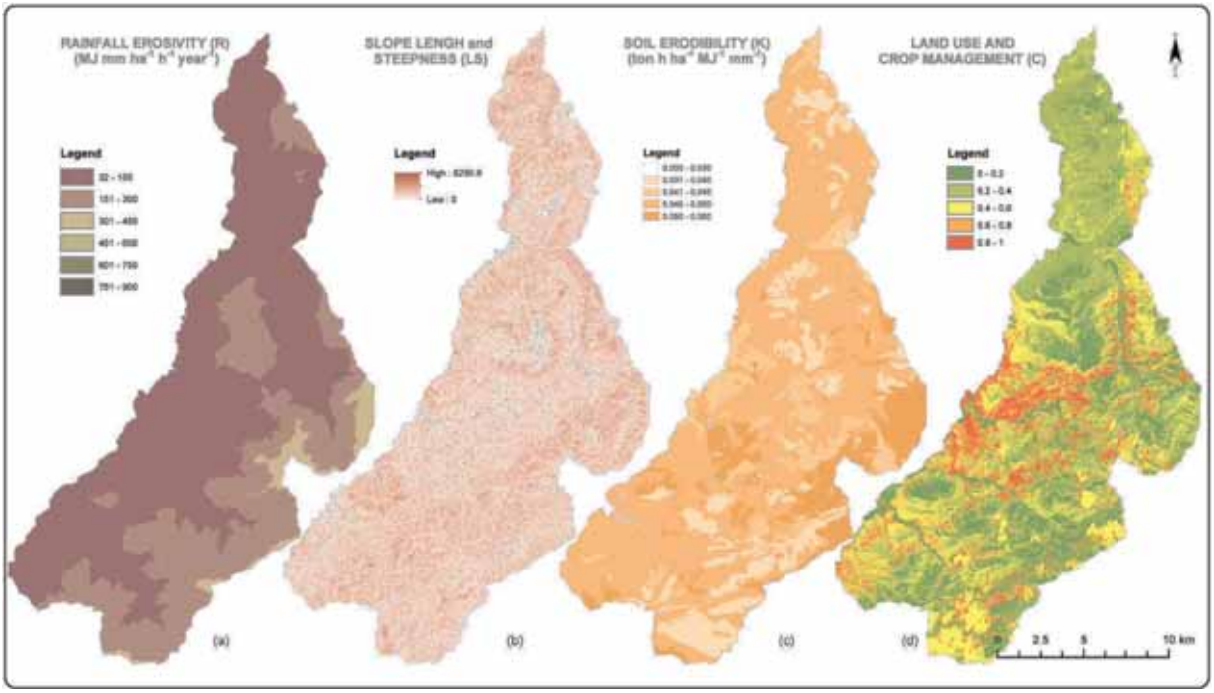

FIGURE 2
(A) Rainfall erosivity; (B) slope length and steepness; (C) soil erodibility; (D) cover and crop management factor maps of Uzundere sub-watershed.

Soil erodibility (K) factor. The descriptive statistics of the K-factor obtained from laboratory analysis for the study area were shown in Table 1. Spatial distribution of the K-factor values within the sub-watershed showed rather homogenous pattern (Fig. 2C). The average K value was 0.13 ton h MJ^{-1} mm^{-1} with a standard deviation of 0.02 ton h MJ^{-1} mm^{-1} (Table 1, Fig. 2C). Most of the study area (90.52%) was under the easily erodible soil type (0.21-0.40 ton h MJ^{-1} mm^{-1}). The light colored volcanic turf spots, sparsely distributed through the area (1.6%) were the main contributor to high erosion potential. K-factor values in these susceptible areas were in the range of 0.4 and 0.6 ton h MJ^{-1} mm^{-1}.

Slope length and steepness (LS) factor. The degree of slopes between 30 and 40 is being most important gradient for soil erosion along with increasing elevation [35]. The DEM data showed that elevation ranges between 540 and 3046 m in the sub-watershed. These values with the tough topography formed the high slope rates especially in the north and east parts of the area. The slope steepness ranges from 0% on the flat surfaces near the streams to 578% on the reels of very sharp terrain throughout the study area. The average slope length and steepness (LS) factor was 16.23 (dimensionless) with a standard deviation of 24.39 (Table 1), and its spatial distribution was given in Fig. 2B. Field observations and the satellite imagery used in this study showed that such steepness caused many rill and gully formation after the event-base storm throughout the study area. This would indicate that significant portion of the soil loss from the area was generated via the rill-interrill and gully erosion.

Land cover and crop management (C) factor. The NDVI image indicated lack of the vegetation cover for the high slope and hill top areas and only riparian areas in the floodplain were vegetated with agricultural crops where irrigation was the main problem for the farmers and landowners. The results by the C-factor map showed an average C-factor value of 0.35 (dimensionless) with a standard deviation of 0.28 for the entire study area. The highest C-factor values were in the central west parts of the study area generally characterized by bare soil surface (Fig 2D).

Sediment delivery ratio (SDR) and sediment yield. According to the Eq.8, sediment delivery ratio was found to be 0.301 for the Uzundere sub-watershed. Each pixel of annual potential soil loss map was multiplied with SDR in order to obtain the sediment yield (soil loss) map (Fig. 3).

Estimated soil loss and risk assessment. The average annual surface soil loss that was estimated from the product of rainfall erosivity (R), slope length and steepness (LS), cover and crop management (C) and soil erodibility (K) factors for the entire Uzundere sub-watersheds was 25.38 ton ha^{-1} yr^{-1} (Table 1). According to the soil loss rate standard used by other researchers [21, 33], estimated soil loss in this study was divided into five different risk categories including very low, low, moderate, high and

very high (Table 2). Using this categorization, nearly half of the study area dominated by the low and very low erosion potential (57.7%) while the combined high and very high erosion risks areas covered more than one-third of the study area (37.2%). This would show that Uzundere sub-watershed is one of the most erosion-prone one within the Coruh River Basin. Obviously these results are attributed to the insufficient vegetative cover on the very tough terrain with an average slope of 58%, despite the low annual rainfall but the contribution of the very heavy downpours in the summer, and a highly erodible volcanic turf bed rock (Fig. 4). The annual potential soil loss and sediment yield map can be seen in Fig. 3. Most of the high and very high potential soil loss areas were found in east and southeast of the sub-watershed where high sloped lands coincide with areas of bare soil surface. The results showed that an average soil loss from the Uzundere sub-watershed was four times higher than that of Turkey's average soil loss rate (approximately 6 t ha^{-1} yr^{-1}) [36] and three times higher than that of Italy's average soil loss (8.46 t ha^{-1} yr^{-1}) which was the highest amongst European countries [37].

This study is the first one to estimates potential surface soil loss from the Uzundere sub-watershed characterized with a hilly terrain with less vegetative cover and semi-arid condition with a few storm events during a year. The results from the study were compared with the results from the other neighboring sub-watersheds of Coruh River Basin and with some other basins showing similar characteristics with Uzundere sub-watersheds. Turkish General Directorate of Combating Desertification and Erosion (CDE) reported 26.02 t ha^{-1} yr^{-1} potential average soil erosion amount for the entire Coruh watershed [38, 39]. This value produced an average of about 4.95 t ha^{-1} yr^{-1} sediment yield (SY) when multiplied with SDR of the 20000 km^2 watershed. Another report by the State Hydraulic Works (SHW) and General Directorate of Renewable Energy (RE) [39], eight observation points using sediment stations across the Coruh River produced an average of 3.79 t ha^{-1} yr^{-1} sediment yield. The computed mean surface soil erosion loss rate (25.38 t ha^{-1} yr^{-1}) for the study area was much higher than the mean soil erosion rates for the entire Coruh River watershed. The main reasons for the significant soil losses from the Uzundere sub-watershed were sparsely distributed least vegetation cover and toughest terrain with many rills and gullies. Primary reason of such a poor vegetative cover was directly related to low rainfall amount throughout the year and lack of soil formation due greater rates of erosion in this particular watershed.

Study by Perovic et al. [40] was conducted in a hilly mountainous terrain of south-eastern part of Serbia (River Nisava basin) showed similar characteristics with Uzundere sub-watershed in terms of topography and climatology. The River Nisava basin study noted a very likely average soil loss estimate (27 t ha^{-1} yr^{-1}) with this study. Study with similar watershed characteristics (mountainous and

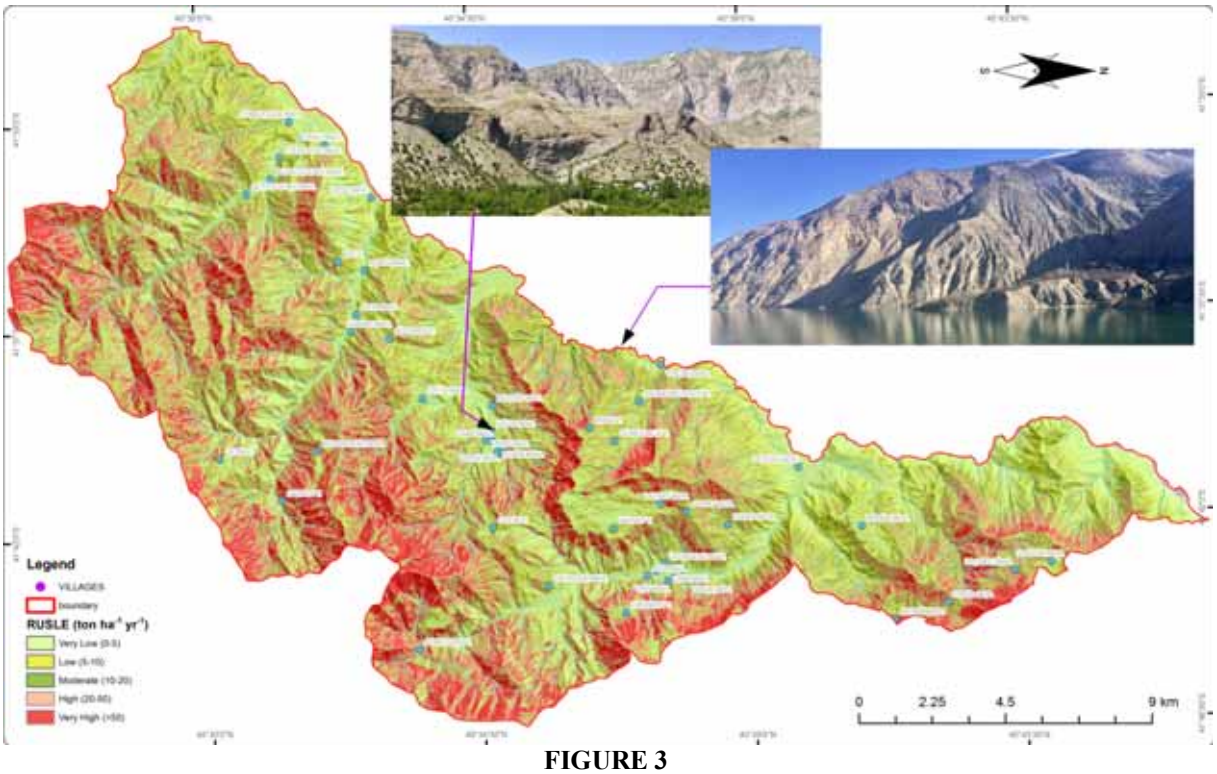

FIGURE 3
Potential surface soil erosion (t $ha^{-1}yr^{-1}$) risk categories for the Uzundere sub-watershed.

TABLE 2
Predefined surface soil erosion risks categories for the Uzundere sub-watershed.

Soil Erosion Risk Categories	Soil Loss (ton ha^{-1} $year^{-1}$)	Area Covered (%)
Very Low	0-5	44.45
Low	5-10	10.25
Moderate	10-20	13.59
High	20-50	17.22
Very High	>50	14.49

FIGURE4
(A) A general view of the study area, (B) wire-cage sills erosion control practices and (C) eroded surfaces and rough terrain near Kirazli Village.

semi-arid) by Arekhi et al. [41] conducted at the Gham Gardalan watershed in the southeast of Ilam Province in the western Iran found average soil loss of 19 t ha^{-1} yr^{-1}. Another study by Irvem et al. [42] conducted at the Seyhan River Basin in southern Turkey found soil loss rate of 16.4 t ha^{-1} yr^{-1}. Climatic condition in the Seyhan River Basin characterized as semi-arid with 600 mm precipitation. The upper part of the basin defined as mountainous while the lower basin is in flat areas. Higher rate of soil loss as 24 t ha^{-1} yr^{-1} was also found at the River Lebna Watershed in the northeast of Tunisia in the Cap Bon region. In the region the elevation ranges from 631 m at the highest to 100 m at the central lowest zone and the average rainfall is around 450 mm [43].

CONCLUSIONS

Rill and interrill erosion are the most important pathways of soil movement and associated land degradation. In this study, the rate of surface soil erosion was estimated using the most known RUSLE methodology coupled with GIS and remote sensing technologies. Results indicated that the rate of the soil erosion in the study area is extremely high. The computed potential annual surface soil loss (25.38 t ha^{-1} yr^{-1}) for the study area was much higher than the mean soil loss for the entire Coruh River Watershed (3.79 ton ha^{-1} yr^{-1}). More than one-third (31.71 %) of the Uzundere sub-watershed is under high (20-50 t ha^{-1} yr^{-1}) and very high (>50 t ha^{-1} yr^{-1}) erosion risk categories. Areas of high erosion potential were located at high elevation belt with mostly southern aspects in the east part of the study area. These results were attributed to the very high slopes (mean: 58%, max: 578%), tough terrain with lesser vegetative cover and a volcanic turf bed rock that can produce very high amount of erosive material during the down-poured storm events.

We recommend that the agricultural and grazing activities on the high elevation and upper part of the study areas are strongly reduced or controlled. Erosion control practices planned by the Turkish General Directorate of Combating Desertification and Erosion should focus on the high and very high erosion risk areas of the watershed to reduce risk of potential soil losses. The implementation of wire-cage, dry-stone sills on the stream and gully channels are highly recommended to reduce soil movement. Finally, it is important to state that use of GIS and RS techniques in very mountainous areas were a low cost and easy to implement tools for modelling surface soil erosion and finding high soil loss potential areas spatially.

ACKNOWLEDGEMENTS

This research is funded by Japan International Cooperation Agency (JICA) and General Directorate of Turkish Forest Services (GDF) through the Coruh River Watershed Rehabilitation Project (2012-2019). We appreciated for their supports in conducting the study. For their input, we also would like thank to Dr. Aydin Tufekcioglu, Dr. Musa Dinc, Dr. Ahmet Duman, Can Vatandaslar and Canan H. Acikgoz from Artvin Coruh University and Deniz Akdeniz from Piramid Photogrammetry Inc.

REFERENCES

[1] Panagos, P., Borrelli, P., Meusburger, K. (2015a) A New European Slope Length and Steepness Factor (LS-Factor) for Modeling Soil Erosion by Water. Geosciences. 5, 117.

[2] Carpenter, S.R., Caraco, N.F., Correll, D.L., Howarth, R.W., Sharpley, A.N., Smith, V.H. (1998) Nonpoint pollution of surface waters with phosphorus and nitrogen. Ecological Applications. 8, 559-568.

[3] Wang, L., Huang, J., Du, Y., Hu, Y., Han, P. (2013) Dynamic Assessment of Soil Erosion Risk Using Landsat TM and HJ Satellite Data in Danjiangkou Reservoir Area, China. Remote Sensing. 5, 3826.

[4] Ozsahin, E., Uygur, V. (2014) The effects of land use and land cover changes (LULCC) in Kuseyr plateau of Turkey on erosion. Turkish Journal of Agriculture and Forestry. 38, 478-487.

[5] Ministry of Environment and Forestry (2006) Desertification. In: Turkey's national action program on combating desertification (in Turkish). Ankara: Ministry of Environment and Forestry Press.

[6] Bayramin, İ., Erpul, G., Erdoğan, H.E. (2006) Use of CORINE methodology to assess soil erosion risk in the semi-arid area of Beypazari, Ankara. Turkish Journal of Agriculture and Forestry. 30, 81-100.

[7] Saygin, S.D., Ozcan, A.U., Basaran, M., Timur, O.B., Dolarslan, M., Yilman, F.E., Erpul, G. (2014) The combined RUSLE/SDR approach integrated with GIS and geostatistics to estimate annual sediment flux rates in the semi-arid catchment, Turkey. Environmental Earth Sciences. 71, 1605-1618.

[8] Stanchi, S., Freppaz, M., Ceaglio, E., Maggioni, M., Meusburger, K., Alewell, C., Zanini, E. (2014) Soil erosion in an avalanche release site (Valle d'Aosta: Italy): towards a winter factor for RUSLE in the Alps. Natural Hazards and Earth System Sciences. 14, 1761-1771.

[9] Berkun, M. (2010) Hydroelectric potential and environmental effects of multidam hydropower projects in Turkey. Energy for Sustainable Development. 14(4), 320-329.

[10] Kibaroglu, A., Klaphake, A., Kramer, A., Scheumann, W., Carius, A. (2005) Cooperation on Turkey's transboundary waters. The German Federal Ministry for Environment, Nature Conservation and Nuclear Safety. Berlin.

[11] Sucu, S., Dinç, T. (2008) Çoruh River Basin Projects. In: TMMOB 2. Congress of Water Policies, Ankara, 33-38 (in Turkish).

[12] Karaburun, A. (2009) Estimating potential erosion risks in Corlu using the GIS-based RUSLE method. Fresen. Environ. Bull. 18, 1692-1700.

[13] Renard, K.G., Foster, G.R., Weesies, G.A., McCool, D.K., Yoder, D.C. (1997) Predicting soil erosion by water—a guide to conservation planning with the Revised Universal Soil Loss Equation (RUSLE). In: Agricultural Handbook Number 703. Washington, D.C.: United States Government Printing Office.

[14] Pan, J.H., Wen, Y. (2014) Estimation of soil erosion using RUSLE in Caijiamiao watershed, China. Natural Hazards. 71, 2187-2205.

[15] Zhang, Y., Degroote, J., Wolter, C., Sugumaran, R. (2009) Integration of Modified Universal Soil Loss Equation (MUSLE) into a GIS Framework to Assess Soil Erosion Risk. Land Degradation and Development. 20, 84-91.

[16] Beskow, S., Mello, C.R., Norton, L.D., Curi, N., Viola, M.R., Avanzi, J.C. (2009) Soil erosion prediction in the Grande River Basin, Brazil using distributed modeling. Catena. 79, 49-59.

[17] Kouli, M., Soupios, P., Vallianatos, F. (2009) Soil erosion prediction using the Revised Universal Soil Loss Equation (RUSLE) in a GIS framework, Chania, Northwestern Crete, Greece. Environmental Geology. 57, 483-497.

[18] Bhattarai, R., Dutta, D. (2007) Estimation of soil erosion and sediment yield using GIS at catchment scale. Water Resources Management. 21, 1635-1647.

[19] State Meteorological Service (2002) Meteorological data for meteorological stations. Ankara: Ministry of Food, Agriculture and Animal Husbandry

[20] Atalay, I., Tetik, M., Yilmaz, O. (1985) Ecosystems of Northeastern Anatolia. Ankara: Forestry Research Institute Press. 141-154. (in Turkish).

[21] Wischmeier, W.H., Smith, D.D. (1978) Predicting Rainfall Erosion Losses - A Guide to Conservation Planning. In: Agriculture Handbook. Washington D.C.: US Department of Agriculture Science and Education Administration.

[22] Toy, T.J., Foster, G.R. (1998) Guidelines for the revised universal soil loss equation (RUSLE) version 1.06 on mined lands, construction sites and reclaimed lands. Denver: The Office of Technology Transfer Western Regional Coordinating Center Office of Surface Mining.

[23] Duman, A. (2017) Determination and modelling of soil properties of degreaded forest and grassland areas in some micro catchments of Artvin, Erzurum and Bayburt using satellite images. Dissertation: Artvin Coruh University Graduate School of Natural and Applied Sciences, Artvin (in Turkish).

[24] Walkley, A., Blake, I.A. (1934) An examination of the Degtjareff method for the determining soil organic matter and a proposed modification of the chromic acid titration method. Soil Science. 37, 29-38.

[25] Bouyoucos, G.J. (1962) Hydrometer method improved for making particle size analyses of soils. Agronomy Journal. 54, 464-465.

[26] Torri, D., Poesen, J., Borselli, L. (1997) Predictability and uncertainty of the soil erodibility factor using a global dataset. Catena. 31(1-2), 1-22.

[27] Torri, D., Poesen, J., Borselli, L. (2002) Predictability and uncertainty of the soil erodibility factor using a global dataset. Catena. 46(4), 309-310.

[28] Moore, I.D., Burch, G.J. (1986) Physical Basis of the Length-Slope Factor in the Universal Soil Loss Equation. Soil Science Society of America Journal. 50, 1294-1298.

[29] De Jong, S.M. (1994) Applications of reflective remote sensing for land degradation studies in a Mediterranean environment. Nederlandse Geografische Studies. 177.

[30] Gundogan, R., Akay, A.E., Okatan, A., Yuksel, A., Oguzkan, E.A. (2010) Land suitability evaluatin for reducing soil losses in Kahraman-maras, Turkey. Fresen. Environ. Bull. 19, 2678-2689.

[31] Demirci, A., Karaburun, A. (2012) Estimation of soil erosion using RUSLE in a GIS framework: a case study in the Buyukcekmece Lake watershed, northwest Turkey. Environmental Earth Sciences. 66, 903-913.

[32] Vatandaslar, C., Yavuz, M. (2017) Modeling cover management factor of RUSLE using very high-resolution satellite imagery in a semiarid watershed. Environmental Earth Sciences. 76, 65.

[33] Boyce, R.C. (1975) Sediment routing with sediment delivery ratios. In: U.D.o. Agriculture. US Department of Agriculture Publication, USA, 61-65.

[34] Tufekcioglu, M. (2018) Gully and streambank erosion and the effectiveness of control measures in a semi-arid watershed. Fresen. Environ. Bull. 27, 8233-8243.

[35] Zhou, Q.W., Yang, S.T., Cai, M.Y., Lu, Y., Zhao, H.G., Luo, Y. (2014) Soil erosion and its relationship with topographical factors in a mountainous watershed in the upper Mekong River in Yunnan Province, China. Fresen. Environ. Bull. 23, 215-222.

[36] Cakal, M.A., Özlü, A., Birhan, H., Bakır, H., Gültepe, N.Z., Ayday, C. (1997) Preparation of the erosion risk map of Tortum Lake Watershed using remote sensing and geographical information system. In: Proceedings of Turkey's Erosion Problem and the Place of Adana Congress, Adana, Turkey (in Turkish).

[37] Panagos, P., Borrelli, P., Poesen, J., Ballabio, C., Lugato, E., Meusburger, K., Montanarella, L., Alewell, C. (2015b) The new assessment of soil loss by water erosion in Europe. Environmental Science and Policy. 54, 438-447.

[38] Ministry of Forest and Water Affairs (2013) Watershed erosion. Ankara: Ministry of Forest and Water Affairs Press (in Turkish).
[39] General Directorate of Combating Desertification and Erosion (2018) DEMIS Turkey water erosion statistics, Technical Summary Report, Ankara, Turkey (in Turkish).
[40] Perovic, V., Zivotic, L., Kadovic, R., Dordevic, A., Jaramaz, D., Mrvic, V., Todorovic, M. (2013) Spatial modelling of soil erosion potential in a mountainous watershed of South-eastern Serbia. Environmental Earth Sciences. 68, 115-128.
[41] Arekhi, S., Bolourani, A.D., Shabani, A., Fathizad, H., Ahamdyasbchin, S. (2012) Mapping soil erosion and sediment yield susceptibility using RUSLE, remote sensing and GIS (Case study: Cham Gardalan Watershed, Iran). Advances in Environmental Biology. 6(1), 109-124.
[42] Irvem, A., Topaloglu, F., Uygur, V. (2007) Estimating spatial distribution of soil loss over Seyhan River Basin in Turkey. Journal of Hydrology. 336, 30-37.
[43] Gaubi, I., Chaabani, A., Ben Mammou, A., Hamza, M.H. (2017) A GIS-based soil erosion prediction using the Revised Universal Soil Loss Equation (RUSLE) (Lebna watershed, Cap Bon, Tunisia). Natural Hazards. 86(1), 219-239.

Received: **21.10.2018**
Accepted: **20.02.2019**

CORRESPONDING AUTHOR

Mehmet Yavuz
Faculty of Forestry,
Department of Forest Engineering,
Artvin Coruh University,
Artvin, 08100 – Turkey

e-mail: myavuz32@gmail.com

© by PSP Volume 28 – No. 4/2019 pages 2599-2607 Fresenius Environmental Bulletin

ANALYSIS OF ACRYLAMIDE IN MEAT-BASED FOOD PRODUCTS BY USING L-CYSTEINE-CAPPED Mn-DOPED ZnS QUANTUM DOTS AS A ROOM TEMPERATURE PHOSPHORESCENT PROBE

Burak Demirhan[1,*], Buket Er Demirhan[1], Hayriye Eda Satana Kara[2]

[1]Department of Pharmaceutical Basic Sciences, Faculty of Pharmacy, Gazi University, Ankara, Turkey
[2]Department of Analytical Chemistry, Faculty of Pharmacy, Gazi University, Ankara, Turkey

ABSTRACT

Meat is a concentrated food source required for optimal human growth. Besides higher biological value proteins, meat has generally rich in micronutrients such as ferrous, selenium, zinc and vitamin B12. Despite its nutrition values and acceptable flavor, cooked meat could be a source of carcinogenic compounds depending on cooking. Acrylamide is produced during thermal processing at 120 °C or higher temperatures by Maillard reaction. The purpose of the study is to determine the content of acrylamide in meat-based food products by using a room temperature phosphorescent quantum dots. Water-soluble L-cysteine capped Mn-doped ZnS quantum dots (QDs) were quenched efficiently by acrylamide. The developed method was applied successfully to the quantitative determination of acrylamide in meat products. Direct determination of acrylamide concentration has been done according to the changing of room temperature phosphorescence (RTP) intensity of QDs. The linearity of the method was achieved between 2-20 µg/mL and the limit of detection was 0.42 µg/mL. Acrylamide was determined in meat samples in the range of 24.6-71.3 µg/kg. According to the results, the developed method was sensitive, selective, fast, cheap, and not time-consuming, has low detection limit and was successfully used for determination of acrylamide in meat-based foodstuffs.

KEYWORDS:
Acrylamide, Meat analysis, Quantum dot, Room temperature phosphorescence.

INTRODUCTION

Meat, which known as a concentrated food source required for optimal growth and evolution of human, is a great source of important nutrients such as proteins, iron, zinc, vitamin A and B, and lipid [1]. Meat is classified as red meat, white meat, fish meat, and processed meat. Higher meat consumption, especially red meat, is widespread in many societies. Meat and meat-based products are usually cooked before eating. The cooking process destroys pathogenic or spoilage microorganism and improves digestion, taste, color, flavor, and texture of meat. Despite its nutrition values and acceptable flavor, cooked meat could be a source of carcinogenic compounds depending on the cooking process. Some carcinogenic compounds such as acrylamide (ACR), heterocyclic amines and polycyclic aromatic hydrocarbons are formed at a higher temperature during the cooking process [2]. Due to the relationship between the increase in the incidence of chronic diseases such as cancer and cardiovascular diseases, and food-borne risks, widespread researches have been carried out in foodstuffs [1]. In many research, the interaction between higher meat consumption and some cancer risk is expressed. Most of the research is epidemiological and therefore only information concerning exposure of the carcinogenic compounds related to the diet is ensured [2].

Harmful effects of toxic chemical contaminants such as ACR in foodstuffs create a major health problem in humans [3]. The presence of toxic chemical contaminants in foodstuffs has an important effect in terms of food safety which is important for human health [2]. ACR exists in many kinds of foods. Several cooking processes such as frying, grilling, and roasting are able to increase significantly the amount of ACR content. The interaction between amino acids especially free asparagine and reducing sugars such as glucose and fructose cause Maillard reaction which is responsible for the flavor and color of the cooked foods [3]. Maillard reaction products present several effects on a human; while melanoidins have health-promoting effects, ACR, furans, and advanced glycations end products have potentially harmful effects [4, 5]. ACR is produced during thermal processing at 120 ^{0}C or higher temperatures by Maillard reaction [6]. Most consumed foodstuffs like coffee, high in starch, potato products, and cereal products may contain large amounts of ACR [3, 7]. The vast majority of consumers may be in

contact with or consume an amount of ACR that cannot be ignored. On the other hand, the occurrence rate of ACR contact or ingestion is uncertain [8]. ACR is metabolized by the liver to glycidamide, which is a reactive genotoxic epoxide. According to the classical detoxification scheme, ACR and glycidamide are conjugated with glutathione and excreted in the urine as mercapturic acid [9]. Owing to the urinary excretion at first 24 hours is approximately 50%, and then 90% within 7 days, ACR metabolites may be evaluated as a biomarker for the exposure [10].

International Agency for Research on Cancer (IARC) labeled the ACR as a probably carcinogenic to human (Group 2A) [11, 12]. ACR exposure could cause neurotoxicity in human and animals, developmental reproductive toxicity, genotoxicity and carcinogenicity in rodents [11]. Occupational exposure of the ACR in humans have mainly resulted in neurotoxicity [13-15]. Exposure levels of ACR by occupational is higher than the diet exposure levels [14].

Rapid and sensitive detection of ACR in food is a major issue for food safety due to the toxicity of ACR [16]. Recently, several analytical methods such as enzyme-linked immunosorbent analysis (ELISA), high-performance liquid chromatography (HPLC), liquid chromatography with mass spectrometry-mass spectrometry (LC-MS-MS) and gas chromatography with mass spectrometry (GC-MS) are improved in order to determine the ACR [17-20].

The quantum dots (QDs), semiconductor nanoparticles, have a spherical shape and their diameters are in the between 2 to 10 nm. At such small sizes, chemical and optical behaviors are different from the bulk form because of their quantum confinement effect. Because of this, these particles have many advantages including a broad excitation range with sharp emission bands, high quantum yield, long phosphorescence lifetime, good photo and chemical stability. In addition, the emission wavelength is adjusted with the changing of diameter [21]. Because of the advantages of QDs, they have been widely used for the analyses of pharmaceuticals [22, 23], nucleic acids [24], food additives [25] and etc.

Room temperature phosphorescence (RTP) turn-off sensor for selective determination of ACR in a different type of meat samples was presented in this article. The mechanism of this system based on quenching of RTP signal of L-cysteine-capped Mn-doped ZnS QDs by adding of ACR. The developed method needs no detailed sample preparation steps, therefore, it is time consuming, economic, avoids the interference coming from chemicals, sensitive, and selective.

MATERIALS AND METHODS

Materials. $ZnSO_4$, $MnCl_2$, Na_2S, and L-cysteine and ACR were obtained from Merck (Darmstadt, Germany). For the preparation of the standard ACR stock solution, 5.0 mg ACR was accurately weighed and dissolved in deionized water in a 10.0 mL volumetric flask and then adjusted to volume with the same solution. The final concentration of the stock solution was 500 µg/mL, which was stored at 5 °C. Phosphate buffer (0.02 M, pH 7.4) was used as a solution for the preparation of standards solutions of ACR. The analytical grade reagents were used in whole experiments. Phosphate buffer (0.02 M, pH 7.4) used for all dilutions was prepared with deionized water and pH was adjusted using sodium hydroxide (5 M).

Deionized water (18.2 MΩ. cm, Simplicity, Milli-Q Millipore water purification system) was used for the preparation of all aqueous solutions.

The used commercial foodstuffs of chicken burger, chicken doner, nuggets, beef burger, and meat doner were obtained from different firms in Ankara, Turkey, and kept under cool, dry conditions.

Apparatus. A Varian Cary Eclipse spectrofluorimeter with a 10 × 10 mm quartz cuvette was used for the phosphorescence measurements. Excitation wavelength and slit widths were 290 nm and 10 nm, respectively. Xenon flash lamp was used as the light source.

In order to pH adjustment, measurements were done by using a combined pH electrode with an Orion model 720 A pH meter. Nuve NF 800R (Turkey) refrigerated type centrifuge, J.P. Selecta (Spain) type sonicator, and vortex (Firlabo, Lyon, France) were used for sample preparation throughout the study. Samples were filtered using 0.45 µm filters (Sartorius, Goettingen, Germany). All experiments were done at room temperature.

Synthesis of the L-cysteine capped Mn-doped ZnS QDs. L-cysteine capped Mn-doped ZnS QDs were synthesized in aqueous solution as per a published method with minor modification [26]. The specific method as follows. In the first step, 50 mL of 0.02 M L-cysteine, 5 mL of 0.1 M $ZnSO_4$, and 1.5 mL of 0.01 M $MnCl_2$ were added to a three-neck flask. With a pH meter, the mixture was adjusted to pH 11 with 1 M NaOH. At room temperature, the mixture was stirring for 30 min and the air was removed with argon gas. After the mixing step, 5 mL of 0.1 M Na_2S were rapidly added to the solution to allow nucleation of the nanoparticles. The mixture was stirred for 20 min, and then the solution was aged at 50 °C under open air for 2 h to form the L-cysteine capped Mn-doped ZnS QDs.

Sample extraction. The sample preparation procedure for the analysis of ACR was performed with modification according to the method described by Kaplan et al. [27]. One gram of each sample was weighed accurately to Falcon flask and 5 mL n-hexane was added. These mixtures were vortexed well for 2 min and then obtained solutions were centrifuged (4100 rpm, 15 min, -5°C). After centrifugation, hexane layer was removed and 0.1 mL Carrez I (15 g of $K_4[Fe(CN)_6]$ in 100 ml water), 0.1 mL Carrez II (30 g of $ZnSO_4$ in 100 ml water), and 9.8 mL 0.2 mM acetic acid were added to the pellets. These mixtures were then vortexed well for 2 min and then obtained solutions were centrifuged (4100 rpm, 15 min, -5°C). After these steps, the supernatant fluid was collected and filtered through a 0.45 µm filter.

Mn-doped ZnS QDs as RTP probe for ACR. To study the effects of ACR on the RTP signal of L-cysteine capped Mn-doped ZnS QDs, the assay solutions containing 100 µL of QDs and varying concentrations of ACR (2-20 µg/mL) were prepared in 0.02 M, pH 7.4 phosphate buffer. Phosphorimetric measurements were carried out 2 min after the reactions with the excitation wavelength of 290 nm. The assay based on the determination of quenched phosphorescence intensity of QDs.

RESULTS AND DISCUSSION

Characterization of the Mn-doped ZnS QDs. Prior studies show that L-cysteine caped Mn-doped ZnS QDs which prepared mentioned above have a spherical shape and nearly uniform size. Brus Equation [1] was also used to determine the diameter of synthesized QDs [25].

$$\Delta E\,(r) = E_g\,(r) + h^2/8r^2\,(1/m_e^* + 1/m_h^*) \quad [1]$$

where ΔE is the emission energy, E_g is band gap energy, r is the radius, h is Planck constant, m_e^* is the effective mass of the excited electron, and m_h^* is the effective mass of excited hole. The diameter of the prepared Mn-doped ZnS QDs was calculated at around 4 nm.

Spectral characterizations of QDs were evaluated by using UV-vis and phosphorimetric technique. The two maxima at 209 and 290 nm were observed (Fig. 1) in the absorption spectra. The phosphorescence spectra showed that the maximum excitation and emission peaks occurred at 290 nm and 590 nm, respectively (Fig. 1). This orange emission band was attributed to the $^4T_1$- $^6A_1$ transition of the Mn^{2+} impurity incorporated into the ZnS host lattice [28]. This orange emission was not observed before aging, however, the QDs were heated at 50 °C under open air for 2 h, the emission at 590 nm occurred.

The quinine reagent was used as a reference standard in order to determine the quantum yield (PL-QY) of synthesized QDs, and it was found as 20.2%. The stability of prepared L-cysteine caped Mn-doped ZnS QDs was showed that QDs and their signals were stable at least 6 months in water without remarkable precipitation in the darkness at 4°C.

Optimum conditions of reactions. Some experimental conditions such as pH and reaction time have a great effect on the RTP intensity of QDs. Hence, to provide that the L-cysteine capped Mn-doped QDs are stable and detect ACR correctly and rapidly, these conditions were optimized.

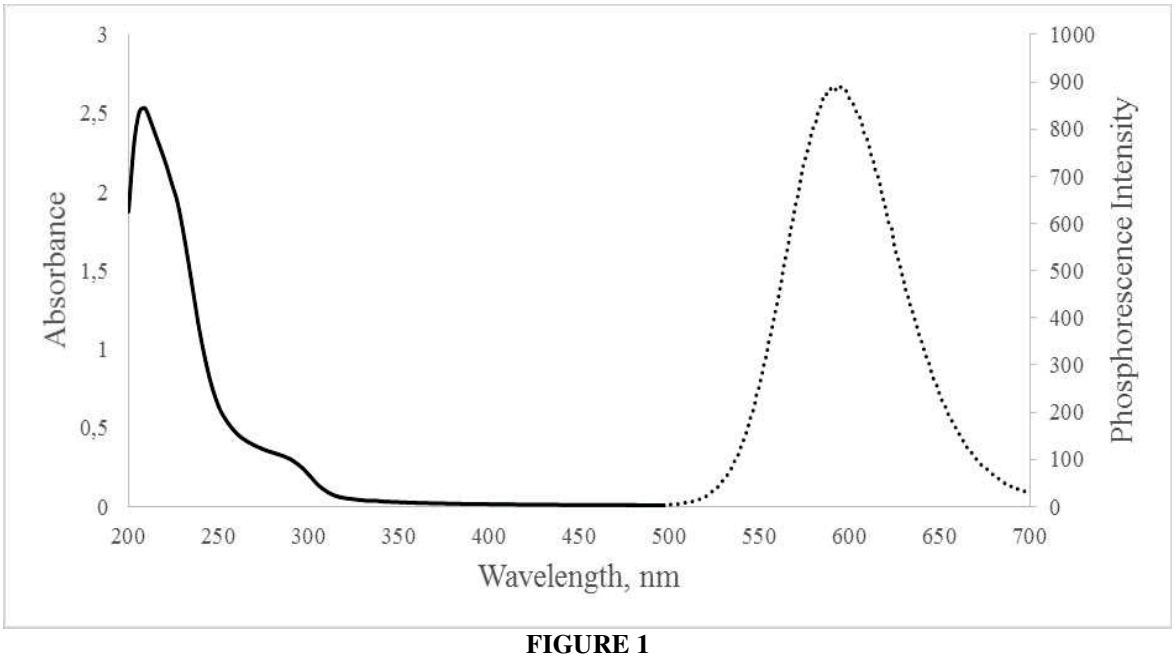

FIGURE 1
The absorption (line) and phosphorescence (dash line) spectra of Mn-doped ZnS QDs.

The effect of pH (5-9) on the RTP intensity of QDs in the presence and absence of ACR was examined. As shown Fig. 2, in the range of 5-7, the RTP intensity of QDs is very weak, which increased with the increase of the pH value. The phosphorescence intensity of QDs reached a maximum value at pH 7.4 and was stable between pH 7.4-8.0. When the pH was changed from 8.0 to 9.2, the intensity decreased significantly. The quenched phosphorescence intensity was also shown similar behavior with changing of pH value. Thus pH 7.4 was selected as an optimum value.

In order to investigate the effect of time on RTP intensity, the time interval of 0-7 min was tried. Phosphorescence intensity of QDs was quenched rapidly with the addition of ACR and reaction was stable after 2 min. Therefore, two min was selected for the analyze time (Fig. 3).

Selectivity of the method. In order to show the potential application of QDs for detecting of ACR in different food samples, the responses of the QDs towards some ingredients such as ions (K^+, Na^+, Ca^{2+}, Mg^{2+}), amino acids and proteins (L-cysteine, dopamine, cholesterol, creatinine, and L-cystine) which may affect the phosphorescence intensity were tested. The results indicated that only ACR had a phosphorescence quenching effect on the QDs and other interferences had a very low effect on quenching. Quenching of the RTP emission due to the addition of ACR was unaffected by 500-fold of ions and 100-fold of amino acids and proteins. These results showed that the proposed method more selective to ACR than other substituent coming from food samples.

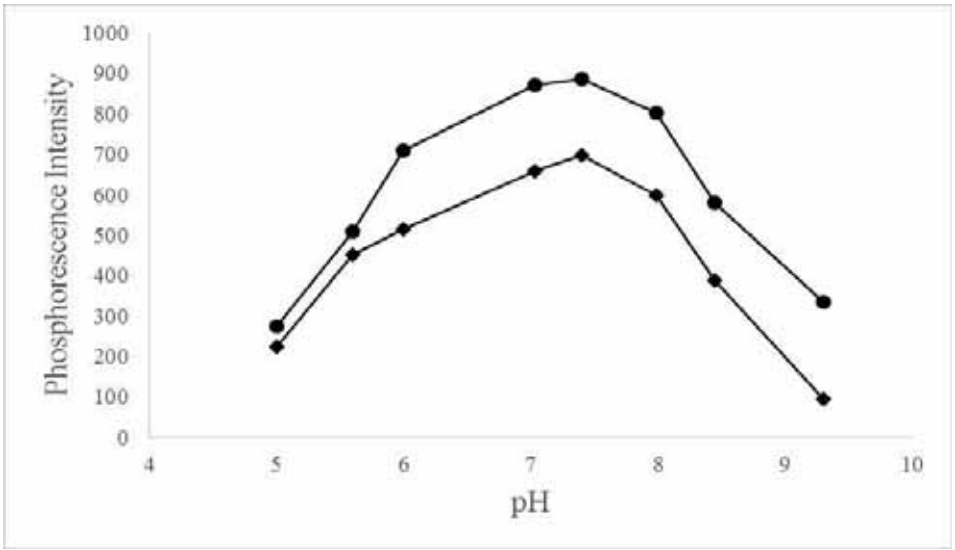

FIGURE 2
Effect of the pH on the RTP intensity of QDs (●) and the quenched RTP intensity of QDs (◆)

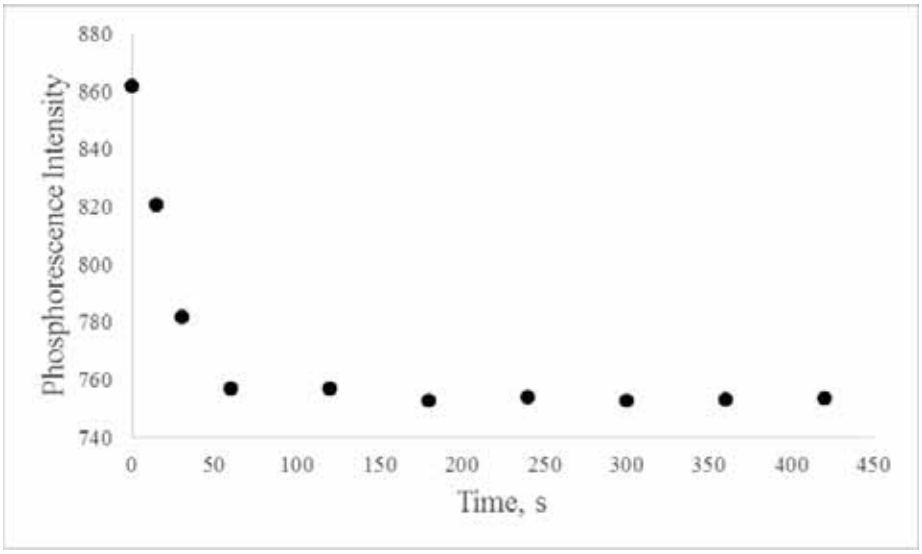

FIGURE 3
Effect of the reaction time on the quenched RTP intensity of QDs (0 s is RTP signal of QDs only).

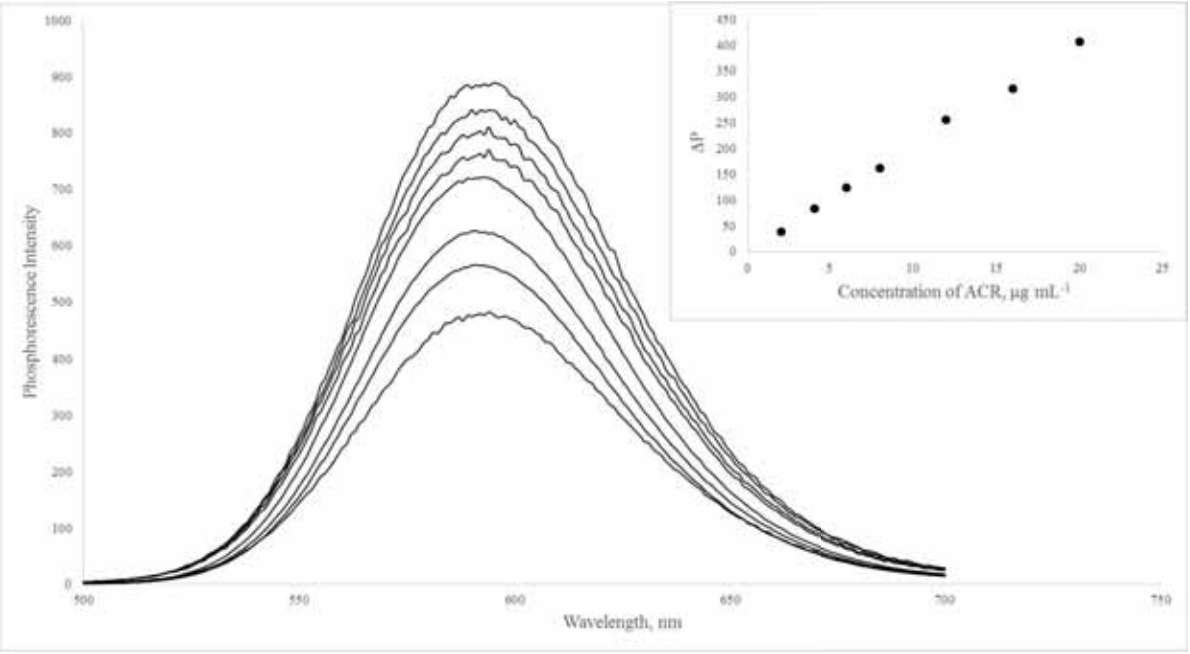

FIGURE 4
Effect of ACR concentrations on the RTP intensity of QDs.
The concentrations of ACR were 0, 2, 4, 6, 8, 12, 16, 20 μg/mL (top to bottom).

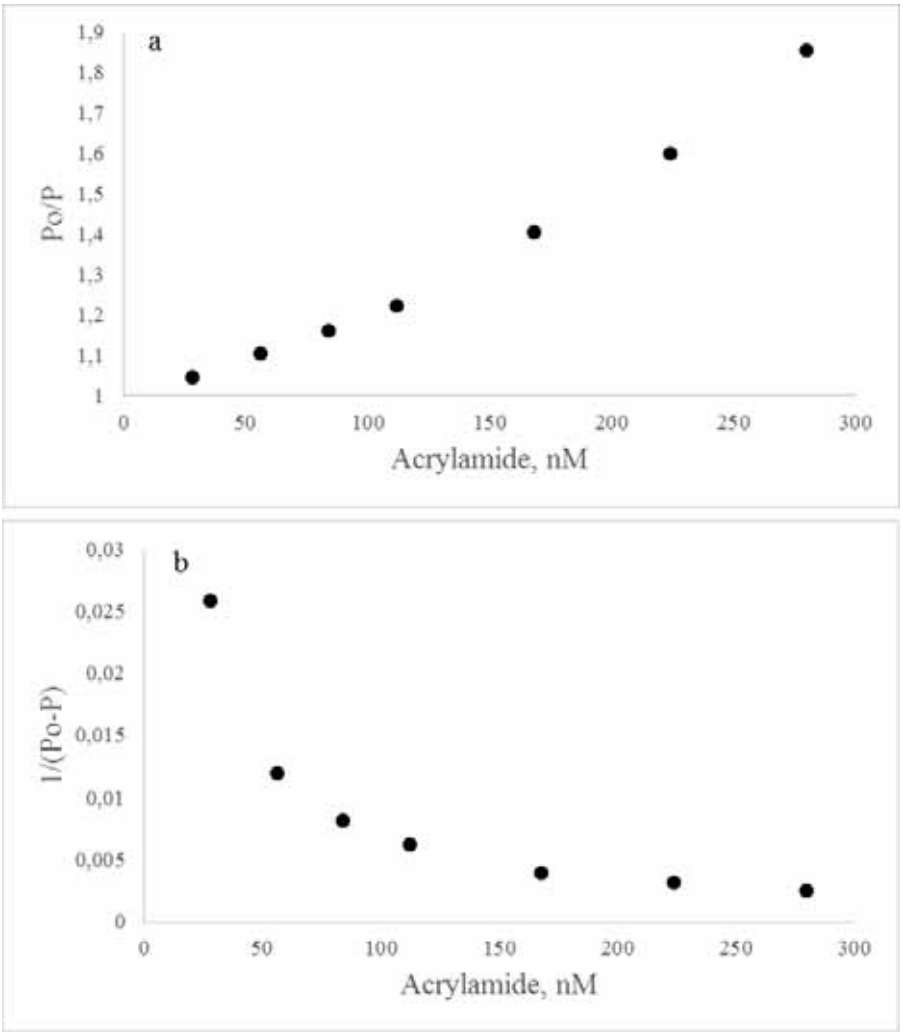

FIGURE 5
Stern-Volmer (a) and Lineweaver-Burk (b) plots for the RTP quenching effect of ACR on QDs.

Response mechanism. The presence of ACR caused gradually quenching of the phosphorescence emission of QDs (Fig. 4) because of the forming of QDs-ACR complex results of the interaction between ACR and L-cysteine.

Quenching mechanism is generally described as dynamic and static quenchings [29]. For quenching with these mechanisms, phosphorescent molecule and the quencher have to interact. If the quencher and phosphorescent molecule contact in the ground state and form a new unphosphorescent complex, this quenching system called static quenching. Besides that, in the static quenching, the lifetime of RTP does not change. However, for dynamic quenching, the decreasing of intensity and lifetime was observed due to the interaction of molecules at an excited state. The static quenching can be described by Lineweaver-Burk equation (Eq. 2) while dynamic quenching can be described by Stern-Volmer equation (Eq. 3)

$$1/(P_0 - P) = 1/P_0 + K_{LB}/(P_0\,[Q]) \quad [2]$$

$$P_0/P = 1 + K_{SV}\,[Q] \quad [3]$$

where P_0 and P are the phosphorescence intensities of QDs in the absence and presence of the quencher, respectively, [Q] is the concentration of the quencher, K_{LB} and K_{SV} are the static and dynamic quenching constants, respectively. K_{LB} is determined by the linear relationship between $1/(P_0\text{-}P)$ and [Q] and K_{SV} can be determined by linear regression of a plot of P_0/P against [Q].

As shown in Fig. 5, the plot of Stern-Volmer's was linear while Lineweaver-Burk was not. The linear curve was $P_0/P = 0.03\,[Q] + 0.91$ with a regression coefficient of r = 0.991 in the concentration range of 28-280 nM. Accordingly obtained results, RTP quenching mechanism of ACR-QDs system was dynamic and K_{SV} was found to be 3.0×10^4 /M which means ACR-QDs interaction was moderate. Obtained results show that developed method allow using as a probe for the determination of ACR in food samples.

Validation parameters of the L-cysteine Mn-doped ZnS QDs for the RTP analysis of ACR. As indicated in Fig. 4, under the optimal conditions, the quenching RTP intensity of QDs was sensitive to ACR and linearly increased with ACR concentration from 2 to 20 µg/mL. In this concentration range, the linear regression was $\Delta P = 20.13\,C + 1.92$ (r= 0.998) where ΔP and C were quenched RTP intensity and concentration of ACR (µg/mL) respectively. The analytical data for the calibration graph are listed in Table 1.

Limit of detection (LOD) and limit of quantification (LOQ) values were indicated the sensitivity of the method. LOD and LOQ were calculated from the equations of LOD= 3s/m and LOQ=10s/m where s is the standard deviation for five replicates and m is the slope of the calibration curve. LOD and LOQ values were calculated as 0.42 µg/mL and 1.39 µg/mL, respectively (Table 1). The obtained values explained that the proposed method has enough sensitivity for the determination of ACR in the meat-based food samples.

System repeatability was determined by five replicates on the same day (intra-day precision) and measurement of RTP intensity. Inter-day precision was assessed by the assay of similar concentration sample on different days. The results summarized in Table 1 indicated a high degree of precisions of the proposed method.

TABLE 1
Statistical Evaluation of Calibration Data for Quantitative Determination of ACR

Linearity range (µg/mL)	2-20
Slope	20.13
Intercept	1.92
Correlation coefficient	0.998
SE of slope	0.38
SE of intercept	0.12
LOD (µg/mL)	0.42
LOQ (µg/mL)	1.39
Inter-day precision* (RSD %)	0.25
Intra-day precision* (RSD %)	0.39

*Mean of the five experiments
SE is the standard error

TABLE 2
Results of Samples and Recovery Analysis of ACR

Sample	Sample value (µg/kg)	RSD (%)	Recovery (%)
Chicken burger	24.6	0.45	100.1
Chicken doner	34.7	1.02	98.7
Nugget	71.3	0.39	99.9
Beef burger	29.6	0.76	99.6
Meat doner	31.3	0.57	100.6

TABLE 3
ACR Levels using Different Methods in Meat-Based Food Products.

Samples	Method	Linearity range	LOD	ACR levels	Recovery (%)	References
Hamburger	GC-MS	150–5000 µg/kg	25 µg/kg	<LOD	82.9-104.2	[30]
Minced meat, meat balls, chicken nugets	LC-MS/MS	34-3750 µg/kg	34 µg/kg	ND-<LOQ	98-109	[31]
Bacon	LC-MS/MS	34-3750 µg/kg	150 µg/kg	ND-<150 µg/kg	98-109	[31]
Fried chicken	GC-ECD	-	0.1 µg/kg	164-225 µg/kg	87-97	[32]
Chicken products	HPLC-UV	45-2000 µg/kg	15 µg/L	0.044-0.925 mg/kg	-	[33]
Chicken, fish and beef bouillon	LC-MS/MS	8-3600 µg/kg	-	<10 µg/kg	95±6	[34]
Hamburger and meat patty	GC-MS	120-1200 µg/kg	10 µg/L	<10-16 µg/kg <10-203 µg/kg	107	[35]
Grilled beef and chicken meat patty	HPLC-MS	5-100 µg/L	0.5 µg/L	23-250 µg/kg	90≤	[27]
Fried beef meat and chicken minced meat	LC-MS/MS	10-5000 µg/kg	10 µg/kg	15-41 µg/kg	99.5	[36]
Hamburger	GC-MS	5-500 µg/kg	5 µg/kg	14-23 µg/kg	98	[36]
Meat samples	GC-MS	150-1000 µg/kg	25 µg/kg	<50 µg/kg 159 µg/kg	79-85	[37]
Chicken and meat products	QDs phosphorescence	2-20 µg/mL	0.42 µg/mL	24.6-71.3 µg/kg	99.8	This method

ND: not detected
LOD: Limit of detection

Recovery studies were performed by spiking pre-analyzed samples with appropriate amounts of the stock solution of ACR in order to find out the accuracy of the developed method and evaluate the possible interferences of the other substances coming from the samples. Recovery values were calculated as 98.7-100.6% (Table 2). These results explained that the developed method can be used for the analysis of ACR in food samples without potential interferences.

Determination of ACR in food samples. In the present work, the application of the developed method for the determination of ACR in food samples such as chicken burger, chicken doner, nugget, beef burger, and meat doner was presented. No interfering peaks were observed from any of the ingredients of the assayed samples. Calibration graphs were constructed by measuring the quenched RTP intensity obtained at mentioned concentrations under the optimized conditions. Table 2 summarizes the calculated sample values of ACR.

Although ACR is mostly determined in high-starch foods such as potato chips, bread, and cookies, there have been a few reports on ACR detection in meat-based food products using different methods (Table 3). These methods generally based on chromatographic techniques such as HPLC, LC-MS, and GC-MS. However, though they are sensitive methods, they need qualify operator, high-quality chemicals, time and cost. On the contrary, the developed method is not only an environmentally friendly method (Green chemistry) but also has enough sensitivity, wide linear range, low relative standard deviation, and high recovery percentage. When it is compared to the chromatographic methods, it was seen that the proposed method was sensitive enough to determine ACR in meat-based food samples.

CONCLUSION

Water-soluble L-cysteine capped Mn-doped ZnS QDs which possess good phosphorescent properties have been synthesized. The QDs were quenched effectively by ACR. The Stern-Volmer plot indicated that the quenching mechanism was dynamic. The developed method avoids interferences such as some cations and amino acids. In addition, lower LOD value showed the method sensitivity. The proposed method was used for the quantitative determination of ACR as successfully in different meat-based food samples. Concentrations of ACR could be directly determined according to the changing of RTP intensity of QDs. The results indicated that the proposed method was sensitive, selective, fast, cheap, not time-consuming, and has a low detection limit.

ACKNOWLEDGEMENTS

This research did not receive any specific grant from funding agencies in the public, commercial, or not-for-profit sectors.

REFERENCES

[1] Pereira, P.M.D.C. and Vicente, A.F.D.B. (2013) Meat nutritional composition and nutritive role in the human diet. Meat Sci. 93(3), 586-592.
[2] Trafialek, J. and Kolanowski, W. (2014) Dietary exposure to meat-related carcinogenic substances: is there a way to estimate the risk? Int J Food Sci Nutr. 65(6), 774-780.
[3] Semla, M., Goc, Z., Martiniakova, M., Omelka, R., Formicki, G. (2017) Acrylamide: A Common Food Toxin Related to Physiological Functions and Health. Physiol Res. 66(2), 205-217.
[4] Martinez-Saez, N., Garcia, A.T., Perez, I.D., Rebollo-Hernanz, M., Mesias, M., Morales, F.J., Martin-Cabrejas, M.A., and del Castillo, M.D. (2017) Use of spent coffee grounds as food ingredient in bakery products. Food Chem. 216, 114-122.
[5] Tamanna, N. and Mahmood, N. (2015) Food Processing and Maillard Reaction Products: Effect on Human Health and Nutrition. Int J Food Sci. 2015, 526762.
[6] Friedman, M. (2003) Chemistry, biochemistry, and safety of acrylamide. A review. J Agr Food Chem. 51(16), 4504-26.
[7] Claus, A., Carle, R., and Schieber, A. (2008) Acrylamide in cereal products: A review. J Cereal Sci. 47(2), 118-133.
[8] Dobrovolsky, V.N., Pacheco-Martinez, M.M., McDaniel, L.P., Pearce, M.G., and Ding, W. (2016) In vivo genotoxicity assessment of acrylamide and glycidyl methacrylate. Food Chem Toxicol. 87, 120-127.
[9] Arribas-Lorenzo, G. and Morales, F.J. (2012) Recent Insights in Acrylamide as Carcinogen in Foodstuffs. Adv Molec Toxicol. 6, 163-193.
[10] Capei, R., Pettini, L., Lo Nostro, A., and Pesavento, G. (2015) Occurrence of Acrylamide in breakfast cereals and biscuits available in Italy. Journal of Preventive Medicine and Hygiene. 56(4), E190-5.
[11] Parzefall, W. (2008) Minireview on the toxicity of dietary acrylamide. Food Chem Toxicol. 46(4), 1360-1364.
[12] Lyon, F. (1994) IARC monographs on the evaluation of carcinogenic risks to humans. Some industrial chemicals. 60, 389-433.
[13] Chu, P.L., Lin, L.Y., Chen, P.C., Su, T.C. and Lin, C.Y. (2017) Negative association between acrylamide exposure and body composition in adults: NHANES, 2003-2004. Nutr Diabetes. 7.
[14] Exon, J.H. (2006) A review of the toxicology of acrylamide. Journal of Toxicology and Environmental Health - Part B: Critical Reviews. 9(5), 397-412.
[15] Spencer, P.S. and Schaumburg, H.H. (1975). Nervous system degeneration produced by acrylamide monomer. Environ Health Perspect. 11, 129-33.
[16] Ning, F., Qiu, T., Wang, Q., Peng, H., Li, Y., Wu, X., Zhang, Z., Chen, L., and Xiong, H. (2017) Dummy-surface molecularly imprinted polymers on magnetic graphene oxide for rapid and selective quantification of acrylamide in heat-processed (including fried) foods. Food Chem. 221, 1797-1804.
[17] Franek, M., Rubio, D., Diblikova, I., Rubio, F. (2014) Analytical evaluation of a high-throughput enzyme-linked immunosorbent assay for acrylamide determination in fried foods. Talanta. 123, 146-150.
[18] Mastovska, K. and Lehotay, S.J. (2006) Rapid sample preparation method for LC-MS/MS or GC-MS analysis of acrylamide in various food matrices. J Agr Food Chem. 54(19), 7001-7008.
[19] Sun, Q., Xu, L., Ma, Y., Qiao, X. and Xu, Z. (2014) Study on a biomimetic enzyme-linked immunosorbent assay method for rapid determination of trace acrylamide in French fries and cracker samples. J Sci Food Agr. 94(1), 102-108.
[20] Zhang, W., Deng, Z., Zhao, W., Guo, L., Tang, W., Du, H., Lin, L., Jiang, Q., Yu, A., He, L., and Zhang, S. (2014) Determination of Trace Acrylamide in Starchy Foodstuffs by HPLC Using a Novel Mixed-Mode Functionalized Calixarene Sorbent for Solid-Phase Extraction Cleanup. J Agr Food Chem. 62(26), 6100-6107.
[21] Kara, H.E.S. and Ertaş, N. (2017) Quantum Dots for Pharmaceutical and Biomedical Analysis. In: Zafar, F. (Ed.) Spectroscopic Analyses-Developments and Applications. InTech.
[22] Jimenez-Lopez, J., Molina-Garcia, L., Rodrigues, S.S.M., Santos, J.L.M., Ortega-Barrales, P. and Ruiz-Medina, A. (2016) Automated determination of Rifamycins making use of MPA-CdTe quantum dots. J Lumin. 175, 158-164.
[23] Pawar, S.P., Gore, A.H., Walekar, L.S., Anbhule, P.V., Patil, S.R., Kolekar, G.B. (2015) Turn-on fluorescence probe for selective and sensitive detection of D-penicillamine by CdS quantum dots in aqueous media: Application to pharmaceutical formulation. Sensor Actuat B-Chem. 209, 911-918.

[24] Ertas, N. and Kara, H.E.S. (2015) L-Cysteine capped Mn-doped ZnS quantum dots as a room temperature phosphorescence sensor for in-vitro binding assay of idarubicin and DNA. Biosens Bioelectron. 70, 345-350.
[25] Demirhan, B.E., Demirhan, B. and Kara, H.E.S. (2015) Room-temperature phosphorescence determination of melamine in dairy products using L-cysteine-capped Mn-doped zinc sulfide (ZnS) quantum dots. J Dairy Sci. 98(5), 2992-3000.
[26] Demirhan, B., Er Demirhan, B., Ertas, N., and Kara, H.E.S. (2018) Rapid Detection of Acrylamide in Food Using Mn-Doped ZnS Quantum Dots as a Room Temperature Phosphorescent Probe. Food Analytical Methods. 11, 1367-1373.
[27] Kaplan, O., Kaya, G., Ozcan, C., Ince, M. and Yaman, M. (2009) Acrylamide concentrations in grilled foodstuffs of Turkish kitchen by high performance liquid chromatography-mass spectrometry. Microchem J. 93(2), 173-179.
[28] Miao, Y., Li, Y., Zhang, Z., Yan, G., and Bi, Y. (2015) "Turn off-on" phosphorescent biosensors for detection of DNA based on quantum dots/acridine orange. Anal Biochem. 475, 32-39.
[29] Lakowicz, J.R. (1999) Principles of fluorescence spectroscopy. Boston, MA: Springer.
[30] Pacetti, D., Gil, E., Frega, N.G., Alvarez, L., Duenas, P., Garzon, A., and Lucci, P. (2015) Acrylamide levels in selected Colombian foods. Food Addit Contam B. 8(2), 99-105.
[31] Eerola, S., Hollebekkers, K., Hallikainen, A., and Peltonen, K. (2007) Acrylamide levels in Finnish foodstuffs analysed with liquid chromatography tandem mass spectrometry. Mol Nutr Food Res. 51(2), 239-247.
[32] Zhang, Y., Dong, Y., Ren, Y., and Zhang, Y. (2006) Rapid determination of acrylamide contaminant in conventional fried foods by gas chromatography with electron capture detector. J Chromatogr A. 1116(1-2), 209-216.
[33] Paleologos, E.K. and Kontominas, M.G. (2007) Effect of processing and storage conditions on the generation of acrylamide in precooked breaded chicken products. J Food Protect. 70(2), 466-470.
[34] Roach, J.A.G., Andrzejewski, D., Gay, M.L., Nortrup, D. and Musser, S.M. (2003) Rugged LC-MS/MS survey analysis for acrylamide in foods. J Agr Food Chem. 51(26), 7547-7554.
[35] Olmez, H., Tuncay, F., Ozcan, N. and Demirel, S. (2008) A survey of acrylamide levels in foods from the Turkish market. J Food Compos Anal. 21(7), 564-568.
[36] Tareke, E., Rydberg, P., Karlsson, P., Eriksson, S. and Tornqvist, M. (2002) Analysis of acrylamide, a carcinogen formed in heated foodstuffs. J Agr Food Chem. 50(17), 4998-5006.
[37] Tateo, F., Bononi, M. and Andreoli, G. (2007) Acrylamide levels in cooked rice, tomato sauces and some fast food on the Italian market. J Food Compos Anal. 20(3-4), 232-235.

Received: **26.10.2018**
Accepted: **19.02.2019**

CORRESPONDING AUTHOR

Burak Demirhan
Department of Pharmaceutical Basic Sciences,
Faculty of Pharmacy,
Gazi University,
06330 Ankara – Turkey

e-mail: burakdemirhan@hotmail.com

© by PSP Volume 28 – No. 4/2019 pages 2608-2616 Fresenius Environmental Bulletin

STUDY ON CARBON-DIOXIDE EMISSIONS IN CHINA BASED ON STRUCTURAL DECOMPOSITION ANALYSIS

Zhiyuan Ge, Jie Hou*

School of Economics and Management, Beijing University of Technology, Beijing, P.R. China

ABSTRACT

Based on the structural decomposition analysis and EORA database, the influence of four driving factors on the change of carbon dioxide emission in China during 1980-2013 was analyzed. The results show that the effect of carbon emission intensity has the greatest contribution to mitigation of carbon dioxide emission increase, and the final demand expanding and the input-output structure effect contribute the most to the growth of carbon dioxide emissions. From the perspective of changing trends, the total amount of carbon dioxide emissions and four factors can be divided into three stages: 1980-1986, 1986-2001 and then 2001-2013, which tend to fluctuation from stable state in early years. From the view of sector level, gas production, cement products, electricity and construction sectors are the main causes of carbon dioxide emissions growth during 2001-2013. With the increase of the use of clean energy, technological change, old plants closeness and improvement of the industrial structure of the final demand are the main ways to reduce carbon dioxide emissions.

KEYWORDS:
Carbon-dioxide Emissions, Environmentally extended Input-output, Structural Decomposition Analysis

INTRODUCTION

With the rapid growth of China's economic development and increase of domestic consumption, energy use, greenhouse gas emissions and environment problems are becoming increasingly alarmed. According to the reports by the World Bank, CO_2 emissions of China exceeded European Union since 2003, and was greater than United States since 2006, and become the largest carbon-dioxide emitter. From 1980 to 2013, the carbon-dioxide emissions of China had increased from 1.47 billion tons to 10.25 billion tons, and reached a proportion of 28.6 percent of the total emission in the world. In recent years, it has been a wide consensus in decreasing emission of carbon-dioxide, energy conservation and environmental protection. At the UN Climate Change Conference Paris 2015 (COP21) China promised that carbon-dioxide emission in China will climb to a peak in 2030, and the ratio of per unit of GDP over carbon-dioxide emission in 2030 will cut down by 60% to 65% in comparison with 2005. Therefore, studies on key economic factors of contributing the emission growth of carbon-dioxide are helpful for the policies and actions in carbon emission reduction [1-3].

Environmentally extended input-output analysis (EEIO) have rapidly become one of the main research methods in industrial ecology. EEIO analysis was proposed by Leontief W [4], in which monetary transaction among economic sectors is used to represent the relationship between the production process of products and service and the emission to environment. EEIO analysis had been applied to evaluate the environmental impact by production and consumption. For example, the assessment of the environmental and economic impacts of greenhouse gas emissions ensuing from the consumption of food and nonalcoholic beverages in the in the EU food supply chain [5]; the use of the Bioeconomic Input-Output model to account for the energy embodied in human labour [6]; the analysis of Sustainability assessment of U.S. final consumption and investments based on triple-bottom-line input–output method [7].

Decomposing analysis is the common method used to find the impact factors which lead to the increase of carbon emission. There are two main kinds of decomposition methods: index decomposition analysis (IDA) and structural decomposition analysis (SDA). Generally SDA is used to decompose the environmentally extended input-output, for example, energy consumptions, carbon-dioxide emissions and other pollutant emissions and demand for sources.

Structural decomposition analysis analyses the components of change over time [8]. The basic components included are the environmental intensity, production technology and the size and composition of final demand.

Yuan and Xu [9] provide a computation on both the China's aggregate CO_2 emission volume and the emission of each sector over the period of 2002-2007, based on the input-output analysis. The changes in emission are analyzed in terms of five different factors. Among the five factors studied in the paper, it is found that emission intensity and

domestic need are the main reasons for the decrease in emission, while production technology, trade structure and scale effect are the more significant causes to the increase in emission.

Nie et al. [10] undertakes a structural decomposition analysis to decompose the changes in CO_2 emissions from 1997 to 2010 into the following six driving forces: emission coefficient, energy intensity, Leontief, sectoral structure, demand allocation and final demand effects. The results show that declines in energy intensity had a decrease impact on CO_2 emissions. The most important driver behind the steady increase in CO_2 emissions is the large increase in final demand. A further analysis at the sectoral level revealed differences and fluctuations in sectors 3.

These studies had made contributions in China's carbon emissions. However, most of these studies based on the input-output table database issued by National Bureau of Statistics of PRC, which only issue China Input-Output Table data every five years and since 2000 there are only three years input-output data, i.e., 2002, 2007, 2012, issued by China National Bureau of Statistics. Moreover, the environment account data were not included in the input-output table, and need to be collected from other resources. As a result, input-output data issued by Chinese government maybe not so accurate with the reality that not suitable for studying the carbon-dioxide emissions year by year. In addition, present studies paid more attention to the whole economy and industries, instead of recognising the key factors for proposing actions to reduce emission.

This paper based on the environmentally extended input-output model and EORA database, analyze the changes of carbon-dioxide emissions in China and factors which affect the emissions, and identify the key factors which have influences on the emissions. Based on the analysis results, we also proposed some actions expected to reduce the emissions.

EXPERIMENTAL

Theoretical background. Input-output Model. The fundamental equation of the Leontief model (consisting of N economic sectors) links an exogenous $N \times 1$ final demand vector y with an $N \times 1$ total output vector x via

$$x = (I - A)^{-1} y \quad (1)$$

where A is a matrix indicating sector intermediate technical coefficients; $(I - A)^{-1}$ is the Leontief inverts matrix.

When emissions, resource use or other sustainability indicators are known, they can be included in an environmentally extended input-output analysis. The matrix of environmental flows is divided by the industry output to obtain unit emission/resource intensities:

$$B = G\hat{x}^{-1} \quad (2)$$

where B=emission or resource use intensity (environmental flow-by-industry); G is emission or resource use matrix (environmental flow-by-industry). The hat symbol ^ denotes a diagonal vector.

These intensities can then be used similar to the value added to give the environmental flows associated with a given technology and final demand:

$$g = B(I - A)^{-1} y = My \quad (3)$$

where g is overall emissions caused by the final demand; M is environmental multiplier matrix.

Structural Decomposition Analysis. There are some techniques that are used for decomposing the development in emission indicators at the sector levels. Structural decomposition analysis (SDA) is one of the techniques, for example, to analyze the demand and technological driving forces of energy use, CO_2 emission and various other pollutant and resources.

Structural decomposition analysis (SDA) analyses the components of change over time. The decomposition analysis is based on equation (3), and given $L = (I - A)^{-1}$ be the input-output structural effect, which reflects the relationship between sectors of production, and the final demand $y = y_s * y_v$ consists of the structure of final demand y_s and the total amount of final demand (scalar) y_v. Then the equation (3) can be changed to the following equation:

$$g = B(I - A)^{-1} y = BLy_s y_v \quad (4)$$

Since the input-output model is linear, the effect of changes from report time 0 to t can be expressed as differences:

$$\Delta g = g_t - g_0 = B_t L_t y_{st} y_{vt} - B_0 L_0 y_{s0} y_{v0} \quad (5)$$

where the Δ symbol denotes the changes over time. Our studies is based on the decomposition techniques proposed by Dietzenbacher & Los [11], which has been found to involve few calculations and yield estimates close to the average value of the full set of decompositions. According to this method, changes of emissions can be expressed as:

$$\Delta g = g_t - g_0 = \Delta B L_0 y_{s0} y_{v0} + B_t \Delta L y_{s0} y_{v0} + B_t L_t \Delta y_s y_{v0} + B_t L_t y_{st} \Delta y_v \quad (6)$$

we finally obtain the final decomposition equation by calculating the average of the two-polar decompositions.

$$\Delta g = \Delta g_B + \Delta g_L + \Delta g_{y_s} + \Delta g_{y_v} \quad (7)$$

$$\Delta g_B = \frac{1}{2}[\Delta B L_t y_{st} y_{vt} + \Delta B L_0 y_{s0} y_{v0}] \quad (8)$$

$$\Delta g_L = \frac{1}{2}[B_0 \Delta L y_{st} y_{vt} + B_t \Delta L y_{s0} y_{v0}] \quad (9)$$

$$\Delta g_{y_s} = \frac{1}{2}[B_0 L_0 \Delta y_s y_{vt} + B_t L_t \Delta y y_{v0}] \quad (10)$$

$$\Delta g_{y_v} = \frac{1}{2}[B_0 L_0 y_{s0} \Delta y_v + B_t L_t y_{st} \Delta y_v] \quad (11)$$

From equations above, the four decomposed factors which influence the carbon-dioxide emissions consists of the emission intensity (Δg_B), Leontief effect (Δg_L), demand allocation (Δg_{y_s}) and final demand (Δg_{y_v}) effects.

Data collection. Our construction of CION is based on the Eora multi-region input-output table (MRIO) database [12,13]. Its main advantage over WIOD database is that Eora provides a time series of high resolution IO tables with matching environmental and social satellite accounts, and continuous coverage for the period 1970-2013 at the time of writing while WIOD dataset only cover data for the period from 2000. By contrast, China Input-Output Table made by National Bureau of Statistics of the People's Republic of China (NBSPRC) issue per five years, and the most recent data released in 2012, and data of environmental accounts is not included in input-output table.

Considering the history of China from 1970 to 1980 which during this time developing economy was not the first place for Chinese government, we studied the emission of China since 1980 when the economic growth of China became significant in the world.

TABLE 1
Overall structure of an input-output framework

	Industries	Final Demand	Total output
Industries	Technology matrix **A** (industry-by-industry	Industry final demand **y**	Industry output **x**
Value added	Value added **v**		
Total output	Industry output **x**		

Table 1 gives the input-output table structure of EORA MRIO database. According to the declaration of EORA website, the country tables published by EORA database use their native/national classification systems if one is available. The China input-output tables include 123 products, primary input and final demand blocks, imports and exports itemized by partner, and environmental satellite accounts.

There are some points in EORA database need to be mentioned here. Generally, all of data in input-output table are positive, especially for intermediate coefficient. However, in EORA database there are some negative number sometimes in China input-output table, for example the primary inputs and a few of final demand items of some industries, which were the consequences of inventory changes, and this phenomenon is not happen in intermediate matrix. Furthermore, in WIOD dataset, even in intermediate matrix there are still a few negative numbers, and it is difficult to explain in physical world. Moreover, negative numbers are hard to interpret in building network model and cannot deal with this case.

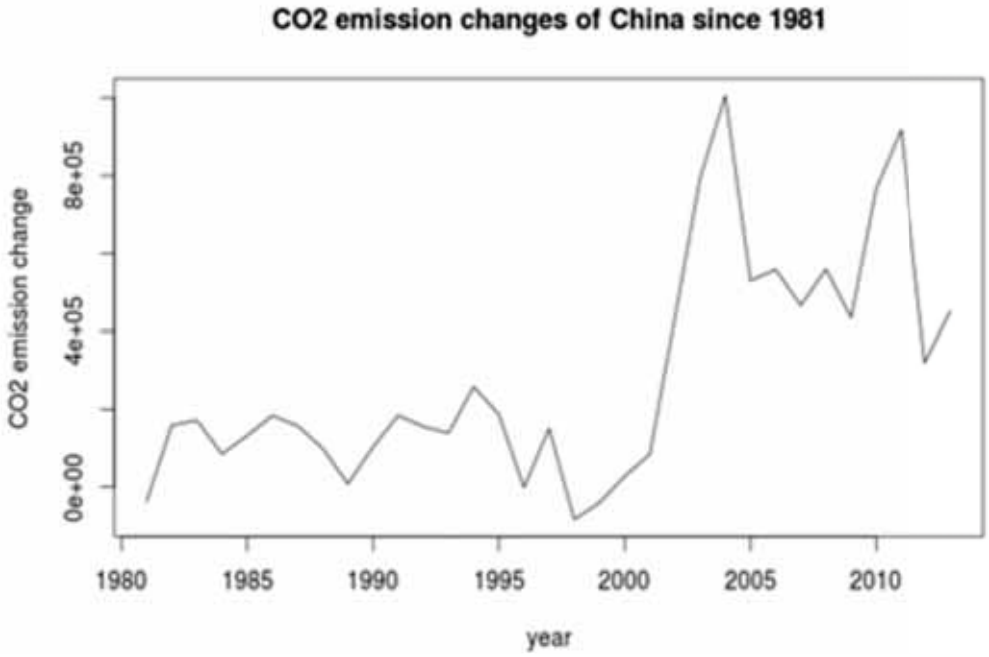

FIGURE 1
Annual CO_2 emission changes of China from 1981 to 2013

RESULTS AND DISCUSSION

An overview of carbon-dioxide emissions during the period 1980-2013. Figure 1 shows the annual changes of total CO_2 emission in China each year from 1980 to 2013. Through the duration from 1980 to 2013 the carbon-dioxide emissions increased 9.35 billion tons. Before 2001 the emission increased slowly each year even during the financial crisis in Southeast Asia from 1996 to 1997 the total emission in China decreased. Since 2002 the augment of CO2 emission rise significantly until recent year.

Table 2 shows the results of structural decomposition analysis from 1980 to 2013. During these years, augment of CO2 emission each year mainly caused by the increase of final demand, which contribute the increment of 1269.6 million tons (281%) of emission for 2013. The second factor for the increment of emission is Leontief effect, which contribute the growth of more than 2643 million tons during the years from 1980 to 2013, and about 28.3%. Emission intensity is the main factor of cutting emissions which reduce 789.9 million tons of CO2 in 2013 and reached -175.7% total deduction since 2000.

Figure 2 shows the tendency of total carbon-dioxide emission changes and decomposition details from 1980 to 2013 of China. According to the change mode the curves shows in the figure 2, we divide the history of emission changes into three stages: the first stage is from 1980 to 1986 which the increases of carbon-dioxide emission are stable in this duration, the second stage is from 1987 to 2001 which each factor fluctuated obviously, and the third stage is after 2002 which each factor fluctuated significantly and total increases of emission are high.

Table 3 shows the details of carbon-dioxide emissions grouped by the three stages, and decomposition of factors during the whole duration from 1980 to 2013. Notice that the value of each factor of 1980-2013 does not equal the sum of three stages because factor changes of each stage does not had a non-linear relationship with the changes in total duration according to the equations (6) to (10). According to the analysis results in table 3 we find that the main factor leading to the increase of carbon-dioxide emission after 1980 is final demand, and then Leontief effect also contributes a lot in the emission increase. However, emission intensity becomes the only factor which lead to decrease the emission.

TABLE 2
Structural decomposition results for CO_2 emissions in China for the period of 1980-2013 (unit: million tons of CO_2)

Factors	1980-1981	1981-1982	1982-1983	1983-1984	1984-1985	1985-1986	1986-1987	1987-1988	1988-1989	1989-1990	1990-1991
Demand Structure	-0.8	-1.1	1.1	5.4	4.8	0.4	5.7	2.2	0.2	2.7	-11.8
Final demand	-71.5	-41.4	130.4	58.0	-23.6	-69.3	254.5	631.7	288.3	-330.8	189.5
Leontief effect	1.2	35.9	-8.4	-36.2	-30.0	21.8	-53.4	-37.1	-7.9	-27.7	243.2
Emission intensity	32.8	165.2	48.5	57.4	181.0	230.3	-49.3	-497.4	-273.1	458.8	-236.9
Total emission changes	-38.2	158.6	171.6	84.6	132.1	183.3	157.5	99.4	7.5	103.0	183.9
Factors	1991-1992	1992-1993	1993-1994	1994-1995	1995-1996	1996-1997	1997-1998	1998-1999	1999-2000	2000-2001	2001-2002
Demand Structure	63.9	-2.8	10.2	21.4	78.0	53.0	-140.3	-0.9	9.9	-11.2	2.5
Final demand	678.5	693.2	-211.4	1053.0	519.5	538.7	315.9	268.3	506.7	290.0	368.1
Leontief effect	-166.4	99.0	-96.5	-99.2	387.5	-169.8	624.1	-42.3	-121.0	68.4	-146.1
Emission intensity	-420.8	-650.9	555.6	-788.0	-986.8	-271.3	-883.8	-265.7	-368.5	-263.0	210.4
Total emission changes	155.3	138.6	257.8	187.2	-1.8	150.6	-84.1	-40.5	27.1	84.2	434.9
Factors	2002-2003	2003-2004	2004-2005	2005-2006	2006-2007	2007-2008	2008-2009	2009-2010	2010-2011	2011-2012	2012-2013
Demand Structure	1.0	21.7	126.8	-85.6	99.5	15.7	-66.9	42.6	28.9	-15.8	-47.2
Final demand	648.3	1073.5	1272.7	1115.1	1826.8	1840.4	478.7	1657.1	2078.9	447.9	1269.6
Leontief effect	-44.9	-117.7	854.2	205.4	1328.1	187.5	425.2	-195.3	-153.4	-302.6	18.0
Emission intensity	189.4	28.3	-1724.6	-677.1	-2789.4	-1485.1	-403.1	-738.7	-1036.5	189.8	-789.9
Total emission changes	793.9	1005.8	529.1	557.7	465.0	558.5	433.8	765.8	917.8	319.4	450.5

TABLE 3
Carbon-dioxide emission changes in three stages and the whole duration from 1980 to 2013

Factors	1980-1986	1986-2001	2001-2013	1980-2013
Demand Structure	9.3	0.3	263.3	166.7
Final demand	-20.5	6820.9	15187.5	33796.1
Leontief effect	-12.3	1257.5	3820.6	12168.9
Emission intensity	715.6	-6653.0	-12039.2	-36781.8
Total emission changes	692.0	1425.7	7232.2	9349.9

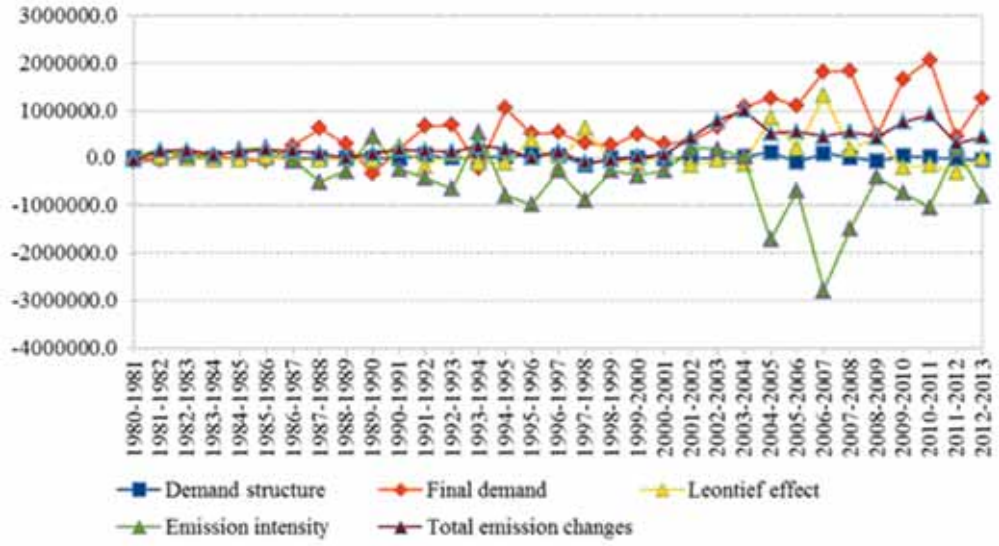

FIGURE 2
Carbon-dioxide emission changes history of China from 1980 to 2013

In the first stage (from 1980 to 1986), the total increase of carbon-dioxide emission contribute 7.4% of the emission through our study duration of 1980-2013, and present stable state in the emission increase. Each factor including emission intensity effect, Leontief effect, demand structure effect and final demand effect, fluctuate lightly. In fact, the economy of China in this duration was small and just started growth with shifting from planned economy to market economy.

In the second stage (from 1986 to 2001), factors fluctuate obviously and total increases of carbon-dioxide emission reach 1.43 billion tons, and contribute 15.2% of the total emission throughout the study duration. Emission intensity effect and final demand effect are the most volatile two factors, and emission intensity effect is negative during each year except for 1989-1990 and 1993-1994, and final demand effect always be positive. That is to say, emission intensity effect is a moderating force on the carbon emission because in this stage emission per unit decreased, and enlarged emission increases by final demand effect illustrate that domestic consumption growth led to the increase of emission. Meanwhile, the China economy developed rapidly and started to focus on the adjustment of industrial structure and trading structure, so that slow down the augment of emission. However, the development of economy still came at the expense of excessive energy consumption and environment pollution in this stage.

In the third stage (from 2001 to 2013), factors fluctuate significantly and total increases of emission came to 7.23 million tons, and contribute 77.4% of the total emission throughout the study duration. After the peak of annual increment of emission in 2004, China kept controlling the carbon-dioxide emission, and only in 2010 and 2011 there is an obvious expanding and soon afterwards the increase of emission has slumped to the lowest since 2003. In this stage the carbon emission intensity effect stay reduction and shows that carbon emission per unit value added decreased. Whereas factor final demand increased significantly and it was approximately induced by the rapid swell of domestic consumption in the context of economy growth. The factor Leontief effect continued to increase in 2004-2009 and this phenomena shows in carbon emission product structure is more important than technical progress. While this factor decreased after 2009 shows that technical progress led to the decrease of emission.

SDA of subsectors during the period of 2001-2013. Until now we just analyzed the total emission with SDA, and next we consider analysis the emission of each industries provided by the database, so that find the dominant influenced industries in the four factors: emission intensity effect, demand allocation effect, final demand effect

and Leontief effect. We only consider the third stage because the first stage and second stage are long ago and no valuable today.

1) Emission intensity effect. Emission intensity effect is the dominant factor slowing down the emission during 2001 to 2013. This factor decrease more than 12 billion tons of carbon-dioxide emission, which comprise -166.5%.

Only one sector scrap and waste have been an increase in emission intensity from 2000 to 2013, and other 121 industries decreased their emission intensity. Table 3 list the top largest 10 in emission intensity decrease during 2001-2013. Gas production and supply rank first in the decrease of emission intensity, which occupy 17.8% of total decrease of emission intensity, and cut 4.94 and 23.4 t/1,000 dollar of carbon-dioxide emission in 2001 and 2013 respectively. Following sectors are cement and cement asbestos products and electricity and steam production and supply which contribute the reduction of 11.8% and 10.2 respectively, and the fourth to tenth place are transports.

Therefore, the dominant sectors in the reduction of emission intensity during 2001-2013 are gas production, cement related products, electricity and steam production and supply, etc. which are energy-intensive, and carbon-dioxide emissions related to production activities have effectively reduced because of large-scale uses of clean energy and promotion of increasing efficiency of energy use . The results shows that the policies of promoting energy usage effectiveness made by Chinese government have been successful during decade years. Furthermore, compared to the developed countries the value of emission intensity is still high and there still are a lot of things to be improved for Chinese government.

2) Leontief effect. Leontief effect (input-output structural effect) is the second factor leading to the increase of carbon-dioxide emissions during 2001-2013. This effect increased 3.82 billion tons of carbon-dioxide emission, which contribute to 52.8% of total emissions.

Leontief inverse matrix represents input-output structure and had been studied by a lot of scholars. Oosterhaven [14] defined the sum of columns of Leontief reverse matrix as multiplier effect, and be used to recognize the key sectors of economy. Afrasiabi and Casler [15] found the changes in the of Leontief inverse matrix comprise technological change and product mix change. As a driving force behind the changes in the Leontief inverse, technological change can cause a decrease in the intermediate output thereby decreasing the total output, and changes of product mix can either increase or decrease total output [16].

The Leontief effect of 109 industries had been increased during 2001-2013, and 14 industries decreased. Table 5 list top 5 increase and decrease industries respectively in Leontief effect. Ferrous ore mining ranks the first place in the increase list and give 3.92% share of effect. The second and third places are other non-metallic mineral products, and agriculture, forestry, animal husbandry and fishing machinery, which contribute 2.37% and 2.13% respectively. Among these industries, effects by product structure are larger than technological changes, and variety of product structure tended to the input-intensive industries, and causing the increase of carbon-dioxide emissions. Whereas the Leontief effect of industry crop cultivation decreased by 0.13 and contribute 0.29%, and following industries are livestock and livestock products and real estate. These industries implemented emission decrease by technological changes.

TABLE 4
Top 10 sectors in the decrease of emission intensity during 2001-2013 (unit: t/1,000 dollar)

Rank	Sector	ΔB	Rank	Sector	ΔB
1	Gas production and supply	-15.68	6	Domestic public transport	-2.25
2	Cement and cement asbestos products	-10.39	7	Highway freight and passangers transport	-2.16
3	Electricity and steam production and supply	-8.96	8	Railway freight transport	-1.97
4	Air passenger transport	-4.57	9	Railway passenger transport	-1.67
5	Air freight transport	-3.42	10	Water freight and passangers transport	-1.48

TABLE 5
Top 5 increase and decrease industries in Leontief effect during 2001-2013

Rank	Industries of increasing ΔL	ΔL	Rank	Industries of decreasing ΔL	ΔL
1	Ferrous ore mining	1.70	1	Crop cultivation	-0.13
2	Other non-metallic mineral products	1.03	2	Livestock and livestock products	-0.11
3	Agriculture, forestry, animal husbandry and fishing machinery	0.92	3	Real estate	-0.09
4	Steel-processing	0.89	4	Wholesale and retail trade	-0.08
5	Alloy iron smelting	0.83	5	Technical services for agriculture, forestry, livestock and fishing	-0.07

TABLE 6
Top 10 increase industries in demand allocation during 2001-2013

Rank	industry	Δy_s	Rank		Δy_s
1	Construction	2.41%	6	Communication equipment	0.25%
2	Other special industrial equipment	0.71%	7	Instruments, meters and other measuring equipment	0.18%
3	Health services	0.42%	8	Business services	0.18%
4	Motor vehicles	0.31%	9	Agriculture, forestry, animal husbandry and fishing machinery	0.14%
5	Other general industrial machinery	0.27%	10	Furniture and products of wood, bamboo, cane, palm, straw, etc.	0.12%

TABLE 7
Top 10 increase industries in final demand during 2001-2013

Rank	industry	y_v	Rank		y_v
1	Construction	1712	6	Wholesale and retail trade	257
2	Public administration and other sectors	485	7	Crop cultivation	255
3	Educational services	332	8	Livestock and livestock products	239
4	Communication equipment	269	9	Health services	239
5	Real estate	269	10	Other special industrial equipment	228
				Unit: 100 million dollars	

So technological changes contributed small in carbon-dioxide emission during 2001-2013. Variety of input-output structure (Leontief inverse matrix) produced more intermediate input demands which are carbon emission intensity, and Leontief effect led to a trend of positive variation in carbon emission intensity. Therefore, technological changes should be encouraged to improve production procedure and promote product efficiency. Furthermore, closing obsolete low-tech old factory is another alternative strategy.

3) Demand allocation effect. The demand allocation effect is the minimum factor influencing carbon emission in all four driver factors, and contribute 263 million tons of emission during 2001-2013, and occupy 3.6% of total emission.

Sixty eight of 123 industries increased in demand allocation effect during 2001-2013. Table 6 list top 10 industries in the increase of demand allocation effect. Some industries which are high carbon emission raised their proportion in demand allocation effect, such as construction, motor vehicles. Construction is the top industry in carbon emission increase by demand allocation effect, and the absolute increase reached 2.41% during 2001-2013. Some industries reduced their proportion in demand allocation effect, for example, public administration and other sectors, crop cultivation, bring down their proportion with 0.80% and 0.73% respectively, and be the highest decrease industries.

Analysis results show that the demand allocation effect increased the carbon-dioxide emissions, especially for some carbon intensive industries which argument the carbon emissions by swelling the proportion in the structure allocation.

4) Final demand. Final demand is the most important factor for the carbon-dioxide emission during 2001-2013, and contribute 15.19 billion tons of emission, a total of 210%. During this period final demand increased to 957 billion dollars from 155 billion dollars in China by an average annual growth rate of 16.38%. With the acceleration of the economic development, consumption increased rapidly along with the improved living standards, therefore, the rapid development of economy is the main driver of carbon emission augment after 2001 in China.

Except re-import and re-export final demand effect of all other industries increased during 2001-2013. Table 7 list top 10 industries in the emissions by final demand effect, and all these top 10 industries contributed 53.5% of emission increase by final demand effect. Construction was the highest industry in the effect and had a more than 171 billion dollars increase, which account for 21.36% of total emission increase. In fact construction is a pillar industry by Chinese government since middle of 1990s and often rank the first place in total outputs during last decade, and social demands for this industry have rise rapidly.

CONCLUSIONS

This paper analyzed the driver factors of carbon-dioxide emission increase during 1980-2013 in China, and based on the structural decomposition analysis (SDA), changes of carbon-dioxide emission had been studied by four driver factors: emission intensity effect, Leontief effect, demand allocation effect and final demand effect. By the analysis of SDA, key industries of leading to the changes of carbon-dioxide emissions were identified and some useful policies can be made by our study results. Some key points by our studies conclude following:

1) Final demand effect brought about 9.35 billion tons of the carbon-dioxide emission increase

during 1980-2013, and final demand effect and Leontief effect are the main driver of emission increase. While emission intensity effect contributed maximum in slowing down the increase of emission.

2) From the perspective of changing trends, the total amount of carbon dioxide emissions and four factors can be divided into three stages: 1980-1986, 1986-2001 and then 2001-2013, which tend to fluctuation from stable state in early years.

3) During 2001-2013 factors fluctuate significantly and total increases of emission came to 7.23 million tons, and contribute 77.4% of the total emission throughout the study duration. In this period the dominant industries in the emission reduction by emission intensity are energy-intensive, such as gas production, cement related products, electricity and transportation. While Leontief effect analysis shows that technological changes had contributed too little, and China economy still go ahead with input-intensive style. The demand allocation effect is the minimum factor influencing carbon emission in all four driver factors. Final demand is the most important factor for the carbon-dioxide emission during this period, and almost all industries led to the emission increase by final demand, in addition construction contributed a lot in this aspect.

4) To decrease the emission increase there are some alternative methods including the use of clean energy and promotion of increasing efficiency of energy use, encouraging technological changes, improving demand allocation structure. Moreover, closing obsolete low-tech old factory is another alternative strategy.

ACKNOWLEDGEMENTS

This work was supported by the National Social Science Fund of China (Grant No. 14CGL003), the National Nature Science Foundation of China (Grant No. 71804017), and the Nature Science Foundation of Beijing (Grant No. KZ20181005010).

REFERENCES

[1] Bolat, P., Bolat, F. (2017) Energy efficiency design index and co2 reduction trend assessment for Turkish flagged ships. Fresen. Environ. Bull. 26, 7065-7073.

[2] Timmer, M.P., Dietzenbacher, E., Los, B., Stehrer, R., de Vries, G.J. (2015) An Illustrated User Guide to the World Input–Output Database: The Case of Global Automotive Production. Review of International Economics. 23, 575–605.

[3] Martin, J.C., Becuwe, S. (2014) Regionalising the Results of a National Structural Decomposition Analysis of Greenhouse Gas Emissions: An Application to Aquitaine Region. Environ Model Assess. 19, 257–269.

[4] Leontief, W. (1970) Environmental Repercussions and The Economic Structure: An Input-Output Approach. Review of Economic Statistics. 52, 262–271.

[5] Camanzi, L., Alikadic, A., Compagnoni, L. (2017) The Impact of Greenhouse Gas Emissions in The EU Food Chain: A Quantitative and Economic Assessment Using An Environmentally Extended Input-Output Approach. Journal of Cleaner Production. 157, 168–176.

[6] Rocco, M.V., Colombo, E., Yan, J. (2016) Internalization of Human Labor in Embodied Energy Analysis: Definition and Application of A Novel Approach Based on Environmentally Extended Input-Output Analysis. Applied Energy. 182, 590-601.

[7] Kucukvar, M., Egilmez, G., Tatari, O. (2014) Sustainability Assessment of U.S. Final Consumption and Investments: Triple-Bottom-Line Input–Output Analysis. Journal of Cleaner Production. 81, 234-243.

[8] Hoekstra, R., Van Den Bergh, J.C.J.M. (2002) Structural Decomposition Analysis of Physical Flows in The Economy. Environmental and Resource Economics. 23, 357-378.

[9] Yuan, L., Xu, Y. (2013) A Structural Decomposition Analysis of CO_2 Emission in China: 2002-2007. Construction Engineering. 1, 1-5.

[10] Nie, H.G., Kemp, R., Vivanco, D.F., Vasseur, V. (2016) Structural decomposition analysis of energy-related CO_2 emission in China from 1997 to 2010. Energy Efficiency. 9, 1351-1367.

[11] Dietzenbacher, E., Los, B. (1998) Structural Decomposition Techniques: Sense and Sensitivity. Economic Systems Research. 10, 307-324.

[12] Lenzen, M., Kanemoto, K., Moran, D. (2012) Mapping The Structure of The World Economy. Environmental Science and Technology. 46, 8374-8381.

[13] Lenzen, M., Moran, D., Kanemoto, K. (2013) Building Eora: A Global Multi-Regional Input-Output Database at High Country and Sector Resolution. Economic Systems Research. 25, 20-49.

[14] Oosterhaven, J. (2004) On the Definition of Key Sectors and The Stability of Net Versus Gross Multipliers. Research Report.

[15] Afrasiabi, A., Casler, S.D. (1991) Product-Mix and Technological Change Within the Leontief Inverse. Journal of Regional Science. 31, 147-160.

[16] Nie, H., Kemp, R., Vivanco, D.F. (2016) Structural decomposition analysis of energy-related CO_2, emissions in China from 1997 to 2010. Energy Efficiency. 9, 1-17.

Received: **31.10.2018**
Accepted: **15.02.2019**

CORRESPONDING AUTHOR

Jie Hou
School of Economics and Management,
Beijing University of Technology,
Beijing – P.R. China

e-mail: 3311018809@qq.com

© by PSP Volume 28 – No. 4/2019 pages 2617-2624 Fresenius Environmental Bulletin

ESTIMATION OF GENETIC PARAMETERS AND GENETIC TREND OF HOLSTEIN FRIESIAN CATTLE POPULATION IN TURKEY

Serdar Genc[1,*], M Ihsan Soysal[2]

[1] Kirsehir Ahi Evran University, Faculty of Agriculture, Department of Agricultural Biotechnology, 40100, Kirsehir, Turkey
[2] Tekirdag Namik Kemal University, Faculty of Agriculture, Department of Animal Science, 59100, Tekirdag, Turkey

ABSTRACT

In this study, 194408 lactation and reproductive records of Holstein Friesian dairy cattle for the period of 1992-2012, which were taken from 23752 farms of Cattle Breeders Association of Turkey located in 10 cities, were evaluated. Variance components, breeding values, heritability, and repeatability of 305-day milk yield (305 DMY), lactation length (LL), dry period (DP), and calving interval (CI) were calculated by using MTDFREML. The effects of the factors (year of birth, lactation number, calving month, location, and calving age) that were thought to affect those traits (305 DMY, LL, DP, and CI) were evaluated. The heritability of 305 DMY, LL, DP, and CI was estimated as 0.22; 0.01; 0.01; and <0.01 respectively. Genetic trend for 305 DMY was also estimated as 7.44 kg/year. The estimated breeding values showed irregular fluctuations, but also the genetic trend increased in recent years. As a result, the estimated variance components, genetic parameters and breeding values could be used as selection criteria to increase the success of the selection in breeding studies for Holstein cattle population in Turkey.

KEYWORDS:
Holstein Friesian, heritability, variance components, breeding values, genetic trend

INTRODUCTION

Aiming to increase the yield taken from unit animal, animal breeding researches need to be examined [1]. Some parameters are needed in order to get successful results and provide the continuation of animal breeding [2]. At the first level, "present circumstances" are determined. Then, variation should be determined in terms of yield or yields about the subject. The rate of this variation is required to be determined based on rates of genotype or environment. If the genotype has high percentage, it needs to be determined which type of gene effects are important. At the second level of breeding process, "the reaching point" is determined. Then, many various programs are organized according to the quality of the data [3]. Correctly estimation of the given parameters depends on correct recording of performance of each animal and an increase on animal numbers used in yield control [4, 5]. Best Linear Unbiased Prediction (BLUP) is widely used on animal models about genetic evaluation of animals [6]. This method uses an animal's information of every relatives known and by that way it highens the hit rate or correctness of the prediction [7, 8]. The success of any breeding program is determined according to genetic improvement seen on populations of subsequent generations [9]. Determination of a genetic structure in a population has a close relationship with the methods used to calculate the predicted breeding value [8]. Thus, in this study, the variance component, genetic parameters, and breeding values of milk yield and progeny traits were predicted by using MTDFREML program by utilizing yield and lactation records of Holstein Friesian dairy cattle taken from Cattle Breeders Association of Turkey located in 10 cities for the period of 1992 - 2012, and the genetic trend was determined with the analysis of breeding values according to years.

MATERIALS AND METHODS

Material. In this study, including at least one province from each geographical region, 10 cities were chosen (Ankara, Antalya, Aydın, Balıkesir, Burdur, Erzurum, Tekirdag, Sanliurfa, Tokat, and Samsun). Yield records of Holstein Friesian dairy cattle of 23752 farms located in those cities were examined. Milk and reproductive records (birth date, calving date, 305-day milk yield (305 DMY), lactation length (LL), lactation number, calving age (CA), calving interval (CI), and dry period (DP)) were used in the present study. The data were obtained from a private farm, which is a member of the Cattle Breeders Association of Turkey. The relevant records covered the period from 1992 to 2012 and lactation number of 1-9.

TABLE 1
Data used in Evaluation and Descriptive Statistics

	Traits				Covariate
	305 DMY	**LL**	**CI**	**DP**	**CA**
Animal	114881	114881	50278	45976	114891
Dam	98067	98067	45075	41355	98074
Sire	4224	4224	2399	2351	4226
All Data	**194280**	**194280**	**78134**	**69381**	**194408**
$\overline{X} \pm S_{\overline{X}}$	6010±3.48	364.3±0,18	416.6±0.27	61.8±0.07	27,795±0,01
CV	25.50	22.27	18.38	28.72	

305 (DMY): 305-Day Milk Yield, LL: Lactation Length, DP: Dry Period, CI: Calving Interval, CA: Calving Age, CV: Coefficient of Variation

Preparation of the Data for Analyzing. Firstly, in the lactation and year groups, the animals whose numbers was less than 100, which gave a stillbirth, dismissed birth, and left from the herd because of the reasons such as illness and disability were excluded from the evaluation during the data preparation. The animals whose lactation length was longer than 600 days and shorter than 220 days, those whose calving age was younger than 20 months and older than 45 months for first lactation and the subsequent lactations, and those except for the ones with 12 months added to previous lowest level and 14 months added to the highest level were excluded from the analysis. Besides, the data concerning calving interval which was below 300 days and above 675 days were not used [10]. As a conclusion, in this study, 194408 lactation records among yield records of Holstein Friesian dairy cattle taken from 23752 farms were evaluated. Table 1 summarizes the data numbers used in these evaluations and descriptive statistics.

Statistical Analyses. First, the analysis of variance (General Linear Model, ANOVA) was used to determine the effect of calving age, calving month, calving year, city, and lactation number on 305 DMY, LL, CA, and DP. Minitab Version 14 and Step-Down Procedure were used in the analyses ($p<0.10$).

At the second stage, genotypic and phenotypic parameters were determined by using the Animal Model MTDFREML including the direct effect of the animal as well as the fixed factors considered as important in preliminary analyses [11]. At the third stage, the breeding values of the animals were predicted and genetic trend was calculated with the Best Linear Unbiased Prediction (BLUP).

Mathematical models of the environmental factors were given.

Model 1:

$Y_{ijklm}=\mu+a_i+c_j+d_k+ f_l +b_{yx}(X_{ijklm}- \overline{X})+e_{ijklm}$

where;

Y_{ijklm} : i. calving age, j. calving month, k. city, l. lactation number m. observation value of the cattle (305-day milk yield, lactation length, dry period, calving interval),

μ : population mean,

a_i : effect of i. calving year (i: 1-20; 1992-2012),

c_j : effect of j. calving month (j: 1-12; January - December),

d_k : effect of k. city (k: 1-10; Ankara, Antalya, Aydin, Balikesir, Burdur, Erzurum, Samsun, Tekirdag, Tokat, Sanliurfa),

f_l : effect of l. lactation number (l: 1-9; 1-9),

b_{yx} : regression coefficient of Y according to X (linear effect),

X_{ijklm} : m. calving age (covariate),

$\overline{X}$: mean of the population calving age

e_{ijklm} : error (random residual effect).

In addition to direct effect of animal and environmental factors which had significant effects, the permanent environmental factor belonging to the animal was added to the mathematical model (Model 2) as a random factor. Variance components, genetic parameters and mathematic model used on breeding value prediction were given below.

Model 2:

where

$Y_{ijklmno}= F_{ijkl}+a_m+P_n+e_{ijklmno}$

$Y_{ijklmno}$: observed values for traits,

F_{ijklm} : (fixed factors): explained in Model 1.

a_m : additive genetic effect of animal

P_n : environmental effect of animal

$e_{ijklmno}$: random residual error.

In Model 3, the variance components, genetic parameters, and matrix form of mathematic model used on breeding value prediction were given.

Model 3: $y=Xb+Za+Wc+e$

Where

y : observation vector,

X : pattern matrix for fixed factors,

b : vector of fixed effects,

Z : pattern matrix for random factors,

a : vector of random effects,

W : pattern matrix for environmental factor,

c : vector of environmental effects,

e : vector of random residual effect

Matrix form of Model 3 is given below.

$$E[y] = [Xb],$$

and

$$V\begin{bmatrix} a \\ c \\ e \end{bmatrix} = \begin{bmatrix} I\sigma_a^2 & 0 & 0 \\ 0 & I\sigma_c^2 & 0 \\ 0 & 0 & I\sigma_e^2 \end{bmatrix}$$

RESULTS

Variance Components, Heritability and Repeatability of Milk and Progeny Traits. Table 2 shows variance components, heritability and repeatability of 305 DMY, LL, DP and CI. Using several traits for dairy breeding is important in terms of reliability of the study. For this purpose, the mostly studied milk yield traits such as 305 DMY, LL, CI and the DP, one of the progeny traits were assessed. Traits of 305 DMY, LL, and CI were the parameters used to determine the economic yield levels of production units and also for breeding process. A production with a high income and a successful herd managing are based on DP, one of the traits of progeny yield.

Genetic Trend and Breeding Values for Milk and Progeny Yield Traits. Figure 1 shows the predicted average breeding value belonging to 305 DMY. The 24-year breeding values of Holstein Friesian Dairy Cattle varied between -1184 and 112 kg. While the highest breeding value belonging to cattle calving in the year of 2000 was determined as 112 kg, the lowest breeding value was determined as -1184 kg in 1988. For the Holstein Friesian Dairy Cattle, the genetic trend based on 305 DMY was determined as 7.44 kg/year.

TABLE 2
Variance Components, Heritability and Repeatability of Milk and Progeny Traits

	Variance Components				Heritability			Repeatability
	σ_a^2	σ_c^2	σ_e^2	σ_p^2	h^2	c^2	e^2	r
305 DMY (kg)	851569	6841	3039607	3898017	0.22	0.018	0.78	0.22
LL(day)	14772	671	1693214	1708657	0.01	0.004	0.99	0.01
DP (day)	133256329	99998439	13998530190	14231794958	0.01	0.070	0.98	0.02
CI (day)	133332959	98859939	13810765433	139042958331	<0.01	0.070	0.98	0.01

σ_a^2 : additive genetic variance, σ_c^2 : permanent environmental effect variance, σ_e^2 : residual variance (error), σ_p^2 : phenotypic variance, h^2 : heritability, c^2 : rate of permanent environmental variance, e^2 : residual error, r : repeatability, 305 DMY : 305-day milk yield, LL: Lactation length, DP: Dry period, CI: Calving Interval

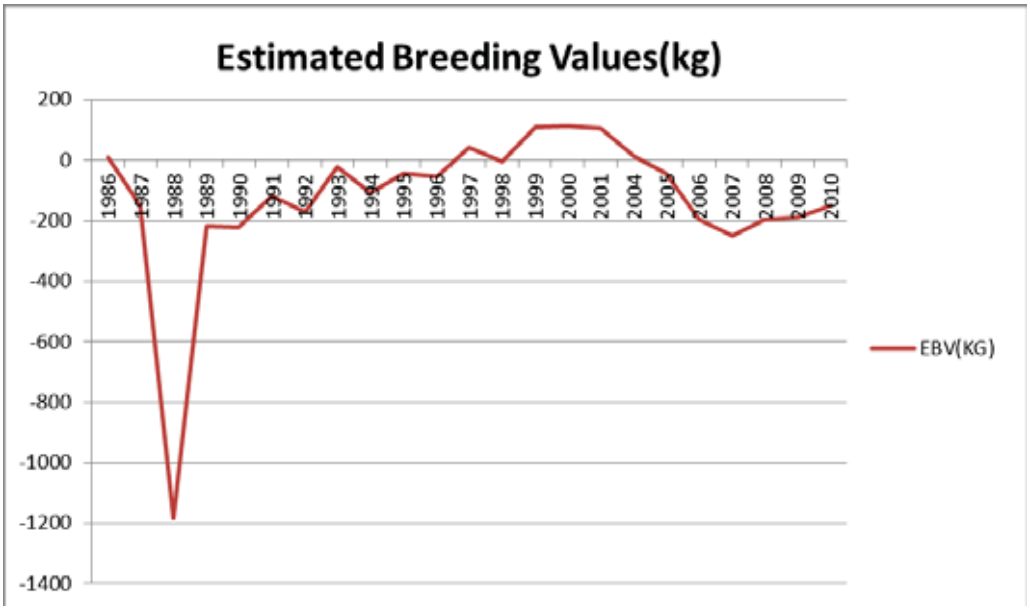

FIGURE 1
Estimated breeding value of 305 DMY according to birth year of Holstein Friesian Dairy Cattle

DISCUSSION

Heritability and Repeatability for 305 DMY. It was seen that there was similar to the national and international studies on one of milk yield traits, the 305 DMY (6010 kg) (Keskin and Boztepe 2011. [12] (5997 kg), Sahin and Ulutas 2011. [13] (6055 kg), Duru et al. 2012. [14] (6010 kg), Galic and Kumlu 2012. [15] (6100 kg), Zavadilova and Zink 2013. [16] (5870 kg)). Also, it was found to be high on the studies seperately conducted on different cities or enterprises throughout Turkey (Akman and Kumlu 2004 [1] (5772 kg), Javed et al. 2004. [17] (3391 kg), Oudah and Zainab 2010. [18] (2737 kg) Hossein-Zadeeh 2012. [19] (5093 kg), Katok and Yanar 2012. [20] (3408 kg) and Kaygısız 2013. [21] (5319 kg)). It was thought that mean 305 DMY of the study showed a recent increase about the milk yield in Turkey.

In the study, the heritability of 305 DMY among milk yield traits was found to be 0.22 in the Holstein Friesian Dairy Cattle. The results of the present study were found to be close to the values of previous studies [14, 16, 21, 22, 23, 24, 25, 26, 27, 28, 29, 30]. However, the heritability predicted for 305 DMY was lower than the values reported [15, 19, 31, 32]. Also, the heritability predicted for 305 DMY was higher than the values reported by [18, 30, 33, 34, 35, 36, 37, 38]. In terms of the desired traits during the breeding process, the heritability is required to be high. The heritability (0.22) of the 305 DMY observed in the study was average as is in many other international studies. High heritability calculated in terms of the studied traits will increase the rate of genotype to be transformed to next generation. By this way, the selection superiority will increase. Therefore, the use of 305 DMY as selection criterion as well as LL, DP and CI were required in the study in order to increase the yield.

In the study, the repeatability of 305 DMY of Holstein Friesian was found to be 0.2202, which was also close to the values reported by [14, 32]. However, it was lower than the values determined by [1, 7, 21, 31, 33, 37, 39, 40, 41, 42] and higher than those determined by [25]. All these effects on repeatability were associated with the inclusion of effect of the fixed environment into the model during the calculation of breeding value. Inclusion of the permanent environment effect to the model provided correct calculation of breeding values [40].

Heritability and Repeatability for LL. In the study, it was calculated that the heritability was 0.009 and repeatability was 0.01 for LL. These values were lower than the results obtained in similar studies [18, 35, 37, 43]. As it was expected, the heritability and repeatability belonging to LL were different and this was considered to be associated with high population number and thus, as the lactation prolonged, number of variation increased. In this case, it was considered that the environmental factors affecting these traits improved more.

Heritability and Repeatability for DP. In the study, the heritability and repeatability calculated as 0.01 and 0.0164 for dry period among Holstein Friesian dairy cattle's yield records, were lower than similar related studies [5, 44, 45, 46, 47, 48, 49]. Generally, on the herds of which the milk yield high may include low rates on progeny yields. In this case, initially, the influencing environmental factors, caring and breeding circumstances, and herd managements had to be improved. Genotypic structure can transmit to individuals, who will create the next generation, only as much as the degree of heritability For this reason, it was considered that along with individual data, the data of the relatives should be benefited from.

Heritability and Repeatability for CI. In the study, it was calculated that heritability and repeatability for calving interval were 0.01 and 0.0017 and were similar with some values in some studies similar [22, 29, 30, 35, 41, 49, 50, 51, 52, 53, 54]. Low heritability of CI affects negatively the selection success to be carried out by taking those traits into consideration. The incidence is reported to be low in the selection to be performed based on phenotypes of animals with low rate of heritability [55].

Breeding Value and Genetic Trend of 305 DMY. In the study, the genetic trend of 305 DMY of Holstein Friesian was determined as 7.44 kg/year. The results obtained in the study were similar with the values calculated by Kunaka et al., 2001. [56] as (8.36 kg/year), Dikmen 2004. [39] as (1.2 kg/year), Kunaka and Makuza 2005. [57] as (8 kg/year), Bakir and Kaygısız 2009. [58] as (7.99 kg/year) and Yousefi-Golverdi et al., 2012 [27] as (6.79 kg/year).

The genetic trend of 7.44 kg/year found for 305 DMY in Holstein Friesian was found to be higher than the values found by Katok and Yanar 2012. [20] as (3.73 kg/year), Sahin et al., 2012. [37] as (-2.46 kg/year), Hossein-Zadeh 2012. [19] as (5.97 kg/year) and Yousefi-Golverdi et al., 2012. [27] as (6.79 kg/year). However, the results of the study were lower than the values determined by Boligon et al., 2005. [59] as (9.25 kg/ year), Farhangfar and Rezaee 2006. [60] as (11 kg/ year), Naeemipour et al., 2006. [61] as (9 kg/ year), Bakır et al., 2009. [58] as (13.42 kg/ year), Oudah and Zainab 2010. [18] as (9.06 kg/ year), and Yaeghoobi et al., 2011. [24] as (19.61 kg/year). Also, the genetic trend was found to be quite lower

by the values reported by Khorshidie et al., 2012. [34] as (52.54 kg/year) and Ramatsoma et al., 2014. [62] as (24 kg/year). In terms of 305 DMY, the genetic trend was observed to be positive and high in some international studies. In order to achieve these increases in Turkey, it has been tried to show that the progeny control and breeding practices applied together with the breeder organizations should be made more carefully.

For this purpose, it is thought that the core herd breeding systems can be constructed in Cattle Breeders Association of Turkey and biotechnological advancements can be used as integrated in traditional breeding methods during selection of male and female cattle to be used as breeding. It needs attention whether or not the used semen is obtained from healthy bulls, is high quality, has a known breeding value and is tried

In this study, it was observed that mean breeding value on Holstein Friesian dairy cattle were negative in some years and were positive in some years. In addition to low genotypic progression value determined on Holstein Friesian, it was observed that there was a fluctuating change instead of ever increasing genotypic trend in following years. It was considered that animals having low genotypic structure were chosen as breeding animal in this period. In next periods, this case may be resulted from the usage of cattle whose breeding values are unknown. In case of not knowing or calculating the breeding values of females during the selection of cattle as breeding, it can be concluded that different criteria (based on phenotypic data) were used instead of pedigree records.

Also, estrous problems, progeny source and progeny quality can be regarded as reasons for not reaching the desired results at breeding values. Thus, width of production unit may cause low breeding values. The data of the study showed that the highest breeding value was calculated as 2475 kg/year in a large-scale production unit no: 1540005 located in Burdur city. The lowest breeding value was predicted as -670kg/year in a small-scale production unit no: 630007 in Sanliurfa city. A similar case was observed in the studies by [9,39,52] and it was stated that the low level of genetic trend was associated with the selection made based on low level of phenotypic values.

In the breeding studies based on selection, as the values of animals chosen as breeding have been determined to be higher than average of the herd and an improvement has been sought in the genetic structure of the herd [3]. Furthermore, it was expected that the studied traits of breeding animals chosen as the parent of next generation transmitted its progeny as the heritability to breeding animals [55]. As a result, it was expected that mean breeding values may increase annually based on breed in a period, evaluated yields and birth dates of grouped animals [40]. However, these results could not be obtained as expected from the study. Because, the observation values included a wide variation. It is thought that this result can be achieved only with a low number of production units which are well-managed, have the predetermined exact goals and are determined in accordance with all breeding and improvement strategies.

A similar result was obtained on a study conducted by Kumlu and Akman 1999 about Holstein Friesian Dairy Cattle for the period of 1987-1994. In these evaluations, consideration of the breeding values calculated with best linear unbiased prediction method instead of selection made based on phenotypic values of Jersey, Holstein Friesian and Brown Swiss Cattle will increase the success of the selection. The application of BLUP method on herd, the realization of selection and filtering based on analyses with BLUP, and recording of animal data as much as possible can provide a constant progress on genetic structure of herd.

CONCLUSION

Breeding values about the traits in breeding studies were calculated and these values were given attention so as to improve the necessary traits of genetic structure of the herd. Regarding the selection of animals going to be chosen as breeding, it is considered that the success can be improved on the selection to be applied by using biotechnological methods which can be integrated in breeding programs as well as breeding values determined based on phenotypic data in selection of breeding animals in farm members from Cattle Breeders Association of Turkey.

ACKNOWLEDGEMENTS

This article carried out part of Serdar GENÇs' Phd thesis in Namık Kemal University Institute of Natural Science and Department of Animal Science.

REFERENCES

[1] Akman, N., Kumlu, S. (2004) Genetic and phenotypic parameters of Turkey Friesian population about 305-day milk yield. Journal of Agricultural Sciences. 10(3), 281-286.
[2] Düzgüneş, O., Akman, N., Eliçin, A. (2012) Animal breeding. Ankara University Agricultural Faculty Department of Animal Science, Book. 1599(551), Ankara.
[3] Soysal, M.İ. (2005) Genetic principles of animal breeding. Trakya University, Tekirdag Agricultural Faculty, Book. Tekirdag, 48(40), 314p.

[4] Kumlu, S. (2000) Breeding and beef cattle. Turkey Cattle Breeders Central Association Publications. 3(166), Antalya.
[5] Ertuğrul, O., Orman M.N., Güneren, G. (2002) Some genetic parameters of milk yield in Holstein Cattle. Turk J. Vet. Anim. Sci. 26, 463-469.
[6] Searle, S.R. (1971) Linear models. John Wiley & Sons, Inc., New York-London-Sydney-Toronto. XXI, 532 S.
[7] Özyurt, A., Akman N. (2009) Use of different methods for estimation of breeding values and estimation of phenotypic and genetic parameters in dairy cattle. Journal of Tekirdag Agricultural Faculty. 6(3), 273-282.
[8] Grosu, H., Schaeffer, L., Oltenacu, P.A., Norman, D., Powell, R. Kremer, V., Banos, G. Mrode, R., Carvalheira, J., Jamrozik, J., Draganescu, C., Lungu, S. (2013) History of genetic evaluation methods in dairy cattle. Romania, 347p.
[9] Ulutas, Z. (2002) Estimation of genetic and phenotypic trends of 305-day milk yield for Holsteins reared at Gelemen State Farm in Turkey. Indian Journal of Animal Sciences. 72(10), 875-877.
[10] Kumlu, S., Akman, N. (1999) Milk yield and reproductive traits of Holstein Friesian breeding herds in Turkey. Lalahan Hay. Araşt. Enst. Derg. 39(1), 1-15.
[11] Boldman, K.G., Kriese, L.A., Van-Vleck, L.D., Kacman, S.D. (1995) Amanual for Use of MTDFREML, USD-ARS, Clay Center, Nebraska, USA.
[12] Keskin, İ., Boztepe S. (2011) Estimation of 305 days milk yield using partial milk yield in Holstein Cattle. Journal of Tekirdag Agricultural Faculty. 8(1),1-7.
[13] Şahin, A., Ulutaş Z. (2011) Some enviromental factors affecting the milk yield and reproductive traits of Holstein Cattle raised at Tahirova State Farm. Anadolu J Agr Sci. 26(2), 156-168.
[14] Duru, S., Kumlu, S., Tuncel, E. (2012) Estimation of variance components and genetic parameters for type traits and milk yield in Holstein Cattle. Turk. J. Vet. Anim. Sci. 36(6), 585-591.
[15] Galiç, A., Kumlu, S. (2012) Application of a random regression model to estimation of genetic parameters of test day milk yields of Turkish Holstein Firesians. Journal of the Faculty of Veterinary Medicine, Kafkas University. 18(5), 719-724.
[16] Zavadilová, L., Zink, V. (2013) Genetic relationship of functional longevity with female fertility and milk production traits in Czech Holsteins. Czech J. Anim. Sci. 58(12), 554–565.
[17] Javed, K., Afzal, M., Sattar, A., Mirza, H. (2004) Environmental factors affecting milk yield in Friesian Cows in Punjab. Pakistan Vet. J. 24(2).
[18] Oudah, E.Z.M., Zainab, A.K. (2010) Genetic evaluation for Friesan Cattle in Egypt using single-trait animal model. J. Animal and Poultry Production, Mansoura University. 1(9), 371-381.
[19] Hossein-Zadeh, N.G. (2012) Genetic Parameters and trends for lactation length in the first three lactations of Holstein Cows. Archiv Tierzucht. 55(6), 533-539.
[20] Katok, N., Yanar, M. (2012) Milk traits and estimation of genetic, phenotypic and environmental trends for milk and milk fat yields in Holstein Friesian Cows. International Journal of Agriculture and Biology. ISSN Online: 1814–9596. 14(2), 311–314.
[21] Kaygısız, A. (2013) Estimation of genetic parameters and breeding values for dairy cattle using test-day milk yield records. The Journal of Animal and Plant Sciences. 23(2), 345-349.
[22] Hossein-Zadeh, N.G. (2011) Estimation of genetic and phenotypic relationships between age at first calving and productive performance in Iranian Holsteins. Trop Anim Health Prod. 43, 967–973.
[23] Pirzada, R. (2011) Estimation of genetic parameters and variance components of milk traits in Holstein-Friesian and British-Holstein dairy cows. Kafkas Univ. Vet. Fak. Derg. 17(3), 463-467.
[24] Yaeghoobi, R., Doosti, A., Noorian, A.M., Bahrami, A.M. (2011) Genetic parameters and trends of milk and fat yield in holstein's dairy cattle of West Provinces of Iran. International Journal of Dairy Science. ISSN: 1811-9743. 6(2),142-149.
[25] Banos, G., Coffey, M.P., Veerkamp, R.F., Berry, D.P., Wall, E. (2012) Merging and characterizing phenotypic data on conventional and rare traits from dairy cattle experimental resources in three countries. Animal. 6(7), 1040–1048.
[26] Rönnegard, L., Felleki, M., Fikse, W.F., Mulder, H.A., Strandberg, E. (2012) Variance component and breeding value estimation for genetic heterogeneity of residual variance in Swedish Holstein Dairy Cattle. J. Dairy Sci. 96, 2627–2636.
[27] Yousefi-Golverdi, A., H. Hafezian, Y. Chashnidel, and A. Farhadi (2012) Genetic Parameters and Trends of Production Traits in Iranian Holstein Population. African Journal of Biotechnology. 11(10), 2429-2435.

[28] Bastin, C., Soyeurt, H., Gengler, N. (2013) Genetic parameters of milk production traits and fatty acid contents in milk for Holstein Cows in parity 1 – 3. J. Anim. Breed. Genet. ISSN 0931-2668. 130(2013), 118-127.
[29] Tiezzi, F., Pretto, D., Marchi, M.D., Penasa, M., Cassandro, M. (2013) Heritability and repeatability of milk coagulation properties predicted by mid-infrared spectroscopy during routine data recording, and their relationships with milk yield and quality traits. Animal. 7(10), 1592–1599.
[30] Nilforooshan, M.A., Jakobsen, J.H., Fikse, W.F., Berglund, B., Jorjani, H. (2014) Multiple-trait multiple-country genetic evaluation of Holstein Bulls for female fertility and milk production traits. Animal. 8(6), 887–894.
[31] Bakır, G., Kaygisiz, A. (2009) Estimation of genetic and phenotypic trends, heritability and repeatability for some milk production traits of Holsteins. Journal of the Faculty of Veterinary Medicine, Kafkas University. 15(6), 879-884.
[32] Irano, N., Braga, B.A., El Faro, L., Luiz, S.M., Lúcia, C.V., Albuquerque, L.G. (2014) Genetic association between milk yield, stayability and mastitis in Holstein Cows under tropical conditions. Trop. Anim Health Prod. 46, 529–535.
[33] Ghorbani, A., Ashtiani, S.M., Noubr, S., Shahriar, A.H., Nikzad, S. (2011) Estimation of genetic parameter in Iranian Holstein crossbred dairy cattle. African Journal of Microbiology Research. 5(12), 1568-1570.
[34] Khorshidie, R., Shadparvar, A.A., Hossein-Zadeh, N.G., Shakalgurabi, S.J. (2012) Genetic trends for 305-day milk yield and persistency in Iranian Holsteins. Livestock Science. 144, 211–217.
[35] Toghiani, S. (2012) Genetic relationships between production traits and reproductive performance in Holstein Dairy Cows. Archiv Tierzucht. ISSN 0003-9438. 55(5), 458-468.
[36] Pretto, D., Lo´ pez-Villalobos, N., Penasa, M., Cassandro, M. (2012) Genetic response for milk production traits, somatic cell score, acidity and coagulation properties in Italian Holstein–Friesian Population undercurrent and alternative selection indices and breeding objectives. Livestock Science. 150, 59–66.
[37] Sahin, A., Ulutas, Z., Yilmaz, A.A., Adkinson, R.W. (2012) Genetic and environmental parameters and trends for milk production of Holstein Cattle in Turkey. Italian Journal of Animal Science. 11(44).
[38] Kheirabadi, K., Alijani, S. (2014) Genetic parameters for milk production and persistency in the Iranian Holstein Population by the multitrait random regression model. Archiv Tierzucht. 57(12), 1-12.
[39] Dikmen, S. (2004) Implementation of best linear prediction method for the determination of breeding value of holsteins milk yield in Karacabey and Tahirova Agricultural Institute. (Phd Thesis), Uludag University, Healt Institute, Bursa.
[40] Ulutaş, Z., Akman, N., Akbulut, Ö. (2004) Estimates of genetic and environmental (co)variances for 305-day milk yield and calving intervals in Holstein Fresian Cattle. Turkish Journal of Veterinary and Animal Sciences. 28(1), 101-105.
[41] Tekerli, M., Gündoğan, M. (2005) Effect of certain factors on productive and reproductive efficiency traits and phenotypic relationships among these traits and repeatabilities in West Anatolian Holsteins. Türk J. Vet. Anim Sci. 29, 17-22.
[42] Hashemi, A., Nayebpoor, M. (2008) Estimates of genetic and phenotype parameters from milk production in Iran Holstein-Friesian Cows. Research Journal of Biological Sciences. 3(6), 678-682.
[43] Hossein-Zadeh, N.G. (2012) Estimation of genetic parameters and trends for energy-corrected 305-d milk yield in Iranian Holsteins. Archiv Tierzucht. ISSN 0003-9438. 55(5), 420-426.
[44] Atıl, H., Khattab, S.A., Yakupoğlu, Ç. (2001) Genetic analysis for milk traits in different herds of Holstein Freisian Cattle in Turkey. On Line Journal of Biological Sciences. 1(8), 737-741.
[45] Veerkamp, R.F., Koenen, E.P.C., De Jong, G. (2001) Genetic correlations among body condition score, yield, and fertility in first-parity cows estimated by random regression models. Journal of Dairy Sci. 84(10), 2327-2335.
[46] Chonkasikit, N. (2002) The impact of adaptive performance on Holstein Breeding in Nothern Thailand. Phd. Thesis. Georg August University, Göttingen, Germany.
[47] Haile, M.M., Morton, J.M., Goddart, M.E. (2003) Estimates of genetic parameters for fertility traits of Australian Holstein Friesian Cattle. Animal Science. 76, 35-42.
[48] Van-Raden, P.M., Sanders, A.H., Tooker, M.E., Miller, R.H., Norman, H.D., Kuhn, M.T., Wiggans, G.R. (2004) Development of a national genetic evaluation for cow fertility. J. Dairy Sci. 87, 2285-2292.
[49] Gonzalez, R.O., Alenda, R. (2005) Genetic parameters for female fertility traits and a fertility index in Spanish Dairy Cattle. J. Dairy Sci. 88, 3282-3289.
[50] Atıl, H., Khattab, A.S. (2005) Estimation of genetic trends for productive and reproductive traits of Holstein Friesian Cows in Turkey. Pakistan Journal of Biological Sciences. 8(2), 202-205.

[51] Biffani, S., Canavesi, R., Samore, A.B. (2005) Estimates of genetic parameters for fertility traits of Italian Holstein Friesian Cattle. Izlaganje Sa Znanstvenog Skupa Conference Paper, Udk 636.082. Stocarstvo. 59(2), 145-153.
[52] Amimo, J.O., Mosi, R.O., Wakhungu, J.W., Muasya, T.K., Inyangala, B.O. (2006) Phenotypic and genetic parameters of reproductive traits for Ayrshire Cattle on large-scale farms in Kenya. Livestock Research for Rural Development. 18(10).
[53] Tekerli, M., Koçak, S. (2009) Relationships between production and fertility traits in first lactation and life time performances of Holstein Cows under subtropical condition. Archiv Tierzucht. ISSN: 0003-9438. 52(4), 364-370.
[54] Perez-Cabal, M.A., Garcia, C., Gonzalez, R.O., Alenda, R. (2006) Genetic and phenotypic relationships among locomotion type traits, profit, production, longevity, and fertility in Spanish Dairy Cows. J. Dairy Sci. 89, 1776-1783.
[55] Şahin, A. (2009) Genetic and phenotypic parameter estimation of fertility and dairy production traits of different dairy cattle breeds reared at state farms in Turkey. Phd Thesis. Gaziosmanpasa University, Naturel Science Institute, Tokat.
[56] Kunaka, K., Makuzo, S.M., Wallny, C.B.A., Bando, J.W. (2001) Genetic trends for milk, fat and protein in the Zimbabwean Holstein Freisian population from 1973 to 1994. Archives of Animal Breeding. 44(1), 1-8.
[57] Kunaka, K., Makuza, S.M. (2005) Genetic and environmental trends for milk traits in The Zimbabwean Holstein Friesian Population. Pakistan Journal of Biological Sciences. 8(7), 1011-1015.
[58] Bakır, G., Kaygisiz, A. Çilek, S. (2009) Estimates of genetic trends for 305-days milk yield in Holstein Friesian Cattle. Journal of Animal and Veterinary Advances. ISSN: 1680-5593. 8(12), 2553-2556.
[59] Boligon, A.A., Rorato, P.R.N., Ferreira, G.B.B., Weber, T., Kippert, C.J., Andreazza, J. (2005) Heritability and genetic trend for milk and fat yields in Holstein Herds raised in The State of Rio. Grande Do Sul R. Bras. Zootec. 34(5), 1512-1518.
[60] Farhangfar, H., Rezaee, H. (2006) Comparison of lactation and test day models for genetic evaluation of 305-day milk trait in Iranian Holstein Heifers. J. Anim. Sci. 84(Suppl. 1).
[61] Naeemipour, H., Farhangfar, H., Moravej, H., Rokoei, M. (2006) Estimation of phenotypic and genetic trends for milk and fat yield traits in Khorasan Province Holsteins of Iran by using a univariate model. J. Anim. Sci. 84(Suppl. 1).
[62] Ramatsoma, N.I., Banga, C.B., Mac-Neil, M.D., Maiwashe, A. (2014) Evaluation of genetic trends for traits of economic importance in South African Holstein Cattle. South African Journal of Animal Science. 44 (1).

Received: **02.11.2018**
Accepted: **20.02.2019**

CORRESPONDING AUTHOR

Serdar Genc
Kirsehir Ahi Evran University,
Department of Agricultural Biotechnology,
40100, Kirsehir – Turkey

e-mail: serdargenc1983@gmail.com

© by PSP Volume 28 – No. 4/2019 pages 2625-2632 Fresenius Environmental Bulletin

STUDY ON MEASURES TO IMPROVE WATER QUALITY IN URBAN LAKES: CASING IN LAKE NANHU IN WUHAN

Hao Huang[1,*], Fan Wan[1], Yan Gao[1], Zhenxing Zhong[2], Shohrat Annanurov[2], Xiangguo Zeng[1]

[1]Wuhan Planning and Design Company, Wuhan, 430014, China
[2]School of Environmental Science and Engineering, Huazhong University of Science and Technology, Wuhan, 430074, China

ABSTRACT

Water pollution is an important factor that plagues urban development and affects human settlements. This study takes Lake Nanhu in Wuhan, China as an example to discuss the water quality improvement of typical urban park lakes. Based on the monitoring results of the water quality in the lake and the quantitative analysis of the pollutant sources in the basin, the engineering measures under various scenarios are proposed as well as the corresponding pollutant reduction. The results show that the total nitrogen (TN) environment capacity of the lake is 315.2 t/a and the total phosphorus (TP) environment capacity is 21.01 t/a, which are calculated by Dillon model. Under the circumstance of the tail water from sewage treatment plant transferring from Lake Nanhu to the Yangtze River, 60% of TN from sediment release and domestic sewage interception are controlled, 67.3% from surface runoff pollution are reduced, the TN emission can be controlled below the water environment capacity and its concentration can reach 1.5mg/L. When the tail water from sewage treatment plant transferring from the lake to river, 75% of TP from domestic sewage and sediment release are controlled, and the reduction rate of TP from surface runoff pollution is 87%, the TP emission can be controlled below the water environment capacity and its concentration can reach 0.1 mg/L. After then, the environment and ecology of the lake can be improved. The feasibility plan of water quality improvement in this lake obtained in this paper can provide experience and case reference for the treatment of the same urban park-type lakes.

KEYWORDS:
Water quality improvement, Urban lakes, Environment capacity

INTRODUCTION

In the past half century, many lakes in the world have suffered from excessive nitrogen, phosphorus and other pollution loads, and the irrational human activities have affected these lakes [1]. The water quality of the lake has decreased significantly and its ecosystem has been degraded. Water environment and ecological security have become one of the major environmental issues that constrain the sustainable development of global and regional economy [2, 3].

Researchers have accumulated a lot of valuable experience in the long-term exploration of lake pollution and treatment [4-6]. In the treatment of Lake Biwa Ko [7], Lake Kasumigaura [8] and Lake Aberka [9], a series of ecological restoration techniques were adopted (such as capturing sand sac and biological manipulation to achieve phosphorus removal and nitrogen removal) to improve lake water transparency and reducing nutrient cycling. At the same time, to reduce the algae biomass and improve water quality by reducing the feeding pressure of fish on zooplankton [10]. The management of lakes requires the development of a scientific plan. Governance of the *Biwa Ko Comprehensive Maintenance and Maintenance Plan* in Japan has established a phased governance goal for lakes [11]. There have been serious blue-green algae pollution in Lake Veluwe in the Netherlands, the lake is muddy, the flora and fauna are drastically reduced, and the lake ecology has been seriously damaged. In the early stages of the project, two sewage treatment plants were built around Lake Veluwe to reduce the input of exogenous phosphorus. However, only reducing the external input cannot quickly restore the lake ecology. In order to reduce the release of internal phosphorus, the lake is diluted in the winter [12]. After the implementation of sewage interception and diversion dilution project in Lake Moses in the United States and Lake Bled in Slovenia, the eutrophication of lake has fundamentally improved [13-14]. The treatment measures of Lake Trummen in Sweden [15] are mainly the dredging of sediments in the whole lake. In the process of urban park lake treatment, the sediments that contaminated by heavy metals in the surface are usually placed in depressions, and then covered with deep uncontaminated sediments. The remaining sediments are constructed in the southern part of the lake to increase the storage of oxygen in the lake and to reduce frequent deaths of fish [16]. The single sediment-dredging project cannot achieve the goal of continuous improvement

FIGURE 1
Location of Lake Nanhu

in the water environment. Lake Finjasjon has undergone more than 40 years of treatment. Through the sediment-dredging project, regulating the structure of the food chain and constructing artificial wetlands, the water quality is gradually improved [17-18].

The development of Chinese economy in recent years has been accompanied by serious environmental pollution [19, 20]. As a typical inland city in China, Wuhan is also facing the same serious problems of water pollution. Lake Nanhu in this study is located in the concentrated construction area and belongs to the typical urban park lake. At present, the water quality of this lake has been inferior to Level V in *Environmental Quality Standards for Surface Water (GB3838-2002)* (TN≤2.0mg/L; TP≤0.2mg/L), which has lost its function as water in urban parks. This paper proposes a feasible plan for improving the water quality of this lake through quantitative analysis to restore the function of its water.

POLLUTION STATUS IN LAKE NANHU

Brief Overview. Lake Nanhu, a freshwater lake formed by river siltation, is located in the main urban area of Wuhan, southeast of the Yangtze River. The geographic coordinates of the lake are 114°22′12.46″N, 30°29′36.37″W. The current location of it is shown in Figure 1. The water area of this lake is 7.67 km^2, the east-west span is about 7.9km, and the north-south span is about 4.2km. Catchment area of the basin is 37.44 km^2 and the water surface rate is 20.5%. The lake has a normal water level of 18.65m and a maximum water level of 19.65m (the Yellow Sea Height System). The population in the catchment area is 469,700 and the population density is 12,545 person/km^2.

The pollution sources of Lake Nanhu can be divided into point source, non-point source pollution and internal pollution source: 1. point source pollution mainly comes from the sewage treatment plant, which is located in the north of this lake. The average daily discharge of tail water from the sewage treatment plant is up to 300,000 cubic meters. The overflowing domestic sewage around this lake is also an important part of point source pollution. 2. Non-point source pollution is mainly based on initial rain. At present, there is still a mixed flow of rain and sewage in the confluence area of Lake Nanhu. The low rate of small flow and large section causes the deposition of pollutants in the rainwater pipeline. When heavy rain occurs, it is discharged into the water with the convergence of rainwater. 3. Internal pollution mainly comes from lake sediments. The organic matter, TN and TP in the sediments of Lake Nanhu have a significant negative impact on the water quality.

Monitoring of the water quality. In August 2017, the monitoring of the water quality for Lake Nanhu was carried out. The monitoring project included eight items, which are temperature, pH, dissolved oxygen, transparency, COD, ammonia nitrogen, TN and TP. According to the size of the water area and the shape of the lake, 15 monitoring points are set. The monitoring points of Lake Nanhu are shown in Figure 2, and the results are shown in Table 1.

It can be seen from Table 1 that the TN and TP in the typical pollutants are of the highest surpassing times, so it is necessary to carry out the pollution sources of TN and TP in Lake Nanhu.

Sources of pollutants in the catchment area. I. Total nitrogen. Through investigation and monitoring, it can be concluded that the TN discharge of domestic sewage in the Lake Nanhu catchment is about 503.9 t/a. According to the water quality of the sewage treatment plant in the district, the TN output from the tail water of the sewage treatment plant was calculated to be 817.3 t/a. By analysis on the land use

function in the catchment area of Lake Nanhu, combined with the rainfall intensity (1269mm/a) in Wuhan, the amount of TN from the surface runoff pollutants is calculated to be 276.1 t/a. According to the air quality situation in Wuhan, the amount of TN from the dust pollution is 1.8 t/a. Through monitoring and analysis of the sediment in Lake Nanhu, the TN content released from the sediment is about 53.8t/a. The current situation of the TN pollution sources in Lake Nanhu is shown in Table 2. The proportion of different sources of TN pollution is shown in Figure 3.

FIGURE 2
Nanhu water quality monitoring layout map

TABLE 1
Nanhu water quality monitoring results

Test items	Temperature (℃)	pH	DO (mg/L)	Transparency (m)	COD (mg/L)	NH_4^+-N (mg/L)	TN (mg/L)	TP (mg/L)
1#	31.1	7.88	5.33	0.43	33	1.94	5.55	0.255
2#	30.0	7.74	5.76	0.44	32	2.42	6.93	0.411
3#	30.2	8.42	5.39	0.43	31	2.21	6.33	0.283
4#	29.9	8.54	5.78	0.41	31	1.87	5.35	0.365
5#	29.8	8.43	3.03	0.36	34	2.81	8.31	0.328
6#	29.2	8.51	3.42	0.35	34	2.82	8.35	0.301
7#	29.5	8.26	3.16	0.34	35	2.79	8.27	0.356
8#	29.5	8.48	5.64	0.40	35	1.98	5.67	0.393
9#	29.6	8.54	5.61	0.42	34	2.07	5.95	0.411
10#	29.2	8.59	4.95	0.44	32	2.84	8.42	0.494
11#	28.9	8.36	5.31	0.40	33	1.89	5.42	0.374
12#	29.5	8.81	5.04	0.42	31	1.77	5.08	0.301
13#	28.8	8.16	4.89	0.39	34	1.71	4.91	0.283
14#	29.1	8.20	5.61	0.44	35	1.87	5.35	0.273
15#	29.0	7.92	5.37	0.41	33	1.84	5.27	0.310

Compared with Level IV in *Environmental Quality Standards for Surface Water (GB3838-2002)* (COD＜30mg/L, NH_4^+-N＜1.5mg/L, TN＜1.5mg/L, TP＜0.1mg/L).

TABLE 2
Current Status of TN Pollutants in Lake Nanhu

	Source of pollution	amount
Amount of external pollutants(t/a)	Sewage treatment plant tail water	817.3
	Domestic sewage discharge	503.9
	Surface runoff pollution	276.1
	Dust pollution	1.8
Amount of internal pollutants(t/a)	Sediment pollution release	53.8
Total		1652.9

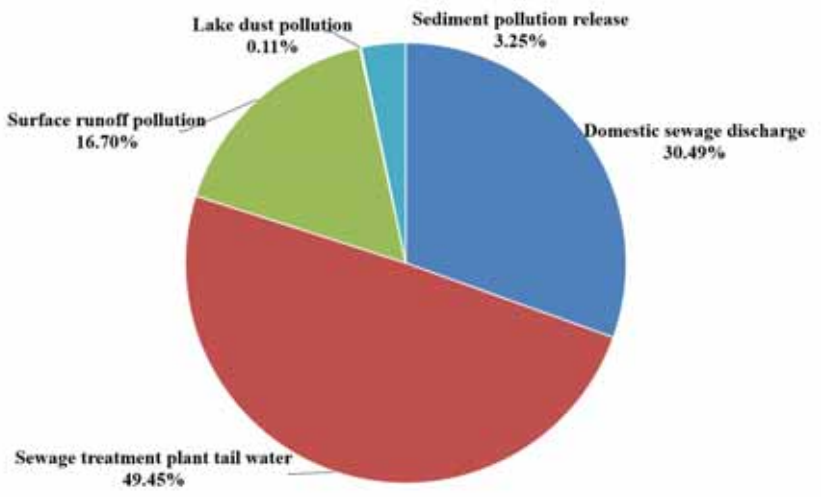

FIGURE 3
Sources of TN pollution

TABLE 3
Status of TP pollutants in Lake Nanhu

	Source of pollution	amount
Amount of external pollutants(t/a)	Sewage treatment plant tail water	22.703
	Domestic sewage discharge	66.689
	Surface runoff pollution	17.155
	Dust pollution	0.317
Amount of internal pollutants(t/a)	Sediment pollution release	8.403
Total		115.267

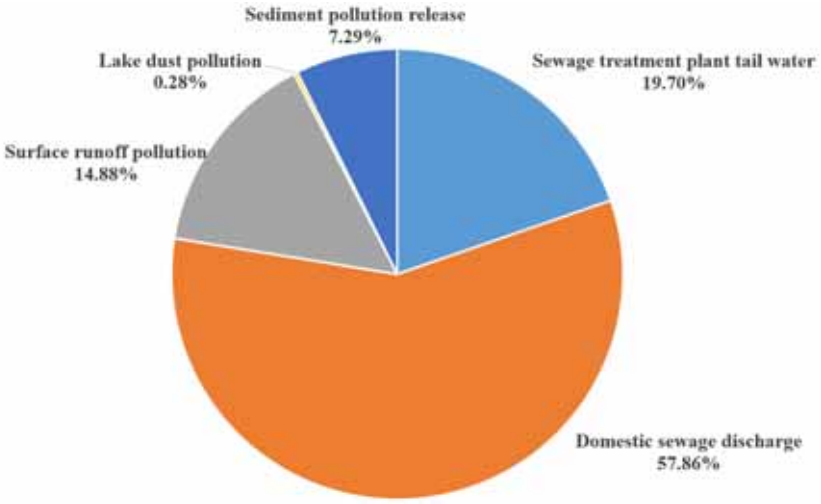

FIGURE 4
Sources of TP pollution

II. Total phosphorus. According to the monitoring data in Table 1, Lake Nanhu not only has the status of TN exceeding the standard, but the TP also exceeds the standard. Therefore, this paper carried out an analysis on different sources of TP pollution for this lake. After investigation and monitoring, it was concluded that the TP discharge of domestic sewage in its confluence area was about 66.69 t/a. Combined with the tail water quality of the sewage treatment plant, the TP content of the tail water into the lake was calculated to be 22.70t/a. Through the land use function in the catchment area of Lake Nanhu, combined with the rainfall intensity (1269 mm/a) in Wuhan, the amount of TP from the surface runoff pollutants is calculated to be 17.16t/a. According to the air quality situation in Wuhan, the amount of TP in the dust pollution is 0.32 t/a. Through the monitoring and analysis of the sediment in this lake, the TP released from the sediment is about 8.40t/a. The status quo of the TP pollution sources in the lake is shown in Table 3. The proportion of different sources of TP pollution is shown in Figure 4.

SYSTEM MEASURES FOR WATER ENVIRONMENT IMPROVEMENT

Environment capacity calculation. In order to formulate scientific measures, according to the analysis on the source of pollutants in Lake Nanhu, it is necessary to grasp the water environment capacity quantitatively. The Dillon model is usually used to calculate the water environment capacity of nitrogen and phosphorus for the eutrophic lake. The Aida Ken model should be used to calculate the water environment capacity of nitrogen and phosphorus, where the water exchange capacity is weak. According to the actual situation of Lake Nanhu, this study selected Dillon model to calculate the environment capacity.

The formula of the Dillon model is:

a. The water environment capacity of nitrogen or phosphorus in a lake can be calculated as Equation 1.

$$M_N = L_s \bullet A \quad (1)$$

Where M_N: nitrogen and phosphorus water environment capacity, t/a;
L_S: environment capacity of nitrogen and phosphorus in a unit water area of the lake, mg/m^2.a;
A: water area of a lake, m^2.

b. Water environment capacity of nitrogen and phosphorus in a unit water area of the lake can be calculated in Equation 2.

$$L_s = \frac{P_s \bullet h \bullet Q_a}{(1-R_p) \bullet V} \quad (2)$$

P_S: the annual average target concentration of phosphorus and nitrogen in a lake, g/m^3;
h: average depth of the lake, m.
Q_a: annual water flow of a lake, m^3/a;
R_p: retention coefficient of nitrogen and phosphorus in a lake, 1/a;
V: annual capacity of a lake, m^3.

c. the retention coefficient R_p of nitrogen and phosphorus in a lake can be calculated as shown in Equation 3.

$$R_p = 1 - \frac{W_{out}}{W_{in}} \quad (3)$$

W_{out}: the amount of nitrogen and phosphorus flowing out of the lake, t/a;
W_{in}: the amount of nitrogen and phosphorus flowing into the lake, t/a;

d. The average concentration of nitrogen and phosphorus in a lake can be calculated as shown in Equation 4.

$$P = \frac{L_p \bullet (1-R_p)}{\beta \bullet h} \quad (4)$$

P: average concentration of nitrogen and phosphorus in the lake, g/m^3;
Lp: annual load of nitrogen and phosphorus in unit area in the lake, g/m^2.a;
R_p: retention coefficient of nitrogen and phosphorus in the lake, 1/a;
β: hydraulic erosion coefficient, 1/a;
h: average depth of the lake, m.

e. The hydraulic erosion coefficient can be calculated as shown in Equation 5.

$$\beta = \frac{Q_a}{V} \quad (5)$$

Q_a: annual water flow of a lake, m^3/a;
V: annual volume of a lake, m^3.

According to the Dillon model, the TN and TP environment capacity of Lake Nanhu is shown in Table 4.

TABLE 4
TN and TP environment capacity of Lake Nanhu

Contaminant	TN	TP
Environment capacity(t/a)	315.2	21.012

TN control. In order to achieve the goal of water quality improvement in Lake Nanhu, combined with the calculation results of the environment capacity, the reduction plan under various scenarios was established to achieve reasonable engineering countermeasures.

In order to make the water quality of Lake Nanhu reach Class IV (TN<1.5mg/L), it is necessary to reduce the pollution load generated by different sources of TN. Through the analysis of environment capacity, concentration of TN corresponding to pollution load in different scenarios is shown in Table 5.

Scenario 1: The diversion of the tail water from the sewage treatment plant into the Yangtze River can reduce the TN load of 817.3t/a. In the case of all the tail water of the sewage treatment plant is reduced, the TN input into the lake is still as high as 835.6 t/a, which is under the case other conditions remain unchanged. The TN concentration in the water quality of Lake Nanhu is expected to decrease to 3.98 mg/L, which cannot be satisfied to Class IV water quality requirements. Scenario 2: On the basis of the tail water discharge of the sewage treatment plant fully reduced, the interception work of the sewage pollutants in Lake Nanhu will be completed, and other conditions are maintained, then the TN load of 503.9t/a will be reduced. The TN concentration is expected to be further reduced to 1.58 mg / L, which is still unable to meet the Class IV water quality requirements. Scenario 3: If the internal source sediment pollution can be further controlled, that is, the TN load of 53.8 t/a will be further reduced, the TN concentration in the lake is expected to be reduced to 1.32 mg/L, meeting the IV water quality requirements.

However, in the actual process, it is impossible to avoid the mismatch of rainwater and sewage pipelines. The discharge of domestic sewage pollutants

cannot be completely controlled by 100%. Similarly, dredging of sediments cannot be completely eliminated. Therefore, based on the tail water drained from the sewage treatment plant, 60% of the TN control in the discharge of domestic sewage and sediment pollution is completed, and then the 67.3% of the amount of non-point source pollutants into the lake is reversed according to the material conservation of TN. Then, the TN concentration in Lake Nanhu is expected to drop to 1.5 mg/L. The relationship between the specific reduction amount and the TN concentration is shown in Table 5. The reduction of TN in different scenarios is shown in Figure 5.

TP control. In order to make the water quality of Lake Nanhu reach Class IV, it is necessary to reduce the pollution load generated by different sources of TP. Through the analysis of the environment capacity of the lake, TP concentration corresponding to pollution load in different scenarios is shown in Table 6.

TABLE 5
Concentration of TN corresponding to pollution load in different scenarios

	Source of pollution	status quo	Scenario 1	Scenario 2	Scenario 3	Scenario 4
Amount of external pollutants(t/a)	Tail water from sewage treatment plant	817.3	0.0	0.0	0.0	0.0
	Domestic sewage discharge	503.9	503.9	0.0	0.0	201.6
	Surface runoff pollution	276.1	276.1	276.1	276.1	90.3
	Dust pollution	1.8	1.8	1.8	1.8	1.8
Amount of internal pollutants(t/a)	Sediment pollution release	53.8	53.8	53.8	0.0	21.5
TN load into the lake(t/a)		1652.9	835.6	331.7	277.9	315.2
Estimated TN concentration(mg/L)			3.98	1.58	1.32	1.50

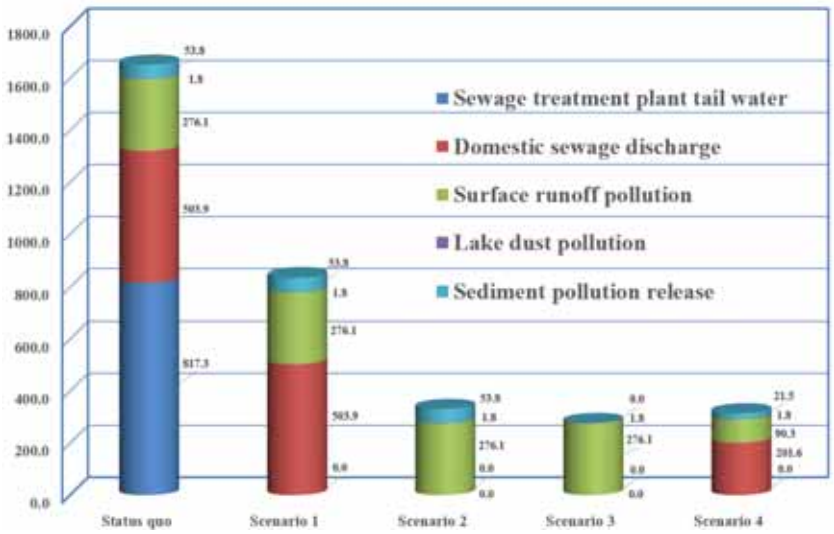

FIGURE 5
TN reduction under different scenarios

TABLE 6
TP concentration corresponding to pollution load in different scenarios

	Source of pollution	Status quo	Scenario 1	Scenario 2	Scenario 3	Scenario 4
Amount of external pollutants(t/a)	Tail water from sewage treatment plant	22.703	0.0	0.0	0.0	0.0
	Domestic sewage discharge	66.689	66.689	0.0	0.0	16.703
	Surface runoff pollution	17.155	17.155	17.155	17.155	3.431
	Dust pollution	0.317	0.317	0.317	0.317	0.317
Amount of internal pollutants(t/a)	Sediment pollution release	8.403	8.403	8.403	0.0	2.101
TP load into the lake(t/a)		115.267	92.564	25.875	17.472	21.012
Estimated TP up to concentration(mg/L)			0.441	0.123	0.083	0.1

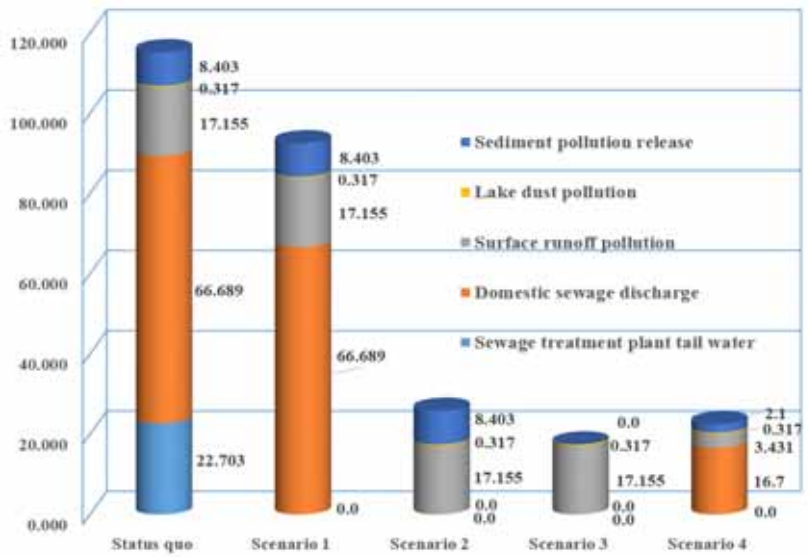

FIGURE 6
TP reduction under different scenarios

Scenario 1: The diversion of the tail water from the sewage treatment plant into the Yangtze River can reduce the TP load of 22.70 t/a. In the case of all the tail water of the sewage treatment plant reduced, the TP input into the lake is still as high as 92.56 t/a, which is under the case other conditions remain unchanged. The TP concentration in the water quality of Lake Nanhu is expected to be reduced to 0.44 mg/L, which cannot be satisfied to Class IV water quality requirements. Scenario 2: On the basis of the tail water discharge from the sewage treatment plant fully reduced, the interception of sewage pollutants in Lake Nanhu will be completed, and other conditions are maintained, then the TP load of 66.69t/a will be reduced. The TP concentration is expected to be further reduced to 0.12 mg/L, which is still unable to meet the Class IV water quality requirements. Scenario 3: If the internal sediment pollution is further controlled, that is, the TP load of 8.4 t/a is further reduced. At this time, the TP concentration in the lake can be reduced to 0.083mg/L, which meets the IV water quality requirements.

However, in the actual process, it is impossible to avoid the mismatch of rainwater and sewage pipelines. The discharge of domestic sewage pollutants cannot be completely controlled by 100%. Similarly, dredging of sediments cannot be completely eliminated. Therefore, based on the tail water discharge of the sewage treatment plant fully reduced, 75% of the TP control in the discharge of domestic sewage and sediment pollution is completed, and then the 87% of the amount of non-point source pollutants into the lake is reversed according to the material conservation of TN. Then, the TP concentration in Lake Nanhu is expected to drop to 0.1 mg/L. The relationship between the specific reduction amount and the TP concentration is shown in Table 6. The reduction of TP in different scenarios is shown in Fig. 6.

CONCLUSIONS

(1) According to the water quality monitoring, the TN and TP are serious pollutants in Lake Nanhu in the typical urban park lake. The main source of pollutants are the tail water from sewage treatment plants, the domestic sewage and surface runoff pollution.

(2) In order to achieve the target of Class IV water quality, it is necessary to make the pollutants with the highest multiple of the current standard reach the Class IV water quality requirements. For TN, based on the tail water drainage of the sewage treatment plant, 60% of the TN control in the discharge of domestic sewage pollutants and the release of sediments fully reduced, and the control rate of TN from the runoff into the lake is 67%. Then, the TN concentration can be reduced to 1.50 mg/L. For TP, based on the tail water drainage of the sewage treatment plant, 75% of the TP in the discharge of domestic sewage pollutants controlled and sediment release fully reduced, and the TP control rate of the surface source is 87%. The TP concentration can be reduced to 0.1 mg/L.

ACKNOWLEDGEMENTS

This work was supported by the Program of Research and Operational Effectiveness Evaluation on Typical Regional Drainage System in Wuhan, China. Thanks for the analytical support from the Analytical and Testing Center of Huazhong University of Science & Technology, and for Wuhan Planning and design institute.

REFERENCES

[1] Gross, C. (2017) Attributes of successful actions to restore lakes and estuaries degraded by nutrient pollution. Journal of Environmental Management. 187, 122-136.

[2] Fischer, E.K., Paglialonga, L., Czech, E., Tamminga, M. (2016) Microplastic pollution in lakes and Lake Shoreline sediments-a case study on Lake Bolsena and Lake Chiusi (central Italy). Environmental Pollution. 213, 648-657.

[3] Sruthy, S., Ramasamy, E.V. (2017) Microplastic pollution in Vembanad Lake, Kerala, India: the first report of microplastics in lake and estuarine sediments in India. Environmental Pollution. 222, 315-322.

[4] Xiong, X., Zhang, K., Chen, X., Shi, H., Luo, Z. Wu, C. (2018) Sources and distribution of microplastics in China's largest inland lake - Qinghai Lake. Environmental Pollution. 235, 899.

[5] Wu, Z., Zhang, Z., Chen, S., He, F., Fu, G., Liang, W. (2007) Nonylphenol and octylphenol in urban eutrophic lakes of the subtropical China. Fresen. Environ. Bull. 16, 227-234.

[6] Barbiero, R.P., Lesht, B.M., Warren, G.J., Rudstam, L.G., Watkins, J.M., Reavie, E.D. (2018) A comparative examination of recent changes in nutrients and lower food web structure in Lake Michigan and Lake Huron. Journal of Great Lakes Research. 44(4), 573-589.

[7] Omura N., Yamashita, K., Sawada, T., Ohaba, M. (1999) Study on characteristics of pollutant runoff into Lake Biwa, Japan. Water Science and Technology. 39(12), 17-25.

[8] Islam, M.N., Kitazawa, D., Park, H.D. (2012) Numerical modeling on toxin produced by predominant species of cyanobacteria within the ecosystem of Lake Kasumigaura, Japan. Procedia Environmental Sciences. 13(3), 166-193.

[9] Coveney, M.F., Stites, D.L., Lowe, E.F., Battoe, L.E., Conrow, R. (2003) Nutrient removal from eutrophic lake water by wetland filtration. Ecological Engineering. 19(2), 141-159.

[10] Dunne, E.J., Coveney, M.F., Marzolf, E.R., Hoge, V.R., Conrow, R., Naleway, R. (2012) Efficacy of a large-scale constructed wetland to remove phosphorus and suspended solids from Lake Apopka, Florida. Ecological Engineering. 42(9), 90-100.

[11] Ballatore, T. (2001) 5.14 Lake Biwa and the world's lakes: rapporteurs: Williams and Ballatore. participants: 50. Water Policy. 3, S205-S207.

[12] Ibelings, B.W., Portielje, R., Lammens, E.H.R.R., Noordhuis, R., Berg, M.S.V.D., Joosse, W. (2007) Resilience of alternative stable states during the recovery of shallow lakes from eutrophication: Lake Veluwe as a case study. Ecosystems. 10(1), 4-16.

[13] Welch, E.B., Patmont, C.R. (1980) Lake restoration by dilution: Moses Lake, Washington. Water Research. 14(9), 1317-1325.

[14] Acharya, S., Pattarkine, V.M., Knudhansen, C.F. (2010) Lake and reservoir management. Water Environment Research. 75(6), 1-63.

[15] Jørgensen, S.E. (2008) Lake restoration methods. Encyclopedia of Ecology. 2093-2098.

[16] Ruley, J.E., Rusch, K.A. (2003) An assessment of long-term post-restoration water quality trends in a shallow, subtropical, urban hypereutrophic lake. Ecological Engineering. 19(4), 265-280.

[17] Annadotter, H., Cronberg, G., Aagren, R., Lundstedt, B., Nilsson, P.A., Ströbeck, S. (1999) Multiple techniques for lake restoration. Hydrobiologia. 395-396(1), 77-85.

[18] Hilt, S., Gross, E.M., Hupfer, M., Morscheid, H., Mählmann, J., Melzer, A., Poltz, J., Sandrock, S., Scharf, E.M., Schneider, S., van de Weyer, K. (2006) Restoration of submerged vegetation in shallow eutrophic lakes– A guideline and state of the art in Germany. Limnologica, 36(3), 155-171.

[19] Hu, X., Jin, X., Lu, S., Chu, Z. (2009) Techniques for sediment pollution control and discussion on the applicability in lakes of China. Engineering Sciences. 9(11), 28-33.

[20] Liu, X., Lu, S., Guo, W., Xi, B., Wang, W. (2018) Antibiotics in the aquatic environments: a review of lakes, China. Science of the Total Environment. 627, 1195-1208.

Received: **02.11.2018**
Accepted: **19.02.2019**

CORRESPONDING AUTHOR

Hao Huang
Wuhan Planning and Design Company,
Wuhan, 430014 – China

e-mail: huanghaoh@163.com

© by PSP Volume 28 – No. 4/2019 pages 2633-2643 Fresenius Environmental Bulletin

EXPERIMENTAL STUDY THE EFFECT OF SULFATE AND RETENTION TIME ON SOLUBLE AL CONCENTRATION AND SPECIES OF PRECIPITATES DURING NaOH NEUTRALIZATION OF AL-BEARING ACID MINE DRAINAGE

Ruifeng Liang, Gaolei Zhao, Xunchi Pu*

State Key Laboratory of Hydraulics and Mountain River Engineering, Sichuan University, Chengdu city, 610065, China

ABSTRACT

The effects of the SO_4^{2-} on the concentration of soluble Al and species of precipitates during Al-bearing acid mine drainage (AMD) treatment with NaOH was investigated. The results showed that SO_4^{2-} affected Al concentration and the content of S in the formed precipitates during AMD neutralization. In short retention time (<=30 minutes), SO_4^{2-} has little effect on Al concentration and solution was approximately in equilibrium with amorphous $Al(OH)_3$. When retention time became longer (48 hour), Al concentration decreased and solution was no longer in equilibrium with amorphous $Al(OH)_3$. X-ray diffraction (XRD) analysis showed that crystalline $Al(OH)_3$ (gibbsite) particles were not detected in precipitates. Thermogravimetric analysis (TGA) and SEM analysis showed the proportion of S in precipitates increased with time and initial SO_4^{2-} concentration. These results indicated that Al ions were immediately precipitated due to the formation of amorphous $Al(OH)_3$ after the addition of NaOH. In retention time, Al concentration ions and suspended Al-solids combined with SO_4^{2-} ions to form Al-SO_4^{2-} precipitates and made Al concentration decrease. The combination of SO_4^{2-} ions with Al-ions to form Al-SO_4^{2-} precipitates lead to the Al concentration in solution less than the solubility of amorphous $Al(OH)_3$ after long retention time.

KEYWORDS:
Al-bearing acid mine drainage, aluminum speciation, X-ray diffraction, Thermogravimetric analysis, Mineql+ model, amorphous

INTRODUCTION

Acid mine drainage (AMD) formed through the oxidation of metal sulfide is a major source of water impairment in both coal and hard rock mining regions throughout the world [1, 2]. A primary contaminants in AMD are Fe and SO_4^{2-}, as well as other metal ions. As the "second substance", Al is found to be highly toxic to aquatic organisms, and can destroy benthic habitat and degrade the aesthetic qualities of water bodies [3, 4] In some cases, Al is the main pollutant in AMD [5]. Data reported from over 150 different mine drainage samples across the United States showed that over 30% of these locations presented minimum Al concentration of 50 $mg \cdot L^{-1}$ [6]. Data reported from 140 abandoned coal mines in Pennsylvania showed that over 50% of these locations present median Al concentration over 1 $mg \cdot L^{-1}$. The concentrations of Al were found in AMD between 1 $mg \cdot L^{-1}$ and 50 $mg \cdot L^{-1}$ in the acidic range of pH 2.7-5[7]. Waters and Webster-Brown [8] reported the total Al range for the ACM sites was between 0.18 and 46.13 $mg \cdot L^{-1}$ in New Zealand.

For applications in the field, the effluent Al from an AMD treatment system is of most concern. Al has only one oxidation state in aqueous systems, Al^{+3}. The concentrations of Al in acid drainage are primarily impacted by the solubility of Al hydroxide [9]. At a pH between 6.0 and 7.0, the theoretical solubility of crystalline $Al(OH)_3$ (gibbsite) in deionized (DI) water at 25ºC is less than 0.01 $mg \cdot L^{-1}$, with lowest solubility at around pH6.5. Al speciation and concentration depend on the pH values and other anions in natural conditions [10, 11].

However, the precipitation of Al from natural acid rock drainage (AMD) is complex. AMD often contains high SO_4^{2-}, which could impact the composition of precipitates. The possible Al precipitates formed as a consequence of pH adjustment of AMD are not only Al hydroxides, but also Al-hydroxyl-SO_4^{2-}. The strong affinity that Al has for SO_4^{2-} in the form of basaluminite and alunite has been observed by Taylor et al. [12] and Bigham and Nordstrom [13]. Several previous studies [14-16] have reported that a jurbanite-like mineral, having a molar stoichiometry of Al:OH:SO_4=1:1:1, might control the activity of Al^{3+} in acidic, SO_4^{2-}-rich waters. Adams and Rawajfih [17] found that amorphous basaluminite [$Al_4(SO_4)(OH)_{10}.5H_2O$] was precipitated during titrations of Al SO_4^{2-} with Na-, K- and Ca-hydroxides, and Nordstrom et al. [18] have also suggested that

the most common phase in mine-drainage systems seems to be an amorphous Al hydroxysulfate with basaluminite stoichiometry. Herrmann and Baumgartner [19] and Kim and Kim [20] have also reported that other compositions of Al precipitates can also be formed in the presence of other anions. Nordstrom et al. [21] also found in both field and laboratory experiments that the precipitates of basaluminite ($Al_4(OH)_{10}SO_4$) /hydrobasaluminite ($Al_4(OH)_{10}SO_4 \cdot 12\text{-}36(H_2O)$) significantly delayed the formation and equilibration of stable minerals.

The actual chemistry of AMD is complexes, and the water could be in nonequilibrium conditions in a treatment system of AMD. Some researchers have reported that the amorphous $Al(OH)_3$ was the primary species of Al-precipitates [9, 18, 23, 24], although the theoretical species of Al-precipitates should be gibbsite and/or Al-SO_4^{2-}. Meanwhile, some researches have reported Al-SO_4^{2-} precipitates were detected in field [12, 13, 20, 22]. In treatment systems, the most important problem is what the lowest solubility the effluent Al could be achieved. However, most of reports focused on the species of precipitates formed and the removal efficiency of Al and other metal ions in treatment [25,26], but few of them involved the aqueous Al [11].

The study was to investigate the effect of SO_4^{2-} and retention time on Al concentration and solid-phase species during active treatment of Al-bearing acidic drainage in controlled laboratory experiments with synthetic acid mine drainage. It focused on the species of Al-precipitates and the relationship of Al concentration to the species of precipitates. This study could provide insight into Al concentration and solid-phase speciation and transformations over time in Al-bearing acidic drainage treatment processes.

EXPERIMENTS AND METHODS

Synthetic Al-bearing AMD. Synthetic AMD used in the experiments contained Na^+, Ca^{2+}, Mg^{2+}, Mn^{3+}, Al^{3+}, Cl^-, and SO_4^{2-}. The composition of synthetic AMD in this study was presented in Table 1. The pH value was adjusted by H_2SO_4 to about 3.5. The concentration of Al was about 50 mg·L^{-1}. The molar ratio of Al/SO_4 was from 1:0, 1:1, and 1:5, therefore the SO_4^{2-} was changed from 0, 180, and 889 mg·L^{-1}, respectively. 866.4 and 1082.8 mg·L^{-1} NaCl was added in the solution when the molar ratio of Al/SO_4 equal 1:1 and 1:0 to keep the ionic strength of solution constant (did not consider the effect of activity).

Experimental procedure and samples collection. Batch experiments were done in a 20 L glass jar with a diameter of ~30cm. During the experiments, 5% NaOH (wt/wt) solution was added into 15L synthetic AMD and stirred for 5 minutes to let the solution completely mixed, then the solution was stopped stirring and the precipitates was allowed to settle down. Supernatant was collected at the position about 10 cm under water surface at 30 mins and 48 hours, respectively.

After the samples (~150-200 ml each time) were collected, they were immediately filtered with 0.45μm Millipore filter and 1 drop of H_2SO_4 (1+1) was added, and the samples were stored at 4ºC in refrigerator for analysis. Duplicate samples were collected each time. The filtered samples represent the dissolved concentration. Three different experiments with molar ratio of Al/SO_4 of 1:0, 1:1, and 1:5 were conducted. The concentration of Al in samples was measured at 30 minutes and 48 hours after settling, respectively. During the experiments, the precipitates were also collected at 30 minutes and 48 hours and separated from water by centrifuge and washed by DI water for three times. The separated precipitates were dried at room temperature before analysis.

Analytic methods. All analysis was performed in accordance with Standard Methods for the Examination of Water and Wastewater [27] and/or Hach methods [28]. All the water samples were digested firstly with microwave digestion before the total and concentration soluble of metal ions were measured. Al were measured with Aluminon method from Hach Chemical Company [28].

The mineralogy of precipitates was analyzed using X-ray powder diffractometer using Rigaku GeigerflexRAD3-C equipped with Cu-Kα source (λ=1.5408Å). The Perkin Elmer TGA 7 Thermogravimetric Analyzer was used for the thermogravimetric analysis. Thermogravimetric analysis (TG) of precipitates were run on heating rate of 10 °C/min. Weight loss was determined for 6-10 mg samples in alumina crucibles at temperatures ranging from 25°C to 1000°C. The compositions of precipitates were also measured with a Philips XL30 scanning electron microscope (SEM). The energy-dispersive x-ray microanalysis system, Oxford Instruments INCA, was used to perform energy dispersive spectroscopy (EDS) analysis. In order to remove the effect of absorbed water, the precipitates were dried at about 80-90ºC before SEM analysis.

TABLE 1
The Constituents of synthetic AMD in the study (mg·L^{-1}).

pH	Na	Al	Mn	Ca	Mg	Cl^-	SO_4
3.5	0~425.7	50	8.4	20.0	16.9	0-657.1	0~888.9

TABLE 2
Dissolved Al after different settling time at different pH values (mg·L^{-1}).

Al: SO_4^{2-}=1:0 (M/M)			Al: SO_4^{2-}=1:1 (M/M)			Al: SO_4^{2-}=1:5 (M/M)		
pH	Retention time		pH	Retention time		pH	Retention time	
	30 min	48 hours		30 min	48 hours		30 min	48 hrs
5.6	1.97	1.21	5.6	1.86	0.31	5.5	1.21	0.21
6.0	0.56	0.33	6.0	0.39	0.14	6.0	0.43	0.03
6.5	0.32	0.27	6.6	0.24	0.09	6.6	0.25	0.02
7.0	0.45	0.37	7.2	0.48	0.13	7.1	0.39	0.04
7.7	1.55	0.89	7.5	0.92	0.36	7.5	1.18	0.16
8.0	3.31	2.62	8.0	3.60	1.80	8.0	3.20	1.32
8.3	10.97	3.91	8.3	8.05	2.92	8.4	5.52	2.81
8.5	10.19	7.42	8.7	13.36	8.19	8.8	13.92	7.53

(Initial Al ~50 mg·L^{-1})

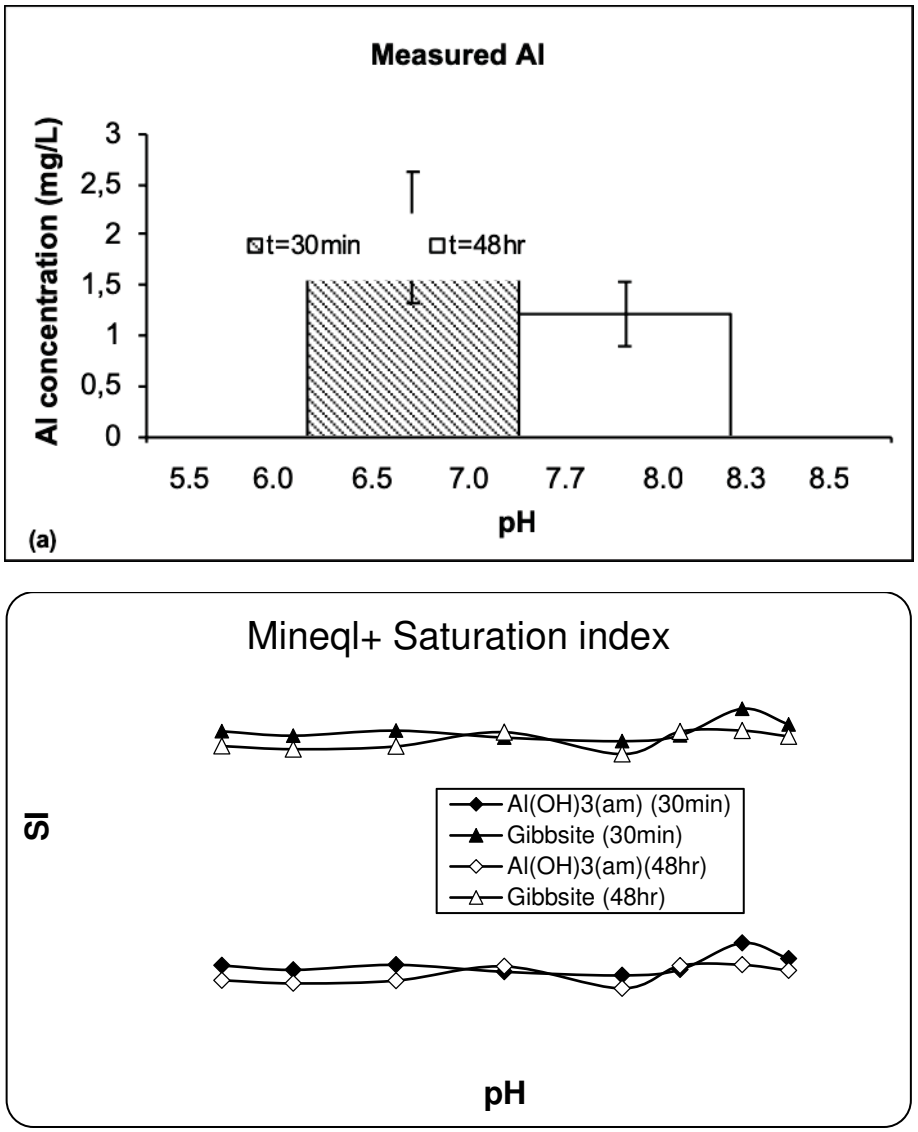

FIGURE 1
(a) Al concentration over settling time at different pH (initial SO_4^{2-} =0); and (b) Saturation indexes of Al-compounds in solution calculated at different settling time calculated by Mineql+ model.
(The initial Al was about 50mg·L^{-1}).

Mineql+ model simulation. The chemical model was conducted by using Mineql+ model (version 4.5) to determine solution speciation and saturation index (SI) for different Al compounds (amorphous Al hydroxide, gibbsite, and basaluminite). Saturation index (SI) is a calculated number used to predict the compound stability of water and defined

as SI=log(IAP/K_{sp}), where IAP is the ion activity product of the dissolved precipitate constituents, and K_{sp} is the solubility product for the precipitates (amorphous $Al(OH)_3$ or basaluminite ($Al_4(OH)_{10}SO_4$)). It indicates whether the water will precipitate, dissolve, or be in equilibrium with this compound. During the calculation of SI of each compound, the input data was the actual measured in the experiments.

RESULTS AND DISCUSSION

Results of experiments without SO_4^{2-} (Al: SO_4^{2-}=1:0). In experiments without SO_4^{2-}, Al concentration at different time were presented in Table 2, where the initial Al was around 50 mg·L^{-1}. As theoretical prediction, the minimum concentration of soluble Al occurred at pH=6.5, then increased with increasing and decreasing pH (Figure 1a). In Table 2, it could be seen that Al concentration decreased a little from 30 minutes to 48 hours. At pH 6.5, Al concentration was 0.27 mg·L^{-1} at 48 hours, which was about 0.05 mg·L^{-1} lower than at 30 minutes. The theoretical solubility is 0.33 mg·L^{-1} for amorphous $Al(OH)_3$ and 0.001 mg·L^{-1} for gibbsite (crystalline $Al(OH)_3$) by Mineql+ model.

The SI value was calculated using Mineql+ model for possible Al compounds. Input data were the concentrations of constituent components in solution at 30 minutes and 48 hours, respectively. Since the possible Al precipitates formed in the experiments were only amorphous and crystalline $Al(OH)_3$, they were selected as the possible Al precipitates. All thermodynamic constants have been taken from the databases of this software. The SI values of the two compounds were plotted as a function of pH shown in Figure 1b (data shown in Table 3).

At 30 minutes, SI values of gibbsite are from 2.5 to 2.9, which were always much larger than zero. The high SI values indicate that the solution was supersaturated with gibbsite. SI values of amorphous $Al(OH)_3$ are from –0.03 to 0.23, which were close to zero (Table 3). Therefore, it is concluded that Al concentration was in theoretical equilibrium with amorphous $Al(OH)_3$ immediately after NaOH addition. When retention time became longer (48hr), SI values of amorphous $Al(OH)_3$ slightly decreased which is from –0.17 to 0.08. The SI values of amorphous $Al(OH)_3$ at different pH values were still close to zero. Therefore, it is reasonable to conclude that the solution was still in equilibrium with amorphous $Al(OH)_3$.

Berkowitz et al. [29] reported that amorphous $Al(OH)_3$ transformed to microcrystalline $Al(OH)_3$ when lake water was treated with alum. However, these mineralogical transformations of precipitates were not found in our experiments. The XRD patterns showed that no crystalline particles were detected in the precipitates formed at pH=6.5 (Figure 2). Since the major gibbsite diffraction peaks appear near *d*-spacing of 4.8 and 4.3 Å [30, 31], the absence of the peaks near the corresponding angle indicates that gibbsite was not produced in the experiments. XRD patterns (Figure 2) of precipitates indicate only amorphous phase with low intensity, broad peaks in the experiments. The XRD patterns of the precipitates at other pH values were similar as the patterns of precipitates at pH=6.5 (not shown). Therefore, it is reasonable to conclude that gibbsite was not formed in the experiments without SO_4^{2-} from pH=5.6 to 8.5 in 48 hour after addition of NaOH.

TABLE 3
The SI value calculated with Mineql+ model

Retention Time	Al:SO_4^{2-}=1:0[1]			Al:SO_4^{2-}=1:1				Al:SO_4^{2-}=1:5			
	pH	am[2]	Gibbsite	**pH**	am	Basaluminite	Gibbsite	**pH**	am	Basaluminite	Gibbsite
30 min	5.6	0.08	2.63	5.6	-0.15	5.80	2.40	5.5	-0.18	5.9	2.4
	6.0	0.03	2.58	6.0	-0.14	4.58	2.41	6.0	-0.14	6.7	2.4
	6.5	0.08	2.63	6.6	0.04	5.34	2.59	6.6	-0.05	5.9	2.5
	7.0	0.01	2.56	7.2	-0.08	3.84	2.48	7.1	-0.10	4.7	2.5
	7.7	-0.03	2.52	7.5	-0.11	1.83	2.44	7.5	0.04	4.3	2.6
	8.0	0.03	2.58	8.0	0.07	2.81	2.62	8.0	0.02	3.3	2.6
	8.3	0.23	2.87	8.3	0.19	2.97	2.74	8.4	-0.04	2.6	2.5
	8.5	0.15	2.70	8.7	0.24	3.88	2.79	8.8	0.02	3.7	2.6
48 hrs	5.6	-0.09	2.46	5.6	-0.74	4.45	1.40	5.5	-1.63	1.73	1.37
	6.0	-0.12	2.43	6.0	-0.56	4.36	1.41	6.0	-1.34	1.91	1.41
	6.5	-0.09	2.46	6.6	-0.48	3.48	1.59	6.6	-1.16	1.44	1.50
	7.0	0.07	2.62	7.2	-0.64	1.50	1.48	7.1	-1.10	0.72	1.45
	7.7	-0.17	2.38	7.5	-0.48	1.52	1.44	7.5	-0.83	0.79	1.59
	8.0	0.07	2.62	8.0	-0.23	1.60	1.62	8.0	-1.02	1.46	1.57
	8.3	0.08	2.63	8.3	-0.25	1.18	1.74	8.4	-0.34	2.57	1.51
	8.5	0.02	2.57	8.7	-0.02	2.03	1.79	8.8	-0.32	1.80	1.57

1: No basaluminite formed;
2: amorphous $Al(OH)_3$.

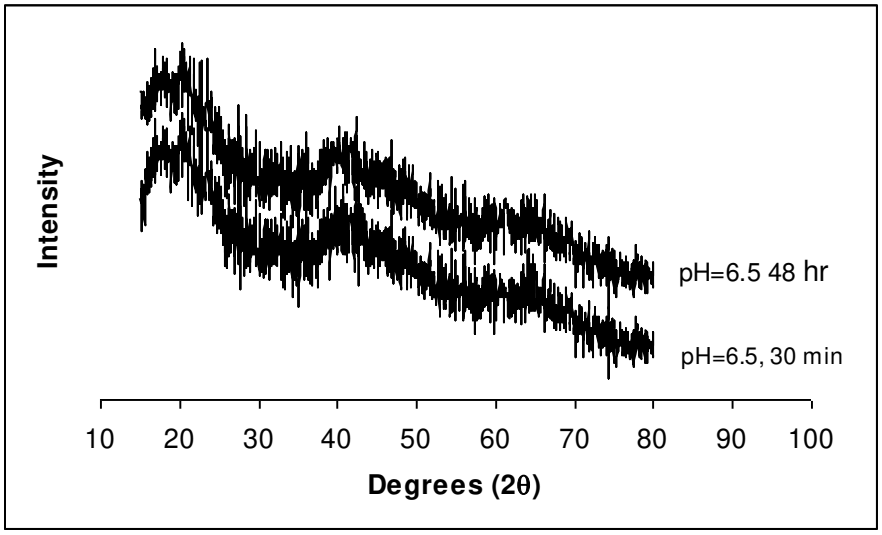

FIGURE 2
XRD pattern of precipitates formed in the experiments without SO_4^{2-}.

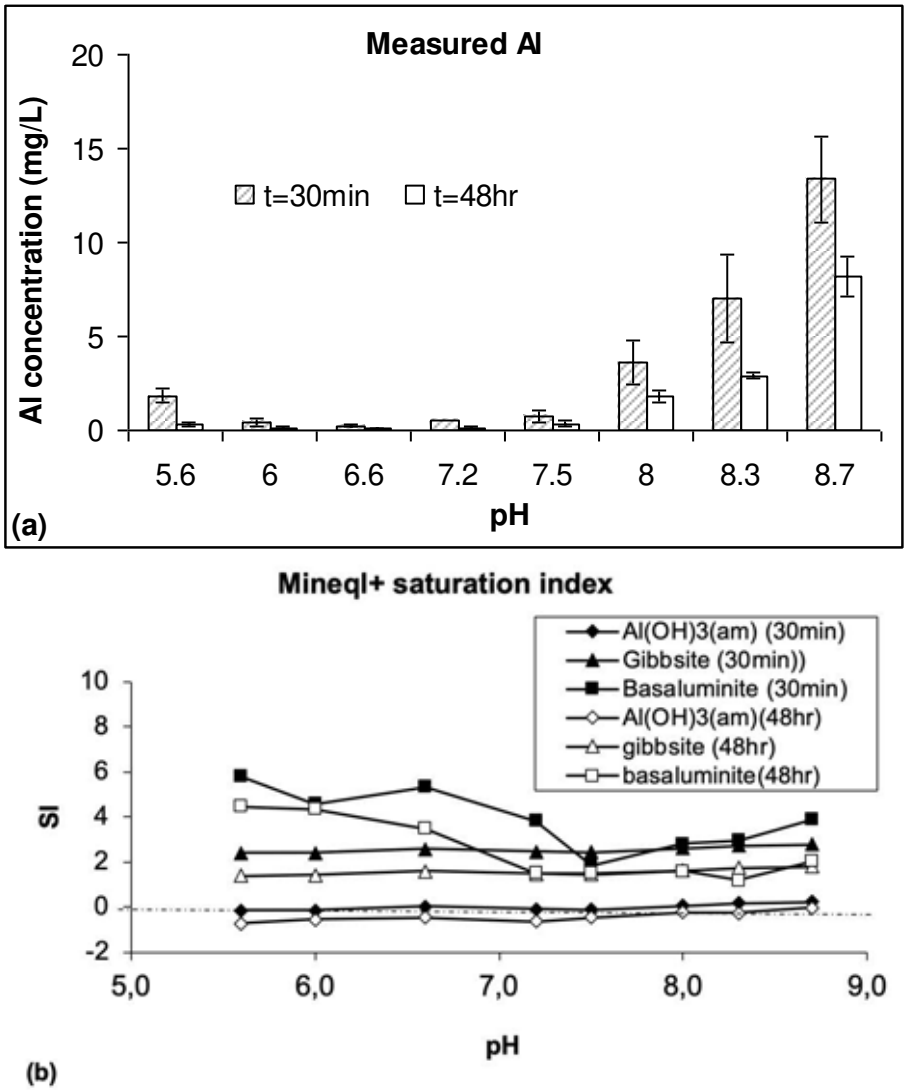

FIGURE 3
(a) Soluble Al over different retention time at different pH, and (b) Saturation indexes of Al-compounds in solution calculated by using Mineql+ model (Molar ratio of Al:SO_4=1:1).
(The initial Al ~50mg·L^{-1} initial SO_4~175mg·L^{-1}).

Results of experiments with Al: SO_4^{2-}=1:1. The Al concentrations at 30 minutes and 48 hours in experiments with low SO_4^{2-} (Al: SO_4^{2-} equal 1:1) were shown in Figure 3a and the corresponding data were presented in Table 2. Concentration of soluble Al at 48 hours in these experiments were less than that in the experiments without SO_4^{2-}, although the soluble Al at 30 minutes was not much different if pH values were close. Unlike the experiments without SO_4^{2-}, the soluble Al decreased significantly from 30 minutes to 48 hours in experiments with SO_4^{2-}.

The SI values were shown in Table 3. Three Al-compounds, amorphous $Al(OH)_3$, gibbsite (crystalline $Al(OH)_3$), and basaluminite ($Al_4(OH)_{10}SO_4$), were selected as the possible Al precipitates. Jurbanite ($Al(OH)SO_4$) was not considered as a possible precipitate of Al-precipitates because the theoretical data shows that jurbanite is not formed when pH is higher than 5.5. The SI values of amorphous $Al(OH)_3$ were close to zero after 30 minutes of neutralizaion. These SI values indicate that the solution was approximately in equilibrium with amorphous $Al(OH)_3$ at 30 minutes, which was similar as the experiment without SO_4^{2-}. All the SI values of gibbsite and basaluminite were higher than 1.5, which means that the solution were supersaturated with gibbsite and basaluminite. When retention time became longer (48hr), all SI values of amorphous $Al(OH)_3$ declined and became less than zero (from –0.12 to –0.74). The negative values of SI indicated that the solution was unsaturated with amorphous $Al(OH)_3$, which indicates that Al concentrations in these experiments were not controlled by amorphous $Al(OH)_3$. The SI values of gibbsite and basaluminite also decreased with longer retention time, but they were still higher than 1.0, which indicates that the solutions were still supersaturated with gibbsite and basaluminite after 48 hours of AMD neutralization.

As sown in the experiments without SO_4^{2-}, no sharp peaks was found in the XRD patterns of precipitates formed in experiments with low SO_4^{2-} contents (Al:SO_4=1:1) (not shown), which indicates that crystalline $Al(OH)_3$ (gibbsite) was not formed in the experiments with SO_4^{2-}. The lack of the *d*-spacing for basaluminite indicated that crystalline basaluminite was also not detected in the precipitates, which means that the Al-SO_4^{2-} precipitates should be amorphous if it had been formed in experiments. Furthermore, the Al concentration in experiments without SO_4^{2-} were higher (as shown in Table 2). These results indicated that the SO_4^{2-} could impact the Al solubility during the active treatment of AMD and the soluble Al will decrease with the presence of SO_4^{2-} contents in solution.

Results of experiments of Al: SO_4^{2-}=1:5. Figure 4a shows the soluble Al at different pH in experiments with higher SO_4^{2-} (Al: SO_4^{2-}=1:5) (data in Table 2). Similar as the experiments with lower SO_4^{2-} contents, the soluble Al at 30 minutes was not significantly different from that in experiments without SO_4^{2-} if pH values were close. With retention time increasing, soluble Al at 48 hours in higher SO_4^{2-} experiments became lower than that without SO_4^{2-} and with lower SO_4^{2-} when the pH was the same. At 48 hours, concentration of soluble Al in the experiments of Al: SO_4^{2-}=1:5 was from 0.02 to 0.21 mg·L^{-1} at pH 5.5 - 7.7, whereas it was from 0.27 to 1.21 mg·L^{-1} and 0.09 to 0.36 mg·L^{-1} in experiment without SO_4^{2-} and with lower SO_4^{2-}, respectively. These results supported the assumption that SO_4^{2-} could decrease the soluble Al in active treatment of Al-bearing acid mine drainage.

Similar as the experiments with low SO_4^{2-}, the SI values at 30 minutes in experiments with higher initial SO_4^{2-} (Al: SO_4^{2-}=1:5) were also close to zero (from –0.18 to 0.02) for amorphous $Al(OH)_3$, whereas the SI values of gibbsite and basaluminite were from 2.4 to 2.6 and 2.5 to 6.7, respectively (shown in Table 3), which shows the solution was strongly supersaturated with gibbsite and basaluminite at 30 minutes. When the retention time became longer (48 hours), all SI values declined. The SI values for amorphous $Al(OH)_3$ decreased particularly, becoming to negative. The negative SI values of amorphous $Al(OH)_3$ was due to the decrease of Al, which indicated that other Al-precipitates could be formed. As shown in Table 3, the SI values of basaluminite at 48hr became smaller when SO_4^{2-} concentration was higher, it is reasonable to hypothesize that Al-SO4 precipitates were formed, which caused the decrease of Al concentration.

The XRD patterns showed that no apparent crystalline peaks were detected in precipitates formed at both short (30 minutes) and longer time (48 hours) when pH=6.6. The high signal-to noise ratio indicated that highly amorphous nature of the precipitates (not shown).

Chemical characteristics of precipitates. TGA analysis of precipitates. Since XRD does not provide a quantitative estimate of the amount of Al hydroxide or other mineral phases present in a sample. TGA was utilized to further characterize and quantify the precipitates formed in the experiments. The TGA curve is well-suited for this since $Al(OH)_3$ and Al-hydroxyl-SO_4^{2-} have a dehydration reaction with an associated weight loss [32] and Al-hydroxyl-SO_4^{2-} has a de-SO_4^{2-} reaction with a weight loss between 800-1000ºC [33]. The weight loss below 100ºC was primarily due to the vaporization of absorbed water [33]. The weight proportion of hydroxyl in precipitates was the part of weight loss between 100-400ºC. The derivation weight loss curves of the precipitates in the experiments without SO_4^{2-} showed that the weight loss primarily occurred between 70-300ºC, which is lower than the reported dehydration temperature for crystalline $Al(OH)_3$ (gibbsite: ~350ºC) [32] and there was no significant

weight loss after 400ºC, which showed that only Al hydroxides were formed and the species of Al hydroxides was in the form of amorphous. This conclusion is supported by the XRD results. It is seen from this result that the crystalline $Al(OH)_3$ (gibbsite) was not formed during the treatment process (48 hours), although the gibbsite could formed in aged sludge [29].

The weight loss proportion of precipitates over temperature is shown in Table 4. The fractional weight loss (as % of original weight) showed that sulfur-trioxide fraction (fraction of weight loss from 800-1000ºC) in precipitates increased with settling time. For the precipitates in low SO_4^{2-} , the weight loss before 90ºC represented the vaporization of absorbed water in precipitates. The second weight loss occurred between 100-400ºC. This part of weight loss was the dehydration of precipitates. The third weight loss occurred among 800-1000ºC, which represents the evaporation of sulfur-trioxide. The residues were the metal hydroxides, most of which are Al_2O_3. In Table 4, it can be seen that the weight loss of dehydration was from 30.8% to 31.2% for 30 minutes, and 29.0% to 30.7% for 48 hours. The weight loss after 800ºC was from the sulfur-trioxide evaporation. The weight fraction of sulfur-trioxide was from 2.2% to 2.7% for 30 minutes, and 3.5% to 7.4% for 48 hours. The TGA data showed that the amount of hydroxyl decreased from 30 minutes to 48 hours, whereas the contents of S increased. Since the fraction of hydroxyl of $Al(OH)_3$ was larger than in Al-SO_4^{2-} compounds (such as basaluminite), the TGA data implied that the proportion of Al-SO_4^{2-} in precipitates increased over retention time if SO_4^{2-} was present in solution.

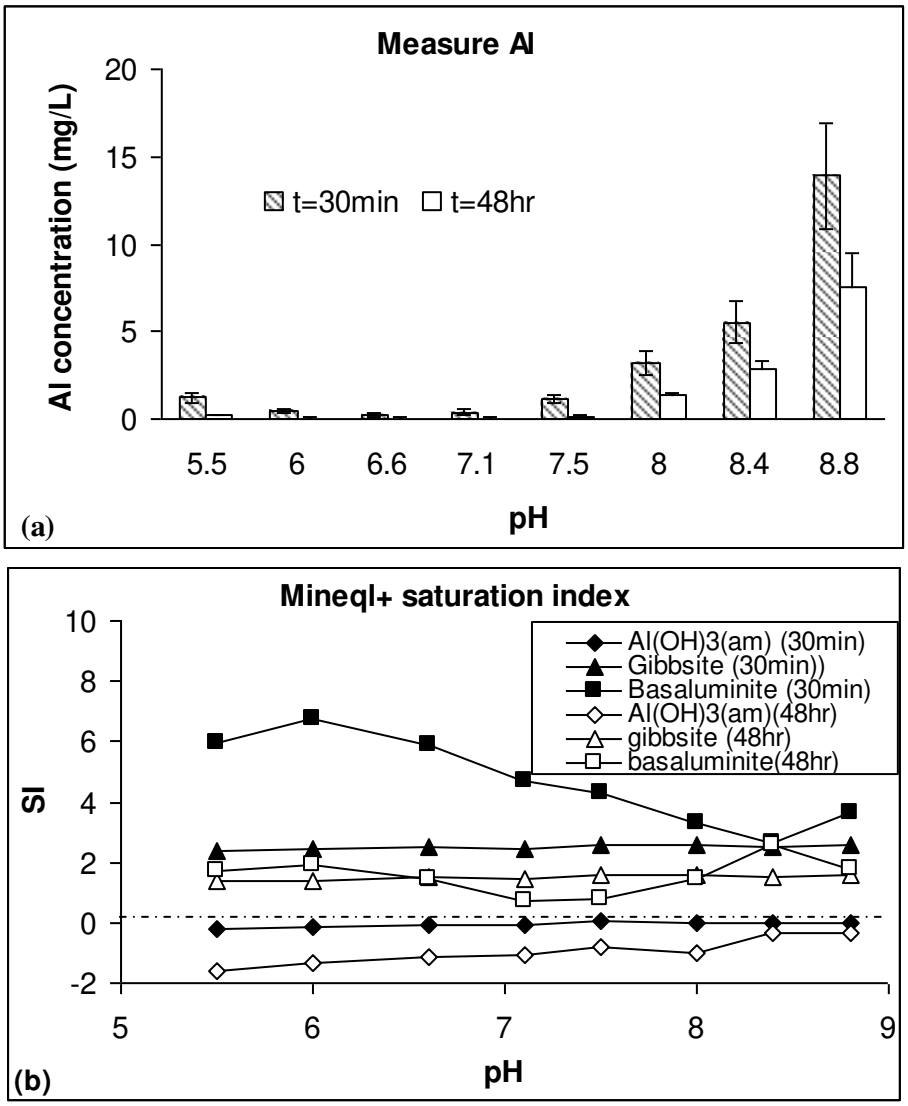

FIGURE 4
(a) Soluble Al over different retention time at different pH value, and
(b) Saturation indexes of Al-compounds in solution calculated by using Mineql+ model.
(The initial Al ~50mg·L^{-1}, initial SO_4~880mg·L^{-1}).

TABLE 4
Fractional weight loss of precipitates (TGA analysis).

Experimental conditions			Thermogravimetric analysis									
			Composition of precipitates (%)						TGA cal[4] (molar ratio)		SEM analysis[5] (molar ratio)	
pH	Al:SO_4	Time	Absorbed H_2O	Dehydro-tion	Other weight loss[1]	sulfur-trioxide	Residues[2] (after 1000ºC)					
			<100ºC	100-400ºC	400-800ºC	800-1000ºC	Al_2O_3	MO[3]	O/Al	Al/S	O/Al	Al/S
5.6	1:1	30 min	5.4	30.8	2.1	2.7	58.8	0.4	2.96	34.67	2.93	32.83
		48 hr	5.4	30.2	2.0	3.7	58.6	ND[6]	2.92	24.84	2.90	24.55
6.6	1:1	30 min	5.0	31.1	2.0	2.5	58.3	1.1	3.01	37.26	2.92	34.15
		48 hr	4.6	30.7	1.6	3.5	58.8	0.7	2.96	26.45	2.89	25.73
8.4	1:1	30 min	5.0	31.2	1.7	2.2	59.6	0.3	2.97	43.53	2.92	43.50
		48 hr	5.1	29.0	1.4	7.4	56.8	0.5	2.88	12.22	2.83	10.73
5.5	1:5	30 min	4.6	30.9	1.2	3.5	59.7	0.2	2.93	27.15	2.94	27.42
		48 hr	5.3	29.4	1.4	5.8	58.0	ND	2.87	15.65	2.80	15.75
6.6	1:5	30 min	4.8	30.8	1.8	3.1	57.8	1.7	3.02	29.71	2.91	28.79
		48 hr	5.3	29.2	2.0	5.8	57.2	0.4	2.89	15.54	2.82	15.95
8.3	1:5	30 min	5.1	30.5	2.1	3.3	58.1	0.9	2.98	28.31	2.86	28.18
		48 hr	5.0	27.8	1.6	9.2	55.4	0.9	2.84	9.55	2.74	9.39

[1]The other weight loss between 400-800ºC could be due to the decomposition of carbonate. The carbonate came from the dissolution of CO_2 during the experiments;
[2]The residue of TAG included the Al oxides and other metal oxides (such as Mn, Ca, and Mg). The proportion of Al_2O_3 and other metal oxides was decided by SEM analysis;
[3]MO represents the total proportion of metal oxides in residues;
[4]TGA cal: calculation with the weight loss of precipitates. During the calculation, the oxygen of O/Al was the part of oxygen combine with Al as OH.
[5]The samples for SEM analysis had been dried at 85ºC to remove the absorbed water.;
[6]ND: not detected.

The weight loss of precipitates in higher SO_4^{2-} has the similar tendency as the precipitates formed with low SO_4^{2-}. The weight loss of dehydration was from 30.5% to 30.8% for 30 minutes, and 27.8% to 29.4% for 48 hours. The weight loss of sulfur-trioxide evaporation (800-1000°C) was from 3.1% to 3.5% for 30minutes, and 5.8% to 9.2% for 48 hours. Compared with the weight loss of precipitates in low SO_4^{2-} experiments, it can be found that the S fraction in precipitates increased with increase of SO_4^{2-} and retention time. The increase of S fraction indicated that SO_4^{2-} ions combined with Al ions (and/or Al complexes) and suspended Al-solids to form precipitates (Al-SO_4^{2-}) and then settle down during the settling processes. In Table 2, it can be seen that soluble Al decreased over time and the SI values showed that the solutions became unsaturated with amorphous $Al(OH)_3$. The unsaturation with amorphous $Al(OH)_3$ was due to the decrease of soluble Al, which was caused by the reaction of SO_4^{2-} with soluble Al.

SEM-EDS analysis of precipitates. SEM and EDS analysis was performed on the precipitates formed in experiments with different SO_4^{2-} contained the partial SEM photos and EDS results). The samples had been dried at 85ºC for two hours to remove the adsorbed H_2O (Brydon and Shah Singh, 1969). The chemical components of precipitates were presented in Table 5 (measured with EDS). In Table 5, it can be seen that precipitates contained different elements, including Al, Mg, Ca, Mn, O, and S, and the contents varied with pH values and initial SO_4^{2-}. In order to calculate the atomic ratio of Al to OH^- of samples, the corrected atomic oxygen percentage was calculated by subtracting the oxygen that was combined with C (as CO_2), S (as SO_4^{2-}), Ca (as $Ca(OH)_2$), Mg (as $Mg(OH)_2$), and Mn (as $Mn(OH)_3$). Because the oxygen in the Al/O ratio did not include the oxygen combined with C, and S, the atomic ratio of Al/OH^- should be equal to the corrected Al/O ratio. The corrected molar ratios of Al/O (or Al/OH^-) were shown in Table 5. At 30 minutes, the contents of S in precipitates did not change much with pH values and the initial SO_4^{2-}. The low S contents in the precipitates indicated that most of the precipitates were in the form of $Al(OH)_3$ at short reaction tine (30 minutes). At 48 hours, the Al/OH^- ratio and S contents increased, and were significant different from the ratios and S contents at 30minute. The increase of Al/OH ratio and S contents indicated that the proportion of Al-SO_4^{2-} compounds increased in the precipitates at with longer retention time.

The calculation of Mineql+ model showed that the solution was approximately in equilibrium with amorphous $Al(OH)_3$ at 30 minutes for all cases, since the SI values are around zero. At long retention time (48 hours), the Al concentration reduced. Furthermore, the higher the initial SO_4^{2-} of solution, the lower the final soluble Al. The change of Al concentration and SI values over time indicated that the reaction of Al-precipitation changed. At the beginning of experiments, the primary reaction of Al-precipitation was the formation of amorphous $Al(OH)_3$. SI values by Mineql+ model calculation supported this conclusion since SI values of amorphous $Al(OH)_3$ in all cases are almost zero at 30 minutes. With the increase of retention time, the Al concentration reduced when SO_4^{2-} was presented in solution, and SI

TABLE 5
Compositions of precipitates formed in the experiments.

	Al:SO_4=1:1											
	pH=5.6				pH=6.6				pH=8.3			
	30min		48 hr		30min		48 hr		30min		48 hr	
	Ave.	Stdev.	Ave.	Stdev.	Ave.	Stdev.	Ave.	Stdev.	Ave.	Stdev.	Ave.	Stdev.
C	3.4	2.3	5.0	1.1	4.8	2.8	6.8	2.1	6.7	1.5	4.3	0.6
O	73.9	3.7	73.5	2.4	73.5	2.6	72.8	3.5	73.0	1.3	73.4	3.2
Mg	ND[3]	ND	ND	ND	0.2	0.3	0.6	0.7	ND	ND	0.2	0.2
Al	21.9	1.9	20.7	1.7	20.6	2.1	19.1	1.7	19.7	1.1	20.1	1.2
S	0.7	0.3	0.8	0.3	0.6	0.1	0.7	0.2	0.5	0.2	1.9	0.4
Ca	ND	ND	ND	ND	0.2	0.1	ND	ND	ND	ND	0.2	0.2
Mn	0.1	0.1	ND	ND	0.1	0.2	ND	ND	0.1	0.1	ND	ND
Al/O[1]	2.93		2.90		2.94		2.89		2.92		2.83	
Al/S[2]	32.86		24.55		34.39		25.73		43.49		12.73	
	Al:SO_4=1:5											
	pH=5.6				pH=6.6				pH=8.3			
	30min		48 hr		30min		48 hr		30min		48 hr	
	Ave.	Stdev.	Ave.	Stdev.	Ave.	Stdev.	Ave.	Stdev.	Ave.	Stdev.	Ave.	Stdev.
C	4.3	1.6	1.2	2.3	3.8	1.0	4.3	1.4	7.7	1.3	6.2	3.6
O	73.8	2.6	73.9	3.6	73.7	2.5	73.3	3.5	72.9	3.2	72.6	1.9
Mg	ND	ND	ND	ND	0.3	0.1	0.2	0.22	0.0	0.0	0.4	0.7
Al	21.1	1.0	23.5	1.8	21.0	0.8	20.8	1.6	18.6	1.1	18.6	2.1
S	0.8	0.1	1.5	0.4	0.7	0.4	1.4	0.3	0.7	0.2	2.0	0.6
Ca	ND	ND	ND	ND	0.3	0.1	0.1	0.1	ND	ND	0.3	0.5
Mn	0.04	0.1	ND	ND	0.2	0.2	ND	ND	0.2	0.1	ND	ND
Al/O	2.94		2.80		2.93		2.81		2.93		2.74	
Al/S	27.42		15.75		28.8		15.95		28.19		9.39	

[1]Al:O: the corrected atomic ratio of Al:O. In this atomic ratio, the O atomic % was subtracted the oxygen that was combined with C (as CO_2), Si (as SiO_2), and S (as SO_4^{2-});
[2]Al:S: the atomic ratio of Al:S;
[3]ND: not detected.

values showed that the solution became unsaturated with amorphous $Al(OH)_3$. The unsaturation state of amorphous $Al(OH)_3$ in solution indicated that the reduction of Al concentration was not due to the formation of amorphous $Al(OH)_3$. Therefore, it is reasonable to assume that the formation of Al-hydroxyl-SO_4^{2-} compounds led to the decrease of Al concentration because gibbsite was not formed. However, the SI values showed that solution was supersaturated with Al-hydroxyl-SO_4^{2-} (basaluminite), which indicates that the solution was not in equilibrium conditions at 48 hours still.

This above supposed reaction was supported by the results of TGA analysis. TGA showed that the proportion of sulfur-trioxide in precipitates increased over time if SO_4^{2-} was present in solution (Table 4). The sulfur-trioxide proportion in precipitates at 30 minutes was less than at 48 hours for all cases. When the initial SO_4^{2-} was low (Al:SO_4=1:1), weight proportion of sulfur-trioxide at 48 hours was 38.1%, 41.2%, and 140.3% more than at 30 minutes when pH=5.6, 6.6, and 8.3, respectively. When initial SO_4^{2-} was high (Al:SO_4=1:5), weight proportion of sulfur-trioxide at 48 hours was 68.2%, 85.4%, and 182.9% more than at 30 minutes when pH=5.5, 6.6, and 8.4, respectively. The calculation with TGA results showed that the molar ratio of Al/S decreased with settling time and the increase of initial SO_4^{2-}. The SEM results showed the similar results (Table 4 and Table 5).

SUMMARY CONCLUSIONS

The SI values at different retention time in the experiments showed that the solution was in equilibrium with amorphous $Al(OH)_3$ when settling time was short (≤30 minutes). When the retention time was longer (~48 hours), the Al concentration decreased and the solution became unsaturation with amorphous $Al(OH)_3$ and supersaturation with gibbsite and Al-SO_4^{2-} (basaluiminite) when SO_4^{2-} was presented in the solution. The Al concentration did not show this tendency when SO_4^{2-} was absent. This indicates that SO_4^{2-} in AMD decreases the concentration of Al in the neutralization process of AMD.

Precipitates analysis showed that the reduction of Al concentration with SO_4^{2-} was due to the formation of Al-SO_4^{2-} precipitates. However, the SI values indicated that the solution was supersaturated with basaluminite, which is the most possible species of Al-SO_4^{2-} formed in the experiments. The data implied that the solution was not in equilibrium state after 48 hours with NaOH addition.

The TGA and SEM analysis showed, the S contents in precipitates were lower and there was no significant different with different pH values at short retention time (30 minutes). At the longer retention time, the S contents increased over time. Under different initial SO_4^{2-} conditions, the higher the SO_4^{2-}, the more S contents in precipitates. These results indicated that the amount of Al-SO_4^{2-} compounds in precipitates increased with the increase of SO_4^{2-} and retention time.

ACKNOWLEDGEMENTS

This study sponsored by The National Key R & D Program of China (grant No. 2016YFC0401701).

REFERENCES

[1] Sasowsky, I., Foos, A., and Miller, C. (2000) Lithic controls on the removal of iron and remediation of acidic mine drainage. Water Res. 34(10), 2742–2746.

[2] Bunce, N.J., Chartrand, M., and Keech, P. (2001) Electrochemical treatment of acidic aqueous ferrous sulfate and copper sulfate as models for acid mine drainage. Water Res. 35(18), 4410-4416.

[3] Koryak, M., Shapiro, M.A., and Sykora J.L. (1972) Riffle zoobenthos in stream receiving acid mine drainage. Water Res. 6, 1239-1247.

[4] Evangelou, V.P., and Zhang, Y.L. (1995) A review: pyrite oxidation mechanisms and acid mine drainage prevention. Critical Reviews in Environmental Science and Technology. 25(2), 141-199.

[5] Yucel, Deniz Sanliyuksel; Baba, Alper, 2013, Geochemical Characterization of Acid Mine Lakers in Northwest Turkey and Their Effect on the Environment. Archives of Environmental contamination and Toxicology, Vol. 64(3):357-376.

[6] Watzlaf, G.R., Schroeder, K.T., Kleinmann, R.L.P., Kairies, C.L. and Nairn, R.W. (2004) The Passive Treatment of Coal Mine Drainage, National Energy Technology Laboratory. US Department of Energy (2004) Information circular.

[7] Cravotta C.A. (2006) Relations among pH, sulfate, and metals concentrations in anthracite and bituminous coal-mine discharges, Pennsylvania. International Conference of Acid Rock Drainage, St. Louis, MO

[8] Waters, A.S., Webster-Brown, J.G. (2013) Assessing aluminum toxicity in streams affected by acid mine drainage. Water Sci. Technol. 67(8), 1764–1772.

[9] Nordstrom, D.K. and Ball, J.W. (1986) The geochemical behavior of aluminum in acidified surface waters. Science. 232, 54–56

[10] Chamier, J., Wicht, M., Cyster, L., Ndindi, N.P., 2015. Aluminium (Al) fractionation and speciation; getting closer to describing the factors influencing Al3+ in water impacted by acid mine drainage. Chemosphere. 130, 17-23.

[11] Simpson, S.L., Vardanega, C.R., Jarolimek, C., Jolley, D.F., Angel, B.M., Mosley, L.M. (2014) Metal speciation and potential bioavailability changes during discharge and neutralisation of acidic drainage water. Chemosphere. 103,172–180.

[12] Taylor, P.D., Jugdaohsingh, R., and Powell, J.J., (1997) Soluble Silica with High Affinity for Aluminum under Physiological and Natural Conditions. J. Am. Chem. Soc. 119(38), 8852–8856

[13] Bigham, J.M., and Nordstrom, D.K. (2000) Iron and aluminum hydroxyl-sulfates from acid sulfate waters. In: Alpers, C.N., Jambor, J.L., Nordstrom, D.K. (Eds.) Sulfate Minerals, Reviews in Mineralogy and Geochemistry. Vol. 40. Mineralogical Society of America, Washington, D.C., 351-403

[14] Karathanasis, A.D., Evangelou, V.P., Thompson, Y.L. (1988) Aluminum and iron equilibria in soil solutions and surface waters of acid mine watersheds. J. Environ. Qual. 17, 534-543.

[15] Sullivan, P.J., Yelton, J.L, Reddy, K.J. (1988) Iron sulfide oxidation and the chemistry of acid generation. Environ. Geol. Water Sci. 11, 289-295.

[16] Van Breemen, N. (1973) Soluble Aluminum in acid sulfate soils and in acid mine waters. Soil Sci. Soc. Am. Proc. 37, 694-697.

[17] Adams, F., Rawajfih, Z. (1977) Basaluminite and alunite: a possible cause of sulfate retention by acid soils. Soil Sci. Soc. Am. J. 41, 686–692.

[18] Nordstrom, D.K., Ball, J.W., Robertson, C.E., Hanshaw, B.B. (1984) The effect of sulfate on aluminum concentrations in natural waters: II. Field occurrences and identification of aluminum hydroxysulfate precipitates. Geol. Soc. Am. Program Abstr. 16(6), 611.

[19] Herrmann, R. and Baumgartner, I. (1992) Aluminum species distribution during mixing of acid coal and slate mine drainage with neutral stream waters. Geologische Rundschau. 81(3), 759-67

[20] Kim, J.J. and Kim, S.J. (2003a) Seasonal factors controlling mineral precipitation in the acid mine drainage at Donghae coal mine, Korea, Science of the Total Environment, 325, 181-191.

[21] Nordstrom, D.K., Alpers, C.N., Ptacek, C.J., and Blowes, D. (2000) Negative pH and extremely acidic mine waters at Iron Mountain Mine, California. Environmental Science and Technology. 34, 254-258

[22] Kim, J.J. and Kim, S.J. (2003b) Environmental, Mineralogical, and Genetic Characterization of Ochreous and White Precipitates from Acid Mine Drainages in Taebaeg, Korea. Environmental Science and Technology. 37(10), 2120-2126.

[23] Lee, G., Bigham, J. M. and Faure, G. (2002) Removal of trace metals by coprecipitation with Fe, Al and Mn from natural waters contaminated with acid mine drainage in the Ducktown Mining District, Tennessee. Applied Geochemistry. 17(5), 569-581

[24] Pu, X., Vazquez, O., Monnell, J.D., Neufeld, R.D. (2010) Speciation of aluminum precipitates from acid mine discharges in Central Pennsylvania. Environ. Eng. Sci. 27(2), 169-180
[25] Seo, E.Y., Cheong, Y.W., Yim, G.J. (2017) Recovery of Fe, Al and Mn in acid coal drainage by sequential selective precipitation with control of pH. Catena. 148(SI), 11-16.
[26] Masindi, V., Gitari, M.W., Tutu, H., De Beer, M. (2016) Fate of inorganic contaminants post treatment of acid mine drainage by cryptocrystalline magnesite: Complimenting experimental results with a geochemical model. Jr. Environ. Chem. Eng. 4(4), 4846-4856.
[27] Standard Methods for the Examination of Water and Wastewater. (2005) 21st Edition. Washington, D.C.: APHA-AWWAWPCF.
[28] Hach Company, (2003) Water Analysis Hand Book. 4th Ed. Hach Company, Loveland, CO.
[29] Berkowitz, J., Anderson, M.A., and Graham, R.C. (2005) Laboratory investigation of aluminum solubility and solid-phase properties following alum treatment of lake waters. Water Res. 39(16), 3919-3928
[30] Leonard, G. (1973) Selected Powder Diffraction Data for Minerals. Joint Committee on Powder Diffraction Standards, Swarthmore, PA.
[31] Huang, P., Wang, M., Kampf, N., Schultze, D., (2002) Aluminum hydroxides. In: Dixon, J.B., Schulze, D.G. (Eds.) Soil Mineralogy with Environmental Applications. Soil Science Society of America, Madison, WI, 261–289.
[32] Karathanasis, A., Harris, W. (1994) Quantitative thermal analysis of soil minerals. In: Amonette, J.E., Zelazny, L.W. (Eds.) Quantitative Methods in Soil Mineralogy. Soil Science Society of America, Madison, WI, 360–411.
[33] Brydon, J.E., and Shah Singh, S. (1969) The nature of the synthetic crystalline basic aluminum sulphates as compared with basaluminite. The Canadian Mineralogist. 9(5), 644-654.

Received: **18.09.2018**
Accepted: **01.03.2019**

CORRESPONDING AUTHOR

Xunchi Pu
State Key Laboratory of Hydraulics and Mountain River Engineering,
Sichuan University,
610065 Chengdu City – China

e-mail: puxunchi@163.com

© by PSP Volume 28 – No. 4/2019 pages 2644-2649 Fresenius Environmental Bulletin

DETERMINATION OF ANTIOXIDANT CAPACITIES, CHEMICAL COMPOSITION AND MELISSOPALYNOLOGICAL CHARACTERIZATION OF *VERBASCUM* SPP. AND *EUPHORBIA* SPP. HONEYS

Asli Ozkok*

Hacettepe University, Bee and Bee Products Applications and Research Center (HARUM), 06800, Beytepe, Ankara, Turkey

ABSTRACT

In this sudy, it has been researched for the first time of two new genus honey type, which were visited by honeybees. These genuses are *Euphorbia* (Euphorbiaceae family) (spurge or milkweed honey) and *Verbascum* (Scrophulariaceae family) (mullein honey). First of all mellissopalynological examinations determined and then total phenolic and total flavonoid capacity, sugar composition and chemical compouns found.

Total phenolic acid content was determined as 146.49±0.11 mgGAE/kg for mullein honey and 136.92±0.06 mgGAE/kg for spurge honey. Total flavonoid content was determined as 35.54±0.05 mgQE/kg for mullein honey and 40.68±0.03 mgQE/kg for spurge honey. The results of sugar analysis performed by HPLC show that, Fructose 45.7%, Glucose 24.8% and F/G rate was 1.84±0.17 for mullein honey and Fructose 38%, Glucose 28.5% and F/G rate was 1.33±0.02 for spurge honey. GC-MS analysis of honey samples revealed alcohols, carboxylic acids and their esters, fatty acids, flavonoids, carbohydrates, ketones, terpenes and other chemical compounds. To the best of our knowledge, this was the first study about spurge and mullein monofloral honeys.

KEYWORDS:
Euphorbia (spurge) honey, *Verbascum* (mullein) honey, melissopalynology, total phenolic and total flavonoid, sugar composition, chemical compound.

INTRODUCTION

Honeybees are important pollinators for our environment. The importance of beekeeping activity for man and nature Albert Einstein explained that "If bees disappear from the earth, human beings will only have 4 years of life. If no bees, fertilization, plants, animals and people will not exist"[1]. Therefore, we must protect and reproduce honeybees and their favorite plants. *Euphorbia* and *Verbascum* plants are one of them.

Euphorbia (Euphorbiaceae family) and *Verbascum* (Scrophulariaceae family) species have cosmopolite distribution in Turkey. *Verbascum* is the second most common genus in Turkey with 232 species, 185 of them are endemic in Turkey [2]. Also *Euphorbia* genus has about 95 species, 15 of them are endemic in Turkey [2]. The nectar and pollen efficiency of *Euphorbia* is trace. But *Verbascum* species has got dominant pollen and trace nectar efficiency [3]. These two genus are frequently visited by honeybees, depending on the flora of the region where they are located. So nectars and pollens are carried into the hive. Although their pollen grains can be found in multifloral honeys, it is very difficult to find them as a monofloral (unifloral) honey. So it is the first time we obtained *Euphorbia* (spurge or milkweed) and *Verbascum* (mullein) monofloral honeys from Turkey and studied some characterizations. At the same time monofloral honeys are important because of high marketing values [4]. For this reason, different monofloral honeys should be investigated and this situation can be significant for the beekeepers, honey producers and consumers etc.

Melissopalynological analysis is the microscopic analysis of honey samples and it is important for the botanical identification of honey. The determination of the botanical origin is based on the relative frequencies of nectariferous species' pollen types. The frequency classes of pollen grains were given as dominant (>45%), secondary (16-45%), minor (3-15%) and trace pollen (<3%) [5, 6].

Usually, a honey is considered as monofloral if the pollen frequency of that plant is >45%. These are general guidelines but many pollen types are underrepresented (*Robinia pseudoacacia*, *Citrus* spp., *Tilia* spp., *Lavandula* spp., *Rosmarinus* spp.) or over-represented (*Castanea sativa* Mill, *Eucaliptus* spp.). For monofloral honey with underrepresented pollen, the minimum percentage of the taxon that gives the honey name is 15% for acacia, 10% for citrus while honey with overrepresented pollen, a content of 70-90% of monofloral pollen is required to classify chestnut and eucalyptus honey, honey as monofloral [6-8].

In this study it has been determined monofloral spurge and mullein honey types via melissopalynological analysis from Diyarbakır and

FIGURE 1
Honey samples obtained from Bingöl and Diyarbakır provinces

Bingöl provinces at the first time in Turkey. Also total phenolic and total flavonoid capacities were made by UV-VIS Spectrophotometer (Genesys 10S UV-VIS Spectrophotometer). Sugar compositions were determined by High Performance Liquid Chromatography (HPLC) (Agilent 1200 Series) and chemical characterization found by Gas Chromatography-Mass Spectrometry (GC-MS). To the best of our knowledge, this was the first study about spurge and mullein honey.

MATERIALS AND METHODS

Collection of Honey Samples. Mullein and spurge honey types were collected as pool samples from Diyarbakır and Bingöl regions of Turkey in 2016 (Fig. 1).

Melissopalynological Analysis. For microscopic analysis Wodehouse (1935) [9] and Sorkun (2008) [5] methods were accepted and honey preparations were examined by Nikon Eclipse E400 microscope.

500 grams of stock honey was well stirred with a sterile glass stick and 10 grams of it was separated for obtain preparats. Then the sample and 20 ml distilled water mixed in a tube and left in a water bath of 45°C for 30-45 minutes. Then this melted honey mixture was centrifuged in 3500 rpm for 45 minutes. Water in centrifuged tubes was removed and tubes were left upside down on a drying mat for full drainage. The material was taken from the bottom of the tube and plated on a lam with basic fucsin-glycerin gelatin mixture.

Basic fucsin-glycerin-gelatine mixture and honey were taken with the edge of a sterile needle was transferred to a microscope slide and put on a hotplate set at 40°C. When the gelatine was melted, 18 × 18 mm^2 cover slips were placed on the samples. Pollen slides were researched with Nikon Eclipse E400 microscope and immersion objective (x100) was used for identification of pollens. During microscopic studies all the area, which is 18x18mm^2, was checked. 200 pollens were counted for every sample and determined pollen types according to their botanical origin.

Identification of Honey Sample Preparates. Relevant sources were used in the identification of the pollen were from Persano Oddo and Piro (2004) [4], Sorkun (2008) [5], Özkök Tüylü and Sorkun (2007) [10], PalDat [11] as well as reference preparats.

Total Phenolic Acid Analysis. The total phenolic content of honey samples was determined by the Folin-Ciocalteu method [12, 13].

Total Flavonoid Analysis. The total flavonoid content of honeys was estimated by aluminium chloride ($AlCl_3$) colorimetric method [12, 13].

High Performance Liquid Chromatography (HPLC) Sugar Analysis. Bogdanov and Baumann (1988) [14] method and HPLC (Agilent 1200 Series) were used for the determination of fructose and glucose at honey samples.

Gas Chromatography-Mass Spectrometry (GC-MS) Chemical Compounds Analysis. GC-MS was used for chemical compound analysis of the honey samples. 1 mg secretion dissolved in 5 ml methanol and mixed for 1 minute by vortex. Next centrifuged at 3500 rpm for 15 minutes. Then upper phase was filtered to vials and 1 µl solution injected to GC-MS. A GC 6890N from Hewlett-Packard (Palo Alto, CA, USA) coupled with mass detector (MS 5973 Hewlett-Packard) was used for the analysis of honey samples. Experimental conditions of GC-MS system were as follows: DB 5MS column (30mx0.25 mm and 0.25 µm of film thickness) was used and flow rate of mobile phase (He) was set at 0.7 ml/min.

RESULTS AND DISCUSSION

Melissopalynological Analysis Results. Melissopalynological analysis is important for the identification of plant origin in honey. As a result of melissopalynological analyses three pollen types belonging to three botanical families were identified in the mullein honey. *Verbascum* sp. pollen was dominant with 97% (Fig. 2) amount and other pollen types (Asteraceae and *Campanula* sp.) were trace amounts with under 3%. In the spurge honey eleven pollen types belonging to ten botanical families were identified. *Vicia* spp. (35%) and *Trifolium* spp. (27%) pollen were identified seconder, Brassicaceae (12.4%), Asteraceae (9.5%) and *Euphorbia* spp. (7.5%) (Figure 3) pollen were identified minor and *Salix* spp. (2.5%), Polygonaceae (2.5%), Cistaceae (1.5%), Apiaceae (1%), *Rumex* spp. (1%), Lamiaceae (0.5%) pollen were identified trace amounts (Table 1). According to Corvucci et al (2014), percent frequency types of pollen grains were given as dominant (≥45%)(D), secondary (15-45%)(S), minor (3-15%)(M) and trace (≤3%) (T). But some honey types can not be comply these rules because of nectar and pollen production situation. For example, chestnut honey characterize with 90% pollen meanwhile, citrus at least 10% or lavender 5-10%. In this study we revealed mullein honey has got high pollen potential like chestnut honey whereas spurge honey has got a low pollen potential. Also D'Albore (1997) [3] found mullein pollen potential is dominant while spurge pollen potential is trace. In the direction of this information, we can say that these honeys showed that monofloral mullein and spurge honey properties.

Total Phenolic and Flavonoid Analysis Results. Total phenolic content was determined as 146.49±0.11 mgGAE/kg for mullein honey and 136.92±0.06 mgGAE/kg for spurge honey. Total flavonoid content was determined as 35.54±0.05 mgQE/kg for mullein honey and 40.68±0.03 mgQE/kg for spurge honey (Table 1). Until this study total phenolic and flavonoid contents did not determine in the spurge and mullein honey. So we couldn't compare the result any other researchers results. However, these results are high and resemble chestnut honey, which has high antioxidant activity. Bertoncelj (2007) [15] found total phenolic content 199.9±34.1 mgGAE/kg in chestnut honey.

Sugar Analysis Results. The results of sugar analysis performed by HPLC show that, Fructose 45.7%, Glucose 24.8% and F/G rate was 1.84±0.17 for mullein honey and Fructose 38%, Glucose28.5% and F/G rate was 1.33±0.02 for

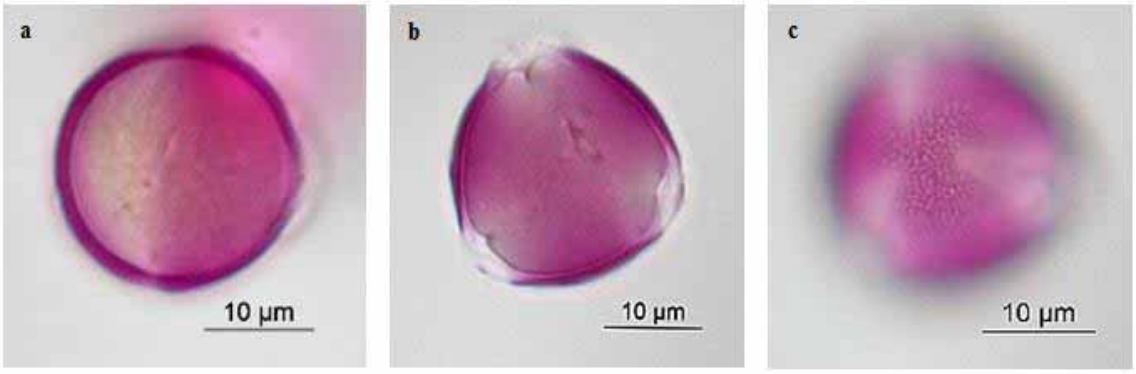

FIGURE 2
Verbascum spp. pollen, a. Equatorial view, b. Polar view, c. Ornemantation view

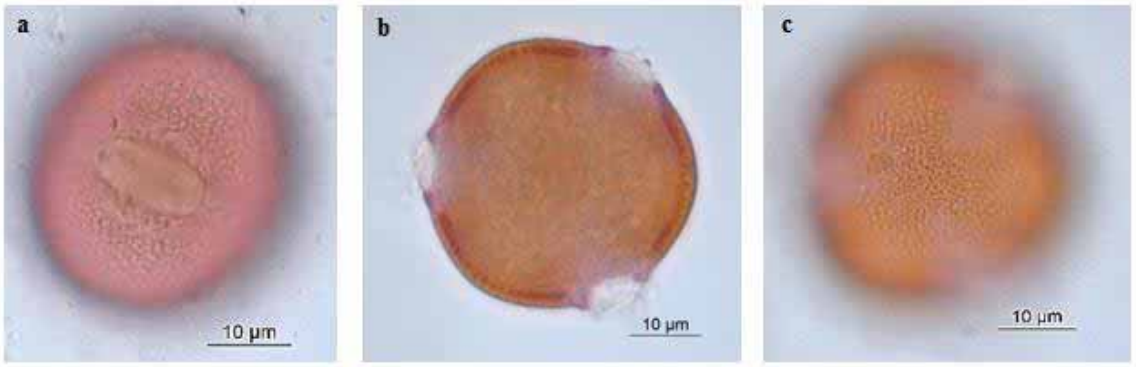

FIGURE 3
Euphorbia spp. pollen, a. Equatorial view, b. Polar view, c. Ornemantation view

spurge honey (Table 1). According to Turkish Food Codex (2012) [16] and Codex Alimentarius Committee on Sugars (2001) [17] Fructose+Glucose amount should be more than 60g/100g and ratio of fructose to glucose should be between 0.9 and 1.4 for the flower honeys. Both of the honey type's Fructose+Glucose amount more than 60g/100. But fructose to glucose ratio of mullein honey result is higher than 1.4. At the same time in the Turkish Food Codex (2012) [16] and Codex Alimentarius Committee on Sugars (2001) [17] fructose to glucose ratio is between 1.0-1.85 for chestnut (*Castanea sativa*) and between 1.2-1.85 for acacia (*Robinia pseudoacacia*) honeys. So 1.84±0.17 amount can be appropriate for the mullein honey and it can use as a data for the monofloral honey studies.

TABLE 1
Mullein and Spurge honey mellissopalynological, total phenolic acid & total flavonoid and sugar analysis results

Honey type	Plant Species in honey	% Pollen*	Region	Total Phenolic Acid Content (mgGAE/kg)	Total Flavonoid Content (mgQE/kg)	Fructose	Glucose	Fructose/Glucose F/G
Mullein	*Verbascum* sp.	97 (D)	Bingöl	146.49±0.11	35.54±0.05	45.7	24.8	1.84±0.17
	Asteraceae	2 (T)						
	Campanula spp.	1 (T)						
	Vicia spp.	35 (S)						
	Trifolium spp.	27 (S)						
	Brassicaceae	12.4(M)						
	Asteraceae	9.5 (M)						
	Euphorbia sp.	7.5 (M)						
Spurge	*Salix* spp.	2.5 (T)	Diyarbakır	136.92±0.06	40.68±0.03	38	28.5	1.33±0.02
	Polygonaceae	2.5(T)						
	Cistaceae	1.5 (T)						
	Apiaceae	1 (T)						
	Rumex spp.	1 (T)						
	Lamiaceae	0.5(T)						

* ≥45% Dominant (D), (16-45%) Seconder (S), (3-15%) Minor (M), (<3%) Trace (T).

TABLE 2
GC-MS chemical compounds analysis results of honey samples

Compounds	Spurge (*Euphorbia* sp.) honey	Mullein (*Verbascum* sp.) honey
Alcohols		
4-Methylcyclohexanol	-	0.34
Total	-	0.34
Carboxylic Acids and Their Esters		
1,3-Butadiene-1-carboxylic acid	-	0.05
Thiocarbamic acid, N,N-dimethyl, S-1,3-diphenyl-2-butenyl ester	0.13	-
Carbonic acid, but-2-yn-1-yl eicosyl ester	-	9.93
6-Chlorohexanoic acid	-	0.22
Hexanoic acid, 4-methyl-	0.57	-
5-Amino-2H-pyrazole-3-carboxamide	0.18	-
Methyl 4-hydroxy-3,5-dimethoxybenzoate (Syringic Acid Methyl Ester)	-	4.29
Total	0.88	14.49
Fatty Acids		
Docosenoic acid (Behenic acid)	-	12.63
Total	-	12.63
Flavonoids		
4H-Pyran-4-one, 2,3-dihydro-3,5-dihydroxy-6-methyl- (DDMP)	-	1.25
Total	-	1.25
Carbohydrates		
Melezitose	-	0.81
Lactose	61.35	-
Total	61.35	0.81
Ketones		
2-(n-Propyl)oxybenzylidene acetophenone	0.22	-
Total	0.22	-
Terpenes		
Furan, 2,5-dimethyl-	1.05	0.06
2,4-Dimethylfuran	0.02	-
Total	1.07	0.06
Others		
1-(Methanesulfonyl)-2-(methylsulfanyl)ethane	0.14	-
Pyrazole, 1,4-dimethyl-	-	0.82

GC-MS Chemical Compounds Analysis Results. In this study we also investigated the chemical content of the these two new monofloral honey type via GC-MS (Table 2).

The most abundant compounds were carboxylic acids and their esters and fatty acids for mullein honey (Table 2). 14.49% and 12.63% amounts found respectively. On the other hand the most abundant compounds were carbohydrates in the spurge honey with 61.35%. Lactose amount is very high. This result is normal because *Euphorbia* genus has got milky latex [2, 18] and lactose is the major carbohydrate of milk [19]. So lactose can be the marker compound for the spurge honey. Beside this, melezitose found in the mullein honey. This sugar type usually found in the honeydew honeys [20-23]. Honeydew honey is prepared from secretions of living parts of plants or excretions of plant-sucking insects on the living part of plants [24, 25]. Melezitose can be the marker compound for the mullein honey.

Furan derivatives (Furan, 2,5-dimethyl- and 2,4-Dimethylfuran) were found generally at the both honey samples but their amounts were low. Also Radovic et al (2001) [26], Cuevas-Glory et al (2007) [27] and Jerkovic & Marijanovic (2010) [28] found furan derivatives in the different type honey samples.

Flavanoids are important compounds because of their antioxidant effects. Flavanones are one of the most important groups of the flavonoids. Yu et al (2013) [29] and Özkök et al (2016) [25] determined 2,3-dihydro-3,5-dihydroxy-6-methyl-4H-pyran-4-one (DDMP) flavanones which is a strong antioxidant in the pine honey samples. Also we found DDMP in the only mullein sample with 1.25% amount.

CONCLUSIONS

In this study, melissopalynologic analysis, total phenolic and flavonoid content, sugar analysis and chemical compounds analysis were done and evaluated for the characterization for two new monofloral honey types. Spurge and mullein honeys characterizations were shown in this study and these datas can be shed light to the honey standart studies.

ACKNOWLEDGEMENTS

I would like to thank Turkish Beekeeping Association for help us to obtain the honey samples for our studies.

REFERENCES

[1] Semerci, A. (2017) Overall Situation of Beekeeping in Turkey and Future Prospects. Journal of Agricultural Faculty of Mustafa Kemal University. 22(2), 107-118.

[2] Seçmen, Ö., Gemici. Y., Görk, G., Bekat, L. and Leblebici, E. (2000) Systematic of Seed Plants. Ege University Publishing House, Bornova, İzmir, 1-394.

[3] D'Albore, G.R. (1997) Textbook of Melissopalynology. Apimondia Publishing House, Bucharest. 1-308.

[4] Persano Oddo, L. and Piro, R. (2004) Main European Unifloral Honeys: Descriptive Sheets. Apidologie. 35(1), 38-81.

[5] Sorkun, K. (2008) Turkey's Nectar Plants, Pollen and Honeys. Palme Publishing House, Ankara, 1-341. (in Turkish)

[6] Corvucci, F., Nobili, L., Mellucci, D. and Grillenzoni, V.T. (2015) The Discrimination of Honey Origin Using Melissopalynology and Raman Spectroscopy Techniques Coupled with Multivariate Analysis. Food Chemistry. 169, 297-304.

[7] Sabatini, A.G., Bortolotti, L. and Marcazan, G.L. (2007) Know the Honey (Conoscere il miele). 2nd ed. Avenue Media, Bologna.

[8] Terrab, A., González, A.G., Díez, M.J. and Heredia, F.J. (2003) Characterization of Moroccan Unifloral Honeys Using Multivariate Analysis. European Food Research Technology. 218(1), 88-95.

[9] Wodehouse, R.P. (1935) Pollen Grains. Mc Graw, Hill N.Y., 106-109.

[10] Özkök Tüylü, A. and Sorkun, K. (2007) The Investigation of Morphologic Analysis of Pollen Grains Which are Economically Important and Collected by *Apis mellifera* L. Hacettepe Journal of Biology and Chemistry. 35(1), 31-38

[11] Palynological Database (PalDat), AutPal-Society for the Promotion of Palynological Research in Austia Department of Botany and Biodiversity Research University of Vienna Rennweg 14 A-1030 Vienna, Austria URL: http://www.paldat.org/ , (Last access December 2017).

[12] Hoerudin, D. (2004) Phenolic and Flavonoid Contents of Australian Honeys from Different Floral Sources. Master Thesis. Queensland University, Australia

[13] Özkök, A., D'Arcy, B. and Sorkun, K. (2010) Total Phenolic Acid and Total Flavonoid Content of Turkish Pine Honeydew Honey. Journal of ApiProduct and ApiMedical Science. 2(2), 65-71.

[14] Bogdanov, S. and Baumann, E. (1988) Determination of Honey Sugars by HPLC, Mitteilungen Aus Dem Gebiete Der Lebensmitteluntersuchung Un Hygiene. 79, 198-206. (in German)
[15] Bertoncelj, J., Doberšek, U., Jamnik, M. and Golob, T. (2007) Evaluation of The Phenolic Content, Antioxidant Activity and Colour of Slovenian Honey. Food Chemistry. 105(2), 822-828.
[16] Turkish Food Codex (2012) Turkish Food Codex. Codex No: 2012/58.
[17] Codex Alimentarius Commission (2001) Revised Codex Standard for Honey Codex Stan 12-1981, Rev. 1(1987), Codex Standard, 1-7.
[18] Öksüz, S., Ulubelen, A. and Barla, A. (2002) Terpenoids and Aromatic Compounds from *Euphorbia heteradena*. Turkish Journal of Chemistry. 26(4), 457-463.
[19] Mahajan, R.T. and Chaudhari, G.M. (2014) Plant Latex as Vegetable Source for Milk Clotting Enzymes and Their Use in Cheese Preparation. International Journal of Advanced Research. 2(5), 1173-1181.
[20] Hudson, C.S., Sherwood, S.F. (1920) The Occurrence of Melezitose in Honey. Journal of the American Chemical Society. 42(1), 116-125
[21] Siddiqui, I.R. (1970) The Sugars of Honey. Advances in Carbohydrate Chemistry and Biochemistry. 25, 285-309
[22] Doner, L.W. (1977) The Sugars of Honey-A review. Journal of the Science of Food and Agriculture. 28(5), 443-456.
[23] Krauze, A. and Zalewski, R.I. (1991) Classification of Honeys by Principal Component Analysis on The Basis of Chemical and Physical Parameters. Zeitschrift fuer Lebensmittel Untersuchung und Forschung. 192(1), 19-23.
[24] Sanz, M.L., Gonzalez, M., Lorenzo, C., Sanz, J. and Martinez-Castro, I. (2005) A Contribution to the Differentiation Between Nectar Honey and Honeydew Honey. Food Chemistry. 91(2), 313-317.
[25] Özkök, A., Sorkun, K. and Salih, B. (2016) The Microscopic and GC-MS Analysis of Turkish Honeydew (Pine) Honey. Hacettepe Journal of Biology and Chemistry. 44(4), 375-383.
[26] Radovic, B.S., Careri, M., Mangia, A., Musci, M., Gerboles, M., Anklam, E. (2001) Contribution of Dynamic Headspace GC-MS Analysis of Aroma Compounds to Authenticity Testing of Honey. Food Chemistry. 72(4), 511-520.
[27] Cuevas-Glory, L.F., Pino, J.A., Santiago, L.S. and Sauri-Duch, E. (2007) A Review of Volatile Analytical Methods for Determining The Botanical Origin of Honey. Food Chemistry. 103(3), 1032-1043.
[28] Jerkovic, I. and Marijanovic, Z. (2010) Oak (*Quercus frainetto* Ten.) Honeydew Honey-Approach to Screening of Volatile Organic Composition and Antioxidant Capacity (DPHH and FRAP assay). Molecules. 15(5), 3744-3756.
[29] Yu, X., Zhao, M., Liu, F., Zeng, S. and Hu, J. (2013) Identification of 2,3-dihydro-3,5-dihydroxy-6-methyl-4H-pyran-4-one as a Strong Antioxidant in Glucose–histidine Maillard Reaction Products. Food Research. International. 51(1), 397-403.

Received: **07.11.2018**
Accepted: **18.02.2019**

CORRESPONDING AUTHOR

Asli Ozkok
Hacettepe University,
Bee and Bee Products Application and Research Center, Biology Department,
06800, Beytepe, Ankara – Turkey

e-mail: asozkok@gmail.com
aozkok@hacettepe.edu.tr

© by PSP Volume 28 – No. 4/2019 pages 2650-2655 Fresenius Environmental Bulletin

THE ORIGIN OF THE OAK HONEYDEW HONEY PRODUCED FROM *QUERCUS FRAINETTO* TEN

Asli Ozkok[1,*], Ahmet Ipek[2], Kadriye Sorkun[1,3]

[1]Bee and Bee Products Application and Research Center (HARUM), Hacettepe University, 06800, Beytepe, Ankara, Turkey
[2]The General Directorate of Forestry, 06560, Yenimahalle, Ankara, Turkey
[3]Department of Biology, Faculty of Sciences, Hacettepe University, 06800, Beytepe, Ankara, Turkey

ABSTRACT

Oak honey is a honeydew honey type. In this study, investigated the source of oak honey and questioned whether it was insect source or extrafloral source. For this purpose, oak species samples were collected from the regions, where the oak honey was produced intensely, in 2016 and 2017. In addition, insect species producing secretion on tree fragments for two years have been observed and studied.

Trunk, leaf and fruit parts were taken from oak trees with dark brown secretion. In these samples, anatomical studies have been done to find both the secretion source and is there any damages in the tree tissues due to insect source. Two types of method were followed for the anatomical investigations. Also chemical composition of oak secretion was determined by GC-MS.

As a result of study has shown that *Quercus frainetto* Ten. fruits have got a great number of secretory glandular trichomes and these trichomes produces sweet secretions. In addition to this, GC-MS chemical substance analyses of the oak secretion revealed alcohols, aldehydes, aromatic acids, aromatic compounds, carbohydrates, carboxylic acids and their esters, fatty acids and other compounds.

KEYWORDS:
Anatomical studies, GC-MS, chemical composition, oak honey, *Quercus frainetto* Ten.

INTRODUCTION

Nectar is the sugary substance which is produced by plants in the glands called nectaries. When nectaries grow in the flowers of plants, they are named as floral nectaries but if they occur in outside of the flower, they are named extrafloral nectaries [1]. Extrafloral nectaries are usually found in the root or trunk of the plant [2-4]. Insects, especially pollinators insects like honeybees prefer floral and extrafloral nectars for making honey. So honey can be broadly categorized as floral or honeydew honey. Floral honey is derived from honeybees collecting nectar from plants, whereas honeydew honey is derived from honeybees collecting sweet substances mainly from the excretions of plant-sucking insects (*Hemiptera*) on the living parts of plants or secretions of the living parts of plants [5, 6]. Clover, thyme, acacia, and citrus are some examples of floral honey varieties, while pine, oak and fir are examples of honeydew honey varieties.

Oak (*Quercus* L.) trees, which belongs to Fagaceae family, are an important plant group for our environment because live long. Most species of oaks live over 200 years. They are widely distributed in the Northern Hemisphere and there are nearly 531 species in the world [7]. There are 18 varieties, 9 subspecies and 2 varieties naturally grown in Turkey [8]. Seven of the oak species found in Turkey are important oak species utilized in the production of honeydew honey in the world. These are; *Quercus frainetto*, *Quercus petraea, Quercus hartwissiana*, *Quercus cerris*, *Quercus robur*, *Quercus pubescens* and *Quercus ilex* (8-10]. But among them *Q. frainetto* Ten. is the most important in the production of honeydew and generally it is located to the northwest of Turkey [11]. Especially Kırklareli province, where is the northwest of Turkey, oak honey is produced intensely and usually oak trees, which belongs to *Q. frainetto* Ten. species, are covered with dark brown secretion. It was unknown whether the source of this dark brown secretion was an insect or an extrafloral source. So in this study, we wanted the find the source of oak honey and questioned whether it was insect source or extrafloral source. For this purpose, oak species samples were collected from the regions, where the oak honey was produced intensely, in 2016 and 2017. In addition, insect species that produce secretions on tree fragments for two years have been observed and studied. Anatomical studies were done at the oak sample parts. Beside this chemical composition of oak secretion was determined by GC-MS.

To the best of our knowledge, there is no information in the literature about the anatomic source of oak honey and GC-MS analysis of oak secretion; thus, the outcomes of this study are important for the classification and characterization oak honey.

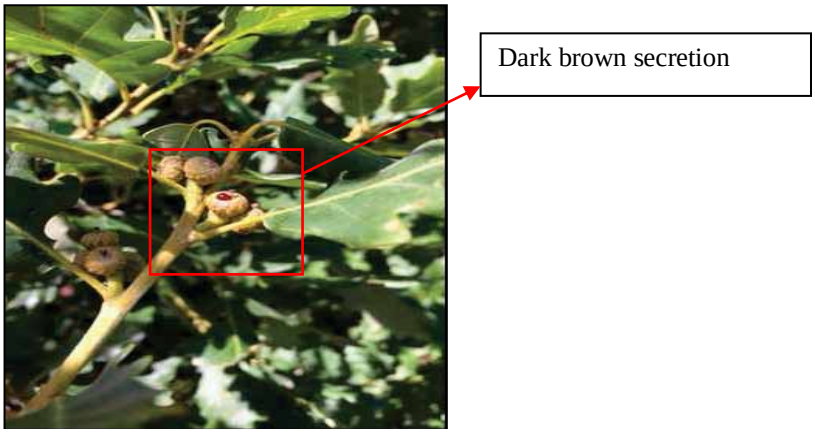

FIGURE 1
***Quercus frainetto* Ten. fruit parts, which were dark brown secretion on it.**

FIGURE 2
Turkey and Kırklareli province in Turkey.

MATERIALS AND METHODS

Collection of oak samples. Dark brown secretory oak species (Fig. 1), which is *Q. frainetto* Ten., trunk, leaf and fruit samples were collected from the Kırklareli province (Fig. 2) in June 2016 and June 2017 with the help of the General Directorate of Forestry. All the samples were placed in jars separately and brought to the laboratory for anatomical studies. Also dark brown secretory of the *Q. frainetto* Ten. was put into the tubes and brought to the laboratory for GC-MS studies.

Anatomical studies. Anatomical studies were done from the trunk, leaf and fruit parts of the oak samples to learn is there any damages in the tree tissues due to insect and find the source of dark brown secretion. Two types of method were followed for the anatomical investigations.

At the first method tree tissue samples sections were taken manually and then preparations were prepared by binary painting method [12]. According to this method all the sections of the samples (trunk, leaf and fruit) were placed in the hypochlorite solution to provide color clarity. After a few seconds they were washed twice in distilled water. Later they were left in the binary dye (mix of aniline/safranine 9/1 or mix of aster blue/safranine 9/1) mixture for 9-10 seconds then they were washed twice in distilled water and sample sections put in the microscope slide for the microscopic examination. Tissue section samples photographs were taken by the microscope (Olympus CX41) and camera (Olympus E330).

At the second method tree tissue samples sections were taken automatically by the Cryotome Cryostat Equipment (Leica CM1520) and directly put in the microscope slide for the microscopic examination. Tissue sections could not be painted because they were very easily disintegrated. Tissue section samples photographs were taken by the microscope (Leica DM1000) and camera (Leica DFC320).

Gas Chromatography-Mass Spectrometry (GC-MS) chemical compounds analysis. Gas Chromatography-Mass Spectrometry (GC-MS) was used for chemical compound analysis of the oak secretion. 1 mg secretion dissolved in 5 ml methanol and mixed for 1 minute by vortex. Next centrifuged at 3500 rpm for 15 minutes. Then upper phase was filtered to vials and 1 µl solution injected to GC-MS. A GC 6890N from Hewlett-Packard (Palo Alto, CA, USA) coupled with mass detector (MS 5973 Hewlett-Packard) was used for the analysis of honey samples. Experimental conditions of

GC-MS system were as follows: DB 5MS column (30mx0.25 mm and 0.25 µm of film thickness) was used and flow rate of mobile phase (He) was set at 0.7 ml/min. In the gas chromatography part, temperature was kept at 150 °C with 10°C/min heating ramp. After this period, temperature was kept at 150 °C for 2 minutes. Finally, temperature was increased to 280 with 20°C/min heating ramp and then kept at 280°C for 49 minutes and chemical substances of the honey samples were identified by using standard Nist Libraries available in the data acquisition system of GC-MS.

RESULTS AND DISCUSSION

Anatomic analysis results. All *Q. frainetto* Ten. parts samples sections investigated by the microscope and microscopic results of trunk, leaf and fruit tissue section samples showed Figs. 3-8.

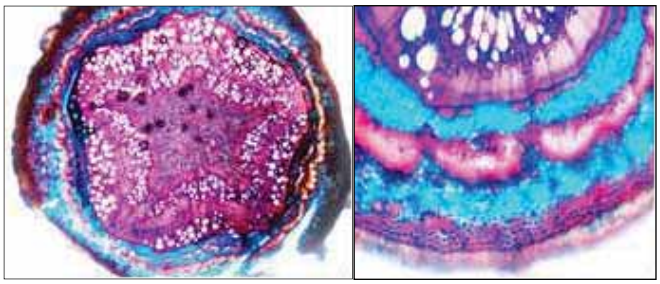

FIGURE 3
***Quercus frainetto* Ten. trunk sections (according to first method).**

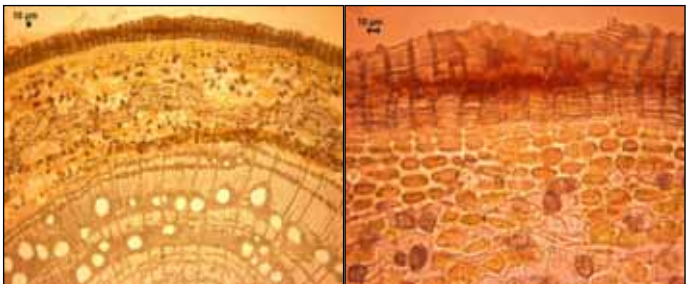

FIGURE 4
***Quercus frainetto* Ten. trunk sections (according to second method).**

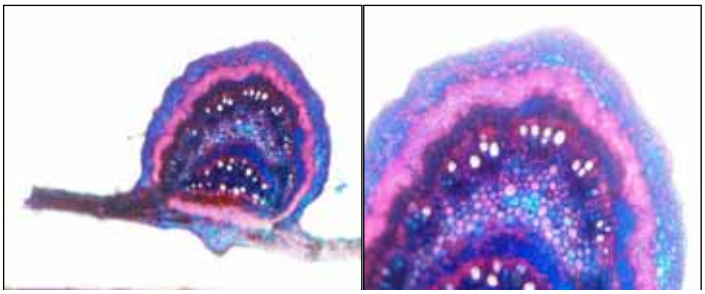

FIGURE 5
***Quercus frainetto* Ten. leaf sections (according to first method)**

FIGURE 6
***Quercus frainetto* leaf sections (according to second method)**

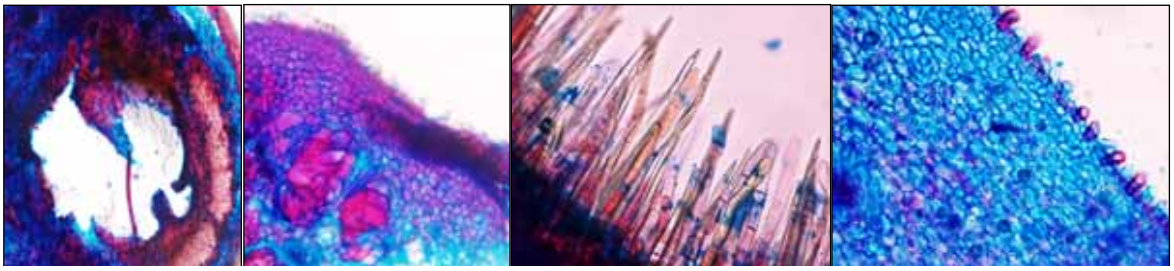

FIGURE 7
Quercus frainetto Ten. fruit sections (according to first method)

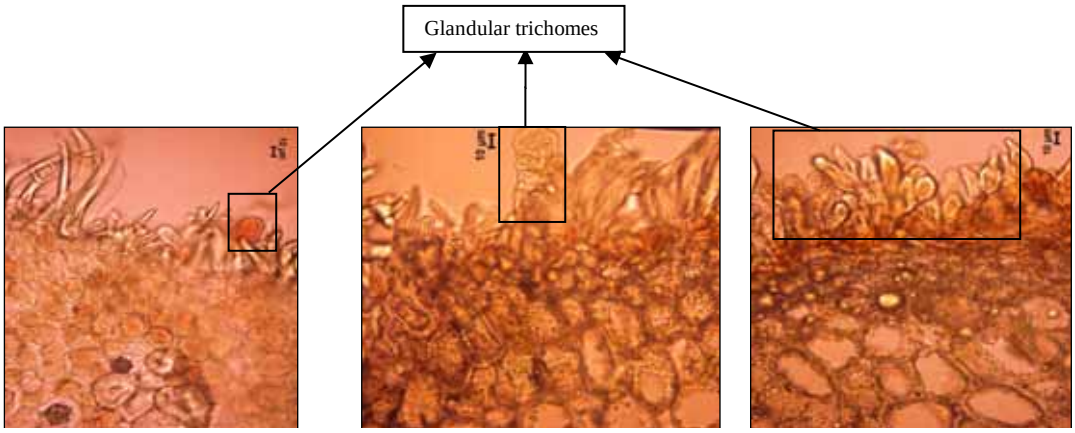

FIGURE 8
***Quercus frainetto* Ten. fruit sections (according to second method)**

TABLE 1
Chemical composition of *Q. frainetto* Ten. dark brown secretion

Chemical component	Retention Time	Area percentage %
Alcohols		
1-Propanol, 3-[(2-hydroxyethyl)thi	8.763	0.36
Phenol, 2,2'-methylenebis[6-(1,1-d	20.210	3.59
Aldehydes		
Furfural	5.093	0.23
Furan, 2,5-dimethyl-	6.025	0.07
Aromatic acids		
Benzenepropanoic acid	23.714	3.59
Aromatic compounds		
3,5-Dimethylpyrazole	5.905	0.07
Carbohydrates		
Melezitose	16.713	2.12
D-Mannoheptulose	9.048	0.39
D-Glucopyranose	17.987	20.26
d-Glycero-l-gluco-heptose	18.530	17.86
Carboxylic Acids and Their Esters		
6-Chlorohexanoic acid	22.651	4.02
3,4- Altrosan	7.151	1.72
Fatty acids		
Tricosanoic acid	21.491	1.00
Other compounds		
2-(n-Propyl)oxybenzylidene acetoph	26.326	1.20

According to the microscopic analysis results, were not observed plant sucking insect traces and damages in the leaf, stem and fruit samples sections (Figs. 3-8). Also there were not detected any honeydew insect species in the oak trees by the entomologist in both years. Beside this, Ülgentürk et al., (2013) [13] found insect species, which are produced honeydew, at the oak species in different regions of Turkey. These insects and oak species are *Lachnus roboris* (*Q. suber*), *Parthenolecanium rufulum* (*Q. cerris*), *Acanthococcus roboris* (*Q. cerris*), *Kermes vermilio* (*Q. ballotae*, *Q. coccifera, Q. ilex, Q. suber*), *Kermes greeni (Q. coccifera*). As seen in all these examples there hasn't been encountered any insect species at the *Q. frainetto* Ten. Also Jerkovic & Marijanovic (2010) [14] mentioned that *Q. frainetto* Ten. fruits had a sweet sap and this was produced without the mediation of plant sucking insects. But they didn't point out exact anatomical source of the secretion. In this

study we noticed that leaf and trunk sections had no any trace about the secretion but fruit parts sections had too many glandular trichomes (Fig. 8). These glandular trichomes were the source of *Q. frainetto* Ten.fruits sweet sap and so also honeydew.

GC-MS Secretion Analysis Results. As a result of the GC-MS chemical substance analyses of the oak secretion revealed alcohols, aldehydes, aromatic acids, aromatic compounds, carbohydrates, carboxylic acids and their esters, fatty acids and other compounds (Table 1).

Glandular trichomes are a specialized structure of epidermal cells and divided into two groups. These are non-secretory glandular trichomes and secretory glandular trichomes. Both of them present in the angiosperms, gymnosperms and bryophytes [15]. On the other hand glandular trichomes play important roles in plant resistance and they act like barrier against environmental stress, diseases and insect pests [16]. For this purpose they can contain chemical compounds such us terpenoids, ketones, sugars, aldehydes etc. [17]. These components react like chemical defense systems against herbivores and pathogens [16]. So in this study we also investigated the chemical content of the oak secretion by GC-MS and carbohydrates amount were found to be high. GC-MS results of the *Q. frainetto* Ten. dark brown secretion is given in Table 1.

Jerkovic & Marijanovic (2010) [14] and Özkök & Sorkun [18] remarked similar chemical components at their studies but they found these components at the oak honey samples and their components number is more. Because honeybees collect the oak secretions from the oak trees and they increase the component amount of the honey while making the honey by adding secretion from their own bodies.

Jerkovic & Marijanovic (2010) [14] and Özkök & Sorkun [18] were found generally furan derivatives (2-Furanmethanol, 2(5H)-Furanone, 1(3H)-Isobenzofuranone, Furfural, Furan, 2,5-dimethyl-) at the all oak honey samples but their amounts were low. We found furfural and furan, 2,5-dimethyl in the oak secretion. At this situation these components are able to migrate from plant sap to honey. Also Radovic et al. (2001) [19] and Cuevos-Glory et al., (2007) [20] found furfural acacia, lime and lavender honeys.

CONCLUSION

As a conclusion of this study has shown that *Q. frainetto* Ten. fruits have got a great number of secretory glandular trichomes and these trichomes produces sweet secretions. So the source of oak honey extrafloral origin and unlike pine honey, there is no insect species in the production of *Q. frainetto* Ten. oak honey. Sweet secretions are collected by honeybees and they made oak honey. Along with that furan derivatives can be at the oak secretion before migrate to honey. To our knowledge, this is one of the first studies on anatomically related to the oak honey and is the only study that proves the source of the oak honey. This information can be used in future studies for the characterization and standardization of oak honey.

ACKNOWLEDGEMENTS

We would like to thank The General Directorate of Forestry for project support and Prof.Dr. Selma Ülgentürk, who is from Ankara University-Faculty of Agriculture, for the entomological examinations at the oak trees and Assist. Prof. Cahit Doğan, who is from Hacettepe University and Prof. Dr. Münevver Nur Pınar, who is from Ankara University for the anatomical studies.

REFERENCES

[1] Yentür, S., and Öz, G.C. (2013) Plant Anatomy. Istanbul University, Faculty of Science, Biology Department, 1-606.

[2] Bentley, B.L. (1977) Extrafloral nectaries and protection by pugnacious bodyguards. Annual Review of Ecology, Evolution, and Systematics. 8(1), 407-427.

[3] Boke, N.H. (1980) Developmental Morphology and Anatomy in Cactaceae. BioScience. 30(59), 605-610.

[4] Mauseth, J.D. (1982) A Morphometric Study of the Ultrastructure of *Echioocereus engelmannii* (Cactaceae). V. Comparison with Shoot Apical Meristems of *Trichocereus pachanoi* (Cactaceae). American Journal of Botany. 69, 551-555.

[5] Sanz, M.L., Gonzalez, M., Lorenzo, C., Sanz, J. and Martinez-Castro, I. (2005) A Contribution to the Differentiation Between Nectar honey and Honeydew Honey. Food Chemistry. 91(2), 313−317.

[6] Karabagias, I.K., Badeka, A., Kontakos, S., Karabournioti, S. and Kontominas, M.G. (2014) Characterisation and Classification of Greek Pine Honeys according to their Geographical Origin Based on Volatiles, Physicochemical Parameters and Chemometrics. Food Chemistry. 146, 548-557.

[7] Govaerts, R. and Frodin D.G. (1998) World Checklist and Bibliography of Fagales *(Betulaceae, Corylaceae, Fagaceae* and *Ticodendraceae),* The Royal Botanic Gardens, United Kingdom.

[8] Seçmen, Ö., Gemici, Y., Görk, G., Bekat, L. and Leblebici, E (2000) Systematic of Seed Plants. Ege University Publishing House, Bornova, İzmir, 1-394.
[9] Davis, P.H. (1965) Flora of Turkey and the East Aegean Islands. University of Edinburgh.
[10] D'Albore, G.R. (1997) Textbook of Melissopalynology. Apimondia Publishing House, Bucharest, 1-308.
[11] Mamıkoğlu, N.G. (2008) Trees and Shrubs of Turkey. NTV, Dogus Publishing House, 1-727.
[12] Çakırlar, H., Doğan, C. and Özmen E. (2009) Atlas of General Botany and Plant Anatomy. Palme Publishing House, 1-176.
[13] Ülgentürk, S., Özdemir, I., Kozar, F., Kaydan, M.B., Dostbil, Ö., Sarıbaşak, H. and Civelek, H.S. (2013) Honeydew Producing Insect Species in Forest Areas in Western Turkey. Turkey Entomology Bulletin. 3, 125-135.
[14] Jerkovic, I. and Marijanovic, Z. (2010) Oak (*Quercus frainetto* Ten.) Honeydew Honey-Approach to Screening of Volatile Organic Composition and Antioxidant Capacity (DPHH and FRAP assay). Molecules. 15(5), 3744-3756.
[15] Tian, N., Liu, F., Wang, P., Zhang, X., Li, X. and Wu, G. (2017) The Molecular Basis of Glandular Trichome Development and Secondary Metabolism in Plants. Plant Gene. 12, 1-12.
[16] Hauser, M.T. (2014) Molecular Basis of Natural Variation and Environmental Control of Trichome Patterning. Frontiers in Plant Science. 5(320), 1-7.
[17] Wang, E., Wang, R., Deparasis, J., Loughrin, J.H., Gan, S. and Wagner, G. J. (2001) Suppression of a P450 Hydroxylase Gene in Plant Trichome Glands Enhances Natural-Product-based Aphid Resistance. Nature Biotechnology. 19, 371-374.
[18] Özkök, A., Sorkun, K. (2018) Characteristic Features of Oak (*Quercus frainetto* Ten.) Honey from Turkey. Fresen. Environ. Bull. 27, 8359-8366.
[19] Radovic, B.S., Careri, M., Mangia, A., Musci, M., Gerboles, M. and Anklam, E. (2001) Contribution of Dynamic Headspace GC-MS Analysis of Aroma Compounds to Authenticity Testing of Honey. Food Chemistry. 72(4), 511-520.
[20] Cuevas-Glory, L.F, Pino, J.A., Santiago, L.S. and Sauri-Duch, E. (2007) A Review of Volatile Analytical Methods for Determining the Botanical Origin of Honey. Food Chemistry. 103(3), 1032-1043.

Received: **07.11.2018**
Accepted: **18.02.2019**

CORRESPONDING AUTHOR

Aslı Ozkok
Hacettepe University,
Bee and Bee Products Application and Research Center, Biology Department,
06800, Beytepe, Ankara - Turkey.

e-mail: asozkok@gmail.com
aozkok@hacettepe.edu.tr

© by PSP Volume 28 – No. 4/2019 pages 2656-2663 Fresenius Environmental Bulletin

NOVEL BIOACTIVITIES OF *CASSIA NEMOPHILA* PODS AGAINST DIABETIC NEPHROPATHY: *IN VITRO* AND *IN VIVO* STUDY

Gauhar Rehman[1], Saba Arshad[1], Muhammad Hamayun[2], Amjad Iqbal[3,*], Waqas Ahmad Shams[1], Anwar Hussain[2], Khair Zaman[4], Ayaz Ahmad[5], Muhib Shah[2], Sahib Gul[6]

[1]Department of Zoology, Abdul Wali Khan University Mardan, 23200, Pakistan
[2]Department of Botany, Abdul Wali Khan University Mardan, 23200, Pakistan
[3]Department of Agriculture, Abdul Wali Khan University Mardan, 23200, Pakistan
[4]Department of Chemistry, Abdul Wali Khan University Mardan, 23200, Pakistan
[5]Department of Biotechnology, Abdul Wali Khan University Mardan, 23200, Pakistan
[6]Department of Biochemistry, Abdul Wali Khan University Mardan, 23200, Pakistan

ABSTRACT

Genetic disorders can actively be treated through wise use of medicinal plants. Plants are natural source that are very cheap to treat life threatening ailments with no side effects. *Cassia nemophila* from genus *Cassia* is one of the best examples that can serve as a best alternative to the expensive synthetic drugs. We have planned to investigate the pharmacological properties of ethanolic extract of *Cassia nemophila* pods (CNPE) against diabetic nephropathy. CNPE at 300 µg/ml has significantly (P= 0.05) improved the albumin urea, weight loss and blood glucose in diabetic mice. Moreover, CNPE has stabilized human red blood cells membrane at 2 mg/ml and scavenged the free radicals at 25 µg/ml. The results implied the pharmacological importance of CNPE and its effectiveness against antioxidant, anti-inflammatory and anti-diabetic nephropathy. Therefore, CNPE is recommended for further investigation and advanced studies.

KEYWORDS:
Cassia nemophila, antioxidant, anti-inflammatory, diabetes, nephropathy

INTRODUCTION

Now a day, diabetes is the foremost cause of death and disability around the globe. It is a disease that is characterized by the presence of high sugar in the blood (hyperglycemia) of a subject. Hyperglycemia mainly caused by malfunctioning or production of insulin [1, 2]. After the prevalence of diabetes, the patient incurred continuous damage, malfunction and/or collapse of vital organs, including eyes, kidneys, nervous system, heart, arteries and veins [3]. In recent years, diabetic nephropathy (DN) got influential interests in the field of nephrology. Diabetes also leads to end-stage renal disease (ESRD), particularly type 2, has been described as a medical catastrophe at international levels [4]. DN is majorly characterized by the presence of high levels of albumin in urine, lesions in glomerular membrane and dysfunctional filtration rate by glomerular membrane [5].

Moreover, oxidative stress can also be linked to the diabetes mellitus. In fact, it has been proven comprehensively that the production of reactive oxygen species (ROS) increases with the commencement of any type of diabetes [6, 7]. A number of sources are responsible for ROS production in diabetes, such as alterations in redox balances, auto-deterioration of glucose and lower amounts of antioxidants in tissues [8, 9]. ROS generation in the subject having higher levels of glucose in his/her blood can be linked with various metabolic disorders allied with diabetes [10]. Substantial evidence has been corroborated to establish a link between oxidative stress and pathogenesis of DN [11]. To tackle this prevailing problem, a number of drugs have been designed, but the drugs are quite expensive and have side effects. Therefore, the interest has been shifted towards the natural products, particularly the plant-based medicines to control metabolic diseases, including diabetes mellitus. Treatment of life threatening diseases, such as diabetic mellitus with plants antioxidants can lead to a cure without any side effects [12-14]. In the present study, ethanolic extract from the pods of *Cassia nemophila* (sub family *Ceasalpiniaceae* of family Leguminosae) were investigated for the *in vivo* anti-inflammatory *and in vitro* antioxidant potential. Also, *in vivo* diabetic nephropathy tests were carried out in a robust mouse model.

MATERIALS AND METHODS

Plant material. *Cassia nemophila* pods were collected from different parts of District Peshawar and Nowshera, KPK, Pakistan in the months of February and March. They were identified by a famous plant taxonomist, Dr. S. I. Ali, University of Karachi.

Plant extraction. The shade dried, dusts free CNP (800 mg) were grind in to coarse powder. The bioactive compounds were then extracted with ethanol in Soxhlet apparatus. The solvent was firstly evaporated in a rotary evaporator under reduced pressure at 48 ºC, to obtain a concentrated extract. The greenish black gummy extract was collected and kept in -20 ºC freezer till further analysis.

***In vivo* Experiment.** Standard protocol of multiple low dose injections of STZ was used to induce diabetes in Albino mice (BALB/c). Latterly, STZ-induced diabetic mice were fed with various concentrations of CNPE to check their anti-diabetic activity.

Animals. Albino mice having weight between 30-40 g was selected for the experiments. Initially, the mice were kept for seven days to acclimatize the conditions and fed with standard diet and water. Fasted animals were kept deprived of only food for 16 h, where water was provided without any restrictions.

Induction of diabetes/ diabetic nephropathy. STZ (Cat. No.41910012-3 Bio plus research chem) was mixed with 0.1 M citrate buffer (pH = 4.5) and provided to the subject mice at a dose of 55 mg/kg body weight (BW). After 15 minutes of mixing, STZ was injected in the peritoneum of mice with the help of 1 mL syringe having 29 gauge needle. The –ive control group (normal mice) was injected with 1.5 ml of citrate buffer without STZ. The process was repeated for five consecutive days. After the required dosage completed, the mice were checked for the hypoglycemia. Mice having low random blood glucose levels (15 mmol/l or 280 mg/dl) after the final STZ injections were removed.

Animal Grouping. Mice (6 each) were grouped as follows:

Group I: Served with distilled water only and were treated as –ive control (normal mice).

Group II: STZ induced diabetic mice, served with distilled water only and were treated as +ive control (diabetic mice).

Group III: STZ induced diabetic mice, served with aqueous CNPE at the dose of 100 mg/kg BW on alternate day for 15 days.

Group IV: STZ induced diabetic mice, served with aqueous CNPE at the dose of 200 mg/kg BW on alternate day for 15 days.

Group V: STZ induced diabetic mice, served with aqueous CNPE at the dose of 300 mg/kg BW on alternate day for 15 days.

After 15 days of treatment, the experiments were stopped and the data was collected. BW was determined with the help of weighing balance at the start and end of the experiment and loss in weight was recorded. Similarly, glucometer (ONCALL EZ II) was used to record blood glucose level at the start and end of the experiment. The blood was taken from tip of the tail, whereas collection of urine was made by pressing the tail and back of the mice. Albumin in urine was checked using kit (Urine/CSF Protein 200ml) on 1st and 15th day of experiment. Institutional animal ethic guidelines were strictly followed during experimental procedures.

HRBC- membrane stabilization assay. This study is based on stabilization and lysis of human red blood cells membrane in hypotonic saline environment. HRBC membrane stabilizing method was used to study anti-inflammatory activity, of CNPE. Healthy volunteers at the Department of Zoology, Abdul Wali Khan University Mardan have been selected and 3-4 ml of the blood was collected in heparinized tubes. The contents were mixed thoroughly and centrifuged (Cntrfg. sigma company mdl 2-16 pk, Germany) for at least five times at 3000 rpm for 12 minutes each. Suspension of packed cells (10% v/v) in hypo saline was prepared after repeated washing with isosaline solution. The final mixture was consisted of 0.5 ml of plant extract at various concentrations (i.e., 0.5 mg, 1 mg, 2 mg, 2.5 mg, 3 mg), 1 ml PBS, 2 ml hypo saline (0.25%), and 0.5 ml human red blood cells suspension (10% v/v). The mixture was incubated for 30 minutes at 37 ºC and was then centrifuged at 3000 rpm for 15 minutes. The collected supernatant was analyzed by using spectrophotometer at 560 nm. The percent stabilization of red blood cells membranes was determined as:

$$\text{Percent protection (\%)} = \frac{absorbance\ control - absorbance\ sample}{absorbance\ control} \times 100$$

DPPH- radical scavenging assay. The in vitro, DPPH-free radical scavenging assay of CNPE was done according to the Brand William's method [15] with some modification. In methanol, 1 ml of 1 mM, DPPH (purchased from sigma Aldrich) and 3ml of CNPE (5µg, 10µg, 15µg, 20µg, 25µg and 30µg) were added and mixed well. The mixture was allowed to set for 30 minutes in dark and then vortexed. The absorbance was determined at 517 nm,

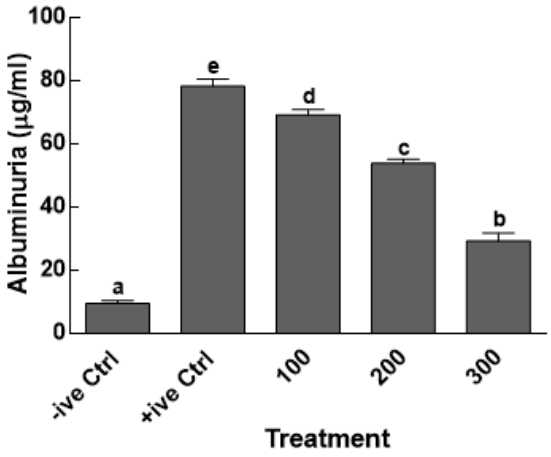

FIGURE 1

Effect of CNPE on urine albumin excretion rate of diabetic mice.

+ive Ctrl= consisted of 6 mice, which served as –ive control (normal mice) and were given distilled water only on daily basis; -ive Ctrl= consisted of 6 STZ induced diabetic mice, which served as +ive control (diabetic mice) and were given distilled water only on daily basis; 100= consisted of 6 STZ induced diabetic mice that were treated orally with aqueous ethanolic extract of *Cassia nemophila* pods (CNPE) at the dose of 100 mg/kg body weight on alternate day for 15 days; 200= consisted of 6 STZ induced diabetic mice that were treated orally with aqueous CNPE at the dose of 200 mg/kg body weight on alternate day for 15 days; 300= consisted of 6 STZ induced diabetic mice that were treated orally with aqueous CNPE at the dose of 300 mg/kg body weight on alternate day for 15 days. The error bars represent ±S.E of replicated data. The bars having different letter are significantly different at P = 0.05.

using spectrophotometer (UV 5100B spectrophotometer) by using the following formula:

$$\text{Scavenging DPPH (\%)} = \frac{\text{absorbance control} - \text{absorbance sample}}{absorbance\ control} \times 100$$

Statistical analysis. The data was analysed by using the Analysis of variance (ANOVA) and the means were further separated by Tuckey's HSD test (P= 0.05), using SPSS 20 software. The graphs were prepared in Graphpad prism 6.

RESULTS

Effect of CNPE on Urine Albumin Excretion Rate (UAER) of mice. The effect of CNPE on blood glucose levels was checked to determine its hypoglycemic activity. Five different groups were created and each group consisted of 20 mice. Diabetes was induced by injecting intraperitoneally, 55 mg of STZ per kg BW of mice. This process was repeated for five consecutive days to induce sufficient diabetes to cause diabetic nephropathy. From each group 6 mice were randomly selected for further analysis. UAER is observed to be increased in STZ induced diabetic rats due to the renal injury (Figure-1). UAER was significantly (P= 0.05) increased (78.3±2.27 µg/ml) in the STZ induced diabetic mice or +ive control as compared to the normal mice or –ive control (9.5±0.96 µg/ml). However, a significant (P= 0.05) decrease in the UAER was observed after oral administration of the CNPE. Moreover, the decrease in the UAER was a dose dependent with maximum decrease (29.3±2.48) observed in the STZ induced diabetic mice fed with 300 mg of CNPE per kg BW, followed by 200 mg per kg BW. The STZ induced diabetic mice fed with 100 mg CNPE per kg BW had also recovered, but the impact was not that great (Figure-1).

Effect of CNPE on body weights of mice. Body weight of the STZ administered +ive control group has been significantly reduced in comparison to the –ive control group (Figure-2). The weight of the mice in –ive control group and the STZ induced diabetic group fed with 300 mg of CNPE per kg BW was significantly (P= 0.05) increased instead. The gain in weight in STZ induced diabetic group fed with 300 mg of CNPE per kg BW reflects on the efficacy of the CNPE. Furthermore, weight losses in the STZ induced diabetic mice fed with 100 and 200 mg of CNPE per kg BW was not as high as STZ induced diabetic mice in +ive control group (Figure-2).

Effect of CNPE on blood glucose levels of mice. Blood glucose level of mice from various groups have been studied (Figure-3). The results indicated that the blood glucose levels in diabetic mice were controlled to maximum extent at a dose of 300 mg/kg of CNPE. The blood glucose level of STZ induced mice fed with 300 mg of CNPE per kg BW was comparable to that of mice from –ive control group. On the other hand, the blood glucose level in STZ induced controlled mice were significantly (P=

0.05) higher than the –ive control and STZ induced mice fed with CNPE (Figure-3). Additionally, the effect of CNPE on blood glucose level at the rate of 100 mg per kg BW was non-significant to 200 mg per kg BW.

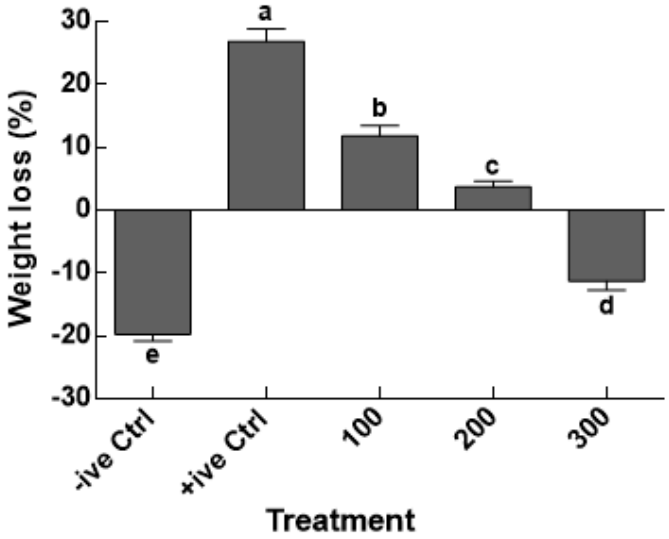

FIGURE 2

Effect of CNPE on body weights of diabetic mice.

+ive Ctrl= consisted of 6 mice, which served as –ive control (normal mice) and were given distilled water only on daily basis; -ive Ctrl= consisted of 6 STZ induced diabetic mice, which served as +ive control (diabetic mice) and were given distilled water only on daily basis; 100= consisted of 6 STZ induced diabetic mice that were treated orally with aqueous ethanolic extract of *Cassia nemophila* pods (CNPE) at the dose of 100 mg/kg body weight on alternate day for 15 days; 200= consisted of 6 STZ induced diabetic mice that were treated orally with aqueous CNPE at the dose of 200 mg/kg body weight on alternate day for 15 days; 300= consisted of 6 STZ induced diabetic mice that were treated orally with aqueous CNPE at the dose of 300 mg/kg body weight on alternate day for 15 days. The error bars represent ±S.E of replicated data. The bars having different letter are significantly different at P = 0.05.

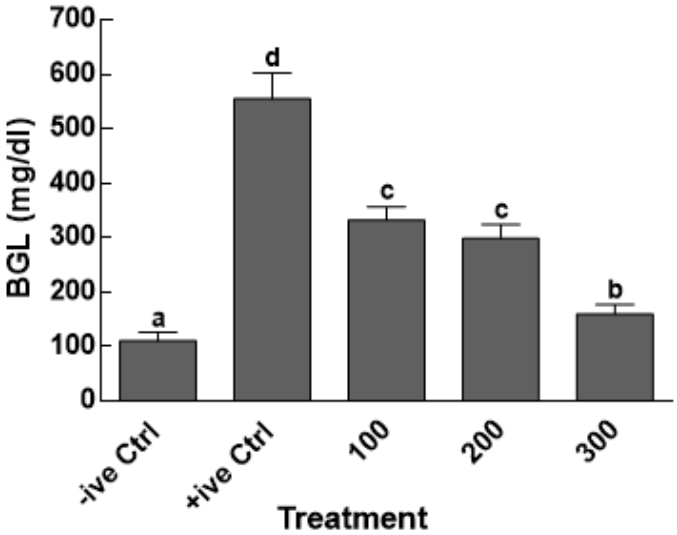

FIGURE 3

Effects of CNPE on blood glucose levels of diabetic mice.

+ive Ctrl= consisted of 6 mice, which served as –ive control (normal mice) and were given distilled water only on daily basis; -ive Ctrl= consisted of 6 STZ induced diabetic mice, which served as +ive control (diabetic mice) and were given distilled water only on daily basis; 100= consisted of 6 STZ induced diabetic mice that were treated orally with aqueous ethanolic extract of *Cassia nemophila* pods (CNPE) at the dose of 100 mg/kg body weight on alternate day for 15 days; 200= consisted of 6 STZ induced diabetic mice that were treated orally with aqueous CNPE at the dose of 200 mg/kg body weight on alternate day for 15 days; 300= consisted of 6 STZ induced diabetic mice that were treated orally with aqueous CNPE at the dose of 300 mg/kg body weight on alternate day for 15 days. The error bars represent ±S.E of replicated data. The bars having different letter are significantly different at P = 0.05.

Effect of CNPE on membrane stabilization. The anti-inflammatory activity of CNPE was determined by studying membrane stabilization of red blood cells. Hypo saline suspension of blood cells treated with varying concentration (0-2.5 mg/ml) of CNPE revealed membrane stabilization with increasing concentrations (Figure-4). The percent stabilization of CNPE was significantly high at 2.0 and 2.5 mg/ml, i.e. 53.7±2.1 and 56.4±1.1%, respectively. The standard drug (indomethacin) showed maximum stabilization of 65.2±2.2% at 2.5 mg/ml. Though, CNPE at lower concentrations (0.5, 1.0 and 1.5 mg/ml) has lower impact on membrane stabilization as compared to the 2.0 and 2.5 mg/ml, but significantly high as compared to the control (Figure-4).

Effect of CNPE on antioxidant scavenging. The antioxidant activity of CNPE was calculated by determining the extent of free radicals scavenged by the test extracts. The result showed an increase in antioxidant activity with an increase in concentration (Figure-5). The percent DPPH activity of CNPE was significantly high at all tested concentrations (5, 10, 15, 20, 25 µg/ml) as compared to the control (0 µg/ml). The DPPH activity was increased steadily till 15 µg/ml of CNPE that increased abruptly afterwards. The highest DPPH activity was observed at 25 µg/ml (78.4±1.9%), followed by 20 µg/ml (55.8±2.3%). Ascorbic acid used as standard drug showed maximum activity (96.7±1.1%) at 20 µg/ml (Figure-5).

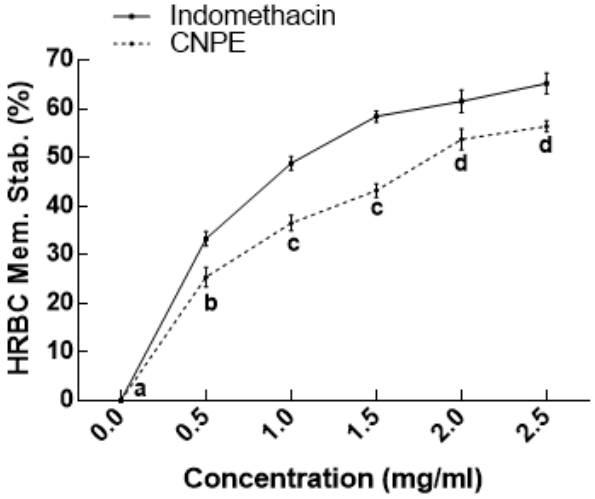

FIGURE 4

***In vitro* Antioxidant activity of CNPE.**

CNPE= ethanolic extract *Cassia nemophilla* pods. HBRC Mem. Stab.= Human red blood cells membrane stabilization. Indomethacin was used as standard drug. The error bars represent ±S.E of replicated data. The bars having different letter are significantly different at P = 0.05.

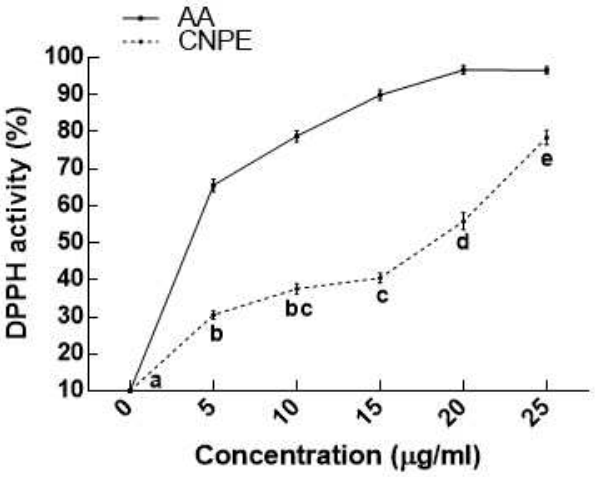

FIGURE 5

***In vitro* anti-inflammatory activity of CNPE.**

CNPE= ethanolic extract *Cassia nemophilla* pods. AA= Ascorbic acid, used as a standard drug. DPPH= 2,2-diphenyl-1-picrylhydrazyl. The error bars represent ±S.E of replicated data. The bars having different letter are significantly different at P = 0.05.

DISCUSSION

Diabetes is a genetic disorder and its occurrence is increasing quickly in most of the countries around the world. The treatment of DM in current scenario is mainly based on parenteral insulin and oral anti-diabetic drugs. Due to serious side effects of oral hypoglycemic agents, there is a need to search newer anti-diabetic agents having minimum side effects and high therapeutic efficacy [16]. This might be fulfilled by curing DM with traditional biomedicine as anti-diabetic agents. Plants offer latent uses, particularly as traditional remedy and pharmacopoeial medicine [17, 18]. A large percentage of the world's populations rely on traditional medicine because of the insufficiency [19]. In Pakistan mostly medicinal plants are use in local, rural population. Our lands are rich in this natural resource, especially our Northern areas, whose lush green mountains serves as a house for unidentified wild plants. It is very essential to have enough knowledge concerning herbs not only because of their extensive uses, but also because they have the ability to initiate reactions or interact with other drugs [20].

Regarding this, different species of genus *Cassia* have shown the presence of many anti diabetic agents. The species are rich in flavonoids, anthrones, anthroquinone, xanthones, sesquiterpenes, steroids, phenyl esters, lactones, and glycosides, making them effective antioxidant and anti-inflammatory drugs [21]. The above arguments, therefore, favored the selection of *C. nemophila* that is widely distributed in Northern part of Pakistan to be evaluated for some medicinal properties. Its antioxidant, anti-inflammatory and hypoglycemic capacity have been targeted that supports the therapeutic effect of *C. nemophila* in diabetes and diabetic nephropathy.

Tissues can be damaged by inflammation and ultimately leading to various types of diseases. Certainly, acute or chronic inflammation can be followed by a number of events, including membrane destabilization [22]. However, inflammation resulting in destabilization of membrane can be regulated by taking drugs. The drugs can either be synthetic with side effects or natural without side effects. Recently, it has been discovered that natural sources can actively relief pains provoked by inflammation [23-26]. In the present study, we have also examined the *in-vitro* anti-inflammatory activity of CNPE in human red blood cell membrane stabilization assay. The assay was done because of the resemblance between erythrocyte and lysosomal membrane [23]. This assay is supposed to provide foundation for the stabilization of lysosomal membrane that have a role in regulation of the inflammatory reactions [24, 27]. The HRBCs, when exposed to hypotonic solution can increase membrane permeability. With an increase in membrane permeability it releases hemoglobin from cells, which can be blocked by anti-inflammatory compounds. The function of anti-inflammatory compounds is to bind the lysosomal enzymes (cyclooxygenases) and inhibit the HRBC membrane lysis [28]. The results of the present study Figure-4) also suggested that CNPE (2-2.5 mg/ml) can stabilize the human erythrocyte membrane in hypotonic solution. Hence, the study validated the stabilizing ability of the CNPE extract in dose depended manner. Moreover, the CNPE was evaluated for antioxidant activity through DPPH free radical scavenging assay. The method is one of the recognized, precise and commonly used approaches for assessing the antioxidant potential of test samples. Free radicals in higher concentration can cause oxidative stress, damages proteins, lipids, DNA and RNA that leads to various diseases [29]. Recently, there is a growing interest in finding natural antioxidants to replace synthetic ones [30, 31]. In the pursuance of natural bioactives, we have observed a strong free radical scavenging ability of CNPE at 20-25 µg/ml (Figure-5). *C. nemophila* reduces radical to hydrazine, when react with hydrogen donors. The potential hydroxyl radical scavenging ability of *Cassia nemophila* fraction might be due to hydroxyl substitution. The antioxidant activity of CNPE might be due to flavonoids, phenols, anthroquinones and lignin.

Furthermore, utilization of carbohydrates is greatly influenced by DM, which leads to imbalance in metabolism of lipids [32]. Therefore, the most important task in managing diabetes is to decrease the abnormally elevated blood glucose concentration. In this regard a test has been carried on STZ induced diabetic mice to mimic human type II diabetes. STZ particularly causes destruction of insulin-producing pancreatic β-cells that leads to abnormal blood glucose. The CNPE has significantly (P= 0.05) decreased the blood glucose levels in the STZ induced diabetic mice fed with 300 mg of CNPE per kg body weight. The hypoglycemic activity of the extract might be resulted due to the antidiabetic active principles in pods. The CNPE might stimulate the release of insulin to restore normal blood glucose levels in diabetic animals. Another possibility in the reduction of blood glucose levels in diabetic mice might be the increased utilization of peripheral glucose.

REFERENCES

[1] A. American Diabetes Association (2010) Diagnosis and classification of diabetes mellitus. Journal of Diabetes Care. 33, S62-S69.

[2] Pratley, R.E., Nauck, M.A., Barnett, A.H., Feinglos, M.N., Ovalle, F., Harman-Boehm, I., Ye, J., Scott, R., Johnson S. and Stewart, M. (2014) Once-weekly albiglutide versus once-daily liraglutide in patients with type 2 diabetes inadequately controlled on oral drugs (HARMONY 7): a randomised, open-label, multicentre, non-inferiority phase 3 study. The Lancet Diabetes and Endocrinology. 2(4), 289-297.

[3] Tesfaye, S. and Gill, G. (2011) Chronic diabetic complications in Africa. African Journal of Diabetes Medicine. 19(1), 4-8.

[4] Narres, M., Claessen, H., Droste, S., Kvitkina, T., Koch, M., Kuss, O. and Icks, A. (2016) The incidence of end-stage renal disease in the diabetic (compared to the non-diabetic) population: a systematic review. PloS One. 11(1), e0147329.

[5] Lim, A.K. (2014) Diabetic nephropathy–complications and treatment. International Journal of Nephrology and Renovascular Disease. 7, 361.

[6] Padgett, L.E., Broniowska, K.A., Hansen, P.A., Corbett, J.A. and Tse, H.M. (2013) The role of reactive oxygen species and proinflammatory cytokines in type 1 diabetes pathogenesis. Annals of the New York Academy of Sciences. 1281(1), 16-35.

[7] Bharath, L.P., Cho, J.M., Park, S.-K., Ruan, T., Li, Y., Mueller, R., Bean, T., Reese, V., Richardson, R.S. and Cai, J. (2017) Endothelial Cell Autophagy Maintains Shear Stress–Induced Nitric Oxide Generation via Glycolysis-Dependent Purinergic Signaling to Endothelial Nitric Oxide Synthase. Arteriosclerosis, Thrombosis, and Vascular Biology. 37(9), 1646-1656.

[8] Matough, F.A., Budin, S.B., Hamid, Z.A., Alwahaibi, N. and Mohamed, J. (2012) The role of oxidative stress and antioxidants in diabetic complications. Sultan Qaboos University Medical Journal. 12(1), 5.

[9] Pitocco, D., Tesauro, M., Alessandro, R., Ghirlanda, G. and Cardillo, C. (2013) Oxidative stress in diabetes: implications for vascular and other complications. International Journal of Molecular Sciences. 14(11), 21525-21550.

[10] Kowluru, R.A. and Mishra, M. (2015) Oxidative stress, mitochondrial damage and diabetic retinopathy. Biochimica et Biophysica Acta (BBA)-Molecular Basis of Disease. 1852(11), 2474-2483.

[11] Asmat, U. Abad, K. and Ismail, K. (2016) Diabetes mellitus and oxidative stress—a concise review. Saudi Pharmaceutical Journal. 24(5), 547-553.

[12] Rajashree, R., Gangolli, D., Patil, S. and Ingawale, K. (2012) Amla, ashwagandha and shatavari formulations as herbal medicines and nutraceuticals. Research Journal of Pharmaceutical Science. 1(3), 10-15.

[13] Afify, A.E.-M.M., El-Beltagi, H.S., Fayed, S.A. and El-Ansary, A.E. (2018) Beneficial and potent effect of olive leaves extract on hyperglycemic state, kidney and liver function in STZ-induced type 2 diabetes mellitus. Fresen. Environ. Bull. 27, 3733-3739.

[14] Afify, A., El-Beltagi, H.S., Fayed, S.A. and El-Ansary, A.E. (2017) Hypoglycemic and iron status ameliorative effects of *Olea europea* CV.'Picual'leaves extract in streptozotocin induced diabetic rats. Fresen. Environ. Bull. 26, 6898-6908.

[15] Brand-Williams, W., Cuvelier, M.-E. and Berset, C. (1995) Use of a free radical method to evaluate antioxidant activity. LWT-Food science and Technology. 28(1), 25-30.

[16] Pulipaka, S., Challa, S.R. and Pingili, R.B. (2012) Comparative antidiabetic activity of methanolic extract of *Operculina turpethum* stem and root against healthy and streptozotocin induced diabetic rats. International Current Pharmaceutical Journal. 1(9), 272-278.

[17] El-Beltagi, H.S., Mohamed, H., Megahed, B.M., Gamal, M. and Safwat, G. (2018) Evaluation of some chemical constituents, antioxidant, antibacterial and anticancer activities of Beta vulgaris L. Root. Fresen. Environ. Bull. 27, 6369-6378.

[18] Afify, A.E.-M.M., El-Beltagi, H.S., Fayed, S.A. and El-Ansary, A. E. (2018) Enhancing effect of olive leaves extract on lipid profile and enzymes activity in streptozotocin induced diabetic rats. Fresen. Environ. Bull. 27, 1875-1883.

[19] Yuan, H., Ma, Q., Ye, L. and Piao, G. (2016) The traditional medicine and modern medicine from natural products. Molecules. 21(5), 559.

[20] Aminabee, S. and Lakshmana Rao, A. (2012) A plant review of *Cassia sophera* Linn. International Journal of Pharmaceutical, Chemical and Biological Sciences. 2(3), 408-414.

[21] Kaur, R. and Kaur, H. (2017) Plant derived antimalarial agents. Journal of Medicinal Plants. 5(1), 346-363.

[22] Leelaprakash, G. and Dass, S.M. (2011) In vitro anti-inflammatory activity of methanol extract of Enicostemma axillare. International Journal of Drug Development and Research. 3(3), 189-196.

[23] Shenoy, S., Shwetha, K., Prabhu, K., Maradi, R., Bairy, K. and Shanbhag, T. (2010) Evaluation of antiinflammatory activity of Tephrosia purpurea in rats. Asian Pacific Journal of Tropical Medicine. 3(3), 193-195.

[24] Babu, N.P., Pandikumar, P. and Ignacimuthu, S. (2011) Lysosomal membrane stabilization and anti-inflammatory activity of Cleroden-drum phlomidis Lf, a traditional medicinal plant. Journal of ethnopharmacology. 135(3), 779-785.

[25] Anosike, C.A., Obidoa, O. and Ezeanyika, L.U. (2012) Membrane stabilization as a mechanism of the anti-inflammatory activity of methanol extract of garden egg (Solanum aethiopicum). DARU Journal of Pharmaceutical Sciences. 20(1), 76.
[26] Zhang, H. and Tsao, R. (2016) Dietary polyphenols, oxidative stress and antioxidant and anti-inflammatory effects. Current Opinion in Food Science. 8, 33-42.
[27] Kuropka, P., Dobrzyński, M., Gamian, A., Gostomska-Pampuch, K., Kuryszko, J. and Całkosiński, I. (2017) Effect of Glucocorticoids on Ultrastructure of Myocardial Muscle in the Course of Experimentally Induced Acute Myocardial Ischemia. BioMed research international. 2017.
[28] Boniface, P.K., Verma, S., Shukla, A., Khan, F., Srivastavan, S.K. and Pal, A. (2014) Membrane stabilisation: a possible anti-inflammatory mechanism for the extracts and compounds from Spathodea campanulata. Natural product research. 28(23), 2203-2207.
[29] Circu, M.L. and Aw, T.Y. (2010) Reactive oxygen species, cellular redox systems, and apoptosis. Free Radical Biology and Medicine. 48(6), 749-762.
[30] Singh, R., Singh, M., Chandra, L., Bhat, D., Arora, M., Nailwal, T. and Pande, V. (2012) In vitro antioxidant and free radical scavenging activity of *Macrotyloma uniflorum* (Gahat dal) from Kumauni region. International Journal of Fundamental and Applied Science. 1(1), 7-10.
[31] Rehman, G., Hamayun, M., Iqbal, A., Ul Islam, S., Arshad, S., Zaman, K., Ahmad, A., Shehzad, A., Hussain, A. and Lee, I. (2018) In Vitro Antidiabetic Effects and Antioxidant Potential of *Cassia nemophila* Pods. BioMed Research International. 2018.
[32] Hardie, D.G. (2012) Organismal carbohydrate and lipid homeostasis. Perspectives in Biology. 4, a006031.

Received: **07.11.2018**
Accepted: **14.02.2019**

CORRESPONDING AUTHOR

Amjad Iqbal
Department of Agriculture,
Abdul Wali Khan University Mardan,
23200 – Pakistan

e-mail: amjadiqbal@awkum.edu.pk

© by PSP Volume 28 – No. 4/2019 pages 2664-2670 Fresenius Environmental Bulletin

SOME WATERSHED CHARACTERISTICS OF MURAT MOUNTAIN OF TURKEY

Nilufer Yazici[1,*], Ismet Celik[2]

[1]Faculty of Forestry of Isparta Applied Sciences University, TR-32260 Isparta, Turkey
[2]Forest District of Ministry of Forestry, TR-43600 Kutahya, Turkey

ABSTRACT

The study was carried out to estimate some watershed characteristics (e.g., circularity ratio, elongation ratio, form factor and compaction ratio, drainage density, stream frequency, drainage intensity) of Basin of Murat Mountain in Turkey to contribute identification and management of the watershed. For this purposes, inventorial data such as topographical and forest maps collected from local and national foundations of the area together with field stage of the study was used by Geographical Information Systems (GIS) based on conversion in Arc Info software to estimate current and potential status of the watershed.

Result of the analysis showed that area of the Murat mountain basin was 25874 ha at 1424 m elevation by 38% of slope. The study area was generally north and south aspect. The basin had 46 streams with a total length of 230.10 km (total of dry and watery streams). Drainage density was 0.88. Stream frequency was 0.5 in the basin showed that the drainage condition of the area was close to optimum.

Natural resource potential within the area estimated by digital maps showed the conditions specific to watershed-specific characteristics and existing conditions were recorded and necessary measures were taken to prevent future changes. Therefore, it was important that the watershed should be dealt with watershed management principles.

KEYWORDS:
Aspect, basin, forest, management, natural resources, slope.

INTRODUCTION

Watershed is one of the most important units in planning and estimation of natural resources. The basin is including many ecological materials such as water resources, agricultural and forest land as a part of ecosystem. So, its management is getting importance based on increasing in human population and sustainability. The management has target to solve the problems in a basin and to ensure that natural resources are fully responded to the wishes of the people and to be operated in a way that makes their welfare steady [1]. Integrated watershed management aims at providing human needs in correspondence with the sustainability of source usage, planning all the other water-based natural sources on the basis of watershed [2]. The management requires the socio-economic structure of the people living in the basin together with natural resources, the hydrological characteristics of the basin, climate, soil and plant existence [3]. It makes necessary interdisciplinary work compulsory such as map engineering and computer science. It is of great importance to transfer the results obtained by studies towards nature to maps recently. Geographic Information Systems (GIS), which serves to decide people in various fields from numerical preparation of simple maps to making complex decisions, has been greatly increased in forestry with the ability to link data to spatial data [4]. It is also cheap and easy application for different purposes. Prior to this time, morphometric parameters were measured using mathematical concepts but Geographic Information System (GIS) modules provide flexible environment and powerful tools for integrating, manipulating and analyzing spatial information [5]. Currently, GIS have gained recognition as preferred data analytical platform for morphometric analyses respectively. For instance, GIS had been extensively utilized in various morphometric analyses [2, 6, 7, 8].

In this study, which was conducted with the purpose of determining the basin characteristics (such as basin shape, slope characteristics, basin area, average elevation) of Murat mountain basin, the present and potential status of the area was evaluated and the watershed characteristics of the research area were tried to be determined by GIS and Arc Info software. In the context of the results obtained, it was aimed to contribute to the development and management of the basin area.

MATERIALS AND METHODS

Material. The basin, located on the slopes of the Murat mountain in the Aegean Region of Turkey, overlooking the town of Gediz in the Kütahya province (Figure 1). The name of the basin was called

from Murat mountain of the region. The borders of the basin started from the Kesiksogut area where the Gediz stream started and then continued in the direction of six villages and a town (Figure 1).

Method. The research was carried out including the primary and field stages. In addition, the collected inventorial documents of the relevant institutions and organizations (maps, etc.) were used. In addition to this, in order to shape the study, a literature review was performed on this subject and the office phase was completed. Before starting the field work, maps were obtained for the determination of the basin where the study could be carried out. The topographic, stand, geology and soil maps of the research area were obtained and all maps were digitized with ArcInfo 9.2 software before the land phase. Elevation, slope and aspect maps were obtained from the topographic map of the scale of 1/25000 and then the maps of the research area were obtained from public institutions (forest management directorate, agriculture district directorate, local administrations etc.). Natural resources potential has been tried to be determined from these maps. Thus, the conditions specific to basin-specific characteristics and current conditions were recorded and necessary measures to be taken against future changes could be identified. The current and potential conditions of the natural resources in the research area have been determined by the primary and field stages of the study.

RESULTS AND DISCUSSION

Identification of the watershed. The microwatershed called from Murat mountain at the area was located between 38° 57'50" and 39° 01'19" N latitude, and between 29° 38'53" and 29° 44'29" E longitude at Gediz district of Kutahya province in Aegean Region of Turkey (Figure 1). The watershed included a town and 6 villages together with hills at different part of studied area as Calova (1739 m) and Turkmen (1688 m) hills at eastern, Kesiksogut hill (1734 m) at northern, Murat mountain (2340 m) and Kazikbatmaz hill (1857 m) at southern part of the basin changed between 1100 and 2300 meters.

The site was in the transition zone from the Central Anatolian climate to the Aegean basin. In this respect, the effect of two different climates was observed according to long periodical climatic data of the region [9]. Summer period was hot and dry winters are relatively rainy and hard. The average temperature was higher 10 ºC between April and October. The average annual rainfall was 548.1 mm.

FIGURE 1
The location of the basin

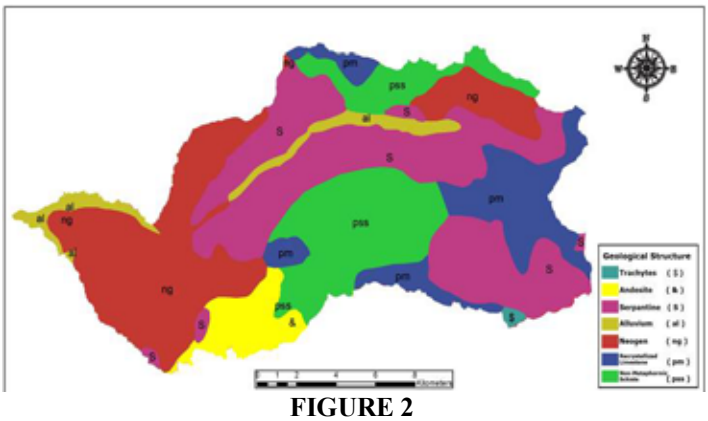

FIGURE 2
Geological structure of the basin

The study area consisted of metamorphic and volcanic structures (Figure 2). Soil depth was very variable in the whole area. Depending on the main structure, the soil was low in the sandy loam slime representing the lightweight structure by low water holding capacity. The soil reaction was slightly acidic with 6.0-6.5 pH levels, and also no salinity problem in the field.

There was 14885 hectares of productive forest of the watershed, 4693.5 hectares of damaged areas and a total of 19578.5 hectares of forest area and 6295 hectares of un-forest areas together with 223 hectares of pasture of which 51.5 hectares was a registered pasture area in the basin. Beside it had also 208 hectares of irrigated and 205 hectares of dry agricultural area (Figures 3 and 4). According to land capability class the land were ordered as 322.46 ha, 1386.16, 3859.69, 9237.40 and 11067.79 ha from first class (I) to sixth (VI) class.

The classification results were compared with the actual data (land use map or ground survey data), and the accuracy of land use classification expressed by the percentage of the total classification area [10]. The result played important roles for different purposes, for instance it was reported that an accurate planning and land management model was required for considering the characteristics of existing land areas, help to conserve soils in a study [11].

Watershed Characteristics, watershed area. Total area of the basin was 25873.5 ha. Therefore, it was classified as very large basin classification (> 10000 ha). The basin area was important in terms of management, hydrological relations, land classification and socio-economic characteristics and also for other practices. Developing the main basin by working in small basins instead of very large basins in basin planning gave higher positive results. In hydrological measurements, the basin area was the first in the relationship between the amount of precipitation and precipitation-flow [12].

Shape factor. While the basin shape grown as the basin area grown, it usually resembled a pear shape in small basins. The basin shape directly affected the time to leave the basin, the drainage system and its hydrological characteristic and other characteristics. When the field grown, the shape factor become smaller and increasing length [13]. Shape factor (S) was found to be 2.92 estimated as $\mathbf{S}=\mathbf{L}^2$ (the length of watershed, km)/**A** (watershed area, km^2) [1]. The estimated value (2.92) emphasized that longitudinal shape.

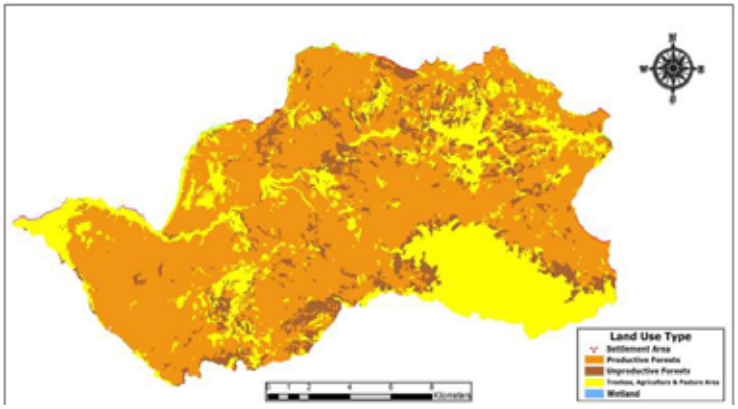

FIGURE 3
Land use status map of the basin

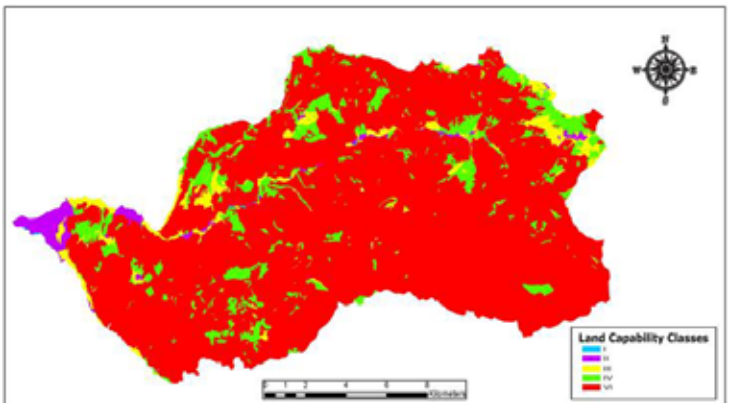

FIGURE 4
Land capability classification map of the basin

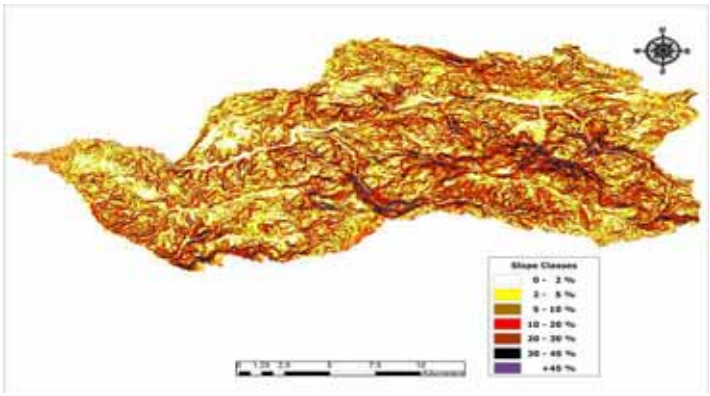

FIGURE 5
Slope classes of basin

TABLE 1
Area and slope (S) classes of the basin

Slope Class	Area (ha)	Percent (%)	Cumulative Percent (%)
Flat areas (S≤ 2%)	322.46	1	-
Less slope (2 >S ≤5%)	1386.16	5	6
Medium slope (5 >S ≤10%)	3859.69	15	21
Very inclined (10 >S ≤20%)	9237.40	36	57
Upright ((20 >S ≤30%)	6477.41	25	82
Steep (30 >S ≤45%)	3736.55	15	97
Very steep (S >45%)	853.83	3	100
Total	25873.50	100	-

Form factor. The form factor (F) was evaluated by **F**= **b** (transverse length of watershed, the width of watershed, km) /**L** (the length of watershed, km) [1]. The form factor of the basin was lower than 1 (0.42) indicated that the length of the basin was larger than the basin width. According to our results, the research area basin had a small form factor and was narrow and long.

Circulatory ratio. The ratio estimated by **Rc** (circularity ratio)= 4π**A** (watershed area, km^2) /**p**^{2} (circumference of watershed, km) [1] was 0.36. It showed small watersheds which exhibit homogeneity in terms of geological structure, this ratio varied in a range of 0.6-0.7, circulatory ratio may between 0.4 and 0.5 in watersheds with a heterogeneous geological structure [14, 15]. As in the research area, the circularity of the waters, with a circularity of less than 0.5, was short, and the slope of the creek was high and the water collected in the creeks could be transformed into peak streams. The area was more similar the basin to the circle, the closer the width and the length values of the basin.

Elongation ratio. This value, calculated as 0.66, showed our area was a mountainous basin for the studied watershed. The ratio, which was calculated as a ratio of diameter of a circle, had an identical area as the watershed to the length of the watershed. It was a parameter that showed the shape of the field. Elongation rate was equal to or smaller than one, and they took small values in mountain basins [1].

Average slope. The slope in the topographic features was of great importance both for hydrological and water erosion. The average slope of the basin was an important factor in the formation of surface flow [14]. Land slope was the degree of roughness of the land. The average slope of the Murat mountain basin was 38%. The high degree of slope of the area increased the formation of erosion and sedimentation. It also emphasized that more than half of the area (57%) seemed unsuitable for agricultural purposes in the basin (Figure 5 and Table 1). In addition, vegetation could have been damaged due to the wrong field practices in the field and in this direction the soils have become sensitive to erosion. Higher slope (S) could be higher drainage density and the stream frequency of the basin [16].

Aspects of the watershed. The basin mainly has northeast aspect (41%) meant shadowy view, while there was four main aspects (Figure 6) which of 11% was flat. In the watershed management studies and ecological aspects, the main direction of the land was sufficient from the ecological point of view for watershed practices.

Average elevation. The height of the highest point on the basin boundary gave the maximum height of the basin and the height at the basin exit point, the minimum height. The average elevation of the basin, watershed management was very important in many ways in management of watershed such as in climate and specially precipitation and temperature relations [17]. The average elevation of

the basin was 1424 m (Figure 7) and it surrounded by high hills. The average elevation of the basin was worth more than an average altitude of 890 m from Turkey. It varied between 710 and 2340 m in the basin.

Drainage condition. The basin had 46 streams with a total length of 230.10 km (total of dry and watery streams). Drainage density, which was an important criterion for determining the drainage status of the basin, calculated by ratio between total stream length to watershed area, was 0.88 (Figure 8). High drainage density indicated a well-developed drainage system and less surface runoff [18]. Low drainage density develops in areas where main rock was present such as granite, quartzite, silica and sandstone which were resistant to hard and erosion [1].

Stream frequency (Ds=Ns (number of streams)/A (watershed area (km^2)) was the ratio of the number of streams in the watershed. It was 0.5 in the basin (Figure 9) showed that the drainage condition of the area was close to optimum.

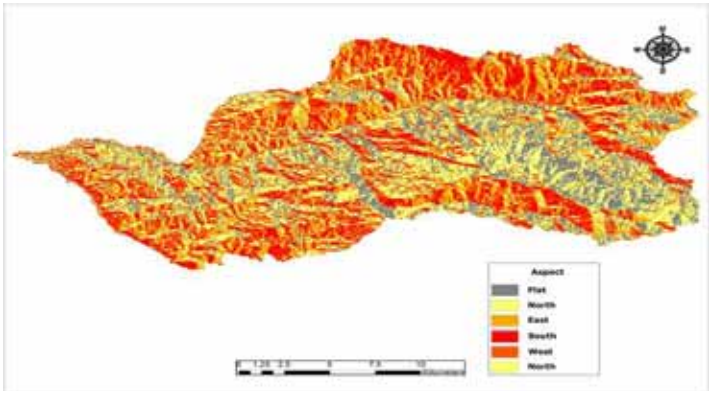

FIGURE 6
The aspects groups of basin

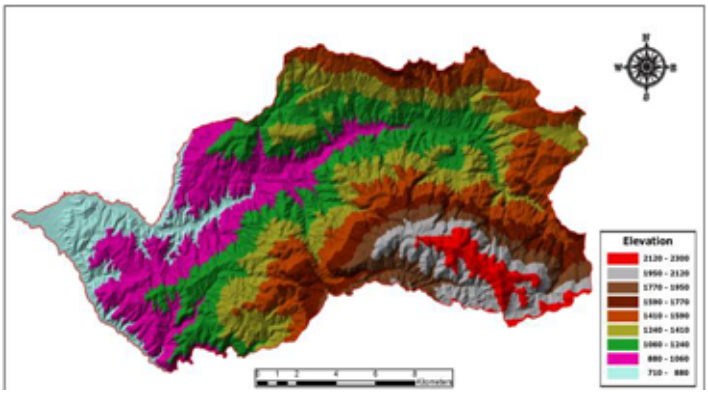

FIGURE 7
Elevation classes of basin

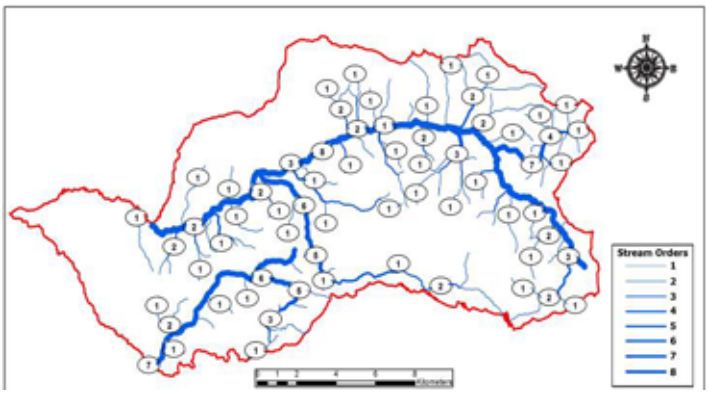

FIGURE 8
Drainage intensity of basin

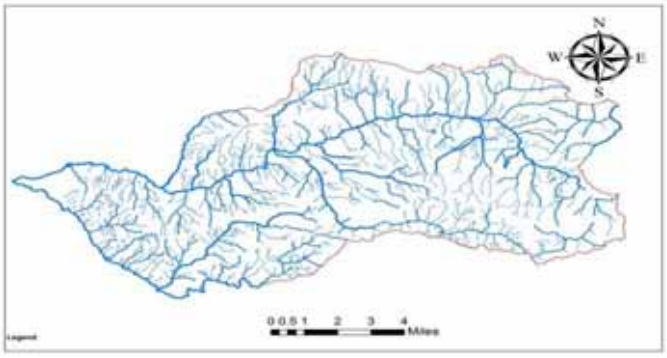

FIGURE 9
Stream frequency of basin

CONCLUSIONS

The integrated watershed management approach proposes to deal with all the characteristics of climate, soil, plants, land and human. The watershed characteristics of the Murat mountain watershed were determined by Geographical Information Systems (GIS). The systems had easy, short, more accurate and cheap in the evaluation of the watershed characteristics. As a result of examining the numerical maps obtained by digitizing, the area of Murat mountain watershed is 25873.5 ha. Murat mountain watershed is classified as large basins. Therefore, it could be said that it was important to management and use the basin in terms of water efficiency and other watershed practices. The form factor of the research area is 0.422, that the small the basin area and the form factor, the lower the danger of natural disasters such as floods. However, the basin of the research area is large; the small form factor showed that the risk of flood and flood hazard can be high.

According to the concept of integrated watershed management, the watershed should be considered as a whole. It is foreseen to start working in the upstream section of the catchment area of the watershed. However, the most problematic region should be taken into consideration primarily in basin improvement practices. The areas should be divided into sub-watershed and concentrated in micro-catchments for higher success in small areas; the entire watershed should be rehabilitated.

Natural resource planning and the eco-tourism potential should be considered on basin watershed. Soil properties should be examined in terms of water production, erosion, flood and the planning in the watershed should be done depending on these characteristics. In order to protect the area, a watershed planning should be carried out with local people and all public foundations.

REFERENCES

[1] Ozhan, S. (2004) Watershed management. Istanbul University Forestry Faculty Publication. No: 4510- 481, Istanbul.

[2] Yilmaz, H., Gol, C. and Edis, S. (2011) The importance of watershed characteristics in integrated watershed management (A case of Gokdere watershed, Turkey). Fresen. Environ. Bull. 20, 3126-3134.

[3] Dengiz, O. and Sarioglu, F.E. (2012) Evaluation of different parametric approaches in land evaluation studies. Soil and Water Journal. 1(2), 82-87.

[4] Ulu, F. (1998) Research on some physical, chemical and hydrological properties of soils under different Land use in Trabzon Uzungol-Haldizen Creek Rainfall basin and their investigation on erosion tendencies. MSc Thesis. Graduate School of Natural and Applied Sciences of Karadeniz Technical University. Trabzon.

[5] Adegoke, K.M. and Bulus, L.G. (2015) Hydrological and morphometric analysis of Upper Yedzam catchment of Mubiin Adamawa State, Nigeria, using GIS. World Environment. 5(2), 63-69.

[6] Nag, S.K. and Anindita, L. (2011) Morphometric analysis of Dwarakeswar watershed, Baukura district, West Bengal, India, using spatial information Technology. International Journal of Water Resources and Environmental Engineering. 3(10), 212-219.

[7] Somashekar, R.K. and Ravikumar, P. (2011) Runoff estimation and morphometric analysis for Hesaraghatta watershed, A remote sensing and GIS approach. Journal of Indian Society of Remote Sensing. 39(1), 95-106.

[8] Akinwumiju, A.S. and Olorunfemi, M.O. (2016) Morphometric analysis of Osun drainage basin, south western Nigeria. Journal of Geography and Geology. 8(4), 9-22.

[9] Anonymous (2013) Murat Mountain Micro-basin Plan. General Directorate of Forestry Division of Soil Conservation and Watershed Improvement, Ankara.
[10] Zhang, Y., Hou, K., Li, X. and Chang, Y. (2018) Study on land use classification and elastic urbanization in Chengguan district of Lhasa city. Fresen. Environ. Bull. 27, 5908-5913.
[11] Yuksek, T. (2009) Effects of land-use management on surface soil properties, erosion indices and green tea yield in humid Blacksea region. Fresen. Environ. Bull. 18, 848-857.
[12] Ozyuvaci, N. (1976) Some plant-soil-water relationships affecting hydrological status in Arnavutkoy creek rainfall basin. Istanbul University Forestry Faculty Publication, No:2082, Istanbul.
[13] Yilmaz, H. (2010) Investigation of Cankiri Gokdere watershed characteristics and some hydrophysical soil properties. MSc Thesis. Graduate School of Natural and Applied Sciences of Ankara University. Cankiri.
[14] Aydın, M. (2009) WEPP (Water erosion prediction project) model determines the soil losses and measures to be taken according to land use in Gumushane-Torul Dam rainfall basin. Kastamonu University Faculty of Forestry Journal. 9(1), 54-65.
[15] Hizal, A. (1984) Investigation of application possibilities of interpretation of basin photographs in basin management (Ova Creek Basin, Kocaeli). Istanbul University Forestry Faculty Publication, No:341, Istanbul.
[16] Reddy, G.P.O., Maji, A.K. and Gajbhiye, K.S. (2004) Drainage morphometry and its influence on landform characteristics in a Basaltic Terrain. International Journal of Applied Earth Observation and Geoinformation. 6, 1-16.
[17] Balci, N. and Ozyuvaci, N. (1988) Watershed management-II. Istanbul University Forestry Faculty Course notes. Unpublished. Istanbul.
[18] Atalay, I. (1986) Applied hydrography. Publications of Ege University Art Faculty No: 38, Izmir.

Received: **14.11.2018**
Accepted: **18.02.2019**

CORRESPONDING AUTHOR

Nilufer Yazici
Faculty of Forestry of
Isparta Applied Sciences University,
TR-32260 Isparta – Turkey

e-mail: niluferyazici@isparta.edu.tr

© by PSP Volume 28 – No. 4/2019 pages 2671-2678 Fresenius Environmental Bulletin

SEASONAL CHANGES IN THE FOOD SPECTRUM AND DAY-TIME RHYTHM OF FEEDING IN RED MULLET *MULLUS BARBATUS* (LINNAEUS, 1758) IN THE SOUTHEAST BLACK SEA

Hatice Onay*, Goktug Dalgic

Recep Tayyip Erdogan University, Fisheries Faculty, Zihni Derin Campus, Rize, 53500 Turkey

ABSTRACT

The diet of the red mullet *Mullus barbatus* was studied in the southeast Black Sea region of Turkey during the autumn, winter, summer and spring. In one year, the stomach contents of 760 individuals of *M. barbatus,* a confirmed omnivorous fish species, were examined (April 2017–March 2018), in addition to those of 180 additional individuals examined within a 24-h period (28 April 2018). Among the 14 prey groups identified in the stomachs of red mullet, the predominant one was Bivalvia, followed by Nematoda, Polychaeta, Brachyura and Cumacea. Data analysis revealed significant differences in prey species composition between seasons (ANOSIM, $R = 0.089$, $p < 0.001$). Moreover, the prey groups that constituted the majority of the diet changed significantly with a season. SIMPER analysis revealed that the prey item contributing the most to the differences between seasons was Bivalvia. Microplastic was also found in the samples. Analysis of the daily rhythm diet variation in stomach contents allowed the identification of 8 prey groups, namely Bivalvia, Amphipoda and Cumacea. In 24-hour examinations, feeding began in the first hours of the day, then showed an increase in the following hours and decreased after the evening. The results of this study could be used to describe the diversity of prey species and intraspecific food competition in the Black Sea.

KEYWORDS:
Mullus barbatus, Black sea, Daily feeding, Seasons feeding, Microplastic.

INTRODUCTION

Red mullet (Mullus barbatus Linnaeus, 1758) is a common benthic fish species living on sandy and muddy bottoms of the continental shelf at depths as low as 200 m [1]. It is distributed all across the Mediterranean basin, including the Black Sea and the Eastern Atlantic along the European and African coasts [2, 3, 1]. Red mullet is one of the most important demersal fish of the Black Sea, has a very high value in Turkish fisheries and is one of the most important fish species traditionally fished and consumed in Black Sea countries [4]. Red mullet is also an important component of the Mediterranean demersal resources exploited by bottom trawl and small-scale fisheries [5, 6]. For Turkey, the total catch of these highly valuable goatfishes summed to 4579 tons in 2016 based on statistics from the Turkish Statistical Institute [7]. Feeding activities provide fish with the necessary nutrition and energy to support their maintenance, growth, reproduction and, subsequently, population development [8, 9, 10]. The study of feeding activities and the factors influencing them is thus critically important in our understanding of the dynamics of fish populations. Knowledge of the feeding habits of a fish may play a key role in research on the following ecological issues: prey selection, predator-prey size relationships, distribution of feeding types with latitude, ontogenetic diet shifts, and species invasions [11]. The diet of the red mullet has been well investigated in the Mediterranean Sea [12, 13, 14, 15, 16, 17, 18, 19, 20, 21, 22, 23, 24, 25, 26, 27]. However, there is no information about this species in the Black Sea, and this study was planned to fill this gap. This work aims to provide a detailed (monthly and daily) description of the feeding habits of the species Mullus barbatus off the Black Sea and to compare them with other areas (e.g. Mediterranean Sea and Atlantic Ocean), which could help provide a basis for understanding trophic levels and interactions in the aquatic food web of the study area. The results of this study can be used in multispecies and ecosystem-based models.

MATERIALS AND METHODS

Fish sampling (annual). A total of 760 red mullet samples were collected monthly using an experimental bottom trawl (12 mm mesh size) between April 2017 and March 2018 off the Rize coast, in the south-eastern Black Sea. Fishing took place within an area defined by the following coordinates: 40o59’29’’N/40o19’52’’E; 40o59’

57''N/40o18' 50''E; 40o01'32''N/40o22'53''E; 41o02'10''N/40o22'04''E (Fig. 1). The average haul duration was 30 min, and towing speed varied from 2.5 to 3.5 knots between 0-30, 30-60 and 60+ m depth contours. Sampled specimens were fixed in 70% alcohol and transferred to the laboratory. The total length of each individual was measured to 0.1 cm, and wet weight was determined to the nearest 0.01 g after the animal was blotted dry on absorbent paper.

Fish sampling (daily). A total of 180 red mullet samples were collected in April at 4-hour intervals during the 24-h sampling period using the same experimental bottom trawl (12 mm mesh size) between 13:00 (28 April 2018) and 09:00 (29 April 2018) off the Rize coast, in the south-eastern Black Sea. The area was defined by the following coordinates: 40o59'29''N/ 40o19'52''E, 40o59' 57''N/40o18'50''E, 40o01'32''N/40 o22'53''E, 41o02'10''N/ 40o22'04''E (Fig. 1). The depth range of the sampling area was from 30 to 40 m. A total of 6 trawl operations were carried out during the 24-h sampling period. The bottom texture in the area was muddy sand. From each haul, 30 specimens were randomly sampled. The total body weight (g) of each fish was measured before dissection for stomach removal. Stomachs were preserved individually in small jars with 10% buffered formaldehyde solution.

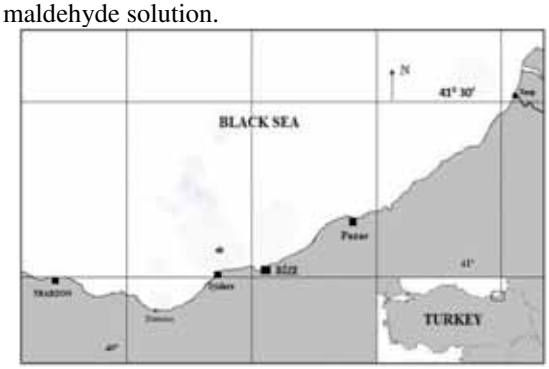

FIGURE 1
Map of the study area

Diet analysis. Stomachs were dissected, and all prey items were identified to the lowest possible taxonomic level after counting and weighing. Sorted prey items were weighed wet to the nearest 0.001 g. The prey group occurrence frequency (F%), prey group numerical frequency (N%), percent prey group weight (W%), relative importance index (IRI) and percent relative importance index (IRI%) (28, 29). were determined as follows:

$$F\% = \frac{n}{Ns} * 100,$$

$$N\% = \frac{n^y}{N_p} * 100$$

$$W\% = \frac{w^y}{W_p} * 100$$

$$IRI = (N\% + W\%).\ (F\%)$$

$$IRI\% = \frac{IRI}{\sum IRI} * 100$$

where, F% = number of stomachs containing prey n / total number of full stomachs x 100 Ns , N% = number of prey n^y/ total number of prey x 100 N_p, W%= weight of prey w^y / total weight of all prey x 100 W_p.

In the annual samples, stomach fullness was determined visually according to (30) using a scale ranging from 0 to 100% and noted as empty (0%), moderately full (25%), half full (50%), quite full (75%) and very full (100%). One-way analysis of similarity (ANOSIM) (31) was used to determine the differences between seasons in the structure of the stomach contents. The most abundant prey species primarily responsible for an observed difference between seasons were examined using similarity percentages (SIMPER) [31] Multivariate analyses were performed with the software package PRIMER 5.

In order to determine the diel feeding intensity and chronology, fullness index (%FI) values (the percentage ratio of the weight of an individual fish stomach contents to its total body weight) and the percentage of empty stomachs (%ES) were calculated for each sampling time [28, 29].

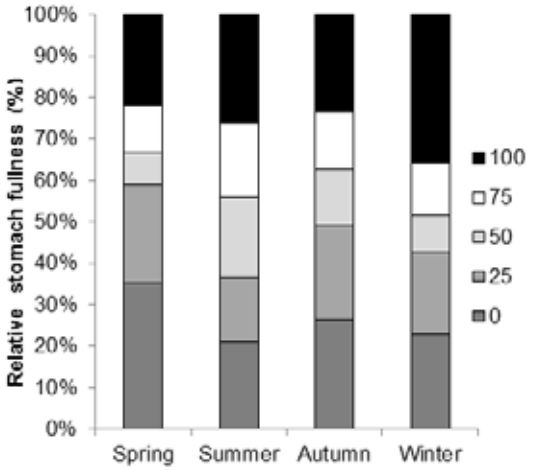

FIGURE 2
Seasonal stomach fullness ratio (empty, 0%; moderately full, 25%; half full, 50%; quite full 75% and very full 100%) of red mullet (M. barbatus) sampled from April 2017 to March 2018 from the Black sea

RESULTS

Empty stomachs were found in all seasons throughout the year. The highest proportion of very full stomachs (35.66%) was found in winter, whereas the highest number of empty stomachs (35.26%) was recorded in the spring (Fig. 2).

Overall diet composition. All stomach contents of red mullet contained Bivalvia (N% = 30.46), Amphipoda (N% = 2.07), Isopoda (N% = 0.87), Cumacea (N% = 13.16), Gastropoda (N% = 3.98), Brachyura (N% = 2.31), Decapoda (N% = 2,17), Teleostei (N% = 0.15), Polychaeta (N% = 4.77), Nematoda (N% = 38.42), Mysidacea (N% = 0.80), Tanaidacea (N% = 0.15), Echinodermata (N% = 0.56) and microplastic (N% = 0.12). According to the percent relative importance index, IRI%, red mullet generally feed on three prey groups: Bivalvia (IRI% = 68.69), Nematoda (IRI% = 14.59) and Polychaeta (IRI% = 5.36) (Table 1).

Seasonal prey variations were observed in the diet of red mullet. The IRI% of food items of red mullet is shown in Table 2. It was clear that Bivalvia was the most important food item in all seasons and showed the highest percentage during the summer, with an average of 70.8%. The prey groups Cumacea, Brachyura and Decapoda followed Bivalvia. In addition, microplastic was found in the samples.

According to the ANOSIM, the global R value was 0.089 [an R value between 0 and 1 indicates that all the most similar samples are within the same groups [32] and the significance level of the sample statistics was 0.001. SIMPER analysis (Table 3) was performed on the number of species found in stomachs in all seasons. The average dissimilarity between spring and summer was 73.57% and showed that the groups Bivalvia and Nematoda were good indicators of spring and Cumacea and Brachyura, of summer. The average dissimilarity between spring and autumn was 69.14% and showed that the groups Bivalvia, Brachyura and Polychaeta were good indicators of spring and Nematoda, of autumn. The average dissimilarity between Summer and Autumn was 67.91% and showed that the groups Bivalvia, Cumacea and Brachyura were good indicators of summer and Nematoda, of Autumn. The average dissimilarity between spring and winter was 69.01% and showed that the groups Bivalvia and Amphipoda were good indicators of spring and Nematoda and Polychaeta, of winter. The average dissimilarity between summer and winter was 72.85% and showed that the groups.

TABLE 1
Overall distribution of prey group occurrence frequency (F%), numerical frequency (N%), weight (W%) and relative importance (IRI%) for the prey groups observed in red mullet stomach.

Species	n	F%	N%	W%	IRI%
Bivalvia	1783	60.75	30.46	41.67	68.69
Amphipoda	121	9.32	2.07	2.60	0.68
Isopoda	51	4.66	0.87	0.11	0.07
Cumacea	770	16.49	13.16	0.27	3.47
Gastrapoda	233	11.29	3.98	1.99	1.06
Brachyura	135	11.65	2.31	23.04	4.63
Decapoda	127	10.75	2.17	5.25	1.25
Teleostei	9	1.25	0.15	4.03	0.08
Polychaeta	279	15.41	4.77	17.40	5.36
Nematoda	2249	22.58	38.42	2.80	14.59
Mysidacea	47	3.23	0.80	0.11	0.05
Tanaidacea	9	0.72	0.15	0.04	0.00
Echinodermata	33	3.58	0.56	0.69	0.07
Microplastic	7	1.08	0.12	0.00	0.00

TABLE 2
Seasonal distribution of prey group occurrence frequency (F%), numerical frequency (N%), weight (W%) and relative importance index (IRI%) values observed in red mullet stomach.

	Spring				Summer				Autumn				Winter			
Prey Groups	**F%**	**N%**	**W%**	**IRI%**	**F%**	**N%**	**W%**	**IRI%**	**F%**	**N%**	**W%**	**IRI%**	**F%**	**N%**	**W%**	**IRI%**
Bivalvia	47.0	42.8	25.2	64.1	63.1	34.9	57.2	70.8	63.7	31.2	39.3	70.3	69.4	20.3	31.0	39.7
Amphipoda	13.4	4.4	13.8	4.9	11.9	2.9	0.6	0.5	6.7	1.4	1.1	0.3	4.1	0.5	1.0	0.1
Isopoda	5.2	0.7	0.4	0.1	2.4	0.3	0.1	0.0	9.6	2.0	0.1	0.3	1.7	0.9	0.0	0.0
Cumacea	8.2	3.2	0.3	0.6	36.3	38.3	0.6	17.2	5.9	1.6	0.0	0.2	9.9	1.6	0.1	0.2
Gastrapoda	12.7	4.2	6.2	2.6	11.9	4.0	0.6	0.7	6.7	7.3	2.9	1.1	14.0	2.3	0.5	0.4
Brachyura	9.7	2.8	32.5	6.9	14.9	3.0	29.2	5.8	13.3	3.0	25.1	5.9	7.4	1.1	5.9	0.6
Decapoda	3.7	0.6	0.1	0.1	22.6	5.6	7.4	3.6	10.4	1.6	5.0	1.1	2.5	0.2	5.2	0.2
Teleostei	2.2	0.4	0.4	0.0	0.6	0.1	1.8	0.0	1.5	0.3	11.6	0.3	0.8	0.1	0.0	0.0
Polychaeta	16.4	6.5	15.4	7.2	3.6	0.5	1.0	0.1	9.6	4.7	10.3	2.3	37.2	7.6	52.0	24.7
Nematoda	18.7	32.2	2.9	13.2	8.9	8.3	1.4	1.0	23.0	46.5	4.5	18.4	45.5	64.0	2.6	33.7
Mysidacea	1.5	0.5	0.4	0.0	7.7	2.2	0.1	0.2	0.0	0.0	0.0	0.0	2.5	0.3	0.0	0.0
Tanaidacea	2.2	0.7	0.3	0.0	0.0	0.0	0.0	0.0	0.7	0.1	0.0	0.0	0.0	0.0	0.0	0.0
Echinodermata	3.7	0.9	2.2	0.2	0.0	0.0	0.0	0.0	0.0	0.0	0.0	0.0	12.4	1.2	1.8	0.4
Microplastic	0.7	0.1	0.0	0.0	0.0	0.0	0.0	0.0	2.2	0.4	0.0	0.0	1.7	0.1	0.0	0.0

TABLE 3
Results of SIMPER analysis: Groups contribution to average dissimilarity between seasons.

Spring-Summer	Average dissimilarity = 73.57					
Groups	**Av.Abund**	**Av.Abund**	**Av.Diss**	**Diss/SD**	**Contrib%**	**Cum.%**
Bivalvia	4.73	4	18.56	1.16	25.23	25.23
Cumacea	0.35	4.37	11.46	0.79	15.57	40.81
Nematoda	3.56	0.95	9.61	0.63	13.06	53.87
Brachyura	0.31	0.33	7.39	0.5	10.05	63.92
Spring-Autumn	Average dissimilarity = 69.14					
Groups	**Av.Abund**	**Av.Abund**	**Av.Diss**	**Diss/SD**	**Contrib%**	**Cum.%**
Bivalvia	4.73	2.86	18.81	1.19	27.2	27.2
Nematoda	3.56	4.27	13.07	0.79	18.9	46.11
Brachyura	0.31	0.28	7.38	0.52	10.67	56.78
Polychaeta	0.72	0.43	7.15	0.57	10.35	67.12
Summer-Autumn	Average dissimilarity = 67.91					
Groups	**Av.Abund**	**Av.Abund**	**Av.Diss**	**Diss/SD**	**Contrib%**	**Cum.%**
Bivalvia	4	2.86	17.79	1.16	26.2	26.2
Cumacea	4.37	0.15	11.28	0.77	16.61	42.8
Nematoda	0.95	4.27	9.95	0.67	14.64	57.45
Brachyura	0.33	0.28	7.64	0.53	11.25	68.7
Spring-Winter	Average dissimilarity = 69.01					
Groups	**Av.Abund**	**Av.Abund**	**Av.Diss**	**Diss/SD**	**Contrib%**	**Cum.%**
Bivalvia	4.73	3.72	17.04	1.21	24.69	24.69
Nematoda	3.56	12.36	16.99	1.03	24.61	49.31
Polychaeta	0.72	1.48	10.8	0.83	15.65	64.96
Amphipoda	0.48	0.09	5.53	0.44	8.01	72.97
Summer-Winter	Average dissimilarity = 72.85					
Groups	**Av.Abund**	**Av.Abund**	**Av.Diss**	**Diss/SD**	**Contrib%**	**Cum.%**
Bivalvia	4	3.72	16.75	1.22	22.99	22.99
Nematoda	0.95	12.36	16.24	1.02	22.3	45.29
Cumacea	4.37	0.31	10.8	0.78	14.82	60.11
Polychaeta	0.06	1.48	8.62	0.72	11.83	71.94
Autumn-Winter	Average dissimilarity = 64.70					
Groups	**Av.Abund**	**Av.Abund**	**Av.Diss**	**Diss/SD**	**Contrib%**	**Cum.%**
Nematoda	4.27	12.36	16.88	1.05	26.09	26.09
Bivalvia	2.86	3.72	16.76	1.23	25.9	51.99
Polychaeta	0.43	1.48	9.63	0.78	14.88	66.87
Brachyura	0.28	0.21	5.41	0.46	8.36	75.23

TABLE 4
Distribution of prey group occurrence frequency (F%), numerical frequency (N%), weight (W%) and relative importance (IRI%) for the prey groups observed in red mullet stomach during 24-h period

Hours	**%**	**Bivalvia**	**Amphipoda**	**Cumacea**	**Gastrapoda**	**Decapoda**	**Polychaeta**	**Nematoda**	**Tanaidacea**
13:00	**F%**	63.64	0.00	0.00	36.36	18.18	63.64	18.18	0.00
	N%	14.47	0.00	0.00	5.26	3.95	73.68	2.63	0.00
	W%	4.89	0.00	0.00	1.04	54.48	39.54	0.05	0.00
	IRI%	12.60	0.00	0.00	2.34	10.86	73.69	0.50	0.00
17:00	**F%**	50.00	0.00	0.00	25.00	0.00	12.50	0.00	0.00
	N%	50.00	0.00	0.00	25.00	0.00	25.00	0.00	0.00
	W%	67.74	0.00	0.00	11.18	0.00	21.08	0.00	0.00
	IRI%	79.91	0.00	0.00	12.28	0.00	7.82	0.00	0.00
21:00	**F%**	27.27	0.00	0.00	9.09	18.18	45.45	18.18	0.00
	N%	20.83	0.00	0.00	4.17	8.33	58.33	8.33	0.00
	W%	27.65	0.00	0.00	0.29	3.58	67.91	0.57	0.00
	IRI%	17.68	0.00	0.00	0.54	2.90	76.72	2.17	0.00
01:00	**F%**	77.78	0.00	0.00	11.11	0.00	66.67	22.22	0.00
	N%	36.11	0.00	0.00	5.56	0.00	47.22	11.11	0.00
	W%	52.96	0.00	0.00	2.07	0.00	44.30	0.67	0.00
	IRI%	51.79	0.00	0.00	0.63	0.00	45.62	1.96	0.00
05:00	**F%**	92.59	0.00	3.70	40.74	3.70	22.22	25.93	3.70
	N%	76.01	0.00	1.01	10.47	1.01	6.42	4.73	0.34
	W%	63.67	0.00	0.08	10.32	0.25	25.47	0.20	0.01
	IRI%	88.42	0.00	0.03	5.79	0.03	4.84	0.87	0.01
09:00	**F%**	68.18	9.09	4.55	27.27	18.18	31.82	4.55	9.09
	N%	51.63	1.63	0.54	9.24	3.26	30.43	0.54	2.72
	W%	21.58	1.22	0.03	3.78	36.92	35.89	0.03	0.56
	IRI%	60.52	0.31	0.03	4.31	8.86	25.58	0.03	0.36

Bivalvia and Cumacea were good discriminators of summer and Nematoda and Polychaeta, of winter. The average dissimilarity between autumn and winter was 64.70% and showed that the group Brachyura was a good discriminator of autumn and Nematoda, Bivalvia and Polychaeta, of winter.

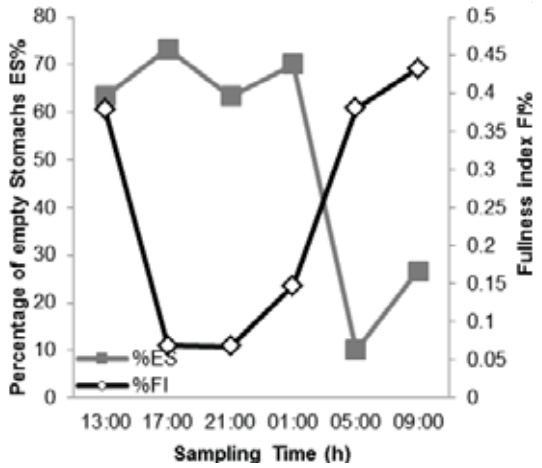

FIGURE 3
Variations in feeding intensity of red mullet during a 24- h sampling period

Daily diet composition. Feeding activity started early in the day (01:00) and increased with the sunrise. It reached the maximum level in the subsequent hours. There was a decrease in feeding activity in the afternoon, towards sunset (Fig. 3).

The daily rhythm in the variation of stomach content analysis allowed the identification of 8 prey groups, namely Bivalvia, Amphipoda, Cumacea, Gastrapoda, Decapoda, Polychaeta, Nematoda and Tanaidacea. The following percent relative importance indices (IRI%) were obtained: at 13:00, Polychaeta IRI% = 73.69; at 17:00, Bivalvia IRI% = 79.91; at 21:00, Polychaeta IRI% = 76.72; at 01:00, Bivalvia IRI% = 51.79; at 05:00, Bivalvia IRI% = 88.42 and at 09:00, Bivalvia IRI% = 60.52 (Table 4).

DISCUSSION

Overall diet composition. Red mullet is a carnivorous fish that scoops up the substratum to detect and feed on a wide range of benthic invertebrates, primarily polychaetes but also crustaceans and molluscs [25, 33, 34, 35, 36, 37]. The diet of red mullet in the Black Sea differs from that of red mullet in the Mediterranean Sea and Atlantic Ocean. This reveals that the presence of Bivalvia in the diet of red mullet predominates in the Black Sea. In the other areas (Mediterranean, Atlantic Ocean and the Aegean Sea), the dominant groups in the stomach contents were reported as Polychaeta [13, 26, 37, 12, 23, 19, 20] and Amphipoda [14]. [27], reported the primary diet group of red mullet as Decapoda in the Mediterranean. Differences in diet of red mullet are generally not important as they could be the results of the areas sampled and/or the biological environment. According to previous studies, the morphological characteristics and foraging behaviour of red mullet accounted for both prey type selection and feeding patterns [25, 35]. In our study and in the study of [27], the Nemotoda prey group was reported. Also, some groups reported in other studies [37, 20, 23, 27] were not reported in our study. Marine plastic litter is slowly broken up by mechanical, chemical and photolytic degradation processes and then fragmented into small sizes. This plastic litter floats on the sea or sinks to the bottom [38]. [39] reported that demersal fish species contain higher levels of microplastics in their stomach contents than pelagic fish species. Microplastic was found in *M. barbatus,* one of the demersal fish species in the study.

Diet composition according to season. In this study the group Bivalvia was determined as the dominant group in all seasons (spring IRI% 64.1, summer IRI% 70.8, autumn IRI% 70.3 and winter IRI% 39.7) (Table 3). [27] and [13] reported the Polychaete group as dominant in all seasons for the same species in the Mediterranean. In several other studies, it was reported that the main feeding group varied between seasons. [14], reported differences between the seasons: in autumn Copepoda was more abundant, whereas in spring Amphipoda was more abundant. In addition, Copepoda was found in abundance in winter and autumn. Amphipoda abundance was higher in summer than in other seasons. Amphipoda and Cumacea were abundant in spring and winter. [23], reported that although the dominant group was Polychaeta in February, May and July, the Bivalvia group was dominant in September. Moreover, in November, Polychaeta and Bivalvia were similar in importance. [19] reported differences between the seasons, but in the spring, there is a higher abundance of food compared with other seasons. Our study also showed differences between the seasons. Such differences in the diet of *M. barbatus* between seasons might be caused by the presence of certain food groups in the environment during a specific season [40].

Diet composition in relation to time of day. Feeding begins in the first hours of the day, then shows an increase in subsequent hours and decreases after the evening. [12, 19] conducted daily rhythm studies in the Aegean Sea and obtained similar results to ours. In two studies, feeding was reported to be intense during the morning, decreasing at night. However, they reported the main group as Polychaeta.

CONCLUSION

Most of the previous studies cited in this manuscript reported Polychaeta as the predominant prey item in the diet of red mullet. However, according to the present study, Polychaeta were not the predominant prey item in the diet of red mullet in the Black Sea. To confirm this, further research is required to investigate the feeding habits of other predators in the Black Sea that consume Polychaeta. In addition, studies on the abundance of Polychaeta in the Black Sea are almost negligible; therefore, it is important to investigate this issue. In the present study, we reported plastic pollution in commercial fishes from the Black Sea. This study provides an important contribution to the knowledge and understanding of plastic occurrence in these commercial fish, given their importance in Black Sea catches and human consumption. The presence of plastic in other commercial fish species has important consequences for human health. The results of this study could be used for ecosystem-based management of *M. barbatus* and to describe the diversity of prey and interspecific food competition in the Black Sea.

ACKNOWLEDGEMENTS

We appreciate the crew members of the Karadeniz Araştırma Gemisi and Yusuf Ceylan, and MSc students Erhan Öztürk and Muhammet Emanet for their help in laboratories.

REFERENCES

[1] Lombarte, A., Recascens, L., Gonzalez, M. and Gil de Sola, L. (2000) Spatial segregation of two species of Mullidae (*Mullus surmuletus* and *M. barbatus*) in relation to habitat. Marine Ecology Progress Series. 206, 239–249.

[2] Hureau, J.C. (1986) Mullidae. In: Whitehead, P.J.P., Bauchot, M.L., Hureau, J.C., Nielsen, J., Tortonese, E. (eds.) Fishes of the North-eastern Atlantic and the Mediterranean. Vol. 2. Paris: UNESCO, 877-82.

[3] Bauchot, M.L. (1987) Bony fish. In: Fischer, W., Bauchot, M.L. and Schneider, M. (eds.) FAO identification sheets for the needs of the fishery. (Revision 1). Mediterranean and Black Sea. Fishing area 37. Vol. II. Commission of the European Communities and FAO, Rome. 891-1421.

[4] STECF (2013) The 2013 Annual Economic Report on the EU Fishing Fleet (STECF 13-15).

[5] Fiorentini, L., Caddy, J.F. and de Leiva, J.I., (1997) Long- and short-term trends of Mediterranean fishery resources. Studies and Reviews. GFCM, No. 69. FAO, Rome, 72 pp.

[6] Tserpes, G., Moutopoulos, D. K., Peristeraki, P., Katselis, G. and Koutsikopoulos, C. (2006) Study of swordfish fishing dynamics in the eastern Mediterranean by means of machine-learning approaches. Fisheries Research. 78, 196–202.

[7] TÜİK (2017) Turkish Statistical Institute, Fishery Statistics 2016.

[8] Beverton, R.J.H. and Holt, S.J. (1957) On the dynamics of exploited fish populations. Fish. Invest. Ser. 2 Mar. Fish. G.B. Minist. Agric. Fish. Food No.19, 533 p.

[9] Backiel, T. and Le Cren, E.D. (1978) Some Density Relationships for Fish Population Parameters, in S.D. Gerking (ed.), Ecology of Freshwater Fish Production, Blackwell, Oxford, pp. 279–302.

[10] Persson, L., Bertolo, B. and De Roos, A.M. (2006) Temporal stability in size distributions and growth rates of three pike (Esox lucius) populations a result of cannibalism. Journal of Fish Biology. 69, 461–472.

[11] Stergiou, K.I. and Karpouzi, V.S. (2002) Feeding habits and trophic levels of Mediterranean fish. Reviews in Fish Biology and Fisheries. 11(3), 217–254.

[12] Ünlüoğlu, A., Cihangir, B., Kaya, M., Benli, H.A. and Katağan, T. (2002) Variations in the feeding intensity and diet composition of red mullet (*Mullus barbatus*) during 24-h period in the summertime in Hisarönü Bay. J. Mar. Biol. Ass. U.K., 82, 527-528.

[13] Mahmoud, H.H., Fahim, M.R., Srour, T.M., El-Bermawi, N. and Ibrahim, M.A. (2017) Feeding ecology of Mullus barbatus and Mullus surmuletus off the Egyptian Mediterranean coast. International Journal of Fisheries and Aquatic Studies. 5(6), 321-325.

[14] Esposito, V., Andaloro, F., Bianca, D. Natalotto, A., Romeo, T., Scotti, G. and Castriota, L. (2014) Diet and prey selectivity of the red mullet, Mullus barbatus (Pisces: Mullidae), from the southern Tyrrhenian Sea: the role of the surf zone as a feeding ground. Marine Biology Research. 10(2), 167178,

[15] Sabates, A., Zaragoza, N. and Raya, V. (2015) Distribution and feeding Dynamics of larval red mullet (Mullus barbatus) in the NW Mediterranean: the important role of cladocera. Journal of Plankton Research. 37(4), 820-833.

[16] Wirszubski, A. (1953) On the biology and biotope of red mullet *Mullus barbatus*. Bull. Sea Fish. Research Stn. Haifa. 7, 1-20.

[17] Gharbi, H. and Ktari, M.H. (1979) Diet of red mullet (*Mullus barbatus* Linnaeus, 1758 and *Mullus surmuletus* Linnaeus, 1758) of the Gulf of Tunis. Bulletin de l'Institut national scientifique et technique d'océanographie et de peche de Salammbô. 6(1-4), 41–52. (French Original).

[18] Focardi, S., Falciai, L., Gambi, C. and Spadini, V. (1980) Analysis of the gastric content of *Mullus barbatus* L. (Perciformes: Mullidae). Rivista di Idrobiologia. 19, 235-248. (Italian Original).

[19] Caragitsou, E. and Tsimenidis, T. (1982a) Seasonal changes and comparative analysis of the food of red mullet (*Mullus barbatus*) in the Guu of Saronikos and Thermaikos. Thalassograph. 5, 41-61.

[20] Caragitsou, E. and Tsimenidis, T. (1982b) Seasonal changes of food spectrum and daytime rhythm of feeding of the red mullet (*Mullus barbatus*) in the Thracian Sea. Thalassograph. 5, 105-115.

[21] Bizsel, K.C. (1987) Seasonal variations in the diel diet of the red mullets (*Mullus barbatus* L.) in the northern Cilician Basin. MSc. Thesis. Middle East Technical University, Mersin, Turkey.

[22] Katağan, T., Kaya, M., Ergen, Z. and Önen, M. (1990) The feeding regime of *Mullus barbatus* Linnaeus, 1758 species living in İzmir Bay. Doğa-Turkish Journal of Zoology. 14, 179-187. (Turkish Original).

[23] Vassilopoulou, V and Papaconstantinou, C. (1993) Feeding habits of red mullet (*Mullus barbatus*) in a gulf in western Greece. Fisheries Research. 16, 69-83.

[24] Golani, D. (1994) Niche separation between colonizing and indigenous goatfish (Mullidae) along the Mediterranean coast of Israel. J. Fish Biol. 45, 503 5033

[25] Labropoulou, M, Eleftheriou, A. (1997) The foraging ecology of two pairs of congeneric demersal fish species: Importance of morphological characteristics in prey selection. Journal of Fish Biology. 50, 324-40.

[26] Vassilopoulou, V, Papaconstantinou, C, Caragitsou, E. (2001) Adaptations of demersal fish species in a nutrient-rich embayment of the Ionia Sea (Greece). In: Thurston, R.V. (ed.) Fish Physiology, Toxicology, and Water Quality. Proceedings of the 6th International Symposium. Athens, GA: Ecosystem Research Division. 107-21.

[27] Cherif, M., Ben Amor, M.M., Selmi, S., Gharbi, H., Missaoui, H. and Capape, C. (2011) Food and feeding habits of the red mullet, *Mullus barbatus* (Actinopterygii: Perciformes: Mullidae), off the northern Tunisian coast (central Mediterranean). Acta Ichthyologica et Piscatoria. 41, 109-16.

[28] Hyslop, E. (1980) Stomach contents analysis-a review of methods and their application. Journal of Fish Biology. 17, 411-429.

[29] Cortés, E. (1997) A critical review of methods of studying fish feeding based on analysis of stomach contents: application to elasmobranch fishes. Canadian Journal of Fisheries and aquatic Science. 54, 726-738.

[30] Kitsos, M.S., Tzomos, T., Anagnostopoulou, L. and Koukouras, A. (2008) Diet composition of the seahorses, *Hippocampusguttulatus* Cuvier, 1829 and *Hippocampus hippocampus* (L.,1758) (Teleostei, Syngnathidae) in the Aegean Sea. Journal of Fish Biology. 72, 1259-1267.

[31] Clarke, K.R. and Warwick, R.M. (1994) Changes in Marine Communities: An Approach to Statistical Analyses and Interpretation. Natural Environment Research Council, Plymouth. 144p.

[32] Clarke, K.R. (1993) Non-parametric multivariate analysis of changes in community structure. Australian Journal of Ecology. 18, 117-143.

[33] Labropoulou, M. and Papadopoulou-Smmh, K.N. (1999) Foraging behaviour patterns of four sympatric demersal fishes. Estuar. Coast. Shelf Sci. 49(Suppl. A), 99-108.

[34] Aguirre, H. (2000) Aspectos biologicos y ecologicos del salmonete de fango *Mullus barbatus* L., 1758 y del salmonete de roca Mullus surmuletus L., 1758, del Mediterraneo Noroccidental. PhD Dissertation. Polytechnic University of Catalunya, Spain. 261p.

[35] Machias, A. and Labropoulou, M. (2002) Intraspecific variation in resource use by Red Mullet, Mullus barbatus. Estuarine Coastal and Shelf Science. 55, 565–578.

[36] Aguirre, A. and Sanchez, P. (2005) Feeding resource partitioning between *Mullus barbatus* and *M. surmuletus* in the Catalan Sea (northwestern Mediterranean). *Cienc. Mar.* 31(2), 429- 439.

[37] Bautista-Vega, A.A., Letourneur, Y., Harmelin-Vivien, M. and Salen-Picard, C. (2008) Difference in diet and size-related trophic level in two sympatric fish species, the red mullets *Mullus barbatus* and *M. surmuletus*, in the Gulf of Lions (NW Mediterranean). J. Fish. Biol. 73, 2402-2420.

[38] Cózar, A., Echevarría, F., González-Gordillo, J.I., Irigoien, X., Úbeda, B., Hernández-León, S., Palma, Á.T., Navarro, S., García-de-Lomas, J., Ruiz, A., Fernández-de-Puelles, M.L., Duarte, C.M. (2014) Plastic debris in the open ocean. Proc. Natl. Acad. Sci. 111, 10239–10244.

[39] Baalkhuyur, F.M., Bin Dohaish, E.A., Elhalwagy, M.E.A., Alikunhi, N.M., AlSuwailem, A.M., Røstad, A., Coker, D.J., Berumen, M.L. and Duarte, C.M. (2018) Microplastic in the gastrointestinal tract of fishes along the Saudi Arabian Red Sea Coast. Marine Pollution Bulletin. 131, 407–415.

[40] Ünlüoğlu, A. 1995. Investigations of the Feeding Habits of Bogue (*B. boops*, Lin. 1758), Horse mackerel (*T. trachurus*, Lin., 1758), Sardine (S. *pilchardus*, Walbaum 1792) and Anchovy (*E. encrasicholus*, Lin 1758) in Izmir Bay, Dokuz Eylül University, Institute of Marine Science and Technology, İzmir.

Received: **19.11.2018**
Accepted: **24.02.2019**

CORRESPONDING AUTHOR

Hatice Onay
Recep Tayyip Erdogan University,
Fisheries Faculty,
Zihni Derin Campus,
Rize, 53500 – Turkey

e-mail: hatice.bal@erdogan.edu.tr

© by PSP Volume 28 – No. 4/2019 pages 2679-2687 Fresenius Environmental Bulletin

EFFECTS OF SOYBEAN OIL SUPPLEMENTATION ON THE GROWTH AND SURVIVAL PERFORMANCE OF RED CLAW CRAYFISH *CHERAX QUADRICARINATUS* IN CULTURE CONDITION

Yavuz Mazlum*, Mehmet N Gunduz, Ozlem Guner Gurlek, Metin Yazici

Faculty of Marine Sciences and Technology, Iskenderun Technical University, 31200, Iskenderun, Hatay, Turkey

ABSTRACT

The current study investigated the effects of soybean oil on the growth and survival of red claw crayfish (*Cherax quadricarinatus*) under culture conditions. An experiment consisting of four dietary soybean oil concentrations (0%, 4%, 8%, and 12%) in commercial trout larvae feed was carried out on a 90-day duration with three replications. Juvenile crayfish (mean ± SD: 25.0±0.6 mm length and 0.51±0.15 g mass) were placed in each of the twelve 0.14-m^2 aquariums with 50 crayfish/m^2 density. Each aquarium contained ten crayfish. At the end of the experiment, the highest mass gain, Specific Growth Rate (SGR) and molting frequency were observed on the crayfish fed with 12% soybean oil diet concentration. Although, 12% soybean oil diet gave the highest mass gain (1.45 g), it resulted in the lowest survival rate (48%) ($p<0.05$). However, no significant difference was found in Feed Conversion Rate (FCR) among soybean oil levels. Moreover, molting frequencies in the diet groups were found as 49.6, 48.0, 46.6, and 73.3% for the dietary soybean oil levels (0%, 4%, 8%, and 12%), respectively. Thus, based on the results, the dietary concentration levels of soybean oil is recommended to be in 8-12% in formulated diets for the optimum growth of crayfish.

KEYWORDS:
Crayfish, *Cherax quadricarinatus*, soybean oil, growth, survival

INTRODUCTION

Red claw crayfish, *C. quadricarinatus* is considered to be a valuable fishery resource for commercial aquaculture. This species has become more popular in recent years [1]. It has such a rapid growth rate and tolerates a wide range of water quality parameters that are available for commercial aquaculture [2, 3]. *C. quadricarinatus* tends to develop very rapidly in tropical and semi-tropical regions of the world. It is capable of surviving and reproducing under various biotic and abiotic conditions. Another characteristic of this species is being a non-burrowing species that is tolerant of a wide variety of habitats such as flowing rivers, lakes and lagoons [4].This species prefers rocky and foraging habitats with plenty of cavities for exploring and finding shelter during molting [5]. *C. quadricarinatus* was introduced into many countries of Asia, North, South and Central America, Africa and Europe [6, 7, 8, 9]. *C. quadricarinatus* is mainly grown in semi-intensive and intensive earthen ponds in the world. Recently, hatchery production has become more common [10, 11, 12, 13]. Crayfish have been described as opportunistic benthic organisms and have well-developed feeding appendages [14, 15, 16]. They are well-adapted for processing both soft and hard food feed types such as a variety of macrophytes, bentic invertebrate and detritus [14]. In Turkey, it is commonly sold as an ornamental aquarium species and was not used for commercial production.

Soybean oil which is used as a source of energy in the larval phase of the crustacean and aquatic animals, also has significant effects on the growth and survival of *C. quadricarinatus* [17]. Soybean oil consists of polyunsaturated fatty acids and is one of the few plant sources with significant amounts of oleic and linolenic acids [17]. It is also cheap and digested well by aquatic animals [18]. High lipid level in feeds may adversely affect the growth, reduce feed intake and decrease the use of nutrients [19, 20]. Moreover, high level also causes an increase in lipid accumulation in fish body and affects quality and nutritional value of fish meat [21]. Therefore, soybean oil can be considered as an alternative dietary lipid in feeds to increase the growth and survival of *C. quadricarinatus*. The levels of required lipid depend on the environmental conditions, life stages and differences among species [22]. In aquaculture, feed consumption has increased in recent years and consequently, extensive research has been carried out on alternative raw and processed materials of plant origin [23]. Increasing growth of the *C. quadricarinatus* is a key factor that supports the aquaculture industry, which includes more knowledge of the culture

requirements of this species and improved nutrition [17]. However, there are still knowledge gaps in relation to nutrient requirements of the crayfish species especially regarding the soybean oil. In this study, soybean oil was added into the diets of crayfish juveniles to observe the effects on their growth and survival under laboratory conditions.

MATERIALS AND METHODS

Source of Animal. Adult female crayfish [*C. quadricarinatus]* were obtained from a pet store located in Iskenderun, Hatay, Turkey. Crayfish were stored in 1000 L tank at Aquaculture Research Facilities at Iskenderun Technical University within a recirculating freshwater where spawning took place. The initial and final length of *C. quadricarinatus* juveniles was measured to the nearest millimeter to determine crayfish size. The experiment was carried out in each of the twelve 0.14 m2 aquariums with the substrate in the bottom. The flow of freshwater was maintained at 0.8 L/min to maintain water quality. Crayfish were checked five days in every week. Water temperature and dissolved oxygen (DO) were recorded by a digital meter (YSI 55, Yellow Springs Instruments Company, Yellow Springs, OH, USA). During the experiments, the pH values of the water were measured by a meter (Accumet 915 pH meter, Fisher Scientific, PA, USA). The concentrations of ammonia nitrogen (Nesler method) and nitrite nitrogen were determined by a spectrophotometer (UV-160 1PC, Shimadzu visible, Tokyo, Japan).

Experimental Design and Setup. The juveniles of *C. quadricarinatus* (mean ± SD: 25.0±0.6 mm length and 0.51±0.15 g mass) were used in this experiment. The experiment was carried out with 50 crayfish/m^2 density in 0.14-m^2 aquariums for about 90 days. Each aquarium contained ten crayfish. The parameters concerning the growth and survival were measured at 30-day intervals during the 90-day period experiment.

Experimental diets and feding. The experimental diets were formulated to contain four levels of soybean oil added to the commercial trout larvae diet with 0% (Control), 4%, 8%, and 12%. Different levels of soybean oil added into the commercial trout larvae diet were mixed homogenously in a kitchen robot. Then, distilled water of 35-40 g was added to the mix to obtain soft dough which was then passed through a mincer with 2 mm diameter holes to produce feed pellets. Then, the pellets were dried in an oven at 40ºC and stored at 4ºC during the experiment. Feed were given twice a day at a quantity of 5% of crayfish body weight for 90 days.

Growth and Survival Parameters. During the 90-day experiment trail, crayfish from each of the twelve aquariums were harvested and weighed on an electronic scale. To determine the growth and survival parameters as well as the molting frequency of crayfish were calculated by using the formulas given below:

SGR =ln (final mass) – ln (initial mass) x100 / time in days

MG= (final mass – initial mass) x100 / initial mass

FCR= feed consumption (g)/ wet mass gain (g)

MF = 100*(Number of molting animal / number of crayfish stocked)

SR= 100*(number of crayfish survived / number of crayfish stocked)

where;

SGR: Specific Growth Rate (%.day^{-1})

Initial mass: The total mass of the crayfish at the beginning of experiment (g)

Final mass: The total mass of the crayfish at the end of experiment (g)

MG: Mass gain (g)

FCR: Feed Conversion Ratio (unitless)

MF: Molting frequency (%)

SR: Survival Rate (%)

Data analysis. Analysis of variance (ANOVA) was used to determine the effects of additional soybean oil levels on the various responses including final wet mass, final length, FCR, and total yield for the diets including different soybean oil levels. Data were analyzed in the SPSS statistics program (version 17, Chicago, IL, USA). Dennett's multiple range test was used to determine the differences in average mass, final length, FCR, survival and total yield. Differences were considered significant at the $p<0.05$ level.

RESULTS AND DISCUSSION

Water quality. Water quality is one of the key factors in determining the success of crayfish culture efficiency. In the study, mean water temperature and Dissolved oxygen (DO) were recorded as 28.1 ± 0.8 ºC and 5.8 ± 0.6 mg O_2/L, respectively. The mean total ammonia nitrogen content, nitrite nitrogen content, and pH value of water was observed as 0.055 ± 0.017 mg NH4-N/ L, 0.025 ± 0.021 mg NO2-N /L and 7.6 ± 0.1, respectively as the average of the 90- day experiment period. These values are considered as suitable for crayfish culture [24]. The plus and minus values represent the standard deviation (SD).

TABLE 1
Growth and survival performances of juvenile *Cherax quadricarinatus* fed with different levels of soybean oil for 90 days*.

Growth parameters	Experimental diets including different levels of soybean oils			
	Control, 0%	4%	8%	12%
Initial length (mm)	25.0±0.6	25.0±0.6	25.0±0.6	25.0±0.6
Final length (mm)	44.2±0.30[a]	42.7±0.20[a]	43.8±0.29[a]	49.2±0.35[b]
Initial mass (g)	0.51±0.15	0.51±0.15	0.51±0.15	0.51±0.15
Final mass (g)	1.20±0.03[a]	1.18±0.01[a]	1.16±0.02[a]	1.45±0.04[b]
Specific growth rate (%.day^{-1} SGR)	0.56±0.02[a]	0.53±0.02[a]	0.56±0.03[a]	0.68±0.03[b]
Molting Frequency (MF, %)	49.6±0.07[a]	46.0±0.08[a]	48.8± 0.05[a]	73.3±0.03[b]
Feed conversion ratio (FCR)	1.12±0.01[a]	1.18±0.02[a]	1.20±0.03[a]	1.28±0.04[a]
Survival rate (SR%)	56.0±8.6[a]	60.0±7.2[a]	64.0±4.5[a]	48.0±4.6[b]
Total Yield (g)	47.2±2.5[a]	37.6±1.38[a]	44.8±4.13[a]	66.7±1.8[b]

*Values (mean ± SD of triplicate values). Means within a row having different letters (a,b) were significantly different among treatments ($p<0.05$).

This study was conducted to determine the optimum level of lipid using soybean oil for the growth and survival of *C. quadricarinatus* juveniles during 90 days are summarized in Table 1.

The study showed that dietary inclusion levels over the 90-days significantly affected growth (Final length, Final mass, SGR, total yield), survival (SR) and molting frequency (MF) of juvenile crayfish. The results showed that the juvenile crayfish fed with the 12% soybean oil diet had higher growth rates than those fed with the other diets with lower oil levels and control group ($p<0.05$). Soybean oil consists of polyunsaturated fatty acids and it is one of the few plant-based sources with significant amounts of oleic and linolenic acids [17]. It is also digested well by aquatic animals [18]. Similar results on the use of lipid on the growth and survival rate of fish were reported. It was reported that higher growth can be achieved with a total lipid level at a dry weight of 2% to 12% in crustaceans [19, 25].

Many factors can be effective in the growth of crayfish such as age, season, stocking density, environmental parameters, nutrient type and nutritional diets [26, 27]. The addition of lipids in diets depends on the permissible levels for aquatic animals including crayfish [28, 29]. Soybean oil is widely used for nutritional supplements of juvenile in the shrimp diet and functional roles of crayfish juvenile [30]. The crayfish feed on a wide variety of feeds such as detritus, algae, macrophytes, invertabrates, fish and fish eggs [1]. It is important to determine the nutritional level of feed in crayfish culture since the low and high levels of nutrient may affect growth negatively [31]. Most of the studies on potential benefits of diets in aquaculture have focused on additions of different nutrients [32, 33, 34]. In recent years, the use of vegetable oils has become very attractive in terms of both price and availability; hence, it can be an alternative to fish oil in aqua feeds [35]. Compared with the fish oil, which is rich in n-3 polyunsaturated fatty acids (n-3 PUFAs), vegetable oils are rich in n-6 polyunsaturated fatty acids (n-6 PUFAs) including soybean oils [36].

In the current study, soybean oil levels over the 90-days significantly improved length, mass, SGR, MF and total yield of juvenile *C. quadricarinatus*. These results are in agreement with several previous studies [37]. SGR was the highest in crayfish fed with 12% soybean oil diet group compared to the control and other groups ($p<0.05$). Similarly, replacement of fish oil by sun flower oil, palm oil, coconut oil and peanut oil showed a significant improvement on growth and survival of *Clarias gariepinus* and *D. puntazzo* [38]. In addition, the better survival and growth were obtained in *C. auratus* fed with coconut oil added feed [39], mud crab (*Scylla serrata)* fed with supplemented corn oil [40] and *S. salar* fed with sunflower oil added feed [41]. However, other studies with Atlantic salmon have shown that addition of fish oil with sunflower oil does not significantly affect the growth [3]. Hence, the present study indicated that the crayfish fed with 12% soybean oil diet exhibited the highest growth rate and molting frequency compared to the diets with lower levels and control groups (Table 1) and it can be beneficial for the freshwater crayfish culture. due to rapid growth. A number of findings have suggested that adding soybean oil in the diets is important for the early stage of crayfish for growth [17, 42, 43]. This study confirms that the growth of juvenile *C. quadricarinatus* increases significantly when the concentrations of soybean oil increase in certain levels. Previous studies have shown that vegetable oils had beneficial effects for many shrimp species [44]. Another researcher mentioned that vegetable oil high in linolenic acid promoted better growth for *P. japanicus* [45]. The results of the present study showed that the diet with soybean oils had no negative effect on the survival and feed intake as reported in other studies [45]. In contrast, the appropriate level of soybean oil in diets provided a higher growth performance than expected for the control diet of crayfish. In the current study, the test diet

with 12% soybean oil positively regulated the FCR (Table 1). However, the difference was found to be statistically insignificant ($p>0.05$). A positive and strong correlation was found between soybean oil addition level and the FCR ($R^2=0.95$) (Fig. 1).

The results the present study showed that the survival rates (SR) of groups fed with diets containing different levels of soybean oil ranged between 48% and 64% (Table 1, Fig. 2). However, it should be noted that the diet with 8% soybean oil gave the relatively higher SR values (64.0%±4.5%) as compared to other diets (Table 1).

Similar findings were reported on the other crayfish and fish species reported by other researchers. Survival rates were during a period of 59–94 days [46] and [47] ranged between 65–85% for *C. destructor* and 60–95% for *C. quadricarinatus*, respectively while it was reported survival rates of 50-71% for experimental diets fed juvenile *C. quadricarinatus* [11]. In the present study, the observations indicated that SGR values of the crayfish were affected by soybean oil concentration levels. SGR was highest (0.68 %.day^{-1}) in the group fed with 12% soybean oil supplemented diet compared to the other groups fed with lower soybean oil levels (Table 1). The SGR values obtained in our study were similar to or higher than those reported by Jones et al. (1996) [46] in *C. destructor.*

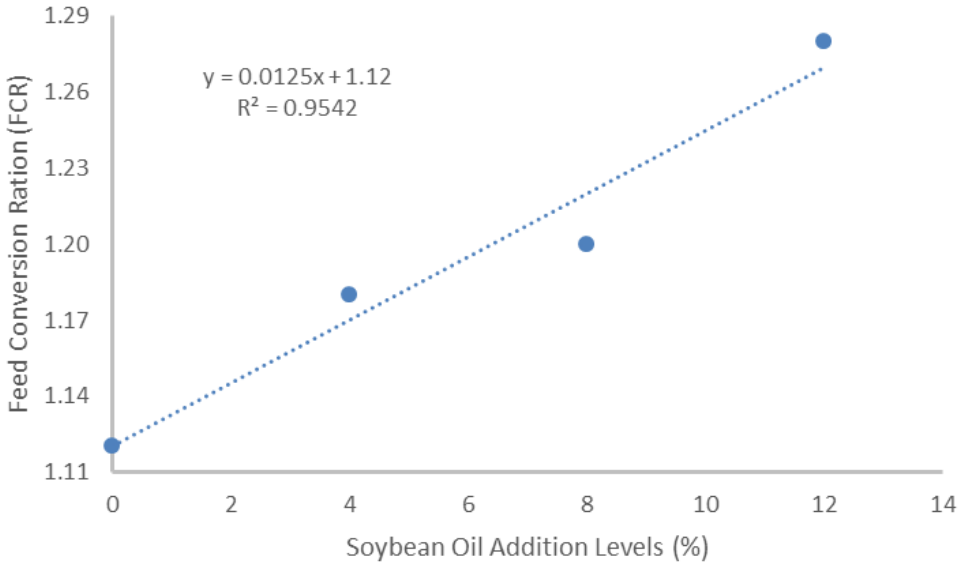

FIGURE 1
Relationship between soybean oil edition levels and FCR of juvenile crayfish fed with diets containing different levels of soybean oil (0, 4, 8, 12%).

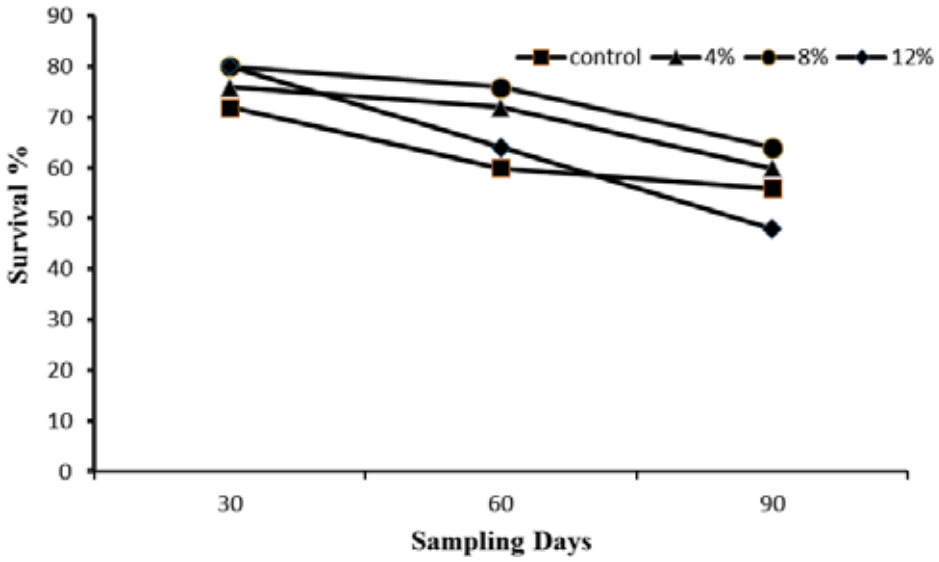

FIGURE 2
Survival (%) of C. *quadricarinatus* fed with different levels of soybean oil for 90 days.

Molting in crustaceans is under the control of many different factors such as temperature, calcium level and hormones [48, 49]. In the current study, the crayfish fed with the diet supplemented with 12% soybean oil molted more frequently than the other groups (73.3%) (Table 1). It is a well-known fact that fast growing and frequent molting crustacean are more vulnerable to cannibalism and predation [50]. In the present study, it was observed a similar trend such that the 12% soybean oil diet group with higher mass gain (1.45 g) and higher molting frequency (73.3%) had lowest survival rate (48%) (Table 1) (Fig. 3).

This study concentrated on the effect of soybean oil on the growth and survival of crayfish juveniles with a 90-day experiment. However, more test should be performed for adults of different sizes to support this result since size can change the effect of soybean oil addition [51]. Also, a longer experiment than 90-days could be more beneficial to understand the long-term effect of soybean oil addition in diets.

In the current study, the relationship between total length and MF and total mass and MF was also studied. It was observed that the MF increased with higher total length and total mass with increased soybean oil levels. Also, high correlations were found between the total length and MF (R^2=0.99) and between the total mass and MF (R^2=0.98) (Fig. 4 and Fig. 5).

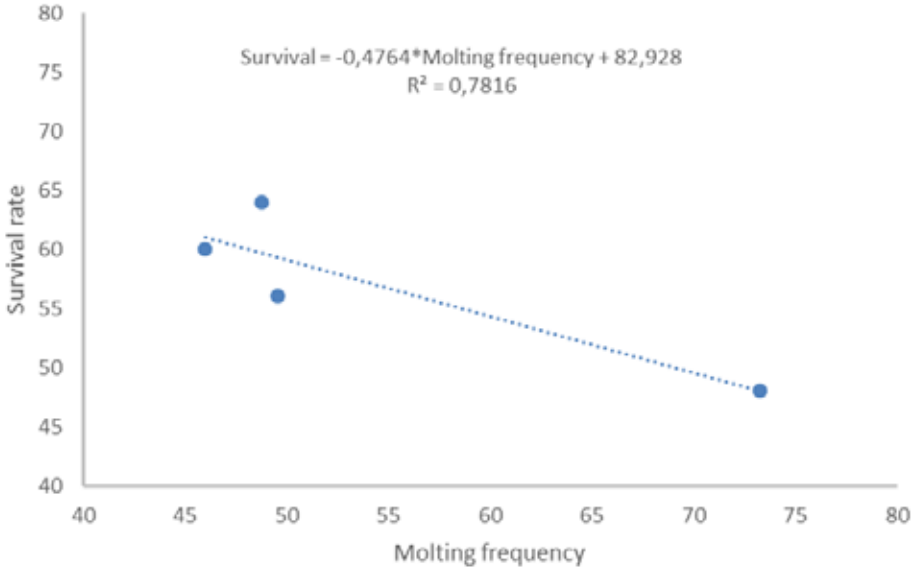

FIGURE 3
Relationship between molting frequency and survival rate of juvenile crayfish fed with diets containing different levels of soybean oil (0, 4, 8, 12%).

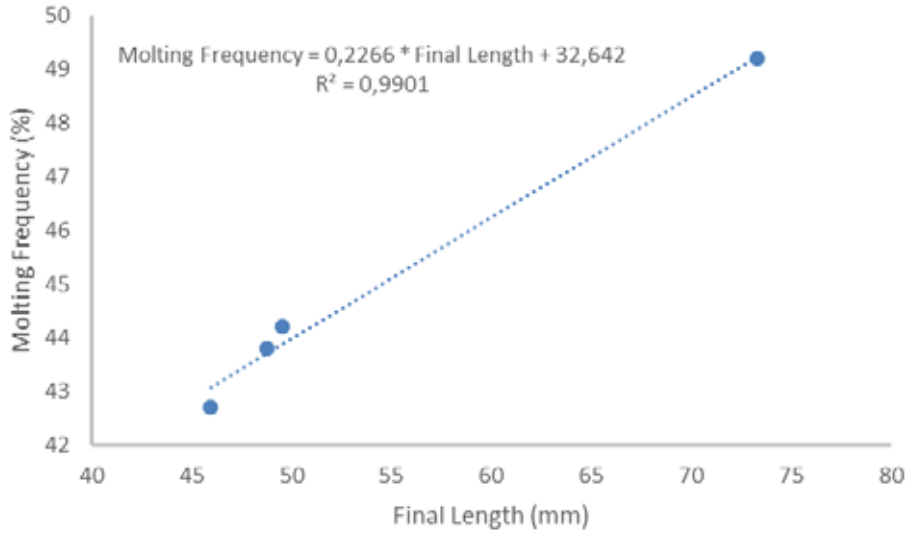

FIGURE 4
Relationship between final length and molting frequency of juvenile crayfish fed with diets containing different levels of soybean oil (0, 4, 8, 12%).

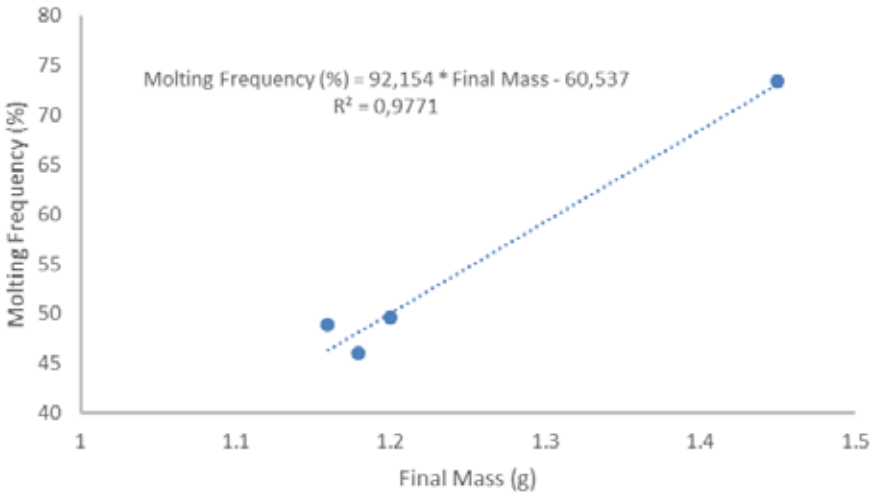

FIGURE 5
Relationship between final mass and molting frequency of juvenile crayfish fed with diets containing different levels of soybean oil (0, 4, 8, 12%).

CONCLUSIONS

In conclusion, this study has shown that the level of soybean oil into the diet have an effect on improving the growth, survival, and molting of red claw crayfish *C. quadricarinatus*. Based on the results, it is recommended to add 8-12% soybean oil in the diet for optimum growth and survival of crayfish.

ACKNOWLEDGEMENTS

The authors would like to thank the Marine Science and Technology Faculty staff for their assistance during the study. Also, they thank Dr. Muharrem Keskin from Mustafa Kemal University for his critical reading of the manuscript.

REFERENCES

[1] Saoud, I.P., Ghanawi, J., Thompson, K.R. and Webster, C.D. (2013) A review of the culture and diseases of redclaw crayfish *Cherax quadricarinatus* (von Martens 1868). Journal of the World Aquaculture Society. 44(1), 1–29.

[2] Naranjo, J. and Villareal, H. (2002) Effects of aeration levels on the growth, survival and biomass of *Cherax quadricarinatus* (redclaw) juveniles reared in ponds. Book of Abstracts of the Conference Aquaculture (s. 230). San Diego, CA: World Aquaculture Society.

[3] Naranjo-Páramo, J., Hernandez-Llamas, A. and Villarreal, H. (2004) Effect of stocking density on growth, survival and yield of juvenile redclaw crayfish *C. quadricarinatus* (Decapoda: Parastacidae) in gravel-lined commercial nursery ponds. Aquaculture. 242(4), 197-206.

[4] Wingfield, M. (2000) An overview of the Australian freshwater crayfish farming industry. In: Whisson and Wingfield, M. (eds) The Australian crayfish Aquaculture Workshop. International Association of Astacology, Perth, Western Australia. 5-13

[5] Souty-Grosset, C., Holdich, D.M., Noel, P.Y., Reynolds, J.D. and Haffner, P. (2006) Atlas of Crayfish in Europe. Muséum national d'Histoire naturelle. Paris: Patrimoines naturels.

[6] Ahyong, S.T. and Yeo, D.C. (2007) Feral populations of the Australian Red-Claw Crayfish (*Cherax quadricarinatus* von Martens) in water supply catchments of Singapore. Biological Invasions. 9(8) 943-946.

[7] Lodge, D.M., Deines, A., Gherardi, F., Yeo, D.C., Arcella, T., Baldridge, A.K. and Zeng, Y. (2012) Global Introductions of Crayfishes: Evaluating the Impact of Species Invasions on Ecosystem Services. Annual Review of Ecology, Evolution, and Systematics. 43, 449-472.

[8] Kouba, A., Buric, M. and Petrusek, A. (2015). Crayfish Species in Europe. In: Kozak, P., Zdenek, D., Petrusek, A., Buric, M., Horka, I., Kouba, A., Policar, T. (eds.) Crayfi Fissh. Biology and Culture. Czech Republic.: University of South Bohemia in Ceske Budejovice, Faculty of Fisheries and Protection of Waters. 79-163.

[9] Nunes, A.L., Zengeya, T.A., Hoffman, A.C., Measey, G.J. and Weyl, O.F. (2017). Distribution and establishment of the alien Australian redclaw crayfish, *Cherax quadricarinatus*, in South Africa and Swaziland. Peer J. 5, e3135, 1-21.

[10] Lawrence, C. and Jones, C. (2002) Cherax. In: Holdrich D. (ed.) Biology of Freshwater Crayϕsh. B. Malden, MA, USA: Blackwell Science. 635-669.
[11] Webster, C.D., Goodgame-Tiu, L.S., Tidwell, J.H. and Rouse, D.B. (1994) Evaluation of practical feed formulations with different protein levels for juvenile red claw crayfish, *Cherax quadricarinatus*. Transactions of the Kentucky Academy of Science. 55, 108-112.
[12] Webster, C.D., Thompson Muzinic, K.L., Yancey, D.H., Dasgupta, S., Xiong, Y.L., Rouse, D.B. and Manomaitis, L. (2004) A preliminary assessment of growth, survival, yield, and economic return of Australian red claw crayfish, *Cherax quadricarinatus*, stoc. Journal of Applied Aquaculture. 15(4), 37-50.
[13] Curtis, M.C., Jones, C.M. (1995) Observation of mono sex culture of redclaw crayfish *Cherax quadricarinatus* von Martens (Decapoda: Parastacidae) in earthen ponds. Journal of World Aquaculture Society. 26(2), 154–159.
[14] Nyström, P. (2002) Ecology. In: Holdich, D.M. (ed.) Biology of freshwater crayfish. London, UK: Blackwell.
[15] Lagrue, C., Podgorniak, T., Lecerf, A., and Bollach, L. (2014) An invasive species may be better than none: invasive signal and native noble crayfish have similar community effects. Freshwater Biology. 59, 1982-1995.
[16] Ercoli, F., Ruokonen, T.J., Koistinen, S., Jones, R.I. and Hamalainen, H. (2015) The introduced signal crayfish and native noble crayfish have different effects on sublittoral macroinvertebrate assemblages in boreal lakes. Freshwater Biology. 60, 1-11.
[17] Noordin, N.M., Zeng, C., Southgate, P.C. and Romano, N. (2015) Effects of Dietary Fish Oil to Soybean Oil Ratio on Survival, Development, and Growth of Early Juveniles of the Blue Swimmer Crab *Portunus pelagicus*. Journal of Shellfish Research. 34(3), 1065-1072.
[18] Turchini, G.M., Ng, W.K., Tocher, D.R. (2010) Fish oil replacement and alternative lipid sources in aquaculture feeds. Boca Raton, FL: CRC Press. 1-551.
[19] Zhang, S.P., Li, J.F., Wu, X.C., Zhong, W.J., Xian, J.A., Liao, S.A. and Wang, A.L. (2013). Effects of different dietary lipid level on the growth, survival and immune-relating genes expression in Pacific white shrimp, *Litopenaeus vannamei*. Fish and Shellfish Immunol. 34(5), 1131-1138.
[20] Toledo, T.M., Silva, B.C., Vieira, F.N., Mourino, J. and Seiffert, W.Q. (2016) Effects different dietary lipid levels and fatty acids profile in the culture of white shrimp *Litopenaeus vannamei* (Boone) in biofloc technology: water quality, biofloc composition, growth and health. Aquaculture Research. 47(6), 1841-1851.
[21] Mohanta, K.N., Mohanty, S.N., Jena, J.K. and Sahu, N.P. (2008) Protein requirement of silver barb, Puntius gonionotus fingerlings. Aquaculture Nutrition. 14, 143–152.
[22] D'Abramo, L. and New, M. (2000) Nutrition, feeds and feeding. M. B. New, and W. C. Valenti Freshwater Prawn Culture. The farming of *Macrobrachium rosenbergii*. Oxford, UK Blackwell Science Ltd. 203-220.
[23] Berntssen, M.G., Lundebye, A.K. and Torstensen, B.E. (2005) Reducing the levels of dioxins and dioxin like PCB's in farmed Atlantic salmon by substitution of fish oil with vegetable oil in the feed. Aquaculture Nutrition. 11(3), 219-231.
[24] Mazlum, Y., Guner, Ö.G. and Sirin, S. (2017) Effect of different substrates on survival and growth of juveniles of the freshwater narrow-clawed crayfish *Astacus leptodactylus* Eschscholtz, 1823 (Decapoda, Astacidae). Crustaceana. 90(12), 1289-1302.
[25] Bowyer, J.N., Qin, J.G., and Stone, D.A. (2013) Protein, lipid and energy requirements of cultured marine fish in cold: temperate and warm water. Reviews in Aquaculture. 5(1) 10–32.
[26] Jones, C.M. and Ruscoe, I. (2000) Assessment of stocking size and density in the production of redclaw crayfish *Cherax quadricarinatus* (von Martens) (Decapoda: Parastacidae), cultured under earthen pond conditions. Aquaculture. 189(2), 63 – 71.
[27] Sirin, S. and Mazlum, Y. (2017) Effect of dietary supplementation of calcium chloride on growth, survival, moulting frequency and body composition of narrow-clawed crayfish, *Astacus leptodactylus* (Eschscholtz, 1823). Aquaculture Nutrition. 23, 805-813.
[28] Carmona-Osalde, C., Rodrigez-Serna, M., and Olvera-Nova, M.A. (2005) Effect of the protein-lipids ratio on growth and maturation of the crayfish. Aquaculture. 250(4), 692–699.
[29] Zhao, J., Wen, X., Zhu, D. and Li, Y. (2015) Effects of dietary lipid levels on growth, feed utilization, body composition and antioxidants of juvenile mud crab *Scylla paramamosain* (Estampador). Aquaculture. 435, 200–206.

[30] Hernandez-Vergara, M.P., Rouse, D.B., Olvera-Novoa, M.A. and Davis, D.A. (2003) Effects of dietary lipid level and source on growth and proximate composition of juvenile redclaw (*Cherax quadricarinatus)* reared under semi-intensive culture conditions. Aquaculture. 223(4), 107-115.

[31] Nakagawa, T., Hu, H., Zharikov, S. and Tuttle, R.A. (2006) A causal role for uric acid in fructose-induced metabolic syndrome. American Journal of Physiology. 290, 625–631.

[32] Dimitroglou, A., Merrifield, D.L., Moate, R., Davies, S.J., Spring, P., Sweetman, J., and Bradley, G. (2009) Dietary mannan oligosaccharides supplementation modulates 317 intestinal microbial ecology and improves morphology of rainbow trout, *Oncorhynchus mykiss* (Walbaum). Journal of Animal Science. 87(10), 3226-3234.

[33] Dimitroglou, A., Merrifield, D.L., Carnevali, O., Picchietti, S., Avella, M., Daniels, C., Davies, S.J. (2011a) Microbial manipulations to improve fish health and production: a Mediterranean perspective. Fish and Shellfish Immunology. 30, 1–16.

[34] Dimitroglou, A., Reynolds, P., Ravnoy, B., Johnsen, F., Sweetman, J. W., Johansen, J., and Davies, S.J. (2011b) The Effect of Mannan Oligosaccharide Supplementation on Atlantic Salmon Smolts (*Salmo salar* L.) Fed Diets with High Levels of Plant Proteins. Journal of Aquaculture Research and Development. 1, 2-6.

[35] Mozanzadeh, M.T., Agh, N., Yavari, V., Marammazi, J.G., Mohammadian, T. and Gisbert, E. (2016) Partial or total replacement of dietary fish oil with alternative lipid sources in silvery-black porgy (*Sparidentex hasta*). Aquaculture. 451, 232–240.

[36] Caballero, M., Obach, A., Rosenlund, G., Montero, D., Gisvold, M. and Izquierdo, M. (2002) Impact of different dietary lipid sources on growth, lipid digestibility, tissue fatty acid composition and histology of rainbow trout, *Oncorhynchus mykiss*. Aquaculture. 214(4), 253-271.

[37] Bhavan, P.S., Jeyanthi, S. and Rebecca, A.A. (2011) Growth performance of the freshwater prawn Macrobrachium rosenbergii post larvae fed with *Ocimum sanctum* (Tulsi) and *Withania somnifera* (Ashwagandha) incorporated feeds. International Journal of Biological Research. 1(1), 34-53.

[38] Turchini, G.M., Francis, D.S., Senadheera, S. P., Thanuthong, T. and De Silva, S.S. (2011) Fish oil replacement with different vegetable oils in Murray cod: evidence of an ‘‘omega-3 sparing effect’’ by other dietary fatty acids. Aquaculture. 315(4), 250–259.

[39] Parameshwaran, K., Edirisinghe, U. and Dematawewa, C. (2002) Replacement of cod liver oil with soybean or coconut oil in diets of larval goldfish, *Carassius auratus* L. Tropical Agricultural Research and Extention. 5(2), 62-67.

[40] Holme, M., Southgate, P.C. and Zeng, C. (2007) Survival, development and growth of mud crab, Scylla serrata, megalopae fed semi-purified diets containing various fish oil: corn ratios. Aquaculture. 269(4), 427-435.

[41] Miller, M.R., Nichols, P.D. and Carter, C.G. (2007) Replacement of fish oil with thraustochytrid Schizochytrium sp. L. oil in Atlantic Salmon parr (*Salmo salar* L) diets. Comparative Biochemistry and Physiology - Part A. 148(2), 382–392.

[42] Coccia, E., Santagata, G., Malinconico, M., Grazia-Volpe, M., Distasio, M. and Paolucci, M. (2010) Juvenile crayfish *Cherax albidus* fed polysaccharide-based pellets: Rheological behavior and effect on growth. Freshwater Crayfish. 17, 13-18.

[43] Kim, Y.C., Romano, N., Lee, K.S., Teoh, C.Y. and Ng, W.K. (2012) Effects of replacing dietary fish oil and squid liver oil with vegetable ils on the growth, tissue fatty acid profile and total carotenoids of the giant freshwater prawn, *Macrobrachium rosenbergii*. Aquaculture. 44(11), 1-10.

[44] Gonzalez-Felix, M.L., and Perez-Velazquez, M. (2002) Current status of lipid nutrition of Pacific white shrimp, *Litopenaeus vannamei*. Avances en Nutricion Acuicola VI. Memorias del VI Simposium Internacional de Nutricion Acuicola.Cancun, Quintana Roo, México. 35-45.

[45] Alvarado, J.L. (2013) The Effect of Dietary Soybean Lecithin on Growth, Survival and Body Amino Acid Composition of Japanese Flounder (*Paralichthys Olivaceus*) Larvae. International Journal of Science and Research. 4(9), 1706-1709.

[46] Jones, P.L., De Silva, S.S. and Mitchell, D.B. (1996) The effect of dietary protein source on growth and carcass composition in juvenile Australian freshwater crayfish. Aquaculture International. 4(4), 361–367.

[47] Ponce-Palafox, J.T., Arredondo-Figueroa, J.L. and Moreno-Rodriguez, M.A. (1998) The effects of varying dietary protein levels on growth and survival of juvenile and pre-adult redclaw (*Cherax quadricarinatus*). In. Klein, J. V and Schram, F. R. (eds). The Biodiversity Crisis and Crustacea - Proceedings of the Fourth International Crustacean Congress. A.A.Balkema. Amsterdam, Netherlands: 715–719.

[48] Hammond, K.S., Hollows, J.W., Townsend, C.R. and Lokman, P.M. (2006) Effects of temperature and water calcium concentration on growth, survival and molting of freshwater crayfish, Paranephrops zealandicus. Aquaculture. 251, 271–279.
[49] Wilder, M.N., Houng, D.T., Jasmani, S., Jayasank, V., Kaneko, T., Aida, K., Wigginton, A. (2009) Hemolymph osmolality, ion concentrations and calciumin the structural organization of the cuticle of the giant freshwater prawn *Macrobracium rosembergii* changes with molt cycle. Aquaculture. 292, 104-110.
[50] Lutz, C.G. (1983) Population dynamics of red swamp crawfish (Procambarus clarkii) and white river crawfish (P*rocambarus acutus acutus)* in two commercial ponds. MSc Thesis. Louisiana State University, Batton Rouge, LA, USA.
[51] Kangpanich, C., Pratoomyot, J. and Senanan, W. (2017) Effects of alternative oil sources in feed on growth and fatty acidcomposition of juvenile giant river prawn (*Macrobrachium rosenbergii)*. Agriculture and Natural Resources. 51(2), 103-108.

Received: **20.11.2018**
Accepted: **20.02.2019**

CORRESPONDING AUTHOR

Yavuz Mazlum
Iskenderun Technical University,
Faculty of Marine Sciences and Technology,
31200, Iskenderun, Hatay – Turkey

e-mail: yavuz.mazlum@iste.edu.tr

© by PSP Volume 28 – No. 4/2019 pages 2688-2696 Fresenius Environmental Bulletin

ENDOPHYTIC FUNGI FROM *CARALLUMA ACUTANGULA* CAN SECRETE PLANT GROWTH PROMOTING ENZYMES

Sajid Ali[1,2], Sumera Afzal Khan[1], Muhammad Hamayun[3], Amjad Iqbal[4,*], Abdul Latif Khan[2], Anwar Hussain[3], Mohib Shah[3]

[1]Center of Biotechnology and Microbiology, University of Peshawar, Pakistan
[2]UoN Chair of Oman's Medicinal Plants & Marine Natural Products, University of Nizwa, Nizwa, Oman
[3]Department of Botany, Abdul Wali Khan University Mardan, Pakistan
[4]Department of Agriculture, Abdul Wali Khan University Mardan, Pakistan

ABSTRACT

Fungal endophytes can establish beneficial relationship with the host plants. The endophytes help in the growth of host plants under stress conditions by secreting various bioactive compounds. To discover potent endophytes, we have isolated some of the fungi from medicinally important plant *Caralluma acutangula*. The isolated endophytes were assessed for extra-cellular enzymes [1-aminocyclopropane-1-carboxylate (ACC) deaminase, cellulases, phosphatases and glucosidases)] and IAA production. The potent endophytes have been identified as *Paecilomyces variotii, Penicillium purpurogenum* and *Epicoccum nigrum* on the basis of internal transcribed spacer (ITS) region homology. The endophytic strains *P. variotii* and *E. nigrum* have produced IAA, phosphatases and glucosidases in significantly higher amounts. Whereas, a higher activity of ACC deaminase (300 nmol α- ketobutyrate mg^{-1} h^{-1}) have been noticed in *P. purpurogenum* and *P. variotii.* The production of IAA, ACC deaminase, celluloses, phosphatases and glucosidases by the isolated endophytes concludes that they can support the host plants under stress conditions.

KEYWORDS:
Caralluma acutangular, extra-cellular enzymes, indole acetic acid, ACC deaminase, fungal endophytes

INTRODUCTION

Over the last three decades, the multifaceted interaction of endophytes has been widely studied as a prolific source of novel bioactive natural products [1-3]. The endophytic microbial flora (fungi/bacteria) encodes for enzymes which offer more stability as compare to other sources. These enzymes can be used in food, medicine, beverages, sweets, textiles, and leather industries to process raw materials [4, 5]. Endophytic fungi favors the resistance, growth and development of their host plant by colonizing the host plant tissues and secreting potential bioactive secondary metabolites [1, 6-8]. Similarly, a variety of substances and enzymes have been identified from these endophytes [9, 10]. Extracellular enzymes can be produced by some endophytic fungi that can be useful in biocontrol programs [11]. The enzymes, such as glucosidases and cellulases from different endophytic microbial flora have been isolated. Production of such enzymes can help the microbes to establish a symptomless symbiotic association with host plants.

The host plant growth and development can be regulated by the production of extra-cellular enzymes and bioactive secondary metabolites, such as phytohormones [6, 12]. Recently, a variety of endophytes (bacteria or fungi) have been documented for the production of plant hormone, indole 3-acetic acid (IAA) [13, 14]. IAA plays a fundamental role in plant growth, development, and overcoming harsh environmental stimuli. The fungal endophytes, *Acremonium coenophialum* and *Phoma glomerata* have been studied intensively that encodes for IAA biosynthesis [15]. Besides IAA, 1-aminocyclopropane-1-carboxylate (ACC) deaminase has also been regarded as important enzyme with the ability to hydrolyze ACC, which is the immediate precursor of ethylene in plants [16]. The reduction of stress ethylene levels by ACC deaminase is considered as one of the major mechanisms employed by the endophytes to facilitate plant growth. ACC deaminase that converts ACC into α-ketobutyrate and ammonia has been found in various bacteria, yeasts, and fungi [17].

Utilization of growth promoting endophytes isolated from various plants as a source of industrially relevant enzymes has been argued and considered over the years. Therefore, exploration of potential plant species around the globe is needed to discover the valuable microbial cell factories. The Arabian Peninsula being the largest peninsula in the world is having relatively high plant diversity [18]. Most of the plant species have been ignored to be investigated for the presence of economically important endophytes, including *Caralluma acutangula*. The medicinally valuable *C. acutangula* belongs to *Asclepiadaceae*, which comprised of about 150 species that are widely distributed from Asia to Africa. The extracts of *Caralluma* are used in

traditional medicine due to the presence of bioactive compounds, especially glycosides of the pregnane group. The glycosides from *Caralluma* species have been reported to possess various biological activities, such as inflammation, rheumatism, anti-diabetic, anti-leprosy, antipyretic, and anti-helminthetic activities [19]. Looking at these perspective and lack of previous knowledge about the presence of endophytes in *C. acutangula*, the current study was planned to characterize endophytes from the species. The potential of identified stains was further evaluated for their ability to produce IAA, ACC deaminase and extra cellular enzymes.

MATERIALS AND METHODS

Plant collection and endophyte isolation. Twenty healthy plants collected from Jabal Al-Akhdar (23° 04' 22.00 N"; 57° 40' 07.00 E") in the Sultanate of Oman was selected to isolate endophytic fungi. The samples were brought to the laboratory in sterilized zip bags. The stem, root and leaf of the plants were separated and treated with 2.5% sodium hypochlorite (NaOCl) to remove epiphytic microorganisms and ecto-mycorrhizae. After surface sterilization, the plant parts were washed thrice with autoclaved distilled water (DDW) to remove any traces of NaOCl [6, 14]. To isolate endophytic fungi the samples were chopped into 0.5 cm with a sterilized cutter and placed on Hagem media (pH 5.6±0.2) containing streptomycin (80 ppm). Fully-grown pure cultures of fungal isolates were inoculated on PDA medium slants for long-term storage.

Screening and identification of fungal endophytes. Fungal isolates were inoculated on Czapek broth medium (pH 7.3±0.2) for the production of secondary metabolites. The composition of the Czapek medium was: 1% glucose, 0.05% $MgSO_4.7H_2O$, 1% peptone, and 0.001% $FeSO_4.7H_2O$, and 0.05% KCl. The pure cultures were grown in a shaking incubator at 30°C with 120 rpm for 7 days. Sophisticated molecular techniques were employed for the precise identification of fungal isolates. The genomic DNA was isolated using the CTAB method as described by Khan et al. [6] and Ali et al. [9]. Afterwards, the gDNA was amplified by polymerase chain reaction (PCR) using Internal Transcribed Spacer (ITS) regions and sequenced [4, 10]. The ITS1–4 region was amplified using the universal primers, i.e. ITS-1F (5´- TCC GTA GGT GAA CCT GCG G-3´) and ITS-4R (5´-TCC TCC GCT TAT TGA TAT GC-3´). In thermal cycler the PCR was performed by using the following steps of amplification: pre-heating at 96 °C for 5 min, followed by 35 cycles of 30 s at 94 °C, 30 sec at 55 °C, 1 min at 72 °C, and a final extension at 72 °C for 3 minutes. Gel electrophoresis was used for the confirmation of amplified PCR products by using 0.8% agarose. The PCR products were purified using PCR purification kits and sequenced. The raw sequences were aligned using MEGA 6.0 [20], edited manually and BLASTn searched for their homologues sequences using NCBI database (http://www.ncbi.nih.gov/index. html). From NCBI, the homologous fungal ITS sequences were retrieved and phylogenetic tree was constructed using the neighbor-joining, maximum parsimony and maximum composite likelihood methods whilst keeping the bootstrap values of 1,000 replicates [20].

ACC deaminase activity and quantification of total protein content. The methodology of Østergaard and Olsen [21] was applied for ACC deaminase activity with some modifications adopted from Shaharoona et al. [22]. In this method, the number of µmol of α-ketobutyrate produced was determined by comparing the absorbance at 540 nm of a sample to a standard curve of α-ketobutyrate ranging between 10 and 200µmol.

The selected endophytes were cultured in Tryptic Soy Broth (TSB) and incubated for four days at 28°C. The cells were harvested by centrifugation at 16,000 rpm for 5 min, washed twice with 0.1 M Tris-HCl (pH 7.5) and incubated for another four days at 28°C in Dowkin and Foster minimal medium (having 5 mM ACC as a nitrogen source). The fungal cells were then centrifuged at 16000 g for 5 min and re-suspended in 5 mL of 0.1 M Tris-HCl (pH 7.6) after discarding the supernatant [21, 22]. The tubes were centrifuged (16,000 rpm for 5 minutes) again and the supernatant was rejected. Tris HCl (2 mL, 0.1 M and pH 8.5) was added to the palette and the suspension was toluenized with 30 µL of toluene and the mixture was vortexed for 30 sec. The toluenized cell suspension (200 µL) was transferred to a new 2-mL microfuge tube and added 20µl (0.5 M) of ACC, vortexed and incubated (30 °C for 15 min). After the incubation, 1 mL of HCl (0.56 M) was added to the mixture, vortexed and centrifuged (16,000 rpm for 5 min). A 1 mL of the supernatant was transferred to a glass test tube and thoroughly mixed with a 2 mL of 2,4-dinitrophenylhydrazine reagent (0.2% 2,4-dinitrophenylhydrazine in 2 M HCl). The mixture in the glass tube was incubated at 30°C for 30 min. Finally, 2 mL NaOH (2 M) was added to the tube and the absorbance of the mixture was measured at 540 nm using SHIMADZU spectrophotometer (Kyoto, Japan) [14, 22].

One of the simple and reliable methods for protein assay is Bradford assay, which is based on an absorbance shift of the Coomassie Brilliant Blue G-250 dye [23]. The dye under acidic conditions has a red colour that converts to blue on binding to the protein being assayed.

A 50 µl aliquot of the toluenized fungal cell suspension was diluted with 350 µl of 0.1 M Tris-HCl (pH 8.0), and boiled with 400 µl of 0.1 N NaOH for 10 min. After the cell sample was cooled to room

temperature, 400 µl of Bradford's reagent were added and the absorbance was measured at 595 nm using the spectrophotometer. Bovine serum albumin (BSA) was used as a standard.

Extracellular enzyme and indole acetic acid quantification of endophytic fungi. The method of Marx et al. [24] was applied for the quantification of extracellular enzymes with some modifications. β-1,4-glucosidase, 4-MUB-β-D-glucopyranoside, 1,4-β-cellobiosidase, 4-MUB-β-D-cellobioside, phosphatase and 4-MUB-phosphate were used for the assay.

Endophytic fungi were collected from Czapek broth cultures by using centrifugation (12,000 rpm / 10 min at 4°C). Turbidity traces were removed from the samples by syringed filtration (0.22 µm) of culture filtrates (CF). For enzyme analysis, substrate and quenched standard were maintained along with substrate control. A minimum of three replicates for each substrate (CF + buffer + substrate), quenched standard (sample + buffer + 4-MUB), and substrate control (media + buffer + substrate) were carried out. Fluorescence spectrophotometer (Shimadzo, Tokyo, Japan) was used to read out the rate of absorbance. The absorbance (360 nm excitation and 460 nm emission) was read at various time intervals, i.e. 0, 30, 60, 90 and 120 min.

$$Activity\ (\mu mol\ h^{-1}\ L^{-1}) = \frac{MSF - MSF1}{\left(\frac{MStF}{0.5\ mol}\right) \times \left(\frac{MQCF}{MSF}\right) \times (0.2\ mL) \times (time\ in\ h)}$$

Where,
MSF = mean sample fluorescence; MSF1 = mean sample initial fluorescence; MStF = mean standard fluorescence; MQCF = mean quenching control fluorescence

IAA was estimated by using a colorimetric-assay as described by Khan et al. [14]. The screened fungi were grown-up in Czapek broth (20 mL) without (0 g/L) and with (0.1 g/L) L-tryptophan and incubated at 30±2 °C in shaking incubator at 200 rpm for one week. The cultured fungi were centrifuged (10,000×g) for 10 minutes at four degrees centigrade. After centrifugation, the cell free cultures were filtered through a 0.45µm cellulose acetate filter (DISMIC®, Denmark). The culture filtrates were acidified with 1N HCl to pH 2.8 and extracted three times with 20mL ethyl acetate. The ethyl acetate fractions were combined and evaporated under vacuum at 45 °C in a rotary evaporator. The filtrate was resuspended in 3 mL 50% methanol. Finally, 1 ml of methanol added filtrate was mixed with 2 mL of Salkowski reagent (12 g $FeCl_3$/L of 7.9 M H_2SO_4) and incubated in the dark for 40 minutes at room temperature. The change in color was read at 535 nm using an ELISA spectrophotometer (BioRad, USA). Standard of pure IAA (Sigma-Aldrich, Korea, Ltd) was prepared separately for the calculation of the IAA amount in the samples.

Statistical Analysis. Each sample was analyzed in triplicate and all the experiment performed was repeated three times. The data presented as a mean ± standard error of the mean (SEM). Mean-values were compared by LSD at P=0.05 (SPSS-20).

RESULTS

Various parameters have been employed to differentiate the isolated endophytes, including colour of aerial hyphae, surface texture, colony, base color, shape, height, growth rate, and pattern. The overall morphological analysis suggested the isolation of six strains. The endophytic fungi were further identified using gDNA extraction, PCR amplification, ITS rRNA region sequencing, and bioinformatics tools (BLASTn search).

Molecular identification and phylogenetic analysis of endophytes. The internal transcribed spacer (ITS) sequences from six endophytic fungi with fragment lengths of rRNA gene regions ranged from 520 to 750 bp have been sequenced and aligned. MEGA 6.0 software was used for the sequence alignment, then BLASTn searched the sequence to find out homology with known fungal strains in NCBI. The correlation of the fungal sequences demonstrated a 96–100% homology with BLASTn hits of fungi (Table 1). Based on sequence similarity and phylogenetic analysis, we identified the fungal strains as *Aspergillus nidulans, Paecilomyces variotii, Epicoccum nigrum, Fusarium proliferatum, Penicillium purpurogenum,* and *Alternaria* sp. (Table 1). The sequences of related species have been deposited in the GenBank, NCBI for accession numbers (Table 1).

Phylogenetic history has been inferred using the neighbor-joining, maximum composite likelihood and maximum parsimony methods. The tree with the sum of branch length 7.97 is shown in Figure 1. The tree is drawn to scale, with branch lengths similar to the evolutionary distances used to infer the phylogenetic tree. The evolutionary distances have been computed using the maximum composite likelihood method and are in the units of the number of base substitutions per site. A total of 59 nucleotide sequences has found to be involved in the analysis (Figure 1). Gaps and missing data have been eliminated from all points to get the final data set with 94 positions. The evolutionary analyses have been carried out by using MEGA 6.0.

TABLE 1
Sequence similarities of isolated endophytic fungal strains from *Boswellia sacra* and *Caralluma acutangula*

ID	Name	Genebank Accessions	Length bp	Identities		
				Match	Total	(%)
LF1	*Aspergillus nidulans*	KY921609	524	521	544	98%
SF2	*Paecilomyces variotii*	KY921608	620	606	680	98%
LF3	*Fusarium proliferatum*	KY921610	554	543	568	97%
SF3	*Epicoccum nigrum*	KY921611	705	703	717	98%
SF5	*Penicillium purpurogenum*	KY921612	567	581	609	100%
RF-6B	*Alternaria* sp.	KY921613	724	648	701	99%

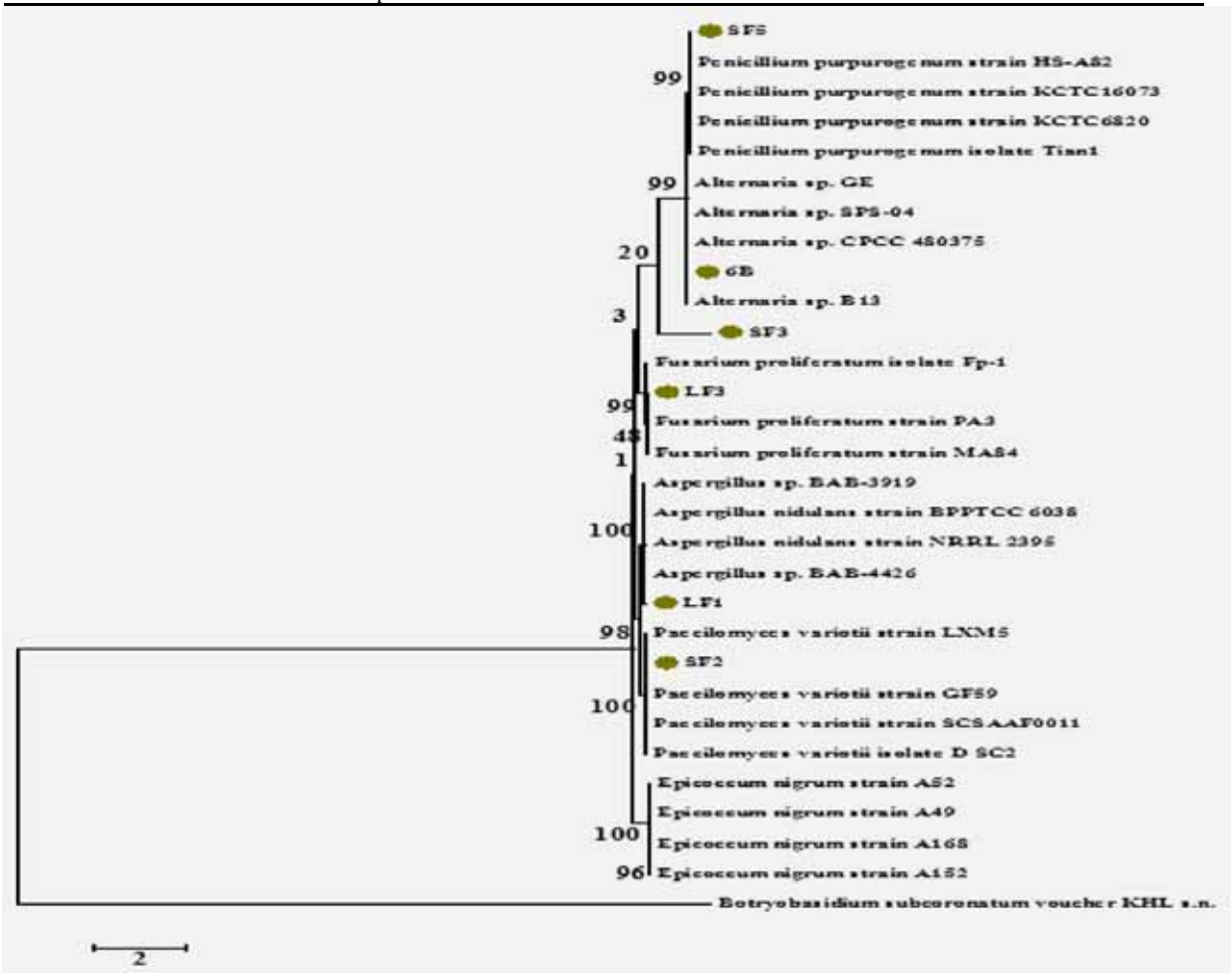

FIGURE 1
The evolutionary relationships of taxa of endophytic fungal strains isolated from *Caralluma acutangula.*
A neighbour joining tree was constructed of homologous ITS sequences using MEGA 6.0 with 1K bootstrap replication. *Botrybasidium subcoronatum* was used as an out group.

Total protein content and ACC deaminase activity of the endophytes. The results of *P. variotii* and *P. purpurogenum* showed higher amounts of total protein in the culture media, followed by *E. nigrum*. The *Alternaria* sp. and *F. proliferatum* endophytic fungal strains showed the least amount of proteins (Figure 2). Among the isolated endophytes, the strain *P. purpurogenum* exhibited higher ACC deaminase activity that produced 355-nmol of α- ketobutyrate mg^{-1} h^{-1}.

Extracellular enzymes and IAA production by endophytic fungi. Extracellular enzymes are encoded by endophytic fungi in axenic conditions. To evaluate this capability of the fungi, all strains have been grown in liquid medium for 14 days and centrifuged to achieve a pure culture. Fluorescence-based MUB standards have been used to analyze the presence of the enzymes β-1,4-glucosidase, 1,4-β-cellobiosidase and phosphatase. A standard curve reading computed the fluorogenic substrate absorbance (excitation and emission) in the presence of the buffer and in combination with the MUB standard. The curve fitting values for cellulases (R^2=0.98; y = 6.35), phosphatases (R^2=0.96; y = 113.04), and glucosidases (R^2=0.98; y = 36.4) have been recorded using the fluorescence spectrophotometer. Variation in concentrations of cellulases, phosphatases, and

glucosidases has been noted among the culture filtrates of different isolated fungal strains (Figure 4, 5 & 6). The pre-optimized fluorescence spectrophotometer (Shimadzo, Tokyo) was used to read the absorbance with 360 nm excitation and 460 nm emission at time zero and 30-minute intervals for 2 hours.

The endophytic fungi from *C. acutangula* generally secreted higher amounts of phosphatase and cellulase enzymes. Among the isolated fungal strains, *P. variotii* and *P. purpurogenum* produced higher quantities of cellulase and phosphatase (Figure 4 & 5). On the contrary, the *Alternaria* sp. secreted comparatively small amounts of these enzymes. Similarly, *P. variotii* exhibited significantly higher amounts of glucosidase, followed by *E. nigrum*, whereas *F. proliferatum* showed the lowest glucosidase production (Figure 6. On the overall basis, both *P. variotii* and *P. purpurogenum* revealed significant potential for the production of extracellular enzymes. Furthermore, *P. variotii and A. nidulans* exposed significantly higher amounts of IAA production (Figure 7).

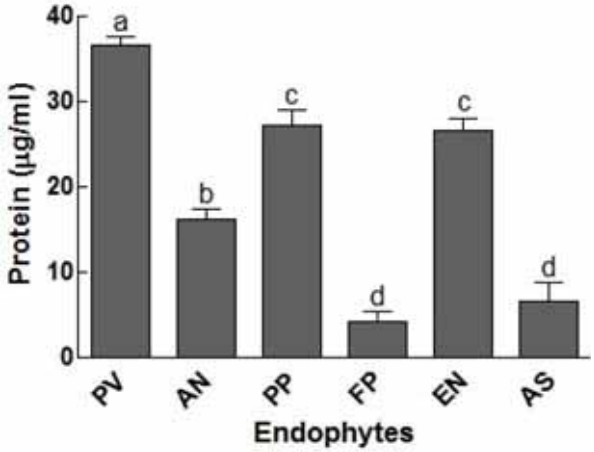

FIGURE 2
Total protein content of the pure culture filtrates of isolated endophytic fungi in (DF) minimal medium.
The bars represent the SE of mean of three replicates. Bars having different letters are significantly different from each at P=0.05.

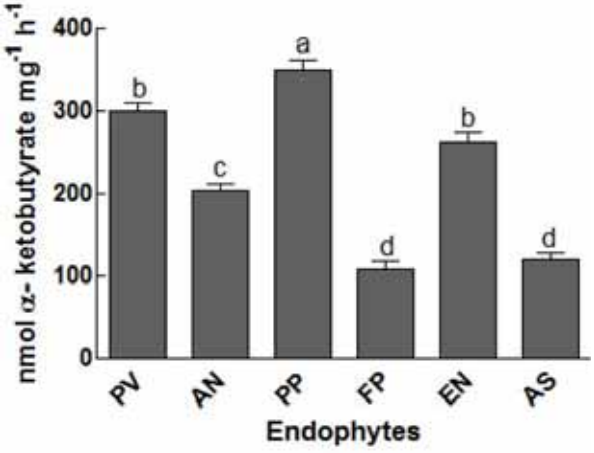

FIGURE 3
ACC deaminase activity of the pure culture filtrates of isolated endophytic fungi in (DF) minimal
medium containing ACC.
The bars represent the SE of mean of three replicates. Bars having different letters are significantly different from each at P=0.05.

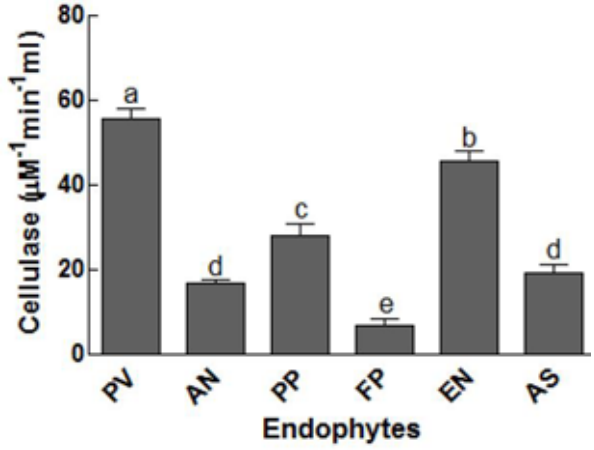

FIGURE 4
Cellulase activity of isolated endophytic fungal strains from *Caralluma acutangula*.
The bars represent the SE of mean of three replicates. Bars having different letters are significantly different from each at P=0.05.

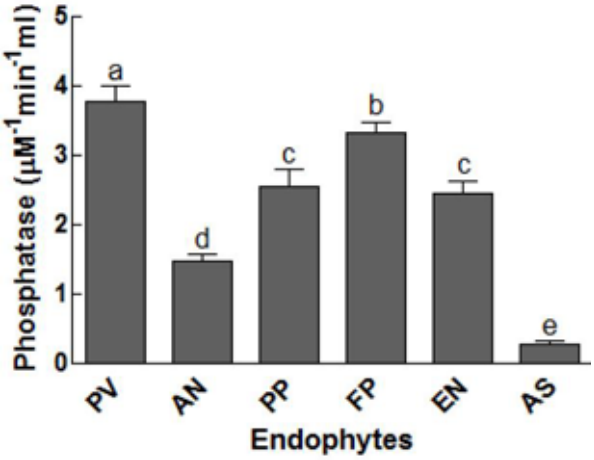

FIGURE 5
Phosphatase activity of isolated endophytic fungal strains from *Caralluma acutangula*.
The bars represent the SE of mean of three replicates. Bars having different letters are significantly different from each at P=0.05.

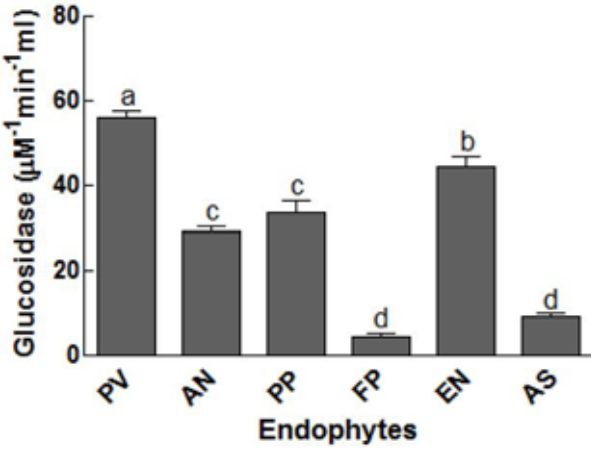

FIGURE 6
Glucocidase activity of isolated endophytic fungal strains from *Caralluma acutangula*.
The bars represent the SE of mean of three replicates. Bars having different letters are significantly different from each at P=0.05.

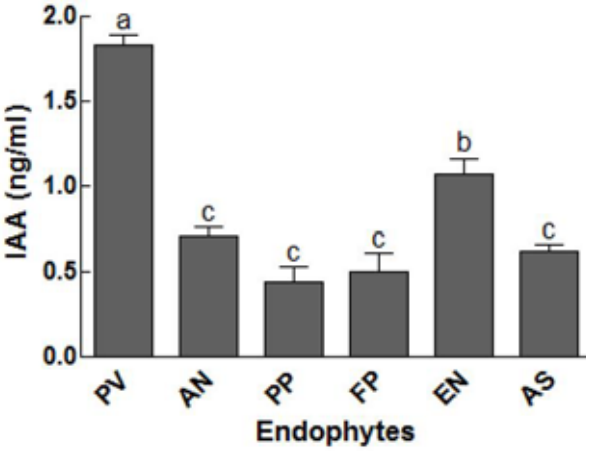

FIGURE 7
Indole acetic acid production by endophytic fungi from *Caralluma acutangula*.
The bars represent the SE of mean of three replicates. Bars having different letters are significantly different from each at P=0.05.

DISCUSSION

Endophytic microbes associated with medicinally important plants have been shown to enhance host plant growth and development. This could possibly be owing to the production of various constituents during the symbiotic processes with the host plants [1, 12]. To further understand the interactions in *in vitro* environments of culturable endophytes from medicinal plants, we isolated and identified endophytic fungal species from *C. acutangula*. To our knowledge, there have been no previous studies on this plant and its associated endophytic microorganisms. In the current study, we isolated and identified various strains of *Paecilomyces*, *Epicucum*, *Fusarium*, *Penicillium*, *Aspergillus*, and *Alternaria* species using molecular techniques. Based on ITS sequence homology, we identified these fungal strains as *A. nidulans, P. variotii, F. proliferatum*, *E. nigrum, P. purpurogenum*, and *Alternaria* sp. These strains have been assessed for their potential to produce ACC deaminase, extra-cellular enzymes, and IAA during their growth.

The production of ACC deaminase is common in bacteria, whereas some of the fungal strains also possessed genes for ACC deaminase synthesis. Among fungal stains, some species of *Penicillium* have been found to produce ACC [17, 25]. The endophytic microbial communities living inside plants and synthesizing ACC deaminase use ethylene. This enzyme cleaves the ethylene precursor ACC to α-ketobutyrate and ammonia. In this way the ethylene level is get lowered in developing or stressed plants [26]. The endophytes which are producing ACC deaminase help in plant growth under stress conditions and also perform an important role in nodulation. This function of ACC deaminase is varible in different plant species. The activity of this enzyme was determined in the extracellular environments of endophytic fungal strains during their growth. The results of the present study suggested a significantly higher amount of ACC deaminase production by the isolated fungal strains, which is in accordance with the previous studies [17, 25, 27].

Although, the biodiversity of fungal species is estimated to be about 1.5 million, a limited number of species (including *Aspergillus, Penicillium, Rhizopus*, and *Trichoderma*) have been characterized to release bioactive molecules mainly fungal enzymes with industrial applications [11, 28]. The wide application of fungal enzyme enhanced the interest of many researchers to explore the microbial strains that can serve as cheap factories for sustainable resources. Likewise, the extracellular enzyme production by endophytes is essential to help the microorganism penetrate the host cell wall, and can contribute to the defense responses and mineral uptake in host-plants [29]. In our study, the extracellular enzyme, β-glucosidase, encoded by endophytic fungi isolated from *C. acutangula* revealed the production of higher amounts of β-glucosidases. The previous data also described the purification, crystallization, and different properties of α-glucosidase from the mycelia of *Mucor* [30]. α-glucosidase activity in the culture filtrates of *Aspergillus niger*, *A. nidulans* and *Penicillium* sp. have been observed in the past [31-33].

In addition, cellulase enzymes produced by the endophytic fungi, *Pycnoporus sanguineus* isolated from *Baccharis dracunculifolia* effectively hydrolyzed cellulose [34]. The production of cellulase enzymes was considerably higher in *P. variotii*, *P. purpurogenum* and *Epicoccum nigrum.* It was also observed that keeping the pH at optimum (i.e., pH 5.5 in our case) can yield greater amounts of cellulase in culture media. Gawas-Sakhalkar et al. [28] reported

intracellular acid phosphatase production from *P. citrinum.* Also, Qureshi et al. [33] observed alkaline phosphatase production from newly isolated *A. fumigatus* EFRL05. The isolated endophytic fungi also showed significant results for phosphatase production. The phosphatase production in *F. proliferatum*, *P. variotii*, and *P. purpurogenum* was significantly higher than that of other strains.

Like enzyme production, it has also been reported that endophytic microbial flora can significantly contribute towards the production of phytohormones [1, 6, 26]. Phytohormones, such as auxins, are produced in the plants and are responsible for the regulation of plant growth and development [35]. Recently, it has been documented that the endophytic microbial flora (bacterial/fungal) of the plant also contribute to the production of these phytohormones [1, 6, 14]. Mei and Flinn [36] observed growth promotion in fungal associated plants under stress conditions. Such promotion in growth might be due to the release of IAA by the endophytes in order to support its host. In our study, *P. variotii* and *A. nidulans* showed considerable IAA production, which supports previous findings regarding IAA-production by endophytes. The results also conclude that endophytic fungi associated with medicinally important plants possess a unique potential to produce bioactive metabolites, which might improve the growth of the host in severe environmental conditions.

REFERENCES

[1] Khan, A.L., Hussain, J., Al-Harrasi, A., Al-Rawahi, A. and Lee, I.-J. (2015) Endophytic fungi: resource for gibberellins and crop abiotic stress resistance. Critical reviews in biotechnology. 35, 62-74.

[2] Martín-Sampedro, R., López-Linares, J.C., Fillat, Ú., Gea-Izquierdo, G., Ibarra, D., Castro, E. and Eugenio, M.E. (2017) Endophytic fungi as pretreatment to enhance enzymatic hydrolysis of olive tree pruning. BioMed research international. 2017, 10p.

[3] Wang, M.-q., Hao, X.-j., Yao, Y.-p. and Xu, M. (2018) Mutation breeding of *Bacillus amyloliquefaciens* HT-Q6. Fresen. Environ. Bull. 27, 4337-4342.

[4] Sunitha, V., Devi, D.N. and Srinivas, C. (2013) Extracellular enzymatic activity of endophytic fungal strains isolated from medicinal plants. World Journal of Agricultural Sciences. 9, 01-09.

[5] Castro, R.A., Quecine, M.C., Lacava, P.T., Batista, B.D., Luvizotto, D.M., Marcon, J., Ferreira, A., Melo, I.S. and Azevedo, J.L. (2014) Isolation and enzyme bioprospection of endophytic bacteria associated with plants of Brazilian mangrove ecosystem. SpringerPlus 3, 382.

[6] Khan, A.L., Hamayun, M., Kang, S.-M., Kim, Y.-H., Jung, H.-Y., Lee, J.-H. and Lee, I.-J. (2012) Endophytic fungal association via gibberellins and indole acetic acid can improve plant growth under abiotic stress: an example of *Paecilomyces formosus* LHL10. BMC microbiology. 12, 3.

[7] Mohd, A., Eyad, A., Syed Amir, A., Kartik, P., Kishan, L. and Mitesh, P. (2018) Physiological and molecular characterization of biosurfactant producing endophytic fungi *Xylaria regalis* from the cones of *Thuja plicata* as a potent plant growth promoter with its potential application. BioMed research international. 2018, 11p.

[8] Wang, M.-q., Hao, X.-j., Yao, Y.-p. and Xu, M. (2018) Study on colonization ability in plants of endophytic *Bacillus amyloliquefaciens* HT-Q6 Isolated From Walnut. Fresen. Environ. Bull. 27, 1152-1156.

[9] Ali, S., Charles, T.C. and Glick, B.R. (2014) Amelioration of high salinity stress damage by plant growth-promoting bacterial endophytes that contain ACC deaminase. Plant Physiology and Biochemistry. 80, 160-167.

[10] Saxena, S., Meshram, V. and Kapoor, N. (2015) *Muscodor tigerii* sp. nov.-Volatile antibiotic producing endophytic fungus from the North-eastern Himalayas. Annals of microbiology. 65, 47-57.

[11] Rytioja, J., Hildén, K., Mäkinen, S., Vehmaanperä, J., Hatakka, A. and Mäkelä, M.R. (2015) Saccharification of lignocelluloses by carbohydrate active enzymes of the white rot fungus *Dichomitus squalens*. PloS one. 10, e0145166.

[12] Kusari, S., Pandey, S.P. and Spiteller, M. (2013) Untapped mutualistic paradigms linking host plant and endophytic fungal production of similar bioactive secondary metabolites. Phytochemistry. 91, 81-87.

[13] Lugtenberg, B.J., Malfanova, N., Kamilova, F. and Berg, G. (2013) Plant growth promotion by microbes. Molecular Microbial Ecology of the Rhizosphere. 1, 2559-573.

[14] Khan, A.L., Halo, B.A., Elyassi, A., Ali, S., Al-Hosni, K., Hussain, J., Al-Harrasi, A. and Lee, I.-J. (2016) Indole acetic acid and ACC deaminase from endophytic bacteria improves the growth of *Solanum lycopersicum*. Electronic Journal of Biotechnology. 21, 58-64.

[15] De Battista, J., Bacon, C., Severson, R., Plattner, R. and Bouton, J. (1990) Indole acetic acid production by the fungal endophyte of tall fescue. Agronomy Journal. 82, 878-880.

[16] Gamalero, E., Berta, G., Massa, N., Glick, B.R. and Lingua, G. (2008) Synergistic interactions between the ACC deaminase-producing bacterium *Pseudomonas putida* UW4 and the AM fungus *Gigaspora rosea* positively affect cucumber plant growth. FEMS Microbiology Ecology. 64, 459-467.

[17] Yim, W., Seshadri, S., Kim, K., Lee, G. and Sa, T. (2013) Ethylene emission and PR protein synthesis in ACC deaminase producing Methylobacterium spp. inoculated tomato plants (*Lycopersicon esculentum* Mill.) challenged with *Ralstonia solanacearum* under greenhouse conditions. Plant physiology and biochemistry. 67, 95-104.

[18] Marwah, R.G., Fatope, M.O., Al Mahrooqi, R., Varma, G.B., Al Abadi, H. and Al-Burtamani, S.K.S. (2007) Antioxidant capacity of some edible and wound healing plants in Oman. Food chemistry. 101, 465-470.

[19] Abdel-Sattar, E., Ahmed, A.A., Hegazy, M.-E.F., Farag, M.A. and Al-Yahya, M.A.-A. (2007) Acylated pregnane glycosides from *Caralluma russeliana*. Phytochemistry. 68, 1459-1463.

[20] Tamura, K., Stecher, G., Peterson, D., Filipski, A. and Kumar, S. (2013) MEGA6: molecular evolutionary genetics analysis version 6.0. Molecular biology and evolution. 30, 2725-2729.

[21] Østergaard, L.H. and Olsen, H.S. (2011) Industrial applications of fungal enzymes, Industrial Applications. Springer, 269-290.

[22] Shaharoona, B., Arshad, M. and Zahir, Z. (2006) Effect of plant growth promoting rhizobacteria containing ACC-deaminase on maize (*Zea mays* L.) growth under axenic conditions and on nodulation in mung bean (*Vigna radiata* L.). Letters in applied microbiology. 42, 155-159.

[23] Zor, T. and Selinger, Z. (1996) Linearization of the Bradford protein assay increases its sensitivity: theoretical and experimental studies. Analytical biochemistry. 236, 302-308.

[24] Marx, M.-C., Wood, M. and Jarvis, S. (2001) A microplate fluorimetric assay for the study of enzyme diversity in soils. Soil biology and biochemistry. 33, 1633-1640.

[25] Jia, Y.-J., Kakuta, Y., Sugawara, M., Igarashi, T., Oki, N., KisAKi, M., Shoji, T., Kanetuna, Y., Horita, T. and Matsui, H. (1999) Synthesis and degradation of 1-aminocyclopropane-1-carboxylic acid by *Penicillium citrinum*. Bioscience, biotechnology, and biochemistry. 63, 542-549.

[26] Hontzeas, N., Richardson, A., Belimov, A., Safronova, V., Abu-Omar, M. and Glick, B. (2005) Evidence for horizontal transfer of 1-aminocyclopropane-1-carboxylate deaminase genes. Applied and Environmental Microbiology. 71, 7556-7558.

[27] Prabavathy, D. and Valli, N.C. (2012) Screening for extracellular enzymes and production of cellulase by an endophytic Aspergillus sp, using cauliflower stalk as substrate. International Journal on Applied Bioengineering. 6, 40-45.

[28] Gawas-Sakhalkar, P., Singh, S., Naik, S. and Ravindra, R. (2012) High-temperature optima phosphatases from the cold-tolerant Arctic fungus *Penicillium citrinum*. Polar Research. 31, 11105.

[29] Wei, H., Wang, W., Yarbrough, J.M., Baker, J.O., Laurens, L., Van Wychen, S., Chen, X., Taylor II, L.E., Xu, Q. and Himmel, M.E. (2013) Genomic, proteomic, and biochemical analyses of oleaginous *Mucor circinelloides*: evaluating its capability in utilizing cellulolytic substrates for lipid production. PloS one. 8, e71068.

[30] Kato, N., Suyama, S., Shirokane, M., Kato, M., Kobayashi, T. and Tsukagoshi, N. (2002) Novel α-glucosidase from Aspergillus nidulans with strong transglycosylation activity. Applied and environmental microbiology. 68, 1250-1256.

[31] Khan, A.L., Al-Harrasi, A., Al-Rawahi, A., Al-Farsi, Z., Al-Mamari, A., Waqas, M., Asaf, S., Elyassi, A., Mabood, F. and Shin, J.-H. (2016) Endophytic fungi from Frankincense tree improves host growth and produces extracellular enzymes and indole acetic acid. PloS one. 11, e0158207.

[32] Liu, C., Liu, T., Yuan, F. and Gu, Y. (2010) Isolating endophytic fungi from evergreen plants and determining their antifungal activities. African Journal of Microbiology Research. 4, 2243-2248.

[33] Qureshi, A.S., Marium, S., Khushk, I. and Bhutto, M.A. (2013) Production of alkaline phosphatase from newly isolated *Aspergillus fumigatus* EFRL05. Top Class Journal of Microbiology. 1, 67-73.

[34] Onofre, S.B., Santos, Z.M., Kagimura, F.Y. and Mattiello, S.P. (2015) Cellulases produced by the endophytic fungus *Pycnoporus sanguineus* (L.) Murrill. African Journal of Agricultural Research. 10, 1557-1564.

[35] Martínez-de la Cruz, E., García-Ramírez, E., Vázquez-Ramos, J.M., de la Cruz, H.R. and López-Bucio, J. (2015) Auxins differentially regulate root system architecture and cell cycle protein levels in maize seedlings. Journal of plant physiology. 176, 147-156.

[36] Mei, C. and Flinn, B.S. (2010) The use of beneficial microbial endophytes for plant biomass and stress tolerance improvement. Recent Patents on Biotechnology. 4, 81-95.

Received: **05.11.2018**
Accepted: **20.02.2019**

CORRESPONDING AUTHOR

Amjad Iqbal
Department of Agriculture,
Abdul Wali Khan University Mardan

e-mail: amjadiqbal@awkum.edu.pk

© by PSP Volume 28 – No. 4/2019 pages 2697-2702 Fresenius Environmental Bulletin

EFFECTS OF MELOXICAM ON STRESS AND OXIDATIVE STRESS IN DAIRY COWS UNDERGOING HOOF TRIMMING

Selvinaz Yakan[1,*], Vesile Duzguner[2]

[1]Agri Ibrahim Cecen University, Eleskirt Celal Oruc School of Livestock Production, Department of Animal Health, Agri, Turkey
[2]Ardahan University, School of Health Sciences, Department of Nursing, Ardahan, Turkey

ABSTRACT

The objective of this study is to investigate meloxicam which is a nonsteroidal anti-inflammatory analgesic of the effect on the antioxidant imbalance this is caused by stress and the oxidative stress may occur in dairy cows undergoing hoof trimming (HT). This research was carried out on 14 female Simmental dairy cows 3 aged with a mean body weight of 450 ± 50 kg that in early lactation period, showing symptoms lameness due to hoof disorder on the commercial dairy farm. Each group had 7 cows: group I (analgesia) and group II (non-analgesia) as were randomly divided into two groups. Group, I (n= 7) was administered intravenously (IV) meloxicam at a dose of 0.5 mg/kg live weight before 30 min HT. Group II (n = 7) was administered saline at the same dose before 30 min the procedure was started. During HT process -30 (30 min before hoof trimming), 15 and 30 mins the heart and respiratory rate was measured. Blood samples were taken in the same time period Total oxidant capacity (TOC), total antioxidant capacity (TAC), glutathione (GSH) enzyme activity, the level of cortisol and glucose level was measured in the serum. There were no significant changes in heart and respiratory rate during HT ($p>0.05$). Cortisol and glucose levels were significantly lower in the analgesia group than in the non-analgesic group ($p<0.05$). TOC measurements at all times in analgesia group ($p<0.001$). TAC level did not change in both groups. GSH level higher at all times in the analgesia group than non-analgesia. Results showed prevented the oxidative stress and support the antioxidant system of meloxicam. The results suggest that analgesia should be used in the process of HT for animal welfare.

KEYWORDS:
Oxidative stress, hoof trimming, meloxicam, dairy cow

INTRODUCTION

Lameness is one of the most important health concerns of dairy cows management, which leads to significant economic losses due to the high prevalence affecting animal welfare and productivity [1−5]. The economic losses caused by lameness are mainly a reduction in milk production, poor reproductive performance, and removal of early production [6−9]. Due to lameness, annual economic losses in countries are reported to be about $ 180 million [10]. The prevalence of lameness in dairy cows herds is quite variable and ranges from 0 to 60% [11]. The distribution of lameness prevalence in such a wide range is related to care and hosting conditions, feeding and hoof care [10, 11]. 75-90% of lameness is caused by foot and hoof diseases [12]. Hoof care is one of the most important factors affecting lameness prevalence [13]. Hoof trimming (HT) is recommended as a protective measure against lameness [14-15].

HT, prevention of excessive elongation of the horn hoof physiologically evolving, thus preventing the formation of distorted and deformed hoof shapes or deformed hoofs to restore normal morphological features made to trimming and correct the process. This procedure creates stress in the animal and the use of analgesic agents to reduce stress reduces oxidative stress and improves animal welfare [11].

Non-steroidal anti-inflammatory drugs (NSAIDs) inhibit the cyclooxygenase (COX) enzyme, which plays a role in the synthesis of prostanoids [16, 17]. Among prostanoids, Prostaglandins E_2 (PGE_2) and PGI_2 exhibit the highest influence on pain signals transformation. NSAIDs decrease PGE_2 production [18]. COX's two forms are COX-1 and COX-2 [15] COX-2 isoforms are usually related to pain and inflammation associated with tissue damage [19]. Meloxicam, oxicam group is a potent nonsteroidal anti-inflammatory analgesic drug that inhibits the activity of the COX-2 enzyme and prevents inflammation and pain relief in painful procedures by inhibiting the production of PGE_2 from arachidonic acid and is used as a painkiller in painful procedures [16, 20].

The objective of this study is to investigate meloxicam which is a nonsteroidal anti-inflammatory analgesic of the effect on the antioxidant imbalance this is caused by and stress and the oxidative stress may occur in cows undergoing HT. The results will guide us to minimize stress during HT.

TABLE 1
Heart rate and respiratory rate of cows in group I (analgesia, n=7) and group II (non-analgesia, n=7) (mean ± SEM).

Time (min)	Group	Heart Rate (Pulse/min)	Respiratory Rate (Beat/Rate)
-30	I	68.85 ± 1.38	24.14 ± 1.14
	II	71.14 ± 1.98	26.14 ± 2.16
15	I	70.28 ± 1.34	24.85 ± 2.27
	II	78.14 ± 3.66	31.00± 3.06
30	I	73.28 ± 3.21	25.14 ± 0.70
	II	70.28 ± 1.50	29.71 ± 1.62

I= Hoof trimming with a painkiller. II= Hoof trimming without painkiller.

MATERIALS AND METHODS

Animal. This research was carried out on 14 female Simmental dairy cows 3 aged with a mean body weight of 450 ± 50 kg that in early lactation period, showing symptoms lameness due to hoof disorder on the Haliloğulları dairy farm, Ağrı, TR. The study was approved by the Animal Ethics Committee of Çukurova University (approval number: 04.07.2018/07). Each group had 7 dairy cows: group I (analgesia) and group II (non-analgesia) as were randomly divided into two groups. Group I (n= 7) was administered intravenously (IV) meloxicam (maxicam X4, 100 mL Sanovel) at a dose of 0.5 mg/kg live weight before 30 min hoof trimming. Group II (n = 7) was administered saline at the same dose before 30 min the procedure was started.

Study design. For the HT process, the animal has detected in the standing of a mobile walk-in crush. HT was started from the medial hoof in the hind legs and the lateral hoof in the anterior feet.

HT was performed by the same person to trimming and correct the horn hoof according to the method and this procedure is completed in about 15 mins. To track changes in the physiological parameters in the animal during HT process -30 (30 min before hoof trimming), 15 and 30 mins the heart rate was measured by auscultation and respiratory rate by counting thoracic excursions.

Biochemical Analysis. Blood samples were taken at -30, 15 and 60th min of the applications then they were brought to the laboratory as soon as possible and centrifuged at 3000 rpm for 10 min at room temperature and kept at -80°C until the samples were tested. Total oxidant capacity (Bovine (TOC) ELISA kit) and total antioxidant capacity (Bovine (TAC) ELISA kit) tests for determination of oxidative stress index in the obtained serum, glutathione (GSH) enzyme analysis (Glutathione Assay kit) was performed by ELISA method for the evaluation of antioxidant potential. The level of cortisol (Bovine (Cortisol) ELISA kit) and glucose (Glucose Colorimetric Assay kit) in the serum was measured using a commercial kit to assess pain in animals.

Statistical Analysis. The one-way analysis of variance (ANOVA) and post hoc Duncan tests were performed on the data to examine the differences among groups using the SPSS statistical software package. The results are presented as average ± SE. A value of $p< 0.05$ was considered significant.

RESULTS

There was no statistically significant in all measurement times in comparisons between and within the groups the results of heart rate both group I and group II ($p>0.05$). However, there was an increase in of the heart rates in the 15th min after HT in the non-analgesia group, but this increase was observed in the physiological limits and was not found statistically significant. Similarly, there was no statistically significant difference within and between the groups in terms of respiratory rate in comparing the results measurements at all times ($p>0.05$). However, there was a slightly increased in respiratory rate likewise as heart rate in the 15th min after HT in the non-analgesia group. The results of measurement of heart and respiratory rate in mins are given in Table 1.

There were no statistically significant differences in cortisol level measurements within the groups in both analgesia and non-analgesia groups ($p>0.05$). The decrease in analgesia group was statistically significant in all-time comparisons between groups ($p<0.05$), (Graph 1). There was no statistically significant difference comparing within the analgesia and non-analgesia groups in glucose level measurements ($p>0.05$). The decrease in the analgesia group in all measurement time was statistically significant ($p<0.05$), (Graph 2).

In TOC measurements, no statistically significant difference was found between all measurement results in within-group comparisons in both analgesia and non-analgesia groups ($p>0.05$). The decrease in analgesia group was statistically significant at all measurement times between groups ($p<0.001$). In TAC was no statistically significant differences comparing within and between the groups at all measurement times in both analgesia and non-

analgesia groups (p>0.05). In within-group comparisons of GSH measurements, there was no statistically significant difference between the -30th and 15th min results in the analgesia group (p>0.05). In the -30th and 30th min measurement results, the increase in the 30th min was statistically significant (p<0.05). The increase between 15 and 30 mins was not statistically significant (p>0.05). There was no statistically significant difference in all measurement times within group comparisons in the non-analgesia groups (p>0.05). There was a statistically significant difference between measurement results -30th comparing between groups (p<0.05). There was a statistically significant difference between the 15th min measurement results (p<0.001). There was a statistically significant difference between the 30th min measurement results (p<0.05), (Table 2).

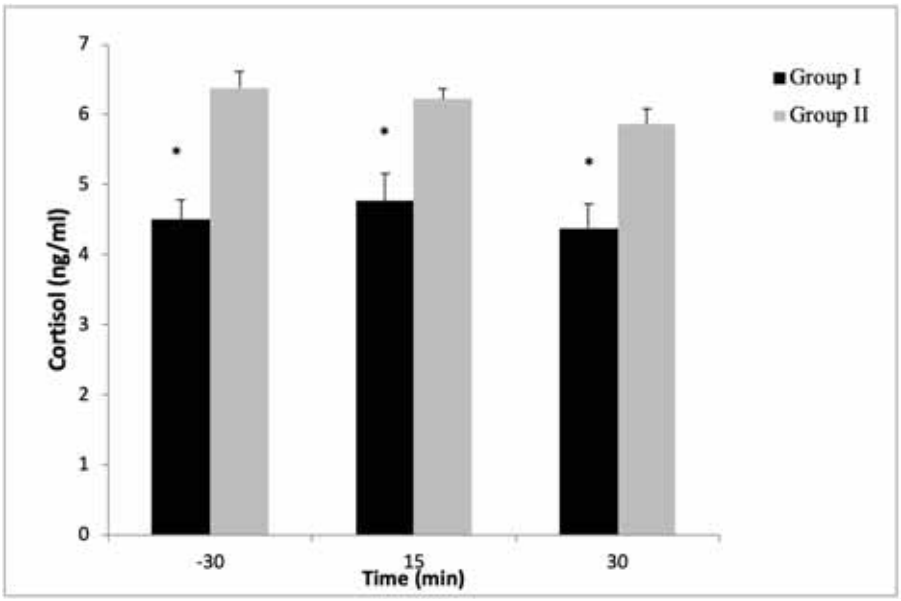

GRAPH 1

Changes in the cortisol level in group I and group II over time.

*In the comparisons between groups, the measurements marked with asterisks at the same time period are considered statistically significant (p<0.05).

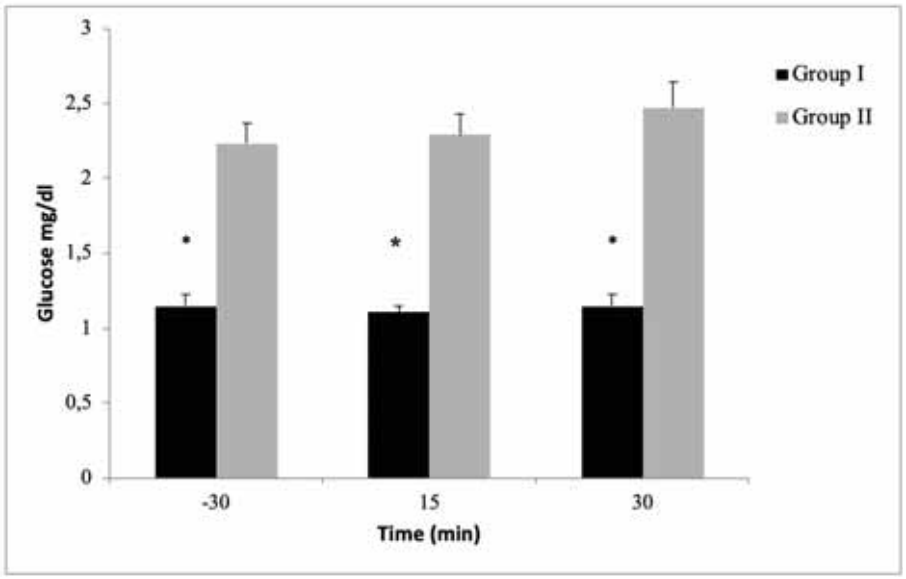

GRAPH 2

Changes in the glucose level in group I and group II over time.

*In the comparisons between groups, the measurements marked with asterisks at the same time period are considered statistically significant (p<0.05).

TABLE 2
Serum TOC, TAC and GSH of cows in group I (analgesia, n=7) and group II (non-analgesia, n=7) (mean ± SEM).

Time (min)	Group	TOC (μmol/L)	TAC (U/mL)	GSH (mmol/L)
-30	I	2.50 ± 0.42**	4.58 ± 0.03	19.70 ± 1.18*[a]
	II	36.66 ± 3.33	4.54 ± 0.11	14.84 ± 0.20
15	I	3.16 ± 0.16**	4.55 ± 0.04	22.66 ± 1.19**
	II	40.00 ± 5.16	4.59 ± 0.04	12.44 ± 1.17
30	I	3.33 ± 0.55**	4.64 ± 0.04	26.80 ± 3.64*[a]
	II	48.33 ± 4.01	4.65 ± 0.03	14.53 ± 1.05

[a]In the within-group comparison, there was a statistically significant difference between the values of same letters in the same column ($p<0.05$).
In the comparisons between groups, the measurements marked with asterisks are considered statistically significant ($p<0.05$, ** $p<0.001$).

DISCUSSION

Hoof trimming (HT) is a common management intervention in the prevention of lameness in dairy cattle [21−25]. However, this HT process has the potential to expose the animal to various stressors including changes in daily routine, preparations made before HT, restriction of animal movement and HT itself with optical, acoustical and mechanical disturbances [13, 14, 26]. To evaluate the welfare effect of a procedure it is important to assess the impact it has on the animal physiologically [13, 14]. Exposure to stress activates multiple neural and endocrine systems of animal and this, in conclusion, leads to a releasing in stress hormones in the bloodstream [13, 27] and can affect physiological functions such as heart and respiratory rate, milk yield, and reproductive functions [13, 14, 28]. HT can impact the heart rate and respiratory rate in cattle and thus these parameters widely accepted criteria used as a measure of relative stress [13]. In the study by Rizk et al. [29], to investigate effects of xylazine hydrochloride on dairy cows undergoing claw trimming after xylazine or saline administration, heart and respiratory rates have slightly risen at 15 min in the saline group but they decreased in xylazine group. A smaller study in study by Korkmaz et al. [14], investigated the effects of dexketoprofen trometamol on oxidative stress that may occur with claw trimming, it is reported that heart and respiration rate increased in the control and analgesia groups but the increase in heart rate was found to be significant in the control group after 15 min. The increase in respiratory rate was found to be significant in the 15th minute in both groups. Unlike other researchers in our study, although there was an increase in heart rate in the 15th min in the non-analgesic group, this increase was not significant. There were no significant changes in heart and respiratory rate during HT.

The level of cortisol in blood is extensively used as an indicator of acute stress response in stressful procedures [27]. Exposure to stressor conditions would stimulate the hypothalamic-pituitary-adrenal axis leading to blatantly incrementing in the ACTH and cortisol level. In a study by Pesenhofer et al. [30], compared the effect on cortisol concentration and milk yield before and after HT with 2 different types of trimming set-ups, a mobile walk-in crush and a tilt table on dairy cattle. Daily milk yield was registered 7 days before and up to 13 days later HT. Cortisol concentration was measured 12 hours before and until 7 days after HT. It is reported that it decreases 0.6 L after 7 days of HT day and decreased by 0.5 L on the HT day milk production. Cortisol concentration was significantly higher 24 hours following. This study is emphasized that HT leads to a stress response and affected the productivity of the animal. In another study, claw trimming was conducted at standing position and similar to other studies cortisol level increased in both groups. This increasing with respect to time was significant in control and analgesia (dexketoprofen trometamol) groups. However, the increase in cortisol level was lower in analgesia group than in the control group [14]. In our study, no significant changes were observed in cortisol level in the HT during in the analgesia and non-analgesia groups. However, in the analgesia and non-analgesia groups, the cortisol level was significantly lower in the analgesia group at all measurement times in the comparisons between the groups. Similar to previous studies cortisol level was higher in the control group than analgesia group. As says of Korkmaz et al. [14], low cortisol level in analgesia group may be due to meloxicam having some pain-relieving effect by the inhibition of prostaglandin synthesis.

Stress causes excessive glucose production and the level of glucose increases with stress [31]. When cows that had a lower glucose concentration were exposed to a stressor an increase in the concentration of glucose but the increase was not as large as what was observed for cows that had higher levels of glucose available before the stressor. However, the relationship between stress and glucose concentration depends on the concentration at the baseline of glucose [29]. So glucose is important components needed for milk production and based on the baseline increased concentration of glucose so varies according to lactation stages of cows increased at the level of glucose due to stress. The increase in glucose level due to stress varies in lactation or non-lactating cows [13, 26, 31, 32]. Early lactation period dairy cows in our study and significant changes were not observed in glucose level in the HT during in the analgesia and

non-analgesia groups. However, in the analgesia and non-analgesia groups, the glucose level was significantly lower in the analgesia group at all measurement times in the comparisons between the groups.

TOC, TAC measurement is recommended to determine their balance and the oxidant and antioxidant status in the organism [33]. In our study, there was a significant decrease in TOC measurements at all times in analgesia group ($p<0.001$). There was no significant change in TAC measurements at all times both Group I and II. GSH, which is involved in the antioxidant defense system in the active and safe removal of reactive oxygen species in living organisms, acts as a non-enzymatic antioxidant [34, 35]. In our study, the GSH level was lower at all times in the group non-analgesia, in which HT during stress occurred and high levels of GSH at all times in the analgesia group indicate that meloxicam supports the oxidant system.

CONCLUSION

As a result, low levels of cortisol and glucose in the HT process showed prevented the stress of meloxicam, in addition to low TOC, prevent oxidative stress and increase the level of glutathione showed that it supports antioxidant system. The results suggest that analgesia (such as meloxicam) should be used in the process of HT for animal welfare.

REFERENCES

[1] Arican, M., Hatipoglu, F., Erol, H., Kanat, O., Yavuz, O., Parlak, K., Koc, O. (2018) Comparison of thermographic imaging and other diagnostic techniques in the diagnosis of cattle with laminitis. Acta Scientiae Veterinariae. 46, 1-7.

[2] Green, L.E., Hedges, V.J., Schukken, Y.H., Blowey, R.W., Packington, A.J. (2002) The impact of clinical lameness on the milk yield of dairy cows. Journal of Dairy Research. 85(9), 2250-2256.

[3] Espejo, L.A., Endres, M.I., Salfer, J.A. (2006) Prevalence of lameness in high producing Holstein cows housed in free stall barns in Minnesota. Journal of Dairy Science. 89, 3052–3058.

[4] Barker, Z.E., Leach, K.A., Whay, H.R., Bell, N.J., Main, D.C. (2010) Assessment of lameness prevalence and associated risk factors in dairy herds in England and Wales. Journal of Dairy Science. 93, 932–941.

[5] Barkema, H.W., Westrick, J.D., Vankeulen, K.A.S., Schukken, Y.H., Brand, A. (1994) The effects of lameness on reproductive performance, milk production and culling in Dutch dairy farms. Preventive Veterinary Medicine. 20(4), 249-259.

[6] Ettema, J.F., Østergaard, S., Kristensen, A.R. (2010) Modeling the economic impact of three lameness causing diseases using herd and cow level evidence. Preventive Veterinary Medicine. 95(1), 64-73.

[7] Hernandez, J.A., Garbarino, E.J., Shearer, J.K., Risco, C.A., Thatcher, W.W. (2005) Comparison of milk yield in dairy cows with different degrees of lameness. Journal of the American Veterinary Medicine Association. 227, 1292–1296.

[8] Peake, K.A., Biggs, A.M., Argo, C.M., Smith, R.F., Christley, R.M., Routly, J.E., Dobson, H. (2011) Effects of lameness, subclinical mastitis and loss of body condition on the reproductive performance of dairy cows. Veterinary Record. 168, 301.

[9] Booth, C.J., Warnick, L.D., Grohn, Y.T., Maizon, D.O., Guard, C.L., Janssen, D. (2004) Effect of lameness on culling in dairy cows. Journal of Dairy Science. 87, 4115–4122.

[10] Kamiloglu, A. (2014) Foot diseases in farm animals. Malatya: Medipress, 3.

[11] Cecen, G. (2014) Lameness and foot diseases in cattle. Bursa: Sentez, 3.

[12] Clarkson, M.J., Downham, D.Y., Faull, W.B., Hughes, J.W., Manson, F.J., Merritt, J.B., Murray, R.D., Russell, W.B., Sutherst, J.E., Ward, W.R. (1996) Incidence and prevalence of lameness in dairy cattle. Veterinary Record. 138, 563–567.

[13] Stoddard, G.C., Cramer, G. (2017) A Review of the relationship between hoof trimming and dairy cattle welfare. Veterinary Clinics of North America- Food Animal Practice. 33(2), 365–375.

[14] Korkmaz, M., Saritas, Z.K., Demirkan, I., Ulutas, E. (2014) Effects of dexketoprofen trometamol on stress and oxidative stress in cattle undergoing claw trimming. Acta Scientiae Veterinariae. 42, 1–6.

[15] Potterton, S.L., Bell, N.J., Whay, H.R., Berry, E.A., Atkinson, O.C., Dean, R.S., Main, D.C., Huxley, J.N. (2012) A descriptive review of the peer and non-peer reviewed literature on the treatment and prevention of foot lameness in cattle published between 2000 and 2011. The Veterinary Journal. 193, 612–616.

[16] Korkmaz, M., Saritas, Z.K., Bulbul, A., Demirkan, I. (2015) Effect of pre-emptive dexketoprofen trometamol on acute cortisol inflammatory response and oxidative stress to hoironson disbudding in calves. Journal of the Faculty of Veterinary Medicine, Kafkas University. 21, 563–568.

[17] Heinrich, A., Duffield, T.F., Lissemore, K.D., Squires, E.J., Millman, S.T. (2009**)** The impact of meloxicam on postsurgical stress associated with cautery dehorning. Journal of Dairy Science. 92, 540–547.

[18] Fraccaro, E., Coetzee, J.F., Odore, R., Edwards-Callaway, L.N., Kukanich, B., Badino, P., Bertolotti, L., Glynn, H., Dockweiler, J., Allen, K., Bergamasco, L. (2013) A study to compare circulating flunixin, meloxicam and gabapentin concentrations with prostaglandin E_2 levels in calves undergoing dehorning. Research in Veterinary Science. 95, 204–211.
[19] KuKanich, B., Bidgood, T., Knesl, O. (2012) Clinical pharmacology of non-steroidal anti-inflammatory drugs in dogs. Veterinary Anaesthesia Analgesia. 39, 69–90.
[20] Mathews, K.A. (2002) Non-steroidal anti-inflammatory analgesics: review of current practice. Journal of Veterinary Emergency Critical Care. 12(2), 89–97.
[21] Kibar, M., Caglayan, T. (2016) Effect of hoof trimming on milk yield in dairy cows with foot disease. Acta Scientiae Veterinariae. 44, 1–7.
[22] Bell, N.J. (2015) Evidence-based claw trimming for dairy cattle. Veterinary Record. 177, 220-221.
[23] Shearer, J.K., Amstel, S.R.V. (2001) Functional and corrective claw trimming. Veterinary Clinics North America Food Animal Practice. 17(1), 53-72.
[24] Maxwell, O.J., Hudson, C.D., Huxley, J.N. (2015) Effect of early lactation foot trimming in lame and non-lame dairy heifers: A randomized controlled trial. Veterinary Record. 177, 100.
[25] Manske, T., Hultgren, J., Begsten, C. (2002) The effect of claw trimming on the hoof health of Swedish dairy cattle. Preventive Veterinary Medicine. 54(2), 113−129.
[26] Janssen, S., Wunderlich, C., Heppelmann, M., Palme, R., Starke, A., Kehler, W., Steiner, A., Rizk, A., Meyer, U., Daenicke, S., Rehage, J. (2016) Short communication: Pilot study on hormonal, metabolic, and behavioral stress response to treatment of claw horn lesions in acutely lame dairy cows. Journal of Dairy Science. 99(9), 7481−7488.
[27] Mostl, E., Palme, R. (2002) Hormones as indicators of stress. Domestic Animal Endocrinology. 23, 67–74.
[28] Hernandez, J., Shearer, J.K., Webb, D.W. (2002) Effect of lameness on milk yield in dairy cows. Journal of the American Veterinary Medicine Association. 220, 640-644.
[29] Rizk, A., Herdtweck, S., Meyer, H., Offinger, J., Zaghloul, A., Rehage, J. (2012) Effects of xylazine hydrochloride on hormonal, metabolic, and cardiorespiratory stress responses to lateral recumbency and claw trimming in dairy cows. Journal of the American Veterinary Medicine Association. 240, 1223–1230.
[30] Pesenhofer, G., Palme, R., Pesenhofer, R.M., Kofler, J. (2006) Comparison of two methods of fixation during functional claw trimming-walk-in crush versus tilt table-in dairy cows using faecal cortisol metabolite concentrations and daily milk yield as parameters. Veterinary Medicine Austria. 93(11-12), 288–294.
[31] Mudron, P., Rehage, J., Sallmann, H.P., Holtershinken, M., Scholz, H. (2005) Stress response in dairy cows related to blood glucose. Acta Veterinaria Brno. 74, 37–42.
[32] Herdt, T.H. (2000) Ruminant adaptation to negative energy balance. Veterinary Clinics North America Food Animal Practice. 16, 215–230.
[33] Kurku, H., Soran, M. (2017) Oxidative stress levels of serum and urine in enuresis. Van Medical Journal. 24(4), 267–271.
[34] Gurgoze, S.Y., Sindak, N., Yilmaz, S., Sertkaya, H., Ozan, S.T. (2003) The effects of corticosteroid treatment of some antioxidant enzymes and the level of lipid peroxidation in cattle with bursitis precarpalis. Van Veterinary Journal. 14, 97–101.
[35] Meral, O., Ercan, N., Fidanci, U.R. (2017) Lipid peroxidation level and antioxidant enzyme activities in septicemic calves. Veterinary Journal of Ankara University. 64, 161–164.

Received: **02.12.2018**
Accepted: **21.02.2019**

CORRESPONDING AUTHOR

Selvinaz Yakan
Agri Ibrahim Cecen University,
Eleskirt Celal Oruc School of
Livestock Production,
Department of Animal Health,
Agri – Turkey

e-mail: syakan@gmail.com

© by PSP Volume 28 – No. 4/2019 pages 2703-2715 Fresenius Environmental Bulletin

ANALYZING THE EFFECTS OF OLIVE LEAVES ON SENSORY AND CHEMICAL PROPERTIES OF REFINED OLIVE OILS USING IMAGE PROCESSING METHODS

Omer Faruk Gamli*

Food Engineering Department, Korkut Ata University, Osmaniye, Turkey

ABSTRACT

Olive leaves are an important source of phenolics and pigments, that leaves are wastes of olive oil industries that enterprise producing olive oil. The main object of this study is to evaluate the chemical and sensory properties of refined olive oils containing different rates of olive leaves that obtained from olive oil factory, which were washed, dried, milled, and sieved, in comparison to virgin olive oil. The second object is to determine the optimal range of olive leaves to be added. The methods used for optimization is transforming the experimental results into images then processing the obtained images. The total phenols, antioxidant activity, chlorophyll and carotenoid, extinction coefficients (K_{232} and K_{270}), bitter index (K_{225}) and positive attributes of sensory evaluations of refined olive oils containing 10 and 15% olive leaves exhibited higher properties than virgin olive oils. These results emphasize the high potential of dried olive leaves as the phenolic constituent's source for refined olive oil and to improve the chemical and sensorial attributes of refined olive oils. Furthermore, the determined optimal olive leaf addition range that will equally satisfy all olive oil constituents is between 12.5%-15%.

Practical application. Adding the olive leaves between 12.5-15% improve the physicochemical and sensorial attributes of refined olive oil and this range is optimal since the lightest gray tone means the optimal. In this case, the center of optimal range is 13.75% and it can be said that this percentage should be preferred to satisfy all attributes equally.

KEYWORDS:
Refined olive oil, olive leaves, sensory profile, phenolic substances, image processing

INTRODUCTION

A high number of by-products and residues derived from both olive tree cultivation and the olive processing industry are obtained yearly; most of them have no practical applications [1]. Olive leaves, one of these by-products, can be found in large amounts in olive oil industries as an agricultural waste by-products. According to Kiristakis et al. [1], olive leaves are mainly found in two different points during the olive oil production process. Firstly, they are found during olive tree pruning, in which they constitute quarter portion of the pruning, and secondly in the olive oil production facility, where leaves are separated from the olives by a blower machine. It is reported that the amount of olive leaves accumulated annually may exceed 1 million tonnes. Harvested olives are accompanied by approximately 6% of leaves and annual world production of olives exceeds 18 million tonnes [2]. Considering the amount of annual olive leaves, the use of olive leaves will help to alleviate the environmental problem of olive oil industries as a waste.

It is reported that Mediterranean nations have used olive oil in their diet since ancient times and it occupies a very important place in nutrition as well as playing roles in medicine, cosmetics and other areas. Because of its beneficial effects, olive oil is considered a medicine, and a source of wealth and power [3]. Additionally olive oil is characterized by nutritional and sensory properties, including bitterness, pungency, fruitiness, and greenness which are considered as positive attributes in olive oils. Phenolic compounds are the major constituents in charge of for pungency and bitterness of olive oils (virgin). Phenolic compounds, which are found in olive leaves especially protect oil against autoxidation, acting as antioxidants, hence attract great interest because of its role in health [1, 4, 5], and their contents in olive oils vary widely, depending on olive fruits, ripening levels, environmental conditions, growing region, crushing and paste malaxation process [6]. Additionally, pigments and tocopherols act as antioxidants that play important roles of olive oil (virgin) stability as well as in the inhibition of some illnesses [7]. The total phenols of virgin olive oils undergo some modifications due to hydrolytic and oxidative reactions during storage (18-25 ºC) at where polyphenol reductions up to 25-31% take place after 18-24 months of storage [8].

Olive oil pigments, carotenoid, and chlorophyll are responsible for colour properties of olive oils and considered as quality parameters of olive oils that affect the consumer choices [7]. The content of

chlorophyll decreases during the maturation of olives which converted to the pheophytin components, turning the oil colour from green to yellow [9]. The oxidation reaction is important for deterioration process in lipid-containing foods and for overcoming the deterioration reaction of many synthetic compounds that contained butyl of anisole, toluene, quinone that were used as additives in lipid-containing foods. In recent years, some reports revealed that the synthetic antioxidants might be implicated in health risks; hence, some countries do not allow the application of these synthetic compounds [10].

Olive oils contain phenolic compounds, which are phenolic acids like caffeic, *p*-coumaric, cinnamic, ferulic, benzoic, gallic, elenolic and vanilic acid; simple phenols like tyrosol, hydroxytyrosol, luteolin, quercetin, apigenin, rutin, and secoiridoid; and glycoside derivatives that contain oleuropein and its constituents [11, 12]. In addition to olive oil composition, olive leaves contain simple phenols such as hydroxytyrosol, the acids of tyrosol, gallic, caffeic, ferulic, *p*-coumaric, cinnamic and verbascoside; flavonoids such as quercetin, rutin, catechin, apigenin, and lutelin; and secoiridoids such as oleuropein, ligstroside, and oleuropein aglycone [13, 14]. A substantial similarity in terms of phenolic compounds is seen by considering the olive oil composition and its leaves.

Although olive oils are produced from olive fruits as olive oils (virgin and extra virgin), and great portions of olive oils are being refined to be edible. The refined olive oils are sensitive to deterioration reactions the storage period due to the lower content of phenolic compounds and pigments, especially chlorophylls. The enrichment of refined oils with natural additives to overcome deterioration reactions becomes of great interest. In especially, natural antioxidants and pigments, especially chlorophyll, carotenoid, tocopherol and polyphenols play important role in preventing oxidation reactions [10]. Olive leaves are the major by-products of oil processing and its industry, which contain numerous phenolic compounds having strong radical scavenging activities. Besides, olive leaves are rich in pigments, antioxidants, and phenolic compounds, which have been used against for neurotic disorders, cancer, hypotensive, hypoglycemic and microbial activities [15-17]. The pharmacological effects of leaves or their extracts are featured to the presence of polyphenols contains mainly oleuropein, hydroxytyrosol, verbascoside, tyrosol, apigenin and luteolin-7-glucoside [18, 19]. In addition, in a study of animals, especially rats based on the pharmacological effects of phenolic constituents, the oral amount of olive leave extracts decreases infarct volume, brain edema, barrier permeability of brain, and ameliorates neurologic deficit scores after impermanent cerebral artery plugging [20]. The addition of olive leaves (3%) before crushing of olive fruits improves phenolic contents, oxidation stability, aroma profiles, and sensory properties that are greenness, fruitiness, bitterness and pungencies of olive oils that perceived by the participants during the sensory evaluation of olive oil samples [21]. The pigment extract of olive leaves, especially chlorophyll, improves the stability of refined oil by inhibiting thermal deterioration and enhancing hydrolytic stability of refined olive oils during the storage [10], and significantly improves resistance to the oxidation, nutritional qualities, as well as enhances the appearances of over mature fruits of olive oils [22].

Olive leaves are important by-products of olive oil factories as waste source and this research was arranged to investigate the changes of physical and chemical properties of refined olive oils as a function of additional olive leaves at different ratios (5-15%). The free acidity (%), peroxide values (meq O_2 kg^{-1}), values of K_{232} and K_{270}, bitter index (K_{225}), chlorophylls (mg kg^{-1}), carotenoid (mg kg^{-1}), phenols, its constituents (mg GAE kg^{-1}), DPPH (%), and sensory evaluations were examined as physical and chemical properties of refined olive oils [23-25]. In addition, the optimal range of olive leave addition to make the parameter values of refined olive oil closer to the desired values was also determined in this research.

MATERIALS AND METHODS

Materials. The refined and virgin olive oils (from Gemlik cultivars) were get from a local olive oil factory in Osmaniye, Turkey. In October, olive leaves were supplied from an olive oil factory especially Gemlik olive cultivars which commonly cultivated in Osmaniye, then, washed, dried at atmospheric conditions (25 ºC), crushed, milled, and sieved. The olive leave particles (< 0.5 mm) were added to the refined olive oils at different ratios (5-15%), and stirred for each day and stored in dark place with glass container for 30 days at 20 ºC. The reagents, chemicals, and phenolic standards were supplied from the companies of Merck (Germany), Sigma (USA), and Fluka (Switzerland).

Methods. Quality Indices. The determined values of the peroxide, free acidity, spectrophotometric absorbance values of K_{232} and K_{270} were met to the EU standards. [26].

Total Phenols (mg GAE kg^{-1}). Refined olive oils containing olive leaves were filtered by filter paper before the analytical process. The olive oil samples obtained from the control, virgin and refined olive oil containing olive leaves were 1 g and the mixture of 5 ml CH_3OH/H_2O was poured to the sample (60:40 v v^{-1}). Thereafter, they were shaken along 2 min. and were filtered from the filter of 0.45 µm (PTFE) after centrifuged for 10 min. at a revolution of 3500 per min. The procedure was repeated for the rest portion by adding 5 ml of CH_3OH/H_2O then 10

ml of pure water was poured to the extracted volume. The mixture of 0.1 ml was taken from the extract and it was poured to 50 ml of volumetric flask. Then, 5 ml distilled water and Folin-Ciocalteu solution (0.5 ml) was poured to these flasks and the mixture was kept for 3 min., the volume was completed by distilled water (50 ml) with adding 1 ml of Na_2CO_3 (35% w v^{-1}). The mixture was kept in a dark place along 2 hours and absorbance value of mixture was evaluated at 725 nm (Shimadzu UV 1800, Japan) against the replicate solution and the results were obtained in terms of mg of GAE per kg. Finally, the same analytical procedures were made for olive leaves [23].

Chromatographic Analysis of Phenolic Constituents. Stock solutions of olive oil phenols were prepared in CH_3OH at 2 mg ml^{-1} and standard stocks of chemicals were prepared by serial dilution of solutions containing CH_3OH/H_2O mixture. Compounds in total phenols were seperated using the HPLC (Thermo Dionex; CA, USA), which is consisted of solvent efficient pump that attached to an array detector (diode) and spectrophotometer. The 1 µl samples obtained from phenolic extracts and olive leaves were splited on the column (250x4.6 mm x5 µ; Interstil, Japan). The separation process on the C_{18} ODS-3 column was made using a gradient elution volume from 10 to 70% CH_3OH along 9 min and 100% CH_3OH along 2 min at a rate of 1 ml per min. The ratio of mobile portion was 19 to 1 (v v^{-1}), water-formalin and methanol-formalin mixtures (solvent A and B). The photodiode array detector and absorbance values were used to determine the phenolic compounds (280 and 320 nm). The quantities of phenolic compounds that are hydroxytyrosol, tyrosol (2-4-hydroxyphenylethanol), oleuropein, the acids of vanillic, caffeic, *p*-coumaric, *o*-coumaric, vanillin, cinnamic, ferulic, apigenin, syringic, luteolin and gallic acid were determined according to the peak areas compared with phenolic standards [18, 24].

DDPH (2,2-diphenyl-1-picrylhydrazyl radical, %). The method of radical scavenging activity (DPPH, %) was used to determine the inhibition % of total phenols (DPPH, %) obtained from the oil samples. The mixture of 0.1 ml of the extracted volume was poured to 2.9 ml DPPH mixture, kept in dark place for 30 min., and the absorbances were measured at 515 nm by spectrophotometer (Shimadzu UV 1800). The radical scavenging activities of olive samples (DPPH, %) were measured in terms of % inhibition as below [25]:

[Eq.1]

$$\text{DPPH \% (Antioxidant Activity)} = \left[\left(A_{control} - A_{sample}\right)/A_{control}\right].100$$

Bitter Index (K_{225}). 1 g of olive oil sample was dissolved in 5 ml of hexane solvent, and after that it was extracted with CH_3OH/H_2O mixture (5 ml,60/40). The extracted solution was mixed by Vortex equipment and centrifuged at a revolution of 3500 for 10 min. The layer of hexane was removed and the polar phase of mixture was transferred to a flask by adding 10 ml of CH_3OH/H_2O mixture (60/40). 5 ml of CH_3OH/H_2O solution was poured to the flask and after that the absorbance values of solution was obtained at 225 nm. Bitter index of olive oil samples was calculated by

$$K_{225} = A_{225}/C \qquad \text{Eq.[2]}$$

where; C: g of olive oil/100 ml and A_{225}: at 225 nm [24].

Pigment Contents (mg kg^{-1}). The chlorophyll contents of refined olive oil samples were evaluated by using the extinction coefficients by dissolving 7.5 g of oil samples in the solution of cyclohexane (25 ml). The extinction coefficient was calculated as E_0= 613 for pheophytin 'α' by the equations as below;

$$\text{Chlorophyll}\left(\text{mg kg}^{-1}\right) = \left(A_{670}.10^6\right)/(613.100.d) \qquad \text{Eq.[3]}$$

$$\text{Carotenoid}\left(\text{mg kg}^{-1}\right) = \left(A_{470}.10^6\right)/(2000.100.d) \qquad \text{Eq.[4]}$$

where; A is the absorbance at 670 and 470 nm and *d* is cell thickness (1 cm) of spectrophotometer [26]. The pigment concentrations were expressed in terms of mg pheophytin α and luteolin per kg of refined olive oil samples, respectively.

Sensory Analysis. 10 proficient person (aged between 29-44) participated in the experiment at which proficient persons were educated to recognize and the perceived rate of bitterness intensity by using standard solutions of quinone monohydrochloride dehydrate as 0.020, 0.035, and 0.045 g/L. During the educating period, proficient persons were inquired to differentiate the bitter index by using a scale from 0 to 10 cm. according to standard process of sensorial analysis. 10 proficient persons were also trained according to bitterness of olive oil by the compution of standard olive oils and like-minded on the description of this property, defined as characteristics taste of the olive oil produced from olive samples.

The oil samples, i.e., enriched with olive leaves, olive oils (refined), and virgin olive oils (control) were presented in coloured glass cups to hide the differences, thus, extinguishing the optical factor. The olive oil temperature was maintained at 28 ºC. The participants were said to get the olive oil samples in their mouth and to allow all the oil samples to reach to the back of their tongue. The positive attributes such as the perceived bitterness, fruitiness, pungency, greenness, and negative attributes were asked to participants to be rated by using a non-structured scale at 10 cm. After the evaluations of samples, participants washed their mouths for 45 second to get

crackers or apple slices [27-29].

Methods for determining the optimal range. In this study, the attribute (chemical and sensorial attributes of olive oil) units of olive oil are different. Therefore, the unique optimal value appropriate for all attributes cannot be determined by averaging the attribute values that calculated by modelling or interpolation. If so, the units of attribute values calculated using modelling or interpolation must be distributed (normalized) to a limited range at first step. Then, the optimal value should be calculated by averaging the normalized attribute values.

In fact, the attribute units can be normalized by distributing values into 0-100 range and each unit can be represented as percentage. In this case, the average of attribute values obtained by interpolating or modelling will have a single optimal value instead of optimal range. But, determining a single optimal value in food engineering experiments is not correct due to various factors [30]. This problem can be eliminated by transforming attributes into representative images then using histogram equalization for the average of images.

For the reasons mentioned above, each attribute was transformed into 4x1 dimensional grayscale image in the first step of this study. Then, dimensions of images were enlarged using bi-linear interpolation method in the second step. Thus, the representative gray tones for all percentages (between 0% - 15%) of olive leaf addition were generated in the second step. Finally, the optimal range was determined by applying histogram equalization to the average of images.

Transforming Attributes into Images. Transforming attributes into images is a recently introduced method in food engineering literature [30-32]. Thanks to this method, attribute values can be matched to gray tones between black and white. Thus, the attribute value that closest to optimal value (assumed as white) can be matched to the lightest gray tone (closest to white) while the attribute value that farthest to optimal value can be matched to the darkest gray tone or black. In this study, the attribute value farthest to optimal value was assumed as black because it is the worst value detected in the experiment (The possible worst value is assumed as black in image transformation method). Other values can be matched to gray tones faithful to relative distances between each other. Transforming attributes into images can be done by Equation 5.

$$\begin{cases} \text{If } O_A \text{ is smaller than } A_{min} & , \quad I = \|(2^n - 1).\left(1 - ((A - A_{min})/(O_A - A_{min}))\right)\| \\ \text{If } O_A \text{ is greater than } A_{max} & , \quad I = \|(2^n - 1).(A - A_{min})/(O_A - A_{min})\| \end{cases} \quad \text{Eq.[5]}$$

In addition, if O_A is between the A_{max} and A_{min}, the values A that greater than O_A should be reduced two times by their distance to O_A, then the second condition of Equation 5 should be applied.

In the Equation 1, I is the values corresponding to gray tones, A is the values of attributes, A_{max} is the maximum of A, O_A is the optimal value for A and n is the bit-depth. Bit-depth is the value that determines the number of possible gray tones in the image. It used to obtain image that identical to attribute values. If it is lower than minimum required, image will not identical to attribute. Optimal bit depth can be determined by trying values from 1 to ∞ until the number of gray tones are stable.

Histogram Equalization. Histogram equalization is a method aims to provide contrast between dissimilar gray tones while making the similar gray tones same. The method actually assigns values corresponding to visually similar gray tones to a single value (creates gray tone segments). This feature allows to make the statistically similar values equal and the values that are not statistically different from single optimal value are determined as optimal range. In the histogram equalization method, the combined values in single value are also distributed between black and white to create better contrast. In other words, the image obtained by combining some gray tones is equally distributed between black and white as far as possible [30,33]. In summary, this method provides to the create optimal range instead of a single optimal value. The flow-chart of analysis methods used in the study can also be seen from Figure 1.

RESULTS AND DISCUSSIONS

Chemical Profiles. The fresh and dried olive leaves contained 52.61% and 0.521% moisture, respectively. The total phenol contents of olive leaves were found as 9013 mg GAE kg^{-1} and the results of quality indices of refined, virgin, and refined olive oils containing olive leaves at different ratios (5-15%) were given in Table 1.

Free acidity of olive oils is considered as a quality factor for classifying the samples. The free acidity of refined, virgin, and enriched with olive leaves of refined olive oil samples whose values ranged between 0.91-1.29% exceeded the upper limit of 0.8% according to council standards of olive oil [26]. The refined olive oils contained olive leaves slightly decreased the free acidity (%) and olive oil that refined with/without leaves had higher acidity value than virgin olive oil samples. This acidity of refined olives showed similarity to the Turkish varieties that is ranged between 0.5 to 1.17% [30] but was higher than Tunisian [21] and Algerian wild olive oil samples [24]. At a ratio of 3% leaves added to the olive varieties increases the free acidity [21] and addition of olive leaves to the refined olive oils showed similarity in respect of olive oils (refined) and the virgin olive oils in our results.

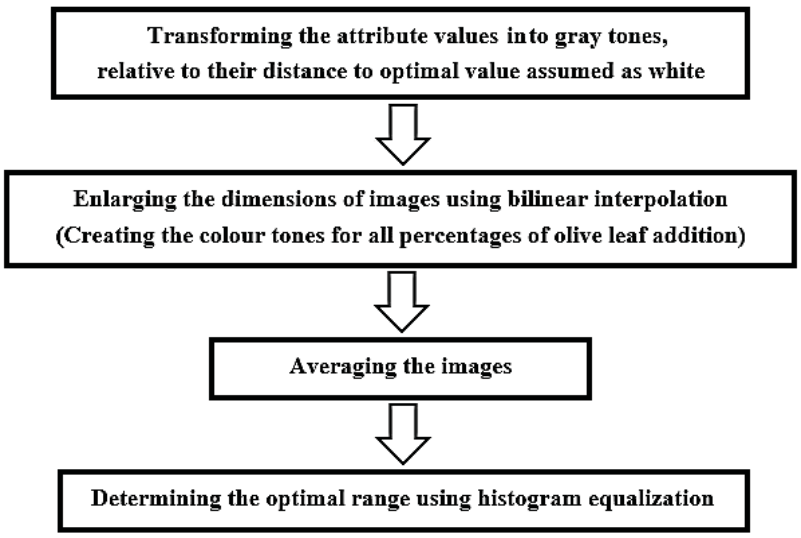

FIGURE 1
Flow-chart of methods used to determine the unique optimal for all attributes

TABLE 1
Quality indices of refined, virgin and olive leaves added refined olive oil samples

Quality index	Refined olive oil (control)	Refined olive oil (5%)	Refined olive oil (10%)	Refined olive oil (15%)	Virgin olive oil (control)
Free acidity (% oleic acid)	1.29[a]	1.15[b]	1.24[a]	1.11[b]	0.95[c]
Peroxide value (meq O_2 kg^{-1})	8.32[d]	8.57[d]	10.93[c]	12.19[b]	15.81[a]
K_{232}	2.73[b]	2.53[c]	2.76[b]	3.53[a]	2.03[d]
K_{270}	0.74[b]	0.67[b]	0.75[b]	0.96[a]	0.210[c]

Different letters in row indicate significantly different values (p<0.05)

The peroxide values of olive oils which are main analytic parameters showing a measurement of lipid oxidation ranged between 8.32 and 15.81 meq O_2 kg^{-1} lower resulting than the upper values indicated by the International Olive Oil Council [26] (EEC 2568/91). The highest peroxide value was observed in the virgin olive oils (15.81 meq O_2 kg^{-1}) and olive leaves added to the refined oil samples at a artio of 10 and 15 (%) resulted an increase in peroxide values, significantly (p<0.05). It is reported that olive oils (Cobrançosa vr.) that contained olive leaves (1-10%) during oil processing increases the peroxide values by favouring respiration process of gases and the obtainable oxygen level [22]. It is reported that addition of olive leaves (3%) before olive oil extraction procedure increases peroxide values significantly (monovarietal Tunisian olives) [21]. Our results are in agreement with the results of Sonda et al. [21] for Chemlali, Zalmati, Chetoui olive varieties in Tunisia and Cobrançosa variety in Portugal [22].

Spectrophotometric characteristics of oil samples were expressed by determining the coefficients of K_{232} and K_{270} at 232 and 270 nm where the absorbance of oxidation products show extensive oxidation reactions in oil/fat-containing products. The olive oil samples showed that K_{232} and K_{270} values varied from 2.03 to 3.53 and from 0.210 to 0.96, respectively. Refined olive oil (control sample) and olive oils containing 5 and 10% olive leaves exhibited similar K_{232} and K_{270} levels. By contrast, olive oil containing 15% olive leaves had significantly higher K_{232} and K_{270} values than virgin olive oil samples. The specific extinction coefficients of olive oil samples that contain 5 and 10% olive leaves were higher than Algerian wild olive oils, K_{232} from 1.69 to 1.78; K_{270} from 0.05 to 0.18 [24]; Tunisia olea star variety, K_{232} from 1.61 to 2.36 and K_{270} from 0.12 to 0.17 [9]; Cobrançosa olive oil that contains different amount of olive leaves, 0-10%, K_{232} from 1.63 to 2.07 and K_{270} from 0.09 to 0.16 [22]; and higher than Memecik and Edremit variety, K_{232} from 1.42 to 1.73 and K_{270} from 0.04 to 0.10 for Memecik, K_{232} from 1.49 to 1.59 and K_{270} from 0.03 to 0.13 for Edremit variety [18]. Determination of K_{232} and K_{270} spectrophotometrically provides information about oil quality and possible changes in olive oil samples. Refined olive oil that contains olive leaves, especially the 15% sample, indicate an increase in the oxidation as well as had higher specific extinction coefficients than other olive oil samples, and these results are in agreement with the results of Malheiro et al. [22] and Sonda et al. [21] respectively.

The values of bitter index ranged between 1.50 to 4.50, refined olive oil exhibiting the lowest K_{225} and refined olive oil containing 15% olive leaves the

highest K_{225} value (Figure 1). Bitterness of olive oil (virgin, control sample) and refined olive oil were 4.18 and 1.50, respectively. Olive leaves added to the refined oils increased the bitterness significantly (Figure 1). The bitter index of Gemlik, Halhali, and Sarı Haşebi cultivars that cultivated in Hatay province changed between 0.31 and 0.72 [34], while for Coratina, Ogliarola, Maiatica, Leccino, and Blend varieties that grow in Italy changed between 0.21 and 0.40 [28], and apparently, our results were higher for these olive cultivars. There is a close resemble between the bitterness of olive oil samples and the phenol contents (mg GAE kg^{-1}), and increase in phenol contents of olive oils increase the bitterness [5, 36]. The total phenols that related to bitterness and pungency of olive oil (virgin) are positively evaluated to the intensities of virgin olive oils and they constitute defence mechanism against phytopathogens with bitter characters [24]. The amount of phenolic compounds in refined and virgin olive oils ranged between 109.8 mg GAE kg^{-1} and 143.4 mg GAE kg^{-1}, and its contents ranged between 138.6 mg GAE kg^{-1}, 217.9 mg GAE kg^{-1}, and 233.2 mg GAE kg^{-1} for refined olive oil containing 5, 10, and 15% olive leaves, respectively (Figure 1). As seen in Figure 1, significant differences were obtained ($p<0.05$) among refined olive oils and refined olive oil samples that contained olive leaves. Olive oils are chemically characterized in terms of phenolic contents having antioxidant properties, beneficial effects for human health and their contents ranged between 50 and 800 mg kg^{-1} (GAE) depending on climatic conditions, varieties, ripening, harvesting time, geographical region, and irrigation [12, 37]. There is an increasing trend for phenolic components of olive oils due to biological attributes [36], consequently, the addition of olive leaves to the refined olive oils increased the total phenol levels more than two times compared to refined and virgin olive oils (Table 2). In fact, the phenolic constituents of olive leaves are similar to the phenolic constituents of olive oil [11, 13], and our results confirmed the results those obtained by Jaber et al. [10] and Sonda et al. [25].

Having green colour, chlorophyll pigments, which are important constituents for olive oil stability, are mainly found in foodstuff. Chlorophyll concentrations ranged between 1.14 mg kg^{-1} and 3.81 mg kg^{-1} for refined and virgin olive oil, its contents changed between 11.03 mg kg^{-1}, 23.54 mg kg^{-1}, and 36.55 mg kg^{-1} for refined olive oils containing 5, 10, and 15% olive leaves, respectively (Table 2). Carotenoid concentrations responsible for yellow colour in foodstuff ranged between 0.625 mg kg^{-1} and 1.84 mg kg^{-1} for refined and virgin olive oils and its concentrations changed between 3.65 mg kg^{-1}, 7.83 mg kg^{-1}, and 11.65 mg kg^{-1} for refined olive oils containing 5, 10 and 15% olive leaves, respectively.

As seen in Table 2, significant differences were determined ($p<0.05$) between refined olive oils and olive oil samples that contain olive leaves in terms of chlorophyll and carotenoid concentrations. Initial concentration of chlorophyll and carotenoids of refined olive oils were similar with those obtained by Rigane et al. [6] and Jaber et al. [10] (1.27 mg kg^{-1} for chlorophyll and 0.94 mg kg^{-1} for carotenoid). Furthermore, an addition of leaves of Chemlali variety to the refined olive oil increased the chlorophyll contents around 3 times more [10]. Additionally, carotenoid contents of Gemlik, Halhali, and Sarı Haşebi are 5.43, 6.63, and 16.57 mg kg^{-1} in terms of lutelin, whereas chlorophyll contents of these cultivars are 16.43, 24.77, and 57.57 mg kg^{-1} in terms of pheophytin, respectively [39]. Carotenoid and chlorophyll concentrations of Memecik and Edremit varieties that are responsible for the colour of olive oils (as virgin) are 12.87 and 25.90 mg kg^{-1}, respectively. These pigment concentrations decrease during the ripening period down to 0.70 and 0.95 mg kg^{-1}, respectively [18]. Pigment extracts of leaves stabilize the olive oil that refined by inhibiting thermal corruption by developing its hydrolytic stability, preventing the conjugation of double bond, and reducing the losses in poly unsaturated fatty acids [10], and again, our results are similar with those obtained by Rigane et al. [6] and Jaber et al. [10], hence, addition of olive leaves increases both carotenoid and chlorophyll pigment concentrations of refined olive oils significantly.

TABLE 2
Antioxidant activities, total phenol levels, K_{225}, chlorophyll and carotenoids of refined, virgin and olive leaves added refined olive oil samples

	Refined olive oil (control)	Refined olive oil (5%)	Refined olive oil (10%)	Refined olive oil (15%)	Virgin olive oil (control)
DPPH (%)	22^{c}	26^{c}	93.5^{a}	92.5^{a}	44.5^{b}
Total Phenols (mg GAE kg^{-1})	109.8^{d}	138.6^{c}	217.9^{b}	233.2^{a}	143.4^{c}
K_{225}	1.5^{d}	2.10^{c}	4.20^{b}	4.50^{a}	4.18^{b}
Chlorophyll (mg kg^{-1})	1.17^{e}	11.03^{c}	23.54^{b}	36.55^{a}	3.81^{d}
Carotenoid (mg kg^{-1})	0.625^{d}	3.65^{c}	7.83^{b}	11.65^{a}	1.84^{d}

Different letters in the same row indicate significantly different values ($p<0.05$)

The DPPH (%) activity of olive oil samples that extracted with methanol/water (80/20) and total phenols were given in Table 2 as percent inhibition of DPPH radical. The refined olive oils containing 10 and15% of olive leaves had higher amounts of phenolic contents with 217.9 mg GAE kg^{-1} and 233.2 mg GAE kg^{-1}, inhibited 93.5 and 92.5% of the DPPH radical, respectively.

Refined olive oils (control sample) had the lowest activity with an inhibition of 22% (109.8 mg GAE kg^{-1}) and virgin olive oil had the activity with an inhibition of 44.5% (143.4 mg GAE kg^{-1}). The refined olive oils containing 10 and 15% olive leaves had higher activities with an inhibition of 93.5 and 92.5% (217.9 mg GAE kg^{-1} and 233.2 mg GAE kg^{-1}), respectively. Hydroxytyrosol and tyrosol, main phenolic alcohols of olive oils are responsible for antioxidant effect and higher amount of these phenolic compounds justify high antioxidant power against to lipid peroxidation. It is reported that inhibition level of lipid peroxidation for seven olive varieties in Spain changed between 23.1 and 45.1% [38]. In our study, there was a slight increase in DPPH (%) for refined olive oil that contain 5% olive leaves and a sharp increase in DPPH (%) for refined olive oil that contain 10 and 15% olive leaves. Therefore, the addition of olive leaves containing higher amounts of phenolic alcohols to the refined olive oils introduces better antioxidant profiles of refined olive oils containing 10 and 15% olive leaves, respectively (Table 2).

The phenolic substances of olive leaves and olive oils were defined and measured by HPLC system by using corresponding standard curves that were linear over the studied range and regression coefficient (r^2)>0.98 for phenolic constituents. The analytical procedure of phenolic constituents allowed the separation and determination of 11 phenolic constituents among 14 phenolic standards; all of them were identified by HPLC (Table 3) whereas caffeic acid, syringic acid, and gallic acid not determined for olive leaves. Among the phenolic constituents, luteolin, ferulic acid, vanillic acid, and *p*-coumaric acid were not found in refined olive oil (control sample). Statistically significant differences were found in phenolic constituents (p<0.05) for olive leaves and olive oil samples. Major phenolic constituent of olive leave was oleuropein and its concentration was found as 739.13 mg GAE kg^{-1}. Additionally, it was determined that olive leave was a good source of apigenin, *o*-coumaric acid, luteolin, ferulic acid, *t*-cinnamic acid, and tyrosol as a phenolic constituent as shown in Table 3. Hydroxytyrosol concentration that is phenolic alcohol with high antioxidant activity was 38.694 mg GAE kg^{-1}. Moreover, vanillin, *p*-coumaric acid, and tyrosol whose concentrations changed from 4.060 to 21.326 mg GAE kg^{-1} were the first group to be identified by HPLC method in olive leave and olive oil samples. Our results showed that leaves are fine sources of luteolin, the flavones and ferulic acid, the hydroxycinnamic acids, and consequently, our results confirmed the study related with olive leaves that conducted by Harp [39] and Talhaoui et al. [13].

Luteolin, ferulic acid, vanillic acid, and *p*-coumaric acid were not found in refined olive oil (control sample) as indicated in Table 3, and the amount of phenolic constituents were low, and their values changed from 0.024 to 1.429 mg GAE kg^{-1}. Vanillic acid, luteolin, and *p*-coumaric acid concentrations that were not found in refined olive oil (control sample) increased significantly. When comparing the increased amount of phenolic constituents of refined olive oils to the virgin olive oil, all the phenolic constituents except ferulic acid increased significantly due to the addition of olive leaves (p<0.05). Oleuropein concentrations that are responsible for bitterness changed from 3.722 to 26.354 mg GAE kg^{-1}, while luteolin changed between 13.127 and 14.438 mg GAE kg^{-1}, which is not found in olive oil (virgin) sample. Increasing in the concentration of oleuropein consisted of bitter intensity and K_{225} values of olive leaves added refined olive oil samples (Table 3).

TABLE 3
Phenolic constituents of olive leave, virgin and refined olive oils that contained olive leaves (mg GAE kg^{-1})

Phenolic Constituents	Olive leave	Refined olive oil (control)	Refined olive oil (5%)	Refined olive oil (10%)	Refined olive oil (15%)	Virgin olive oil (control)
Hydroxytyrosol	38.694^{c}	$0.801^{c,D}$	$1.423^{e,C}$	$2.885^{d,B}$	$3.144^{d,A}$	2.754^{c}
Tyrosol	21.326^{d}	$1.024^{b,D}$	$2.806^{c,C}$	$3.778^{c,B}$	$5.876^{c,A}$	3.698^{b}
Oleuropein	734.13^{a}	$1.429^{a,D}$	$3.722^{b,C}$	$13.028^{b,B}$	$26.354^{a,A}$	12.120^{a}
o-coumaric acid	70.918^{b}	$0.184^{d,D}$	$2.144^{d,C}$	$2.574^{d,B}$	$3.025^{d,A}$	0.800^{f}
t-cinnamic acid	17.151^{e}	$0.049^{e,C}$	$0.101^{g,B}$	$0.462^{h,A}$	$0.524^{h,A}$	0.077^{h}
Luteolin	39.177^{c}	-	$13.127^{a,B}$	$15.028^{a,A}$	$14.438^{b,A}$	-
Ferulic acid	33.261^{c}	-	-	-	-	-
Apigenin	87.14^{b}	$0.045^{e,C}$	$0.905^{f,B}$	$1.215^{g,A}$	$1.314^{g,A}$	1.141^{e}
Vanillin	4.060^{g}	$0.024^{f,D}$	$0.418^{e,C}$	$0.591^{h,B}$	$0.740^{h,A}$	0.560^{g}
Vanillic acid	3.651^{g}	-	$1.490^{e,C}$	$1.794^{f,B}$	$1.988^{f,A}$	1.611^{d}
p-coumaric acid	13.821^{f}	-	$1.854^{d,C}$	$2.148^{e,B}$	$2.497^{e,A}$	0.834^{f}

Small letters in column, capital letters in row indicate significantly different values (p<0.05)

t-cinnamic acid content that describing an important marker of Turkish olive cultivars [40], changed between 0.101 and 0.524 mg GAE kg^{-1}. In studies regarding the amount of phenolic constituents, the concentration of these substances varies with a wide range for olive oils from different cultivars. Tyrosol changed from 5.1 to 105, luteolin concentrations from 0.97 to 13 mg GAE kg^{-1}, hydroxytyrosol from 0.68 to 10, apigenin from 0.07 to 1.1, and oleuropein from 24 to 90 mg GAE kg^{-1} for Algerian wild olive cultivars, respectively [20]. For Turkish olive cultivars, tyrosol concentrations changed from 4.1 to 22, hydroxytyrosol from 1.1 to 26 mg GAE kg^{-1}, and oleuropein from 0.48 to 0.72 mg GAE kg^{-1}, respectively [40]. For Spanish olive cultivars, luteolin concentrations changed from 0.72 to 2.96 and apigenin from 0.17 to 0.91 mg GAE kg^{-1} [38]. For the Edremit and Memecik varieties of Turkish olive cultivars, luteolin changed from 29.26 to 63.42 mg GEA kg^{-1} and apigenin concentrations from 21.60 to 76.35 mg GAE kg^{-1}, respectively [18]. Our results showed that addition of olive leaves led the refined olive oils to become superior in terms of phenolic constituents, particularly oleuropein, luteolin, vanillic acid, *p*-coumaric acid, tyrosol and hydroxytyrosol. Finally, these results in terms of phenolic constituents consisted with the studies that conducted by Franco et al. [38], Yorulmaz et al. [18], and Bayram et al. [40].

Sensory Profiles. Sensory profiles of refined, olive leaves containing oils, and virgin olive oils were illustrated in Figure 3. Sensory profiles of olive oils were endowed with positive attributes (fruitiness, greenness, pungency, bitterness) and negative attributes [21, 28, 29]. Bitter intensities of refined and virgin olive oils changed between 3.19 and 4.14, whereas the bitterness of refined olive oils contained olive leaves changed from 4.71 to 5.49 (Figure 2), so the olive leaves addition to the refined olive oils increased the bitterness significantly, and these results consisted with the bitter index (K_{225}) of olive oil samples whose indices changed from 1.5 to 4.50. K_{225} values of refined olive oils containing olive leaves (10-15%) changed between 4.18 and 4.50 and these indices values were similar to the virgin olive oil sample that values were given in Table 2.

It is reasonable to assume that higher phenolic content of olive leaves increases the bitterness and K_{225}. Although there is a close relationship between total phenols, bitter intensity, and K_{225}, higher phenol contents do not mean higher perceived bitterness and higher K_{225}. It is reported that the highest total phenol levels are not correlated with the highest bitter intensity [41]. The pungency of refined olive oil and virgin olive oil changed between 4.25 and 5.99, respectively. Olive leaves affected the perceived pungency of refined olive oils significantly and whose values changed between 4.61 and 5.49. There was a great effect on the greenness of refined olive oils, and olive leaves addition increased the colour intensity of refined olive oils. Its value changed between 2.87 and 5.5 for refined and virgin olive oils, respectively. The greenness of refined olive oils containing olive leaves (5-15%) changed between 6.66 and 7.60, respectively. The degree of crushing and milling of olive leaves improves the pigment transition to the refined olive oils and sensory results of greenness refined olive oils containing olive leaves consistent with the results for chlorophyll in Figure 2, and the results of studies that conducted by Rigane et al. [6].

The olive leaves addition to the refined olive oils increased the perceived fruitiness, and these fruitiness values that changed between 6.36 and 7.84. The fruitiness of refined and virgin olive oil changed between 5.27 and 6.36, respectively. Adding olive leaves to the refined olive oils significantly affected the fruitiness value ($p<0.05$). The negative attributes of olive oils such as rancid, musty/muddy sediment, winey/vinegary acid/sour, and frostbitten olive taste were evaluated by participants and perceived negative attributes were lower than 2.20. Addition of olive leaves to the refined olive oils improved greenness, bitterness, and pungency of refined olive oils significantly, and there was a slight increase in fruitiness of refined olive oils. The aromatic profiles of refined olive oils were not distorted, and participants perceived higher intensities of greenness, pungency and bitterness. Addition of olive leaves at different ratios affect the sensory profiles of refined olive oils for Gemlik variety and our results are consistent with that of Cobrançosa olive variety which was conducted by Malheiro et al. [22] and monovarietal olive cultivars which was conducted by Sonda et al. [21].

The optimal olive leaves addition range. According to the findings obtained in the study, 10% and 15% added olive leaves are optimal for most of the refined olive oil properties (attributes). However, it will be more accurate to determine the optimal range that satisfies all attributes as much as possible and the center of this range should be suggested to avoid the experimental and environmental factors that can change the result. Therefore, the experimental results of chemical and sensory attributes were first transformed into grayscale images then the images were enlarged using image interpolation. Thus, all attributes were represented with same unit. The bit-depth was selected as 32 to obtain gray tones identical to attribute values and the agreed (selected) optimal values for the attributes can be seen in Table 4. Also, the representation of chemical and sensory attributes with grayscale images are represented in Figure 3.

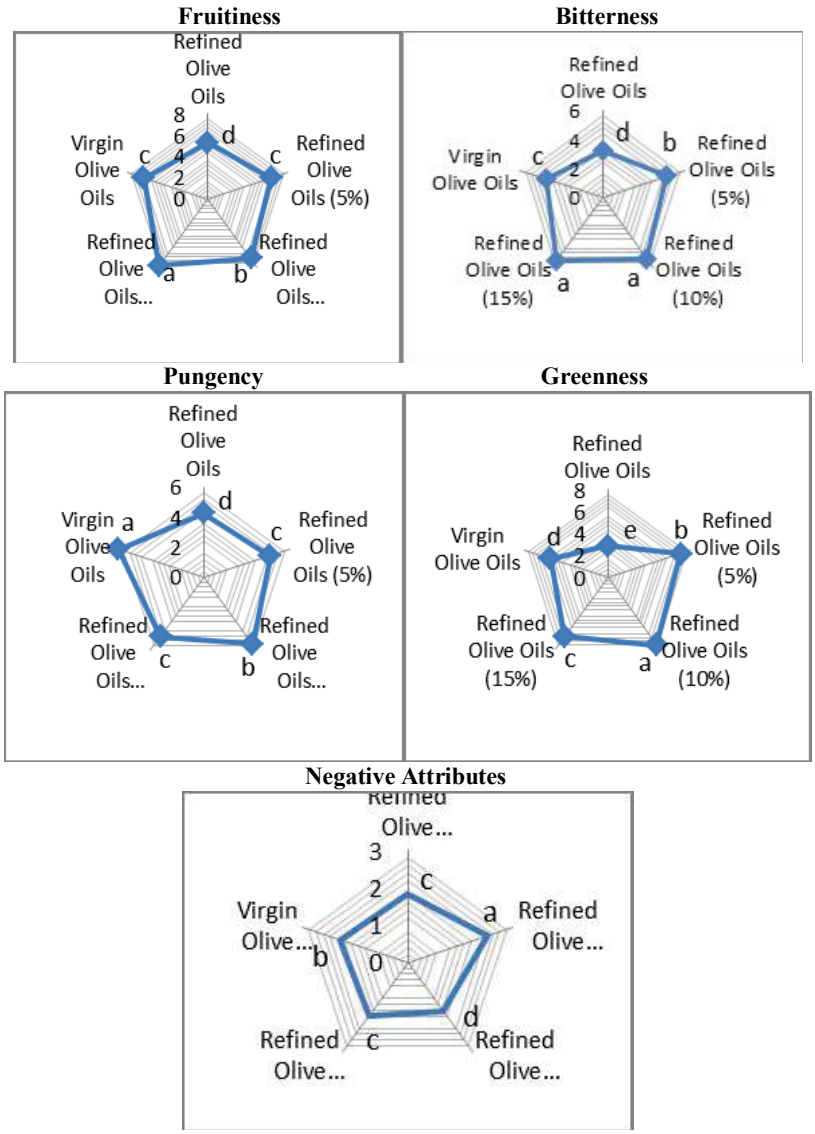

FIGURE 2

Sensory spider plots of refined, olive leaves added (5-15%) refined olive oils and virgin olive oil for Gemlik olive cultivar for fruitiness, bitterness, pungency, greenness and negative attributes.

The values of named by letters [a, b, c, d] show significantly different ($p<0.05$)

TABLE 4

The agreed (selected) optimal values for the attributes

Quality Index	Agreed (Selected) Optimal Value
Free Acidity (% Oleic Acid)	Values of virgin olive oil
Peroxide Value (meq O_2kg^{-1})	
K_{232}	
K_{270}	
DPPH (%)	100
Total Phenols (mg GAE kg^{-1})	Maximum value measured from the olive leave added olive oils
Chlorophyll (mg kg^{-1})	
Carotenoid (mg kg^{-1})	
K_{225}	Value of virgin olive oil
Fruitiness	9
Bitterness	
Pungency	
Greenness	
Negative Attributes	0

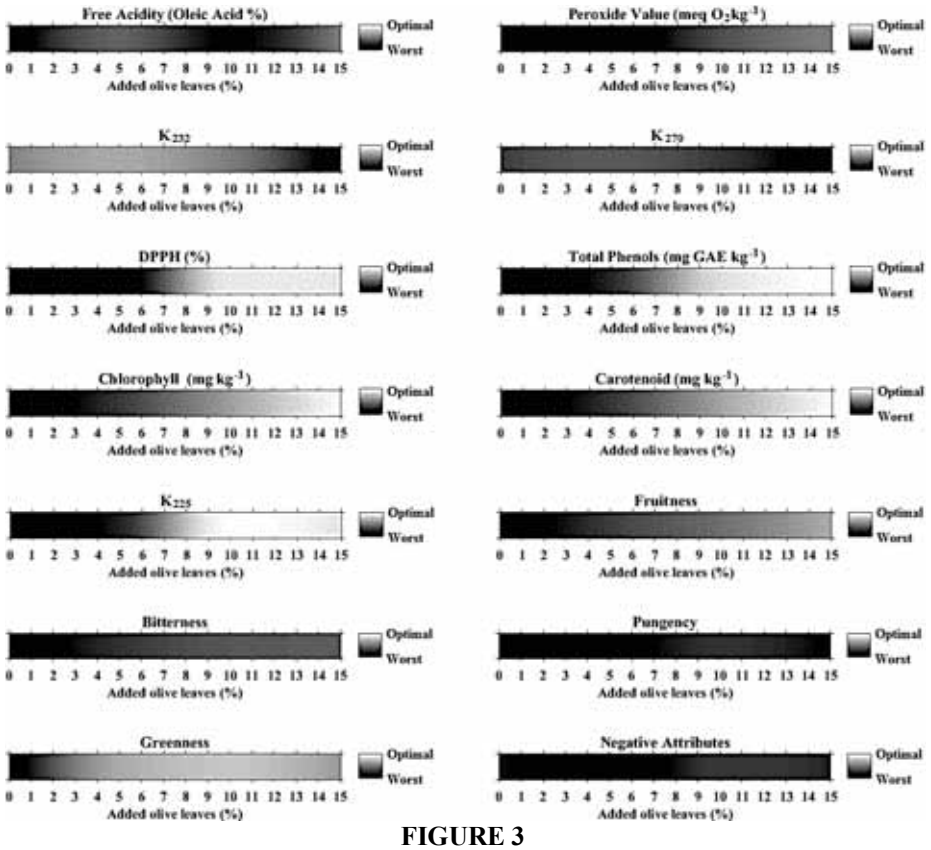

FIGURE 3
Image representation of chemical and sensory attributes of the olive leave added olive oil

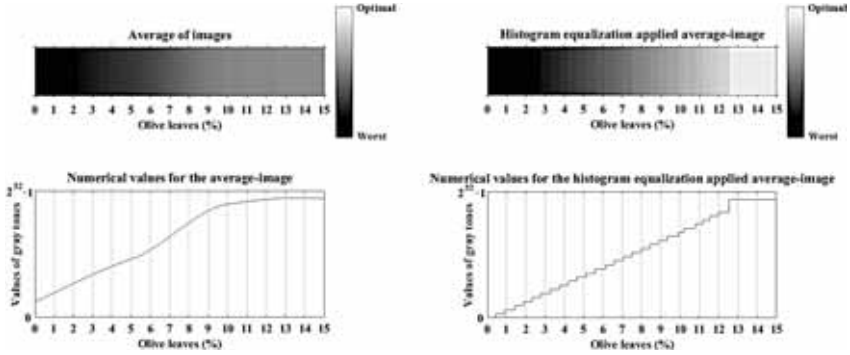

FIGURE 4
Average of attribute images and its enhanced from obtained by histogram equalization

As shown in the Figure 3, all the images are consistent with the ratio between the values of the experimental results. Then, the Figure 4 shows the average image that will satisfy all attributes equally. As can be seen in the Figure 4, adding the olive leaves between 12.5-15% provides statistically same results and this range is optimal since the lightest gray tone means the optimal. In this case, the center of optimal range is 13.75% and it can be said that this percentage should be preferred to satisfy all attributes equally.

CONCLUSIONS

The use of olive leaves in any ways will help preventing environmental waste problem of olive oil industries. Olive leaves, which are important by-products of olive oil processing and its industry, contain a large variety of phenolic constituents, simple phenols, secoiridoids, pigments and these constituents are similar to the olive oil composition. Olive leaves affected the quality indices of refined olive oils in terms of peroxide values and extinction coefficients (K_{232} and K_{270}) but decreased the free acidity significantly. Bitter index (K_{225}), chlorophyll, carotenoid, DPPH (%), and total phenols increased with the increasing addition of olive leaves to the refined

olive oils. 11 phenolic constituents out of 14 compounds were identified in olive leaves and particularly oleuropein, luteolin, hydroxytyrosol, tyrosol, and vanillic acid concentrations of refined olive oils increased significantly. Olive leaves addition to the refined olive oils positively affected the greenness, bitterness, pungency, as well as fruitiness of refined olive oils in terms of positive attributes. Chlorophyll and carotenoid concentrations increased up to 10 times. In summary, it was determined that the refined olive oils containing olive leaves at optimal range (between 12.5 and 15%) had superior properties compared to virgin olive oils with respect to chemical and sensorial properties. Then the center (13.75%) of optimal range was proposed to avoid the possible negative effects. Additional researches are necessary to approve these obtained results, to better characterize the transition of phenolic constituents from olive leaves; therefore, to improve the chemical and sensorial properties of refined olive oils.

In the study, the change of the properties of refined olive depending on the olive leave addition percentage has also presented by visually interpretable images. These easy interpretable images and the methods used for obtaining images will be useful resource for future studies.

REFERENCES

[1] Kiritsakis, K., Goula, M.A., Adamopoulos, G.K., Gerasopoulos, D. (2017) Valorization of Olive Leaves: Spray Drying of Olive Leaf Extract. Waste Biomass Valor. 9, 619–633.

[2] FAOSTAT (2015) Database.

[3] Jacimovic, D., Kosovic, M., Sukovic, D., Pekic, M., Radulovic, D., Jacimovic, Z. (2017) Ecological entrepreneurship-olive production potential in Montenegro. Fresen. Environ. Bull. 26, 2678-2683.

[4] Ozden, A., Dios-Palomares, R. (2015) Environmental, quality and technical efficiency in olive oil industry: a metafrontier comparison between Turkey and Spain. Fresen. Environ. Bull. 24, 4353-4363.

[5] Aguilera, M.P, Jimenez, A., Sanchez-Villasciaras, S., Uceda, M., Beltran, G. (2015) Modulation of bitterness and pungency in virgin olive oil from unripe 'Picual' fruits. European Journal of Lipid Science and Technology. 117, 1463-1472.

[6] Rigane, G., Bouaziz, M., Sayadi, S., Salem, R.B. (2013) Effect of storage on refined olive oil composition: stabilization by addition of chlorophyll pigments and squalene. Journal of Oleo Science. 62(12), 981-987.

[7] Bengana, M., Bakhouche, A., Lozano-Sanchez, J., Amir, Y., Youyou, A., Segura-Carretero, A., Fernandez-Gutierrez, A. (2013) Influence of olive ripeness on chemical properties and phenolic composition of Chemlal extra-virgin olive oil. Food Research International. 54, 1868-1875.

[8] Kotsiou, K., Tasioula-Margari, M. (2016) Monitoring the phenolic compounds of Greek extra-virgin olive oils during storage. Food Chemistry. 200, 255-262.

[9] Dabbou, S., Selvagginib, R., Urbanib, S., Taticchib, A., Servili, M., Hammami, M. (2011) Comparison of the chemical composition and the organoaleptic profile of virgin olive oil from two wild and two cultivated Tunisian Olea europaea. Chemical Biodiversity. 8,189-202.

[10] Jaber, H., Ayadi, M., Makni, J., Rigane, G., Sayadi, S., Bouaziz, M. (2012) Stabilization of refined olive oil by enrichment with chlorophyll pigments extracted from Chemlali olive leaves. European Journal of Lipid Science and Technology. 114, 1274-1283.

[11] Caruso, D., Colombo, R., Patelli, R., Giavarini, F., and Galli, G. (2000) Rapid evaluation of phenolic profile and analysis of oluropein aglycon in olive oil by atmospheric pressure chemical ionization-mass spectrometry (APCI-MS). Journal of Agriculture and Food Chemistry. 48, 1182-1185.

[12] Ryan, D., Antolovich, M., Prenzler, P., Robards, K., Shimon L. (2002) Biotransformations of phenolic compounds in Olea europaea L. Scientia Horticulturae. 92, 147-176.

[13] Talhaoui, N., Taamalli, A., Gomez-Caravaca, A.M., Fernandez-Gutierrez, A., Segura-Carretero, A. (2015) Ohenolic compounds in olive leaves: analytical determination, biotic and abiotic influence, and health benefits. Food Research International. 77, 92-108.

[14] Tsimidou, M.Z., Papoti, P.V. (2010) Bioactive ingredients in olive leaves. In: Preedy, V.R., Watson, R.R. (Eds.) Olives and olive oil in health and disease prevention. Chapter 39. Elsevier, London, 349-356.

[15] Bouaziz, M., Grayer, R.J., Simmonds, M.S.J., Damak, M. and Sayadi, S. (2005) Identification and antioxidant potential of flavonoids and low molecular weight phenols in olive cultivar Chemlali growing in Tunisia. Journal of Agriculture and Food Chemistry. 53, 236-241.

[16] Mkaouar, S., Bahloul, N., Gelicus, A., Allaf, K., Kechaou, N. (2015) Instant controlled pressure drop texturing for intensifying ethanol solvent extraction of olive leaf polyphenols. Separation and Purification Technology. 145, 139-146.

[17] Lafka, T.I., Lazou, A.E, Sinanoglou, V.J., Lazoz, E.S. (2013) Phenolic extracts from wild olive leaves and their potential as edible oils antioxidants. Foods. 2, 18-31.

[18] Yorulmaz, A., Erinc, H., Tekin, A. (2013) Changes in olive and olive oil characteristics during maturation. Journal of American Oil Chemists Society. 90, 647-658.
[19] Arslan, D. (2012) Physico-chemical characteristics of olive fruits of Turkish varieties from the province of Hatay. Grasas Y Aceites. 63(2), 158-166.
[20] Mohaghegi, F., Bigdeli, M.R., Rasoulian, B., Hashemi, P., Pour M.R. (2011) The Neuroprotective effect of olive leaf extract is related to improved blood-brain barrier permeability and brain edema in rat with experimental focal cerebral ischemia. Phytomedicine.18, 170-175.
[21] Sonda Akram, Z., Boutheina, G., Guido, F., Mohamed, B. (2014) Effect of addition of olive leaves before fruits extraction process to some monovarietial Tunisian extra-virgin olive oils using chemometric analysis. Journal of Agriculture and Food Chemistry. 62, 251-263.
[22] Malheiro, R., Casal, S., Teixeira, H., Bento, A., Pereira J.A. (2013) Effect of olive leaves addition during the extraction process of overmature fruits on olive oil quality. Food Bioprocess Technology. 6, 509-521.
[23] Hrncirik, K., Fritsche, S. (2004) Comparability and reliability of different techniques for the determination of phenolic compounds in virgin olive oil. European Journal of Lipid Science and Technology. 106, 540.
[24] Bouarroudj, K., Tamendjari, A., Larbat, R. (2016) Quality, composition and antioxidant activity of Algerian wild olive (Olea europaea L. subsp. Oleaster) oil. Industrial Crops and Products.
[25] Ferreira, I.C.F.R., Barros, L., Soares, M.E., Bastos, M.L., Pereira, J.A. (2007) Antioxidant activity and phenolic contents of olea europaea L. leaves sprayed with different copper formulations. Food Chemistry.103, 188-19.
[26] IOOC. (2011) Guide for the determination of the characteristics of oils-olives. International Olive Oil Council. European Union Commission Regulation EEC 2568/91
[27] Predieri, S., Medoro, C., Magli, M., Gatti, E., Rotondi, A. (2013) Virgin olive sensory properties: comparing trained panel evaluation and consumer preferences. Food Research International. 54, 2091-2094.
[28] Favati, F., Condelli, N., Galgano, F., Caruso, M.C. (2013) Extra virgin olive oil bitterness evaluation by sensory and chemical analyses. Food Chemistry. 139,949-954
[29] Amelio, M. (2016) The official method for olive oil sensory evaluation: an expository revision of certain sections of the method and a viable means for confirming the attribute intensities. Trends in Food Science and Technology. 4.
[30] Akben, S.B. (2018) A new approach to reduce the effects of omitted minor variables on food engineering experiments: Transforming the variable-result interaction into image. Measurement. 114, 162-168.
[31] Akben, S.B., Kalkan, S., Çanga, D. (2017) The Optimization Method by Using the Transformation of Two Variable Dependent Experiment Results into Image Data and Its Usability in the Food Engineering Applications. Eurasian Journal of Food Science and Technology. 1(1), 58-65.
[32] Gamli, Ö., Eraslan, Z., Akben, S.B. (2018) Determination of the protective effects of olive leaf extracts on microbiological and physicochemical properties of pepper paste using the image processing methods. Journal of Food Process Engineering. 41(7).
[33] Russ, J.C. (2016) The image processing handbook. Sixth Edition. CRC press. taylor&Francis Group.
[34] Tanilgan, K., Ozcan M., Unver A. (2007) Physical and chemical characteristics of five Turkish olive (olea europaea L.) varieties and their oils. Grasas Y Aceties. 58(2), 142-147.
[35] Konuskan, D.B (2008) Determination of some properties of solvent extracted oils of olive oil Halhalı, Sarı Hasebi and Gemlik varieties grown in Hatay and comparison with olive oils obtained by mechanical method. Phd. Thesis. Institute of Naturel and Applied Science. University of Cukurova.
[36] Condelli, N., Caruso, M.C., Galgano, F., Russo, D., Milella, L., Favati, F. (2015) Prediction of the antioxidant activity of extra virgin olive oils produced in the Mediterranean. Food Chemistry. 177, 233-239.
[37] Servili, M., Selvaggini, R., Esposto, S., Taticchi, A., Montedoro, G.F., Morozzi, G. (2004) Health and sensory properties of virgin olive oil hydrophilic phenols: agronomic and technological aspects of production that affect their occurrence in the oil. Journal of Chromatography A. 1054, 113-127.
[38] Franco, M.N., Galeano-Diaz, T., Lopez, O., Fernandez-Bolanos, J.G., Sanchez, J., De Miguel C., Gil, M.V., Martin-Vertedor, D. (2014) Phenolic compounds and antioxidant capacity of virgin olive oil. Food Chemistry. 163, 289-298.
[39] Harp, F. (2011) Determination of antioxidant effects of Gemlik, Domat, Adana Topagı and Adana local type olive leaves. MSc Thesis. Cukurova University, Natural and Applied Science. Adana
[40] Bayram, B., Esatbeyoglu, T., Schulze, N., Ozçelik, B., Frank, J., Rimnach, G. (2012) Comprehensive analysis of polyphenols in 55 extra virgin olive oils by HPLC-ECD and their correlation with antioxidant activities. Plant Foods for Human Nutritions. 67, 326-336.

[41] Esti, M., Contini, M., Moneta, E., Sinesio, F. (2009) Phenolic compounds and temporal perception of bitterness and pungency in extra-virgin olive oils: changes occurring throughout storage. Food Chemistry. 13, 1095-1100.

Received: **05.12.2018**
Accepted: **21.02.2019**

CORRESPONDING AUTHOR

Omer Faruk Gamli
Food Engineering Department,
Korkut Ata University,
Osmaniye – Turkey

e-mail: omergamli@osmaniye.edu.tr

© by PSP Volume 28 – No. 4/2019 pages 2716-2724 Fresenius Environmental Bulletin

ANALYSING THE NATIONAL DATA FOR AGRICULTURAL TECHNOLOGY PENETRATION IN TURKEY

Arif Behic Tekin*

Ege University, Faculty of Agriculture, Department of Agricultural Engineering & Technology 35100 Bornova, Izmir, Turkey

ABSTRACT

Agriculture is a strategic sector to supply basic human requirements. Over the last centuries, its strategic importance has been escalated. Global trends such as increasing world population, climate change, and digital developments are shaping the sector. Agriculture is the largest user of the limited global sources like water and energy and conventional techniques deteriorate environment while being affected by environmental changes. It is a cycling process. World population is seeking more fibre and food; the sector is trying to survive in the unstable environment. The uncertainty could be managed through the effective use of digital technologies. This paper aims to develop a method for monitoring ICT penetration in agriculture and to project current state of digital change on Turkish agriculture by analysing data published by the Turkish Statistical Institute (TUIK). Besides, the paper discusses latest developments and shift to Agriculture 4.0.

KEYWORDS:
Data analyses, digital divide, ict adoption, Turkish agriculture

INTRODUCTION

Food security is an important issue of all nations since more than a billion people are undernourished. The poverty is even getting more important for undeveloped countries. Pressures are getting worse due to changes faced for last 30 years. In this period, there have been tremendous changes in world agriculture and food domain. Major drivers are the global and local trends listed below [1]

Global warming and climate change are bringing indefiniteness on known crop production calendar and cycles. This uncertainty is resulting in difficulties on doing agricultural operations in certain time. The operations have to be completed in indefinite period and shortest time [2-3].

For food and fibres, the world uses primary source of the world such as soil, water etc. Due to overdose and misapplication of inputs such as fertilizer, other chemicals etc. are triggering environmental pollution which also threatening agricultural production. In order to interrupt the cycle, environmental friendly methods and tools must be implemented.

The world's limited sources such as soil, clean water, energy etc. are continuously gaining importance due to increasing demand. In this respect, in order to carry on sustainable production, efficiency of input use needs to be amplified.

While cost of energy is scaled up, in parallel, agricultural input price is increasing that makes difficult to keep sustainability on production.

Although agriculture depends on massive public interventions and subsidies for promoting production, recently there is strong resistance rising from the people to decrease even to extinguish financial supports. Therefore, small-scale farms have been leaving the sector.

Policies of protecting the domestic farmers have been low levelled by reducing subsidies that trigger global competition on agricultural trade. This trend has been leading to global threat on domestic farmers while opening new doors to them.

Food and fibre demand are rising dramatically due to increasing population, which will be expected to be 9 billion by 2050 and increased living standards. This development brings about awareness of strategic importance of agriculture by humankind, but this perception is not leading to realization on investment policies with the same extent. Accordingly, despite booming food demand that causes market price rise, field price is still low and unsustainable agricultural production cannot meet that request.

Due to low income and low level of comfort and wealth on rural area, young generation tends to prefer emigration to urban and works on other sectors such as manufacturing and service industry. Therefore, their parents with an average age of 57 who are planning to be retired within 5-10 years have carried agricultural production.

Consequently, agricultural production must be increased under these global trends listed above while improving input use efficiency, low input use, with few operations, at low cost and by protecting environment. Under these circumstances, conventional production approach must be neglected and management of heterogeneity approach by using information and communication technology must be applied.

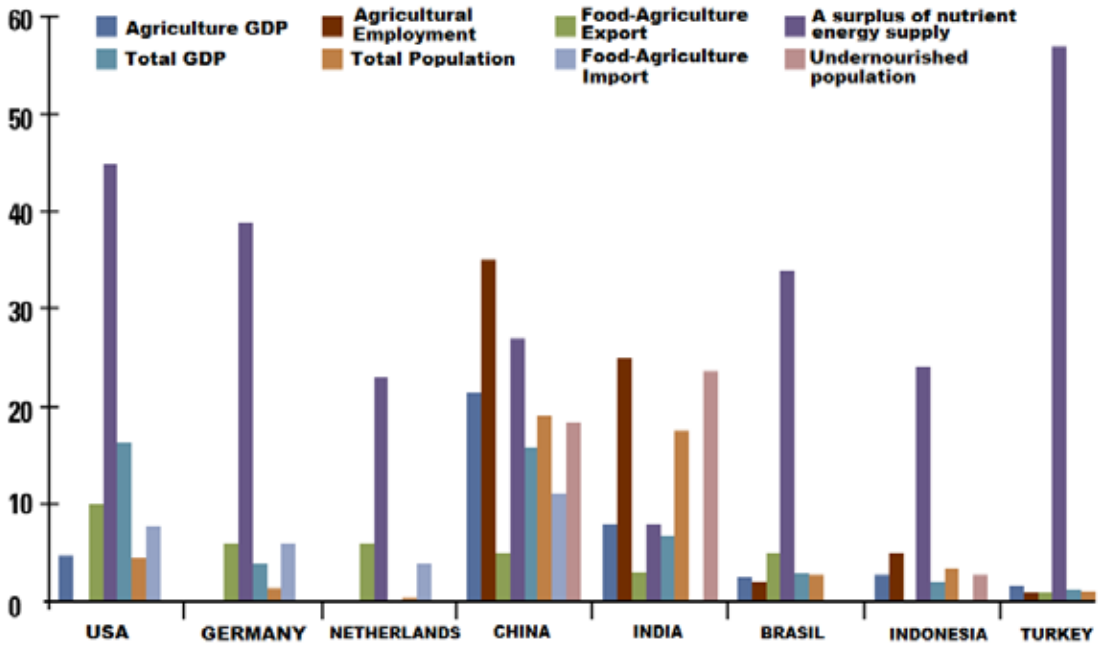

FIGURE 1
Share of selected country's supply and demand shares (%)

Therefore, the aim of this article is to focus on Turkey's position in various world's production and productivity trends and developments in politics, in parallel with the agenda and change that are stated above in the world agriculture-food sector. Latest analyses show that smart agriculture approach will be the solution for overcoming the increasing limits such as environmental and economic pressure. Although there is no certain indicator on penetration of smart agriculture for global and national evaluation, ICT indicators would be useful for assessing the penetration and potential [4]. Accordingly, the paper will also evaluate status and future projection of Turkish agriculture sector and specifically information technology penetration by using those ICT indicators.

Agricultural Structure, Labour and Income. Agricultural structure, human resources and income are the main concerns for overall sustainability of food and agricultural systems. Variables such as geography, climate etc. that directly result in crop diversity and alteration on production for certain location. These are the natural wealth/ destitution of each country. The property belong to country could determine if it can meet the needs of a national population. Moreover, the people who are living in rural areas are extremely poor. Therefore, they are strictly not willing to work without enough revenues. Thus, poverty affect the labour shift from the sector to other industries. The statistical data will shed light developments on the issue in terms of Turkish agricultural domain.

Crop Pattern and Holding Structure. Turkey with a natural wealth and climate, large agricultural land, and plentiful water potential, is one of the leading countries in the world following USA, European Union, China, India, Brasil and Indonesia. According to eight indicators that reveals the performance of the country in terms of agriculture, share of them are given in Fig. 1 [5]. While first four indicators reveal the power of national supply, others represent the power of national demand at global agricultural market. Turkey is taking eighth position in world agricultural league with a highest surplus of energy nutrient supply.

Table 1 summarises the Turkish agricultural land use and its sectorial shares that are because of it. There has been significant alteration of the land use in Turkey for two decades that contribute the performance. While witnessing slightly decrease in total utilized agricultural land, the data belong to land under permanent meadows and pastures land have been fixed for a long time. This data needs to be discussed. The table reveals the decrease in total utilized agricultural land that is related to decline in sown area and follow land. Moreover, area of vegetable production is slightly dropped at that period. Nevertheless, area of fruit production and ornamental plants have been increased. The drivers for this variation in land use are highest income from vegetable, fruits and ornamental production, population increase, increasing input demand from food industry and tourism.

TABLE 1
Agricultural land use and sectorial share (1000 ha)*

Agricultural land							(Thousand hectares)
Year	Total utilized agricultural land	Area of cereals and other crop products		Area of vegetable gardens	Area of ornamental plants	Area of fruits, beverage and spice crops	Land under permanent meadows and pastures
		Sown area	Fallow land				
2001	40 967	17 917	4 914	909	-	2 610	14 617
2002	41 196	17 935	5 040	930	-	2 674	14 617
2003	40 644	17 408	4 991	911	-	2 717	14 617
2004	41 210	17 962	4 956	895	-	2 780	14 617
2005	41 223	18 005	4 876	894	-	2 831	14 617
2006	40 493	17 440	4 691	850	-	2 895	14 617
2007	39 504	16 945	4 219	815	-	2 909	14 617
2008	39 122	16 460	4 259	836	-	2 950	14 617
2009	38 912	16 217	4 323	811	-	2 943	14 617
2010	39 011	16 333	4 249	802	-	3 011	14 617
2011	38 231	15 692	4 017	810	4	3 091	14 617
2012	38 399	15 463	4 286	827	5	3 201	14 617
2013	38 423	15 613	4 148	808	5	3 232	14 617
2014	38 558	15 782	4 108	804	5	3 243	14 617
2015	38 551	15 723	4 114	808	5	3 284	14 617
2016(*)	38 380	15 574	4 050	804	5	3 329	14 617

*TUIK, 2016
Data are grouped according to Statistical Classification of Products by Activity in European Economic Community [6]

TABLE 2
Global employment trends in agriculture as share of total employment

Region	1991	2013	% Change
World	44.5	31.3	-29.7
Development Economies & EU	6.9	3.6	-47.8
Central & SE Europe (non-EU) & CIS	28.8	17.7	-38.5
East Asia	56.8	30.3	-46.7
South-East Asia & the Pacific	58.9	39.3	33.3
South Asia	62.1	46.3	-25.4
Latin America & the Caribbean	24.7	14.8	-40.1
Middle East	24.5	14.3	-41.6
North Africa	34.9	28.0	-19.8
Sub-Saharan Africa	65.9	62.0	-5.9

Source: ILO, "Key indicators of the labour market" Geneva, 2014 [7]

TABLE 3
Employment and its sectorial share

Years	2005	2010	2011	2012	2013
Total Employment (Thousand person)	21.667	24.618	25.557	26.158	27.101
Total Agricultural Employment (Thousand person)	5.154	5.039	6.143	6.097	6.015
Share of Agr. Sector (%)	23,2	20,8	21,1	20,2	19,2
Industry, Mining and Construction Sec. Share (%)	24,6	24,5	25,5	25,4	25,5
Service Sec. Share (%)	42,7	43,6	44,3	46,0	46,3
Unemployment (%)	9,5	11,1	9,1	8,4	9,0

*TUİK, (2005...2013) [6]
1. Agricultural Employment, and unemployment were calculated based on even distribution to all sector
2. In order to be clear, Labour data belong to Mining and Construction sectors were included in Industry,

Agricultural Population and Labour. As it is well known that income in agricultural domain mostly annual based except livestock and greenhouse production. In addition, economic uncertainties are high. Therefore, revenue offering is not flexible that cause shifting of young population from the sector to other industrial domains. International Labour Organisation (ILO) has been releasing key indicators for revealing progress on world level. Turkish national organisation gathered data, but ILO plays key role in assessing the data and releasing the labour market report. The key indicators revealed dramatically decline in labour market in the sector since 1991 (Table 2). Therefore, the world agricultural population has been getting older. As the ILO announced that, the global average farmer age is around 58.

TABLE 4
Value of agricultural production*

Years	Value of Agricultural Production			Value of Crop Production ([1])			Values of animal production ([1])		
	Total			Total			Total		
	Value of Production	Value of Marketable	%	Value of Production	Value of Marketable	%	Value of Production	Value of Marketable	%
2005	88.364.969	62.734.237	71	50.939.687	42.206.851	83	37.425.282	20.527.386	55
2010	165.039.292	116.710.776	71	80.038.126	67.393.773	84	85.001.166	49.317.003	58
2011	191.627.972	132.412.900	69	88.979.273	74.166.678	83	102.648.699	58.246.222	57
2012	200.815.472	138.078.554	68	87.946.988	73.400.236	83	112.868.484	64.678.318	57
2013	190.605.101	130.482.573	68	92.489.688	76.661.249	83	98.115.413	53.821.324	55
2014	204.967.741	140.077.778	68	98.123.089	81.742.278	83	106.844.652	58.335.500	55
2015	248.925.103	172.305.825	69	120.152.079	100.363.684	84	128.773.024	71.942.141	56
2016	271.001.302	183.877.847	68	118.969.018	99.491.652	84	152.032.284	84.386.195	56

*TÜİK, (2005...2016) [6]
([1]) Cpa 2002/2008 Classification
Sources: Turkstat, Agricultural Structure (Production, Price, Value) Publication

Besides assessing the global trends, in order to have clear information on national development, TUIK data was evaluated (Table 3). Although total employment in Turkey has been increasing by years, the agricultural employment has been decreasing. The trends coincidence with global trends. The agricultural labour transition results in several developments in sector such as increasing mechanization level, holding scale and efficiency.

Agricultural Income. The sector is a strategic importance in terms of adding value to Turkish economy Tekin and Unal 2011. [8] analysed the economic status of the sector in national economy by input-output analysis. They reported that agriculture was fourth biggest input user of the economy for the production. Nevertheless, the sector provided 44% of the direct input requirement by itself. The sector has a fewer "Backward Dependency Coefficient" compared to other sectors; the input used at production is supported by mostly itself. The rank was 46 among 59 sectors. On the contrary, it has one of the highest "Forward Dependency Coefficient" among all sectors that means it transfers most of its products to other sectors.

Since, equity capital of agricultural holding determines investment capacity on agricultural infrastructure and technology. The ratio between value of marketable and production is an indicator in terms of investment capacity. If that is elevated, the level of income and welfare will be high. Nevertheless, the ratio is still low although there has been development on logistic sector and market chain (Table 4). On the other hand, labour and land (field) efficiency were very low and 30% and 20% respectively [7]. Therefore, due to lack of equity capital, the sector seeks subsidies for investment and production in order to increase production and efficiency.

Agriculture 4.0. People are aware of the heterogeneity in nature from the beginning of life. Although ancient farmers applied the strategy of heterogeneity management, population increase, and industrialization have forced to shift latest conventional production techniques. The reason were the lack of technology and knowledge to assist the management strategy and limited access to products at affordable prices. However, the world has experienced a great revolution in information and communication technology (ICT) over the last several decades. It is identified as a generic technology, capable of changing the economic and social environment. Innovation and knowledge are the new drivers of economies [9]. That leads agricultural revolution named previously smart agriculture lately Agriculture 4.0.

The technology behind the revolution in information and communication technology (ICT) is internet. It connects business, people, and things respectively than will connect artificial intelligences. Within the concept of Internet of Things (IoT) all devices are communicating each other via internet facilities. This includes cell phones, refrigerator, oven, wearable devices, cars, and so on. The reflection of this concept in agricultural domain is Agriculture 4.0. It is a way of sustainable agricultural production by producing more food and supplying them at affordable price in the market. It is an integration of technologies such as sensors, tools, devices and vehicles. All elements in farm are communicating with each other in order to produce more with less input use in environment-friendly manner.

The goal of this paper was to develop a method for monitoring ICT penetration in agriculture and to project current state of digital change on Turkish agriculture by analysing data published by the Turkish Statistical Institute (TUIK). Besides, the paper discusses latest developments and shift to Agriculture 4.0.

MATERIALS AND METHODS

The data gathering method is based on face-to-face survey applied by Turkish Statistic Institute (TUIK). Turkish Statistic Institute, within the EU

harmonization work, have used Address Based Population Registration System (ABPRS) for the ICT Usage in Households and by Individuals Survey since 2009. OECD Working Party on Indicators for the Information Society has developed a list of core ICT indicators that assists countries to measure the level of ICT penetration. Therefore, Turkey has started to collect data by applying "ICT Usage in Households and by Individuals Survey" annually since 2005.

Results. Information and Communication Technology Access. It is well known the fact that creation of internet plays key role in latest invention and development in all sectors. The technology beside ICT' tools result in moving towards an increasingly globalized world while creating new economic and social environments and fundamentally changing economies [10]. They affect all segments of society and the economy. The statistical data on access to and use of ICTs (see Table 1) reveals impact and penetration in all domain. They are strategic assets to monitor and to develop policies and strategies for checking and evaluating the progress. Therefore, the study used the ICT data, which has a yearly resolution spanning 2004 to 2016.

Fig. 2-5 summarizes the level of penetration of important ICT technologies in Turkey in that period. Fig.2 graphed the availability of desktop and laptop, which are fundamental tools of information society. Desktop use had a curve line that reach its peak point in 2012 than declined. Whereas, laptop use is getting increase in surveyed years. Although there is missing data for the latest year, the variation in lines to be expected in the same direction. There were differences between rural and urban; rural laptop penetration level was one of third comparing with urban. Moreover, the difference for desktop is one of two.

The data gathering method is based on face-to-face survey applied by TUIK within the EU harmonization work and classified according to EU Typology Classification.

Agricultural Holding structure; data was compiled from agricultural holdings that are engaged in crop production or bovine animal (cattle and buffaloes) husbandry or sheep and goat husbandry on their own account. Agricultural Holding Structure Survey was conducted by face-to-face interview with agricultural holdings selected by sampling method and Public Agricultural Holdings were covered by complete enumeration.

Figure 3 represents the use of ICT tools in households and by individuals in Turkey. The figure allows making several inferences about the ICT penetration for the period. Penetration of all ICT devices are dramatically increased. Internet connection at houses has been very popular comparing with computer usage. Moreover, males are more aggressive on using both technologies.

In addition, ICT penetration in enterprises would give a bit clearer vision. Figure 4 reveals computer use and internet access besides having website in business. While the ratio of companies with website is fluctuating, computer use, and internet access have been high and stable. Although, there is no data for benchmarking of urban and rural, reflection of other ICT tools such as smart phone would allow to inference.

The figure 5 represents variation in penetration level of fixed line telephone and smart phone. Although, fixed line telephone was very popular at the beginning of period, year by year the service lost its availability. Due to technological development, decreasing device and service cost, people replace it with smart phone. On the other hand, variation at the lines following each other very closely. Benchmarking of urban and rural reveals that they were following same trends.

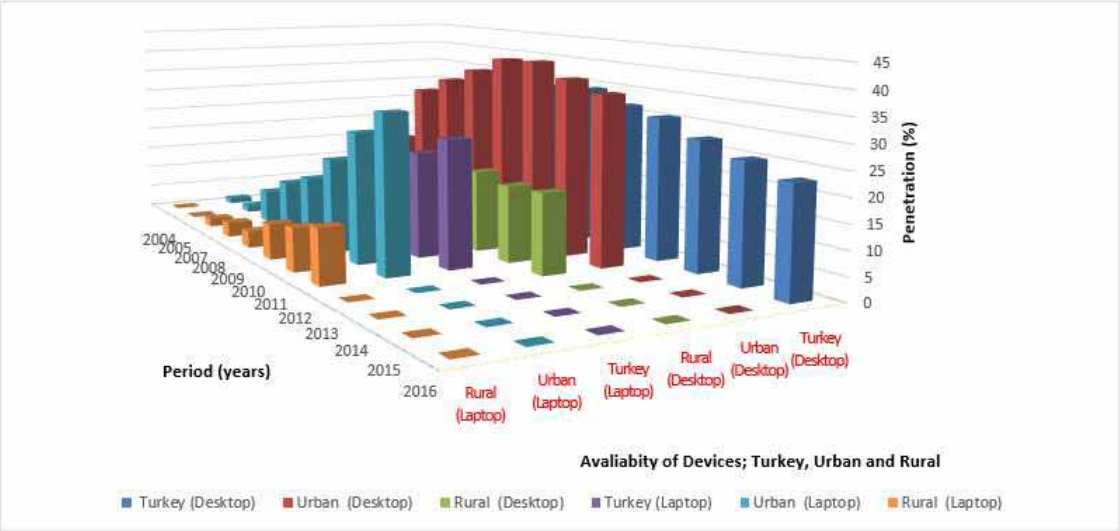

FIGURE 2
Availability of devices in households

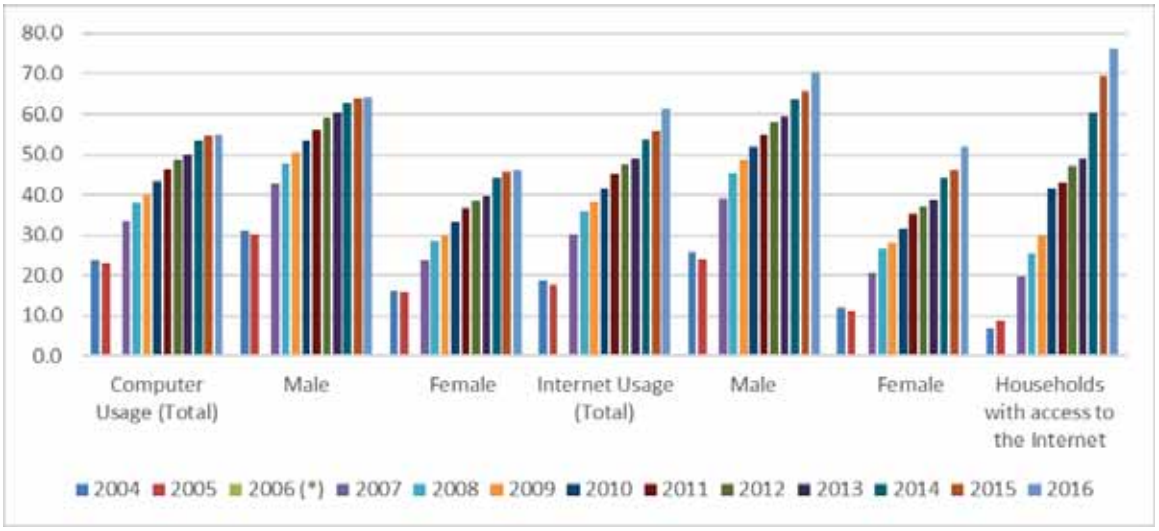

FIGURE 3
ICT usage in households and individuals

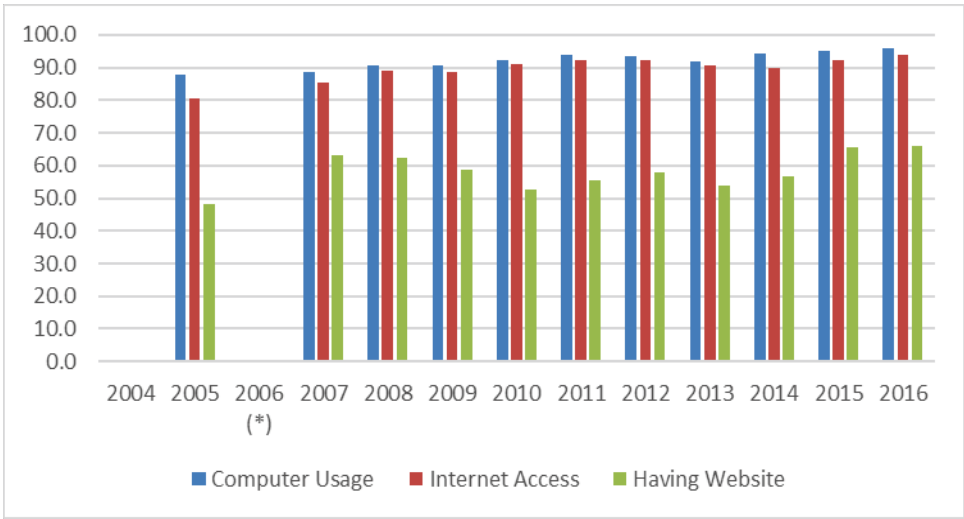

FIGURE 4
Ict usage in enterprises

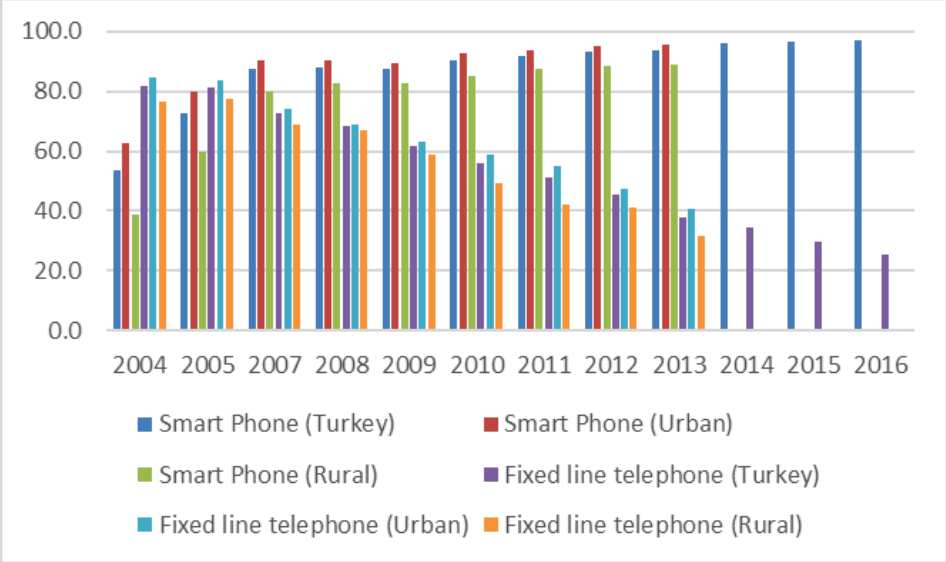

FIGURE 5
Availability of communication devices

RESULTS AND DISCUSSION

Human beings have left primitive input application that is taking heterogeneity of agricultural domains into account due to necessity of cultivating larger fields and lack of appropriate technology through the history. This development lead to agronomical, economic and environmental problems originated from agricultural activities. Whereas, current technological development is assisting farmers to deal with natural heterogeneity of agricultural domain since 2000. Moreover, latest development will allow farmer to manage the heterogeneity more effectively since all devices and units in agricultural domain will communicate each other via internet to optimise the production. It will allow recording all data for each parcel and location. Then process it, create information and knowledge for better benefit for farmers. The record keeping is also potential for increase in land value. Since, one who will own or manage the land will have opportunity of better understanding from historical data.

On the other hand, adoption of these new technologies has barriers arising from different sources. Penetration of these technologies alter due to constraints such as lack of effective training, fear of technology, lack of technological infrastructure [11]. Previous study reported that despite Turkey's performance in international arena, there were significant difference in ICT adoption between urban and rural communities [10]. In addition, he added that without preventative policy, the difference become steady. The gap will become larger year by year although at present both urban and rural; areas have the same growth rate.

Unluckily there is no direct indicator developed for measuring the level of ICT penetration in agricultural holdings around the world. Therefore, the study focused on the trends of ICT indicators to infer progress on agricultural revolution in terms of ICT. People, who live in rural, are taking advantage of having ICT tools in their social and professional life. The penetration of such tools was mostly limited by infrastructure, acquisition cost and familiarity. On the other hand, as it is clear from the graphs that penetration is getting high for the period of under assessment. There is a positive progress in Turkey.

There are evidences of similar progress on shifting from conventional agriculture to Agriculture 4.0. The experience on the penetration of ICT tools sympathize with the conclusion of the data. The studies have been conducted in order to develop awareness on the "management of heterogeneity" [12 - 15] Accordingly some of them prototyped related technologies with the leading of several scientists [9] and [16-19].

While scientists imported several tools and devices such as GPS, sensors, yield monitoring systems and mapping software from international companies in order to conduct studies and gain experiences on the topic. The first PhD was completed in 2005 titled with "A Study on Modifying Granule Fertilizer Applicator for Variable Rate Fertilizer Application" [20]. Then, other scientists followed the study to gain experience on the new domain [21 – 24]. While many academic studies funded by private sector, governmental organization and universities, lately, ministry of agriculture with the help of experts from universities has carried out several nation-wide projects in order to demonstrate the results of the studies and train people such as experts from government and institutes, farmers and agricultural implement manufacturers. Moreover, in order to supply correction signal for increasing GPS accuracy government went out to tender for correction signal network and put it into service [25].

While scientific and governmental activities assisting to increase the awareness, pioneer investors have started to apply the philosophy for 10 years. They have started yield mapping of their production and applying input at variable rate [26 – 30]. Recently, auto guidance systems for agricultural vehicles have been very popular in the market as it was the case for developed countries. Several studies dealt with the accuracy of the system in order to reveal outcome [31-32] Ministry of agriculture has been evaluating the application of yield monitoring system in order to gather ground-based data very precisely so that it can serve parcel-based maps to farmers.

Furthermore, livestock and greenhouse production are very attractive for the ICT tools and technologies. Fully atomised systems have been installed into barn and greenhouses. Milking robots are penetrating after introducing herd management systems beside other automation in livestock production. Automatic systems are controlling air quality and temperature in buildings. Local companies developed national herd management systems beside milk sensors. Traceability from field to customer is getting importance for more than 5 years due to public awareness on the good management practice.

Lately, robotic farm is getting popular at the global agenda. Turkish scientific teams have been partnering of international projects about development of unmanned vehicle for agricultural operations [33 – 36]. First robotic vehicle was an output of Robofarm project in 2015. In a five year, it was planned that the vehicle will take place in agricultural field for carrying on agricultural operations and data gathering. Several farmers have started to monitor their field via unmanned air vehicle while scientist have been dealing with development of knowledge.

CONCLUSIONS

Although there are social, technical and economic challenges, Turkey has been shifting to Agriculture 4.0. All statistical data and experience reveal the positive progress. Nevertheless, in order to catch the global penetration trends, the country must focus on several steps such as creating financial resources for investment, creating social and economic environment for attracting teenagers, encouraging manufacturer for investment on innovations.

REFERENCES

[1] Evcim, H.Ü., Tekin, A.B., Gülsoylu, E., Demir, V., Yürdem, H., Güler, H., Bilgen, H., Alayunt, F. and Evrenosoğlu, M. (2015) Situation in Agricultural Mechanization, Problems and Possible Solutions. Agriculture Engineering VII. Technical Congress Handbook. 2, 1080-1106

[2] Pechanec, V., Machar, I., Kilionova, H., Vlckova, V., Bucek, Antonin, Plasek, Vitezslav (2017) Prediction of climate change impacts on WKH Czech Republic. Fresen. Environ. Bull. 26, 7580 - 7586

[3] Hongzhou, Y., Jifeng, D., Hangyong, Z (2018). Comparison of three vapour-exchange Methods for describing hourly litter moisture content of typical forest stands in Daxingangling prefecture, Northeastern China. Fresen. Environ. Bull. 27, 7316 – 7325

[4] ITU (2016) The World Telecommunication/ICT Indicators Database. http://www.itu.int/en/ITU-D/Statistics/Documents/statistics/2016/WTID_2016_ListOfIndicators.pdf. (accessed 10 April 2017).

[5] Çakmak, E.H., Kasnakoğlu, H. (2017) Agriculture Report 2016. Turkish Exporters Assembly, İstanbul/Turkey. Available at: www.tim.org.tr (accessed 25 March 2018)

[6] TUIK (2017) Turkish Statistical Institute Database. http://www.turkstat.gov.tr/Start.do (accessed 10 April 2017).

[7] World Bank. World Development Indicators (WDI) Data Catalog. www.worldbank.org (accessed 10 April 2017)

[8] Tekin, A.B., Evcim, H.Ü (2011). Input-Output Structure of Turkish Agriculture. Bulgarian Journal of Agricultural Science. 17(2), 258-268

[9] Tekin, A.B. and Sındır, K.O. (2002) Prospects and Challenges for Precision Farming in Turkey. In: Proceeding of The Union of Scientist Rousse. Energy Efficiency and Agricultural Engineering (EE&AE'2002) April 4-6, 2002. Rousse, Bulgaria.

[10] Tekin, A.B. (2011) Information and Communication Technology: An Assessment of Turkish Agriculture. Outlook on Agriculture. 40(2), 147-156.

[11] Gelb, E. and Parker, C. (2005) Is ICT adoption for agriculture still an important issue? In: The 5th Conference of the European Federation for Information Technology in Agriculture, Food and Environment and the 3rd World Congress on Computers in Agriculture and Natural Resources. 25–28 July 2005, Portugal.

[12] Sındır, K.O. and Tekin, A.B. (2002) Economics of Variable Rate Fertilizer Application. Balkan Agricultural Engineering Review. (ISSN 1312-5443). 2. Rousse, Bulgaria.

[13] Tekin, A.B. and Sındır, K.O. (2004) Application Accuracy and Distribution Uniformity of Variable Rate Fertilizer Application. Balkan Agricultural Engineering Review (ISSN 1312-5443). 5. Rousse, Bulgaria.

[14] Akdemir, B., Bellitürk, K., Şişman, C.B. and Simon, B. (2005) Spatial Distribution in A Dry Onion Field (A Precision Farming Application in Turkey). Journal of Central European Agriculture. 6, 211-221.

[15] Tekin, A.B. (2010) Variable rate fertilizer application in Turkish wheat agriculture: Economic assessment. African Journal of Agricultural Research. 5(8), 647 – 652

[16] Tekin, A.B., Sındır, K.O. (2014). Performance Assessment of Variable Rate Spinner Disc Fertilizer Spreader – "PreFer". Agricultural Engineering. 2, 43–52.

[17] Bellitürk, K., Sağlam, C., Akdemir, B., Şişman, C.B., Sözübek, B. (2010) Determination of Spatial Variability in Olive Production Part I-Soil. Bulgarian Journal of Agricultural Sciences. 16, 468-475.

[18] Bellitürk, K., Sağlam, C, Akdemir, B, Şişman, C.B. and Sözübek, B. (2010) Determination of Spatial Variability in Olive Production Part II-Leaf. Bulgarian Journal of Agricultural Sciences. 16, 713-718.

[19] Karayel, D., Topakci, M., Ünal, İ., Šarauskis, E. and Çanakci, M. (2012) Using real-time kinematic (RTK) global positioning system (GPS) for the determination of seedling distributions over the field. Zemdirbyste-Agriculture. 99(4), 425-430.

[20] Tekin, A.B. (2005) A Study on Modifying Granule Fertilizer Applicator for Variable Rate Fertilizer Application. PhD Thesis. Ege University. İzmir/Turkey.

[21] Dalmış, İ.S., Akdemir, B., Bellitürk, K. and Türen, N. (2016) Development of an Automatic Soil Sampling Machine. Tekirdağ Ziraat Fakültesi Dergisi. 13, 1-12.

[22] Topakci, M., Ünal, İ., Çanakci, M., Çelik, H.K. and Karayel, D. (2010a) Design of a Horizontal Penetrometer for Measuring On-The-Go Soil Resistance. Sensors. 10(10), 9337-9348
[23] Eroğlu, M.C., Öğüt, H. and Türker, U. (2011) Effects of Some Operational Parameters in Combine Harvester on Grain Loss and Comparison Between Sensor and Conventional Measurement Method. Energy Education Science and Technology Part A: Energy Science and Research. 28(1), 497-504.
[24] Tekin, A.B. and Yalçın, H. (2014) Development of Online Soil Profile Sensor for Variable Depth Tillage. In: 12th International Conference on Precision Agriculture. 20 – 23 July 2014. Sacramento, CA. USA.
[25] CORS-TR (2013) Continuously Operating Reference Station – TR. Available at: http:// cors-tr.iku.edu.tr/ENGLISH.htm (accessed 10 April 2017).
[26] Tekin, A.B., Günal, H., Sındır, K.O. and Balcı, Y. (2011) Spatial structure of available micronutrient contents and their relationships with other soil characteristics and corn yield. Fresen. Environ. Bull. 20, 783-791.
[27] Turker, U., Erdem, T., Arostotelis, T., Fountas, S., Mitev, G., Gemtos, T. and Akdemir, B. (2011) Feasibility Study of Variable Rate Irrigation in Black Sea Area: Water and Energy Saving from the Application. Journal of Information Technology in Agriculture. 4, 1-8.
[28] Türker, U, Dayıoğlu, M.A., Eroğlu, M.C. (2012) A Research on Site Specific Irrigation in Irrigated Maize in Çukurova Region for Energy and Water Saving. Energy Education Science and Technology Part A. Energy Science and Research. 28(2), 821-826.
[29] Türker, U., Erdem, T., Tagarakis, A., Fountas, S., Mitev, G., Akdemir, B. and Gemtos, T.A. (2011) A Feasibility Study of Variable Rate Irrigation in Black Sea Area: Water and Energy Saving from the Application. Journal of Information Technology in Agriculture. 4(1),1-8.
[30] Türker, U., Talepbour, B. and Yegül, U. (2011) Determination of the Relationship Between Apparent Soil Electrical Conductivity with Pomological Properties and Yield in Different Apple Varieties. Zemdirbyste-Agriculture. 98(3), 307-314.
[31] Topakci, M., Has, M., Ünal, İ., Çanakci, M., Karayel, D. and Koç, A. (2011) Determination of Efficiency of Lightened Guidance System on Agricultural Machinery: A Case Study on Fertilizer Broadcaster. Journal of Agricultural Machinery Science. 1, 13-17.
[32] Topakci, M., Ünal, İ., Çanakci, M., Yiğit, M. and Karayel, D. (2010b) Improvement of Field Efficiency Measurement System Based on GPS For Precision Agriculture Applications. Journal of Food Agriculture. 8, 288-292.
[33] I-LEED (2017) Advanced cattle feeding on pasture through innovative pasture management. Available at: http://www.lfl.bayern.de/ ilt/i-leed/en/
[34] Robofarm (2013) Integrated robotic and software platform as a support system for farm level business decisions. http://robofarm.unibo.it/
[35] Tsiropoulos, Z., Fountas, S., Vasileios, L., Tekin, A.B., Aygun, T. and Blackmore, S. (2013) Web-based Farm Management Information System for Agricultural Robots. In: EFITA-WCCA-CIGR Conference "Sustainable Agriculture through ICT Innovation", Turin, Italy, 24-27 June 2013.
[36] Ünal, İ. and Topakci, M. (2015) Design of a Remote-controlled and GPS-guided Autonomous Robot for Precision Farming. International Journal of Advanced Robotic Systems. 12(12), 1-10.

Received: **05.12.2018**
Accepted: **21.02.2019**

CORRESPONDING AUTHOR

Arif Behic Tekin
Ege University,
Faculty of Agriculture,
Department of Agricultural
Engineering & Technology
35100 Bornova, Izmir – Turkey

e-mail: behic.tekin@ege.edu.tr

© by PSP Volume 28 – No. 4/2019 pages 2725-2732 Fresenius Environmental Bulletin

RESEARCH ON WATER RESOURCES CARRYING CAPACITY OF CHANGZHOU CITY BASED ON NEURAL NETWORK

Mengyu Liu[1,*], Jianyong Zhang[2], Chenhui Wang[1], Hui Lu[1]

[1]School of Business Administration, Hohai University, Changzhou 213022, China
[2]Department of Mathematics and Physics, Hohai University, Changzhou 213022, China

ABSTRACT

In order to predict and evaluate the future water resources carrying capacity (WRCC) of Changzhou, a prediction method (PM) is proposed based on BP neural network. The neural network is used to predict the indicators of WRCC in Changzhou in 2020, and the overall effect is predicted to be good. Finally, it is concluded that Changzhou's future COD concentration, water efficiency and per capita GDP are at level 3, indicating that Changzhou will perform better in terms of water resources quality, water resources utilized level and socioeconomic level in the future. However, the utilization rate of water resources is at level 2, indicating that the water supply capacity is somewhat insufficient in the future, and the per capita water resources are at level 1, indicating that there is a shortage of water resources. Finally, the article puts forward reasonable suggestions for the specific situation of water resources in Changzhou.

KEYWORDS:
Water Resources Carrying Capacity, BP Neural Network, Water Resource Forecast

INTRODUCTION

Water resources are an important and basic natural resources and economic resources for human survival and development, and an indispensable development factor for a city. However, traditional utilization patterns of water resource result in an increasingly scarce water resource and serious pollution of water resources. The status quo of water resources utilization, “water-based production and water-based city”, has affected social stability and human survival. The bottleneck of water resources has become an important factor restricting global economic and social development in the 21st century [1]. The study of WRCC has received extensive attention from governments and academia at all levels, and has become a hot issue in the current research of water resources.

As a kind of multi-layer feedforward of neural network [2] trained by error back propagation, BP neural network can approximate arbitrary continuous functions with arbitrary precision, so it is widely used in various aspects, such as sNonlinear Modeling, Function Approximation and Pattern Classification [3]. In this paper, MATLAB is used to build BP neural network, and a relatively mature network model is obtained through training. The neural network is used to obtain the predicted value of the evaluation index, and the WRCC of Changzhou City is predicted and evaluated, and reasonable suggestions are put forward.

RESEARCH SUMMARY ON WRCC

Foreign research on WRCC is relatively rare, and it is only mentioned in the study of sustainable development. For example, URS Company of the United States used mathematical analysis model to study the WRCC of the Keys Basin in Florida [4]; Joardor et al. conducted a related study on urban WRCC from the perspective of water supply in 1998 [5]; Rijiberman et al. used bearing capacity as a measure of urban water security assurance in the study of urban water resources assessment and management systems [6]; Harris focused on the water resources agricultural capacity of agricultural production areas as a measure of regional development potential [7-8]; Falkenmark et al. believed that WRCC is a long-term sustainability capability and uses system dynamics to reveal the dynamic relationship between population size and water carrying capacity [9].

China's research on WRCC started in the late 1980s [10]. Afterwards, scholars have carried out a lot of exploration on the connotation and research methods of WRCC.

In terms of the concept of WRRC, the likes of Shi Yafeng believe that WRRC refers to the water resources in a region which can bear the maximum level of agriculture, industry, city size and population in a certain social and scientific development stage without destroying society and ecosystem. WRRC is an optimization goal that changes with the

socio-economic and scientific and technological levels [11]. Considering the foreseeable impact of technology, culture, system and personal value choice, the likes of Cheng Guodong, Xia Jun define WRRC as a region under a specific historical development stage, which is the supporting ability of water resources to the benign development of the eco-economic system under the condition of using reasonable management techniques [12-13]. The likes of Fang Guohua, Han Junli and Zhang Juncheng believe that WRRC is the regional water resources that can support the largest and coordinated development of social economy, environment and population scale after reasonable rational allocation under a certain historical development stage, with the basis of the foreseeable level of technology, economy and society development, with the principle of sustainable development, and with the premise of meeting ecological water use [14-16].

In the research methods of WRRC, commonly there are routine trend method, fuzzy comprehensive evaluation method, system dynamics method, multi-objective decision method and principal component analysis method.The system dynamics method applies the principle of system dynamics, comprehensively considers many factors such as social economy, resource environment and their mutual relationship, and uses the feedback model of dynamic system to evaluate the WRRC of a region. For example, Fang Chuanglin and others analyzed the water resources carrying capacity in Qaidam Basin by using this method [17]. The multi-objective decision-making method is based on the social, economic, demographic, environmental and other interrelated goals that can reflect the characteristics of WRCC, which is to study scales of ecology, economy and population that water resources can carry under different level years and different strategies through model building, with the principle of social sustainable development, and methods of system analysis and dynamic analysis [18]. For example, Wang Yuan et al. used this method to quantitatively study the economic scale that water resources in Tianjin can carry [19]. The principal component analysis method uses dimensionality reduction to transform multiple indicators into a few comprehensive indicators, which can objectively determine the weight of each indicator. For example, Li Weikun applied this method to analyze and evaluate the water resources carrying capacity of Chongqing [20].

In addition, from the definition of research area, the current research on WRCC generally includes three spatial scales of watershed, region and city. The research on urban WRCC is the latest to start, and the related research is still in the exploration stage [6].

The Principle of the PM based on BP Neural Network. The Principle of the Model. BP neural network is a multi-layer feedforward network based on error back-propagation algorithm which consists of input layer, hidden layer and output layer. The number of hidden layer can be non-unique, and each layer includes several neurons. There is no connection between the neurons in the same layer, and the neurons between the adjacent layers are fully connected. Since any continuous function in the closed interval can be approximated by a neural network containing a hidden layer [21], if the neural network is taken as a mapping from input to output, the mapping is a highly nonlinear mapping [22].

As shown in Figure 1, there is a corresponding weight between each connected neuron. ω_{ij} represents the connection weight between the neuron **i** of the input layer and the neuron **j** of the hidden layer, and V_{jt} represents the connection weight between the neuron **j** of the hidden layer and the neuron **t** of the output layer.

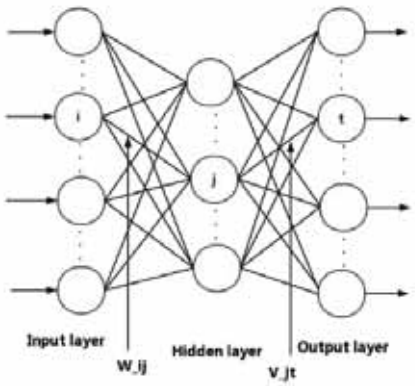

FIGURE 1
Three-layer BP Neural Network Topology

The input vector is main factors ΔX that affect WRCC, and output vectors are the predicted target ΔY of WRCC. The neural network is trained by the collected input sample ΔX_K and the output sample ΔY_K. The trained neural network can be used to predict the WRCC until a certain precision is reached as require.

The Architecture of the Model. In order to predict WRCC and propose improvement suggestions according to specific situations, this paper establishes a PM of urban WRCC based on neural network. Firstly, it is necessary to determine the indicator system, including the impact indicators and evaluation indicators of WRCC, and then collect data through multiple channels according to the indicators and have a pre-process for the data, and use MATLAB to train the neural network to achieve a certain precision, thereby a model of knowledge base is constructed.

When it is necessary to judge whether a city's planning is reasonable for the city's WRCC, it is only necessary to use the influencing factors of WRCC in urban planning as input variables. Through the prediction mechanism of neural network, the predicted

value for evaluation index of the WRCC can be obtained, and then the prediction results are evaluated, and reasonable suggestions and countermeasures are proposed.

The entire model architecture is shown in Figure 2.

Construction of Index System. In order to predict and judge the urban WRCC, it is necessary to establish the prediction index system of neural network and the evaluation index system of WRCC. As the WRCC system is a mutually influential and complex system including social economy system, ecological environment system and other systems, water resources is supporting the good development of social economy and ecological environment and the social economy and ecological environment's development and utilization also affect WRCC at all times. Therefore, it is necessary to establish a reasonable evaluation index system with operational possibilities and multiple aspects. The existing reference index system for WRCC is shown in Figure 3.

On the basis of the comprehensive evaluation index system of WRCC, it should be considered that the regional characteristics and socio-economic development of Changzhou. Based on the five aspects of water resources quantity, water resources quality, water resources use, water use and socio-economic level, five main factors were selected as evaluation indicators, and the threshold value of the evaluation indicators were determined based on the relevant indicators of sustainable development.

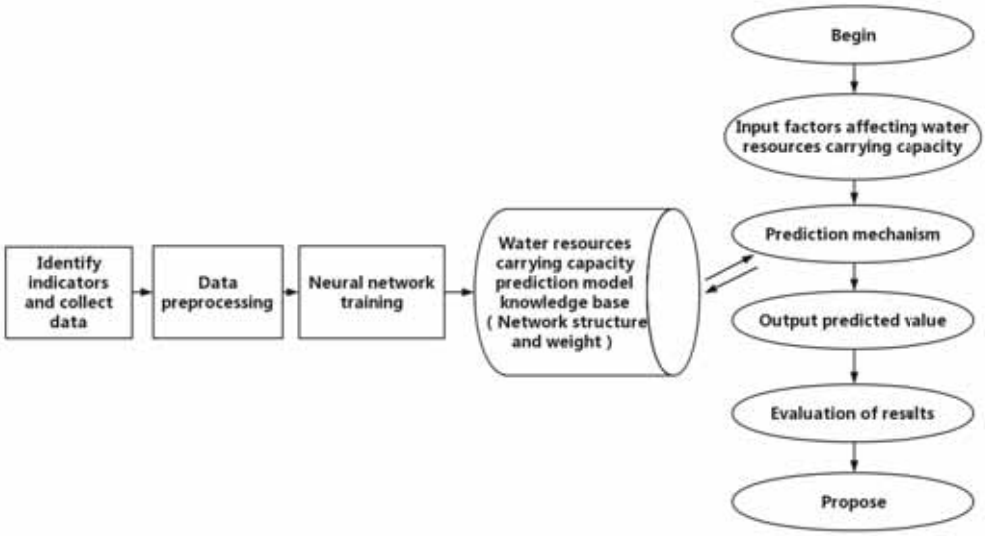

FIGURE 2
The Architecture of WRCC Prediction Model based on BP

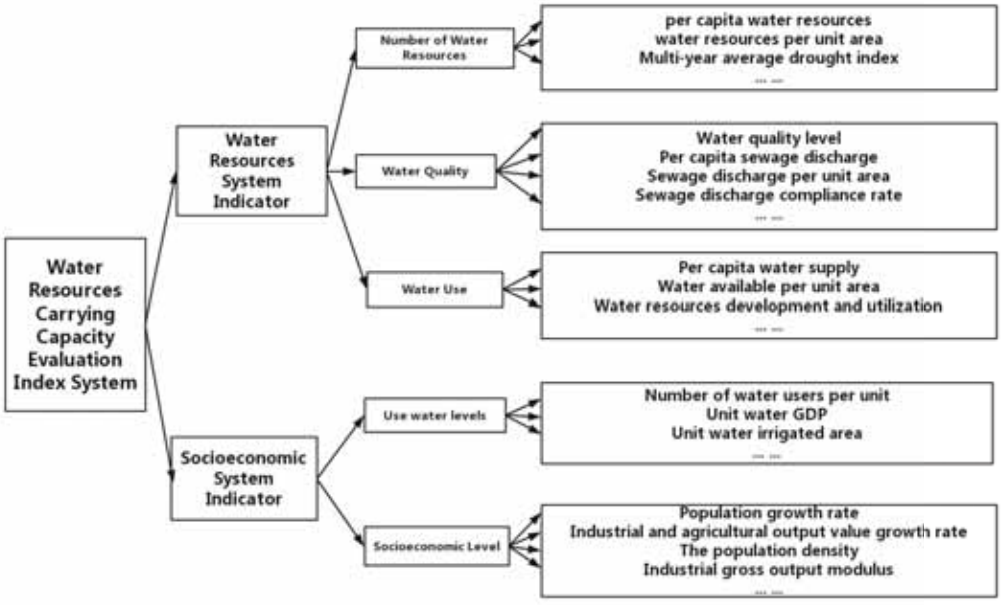

FIGURE 3
The Comprehensive Evaluation Index System for WRCC [23]

TABLE 1
The Prediction Indicators for WRCC of Neural Network

Input indicators	Output indicators
Water Supply Amount, Industrial Wastewater Discharge Amount, Sales of Social Consumer Goods, Foreign Export Value, Natural Population Growth Rate	Population, Industry and Agriculture Output Value, GDP, COD Emissions

TABLE 2
The Evaluation Index System of WRCC and the Threshold Value [24~25]

Criterion Layer	Factor Layer	1st Grade	2nd Grade	3rd Grade
Water Resources Quantity	Water Resources per capita (m^3)	<200	200~400	>400
Water Resources Quality	COD Concentration (mg/L)	>30	15~30	<15
Water Supply Capacity	Utilization Rate of Water Resources (%)	<20	20~30	>30
Water Resources Utilized Level	Water Efficiency (yuan/m^3)	<3.07	3.07~408.6	>408.6
Socioeconomic Level	GDP per capita (yuan)	<3280	3280~32800	>32800

The Table 2 divides the WRCC into three grades. The 1st Grade indicates that WRCC in the current region is poor and in an unbearable state. If the development strategy is not changed, there will be a shortage of water resources. The 3rd Grade indicates that WRCC in the current region is very good and can provide a strong support for the development of the city. The 2nd Grade is somewhere in between, indicating that the water use in the current region has a considerable scale, but still provides a certain degree of support for the city.

The Research on WRCC of Changzhou. The Overview for the Survey Area. Located in the center of the Yangtze River Delta, Changzhou is one of the central cities in the Yangtze River Delta and an advanced manufacturing base. It is an important part of the Jiangsu -Yangtze River economic zone. It forms the Suzhou-Wuxi metropolitan area with Suzhou and Wuxi, and now has a jurisdiction over 5 districts of Jintan, Wujin, Xinbei, Tianning, and Zhonglou, hosting a county-level city of Liyang, with a total area of 438,500 hectares, including 361,800 hectares of land and 73,300 hectares of water.

At the end of 2016, the total registered population of Changzhou was 3.479 million, and the resident population was 4,708,300. In 2016, the city's gross domestic product (GDP) was 577.4 billion yuan, GDP per capita was 122,721 yuan, fixed assets investment was 311.852 billion yuan, industrial output value was 1007.34 billion yuan, social consumer goods totaled 220.283 billion yuan, total import and export volume was 27.584 billion yuan.

Changzhou is located in the western part of the Taihu Lake Basin. It faces the Yangtze River in the north and Taihu Lake in the east. The mountains are connected, the lakes are also connected, and the river network is dense. By the end of 2016, the city had built 91 large and small reservoirs, including 5 large and medium-sized reservoirs and 86 small reservoirs with a total water storage capacity of 400 million cubic meters.

Data Collection and Processing. Since training neural network model requires a large amount of historical data, the numerical values of the input and output indicators of the neural network from 1990 to 2016 were collected according to the Changzhou Statistical Yearbook and other statistical data. The data set from 1990 to 2011 was selected for training, and the data set from 2012 to 2016 was tested.

In terms of data processing, the data related to prices are the current year's prices, such as foreign export value, sales of social consumer goods, industry and agriculture output value and GDP. As the lack of comparability among nominal prices due to inflation, they are converted into comparable prices based on the following formula (Based on 1990).

$$\text{Actual Price of year Y} = \text{Nominal Price of year X} \times \frac{\text{Price Index of Year Y}}{\text{Price Index of Year X}}$$

At the same time, when using the MATLAB toolbox to train the neural network, in order to avoid numerical problems and make the network converge quickly, the input data needs to be value normalized, and the output data is inversely normalized. At the same time, when using the MATLAB toolbox to train the neural network, in order to avoid numerical problems and make the network converge quickly, the input data needs to be value normalized, and the output data is inversely normalized. First, the maximum and minimum values are defined for the input matrix. The maximum matrix is defined as 1.2 times the original matrix, and the minimum matrix is defined as 0.8 times the original matrix. Then the actual value is distributed in the interval (0, 1) by the following formula. When output values, the formula is transformed accordingly to obtain the actual output value.

$$\text{Normalized Data} = \frac{\text{Original Matrix} - \text{Minimum Matrix}}{\text{Maximum Matrix} - \text{Minimum Matrix}}$$

Prediction and Calculation of WRCC in Changzhou. For the four output indicators in the Table 1, a neural network is constructed with five input indicators as input variables and output indicators as

TABLE 3
The Test Results of Neural Network

	Population (million)		Industry and Agriculture Output Value (100 million yuan)		COD Emissions (10,000 tons)		GDP (100 million yuan)	
	Actual	Predicted	Actual	Predicted	Actual	Predicted	Actual	Predicted
2013	365.91	366.54	192.43	191.03	6948	7605.9	260.76	258.24
2014	368.64	363.00	196.28	186.26	7046	7456.1	265.97	257.24
2015	370.85	366.17	199.03	184.65	7446	7541.7	269.70	261.05
2016	374.9	366.37	203.01	179.37	7232	7749.2	275.09	262.50

TABLE 4
The Test Errors of Neural Network

	Population (million)		Industry and Agriculture Output Value (100 million yuan)		COD Emissions (10,000 tons)		GDP (100 million yuan)	
	error amount	error rate	error amount	error rate	error amount	error rate	error amount	error rate
2013	0.63	0.00172	-1.4	-0.00728	657.9	0.09469	-2.52	0.00966
2014	-5.64	-0.01530	-10.02	-0.05105	410.1	0.05820	-8.73	0.03282
2015	-4.68	-0.01262	-14.38	-0.07225	95.7	0.01285	-8.65	0.03207
2016	-8.53	-0.02275	-23.64	-0.11645	517.2	0.07152	-12.59	0.04577

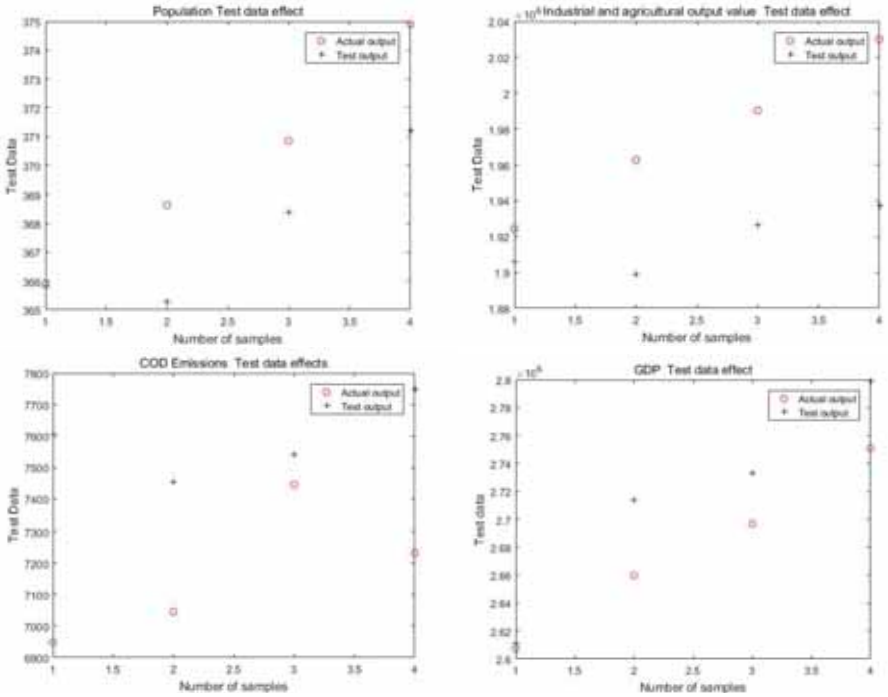

FIGURE 4
The Prediction of Neural Network

output variables, and then the collected planning data is used as an input matrix to obtain predicted values.

Determination of Neural Network Basic Parameters. In this study, the number of network layers is 3. In detail, the number of hidden layers is 1, the number of neurons in the input layer of the BP network is 5, the number of neurons in the output layer is 1, and the number of neurons in the hidden layer is 10. The transfer function of the hidden layer uses the S-type tangent function (tansig), the transfer function of the output layer uses the S-type logarithmic function (logsig), and in order to adjust the speed of the gradient descent, the BP training function Levenberg-Marquardt is used. Set BP network training times to 30,000, learning rate to 0.1, and training target minimum error to the smallest positive eps in MATLAB.

Model Training and Testing. By continuously training and checking the sample data, the corresponding test data is obtained as shown in Table 3, where the value related to price is the converted comparable price. Based on the test results, the relative error and error rate are calculated as shown in Table 4.

TABLE 5
The 2020 Urban Planning Data of Changzhou

The Amount of Water Supply (10,000)	The Amount of Industrial Wastewater Discharge (10,000 tons)	Sales of Social Consumer Goods (100 million yuan)	Foreign Export Value (100 million US dollars)	Natural Population Growth Rate (permillage)
68000	20000	3000	250	4

Note: The planning data comes from Changzhou Master Plan (2011-2020) and Changzhou planning library.

TABLE 6
Evaluation indexes Changzhou WRRC in 2020

	Water resources per capita (m^3/person)	COD concentration (mg/L)	Water resource utilization (%)	Water use efficiency (yuan/m^3)	GDP per capita (yuan)
Value	170.64	12.34	26.86	2500	187205
Grade	1st	3rd	2nd	3rd	3rd

It can be seen from Table 4 that the trained neural network can better obtain the target value of WRCC. In addition to several large error rates (maximum error rate of 11%), most of the rest are maintained within ± 5%, indicating that the neural network is better and can be applied to the forecast.

Prediction of the Model. According to Changzhou Master Plan (2011-2020), Changzhou Water Supply Plan (2004~2020) and Changzhou Drainage Plan (2004~2020), Changzhou's 2020 urban planning data is collected, as shown in Table 5.

Convert the price into a comparable price in 1990 as the input value of the neural network to get these following forecast values. The predicted population of Changzhou in 2020 is 4.0063 million, the predicted value of industrial and agricultural output is 23.109 billion yuan, the predicted COD emissions is 671 tons and the GDP forecast value is 31.348 billion yuan. It is necessary to mention that the price data obtained is a comparable price based on 1990.

The Reasonable Analysis of Forecast Results. Due to the uncertainty, periodicity and volatility of future social and economic development, it is difficult to predict accurately for the prediction model. However, indicators such as population and economy are with trending and regularity. The forecast data is in line with the law of actual development and can be used as a basis for evaluating the water resources carrying capacity of Changzhou.

Evaluation of Changzhou WRCC. In order to ensure the comprehensiveness of the evaluation, the WRCC of Changzhou in 2020 was judged by the five indicators in Table 2: water resources per capita, COD concentration, the utilization rate of water, water use efficiency and GDP per capita. Water resources per capita (m^3/person): the ratio of the water supply to the total population when the water supply guarantee rate is 75%. COD concentration (mg/L): the amount of oxidant consumed by the reducing substances in 1L oxidized wastewater. The utilization rate of water resources (%): the ratio of water supply to total available water resources when water supply frequency is 75%. Water use efficiency (yuan/m^3): the ratio of the gross output value of industry and agriculture to the water consumption of industry and agriculture (yuan/m^3). GDP per capita: the ratio of GDP to population (yuan).

It is needed to convert the predicted comparable price into the price of the corresponding year. Using the values predicted by the neural network and the data appearing in the urban planning, the values of the following evaluation indicators are calculated.

It can be seen from Table 6 that the COD concentration, water use efficiency and GDP per capita are all at 3rd grade, indicating that WRCC of Changzhou in the future is better in terms of water quality, water consumption and social economic level. The utilization rate of water resources is at 2nd grade, indicating that Changzhou has a common water supply capacity in the future. However, the grade of water resources per capita is poor, indicating that there is a shortage of water resources in Changzhou.

CONCLUSION

When predicting the evaluation index of WWRC, there is a problem that it is difficult to determine the weight of the influencing factors. However, BP neural network does not need to determine the weight by people, which greatly reduces the distortion of the result caused by subjective weighting, and the prediction result is more effective and objective. At the same time, NNs is an implicit mathematical processing method compared to System dynamics and Multi objective decision making. First, the network is trained until a certain precision is reached. Then, as long as the processed data is inputted into the network, the result can be obtained. The overall process is relatively simple and the results are more reliable.

This paper uses MATLAB data network toolbox to establish the neural network with low error rate through multiple trainings. Through neural

network prediction, the evaluation index value of Changzhou WRRC in 2020 is obtained. It can be seen from the analysis that Changzhou performs well in terms of water quality, water consumption grade and socio-economic level in the future, but the water supply capacity is common in the future. In addition, there may be a shortage of water resources. In order to cope with this unfavorable situation, it is necessary to strengthen the government's macro-control: 1. It is necessary to further improve the city's water conservancy facilities, improve the water intake capacity of Changzhou, and ensure local water demand; 2. Since Changzhou's sewage is mostly derived from industrial wastewater, therefore, it is necessary to accelerate industrial transformation to reduce industrial wastewater discharge, and at the same time, it is necessary to promote scientific and technological development and improve industrial water use processes; 3. Improve residents' awareness of water conservation and improve the treatment capacity of urban residents' domestic wastewater; 4. Strengthen regional linkage, Changzhou is located in the Taihu Basin, it is necessary to strengthen cooperation with surrounding cities to achieve optimal allocation of water resources and water environmental protection.

ACKNOWLEDGEMENTS

This thesis is the training project of college students' innovative entrepreneurship—"Prediction of Urban Water Resources Carrying Capacity Based on Neural Network——Taking Changzhou City as an Example" (No. 2018102941366).

REFERENCES

[1] Xu, Y. (1993) Study on Comprehensive Evaluation of Water Resources Carrying Capacity in Arid Area—Taking the Hetian River Basin in Xinjiang as an Example. Journal of Natural Resources. 1993(03), 229-237.
[2] Wen, X., Zhang, X., Zhu, Y., Li, X. (2015) Intelligent Fault Diagnosis Technology: MATLAB Application. Beijing: Beijing University of Aeronautics and Astronautics Press.
[3] Hagan, M.T., Demuth, H.B., Beale, M.H. (2015) MATLAB Application. Beijing: Beijing University of Aeronautics and Astronautics Press.
[4] Committee to review the Florida Keys Carrying Capacity Study (2001) National Research Council. Interim review of the Florida Keys carrying capacity study. Washington D.C. National Academy.
[5] Harris, J.M. (1999) Carrying capacity in Agriculture: Globe and regional issue. Ecological Economics. 29(3), 443-461.
[6] Rijisberman, M.A., Frams, H.M. (2000) Different approaches to assessment of design and management of sustainable urban water system. Environment Impact Assessment Review. 20(3), 333-345.
[7] Haddadin, M.J. (2000) Water issue in Hashemite Jordan. Arab Study Quarterly. 22(5), 54- 67.
[8] Hrlich, A.H. (1996) Looking for the ceiling: estimates of the earth's carrying capacity. American Scientist, Research Triangle Park. 84(5), 494-499.
[9] Falkenmark, M., Lundqvist, J. (1998) Towards water security: political determination and human adaptation crucial. Natural Resources Forum. 21(1), 37- 51.
[10] Xinjiang Water Resources Soft Science Research Group. (1989) Xinjiang Water Resources and Its Bearing Capacity Development Strategy. Water Resources and Hydropower Technology. 1989(6), 2-9.
[11] Shi, Y., Qu, Y. (1992) Water Resources Carrying Capacity and Its Rational Utilization in the Urumqi River Basin. Beijing: Science Press, 94-111
[12] Cheng, G. (2002) The Evolution of the Concept of Carrying Capacity and the Application Framework of Water Resources Carrying Capacity in Northwest China. Journal of Glaciology and Geocryology, 2002(04), 361-367.
[13] Xia, J., Zhu, Y. (2002) Measurement of Water Resources Security: Research and Challenges of Water Resources Carrying Capacity. Journal of Natural Resources. 2002(03), 262-269.
[14] Fang, G., Hu, Y., Xu, Y. (2006) Multi-objective Analysis and Evaluation Model of Regional Water Resources Carrying Capacity and Its Application. Water Resources Protection. 22(6), 9-13.
[15] Han, J., Duan, W. (2004) Basic Theory Research on Water Resources Carrying Capacity in Urban. China Water Resources. 2004(07), 12-14.
[16] Zhang, J., Zheng, Z., Li, Y., Yu, J. (2010) Study on Water Resources Carrying Capacity in Zoucheng. Resources Environment and Development. 2010(1), 11-15.
[17] Fang, C., Yu, D. (1999) The Experimental Control of the Regional Sustainable Development of SD Planning Model—Taking the Qaidam Basin in the Arid Area as an Example. Acta Ecologica Sinica. 1999(06), 767-774.
[18] Jiao, X., Liu, G. (2013) The Research Theory and Method of Regional Water Resources Carrying Capacity. International Seabuckthorn Research and Development. 11(01), 28-33+46.
[19] Wang, Y., Xu, L. (2003) Research on the Coordinated Development of Water Resources Carrying Capacity and Economy in Tianjin. Journal of Tianjin Normal University (Natural Science Edition). 2003(01), 68-72.

[20] Li, K., Xie, S. (2008) Evaluation of Impact Factors of Water Resources Carrying Capacity in Chongqing Based on Principal Component Analysis. Water Sciences and Engineering Technology. 2008(S2), 38-41.
[21] Hecht-Nielsen, R. (1989) Theory of the back propagation neural network. In: Proceedings of the International Joint Conference on Neural Network. [S.l.]: IEEE Press. 1, 121- 125.
[22] Khotanzad, A., Afkhami-Rohani, R., Lu, T., Abaye, A., Davis, M., Maratukulam, D.J. (1997) ANNSTLF-A neural-net-work-based electric load forecasting system. IEEE Transaction on Neural Networks. 8(4), 835-845
[23] Liu, S., Chen, J. (2007) Research on Water Resources Carrying Capacity Based on Neural Network Theory. Resources Science. 2007(01), 99-105.
[24] Zhu, Y., Xia, J., Tan, G. (2003) Analysis, Prediction and Evaluation of Water Resources Carrying Capacity in Northwest China. Resources Science. 2003(04), 43-48.
[25] Xu, L., Zhao, S., Yang, H. (2008) Research on the Evaluation Model of BP Neural Network of Water Resources Carrying Capacity. Computer Engineering and Applications. 2008(08), 217-219.

Received: **13.12.2018**
Accepted: **22.02.2019**

CORRESPONDING AUTHOR

Mengyu Liu
School of Business Administration,
Hohai University,
Changzhou 213022 – China

e-mail: 18261195600@163.com

© by PSP Volume 28 – No. 4/2019 pages 2733-2738 Fresenius Environmental Bulletin

ANALYSIS OF THREE RELATIONS IN RURAL TOURISM DEVELOPMENT OF CHINA GUIZHOU UNDER THE STRATEGIC BACKGROUND OF RURAL VITALIZATION

Wei Wang*

Guizhou University, College of Law, Guiyang City, Guizhou Province, 550025, China

ABSTRACT

Rural vitalization is an important content for the construction of a great modern socialist country in the new era, and development of rural tourism is a vital means of such vitalization. In Guizhou province, rural tourism was conducted earlier, and the prosperity of rural tourism greatly promoted its rural economic and social development. Under the strategic background of rural vitalization in China, to further boost rural tourism, Guizhou must accurately grasp three relations to reach the purpose of rural tourism development, that is to get rid of poverty for all rural impoverished population. Hence, in the process of developing rural tourism, measures must be precisely and accurately taken in order to achieve the goal of poverty elimination. Rural area in Guizhou boasts beautiful natural scenery and abundant ethnic customs, but its ecological environment is fragile. As a result, "development" of rural tourism is based on the perquisite of "protection" in rural vitalization. To make rural tourism of Guizhou advance in a healthy manner, we must regard the market as the foundation and the government as the leading role to avoid malignant competition and resource waste.

KEYWORDS:
Rural tourism, rural vitalization, Western China

INTRODUCTION

To address the issues of agriculture and rural areas in China and build a great modern socialist country in the new era, in October 2017, the report of the CPC at the 19th National Congress proposed the significant strategy of "rural vitalization". In September 2018, the CPC Central Committee and the State Council announced *The Strategy of Rural Vitalization* (2018-2022) which presented exhaustive regulations on the development goals, vision planning and detailed measures regarding Chinese rural vitalization. The implementation of the rural vitalization strategy is the key and integral part of China's efforts to establish a moderately prosperous society and a great modern socialist country. Rural tourism can not only provide new employment opportunities and stable economic income sources for rural people, but also improve infrastructure construction and living environments in rural areas, and push agriculture towards modernization. Therefore, rural tourism has become the core industry and important channel for many rural areas to vitalize their industries and get rid of poverty. Besides, it is one of the most effective and direct means to systematically solve the three rural issues and materialize the rural vitalization strategy [1].

Over the years, Guizhou province in China has started with its own conditions to combine tourism development with promotion of poverty elimination in needy areas, industrial structure adjustment and resolution of three rural issues. It carried out the strategy of enriching people through tourism development, which generated distinct effect in increasing local farmers' income, facilitating adjustment of rural industrial structure, local economic and social development. According to the data in Guizhou Statistical Yearbook 2017, in 2015, tourism revenue accounted for 33.33% of Guizhou's gross regional product, and it was reached 42.67% in 2016. Rural tourism constitutes an essential component of Guizhou's tourism industry and in 2017, the rural tourism revenue occupied 1/4 of the total provincial tourism revenue [2]. Rural tourism plays an irreplaceable role in advancing Guizhou's rural economic development and facilitating sustainable development of rural economy, society, culture and environment. In the new era, to develop rural tourism better, realize the great strategy of rural vitalization, make Guizhou become moderately prosperous in sync and build a great modern socialist country, we must correctly handle three relationships in rural tourism, that is, poverty alleviation and poverty elimination, protection and development, government and market.

MATERIALS AND METHODS

The relationship between poverty alleviation and poverty elimination in Guizhou's rural tourism under the strategic background of rural vitalization: process or goal. Compared with other provinces, Guizhou has the largest poor population, the

largest area of poverty and the severest degree of poverty, therefore, Guizhou has been the main battlefield for China's fight against poverty. The tourism industry with prominent driving capacity and high industrial integration power is strongly linked with other industries. Guizhou has exceptional advantages to develop rural tourism for its cool weather, splendid natural scenery and unique folk customs. Being one of the earliest provinces which conducted rural tourism practice, Guizhou started rural tourism in 1980s and 1990s, and regarded it as the important aspect of rural poverty relief [3]. In the new era, Guizhou takes advantage of rural tourism construction to build a poverty relief network centering on rural tourism, raise poverty relief funds, develop rural tourism projects, promote construction of tourism products, and closely combine rural tourism and poverty relief. The Poverty Alleviation and Development Office of Guizhou Province arrange special funds of RMB 80 million for rural tourism poverty relief projects every year. Today, rural tourism has turned into one of the effective means of targeted poverty alleviation in Guizhou. During the 12th Five-Year Plan, rural tourism of Guizhou provided 2.8761 million jobs, benefited more than 5.77 million people with annual income of more than RMB 55 billion, and got rid of poverty or alleviated poverty for 647,000 people [4]. In 2017, the number of natural villages engaged in rural tourism that exceeded 3,000, among them, 517 natural villages were listed as the national key villages for rural tourism poverty alleviation. Rural tourism realized an annual income of RMB 76.316 billion, offered 480,000 direct employment opportunities and more than 600,000 indirect employment opportunities [5].

Winning the tough fight against poverty alleviation is the bottom line target and symbolic target of China's construction of a moderately prosperous society, and the essential requirement of socialism with Chinese characteristics, that is, every poor household must be free from poverty. China's rural vitalization strategy aims to make rural residents live a well-off life. Over the years, Guizhou has driven poor population to start businesses and make them gain extensive earnings from the development of rural tourism, which facilitated harmonious development of rural economy and society, and reaped distinct benefits in poverty relief. However, we must be aware that poverty alleviation is a process, and our ultimate goal is to remove poverty for all households. When the goal is achieved, the requirements of rural vitalization strategy are met. Some new problems appeared in the process of poverty alleviation and province development: all places where rural tourism can be developed which have been covered, and now it still has more than five million population stuck in poverty in Guizhou province, many of which live in a scattered way, so the cost for road construction, water and electricity supply is overly high. How to give scope to the poverty relief function of rural tourism and make the remaining poor population get rid of poverty at the earliest date is an urgent and severe issue at present.

To solve the realistic problem and carry out China's rural vitalization strategy, poverty alleviation by rural tourism needs to targeted poverty alleviation which will remove poverty for the last batch of poor people or poverty-stricken people so that all households and people will become affluent. To be targeted, precise measures should be implemented. Local resources should be properly utilized to help them develop. For instance, some places may have convenient transportation, so rural tourism can focus on accommodation; while some places possess the advantage of flower and fruit planting, so special breeding can be conducted to develop leisure and sightseeing agriculture. At the same time, targeted poverty alleviation should consider specific conditions of different households and people to find out the entry point on the chain of rural tourism that can increase the income of poor households. Now, Guizhou combines large scenic spots with small villages, that is, it can drive tourism development in the neighborhood through large scenic spots, list poverty alleviation through tourism in management measures for provincial level A tourism sites, and guide 250 tourism sites of the province to boost employment of poor population. In the process, 90,000 poor populations have benefited. In the meantime, Guizhou applied big data census on tourism resources to summarize 2,689 favorable resources and 960 new resources spot in extremely poor towns, which will be given priority in planning and development. Besides, an exquisite tourism scenic spot is constructed in 14 deeply impoverished towns. Guizhou set up exquisite tourism model places, and meanwhile built exquisite tourism routes with combination of points and lines. First, it conducts trial development in poor mountainous areas where conditions are met, and connects model places through exquisite tourism routes. Then, these routes are stringed into belts, and eventually, three theme functional zones of "red tourism + folk customs + ecological recreation" are formed around the province. Guizhou propels poverty alleviation and accelerates the process of poverty removal through sustainable development of rural tourism.

The relationship between development and protection in Guizhou's rural tourism under the strategic background of rural vitalization: way out or prerequisite. The core of tourism lies in local characteristic resources and maintenance of these characteristics [6]. Rural areas of Guizhou have natural beauty, beauty of harmonious humanity and beauty of simplistic rural charm, and the favorable ecological environment and profound ethnic cultural connotations are two precious treasures for rural tourism development in Guizhou. With scientific and reasonable development of rural tourism

resources, it converts these resources into appealing tourism products and further capital, gives play to the role of these resources and presents them to the public. Therefore, rural tourism development under the rural vitalization strategy is an effective way out for the three rural issues. However, rural tourism should not only provide quality services for tourists and develop economy, but also ensure intactness of nature and humanistic ecology as well as continuity of economic growth. Hence, protection of resources is the prerequisite for development and both of them should be well coordinated.

Guizhou is lauded by the general secretary XI Jinping as a "park province", of which beautiful villages are the most colorful and abundant elements. The beauty in Guizhou rural areas lies in their blue hills, green waters, characteristic villages and ecological and comfortable living environments. The natural scenery, fresh air and pleasant climate provide integral environmental resources and quality material elements for the development of rural tourism in Guizhou [7]. Meanwhile, Guizhou rural areas have rich and unique minority ethnic cultures. At present, 545 villages of Guizhou are listed in China Directory of Traditional Villages Protection, ranking the second in China; 213 villages are included in the list of villages with Chinese ethnic characteristics. It's deemed as the original ecological ethnic museum. However, the majority of its rural areas are located in the intensive karst landscape. As a result, despite abundant, beautiful and peculiar landscape, the karst area is characterized by fragile environment and low environmental capacity, thus being likely to be disturbed by artificial activities, and further causing environmental problems such as water and soil loss and damaged terrain. The construction of infrastructure in the rural tourism development of Guizhou has brought about immense people flow and material flow to natural villages that produce plenty of waste. Moreover, uncivilized behavior of tourists also destroys the rural ecological environment. As rural tourism is highly dependent on the desirable ecological environment, we must keep in mind that improving ecological environment is to protect and develop productivity, and that green waters and blue hills are gold and silver mountains. In addition, we should make economic benefits, social benefits and ecological benefits consistent, and take into account the bearing capacity of resources and environment. While guaranteeing facilities, we should pay greater attention to the protection of rural ecological environment and rural landscape so that urban residents are more willing to come to villages. Rural tourism is developed in rural areas, so rural environment, buildings, folk customs and food are all what attracts tourists; if these are missing, the development of tourism will lose support. Rural tourism shall stick to five originals, that is, original houses, original residents, original life, original production and original ecology [8]. In recent years, Guizhou has abided by the two bottom lines of development and ecology, carried out three strategic actions of large poverty alleviation, big data and large ecology, fully implemented the action plan of "experience in agricultural households and beautiful villages", and made great efforts to expedite rural tourism. Only rural characteristic landscape is built and original ecological environment is supplied, rural tourism realized sustainable development.

The relationship between government and market in Guizhou's rural tourism under the strategic background of rural vitalization: dominance or foundation. Being local and rural, rural tourism regards local beautiful natural landscape and abundant humanistic landscapes as its attracting points, and eventually realizes the development of rural economy and society by making rural tourism resources more intriguing to tourists and satisfying tourists' needs. In essence, it is a kind of market behavior which underlines market products and service value exchange. Operators maximize their profits, that is, pursuit of profit is the most typical feature of market behavior. Under such circumstance, it's likely that subjects of rural tourism develop blindly and put economic benefits in the first place in terms of value judgment, being anxious to attain success. On the one hand, this gives rise to homogenous malignant competition, that is, all tourism projects are the same, eating rural food and going sightseeing. Besides, the form of tourism products is dull and deep experience projects are missing, so projects with unique charm should be designed. On the other hand, chaotic development causes damages to rural ecological environment. Rural tourism, as a comprehensive industry that involves politics, economy, culture, society and ecology, produces positive impact on local economic and social development, but negative influences should not be overlooked. Hence, the pursuit of profit determined by the market implies that rural tourism development should not be completely left to the market; instead, governments must take the lead in it to gain balanced development of local politics, economy, culture and ecology [9], that is, to reinforce governments' macroscopic functions in development and improve the tourism management mechanism, which are leading factors [10].

Guizhou is a place with severe poverty, weak economy and low degree of marketization. Moreover, once the fragile ecological environment in rural karst areas of Guizhou is sabotaged, it will be difficult to restore. To orderly develop rural tourism and achieve coordinated and sustainable development of rural economy, society and environment, it is necessary to develop government-dominated tourism. In the process, government should work out a scientific plan first to reasonably determine goals of tourism development. Guizhou is pioneering in formulating the rural tourism plan *Rural Tourism Plan of Guizhou*, and also established related standards and systems, such

as *Standards for Assessment and Management of Rural Hotel in Guizhou*, *Rural Tourism Standards Based on the Unit of Villages* and *Rural Tourism Standards of Guizhou*, which promoted standardization of rural tourism in Guizhou. Second, governments should stipulate regulations on rural tourism so as to ensure standard management, correct guide and proper development with order [11]. Guizhou has successively announced documents such as *Opinions on Accelerating Rural Tourism Development*, *Rural Tourism Plan of Guizhou*, *Rural Tourism Development Plan for Key Tourist Villages*, *Implementation Plan for Poverty Alleviation of Guizhou*, *Implementation Plan for the Poverty Alleviation Fight through Tourism Development of Guizhou*, *Working Plan for Standardized and High-quality Development of Rural Tourism in Guizhou*, *Implementation Plan for Assistance of Ten Thousands of Enterprises and Villages in Guizhou*, *Opinions of Guizhou People's Government on Implementing Six Action Plans for Infrastructure Construction with the theme of "Experience in Agricultural Households and Beautiful Villages"*, *Standards for Assessment and Management of Rural Hotels in Guizhou*, *Standards for Village Construction and Services of Rural Villages in Guizhou*, *Grading and Evaluation of Service Quality of Rural Tourism Inns in Guizhou*, and *Management Measures for Quality Grading and Rating of Rural Tourism Villages*, *Operating Households (Agritaiment) and Inns*. These normative documents that focus on the manifestation of Guizhou's mountain environment, natural ecology and ethnic cultural characteristics have pointed out pertinent measures for orderly development of tourism, especially problems such as environmental and ecological damage, and hidden risks. Third, in the process, governments need to improve rural infrastructure and increase the level of public service [12]. Infrastructure belongs to public products whose exclusive and non-competitive characteristics determine that governments must shoulder the main responsibility of infrastructure construction, including rural roads, parking lots, washrooms, wastewater treatment facilities, fire control facilities and water & electricity supply facilities, etc. As China's first province where expressways are built in every county, Guizhou has convenient transportation that provides powerful support for the development of rural tourism. At the same time, in 2018, governments of Guizhou invested RMB 500 million in constructing 100 rural tourism model sites. In recent three years, Guizhou put RMB 278 million in building and expanding public service facilities including 803 toilets, parking lots, service stores and signboards, etc. Besides, governments held promotion meetings to introduce tourism routes of Guizhou [13]. To further speed up the development of rural tourism, Guizhou needs to focus on the following aspects: first, building highways in all rural groups of rural areas for the sake of rural tourism; second, accelerating intensification of expressways and construction of high-speed railways between cities and prefectures, as well as construction of civil airports and general airports; third, making sure every village is supplied with safe and stable water by to strengthening construction rural water conservancy infrastructure; fourth, rectifying rural living environment and ecological environment, and improving the living and environmental quality for rural residents; fifth, ensuring every village has access to quick internet services by heightening network infrastructure construction; sixth, promoting rural tourism operators to establish cooperative relations with tourism e-commerce and modern logistics enterprises; last but not least, strengthening training of employees in the rural tourism industry to enhance their management and service skills.

RESULTS

Much as the development of rural tourism entails the leading role of governments, in essence, it is a market behavior. Therefore, it should receive the test of the market, and only in this way can maintain its vitality. In the process, governments should clarify the marketization orientation, subdivide the markets and work out a strategic direction so that tourists' personalized consumption demands can be satisfied. Market is the foundation for rural tourism development which must observe the market mechanism. To meet the market demand, governments should select, process and re-create rural tourism resources, study these resources in detail on the basis of the market and design characteristic tourism products and routes that cater to the market demand. All in all, governments should not only guide the market but also pander to the market demands. Guizhou adopted the "two mountains" strategy along with Guizhou-Cloud Big Data to promote in-depth integration of big data and rural tourism, and utilized data analysis and mining technology to provide more scientific operation and decision making models for rural tourism. It has worked out many tourism routes and products that conform to tourists' preferences, cultivated tourism brands with distinct regional features based on local conditions at the right time, and highlighted rural characteristics. Sticking to "one village one product", "one village one scenery", "one village one charm", "one family one skill", and "one household one specialty" [14], Guizhou has achieved personalization, characterization and differentiation, and meanwhile maintained lasting development. Guizhou's rural tourism is led by governments on the basis of the market to meet diversified market demands and reinforce standardized market management [15]. By doing this, it not only compensates for the flaw of market failure, avoids malignant competition, resource waste and environmental damage, but also brings diverse operators and lively mechanisms, fully mobilizes operating subjects'

enthusiasm about rural tourism, and makes the development more scientific, reasonable, healthy and sustainable.

DISCUSSION AND CONCLUSION

As a significant strategy proposed at the 19th National Congress of the CPC, rural vitalization is the general initiative for three rural issues in the new era. As pointed out by *The Strategy of Rural Vitalization* (2018-2022), the recreational function of agriculture should be expanded while basic production tasks are accomplished; while basic life and product conditions are guaranteed for rural people, conditions should be created to develop rural tourism. Rural tourism connects the primary industry and the tertiary industry which can directly enhance the added value of agricultural products, boost integrated development of varied industries in rural areas, transform single agriculture mode into diversified agriculture mode, and accelerate the shift from extensive economy to benefit economy [16]. Rural tourism is a favorable image of Guizhou and the main channel of increasing income for impoverished population. The *13th Five-Year Plan for Economic and Social Development of Guizhou* proposed to expedite integrated development of the primary, secondary and tertiary industries, proactively extend agricultural functions, rely on natural sceneries, ethnic villages, ancient towns and villages and the program of "experience in agricultural households and construction of beautiful villages" to invigorate rural tourism based on local conditions, focus on construction of rural tourism model sites in the mountain areas, and build more than 2000 such villages by 2020. The development of rural tourism products should be strengthened to help with targeted poverty alleviation. Guided by the strategy of rural vitalization in the new era, Guizhou should correctly handle the three relationships between poverty alleviation and poverty elimination, development and protection, government and market so as to gain prosperity of rural tourism, enhance agricultural synergy, raise income of rural people and make the rural areas flourish. The active effect of rural tourism has been verified in promoting and protecting agricultural ecology and local culture, increasing rural people's income, alleviating poverty, transforming and upgrading agriculture, providing job opportunities for rural people, and enriching tourism products, etc.

ACKNOWLEDGEMENTS

Thanks for the support of Talent Introduction Research Project of Guizhou University (GZU Talent Introduction Contract Fund [2019] Reference No. 003).

REFERENCES

[1] Liu, Y. (2015) Orientation of Chongqing "five functional zones" towards new development of rural tourism. Journal of Chongqing University of Education. 29(4), 26-29.
[2] Zhang, Y., Hou, K., Li, X., Chang, Y. (2018) Study on land use classification and elastic urbanization in Chengguan district of lhasa city. Fresen. Environ. Bull. 27(9), 5908-5913.
[3] Che, J.X., Su, W.C., Liu, R. (2007) Development model and strategies of rural ecological tourism in mountain areas of Guizhou. Rural Economy. 27(11), 38-41.
[4] He, J.L. (2011) Development and utilization of catering culture and new countryside construction in Guizhou of China. Journal of Anhui Agricultural Sciences. 39(13), 76-79.
[5] Xiao, H.G., Li, L. (2004) Villagers' perceptions of traditions: some observations on the development of rural cultural tourism in china. Tourism Recreation Research. 29(2), 69-80.
[6] Zhang, S.J. (2017) On resource development and ecological protection in rural tourism: a case study on Taizhou city of Jiangsu province. Journal of Sichuan Tourism University. 17(6), 39-42.
[7] Xu, L., Cao, S.T., Liu, D.C. (2017) Exploration of Integrated Development between Rural Tourism and Ecological Civilization. Geography and Geo-Information Science. 17(6), 106-111.
[8] Lu, C., Wang, Y.C. (2017). How to develop farmhouse based on market demand? Asian Agricultural Research. 1, 13-14.
[9] Li, J.H. (2009) A study on sustainable development of rural tourism in karst areas. Beijing: Beijing Forestry University, 20.
[10] Wang, J.J. (2008) A study on ecosystem services for poverty alleviation in the basin of Lijiang River. Guilin: Guangxi Normal University, 8.
[11] Chen, Q. (2011) Government behavior and ecological protection in rural tourism sites: a case study on Kaifu district of Changsha city. Journal of Anhui Agricultural Sciences. 21(5), 2920-2922.
[12] Zhu, Y.H. (2016) A study on optimization of government functions in ecological tourism: a case study on Chongming county of Shanghai. Shanghai: East China University of Political Science and Law, 51.
[13] Almeida, A.M.M., Correia, A., Pimpão, A. (2014) Segmentation by benefits sought: the case of rural tourism in madeira. Current Issues in Tourism. 17(9), 813-831.
[14] Madan R. (2014) Agri-tourism in peri-urban Mumbai and Pune: ecological citizenship and rural-urban linkages in the global south. Cardiff University, 26.

[15] Wang, J., Dong, Q., Wang, Z.L., Liu, X.J. (2008) On marketing of cultural brand in rural ecological tourism. Research of Agricultural Modernization. 29(1), 81-84.
[16] Ma, Y. (2016) A study on legal guarantee issues of rural ecological tourism in construction of new rural areas. Agricultural Economy. 26(6), 53-54.

Received: **14.01.2019**
Accepted: **22.02.2019**

CORRESPONDING AUTHOR

Wei Wang
Guizhou University,
College of Law,
Guiyang City,
550025, Guizhou Province – China

e-mail: liangzzw@126.com

© by PSP Volume 28 – No. 4/2019 pages 2739-2746 Fresenius Environmental Bulletin

BIOLOGICAL EVALUATION OF 1-(4-(HYDROXY(1-OXO-1,3-DIHYDRO-2H-INDEN-2-YLIDENE)METHYL)PHENYL)-3-PHENYLUREA DERIVATIVES: ANTICHOLINERGICS AND ANTIEPILEPTIC POTENTIALS

Umit Muhammet Kocyigit*

Vocational School of Health Services, Sivas Cumhuriyet University, 58140 Sivas, Turkey

ABSTRACT

In this work, a class of phenylurea compounds containing 2-benzoylindan-1-one molecules 3a–3j was designed and synthesized from the reaction of phenylurea-substituted acetophenone compounds with phthalaldehyde molecule under mild action situations in good yields. The inhibitory effect of these compounds on some metabolic enzymes was examined and compared with a standard compound. IC_{50} values were obtained from the phenylurea-Induced Activity (%)-[phenylurea compounds] graph and from the Lineweaver-Burk graph. According to the results, the IC_{50} values of these molecules were in the range 18.23-63.01 nM for hCA I, while the mean K_i values were in the range 7.79±0.94-122.64±32.15 nM for this enzyme. The results obtained are expected to make an important contribution to drug design and pharmacological applications. Additionally, these compounds demonstrated well inhibitory effects against acetylcholineesterase (AChE) enzyme. Finally, the K_i values of hCA II were in the range 15.09±4.48-65.72±6.64 nM and 1.54±0.21-22.44±3.83 nM against AChE, respectively.

KEYWORDS:
Phenylurea, carbonic anhydrase, acetylcholinesterase, enzyme inhibition, antiepileptic potentials.

INTRODUCTION

1,3-Diketone compounds have a significant location in the medicinal and organic chemistry as a synthetic building block. These molecules play an outstanding role in the synthesis act of many heterocyclic molecules and bioactive molecules. Great reactivity of 1,3-diketone molecules performed molecular variety in the synthesis action of natural and organic compounds. Additionally, between the molecules exhibiting biological activity, it recognized that molecules comprising the diaryl urea unit have a wide spectrum of activity [1-3]. Also, we synthesized some phenylurea derivatives 3a – 3j, which are diphenylurea motif and 1,3-diketone, by the reaction of phthalaldehyde with phenylurea substituted acetophenones in basic medium (Figure 1).

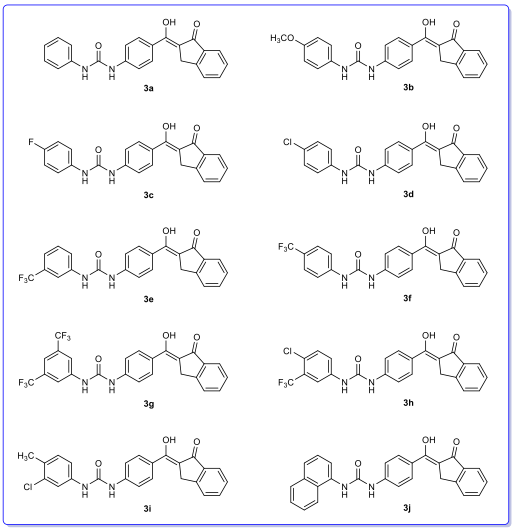

FIGURE 1
Structures of 3a-j derivatives

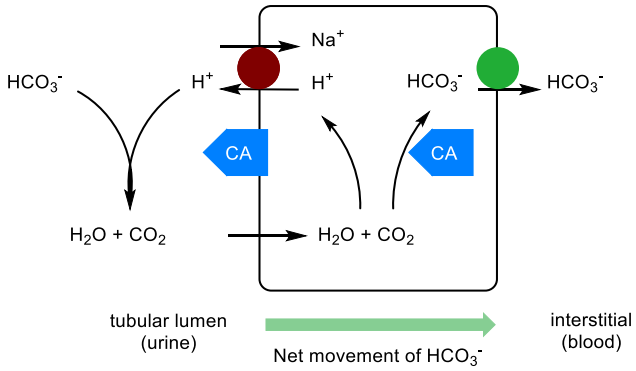

FIGURE 2
Mechanism of carbonic anhydrase enzyme

Carbonic anhydrase (CA, E.C.4.2.1.1) enzymes play a main role in the base-acid equilibrium by using a necessary buffering system for the tissues and body fluids [4-7]. Also, they transform CO_2 molecule that is created by metabolic mechanisms to H_2CO_3, which is transported in the blood via tissue cells [8]. CA enzymes are very efficient enzymes, which catalyze the rapid conversion of carbon dioxide (CO_2) to bicarbonate (HCO_3^-) and a proton (H^+) [9, 10]. This act is current for most organisms during the evolution of life seven genetically diverse classes of this enzyme, which classified as α-, β-, γ-, δ-, ζ-, η- and θ-CAs. Many CA isoforms involved in these mechanisms are significant therapeutic goals with the potential to be inhibition or activation for the therapy of a large disorders spectrum [11-14]. Up to now, sixteen isozymes have been determined that differ in their catalytic activity and subcellular site with different affinity to inhibitors. CA is one of the most studied enzymes and both CA I, and II are the most common isoenzymes conforming to situations and necessities of the middle [15-17] (Figure 2).

Cholinesterase (ChE) enzymes hydrolyze the choline ester molecules. Indeed, in mammalian cells, there are two main forms of cholinesterase enzymes, namely, butyrylcholinesterase (BChE) and AChE, determined by very great concentrations in the nerve cells, placental tissue, muscle, erythrocytes, and brain [18, 19]. AChE enzyme is a special choline esterase enzyme and also it is a hydrolytic catalyst of the serine type [20]. Alzheimer's disease (AD) affects frequently the elderly human and superior resulting in spoiled behavior and memory [21]. This disturbance clinically involves the advanced decline of brain tissue cells that are influenced by the deficit in acetylcholine (ACh) [22]. Cerebral amyloid-β aggregation, a deficiency in ACh and a deficiency in cholinergic neurotransmission, was considered in sicks with AD. AChE enzyme, a main element of the cholinergic system in the central and peripheral nervous system, is capable to convert ACh molecule to choline and acetate. It is caused by genetic influences and environmental [23-27].

In this work, we have determined the inhibition effects of phenylurea compounds on some metabolic enzymes like AChE, hCA I and II enzymes, using the acetylcholine iodide solution as substrate for AChE enzyme.

MATERIALS AND METHODS

Chemicals. A series of 1-(4-(hydroxy(1-oxo-1,3-dihydro-2H-inden-2-ylidene)methyl)phenyl)-3-phenylurea molecules (3a – 3j) have been synthesized from the phenylurea substituted acetophenone molecules in high yields (73 – 85%). The main structures of these molecules were established on the basis of spectroscopic methods (Table 1) [28].

TABLE 1
Synthesized 3a-j derivatives.

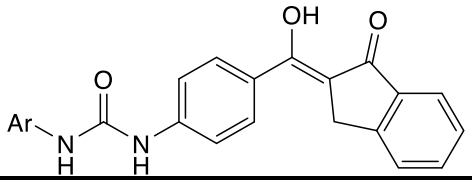

Entry	Ar	Product
1	Ph	**3a**
2	4-MeOPh	**3b**
3	4-FPh	**3c**
4	4-ClPh	**3d**
5	3-CF_3Ph	**3e**
6	4-CF_3Ph	**3f**
7	3,5-CF_3Ph	**3g**
8	3-CF_3-4-ClPh	**3h**
9	3-Cl-4-CH_3Ph	**3i**
10	1-Naphthyl	**3j**

Enzyme studies. Carbonic anhydrase inhibition assay. In CA enzyme section, changes in absorbance and inhibitory effects of phenylurea molecules (3a – 3j) were recorded during 3 min at 348 nm using p-Nitrophenylacetate was utilized as a substrate which converted by both isoenzymes to the p-nitrophenolate and performed conforming to Verpoorte [29] method and previous studies [30, 31].

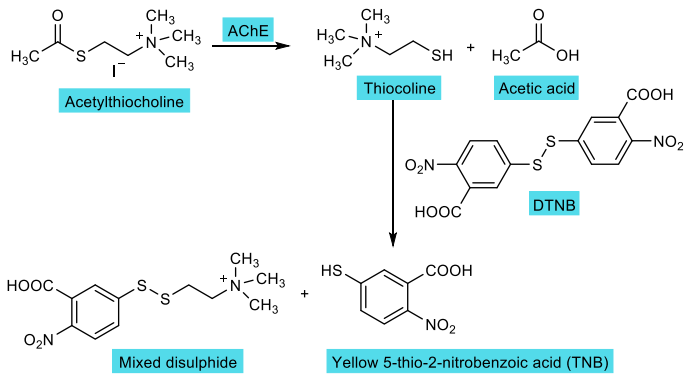

FIGURE 3
Mechanism of Acetylcholinesterase enzyme with DTNB and AChI

TABLE 2
The half maximal inhibition concentration (IC_{50}) and inhibition constants (K_i) of phenolic compounds against human carbonic anhydrase isoenzymes I and II (hCA I and II), and AChE enzymes.

Compounds	IC_{50} (nM)						K_i (nM)		
	hCA I	r^2	hCA II	r^2	AChE	r^2	hCA I	hCA II	AChE
3a	53.30	0.9808	30.12	0.9480	5.54	0.9859	43.02±4.44	49.26±3.58	1.72±0.53
3b	25.66	0.9879	29.98	0.9719	9.11	0.9905	24.77±9.51	50.51±6.46	4.42±0.32
3c	49.50	0.9883	28.87	0.9674	4.31	0.9360	43.60±11.38	34.40±7.81	1.54±0.21
3d	36.47	0.9760	13.31	0.9810	5.87	0.9621	21.51±6.54	16.54±3.07	7.11±1.18
3e	18.23	0.9820	14.37	0.9735	15.06	0.9830	7.79±0.94	15.09±4.48	8.52±0.67
3f	53.33	0.9690	40.52	0.9897	12.37	0.9602	35.36±4.31	65.72±6.64	14.67±4.76
3g	49.14	0.9729	26.65	0.9713	8.55	0.9727	122.64±32.15	32.60±10.44	5.80±2.15
3h	63.01	0.9557	53.32	0.9901	23.10	0.9842	92.42±32.26	51.31±2.55	22.44±3.83
3i	62.37	0.9384	30.13	0.9780	15.41	0.9596	47.37±16.28	59.18±5.55	6.32±0.88
3j	45.88	0.9880	21.01	0.9681	7.21	0.9855	76.22±33.12	14.27±3.78	2.57±0.53
AZA*	173.28	0.9778	115.52	0.9642	-	-	271.15±74.62	113.07±20.98	-
Tacrine⁰	-	-	-	-	53.31	0.9698	-	-	12.44±3.42

*AZA (acetazolamide) was used as positive control for hCA I, and II isoenzymes.
⁰Tacrine was used as positive control for AChE enzyme.

Acetylcholinesterase inhibitions assays. Acetylthiocholine iodide was used as substrates of the reaction and DTNB method was used for the measurement and inhibitory effects of phenylurea molecules (3a – 3j) as anticholinesterase activity and performed conforming to Ellman method [32] and previous studies [33, 34]. For investigation inhibitory effects and hydrolysis of this substrate by spectrophotometrically and the formation of yellow 5-thio-2-nitrobenzoate anion as a result of the reaction of DTNB with thiocholine molecule, released in this study by the enzymatic hydrolysis of acetylthiocholine iodide, at a wavelength of 412 nm.

RESULTS AND DISCUSSION

In this article, AChE as a metabolic enzyme was investigated. phenolic compounds were determined for their inhibition confidants against some metabolic enzyme, which demonstrated commonly an effective inhibition. The chemical structure of phenolic compound is shown in Figure 1. Also, these metabolic enzymes inhibiting results of the phenolic compound are seen in Table 2 and Figure 4. The following results of this work of Table 2:

(i) Both physiologically pertinent hCA I, hCA II, and AChE were investigated in the enzyme inhibition stage of this work using esterase activity. CA has both esterase and hydratase activities, however, esterase activity had common usage than hydratase activity in inhibition studies because of the determination of Ki values of inhibitors. CA II was chosen since of its antiglaucoma drug goals while CA I, due to it makes dispensation gastrointestinal tract and in the blood is one of the main off-goals for such pharmacologic factors [35]. Results of these isoforms:

For the cytosolic hCA I isoform, phenylurea derivatives (3a – 3j) had K_i values form 7.79±0.94 nM to 122.64±32.15, also had IC_{50} values from 18.23 nM to 63.01, respectively (Table 2 and Figure 4). Additionally, For the hCA II isoform, phenylurea derivatives (3a – 3j) had K_i values from 15.09±4.48 nM to 65.72±6.64, also obtained IC_{50} values from 13.31 nM to 53.32, respectively (Table 2 and Figure 4). In this work, acetazolamide (AZA), used as a control CA inhibitor for the medical therapy of glaucoma, idiopathic intracranial hypertension, altitude sickness, dural ectasia, and epileptic seizure. This standard inhibitor (AZA) showed K_i values of 271.15±74.62 and 113.07±20.98 nM, for both physiologically relevant hCA I, and II respectively (Table 2 and Figure 4). IC_{50} values of phenylurea

derivatives (3a – 3j) and standard (acetazolamide) compounds exhibited the following order: 3e (18.23 nM, r^2: 0.9820) < 3b (25.66 nM, r^2: 0.9879) < 3d (36.47 nM, r^2: 0.9760) < 3j (45.88 nM, r^2: 0.9880) < 3g (49.14 nM, r^2: 0.9729) < 3c (49.50 nM, r^2: 0.9883) < 3a (53.30 nM, r^2: 0.9808) < 3f (53.33 nM, r^2: 0.9690) < 3i (62.37 nM, r^2: 0.9384) < 3h (63.01 nM, r^2: 0.9557) < acetazolamide (173.28 nM, r^2: 0.9778) for hCA I while these compound exhibited for hCA II the following order: 3d (13.31 nM, r^2: 0.9810) < 3e (14.37 nM, r^2: 0.9735) < 3j (21.01 nM, r^2: 0.9681) < 3g (26.65 nM, r^2: 0.9713) < 3c (28.87 nM, r^2: 0.9674) < 3b (29.98 nM, r^2: 0.9719) < 3a (30.12 nM, r^2: 0.9480) < 3i (30.13 nM, r^2: 0.9780) < 3f (40.52 nM, r^2: 0.9897) < 3h (53.32 nM, r^2: 0.9901) < acetazolamide (115.52 nM, r^2: 0.9642). CAIs have been utilized in clinic for the therapy of diverse diseases like glaucoma, epilepsy and high altitude sickness. Indeed, these inhibitors are under large research for their use in the therapy of cancer and obesity while CA activators have been studied for the therapy of memory disturbances [36]. (Figure 5).

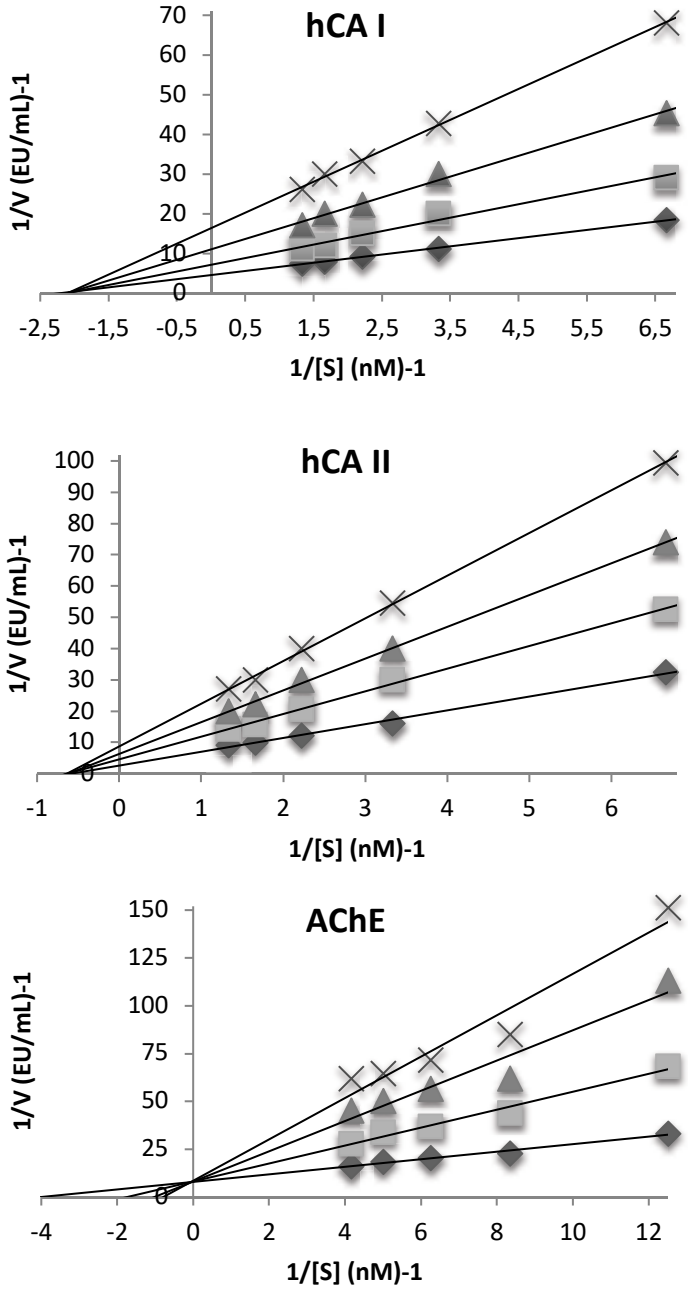

FIGURE 4
K_i graphs of best inhibitors

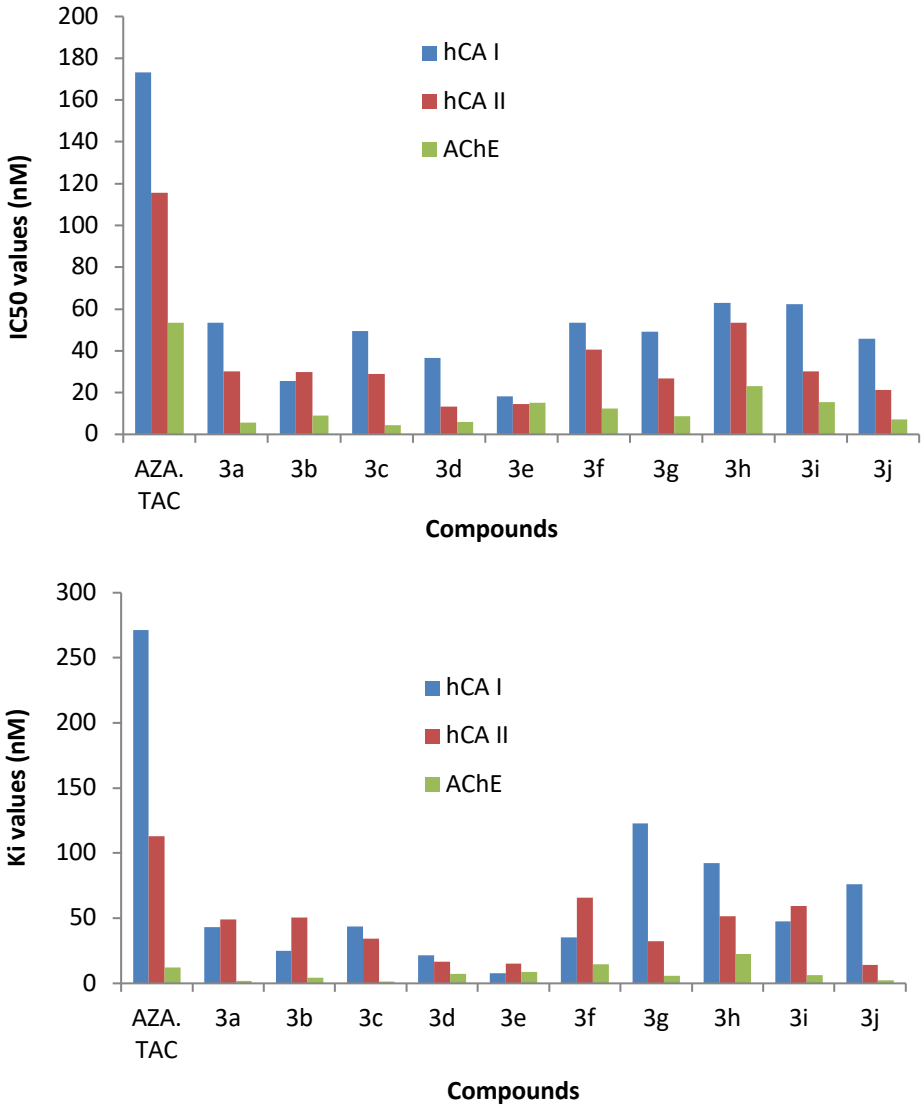

FIGURE 5
Ki and IC_{50} values which shown by graphs

(ii) Phenylurea derivatives (3a – 3j) effectively inhibited AChE, which is the primary cholinesterase in the body. It was obtained that K_i values were in the range 1.54±0.21-22.44±3.83 nM for AChE. (Table 2 and Figure 4). In addition, Tacrine (TAC) was used as positive control AChE inhibitor it had K_i value 12.44±3.42. IC_{50} values of phenylurea derivatives (3a – 3j) and standard (Tacrine) compounds exhibited the following order: 3c (4.31 nM, r^2: 0.9360) < 3a (5.54 nM, r^2: 0.9859) < 3d (5.87 nM, r^2: 0.9621) < 3j (7.21 nM, r^2: 0.9855) < 3g (8.55 nM, r^2: 0.9727) < 3b (9.11 nM, r^2: 0.9905) < 3f (12.37 nM, r^2: 0.9602) < 3e (15.06 nM, r^2: 0.9830) < 3i (15.41 nM, r^2: 0.9596) < 3h (23.10 nM, r^2: 0.9842) < Tacrine (53.31 nM, r^2: 0.9698). New attention has focused on AChE enzyme and its possible relation in the therapy of AD. BChE and AChE enzymes have been recognized in neurofibrillary tangles and amyloid plaque cells. AChE enzyme defined as predominates enzyme in the normal brain while BChE enzyme is thought to be relevant with a secondary role in the brain for adjustment of ACh levels. A considerable increase in the AChE enzyme activity is monitored in AD early phase. For this reason, AChE enzyme is substantial remedial and therapeutic aims for the recovery of cholinergic deficiency and can to be the AD hallmark [37].

Investigation of the effects of these compounds on AChE enzyme, and hCA I and II isoenzymes was the main purpose of this work, and inhibition results of these molecules are present in Table 2. Also, the chemical structures of phenylurea derivatives (3a – 3j) are clearly seen in Table 1 and Figure 1. IC_{50} value is the exponent of these molecules in inhibiting metabolic enzymes activities. Additionally, the calculated Ki values for these molecules were evaluated for each enzyme. As we described above, phenylurea derivatives (3a – 3j) can be alright factors drugs, the

same as AChE enzyme, for treatment of AD, and CAI compounds, for the therapy of some diseases, like glaucoma, mountain sickness, gastric and duodenal ulcers, osteoporosis, epilepsy, or neurological disturbances. These molecules can be utilized as a significant tool in important biological mechanisms and in the modern chemistry branch [38]. For AChE, Ki values of phenylurea derivatives (3a – 3j) and standard (Tacrine) compounds exhibited the following order: 3c (1.54±0.21 nM) < 3a (1.72±0.53 nM) < 3j (2.57±0.53 nM) < 3b (4.42±0.32 nM) < 3g (5.80±2.15 nM) < 3i (6.32±0.88 nM) < 3d (7.11±1.18 nM) < 3e (8.52±0.67 nM) < 3f (14.67±4.76 nM) < 3h (22.44±3.83 nM) < Tacrine (12.44±3.42 nM).

When we defined to enzyme results, all compounds had lower IC_{50} degree than the control molecule and compound 3e was the most beneficial and effective one for hCA I. phenylurea derivatives (3a – 3j) have also lower IC_{50} value than the control molecule AZA for hCA II and the molecule 3j is the best hCA II inhibitor. As find in the results, these compounds of phenylurea derivatives (3a – 3j) have the potential to inhibit metabolic enzymes for example AChE enzyme, which is very necessary ChE for humans.

Recently, our group could the interactions of BChE and AChE with Mannich bases, cyclic thioureas, ureas derived from phenethylamines, hetaryl sulfonamides, tetrahydropyrimidines, diaryl ethers, benzenesulfonamides, and tetrahydropyrimidine-5-carboxylates, and β-lactams, as well as the interactions for both CA enzymes with polyphenols and phenolic acids, caffeic acid, bromophenols, 1,3,5-trisubstitutedpyrazolines, tetralone-based derivatives, dopaminergic compounds, benzotropones, sulfamides, sulfonamides, benzenesulfonamides, novel eugenol derivatives, acylsulfonamides, some natural sulfonamide derivatives, and benzylsulfamides have been studied [39, 40].

CONCLUSIONS

AChEI compounds, acting with AChE enzyme as their key goal, are applied as toxin materials and relevant drugs. A good-recorded CA inhibitor compound as control factor, AZA, also some other CA inhibitors such as methazolamide, zonisamide, topiramate, were agreed for the treatment of epileptic perturbations and epilepsy. These compounds utilized in the present study recorded efficient inhibition profiles against as important metabolic enzymes. In this study, nanomolar levels of IC_{50} and K_i values were obtained for these important compounds on metabolic enzymes which are hCA I and II and AChE enzymes.

ACKNOWLEDGEMENTS

The authors declare that there are no conflicts of interest.

REFERENCES

[1] Vigato, P.A., Peruzzo, V. and Tamburini, S. (2009) The evolution of β-diketone or β-diketophenol ligands and related complexes. Coordination Chemistry Reviews. 253(7-8), 1099-1201.

[2] Kim, J., Shokova, E., Tafeenko, V. and Kovalev, V. (2014) $(CF_3CO)_2O/CF_3SO_3H$-mediated synthesis of 1, 3-diketones from carboxylic acids and aromatic ketones. Beilstein journal of organic chemistry. 10(1), 2270-2278.

[3] Abdel-Aziz, M., Abuo-Rahma, G.E.D.A. and Hassan, A.A. (2009) Synthesis of novel pyrazole derivatives and evaluation of their antidepressant and anticonvulsant activities. European journal of medicinal chemistry. 44(9), 3480-3487.

[4] Taslimi, P., Sujayev, A., Garibov, E., Nazarov, N., Huyut, Z., Alwasel, S.H. and Gulçin, İ. (2017) Synthesis of new cyclic thioureas and evaluation of their metal-chelating activity, acetylcholinesterase, butyrylcholinesterase, and carbonic anhydrase inhibition profiles. Journal of biochemical and molecular toxicology. 31(7), e21897.

[5] Kocyigit, U.M., Taslimi, P. and Gulçin, İ. (2018) Characterization and inhibition effects of some metal ions on carbonic anhydrase enzyme from Kangal Akkaraman sheep. Journal of biochemical and molecular toxicology. 32(8), e22172.

[6] Ökten, S., Ekiz, M., Koçyiğit, Ü.M., Tutar, A., Çelik, İ., Akkurt, M. and Gülçin, İ. (2019) Synthesis, characterization, crystal structures, theoretical calculations and biological evaluations of novel substituted tacrine derivatives as cholinesterase and carbonic anhydrase enzymes inhibitors. Journal of Molecular Structure. 1175, 906-915.

[7] Kocyigit, U.M. (2018) Investigation of Inhibition Effect of Oxytocin on Carbonic Anhydrase and Acetylcholinesterase Enzymes in the Heart Tissues of Rats Iğdır Univ. J. Inst. Sci. and Tech. 8(1), 199-207.

[8] Tutar, U., Koçyiğit, Ü.M. and Gezegen, H. (2018) Evaluation of antimicrobial, antibiofilm and carbonic anhydrase inhibition profiles of 1, 3-bis-chalcone derivatives. Journal of biochemical and molecular toxicology. e22281.

[9] Eruygur, N., Ataş, M., Tekin, M., Taslimi, P., Koçyiğit, U.M., and Gulçin, İ. (2018) In vitro antioxidant, antimicrobial, anticholinesterase and antidiabetic activities of Turkish endemic Achillea cucullata (Asteraceae) from ethanol extract. South African Journal of Botany. 12, 5p.

[10] Ekiz, M., Tutar, A., Ökten, S., Bütün, B., Koçyiğit, Ü.M., Taslimi, P. and Topçu, G. (2018) Synthesis, characterization, and SAR of arylated indenoquinoline-based cholinesterase and carbonic anhydrase inhibitors. Archiv der Pharmazie. 351(9). 1800167.

[11] Eruygur, N., Koçyiğit, U.M., Taslimi, P., Ataş, M., Tekin, M. and Gülçin, İ. (2019) Screening the in vitro antioxidant, antimicrobial, anticholinesterase, antidiabetic activities of endemic Achillea cucullata (Asteraceae) ethanol extract. South African Journal of Botany. 120, 141-145.

[12] Garibov, E., Taslimi, P., Sujayev, A., Bingol, Z., Çetinkaya, S., Gulçin, İ., Beydemir, S. Farzaliyev, W., Alwasel, S.H., Supuran, C.T. (2016) Synthesis of 4, 5-disubstituted-2-thioxo-1, 2, 3, 4-tetrahydropyrimidines and investigation of their acetylcholinesterase, butyrylcholinesterase, carbonic anhydrase I/II inhibitory and antioxidant activities. Journal of enzyme inhibition and medicinal chemistry. 31(sup3), 1-9.

[13] Aksu, K., Özgeriş, B., Taslimi, P., Naderi, A., Gülçin, İ. and Göksu, S. (2016) Antioxidant activity, acetylcholinesterase, and carbonic anhydrase inhibitory properties of novel ureas derived from phenethylamines. Archiv der pharmazie. 349(12), 944-954.

[14] Taslimi, P., Gulcin, I., Ozgeris, B., Goksu, S., Tumer, F., Alwasel, S.H. and Supuran, C.T. (2016) The human carbonic anhydrase isoenzymes I and II (hCA I and II) inhibition effects of trimethoxyindane derivatives. Journal of enzyme inhibition and medicinal chemistry. 31(1), 152-157.

[15] Gul, H.I., Tugrak, M., Sakagami, H., Taslimi, P., Gulcin, I. and Supuran, C.T. (2016) Synthesis and bioactivity studies on new 4-(3-(4-Substitutedphenyl)-3a, 4-dihydro-3 H-indeno [1, 2-c] pyrazol-2-yl) benzenesulfonamides. Journal of enzyme inhibition and medicinal chemistry. 31(6), 1619-1624.

[16] Gul, H.I., Demirtas, A., Ucar, G., Taslimi, P., and Gulcin, I. (2017) Synthesis of Mannich bases by two different methods and evaluation of their acetylcholine esterase and carbonic anhydrase inhibitory activities. Letters in drug design and discovery. 14(5), 573-580.

[17] Bayrak, Ç., Taslimi, P., Gülçin, İ. and Menzek, A. (2017) The first synthesis of 4-phenylbutenone derivative bromophenols including natural products and their inhibition profiles for carbonic anhydrase, acetylcholinesterase and butyrylcholinesterase enzymes. Bioorganic chemistry. 72, 359-366.

[18] Kocyigit, U.M., Taslimi, P., Gezegen, H., Gulçin, İ. and Ceylan, M. (2017) Evaluation of acetylcholinesterase and carbonic anhydrase inhibition profiles of 1, 2, 3, 4, 6-pentasubstituted-4-hydroxy-cyclohexanes. Journal of biochemical and molecular toxicology. 31(9), e21938.

[19] Dastan, T., Kocyigit, U.M., Durna Dastan, S., Canturk Kilickaya, P., Taslimi, P., Cevik, O., and Cetin, A. (2017) Investigation of acetylcholinesterase and mammalian DNA topoisomerases, carbonic anhydrase inhibition profiles, and cytotoxic activity of novel bis (α-aminoalkyl) phosphinic acid derivatives against human breast cancer. Journal of biochemical and molecular toxicology. 31(11), e21971.

[20] Kocyigit, U.M., Taşkıran, A.Ş., Taslimi, P., Yokuş, A., Temel, Y. and Gulçin, İ. (2017) Inhibitory effects of oxytocin and oxytocin receptor antagonist atosiban on the activities of carbonic anhydrase and acetylcholinesterase enzymes in the liver and kidney tissues of rats. Journal of biochemical and molecular toxicology. 31(11), e21972.

[21] Kocyigit, U.M., Budak, Y., Gürdere, M.B., Tekin, Ş., Köprülü, T.K., Ertürk, F. and Ceylan, M. (2017) Synthesis, characterization, anticancer, antimicrobial and carbonic anhydrase inhibition profiles of novel (3aR, 4S, 7R, 7aS)-2-(4-((E)-3-(3-aryl) acryloyl) phenyl)-3a, 4, 7, 7a-tetrahydro-1H-4, 7-methanoisoindole-1, 3 (2H)-dione derivatives. Bioorganic chemistry. 70, 118-125.

[22] Bulut, N., Kocyigit, U.M., Gecibesler, I.H., Dastan, T., Karci, H., Taslimi, P., Dastan, S.D., Gulcin, I. and Cetin, A. (2018) Synthesis of some novel pyridine compounds containing bis-1, 2, 4-triazole/thiosemicarbazide moiety and investigation of their antioxidant properties, carbonic anhydrase, and acetylcholinesterase enzymes inhibition profiles. Journal of biochemical and molecular toxicology. 32(1), e22006.

[23] Kocyigit, U.M., Budak, Y., Gürdere, M.B., Ertürk, F., Yencilek, B., Taslimi, P., Gulcin, I., and Ceylan, M. (2018) Synthesis of chalconeimide derivatives and investigation of their anticancer and antimicrobial activities, carbonic anhydrase and acetylcholinesterase enzymes inhibition profiles. Archives of physiology and biochemistry. 124(1), 61-68.

[24] Kocyigit, U.M., Taslimi, P., Gurses, F., Soylu, S., Durna Dastan, S. and Gulcin, İ. (2018) The effects of wireless electromagnetic fields on the activities of carbonic anhydrase and acetylcholinesterase enzymes in various tissues of rats. Journal of biochemical and molecular toxicology. 32(3), e22031.

[25] Güzel, E., Koçyiğit, Ü.M., Arslan, B.S., Ataş, M., Taslimi, P., Gökalp, F. and Gulçin, İ. (2019) Aminopyrazole-substituted metallophthalocyanines: Preparation, aggregation behavior, and investigation of metabolic enzymes inhibition properties. Archiv der Pharmazie. 1800292.
[26] Taslimi, P. and Gulçin, İ. (2018) Antioxidant and anticholinergic properties of olivetol. Journal of food biochemistry. 42(3), e12516.
[27] Türker, F., Barut Celepci, D., Aktaş, A., Taslimi, P., Gök, Y., Aygün, M. and Gülçin, İ. (2018) meta-Cyanobenzyl substituted benzimidazolium salts: Synthesis, characterization, crystal structure and carbonic anhydrase, α-glycosidase, butyrylcholinesterase, and acetylcholinesterase inhibitory properties. Archiv der Pharmazie. 351(7), 1800029.
[28] Kocyigit, U.M., Budak, Y., Eligüzel, F., Taslimi, P., Kılıç, D., Gulçin, İ. and Ceylan, M. (2017) Synthesis and carbonic anhydrase inhibition of tetrabromo chalcone derivatives. Archiv der Pharmazie. 350(12), 1700198.
[29] Verpoorte, J.A., Mehta, S., and Edsall, J.T. (1967) Esterase activities of human carbonic anhydrases B and C. Journal of Biological Chemistry. 242(18), 4221-4229.
[30] Temel, Y. and Kocyigit, U.M. (2017) Purification of glucose-6-phosphate dehydrogenase from rat (Rattus norvegicus) erythrocytes and inhibition effects of some metal ions on enzyme activity. Journal of biochemical and molecular toxicology. 31(9), e21927.
[31] Öztaskın, N., Taslimi, P., Maraş, A., Gülcin, İ., and Göksu, S. (2017) Novel antioxidant bromophenols with acetylcholinesterase, butyrylcholinesterase and carbonic anhydrase inhibitory actions. Bioorganic chemistry. 74, 104-114.
[32] Ellman, G.L., Courtney, K.D., Andres Jr., V. and Featherstone, R.M. (1961) A new and rapid colorimetric determination of acetylcholinesterase activity. Biochemical pharmacology. 7(2), 88-95.
[33] Timur, İ., Kocyigit, Ü.M., Dastan, T., Sandal, S., Ceribası, A.O., Taslimi, P., Gulçin, I., Koparir, M., Karatepe, M.,and Çiftçi, M. (2019) In vitro cytotoxic and in vivo antitumoral activities of some aminomethyl derivatives of 2, 4-dihydro-3H-1, 2, 4-triazole-3-thiones—Evaluation of their acetylcholinesterase and carbonic anhydrase enzymes inhibition profiles. Journal of biochemical and molecular toxicology. 33(1), e22239.
[34] Atmaca, U., Yıldırım, A., Taslimi, P., Çelik, S. T., Gülçin, İ., Supuran, C.T. and Çelik, M. (2018) Intermolecular amination of allylic and benzylic alcohols leads to effective inhibitions of acetylcholinesterase enzyme and carbonic anhydrase I and II isoenzymes. Journal of biochemical and molecular toxicology. 32(8), e22173.
[35] Bayrak, Ç., Taslimi, P., Gülçin, İ. and Menzek, A. (2017) The first synthesis of 4-phenylbutenone derivative bromophenols including natural products and their inhibition profiles for carbonic anhydrase, acetylcholinesterase and butyrylcholinesterase enzymes. Bioorganic chemistry. 72, 359-366.
[36] Zengin, M., Genc, H., Taslimi, P., Kestane, A., Guclu, E., Ogutlu, A., Karabay, O. and Gulçin, İ. (2018) Novel thymol bearing oxypropanolamine derivatives as potent some metabolic enzyme inhibitors–Their antidiabetic, anticholinergic and antibacterial potentials. Bioorganic chemistry. 81, 119-126.
[37] Huseynova, M., Taslimi, P., Medjidov, A., Farzaliyev, V., Aliyeva, M., Gondolova, G., Sahin, O., Yalcın, B., Sujayev, A., Orman, E.B. and Özkaya, A.R. (2018) Synthesis, characterization, crystal structure, electrochemical studies and biological evaluation of metal complexes with thiosemicarbazone of glyoxylic acid. Polyhedron. 155, 25-33.
[38] Huseynova, M., Medjidov, A., Taslimi, P. and Aliyeva, M. (2018) Synthesis, Characterization, Crystal Structure of the Coordination Polymer Zn (II) with Thiosemicarbazone of Glyoxalic Acid and Their Inhibitory Properties Against Some Metabolic Enzymes. Bioorganic chemistry. 83, 55-62.
[39] Biçer, A., Taslimi, P., Yakalı, G., Gülçin, I., Gültekin, M.S. and Cin, G.T. (2019) Synthesis, characterization, crystal structure of novel bisthiomethylcyclohexanone derivatives and their inhibitory properties against some metabolic enzymes. Bioorganic chemistry. 82, 393-404.
[40] Yiğit, B., Kaya, R., Taslimi, P., Işık, Y., Karaman, M., Yiğit, M. and Gulçin, İ. (2019) Imidazolinium chloride salts bearing wingtip groups: Synthesis, molecular docking and metabolic enzymes inhibition. Journal of Molecular Structure. 1179, 709-718.

Received: **21.01.2019**
Accepted: **20.02.2019**

CORRESPONDING AUTHOR

Umit M Kocyigit
Cumhuriyet University
Vocational School of Health Services
TR-58140-Sivas – Turkey

e-mail: ukocyigit@cumhuriyet.edu.tr

© by PSP Volume 28 – No. 4/2019 pages 2747-2753 Fresenius Environmental Bulletin

A STUDY ON THE EFFECTS OF WOOD VINEGAR ON WEEDS AND CULTIVATED PLANTS IN THE WHEAT AGRO-ECOSYSTEMS

Ibrahim Koc[1,*], Ayten Namli[2], Mehmet Mendes[3], Suleyman Mesut Pinar[4], Fatih Cig[5], Erdal Necip Yardim[6]

[1]Bitlis Eren University, Faculty of Engineering and Architecture, Department of Environmental Engineering, 13000, Bitlis, Turkey
[2]Ankara University, Faculty of Agriculture, Department of Soil Science and Plant Nutrition, 06110, Ankara, Turkey
[3]Canakkale Onsekiz Mart University, Faculty of Agriculture, 17000, Canakkale, Turkey
[4]Van Yuzuncu Yil University, Van School of Health, 65080, Van, Turkey
[5]Siirt University, Faculty of Agriculture, Department of Field Crops, 56100, Siirt, Turkey
[6]Bitlis Eren University Rectorship, 13000, Bitlis, Turkey

ABSTRACT

This study was conducted to determine the effects on the weeds and cultivated plants in the wheat agro-ecosystems of the wood vinegar in the biopesticide potential obtained from hazelnut shells on certain growth and yield parameters. The study was conducted based on the Randomized Blocks Testing Design with repeated four times. In the experiment, treatments of 0.5%, 1.0%, 2.0%, 3.0%, 4.0%, and 5.0% mL doses of wood vinegar were administered, and only tap water was given to the control group. It was found that the 4% mL dose had positive effects on cultivated plant height and that the 1% mL dose had positive effects on thousand kernel weight and seed per spike compared with the control. It was seen that its effect on weeds dry weight is changed according to the years (P=0.011). In 2015-2016, it was found that 3% mL increased and 0.5%, 1% and %5 mL decreased the weight of dry grass. In the test field; weeds determination is made from 12 families. In 2014-2015, *Polygonum bellardii*, *Eremopoa altaica* and *Microthlaspi perfoliatum*; and in 2015-2016, *Eremopoa altaica*, *Erodium absinthoides*, *Lactuca serriola* and *Polygonum bellardii* was seen most.

KEYWORDS:
Agro-ecosystems, growth and yield parameters, nutshell, weeds, wheat, wood vinegar.

INTRODUCTION

Wood vinegar (WV) and other weak pyrolysis liquids are produced as a byproduct of carbonization processes. And it was found in previous archeological studies that these liquids were used in the time of Neanderthals as a biopesticide [1]. [2] reported with reference to Jang that WV is approximately 80-90% water and that the remaining portion is composed of more than 200 different organic compounds. [3] determined that WV is composed of acetic acids and organic acids, phenolic, alkane, alcohol, and ester compounds. [4] stated that WV is toxic or lightly toxic for untargeted organisms in water and soil. [5] reported, with regard to Ikeshima, that WV was used in the fundamental fertilizer that plants need in the development of plants and soil quality and in plant growth in agriculture. [6] revealed that a 3-5% dose of WV significantly increases height, leaf length, and bud/twig development in plants. [7] determined that the mixture (WV and fermented organic liquid fertilizer) they sprayed on plant leaves didn't create a significant difference in yield. [8] reported that when they administered WV and bioextracts to tomato plants, it marginally increased the total dry weight, fruit count, fresh fruit weight, and dry fruit weight. [9] found that the mixture they applied to cucumber plants increased plant height, root length, root volume, and root tips by 29.7%, 117%, 121%, and 76.1%, respectively. [3] stated that did not significantly increase hazelnut yield but, although marginally, increased hazelnut shell. [10] determined in their study that WV (50 mL/L) increase the diameter of papaya stems. [6] determined in their study that WV created a 40.3% increase in yield. They also reported that WV (3-5% mL) provide significant positive growth for *Zingiber offtcinale* Roscoe var. white ginger (height, leaf length, and bud/twig development). [11] reported that WV and a mixture (WV+charcoal powder) increased the length, chlorophyll contents, and photosynthesis rate of pepper plants, and that the mixture effectively increased fruit length, fruit diameter, and pericarp thickness. [12] determined that the treatment of the 10%, 20%, and 30% dose of the WV they acquired from hazelnut shells didn't statistically affect the grow of the soy bean plants but had significant effects on yield. As a result, pesticides and chemical fertilizers used for agricultural purposes negatively affect us and the environment in many regards. Because of this situation, it has become essential that we search for alternatives. The purpose of this study is to deter-

mine the effect of the wood vinegar (acquired through the carbonization of hazelnut shells), which has the potential to be a biopesticide, on wheat cultivate plants and weeds.

MATERIALS AND METHODS

Materials. This study was conducted at the Krasunia odeska wheat field belonging to the BERCE Alparslan Agricultural Business located approximately 12 km from the Muş provincial center (height: 1276, lateral: 380 47' 33. 1815", long: 410 32' 45. 700"). In the brief 10-year history of the area in which the experiment was established, fungicide (Duet ultra® and Input®), herbicide (Axial®, Lancelot Super®, Roundup®, Guardian®, and Harmony Extra®), and insecticide (Tekvando®) were used. Table 1 provides the climate data for the study region for the values of total precipitation, mean temperature, and mean relative humidity the first year (2014-2015), second year (2015-2016), and final ten years (long year mean) [13].

WV, which is used in this study, was obtained from a company that develops biochar and wood vinegar products with gasification machine [14]. In the test, the base fertilizer (NP 20-20-0, 13.7 kg/ha^{-1}) with the planting and the height fertilizer (46% urea, 10 kg/ha^{-1}) were used. In addition, on May 26, 2015 one time was applied and 24 April, 30 April, 8 May and 6 June 2016, WV Treatments was applied four times and only tap water was given to control group.

Methods. This study was carried out in Muş province in 2014-2015 and 2015-2016 production seasons, in field conditions according to Randomized Block Design with four repeats. Each parcel is 5m × 5m = 25m^2 and has a minimum distance of 2 m between blocks and parcels [15]. Treatments in the test were carried out following the fertilizer and spraying schedule of BERCE Alparslan Agricultural Enterprise. Spraying was done with the help of a backpack sprayer. The following procedures were carried out in the study: It made as 1) %0.5 mL WV, 2) %1 mL WV, 3) %2 mL WV, 4) %3 mL WV, 5) %4 mL WV, 6) %5 mL WV and 7) control which is only given tap water. Weeds collected from the treatments field; dried according to herbarium technique and turned into herbarium material, after counting the required records. In the identification of plants "Flora of Turkey and the East Aegean Islands" [16, 17, 18] were used. Van Yüzüncü Yıl University Faculty of Science Department of Biology (VANF) herbarium samples were also used, and comparisons were made. The collected plant samples are made into herbarium material and stored at Herbarium. Author and plant names have been checked according to [19]. The density of weeds in the test field was determined by counting with a wooden frame of one square meter to represent that parcel from three different locations of each parcel. After the weeds, which are in one square meter frame field, were cut from the soil

TABLE 1
Some climate data for 2014-15, 2015-16 years and last ten years (LTY) in Muş province

Total rainfall (mm)			Mean temperature (C^0)			Mean relative humidity (%)		
2014-15	2015-16	LTY	2014-15	2015-16	LTY	2014-15	2015-16	LTY
740.4	790.1	740.5	11.55	11.48	10.62	55.02	54.00	60.79

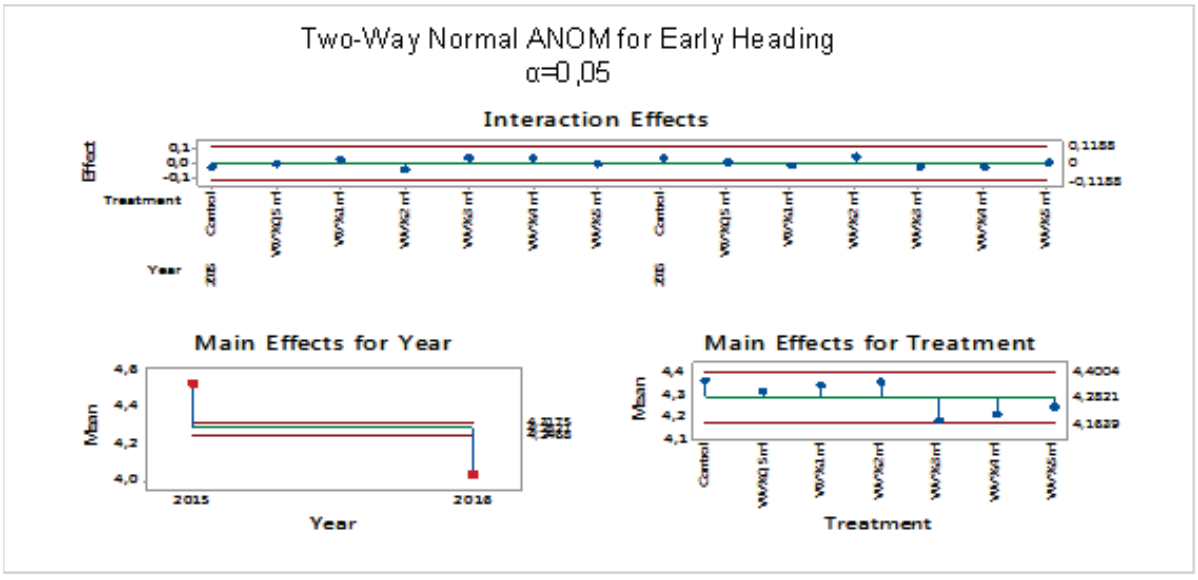

FIGURE 1
Effect of wood vinegar doses on early heading

surface, they were dried at 70 °C for 48 hours in the drying cabinet and after that their biomass was determined [20]. In order to determine the effect of the treatments on the cultivated plant, 10 plants', which are randomly selected from each plot, plant height, harvest index, grain number per spike, grain yield per spica with thousand kernel weight [21] and early spica status were analyzed. In the statistical analysis; Minitab (Ver. 17) and IBM SPSS (Ver. 24) statistical package programs were used. Analysis of Means (ANOM) Technique was used to compare the effects of wood vinegar treatments on weeds and cultivated plant weight. In order to determine the effect of the treatments on weeds dry weight and cultivated plant, Variance Analysis Technique (Repeated Measurement ANOVA) was used in Repeated Measured Experiments [22].

RESULTS

Effects of Treatments on the cultivated plant. The ANOM figures for investigating effect of different treatments and years on early heading, plant height, harvest index, numbers of seed per spike**,** grain yield per spike**,** thousand kernel weight have been given in figure 1-6, respectively.

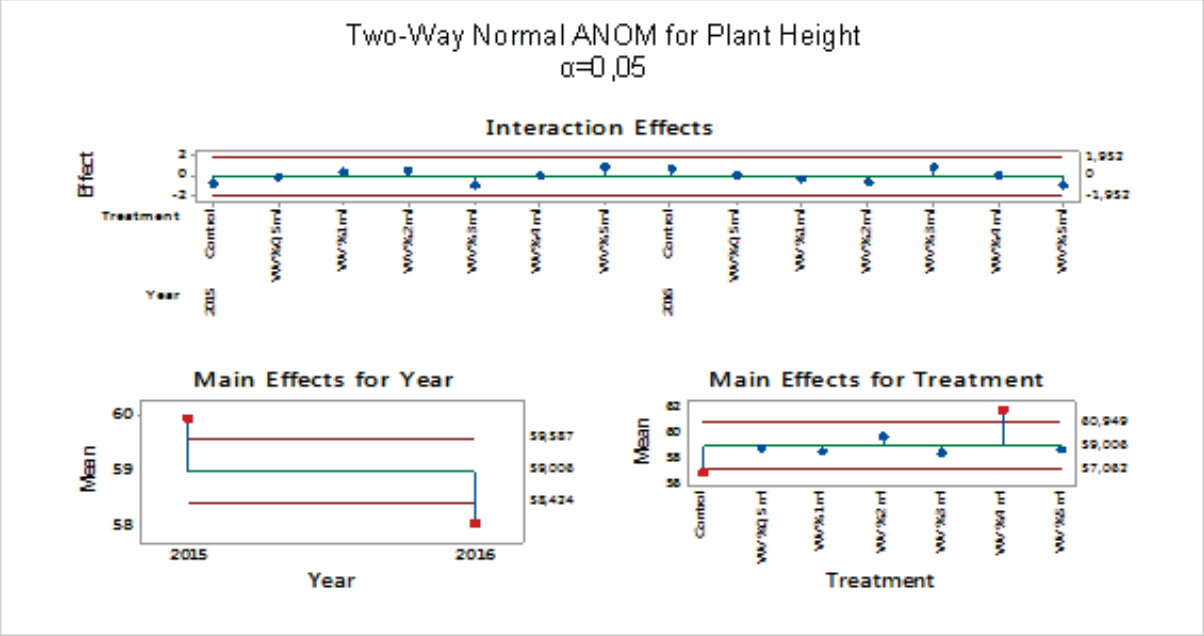

FIGURE 2
Effect of wood vinegar doses on plant height

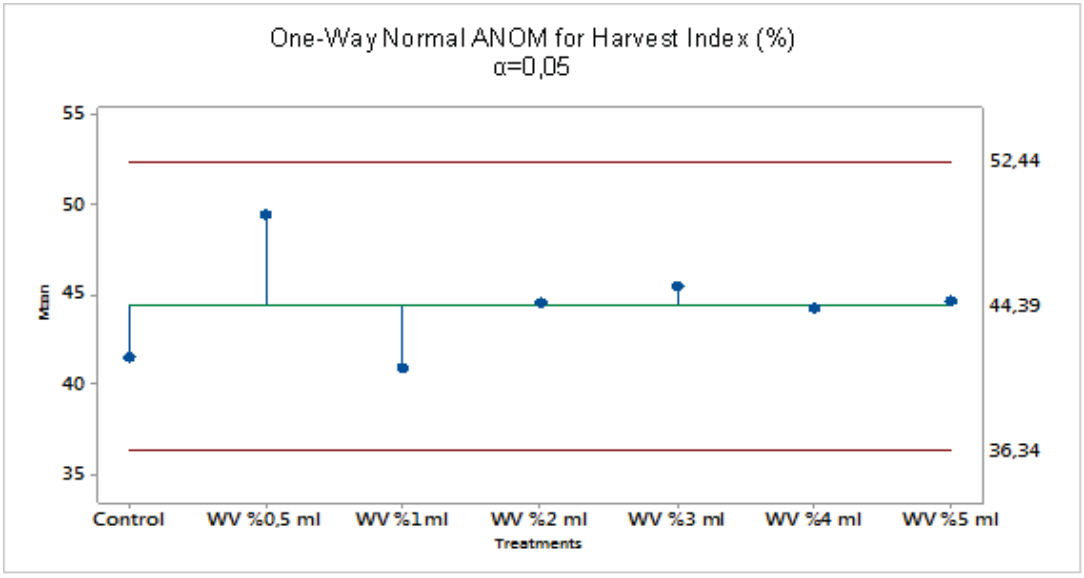

FIGURE 3
Effect of wood vinegar doses on harvest index (%)

For plant height (Figure 2), as it is seen from the figure 2, interaction effect is not statistically significant while the main effect of the treatments and years are significant. When effect of treatments on plant height is examined, it is seen that the mean of the plant height in 2014-2015 is significantly higher than that of the 2015-2016. For treatment effect, the most effective treatment is WV 4% mL while the least effective one is control.

When figures 3, 4, 5 and 6 are examined, it is seen that all means fall between the lower and upper decision lines. That means the effect of the treatments on these variables is not statistically significant. Although there are not any statistically significant differences in terms of these variables among the treatments, especially the observed difference in terms of number of seed per spike may be practically significant for the researchers. Because as it can be seen from the figure 6, the mean line of the treatment WV 1% mL is very close to the lower decision line. That means the effect of the treatment WV 1% mL on number of seed per spike may be practically significant. The ANOM figure for investigating the effect of treatments on thousand kernel weight is given in figure 6. As it can be seen from the figure 6, the least thousand kernel weight is obtained when treatment WV 1% mL is applied. On the other hand, although the effect of the treatment WV 2% mL is not exceeded the upper decision line, this effect or difference may be practically significant for the researcher.

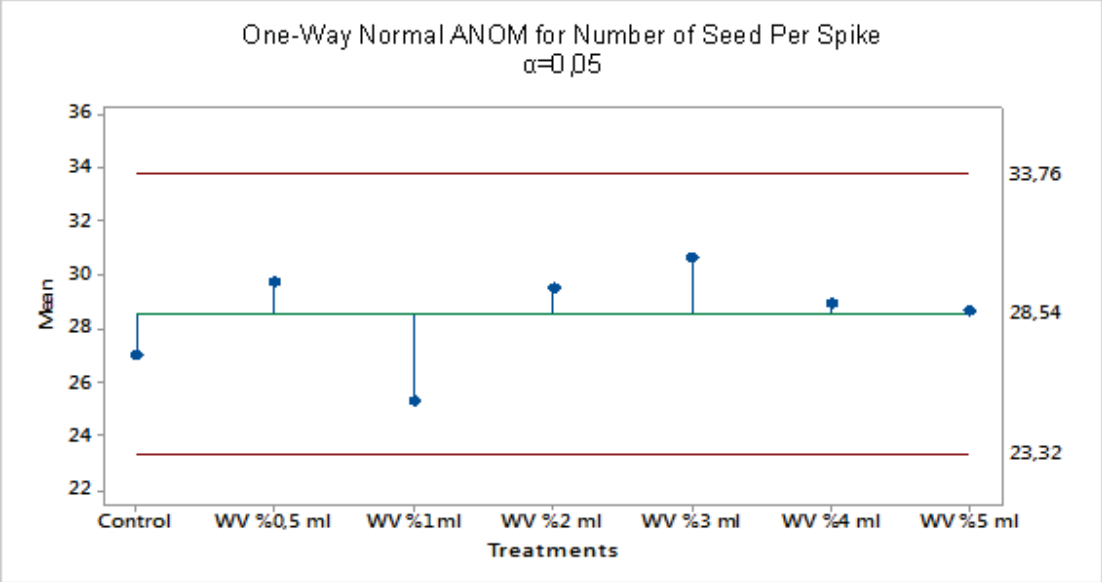

FIGURE 4
Effect of wood vinegar doses on number of seed per spica

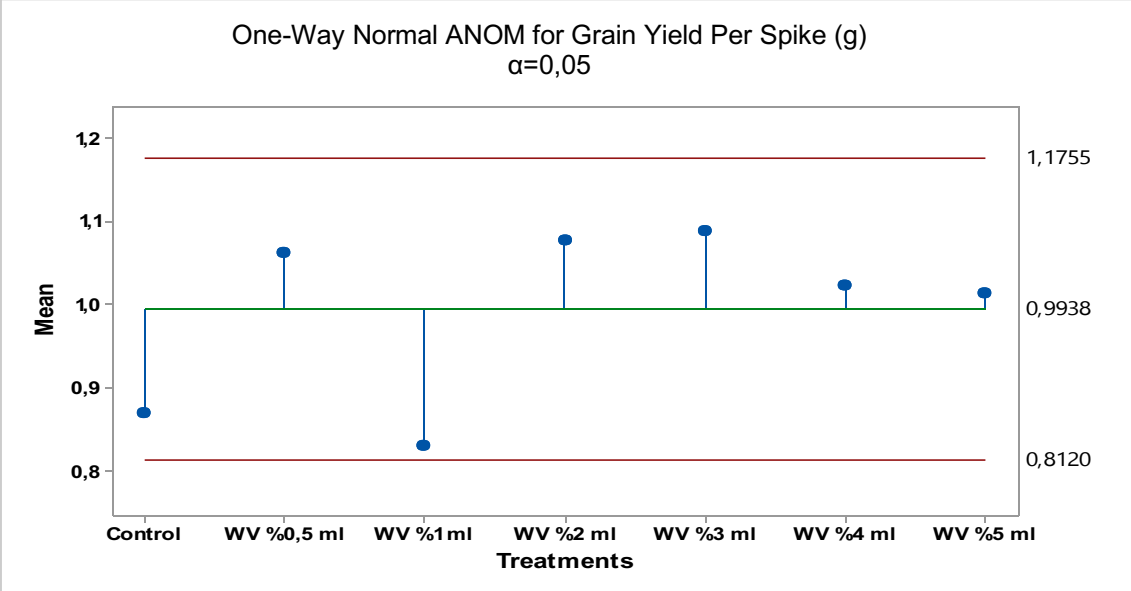

FIGURE 5
Effect of wood vinegar doses on grain yield per spica (g)

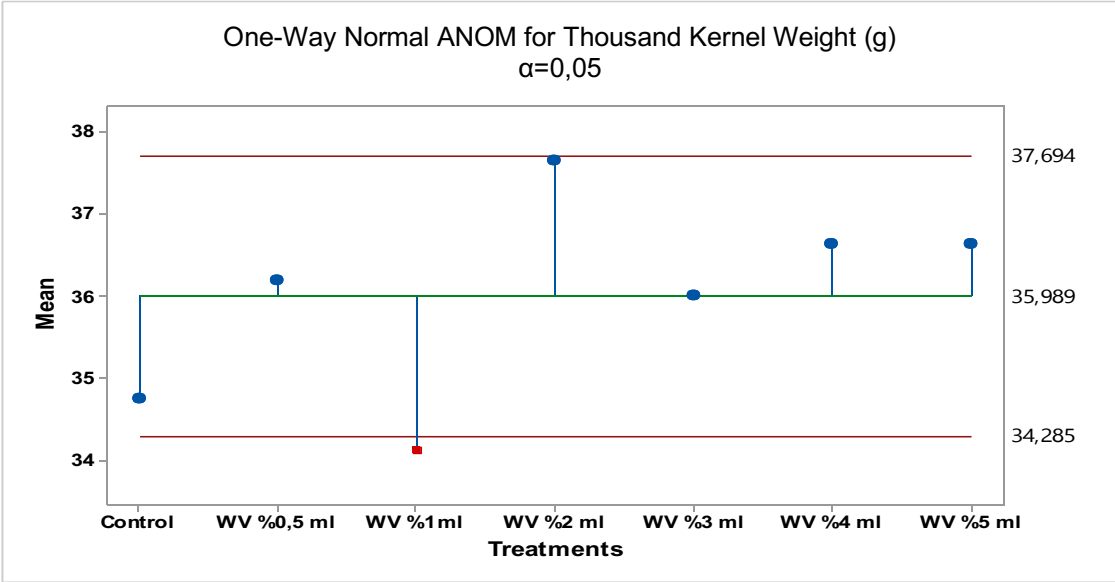

FIGURE 6
Effect of wood vinegar doses on thousand kernel weight (g)

TABLE 2
The change of the effect of Treatments on weeds weight and the results of TUKEY test

Year	2014-2015	2015-2016
Treatments	$\bar{X} \pm S_{\bar{X}}$	$\bar{X} \pm S_{\bar{X}}$
WV %0.5 mL	20,2±4,3 Ab	143,4±19,0 Da
WV %1 mL	13,9±3,1 Ab	177,9±21,3 Ca
WV %2 mL	22,8±1,9 Ab	233,4±31,9 ABa
WV %3 mL	23,6±2,8 Ab	262,5±43,8 Aa
WV %4 Ml	18,4±4,2 Ab	219,6±25,0 Ba
WV %5 mL	20,9±7,9 Ab	171,5±11,3 Ca
Control	25,5±1,6 Ab	154,3±20,1 CDa

Note 1. Differences between Treatments averages shown in different capital letters in the same year are important.
Note 2. Differences between year averages shown in different lower-case letters in the same Treatments are important.

TABLE 3
Weeds identified in the test field

Line no	Name	The year it was identified	
		2014-2015	2015-2016
1	*Vicia anatolica* Turrill (Fabaceae)	X	X
2	*Trifolium echinatum* M.Bieb (Fabaceae)	--	X
3	*Lathyrus inconspicuus* L. var. (Fabaceae)	X	X
4	*Trifolium* sp. (Fabaceae)	X	X
5	*Lathyrus gloeosperma* Warb. & Eig (Fabaceae)	--	X
6	*Lathyrus aphaca* L. var *modest*us P.H.Davis (Fabaceae)	X	X
7	*Tripleurospermum disciforme* (C.A.Mey) Sch.Bip. (Asteraceae)	X	X
8	*Lactuca serriola* L. (Asteraceae)	X	X
9	*Lapsana communis* L. (Asteraceae)	--	X
10	*Senecio vernalis* Waldst. & Kit. (Asteraceae)	X	X
11	*Erodium absinthoides* Willd. subsp. *armenum* (Trautv.) P.H.Davis (Geraniaceae)	X	X
12	*Galium verum* L. subsp. *verum* (Rubiaceae)	X	X
13	*Microthlaspi perfoliatum* (L.) F.K.Mey. (Brassicaceae)	X	X
14	*Polygonum bellardii* All. (Polygonaceae)	X	X
15	*Cerastium longifolium* Willd. (Caryophyllaceae)	X	X
16	*Cerastium dichotomum* L. subsp. *dichotomum* (Caryophyllaceae)	X	X
17	*Eremopoa altaica (Trin.) Roshev.* (Poaceae)	X	X
18	*Alopecurus myosuroides* Huds. var. *myosuroides* (Poaceae)	X	X
19	*Cynodon dactylon* (L.) Pers var. *villosus* Regel (Poaceae)	X	X
20	*Ranunculus arvensis* L. (Ranunculaceae)	X	X
21	*Orobanche alba* Stephan ex Willd. subsp. *alba* (Orobanchaceae)	--	X
22	*Veronica* sp. (Plantaginaceae)	X	X
23	*Euphorbia* sp. (Euphorbiaceae)	X	X

Effect of treatments on dry weights of weeds. As a result of analysis of variance made, it was observed that the effect of Year × Treatments interaction was statistically significant (P = 0.011). Therefore, the effect of the Treatments on weeds weight showed significant changes over the years.

According to TUKEY test results; while the effects of WV Treatments were similar in 2014-2015, it was observed that it was obtained at most in 3% WV and at least from control, and 0.5%, 1% and 5% from vinegar treatments in 2015-2016, (Table 2). Weeds identified in the test field; 12 families of weeds were identified from the Treatments field, (Table 3). The most common weeds found in 2014-2015 are; *Polygonum bellardii* All. (Polygonaceae), *Eremopoa altaica* (Trin.) Roshev. (Poaceae) and *Microthlaspi perfoliatum* (L.) F.K.Mey. (Brassicaceae). The most common weeds found in 2015-2016 are; *Eremopoa altaica* (Trin.) Roshev. (Poaceae), *Erodium absinthoides* Willd. subsp. *armenum* (Trautv.) P.H.Davis (Geraniaceae), *Lactuca serriola* L. (Asteraceae) and *Polygonum bellardii* All. (Polygonaceae). Also, unlike the previous year, in 2015-2016; *Trifolium echinatum* M.Bieb (Fabaceae), *Lathyrus gloeosperma* Warb. & Eig (Fabaceae), *Lapsana communis* L. (Asteraceae) and *Orobanche alba* Stephan ex Willd. subsp. *alba* (Orobanchaceae) were found.

DISCUSSION

Pesticide and chemical fertilizers used in agro-ecosystems increase the yield while adversely affecting the environment. In this context, we should tend to alternative products that will not leave any harmful residue in the products and will not harm the biological circle and the environment. Wood vinegar (WV) is an organic product with a potential for being biopesticide and biofertilizer. Some studies have been conducted about this product, however they are not enough. In this study; according to the control, it was determined that the dose of 4% mL WV had a positive effect on the plant height, the WV 1% mL thousand kernel weight and the grain number per spica. It is seen that this obtained positive result is supported by the works of [3], [6], [9], [10] and [11]. Also, it was determined that [12] coincided with the findings on plant yield but not with the plant growth parameter. It was seen that the treatments of WV's effect on weeds weight is changed according to the years (P = 0.011). The similarity of the 2014-2015 data (unlike the 2015-2016 data) is thought to be due to the continuation of the effects of the pesticides used in the test field history. In 2015-2016, it was found that 3% mL WV, compared to control, increased weeds weight but 0.5%, 1% and 5% mL WV decreased the weeds dry weight. As a result; it has been determined that 1% mL of the wood vinegar dose increases the plant yield and reduces the dry weight of the weeds, and 4% mL of it has a positive effect on the plant growth.

ACKNOWLEDGEMENTS

A small part of this study has been presented in UGAP2018-1ST International GAP Agriculture and Livestock Congress 2018-Şanlıurfa/Turkey as an oral presentation.

REFERENCES

[1] Tiilikkala, K., Fagernäs, L., Tiilikkala, J. (2010) History and use of wood pyrolysis liquids as biocide and plant protection product history and use of wood pyrolysis liquids as biocide and plant protection product. The Open Agriculture Journal. 4, 111-118.

[2] Kim, D.H., Seo, H.E., Lee, S., Lee, K. (2008) Effects of wood vinegar mixed with insecticides on the mortalities of *Nilaparvata lugens* and *Laodelphax striatellus* (Homoptera: Delphacidae). Anim Cells Syst. 12, 47-52.

[3] Jothityangkoon, D., Koolachart, R., Wanapat, S., Wongkaew, S., Jogloy, S. (2008) Using wood vinegar in enhancing peanut yield and in controlling the contamination of aflatoxin producing fungus. International Crop Science. 4, 253-253.

[4] Hagner, M. (2013) Potential of the slow pyrolysis products birch tar oil, wood vinegar and biochar in sustainable plant protection-pesticidal effects, soil improvement and environmental risks. Thesis. Department of Environmental Sciences Faculty of Biological and Environmental Sciences University of Helsinki, Finland.

[5] Rakmai, J. (2009) Chemical determinations, antimicrobial and antioxidant activities of Thai wood vinegars. (Thesis). Prience of Songkla University, Thailand.

[6] Nurhayati, T., Roliadi, H., Bermawie, N. (2005) Production of mangium (*Acacia mangium*) wood vinegar and its utilization. Indonesian Journal of Forestry Research. 2, 13-25.

[7] Pangnakorn, U., Watanasorn, S., Kuntha, C., Chuenchooklin, S. (2009) Treatment of wood vinegar to fermented liquid bio-fertilizer for organic agriculture on soybean. As. J. Food Ag-Ind. 189-196.

[8] Mungkunkamchao, T., Kesmala, T., Pimratch, S., Toomsan, B., Jothityangkoon, D. (2013) Wood vinegar and fermented bioextracts: Natural products to enhance growth and yield of tomato (*Solanum lycopersicum* L.). Sci Hortic-Amsterdam. 154, 66-72.

[9] Pan, X., Zhang, Y., Wang, X., Liu, G. (2017) Effect of adding biochar with wood vinegar on the growth of cucumber. In IOP Conference Series: Earth and Environmental Science. 61, 1.
[10] Rahmat, B., Pangesti, D., Natawijaya, D., Sufyadi, D. (2014) Generation of wood-waste vinegar and its effectiveness as a plant growth regulator and pest insect repellent. Bioresources. 9, 6350-6360.
[11] Jeong, C., Yun, I., Park, J., Kyoung, J., Kang, J., Lee, S., Jo, T., Ahn, B. (2006) Effect of wood vinegar and charcoal on growth and quality of sweet pepper. Korean J Hortic Sci. 24, 177-180.
[12] Travero, J.T., Mihara, M. (2016) Effects of pyroligneous acid to growth and yield of soybeans (glycine max). International Journal of Environmental and Rural Development. 7, 50-54.
[13] Anonymous. (2016a) Muş meteorological provincial directorate records. (Accessed: 05/11/2016). (In Turkish).
[14] Namlı, A., Akça, M.O., Turgay, E.B., Soba, M.R. (2014) Investigation of potential agricultural use of wood vinegar. Soil-Water Journal. 3, 44-52.
[15] Anonymous. (2016b) Plant pests standard drug testing methods: Cereal pests. https://www.tarimorman.gov.tr/tagem/belgeler/yayin/9.pdf. (Accessed: 27/11/2016). (in Turkish).
[16] Davis. P.H. (1965-1985) Flora of Turkey and the East Aegean Islands. Vol.1-9, Edinburgh Univ. Press., Edinburgh.
[17] Davis, P.H., Mill, R.R., Tan, K. (1988) Flora of Turkey and the East Aegean Islands. Vol.10, Edinburgh Univ. Press., Edinburgh.
[18] Güner, A., Özhatay, N., Ekim, T., Başer, K.H.C. (2000) Flora of Turkey and the East Aegean Islands. Vol. 11. Edinburgh University Press., Edinburgh.
[19] Güner, A., Aslan, S., Ekim, T., Vural, M., Babaç, M.T. (2012) Turkey plant list (vascular plants). Nezahat Gökyiğit Botanik Bahçesi ve Flora Araştırmaları Derneği Yayını, İstanbul.
[20] Kaydan, D., Tepe, I., Yağmur, M., Yergin, R. (2012) Effects of sowing methods and rates on weeds, grain yield and some yield components of wheat. Tarim Bilim Derg. 310-323.
[21] Tuğay, M.E., Abacı, Y. (1989) Research on yield and yield components of 40 barley lines cultivated in autumn of 1987 in Tokat region. Cumhuriyet University Faculty of Agriculture Journal. 5, 1.
[22] Winer, B.J., Brown, D.R., Michels, K.M. (1971) Statistical principles in experimental design. Vol. 2. McGraw-Hill, New York.

Received: **21.01.2019**
Accepted: **18.02.2019**

CORRESPONDING AUTHOR

Ibrahim Koc
Bitlis Eren University,
Faculty of Engineering and Architecture,
Department of Environmental Engineering,
13000, Bitlis – Turkey

e-mail: ibrahimkoc47@gmail.com

© by PSP Volume 28 – No. 4/2019 pages 2754-2770 Fresenius Environmental Bulletin

TIME-DRIVEN ACTIVITY-BASED COSTING IN THE OPHTHALMOLOGY DEPARTMENT OF STATE HOSPITAL: A CASE STUDY

Pinar Kurt[1,*], Metin Saban[2], Fikret Cankaya[3], Mehmet Cengiz Annac[4]

[1]Department of Opticianry, Vocational School of Health Services, Bandirma Onyedi Eylul University, 10200, Bandirma, Turkey
[2]Department of Business, Faculty of Economics and Administrative Sciences, Bartin University, 74100, Bartin, Turkey
[3]Department of Business, Faculty of Economics and Administrative Sciences, Karadeniz Technical University, 61080, Trabzon, Turkey
[4]Department of Ophthalmology, Bartin State Hospital, 74100, Bartin, Turkey

ABSTRACT

Today, competition is becoming increasingly intense throughout the world, and traditional cost methods fail to provide the information necessary for the sustainability of businesses. This information is of vital importance regarding the decision-making process in business management. As is the case in all businesses, successful management decisions are associated with accurate cost information. For hospital administrations to be able to handle the decision-making and control functions both effectively and efficiently, and to be sustainable, they have to be completely familiar with the costs of their health services. For this reason, the use of Time Driven Activity Based Costing (TDABC), a modern cost method, has become important to obtain more accurate and realistic cost information in evaluating health care interventions in complex hospital businesses.

In this study, information on TDABC has been presented and a summary has been given on what needs to be done to increase the success of the method. Subsequently, studies on TDABC have been discussed and a case study sample application has been carried out. This study aimed to show why the TDABC method is applicable and how it can be efficiently applied. The study was carried out at the ophthalmology department of a state hospital, and the costs of five surgical procedures which performed on under local anesthesia, fluorescein fundus angiography (FFA) and laser treatments (argon laser photocoagulation, Nd:YAG (neodymium-doped yttrium aluminum garnet) laser capsulotomy-synechiotomy, electrolysis (via argon laser) applied in distichiasis), per patient were calculated according to the TDABC method.

As a result, the study showed that the TDABC method can be applied in hospital businesses to obtain accurate cost information, and it is useful in helping hospital management to make strategic decisions. Also, hospital businesses will be able avoid waste of resources by calculating their costs in a realistic way through TDABC method, which will also contribute positively to the environment as the use of medical supplies and the amount of medical waste will be reduced. In addition to all these, it is believed that the study will be motivating and guiding for other hospital businesses realistic cost calculation and therefore it will be beneficial for the society.

KEYWORDS:
TDABC, Time Driven Activity Based Costing, Hospital, Patient, Cost, Value-Based Health Care, Unused Capacity, Medical Waste

INTRODUCTION

Although health costs are high in Turkey (total health costs in 2017 were approximately 37.1 billion USD) [1], worse outcomes have been observed compared to those of other countries suffering high levels of chronic illnesses and shorter life spans. Improper health system structures, lack of flexibility in this structure and other similar reasons have increased health costs. This has led to the establishment of important health reforms to reduce the cost of health care. Policies on health reform emphasize value-based health care services. The value in health care is defined as the ratio of health results to USD spent [2]. In this manner, stakeholders should collaborate to improve quality, reduce costs and provide better value in the health sector [3, 4].

In a value-based system, quality and costs must be measured when it is applied. Therefore, new cost methods need to be adopted by health care providers [2]. Health care providers should have a better understanding of the costs and outcomes associated with health interventions to increase the value of health care provision. If the costs and results cannot be measured in sufficient detail, it will be impossible to have accurate information on the business, to find the parts that fail in service, to determine the costs that do not add value to the service provided, and thereby evaluate the effect of changes in the health system and in the maintenance processes [5]. Due to time and cost limitations, businesses often avoid calculating costs. This is no different in the health sector, and the study is important when this aspect is

considered. In addition, such studies carried out in the health sector are important as an example to help guide other organizations.

On the other hand, wastes from health institutions are called hospital wastes and cause serious environmental pollution. These wastes represent important health risks for hospital workers, patients and the community. Hospital wastes are classified as domestic wastes, medical wastes, chemical wastes, infective wastes and radioactive wastes [6-8]. Generally, 80% of hospital wastes are domestic waste, 15% are pathological and infective wastes, 3% are chemical and pharmaceutical wastes and 1% are radioactive and cytotoxic wastes [9]. According to the 2017 data, the medical waste cost of the hospital where the study was conducted is 92.805 USD. The cost of medical drugs and consumables for the hospital is 3.438.816 USD.

In hospital businesses, excessive use of medical materials cause waste problems and therefore damages the environment. These damages can be examined from different angles. First, the use of fossil fuels in the production of medical devices has damage to the environment. Secondly, there are damages caused by the use of non-renewable energy sources in the production of fossil fuels. Finally, there are medical wastes and their damages to the environment. Therefore, excessive use of medical materials and medical wastes are significant cost factors both for businesses and the environment.

Businesses must use the resources optimally to minimize their own costs and environmental costs. Here, a realistic calculation of costs will contribute to the optimal use of medical devices. This will provide a significant cost advantage to the business. As a result, the use of TDABC will contribute significantly to the reduction of environmental pollution as well as contributing to the operation by minimizing the waste of resources. In addition, optimal use of resources will reduce the medical waste from excessive use and the cost of eliminating them [10].

In traditional cost determination methods, those which are not directly related to the products based on their cost items are distributed among the products produced with the help of volume-based measures (distribution keys). This method gives inaccurate results in the distribution of costs to products or services and yields inaccurate cost information. In this manner, using the information obtained by traditional methods can lead to wrong decision making in the hospital businesses where the organizational structure is complex.

Traditional cost methods are designed for production structures that are mainly based on labor, where the product variety is low, the production quantity is high and the automation is low [11]. To evaluate the limitations of these methods, the novel Time Driven Activity Based Costing (TDABC) method was developed to estimate realistic costs more accurately. With the application of the TDABC method in hospital businesses, health care providers can get a better idea of the business, help eliminate the activities that do not create value and make more accurate decisions with the help of more accurate cost information.

The TDABC method was first developed by Steven Anderson in 1997 [12] and applied by Acorn Systems, Inc. This method is a tool that increases the efficiency of health services, by allowing a more realistic calculation of the direct and indirect costs involved in the delivery of a particular service [13-15]. TDABC helps to deliver a health service offering to a patient at a lower cost [14]. In other words, the TDABC method allows service providers and hospital managers to accurately identify and evaluate the costs of clinical, administrative and operational processes [16]. TDABC is a new method distributing direct and indirect costs in health service that increases the feasibility of cost management by taking unused capacity costs into account and which is easier to update [17]. Two parameters are required in the application of this novel method. These are the unit cost of supply sources and the time required to perform each activity [18]. Business costs can be calculated by multiplying the unit cost of supply sources by the time required to perform a particular activity based on these two parameters [19]. As stated in the equation below, the unit cost of the supply resources (unit capacity cost) is the ratio of the cost of the supplied capacity to the practical capacity of the supplied resources [20].

$$Unit\ Capacity\ Cost\ = \frac{Cost\ of\ capacity\ supplied}{Practical\ capacity\ of\ the\ resources\ supplied}$$

The general aim of the TDABC method is to maintain accurate cost information by eliminating the processes that cost unnecessary time and those that are high-cost methods [21]. Also, in those companies that apply the TDABC method, the conditions for using modern cost methods (lean production, agile production, lean-agile production, kaizen) will be automatically created. According to Kaplan and Anderson, the TDABC method comprises six stages [5]:

1. Definition of the various resource groups that the activities use.
2. Estimation of the cost of each resource group.
3. Estimation of the practical time capacity of each resource group.
4. Calculation of the unit cost of each resource group by dividing the total costs of the resource groups by the practical working capacity.
5. Determination of the duration required for each different time driven activity.
6. Multiplication of the unit costs by the duration required to monitor the unit costs.

TABLE 1
Previous Studies in The Literature

Year of publication	Authors [Ref. Number]	Method used	Studied Area	Country of origin	Application Area	Review (R) or Application (A)
2018	Alves et al. [25]	ABC[a] TDABC	Oncology	U.S.A	Clinic	R
2018	Burns et al.[26]	TDABC	Blood[b]	Australia	Monash Medical Centre	A
2018	Pollard et al. [12]	TDABC	Kidney and Ureteral Stone	U.S.A	Academic Medical Center	A
2018	Ruhumuriza et al. [27]	TDABC	Acute Abdominal Condition	Rwanda	Rural District Hospital	A
2018	Koehler et al. [28]	TDABC	Endoscopic and Open Carpal Tunnel	U.S.A	Hospital	A
2018	Bauer-Nilsen[29]	TDABC	Definitive Radiation Therapy For Locally Advanced Cervical Cancer	U.S.A	Clinic	A
2018	Laviana et al. [30]	TDABC	Retroperitoneal and Transperitoneal	U.S.A	UCLA[c] Health and University of Michigan	A
2017	Keel et al. [31]	TDABC	Review	Sweden		R
2017	Garcia et al. [32]	TDABC	Aerodigestive	U.S.A	MEEI[d] Multidisciplinary Aerodigestive Center	A
2017	Çetiner [33]	TDABC	Polyclinic*	Turkey	Training and Research Hospital	A
2017	Andreasen et al. [34]	TDABC	Hip and Knee Arthroplasty	Denmark	Hospital	A
2016	El Alaoui et al. [35]	TDABC	Clinical Psychiatry	Sweden	Health Care Services	A
2016	Yun et al. [36]	TDABC	Emergency Department	U.S.A	Clinic	A
2016	Yu et al. [2]	TDABC	Appendicitis	U.S.A	Hospital	A
2016	Thaker et al. [37]	TDABC	Prostate Brachytherapy	U.S.A	Clinic	A
2016	Luther et al. [38]	TDABC RVU[f]	Pediatric Forearm Fractures	U.S.A	Hospital	A
2016	Laviana et al. [39]	TDABC	Prostate Cancer	U.S.A	UCLA Health	A
2016	Ilg et al. [40]	TDABC	Prostate Cancer	U.S.A	Academic Referral Center	A
2016	Gregorio et al. [41]	TDABC	Pharmaceutical	Portugal	Pharmaceutical Services	A
2016	Schutzer et al. [42]	TDABC	Breast Cancer	U.S.A	Hospital	A
2016	Laviana et al. [16]	TDABC	Treating Small Renal Masses	U.S.A	UCLA Health	A
2015	Akhavan et al. [3]	TDABC-TA[g]	Arthroplasty Surgery	U.S.A.	University of California	A
2015	Balakrishnan [15]	TDABC	Outpatient Pediatric Adenotonsillectomy	U.S.A	Tertiary Pediatric Hospital	A
2015	Mandigo et al. [43]	TDABC	Obstetric and Breast Cancer Care	Haiti	HUM[h]	A
2015	Lievens et al. [44]	TDABC	Lung Cancer	Belgium	Radiotherapy Centers	A
2015	Inverso et al. [14]	TDABC	Plagiocephaly	U.S.A	Hospital	A
2015	Erhun et al. [45]	TDABC	Coronary Artery Bypass Graft	U.S.A India	Hospital	A
2015	Digioia et al. [46]	TDABC	Hip and Knee Arthroplasty	U.S.A	Hospital	A
2015	Chen et al. [47]	TDABC	Knee Replacement Surgery	England	Hospital	A
2015	Ozkan [48]	TDABC	Polyclinic[i]	Turkey	Hospital	A
2014	McLaughlin et al. [49]	TDABC	Neurosurgery and Urology	U.S.A	UCLA Health	A
2014	Kaplan et al. [50]	TDABC	Benign Prostatic Hyperplasia	U.S.A	Hospital	A
2014	Atalay et al. [51]	TDABC	ENT[j] Clinic	Turkey	Hospital	A
2013	Oker et al [52]	ABC TDABC	Laparoscopic Surgery	Cyprus	Magusa Yasam Hospital	A
2011	Aydin [53]	ABC TDABC	Dental Diseases	Turkey	Dentistry Hospital	A
2009	Demeere et al. [54]	TDABC	Outpatient	Belgium	Hospital	A

[a]Activity-Based Costing; [b]Beta Thalassaemia Major; [c]University of California Los Angeles; [d]Massachusetts Eye and Ear Infirmary; [e]Urology, Internal Medicine, Pediatric, Neurology, Gynecology and Obstetrics; [f]Relative Value Unit; [g]Tradinational Accounting; [h]Hospital University of Mirebalais; [i]Emergency, General Surgery, Cardiovascular Surgery, Cardiology, Neurosurgery, Orthopedics, Internal Diseases, Urology; [j]Ear, Nose and Throat

The TDABC method provides many advantages to logistics, distribution, hospital and service businesses in providing an accurate cost model for complex activities [22]. The most important advantages of the TDABC method are as follows [23, 24]:

1. It can be applied to any company, industry or hospital business where there are complex cost objects.
2. It is not costly and time consuming in the initial application stage.
3. It simplifies the cost calculation process.
4. It is a simple and rapid method.
5. It does not require costly and time consuming interviews with the employees.
6. It provides information to the administration to make decisions.
7. It provides reports on the exact quantities and values of the unused capacity, and on the process efficiency of the business.

TABLE 2
Durations of Angiography, Types of Laser and Surgery

Angiography and Laser Treatment Types	Time (min)	Surgery Treatment Types	Time (min)
Fluorescein Fundus Angiography (FFA)	15	Phacoemulsification + İOL	30
Nd. YAG Laser Capsulotomy-Synechotomy	5	Conjunctival Plastic, With Grafts	45
Argon Laser Photocoagulation	15	Pterygium Surgery	30
Electrolysis (Via Argon Laser) Applied in Distichiasis	5	Blepharoplasty Surgery(for one eye)	30
		Eyelid Reconstruction (With Grafts or Flaps)	45

In the present study, the TDABC method, which measures the costs of the health services, was applied in the ophthalmology department of a state hospital in Turkey. The aim of the study was to emphasize the importance of the TDABC method, to show that more accurate cost information can be gathered in hospital businesses and to explain how the method is applied. Another aim was to create guidelines for other businesses to use this method.

Literature. Numerous studies on TDABC have been conducted in numerous businesses in different sectors. The studies on the health sector, and especially hospital businesses, on this subject are given in Table 1.

Examining Table 1, 21 of these studies were carried out in the USA, 4 in Turkey, 2 in Sweden, 2 in Belgium, 1 in Australia, England, Denmark, Portugal, Northern Cyprus, Haiti and Rwanda. Compared to those in the USA, such cost calculation studies in hospitals in Turkey are inadequate. This can be explained by the difficult, costly and time consuming calculations for service production costs in hospital businesses that have a complex structure and inadequate staff numbers.

Also, in some of the studies, the costs were compared using the ABC and the TDABC methods, while in the other studies, costs were only calculated using the TDABC method. In the majority of the studies, it was seen that the TDABC method was applied to only one part of the hospital. It is important to emphasize that the application of these practices to the entire hospital will provide advantages, including calculating all hospital costs in a more realistic way and eliminating activities that do not provide any added value to the service.

Furthermore, it was seen that all the researchers studying this subject were in agreement that the TDABC method is an applicable method, and that it can calculate the costs in a more realistic way and provide managers with the information that will allow them to make successful decisions.

MATERIALS AND METHODS

Information on the hospital. In this single-center, retrospective study, the records of the patients, who were treated between January to December 2017 in ophthalmology department of a state hospital in Turkey, were reviewed. Aim of this study calculating the cost of treatments, which surgical treatments with under local anesthesia, fluorescein fundus angiography (FFA) and laser treatments (argon laser photocoagulation, Nd:YAG laser capsulotomy-synechiotomy, electrolysis (via argon laser) applied in distichiasis), per patient using the TDABC method. The state hospital occupies a 30,396 m^2 area with a capacity of 452 beds and a 24-hour service with 1128 staff. In 2017, 981,482 patients attended different units of the hospital and 22,019 of these received surgical treatments. In the ophthalmology department, 63,698 polyclinic patients and 925 clinical patients received, 2003 patients who received FFA and laser treatments and 1728 patients who received surgical treatments during this period. Angiography, laser and surgery treatments types are given with their durations in Table 2.

Assumptions used in the application. As in all studies, there are limitations. A more realistic cost would be obtained by a study with no limitations. Due to the wide range of services provided in the hospital and the large number of activities along with time, cost and similar limitations some assumptions were made. These are as follows:

- The entire hospital was not included in the study, only the ophthalmology department.
- The four surgical procedures performed with general anesthesia regarding ophthalmologyin 2017, were not taken into consideration.
- Since the study was carried out in Turkey, 1 USD Dollar was taken to be 3.80 TRY, and the calculations were made accordingly.

Method adopted in the application. The application carried out in the ophthalmology department of a state hospital was in accordance with the recommendations for the application of TDABC introduced by Kaplan and Anderson (2004). Six stages of the TDABC method were applied in the department. In the study, the service production process of the ophthalmology department was examined and a process map was established accordingly. The process map is given in Figure 1.

According to the process map given in Figure 1, the process consisted of six activity groups from the patient's admission to the hospital until their discharge from the ophthalmology department. These activity groups are given in Table 3. Since the same staff provides the services for patient admission and

discharge, a single activity group was formed to include both patient admission and discharge services. Then, the duration required for the sub-activities in these activity groups was determined in minutes using the average time estimates, and observational data and interviews conducted directly with the related personnel. Also, the costs of the activity groups were estimated based on the data from hospital health and administrative staff. Following the estimation of the activity groups, the practical working capacity calculation for each activity group was carried out and unit time costs were determined. The costs of the activities were calculated by multiplying the unit cost of activities by the time to perform the activities. Finally, the total operating costs were added to the cost objects (services) using the time factor that forms the basis of the TDABC method.

Step 1: Definition of the various resource groups that the activities use. In the first step of the TDABC application method, the activities performed in the ophthalmology department were grouped. These activity groups and the costs of the activity groups are given in Table 3 and are numbered from A1 to A6, respectively.

Ophthalmology department activity groups and costs are given in Table 3, while the time to implement the sub-activities of each activity group are given in Table 4.

Step 2: Estimation of the cost of each resource group. In the second step, the estimated direct costs of each activity group are shown in Table 3 based on the clinical and hospital costs, and on data obtained from hospital health and administrative staff. These direct costs include the costs of the salaries of doctors, nurses, administrative and support staff, the depreciable costs of medical devices and equipment and their maintenance, the costs of medical equipment and other costs (electricity, water, energy, communications, stationery, laundry, food, cleaning, medical waste and software automation).

Step 3: Estimation of the practical time capacity of each resource group. In this step, the capacity of each resource was estimated and the total minutes that each staff can work in a year was calculated. In calculating the total duration, the periods not related to the patient, such as breaks, meals and education were not included.

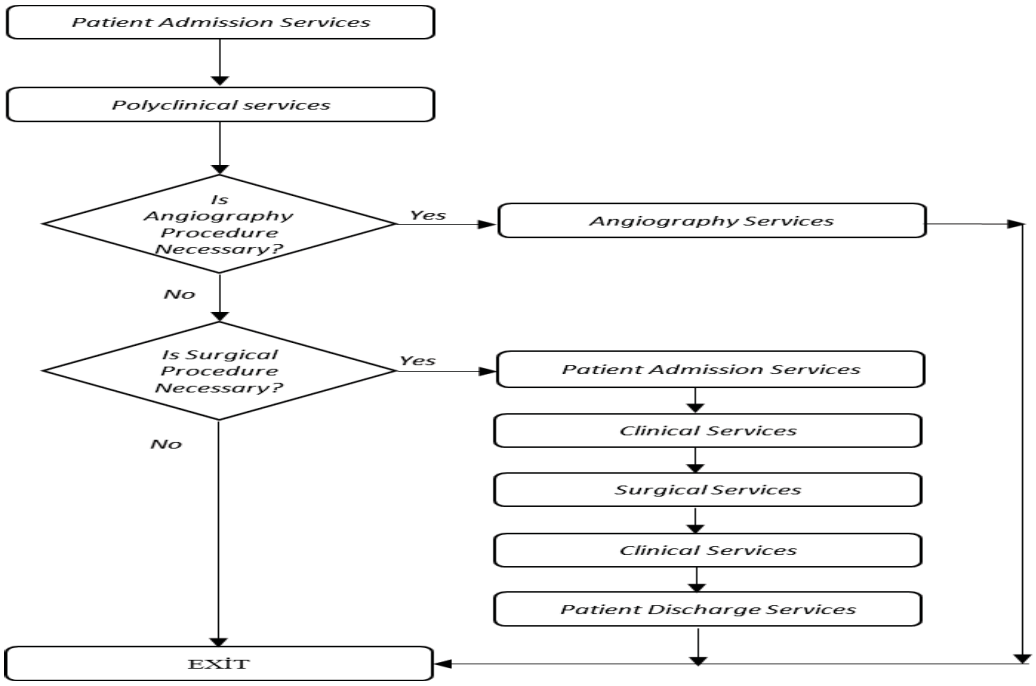

FIGURE 1
Process Map of Ophthalmology Department

TABLE 3
Ophthalmology Department Activity Groups and Costs

Activity Groups	Cost ($)
A1. Patient Admission Services	12,722
A2. Polyclinic Services	261,631
A3. Angiography and Laser Services	30,968
A4. Patient Admission and Discharge Services	3,673
A5. Surgical Services	152,505
A6. Clinical Services	81,554

TABLE 4
Sub-Activities of Activity Groups and Durations

A1. Patient Admission Services Sub-Activities	Time (min)	A2. Polyclinic Services Sub-Activities	Time (min)
Meeting the Patient, Providing Counseling Services	1	Doctor's Pre-Interview with the Patient	1
Checking Patient Information	1	Taking the Anamnesis (history) of the Patient	2
Patient Appointment Control and File Opening	2	Preparing the Patient for Examination	1
Verification of the Patient's Account And Insurance	1	Making the Eye Measurements of the Patient	3
Informing the Patient about Time	1	Patient's File Control	1
Sending the Patient to the Waiting Room of the Related Department	1	Present, New and Consulted Patient Examination	3
General Follow-up of Patient Appointments	10	Performing Result Control Procedures	1
In- and Out- Hospital Phone Calls	10	Informing the Patient	2
Other Administrative Tasks	15	Guiding the Patient	1
		In-House Phone Calls	10
		Other Administrative Tasks	30
A3. Angiography and Laser Services Sub-Activities	**Time (min)**	**A4. Patient Admission and Discharge Services Sub-Activities**	**Time (min)**
Preparing the Patient	4	Patient Hospitalization and Room Planning	5
Application of the Treatment Procedure	10.8	Completing the Patient File	7
Informing the Patient	3	Sending the Patient File to the Service	5
		Information Exchange of the Secretary and Nurse	3
		Taking the Patient into the Room	10
		Adding the Nurse Observations in the Patient File	2
		Exiting the Discharged Patient from the Program	2
		In- and Out-Hospital Phone Calls	25
		Filling Forms, Reports and Other Documents	30
		Other Administrative Tasks	20
A5. Surgical Services Sub-Activities	**Time (min)**	**A6. Clinical Services Sub-Activities**	**Time (min)**
Filling the Preoperative Form	5	Shift Change	30
Preparing the Patient for Surgical Operation	7	Taking the New Patient to the Room and First Care	20
Taking the Patient to the Operating Table	5	Visitation (In the Morning and After Surgery 15.00-16.00)	30
Preparing the Medical Drugs and Consumables	10	Taking Blood, Opening Vascular Path, Hygienic Care	10
Doctor's Interview with the Patient	3	Fever, Pulse and Blood Pressure Measurement	15
Application of Local Anesthesia	2	Daily Medicine and Medical Consumables Control	17.5
Surgical Procedure Application Activities	21.8	Patient Examination	20
Cleaning the Patient and Dressing the Wound(s)	10	Application of the Patient Treatment Plan	20
The Patient Leaving the Operating Table	10	Patient File Control	5
Filling the Postoperative Form	10	Informing the Patient's Relatives	5
Sending the Patient to the Clinical Service	10	Bed Sheets and Clothing Control	10
Recording of the Duration and Material of the Surgical Operation	7	Organizing the Food Program	15
Other Administrative Tasks	20	Other Administrative Tasks	30
Filling Forms and Other Documents	30	Providing Information to the Department of Surgical Services and to the Doctor	10
		Examination Inputs and Medical Consumables Control	10
		Dilating the Patient's Eyes on the Day of the Surgical Operation	30
		Preparing the Patient for the Department of Surgical Services	10
		Obtaining Consent Form Specific to the Surgical Operation	5
		Filling Forms, Reports and Other Documents	37.5
		Delivering the Patient to the Department of Surgical Services	10
		Taking the Patient from the Department of Surgical Services	10
		Taking the Patient to the Room and First Care	15
		Giving the Patient Drops According to the Treatment Plan	35
		Preparing the Patient for Discharge	10

In the A1 *Patient Admission Services* activity group, 8 staff works to provide the same service to each department. Since 63,698 of the 981,482 patients who received service from all departments in 2017 received service from the ophthalmology department, 0.52 staff was allocated to the department by distribution (8 staff × 63,698 patients / 981,482 patients). Since staff work for 8 hours a day, 22 days a month, they provide service for 264 days or 126,720 minutes per year. As a result of observations and interviews, it was found that a staff member in the A1 activity group spent 15,840 minutes per year on breaks, meals and training. Therefore, this value shows the unused capacity, and the remaining 110, 880 minutes (126, 720 minutes − 15, 840 minutes) represents the practical working capacity of the staff in the A1 activity group. The practical working capacity period of the 8 staff in the A1 activity group was calculated to be 887,040 min (8 staff × 110,880 min). The practical working capacity period of 0.52 staff distributed to the ophthalmology department was calculated to be 57,657.60 minutes (0.52 staff × 110,880 minutes).

In the A2 *Polyclinic services* activity group, the staff in the ophthalmology department dedicated to this function consists of 4 doctors, 4 nurses and 4

secretaries. Since doctors work 7 hours a day, 18 days a month, 4 doctors work 864 days or 362,880 minutes per year. As a result of observations and interviews, it was found that doctors spend 51,840 minutes per year on breaks, eating and training. The remaining 311,040 minutes (362,880 minutes − 51,840 minutes) show the practical working capacity of the doctors. Since nurses work 7 hours a day, 22 days a month, 4 nurses work 1056 days or 443,520 minutes per year. Nurses spend 63,360 minutes per year for breaks, eating and training. The remaining 380,160 minutes (443,520 minutes − 63,360 minutes) show the practical working capacity of the nurses. Finally, since secretaries work 8 hours a day, 22 days a month, 4 secretaries work 1056 days or 506,880 minutes per year. Secretaries spend 63,360 minutes per year for breaks, eating and training. The remaining 443,520 minutes (506,880 – 63,360 minutes) show the practical working capacity of the secretaries. As a result, the total practical working capacity of doctors, nurses and secretaries was calculated to be 1,134,720 minutes (311,040 minutes + 380,160 minutes + 443,520 minutes).

In the A3 activity group, *Angiography and Laser Services*, there were 4 doctors and 4 nurses working 1 hour per day, 18 hours per month. Therefore, the practical working capacity of the doctors and nurses was calculated to be 1728 days per year or 103,680 minutes per year.

There was one staff member working in the A4 *Patient Admission and Discharge Services* activity group. The staff working in this group served 925 patients in the ophthalmology department and 765 patients in the other departments, a total of 1690 patients. Therefore, 0.55 staff allocated by distribution served in the ophthalmology department (1 staff × 925 patients / 1690 patients). Also, since the staff member worked 8 hours a day, 22 days a month they provided service for 264 days or 126,720 minutes per year. The staff spends 15,840 minutes per year on breaks, eating and training. The remaining 110,880 minutes shows the practical working capacity of the staff. The practical working capacity period of 0.55 staff distributed to the ophthalmology department was calculated to be 60,984 minutes (0.55 staff × 110,880 minutes).

Four doctors, 20 nurses and 1 secretary work in the A5 *Surgical Services* activity group. Since the doctors work 8 hours a day, 4 days a month they provide service for 192 days or 92,160 minutes per year. As a result of observations and interviews, it was found that doctors spend 11,520 minutes on breaks, meals and training, and the remaining 80,640 minutes (92,160 minutes − 11,520 minutes) represents the practical working capacity of the doctors. Nurses serve all the departments of the hospital. In the hospital, 1728 of 22,019 patients received surgical services in the ophthalmology department. Therefore, 1.57 staff – placed by distribution across the service in the ophthalmology department (20 nurses × 1728 patients / 22,019 patients). Also, since the nurses work for 12 hours a day, 24 days a month they provide service for 452.16 days or 126,720 minutes per year. The nurses spend 27,129.60 minutes for breaks, meals and training, and the remaining 298,425.60 minutes (325,555.20 minutes − 27,129.60 minutes) show the practical working capacity of the nurses. Finally, since the secretary serving in the A5 activity group serves all the patients that receive surgical service, 0.08 secretaries (1 secretary × 1,728 patients / 22,019 patients) serves the ophthalmology department. Also, since the secretary serving in this groups work for 8 hours a day, 22 days a month service is provided for 264 days or 126,720 minutes per year. The secretary spent 15,840 minutes for breaks, meals and training per year, and the remaining 110,880 minutes shows the practical working capacity of the secretary. The secretary in the ophthalmology department works for 8,870.40 minutes (0.08 staff × 110,880 minutes). As a result, the total practical working capacity of doctors, nurses and secretaries was calculated to be 387,936 min (80,640 minutes + 298,425.60 minutes + 8,870. 40 minutes).

There were four nurses working in the A6 *Clinical Services* activity group serving 925 patients in the ophthalmology department, a total of 1690 patients including the patients from other departments. Therefore, 2.19 staff placed by distribution across the service works in the ophthalmology department (4 nurses × 925 patients / 1690 patients). Since the nurses in the ophthalmology department work for 12 hours a day, 24 days a month they provide service for 630.72 days or 454,118.40 minutes per year and spent 37,843.20 minutes for breaks, meals and training. Therefore, the remaining 416,275.20 minutes (454,118.40 minutes − 37,843.20 minutes) shows the practical working capacity of the nurses.

Step 4: Calculation of the unit cost of each resource group by dividing the total costs of the resource groups by the practical working capacity. The unit cost of each resource group is calculated by dividing the total costs of the resource groups by the practical working capacity. To calculate the unit capacity cost, the cost totals of the resource groups shown in Table 3 were divided by the calculated practical working capacity durations from the third stage to obtain the cost per unit capacity (cost per minute). Unit capacity costs of staff working in the activity groups are given in Table 5.

TABLE 5
Total Practical Capacities and Unit Time Costs of Activity Groups

Activity Groups	(a) Total Cost ($)	(b) Practical Capacity (min)	(c)=(a/b) Unit Time Cost ($/min)
A1. Patient Admission Services	12,722	57,657.60	0.22
A2. Polyclinic Services	261,631	1,134,720	0.23
A3. Angiography and Laser Services	30,968	103,680	0.30
A4. Patient Admission and Discharge Services	3,673	60,984	0.06
A5. Surgical Services	152,505	387,936	0.39
A6. Clinical Services	81,554	416,275.20	0.19*

*0.196

TABLE 6
Time and Cost of A1 Patient Admission Services Activity Group

Activities	(a) Time (min)	(b) Time Driver	(c) Unit Time Cost ($\min)	(d)=(axb) Total Consumed Time (min)	(e)= (cxd) Total Activity Cost ($)	(f)= [d/(8x0.52)] Total Consumed Time (min)	(g)= [e/(8x0.52)] Total Activity Cost ($)
Meeting the Patient, Providing Counseling Services	1	63,698 patient	0.22	63,698	14,013.56	4,140.37	910.88
Checking Patient Information	1	63,698 patient	0.22	63,698	14,013.56	4,140.37	910.88
Patient Appointment Control and File Opening	2	63,698 patient	0.22	127,396	28,027.12	8,280.74	1,821.76
Verification of the Patient's Account And Insurance	1	63,698 patient	0.22	63,698	14,013.56	4,140.37	910.88
Informing the Patient about Time	1	63,698 patient	0.22	63,698	14,013.56	4,140.37	910.88
Sending the Patient to the Waiting Room of the Related Department	1	63,698 patient	0.22	63,698	14,013.56	4,140.37	910.88
General Follow-up of Patient Appointments	10	260 day	0.22	2,600	572	169	37.18
In- and Out-Hospital Phone Calls	10	260 day	0.22	2,600	572	169	37.18
Other Administrative Tasks	15	260 day	0.22	3,900	858	253.50	55.77
Total Performed (1)				**454,986**	**100,096.92**	**29,574**	**6,506.29**
Practical Capacity (2)				**887,040**	**195,720***	**57,657.60**	**12,722**
Unused Capacity (3)= (1-2)				**432,054**	**95,623.08**	**28,083.60**	**6,215.71**
Unused Capacity Ratio (4)=(3/2)				**49%**	**49%**	**49%**	**49%**

(c): Unit time cost was calculated in Table 4.
(d): A1 activity group total time consumed by 8 personnel
(e): A1 activity group total activity cost of 8 personnel
(f): A1 activity group total time consumed by 0.52 personnel distributed to the ophthalmology department
(g): A1 activity group total activity cost of 0.52 personnel distributed to the ophthalmology department
* : A1 activity group total practical capacity cost of 8 personnel=$195,720

Step 5: Determination of the duration required for each different time driven activity. The duration of each activity is given in Table 4 where the sub-activities of the activity groups were determined in the first stage, and the duration of the surgical procedures performed with local anesthesia, angiography and laser treatments, which are the cost objects, are given in Table 2. To prevent repetition, the same information is not shown at this stage. The treatment of angiography and laser treatments are short-term and does not require in-patient treatment. For each surgical procedure, the patient is treated in hospital for three days.

Step 6: Multiplication of the unit costs by the duration required to monitor the unit costs. In the TDABC method, for step 6, the operating costs must be charged to the cost objects using the time factor. To calculate the costs of the cost objects, the activities in each activity group were separately examined.

Since 0.52 people calculated in the third stage of the activities of the A1 *Patient Admission* Services activity group serve the ophthalmology department, the cost calculation was carried out accordingly. Regarding the A1 activity group, since the number of eye patients in polyclinic and daily routine jobs are represented by a cost factor requiring five days of labor per week, the cost effect was calculated to be 260 days (52 weeks × 5 days). Table 6 shows the total duration, the total costs of the activities of the A1 activity group, the unit duration and the unit duration cost of these activities.

As seen in Table 6, the activity costs of the A1 activity group in ophthalmology department were calculated to be 6,506.29 USD and the patient unit cost of the A1 activity group was calculated as follows:

$$\text{The Unit Patient Cost of Activity Group A1} = \frac{\text{Sum of the Activity Cost}}{\text{The Number of Patients}}$$
$$= 6{,}506.29\text{USD}/63{,}698\ \text{Patients} = 0.10\ \text{USD (Per Patient)}$$

TABLE 7
Time and Cost of A2 Polyclinic Services Activity Group

Activities	(a) Time (min)	(b) Time Driver	(c) Unit Time Cost ($\min)	(axb)=(d) Total Consumed Time (min)	(e)=(cxd) Total Activity Cost ($)
Doctor's Pre-Interview with the Patient	1	63,698 patient	0.23	63,698	14,654.54
Taking the Anamnesis (history) of the Patient	2	63,698 patient	0.23	127,396	29,301.08
Preparing the Patient for Examination	1	63,698 patient	0.23	63,698	14,654.54
Making the Eye Measurements of the Patient	3	63,698 patient	0.23	191,094	43,951.62
Patient's File Control	1	63,698 patient	0.23	63,698	14,654.54
Present, New and Consulted Patient Examination	3	63,698 patient	0.23	191,094	43,951.62
Performing Result Control Procedures	1	63,698 patient	0.23	63,698	14,654.54
Informing the Patient	2	63,698 patient	0.23	127,396	29,301.08
Guiding the Patient	1	63,698 patient	0.23	63,698	14,654.54
In-House Phone Calls	10	260 day	0.23	2,600	598
Other Administrative Tasks	30	260 day	0.23	7,800	1,794
Total Performed (1)				**965,870**	**222,170.10**
Practical Capacity (2)				**1,134,720**	**261,631**
Unused Capacity (3)=(1-2)				**168,850**	**39,460.90**
Unused Capacity Ratio (4)= (3/2)				**15%**	**15%**

TABLE 8
Time and Cost of the A3 Angiography and Laser Services Activity Group

Activities	(a) Time (min)	(b) Time Driver (patient)	(c) Unit Time Cost ($/min)	(axb)=(d) Total Consumed Time (min)	(cxd)=(e) Total Activity Cost ($)
Preparing the Patient	4	2,003	0.30	8,012	2,403.60
Application of the Treatment Procedure	10.8*	2,003	0.30	21,705	6,511.50
Informing the Patient	3	2,003	0.30	6,009	1,802.70
Total Performed (1)				**35,726**	**10,717.80**
Practical Capacity (2)				**103,680**	**30,968**
Unused Capacity (3)=(1-2)				**67,954**	**20,252.20**
Unused Capacity Ratio (4)= (3/2)				**66%**	**66%**

*10,836.25

Regarding the A2 activity group, since the number of eye patients in polyclinic patients and daily routine jobs are represented by a cost factor requiring five days of labor per week, the cost effect was calculated to be 260 days (52 weeks × 5 days). The activities in the A2 activity group and the total duration and total activity costs calculated according to the unit duration, unit duration cost and time factor are given in Table 7.

As shown in Table 7, the cost of the activities in the A2 activity group (polyclinic services) was calculated to be 222,170.10 USD. Accordingly, the patient unit cost of the activity group A2 was calculated as follows:

$$\text{The Unit Patient Cost of Activity Group A2} = \frac{\text{Sum of the Activity Cost}}{\text{The Number of Patients}}$$
$$= 222{,}170.10\text{USD}/\ 63{,}698\ \text{Patients}$$
$$= 3.49\ \text{USD (Per Patient)}$$

The number of angiography and laser service patients was regarded as the cost factor for the activities in the A3 *Angiography and Laser Services* activity group. Also, the duration of angiography and laser procedures was determined to be 21,705 minutes according to the hospital's electronic medical record system. When the 21,705 minute total duration was divided by the annual number of angiography and laser procedures (2003), the application duration of one angiography and laser procedure was found to be 10.83625 minutes (21,705 minutes / 2003 angiography and laser applications). The activities in the A3 activity group and the total duration and total activity costs calculated according to the unit duration, unit duration cost and time factor are given in Table 8.

As shown in Table 8, the cost of the activities in the A3 activity group was calculated to be 10,717.80 USD. Accordingly, the patient unit cost of the activity group A3 was calculated as follows:

$$\text{The Unit Patient Cost of Activity Group A3} = \frac{\text{Sum of the Activity Cost}}{\text{The Number of Patients}}$$
$$= 10{,}717.80\ \text{USD}/2003\ \text{Patients}$$
$$= 5.35\ \text{USD (Per Patient)}$$

Also, since the durations of the cost objects of the angiography and laser procedures were different, the angiography and laser procedures costs were calculated and are given in Table 9.

TABLE 9
Unit Costs of Angiography and Laser Procedure Types

Activities	Argon Laser Photocoagulation ($)	Nd:YAG Laser Capsulotomy-Syn-echotomy ($)	Fluorescein Fundus Angi-ography (FFA) ($)	Electrolysis (Via Argon La-ser) Applied in Distichiasis ($)
Preparing the Patient	1.20	1.20	1.20	1.20
Applying the Treatment Procedure	4.50[a]	1.50[b]	4.50[a]	1.50[b]
Informing the Patient	0.90	0.90	0.90	0.90
TOTAL	**6.60**	**3.60**	**6.60**	**3.60**

[a]:As Photocoagulation and Fluorescein Fundus Angiography procedure times were 15 min, 15 min x 0.30 USD= 4.50 USD
[b]:As Nd:YAG Laser Capsulotomy-Synechotomy and Electrolysis (Via Argon Laser) in Distichiasis procedure times were 5 min, 5 min x 0.30 USD = 1.50 USD

TABLE 10
Time and Costs of the A4 Patient Admission and Discharge Services Activity Group

	(a)	(b)	(c)	(d)=(axb)	(e)=(cxd)
Activities	Time (min)	Time Driver (patient)	Unit Time Cost ($/min)	Total Consumed Time (min)	Total Activity Cost ($)
Patient Hospitalization and Room Planning	5	925	0.06	4,625	277.50
Completing the Patient File	7	925	0.06	6,425	388.50
Sending the Patient File to the Service	5	925	0.06	4,625	277.50
Information Exchange of the Secretary and Nurse	3	925	0.06	2,775	166.50
Taking the Patient into the Room	10	925	0.06	9,250	555
Adding the Nurse Observations in the Patient File	2	925	0.06	1,850	111
Exiting the Discharged Patient from the Program	2	925	0.06	1,850	111
In- and Out-Hospital Phone Calls	25	925	0.06	6,500	390
Filling Forms, Reports and Other Documents	30	925	0.06	7,800	468
Other Administrative Tasks	20	925	0.06	5,200	312
Total Performed (1)				**50,950**	**3,057**
Practical Capacity (2)				**60,934**	**3,673**
Unused Capacity (3)=(1-2)				**9,984**	**616**
Unused Capacity Ratio (4)= (3/2)				**16%**	**16%**

Regarding the activities in the A4 *Patient Admission and Discharge Services* activity group, since the number of eye patients in polyclinic and daily routine jobs are represented by a cost factor requiring five days of labor per week, the cost effect was regarded to be 260 days (52 weeks × 5 days). The total duration and total activity costs of the A4 group, calculated according to the unit duration, unit duration cost and time factor, are given in Table 10.

As seen in Table 10, the operating cost of the A4 activity group was calculated to be 3,057 USD. Accordingly, the patient unit cost of the activity group A4 was calculated as follows:

$$\textit{The Unit Patient Cost of Activity Group A4} = \frac{\textit{Sum of the Activity Cost}}{\textit{The Number of Patients}}$$
$$= 3{,}057\ \textit{USD} / 925\ \textit{patients}$$
$$= 3.31\ \textit{USD (Per Patient)}$$

Regarding the cost factor for the activities in the A5 *Surgical Services* activity group, considering the number of eye surgery patients and the fact that the A5 activity center provides service 24 hours a day, the cost factor for routine jobs was determined to be 365 days. Also, the duration of surgical procedures was determined to be 37,733 minutes according to the hospital's electronic medical record system. When the 37,733 minutes total duration was divided by the annual number of surgical procedures (1728 patients), the application duration of one surgical procedure was found to be 21.836226 minutes (21,705 min / 1728 patients). The total duration and total activity costs for the A5 group, calculated according to the unit duration, unit duration cost and time factor, are given in Table 11.

As shown in Table 11, the cost of the activities in the A5 group was calculated to be 75,074.05 USD. Accordingly, the patient unit cost of the activity group A5 was calculated as follows:

$$\textit{The Unit Patient Cost of Activity Group A5} = \frac{\textit{Sum of the Activity Cost}}{\textit{The Number of Patients}}$$
$$= 75{,}074.05\textit{USD}/1{,}728\ \textit{Patients}$$
$$= 43.45\ \textit{USD (Per Patient)}$$

Also, since the durations of the cost objects of the surgical procedures were different, the costs of these surgical procedures were calculated and are given in Table 12.

Regarding the cost factor for the activities in the A6 *Clinical Services* activity group, considering the number of in-patients in the ophthalmology polyclinics and the fact that the A6 activity center provides service 24 hours a day, the cost factor was determined to be 365 days. The total duration and total activity costs of the activities in the A6 group, calculated according to the unit duration, unit duration cost and time factor, are given in Table 13.

TABLE 11
Time and Cost of the A5 Surgical Services Activity Group

	(a)	(b)	(c)	(d)=(axb)	(e)=(cxd)
Activities	**Time (min)**	**Time Driver**	**Unit Time Cost ($/min)**	**Total Consumed Time (min)**	**Total Activity Cost ($)**
Filling the Preoperative Form	5	1,728 patient	0.39	8,640	3,369.60
Preparing the Patient for Surgical Operation	7	1,728 patient	0.39	12,096	4,717.44
Taking the Patient to the Operating Table	5	1,728 patient	0.39	8,640	3,369.60
Preparing the Medical Drugs and Consumables	10	1,728 patient	0.39	17,280	6,739.20
Doctor's Interview with the Patient	3	1,728 patient	0.39	5,184	2,021.76
Application of Local Anesthesia	2	1,728 patient	0.39	3,456	1,348.84
Surgical Procedure Application Activities	21.8*	1,728 patient	0.39	37,733*	14,715.87
Cleaning the Patient and Dressing the Wound(s)	10	1,728 patient	0.39	17,280	6,739.20
The Patient Leaving the Operating Table	10	1,728 patient	0.39	17,280	6,739.20
Filling the Postoperative Form	10	1,728 patient	0.39	17,280	6,739.20
Sending the Patient to the Clinical Service	10	1,728 patient	0.39	17,280	6,739.20
Recording of the Duration and Material of the Surgical Operation	7	1,728 patient	0.39	12,096	4,717.44
Other Administrative Tasks	20	365 day	0.39	7,300	2,847
Filling Forms and Other Documents	30	365 day	0.39	10,950	4,270.50
Total Performed (1)				**192,495**	**75,074.05**
Practical Capacity (2)				**387,936**	**152,505**
Unused Capacity (3)=(1-2)				**195,441**	**77,430.95**
Unused Capacity Ratio (4)= (3/2)				**50%**	**50%**

*21.836226

TABLE 12
Unit Costs of Surgical Procedure Types

Activities	**Phacoemulsification IOL ($)**	**Conjunctival Plastic, With Grafts ($)**	**Pterygium Surgery ($)**	**Blepharoplasty Surgery (for one eye) ($)**	**Eyelid Reconstruction with Grafts or Flaps($)**
Filling the Preoperative Form	1.95	1.95	1.95	1.95	1.95
Preparing the Patient for Surgical Operation	2.73	2.73	2.73	2.73	2.73
Taking the Patient to the Operating Table	1.95	1.95	1.95	1.95	1.95
Preparing the Medical Drugs and Consumables	3.90	3.90	3.90	3.90	3.90
Doctor's Interview with the Patient	1.17	1.17	1.17	1.17	1.17
Application of Local Anesthesia	0.78	0.78	0.78	0.78	0.78
Surgical Procedure Application Activities	11.70[a]	17.55[b]	11.70[a]	11.70[a]	17.55[b]
Cleaning the Patient and Dressing the Wound(s)	3.90	3.90	3.90	3.90	3.90
The Patient Leaving the Operating Table	3.90	3.90	3.90	3.90	3.90
Filling the Postoperative Form	3.90	3.90	3.90	3.90	3.90
Sending the Patient to the Clinical Service	3.90	3.90	3.90	3.90	3.90
Recording of the Duration and Material of the Surgical Operation	2.73	2.73	2.73	2.73	2.73
Other Administrative Tasks	7.80	7.80	7.80	7.80	7.80
Filling Forms and Other Documents	11.70	11.70	11.70	11.70	11.70
TOTAL	**62.01**	**67.86**	**62.01**	**62.01**	**67.86**

[a]:As Phacoemulsification-IOL, Pterygium and Blepharoplasty Surgery (for one eye) surgical procedure times are 30 min, 30 min. x 0.39 USD = 11.70 USD
[b]:As Conjunctival Plastic, with Grafts and Eyelid Reconstruction with Grafts or Flaps surgical procedure times are 45 min, 45 min. x 0.39 USD = 17.55 USD

As shown in Table 13, the cost of the activities in the A6 group was calculated to be 65,682.75 USD. Accordingly, the patient unit cost of the activity group A6 was calculated as follows:

$$\textit{The Unit Patient Cost of Activity Group A6} = \frac{\textit{Sum of the Activity Cost}}{\textit{The Number of Patients}}$$
$$= 65{,}682.75\ \text{USD} / 925\ \text{Patients}$$
$$= 71.01\ \text{USD (Per Patient)}$$

The costs for each activity group were charged to the cost objects that were the subject of the application study, i.e., the types of angiography, laser and surgical procedures. The shares of the types of angiography, laser and surgical procedures from the activity groups are shown in Table 14.

After all the charges were calculated for the activity groups, the total cost of a patient that receives polyclinic, angiography and laser or surgical services in the ophthalmology department is given in Table 15.

TABLE 13
Time and Cost of the A6 Clinical Services Activity Group

Activities	(a) Time (min)	(b) Time Driver	(c) Unit Time Cost ($/min)	(d)=(axb) Total Consumed Time (min)	(e)=(cxd) Total Activity Cost ($)
Shift Change	30	365 day	0.19*	10,950	2,146.20
Taking the New Patient to the Room and First Care	20	925 patient	0.19	18,500	3,626
Visitation (In the Morning and After Surgery 15.00-16.00)	30	925 patient	0.19	27,750	5,439
Taking Blood, Opening Vascular Path, Hygienic Care	10	925 patient	0.19	9,250	1,813
Fever, Pulse and Blood Pressure Measurement	15	925 patient	0.19	13,875	2,719.50
Daily Medicine and Medical Consumables Control	17.5	925 patient	0.19	16,187.50	3,172.75
Patient Examination	20	925 patient	0.19	18,500	3,626
Application of the Patient Treatment Plan	20	925 patient	0.19	18,500	3,626
Patient File Control	5	925 patient	0.19	4,625	906.50
Informing the Patient's Relatives	5	925 patient	0.19	4,625	906.50
Bed Sheets and Clothing Control	10	925 patient	0.19	9,250	1.813
Organizing the Food Program	15	925 patient	0.19	13,875	2,719.50
Other Administrative Tasks	30	365 day	0.19	10,950	5,439
Providing Information to the Department of Surgical Services and to the Doctor	10	925 patient	0.19	9,250	1,813
Examination Inputs and Medical Consumables Control	10	925 patient	0.19	9,250	1,813
Dilating the Patient's Eyes on the Day of the Surgical Operation	30	925 patient	0.19	27,750	2,146.20
Preparing the Patient for the Department of Surgical Services	10	925 patient	0.19	9,250	1,813
Obtaining Consent Form Specific to the Surgical Operation	5	925 patient	0.19	4,625	906.50
Filling Forms, Reports and Other Documents	37.5	925 patient	0.19	34,687.50	6,798.75
Delivering the Patient to the Department of Surgical Services	10	925 patient	0.19	9,250	1,813
Taking the Patient from the Department of Surgical Services	10	925 patient	0.19	9,250	1,813
Taking the Patient to the Room and First Care	15	925 patient	0.19	13,875	2,719.50
Giving the Patient Drops According to the Treatment Plan	35	925 patient	0.19	32,375	6,345.50
Preparing the Patient for Discharge	10	925 patient	0.19	9,250	1,813
Total Performed (1)				**345,650**	**67,747.40**
Practical Capacity (2)				**416,275.20**	**81,554**
Unused Capacity (3)=(1-2)				**70,625.20**	**13,806.60**
Unused Capacity Ratio (4)= (3/2)				**17%**	**17%**

*0.196

TABLE 14
The Shares the Angiography, Types of Laser and Surgery Procedures Took from the Activity Groups

	Angiography, Types of Laser and Surgery Procedures	A1 ($)	A2 ($)	A3 ($)	A4 ($)	A5 ($)	A6 ($)	Total Cost ($)
Angiography/ Laser	Argon Laser Photocoagulation	0.10	3.49	6.60	-	-	-	10.19
	Nd: YAG- Laser Capsulotomy-Synechotomy	0.10	3.49	3.60	-	-	-	7.19
	Fluorescein Fundus Angiography (FFA)	0.10	3.49	6.60	-	-	-	10.19
	Electrolysis (Via Argon Laser) Applied in Distichiasis	0.10	3.49	3.60	-	-	-	7.19
Surgery	Phacoemulsification - IOL	0.10	3.49	-	3.31	62.01	213.03*	281.94
	Conjunctival Plastic, With Grafts	0.10	3.49	-	3.31	67.86	213.03	287.79
	Pterygium Surgery	0.10	3.49	-	3.31	62.01	213.03	281.94
	Blepharoplasty Surgery (for one eye)	0.10	3.49	-	3.31	62.01	213.03	281.94
	Eyelid Reconstruction (with Grafts or Flaps)	0.10	3.49	-	3.31	67.86	213.03	287.79

*Since 3 days of hospitalization was done for the surgical procedures in the A6 activity group, 71.01 USD x 3 days= 213.03 USD

TABLE 15
Patient Unit Costs of Polyclinic, Angiography and Laser and Surgical Services

Cost Objects	A1 ($)	A2 ($)	A3 ($)	A4 ($)	A5 ($)	A6 ($)	Total Cost ($)
Polyclinic Patient Cost	0.10	3.49	-	-	-	-	3.59
Angiography Patient Cost	0.10	3.49	5.35	-	-	-	8.94
Surgical Service Patient Cost	0.10	3.49	-	3.31	43.45	71.01	121.36

RESULTS AND DISCUSSIONS

The success of today's business world in which the economic life of information is very short depends on making decisions supported by accurate information. Considering that resources used are often scarce and costly, and damage can be caused to the environment by the production of new resources, it is necessary to act more rationally in their use. The best way to get the highest efficiency from resources in business is to base decisions on accurate cost information.

The TDABC method not only provides accurate cost information for businesses, but also provides opportunities to identify and eliminate activities that do not provide added value. Managers will reduce any waste of resources by making accurate decisions thanks to accurate cost information. Therefore, as is the case in all businesses that want to be ahead of their competitors, the cost advantage delivered by the TDABC method benefits hospital businesses by obtaining accurate cost information. The shortcomings in the health services delivered can be determined by the TDABC method. With this method, hospital managers can detect the activities that are unnecessarily time consuming, and they can obtain better information on their staff costs and on the efficiency of their staff. Also, since the cost is calculated in an accurate way, unused capacity costs can be identified. Thus, unused capacity costs will not be reflected in the cost objects: angiography, laser and surgical services, so that more realistic cost information is obtained.

In the present study, since the TDABC method carries out cost calculation by considering the practical working capacity, information on the unused capacities of the ophthalmology department is highlighted along with the costs of these capacities. In this manner, examining the unused capacity ratios and the costs of the activity groups in the ophthalmology department of the state hospital according to the TDABC method, these values were found to be 49% and 6,215.71 USD in the A1 *Patient Admission Services* activity group; 15% and 39,460.90 USD in the A2 *Polyclinic Services* activity group; 66% and 20,252.20 USD in the A3 *Angiography and Laser Services* activity group; 16% and 616 USD in the A4 *Patient Admission and Discharge Services* activity group; 50% and 74,430.95 USD in the A5 *Surgical Services* activity group, and 17% and 13,806.60 USD in the A6 *Clinical Services* activity group.

Regarding the unused capacity ratios, the A3 activity group produced the highest, while the A2 activity group produced the lowest. In the A3 activity group, the unused capacity ratio was high because it operated 1 hour a day and 5 days a week. Since the health services in the A3 activity group were provided by the staff in the A2 activity group, the hospital management can deliver the health services provided here together with the services provided in the A2 activity group to reduce or eliminate the unused capacity. Thus, the unused capacity ratio of the A3activity group will be reduced, and the area where the A2 activity group health services are provided will be available for other services. Also, to decrease or eliminate the unused capacities in other activity groups, the staff working in these activity groups will be diverted to the busier departments that are in need of staff, and this will contribute to improving the hospital administration's efficient management of capacity.

Examining the unit costs per patient in the activity groups in the ophthalmology department, the activity groups A1, A2, A3, A4, A5 and A6 were calculated to be 0.10, 3.49, 5.35, 3.31, 43.45 and 71.01 USD, respectively. The lowest cost was in the A1 activity group where consultation services are given, while the highest cost was in the A6 activity group where clinical care service is provided.

Examining the costs of angiography, laser and surgical procedures given in Table 14, the unit cost for argon laser photocoagulation and fundus fluorescein angiography procedures applied was found to be 10.19 USD, while the unit costs of Nd:YAG laser capsulotomy- synechiotomy and distichiasis-electrolysis (via argon laser) procedures were found to be 7.19 USD. Also, the unit costs of each of the phacoemulsification with IOL, blepharoplasty surgery (for one eye) and pterygium surgery were calculated to be 281.94 USD, and the unit costs of each of the conjunctivoplasty and eyelid reconstructions with (graft or flap) were calculated to be 287.79 USD.

In Table 15, the cost of a patient receiving polyclinic services in the ophthalmology department was calculated to be 3.59 USD, the cost of a patient receiving angiography and laser was 8.94 USD and a patient receiving a surgical procedure was 121.36 USD.

Hospital management can make more accurate decisions about capacity and cost objects thanks to the TDABC method, and more reliable and up-to-date results can be acquired about the source, activity and process. The TDABC method not only provides a more accurate calculation of the unit costs of the activities it also provides important information to the hospital management about these activities. As a result of the activity analyses that can be performed, activities that do, or do not, provide added value to the hospital business can be determined clearly. Consequently, patient treatment cycle duration can be optimized, workflow regarding the related process can be improved and hospital management will be able to provide activities efficiently thanks to this information resulting in an increase in profitability.

Since there were no previous studies conducted on this subject in a state hospital, this study provided an opportunity to hospital administration to apply

this study in other hospital units. Hospital administrations will have the chance to gain a better understanding of the amount and location of their unused capacity. Also, hospital administrations will have an idea about which units they should focus on and in which units they should pay more attention to costs. Calculation of the costs by the TDABC method will be important for the future of hospital businesses. Furthermore, state hospitals will have a system that provides easier, faster, cheaper and more accurate cost data thanks to the continuous application of the TDABC method. This study provides hospital management with the opportunity to increase control of hospital activities, to increase their efficiency and to easily update cost management when service provision is redesigned.

Also, with the increasing technology and increasing population, the amount of medical waste from hospital businesses is increasing. The environmental impact of controlling this increase is very important. Businesses using the TDABC method will contribute significantly to both the operation and the natural environment by eliminating the waste of consumed materials and controlling the production of waste. In addition to calculating the costs according to the TDABC method, these hospital businesses should carry out an effective waste management program and related training programs. Thus, the medical wastes will be taken under control and a positive contribution to the natural environment will be achieved.

The present study showed that the TDABC method can be applied to hospital businesses, which have an important place in health institutions, and that this method is necessary for those hospital businesses and will make a significant contribution to hospital management in making strategic decisions. Also, the study will contribute to published literature and to society by encouraging hospital businesses which currently avoid calculating costs to use this as a model.

REFERENCES

[1] TUIK (2018) Health Expenditure Statistics, Turkish Statistical Institute, 27621, 1-2. (In Turkish).

[2] Yu, Y.R., Abbas, P.I., Smith, C.M., Carberry, K.E, Ren, H., Patel, B., Nuchtern, J.G. and Lopez, M.E. (2016) Time-Driven-Activity-Based Costing to Identify Opportunities for Cost Reduction in Pediatric Appendectomy. J Pediatr Surg. 51(12), 1962-1966.

[3] Akhavan, S., Ward, L. and Bozic, K.J. (2016) Time-driven activity-based costing more accurately reflects costs in arthroplasty surgery. Clin Orthop Relat Res. 474, 8-15.

[4] Porter, M.E. (2010) What is value in health care? N Engl J Med. 363, 2477-2481.

[5] Kaplan, R.S. and Anderson, S.R. (2004) Time-driven activity-based costing. Harv Bus Rev. 82, 131-150.

[6] Ozder, A., Teker, B., Eker, H.H., Altındis, S., Kocaakman, M. and Karabay, O. (2013) Medical waste management training for healthcare managers - a necessity? Journal of Environmental Health Science and Engineering. 11(20), 1-8.

[7] Hasçuhadar, M., Kaya, Z., Şerbetçioğlu, S., Arslan, T. and Altınkaya, S. (2007) The awareness level among the employees working in Ankara Ataturk Training and Research Hospital about medical wastes. Turk Med J. 1, 138-144.

[8] Rahman, S., Acık, Y., Gülbayrak, C., Erhan, D., Nazlıer, K. and Deveci, E. (2009) Methods of collecting, storing and disposal of medical wastes in healthcare institutions. Firat Healthcare Journal. 4(11), 3-14.

[9] Ege, H. (2009) Management of medical wastes in province of Adana; Problems and solution offers. Unpublished Master Thesis. Cukurova University, Social Science Institute, Department of Environmental Engineering publication, Adana, Turkey.

[10] Ekiz, C.U. and Ekiz, C. (2013) State of The World 2013 is Sustainability Still Possible? Worldwatch Institute, Turkey WorkBank Culture Series, 11931.

[11] Öker, F. (2003) Activity Based Costing, Production and Service Business Applications. Literature Publishing, Istanbul, Turkey, 185p. (In Turkish).

[12] Pollard, M.E, Laviana, A.A, Kaplan, A.L, Pagan, C. and Saigal, C.S. (2018) Time-Driven Activity-Based Costing Analysis of Urologic Stone Disease. Urology Practice. 5(5), 327-333.

[13] Sharan, A.D., Schroeder, G.D., West, M.E. and Vaccaro, A.R. (2016) Understanding time-driven activity-based costing. Clin Spine Surg. 29(2), 62–65.

[14] Inverso, G., Lappi, M.D., Flath-Sporn, S.J., Heald, R., Kim, D.C. and Meara, J.G. (2015) Increasing Value in plagiocephaly care: a time driven activity-based costing pilot study. Ann Plast Surg. 74, 672-676.

[15] Balakrishnan, K., Goico, B. and Arjmand, E.M. (2015) Applying cost accounting to operating room staffing in otolaryngology: time-driven activity-based costing and outpatient adenotonsillectomy. Otolaryngol Head Neck Surg. 152, 684-90.

[16] Laviana, A.A., Kundavaram, C.R., Tan, H.J., Burke, M.A., Niedzwiecki, D., Lee, K.R. and Hu, J.C. (2016) Determining the True Costs of Treating Small Renal Masses Using Time Driven, Activity Based Costing. Urology Practice. 3, 180-186.

[17] Taniş, V.N. and Özyapici, H. (2012) The Measurement and Management of Unused Capacity in A Time Driven Activity Based Costing System. Jamar. 10(2), 43-55.
[18] Bruggeman, W., Everaert, P., Steven, R.A. and Levant, Y. (2005) Modeling Logistics Costs Using TimeDriven ABC: A Case in a Distribution Company. Gent University Working Paper, 2005/332.
[19] Bruggeman, W. and Moreels, K. (2003) Time-Driven Activity Based Costing a New Paradigm in Cost Management. Bimac Newsletter. 1-2.
[20] Barros, R.S. and Dias, A.C.F. (2017) Time-Driven-Activity-Based Costing: Designing A Model in A Portuguese Production Environment. Qualitative Research in Accounting and Management. 14(1), 2-20.
[21] Barrett, R. (2005) Time-Driven Costing: The Bottom Line on the New ABC. Business Performance Management. 3, 1-3.
[22] Saban, M. and Irak Gugercin, G. (2009) Modern Cost Management System: Time Driven Activity Based Costing. ZKU Journal of Social Sciences. 5(10), 97-108. (In Turkish).
[23] Namazi, M. (2016) Time-driven activity-based costing: Theory, applications and limitations. Iranian Journal of Management Studies (IJMS). 9(3), 457-482.
[24] Irak Gugercin, G. and Saban M. (2018) Distribution Of Manufacturing Overhead Costs By Time Driven Activity Based Costing Method: An Application in Shipbuilding Construction Projects. Business and Management Studies: An International Journal. 6(3), 590-604. (In Turkish).
[25] Alves, R.J.V., Etges, A., Neto, G.B. and Polanczyk, C.A. (2018) Activity-Based Costing and Time-Driven Activity-Based Costing for Assessing the Costs of Cancer Prevention, Diagnosis, and Treatment: A Systematic Review of the Literature. Value Health Reg. 24(17), 142-147.
[26] Burns, K.E., Haysom, H.E., Higgins, M.A., Waters, N., Tahiri, R., Rushford, K., Dunstan, T., Saxby, K., Kaplan, Z., Chunilal, Z., McQuilten, Z.K. and Wood, E.M. (2019) A time-driven, activity-based costing methodology for determining the costs of red blood cell transfusion in patients with beta thalassaemia major. Transfusion Medicine. 29(1), 33-40.
[27] Ruhumuriza, J., Odhiambo, J., Riviello, R., Lin, Y., Nkurunziza, T., Shrime, M., Maine, R., Omondi, J.M., Mpirimbanyi, C., de la Paix Sebakarane, J., Hagugimana, P., Rusangwa, C. and Hedt-Gauthier, B. (2018) Assessing the cost of laparotomy at a rural district hospital in Rwanda using time-driven activity-based costing. BJS Open. 2(1), 25-33.
[28] Koehler, D.M., Balakrishnan, R., Lawler, E.A. and Shah, A.S. (2019) Endoscopic versus open carpal tunnel release: A detailed analysis using time-driven activity-based costing at an academic medical center. J Hand Surg. Am. 44(1), 62.e.1- 62.e.9.
[29] Nilsen, K.B., Hill, C., Trifiletti, D.M., Libby, B., Lash, D.H., Lain, M., Christodoulou, D., Hodge, C. and Showalter, T.N. (2018) Evaluation of delivery costs for external beam radiation therapy and brachytherapy for locally advanced cervical cancer using time-driven activity-based costing. Int J Radiat Oncol Biol Phys. 102(5), 1598-1599.
[30] Laviana, A.A., Tan, H.J., Hu, J.C., Weizer, A.Z., Chang, S.S. and Barocas, D.A. (2018) Retroperitoneal versus transperitoneal robotic-assisted laparoscopic partial nephrectomy: a matched-pair, bicenter analysis with cost comparison using time-driven activity-based costing. Curr Opin Urol. 28, 108-114.
[31] Keel, G., Savage, C., Rafiq, M. and Mazzocato, P. (2017) Time-Driven Activity-Based Costing In Health Care: A Systematic Review of the Literature. Health Policy. 121, 755-763.
[32] Garcia, J.A., Mistry, B., Hardy, S., Fracchia, M.S., Hersh, C., Wentland, C., Hartnick, C.J. and Vadakekalam, J. (2017) Time-driven activity-based costing to estimate cost of care at multidisciplinary aerodigestive centers. Laryngoscope. 127(9), 2152–2158.
[33] Çetiner, A. (2017) Time-based activity-based costing in public hospitals. Unpublished Master Thesis. Istanbul Aydin University, Social Science Institute, Istanbul.
[34] Andreasen, S.E., Holm, H.B., Jørgensen, M., Gromov, K., Kjærsgaard-Andersen, P. and Husted, H. (2017) Time-drivenActivity-based Cost of Fast-Track Total Hip and Knee Arthroplasty. J Arthroplasty. 32, 1747-1755.
[35] El Alaoui, S. and Lindefors, N. (2016) Combining Time-Driven Activity-Based Costing with Clinical Outcome in Cost-Effectiveness Analysis to Measure Value in Treatment of Depression. Plos One, 11(10), 1-15.
[36] Yun, B.J., Prabhakar, M.A., Warsh, J., Kaplan, R., Brennan, J., Dempsey, K.E. and Raja, S.A. (2016) Time-Driven Activity-Based Costing in Emergency Medicine. Annals of Emergency Medicine. 67(6), 765-772.
[37] Thaker, N.G., Pugh, T.J., Mahmood, U., Spinks, E.T., Martin, N.E., Kudchadker, R.J., Guzman, A.B., Jones, T.M., Tatum, L.S., Incalcaterra, J.R., Frank, B.D., Bingham, J., Kaplan, R.S., Stowell, C., Bucholz, T.A., Kuban, D.A., Feeley, T.W. and Frank, S. (2016) Defining the Value Framework for Prostate Brachytherapy Using Patient-Centered Outcome Metrics and Time-Driven Activity-Based Costing. Brachytherapy. 15, 274-282.

[38] Luther, G., Miller, P., Waters, P.M. and Bae, D.S. (2016) Radiographic Evaluation During Treatment of Pediatric Forearm Fractures: Implications on Clinical Care and Cost. J Pediatr Orthop. 36, 465-471.

[39] Laviana, A.A., Ilg, M.A., Veruttipong, D., Tan, H.J., Burke, M.A., Niedzwiecki, D.R., Kupelian, P.A., King, C.R., Steinberg, M.L., Kundavaram, M.L., Kamrava, M., Kaplan, A.L., Moriarity, A.K., Hsu, W., Margolis, D.J.A., Hu, J. and Saigal, C.S. (2016) Utilizing Time-Driven Activity-Based Costing to Understand the Short- and Long-Term Costs of Treating Localized, Low-Risk Prostate Cancer. Cancer. 122, 447-55.

[40] Ilg, M.A., Laviana, A.A., Kamrava, M., Veruttipong, D., Steinberg, M.L., Park, S.J., Burke, M.A., Niedzwiecki, D.R., Kupelian, P.A. and Saigal, C.S. (2016) Time-driven activity-based costing of low-dose-rate and high-dose-rate brachytherapy for low-risk prostate cancer. Brachytherapy. 15(6), 760-767.

[41] Gregorio, J., Russo, G. and Lapao, L.V. (2016) Pharmaceutical Services Cost Analysis Using Time-Driven Activity-Based Costing: A Contribution to Improve Community Pharmacies' Management. Research in Social and Administrative Pharmacy. 12(3), 475-485.

[42] Schutzer, M.E., Douglas, D.W., Arthur, M.D., Mitchell, S. and Anscher, M.D. (2016) Time-Driven Activity-Based Costing: A Comparative Cost Analysis of Whole-Breast Radiotherapy Versus Balloon-Based Brachytherapy in the Management of Early-Stage Breast Cancer. Journal of Oncology Practice. 12(5), 476-593.

[43] Mandigo, M., O'Neill, K., Mistry, B., Mundy, B., Millien, C., Nazaire, Y., Damuse, R., Pierre, C., Mugunga, J.C., Gillies, R., Lucien, F., Bertrand, K., Luo, E., Costas, A., Greenberg, S.L.M., Meara, J.G. and Kaplan, R.A. (2015) Time-driven Activity-based Costing Model to Improve Health-care Resource Use in Mirebalais, Haiti. Harvard Medical School. 385, 22.

[44] Lievens, Y., Obyn, C., Mertens, A.S., Van Halewyck, D. and Hulstaert, F. (2015) Stereotactic Bodyradiotherapy For Lung Cancer: How Much Does It Really Cost? Journal of Thoracic Oncology. 10, 454–61.

[45] Erhun, F., Mistry, B., Platchek, T., Milstein, A., Narayanan, V.G. and Kaplan, R.S. (2015) Time-Driven Activity-Based Costing of Multivessel Coronary Artery Bypass Grafting Across National Boundaries to Identify Improvement Opportunities: Study Protocol. BMJ Open. 5(8), e008765.

[46] DiGioia, M.A., Greenhouse, P.K., Giarrusso, M.L. and Kress, J.M. (2015) Determining The Truecost to Deliver Total Hip and Knee Arthroplasty Over The Full Cycle of Care: Preparing For Bundling and Reference-Based Pricing. The Journal of Arthroplasty. 31, 1-6.

[47] Chen, A., Sabharwal, S., Akhtar, K. Makaram, N. and Gupte, C.M. (2015) Time-Driven Activity Based Costing of Total Knee Replacement Surgery at A London Teaching Hospital. The Knee. 22, 640-645.

[48] Özkan, Ö. (2015) Time driven activity based costing and a hospital application. Unpublished PhD Thesis. Marmara University, Social Science Institute, Istanbul.

[49] McLaughlin, N., Burke, M.A., Setlur, N.P., Niedzwiecki, D.R., Kaplan, A.L., Saigal, C., Mahajan, A., Martin, N.A. and Kaplan, R.S. (2014) Time-Driven Activity-Based Costing: A Driver For Provider Engagement in Costingactivities and Redesign Initiatives. Neurosurg Focus. 37, E3.

[50] Kaplan, A.L., Agarwal, N., Setlur, N.P., Tan, H.J., Niedzwiecki, D., McLaughlin, N., Burke, M.A., Steinberg, K., Chamie, K. and Saigal, C.S. (2014) Measuring The Cost of Care in Benign Prostatic Hyperplasia Using Time-Driven Activity-Based Costing (TDABC). Healthcare. 3(1), 43-48.

[51] Kırlıoğlu, H. and Atalay, B. (2014) A Capacity Management Evaluation of Time Driven Activity Based Costing and A Hospital Management Practice. Int. Journal of Management Economics and Business. 10(23), 99-119.

[52] Oker, F., Ozyapici, H. (2013) A New Costing Model in Hospital Management: Time-Driven-Activity-Based Costing System. The Health Care Manager. 32(1), 23-36.

[53] Aydın, A. (2011) Service Profitability Analysis with Time Driven Activity Based Costing System: Practice in Faculty of Dentistry. Unpublished Master Thesis. Karadeniz Technical University, Social Science Institute, Trabzon.

[54] Demeere, N., Stouthuysen, K. and Roodhooft, P. (2009) Time-Driven-Activity-Based Costing in an Outpatient Clinic Environment: Development, Relevance and Managerial Impact. Health Policy. 92, 296-304.

Received: **01.11.2018**
Accepted: **14.02.2019**

CORRESPONDING AUTHOR

Pınar Kurt
Department of Opticianry
Vocational School of Health Services
Bandirma Onyedi Eylul University
Bandirma 10200 – Turkey

e-mail: kurt.pnr@yahoo.com

© by PSP Volume 28 – No. 4/2019 pages 2771-2779 Fresenius Environmental Bulletin

THE OPTIMIZATION OF STARCH GELATINIZATION AND QUALITY ATTRIBUTES UNDER HYDROTHERMAL TREATMENT OF PADDY BY RESPONSE SURFACE METHOD

Khurram Yousaf[1], Adnan Abbas[2], Xuejin Zhang[3], Rui Kang[1], Eisa Belal[4], Fiaz Ahmad[5,6], Kunjie Chen[1,*]

[1]College of Engineering, Nanjing Agricultural University, Nanjing, Jiangsu 210031, P.R. China
[2]College of Engineering, China Agricultural University, Beijing, 100083, P.R. China
[3]Nanjing Research Institute for Agricultural Mechanization, Ministry of Agriculture, Nanjing, 210014, China
[4]Department of Agricultural Engineering, University of Zalingei, Central Darfur State, Zalingei, POX6, Republic of Sudan
[5]Department of Agricultural Engineering, Bahauddin Zakeriya University, Multan, 60800, Pakistan
[6]School of Agricultural Equipment Engineering, Jiangsu University, Zhenjiang, 212013, China

ABSTRACT

The effect of soaking temperature, soaking time, and steaming time min up to five levels on DSG, percentage head rice yield (HRY), hardness, lightness, and color of japonica rice variety Huaidao 5 were taken under consideration. The most appropriate model in prediction of DSG, HRY, hardness, lightness and color was quadratic with R^2 values of 0.92, 0.91, 0.94, 0.91, and 0.94 respectively by response surface method (RSM). Although, the DSG, HRY, hardness, and color increased with the process severity thereby lightness decreased. However, HRY increased only up to some level before it started to reduce. The predicted optimum soaking temperature, soaking time and steaming time were 65˚C, 135 min and 10.66 min respectively and the predicted DSG, HRY, hardness, lightness and color under this condition was 82.38%, 73.44%, 32.38 N, 81.54, and 13.62 respectively with 0.897 composite desirability.

KEYWORDS:
Gelatinization, hydrothermal, optimization, response surface method, rice quality

INTRODUCTION

Rice being a staple food is utilized by more than half of the world's population [1]. Parboiling is a hydrothermal process of paddy rice where it is subjected to a number of treatments such as soaking, steaming, and drying before milling [2]. Parboiling helps rice to absorb water until it is hydrated during soaking, and further in steaming process isolation of starch in endosperm of grain. It turns the rice harder which decreases milling breakage, and improves HRY during milling, the nutritional value, and resistance to spoilage by insects [3, 4]. The hydrothermal treatment affects the rice starch structure by changing its amorphous form into a strongly packed endosperm. Starch has an important role in making the rice harder and improving its quality. The degree of starch gelatinization (DSG) provides an idea of the behavior of starch in endosperm, which is mainly responsible for the most of the properties of parboiled rice [5].

The response surface methodology (RSM) is a unique combination of mathematical and statistical approaches to evaluate the optimal conditions by reducing the number of experiments between factors and responses [6]. It is an excellent approach which has been used by many researchers for optimization of the different factors in their research studies. For instance, [7] has applied RSM to predict starch gelatinization in wheat, bread and potato while using initial moisture content and baking temperature to predict starch gelatinization and crumb softness of the bread. In another study, [8] used RSM to study combined effects of different components on biomass growth. [9] has optimized the effect of two independent variables (soaking temperature and steaming time) on quality properties of parboiled rice by RSM. RSM has also been used in optimization studies involving parboiling. For illustration, [10] used RSM for optimization of parboiling conditions (soaking temperature, steaming time, and drying time) for HRY maximization. In addition, RSM has been successfully applied in optimization of two-step hydrolysis of sweet potato starch [11].

The scope of this study covers the mathematical modeling of degree of starch gelatinization (DSG) and rice quality properties during parboiling, by considering three independent variables (soaking temperature, soaking time, and steaming time). To the best of our knowledge, no optimization study has focused on predicting the combined effect of soaking temperature, soaking time, and steaming time on DSG and quality parameters of parboiled rice. Therefore, this study was conducted to fill this research gap. We aim to investigate the prediction of DSG and parboiled rice quality indicators (HRY, hardness, lightness, and color) by mathematical

modeling by considering three independent variables (soaking temperature, soaking time, and steaming time).

MATERIALS AND METHODS

Sample preparation and parboiling of paddy. The japonica rice Huaidao 5 (H_5) variety with intermediate amylose content 16.85% was selected for experimentation. The H_5 was harvested in the year 2014 at experimental site of Nanjing Agricultural University, China. After harvesting, paddy was dried at safe moisture content (13±1) and stored for two months at 4˚C for parboiling experimentation [12].

The paddy was processed using parboiling technique to improve rice quality. The soaking and steaming conditions were followed according to design expert 8.0.6 (Stat-Ease, Inc. USA) as shown in Table 1 and values were rounded off to nearest digit. The hydrated rice was obtained by hot soaking (97˚C) in deionized water using electronically controlled water bath (DK-600A, China). Moreover, extra water was drained out after soaking and samples were tempered for 1 hour. The rice samples were steamed in auto clave at 1 kg/cm^2 pressure (121˚C) as proposed by design expert up to five levels [13], presented in Table 2. Each sample was tempered for 30 min after steaming and moisture content of samples was found in the range of 22.61-34.31% (w.b). The two-stage drying method was applied for fast removal of moisture content. Two temperatures 60 and 40˚C were used during first and second stage drying respectively with three hours tempering time between two stages [14]. The initial moisture content was measured at 120˚C for 16 hours. After drying, samples were packed in polyethylene bags and coded according to the treatment applied and stored for further processing.

Determination of degree of starch gelatinization (DSG). The DSG was calculated by using following Eq. 1

$$DSG = \left[1 - \frac{\Delta H}{\Delta H*}\right] \times 100 \quad (1)$$

Where, ΔH and $\Delta H*$ are enthalpy changes due to gelatinization of parboiled and raw rice respectively. The instrument simultaneously thermal analyzer (STA 449 F3 Jupiter, Germany) was used to measure the enthalpies. The 10 g of each sample was ground in fine powder and sieved (160 microns). The instrument was first calibrated using indium as reference material and then 3 mg sample was selected from each treatment for DSG measurement. The samples were then heated from 30˚C to 120˚C with the rate 10˚C/min. The procedure was repeated for all samples.

Determination of HRY. Approximately after four days of drying, paddy was de-husked using laboratory stake rubber roller rice husker (THU35C, China). The HRY was calculated as a percentage of whole grains; the average of triplicate was considered [15, 16].

Determination of hardness. TMS-Pro hardness tester was used to calculate the hardness, three-point breakage mechanism was considered in terms of bending force. The load cell consisted of 500 N was applied with accuracy level of 5% to measure force using lab texture pro-computer program. Furthermore, the flat loading head of 1.0 mm thickness with deformation rate of 0.5 mm/s was used to apply force on horizontally placed rice kernel. The total fifty randomly selected healthy grains were incorporated and average value was considered final hardness [2, 17].

Lightness and Color measurement. In order to measure the color and lightness, precision color reader model HP-200 was used. Prior to measurement, the instrument was calibrated with white and black plates provided by the manufacturer. The results were expressed in term of L^*, a^*, b^* values, L^* represents brightness from black to white, positive and negative "a^*" values represents redness/greenness and "b^*" value represents yellowness/ blueness respectively. The total ten measurements were done on each sample by shaking sample gently to avoid measurement error, and to gain more realistic results the average values were encountered for further analysis. The color value (B) of parboiled rice determined by using following Eq. 2 [20-22].

$$B = \sqrt{a^{*2} + b^{*2}} \quad (2)$$

Experimental design. The Central composite design (CCD) was utilized for model fitting to determine the polynomial equation, by using response surface methodology (RSM). The experimental data was executed using statistical software Design Expert 8.0.6 (Stat-Ease, Inc. USA). The coded and actual values of independent variables up to five levels are presented in Table 1. The fourteen experiments were investigated with combination of six replicates to estimate pure error as shown in Table 2. A CCD with three factors at five levels was investigated [23, 24]. The Investigated factors which were considered to have a maximum effect on DSG, HRY and other quality properties in literature were soaking temperature, soaking time and steaming time [9]. In current study, with three (Soaking temperature, soaking time and steaming time) independent variables and total number A total of 20 experiments were performed, and following relationship 2^k+2k+6 were used for calculation, where k is total number of factors.

In optimization, the responses can be related to the factors by linear or quadratic models. A quadratic model include linear model shown in Eq. 3 [24].

$$y = \beta o + \sum_{i=1}^{k} \beta_i X_i + \sum_{i=1}^{k} \beta_{ii} X_i^2 + \sum_{i=1}^{k} \sum_{i=1}^{k} \beta_{ij} X_i X_j + e \quad (3)$$

Where Y is dependent variable, X_i and X_j are independent variables; k is number of independent variables, β_o is intercept of the model. The coded values were calculated by following Eq. 4.

$$X_i = (X_i - X_o)/\delta X \quad (4)$$

The run number and experimental conditions arranged by central composite design with coded and actual values are shown in Table 2. The design expert program was used to process the data by using Eq. 2 as well as Analysis of variance (ANOVA), to find the interactions between independent variables and responses. The fitness of polynomial model was expressed by the coefficient of determination R^2, and its significance was also checked by F-test.

RESULTS AND DISCUSSION

CCD and model development. The parboiling consists of soaking, steaming and drying of rough rice. Generally, parboiling increases HRY, nutritional value and protects grain from insects due to starch blindness. The actual and predicted values are shown in Table 3.

TABLE 1
Experimental ranges and levels in actual and coded form

Variable	Symbol	Coded variable levels				
		-α	Low	Medium	High	α
		-1.68	-1	0	1	1.68
Soaking temperature (˚C)	X_1	31.48	40	52.50	65	73.52
Soaking time (min)	X_2	54.55	75	24.79	135	155.45
Steaming time (min)	X_3	6.59	10	15.00	20	23.41

TABLE 2
Design of CCD for independent variables

Std. order	Run	Coded variables			Actual variables		
		X_1	X_2	X_3	X_1	X_2	X_3
1	20	-1	-1	-1	40	75	10
2	1	1	-1	-1	65	75	10
3	19	-1	1	-1	40	135	10
4	9	1	1	-1	65	135	10
5	10	-1	-1	1	40	75	20
6	16	1	-1	1	65	75	20
7	18	-1	1	1	40	135	20
8	17	1	1	1	65	135	20
9	13	-1.68	0	0	31.48	105	15
10	11	1.68	0	0	73.52	105	15
11	14	0	-1.68	0	52.5	54.55	15
12	2	0	1.68	0	52.5	155.45	15
13	6	0	0	-1.68	52.5	105	6.59
14	7	0	0	1.68	52.5	105	23.41
15	12	0	0	0	52.5	105	15
16	5	0	0	0	52.5	105	15
17	3	0	0	0	52.5	105	15
18	15	0	0	0	52.5	105	15
19	4	0	0	0	52.5	105	15
20	8	0	0	0	52.5	105	15

* X_1= Soaking temperature, X_2= Soaking time, X_3= Steaming time

TABLE 3
Observed and predicted values for DSG, HRY, hardness, lightness and color of parboiled rice

Std. order	Run	DSG (%)		HRY (%)		Hardness (N)		Lightness		Color (b-value)	
		Observed	Predicted	Observed	Predicted	Observed	Predicted	Observed	Predicted	Observed	Predicted
1	20	76.79	77.82	67.97	67.36	27.79	28.47	84.90	83.91	13.59	13.67
2	1	80.03	79.65	69.99	70.03	31.03	30.66	81.57	81.66	14.04	13.94
3	19	81.69	81.03	68.17	68.24	31.69	31.24	81.58	80.95	13.81	13.38
4	9	82.33	81.77	74.31	73.50	32.33	31.84	82.13	81.39	13.33	13.35
5	10	83.25	84.08	67.46	68.05	33.25	34.05	77.01	76.49	15.72	15.73
6	16	85.18	86.11	68.40	68.10	35.18	35.93	77.88	77.24	15.61	16.07
7	18	84.88	85.53	68.23	67.96	34.88	35.56	78.74	77.39	15.81	15.94
8	17	87.23	86.47	70.21	70.59	36.23	35.85	81.11	80.83	16.02	15.97
9	13	83.47	82.50	67.52	67.54	33.47	32.60	78.51	79.48	15.09	15.23
10	11	84.25	84.83	71.70	72.00	34.25	34.69	80.65	80.48	15.67	15.49
11	14	83.59	82.28	69.70	69.76	33.59	32.63	79.95	79.72	15.35	15.09
12	2	84.35	85.28	72.34	72.60	34.35	34.88	79.93	80.25	14.55	14.76
13	6	76.25	76.72	66.82	67.49	27.25	27.77	82.67	83.34	11.82	12.09
14	7	86.79	85.94	65.97	65.62	36.79	35.84	75.65	76.63	16.35	16.03
15	12	84.48	84.85	69.50	68.20	34.48	35.02	79.31	79.98	15.24	15.22
16	5	86.08	84.85	67.97	68.20	36.08	35.02	80.17	79.98	15.37	15.22
17	3	85.13	84.85	67.09	68.20	35.13	35.02	80.09	79.98	14.73	15.22
18	15	84.63	84.85	68.96	68.20	34.63	35.02	79.27	79.98	15.24	15.22
19	4	83.88	84.85	68.11	68.20	34.88	35.02	79.77	79.98	15.68	15.22
20	8	84.86	84.85	67.63	68.20	34.86	35.02	78.78	79.98	15.03	15.22

*DSG= Degree of starch gelatinization, HRY= Head rice yield

TABLE 4
Regression equations for response variables

Response	Equation
DSG (%)	$84.85 + 0.69X_1 + 0.89X_2 + 2.74X_3 - 0.27X_1X_2 + 0.05X_2X_3 - 0.44X_2X_3 - 0.42X_1^2 - 0.38X_2^2 - 1.25X_3^2$
HRY (%)	$68.20 + 1.33X_1 + 0.84X_2 - 0.55X_3 + 0.65X_1X_2 - 0.65X_1X_3 - 0.24X_3 + 0.56X_1^2 + 1.05X_2^2 - 0.58X_3^2$
Hardness (N)	$35.02 + 0.62X_1 + 0.67X_2 + 2.40X_3 - 0.40X_1X_2 - 0.07X_1X_3 - 0.31X_2X_3 - 0.49X_1^2 - 0.45X_2^2 - 1.14X_3^2$
Lightness	$79.53 + 0.30X_1 + 0.16X_2 - 2.00X_3 + 0.67X_1X_2 + 0.75X_1X_3 + 0.97X_2X_3 + 0.23X_1^2 + 0.36X_2^2 + 0.08X_3^2$
Color (b-value)	$15.22 + 0.07X_1 - 0.09X_2 + 1.17X_3 - 0.07X_1X_2 + 0.01X_2X_3 + 0.12X_2X_3 + 0.05X_1^2 - 0.10X_2^2 - 0.41X_3^2$

*DSG= Degree of starch gelatinization, HRY, Head rice yield, X_1= Soaking temperature, X_2= Soaking time, X_3= Steaming time

TABLE 5
Effect of independent variables on response variables

Coefficient	DSG (%)	HRY (%)	Hardness (N)	Lightness	Color (b-value)
β_o	84.85	68.20	35.02	79.53	15.22
X_1	0.69*	1.33*	0.62*	0.30^{NS}	0.08^{NS}
X_2	0.89*	0.84*	0.67*	0.16^{NS}	-0.10^{NS}
X_3	2.74*	-0.55*	2.40*	-2.00*	1.17*
X_{12}	-0.27	0.65*	-0.40*	0.67	-0.08
X_{13}	0.05	-0.65*	-0.07	0.75*	0.02
X_{23}	-0.44	-0.24	-0.31	0.97*	0.12
X_1^2	-0.42	0.56*	-0.49	0.23*	0.05
X_2^2	-0.38	1.05*	-0.45*	0.36	-0.10
X_3^2	-1.25*	-0.58*	-1.14*	0.08	-0.41*
R^2	0.92	0.91	0.94	0.91	0.94
Adjusted R^2	0.85	0.84	0.88	0.83	0.89
Lack of fit	0.1	0.11	0.08	0.08	0.33

*All values (*) are significant at confidence of interval 5%, NS; Non-significant coefficients

Table 5 represented the effect of soaking temperature, soaking time and steaming time on response variables with correlation coefficient R^2, adjusted R^2 and co-efficient of equation. The quadratic model properly studied the responses and R^2 values are in acceptable fitting. However, soaking temperature strongly affected DSG, HRY and Hardness but lightness and color were found non-significant. In case of soaking time, it affects DSG, HRY and hardness, and found significant ($P<0.05$), other

coefficients were not affected by soaking time. Furthermore, steaming time had strongly affected all variables but HRY and lightness were affected negatively. The goodness of fit was also evaluated by coefficient of determination R^2, for a good fitted regression model R^2 value should be more than 80%, for all these responses R^2 values were found more than 80% as presented in Table 5 [10]. Moreover, lack of fit test was also found non-significant which indicated the validation of treatment applied [25, 26]. Table 4 showed the regression equations of DSG, HRY, hardness, lightness and color respectively.

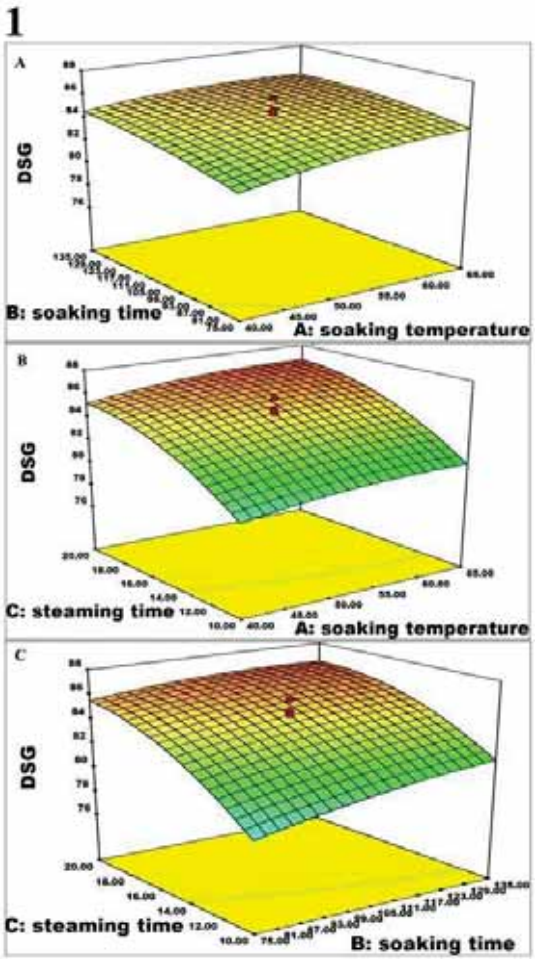

FIGURE 1
Effect of soaking temperature, soaking time and steaming time on DSG

Effect of hydrothermal treatment on degree of Starch Gelatinization. The gelatinization of starch plays an important role in rice quality. Table 3 showed that DSG varies from 76.25 to 87.23% which is relatively similar to the findings reported by other researchers [27, 28]. The soaking temperature, soaking time and steaming time significantly affected DSG as shown in Figure 1. The Figure 1A showed interactional relationship between soaking temperature and time, with the increase of these two variables DSG also increased. As shown in Figure 1 (A, B) the steaming time significantly affected DSG as compared to soaking temperature and time, the sharp curve indicated that DSG increased with increasing soaking temperature (31.48-73.52) ˚C, soaking time (54.55-155.45) min and steaming time (6.59-23.41) min. Similar observations were reported by [9, 29, 30]. The rice grains absorbed enough water and it increased with the increase of soaking temperature and time, which leads transformation of starch granules and gelatinization. DSG increased with steaming time and same results were observed in current study [18, 31].

HRY. The maximum HRY 74.31% was obtained at run nine, when rice were soaked at 65˚C for 135 min and steamed at 10 min at 121˚C; predicted HRY was found 73.50% on the same condition. The maximum HRY at 65˚C soaking time for 6 min steaming was similar with findings of [9]. Moreover, the analysis of variance for quadratic model was found significant (prob>F 0.0002 less than F-value 12.66) and goodness of fit was also evaluated by coefficient of determination R^2 as shown in Table 5. However, the current model was appropriate to navigate the design space.

The minimum HRY was observed at run seven (65.97%), when paddy was soaked at 52.50˚C for 105 min and steamed for 23.41 min at 1 kg/cm^2 pressure. The appropriate condition of parboiling increased HRY, which facilitates milling process of parboiled rice [20]. The Figure 2 showed relationship between three independent variables and HRY. The HRY greatly influenced by all three variables but steaming time has more effective on it. Figure 2A depicted that with increase of soaking temperature and time, HRY initially increased then slightly decreased and then increased again for longer duration soaking at higher temperature. The relationship between soaking temperature and steaming time was showed abrupt change in HRY as shown in Figure 2B, when soaked paddy was steamed, initially HRY increased with steaming duration but for longer steaming time HRY decreased. The decreasing trend of HRY for longer duration of steaming showed that starch granular fully gelatinize because of higher soaking temperature for longer duration of steaming. The physical appearance showed that for longer duration of steaming, grain shape was changed and highly deformed. The Figure 2C clearly showed same decreasing trend of HRY for longer soaking and steaming durations. In addition, for longer steaming time rice grain absorbed excessive water, husk was also observed splitting [27]. Additionally, parboiling process specially steaming time effect gelatinization of starch, if degree of gelatinization is high then deformed grain would be obtained during parboiling and deformed grains would lose along with exuded part of endosperm. The experimental results for HRY was found agreed with [32], maximum HRY (73.88%) was obtained at lower steaming time.

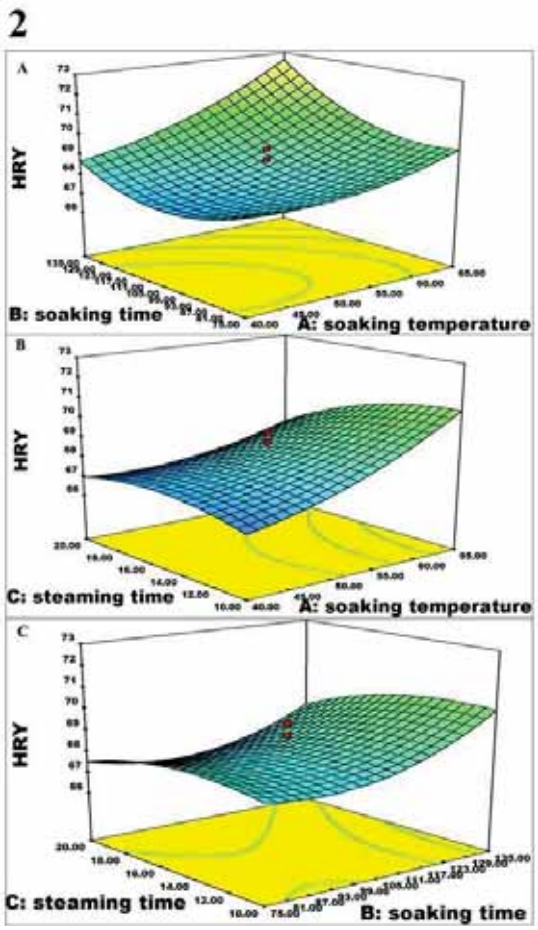

FIGURE 2
HRY affected by hydrothermal treatment

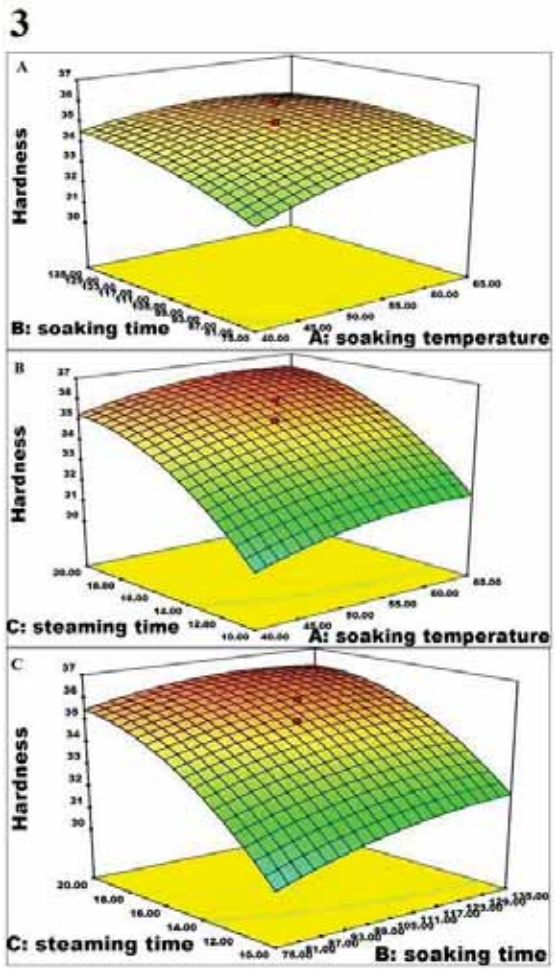

FIGURE 3
Interactional effect of three variables on hardness of rice kernel

Hardness. The hardness is important parameter in rice quality measurement, during parboiling process because of high temperature application rice turns harder as compared to unprocessed grains [33]. The R^2 and adjusted R^2 were 94% and 88% respectively, which suggested that quadratic model suitably described relationship between selected factors. Figure 3 explained the effect of three independent variables on grain hardness during parboiling. Furthermore, Figure 3 (A, B and C) showed that with the increases of soaking temperature and time, it increased slightly, moisture absorbed by rice grains during steaming cause melting of starch and decrease in ΔH at longer steaming duration [19, 34], steaming time play vital role to harden the rice grains. Similarly, soaking temperature and steaming time in combination were shown in Figure 3, it can be seen clearly steaming time influenced hardness up to great extent. Furthermore, similar results were found in soaking and steaming duration combination. The maximum hardness (36.79 N) was observed at run seven where steaming duration was maximum 23.41 min and lowest hardness (27.25 N) was seen at 6.59 min steaming duration. The results revealed that the hardness increased with severity of parboiling process [35].

Lightness. The lightness ranges from 75.65 to 84.90, lightness values were relatively similar to those reported by [29]. The R^2 and adjusted R^2 were observed 91% and 83% respectively. The darkest rice was observed when rice treated at 52.50˚C, 105 min and 23.41 min soaking temperature, soaking time and steaming time respectively. Figure 4 represents response surface curves for lightness. The quadratic effects of independent variables were revealed that lightness decreased with severity of parboiling process. Figure 4A showed that with the increase of soaking temperature and time, lightness decreased continuously. Similarly, lightness is highly inclined by the steaming time [4, 36, 37]. The steep curve in Figure 4B exhibited the effect of steaming time on lightness of rice. The same results were observed in combination of soaking and steaming time (Figure 4C). Consequently, based on the observations of Figure 4 it can be concluded that rice should not be treated under severe hydrothermal treatment. Higher temperature application could affect lightness of rice that leads to poor quality of rice and less demand in market [38].

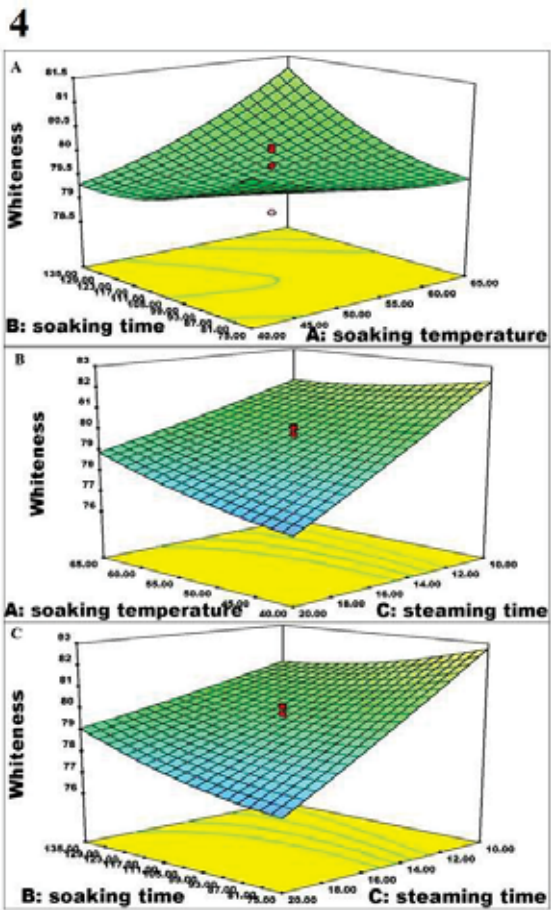

FIGURE 4
Effect of soaking temperature, soaking time and steaming time on lightness

Color. The color of rice is very important indicator to measure quality of processed rice. Figure 5 (A, B and C) signified that color value highly affected by soaking temperature, soaking time and steaming duration. The color was varied from 11.82 to 16.35, that is quite close to the findings of [9, 29], darkest color was observed at run seven when soaking temperature, soaking time and steaming time were 52.50˚C, 105 min and 23.41 min respectively. The discoloration of rice caused by reaction of released sugar with amino acid of grain treated under high temperature. Furthermore, rice bran pigments penetrated into endosperm during parboiling leads to dark color [30, 39]. The sharp curves in Figure 5 (B and C) showed that steaming time highly affected color during hydrothermal treatment of rice. Therefore, in rice parboiling process, it is necessary to cook rice at lower temperature for better quality.

Optimization. The optimal condition for paroling process was estimated as soaking temperature= 65˚C, soaking time= 135 min and steaming duration= 10.66 min. The predicted responses given by design expert under above condition were DSG= 82.23%, HRY= 73.44%, hardness= 32.38 N, lightness= 81.54 and color value= 13.62. The optimal values of independent variables for responses were calculated by solving regression equations using design expert presented in Table 4. Furthermore, above predicted optimal condition was applied on three independent replicates to validate the predicted model. The finding and results of current study showed that RSM can be used to optimize the DSG, HRY, hardness, lightness and color in parboiling process by using soaking temperature, soaking time and steaming time as independent variables.

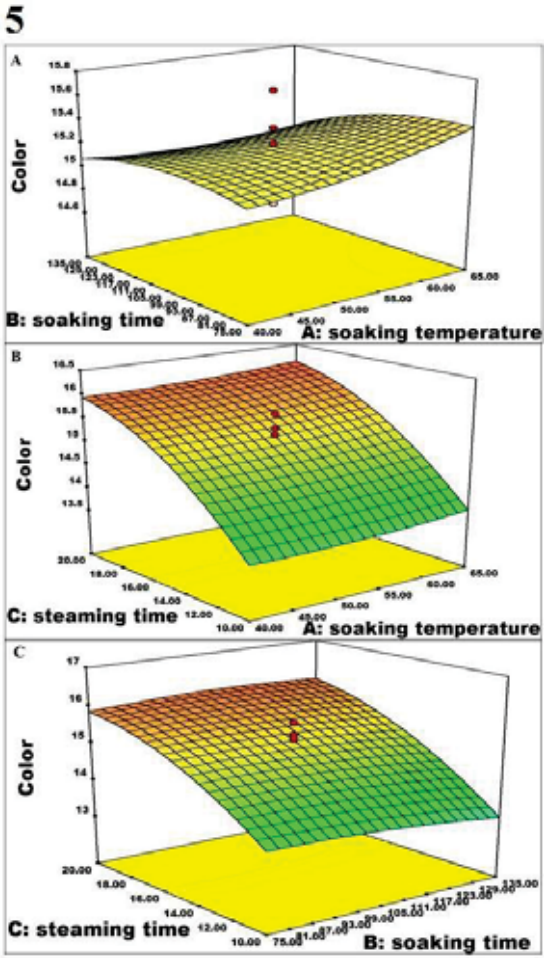

FIGURE 5
Effect of soaking temperature, soaking time and steaming time on color

CONCLUSION

The RSM was used to jointly optimize the set of responses. The DSG, HRY, hardness, lightness and color of parboiled rice were tried to predict by taken three independent variables (soaking time, soaking time and steaming time). Results showed that responses are in acceptable limit in parboiled rice quality measurement. Based on RSM data analysis, the predicted optimum soaking temperature, soaking time and steaming time were 65˚C, 135 and 10.66 min respectively and predicted DSG, HRY, hardness, lightness and color under this condition were 82.23%, 73.44%, 32.38 N, 81.54, and 13.62

respectively with composite desirability equal to 0.897. Findings of this study can be useful for industry to get desired quality of parboiled rice. This research is particularly helpful for peoples working worldwide on commercialization of parboiled rice. We intend to validate following technique in our further research.

ACKNOWLEDGEMENTS

All experimentation and study was conducted with the help and funding under the project Jiangsu Agricultural Science and Technology Innovation Fund CX-(17)1003. The first author is thankful to College of Engineering, Nanjing Agriculture University, China for providing all kinds of possible facilities during research in China.

REFERENCES

[1] Swasdisevi, T., Sriariyakula, W., Tia, W. and Soponronnarit, S. (2010) Effect of Pre-Steaming on Production of Partially-Parboiled Rice Using Hot-Air Fluidization Technique. Journal of Food Engineering. 96(3), 455-462.

[2] Buggenhout, J., Brijs, K. and Delcour, J.A. (2014) Soaking Conditions During Brown Rice Parboiling Impact the Level of Breakage-Susceptible Rice Kernels. Cereal Chemistry. 91(6), 554-559.

[3] Bauer, B.A. and Knorr, D. (2004) Electrical Conductivity: A New Tool for the Determination of High Hydrostatic Pressure-Induced Starch Gelatinisation. Innovative Food Science and Emerging Technologies. 5(4), 437-442.

[4] Elbert, G., Tolaba, M.P. and Suarez, C. (2001) Effects of Drying Conditions on Head Rice Yield and Browing Index of Parboiled Rice. Journal of Food Engineering. 47(1), 37-41.

[5] Bello, M.O., Loubes, M.A., Aguerre, R.J. and Tolaba, M.P. (2015) Hydrothermal Treatment of Rough Rice: Effect of Processing Conditions on Product Attributes. Journal of Food Science and Technology. 52(8), 5156-5163.

[6] Ghosh, D. and Hallenbeck, P.C. (2010) Response Surface Methodology for Process Parameter Optimization of Hydrogen Yield by the Metabolically Engineered Strain Escherichia Coli Djt135. Bioresource Technology. 101(6), 1820-1825.

[7] Chhanwal, N. and Chinnaswamy, A. (2014) Temperature and Moisture Based Modeling for Prediction of Starch Gelatinization and Crumb Softness During Bread - Baking Process. Journal of Texture Studies. 45(6), 462–476.

[8] Sharma, S., Malik, A. and Satya, S. (2009) Application of Response Surface Methodology (Rsm) for Optimization of Nutrient Supplementation for Cr (Vi) Removal by Aspergillus Lentulus Aml05. Journal of Hazardous Materials. 164(2-3), 1198-1204.

[9] Taghinezhad, E. and Brenner, T. (2017) Mathematical Modeling of Starch Gelatinization and Some Quality Properties of Parboiled Rice Based on Parboiling Indicators Using Rsm. Journal of Food Process Engineering. 40(3), e12483.

[10] Danbaba, N., Nkama, I., Badau, M.H., Ukwungwu, M.N., Maji, A.T., Abo, M.E., Hauwawu, H., Fati, K.I. and Oko, A.O. (2014) Optimization of Rice Parboiling Process for Optimum Head Rice Yield: A Response Surface Methodology (Rsm) Approach. International Journal of Agriculture and Forestry. 4(3), 154-165.

[11] Betiku, E. and Adesina, O.A. (2013) Optimization of Sweet Potato Starch Hydrolyzate Production and Its Potential Utilization as Substrate for Citric Acid Production. British Biotechnology Journal. 3(2), 169-182.

[12] Bello, M.O., Aguerre, R.J., Tolaba, M.P. and Suárez, C. (2012) Effect of Hydrothermal Conditions on Translucence of Milled Rice. José Luis Caivano and María del Pilar Buera CRC Press.

[13] Cherati, F.E., Kamyab, S., Shekofteh, M. and Derikvan, R. (2012) Analysis and Study of Parboiling Method and the Following Impact on Waste Reduction and Operation Increase of Rice in Paddy Conversion Phase. Research Journal of Applied Sciences, Engineering and Technology. 4(16), 2649-2652.

[14] Thakur, A.K. and Gupta, A.K. (2006) Two Stage Drying of High Moisture Paddy with Intervening Rest Period. Energy Conversion and Management. 47(18-19), 3069-3083.

[15] Bello, M., Baeza, R. and Tolaba, M.P. (2006) Quality Characteristics of Milled and Cooked Rice Affected by Hydrothermal Treatment. Journal of Food Engineering. 72(2), 124-133.

[16] Latifi, A. and Alizadeh, M.R. (2014) Effect of Parboiling on Qualities and Milling of Iranian Rice. Journal of Agricultural and Engineering Research. 15(1), 77-88.

[17] Buggenhout, J., Brijs, K., Van, O.J., and Delcour, J.A. (2014) Milling Breakage Susceptibility and Mechanical Properties of Parboiled Brown Rice Kernels. LWT - Food Science and Technology. 59(1), 369-375.

[18] Juliano, B.O. (1982) An International Survey of Methods Used for Evaluation of Cooking and Eating Qualities of Milled Rice. International Rice Research Institute, Los Bafios, Laguna, Philippines.

[19] Singh, N., Kaur, L., Singh, S.N., and Singh, S. K. (2005) Physicochemical, Cooking and Textural Properties of Milled Rice from Different Indian Rice Cultivars. Food Chemistry. 89(2), 253-259.
[20] Islam, M.R., Shimizu, N. and Kimura, T. (2004) Energy Requirement in Parboiled and Its Relationship to Some Important Quality Indicators. Journal of Food Engineering. 63(4), 433-439.
[21] Lamberts, L., Bie, Els. De., Vandeputte, G.E., Veraverbeke, W.S., Derycke, V., Man, W. De., and Declour, J.A. (2007) Effect of Milling on Colour and Nutritional Properties of Rice. Food Chemistry. 100(4), 1496-1503.
[22] Sareepuang, K., Siriamornpun, S., Wiset, L., and Meeso, N. (2008) Effect of Soaking Temperature on Physical, Chemical and Cooking Properties of Parboiled Fragrant Rice. World Journal of Agricultural Sciences. 4(4), 409-415.
[23] Khuri A.I., Cornell, J.A. (1996) Response Surfaces: Designs and Analyses. Vol. 2nd ed. New York: Marcel Dekker.
[24] Khuri, A.I. and Cornel, L.J.A. (1987) Response Surfaces. New York: Marcel Dekker.
[25] Vázquez, M., Delgado, R. and Castro, A.J. (2009) Modelling of the Enzymatic Hydrolysis of Potato (Solanum Tuberosum) Using Response Surface Methodology. Starch. 61(10), 601–609.
[26] Aghaie, E., Pazouki, M., Hosseini, M.R., Ranjbar, M. and Ghavipanjeh, F. (2009) Response Surface Methodology (Rsm) Analysis of Organic Acid Production for Kaolin Beneficiation by Aspergillus Niger. Chemical Engineering Journal. 147(2-3), 245-251.
[27] Ayamdoo, J.A., Demuyakor, B., Dogbe, W., Owusu, R. and Ofosu, M.A. (2013) Effact of Varying Parboiling Conditions on Physical Qualities of Jasmine 85 and Nerica 14 Rice Varieties. American Journal of Food Technology. 8(1), 31-42.
[28] Ahromrit, A., Ledward, D.A., and Niranjan, K. (2007) Kinetics of High Pressure Facilitated Starch Gelatinisation in Thai Glutinous Rice. Journal of Food Engineering. 79(3), 834-841.
[29] Islam, M.R., Roy, P., Shimizu, N. and Kimura, T. (2002) Effect of Processing Condition on Physical Properties of Parboiled Rice. Food Science and Technology Research. 8(2), 106-112.
[30] Lamberts, L., De Bie, E., Derycke, V., Veraverbeke, W.S., De Man, W. and Declour, J.A. (2006) Effect of Processing Conditions on Color Change of Brown and Milled Parboiled Rice. Cereal Chemistry. 83(1), 80-85.
[31] Manful, J.T., Grimm, C.C., Gayin, J. and Coker, R.D. (2008) Effect of Variable Parboiling on Crystallinity of Rice Samples. Cereal Chemistry. 85(1), 92-95.
[32] Taghinezhad, E., Khoshtaghaza, M.H., Minaei, S., Suzuki, T. and Brenner, T. (2016) Relationship between Degree of Starch Gelatinization and Quality Attributes of Parboiled Rice During Steaming. Rice Science. 23(6), 339-344.
[33] Islam, M.R., Shimizu, N., and Kimura, T. (2001) Quality Evaluation of Parboiled Rice with Physical Properties. Food Science and Technology Research. 7(1), 57-63.
[34] Saif, S.M.H., Suter, D.A. and Lan, Y. (2004) Effects of Processing Conditions and Environmental Exposure on the Tensile Properties of Parboiled Rice. Biosystems Engineering. 89(3), 321-330.
[35] Nasirahmadi, A., Emadi, B., Abbaspour-Fard, M.H. and Aghagolzade, H. (2014) Influence of Moisture Content, Variety and Parboiling on Milling Quality of Rice Grains. Rice Science. 21(2), 116-122.
[36] Bhattacharya, S. (1996) Kinetics on Colour Changes in Rice Due to Parboiling. Journal of Food Engineering. 29(1), 99-106.
[37] Lv, B., Li, B., Chen, S., Chen, J. and Zhu, B. (2009) Comparison of Color Techniques to Measure the Color of Parboiled Rice. Journal of Cereal Science. 50(2), 262-265.
[38] Parnsakhorn, S. and Noomhorm, A. (2008) Changes in Physicochemical Properties, Agricultural Engineering International: CIGR E-journal, X, 20p.
[39] Miah, M.A.K., Haque, A., Douglass, M.P., and Clarke, B. (2002) Parboiling of Rice. Part Ii: Effect of Hot Soaking Time on the Degree of Starch Gelatinization. International Journal of Food Science and Technology. 37(1), 539-545.

Received: **06.11.2017**
Accepted: **16.02.2019**

CORRESPONDING AUTHOR

Kunjie Chen
College of Engineering,
Nanjing Agricultural University,
Nanjing, Jiangsu 210031 – P.R. China

e-mail: kunjiechen@njau.edu.cn

© by PSP Volume 28 – No. 4/2019 pages 2780-2786 Fresenius Environmental Bulletin

THE ROLE OF TiO_2 NANOPARTICLES IN DISINFECTION OF GRAM (+) BACTERIA UNDER VISIBLE LIGHT

Merve Ozkaleli Akcetin, Ayca Erdem*

Akdeniz University, Faculty of Engineering, Department of Environmental Engineering, Antalya, 07058, Turkey

ABSTRACT

In this study, photocatalytic semiconductor TiO_2 nanoparticles were used to remove gram- positive *Staphylococcus aureus* and *Bacillus subtilis* bacteria which are important drinking water pollutants from aqueous solutions. Within the scope of study, *S. aureus* and *B. subtilis* bacteria were exposed to different concentrations of TiO_2 nanoparticles (10– 1000 mg/L), pH (6.5), different water contents (ionic strengths: 10– 100 mM). The results were depicted as specific die-off rate (k') and survival fractions (N/N_o). TiO_2 nanoparticles provided cell inactivation in absence and presence of light conditions. In addition, photocatalytic activity has been observed even when visible light condition was applied. The compared k' values for both bacterial strains showed that *B. subtilis* bacteria were found to be more resistant to TiO_2 nanoparticles than *S. aureus* bacteria.

KEYWORDS:
Bacillus subtilis, Disinfection, *Staphylococcus aureus*, TiO_2 nanoparticles, Visible light

INTRODUCTION

In recent years, accessing to clean water is one of the most important environmental problems that one of 10 people has to use polluted water instead of clean water [1]. According to a study [2], 9.7% of the European population do not have access to adequate sanitation, and moreover several countries in The United Nations Economic Commission for Europe (UNECE) region still do not have access to safe drinking water and/or improved sanitation. US-EPA (United States Environmental Protection Agency) classifies water pollutants into six categories, namely: plant nutrients, biodegradable waste, heat, sediment, hazardous and toxic chemicals, and radioactive pollutants. Additionally, water pollutants can be classified as organic pollutants, pathogens, industrial pollutants, and heavy metals [3].

The Gram (+) *Staphylococcus aureus* and *Bacillus subtilis* are highly infective pathogens. They cause gastrointestinal and infectious illnesses in humans [4, 5]. In traditional disinfection systems, chlorine, ozone, chlorine dioxide and chloramines have been widely used, however harmful disinfection by-products (DBPs) can be formed. Among the most dangerous DBPs, the trihalomethanes (THMs) have the highest carcinogenic potential [6-11]. In order to overcome the potential serious consequences of those infectious pathogens and conventional disinfectants, nanotechnology and its products (nanomaterials, nanoparticles) for disinfection purposes have been prompted [12-15]. The ideal disinfectant should possess the following properties: (i) broad antimicrobial spectrum within short time; (ii) no generation of harmful by-products; (iii) low toxicity to human health and ecosystems; (iv) low energy cost and easy operation; (v) easy to store and must not be corrosive; and (vi) capable of safe disposal [6]. Therefore, to reduce the formation of DBPs, to inactivate water pathogens and to mineralize the refractory organic compounds, advanced oxidation processes (AOPs) can be applied [16]. Among these AOPs, heterogeneous photocatalysis employing semiconductor nanoparticles (TiO_2, ZnO, Fe_2O_3, etc. NPs) has demonstrated its efficiency in disinfection of pathogenic bacteria. Especially TiO_2 NPs are excellent adsorbents and catalysts due to their large specific surface area and high reactivity [17-19]. Matsunaga et al. [20] reported for the first time that TiO_2 photocatalyst could kill bacterial cells in water by illumination, which could generate reactive oxygen species (ROS) in water medium. Since then, numerous photocatalytic disinfection studies under UV light [21-24] and fewer studies under solar light [25, 26] using TiO_2 photocatalyst studies have been reported. In addition to those studies, TiO_2 NPs [27-29], TiO_2 thin films [30], Ni doped TiO_2 NPs [31], Fe doped Ti-CNTs [32], Ce_2O_3/ TiO_2 composites [33], Ag doped TiO_2 NPs [34], Al_2O_3-TiO_2-Ag composites [35], solar and solar/H_2O_2 process [36], H_2O_2 electrophotocatalytic system [37] were employed to inactivate *S. aureus* and/or *B. subtilis* bacteria.

In this study, the disinfection efficiency of TiO_2 NPs on gram-positive *S. aureus.* and *B. subtilis* was compared, and the objectives of this study were to determine (a) the antibacterial NP concentrations, (b) whether ionic strength of the suspensions affects antibacterial activity, and (c) whether inactivation of bacteria occurs in the absence of light.

MATERIALS AND METHODS

Culture of microorganisms. The Gram (+) *S. aureus* (ATCC 43300) and *B. subtilis* (ATCC 6633) were cultivated in 100 mL of Luria-Bertani (LB) broth at 37°C on a rotary shaker (150 rpm) for 18 h. The cells were harvested by centrifugation at 7,800×g for 10 min, and then resuspended in 10% glycerol and LB Broth mixture. The stock cultures with an initial population of $10^8 \pm 10^2$ CFU mL^{-1} were then kept in -20°C for further reactions. The final optical density at 600 nm of the suspension was determined as 1.30 with a Hach DR/2800 spectrophotometer.

TiO_2 Nanoparticles. TiO_2 NPs (32 nm) used in experiments were purchased from Alfa Aesar. The particle size, zeta potential and surface area of the NPs were analyzed using dynamic light scattering technique in DynaproNanostar (Wyatt Inc), NanoZ90 zetasizer (Malvern Inc) and N_2 gas adsorption BET analyzer (QuadraSorb Station, Quantochrome Ins., FL), respectively. A 1000 mg/L stock suspension for each NP was prepared in 0, 10, 50 and 100 mM of deionized water immediately before the experiments. The final concentrations of 10, 100 and 500 mg L^{-1} NPs were prepared by serially diluting of the stock suspensions having different ionic strength. All experiments were conducted in continuously shaken aqueous slurry solutions to ensure mixing and to prevent settling of the NPs. The bacteria were added to the suspensions immediately prior to the disinfection runs.

Exposure Experiments. An orbital platform shaker holding 100 mL plastic beakers was used to conduct the exposure experiments in a covered biosafety cabinet. Four artificial light sources (color temperature of 4300 K, and total light intensity of 7000 lux), mimicking the spectrum of natural solar light, were placed 30 cm above the orbital shaker to produce light intensity of 2.1 W cm^{-2}. The temperature inside the cabinet was maintained at 25.0 ± 1.5◦C. The shaker was set to mix at 150 rpm throughout all experiments. All antibacterial tests in presence and absence of light lasted 1 h. To determine the effect of particle concentration and ionic strength of the test media on the survival of bacteria, dose-response experiments were conducted. Each beaker contained an initial bacterial concentration of $10^6 \pm 10^2$ CFU mL^{-1}. A stock solution of each NP was freshly prepared in sterile deionized water (as control, 0 mM), 10, 50 and 100 mM using Na_2HPO_4, KH_2PO_4, NH_4Cl, and NaCl prior to the experiments. A 45 mL of NP solution and 5 mL of bacteria prepared in 0, 10, 50 and 100 mM sterile test media were added to each beaker to make initial NP concentrations of 0, 10, 100, and 500 mg L^{-1}.

Dose-Response Test. The numbers of viable cells in cell suspensions were determined by plating serially diluted suspensions onto LB agar plates. The plates were incubated at 37°C for 24 h, and then the numbers of colonies on the plates were counted by using Lassany model digital colony counter. The survival fractions (N/N_0) and the specific die-off rates (k', Eq 1) [36] were calculated by the following equation from triplicated results:

$$k'\ (L\ mg^{-1}) = \frac{-\ln(N/N_0)}{C} \qquad (1)$$

where N_0 (CFU, colony forming unit) is the population of the control cultures, N (CFU) is the population of the NP exposed cultures after 1 h in presence and absence of light, and C (mg L^{-1}) is the NP concentration.

RESULTS AND DISCUSSION

The size and type are important attributes of NPs. The major objective of the present research was to determine the antimicrobial effect of NPs on the survival of bacteria exemplified by *S. aureus and B. subtilis*. The bacteria were exposed toTiO_2 NPs for 1 h at various size classes and concentrations. During the time of exposure, the average temperature was 25.0 ± 1.5◦C and the average pH was 6.5 ± 0.2.

In order to characterize the NPs, particle size, surface area and zeta potential of the NPs were measured. Table 1 shows the NP characterization results and Figure 1 depicts the SEM imaging results and amorphous background with aggregates of NPs.

TABLE 1
Characterization results of the TiO_2 nanoparticles used in the experiments.

Analysis Applied	Results
Primary Particle Size by DLS (nm)	26.4
Primary Surface Area (BET, m^2g^{-1})	176.34
Zeta Potential at pH 6.5 (mV)	-20.3
Particle Size by DLS (nm) (10 mM, pH 6.5)	287±25

Primary particle size shows the measured particle size directly sampled from the box. Nano-TiO_2 primary particle sizes measured by DLS were smaller than the measurement given by the manufacturer. When NPs were used in 10 mM and 50 mM test media, a 10 - 55× increase was observed in average particle size. The surface areas were inversely correlated to the particle sizes as expected. Zeta potential results showed that the NPs were not stable in the test media.

Four different NP concentrations (10, 100, 500 and 1000 mgL^{-1}), and dark and light (light intensity: 2.1 W cm^{-2}) conditions were used to determine the effect of NP concentration and light on the survival of *S. aureus* and *B. subtilis* (Figure 2). Both NP concentration increase and changing the light condition from dark to light increased the mortality rate of the bacteria when 10 mM ionic strength of test media

was used. However, the most effective antibacterial impact was observed when 1000 mg L^{-1} of TiO_2 NPs were used in presence of light. In absence of light, when NP concentration increased, the most increase in mortality rates were observed as 57 % (500 mg L^{1}) in TiO_2 NP setup. The results in Figure 2 confirms that antibacterial effect of TiO_2 NPs can be in absence of light. One possible explanation for higher bacterial sensitivity in absence of light may be linked to the NP-bacteria interaction or NP-specific mechanisms, since membrane damage due to the NP attachment to the cell membrane was shown in other studies [38-40].

The effect of ionic strength and TiO_2 NP concentration on the survival of *S. aureus* and *B. subtilis* are depicted in Figure 3 and Figure 4, respectively. The survival fraction of bacteria (N/N_0) against TiO_2 NPs decreased with increasing the concentration of NPs and the ionic strength in absence of light. However, in presence of light, increase in ionic strength inversely correlated with the survival fractions. *S. aureus* and *B. subtilis* bacteria were not completely killed at any NP concentration during 1 h of exposure. The highest antibacterial effect for *B. subtilis* were 85 % (50 mM) and 75 % (100 mM) at 1000 mgL^{-1} NP concentration, while the highest antibacterial effect for *S. aureus* were observed at same NP concentration were calculated as 83 % (100 mM) and 93 % (10 mM) in absence and presence of light, respectively. Figure 3 and 4 also depict the curve fits obtained from the calculated survival fractions.

Ionic strength condition, and k' values were averaged (k'_{ave}), where lower k'_{ave} value means higher antibacterial effect (Table 2). The lowest k'_{ave} values of *S. aureus* treated with TiO_2 were calculated as 0.003 L mg^{-1} (Control) and 0.004 L mg^{-1} (50mM) under dark and light conditions, respectively. On the other hand, higher k'_{ave} values of *B. subtilis* treated with TiO_2 were calculated as 0.017 L mg^{-1} (10 mM-Dark) and 0.007 L mg^{-1} (50 mM- Light).

In order to control the experimentally verified k'_{ave} values were used in Eq 1, the calculated survival fractions were estimated. R^2 values were presented in order to correspond the curve fits with experimental results. Highest correspondence (R^2) values were obtained from *B. subtilis* data than that of *S. aureus* data.

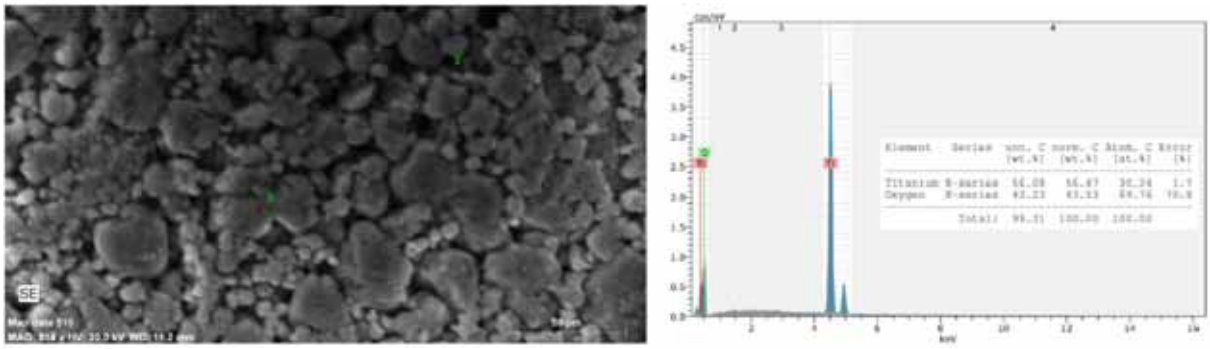

FIGURE 1
SEM image of TiO_2 nanoparticles

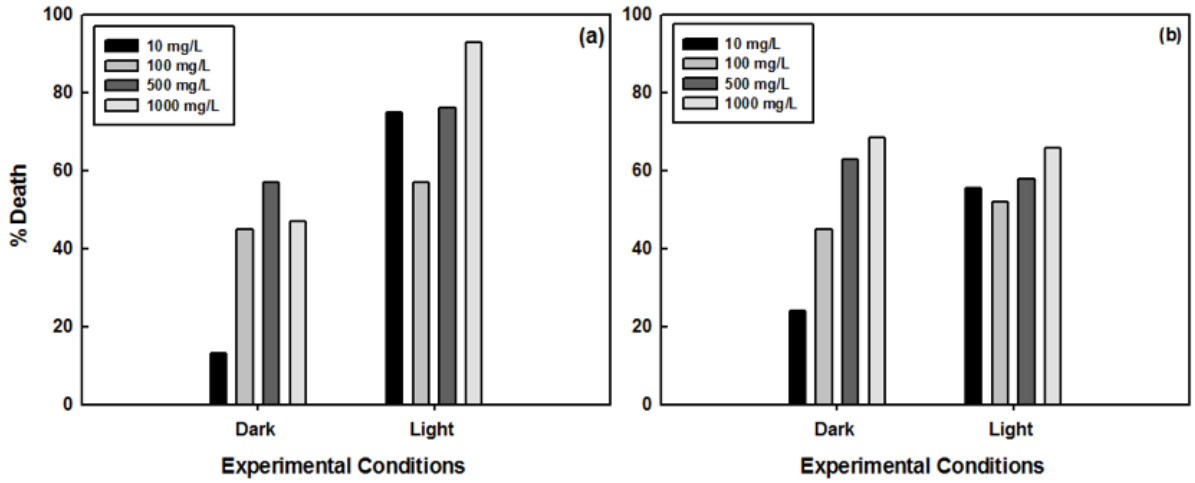

FIGURE 2
The effect of nanoparticle concentration on the survival of *S. aureus* (a) and *B. subtilis* (b) under dark and light conditions.

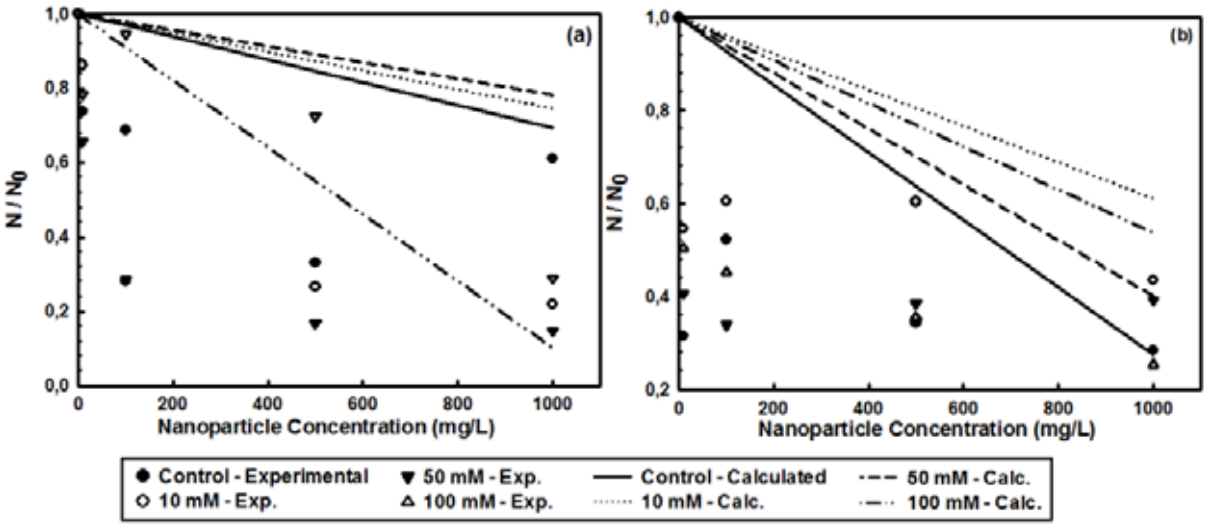

FIGURE 3
The effect of ionic strength and TiO_2 nanoparticle concentration on *S. aureus* under dark (a) and light (b) condition.

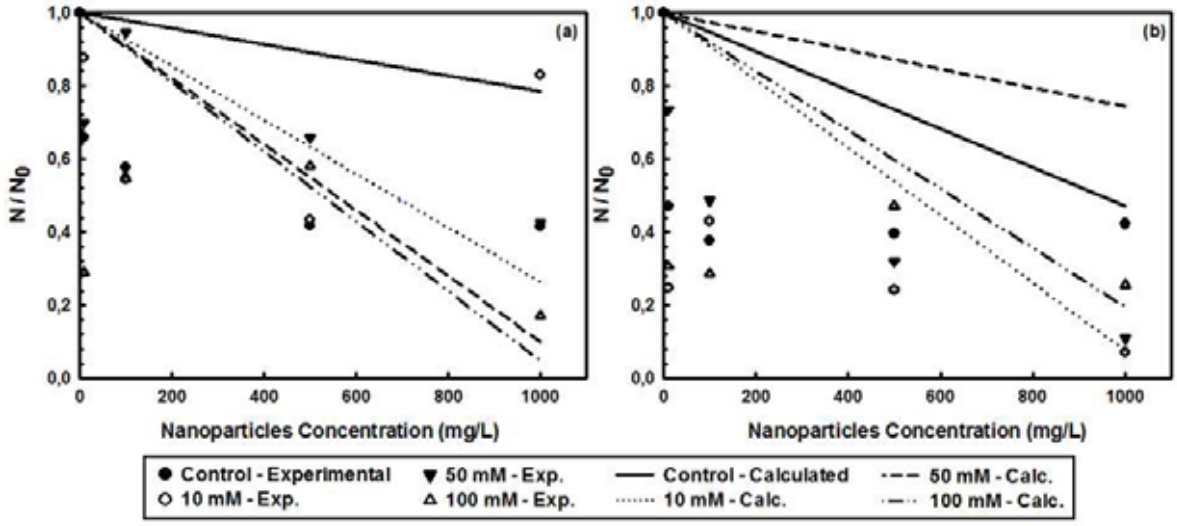

FIGURE 4
The effect of ionic strength and TiO_2 nanoparticle concentration on *B. Subtilis* under dark (a) and light (b) condition.

TABLE 2
Averaged specific die-off rates (k'_{ave}) and R^2 values obtained from bacterial survival fractions.

Bacteria and Condition / Ionic Strength	*S. aureus*				*B. subtilis*			
	Dark		Light		Dark		Light	
	k'_{ave}	R^2	k'_{ave}	R^2	k'_{ave}	R^2	k'_{ave}	R^2
Control	0.003	0.919	0.004	0.859	0.031	0.823	0.009	0.877
10 mM	0.008	0.730	0.005	0.839	0.017	0.876	0.008	0.926
50 mM	0.007	0.759	0.004	0.869	0.026	0.836	0.007	0.928
100 mM	0.006	0.786	0.005	0.823	0.020	0.859	0.027	0.697

CONCLUSIONS

Specific die-off rates of the NPs were calculated and were used in defining a factor promoting the disinfection of the *S. aureus* and *B. subtilis.* It was clearly shown that TiO_2 NPs promoted the inactivation of gram (+) bacteria. Based on the experimental results, *S. aureus* and *B. subtilis* showed higher sensitivity to TiO_2 NPs in both absence and presence of light. Though TiO_2 NPs showed more antibacterial effect on *S. aureus* than that of on *B.*

subtilis. However, the ionic strength of the water lead to an aggregation of NPs which resulted in bigger particles and negation of antibacterial effect. Therefore, dispersion and retention of NPs and the sustainability of antimicrobial activity need to be considered significantly. Since this study was conducted in relatively simple and clean solutions, the sustainability of antimicrobial activities of NPs in natural or waste water, whose constituents may interfere with the NP–bacteria interactions, is still unclear. Therefore, more research to further assess the applicability and sustainability of NPs in disinfection processes and to address the limitations.

ACKNOWLEDGEMENTS

The authors would like to thank Akdeniz University, The Scientific research Projects Coordination Unit for supporting this research within the project FDK-2015-27.

REFERENCES

[1] WHO (World Health Organization) (2012) Global costs and benefits of drinking-water supply and sanitation interventions to reach the MDG target and universal coverage (WHO/HSE/WSH/12.01). Hutton, G. (Ed.) Switzerland.

[2] Kochubovski, M. (2011) Water Safety in Small-Scale Supplies and New Approaches. J Environ Protection and Ecology. 12(4A), 2011-2018.

[3] Ibrahim, R., Hayyan, M., Alsaadi, M.A., Hayyan, A., Ibrahim, S. (2016) Environmental application of nanotechnology: air, soil, and water. Environ. Sci. Pollut. Res. 23(14), 13754-13788.

[4] Lowy, F. (1998) Medical progress: *Staphylococcus aureus* infections. The New England Journal of Medicine. 339(8), 520-532.

[5] Kadariya, J., Smith, T.C., Thapaliya, D. (2014) *Staphylococcus aureus* and Staphylococcal Food-Borne Disease: An Ongoing Challenge in Public Health. BioMed Research International. 2014, Article ID: 827965, 1-10.

[6] Zhang, Y., Wu, B., Xu, H., Liu, H., Wang, M., He, Y., Pan, B. (2016) Nanomaterials-enabled water and wastewater treatment. NanoImpact, 3-4, 22-39.

[7] Nieuwenhuijsen, M., Toledano, M.B., Eaton, N.E., Fawell, J., Elliott, P. (2006) Chlorination disinfection byproducts in water and their association with adverse reproductive outcomes: a review. Occup Environ Med. 57, 73-85.

[8] Krasner, S. (2009) The formation and control of emerging disinfection by-products of health concern. Phil. Trans. R. Soc. A. 367, 4077-4095.

[9] Culea, M., Iordache, A., Cozar, O., Ristoiu, D. (2009) Trihalomethanes Analysis in Drinking Water. J Environ Protection and Ecology. 10(2), 342-350.

[10] Cosma, C., Nicolau, M., Patroescu, V., Stefanescu, M., Ballo, A., Florescu, S. (2009). The Incidence of by-Products (THMs) Disinfection in Drinking Water. J Environ Protection and Ecology. 10(1), 14-22.

[11] Babaei, A.A., Alavi, N., Hassani, G., Yousefian, F., Shirmardi, M., Atari, L. (2015). Occurrence and Related Risk Assessment of Trihalomethanes in Drinking Water, Ahvaz, Iran. Fresen. Environ. Bull. 24, 4807-4815.

[12] Hu, C., Hu, X., Guo, J., Qu, J. (2006) Efficient destruction of pathogenic bacteria with NiO/$SrBi_2O_4$ under visible light irradiation. Environ. Sci. Technol. 40, 5508-5513.

[13] Parnia, F., Hafezeqoran, A., Moslehifard, E., Mahboub, F., Nahaei, M., Dibavar, M.A. (2009) Effect of Different Disinfectants on Staphylococcus aureus and Candida albicans Transferred to Alginate and Polyvinylsiloxane Impression Materials. J of Dental Research, Dental Clinics, Dental Prospects. 3(4), 122-125.

[14] Oliveira, P., Souza, S.G., Campos, G.B., Da Silva, D.C.C., Sousa, D.S., Araújo, S.P.F., Ferreira, L.P., Santos, V.M., Amorim, A.T., Santos, A.M.O.G., Timenetsky, J., Cruz, M.P., Yatsuda, R., Marques, L.M. (2014) Isolation, pathogenicity and disinfection of Staphylococcus aureus carried by insects in two public hospitals of Vitória da Conquista, Bahia, Brazil. Braz J Infect Dis. 18(2), 129-136.

[15] Felekis, T.A., Katsaros, N. (2009) Environment and Nanotechnology: A Promising Challenge. J Environ Protection and Ecology. 10(4), 1146-1154.

[16] Chong, M.N., Jin, B., Chow, C.W.K., Saint, C. (2010) Recent developments in photocatalytic water treatment technology: A review. Water Res. 44, 2997-3027.

[17] Li, Q.L., Mahendra, S., Lyon, D.Y., Brunet, L., Liga, M.V., Li, D., Alvarez, P.J.J. (2008) Antimicrobial nanomaterials for water disinfection and microbial control: Potential applications and implications. Water Res. 42(18), 4591-4602.

[18] Petrov, L., Iliev, V., Eliyas, A., Tomova, D., Puma, G.L. (2007) Photocatalytic properties of modified TiO_2 coatings for purification of waste water and air. J Environ Protection and Ecology. 8(4), 881-909.

[19] Stefchev, P., Ivanova, K., Dikov, H., Trapalis, C. (2006) Photocatalytic Activity of TiO_2 Sol-Gel Films. J Environ Protection and Ecology. 7(4), 896-902.

[20] Matsunaga, T., Tomoda, R., Nakajima, T., Wake, H. (1985) Photoelectrochemical sterilization of microbial-cells by semiconductor powders. Fems Microbiology Letters. 29(1-2), 211-214.

[21] Wei, C., Lin, W.Y., Zainal, Z., Williams, N.E., Zhu, K., Kruzic, A.P., Smith, R.I., Rajeshwar, K. (1994) Bactericidal activity of TiO_2 photocatalyst in aqueous media: toward a solar-assisted water disinfection system. Environ. Sci. Technol. 28, 934-938.

[22] Christensen, P.A., Curtis, T.P., Egerton, T.A., Kosa, S.A.M., Tinlin, J.R. (2003) Photoelectrocatalytic and photocatalytic disinfection of *E-coli* suspensions by titanium dioxide. Appl. Cat. B-Environ. 41(4), 371-386.

[23] Gogniat, G., Thyssen, M., Denis, M., Pulgarin, C., Dukan, S. (2006) The bactericidal effect of TiO_2 photocatalysis involves adsorption onto catalyst and the loss of membrane integrity. Fems Microbiology Letters. 258(1), 18-24.

[24] Bonetta, S., Bonetta, S., Motta, F., Strini, A., Carraro, E. (2013) Photocatalytic bacterial inactivation by TiO_2-coated surfaces. AMB Express. 3(59), 1-8.

[25] Hu, C., Guo, J., Qu, J., Hu, X. (2007) Photocatalytic Degradation of Pathogenic Bacteria with AgI/TiO_2 under Visible Light Irradiation. Langmuir. 23(9), 4982-4987.

[26] Helali, S., Polo-López, M.I., Fernández-Ibánez, P., Ohtani, B., Amanoc, F., Malato, S., Guillard, C. (2014) Solar photocatalysis: A green technology for *E. coli* contaminated water disinfection. Effect of concentration and different types of suspended catalyst. J Photochem Photobiol A: Chem. 276, 31-40.

[27] Barnes, R., Molina, R., Xu, J.B., Dobson, P.J., Thompson, I.P. (2013) Comparison of TiO_2 and ZnO nanoparticles for photocatalytic degradation of methylene blue and the correlated inactivation of gram-positive and gram-negative bacteria. J Nanopart Res. 15(2), 1432, 11p.

[28] Shah, R., Kaewgun, S., Lee, B.I., Tzeng, T.R.J. (2008) The Antibacterial Effects of Biphasic Brookite-Anatase Titanium Dioxide Nanoparticles on Multiple-Drug-Resistant *Staphylococcus aureus*. J Biomed Nanotechnol. 4(3), 339-348.

[29] Xing, Y., Li, X.H., Zhang, L., Xu, Q.L., Che, Z.M., Li, W.L., Bai, Y.M., Li, K. (2012) Effect of TiO_2 nanoparticles on the antibacterial and physical properties of polyethylene-based film. Prog Org Coatings. 73(2-3), 219-224.

[30] Kambala, V., Naidu, R. (2009) Disinfection Studies on TiO_2 Thin Films Prepared by a Sol-Gel Method. J Biomed Nanotechnol. 5(1), 121-129.

[31] Yadav, H., Otari, S.V., Bohara, R.A., Mali, S.S., Pawar, S.H., Delekar, S.D. (2014) Synthesis and visible light photocatalytic antibacterial activity of nickel-doped TiO_2 nanoparticles against Gram-positive and Gram-negative bacteria. J Photochem Photobiol: A Chem. 294, 130-136.

[32] Latif, W., Qazi, I.A., Hashmi, I., Arshad, M., Nasir, H., Habib, A. (2014) Novel Method for Preparation of Pure and Iron-Doped Titania Nanotube Coated Wood Surfaces to Disinfect Airborne Bacterial Species Pseudomonas aeruginosa and *Staphylococcus aureus*. Environ Eng Sci. 31(12), 681-688.

[33] Hassan, M., Amna, T., Al-Deyab, S.S., Kim, H.C., Oh, T.H., Khil, M.S. (2012) Toxicity of Ce_2O_3/TiO_2 composite nanofibers against *S. aureus* and *S. typhimurium*: A novel electrospun material for disinfection of food pathogens. Colloids and Surfaces A. 415, 268-273.

[34] Kowal, K., Wysocka-Krol, K., Kopaczynska, M., Dworniczek, E., Franiczek, R., Wawrzynska, M., Vargova, M., Zahoran, M., Rakovsky, E., Kus, P. (2011) In situ photoexcitation of silver-doped titania nanopowders for activity against bacteria and yeasts. J Colloid Interface Sci. 362(1), 50-57.

[35] Tartanson, M., Soussan, L., Rivallin, M., Chis, C., Penaranda, D., Lapergue, R., Calmels, P., Faur, C. (2014) A new silver based composite material for SPA water disinfection. Water Res. 63, 135-146.

[36] Eleren, S.C., Alkan, U., Teksoy, A. (2014) Inactivation of *E. coli* and *B. subtilis* by Solar and Solar/H_2O_2 Processes in Humic Surface Waters. Fresen. Environ. Bull. 23, 1397-1406.

[37] Rezaee, A., Kashi, G., Jonidi-Jafari, A., Khataee, A., Nili-Ahmadabadi, A. (2011) Effect of Hydrogen Peroxide on Bacillus subtilis Spore Removal in an Electrophotocatalytic System. Fresen. Environ. Bull. 20, 2750-2755.

[38] Erdem, A., Metzler, D., Cha, D., Huang, C.P. (2015) Inhibition of bacteria by photocatalytic nano-TiO_2 particles in the absence of light. Int J Environ Sci Technol. 12(9), 2987-2996.

[39] Dalai, S., Pakrashi, S., Kumar, R.S.S., Chandrasekarana, N., Mukherjee, A. (2012) A comparative cytotoxicity study of TiO_2 nanoparticles under light and dark conditions at low exposure concentrations. Toxicol Res. 1, 116-130.

[40] Adams, L.K., Lyon, D.Y., Alvarez, P.J.J. (2006) Comparative eco-toxicity of nanoscale TiO_2, SiO_2, and ZnO water suspensions. Water Research. 40, 3527-3532.

Received: **04.01.2018**
Accepted: **19.02.2019**

CORRESPONDING AUTHOR

Ayca Erdem
Akdeniz University
Faculty of Engineering
Department of Environmental Engineering
Konyaalti, 07058, Antalya – Turkey

e-mail: ayerdem@akdeniz.edu.tr

© by PSP Volume 28 – No. 4/2019 pages 2787-2794 Fresenius Environmental Bulletin

BIOLOGICAL ACTIVITY OF FOUR TYPES OF CHITOSAN AGAINST SOME PLANT PATHOGENIC FUNGI

Abdurrahman Onaran[1*], Kader Tokatli[2], Aslihan Demirdoven[3], Mustafa Bayram[3], Yusuf Yanar[1]

[1]Department of Plant Protection, Faculty of Agriculture, Gaziosmanpasa University, Tokat, Turkey
[2]Department of Nutrition and Dietetics, Faculty of Health Science, Gaziosmanpasa University, Tokat, Turkey
[3]Department of Food Engineering, Faculty of Engineering and Natural Sciences, Gaziosmanpasa University, Tokat, Turkey

ABSTRACTS

Chitosan is a natural carbohydrate polymer acquired by deacetylation of chitin, the second most common polysaccharide in nature, has strong biological activity. Antifungal activities of four types of chitosan were determined against plant pathogens of *Verticillium dahliae*, *Alternaria solani*, *Monilia fructigena*, *Botrytis cinerea* and *Rhizoctonia solani*. Biological activity studies were carried out using the agar plate method with doses 0.2, 0.3, 0.5, 1 and 2 mg/ml of chitosan. Each chitosan type showed strong antifungal activity against test fungi. Mycelial growth inhibition (MGI) rates, Minimum fungicidal Concentration (MFC) and, LD_{50} and LD_{90} values of chitosan were calculated. 100% MGI ratios were found in doses of 2 mg/ml for each chitosan. Mycelial growth inhibition was observed even at the lowest dose when compared to the control. According to these results, all doses of chitosan applied against the test fungi were obtained promising results. For the first time with this study, antifungal activity of chitosans was examined against *M. fructigena* plant pathogen. The result showed that the biological activity of chitosan has been obtained different result according to molecular weight and test fungi. Because of that chitosan is a natural, non-toxic and inexpensive compound, it can be easily used to control plant pathogens.

KEYWORDS:
Natural compounds, Chitosan, Plant pathogenic fungi, Biological activity, Lethal doses

INTRODUCTION

Natural antifungal materials are used to control plant diseases from past to present day. The research for these materials continues with the advance of technology rapidly. Today, excessive use of fungicides leads to environmental pollution as well as increased fungicide resistance of pathogens. Therefore, alternative methods should be developed against fungicides. In this study, the antifungal property of chitosan, a natural carbohydrate polymers obtained by distillation of chitin, (second most common polysaccharide in nature) has been investigated. Chitosan is an important polymer with antimicrobial activity [1-2] and antioxidant properties [3-4].

Verticillium dahliae Kleb., and *Alternaria solani* (Ellis & G. Martin) L.R. Jones & Grout, which cause intense damage in tomato both in the world and in our country, are two large groups of pathogens. *A. solani* is an early blight agent, which is very common in tomatoes in Turkey [5]. *V. dahliae* is a soil-borne pathogen causing verticillium wilt disease in tomatoes [6]. *Monilia fructigena* Honey is the cause of brown rot disease in areas where apple farming is made [7]. *Rhizoctonia solani* Kuhn is the agent of disease named root rot in root and tuber of the potatoes, causes significant crop losses in the potato [8]. *Botrytis cinerea* Pers., causes grey mold disease in strawberries all around the world [9].

Chitosan is a cheap and non-toxic compound which has reactive amino group [10] can be easily used in agriculture fields [11]. It has been mentioned in many studies that chitosan prevent disease spreading in plants [12] increase the natural immunity of plants [13], and reduce the development of phytopathogenic fungi in fruit and vegetables. They stated that chitosan showed antifungal activity against *Rhizoctonia solani* [14-15], *Verticillium dahliae* [16], *Alternaria solani* [17-18] and *Botrytis cinera* [19-21] disease agents. Furthermore, they observed that the antimicrobial activity of chitosan produced at different molecular weights and structure and that this activity revealed dissimilar effects to the test fungi [1]. However, the biological activity of chitosan depends on the viscosity and the degree of distillation [22].

In our study, the biological activity of four different types (different molecular weight) of chitosan was investigated against five fungi species (*Verticillium dahliae*, *Alternaria solani*, *Monilia fructigena*, *Botrytis cinerea* and *Rhizoctonia solani*) causing disease in plants.

TABLE 1
List of test fungi

Test Fungi	Origin	Isolation place
Verticillium dahliae	Tomato (*Solanum lycopersicum* L.)	Antalya/Turkey
Alternaria solani	Tomato (*Solanum lycopersicum* L.)	Antalya/Turkey
Monillia fructigena	Apple (*Malus domestica* Borkh.)	Gümüşhane/Turkey
Botrytis cinerea	Strawberry (*Fragaria spp.* L.)	Antalya/Turkey
Rhizoctonia solani	Potato (*Solanum tuberosum* L.)	Tokat/Turkey

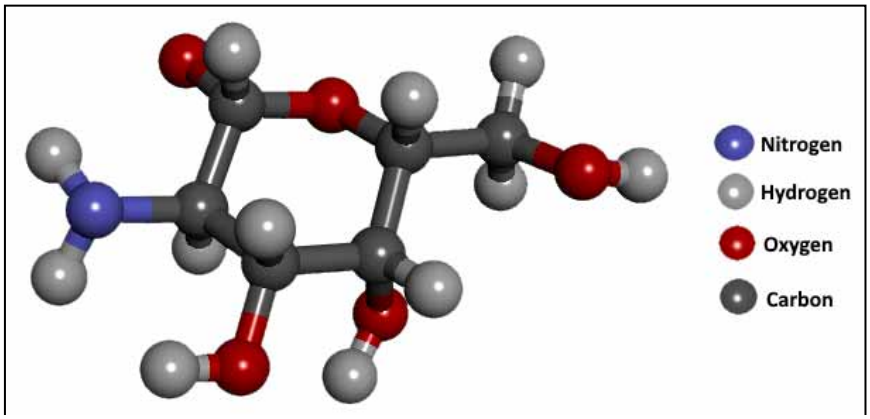

FIGURE 1
Molecular structure of Chitosan

MATERIALS AND METHODS

Fungi culture. Five plant pathogens (Table 1) isolates were obtained as a pure culture from Gazi-osmanpasa University, Plant Protection Department in Tokat. Each pathogen was inoculated on potato dextrose agar (PDA) plates (~20 mL plate^{-1}) and incubated at 25±2ºC. Seven-days-old fungal cultures were used for the experiment.

Chitosan production. Shrimp waste sourced from Marmara Sea (Turkey) was used for chitin and chitosan production. The shrimp waste washed with tap water, dehydrated at room temperature and shred into pieces smaller than 2 mm using a blender (Fakir Harmony 400, People's Republic of China). Optimum extraction conditions were carried out by using the response surface methodology (RSM). The chitin was experimented using 0.73-mol I^{-1} hydrochloric acid for 132.61 min at room temperature for demineralization and 0.95-mol I^{-1}sodium hydroxide for 75.65 min at 60.49°C for deproteinization. The obtained chitin was used to optimize chitosan production and two chitosans were defined as Chitosan-1 and Chitosan-2. Chitosan-1 was obtained by deacetylation with 40% sodium hydroxide at 120°C for 300 minute and Chitosan-2 was carried out by deacetylation with 50% sodium hydroxide at 100°C for 720 minutes. The detailed information about optimization was provided by [23]. Chitosan-1 has deacetylation degree of 78.2%, molecular weight of 182 kDa, viscosity of 120 cPs and Chitosan-2 has deacetylation degree of 84.95%, molecular weight of 127 kDa, viscosity of 40 cPs [23]. Chitosan -3 [Low molecular weight (50-190 kDa); Sigma Aldrich-448869] and Chitosan -4 [Medium molecular weight (190-310 kDa); Sigma Aldrich-448877] were obtained from Sigma-Aldrich.

***In vitro* antifungal activity.** The antifungal activities of the chitosans (Chitosan-1, Chitoan-2, Chitosan-3 and Chitosan-4) were determined by agar plate method [24]. Chitosans were added to PDA at 40 ºC to give the final concentration of 0.2, 0.3, 0.5, 1 and 2 mg/mL for each chitosan (prepared in 1% (v/v) acetic acid) and then the PDA with chitosans were poured (~10 mL/plate^{-1}) each alone in petri plates (60mm in diameter). Seven-day-old agar discs (5mm in diameter) bearing the desired fungi mycelial growth was transferred in the petri plates. These fungi cultures were incubated at 25±2 ºC for 10 days. Fungi mycelial growth were recorded daily [25]. Commercial fungicide [Thiram 80% (w/v)] was used as a positive control. Acetic asid 1% (v/v) was used as a negative control. Each chitosan was adjusted for pH 6.0 by NaOH. Experiment was set up 4 replications and repeated 2 times [15]. The percentage of mycelial growth inhibition was calculated accordingly the formula mentioned by [26].

$$I=100\times(dc-dt)/dc$$

I; Mycelial growth inhibition
dc; Is the mycelial growth in control
dt; Is the mycelial growth in treatment

Statistical Analysis. Data were analyzed statistically using SPSS 16.0 program (SPSS, Chicago, IL). Comparison of means was analyzed by Duncan's multiple range test and differences were considered significant when $P<0.05$. Lethal doses (LD) were determined by Polo Plus program (LeOra software).

RESULTS AND DISCUSSION

One of the most important bioactive properties of chitosan is the antifungal activity. In our study, it was observed that at each doses of chitosan 0.2, 0.3, 0.5, 1 and 2 mg/ml the inhibition of mycelial growth was noticeable when compared to control (Figure 2, 3 and 4). Mycelial growth inhibitions depending on the dose increased. The rations have been realized at different levels according to the test fungi and each chitosan. Which is thought to be due to the different molecular weight (MW) of chitosan. A study has reported that the antimicrobial effect of chitosan MW was decreases against *E. coli* but increases against *Staphylococcus aureus*. At 0.75% concentration against *E. coli* 305 kDA inhibition was 50% while 48.5 kDA was 90%. Against *S. aureus*, these rates were found 100% and 99% respectively. Nevertheless, 100% inhibition was observed at 1% concentration of Chitosan against *E. coli* [1]. According to these results, each chitosan used in our study exhibits antifungal effects at different levels against the test fungi (Figure 2, 3 and 4). Chitosan-4 (C4) which has been shown the highest MW ratio and found to be more effective. However, it was found less effective against *V. dahliae* than other chitosans. The growth of mycelium against *V. dahliae* at a dose of 2 mg/ml of C4 was 8.14 mm whereas 1.41 mm in Chitosan-1 (C1) and it was not observed any growth in chitosan-2 (C2) and chitosan-3 (C3). Similarly, C2 was found to be more effective than C1 against test fungi. Statistically, significant rate of mycelium growth inhibitions was observed for each chitosan dose (Figure 2 and 3). All test fungi showed, *V. dahliae* 59.05 mm, *A. solani* 60 mm, *M. fructigena* 56.95 mm, *B. cinerea* 60 mm and *R. solani* 60 mm mycelium growth in negative control 10 days after inoculation. When compared to the negative control, the average upper and lower bound mycelium growth for each chitosan of *V. dahliae* was found to be from 35.01 to 0.00 mm. These rates were observed respectively for the other test fungi. For *A. solani* from 34.49 to 0.00 mm, for *M. fructigena* from 29.76 to 0.00 mm, for *B. cinerae* from 27.28 to 0.00 mm and for *R. solani* from 34.59 to 0.00 mm (Figure 2 and 3).

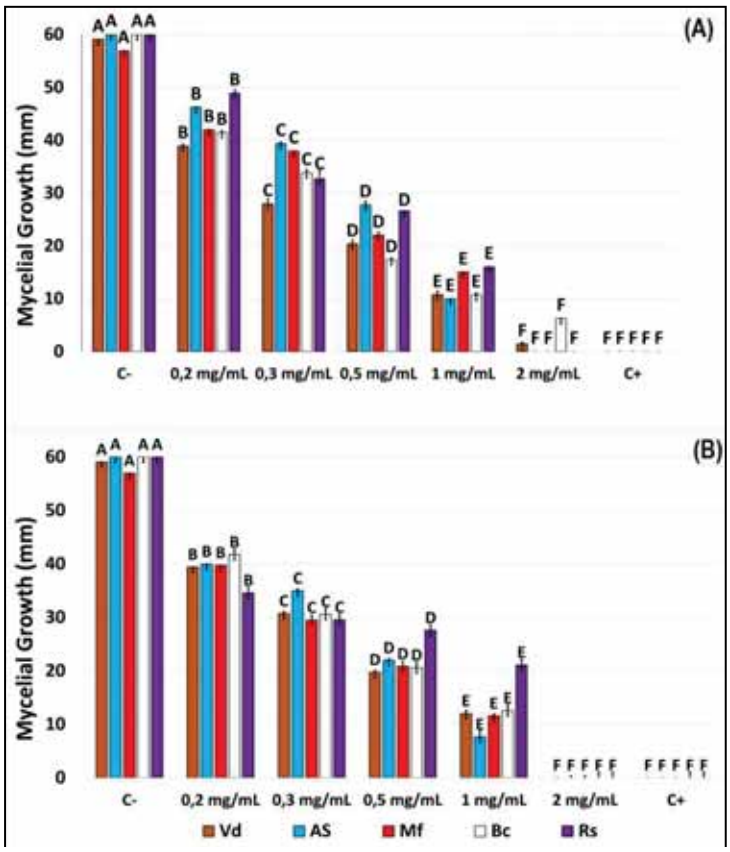

FIGURE 2

Mycelium growth of test fungi against Chitosan-1 (A) and Chitosan-2 (B). Mycelial colony diameter was calculated 10 d after treatment. *Verticillium dahliae*= Vd, *Alternaria solani*= As, *Monillia fructigena*=Mf, *Botrytis cinerea*= Bc, *Rhizoctonia solani*=Rs, Negative control=C-, Positive Control=C+

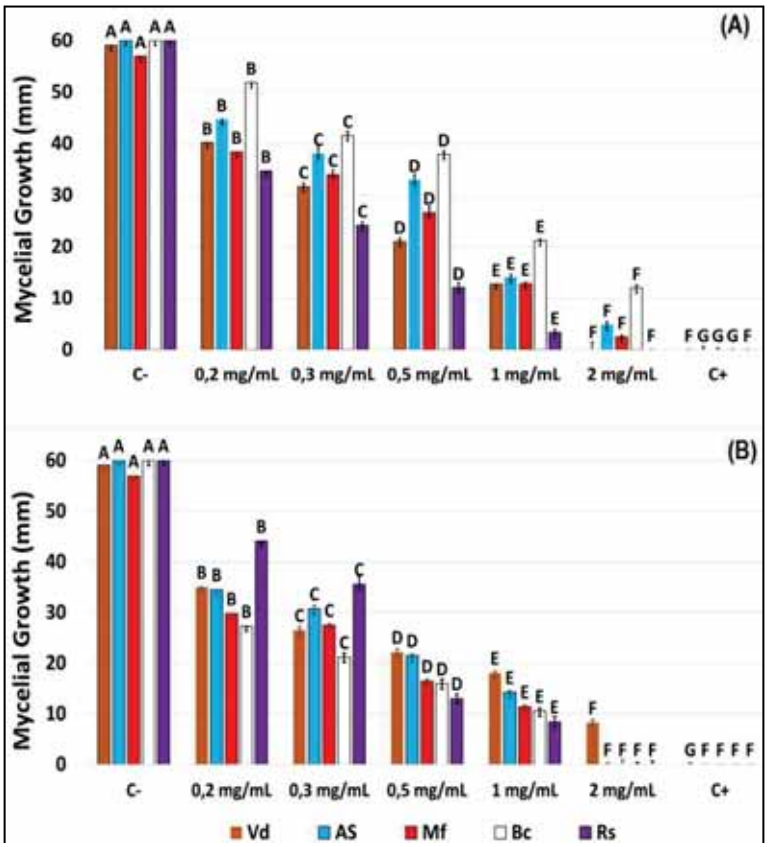

FIGURE 3

Mycelium growth of test fungi against Chitosan-3 (A), and Chitosan-4 (B). Mycelial Colony diameter was calculated 10 d after treatment. *Verticillium dahliae*= Vd, *Alternaria solani*= As, *Monillia fructigena*=Mf, *Botrytis cinerea*= Bc, *Rhizoctonia solani*=Rs, Negative control=C-, Positive Control=C+

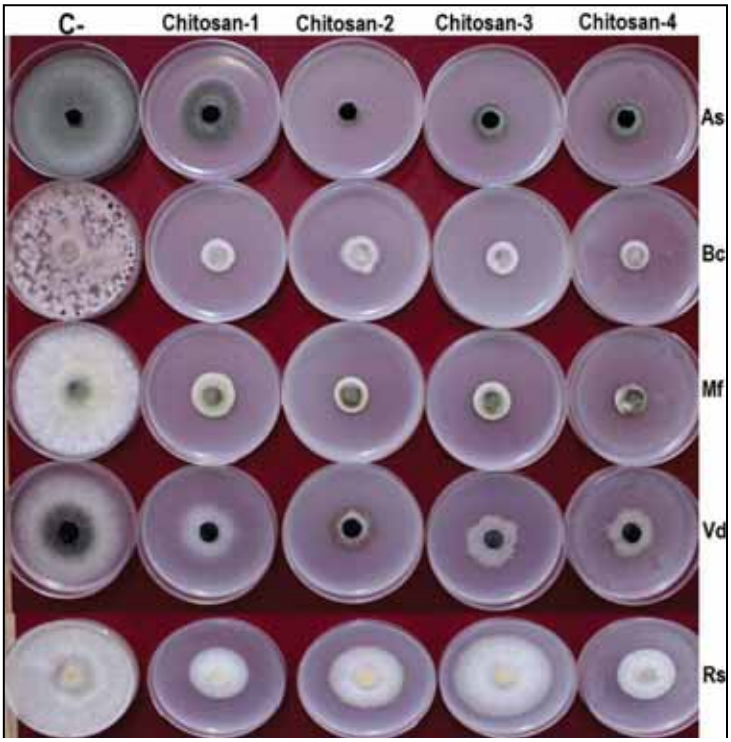

FIGURE 4

Mycelial growth in 1 mg/ml doses of chitosans against test fungi. *Verticillium dahliae*= Vd, *Alternaria solani*= As, *Monillia fructigena*=Mf, *Botrytis cinerea*= Bc, *Rhizoctonia solani*=Rs, Negative control=C-.
Photographs were taken at 10 days after incubated.

TABLE 2
Mycelium growth inhibition (%) of chitosans against test fungi

Chitosans	Doses (mg/mL)	Test Fungi				
		Vd	As	Mf	Bc	Rs
Chitosan-1	C-	0,0±0,0	0,0±0,0	0,0±0,0	0,0±0,0	0,0±0,0
	0.2	34[a]±0,38[b]	23±0,29	26±1,67	31±0,85	18±0,87
	0.3	53±1,44	34±0,50	33±0,41	44±0,89	46±2,57
	0.5	66±0,94	54±0,78	61±1,16	71±0,90	56±0,05
	1	82±0,94	83±0,14	74±0,33	82±0,35	73±0,18
	2	97±0,63	100±0,0	100±0,0	90±0,22	100±0,0
	C+	100±0,0	100±0,0	100±0,0	100±0,0	100±0,0
Chitosan-2	C-	0,0±0,0	0,0±0,0	0,0±0,0	0,0±0,0	0,0±0,0
	0.2	33±0,54	33±0,51	30±1,44	30±0,63	42±1,14
	0.3	48±0,34	42±0,48	48±1,60	49±0,70	51±0,51
	0.5	67±0,92	63±1,63	63±0,77	66±0,70	54±0,59
	1	80±0,26	87±0,40	80±0,64	79±0,89	65±0,39
	2	100±0,0	100±0,0	100±0,0	100±0,0	100±0,0
	C+	100±0,0	100±0,0	100±0,0	100±0,0	100±0,0
Chitosan-3	C-	0,0±0,0	0,0±0,0	0,0±0,0	0,0±0,0	0,0±0,0
	0.2	32±0,73	26±2,56	33±1,77	14±1,46	42±0,91
	0.3	46±0,73	37±1,45	40±1,94	31±0,69	60±1,37
	0.5	64±0,18	45±0,90	53±0,74	37±1,11	80±1,00
	1	78±2,07	77±0,69	78±0,47	65±0,54	94±0,19
	2	100±0,0	92±0,78	96±0,55	80±0,73	100±0,0
	C+	100±0,0	100±0,0	100±0,0	100±0,0	100±0,0
Chitosan-4	C-	0,0±0,0	0,0±0,0	0,0±0,0	0,0±0,0	0,0±0,0
	0.2	41±0,95	43±0,95	48±0,35	55±1,22	27±2,96
	0.3	55±0,96	49±0,64	52±0,54	65±1,23	41±1,40
	0.5	62±1,11	64±0,55	71±0,74	73±1,11	78±1,45
	1	69±0,60	76±0,24	80±1,26	82±0,59	86±1,05
	2	86±0,33	100±0,0	100±0,0	100±0,0	100±0,0
	C+	100±0,0	100±0,0	100±0,0	100±0,0	100±0,0

[a]Mycelial growth inhibition±[b]Standard error mean (SEM), *Verticillium dahliae*= **Vd**, *Alternaria solani*= **As**, *Monillia fructigena*=**Mf**, *Botrytis cinerea*= **Bc**, *Rhizoctonia solani*=**Rs**, Negative control=**C-,** Positive Control=**C+**

TABLE 3
Minimum fungicidal concentration values of chitosans against test fungi.

Chitosans (mg/ml)	Test Fungi				
	V. dahliae	*A. solani*	*M. fructigena*	*B. cinera*	*R. solani*
1	++[a]	++	++	++	++
2	++	++	++	++	++
3	++	++	++	+++	+
4	+++	++	++	+	+

[a] Doses; 0.5 to 1.0= (+), 1.0 to 2.0= (++), >2.0=(+++)

Chitosan has been shown to inhibit mycelial growth by causing morphological and structural changes to the tested fungi. These changes have occurred in the form of aerial mycelium growth, stopping or reducing the formation of spores (Figure 4). In addition, at the same dose for each chitosan (1 mg/ml), C4 showed stronger antifungal activity than C3, and C2 inhibited more mycelial growth than C1 (Figure 4). It has been reported that chitosan inhibits enzyme activities responsible for mycelial growth in fungi, leading to morphological abnormalities [27].

Fungicidal and fungistatic percent effects were observed against test fungi of chitosan. These effects occurred between the chitosans C1, C2, C3 and C4 and at doses of 0.2, 0.3, 0.5, 1 and 2 mg/ml

and for Vd from 32 to 100%, for As from 23 to 100%, for Mf from 26 to 100%, for Bc from 14 to 100 and for Rs from 18 to 100% (Table 2).

The minimum fungicidal concentration (MFC) was determined as the lowest test concentration that allows no mycelial growth of the plant pathogens on agar medium (Table 3). Chitosan has been shown to be antifungal activity against *Botrytis cinerea*, *Fusarium oxysporum* and *Rhizoctonia solani*. The minimum inhibitory concentrations (MIC) reported for test fungi range from 10 to 1000 ppm [28].

Many studies have reported that chitosan has strong antifungal effects against the disease agents used in our studies. They determined that chitosan increased the growth against *V. dahliae* at doses of 0.5 and 1 mg/ml but decreased the growth at the dose of 2 mg/ml [16]. Another study showed that antifungal activities of chitosan and chitosan derivatives were different against *A. solani*, that derivatives showed better inhibitory effect [17], and that spraying chitosan into tomato leaves could be used as a protective measure against *A. solani* [29], and that 1 mg/ml of chitosan inhibited the growth of *A. solani* and reduced the severity of early blight disease in tomato leaves [18]. A study about the activity of chitosan against *M. fructigena* was not found. First time with this study was determined effect of chitosan against *M. fructigena.* But, 5 and 10 mg/ml doses of chitosan were used against *M. fructicola* disease agents which is belonging to the same genus. They stated that both doses used, significantly inhibited the growth of the disease [30]. They reported that the concentrations of 2, 4 and 6 g/l of chitosan were sprayed on the strawberry fruit against *B. cinerea*, and that disease growth was significantly reduced [19]. They determined that conidia germination 1 h after inoculation of chitosan on the fruit against grey mold caused by *B. cinerea* in cucumbers decreased disease growth 65%, after 4 h and 24 h the rates were respectively 85% and 87% but the disease growth inhibited 51% on leaves [31]. Some researchers have indicated that chitosan provides protection against *B. cinerea* in *Vitis vinifera* [20-21-32]. In a different study, they stated that three types of chitosan showed strong antifungal effects against *R. solani* in rice and that these chitosans protected rice seeds against disease and inhibited mycelium growth from 69% to 91% [15]. In another research it has been reported that chitosan protects tomato plants against *R. solani* [33].

TABLE 4
Lethal Doses (LD) of chitosan against test fungi

Test Fungi		Chitosan-1 (mg/ml) 95% limits			Chitosan-2 (mg/ml) 95% limits			Chitosan-3 (mg/ml) 95% limits			Chitosan-4 (mg/ml) 95% limits		
		LD	Low.	Upr.	LD	Low.	Upr.	LD	Low.	Upr.	LD	Low.	Upr.
Vd	LD_{50}	0.31	0.27	0.34	0.33	0.28	0.36	0.34	0.29	0.38	0.28	0.22	0.34
	LD_{90}	1.15	0.97	1.45	1.21	1.01	1.53	1.25	1.03	1.62	3.53	2.42	6.25
	Slope	2.23+/-0.17			2.25+/-0.16			2.26 +/- 0.16			1.16+/-0.13		
	Het.	1.07			1.10			1.32			0.37		
	X^2	13.87			14.35			17.13			4.77		
As	LD_{50}	0.41	0.38	0.45	0.34	0.31	0.37	0.46	0.42	0.51	0.30	0.24	0.35
	LD_{90}	1.19	1.05	1.40	1.06	0.92	1.26	1.96	1.62	2.48	1.39	1.08	2.02
	Slope	2.78 +/- 0.17			2.57+/-0.17			2.05+/-0.14			1.91+/-0.15		
	Het.	0.81			0.83			0.62			1.72		
	X^2	10.51			10.77			8.05			22.37		
Mf	LD_{50}	0.41	0.36	0.47	0.34	0.30	0.38	0.39	0.34	0.43	0.25	0.20	0.30
	LD_{90}	1.38	1.12	1.85	1.20	1.01	1.51	1.68	1.39	2.14	1.22	0.96	1.73
	Slope	2.43+/-0.16			2.33+/-0.17			2.01+/-0.15			1.88+/-0.16		
	Het.	1.70			1.05			0.56			1.48		
	X^2	22.07			13.67			7.26			19.28		
Bc	LD_{50}	0.33	0.29	0.38	0.33	0.29	0.38	0.68	0.61	0.76	0.19	0.14	0.23
	LD_{90}	1.62	1.34	2.07	1.21	1.01	1.56	3.34	2.63	4.56	1.10	0.87	1.55
	Slope	1.87+/-0.14			2.28+/-0.16			1.85+/-0.13			1.68+/-0.16		
	Het.	0.69			1.26			0.50			1.30		
	X^2	8.94			16.33			6.47			16.90		
Rs	LD_{50}	0.42	0.36	0.48	0.33	0.22	0.43	0.24	0.21	0.27	0.33	0.29	0.37
	LD_{90}	1.38	1.10	1.91	2.04	1.31	4.87	0.70	0.62	0.82	0.92	0.78	1.14
	Slope	2.48+/-0.16			1.62+/-0.140			2.76+/-0.22			2.89+/-0.19		
	Het.	2.17			1.67			0.17			1.53		
	X^2	28.20			21.52			2.17			19.84		

Vd=*Verticillium dahliae*; As=*Alternaria solani*, Mf=*Monillia fructigena*; Bc=*Botrytis cinerea*; Rs=*Rhizoctonia solani;* LD: Lethal Dose, Low.=Lower bound, Upr.=Upper bound, Het.= Heterogeneity, X^2= Chi-square

The lethal doses of the chitosans against the tested fungi are given in table 4. Effective doses LD_{50} (50% test fungi killing dose) and LD_{90} (90% test fungi killing dose) values were determined separately for each fungus species. It was stated that the most effective lethal doses and chitosans for the LD_{50} value against the tested fungi were, C4 with 0.28 mg/ml in Vd, C4 with 0.30 mg/ml in As, C4 with 0.25 mg/ml in Mf, C4 with 0.19 mg/ml in Bc, and C2 and C4 with 0.33 mg/ml in Rs. Similarly, these rates for LD_{90} were found respectively, C1 with 1.15 mg/ml in Vd, C2 with 1.06 mg/ml in As, C2 with 1.20 mg/ml in Mf, C4 with 1.10 mg/ml in Bc and C3 with 0.70 mg/ml in Rs (Table 4).

CONCLUSION

Chitosan is preferred product the fact that it has cheap, non-toxic, high antimicrobial properties and positive effects on environment and human health and because of the presence of many field uses. Today, it is possible to obtain more effective results by improving the derivatives of chitosans. It is important that the chitosan types used in our study show high antifungal activity against test fungi, in order to be considered as an alternative method of struggle for these phytopathogenic fungi species, which have high level of problems in agricultural areas. According to our knowledge, for the first time, the activity of chitosan was examined against *M. fructigena* pathogen in this study. For other used pathogen groups, similar results were obtained with other studies. In addition, the fact that the produced chitosan types are derived from materials from different regions adds to innovation to our study. Because of that, the reasons for the different pathogenicity and virulence of each pathogen group and the different resistance against to the used fungicides add to this study individuality.

REFERENCES

[1] Zheng, L.Y., Zhu, J.F. (2003) Study on antimicrobial activity of chitosan with different molecular weight. Carbohydr Polym. 54, 527–530.

[2] Dutta, P.K., Tripathi, S., Mehrotra, G.K., Dutta, J. (2009) Perspectives for chitosan based antimicrobial films in food applications. Food Chem. 114, 1173-1182.

[3] Xing, R.E., Yu, H.H., Liu, S., Zhang, W.W., Zhang, Q.B., Li, Z.E., Li, P.C. (2005) Antioxidant activity of differently regioselective chitosan sulfates *in vitro*. Bioorg. Med. Chem. 13, 1387–1392.

[4] Sun, T., Zhou, D., Xie, J., Mao, F. (2007) Preparation of chitosan oligomers and their antioxidant activity. Eur Food Res Technol. 221, 421-456.

[5] Yazıcı, S., Yanar, Y., Karaman, I. (2011) Evaluation of bacteria for biological control of early blight disease of tomato. Afr J. Biotechnol. 10, 1573–1577.

[6] Diwan, N., Fluhr, R., Eshed, Y., Zamir, D., Tanksley, S.D. (1999) Mapping of Ve in tomato: a gene conferring resistance to the broad-spectrum pathogen, *Verticillium dahliae* race 1. Theor Appl Genet. 98, 315-319.

[7] Buza, N.L., Krinitsyna, A.A., Protsenko, M.A., Vartapetyan, V.V. (2004) Intensity of apple fruit attack by brown rot fungus *Monilia fructigena* during ripening. Mikol Fitopatol. 38, 62-67.

[8] Carling, D.E., Leiner, R.H., Westephale, P.C. (1989) Symptoms, signs and yield reduction associated with Rhizoctonia disease of potato induced by tuber borne inoculum of *Rhizoctonia solani* AG-3. Am Potato J. 6, 639–697.

[9] Grabke, A., Fernández-Ortuño, D., Amiri, A., Li, X., Peres, N.A., Smith, P., Schnabel, G. (2014) Characterization of iprodione resistance in *Botrytis cinerea* from strawberry and blackberry. Phytopathology. 104, 396-402.

[10] Rabea, E.I., Badawy, M.E.T., Stevens, C.V., Smagghe, G., Steurbaut, W. (2003) Chitosan as antimicrobial agent: applications and mode of action. Biomacromolecules. 4, 1457-1465.

[11] Kurita, K. (1998) Chemistry and application of chitin and chitosan. Polym Degrad. Stabil. 59, 117–120.

[12] Robles-Martínez, L., Guerra-Sánchez, M.G., Hernández-Lauzardo, A.N., Pardo, J.P., Velázquez-del Valle, M.G. (2014) Effects of chitosan and oligochitosan on development and mitochondrial function of *Rhizopus stolonifera*. J. Basic Microbiol. 54, S42–S49.

[13] Hadwiger, L.A. (2013) Multiple effects of chitosan on plant systems: solid science orhype. Plant Sci. 208, 42–49.

[14] Wade, H.E., Lamondia, J.A. (1994) Chitosan inhibits *Rhizoctonia fragariae* but not strawberry black root rot. Adv. Strawberry Res. 13, 26–31.

[15] Liu, H., Tian, W., Li, B., Wu, G., Ibrahim, M., Tao, Z., Wang, Y., Xie, G., Li, H., Sun, G. (2012) Antifungal effect and mechanism of chitosan against the rice sheath blight pathogen, *Rhizoctonia solani*. Biotechnol Lett. 34, 2291–2298.

[16] Palma-Guerrero, J., Jansson, H.B., Salinas, J., Lopez-Llorca, L.V. (2007) Effect of chitosan on hyphal growth and spore germination of plant pathogenic and biocontrol fungi. Journal of Applied Microbiology. 104, 541–553.

[17] Guo, Z., Chen, R., Xing, R., Liu, S., Yu, H., Wang, P., Li, C., Li, P. (2006) Novel derivatives of chitosan and their antifungal activities in vitro. Carbohydr Res. 341, 351–354.

[18] Sathiyabama, M., Akila, G., Einstein, C. (2013) Chitosan-induced defence responses in tomato plants against early blight disease caused by *Alternaria solani* (Ellis and Martin) Sorauer. Arch Phytopathol Plant Protect. 47, 1963–1973.
[19] Reddy, M.B., Belkacemi, K., Corcuff, R., Castaigne, F., Arul, J. (2000) Effect of pre-harvest chitosan sprays on postharvest infection by *Botrytis cinerea* and quality of strawberry fruit. Postharvest Biol Technol. 20, 39–51.
[20] Romanazzi, G., Nigro, F., Ippolito, A., Divenere, D., Salerno, M. (2002) Effects of pre- and postharvest chitosan treatments to control storage grey mold of table grapes. J. Food Sci. 67, 1862–1866.
[21] Nascimento, T., Rego, C., Oliveira, H. (2007) Potential use of chitosan in the control of grapevine trunk diseases. Phytopathol Mediterr. 46, 218–224.
[22] El Hadrami, A., Adam, L.R., El Hadrami, I., Daayf, F. (2010) Chitosan in plant protection. Mar. Drugs. 8, 968–987.
[23] Tokatlı, K., Demirdöven, A. (2016) Optimization of cihitin and chitosan production from shrimp waste and characterization. Journal of Food Processing and Preservation. 42(2), e13494.
[24] Nwosu, M.O., Okafor, J.l. (1995) Preliminary studies of the antifungal activities of some medicinal plants against Basidiobolus and some other pathogenic fungi. Mycoses. 38, 191-195.
[25] Onaran, A., Yılar, M. (2012) Antifungal activity of *Trachystemon orientalis* L. aqueous extracts against plant pathogens. J. Food Agric. Environ. 10, 287-291.
[26] Pandey, D.K., Tripathi, N.N., Tripathi, R.D., Dixit, S.N. (1982) Fungitoxic and phytotoxic properties of essential oil of *Hyptis suaveolens*. Z. Pflanzenk. 89, 344–349.
[27] Jia R., Duan, Y., Fang, Q., Wang, X., Huang. J. (2016) Pyridine-grafted chitosan derivative as an antifungal agent. 2016. Food Chem. 196, 381–387.
[28] Liu, X.F., Guan, Y.L., Yang, D.Z., Li, Z., Yao, K.D. (2001) Antibacterial action of chitosan and carboxymethylated chitosan. J. Appl. Polym. Sci. 79, 1324-1335.
[29] Ge, Y., Li, D.A. (1996) A molecular study on tomato induced resistance to *Alternaria solani*. In: 8th International Congress of Molecular Plant–Microbe Interaction, Knoxville, TN, USA, 14–19.
[30] Li, H., Yu, T. (2000) Effect of chitosan on incidence of brown rot, quality and physiological attributes of postharvest peach fruit. J. Sci. Food Agric. 81, 269–274.
[31] Ben-Shalom, N., Ardi, R., Pinto, R., Aki, C., Fallik, E. (2003) Controlling gray mould caused by *Botrytis cinerea* in cucumber plants by means of chitosan. Crop Protect. 22, 285–290.
[32] Barka, E.A., Eullaffroy, P., Clément, C., Vernet, G. (2004) Chitosan improves development, and protects *Vitis vinifera* L. against *Botrytis cinerea*. Plant Cell Rep. 22, 608–614.
[33] Abd-El-Kareem, F., El-Mougy N.S., El-Gamal, N.G, Fotouh, Y.O. (2006) Use of chitin and chitosan against tomato root rot disease under greenhouse conditions. Res J Agric Biol Sci. 2, 147–152.

Received: **09.02.2018**
Accepted: **21.02.2019**

CORRESPONDING AUTHOR

Abdurrahman Onaran
Gaziosmanpasa University
Department of Plant Protection
Faculty of Agriculture
60250, Tokat – Turkey

e-mail: abdonaran@hotmail.com
abdurrahman.onaran@gop.edu.tr

© by PSP Volume 28 – No. 4/2019 pages 2795-2801 Fresenius Environmental Bulletin

EFFECT OF PLANT DENSITY ON GROWTH AND GRAIN YIELD OF SOME HYBRID CORN (*ZEA MAYS* L.) VARIETIES UNDER MEDITERRANEAN ENVIRONMENT

Omer Konuskan*, Cengiz Kilinc

Department of Field Crops, Faculty of Agriculture, Mustafa Kemal University, Hatay, Turkey

ABSTRACT

Corn production in less planr sensity has been struggled over the last decades with differnt degrees of accomplishment. This research was conducted on the second crop growing season in 2016 at the Mustafa Kemal Univertiy, Turkey to determine the optimum plant density (8, 9, 10, and 11 plant/m^2) for two different maturitiy groups hybrid corn varieties of P31 P 41 (FAO 650) and DKC 5741 (FAO 500). Tasseling time, plant height, stem diameter, stalk length, cob thickness, wedge weight, SPAD, leaf area index, harvest index and grain yield were measured. The results indicated that there were sinificant differences among the plant densities, and between the varieties, and their intercations for almost all the growth and yield trains of hybrid corn varieties. For the plant density, wider spaced plants (8 plants/m^2) produced the highest values of stem diameter (SD), SPAD reading, ear diameter (ED), grain weight (GW), and grain yield (GY) followed by nearest spaced plants (9 plants/m^2) as compared to closed spaced plants (10 and 11 plants/m^2). Significant varietal differences were recorded in all studied traits except SPAD falue and ED. However, the variety DKC 5741 produced shorter plant, lesser LAI and tasseled earlier but generated higher SD, EL (ear length), GW, and GY than the variety P31 P 41. Therefore, the early maturing maize variety DKC 6547 can be grown with maintaining 8-9 plants/m2 for obtaining maximum grain yield corn.

KEYWORDS:
Corn (*Zea mays*), plant density, varieties, leaf area index, SPAD value, grain yield

INTRODUCTION

Maize (*Zea mays* L.) is one of the most warm season creals crop in the World [1]. It is an important cereal which is used as human consumption, animal feeding and a raw material for various agro-based industries throughout the globe. Several environmental factors, management practises, and genetic factors effect of forage maise productivity and quality properties [2]. It belongs to family poeaceae, ranked third among production fo ceral crop, in addition, it is cultivated for grain production as well as fodder in tropical, sub-tropical and temperate area of the globe [3, 4]. It is one of essential plants global due tothe production is high from grain and forage. It has wide adapting attributes and is intensely cultivated in Turkey [5, 6, 7].

Crop phenology is the major essential aspects of crop yield evaluation, and it is imprtant to predicting physiological performance under different field conditions [8]. Moreover, seed row spacing is an agronomical management strategy used by producers to maximize the husbandry of thensoil and plant ecosystem from planting to harvest with the target of bolstering the crop production [8]. Gözübenli et al. [9] revealed that optimum grain yield was achieved from 7 plant/m^2 in the East Mediterennean in second crop season. While, Gözübenli et al. [1] steated that cultivars and density variences was important while interaction was not important and the maximum yield is obtained with the plant density of 9 plants/m^2. The planting densities have been observed to contribute towards positive increase in production of grain [10]. Maize yield response to density depends on the variety [11]. In addition, biomass yield, plant height, and ear length have been observed to improve with increase in density of plant [10], thus leading to leaf area [12].

Recently, the improvment of hybrids are more prone to withstand higher density of plant than older hybrids and inbreds. The plant controlling is essential strategy of managing of plant because it can lead to an increase in solar radiation interception, better use of water and nutrients, resulting higher productivity [13]. To achieve high grain productivity it is essential to maintain optimum plant density for achieving available resources from the environment, allowing better conditions for the plant growthand development [14]. The objective of this research was to determine the optimum plant densities for growth and yields of corn in East Mediterenean conditions.

TABLE 1
Nutrient status of soil with critical value before sowing of maize

Soil properties	Method	Hatay
Organic matter (%)	Walkley-Black	1.39
Lime (%)	Calcimetric	23.42
Saturation (%)	With water	101
Sand (%)		17
Silt (%)		25
Clay (%)		59
Teksture		Clay
pH	Potentiometric	8.22
Conductivity(µS/cm)	Potentiometric	974.6
Salinity	(EC meter)	0.05
N (%)	Kjeldahl	0.036
P (ppm)	Spektrofotometrik	6.40
K (ppm)	Flame photometer	287.3
Na (ppm)	Flame photometer	231.3
Li (ppm)	Flame photometer	4.0
Ca (ppm)	Flame photometer	4010.0
Fe (ppm)	MP-AES	9.523
Zn (ppm)	MP-AES	0.244
Cu (ppm)	MP-AES	2.914
Mn (ppm)	MP-AES	12.025
Mg (ppm)	MP-AES	992.0

TABLE 2
Climatological conditions during the present study and long years

Locations	Mean heat (°C)		Precipitation (mm)		Humidity (%)	
	1940-2016	2016	1940-2016	2016	1940-2016	2016
May	21.9	21.7	14.2	26.8	63.1	56.8
June	25.2	26.4	1.5	0	63.2	54.4
July	27.7	30.1	0.1	0	64.0	49.6
August	28.8	29.3	0.1	0	63.2	61.3
September	26.4	28.4	9.9	0	61.0	57.1
October	21.4	22.7	29.5	24.6	59.2	62.8

MATERIALS AND METHODS

Location and growing conditions. This research was conducted at the Mustafa Kemal University, Turkey in 2016, to determine the optimum plant for two different maturitiy groups hybrid corn on second crop growing season. The soil was clay loam having pH 7.12, low in available phosphosus (7.41 kg/ha^{-1}), and organic matter (1.93%). Nitrogen fertilizer was added as urea at rates of 240 kg N ha^{-1}. It was applied at planting process 80kg K ha-1 as K_2O and 80kg P_2O_5 ha-1 as basal doses during final land prepararion. Regarding N implementation, half of each rate was applied at planting as a band close to the seed with a combine drill, and the other half was applied by broadcasting when the plants were about 50 cm high. Plants were irrigated every 10 to 15 days intervals to avoid any growth restrictions due to drought. Grain yield (adjusted to 15% moisture), and other treits were determined in the centre 2 rows of each sub-plot. Soil samples were collected and analyzed for various physicochemical properties (Table 1). Mean temperature and precipitation in the growing season are presented in (Table 2).

Experimental design and treatments. The experiment was laid out in Split Plot design with three replications. Experimental factors were: Maize hybrid cultivars represented in main plots and densities represented in sub-plots. Sub-plots were 4 rows (70 cm) wide by 5 m long. Two different maturitiy groups hybrid corn varieties viz. 31 P 41(FAO 650), and DKC 5741 (FAO 500) were cultivated at four plant density (8, 9, 10, and 11 plants/m^2).

Sampling and measurements of grain yield traits. At harvesting time, data on various yield components was collected by using standard procedures. The number of plants and ears were counted separately. Yield components like plant height (cm), ear height (cm), ear-up stem length (cm), ear diameter (mm), grain weight (g), grain yield (kg m^{-2}) and harvest index (%) were measured [15].

LAI. LAI = Leaf area/ plant, Area. LAI: Leaf area index, YA: leaf area (cm^2), PA: Plant area (cm^2).

SPAD. The SPAD value of 10 plants ear leaf were measured (SPAD-502, Minolta Ltd. Osaka, Japan) during the tasseling time.

Harvest Index (%): Harvest index was measured with the help of the following formula:

HI= [grain weigth/total plant weigth)*100].

TABLE 3
Analysis of variance (ANOVA) some plant paremeteristics

Source of variation	D.F	F values									
		TT	PH	SD	LAI	SPAD	EL	ED	GW	HI	GY
Replication	2	0.5135	16.44	0.1258	0.6316	0.2708	2.412	0.5172	0.6138	0.3328	1.2001
Cultivars(C)	1	132.43**	917.15**	77.21*	47.162*	2.0315	34.03*	0.1488	42.5979*	442.891*	58.219*
Error	2										
Density (D)	3	2.33	2.76	5.91*	9.089**	18.462**	2.751	5.5656*	8.1015**	0.1267	9.225**
CX D	3		3.21	1.63	3.3026	19.896**	0.974	0.1888	0.6499	0.1751	0.6610
Error	12	1.79									
Total	23										
CV (%)		2.14	2.52	4.32	7.76	3.03	3.83	2.03	9.02	19.65	14.43

*, ** significant P<0.05, P<0.01 levels, respectively; ns: not significant; CV: coefficient of variation; TT: tasseling time; PH: plant height; SD: stem diamete; LAI: Leaf area index, EL: ear length; ED: ear diameter; GW: grain weight; HI: harvest index; GY: grain yield.

Statistical analysis. All data collected for two years average and obtained results were calculated to analyses of variance according to Gomez and Gomez [16]. Significant means were separated by the Least Significant Difference (LSD) at the 0.05 significance level (P≤0.05). The estimation of correlation for traits was calculated by MSTAT-C software package.

RESULTS AND DISCUSSION

The analysis of variance showed that the effect of all treatments on all traits under studied were significant. It was found that the cultivars and plant density significantly influenced almost al the the studied charecteristics for hybrids. The interaction effect between the plant population x cultivars on the SPAD value was significant (Table 3). The previous studies revealed that plant desnsity significantly influenced the growth and yield of maize cultivars [1]. According to Calonego et al. [17], it was observed that the spacings of 0.45 m and 0.90 m, and three plant populations viz. 45, 60 and 75 000 plants ha^{-1} did not record any positive interaction effect between spacing x plant population influencing agronomic traits and grain yield. Plant population increase could lead to morphological and physiological changes in plants, higher plant height, higher height of the cob insertion and lower stem diameter, enabling greater lodging and caused reduction in productivity [14].

Tasseling time. The tasseling time is an essential yield-related properties and influences the productivity. Early maturing hybrids are favour in corn cultivation. The tasseling time was not affected by plant dentsities. The differences of tasseling period between the two hybrids were statistically significant. However, the hybrid DKC 5741 had the earliest tasseling time (50.92 days) over the cultivar P31 P 41 (56.75 days) (Table 4). The earlier-flowering corn plants produced smaller plant size and longer kernel-filling stages [18]. A significant variation in the days up to tasseling stage of popcorn with different nitrogen levels and plant densities was reported by Gökmen et al. [19].

Plant height (cm). Plant height is an essential attributes which helps determining the growth attained during the growing stage [20]. In our study, it was found that plant height was significantly influenced by cultivras, but the variables plant height were not affected by an increase in plant dentsities. Nonetheless, the plant height gradually increased from 8 to 10 plants/m^2 in both the cultivars but the cultuvar P31 P 41 was more responsive the another one. The cultuvar P31 P 41 produced remarkably higher plant height (173.617 cm) than the plant highet (162.350 cm) of DKC 5741 (Table 2). [1] Calonego et al. [17] and [1] Gilo et al. [21] reported that the reduction of the spacing between the lines did not influenced plant height. Lima et al. [22] observed no statistical differences for plant height, when studying three plant populations (50,000, 55,000 and 60,000 plants ha^{-1}). [1] Silva et al. [23] observed higher plants for larger populations, due to the increased inter plants competition for light, water, and nutrients.

Stem diameter (mm). Plant density significantly influenced the stem diameter and stem diameter was decreased with the increase in plant density, and the highest stem diameter (19.0 mm) was obtained at 8 plants/m^2 and the lowest stem diameter (17.1 mm) was recorded at 11 plants/m^2 (Table 4). The comparison of the mean values of hybrids showed that DKC 5741 cultivar had the highest stem diameter. Similar results were also observed by Calonego et al. [17] who reported that the stem diameter decreased with the increase in plan population and the highest plant population of 75,000 plants ha^{-1} produced the minimum stem diameter. Stem diameter was lower in the high reat of plant densities as a consequence of inter plant competition, and maize hybrids did not achieve significant inffluence on stem diameter [24].

TABLE 4
Effects of Plant density on TT, OH, SD, LAI and SPAD of corn hybrids in growing season.

Parameters		Plant density (plant/ m^2)				
	Cultivars	8	9	10	11	Mean
TT (day)	DKC 5741	50	50.33	51.66	51.66	50.92 b
	P31 P 41	57.66	55.33	56.66	57.33	56.75 a
	Mean	53,83	52,83	54,16	54,5	
	LSD					
PH (cm)	DKC 5741	163.467	164.933	165.433	155.567	162.350 a
	P31 P 41	167.967	175.167	176.267	175.067	173.617 b
	Mean	165.717	170.050	170.850	165.317	
	LSD					
SD (mm)	DKC 5741	20.183	19.633	19.153	17.530	19.125 a
	P31 P 41	17.823	16.967	17.453	16.717	17.240 b
	Mean	19.0 a	18.3 a	18.3 a	17.1 b	
	LSD (Density)	0.9881				
LAI (cm^2/cm^2)	DKC 5741	3.593	3.847	3.920	4.040	3.850 a
	P31 P 41	4.317	5.527	5.380	5.717	4.985 b
	Mean	3.955 b	4.187 b	4.650 a	4.878 a	
	LSD (Density)	0.43				
SPAD	DKC 5741	56.3 a	52.4 c	52.5 bc	44.4 e	51.3
	P31 P 41	54.9 ab	52.6 bc	48.9 d	53.9 abc	52.5
	Mean	55.6a	52.4 b	50.7 bc	49.2 c	
	LSD	Densty 1.981		Interaction 2.65		

TT: tasseling time; PH: plant height; SD: stem diamete; LAI: Leaf area index

TABLE 5
Effects of Plant density on ED, EL, HI, GW and GY of corn hybrids in growing season.

		Plant density (plant/ m^2)				
	Cultivars	8	9	10	11	Mean
ED (mm)	DKC 5741	39.9	39.6	38.9	38.5	39.2
	P31 P 41	39.7	39.6	38.3	37.9	38.9
	Mean	39.8a	39.6 ab	38.6 bc	38.2 c	
	LSD(Density)	0.995				
EL (cm)	DKC 5741	17.6	17.1	17.5	16.2	17.1 a
	P31 P 41	15.9	15.4	15.4	15.3	15.5 b
	Mean	16.8	16.3	16.4	15.8	
	LSD					
HI (%)	DKC 5741	31.6	31.9	32.8	31.5	31.9 a
	P31 P 41	23.5	27.1	23.8	25.5	24.9 b
	Mean	27.5	29.5	28.3	28.5	
	LSD					
GW (g)	DKC 5741	206.7	207.0	173.3	171.9	189.7 a
	P31 P 41	133.6	136.2	120.9	105.9	124.2 b
	Mean	170.1 a	171.6 a	147.1 b	138.9 b	
	LSD(Density)	17.80				
GY (kg/da)	DKC 5741	734.7	660	540.5	497.4	608.1 a
	P31 P 41	459.6	477.1	344.9	331.8	403.3 b
	Mean	597.2 a	568.5 a	442.7 b	414.6 b	
	LSD(Density)	91.81				

EL: ear length; ED: ear diameter; GW: grain weight; HI: harvest index; GY: grain yield.

LAI (Leaf area index). LAI is an important growth trait which influences the yield of maize. In this study, plant density and cultivar significantly influenced the important growth paramerer of LAI. However, the higher LAI was recorded at the cultivar P31 P 41 (4.985 cm^2/cm^2) than the the cultivar DKC 5741 (3.850 cm^2/cm^2). The LAI gradually increased with increasing plant density for both the cultuvars. The plant density of 11 plants/m^2 produced the highest average LAI (4.878 cm^2/cm^2) which was statistically identical with the plant density of 10 plants/m^2. On the other hand, the lowest LAI (3.955 cm^2/cm^2) was recorded at the plant density of 8 plants/m^2 that was staitistically similar (4.187cm^2/cm^2) with the plant density of 9 plants/m^2 (Table 4). Valadabadi and Farahani [25] concluded that leaf area is influenced by genotype, plant population, climate and soil fertility. The increase in plant density improved plant morphological traits and thereby increased maize yield [26]. Previous studies

revealed the relationship between LAI and plant density to be generally positive as density increases until optimum, but at the expense of LAI per plant, which decreases as plant density increases [27]. It was reported taht higher maize density increased leaf area index than lower density during maize growth [28].

SPAD values. The effect of plant densitities and cultivars on the SPAD value was significant (Table 4). The comparison of the mean values of the SPAD for plant density showed that the closer plant density of 8 plans/m^2 treatment had the highest SPAD value, wheareas the wider plant spacing of 11 plants/m^2 treatment had the lowest SPAD value. However, the comparison of the mean values of the SPAD values for hybrid cultivar treatments did mot show any significant differences between them regarding the SPAD values. The increase of panting density accelerated leaf senescence [29], increased the shading of leaves [30], and caused a reduction in net assimilation of individual plants.

Ear diameter (mm). The ear diameter decreased with increases in plant density, and the thickest ears (39.8 mm) were produced at low plant density (8 plants/m^2) treatment that was statistically identical with 9 plants/m^2 density treatment, while the narrower ears (38.2 mm) was recorded at wider plant spacing (9 plants/m^2). The comparison of the mean values of the ear diameter for hybrid cultivars did not show any statistical differences (Table 5). Konuskan and Gozubenli [24] revealed that plant densities influenced the ear diameter and the thinner of ears were produced at high densities. Contrary, plant populations did not influence considerably on the cob diameter as reported by Lima et al. [22].

Eear length (cm). The comparison of the mean values of the ear length among four levels of plant densities, no statistical differences were recorded in this study. However, the ear length of the cultivars varied significantly, and the levated ear length (17.1cm) was obtained in the DKC 5741 hybrid cultivar and the lower ear length (15.5 cm) was recoded in P31 P 41 cultivar (Table 5). Lima et al. [22] found did not observe any differences for cob length, when studying with three plant populations. The cob length did not differe between the different spacing and plant populations [14].

Grain weight (g). The findings regarding 1000-grain weight are showed in table (Table 5). The result indicated that grain weight was significantly influenced by variance plant densities and cultivars. Moreover, the cultivar DKC 5741 showed that the higher grain weight than the cultivar P31 P 42. The GW gradually decreased with increasing plant densities (Table 5). The differences were significant for plant densities and 8 cm and 9 cm plant density treatments had the optimum grain weight. The thousand grain mass was influenced by the change in plant spacing [14]. The Low rate of grain weight in high rate of plant density could be due to availability of less photosynthates for grain development on account of high inter-specific competition which resulted in low rate of photosynthesis and high rate of respiration [31, 20]. This characteristic is greatly influenced by environmental factors, and resulted a reduction in growth and productivity [32, 33, 34].

Grain yield (kg/da). The data on grain yield indicated that grain yield was significantly affected by plant population densities and hybrid cultivars (Table 5). The grain yield was influenced by plant densities, and the highest yield (597.2 kg/da) were obtained from the plant densities of 8 plants/m^2, followed by 9 plants/m^2 treatment (568.5 kg/da), However, the lowest GY was recorded with ple plant density of 11 plants/m^2 which was statistically similar to 10 plants/m^2 (Table 5). The performance of the cultivar DKC 5741 (608.1 kg/da) considering grain yield was superior to the cultivar P31 P 41 (403.3 kg/da). Sharratt & McWillians [35] observed that the corn yield increased with decrease in plant spacing. Silva et al. [36] achieved an increase of 11% grain yield with an increase of plant density from 78 to 100 thousand plants ha^{-1}. Abuzar et al. [20] revealed taht the highest grain yield was achieved with the highest plant population of 80000 plants ha^{-1} which possibly due to higher number of ears ($plant^{-1}$) and number of grain rows (ear^{-1}) in that treatment. A reduction in the spacing between plant rows (0.90 to 0.45 m) and an increase in population density (from 60,000 to 90,000 plants ha^{-1}) resulted in higher yield for the hybrid 30K75, without changing their agronomic attributes [37, 14]. Yield differences across planting density have also been reported by Seyed Sharifi et al. [38] and Zhang et al. [39].

Harvest Index. Harvest index was not significantly influenced by different plant densities (Table 5). The mean values of the HI for hybrids showed that the cultivar DKC 5741 hybrid had the significantly higher HI (31.9%) than the HI (24.9%) of the hybrid cultivar P31 P 41. It is reported that the biomass yield decreases progressively as the number of plants increases in a given area because the production of the individual plant reduces [40]. The harvest index declines when plant density increases above the critical plant density in maize [31].

CONCLUSION

The present study indicated that adequate plant densities per unit area significantly influenced the most of yield contributing traits which finally produced a good yield of maize hybrids. The performance of the cultivar DKC 5741 was better than the cultivar P31 P41 considering yield traits and yield. It

can be concluded that the hybrid maize cultivar DKC 5741 can be grown with maintaining plant density of 8-9 plant/m^2 for achieving maximum grain yield in Turkey.

ACKNOWLEDGEMENTS

The authors have no any conflicts of interest

REFERENCES

[1] Gozubenli, H., Sener, O., Konuskan, O., Kilinc, M. (2003) Effect of hybrid and plant density on grain yield and yield components of maize (*Zea mays*). Ind. J. Agron. 48, 203-205.

[2] Carpıcı, E.B., Celik, N. (2010) Determining possible relationships between yield and yield-related components in forage maize (*Zea mays* L.) using correlation and path analyses. Notulae Botanicae Horti Agrobotanici Cluj-Napoca. 38(3), 280- 285.

[3] Molla, S.H., Nakasathien, S., Ali, A., Khan, A., Alam, R., Hossain, A., Farooq, M., EL Sabagh, A. (2018) Influence of nitrogen application on dry biomass allocation and translocation in two maize varieties under short pre-anthesis and prolonged bracketing flowering periods of drought. Archives of Agronomy and Soil Science. (In Press).

[4] Abdelaal, Kh., A.A., Hafez, Y. M., EL Sabagh, A. (2017) Ameliorative effects of abscisic acid and yeast on morpho-physiological and yield characters of maize (*Zea mays* L.) plants under water deficit conditions. Fresen. Environ. Bull. 26, 7372-7383.

[5] Barutcular, C., Dizlek, H., EL Sabagh, A., Sahin, T., EL Sabagh, M., Islam, M.S. (2016) Nutritional quality of maize in response to drought stress during grain-filling stages in Mediterranean climate condition. Journal of Experimental Biology and Agricultural Sciences. 4(6), 644-652.

[6] Erol, H., Barutçular, C., EL Sabagh, A., Erol, R. (2017) Data mining models for selection of the best spectral reflectance indices in estimation of crop yields and data mining classification of crop hybrid types using spectrometer data. European Conference on Electrical Engineering and Computer Science. Bern, Switzerland, November 17-19.

[7] EL Sabagh, A., Barutcular, C., Hossain, A., Islam, M.S. (2018) Response of maize hybrids to drought tolerance indices in relation to grain weight. Fresen. Environ. Bull. 27, 2476-2482.

[8] Sharifi, R.S., Namvar, A. (2016) Plant density and intra-row spacing effects on phenology, dry matter accumulation and leaf area index of maize in second cropping. Biologija. 62(1), 46–57.

[9] Gozubenli, H., Kılınc, M., Sener, O., Konuskan, O. (2004) Effect of single and twin row planting on yield and yield components in maize. Asian Journal of Plant Science. 3(2), 203-206.

[10] Cardwell, V.B. (1992) Fifty years of Minnesota corn production: sources of yield increase. Agron. J. 74, 984–995.

[11] Chandra, D., Gautan, R.C. (1997) Performance of maize varieties at varying plant densities. Ann. Agric. Res. 18, 375–376.

[12] Modarres, A.M., Hamilton, R.I., Dijak, M., Dwyer, L.M., Stewart, D.W., Mather, D.E., Smith, D.L. (1998) Plant density effects on maize inbred lines grown in short season environments. Crop Science. 38, 104–108.

[13] Sangoi, L. (2000) Understanding plant density effects on maize growth and development: an important issue to maximize grain yield. Ciência Rural, Santa Maria. 31(1), 159-168.

[14] Buso, W.H.D., Silva, L.B., Rios, A.D.F., Firmiano, R.S. (2016) Corn agronomic characteristics according to crop year, spacing and plant population densities. Comunicata Scientiae. 7(2), 197-203.

[15] Ulger, A.C. (1986) Reaction of various maize inbred lines and hybrids to increasing nitrogen supply (Reaktion Verschiedener Mais-Inzuchtlinien und Hybryden auf steigendes Stickstoffangebot). Dissertation. Hohenheim-Stutgart/ West Germany, 83p.

[16] Gomez, K.A., Gomez, A.A. (1984) Statistical Procedures for Agricultural Research. John Wiley and Sons. New York, 680p.

[17] Calonego, J.C., Poleto, L.C., Domingues, F.M., Tiritan, C.S. (2011) Yield and growth of maize in different arrangements (Produtividade e crescimento de milho em diferentes arranjos de plantas). Agrarian. 4, 84-90.

[18] Troyer, F. (2001) Temperate Corn-Background, Behavior, and Breeding. In: Hallauer, A.R. (Ed.) Specialty Corns. 2. Edition. Florida, CRS Press, 395-469.

[19] Gökmen, S., Sencar, Ö. and Sakin, M.A. (2001) Response of popcorn (*Zea mays everta*) to nitrogen rates and plant densities. Turkish J. of Agric. and Forestry. 25, 15-23.

[20] Abuzar, M.R., Sadozai, G.U., Baloch, M.S., Shah, A.A., Javaid T., Hussain N. (2011) Effect of plant population densities on yield of maize. The J. of Ani. and Plant Sci. 21(4), 692-695.

[21] Gilo, E.G., Silva Junior, C.A., Torres, F.E., Nascimento, E.S., Lourenção, A.S. (2011) Behavior of corn hybrids in cerrado Sul-Mato-Grossense under different row spacing. Biosci. J. Uberlândia. 27(6), 908-914.

[22] Lima, C.F., Arnhold, E., Araújo, B.L., Oliveira, G.H.F., Oliveira Junior, E.A. (2012) Evaluation of maize hybrids under three population densities in agricultural frontier in Maranhão. Comunicata Scientiae. 3, 30-34.
[23] Silva, A. da F., Schoninger, E.L., Caione, G., Kuffel, C., Carvalho, M.A.C. (2014) Productivity of maize hybrids in relation to spacing and plant population under conventional tillage. Journal of Maize and Sorghum. 13(2), 162-173.
[24] Konuskan, O., Gozubenli., H. (2004) Effects of plant density on grain yield and yield- related traits in some hybrids maize varietes second-crop. Journal of Field Crops Central Research Institute. 10(1), 50-57.
[25] Valadabadi, S.A., Farahani, H.A. (2010) Effects of planting density and pattern on physiological growth indices in maize (*Zea mays* L.) under nitrogenous fertilizer application. J. Agric. Ext. and Rural Dev. 2(3), 40-47.
[26] Farnia, A., Mansouri, M. (2015) Study on morphological characteristics of maize (*Zea mays* L.) cultivars under different plant densities. Indian Journal of Natural Sciences. 5(30), 8393-8397.
[27] Bavec, F., Bavec, M. (2002) Effect of plant population on leaf area index, cob characteristics and grain yield of early maturing maize cultivars. Europ. J. Agron. 16, 151-159.
[28] Saberali, S.F. (2007) Influence of plant density and planting pattern of corn on its growth and yield under competition with common Lambesquarters (Chenopodium album L.). Pajouhesh and Sazandegi. 74, 143-152
[29] Tetio-Kagho, F., Gardner, F.P. (1987) Responses of maize to plant population density: II Reproductive development, yield and yield adjustments. Agron J. 80, 935-940.
[30] Hashemi-Dezfouli, A., Herbert, S.J. (1992) Intensifying plant population response of corn with artificial shade. Agron J. 84, 547-551.
[31] Zamir, M.S.I., Ahmad, A.H., Javeed, H.M.R., Latif, T. (2011) Growth and yield behaviour of two maize hybrids (*Zea Mays* L.) towards different plant spacing. Cercetări Agronomiceîn Moldova. 2(146), 33-40.
[32] Jahan, M.A.H.S., Hossain, A., Teixeira da Silva, J.A., EL Sabagh, A., Rashid, M.H., Barutçular, C. (2019) Effect of naphthaleneacetic acid on root and plant growth and yield of ten irrigated wheat genotypes. Pakistan Journal of Botany. 51(2).
[33] Barutcular, C., EL Sabagh, A., Koç, M., Ratnasekera, D. (2017) Relationships between grain yield and physiological traits of durum wheat varieties under drought and high temperature stress in Mediterranean conditions. Fresen. Environ. Bull. 26, 4282-4291.
[34] Hossain, M.M., Hossain, A., Alam, M.A., EL Sabagh, A., Ibn Murad, K.F., Haque, M.M., Muriruzzaman, M., Islam, M.Z., Das, S. (2018) Evaluation of fifty spring wheat genotypes grown under heat stress condition in multiple environments of Bangladesh. Fresen. Environ. Bull. 27, 5993-6004.
[35] Sharratt, B.S., McWillians, D.A. (2005) Microclimatic and rooting characteristics of norrow-row versus conventional-row corn. Agronomy Journal. 97, 1129-1135.
[36] Silva, R.R., Theodoro, G.F., Libório, C.B., Pessoa, L.G.A. (2012) Effect of crop density of two genotypes of maize in the severity of gray leaf spot and yield in the second season crop. (Influência da densidade de cultivo de dois genótipos de milho na severidade de mancha de cercospora e no rendimento de grãos na "safrinha"). Semina: Ciencias Agrárias. 33, 1449-1454.
[37] Stacciarini, T.C.V., Castro, P.H.C., Borges, M.A., Guerin, H.F., Moraes, P.A.C., Gotardo, M. (2010) Effect of row spacing reduction and increase in population density on agronomic traits of corn. Revista Ceres. 57, 516–519.
[38] Seyed Sharifi, R., Sedghi, M., Gholipouri, A. (2009) Effect of population density on yield and yield attributes of maize hybrids. Research J. Biological Sci. 4(4), 375- 379.
[39] Zhang, J., Dong, S., Wang, K., Hu, C., Liu, P. (2006) Effects of shading on the growth, development and grain yield of summer maize. Ying Yong Sheng Tai Xue Bao. 17(4), 657-662.
[40] Hamidia, A., Khodabandehb, N. and Mohammady-Nasabc, A.D. (2010) Plant density and nitrogen effects on some traits of maize (Zea mays L.). Plant Ecophysiol. 2, 47-52.

Received: **07.05.2018**
Accepted: **05.03.2019**

CORRESPONDING AUTHOR

Omer Konuskan
Department of Field Crops,
Faculty of Agriculture,
Mustafa Kemal University,
Hatay – Turkey

e-mail: okonuskan@mku.edu.tr

© by PSP Volume 28 – No. 4/2019 pages 2802-2806 Fresenius Environmental Bulletin

AFLATOXIN M_1 IN TRADITIONAL HOMEMADE YOGHURTS MARKETED IN SOUTHEASTERN TURKEY

Semra Gurbuz[1,*], Serap Kilic Altun[2]

[1]University of Mardin Artuklu, Tourism Faculty, Gastronomy and Culinary Arts, 47060, Mardin, Turkey
[2]University of Harran, Faculty of Veterinary Medicine, Department of Food Hygiene and Technology, Sanliurfa, Turkey

ABSTRACT

This study was performed to determine the presence and levels of aflatoxin M_1 (AFM_1) in yoghurt produced by traditional methods in small scale enterprises in Mardin and Şanlıurfa provinces located in Southeastern Turkey and to evaluate the yoghurt in terms of food safety. A total of 90 yoghurt samples, 42 from Mardin and 48 from Şanlıurfa were collected from small-scale retailers and tested for AFM_1 by enzyme-linked immunosorbent assay (ELISA). AFM_1 was detected in 34 (37.8 %) of 90 yoghurt samples at the levels ranging from 10 to 515 ng/kg. Five (11.9 %) samples (ranging from 10 to 515 ng/kg) from Mardin and 29 (60.4 %) samples (ranging from 10 to 101 ng/kg) from Şanlıurfa were found to be contaminated with AFM_1. There was a statistically significant difference between the samples collected Mardin and Şanlıurfa concerning the presence frequency of AFM_1 ($p=0.000$). The AFM_1 levels of 16 (17.8 %) positive yoghurt samples were higher than the legal limits. The results of this study have revealed that the traditionally produced homemade yoghurt is contaminated with AFM_1 and poses health risk for consumers.

KEYWORDS:
Aflatoxin M_1, ELISA, milk product, traditional yoghurt, Turkey

INTRODUCTION

Yoghurt constitutes an important part of the daily diet in Turkey and it is still produced with traditional methods in small farming businesses in rural areas besides industrial production.

Aflatoxins are naturally occurring highly toxic secondary metabolites mainly produced by *Aspergillus flavus*, *Aspergillus parasiticus* and rarely by *Aspergillus nominus* [1]. Among the main classes of the aflatoxins (B_1 B_2, G_1, and G_2), aflatoxin B_1 (AFB_1) is the most important compound because of being frequently produced mycotoxin [2, 3] and has toxic, carcinogenic, mutagenic and teratogenic effects [4]. Animals are exposed to AFB_1 by consumption of contaminated feeds [5]. AFB_1 is metabolized to aflatoxin M_1 (AFM_1) in the liver, and can be found in milk after 12-24 hours of the consumption of contaminated feed [6]. Although carcinogenic potential of AFM_1 is about ten times lesser than AFB_1, AFM_1 has been classified as group 2B, a possible human carcinogen [7].

The previous studies have shown that milk and milk products such as yoghurt, cheese, butter, cream, milk powder and breast milk are often contaminated with AFM_1. [1, 3, 8-10].

According to the European Commission Regulation and Turkish Food Codex, the maximum AFM_1 level is 0.050 µg/kg for raw milk, heat-treated milk and milk for the manufacture of milk-based products [11, 12].

Aflatoxin production is strongly associated with environmental conditions, especially high temperature and water stress as well as cropping system, harvesting time and storage condition [1]. Almost a quarter of the crops harvested in the world are contaminated with mycotoxins every year [13]. Therefore, monitoring of aflatoxins is important in order to take necessary preventive measures.

The aim of this study was to investigate the presence and level of AFM_1 in homemade yoghurt marketed in Şanlıurfa and Mardin provinces located in Southeastern region of Turkey.

MATERIALS AND METHODS

Sample collection. In this study, a total of 90 yoghurt samples traditionally produced from cow milk were analyzed. The 42 of the samples from Mardin and 48 samples from Şanlıurfa provinces were purchased from different small retailers selling local products between May and July 2016. The samples were transported to the laboratory in refrigerated containers (4 °C) and stored at – 20 °C until analysis.

Sample preparation. Yoghurt samples were heated at 80 °C for 3 minutes in a water bath for pasteurization [14]. Then 10 grams of the sample that was cooled to room temperature was diluted 1:10 by adding 100 ml of PBS-buffer (pH 7.2). The diluted samples were homogenized for 3 minutes with a Stomacher Lab-Blender and 100 ml of ho-

mogenized samples were used for the ELISA test.

Analysis of the samples. The detection of AFM_1 in the samples was performed by a commercially available competitive ELISA (R-Biopharm GmbH, Germany (RIDASCREEN, Art No.: R1121) kit with 5 ng/kg detection limit. The AFM_1 standard solutions (0, 5, 10, 20, 40 and 80 ng/kg) supplied by the kit were used in the assay.

The ELISA procedure was briefly as follows: A 100 µl of diluted antibody solution was added at the bottom of the each well and mixed gently by shaking manually and then the liquid was poured out and the well was manually washed twice with 250 µl of washing buffer following incubation at room temperature (20-25 °C) for 15 minutes. Then 100 µl from each standard solutions and 100 µl from each diluted sample solutions were poured into wells in duplicate and manually mixed gently and incubated 30 minutes at room temperature in the dark. Then wells were manually washed twice with washing buffer as described above. In the next step, a 100 µl of diluted enzyme conjugate was added into each well and mixed gently. After 15 minutes incubation at room temperature in the dark, washing process was repeated. The 100 µl of substrate/chromogen was added into each well and the reaction was stopped with the stop solution after 15 minutes incubation at the same conditions mentioned above. The plate was read within 15 minutes after addition of stop solution. The optical density was measured at 450 nm by an ELISA plate reader (Perkin Elmer Victor 3-1420 Microplate Reader).

Evaluation of data. The mean value of the absorbances for the standards and the samples was evaluated with the Rida- Soft Win program (Ridavin.exe) prepared by R-Biopharm AG. The recoveries of AFM_1 from the samples spiked at levels of 5, 10, 20, 40 and 80 ng/kg were 104 %, 93 %, 95 %, 102 % and 98 % respectively. The mean recovery rate was 98.4 %.

Statistical analysis. Descriptive statistical analysis was carried out with SPSS ver. 21.0. Sign Test, Chi-Square Test and Mann-Whitney U Test were used to determine the differences between Şanlıurfa and Mardin concerning presence and level of AFM_1 in yoghurt samples. Value of $p < 0.05$ was considered statistically significant.

RESULTS

In this study, AFM_1 was detected in 34 (37.8 %) of 90 yoghurt samples at the levels ranging from 10 to 515 ng/kg. Fifty-six samples (62.2 %) did not reveal the presence of AFM_1. Five (11.9 %) of the 42 samples taken from Mardin and 29 (60.4 %) of the 48 samples taken from Şanlıurfa were found to be contaminated with AFM_1 at the levels ranging between 10-515 and 10-101 ng/kg respectively.

The AFM_1 level of 16 (17.8%) yoghurt samples was above the legal permissible limit. The number of the samples had AFM_1 positive results higher than 50 ng/kg was 4 (9.5 %) and 12 (25 %) in Mardin and Şanlıurfa respectively (Table 1).

The presence frequency of AFM_1 in the samples collected from Şanlıurfa was significantly higher than Mardin ($p=0.000$). There was no significant difference between Mardin and Şanlıurfa concerning the presence level of the AFM_1 ($p=0.089$) and AFM_1 level of the positive samples containing AFM_1 above 50 ng/kg ($p=0.855$) (Table 1).

DISCUSSION

The presence of AFM_1 in milk and subsequently milk-based products pose an important public health problem. The results of this study showed that 37.8 % of yoghurt samples were contaminated with AFM_1 on the ranges between 10-515 ng/kg. Studies in different parts of Turkey revealed variable results; the frequency of AFM_1 in yoghurt samples ranges from 3.3 to 100 % (Table 2). The 11.9 % AFM_1 positive result detected in Mardin was highly lower than the results ranged from 44.4 to 100 % in the previous studies [14-19]. On the other hand, the result was higher than the results of Şahin et al. [20]. In our study, 60.4 % of the AFM_1 positive results detected in samples taken from Şanlıurfa were higher than the findings of Kocasarı et al. [17] and Şahin et al. [20]. However our result was similar to the results of Ertaş et al. [15] and was lower than those reported by some other researchers in Turkey [14, 16, 18, 19, 21] (Table 2).

TABLE 1
Presence of AFM_1 in yoghurt in Mardin and Şanlıurfa provinces, Turkey

	Total n	Positive n (%)	AFM_1 (ng/kg) Mean±sd (min-max)	Samples with AFM_1 >50 ng/kg, n(%)
All samples	90	34 (37.8)	65,7 ± 87.8 (10-515)	16 (17.8)
Mardin	42	5^{ab} (11.9)	174.6 ± 203.4 (10-515)	4^{c} (9.5)
Şanlıurfa	48	29^{ab} (60.4)	47 ± 26.2 (10-101)	12^{c} (25)

P values: ^{a}p 0.000, ^{b}p =0.089, and ^{c}p =0.855

TABLE 2
Compilation of data concerning AFM_1 in yoghurt in Turkey

Location	Total n	Positive n (%)	Min-max (ng/kg)	Samples with AFM_1 >50 ng/kg, n (%)	References
Ankara	40	32 (80)	61.6-365.6	32(100)	[14]
Kayseri	50	28 (56)	2.5-78	7(14)	[15]
Erzurum	80	70 (87.5)	10-475	16 (20)	[16]
Burdur	45	20 (44.4)	50-360	20 (44.4)	[17]
Şanlıurfa	50	50 (100)	40.6-72	10 (20)	[21]
Kayseri	100	100 (100)	2.7-79.3	7 (7)	[18]
Ankara	19	17 (89.5)	7.3-107.2	5 (29.4)	[19]
Çorum	60	2 (3.3)	23-28	0 (0.0)	[20]
Şanlıurfa-Mardin	90	34 (37.8)	10-515	16 (17.8)	This study

The contamination frequency with AFM_1 in the samples taken from Şanlıurfa was significantly higher than those of Mardin. These provinces are located in the same geography. Samples were collected in the same period and tested in the same laboratory. Considering the detection of AFM_1 in 60.4 % of the samples with the levels of 10-101 ng/kg in the present study, it can be concluded that the yoghurts sold in Şanlıurfa may be produced in the small scale enterprises from the mixed milk obtained from different farms. The less frequent AFM_1 positive result obtained the samples taken from Mardin may be due to the fact that the farmers in this province are more effective in taking measures against contamination of feeds with aflatoxin.

In several countries, studies have shown the AFM_1 contamination frequency for yoghurt as 80 % and 68.8 % in 1996 and 2001 respectively in Italy [22, 23] and 61% in Pakistan [3]. In different studies conducted in Iran AFM_1 contamination were reported as 66.1 %, 98.3 % and 96.2 % by Fallah [4], Issazadeh et al. [24] and Mason et al. [25] respectively. In Portugal, Martin and Martin [26] reported 4.2 % whereas in Lebanon, Hassan and Kassaify [27] found 72 % of the yoghurt samples contaminated with AFM_1. The different results may be due to various factors such as the contamination level of the milk used for the yoghurt production, climate, season, geographical differences, farm management, applied feeding systems, feed storage conditions, yoghurt production technology, sampling, analytical methods and laboratory conditions [4, 28-31].

In this study, a total of 16 (17.8 %) samples, 4 (9.5 %) from Mardin and 12 (25 %) from Şanlıurfa were above the permissible level of 50 ng/kg (Table 1). Therefore, the detection of higher level of AFM_1 than the allowed limit in the investigated yoghurt samples in both provinces have shown that traditionally produced homemade yoghurt poses a risk for public health. The difference between Mardin and Şanlıurfa concerning the frequency of the AFM_1 positive samples containing AFM_1 above 50 ng/kg ($p > 0.05$) was not significant. In the studies performed in Turkey, the samples contaminated with AFM_1 above 50 ng/kg varied between 0 and 100 % (Table 2). Şahin et al. [20] reported no sample contaminated with AFM_1 above 50 ng/kg whereas Gürbay et al. [14] found that all of the investigated samples contaminated with AFM_1 at the levels between 61.6 and 365.6 ng/kg. In Portugal, Martin and Martin [26] found no value greater than 50 ng/kg in any samples that they investigated. On the other hand, Hassan and Kassaify [27] reported that 13 % of the samples in Lebanon, Tomasevic et al. [31] reported that 39.2 % of the samples in Serbia were contaminated with AFM_1 above the legal limit of 50 ng/kg. Thermal processing such as pasteurization and sterilization do not cause a significant change in the level of AFM_1 in the milk [1, 27, 32]. However, it is reported that following the fermentation and storage, the level of AFM_1 in yoghurt is lower than the initial level [28]. It has been concluded that the differences of AFM_1 levels in the investigated yogurt samples may be due to the level of AFM_1 in the milk used and the difference in yoghurt production technology.

In conclusion, the contamination levels of yoghurt with AFM_1 appear to be a potential public health hazard for consumers in both provinces. The most effective way to control AFM_1 contamination in milk and milk products is to take preventive measures against contamination of feed with aflatoxin-producing molds. Farmer training by the public authorities to improve the farmers' knowledge for good storage conditions is quite important.

In order to be able to make the necessary interventions to reduce the frequency and level of exposure to toxins, it is necessary to monitor the presence of AFB_1 in feeds and the presence of AFM_1 in milk and dairy products. Products that are produced locally by traditional methods are consumed by the people living in the rural area and are increasingly being consumed by the people who live in cities with the thought that these products are more delicious, natural and healthy. Therefore, besides industrial production, regular control of such products is also important.

ACKNOWLEDGEMENTS

This study was presented as a summary at the 7th Veterinary Food Hygiene Congress.

REFERENCES

[1] Prandini, A., Tansini, G., Sigolo, S., Filippi, L., Laporta, M. and Piva, G. (2009) On the occurrence of aflatoxin M1 in milk and dairy products. Food and Chemical Toxicology. 47, 984–991.

[2] EFSA (European Food Safety Authority) (2004) Opinion on the scientific panel on contaminants in the food chain on a request from the commission related to aflatoxin B1 as undesirable substance in animal feed. EFSA J. 39, 1–27.

[3] Iqbal, S.Z. and Asi, M.R. (2013) Assessment of aflatoxin M1 in milk and milk products from Punjab, Pakistan. Food Control. 30, 235-239.

[4] Fallah, A.A. (2010) Aflatoxin M1 contamination in dairy products marketed in Iran during winter and summer. Food Control. 21, 1478–1481.

[5] Iha, M.H., Barbosa, C.B., Okada, I.A. and Trucksess, M.W. (2013) Aflatoxin M1 in milk and distribution and stability of aflatoxin M1 during production and storage of yoghurt and cheese. Food Control. 29, 1-6.

[6] Shundo, L., Navas, S.A., Lamardo, L.C.A., Ruvieri, V. and Sabino, M. (2009) Estimate of aflatoxin M1 exposure in milk and occurrence in Brazil. Food Control. 20, 655–657.

[7] IARC (International Agency for Research on Cancer) (2002) Some traditional herbal medicines, some mycotoxins, naphthalane and styrene IARC monographs on the evaluation of carcinogenic risks to humans. Vol. 82. 171–300 p. Lyon, France: IARC Press.

[8] Kamber, U. (2005) Aflatoxin M_1 Contamination of Some Commercial Turkish Cheeses from Markets in Kars, Turkey. Fresen. Environ. Bull. 14, 1053-1056.

[9] Aksoy, A., Das, Y.K., Yavuz, O., Guvenc, D., Cetinkaya, M.B., Kokcu, A., Celik, S. (2009) Aflatoxin M1 Level of Human Breast Milk Samples in Samsun and Neighbour Provinces, Turkey. Fresen. Environ. Bull. 18, 832-834.

[10] Kara, R. and Ince, S. (2018) Presence of Aflatoxin M1 in Kaymak Produced in Afyonkarahisar Province. Fresen. Environ. Bull. 27, 5033-5036.

[11] European Commission. (2010) Commission Regulation (EU) No 165/2010 of 26 February 2010 setting maximum levels for certain contaminations in foodstuffs as regards aflatoxins. Official Journal of the European Union. L 50, 8-11.

[12] Turkish Food Codex. (2011) Turkish Food Codex Regulation on Contaminants. Official Journal No. 28157 Ankara, Turkey.

[13] Marin, S., Ramos, A.J., Cano-Sancho, G. and Sanchis, V. (2013) Mycotoxins: Occurrence, toxicology, and exposure assessment. Food and Chemical Toxicology. 60, 218-237.

[14] Gürbay, A., Engin, A.B., Çağlayan, A. and Şahin, G. (2006) Aflatoxin M1 levels in commonly consumed cheese and yoghurt samples in Ankara, Turkey. Ecology of Food and Nutrition. 45, 449-459.

[15] Ertas, N., Gonulalan, Z., Yildirim, Y. and Karadal, F. (2011) A survey of concentration of aflatoxin M1 in dairy products marketed in Turkey. Food Control. 22, 1956-1959.

[16] Atasever, M.A., Atasever, M. and Özturan, K. (2011) Aflatoxin M1 levels in retail yoghurt and ayran in Erzurum in Turkey. Turk J Vet Anim Sc. 35, 59-62.

[17] Kocasari, F.S., Taşcı, F. and Mor, F. (2012) Survey of aflatoxin M_1 in milk and dairy products consumed in Burdur, Turkey. International Journal of Dairy Technology. 65(3), 365-371.

[18] Kayaalp, O., Ertaş, N. and Al, S. (2015) Determination of Aflatoxin M1 Level in Water Buffalo Yoghurt Consumed in Kayseri Region. Journal of Faculty of Veterinary Medicine, Erciyes University. 12(1), 19-23.

[19] Sarıca, D.Y., Has, O., Taşdelen, S. and Ezer, U. (2015) Occurrence of Aflatoxin M1 in milk, white cheese and yoghurt from Ankara, Turkey Markets. Biological and Chemical Research. 2015, 36-49.

[20] Sahin, H.Z., Celik, M., Kotay, S. and Kabak, B. (2016) Aflatoxins in dairy cow feed, raw milk and milk products from Turkey. Food Additives and Contaminants: Part B. 9(2), 152-158.

[21] Temamogullari, F. and Kanici, A. (2014) Aflatoxin M1 in dairy products sold in Şanlıurfa, Turkey. Journal of Dairy Science. 97(1), 162–165.

[22] Galvano, F., Galofaro, V. and Galvano, G. (1996) Occurrence and stability of aflatoxin M1 in milk and milk products: a worldwide review. Journal of Food Protection. 59, 1079-1090.

[23] Galvano, F., Galofaro, V., Ritieni, A., Bognanno, M., Angelis, A.D. and Galvano, G. (2001) Survey of the occurrence of aflatoxin M1 in dairy products marketed in Italy: Second year of Observation. Food Additives and Contaminants. 18(7), 644-646.

[24] Issazadeh, K., Darsanaki, R.K. and Pahlaviani, M.R.M.K. (2012) Occurrence of aflatoxin M1 levels in local yogurt samples in Gilan Province, Iran. Annals of Biological Research. 3(8), 3553-3855.

[25] Mason, S., Arjmandtala, H., Hajimohammadi, B., Arsanjani, A.K., Karami, S., Sayadi, M. and Oryan, A. (2015) Aflatoxin M1 Contamination in Industrial and Traditional Yogurts Produced in Iran. Journal of Food Quality and Hazards Control. 2, 11-14.
[26] Martins, M.L. and Martins, H.M. (2004) Aflatoxin M1 in yoghurts in Portugal. International Journal of Food Microbiology. 91, 315-317.
[27] Hassan, H.F., Kassaify, Z. (2014) The risks associated with aflatoxins M1 occurrence in Lebanese dairy products. Food Control. 37, 68-72.
[28] Govaris, A., Roussi, V., Koidis, P.A. and Botsoglou, N.A. (2002) Distribution and stability of aflatoxin M1 during production and storage of yoghurt. Food Additives and Contaminants. 19(11), 1043-1050.
[29] Warth, B., Parich, A., Atehnkeng, J., Bandyopadhyay, R., Schuhmacher, R., Sulyok, M. and Krska, R. (2012) Quantitation of mycotoxins in food and feed from Burkina Faso and Mozambique using a modern LC-MS/MS multitoxin method. J Agricultural and Food Chemistry. 60, 9352-9363.
[30] Iqbal, S.Z., Jinap, S., Pirouz, A.A. and Faizal, A.A.R. (2015) Aflatoxin M1 in milk and dairy products, occurrence and recent challenges: A review. Trends in Food Science and Technology. 46, 110-119.
[31] Tomasevic, I., Petrovic, J., Jovetic, M., Raicevic, S., Milojevic, M. and Miocinovic, J. (2015) Two year survey on the occurrence and seasonal variation of aflatoxin M1 in milk and milk products in Serbia. Food Control. 56, 64-70.
[32] Çelik, T.H., Sarimehmetoğlu, B., Küplülü, O. (2005) Aflatoxin M1 contamination in pasteurised milk. Veterinarski Arhiv. 75(1), 57-65.

Received: **11.06.2018**
Accepted: **28.02.2019**

CORRESPONDING AUTHOR

Semra Gurbuz
University of Mardin Artuklu,
Tourism Faculty,
Gastronomy and Culinary Arts
Mardin – Turkey

e-mail: semragurbuz@gmail.com

© by PSP Volume 28 – No. 4/2019 pages 2807-2815 Fresenius Environmental Bulletin

PROPERTIES OF COPPER-CONTAMINATED SAND BEFORE AND AFTER STABILIZATION USING ELECTRICAL RESISTIVITY MEASUREMENT

Xiaofeng Liu[1], Xin Xu[2], Xiaoqiang Dong[1], Junboum Park[2,*], Jiwei Shen[3], Shahabaldin Rezania[2]

[1]College of Architecture and Civil Engineering, Taiyuan University of Technology, Taiyuan 030024, China
[2]Department of Civil and Environmental Engineering, Seoul National University, Seoul 08826, S. Korea
[3]College of Civil Engineering, Chongqing Three Gorges University, Chongqing, 404100, China

ABSTRACT

In this study, the electrical resistivity properties of copper-contaminated sand before and after cement solidified/stabilized, the effect of curing time on unconfined compressive strength and leaching toxicity of cement-treated sand were investigated. The results showed that the electrical resistivity of copper-contaminated sand increased with the increase of porosity and decreased with the increase of copper ion content and water content. An accurate electrical resistivity formula of copper-contaminated sand was also obtained. For the cement-treated copper-contaminated sand, the unconfined compressive strength increased with the increase of curing time, and high copper concentration could suppress the unconfined compressive strength. The electrical resistivity increased with the increase of the curing time and decreased with the increase of the copper ion content. In addition, there was a positive correlation between the electrical resistivity and unconfined compressive strength. The leaching toxicity increased with the increase of the copper ion content and the curing time. Through this study, electrical resistivity measurement can be possibly used as a non-destructive method to evaluate the pollution situation of copper-contaminated sand before and after cement solidification/stabilization.

KEYWORDS:
copper-contaminated sand, electrical resistivity, stabilization, unconfined compressive strength

INTRODUCTION

In recent years, copper pollution has become a hot topic in the field of environmental geotechnics which is caused by abandoned mines, industrial zones, unsanitary landfills, etc [1]. The copper pollution situation in water, air, soil, and other areas have become more and more serious [2, 3]. Therefore, it is of great public value to take effective remediation measure for copper soil pollution caused by copper [4]. Many researchers have studied about the copper pollution problem [5, 6]. The most commonly used methods for copper pollution treatment in soil include immobilization, soil washing, and phytoremediation. The soil washing is not suitable for large-scale site because of its high cost while phytoremediation is always affected by local climate and other factors that can influence plant growth [7]. Thus, immobilization has been proved to be a promising treatment for heavy metal pollution [8, 9].

Solidification/stabilization (S/S) technology for immobilization of hazardous wastes have been used for many years [10, 11, 12]. Presently, this technology is widely applied for the immobilization of pollutants in contaminated soils [13, 14]. Cement is a kind of inorganic cementitious materials that can induce hydration reaction when adding water. Hydration product can also fix the waste and then produce a hydration reaction to form a hard cement block [15]. Cement-based S/S has been used widely in inorganic solid wastes treatment that contain heavy metals such as As, Cd, Cr, Cu, NI, Pb and Zn. For instance, Cu can be effectively immobilized using cement-based materials [16, 17, 18].

It's of great importance to detect the pollution degree and the S/S effect of copper-contaminated soil. A traditional detection method that combines chemical sampling with laboratory analysis is not suitable for pollution detection because of its long period and weak practicality. The electrical resistivity is a basic parameter of the soil, which is defined in the formula $\rho = RS/L$, where ρ is the electrical resistivity, L is the length of the material, S is the area, and R is the resistance. Initially, electrical resistivity method was used to study the microstructure of saturated sandstones. and an electrical resistivity structure model of cohesionless saturated sand and rocks called Archie formula was proposed by Archie [19].

The electrical resistivity method can also provide an effective method for pollution control in environmental engineering. Many studies applied this method in groundwater pollution and original waste disposal research, contaminated soil analysis, and landfill leachate contamination sandy soil studies [20, 21, 22, 23]. The value of soil electrical resistivity depends on soil properties such as porosity, water content, saturation degree, soil particle ingredients,

shape and orientation, particle-size distribution, cation exchange capacity, ion composition, and ionic strength of soil solution [24, 25]. The electrical resistivity method has been applied in different kinds of saturated and unsaturated soil in geo-environmental engineering. The resistivity characteristics of unsaturated soils was quantitatively analyzed and the resistivity formula by generalized Archie law that applied in the assessment of soil electrical conductivity was founded by Shah and Sing [26]. The electrical resistivity structure model of unsaturated clay soil based on the experimental results was established by Zha [27]. Literature shows that electrical resistivity can be used as a timely and cost-effective way to evaluate the physical and mechanical properties of cement-stabilized heavy metal-contaminated soils [28, 29, 30]. It is expected that the electrical resistivity method can be widely used for checking/controlling the quality of soil–cement in practice [31].

The aim of this paper is to evaluate the related properties of copper-contaminated sand before and after S/S using the electrical resistivity method. Specially, the paper addresses two aspects: 1) the electrical resistivity of copper-contaminated sand under different current frequency, water content, copper content and porosities; 2) the unconfined compressive strength (UCS) and electrical resistivity of cement-treated copper-contaminated sand.

MATERIALS AND METHODS

International Organization for Standardization (ISO) standard sand was used in this study. Figure 1 shows the particle-size distribution of sand which was classified as medium-sized soil. $Cu(NO_3)_2 \cdot 3H_2O$ with analytic grade was used to form contaminants. The reagent was bought from Taiyuan Jiejin Chemicals Company Limited in China. The copper-contaminated sand with representative ratios were selected to be stabilized. Ordinary Portland cement with strength grade of 42.5 was used as the S/S blinder.

Copper-contaminated sands with different copper ion contents, water contents, and porosities were artificially prepared in the laboratory by mixing DI water, ISO standard sand and $Cu(NO_3)_2 \cdot 3H_2O$ in designed ratios. The test parameters are shown in Table 1. The predetermined sands were put into a polyvinyl chloride column in diameter of 10mm and height of 20mm by compaction test in five layers. Two circular copper electrodes were placed on the top and bottom sides of the specimen. The electrical resistance was measured using TH2828A Digital Bridge, which was connected with two copper electrodes of the specimen.

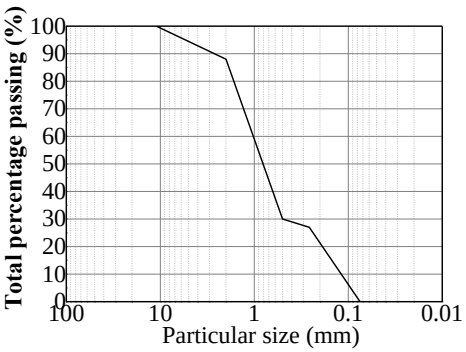

FIGURE 1
Particle-size distribution of standard sand

Cement and standard sand were mixed in the mixer evenly to produce cement sand. Copper nitrate solution with designed concentration was poured into the cement sand and was sufficiently mixed; The mixtures were then compacted into standard steel molds with the dimensions 70.7×70.7×70.7 mm. The test parameters are shown in Table 2. After standing without disturbance in the molds for 2 days, the specimens were carefully removed from the mold and cured under a constant temperature of 20°C and relative humidity of 95%. At the curing time of 3, 7, 14, 28, and 60 days, the electrical resistance and UCS of the specimens were tested.

The electrical resistance was measured by TH2828A Digital Bridge and then was converted into electrical resistivity by following equation:

$$\rho = RA/L \quad (1)$$

TABLE 1
Test parameters of copper-contaminated sand

Parameters	Values
Porosity (%)	33; 36; 39; 41
Water content (%)	3; 6; 9; 12
Current frequency (Hz)	50; 10^2; 5×10^2; 10^3; 5×10^3; 10^4; 5×10^4; 10^5; 5×10^5; 10^6
Copper content (mg/kg)	0; 10; 25; 50; 100; 250; 500; 1000; 2500; 5000

TABLE 2
Test parameters of cement-treated copper-contaminated sand

Parameters	Values
Dry soil: cement: water (mass ratio)	1:0.15:0.173
Copper ion content (mg/kg)	0; 50; 100; 250; 500; 1000; 2500
Current frequency (Hz)	50; 10^2; 5×10^2; 10^3; 5×10^3; 10^4; 5×10^4; 10^5; 5×10^5; 10^6
Curing age (d)	3;7;14;28;60

where R is the electrical resistance of the specimen, A is the area of the electrode piece, L is the distance between the two electrode pieces, ρ is the electrical resistivity of the sand.

The cement-treated sand samples were crushed and the specimen particles were sieved through a 9.5 mm diameter mesh. The leaching toxicity test was conducted according to a standard solid waste-extraction procedure while the copper content analyzed by Shanghai Jingke instrument 361MC atomic absorption spectrophotometer [32].

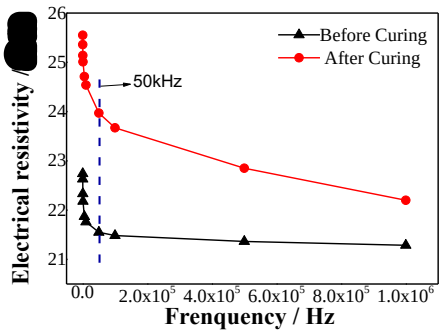

FIGURE 2
The relationship between the electrical resistivity and current frequency

RESULTS AND DISCUSSION

Relationships between electrical resistivity and current frequency. In comparison with direct current (DC), the alternating current (AC) test can avoid the undesirable influences caused by dynamic phenomenon and electrochemical phenomena in the DC test. The current frequency is an important factor for electrical resistivity. As shown in Figure. 2, the electrical resistivity decreased with the increase of current frequency in both copper-contaminated sand and solidified copper-contaminated sand. 50kHz was a turning point of the changing trend. When the current frequency was less than 50kHz, the electrical resistivity decreased quickly. In current frequency higher than 50kHz, the electrical resistivity decreased slowly and tended to be stable. This was similar to the change situation of water and saturated sand with current frequency [33]. Thus 50kHz was chosen as the current frequency of electrical resistivity in this research.

Electrical resistivity characteristics of copper-contaminated sand. The relationships between the electrical resistivity and the copper ion content under different water contents and porosities are shown in Figure 3. It can be seen that the electrical resistivity decreased with the increase of copper ion content. When the copper ion content was less than 250mg/kg, the electrical resistivity was very sensitive to the copper ion content. That is, a small change in copper ion content could lead to dramatic change in electrical resistivity. When the copper ion content was higher than 250mg/kg, the influence of the copper ion content caused on the electrical resistivity of copper-contaminated sand would be obviously smaller, and the trend gradually tended to be stabilized. This is because the conductivity of copper-contaminated sand is mainly determined by the conductivity of the pore solution. As the water content remains constant, the number of charged ions in the pore solution is the main factor that can determine the conductivity of the pore solution. The increase of copper ion content can lead to an increase of charged ions in the pore solution that can improve the conductivity of copper-contaminated sand and reduce the electrical resistivity. When the copper ion content reaches a certain value and the number of charged ions reach a saturation state, the influence of the copper ion content caused on the electrical resistivity is reduced and the electrical resistivity gradually become stable [24, 34].

The relationships between the electrical resistivity and the copper ion content can be fitted as follows:

$$\rho = a_1(1+c)^{b_1} \quad (2)$$

where ρ is electrical resistivity of copper-contaminated sand (Ω•m); c is copper ion content (mg/kg); a_1 and b_1 are the fitting parameters.

Table 3 shows the fitting parameters of relationships between copper ion content and the electrical resistivity. Since b_1 is very close, the average value of b_1 (-0.35) was chosen in this equation. Equation (2) can be expressed as follows:

$$\rho = a_1(1+c)^{-0.35} \quad (3)$$

The relationships between the electrical resistivity and the water content under different copper contents and different porosities are shown in Figures 4(a) and 4(b). It can be seen that electrical resistivity decreased with the increase of the water content. Once the water content was less than 6%, the sand was in a dry state and the electrical resistivity value had highest value. A little change of the water content can greatly influence the electrical resistivity. When the water content was higher than 9%, the electrical resistivity decreased slightly with the increase of water content. This is because the sand particles in copper-contaminated sand are of great impedance and the main conductive medium is the pore solution [35, 36]. In lower water content, there were little adsorbed solution in the sand surface, which could not form enough current paths. This resulted in the weak conductivity of copper-contaminated sand. With the water content increasing from 3% to 6%, the current paths established by the solutions gradually increases. Similarly, the conductivity also increased by reducing electrical resistivity. As the water content value exceeds 6%, most current paths were established and the influence of the water content on the electrical resistivity was less. As found by Zha,

increasing of water content changed magnitude of electrical resistivity in small values [27].

The relationships between the electrical resistivity and the water content can be fitted as follows:

$$\rho = a_2(1+w)^{b_2} \quad (4)$$

where, ρ is electrical resistivity of copper-contaminated sand (Ω • m); w is water content (%); a_2 and b_2 are the fitting parameters.

The relation between the water content and the electrical resistivity is shown in Table 4. Since all b_2 are very close, the average value of b_2 (-1.15) is chosen in this equation. Thus, Equation (4) can be expressed as follows:

$$\rho = a_2(1+w)^{-1.15} \quad (5)$$

The relationships between the electrical resistivity and porosity under different copper contents and different water contents are shown in Figures 5(a) and 5(b). It can be seen that the electrical resistivity increases with the increase of the porosity. The electrical resistance of sand particles is so large that its conductivity can be overlooked. The conductivity of copper-contaminated sand is mainly realized by the pore solution. The greater the porosity is, the looser the sand is and the less touch areas there are between the sand particles. As a result, the current paths formed by the pore solution become lesser. Then, the conductivity of the copper-contaminated sand decreases and the electrical resistivity increases [29].

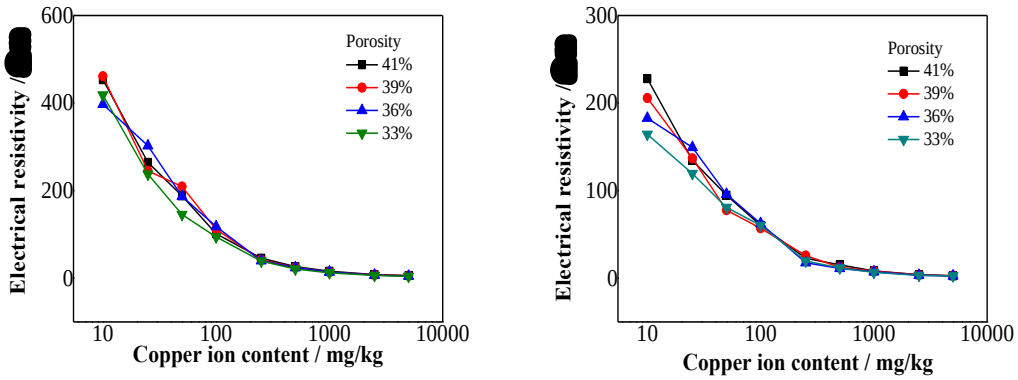

(a) *w*: 6% **(b) *w*: 12%**

FIGURE 3
The relationships between the copper ion content and the electrical resistivity of copper-contaminated sand

TABLE 3
Parameters of fitting relationships between the copper ion content and the electrical resistivity of copper-contaminated sand

w / %		6				12			
n / %		41	39	36	33	41	39	36	33
Parameters	a_1	887.91	719.41	685.7	607.4	341.48	350.02	372	26.26
	b_1	-0.39	-0.35	-0.34	-0.34	-0.33	-0.35	-0.37	-0.3
	R^2	0.96	0.91	0.92	0.88	0.9	0.93	0.95	0.88

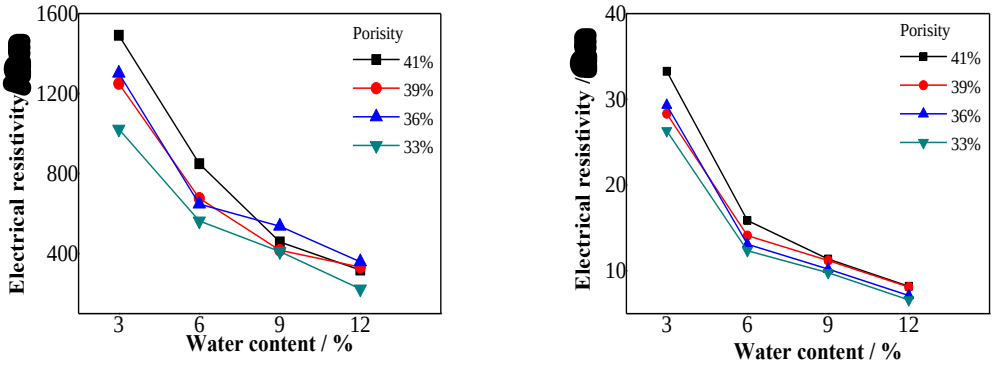

(a) *c*: 0mg/kg **(b) *c*: 1000mg/kg**

FIGURE 4
The relationships between the water content and the electrical resistivity of copper-contaminated sand

TABLE 4
Parameters of fitting relationships between the water content and the electrical resistivity of copper-contaminated sand

C / mg/kg		0				1000			
n / %		41	39	36	33	41	39	36	33
Parameters	a_2	8130.62	6123.67	5734.28	4826.37	178.91	125.82	142.33	134.25
	b_2	-1.21	-1.14	-1.08	-1.11	-1.22	-1.08	-1.17	-1.18
	R^2	0.98	0.99	0.98	0.98	0.99	0.98	0.99	0.99

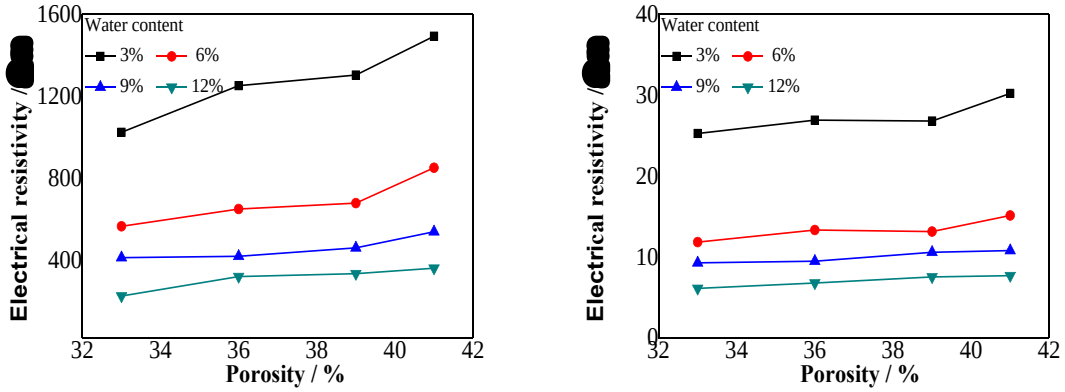

(a)*c*: 0mg/kg **(b) *c*: 1000mg/kg**

FIGURE 5
The relationships between the porosity and the electrical resistivity of copper-contaminated sand

TABLE 5
Parameters of fitting relationships between the porosity and the electrical resistivity of copper-contaminated sand

C / mg/kg		0				1000			
W / %		3	6	9	12	3	6	9	12
Parameters	a_3	3.41	0.87	4.18	0.26	0.554	0.19	0.86	0.16
	b_3	1.62	1.33	1.29	1.43	1.42	1.24	1.45	1.05
	R^2	0.91	0.8	0.72	0.79	0.97	0.88	0.87	0.94

The relationship between the electrical resistivity and the porosity can be fitted as follows:

$$\rho = a_3(1+n)^{b_3} \quad (6)$$

where ρ is electrical resistivity of copper-contaminated sand (Ω • m), n is porosity (%), a_3 and b_3 are the fitting parameters

The parameters are shown in Table 5. Since all b_3 are very close, the average value of b_3 (1.35) is chosen in this equation. Equation (6) can be expressed as follows:

$$\rho = a_3(1+n)^{1.35} \quad (7)$$

In this study, all the parameters (copper ion content, water content, porosity) can affect the electrical resistivity of copper-contaminated sand and the calculation formulas between the electrical resistivity and single variable were obtained. Based on the above three mentioned calculation equations, a calculation formula of copper-contaminated sand can be obtained in which copper ion content, porosity and water content are considered, this equation can be developed as follows:

$$\rho = 108.33(1+c)^{-0.35}(1+w)^{-1.15}(1+n)^{1.35} \quad (8)$$

In order to verify the accuracy of the electrical resistivity calculation, the electrical resistivity values of copper-contaminated sand with other copper ion contents, water contents, and porosities were tested and compared with the calculated values obtained by this formula. As shown in Figure 6, corresponding points between measured values and calculated values were in the vicinity of a straight line of 1:1, and all points are between the + 10% error line and the -10% error line. When the copper ion content is low, a few points were distributed near the ± 10% error line. By increasing copper ion content, most of the points were in the vicinity of a straight line of 1:1. It was indicate that the electrical resistivity calculation formula was close to the actual situation. Therefore, the electrical resistivity calculation formula can be applied in the detection of an actual copper ion pollution site.

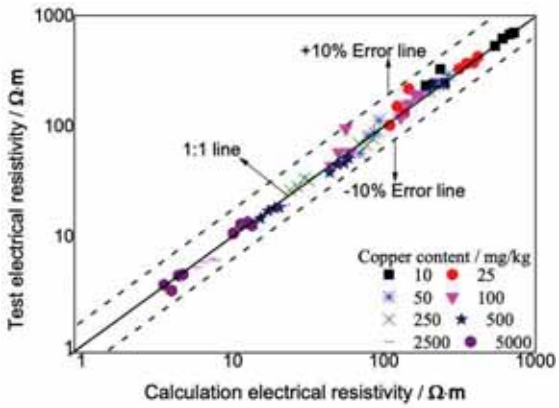

FIGURE 6
Comparison between calculated values and measured values

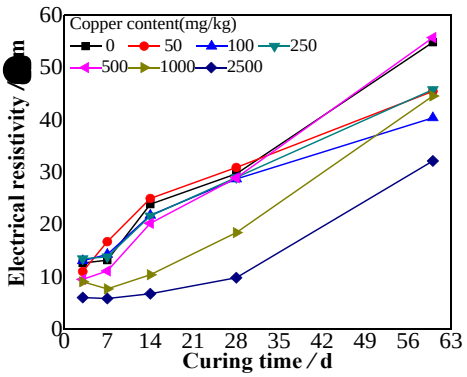

FIGURE 7
Relationship between electrical resistivity and curing time

Electrical resistivity and UCS characteristics of cement-treated copper-contaminated sand. Figure 7 shows that the electrical resistivity of cement-treated copper-contaminated sand increased with the increase of curing time. These results are similar to the case of cement-treated non-contaminated sand as reported by other researchers [37, 38]. This phenomenon is attributable to the development of hydration reaction in the cement-sand system. As the curing time increasing, more hydration products such as crystalline calcium hydroxides and precipitated copper compounds were generated. These products filled the pore spaces of sand, resulting in a denser structure and generating a more tortuous pathways for electric current. On the other hand, the free copper ions are gradually fixed by chemical fixation, adsorption and physical inclusion, which can also reduce the conductivity and increase the electrical resistivity. Consequently, all of these above actions lead to the same result: The electrical resistivity of the cement-treated copper-contaminated sand increased with the increase of curing time [39].

Figure 8 shows that the UCS of cement-treated copper-contaminated sand increased with the increase of curing time. The change tendency of UCS with curing time was very similar to the electrical resistivity. With the increase of curing time, the hydration reaction gradually enhanced and the UCS gradually increased. Further analysis showed that in copper ion content of less than 1000mg/kg, the strength increased rapidly with the increase of curing time. When the copper ion content was more than 1000mg/kg, the strength increases rapidly at first (T ≤14d), and then increases (T>14d) slowly with the increase of curing time. This showed the hydration of cement throughout the total curing process of cement-based materials, and that the cement hydration process can be influenced by the copper pollutants [40].

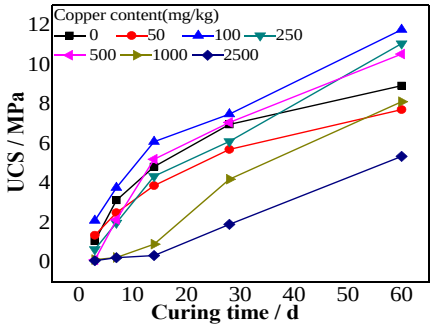

FIGURE 8
Relationship between UCS and curing time

Figure 9 shows the relationships between UCS and copper ion content. It can be seen that copper ions at a certain concentration enhanced the UCS of cement-treated sand. The maximum strength value can be obtained when the copper ion content was 100 mg/kg. The reason may be that a certain concentration copper can significantly promote the hydration reaction and the formation of ettringite. However, at high concentrations, hydration is considerably suppressed to some extent and UCS tends to reduce [37, 41]. Therefore, the curing effect was the best when the copper-contaminated sand of a copper ion concentration was solidified by cement in a practical application.

Figure 10 shows that the electrical resistivity decreases with the increase of copper content. This phenomenon can be attributed to the influence of copper concentration on hydration development. As discussed in the previous section, the generation of hydration products can be suppressed with the copper content growing, which consequently causes the downward tendency of electrical resistivity [30].

With the development of cement hydration, both UCS and electrical resistivity increased as analyzed in the previous section. The curing time and the copper content are two important factors that can influence the cement hydration. The use of electrical resistivity to represent the UCS of copper-contaminated sand can offer a monitoring means for the field of engineering.

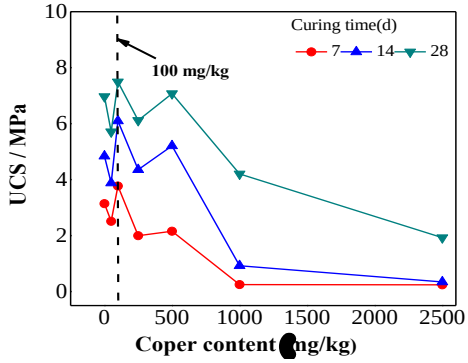

FIGURE 9
Relationships between UCS and copper ion content

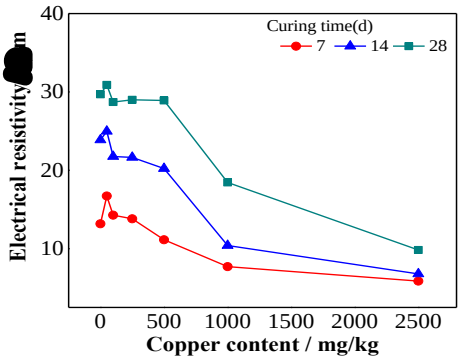

FIGURE 10
Relationships between electrical resistivity and copper content

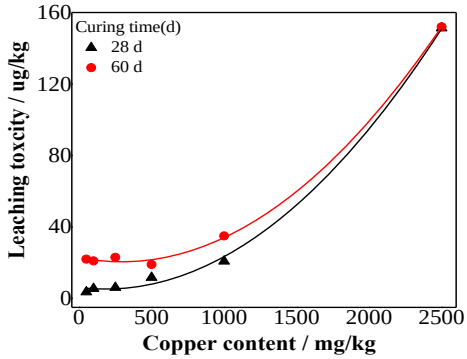

FIGURE 11
Fitting curve of copper ion content in leaching solution

Leaching toxicity of cement-treated copper-contaminated sand. Figure 11 shows the relationship between the leaching toxicity and the copper ion content of cement sand with 28 and 60 days of curing time. It can be seen that in higher copper ion content, the leaching toxicity was higher. Furthermore, the leaching toxicity was very small and increases slowly in ion content less than 1000 mg/kg. When the copper ion content was more than 1000 mg/kg, the leaching toxicity increased rapidly.

With increase of curing age, the leaching toxicity increased by comparison of day 28 and day 60 toxic leaching. This indicates that the curing effected the cement on the copper-contaminated sand may deteriorate when the curing age was relatively long. The relationship between the leaching toxicity and the copper ion content can be fitted with a good fitting degree as shown in Table 6. This fitting formula can be used to predict the leaching toxicity of the cement-treated copper-contaminated sand and the stability of S/S situation in a copper-contaminated site.

TABLE 6
Regression equation of copper ion content in leaching solution

Formula	$L = A + B_1c + B_2c^2$			
Parameter	A	B_1	B_2	R^2
28d (Curing time)	6.18	-0.00998	2.39	0.997
60d (Curing time)	22.84	-0.0158	2.34	0.998

where L is leaching toxicity; A, B_1, B_2 are fitting parameters; C is the initial copper content.

CONCLUSIONS

Based on the results, the following conclusions can be drawn.

1) The electrical resistivity of copper-contaminated sand before and after stabilization decreases with the increase of current frequency, and 50KHz is a turning point.

2) The electrical resistivity of copper-contaminated sand decreases with the increase of copper ion content and water content, but increases with the increase of porosity.

3) The electrical resistivity calculation formula was related to the copper ion content, water content and porosity was established and verified accurately.

4) When the copper-contaminated sand was stabilized by cement, the electrical resistivity and UCS increased with the increase of curing time. A high copper concentration can suppress the cement hydration, and influence the electrical resistivity and UCS.

5) The leaching toxicity increased with the increase of the copper ion content.

ACKNOWLEDGEMENTS

This study was financially supported by Shanxi Scholarship Council of China (2017-039), Scientific Research Foundation of Shanxi Province of China (201701D121121), the National Research Foundation of Korea (NRF)(2016R1D1A1A02937267) funded by the Ministry of Education, the Institute of Engineering Research at Seoul National University, China Scholarship Council.

REFERENCES

[1] Li, Z., Ma, Z., van der Kuijp, T.J., Yuan, Z., Huang, L. (2014) A review of soil heavy metal pollution from mines in China: pollution and health risk assessment. Science of the total environment. 468, 843-853.

[2] Chen, S., Wang, W.B. (2014) Study on Environmental Pollution Problems in the Copper Industry. Advanced Materials Research. 889, 1600-1603.

[3] Veli, S. and Pekey, B. (2004) Removal of copper from aqueous solution by ion exchange resins. Fresen. Environ. Bull. 13, 244-250.

[4] Lim, S.Y., Min, S.H. and Yoo, S.H. (2016) The public value of contaminated soil remediation in Janghang copper smelter of Korea. Resources Policy. 50, 66-74.

[5] Yue, Q., Lu, Z.W. and Zhi, S.K. (2009) Copper cycle in China and its entropy analysis. Resources, Conservation and Recycling. 53(12), 680-687.

[6] Medyñska-Juraszek, A. and Kabala, C. (2012) Heavy metal pollution of forest soils affected by the copper industry. Journal of Elementology. 17(3), 441-451.

[7] Xu, Y., Liang, X., Xu, Y., Qin, X., Huang, Q., Wang, L. and Sun, Y. (2017) Remediation of heavy metal-polluted agricultural soils using clay minerals: A review. Pedosphere. 27(2), 193-204.

[8] Li, J., Yu, G., Xie, S., Pan, L., Li, C., You, F., and Wang, Y. (2018) Immobilization of heavy metals in ceramsite produced from sewage sludge biochar. Science of The Total Environment. 628, 131-140.

[9] Lu, K., Yang, X., Gielen, G., Bolan, N., Ok, Y.S., Niazi, N.K., Xu, S., Yuan, G., Chen, X., Zhang, X., Liu, D., Song, Z., Liu, X., and Wang, H. (2017) Effect of bamboo and rice straw biochars on the mobility and redistribution of heavy metals (Cd, Cu, Pb and Zn) in contaminated soil. Journal of environmental management. 186, 285-292.

[10] Glasser, F.P. (1997) Fundamental aspects of cement solidification and stabilisation. Journal of Hazardous Materials. 52(2-3), 151-170.

[11] Hills, C.D. and Pollard, S.J. (1997) The influence of interference effects on the mechanical, microstructural and fixation characteristics of cement-solidified hazardous waste forms. Journal of Hazardous Materials. 52(2-3), 171-191.

[12] Zhou, X., Zhou, M., Wu, X., Han, Y., Geng, J., Wang, T., Sha W., Hou, H. (2017) Reductive solidification/stabilization of chromate in municipal solid waste incineration fly ash by ascorbic acid and blast furnace slag. Chemosphere. 182, 76-84.

[13] Li, J. and Poon, C.S. (2017) Innovative solidification/stabilization of lead contaminated soil using incineration sewage sludge ash. Chemosphere. 173, 143-152.

[14] Liao, X., Yan, X., Ma, D., Zhao, D., Sun, L., Li, Y., Fei, Y., Li, P., Lin, L., Tao, H. (2018) The Research and Development of Technology for Contaminated Site Remediation. In: Luo Y., Tu C. (eds.) Twenty Years of Research and Development on Soil Pollution and Remediation in China. Springer, Singapore. 785-798.

[15] Paria, S. and Yuet, P.K. (2006) Solidification–stabilization of organic and inorganic contaminants using portland cement: a literature review. Environmental reviews. 14(4), 217-255.

[16] Yin, C.Y., Mahmud, H.B., and Shaaban, M.G. (2006) Stabilization/solidification of lead-contaminated soil using cement and rice husk ash. Journal of hazardous materials. 137(3), 1758-1764.

[17] Du, Y.J., Jiang, N.J., Liu, S.Y., Jin, F., Singh, D.N. and Puppala, A.J. (2013) Engineering properties and microstructural characteristics of cement-stabilized zinc-contaminated kaolin. Canadian Geotechnical Journal. 51(3), 289-302.

[18] Eker, G. and Pinarli, V. (2018) Immobilization of Heavy Metals in Waste Phosphate Coating Sludge Using Kiln Dust as Portland Cement Substitute. Civil Engineering and Architecture. 6(2), 65-70.

[19] Archie, G.E. (2003) The electrical resistivity log as an aid in determining some reservoir characteristics. SPE reprint series, 9-18.

[20] Chambers, J.E., Kuras, O., Meldrum, P.I., Ogilvy, R.D. and Hollands, J. (2006) Electrical resistivity tomography applied to geologic, hydrogeologic, and engineering investigations at a former waste-disposal site. Geophysics. 71(6), B231-B239.

[21] Han, L.H., Liu, S.Y. and Du, Y.J. (2006) New method for testing contaminated soil-electrical resistivity method. Chinese Journal of Geotechnical Engineering. Chinese Edition. 28(8), 1028.

[22] Kim, Y.S., Oh, M.H. and Park, J. (2009) Analysis of resistivity data obtained from cone penetrometer in contaminated soil layers. Environmental geology. 58(6), 1309-1317.

[23] Guo, X.J., Wu, S.J. and Ma, Y.Y. (2012) Quantitative investigation of landfill-leachate contaminated sand soil with electrical resistivity method. Chinese Journal of Geotechnical Engineering. 34, 2066-20.

[24] Chen, L., Du, Y.J., Liu, S.Y. and Jin, F. (2010) Evaluation of cement hydration properties of cement-stabilized lead-contaminated soils using electrical resistivity measurement. Journal of Hazardous, Toxic, and Radioactive Waste. 15(4), 312-320.

[25] Cai, J., Wei, W., Hu, X., and Wood, D.A. (2017) Electrical conductivity models in saturated porous media: a review. Earth-Science Reviews. 171, 419-433.
[26] Shah, P.H. and Singh, D.N. (2005) Generalized Archie's law for estimation of soil electrical conductivity. Journal of ASTM International. 2(5), 1-20.
[27] Zha, F.S., Liu, S.Y. and Du, Y.J. (2010) Prediction of matric suction of unsaturated soil based on electrical resistivity. J. Rock and Soil Mechanics. 31(3), 1003-1008.
[28] Wei, X. and Li, Z. (2006) Early hydration process of Portland cement paste by electrical measurement. Journal of materials in civil engineering. 18(1), 99-105.
[29] Liu, S.Y., Du, Y.J., Han, L.H. and Gu, M.F. (2008) Experimental study on the electrical resistivity of soil–cement admixtures. Environmental Geology. 54(6), 1227-1233.
[30] Chu, Y., Liu, S., Wang, F., Cai, G. and Bian, H. (2017) Estimation of heavy metal-contaminated soils' mechanical characteristics using electrical resistivity. Environmental Science and Pollution Research. 24(15), 13561-13575.
[31] Dong, X., Zhang, S., Su, N., Huanf, X. and Bai X. (2015) Effects of contaminated soil on electrical resistivity and strength of cemented soil." Tumu Gongcheng Xuebao/China Civil Engineering Journal. 48(4), 91-98.
[32] HJ/T300-2007: (2007) Solid waste-extraction procedure for leaching toxicity-acetic acid buffer solution method. Beijing Standards Press of China, China.
[33] Liu, X.F., Qiu, B., Liu, D., Zhang Y. and Dong, X.Q. (2014) On Ac resistivity characteristics of saturated sand, Journal of Taiyuan University of Technology. 45(5), 653-656.
[34] Liu, S.Y., Du, Y.J., Chen, L., Liu, Z.B. and Jin, F. (2010) Application of Electrical Resistivity for Cement Solidified/Stabilized Heavy Metal Contaminated Soils. In: Chen, Y., Zhan, L., Tang, X. (eds.) Advances in Environmental Geotechnics. Springer, Berlin, Heidelberg, 259-264.
[35] Samouëlian, A., Cousin, I., Tabbagh, A., Bruand, A. and Richard, G. (2005) Electrical resistivity survey in soil science: a review. Soil and Tillage research. 83(2), 173-193.
[36] Pandey, L.M.S., and Shukla, S.K. (2019) Detection of leachate contamination in Perth landfill base soil using electrical resistivity technique. International Journal of Geotechnical Engineering. 3, 249-260.
[37] Ouki, S.K. and Hills, C.D. (2002) Microstructure of Portland cement pastes containing metal nitrate salts. Waste management. 22(2), 147-151.
[38] Qiao, X.C., Poon, C.S. and Cheeseman, C.R. (2007) Investigation into the stabilization/solidification performance of Portland cement through cement clinker phases. Journal of hazardous materials. 139(2), 238-243.
[39] Vincent, N.A., Shivashankar, R., Lokesh, K.N. and Jacob, J.M. (2017) Laboratory Electrical Resistivity Studies on Cement Stabilized Soil. International scholarly research notices. 2017, 15p.
[40] Zha, F.S., Liu, J.J., Cui, K.R. and Xu, L. (2012) Utilization of cement for solidification/stabilization (s/s) of heavy metal contaminated soils. Disaster Advances. 5(4), 1574-1577.
[41] Du, Y.J., Liu, S.Y., Liu, Z.B., Chen, L., Zhang, F. and Jin, F. (2010) An overview of stabilization/solidification technique for heavy metals contaminated soils. In: Chen, Y., Zhan, L., Tang, X. (eds.) Advances in Environmental Geotechnics. Springer, Berlin, Heidelberg. 760-766.

Received: **29.06.2018**
Accepted: **20.02.2019**

CORRESPONDING AUTHOR

Junboum Park
Department of Civil and Environmental Engineering,
Seoul National University,
Seoul – Korea

e-mail: junbpark@snu.ac.kr

© by PSP Volume 28 – No. 4/2019 pages 2816-2824 Fresenius Environmental Bulletin

ASSESSMENT OF AQUIFER RECHARGING USING DAMS IN TERMS OF GEOTECHNICAL CHARACTERIZATION AND HYDROGEOLOGICAL CONDITIONS IN ARID REGIONS

Mustafa Can Canoglu*

Sinop University, Faculty of Engineering and Architecture, Environmental Engineering Department, 57000, Osmaniye Village Nasuhbasoglu District, Sinop, Turkey

ABSTRACT

Under favour of advancing pumping technologies, groundwater is utilized all around the world for many purposes such as agriculture, potable water supply, industry etc. Due to the benighted use of groundwater, irreparable damages are occurred in phreatic surfaces. To recover the decreased groundwater level water retaining structures are widely used for aquifer recharge. In this study, feasibility stage design of groundwater recharge Wadi Keed dam (Bahla, Sultanate of Oman) was assessed considering hydrogeological conditions and geotechnical parameters of dam location and proximity. Within this context, field, office, and laboratory works had been conducted. Field works consist of a drilling program, excavation of trial pits and in-situ tests such as falling head permeability tests and Lugeon tests. The laboratory works had been performed on the core samples handled from the drill-holes and the soil samples obtained from trial pits. In context of office studies, the results obtained from field and laboratory works had been evaluated and the recharge dam was designed based on the geotechnical properties and hydrogeological conditions of dam location. In this regard, Wadi Keed dam is optimized for a groundwater recharge purpose based on the geotechnical and hydrogeological data. It is predicted to percolate 400 000 m^3 water per year for recharging the Bahla aquifer and this percolation will uplift 8 m the phreatic surface around Bahla City.

KEYWORDS:
Aquifer recharging, Geotechnical characterization, Environmental Justice, Infiltration characteristics, Bahla Aquifer, Wadi Keed Dam

INTRODUCTION

Rapid increase in population due to the unforeseeable refugee influx in a very short period of time caused a notable demand on water in Middle East [1]. This situation reveal the importance of effective use water resources for agricultural irrigation, and domestic use. Especially in semi-arid and arid regions groundwater resources are widely utilized and the acute increased water demand have caused important decrease of phreatic surface and well yields. A number of dramatic environmental disasters occur due to the decrease of groundwater level such as disappear of lakes, endemic species, landslide triggering etc. Apart from these, the natural disaster risks by uncontrolled urbanization such as flood is an invisible negative effect of the acute population increase especially in arid regions. To achieve these problems, a multipurpose engineering approach which consist of a water retaining structure (aquifer recharge dam) in Bahla city is applied in order to recharge the Bahla aquifer and protect the city from flood disaster.

Aquifer recharging is an engineering work which should be well planned and requires a detailed knowledge of hydrogeology. Artificial recharge systems and aquifer recharging are studied by many researchers [2 - 7]. Various techniques of aquifer recharging such as bank filtration, dune filtration, percolation tank, rainwater harvesting and underground dam have been noted by many researchers [8]. The main advantages of the aquifer recharge are the economic yield and safety potable water supply.

One of the water accumulation technique is the construction of dam. Dams are studied by many researchers in terms of geotechnics and hydrogeology from different perspectives such as grout curtain optimization, natural structural materials, landsliding, liquefaction etc. [9 - 25]. In fact, dams as water retaining structures are mainly used techniques for water storage all around the world such as Atatürk Dam (Turkey), Keban Dam (Turkey), Al Wehdah Dam (Jordan), Douera Dam (Algeria), Berke Dam (Turkey) etc. However, the environmental impacts of these dams negatively affect the local communities in terms of social, economic and civil life. Finding also a suitable dam axis location consists of complex engineering processes. Apart from these, the cost of feasibility, planning and application stages of a dam is too much. In addition, for arid and semi-arid regions such as Oman, long term water accumulation in dams is not efficient and productive due to the evaporation losses and

precipitation regime. The risk of terrorist attacks (such as attack on the dam embankment which can lead a sudden discharge or mixing a hazardous substance to the dam reservoir) is also a weak point of dams.

The objective of this study is to project an aquifer recharge dam for arising the groundwater level and increase the well yields of Bahla Aquifer which is over-exploited. In this region, rainfall cause flooding generally due to the unstable precipitation regime. The root engineering idea behind the projection of Wadi Keed dam which is planned to be located in the upstream of Bahla city is to impound the surface runoff and reducing the flow rate. With this reduction of flow rate it is planned to be protected from flood disaster and to infiltrate the retarded surface water. In infiltration excess runoff phenomenon the flow rate and the percolation amount are inversely proportional. For this reason, reduced flow rate in Wadi Keed Valley will lead to recharge Bahla aquifer and arise the groundwater level around Bahla City.

Within the context of this study, office pre-studies, field pre-studies, field studies and drilling program, laboratory studies, and detailed office works have been conducted. A suitable dam axis was found with the use of aerial photographs and 1/25 000 scaled topographical map with office pre-studies. Within the field pre-studies detailed geology of the study area and the borehole locations to be drilled are determined. Based on these works a drilling program is followed and the in-situ tests have been conducted within field studies. The laboratory works have been performed on the core samples handled from the drill-holes. Ultimately, the feasibility stage design of the Wadi Keed Dam for aquifer recharging was assessed in terms of geotechnical characterization and hydrogeological conditions of the studied site.

GENERAL CHARACTERISTICS OF STUDY AREA

Project area is located in Bahla City, North Sultanate of Oman. The Wadi Keed dam which is planned to be constructed for aquifer recharging and flood protection purposes is projected to construct on Keed River, Wilayat Bahla, Al-Dakhiliyah Governorate. The dam axis is planned to be located at 4.5 km northwest of Bahla Settlement. Transport to the study area is provided by asphalt road for four seasons (Figures 1 and 2).

The terrain is characterized by the Batinah coastal plains between the gulf of Oman on the east and the piedmonts with increasing relief towards the west. The N – S trending Oman Mountain range lie further west of the piedmonts. The highest elevation is 1100 m in the western mountains. The main drainage flows from West to East and feed the aquifers in Batinah coastal plains. The groundwater level surveys conducted in the boreholes drilled in the study area show that the phreatic surface varies between 12 – 15m depth from the soil surface in the study area. This finding indicates that the effect of rainfall on the groundwater level fluctuations is not prepotent because of the high flow rate of surface runoff and infiltration characteristics of the existing soil. Limited agricultural lands exist in gentle slopes which are irrigated by groundwater while extensive desert and sand dunes cover the highest and steepest elevations.

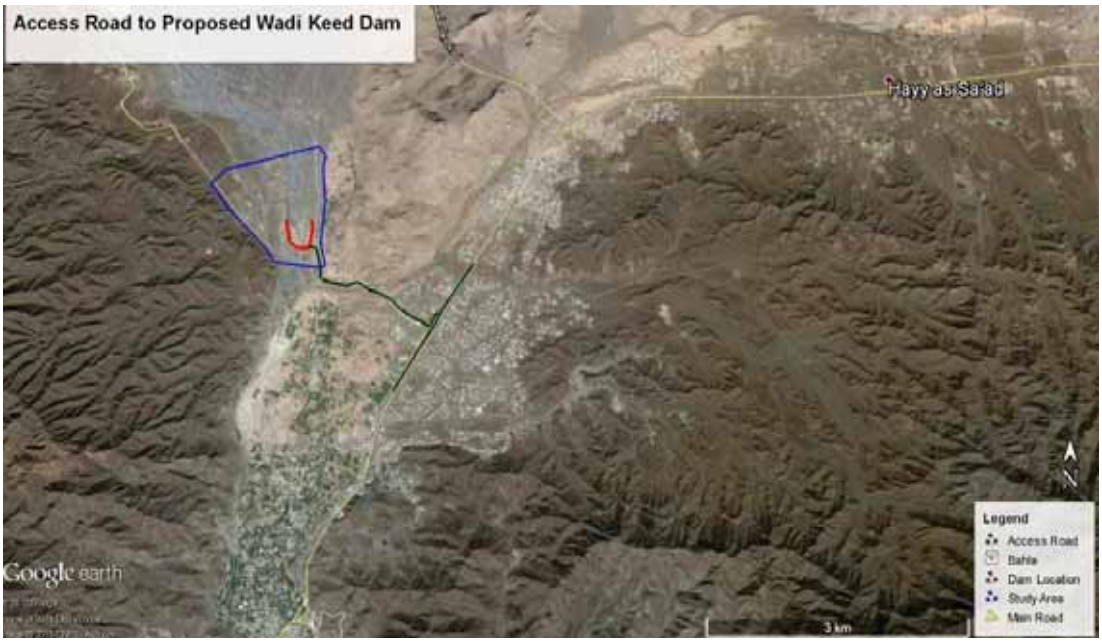

FIGURE 1
Location map of the study area (Google Earth, 2015)

FIGURE 2
General views of study area

The climate can be defined as arid or semi- arid which is also known as desert climate. The weather is generally hot and dry. The mean annual rainfall of this climate is 70 mm/year with an unstable precipitation regime. Due to the mountainous topography of the study area, the moisture income from Red Sea becomes sudden and abundant precipitation on the windward sides of the mountain and generally leeward slopes persist dry. The study area is located trough the windward side of the Hajar Mountain chain which cause flood hazards due to the sudden and abundant precipitation regime.

Geological Setting of Study Area. The topography of Oman is dominated by a west -east oriented mountain chain in the north of the country (Figure 3). This chain is known as the Hajar Mountains, comprises elevations of up to 3000 m and stretches from Musandam Peninsula in the north to Ras al Hadd in the southeast. The arcuated mountain chain is bordered by huge alluvial fans to the north and south. The Batinah coastal plain in the North of the country is composed of gravel and sand, eroded from the adjacent Hajar Mountains. The mountains form a dome structure representing basement cored anticlines. Jebel Akhdar, Jebel Nakhl and the Saih Hatat culminations form geological windows, which allow insight down to the pre-Mesozoic and partly pre- Paleozoic basement.

The terrain is characterized by the Batinah coastal plains between the gulf of Oman on the east and the piedmonts with increasing relief towards the west. The N – S trending Oman Mountain range lie further west of the piedmonts. The highest elevation is 1100 m in the western mountains. The main drainage flows from West to East and feed the aquifers in Batinah coastal plains.

The Oman Mountains constitute a composite hill range, uplifted during two major tectonic events/ cycles. The Eoalpine cycle of late Permian to late cretaceous age resulted in the building of Eoalpine belt. The Alpine cycle led to the building of the present day Oman Mountains which superposed on the earlier Eoalpine Mountains. The Alpine Oman Mountain belt, extending along the north eastern edge of the Arabian platform for over 700 Km, from the Musandam peninsula in the north to the Batain coast in the south east, was uplifted by the end of Miocene.

In the Wadi Keed Dam axis location Paleozoic, Mesozoic and Cenozoic aged geological units are dominantly observed. Permian aged Tectonized Harzburgites (Hz) are founded in base of stratigraphic array. Tectonized Harzburgites is covered discordantly by Late Cretaceous aged Ophiolites (Pd) and Upper Cretaceous aged Conglomerates (Cg). Finally, Quaternary aged Alluvium deposits (Qal) cover all these units discordantly (Figure 3).

In the study area Quaternary is represented by the Alluvium Deposits (Qal) and Clay Deposits. The Alluvium Deposits are made of quaternary gravels (pebbles & cobbles) present in the active streams throughout the Dam area. The origin of fluvial sediments are peridotite and limestone gravels and sand of different sizes ranging between 1-40 cm. These sediments are considered to be efficient to infiltrate the groundwater for aquifer recharging. There are partial clay deposits observed around the quaternary sediments which are potentially residual soil. The Quaternary deposits represent more than 30% of the total mapped area.

Comprising the Eastern part of the proposed Dam site (Left Bank of Wadi Keed Dam), the cemented gravels and sand forms the conglomerate (Cg) rock unit. Mainly consisting of 30 cm size gravels and sand size sediments. The cementing matrix is mostly calcareous. The conglomerate is made of limestone, dolomites, chert and shale, derived from the Hawasinah Mountains at the northern and eastern part of the proposed dam site. This rock unit occupies about 25% of the total Dam area. This sediments are considered to be efficient for groundwater storage.

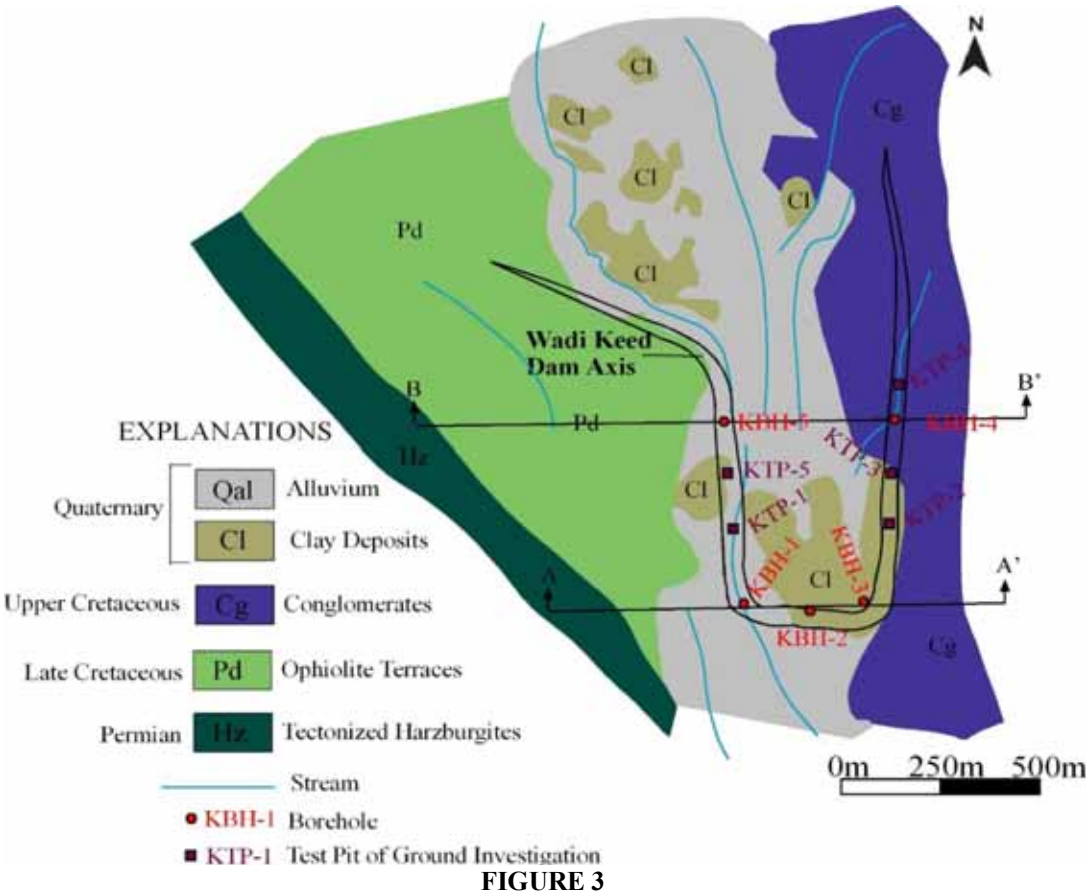

FIGURE 3
Geology map of the dam axis location and surrounding

The Ophiolite Terraces lie at the vicinity of the tectonized mountain chain, the gravels are of different sizes ranging in size between 40 cm- sand size. The origin of this unit mainly consists of Harzburgite, dunite and other sedimentary rocks gravel that occupy about 30% of the total study area. This rock unit forms the Western bank of the proposed dam (Right Bank of Wadi Keed Dam). These sediments are also considered to be efficient for groundwater storage.

This rock unit is the lower part of the ophiolite sequence, and occupies vast areas at the upstream of the Dam site. The Harzburgite is highly weathered fragile rocks, and subject to erosion by wind and water. It forms the Western Edge of the Dam site, it is anticipated that this rock unit extends in the subsurface to form the bed rock under the Quaternary sediments.

GEOTECHNICAL CHARACTERIZATION

Wadi Keed Dam body is projected as clay core homogenous earth fill dam with a crest length of 2356 m. The height of dam from thalweg is 8.7 m and from the foundation is 10.7 m. The maximum water elevation of the reservoir area is 584.8 m and any spillway, sluice, cofferdam, grout curtain were not designed due to the groundwater recharge purpose of the dam. The Wadi Keed Dam body is extended over large area to increase the infiltration pattern and cross 4 different geological units (Figure 3).

Because of the heterogeneity of ground conditions in Wadi Keed Dam axis in terms of bearing capacity and hydraulic conductivity, a number of geotechnical and hydrogeological works have been conducted in the study area. In order to enlighten the ground condition, a drilling program including in-situ tests was followed. Within this context, 5 boreholes and 75 m total depth of drilling were performed and 5 test pits for foundation investigations were excavated along the Wadi Keed Dam axis (Figure 3).

In the drilled boreholes standard penetration tests, falling head permeability tests and Lugeon tests were carried out as in-situ tests. The core samples obtained from the boreholes and the soil samples handled from the trial pits have been subjected to the laboratory tests for the hydrogeological and geotechnical characterization of the study area. Based on these studies the geological description and geotechnical properties of the subsurface material encountered in the boreholes for each depth interval are shown in Table 1. In addition, the A-A' and B-B' subsurface profiles mentioned in Figure 3 was determined (Figure 4).

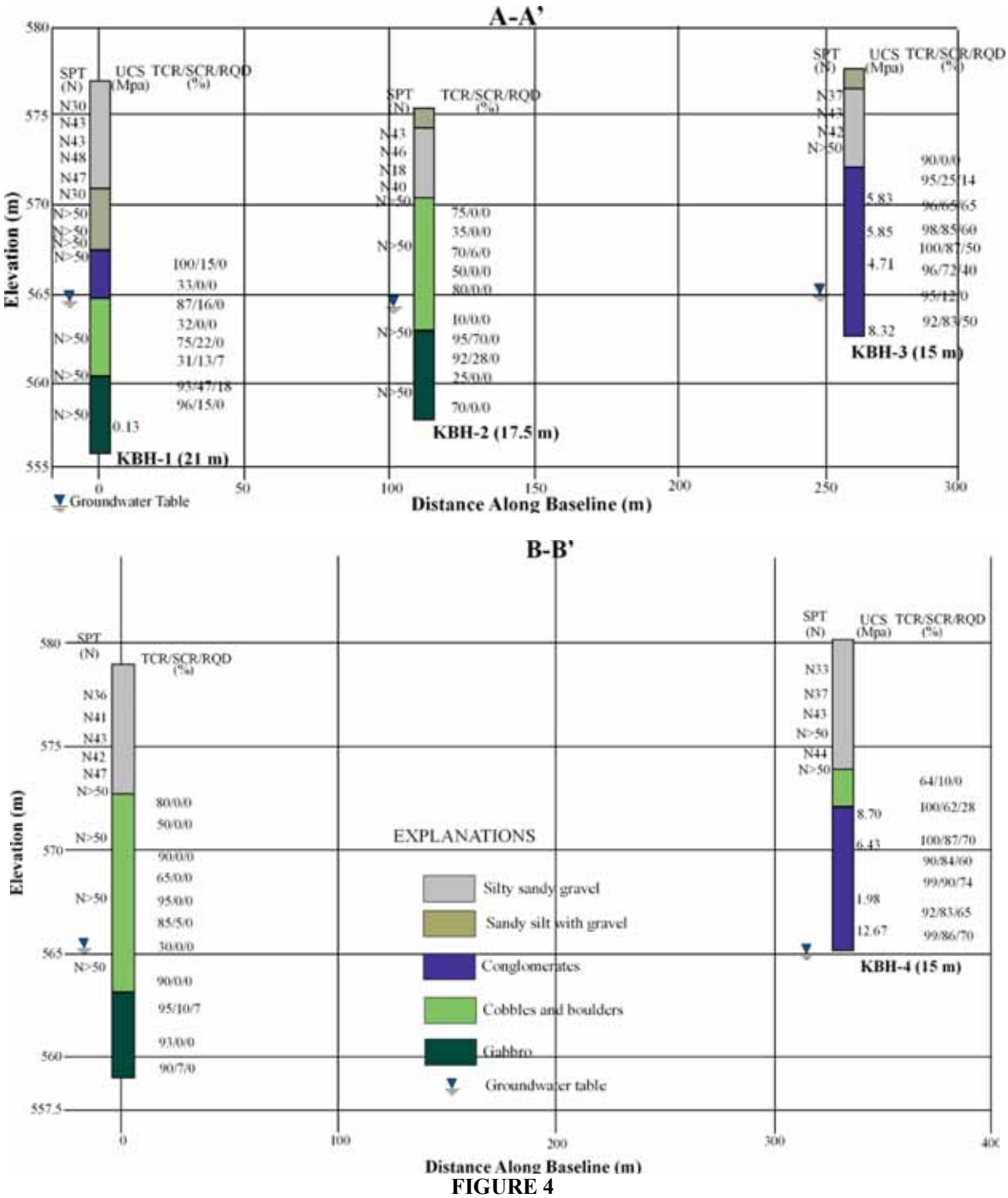

FIGURE 4
Generalized subsurface profiles of A-A' and B-B'sections

The maximum dry density of the core and soil samples obtained from field studies varies between 2.00 – 2.18 g/cm^3 based on the standard proctor tests and the optimum moisture contents varies between %3.90 – %9.80. The Unconfined Compressive Strength (UCS) of the core samples shows that the ground is weak. The UCS values varies generally between 1 – 13 kg/cm^2.

HYDROGEOLOGICAL CONDITIONS AND GROUND INFILTRATION CHARACTERISTICS

The principal aim of Wadi Keed Dam is to transfer the surface water into the subsurface with reducing the flow rate. For this purpose, the ground permeability and infiltration characteristics of the study area should be enlighten by hydrogeological investigations. To determine the permeability of alluvium and soil like material falling head permea-

bility tests have been conducted. For the permeability of rock units Lugeon tests have been performed. These tests are realized in ground investigation boreholes drilled on dam axis.

Lugeon test is an in-situ test applied in a borehole with the purpose of hydraulic conductivity determination of rock masses under variable hydraulic heads [26]. Lugeon test is called as water pressure test and packer tests also. The application of Lugeon test in Turkey is generally performed with test intervals of 2 m to 5 m. Relevant to this matter, Akyuz [27] mentioned that engineering judgement should be considered as for the permeable rock masses, the test interval could be diminuted down to 1m to reflect the heterogeneous character of the formation, contrarily, for impermeable rock masses the test interval could be raised up until 10 m due to the uniform and homogeneous character of rock medium.

The Lugeon tests performed under field studies were carried out on the rock formations at the depths specified by the engineering judgements. The Lugeon test comprises of the measurement of the volume of clear water that can escape from an uncased section of borehole in a given time under a given pressure. The flow is confined between known depths by means of packers- two packers in the double packer test and between one packer and the bottom of the borehole in the single packer test. In all the boreholes double packer test method was used as specified by Akyuz [27]. The results of the Lugeon tests are shown in Table 2 and in that table the equivalence of hydraulic conductivity of Lugeon values are calculated based on the method proposed by Canoglu and Kurtulus [10].

TABLE 1
Geotechnical summary of ground material for each boreholes

Depth (From Sea Level in m)		Thickness (m)	Borehole ID	Geological Description	Summary of Test Results	Material Classification
From	To					
577.03	567.5	9.53	KBH-1			
575.48	570.48	5	KBH-2	Brownish grey slightly silty to silty, sandy to very sandy fine to medium GRAVEL	Standard Penetration Test N results: 18 to >50	Relative Density: Medium dense to very dense
577.74	573.36	4.38	KBH-3			
580.27	573.92	6.35	KBH-4			
578.94	572.63	6.31	KBH-5			
567.5	560.53	6.97	KBH-1			
570.48	562.98	7.5	KBH-2	Light brown to grey Pebble, Cobble and Boulder originated from various rocks	Rock Quality Design (RQD) (%): 0	Strength of Rock (SR): Granular material
573.36	572.24	1.12	KBH-3			
573.92	572.27	1.65	KBH-4			
572.63	562.94	9.69	KBH-5			
572.24	562.74	9.5	KBH-3	Brownish grey CONGLOMERATE	RQD (%): 0 - 74 UCS (kg/cm^2): 1.98 - 12.67	SR: Very weak to weak
572.27	565.27	7	KBH-4			
560.53	556.03	4.5	KBH-1	Greenish grey to dark grey GABBRO, moderately to highly weathered, fractures are close to extremely close spaced.	RQD (%): 0 - 18 UCS (kg/cm^2): 0.13	SR: Extremely weak to locally very weak
562.98	557.98	5	KBH-2			
562.94	558.94	4	KBH-5			

TABLE 2
The results of Lugeon tests and the material types

Borehole ID	Test Interval (From Ground Level in m)	Lugeon Values	Hydraulic Conductivity Equivalence (m/s)	Material Type
KBH-1	17.00 - 18.00	36.8	3.79E-02	GABBRO
KBH-1	19.00 - 20.00	27.5	2.83E-02	GABBRO
KBH-2	13.50 - 14.50	54.5	5.63E-02	GABBRO
KBH-2	15.50 - 16.50	69.3	7.18E-02	GABBRO
KBH-3	7.50 - 8.50	177.8	1.86E-01	CONGLOMERATE
KBH-3	10.00 - 11.00	130.6	1.36E-01	CONGLOMERATE
KBH-3	13.00 - 14.00	139.4	1.45E-01	CONGLOMERATE
KBH-4	8.50 - 9.50	82.5	8.55E-02	CONGLOMERATE
KBH-4	11.00 - 12.00	80.2	8.31E-02	CONGLOMERATE
KBH-4	13.50 - 14.00	57.7	5.97E-02	CONGLOMERATE
KBH-5	16.50 - 17.50	25.3	2.60E-02	GABBRO
KBH-5	18.50 - 19.50	14.4	1.47E-02	GABBRO

TABLE 3
Test results of falling head permeability tests

Borehole ID	Test Interval (From Ground Level in m)	Hydraulic Conductivity (m/s)
KBH-1	3.00 - 4.00	3.61E-05
KBH-1	6.50 - 7.50	2.89E-05
KBH-2	1.50 - 2.50	6.57E-06
KBH-2	3.50 - 4.50	3.40E-06
KBH-2	7.50 - 8.50	3.12E-05
KBH-3	1.50 - 2.50	7.22E-06
KBH-3	3.00 - 4.00	9.17E-06
KBH-4	1.50 - 2.50	2.63E-05
KBH-4	4.00 - 5.00	3.61E-05
KBH-5	2.00 - 3.00	5.50E-06
KBH-5	4.50 - 5.50	4.90E-06
KBH-5	9.00 - 10.00	3.61E-05

In addition to the Lugeon tests, falling head permeability tests have been performed in order to determine the hydraulic conductivity of the soil type material. In falling head permeability test the pressure in the borehole is increased by introducing water into it, commonly referred as falling head or inflow test to assess the permeability of the soil/rock. Subsequent monitoring is realized at given time intervals with respect to head drop. The tests were carried out in the selected boreholes at selected depths with the consideration of engineering judgement as for the Lugeon tests. The results of the falling head permeability test results are shown in Table 3.

Determination of Infiltration Rate. The infiltration rate is calculated considering the vertical saturated flow in the alluviums under a hydraulic gradient based on the hydraulic conductivity of the alluviums. The vertical flow rate of groundwater can be estimated by Darcy law with the assumption of alluvium is homogenous and isotropic. Hereunder;

Darcy Law is expressed as

$Q = A \times K \times i$ Eq. 1

In this formula "Q" is the vertical flow rate of the infiltrated water, "A" is the cross-section of alluvium perpendicular to the water flux (infiltration area), "K" is the hydraulic conductivity of alluvium, "i" is hydraulic gradient. For the calculation of the flowrate it is assumed that the mean alluvium thickness is estimated to be 5 m based on the subsurface profile of the study area. In addition, the infiltration area is considered as the reservoir area of Wadi Keed Dam which is 350 000 m^2 and the hydraulic head is assumed as the free water level (9 m). Finally, the hydraulic conductivity is assumed as the average of the falling head permeability test results.

In this case,

i= hydraulic head / horizontal distance Eq. 2

= 9 m / 800 m

i = 0.01125

$A = 350\,000\ m^2$ Eq. 3

$K=1.93 \times 10^{-5}$ m/s Eq. 4

So,

$Q = 1.93 \times 10^{-5} \times 350\,000 \times 0.01125 = 0.076\ m^3/s$ Eq. 5

The total infiltration rate of the alluviums in the reservoir area of Wadi Keed dam is 76 l/s. Considering the mean phreatic surface (13 m depth approximately) the groundwater level uplift in Bahla aquifer around the study area is expected to be 8 m approximately.

RESULTS AND CONCLUSIONS

The aim of the study was to assess the geotechnical feasibility and the characterization of hydrogeological conditions of the Wadi Keed Dam which is an aquifer recharge dam. For this assessment field and laboratory works have been conducted. As a result of these works the projected Wadi Keed Dam will contribute to the groundwater 76 l/s in case of precipitation. This value would rise approximately 8 m the groundwater level of Bahla Aquifer around the study area.

The ground conditions and the geotechnical suitability of Wadi Keed Dam are investigated. It can be deduced from the UCS and the SPT tests results that the dam axis location is suitable for the construction of Wadi Keed Dam. As Wadi Keed dam will be constructed for aquifer recharge purpose, any slurry trench or grout curtain was not projected for construction. For this reason, there is a risk of piping in the alluviums under Wadi Keed Dam embankment due to the hydraulic pressure. This is an important matter which has the potential of fatal accidents. Construction of a blanket on the upstream side of the dam embankment is expected to avert the risk of piping. In addition, 2 m of stripping excavation is planned to ensure the stability of dam embankment in order to be on safe side.

Another important benefit of the Wadi Keed Dam is the prevention of the flood risk caused by the irregular precipitation regime. It is foreseen that after the construction of the Wadi Keed Dam the flowrate of the surface water would be reduced and the potential flood events which run out of patience of the local people in Bahla city would be avoided.

It is inferred that with the aquifer recharge dam projected around Bahla city, the use of groundwater in agricultural activities is augmented and the utilization of the arable lands would be more effective. In addition the water losses caused by the evaporation would be minimized with underground storage. Finally, with the contribution on the groundwater level, many environmental complications were averted.

ACKNOWLEDGEMENTS

This work is performed in the context of the "Consultancy Services for Detailed Design and Construction Supervision of Recharge Dam for Wadi Keed – Wilayat Bahla" project of the Sultanate of Oman Ministry of Regional Municipalities and Water Resources with the contribution of SuYapi Engineering and Consulting Inc. and Atlas International Engineering Consultants. The author thanks to The Sultanate of Oman Ministry of Regional Municipalities and Water Resources staff who spearhead for this article and share their engineering experiences. Many thanks, also to SuYapi Engineering and Consulting Inc. family for their exchange of ideas especially to Department of Geotechnical Services.

In addition, author thank sincerely to Arab Centre for Engineering Sciences LLC. staff for their contributions in meticulous filed and laboratory works.

REFERENCES

[1] Canoğlu, M.C. (2017) Determination of hydrologic characteristics of Sinop Demircikoy Watershed and production of monthly saturation degree maps. Bulletin of Mineral Resource and Exploration. 155, 203-212.

[2] Dillon, P. (2009) Water recycling via managed aquifer recharge in Australia. Boletín Geológico y Minero. 120(2), 121-130.

[3] Parimala Renganayaki, S. and Elango, L. (2013) A Review on Managed Aquifer Recharge by Check Dams: A Case Study Near Chennai, India. International Journal of Research in Engineering and Technology. 2(4), 416-423.

[4] Bouwer, H., Back, J.T., Olivier, J.M. (1999) Predicting infiltration and groundwater mounding for artificial recharge. Journal of Hydrologic Engineering. 4(4), 350-357.

[5] Bouwer, H. (2002) Artificial recharge of groundwater: hydrogeology and engineering. Hydrogeology Journal. 10, 121–142.

[6] Abdalla, O.A.E., Al-Rawahi, A.S. (2013) Groundwater recharge dams in arid areas as tools for aquifer replenishment and mitigation seawater intrusion: example of AI Khod, Oman. Environ Earth Sci. 69(6), 1951–1962.

[7] Ishaq A.M., Khan, A.A. (1997) Recharge of aquifers with reclaimed wastewater: a case for Saudi Arabia. Arabian Journal for Science and Engineering. 22(1C), 133–141.

[8] Dillon, P. (2005) Future management of aquifer recharge. Hydrogeology Journal. 13, 313-316.

[9] Canoğlu, M.C., Kurtuluş, B. (2016) Body Type Optimization of Water Structures and Engineering Parameters Determination of Natural Structural Materials: An Example of Kışlademirli Dam (Kütahya). Karaelmas Science and Engineering Journal. 6(2), 250-264.

[10] Canoğlu, M.C. and Kurtuluş, B. (2017) Permeability of Savcıbey dam (Bilecik) axis location and design of grout curtain. Bulletin of Mineral Research Exploration. 154, 157-168.

[11] Canoğlu, M.C. (2017) Determination of hydrologic characteristics of Sinop Demircikoy Watershed and production of monthly saturation degree maps. Bulletin of Mineral Research Exploration. 155, 203-212.

[12] Canoğlu, M.C. (2017) Deterministic landslide susceptibility assessment with the use of a new index (factor of safety index) under dynamic soil saturation: an example from Demirciköy Watershed (Sinop/Turkey). Carpathian Journal of Earth and Environmental Science. 12(2), 423-436.

[13] Canoğlu, M.C. (2018) Investigation of the Suitability of a Pipe Stock Site in Terms of Geotechnical Characterization and Engineering Design Parameters Considering the Economic Aspects. Hitite Journal of Science and Engineering. 5(2), 147-154.

[14] Canoğlu, M.C. (2018) Geotechnical investigations and geological engineering approaches in landsliding on pipelines. International Journal of Engineering Research and Development. 10(1), 12-21.

[15] Canoglu, M.C., Aksoy, H. and Ercanoglu, M. (2018) Integrated approach for determining spatio-temporal variations in the hydrodynamic factors as a contributing parameter in landslide susceptibility assessments. Bulletin of Engineering Geology and the Environment. online first. 16p.

[16] Karagüzel, R. and Kılıç, R. (2000) The effect of the alteration degree of ophiolitic melange on permeability and grouting. Engineering Geology. 57, 1–12.
[17] Ulusay, R., Tuncay, E. and Hasançebi, N. (2007) Liquefaction assessments by field-based methodologies for the foundation soils at a dam site in northeast Turkey. Bulletin Engineering Geology Environment. 66, 361–375.
[18] Gürocak, Z. and Alemdağ, S. (2012) Assessment of permeability and injection depth at the Atasu dam site (Turkey) based on experimental and numerical analyses. Bulletin Engineering Geology Environment. 71, 221–229.
[19] Uromeihy, A. and Farrokhi, R. (2012) Evaluating groutability at the Kemal-Saleh dam based on Lugeon tests. Bulletin Engineering Geology Environment. 71, 215–219.
[20] Tunar, N.Ö., Ulusay, R. and Işık, N.S. (2013) A study on geotechnical characterization and stability of downstream slope of a tailings dam to improve its storage capacity (Turkey). Environmental Earth Sciences. 69, 1871–1890.
[21] Eryılmaz Türkkan, G. and Korkmaz, S. (2015) Determination of hydraulic conductivity using analytical and numerical methods applied to well and aquifer tests. Technical Journal of Turkish Chamber of Civil Engineers. 26, 6969–6991.
[22] Aldemir, A., Yılmaztürk, S.M., Yücel, A.R., Binici, B., Arıcı, Y. and Akman, A. (2015) Analysis methods for the investigation of the seismic response of concrete dams. Technical Journal of Turkish Chamber of Civil Engineers. 26, 6943–6968.
[23] Cato, K.D. and Rogers, J.D. (2017) Failure of the Alexander Dam embankment and reconstruction using drainage mitigation on Kauai, 1930-1932. Environmental and Engineering Geoscience. 23(4), 1-21.
[24] Ekmekci, M., Kalaycioglu, N.E., Acikel, S., Namkhai, O. and Akman, S.B. (2017) Numerical simulation of uplift pressure and relief drains at a dam reservoir. Environmental and Engineering Geoscience. 23(2), 79-96.
[25] Nield, M.C. (2017) Grout Curtain construction at Bolivar Dam, Ohio. Environmental and Engineering Geoscience. 23(4), 1-16.
[26] Canoglu, M.C. (2019) Selection of suitable dam axis location considering permeability and grout curtain optimization. Environmental and Engineering Geoscience. 25(1), 15-25.
[27] Akyuz, S. (2010) Investigation of permeability features of lithologic units on Kargı dam site (Çorum). M.Sc. Thesis. Çukurova University, Institute of Natural and Applied Sciences, Adana.

Received: **18.07.2018**
Accepted: **05.01.2019**

CORRESPONDING AUTHOR

Mustafa Can Canoglu
Sinop University
Faculty of Engineering and Architecture,
Environmental Engineering Department,
57000 Sinop – Turkey

e-mail: mccanoglu@sinop.edu.tr

© by PSP Volume 28 – No. 4/2019 pages 2825-2834 Fresenius Environmental Bulletin

EVALUATION OF IN VIVO EFFECTS OF *VISCUM ALBUM L.* AND ITS CONSTITUENT *O-COUMARIC ACID* ON BILE ACID SYNTHESIZING CYPS

Tuba Ege[1,*], Ayse Mine Gencler Ozkan[2], Alaattin Sen[3], Orhan Adali[4]

[1]European University of Lefke, School of Applied Science, Lefke, Turkish Republic of Northern Cyprus
[2]Ankara University, Faculty of Pharmacy, Department of Pharmaceutical Botany, Ankara, Turkey
[3]Pamukkale University, Faculty of Sciences, Department of Biology, Denizli, Turkey
[4]Middle East Technical University, Department of Biological Sciences and Joint Graduate Program in Biochemistry, Ankara, Turkey

ABSTRACT

This research was designed to determine about the possible potency of medicinal plants *Viscum album L.* and its major polyphenolic ingredient, *o*-coumaric acid on rat liver cholesterol and bile acid metabolizing enzymes. Bioactive compounds of *V. album* extracts were identified using LC-MS technique. The water extracts of *V. album* (10 mg/kg) and *o*-coumaric acid (30 mg/kg) were injected intraperitoneally for 9 days. Then, *in vivo* effects of this plant and its major phenolic ingredient (*o*-coumaric acid) on rat liver cholesterol and bile acid metabolizing cytochromes P450s were analyzed by determining protein and mRNA expression levels using western blotting and qRT-PCR techniques, respectively. The results showed that *V. album* caused a 0.9 fold decrease in protein expression of CYP7A1 and CYP7B1, but 1.4 and 1.3 fold increases in protein expression of CYP27A1 and CYP8B1, respectively. *V. album* caused 9, 1.3 and 2.4 fold decrease in mRNA expression of CYP7A1, CYP27A1, CYP7B1, respectively, however, 4.2 fold increase in mRNA expression of CYP8B1. Injection of *o*-coumaric acid to rats resulted 0.8 fold decrease in protein expression of CYP7A1, CYP27A1, CYP8B1 and CYP7B1. However, *o*-coumaric acid caused 1.8, 1.3, 2.3 and 2.3 fold increase in mRNA expression of CYP7A1, CYP27A1, CYP8B1 and CYP7B1, respectively. According to results, even though *V. album* and *o*-coumaric acid caused fold change in protein and mRNA expressions of bile acid metabolizing CYPs, serum cholesterol levels remained unchanged. Thus, the idea can be taken about the role of this plant and its major polyphenolic ingredient in drug discovery and development.

KEYWORDS:
Viscum album L., *o*-coumaric acid, bile acids, CYP450s, medicinal plants.

INTRODUCTION

In mammals, excessive cholesterol is removed mainly through conversion to bile acids. Cytochromes P450s initiate all quantitatively significant pathways of cholesterol metabolism and bile acid biosynthesis [1, 2]. The bile acid pathway is very important in maintaining normal cholesterol levels. If cholesterol homeostasis is changed, some conditions such as atherosclerosis, cholestasis and neurological diseases can be seen because of accumulation of cholesterol in one or more compartment in the body [3].

There is a great promise towards traditional medicine such as herbal remedies or dietary supplements. European mistletoe is named as *Viscum album (VAT)* in Latin because it has white, viscous and sticky fruit [4]. *V. album* includes many active ingredients such as viscotoxins, oligo- and polysaccharides, alkaloids, flavonoids and phenolic acids (digallic and *o*-coumaric acid) [5- 9]. Due to having a huge phenolic profile, mistletoe has many different biological functions. These include anti-tumor, apoptosis-inducing, anti-oxidant, anti-mitotic, anti-bacterial, anti-viral, anti-diabetic, anti-epileptic, anti-cancer and immunomodulatory activities [10-16].

VAT and its major polyphenolic ingredients, *o*-coumaric acid (2-hydroxycinnamic acid-OCA) have been used as CAM (Complementary and Alternative Medicine). It has been very popular to research effects of total plant extract, but there is a big dilemma about using total plant extract because plants include many different polyphenolic compounds. To solve this problem, researchers began to prefer investigate polyphenolic compounds which are isolated from plants rather than use of total plant extracts.

So far, it has been generally studied anti-oxidant activity of herbs. This study was to investigate the relevance of the biosynthesis of bile acids from cholesterol and phytochemicals. The specific aims were to research and compare possible effects of *VAT* and its major ingredient OAC on rat liver cholesterol and bile acid metabolizing CYPs.

MATERIALS AND METHODS

Chemicals. Primary antibody CYP7A1 (sc-25536), CYP27A1 (sc-14835), CYP8B1 (sc-23515) and CYP7B1 (sc-26087) were purchased from Santa Cruz Biotechnology, Texas, USA. Secondary antibody AP rabbit (A3687), sodium dodecyl sulfate (SDS; L4390), sodium-potassium tartarate (S-2377), trisma base (T1503), tween 20 (P1379) were the products of Sigma-Aldrich, Germany. Nitrotetrazolium blue chloride (NBT; A1243) was obtained from AppliChem GmbH, Darmstadt, Germany. 5-bromo 4-chloro 3-indoyl phosphate (BCIP; R0821), dichlorodiphenyltrichloroethane (DDT; R0861), gene rulerTM 50 bp DNA ladder (SM0371) and pre-stained protein ladder (SM0671) were taken from Fermentas, USA.

Plant material. The location, habitat, distribution, and blooming time of *Viscum album L.* was identified based on publishes of Davis [17, 18]. The plant was collected from unpolluted field and their locations from Melikgazi Village, Pınarbaşı, Kayseri, Turkey, 1800 m altitude in August. Voucher specimen (No: AEF 25945) of *Viscum album L.* was deposited in the Herbarium of Faculty of Pharmacy at Ankara University. Air dried and powdered plant samples (50 g) were subjected to maceration in sterile ddH2O. Plant extracts obtained were filtered through Whatman filter paper, dried in freeze dryer (Christ Gamma 2-16 LSC), and weighed. The extracts of plant were gassed with nitrogen, and held in at -20°C until use for the assays.

Plant Profile. Identification and quantification of *VAT* bioactive compounds was carried out by Liquid Chromatography Mass Spectrometry (LC-MS). Mobile phase was prepared using 2 solvent systems; Solvent 1: 0.05 % Formic acid + 5 mM ammonium formate (10 mM Ammonium acetate for ellagic acid) and Solvent 2: Methanol (MS grade). The spectra of eluted samples were monitored between 200 and 500 nm. Flow rate was arranged as 0,3 ml/min., analysis length was 13 minutes with gradual mobile phase flow and injection volume was 5 µL. Standard curve was drawn based on the serial dilution of samples (0,15-0,31-0,625-1,25-2,5-5-10 ppm). Mass Spectrometry was carried out in Agilent 6460 LC-MS. After choosing MRM (Multiple reaction monitoring) as an analysis mode, gas temperature, sheath gas temperature, gas flow rate, nozzle voltage and capillary voltage were arranged to 350°C, 350°C, 10 ml/ml, 500 V and 4000V, respectively. The following pure standards were used for analysis of phenolic content of *VAT* extract; chlorogenic acid, gallic acid, caffeic acid, quercetin dehydrate and o-coumaric acid. Agilent G3793AA Mass Hunter Optimizer software was used for analysis.

Folin-Ciocalteu method [19] was used to determination of total phenolic content. *VAT* extracts were diluted in dH_2O with serial dilutions as 1 mg/ml and 2 mg/ml. 23 µl of samples was mixed with 1817 µl distillated water, 115 µl Folin-Ciocalteu reagent (dilution 1:10, v/v) and 345 µl of 15% Na2CO3 solution. Then, the mixture incubated at room temperature for 2 hours in the dark. The absorbance was measured at 765 nm using a spectrophotometer (Shimadzu). The results were expressed in mg gallic acid equivalents (GAE)/g fresh matter.

Determination of total flavonoid content was performed by colorimetric method of Chang *et al.* [20]. *VAT* extracts were diluted in dH_2O with serial dilutions as 1 mg/ml and 2 mg/ml. 10 % (w/v) sample in methanol was mixed with 1.5 mL of methanol, 0.1 mL of 10 % aluminum chloride, 0.1 mL of 1 M potassium acetate, and 2.8 mL of distilled water, and incubated at room temperature for 30 min. The absorbance of the mixture was measured at 510 nm using a spectrophotometer (Shimadzu). Total flavonoid content was calculated based on the calibration curve prepared by using catechin solutions at concentrations from 50 to 300 µg/ml.

Animals. This part of the study was carried out with the collaboration of Pamukkale University, Biology Department. Permissions of Ethical Committee were taken from Pamukkale University Experimental Animal Ethics Committees and METU. 12 weeks old healthy male Wistar Albino rats (*Rattus norvegicus*) which weighing 200-250 g were purchased from Experimental Research Department of Pamukkale University, Denizli. They were housed University Animal House in standard conditions and fed with standard diet with water and libitum. The water extracts of *VAT* and its major polyphenolic ingredients (*o*-coumaric acid-OCA) were intraperitoneally (i.p.) injected to the rats. For the experiment, animals were divided into 3 groups: **C-** Control (no injection): Rats in this group never made any application but they were kept under the same conditions with other groups during the experiment. ***VAT*:** The water extract of *Viscum album L.* was injected intraperitoneally as 10 mg/kg for 9 days. **OCA:** *o*-Coumaric acid was injected intraperitoneally as 30 mg/kg for 9 days. At the end of the treatment protocol given above and after 16 h of fasting, the rats were euthanized with decapitation. Blood was collected by heart puncture and the livers were isolated and stored at -80 °C till preparation of microsomes and S1.5 fractions.

Protein Expression. The impacts of *VAT* and its major polyphenolic ingredient (*o*-coumaric acid-OCA) on protein expressions of cholesterol and bile acid metabolizing CYP7A1, CYP27A1, CYP8B1 and CYP7B1 were determined according to the method of Towbin et al. [21] with some optimiza-

tions. Before application of Western Blot immune-detection technique, proteins were separated using SDS-PAGE (sodium dodecyl sulfate polyacrylamide gel electrophoresis) method as reported by Laemni et al. [22]. Protein samples were diluted with 4X sample dilution buffer in a ratio 1:3 (1 part buffer and 3 parts sample) to obtain 2 mg/ml of protein. Before the electrophoresis unit was connected with power supply (Bio Rad Laboratories, CA, USA) to run at 15 mA-150 V for stacking gel and 30 mA-300 V for separating gel, gel running module was put in running tank. Samples transferred from gel to PVDF membrane was carried out at 400 mA-90 V for 90 minutes in cold room. End of this process, 'blot', a membrane including transferred proteins, was obtained. The blot was incubated with primary antibody and secondary antibody. Finally, the image was photographed by a gel imaging instrument which based on a computer, (Infinity 3000, Vilber Lourmat, Marne-la-Vallee Cedex1, France) through Infinity-Capt Version 12.9 software. The density of protein bands was quantified using Image J visualization software (Scion Image Version Beta 4.0.2).

Gene Expression. The impacts of *VAT* and OCA on CYP7A1, CYP27A1, CYP8B1 and CYP7B1 gene expressions were analyzed by quantitative Real Time PCR (qRT-PCR) using Corbett Rotor Gene 6000 (Corbett life Science, PO Box 435, Concorde, NSW 2137). Quantitative Real Time PCR was carried out by using Light Cycler FastStart DNA Master^{Plus} SYBR Green I (Roche Applied Science, Basel, Switzerland). Assay was performed manufacturer's protocols. The primers were designed using NCBI and the blasts were confirmed the based on *Rottus norvegius.*

Total Cholesterol. Total cholesterol was determined in the Düzen Clinical Laboratory, Ankara. Cholesterol is found in two forms in the blood as free form or esterified form. In this method, enzymes (cholesterol esterase and cholesterol oxidase) are very specific to determine the forms of cholesterol. Cholesterol esterase converted the cholesterol esters into the cholesterol. Next, the cholesterol was oxidized by cholesterol oxidase to produce ketone cholest-4-en-3-one and hydrogen peroxide. After reaction, a colored compound obtained gave an absorbance at 570 nm. Different concentrations of standard (cholesterol) were prepared. After 45 minutes incubation of samples with enzymes, samples were compared to known concentrations of cholesterol.

TABLE 1
Quantitative LC-MS analysis of selected bioactive compounds from *VAT*; and total phenolic and flavonoid content of this plant.

Bioactive compound	*Viscum album L.*
Gallic acid	≤ 0,31 ppm
Cafeic acid	≤ 0,15 ppm
Quercetin dhydrate	≤ 0,31 ppm
Chlorogenic acid	1,0528±0,0453
o-coumaric acid	≤ 0,27 ppm
Total phenolic content	57 ±1,756 (mgGAE/g dried extract±SD)
Total flavonoid content	19,0278 ±1,2615 (mg CE/g dried extract±SD)

RESULTS

Biological compound. LC-MS chromatogram of phenolic compounds of *VAT* is presented in the chromatogram was used as a fingerprint of *VAT* and to quantify its phenolic compounds (Fig. 1). According to quantitative LC-MS analysis carried out in the present study, chlorogenic acid (1.0528 ppm) was the dominant compound in the *VAT*. Gallic acid

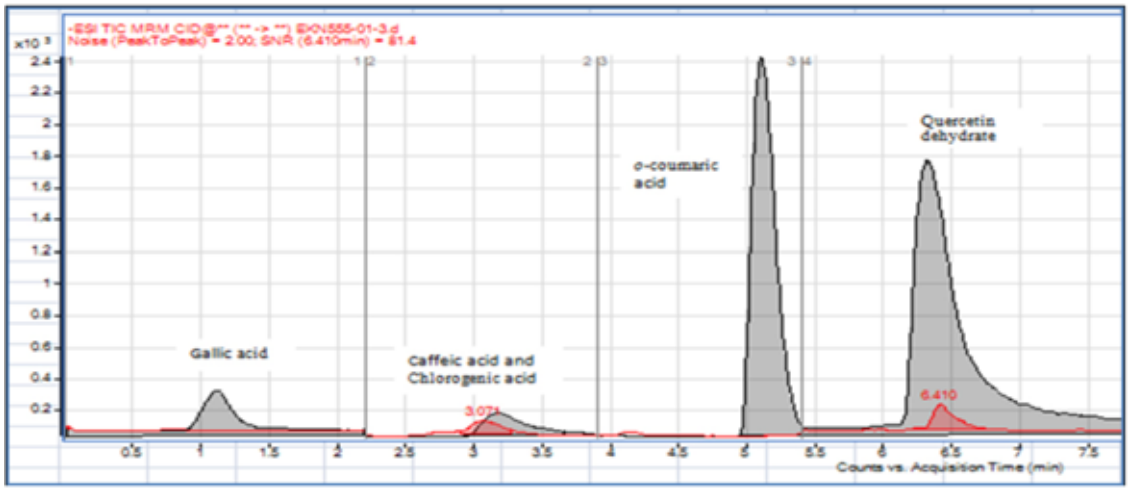

FIGURE 1
LC-MS chromatogram of *VAT* extract. Grey line shows mixture of standards (total 1.25 ppm).
Red line shows *VAT* extract (10 mg/ml).

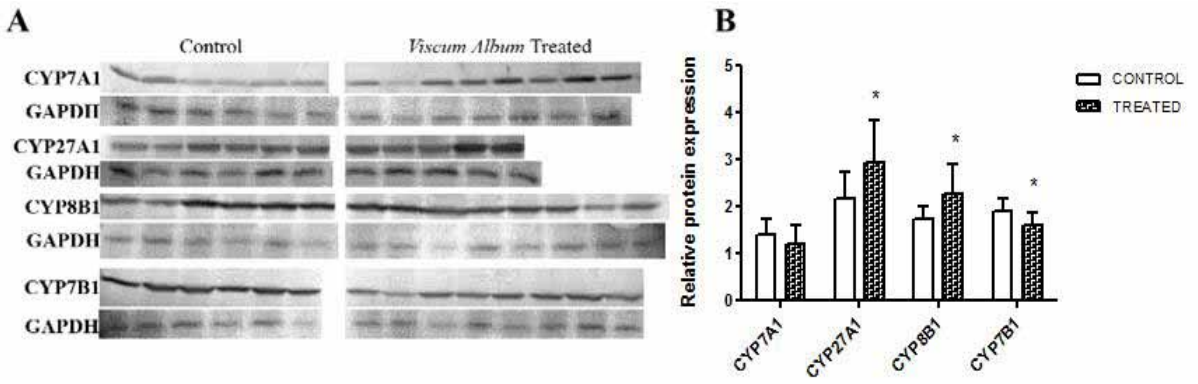

FIGURE 2

(A) Representative immunoblot of liver CYP7A1 (58 kDa), CYP27A1 (60 kDa), CYP8B1 (57 kDa), and CYP7B1 (58 kDa) proteins in experimental control and *Viscum album L.* treated animals. (B) Comparison of CYP7A1, CYP27A1, CYP8B1, and CYP7B1 protein expressions of the control (n=11) and *VAT*- treated (n=11) groups.

Band quantification was expressed as the mean ±SD of the relative intensity with respect to that of the internal control GAPDH. *Significantly different from the respective control value p<0.005.

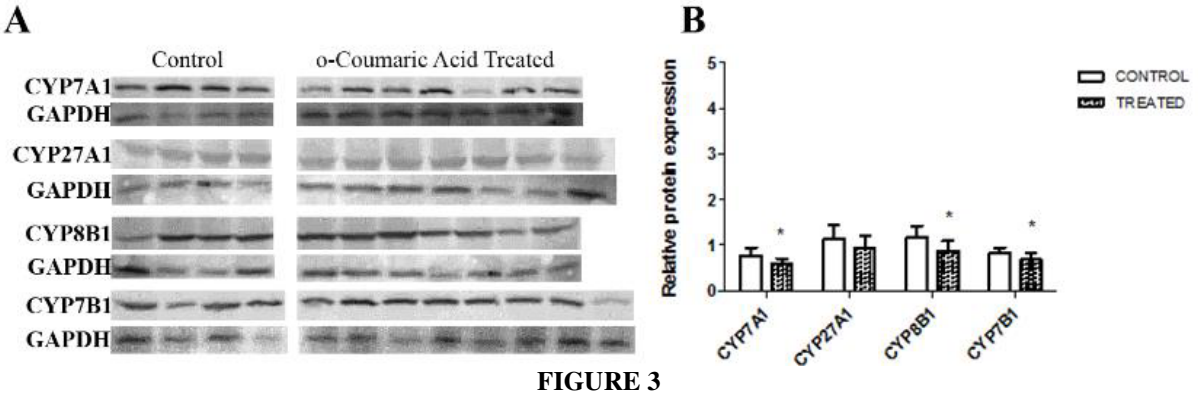

FIGURE 3

(A) Representative immunoblot of liver CYP7A1 (58 kDa), CYP27A1 (60 kDa), CYP8B1 (57 kDa), and CYP7B1 (58 kDa) proteins in experimental control and *o*-coumaric acid treatment. (B) Comparison of CYP7A1, CYP27A1, CYP8B1, and CYP7B1 protein expression of the control (n=6) and OCA-treated (n=9) groups.

Band quantification was expressed as the mean ±SD of the relative intensity with respect to that of GAPDH, used as the internal control. *Significantly different from the respective control value *p<0.05.

and quercetin dehydrate amounts were less than 0.31 ppm. Caffeic acid and OCA values were calculated less than 0.15 ppm and 0.27 ppm, respectively (Table 1). Also, the data represented in Table 1 revealed that the amount of total phenolic content of *VAT* was 57±1.756 mg GAE/g dried extract and, the result of total flavonoid of *VAT* was 19.0278 ±1.2615 mg CE/ g dried extract.

Biological activity. The effects of *VAT* and OCA on rat liver CYP7A1 (58 kDa), CYP27A1 (60 kDa), CYP8B1 (57 kDa), and CYP7B1 (58 kDa) protein expression was measured via western-blot by using glyceraldehyde 3-phosphate dehydrogenase (GAPDH) (37 kDa) as an internal control. Protein levels were compared relative to GAPDH expression. Fig. 2-A and Fig 3-A illustrated the results of Western-blot analysis of CYP proteins with GAPDH co-immunostaining. The intensity of each band was analyzed as an arbitrary unit, relative peak area (RPA), with the help of the Image J software program. The protein expressions of CYP7A1, CYP27A1, CYP8B1 and CYP7B1 in *VAT*-treated rats were significantly different from control rats (p<0.005). *VAT* caused a 0.9 fold decrease in protein expression of CYP7A1 and CYP7B1, but a 1.4 and 1.3 fold increase in protein expressions of CYP27A1 and CYP8B1, respectively (Fig. 2B). Protein expression of CYP7A1, CY8B1, and CYP7B1 in *O*AC treated rats was significantly decreased compared to control (p<0.05). *O*AC caused a 0.8 fold decrease in the protein expressions of CYP7A1, CYP27A1, CYP8B1 and CYP7B1 (Fig. 3B).

The effects of *VAT* and OCA on the mRNA expression of CYP7A1, CYP27A1, CYP8B1, and CYP7B1 was evaluated using quantitative real time PCR (qRT-PCR). Real time-PCR results of CYP7A1, CYP27A1, CYP8B1, and CYP7B1 mRNA levels are shown in Fig. 4-5. The Livak method [23] was applied to determine the mRNA expression changes of CYPs. *VAT* treatment caused

significant changes in the mRNA expressions of CYP7A1, CYP8B1, and CYP7B1. *VAT* caused 9, 1.3, and 2.4 fold reductions in mRNA expression of CYP7A1, CYP27A1, and CYP7B1 respectively, with respect to controls, and a 4.2 fold increase the expression of CYP8B1 ($p<0.05$). Relative mRNA expression of CYP7A1, CY8B1, and CYP7B1 in OCA-treated rats was significantly increased compared to control animals ($p<0.05$) (Fig. 5). OCA treatment induced a 1.8, 1.3, 2.3, and 2.3 fold increase in mRNA expression of CYP7A1, CYP27A1, CYP8B1, and CYP7B1 respectively, compared to controls and normalized with GAPDH expression as an internal reference.

Serum samples obtained from *VAT* and OCA treated rats were determined and results were given in Table 2. When cholesterol concentration of serum samples from *VAT* and OCA treated rats were compared to control animals, no significant change was found.

TABLE 2
Blood serum total cholesterol values of control, *VAT* and *O*CA treated animals.

Sample	Total cholesterol (mg/dL)
Control	70.5±1.905
Viscum album L.	61.25±2.333
o-coumaric acid	68±2.793

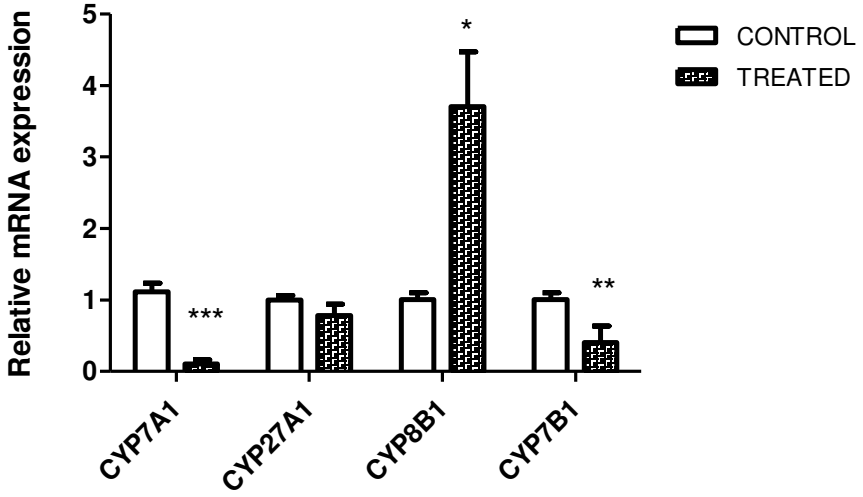

FIGURE 4
Comparison of *in vivo* effects of *VAT* on rat liver CYP7A1, CYP27A1, CYP8B1, and CYP7B1 mRNA expressions.
The quantities are expressed as mean ±SD of the relative expression.

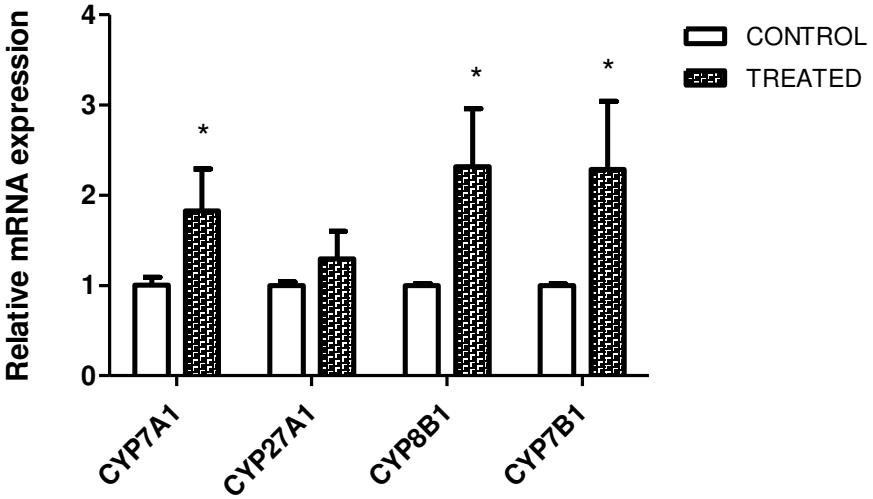

FIGURE 5
Comparison of *in vivo* effects of OCA on rat liver CYP7A1, CYP27A1, CYP8B1, and CYP7B1 mRNA expression.
The quantities are expressed as mean ±SD of the relative expression.

DISCUSSION

Until now, it has been proved that *Viscum album L.* has important pharmacological impacts. Since ancient times this plant has been used to cure of different diseases such as diabetes mellitus, dizziness, nervous tachycardia, hysteria, hypertensive headache, atherosclerosis, stroke, chorea, periarthritis, and arthritis [24 -26]. Also, since 1927, the plant has been used as a supportive element especially oak mistletoe for cancer treatment since it stimulates immune response-system [27]. According to clinical experiments, total mistletoe extracts and its isolated polyphenolic compounds have essential effects in treatment of cancer. *Viscum album* includes many bioactive compounds and we chose to work with o-coumaric acid. *o*-Coumaric acid, which also named as trans-*o*-hydroxycinnamic acid, is found in many plant products, such as vinegar, coffee, tea, beer, oats and peanuts. Researches evaluated that *o*-coumaric acid has many biological activities, such as anti-lipidemic, anti-obesity, antioxidant, and anti-carcinogenic activities [28, 29].

According to quantitative LC-MS analysis carried out in the present study, chlorogenic acid (1.0528 ppm) was the dominant compound in the *Viscum album L.* Gallic acid and quercetin dehydrate amounts were less than 0.31 ppm. Caffeic acid and *o*-coumaric acid values were calculated less than 0.15 ppm and 0.27 ppm, respectively (Table 1). Also, the data represented in Table 1 revealed that the amount of total phenolic content of *VAT* was 57±1.756 mg GAE/g dried extract and, the result of total flavonoid of *VAT.* was 19.0278 ±1.2615 mg CE/ g dried extract.

Vicaş et al. [8] worked with *Viscum album* from different host trees (*Acer campestre*, *Fraxinus excelsior*, *Populus nigra*, *Malus domestica*, and *Robinia pseudoacacia*). Gallic acid, a phenolic acid, was only found in *Viscum album* hosted by *Robinia pseudoacacia.* The mistletoe hosted by *Fraxinus excelsior* contains very high concentration of caffeic acid in leaves (13.98 µg/g dry matter) and stems (15.86 µg/g dry matter). Trans-cinnamic acid (*o*-coumaric acid), a phenolic compound, was identified in stem of *Viscum album* hosted by *Acer campestre.* Moreover, Haas et al. [6] and Materska [30] showed that quercetin, a flavanol, and its methyl derivatives founded in mistletoe, have strong antioxidant activity. Also, Condrat et al. [31] determined that quercetin was found very low concentration in mistletoe extracts (0.20 µmol/g dry matter). Luczkiewicz et al. [5], analyzed the *Viscum album* hosted by *Populus nigra*, they displayed the main component of mistletoe was chlorogenic acid (12.34 mg %). In the same research, Vicaş *et al.* [8] identified the highest total phenolic content of mistletoe hosted by *Robinia pseudoacacia* was 200.51 ± 0.00 mg GAE/g fresh matter, while the lowest value of misletoe hosted by *Malus domestica* was 176.87 ± 0.003 mg GAE/g fresh matter. The highest total flavonoid content in *Viscum album* by hosted *Robinia pseudoacaci* was determined as 21.86 mg CE/ g fresh matter whereas the lowest total flavonoid content in *Viscum album* by hosted *Malus domestica* was 0.36 mg CE/ g fresh matter. Sengül et al. [32] determined of total phenolic content of *Viscum album* as 42.29 mgGAE/g dry extract. Also, Pietrzak *et al.* [9] analyzed total phenolic and flavonoid content of *Viscum album* subsp *abietis* as 37.152 ±1.895 mgGAE/g dry extract and 9.955±0.482 mgCE/g dry extract, respectively. As a result of these experiments total phenolic and flavonoid content are correlated with LC-MS result and also our results are very similar with literature for *Viscum album* extract.

Mengarelli, et al. [33] worked with Argentinean mistletoe to investigate the effect of blood fluidity through the hemorheological behavior on treated wistar rats. The red blood cell membrane composition was changed by blood cholesterol content. Argentinean mistletoe-treatment decreased plasma cholesterol levels and increased the viscosity and reduced deformation of red blood cell. Cholesterol excretion (bile acids) and cholesterol biliary secretion also lead to reduction of plasma cholesterol level. Increment of bile acid excretion was same with bile flow increment. Later, Poruthukaren et al. [34] evaluated the anti-hypertensive effect of *Viscum album*. *Viscum album* was given patients newly diagnosed and had not used any drug for hypertension. After 12 weeks administration of mistletoe, serum total cholesterol and serum triglyceride levels was statistically evaluated. There was not any significant change of serum cholesterol level while serum triglyceride was significantly decreased. Another research about anti-hypertensive activity elucidated that *Viscum album* decreased the blood pressure in hypertensive rats [35]. Also, Avcı et al. [36] chose five plants including *Viscum album* from Turkish flora to research anti-hypercholesterolemic and antioxidant activity of these five plants. They investigated the impacts of water and ethanol extracts of plants on serum total cholesterol, triglyceride, HDL-C, LDL-C, glucose, AST and ALT concentrations in mice fed with cholesterol-rich diet. The ethanol extracts of *Viscum album* decreased the total serum cholesterol level while water extract did not affect significantly the total serum cholesterol concentration. Level of HDL was increased and, meanwhile LDL level was decreased by the ethanolic extract of *Viscum album*. Under the light of the data they suggested that ethanolic extract of *Viscum album* has a beneficial effect in the deal with atherosclerosis and cardiovascular diseases.

Sen et al. [37] investigated anti-cancer activity of OCA in human breast cancer cells. Since OCA stimulates apoptosis and tumor suppression, they suggested that OCA can be used an alternative

agent for curing of breast cancer. Sen et al. [38] continued to research anti-cancer activity of OCA and studied the impact of OCA on mRNA and protein expression of CYPs in human hepatocarcinoma cell line. They suggested that OCA induces expression of CYP2E1 and CYP1A2 which metabolize some toxic chemicals such as benzene and pyridine. Thus, it has been offered OCA may be used for treatment of some hepatic diseases. Hsu et al. [29] looked into anti-obesity impacts of *o*-coumaric acid and rutin in obese rats. Rats separated into 2 groups as obese and control. *o*-Coumaric acid and rutin were administrated 100 mg/kg and 50 mg/kg respectively. Tissues weight and serum profile of lipid, insulin, leptin, hepatic cholesterol and triacylglycerol were compared between control and obese rats. Research parameters showed a decrease in *o*-coumaric acid and rutin treated obese-rats compare to non-treated obese rats. Especially, hepatic cholesterol and triacylglycerol levels were drastically diminished. They determined the total cholesterol level as 53±5.0 mg/dl in normal rats, 76.2±13.0 mg/dl in fed with high fat diet. After administration of low and high doses of *o*-coumaric acid, total cholesterol levels were determined as 67.3±11 and 65.2±7.0 respectively. According to these results, they suggested that intake of *o*-coumaric acid and rutin may be important agent for repression of oxidative stress, hepatosteatosis and dyslipidemia in rats, and also *o*-coumaric acid can be promising parameter for the treatment of obesity.

Determination of serum total cholesterol level is one of the important biomarker for especially to identify of cardiovascular diseases. When we compared the total cholesterol level of the water extracts of *VAT* (61.25±2.333) and OCA (68±2.793) treated samples to control (70.5±1.905) in this study there was no significant change in total cholesterol levels and also our results are very similar with literature for *Viscum album* extract.

In this study, protein and mRNA expressions of bile acid metabolizing enzymes were analyzed in *VAT* and OCA acid-treated samples. According to results, *VAT* caused 0.9 fold a decrease in protein expression of CYP7A1 and CYP7B1, but 1.4 and 1.3 fold increase in protein expression of CYP27A1 and CYP8B1, respectively. *VAT* caused 9, 1.3 and 2.4 fold decrease in mRNA expression of CYP7A1, CYP27A1, CYP7B1, respectively, with respect to controls and normalized with GAPDH expression as an internal reference, however, 4.2 fold increase in mRNA expression of CYP8B1. It indicates that the decrease of CYP27A1 mRNA expression does not interpret with a proper decrease of CYP27A1 protein levels (Fig. 4).

In present study, OCA caused 0.8 fold decrease in protein expression of CYP7A1, CYP27A1, CYP8B1 and CYP7B1. OCA caused 1.8, 1.3, 2.3 and 2.3 fold increase in mRNA expression of CYP7A1, CYP27A1, CYP8B1 and CYP7B1 respectively, with respect to controls and normalized with GAPDH expression as an internal reference. There is no correlation between relative mRNA and protein expressions of OCA treated CYP7A1, CYP27A1, CYP8B1 and CYP7B1 as shown Fig. 5.

There is a correlation relative to protein and mRNA expression of CYP7A1, CYP8B1 and CYP7B1 in *VAT*-treated samples. While according to all western-blot and qRT-PCR results clearly not corroborated for OCA-treated samples. Bussing et al. [39] theorized that whole plant extract of *Viscum album* is more efficient than purified phenolic and flavonoid compounds. According to our data (Fig. 4), we obtained same conclusion. When we compared *VAT* and its phenolic compound (OCA), *VAT* is more effective than *o*-coumaric acid. European mistletoe extracts are still provoking intense discussion; hence research should be conducted with a lot of caution.

Herbs are one of the members of the inducers and/or inhibitors. It appears that in Fig. 4 and Fig. 5 when mRNA and protein expression of CYPs were compared, there was no significant correlation. The expressions of CYPs gene is regulated transcriptionally, post-transcriptionally, translationally and post-translationally. These mechanisms are important for steady-state protein concentration. There are some reasons for these poor correlation or non-correlation. Translation and protein degradation are as important as mRNA transcription and stability of the final product of protein.

The first and rate limiting enzyme of neutral pathway is cholesterol 7α-hydroxylase (CYP7A1). Bile acids can regulate cholesterol homeostasis via bile acid synthesis pathway. Bile acid synthesis is regulated by many factors, including bile acids, nutrients, diets, and hormones, especially through regulating transcription of CYP7A1 gene. Besides, many liver specific transcription factors, commonly nuclear receptors have an important role in cholesterol and bile acid metabolism [3, 40-42].

According to our protein and mRNA expression results, *VAT* repressed the CYP7A1 transcription. A mentioned above, regulating transcription of CYP7A1 gene is very important bile acid synthesis. LXR and FXR play a crucial role coordinately way on bile acid synthesis, transport and absorption in liver and intestine, and cholesterol metabolism in the liver and peripheral tissues. When cholesterol increases in liver, oxysterols activate LXRα, which stimulates conversion of cholesterol to bile acids by inducing CYP7A1 transcription. Increased bile acid synthesis and pool stimulate FXR, which inhibits CYP7A1 to decrease bile acid synthesis but stimulates BSEP (bile salt export pump) expression to excrete bile acids into bile. Thus, bile acid- regulated genes and nuclear receptors are promising target for drug development for decreasing the serum cholesterol and triacylglycerol levels, and liver and

cardio-vascular diseases [3, 40].

Nuclear receptors involved in bile acid and cholesterol metabolism RXR, LXR, FXR, PPARα, HNF4α, FTF, SHP and PXR) can regulate not only the main transcription but also feedback regulation of CYP7A1 gene and other bile acid metabolizing related enzymes [3]. For example, peroximal proliferator activator receptors (PPARs) are activated by polyunsaturated fatty acids. PPARs show a dual role in the regulating cholesterol metabolism as well as regulating of fatty acid metabolism. PPARα stimulates LXR, so LXR promotes reverse cholesterol transport pathway to liver. In the liver, PPARα induces the expression of CYP8B1 and represses the expression CYP7A1 enzyme.

Addition to nuclear receptors, there are other factors to regulate the CYP7A1 expression. Rodent model studies have established that CYP7A1 is highly regulated by physiological factors that influence hepatic bile acid biosynthesis, including cholesterol feeding, diurnal factors, and bile acids, which feedback inhibit the overall biosynthetic pathway in large part at the level of CYP7A1 gene expression. CYP7A1 is down-regulated via chenodeoxycholic acid and induced via dietary cholesterol. Moreover, the disruption of CYP7A1 gene leads to reduce of bile acid biosynthesis, so CYP7A1 gene is upregulated to compensation of bile acid synthesis. As a same way, the CYP27A1 gene expression is upregulated via cholesterol and down regulated via bile acids. Also, CYP8B1 gene is inhibited at the pretranslational level by thyroid hormone and insulin, and induced by bile acids, subsequent CYP7A1 mRNA increases.

Cholesterol homeostasis is essential for the living organisms. If cholesterol levels increase in blood, dangerous consequences can be occurred. In mammals, excessive cholesterol is removed mainly through conversion to bile acids, and only a small portion is utilized for production of steroid hormones and other endogenous compounds. Cytochromes P450 (P450s or CYPs) play an important role all quantitatively significant pathways of cholesterol metabolism and bile acid biosynthesis. Consequently, our results showed that *Viscum album L.* and *o*-coumaric acid are considerable for drug discovery and development.

REFERENCES

[1] Russell, D.W. (2003) The Enzymes, Regulation, and Genetics of Bile Acid Synthesis. Annual Review of Biochemistry. 72, 137–174.

[2] Pikuleva, I.A. (2006) Cholesterol-Metabolizing Cytochromes P450. Drug Metabolism and Disposition. 34(4), 513-520.

[3] Chiang, J.Y.L. (2002) Bile Acid Regulation of Gene Expression: Roles of Nuclear Hormone Receptors. Endocrine Reviews. 23(4), 443–463.

[4] Ergun, F., Deliorman, D. (1995) *Viscum album L.* (Mistletoe) Chemical Composition. Ankara Faculty of Pharmacy Journal. 24(2), 95-107.

[5] Luczkiewicz, M., Cisowski, W., Kaiser, P., Ochocka, R., Piotrowski, A. (2001) Comparative analysis of phenolic acids in mistletoe plants from various hosts. Acta Poloniae Pharmaceutica-Drug Research. 58(5), 373-379.

[6] Haas, K., Bauer, M., Wollenweber, E. (2003) Cuticular waxes and flavonol aglycones of mistletoes. Z Naturforsch. 58, 464-470.

[7] Vicaş, S.I., Rugin, D., Leopold, L., Pintea, A., Socaciu, C. (2011a) HPLC Fingerprint of Bioactive Compounds and Antioxidant Activities of Viscum album from Different Host Trees Notulae Botanicae Horti Agrobotanici Cluj. 39(1), 48-57.

[8] Vicaş, S.I., Rugina, D., Sconta, Z., Pintea, A., Socaciu, C. (2011b) The In Vitro Antioxidant and Anti-Proliferative Effect and Induction of Phase II Enzymes by a Mistletoe (*Viscum album*) Extract. Bulletin of University of Agricultural Sciences and Veterinary Medicine Cluj-Napoca Agriculture. 68(2), 482-491.

[9] Pietrzak, W., Nowak, R., Olech, M. (2014) Effect of extraction method on phenolic content and antioxidant activity of mistletoe extracts from *Viscum album* subsp. abietis. Chemical Papers. 68 (7), 976–982.

[10] Hajtó, T., Hostanska, K., Berki, T., Pálinkás, L., Boldizsár, F., Németh, P. (2005) Oncopharmacological perspectives of a plant lectin (*Viscum album* Agglutinin-I): overview of recent results from in vitro experiments and in vivo animal models, and their possible relevance for clinical applications. Evidence-based Complementary and Alternative Medicine. 2, 59-67.

[11] Orhan, D.D., Aslan, M., Sendogdu, N., Ergun, F., Yesilada, E. (2005) Evaluation of the hypoglycemic effect and antioxidant activity of three *Viscum album* subspecies (European mistletoe) in streptozotocindiabetic rats. Journal of Ethnopharmacology. 98, 95-102.

[12] Onay-Ucar, E., Karagöz, A., Arda, N. (2006) Antioxidant activity of *Viscum album* spp. Fitoterapia. 77, 556-560.

[13] Çetin, E.A., Özçelik, N. (2007) A poptotic mechanism of Mistletoe (*Viscum album*) extract used in the treatment of cancer. Reviews: Journal of Medical and Health Sciences. 27, 533-539.

[14] Oluwaseun, A.A., Ganiyu, O. (2008) Antioxidant properties of methanolic extracts of mistletoes (*Viscum album*) from cocoa and cashew trees in Nigeria. African Journal of Biotechnology. 7(17), 3138-3142.

[15] Choudhary, M.I, Maher, S., Begum, A., Abbaskhan, A., Ali, S., Khan, A., Rehman, S., Rahman, A. (2010) Characterization and Antiglycation Activity of Phenolic Constituents from *Viscum album* (European Mistletoe). Chemical and Pharmaceutical Bulletin. 58(7), 980-982.

[16] Lee, S., An, H., Jung, Y. W., Lee, E., Lee, H., Chio, E., An, S., Son, H., Lee, S., Kim, J., Min, K. (2014) Korean mistletoe (*Viscum album coloratum*) extract extends the lifespan of nematodes and fruit flies. Biogerontology. 15, 153–164.

[17] Davis, P.H. (1978) Flora of Turkey and the East Aegean Islands. Vol. 6, Edinburgh University Press, Edinburgh.

[18] Davis, P.H. (1984) Flora of Turkey and the East Aegean Islands. Vol. 8, Edinburgh University Press, Edinburgh.

[19] Singleton, V.L., Orthofer, R. and Lamuela-Raventos, R.M. (1999) Analysis of total phenols and other oxidation substrates and antioxidants by means of folin-ciocalteu reagent. Methods in Enzymology. P. Lester, Academic Press. 299, 152-178.

[20] Chang, C., Yang, M., Wen, H., Chern, J. (2002) Estimation of total flavonoid content in propolis by two complementary colorimetric methods. Journal of Food and Drug Analysis. 10, 178-182.

[21] Towbin, H., Staehelin, T., Gordon, J. (1979) Electrophoretic transfer of proteins from polyacrylamide gels to nitrocellulose sheets: procedure and some applications. Proceedings of the National Academy of Sciences. 76(9), 4350-4354.

[22] Laemmli, U.K. (1970) Cleavage of Structural Proteins during the Assembly of the Head of Bacteriophage T4. Nature. 227, 680-685.

[23] Livak, K.J., Schmittgen, T.D. (2001) Analysis of relative gene expression data using real-time quantitative PCR and the 2(-Delta Delta C (T)) Method. Methods. 25(4), 402-428.

[24] Murray, T.M. (1995) The Healing Power of Herbs. 2nd ed. Prima, Rocklin, CA, 253–260.

[25] Newall, C.A., Anderson, L.A., Phillipson, J.D. (1996) Herbal Medicines. Pharmaceutical Press, London, 193–196.

[26] Ohiri, F.C., Esimone, C.O., Nwafor, S.V., Okoli, C.O., Ndu, O.O. (2003) Hypoglycemic properties of *Viscum album* (Mistletoe) in alloxan induced diabetic animals. Pharmaceutical Biology. 41, 184–187.

[27] Ramm, H. (2015) Mistletoe through Cultural and Medical History: The All-Healing Plant Proves to Be a Cancer-Specific Remedy. Karger Medical and Scientific Publishers, Mistletoe: From Mythology to Evidence-Based Medicine. Translational Research in Biomedicine, Basel, Karger. 4, 1-10.

[28] Yeh, C.T., Huang, S.M., Yen, G.C. (2005) Induction of phenolsulfotransferase expression by phenolic acids in human hepatoma HepG2 cells. Journal of Agricultural and Food Chemistry. 53, 4766–73.

[29] Hsu, C., Wu, C., Huang, S., Yen, G. (2009) Phenolic Compounds Rutin and o-Coumaric Acid Ameliorate Obesity Induced by High-Fat Diet in Rats. Journal of Agricultural and Food Chemistry. 57, 425–431.

[30] Materska, M. (2008) Quercetin and its derivatives-a review. Polish Journal of Food and Nutrition Sciences. 58(4), 407-413.

[31] Condrat, D., Szabo, M.R, Crisan, F., Lupea, A.-X. (2009) Antioxidant activity of some phanerogam plant extracts. Food Science and Technology Research. 15(1), 95-98.

[32] Sengül, M., Yıldız, H., Güngör, N., Çetin, B., Eser, Z., Ercisli, S. (2009) Total Phenolic Content, Antioxidant and Antimicrobial Activities of Some Medicinal Plants. Pakistan Journal of Pharmaceutical Sciences. 22, 1, 102-106.

[33] Mengarelli, G., Alvarez, L., Wagner, M., Gurni, A., Carnovale, C. and Luquita, A. (1999) Effect of Ligaria cuneifolia (Lc) on the hemorheology parameters and on the biliary secretion on the rat. 2nd Congress of Pharmaceutical Sciences.

[34] Poruthukaren, K.J., Palatty, P.L., Baliga, M.S., Suresh, S. (2014) Clinical Evaluation of Viscum album Mother Tincture as an Antihypertensive: A Pilot Study. Journal of Evidence-Based Complementary and Alternative Medicine. 19(1), 31-35.

[35] Radenkovic, M., Ivetic, V., Popovic, M., Brankovic, S., Gvozdenovic, I. (2009) Effects of mistletoe (*Viscum album L.*, Loranthaceae) extracts on arterial blood pressure in rats treated with atropine sulfate and hexocycline. Clinical and Experimental Hypertension. 31(1), 11–19.

[36] Avci G., Kupeli E., Eryavuz, A., Yesilada E., Kucukkurt, I. (2006) Antihypercholesterolaemic and antioxidant activity assessment of some plants used as remedy in Turkish folk medicine. Journal of Ethnopharmacology. 107, 418-423.

[37] Sen, A., Atmaca, P., Terzioglu, G., Arslan, S. (2013) Anticarcinogenic effect and carcinogenic potential of the dietary phenolic acid: o-coumaric acid. Natural Product Communications. 9, 1269-1274.

[38] Sen, A., Terzioğlu, G., Atmaca, P., Çelik, G., Ozgun, O., Arslan, S. (2015) Modulatory actions of *o*-coumaric acid on carcinogen-activating cytochrome P450 isozymes and the potential for drug interactions in human hepatocarcinoma cells. Pharmaceutical Biology. 53(9), 1391-1398.
[39] Bussing, A. (1997) Mistletoe therapy and immunological research. Anti-Cancer Drugs. 8(1), 65.
[40] Davis, R.A., Miyake, J.H., Hui, T.Y. and Spann N.J. (2002) Regulation of cholesterol 7 α-hydroxylase: BAREly missing a SHP. Journal of Lipid Research. 43, 533-543.
[41] Fuchs, M. (2003) Bile Acid Regulation of Hepatic Physiology III. Regulation of bile acid synthesis: past progress and future challenges. Gastrointestinal and Liver Physiology. 284, 551–557.
[42] Li, T., Chiang, J.Y.L. (2012) Bile Acid Signaling in Liver Metabolism and Diseases. Hindawi Publishing Corporation Journal of Lipids. Article ID 754067, 1-9.

Received: **29.07.2018**
Accepted: **28.02.2019**

CORRESPONDING AUTHOR

Tuba Ege
Faculty of Health Science,
European University of Lefke,
Turkish Republic of Northern Cyprus

e-mail: tubacege@gmail.com

© by PSP Volume 28 – No. 4/2019 pages 2835-2841 Fresenius Environmental Bulletin

LAND USE PATTERN CHANGE AND FORECAST ANALYSIS OF ENERGY AND CHEMICAL INDUSTRY BASE IN THE LOESS PLATEAU

Hou Kang[1], Haihong Li[1,*], Shijun Zhao[2], Juan Wang[1], Ke Yang[1], Yue Wang[1], Doudou Han[1],Yanan Lu[1]

[1]School of Environmental and Chemical Engineering, Xi'an Polytechnic University, Xi'an,710048, China
[2]Xingtai City Environmental Protection Bureau, Xingtai, 054001, China

ABSTRACTS

The Energy and Chemical Industry Base (ECIB) in the Loess Plateau is the key area for soil erosion in the Loess Plateau. The implementation of the project of returning farmland to forests (grass) has a significant impact on the structure and pattern of land use in this region. Based on the interpretation of the TM images of the ECIB in 1997, 2004 and 2011, the GIS spatial analysis and mathematical statistics analysis methods were used to analyze temporal and spatial variation characteristics of land use. In order to better respond to the impact of land use change, the gray system dynamic model (GM) was used to predict the dynamic change of land use in the study area. The results showed that the area of woodland, grassland and building land increased significantly, but the water body, cultivated land and unutilized land area all showed a significant decrease trend. From 1997 to 2011, the *R* index of the ECIB was less than 0, indicating that the rate of land use change was small and in an adjustment period. Using this predictive model, the proportion of woodland, water body and building land in the study area would continue to increase, and the rate would be slowed down compared with the previous period. Then the area of grassland, unutilized land and cultivated land would be further reduced by 2020, and the policy factors had a greater impact on land use types and patterns.

KEYWORDS:
Land use pattern, energy and Chemical Industry Base, gray system dynamic model (GM)

INTRODUCTION

Land use change directly affects human living environment and agricultural food security, meanwhile human economic and social development plays an important role in land use [1-2]. On a global scale, land use has a significant effect on the hydrothermal cycle in the water and land cycle [3]. At the end of the twentieth century, research on land use change was jointly proposed by the International Geosphere-Biosphere Programme (IGBP) and International Human Dimensions Programme Change (IHDP), which promoted the in-depth study of the response relationship between human activities and land use [4-6]. So the ecological environment affected by land use is evaluated in the space and time, and appropriate interventions are carried out to achieve the coordinated and sustainable development of land use and ecological environment. In the past few decades, most research has focused on the causes, the results, driving factors of land use for policy makers to optimize land use [7-9]. However, there is a lack of analysis of trends in land use patterns in a typical energy and chemical area.

As one of the regions with the richest reserves of mineral resources in China, the study area has the most abundant coal and oil reserves. With the development of economy and the intensification of urbanization, large-scale energy and mineral resources have been developed, and the exploitation of large-scale energy minerals has led to rapid changes in land use. The land use pattern in this region has a huge impact on the stability of the regional ecological environment, which makes the ecological vulnerability of the study area increase, and the regional sustainable development is seriously threatened [10-11]. By analyzing the spatiotemporal variations of land use in the region, it can provide reasonable suggestions for the sustainable development of social economy and environment, and promote the rational use of regional water resources and land resources. Strengthening the monitoring of land use in the region can effectively prevent the damage caused by the unreasonable activities of human society to the ecological environment, and ensure the safety of the production in China's energy and chemical bases. At the same time, it can also improve the research on the impact mechanism of human activities on environmental change and promote research in interdisciplinary fields.

The purpose of land use prediction is to analyze the trend of future land use structure change through reasonable mathematical model, so as to provide reference for regional land use policies [12-13]. The gray model GM (1,1) is suitable for predicting regional objects with short time span and obvious changes, and can well reveal the development trend

of the predicted series[14-16]. Based on regional natural characteristics, economic and social factors, land use type should be predicted [17-18]. It is fully considering the development needs of human society production and life, and the land use in the early and present. On the basis of the type, quantitative analysis of future land use development aims to grasp the trend of future land use change and provide decision-making basis for the optimal allocation of agricultural industry. In this study, the grey system prediction model[19] was used to predict land use trends according to the result of land use interpretation from 1997 to 2011.

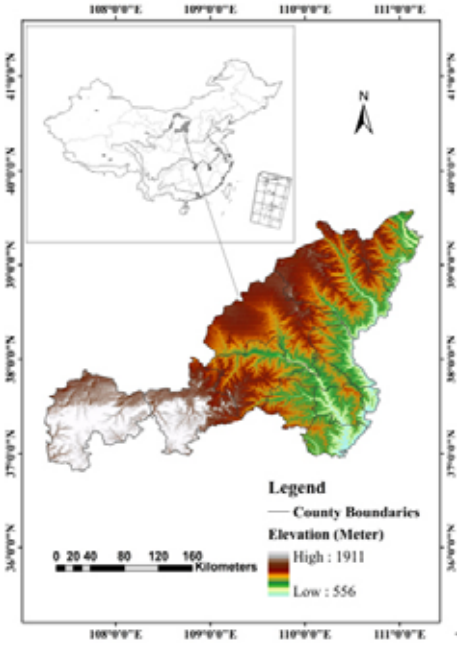

FIGURE 1
Location and elevation change of the study area

MATERIALS AND METHODS

Description of study area. Energy and Chemical Industry Base is located at 36 ° 57' to 39 ° 34'N and 108 ° 28 ' to 111 ° 15'E, which is in the boundary of Loess Plateau and Mu Us Desert. It is the gully region with the elevation descending from southwest to northeast, varying from 556 m to 1911 m. The study area covers 12 counties with an area of 43578 Km^2. This region includes Yuyang District, Fugu County, Shenmu County, Hengshan County, Jingbian County and Dingbian County Suide County, Mizhi County, Jiaxia County, Qingjian County, Wubu County and Zizhou County. The northern region is rich in mineral resources, while the southern region has a developed agricultural economy. Therefore, the ecological environment of the southern region is good for the northern region. There are large amounts of the mineral resources such as coal, gas and oil. Because of the excessive exploitation and harsh weather conditions, it is one of most fragile ecological regions, which suffer from serious soil erosion.

Data acquisition. The original data mainly involves TM5 remote sensing image. The sequence Numbers of remote sensing images are (127, 33), (127, 34) and (128,34)respectively. And the acquisition time of remote sensing image is June of corresponding year. Remote sensing data could be obtained from the Geospatial data cloud (http://www.gscloud.cn/). Meanwhile, the cloud quantity of the selected remote sensing image is controlled below 5% (Table 1).

Land use change magnitude and degree model. Based on the comprehensive analysis method of land use degree, the land use degree was divided into four levels according to the natural equilibrium state of the land natural complex under the environment of social factors, and the classification index was given respectively (Table 1) [20-21].

The quantitative expression of the land use comprehensive index [17] is:

$$L = 100 \times \sum_{i=1}^{n} A_i C_i \quad (1)$$

L is the comprehensive land use degree index of a research area; A_i is the i-level land use degree classification index of the study area, and C_i is the i-level land use degree percentage of the study area.

The expression of the land use change model [17] is as follows:

$$\Delta L_{y-x} = L_y - L_x \quad (2)$$

$$R = \frac{L_y - L_x}{L_x} \quad (3)$$

ΔL_{y-x} is the amount of change in land use; R is the rate of change in land use; L_y and L_x are the comprehensive index of land use degree of time period y and x respectively. If $\Delta L_{y-x}>0$ or $R>0$, the land use of this area is in the development period, otherwise it is in the adjustment period or the recession period (Table 2).

Predictive model. This study selected the gray system dynamic prediction model GM(n,h), which was mainly used in many research fields of social and economic development, and could well predict the future land dynamic change process [22-23]. This study used the dynamic prediction model, based on the cumulative characteristics, and then the land use system was applied to different types. The woodland, grassland, cultivated land, water body, building land and unutilized land were analyzed, and the specific model was selected as the GM (1, 1) model. The general form of the model is as follows:

TABLE 1
Remote sensing data required for the study area

Row number	Resolution	Time
12733	30m	1997.06.13 2004.05.31 2011.06.30
12734		1997.06.13 2004.05.31 2011.06.30
12834		1997.06.23 2004.06.07 2011.07.23

TABLE 2
Land use rating scale [17]

Type classification	Unutilized land level	Extensive use of land level	Intensive land use level	Urban settlement land level
Land use type	Unutilized land	Woodland, Grassland, Water body	Cultivated land	Building land
Graded index	1	2	3	4

The variable X(0)=[X(0)(i), i=1,2,...,n] is a non-negative monotonic raw data column of a certain prediction object, in order to establish a gray prediction model. Firstly, X(0) performs an accumulating sequence by generating an accumulating sequence [25-28]:

$X^{(1)}=[X^{(1)}(k),\ k=1,\ 2,\ \ldots,\ n]$

Among them

$$X^{(1)}(k)=\sum_{i=1}^{k} X^{(0)}(\mathrm{i})$$

$$=X^{(1)}(k-1)+X^{(0)}(k) \quad (4)$$

The following albinism differential equation can be established for $X^{(1)}$:

$$\frac{dX^{(1)}}{dt}+aX^{(1)}=u \quad (5)$$

That is the GM (1, 1) model.

The parameter sequence is $\hat{a}$, $\hat{a}=[a,u]^{\mathrm{T}}$, $\hat{a}$ can be solved by :

$$\hat{a}=(B^{T}B)^{-1}B^{\mathrm{T}}Y \quad (6)$$

In the formula:

B—data array;

Y—data column.

$$B=\begin{bmatrix} -\frac{1}{2}(X^{(1)}(1)+X^{(1)}(2)) & 1 \\ -\frac{1}{2}(X^{(1)}(2)+X^{(1)}(3)) & 1 \\ \cdots & \\ -\frac{1}{2}(X^{(1)}(\mathrm{n}-1)+X^{(1)}(\mathrm{n})) & 1 \end{bmatrix} \quad (7)$$

$$Y=(X^{(0)}(2), X^{(0)}(3),\ldots, X^{(0)}(n))^{\mathrm{T}} \quad (8)$$

The solution of the above whitening differential equation is (discrete response):

$$\hat{X}^{(1)}(k+1)=(X^{(0)}(1)-\frac{u}{a})\,e^{-ak}+\frac{u}{a} \quad (9)$$

k is a time series and can be taken in years, quarters or months.

It refers to a system with completely clear information as a white system and a system with unknown information as a black system. A system with some clear information and some unclear information is called a gray system [29].

RESULTS AND DISCUSSIONS

Remote sensing image interpretation and result verification. With the support of remote sensing image processing system, according to the spectral characteristics of the features and the established interpretation marks, the typical regions of each type were selected on the image, and the classification template was established. The maximum likelihood method was used to supervise and classify the image of the study area. After repeated selection, calculation, observation, verification and evaluation, until the classification results meet the required accuracy. Finally, post-processing was carried out, and then the three-stages of classification data were obtained. Through classification accuracy assessment, the overall accuracy of classification in 1997 reached 85.52%, and Kappa statistic value was 0.80. The overall accuracy of classification in 2004 reached 85.35%, and the statistical value of Kappa was 0.81, which achieved better accuracy. The overall accuracy of classification in 2011 reached 83.17% and the statistical value of Kappa was 0.79, which achieved better accuracy. Then statistical analysis of land use in 1997, 2004 and 2011 TM images of the ECBI was conducted.

Changes in the number of land use types. From 1997 to 2011, various land areas had undergone varying degrees of changes in the study area. The main changes were shown in Figure 2.

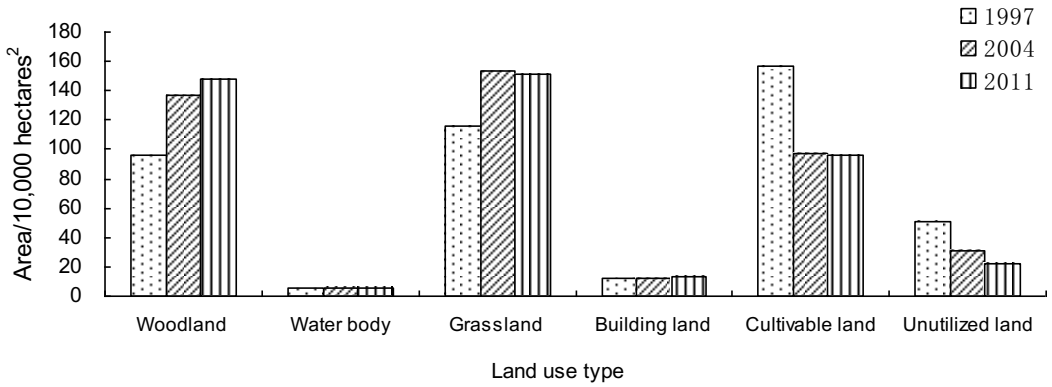

FIGURE 2
Land use area change from 1997 to 2011 in ECIB

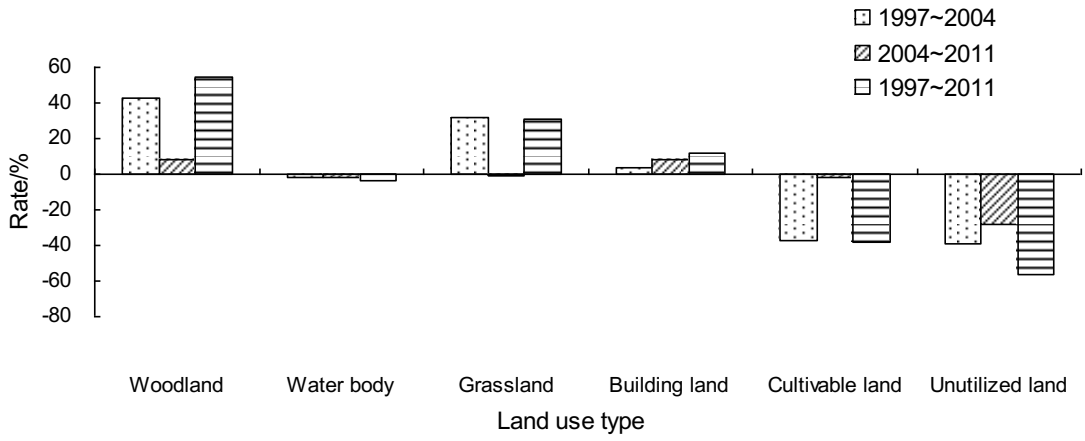

FIGURE 3
Rate of change in land use area from 1997 to 2011 in ECIB

During 1997-2011, the cultivated land in ECIB had been decreasing, and the reduction of cultivated land area in the previous period was higher than that in the later period. 1997-2004 and 2004-2011, the area of cultivated land reduced by 586667 hectares and 36600 hectares respectively. Through data analysis, the previous period of reduction was significantly larger than the latter period, mainly due to the impact of the state's policy of protecting the cultivated land, coupled with a slowdown in population growth.

From 1999 to 2004, the area of grassland had been increasing. Conversely, from 2004 to 2011, the grassland area began to decrease again. From 1997 to 2011, it increased by 372,666 hectares, and the later period decreased by 114,400 hectares. Relatively speaking, the growth rate of grassland in the early stage was relatively high. Obviously, it reached 372,667 hectares, which was second only to the increase in woodland. The area in the later period was relatively reduced, but the reduction was small.

Woodland had been increasing from 1997 to 2011. The area of woodland increased significantly from 1997 to 2004, but the increase rate was relatively slow from 2004 to 2011. It increased by 418,800 hectares and 141,133 hectares in 1997~2004 and 2004 ~2011 respectively.

The area of building land had been increasing from 1997 to 2011. However, unutilized land had been declining for the past 15 years, and the magnitude of the change had been large, during that time it was reduced by 50%. The water body area was also decreasing less, but the latter reduction was in a small state.

It can be seen from Figure 3 that the area of woodland, grassland and building land had increased significantly within 15 years. The increase areas of woodland, grassland and building land were 54.21%, 30.52%, 12.03%, respectively. The area of woodland and grassland and their proportion varied greatly from 1997 to 2004, but they changed little during the period from 2004 to 2011, which was extremely slow. The change of building land was in a growing trend, and the later period was larger than the previous period.

The water body, cultivated land and unutilized land area all showed a significant decrease trend, with the reductions being 3.66%, 38.45% and

56.53%, respectively. The area of cultivated land and unutilized land and its proportion varied greatly from 1997 to 2004. The rate of change of unutilized land was greater than that of cultivated land between 2004 and 2011. From 1997 to 2011, the proportion of water body had been decreasing, but the reduction was small.

Comprehensive land utilization analysis. The degree of land use could describe the extent to which humans and the environment interact on the land. It not only reflected the natural attributes of the land itself, but also reflected the combined effects of human factors and natural environmental factors. It could be seen from Table 3 that the land use in the study area had developed to a certain extent. The comprehensive index of land use degree had decreased from 234.01 in 1997 to 224.74 in 2004, and then increased to 225.99 in 2011. The change in comprehensive index of land use degree was 8.023. The land use index was 2, which was divided by 100, 2.34 for 1997, 2.24 for 2004, and 2.25 for 2011, indicating that the overall land use of the study area was from extensive use to intensive land use. From 1997 to 2011, the *R* of the ECIB was less than 0, indicating that the rate of change in land use during this period was small and in an adjustment period.

Land use prediction. This paper examined the land use of three spans and representative periods in 1997, 2004 and 2011, using the GM (1, 1) gray system dynamic prediction model for woodland, cultivated land, grassland, water body, building land and unutilized land to solve the prediction equation. Land use data for 2011 was obtained by using the prediction equation and compared with the results of interpretation, which was the original means of verification. Finally, the land use prediction in the ECIB was carried out (Figure 4).

The difference between each type of land data and actual data was not more than 5%, so it could be used to predict changes in land use structure in the area. According to the analysis results, the area of cultivated land, water body and unutilized land in study area would continue to decrease in the future, and the reduction of cultivated land would be small. By 2025, the area of cultivated land will be reduced by 38.15%. Grassland and building land will continue to increase the trend, but the rate of growth will be smaller than the previous period.

Since 1997, woodland has increased by 73.89% by 2025, and the grassland will increase by 21.25%. It shows that the country's policy of returning farmland to forests plays a considerable role [30], and the results are based on the assumption that the factors affecting land use remain unchanged. However, most of the factors affecting land use are always changing, such as socio-economic factors and natural factors, which lead to the changing types of land use. In the past few years, the implementation of returning farmland to forests was mainly affected by socio-economic factors and natural factors, which slowed the relative change rate of cultivated land and building land, could promote changes in other land use types.

TABLE 3
Land use comprehensive index

Index 1	L_{1997} 234.01	L_{2004} 224.74	L_{2011} 225.99
Index 2	$L_{(2004\sim1997)}$ -9.27	$L_{(2011\sim2004)}$ 1.25	$L_{(2011\sim1997)}$ -8.02
Index 3	$R_{(2004\sim1997)}$ -0.03961	$R_{(2004\sim1997)}$ 0.005562	$R_{(2011\sim1997)}$ -0.03427

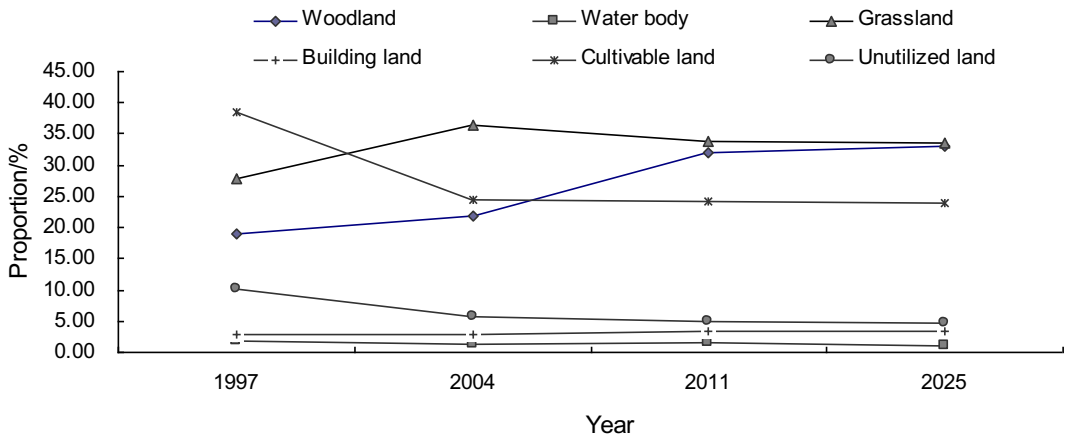

FIGURE 4
Prediction of land use in ECIB

CONCLUSIONS

From 1997 to 2011, the land use type of ECIB had undergone great changes. The area occupied by cultivated land was the largest, and the area transformed into grassland was the largest. The area of cultivated land decreased first and then increased slightly, but eventually it was in a decreasing trend. The area of grassland increased from 1997 to 2004, but gradually decreased between 2004 and 2011. The woodland had been increasing during this period; however the increase rate in the previous period was obviously greater than that in the latter stage. The building land was always growing, and the unutilized land and water body decreased between 1997 and 2011, and the area of unutilized land decreased by 50%.

Through the analysis of the comprehensive degree of land use, the results showed that the overall land use of the study area was from extensive use to intensive land use. From 1997 to 2011, the *R* of the ECIB was less than 0, indicating that the rate of change in land use during this period was in an adjustment period.

Using the grey dynamic forecasting model, by 2025, the proportion of woodland and building land in the region will continue to increase, but the speed will slow down significantly. Unutilized land, water body and cultivated land will be further reduced, and then policy factors have a greater impact on future land use types and patterns.

ACKNOWLEDGEMENTS

We are grateful for constructive comments of the Zhao Shijun (Xingtai City Environmental Protection Bureau). Then we would like to thank Prof. Tao Wendong (SUNY, USA) for the further grammar modification of the language of this manuscript.

REFERENCES

[1] Black, R., Adger, W.N., Arnell, N.W., Dercon, S., Geddes, A., Thomas, D. (2011) The effect of environmental change on human migration. Global environmental change. 21, S3-S11.

[2] Horrigan, L., Lawrence, R.S., Walker, P. (2002) How sustainable agriculture can address the environmental and human health harms of industrial agriculture. Environmental health perspectives. 110(5), 445.

[3] Raich, J.W., Schlesinger, W.H. (1992) The global carbon dioxide flux in soil respiration and its relationship to vegetation and climate. Tellus B. 44(2), 81-99.

[4] Liu, J., Liu, M., Zhuang, D., Zhang, Z., Deng, X. (2003) Study on spatial pattern of land-use change in China during 1995–2000. Science in China Series D: Earth Sciences. 46(4), 373-384.

[5] Liu, J., Zhang, Z., Xu, X. (2010) Spatial patterns and driving forces of land use change in China during the early 21st century. Journal of Geographical Sciences. 20(4), 483-494.

[6] Duran, Z., Musaoglu, N., Seker, D.Z. (2006) Evaluating urban land use change in historical peninsula, Istanbul, by using GIS and remote sensing. Fresen. Environ. Bull. 15, 806-810.

[7] Lambin, E.F., Turner, B.L., Geist, H.J., Agbola, S.B., Angelsen, A., Bruce, J.W., George, P. (2001) The causes of land-use and land-cover change: moving beyond the myths. Global environmental change. 11(4), 261-269.

[8] Lambin, E.F., Geist, H.J., Lepers, E. (2003) Dynamics of land-use and land-cover change in tropical regions. Annual review of environment and resources. 28(1), 205-241.

[9] Lambin, E.F., Rounsevell, M.D.A., Geist, H.J. (2000) Are agricultural land-use models able to predict changes in land-use intensity? Agriculture, Ecosystems and Environment. 82(1-3), 321-331.

[10] Dewan, A.M., Yamaguchi, Y. (2009) Land use and land cover change in Greater Dhaka, Bangladesh: Using remote sensing to promote sustainable urbanization. Applied Geography. 29(3), 390-401.

[11] Lambin, E.F., Meyfroidt, P. (2010) Land use transitions: Socio-ecological feedback versus socio-economic change. Land use policy. 27(2), 108-118.

[12] Pijanowski, B.C., Brown, D.G., Shellito, B.A., Manik, G.A. (2002) Using neural networks and GIS to forecast land use changes: a land transformation model. Computers, environment and urban systems. 26(6), 553-575.

[13] Seto, K.C., Kaufmann, R.K. (2003) Modeling the drivers of urban land use change in the Pearl River Delta, China: integrating remote sensing with socioeconomic data. Land Economics. 79(1), 106-121.

[14] Liu, S.F., Deng, J.L. (2000) The range suitable for GM (1, 1). Systems Engineering-Theory and Practice. 5, 022.

[15] Li, Z., Zhao, Q.G. (2009) Comparative Research about Forecast Methods of Demanded Quantity of Construction Land-Use. Surveying and Mapping of Geology and Mineral Resources. 1, 003.

[16] Zhao, L.L., Xia, L.T. (2007) Improved gray Markov SCGM (1, 1) model and its application. Journal of Hohai University (Natural Sciences). 4, 027.

[17] Liang, J., Zhong, M., Zeng, G., Chen, G., Hua, S., Li, X., Yuan, Y.J., Wu, H.P., Gao, X. (2017) Risk management for optimal land use planning integrating ecosystem services values: A case study in Changsha, Middle China. Science of the Total Environment. 579, 1675-1682.
[18] López, E., Bocco, G., Mendoza, M., Duhau, E. (2001) Predicting land-cover and land-use change in the urban fringe: a case in Morelia city, Mexico. Landscape and urban planning. 55(4), 271-285.
[19] Wu, Q., Li, H.Q., Wang, R.S., Paulussen, J., He, Y., Wang, M., Wang, B.H., Wang, Z. (2006) Monitoring and predicting land use change in Beijing using remote sensing and GIS. Landscape and urban planning. 78(4), 322-333.
[20] Liu, J., Liu, M., Zhuang, D., Zhang, Z., Deng, X. (2003) Study on spatial pattern of land-use change in China during 1995–2000.Science in China Series D: Earth Sciences. 46(4), 373-384.
[21] Song, K., Liu, D., Wang, Z., Zhang, B., Jin, C., Li, F., Liu, H. (2008) Land use change in Sanjiang Plain and its driving forces analysis since 1954. Acta Geographica Sinica-Chinese Edition. 63(1), 93.
[22] Liu, J., Liu, M., Zhuang, D., Zhang, Z., Deng, X. (2003) Study on spatial pattern of land-use change in China during 1995–2000. Science in China Series D: Earth Sciences. 46(4), 373-384.
[23] Wang, S.Y., Liu, J.Y., Zhang, Z.X., Zhou, Q.B., Zhao, X.L. (2001) Analysis on Spatial-Temporal Features of Land Use in China. Acta Geographica Sinica. 6, 631-639.
[24] Shen, L., Cheng, S., Gunson, A.J., Wan, H. (2005) Urbanization, sustainability and the utilization of energy and mineral resources in China. Cities. 22(4), 287-302.
[25] Zhang, D.H., Jiang, S.F., Shi, K. (2002) Theoretical defect of grey prediction formula and its improvement. Systems Engineering-Theory and Practice. 22(8), 140-142.
[26] Ji, M., Wang, S.X., Chen, S.Q. (2005) The application of grey theory in geophysical exploration. Progress in Geophysics. 4, 041.
[27] Mao, S., Gao, M., Xiao, X., Zhu, M. (2016) A novel fractional grey system model and its application. Applied Mathematical Modelling. 40(7-8), 5063-5076.
[28] Gao, C.Y., Gao, N. (2009) A new kind of optimized method of grey prediction model and its applications in deformation. In: Information Engineering and Computer Science, 2009. ICIECS 2009. International Conference on IEEE. 1-4.
[29] Hao, Y., Yeh, T.C.J., Gao, Z., Wang, Y., Zhao, Y. (2006) A gray system model for studying the response to climatic change: The Liulin karst springs, China. Journal of Hydrology. 328(3-4), 668-676.
[30] Hou, K., Li, X., Jing Wang, J., Zhang, J. (2016) An analysis of the impact on land use and ecological vulnerability of the policy of returning farmland to forest in Yan'an, China. Environmental Science and Pollution Research. 23(5), 4670-4680.

Received: **31.07.2018**
Accepted: **03.02.2019**

CORRESPONDING AUTHOR

Haihong Li
School of Environmental and
Chemical Engineering,
Xi'an Polytechnic University,
Xi'an, 710048 – China

e-mail: lihhcn@163.com

© by PSP Volume 28 – No. 4/2019 pages 2842-2847 Fresenius Environmental Bulletin

DETERMINING THE BEST NORMALIZATION TECHNIQUE FOR ESTIMATION USING ARTIFICIAL NEURAL NETWORKS: CASE OF BRUSHTOOTH LIZARDFISH

Levent Sangun*

University of Cukurova, Vocational School of Adana, P.O. Box 01160, Çukurova, Adana, Turkey

ABSTRACT

In this study, the bodyweight of Brushtooth lizardfish was estimated through the use of artificial neural networks (ANNs) by applying various normalization techniques to the morphometric data (total length, fork length, standard length) of the fish, and the best normalization method was selected based on the results. Z-Score, Median, Sigmoid, Min-max and D-Min-Max methods were applied in the given order, and the best MAPE and MSE values in the ANNs were calculated to be 3.187–0.001 for D-Min-Max and 3.784–0.001 for Min-max. Since the estimates obtained from the application of these two methods will turn out to be more accurate according to the results of ANN analyses, they are the methods recommended to be employed.

KEYWORDS:
Artificial Neural Networks, normalization, estimation, Brushtooth lizardfish

INTRODUCTION

The functioning of Artificial Neural Networks (ANNs) is inspired by the human brain. These programs are logical software that learn by reviewing the obtained data, that formulate results based on what they learn and that can be developed to generalize these conclusions, just like in a human [1]. They can be used in many areas as a result of such advantages they offer as, for example, their ability to be run quickly and reliably for the resolution of nonlinear complex problems; the store calculation methods within their databases; their toleration of errors; their ability to make generalizations about circumstances that they have never encountered before using known examples by means of their ability to learn; their ability to be run with missing data; and their ability to process an unlimited number of parameters [2, 3]. In modeling systems that lack classification, conceptualization, clustering or linearity, statistical analyses commonly used in aquaculture studies, such as optimization and time series, can be easily conducted through ANN [4, 5].

The training of an ANN in relation to data can be made more effective by carrying out certain processes on the inputs and outputs. Normalization methods in particular are the most significant among such processes, being employable in cases where data is recorded at different scales or codes such that they disrupt data integrity, and it may also be used to prevent the repetition, loss or insufficiency of data during the design of the database. Training a network with a non-normalized data set will both prolong the training time of the network and decrease its efficiency.

There are various normalization methods, and so researchers should attempt to estimate the best result using several methods rather than a single normalization technique in their studies [6].

Although ANN has been used in many branches of science for a long time, it has only been used in ecological modeling studies since the early 1990s [7]. Recently, it has been employed in studies of aquaculture [8, 9, 10, 11, 12, 13, 14, 15, 16] as an alternative to conventional statistical methods.

In this study, various normalization methods were applied to morphometric data (total length, fork length, standard length) of Brushtooth lizardfish, and the method that gave the best result in estimating the body weight by means of ANNs was determined.

MATERIALS AND METHODS

Brushtooth lizardfish is a Lessepsian species that originated in the Indo-Pacific region and migrated to the Mediterranean Sea via the Suez Canal [17, 18]. Having found a suitable habitat, Brushtooth lizardfish colonized almost all of the Mediterranean Sea and became a species of significant commercial value [19, 20]. It reaches a maximum length of 50 cm, and is caught in a range of 20–30 cm [21].

Artificial Neural Networks. Certain preliminary processes are carried out on the inputs and outputs of Artificial Neural Networks, rendering training more efficient. Normalization processes are carried out on raw data to ensure the preparation of a data set suitable for the training of the network. If the

raw data is not normalized, it may slow the functioning of the network. The normalization of data in multi-layered networks severely affects the performance of the network, in that it makes the distribution of the values in the data set regular.

This study was conducted on 321 *Saurida undosquamis* obtained from commercial fishermen in Karataş, Adana between 2012 and 2013. In the ANN created using this fish, the input values were total length (TL), fork length (FL) and standard length (SL), whereas the estimated output value was weight (W). The structure of the network created for the input and output data in the ANN is presented in Figure 1.

A Feed Forward Backpropagation Algorithm was used in the network, and the training function used was the Trainlm function; the learning function used was learngdm (backpropagation), and the activation functions were Tansig and Logsig. Additionally, a multi-layered network consisting of 1 to 10 strata was used [10], and the iteration was run between 300 and 800.

The output values obtained were the body weights of *Saurida undosquamis*. Of the 321 input values, 70 percent (224) were used as the training set and 30 percent (97) were used as the test set. A Matlab R2013b was employed for the application of ANN.

In order to measure the performance of the network, Mean Absolute Percentage Error (MAPE) (Equation 1) and Mean Square Error (MSE) (Equation 2) values were calculated.

$$MAPE = \frac{\sum_{i}^{N} \frac{|t_i - t_{di}|}{t_i}}{N} * 100(\%) \quad (1)$$

$$MSE = \frac{1}{N}\sum_{1}^{N}(t_i - t_{di})^2 \quad (2)$$

In which t_i is the actual value, t_{di} is the estimated/calculated value and N is the number of items of data [22, 23].

Normalization Methods. The normalization methods used in this study are Z-Score, Medyan, Sigmoid, Min-max and D-Min-Max, respectively.

Z-Score Method. The fact that some of the values in the data set are less than 0 and some are more than 0 indicates that the distances between the data, particularly the outliers, will have a strong impact on the results. The normalization of the data ensures that each parameter in the input set of the training contributes equally to the estimation of the model. The application of the Z-score method eliminates the distances between the data and reduces the outliers among the data (Equation 3).

$$\chi' = \frac{\chi_i - \mu_i}{\sigma_i} \quad (3)$$

In which χ' is the normalized data, χ_i is the input value, μ_i is the mean of the input set, and σ_i is the standard deviation of the input set [6, 24, 25].

Median Normalization. A median normalization method is applied to each sample, being unaffected by extreme deviations (Equation 4).

$$\chi' = \frac{\chi_i}{Median(a_i)} \quad (4)$$

In which χ' is the normalized data, χ_i is the input value, and $Median(a_i)$ is the median of the input set.

Sigmoid Normalization. In sigmoid normalization, data is classified between 0 and 1 or -1. There are various non-linear sigmoid functions. The applied sigmoid model is given in Equation (5).

$$\chi' = \frac{e^{\chi i} - e^{-\chi i}}{e^{xi} + e^{-xi}} \quad (5)$$

In which χ' is the normalized data, χ_i is the input value and "e" is the natural logarithm value.

Min-Max Normalization. In this method, the minimum and maximum values in a group of data are addressed, and all remaining data is normalized according to these values. The purpose is to normalize the data such that the minimum value is 0 and the maximum value is 1, and to propagate all remaining data to the range of 0–1 (Equation 6).

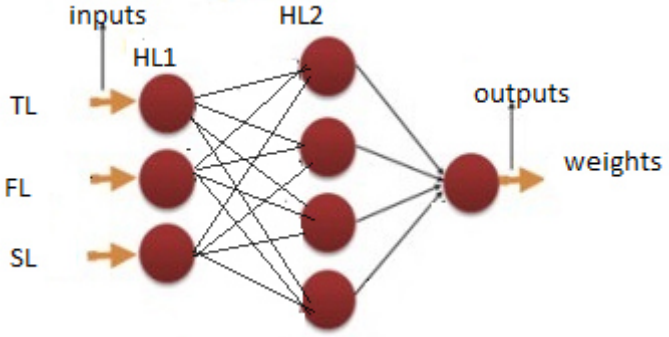

FIGURE 1
Structure of Network

$$\chi' = \frac{\chi_i - \chi_{\min}}{\chi_{\max} - \chi_{\min}} \quad (6)$$

In which χ' is the normalized data, χ_i is the input value, $\chi_{\min}$ is the minimum number in the input set and $\chi_{\max}$ is the maximum number in the input set ([6, 22, 26].

D_Min-Max Normalization. Using the equation below, all data were normalized between 0.1 and 0.9 (Equation 7).

$$\chi' = 0,8 * \frac{\chi_i - \chi_{\min}}{\chi_{\max} - \chi_{\min}} + 0,1 \quad (7)$$

In which χ' is the normalized data, χ_i is the input value, $\chi_{\min}$ is the minimum number in the input set and $\chi_{\max}$ is the maximum number in the input set [27, 28].

RESULTS AND DISCUSSION

This study identifies which normalization technique gives the best result in estimating the body weight of Brushtooth lizardfish caught in the Gulf of Iskenderun between 2012 and 2013 based on morphometric data (total length, fork length and standard length) of the fish. The activation functions used in the ANN, namely, tangent sigmoid (tansig) and logarithmic sigmoid (logsig), are given in Table 1, and the best MAPE and MSE results for the values obtained are given in Table 2.

The MAPE and MSE results of the various models are given in Tables 1 and 2. The MAPE value of 3.187 and the MSE value of 0.001 were found to be the best values in the Tansig (10,1,2) model, and the MAPE value of 3.784 and MSE value of 0.001 were found to be the best values in the Logsig (10,1,4) model. There are extremely high and low values among the inputs and outputs of ANNs, and when calculating net inputs, these outliers may result in the network being misled [27, 29]. Network can be trained without performing normalization, and can give goods results, as in the case in Table 1. This indicates that the data has an even distribution.

Comparisons of the MAPE and MSE values obtained performing normalization are given in Figures 2 and 3, respectively.

Figures 2 and 3 show the MAPE and MSE results of the values calculated from the normalization. According to the two figures, two methods (Min-max and D-Min-Max) gave better results, as their means are low. A comparison of the estimation values obtained by the D_Min_Max normalization method and the actual values is presented in Figure 4.

Figure 4 indicates that the values calculated using the D_Min_Max normalization method are closest to the actual values, and it can therefore be considered the best method.

CONCLUSION

In conclusion, various normalization techniques were applied, one-by-one, to the morphometric data of *S.undosquamis* to estimate its body weight by means of ANN. D_Min_Max and Min_Max methods were found to perform better in the ANN, meaning that they gave results closer to the actual values. It was found that the results of the data analyzed through the use of ANNs after applying normalization techniques were close to the actual values. Since normalization renders the distribution of the values in the data set regular, it also makes the performance of the network regular, and thus an ANN can provide answers to questions it has never seen before with an acceptable level of error. As more accurate results will be obtained after using the appropriate normalization techniques in estimating the relationship between dependent and independent variables in the ANN, it can be used as an alternative to conventional statistical methods. It is recommended in particular to be used as a quite successful means of evaluating data that cannot be resolved by means of conventional methods.

TABLE 1
Trial Results of the Models for Artificial Neural Networks

	Tansig(10,1,4)	**Tansig(10,1,2)**	**Logsig(10,1,4)**	**Logsig(10,1,2)**
Results	MAPE(%)-MSE	MAPE(%)-MSE	MAPE(%)-MSE	MAPE(%)-MSE
Z–Score	7,854–0,032	7,921–0,033	8.317–0.38	8,915–0,031
Min_Max	4,458–0,002	3,974–0,001	3,784–0,001	4,074–0,001
Median	6,921–0,005	6,998–0,005	6,923–0,005	6,930–0,004
D_Min_Max	3,215–0,001	3,187–0,001	3,205–0,001	3,478–0,001
Sigmoid	16,750–0,216	16,345–0,184	16,059–0,187	15,784–0,187
Raw data	4,624–2,845	4,023–2,174	4,892–3,032	4,154–2,418

Tansig (10,1,2) refers to the number of layers, number of hidden layers and number of neurons in the hidden layer, respectively.

TABLE 2
Best MAPE and MSE results

	Input Parameters	MAPE (%)-MSE
D_Min_Max	**Tansig(10,1,2)**	3,187–0,001
Min_Max	**Logsig(10,1,4)**	3,784–0,001
Median	**Tansig(10,1,4)**	6,921–0,005
Z-Score	**Tansig(10,1,4)**	7,854–0,032
Sigmoid	**Logsig(10,1,2)**	15,784–0,187

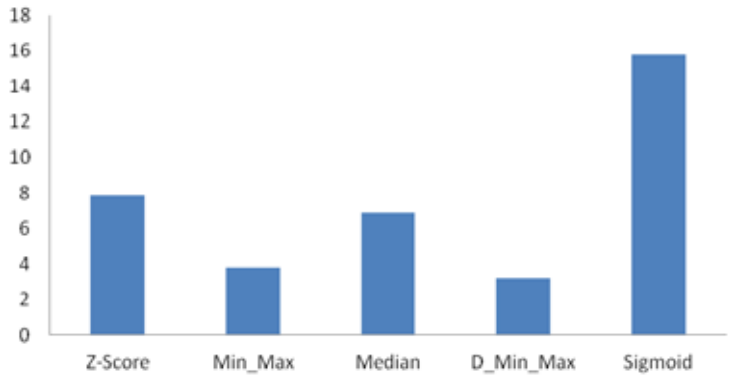

FIGURE 2
Comparison of MAPE results after normalization

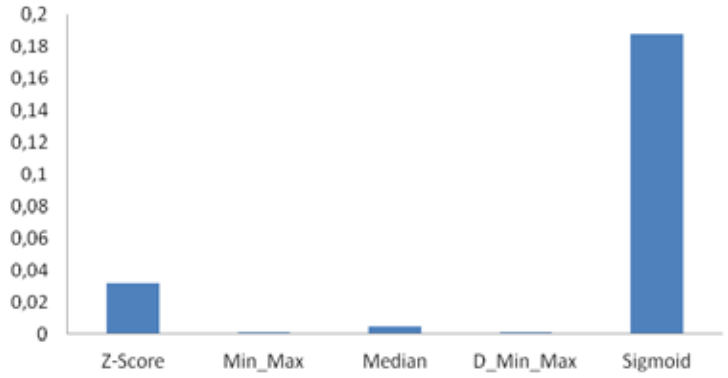

FIGURE 3
Comparison of MSE results after normalization

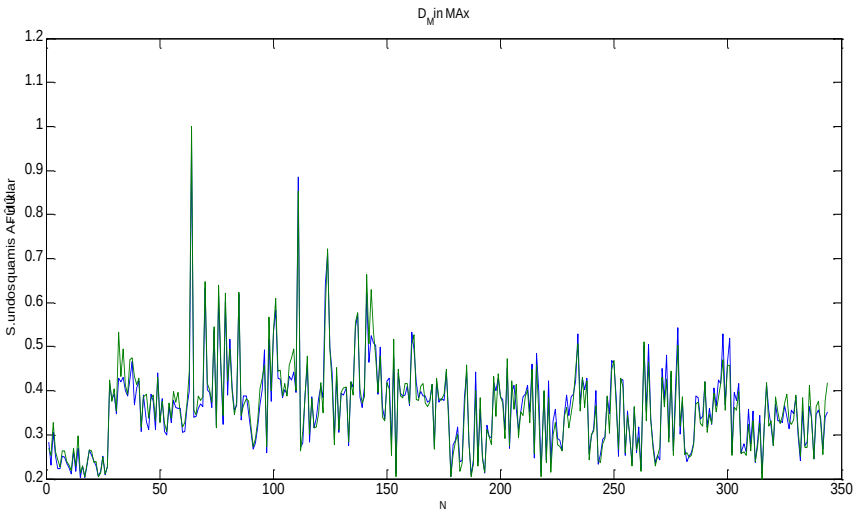

FIGURE 4
Comparison of the Estimation Values Obtained by D_Min_Max Normalization Method and the Actual Values

ACKNOWLEDGEMENTS

This study was supported financially (AMYO2011BAP4) by the Resource Fund of Cukurova University (Turkey).

REFERENCES

[1] Yazıcı, A.C., Öğüş, E., Ankaralı, S., Canan, S., Ankaralı, H. and Akkuş, Z. (2007) Artificial Neural Networks Overview Turkey Clinics. J. Med Sci. 27, 65-71. (in Turkish).

[2] Bayır, F. (2006) An Application on Artificial Neural Networks and Prediction Modeling. Master Thesis. Istanbul University Institute of Social Sciences. İstanbul.

[3] Mammadova, N.M. and Keskin, I. (2015) Application of neural network and adaptive neuro-fuzzy inference system to predict subclinical mastitis in dairy cattle. Indian J. Anim. Res. 49, 671-679.

[4] Warner, B. and Misra, M. (1996) Understanding Neural Networks as Statistical Tools. The American Statistician. 50(4), 284-293.

[5] Dunis, C. and Huang, X. (2002) Forecasting and Trading Currency Volatility: An Application of Recurrent Neural Regression and Model Combination. Journal of Forecasting. 21(5), 317-354.

[6] Nayak, S.C. Misra, B.B. and Behera, H.S. (2014) Impact of Data Normalization on Stock Index Forecasting. International Journal of Computer Information Systems and Industrial Management Applications. 6, 257 – 269.

[7] Özesmi, S.L., Tan, C.O. and Özesmi, U. (2006) Methodological issues in building, training, and testing artificial neural networks in ecological applications. Ecological Modelling. 195(1-2), 83-93.

[8] Brosse, S., Guegan, J., Tourenq, J. and Lek, S. (1999) The use of artificial neural networks to assess fish abundance and spatial occupancy in the littoral zone of a mesotrophic lake. Ecological Modelling. 120(2-3), 299-311.

[9] Suryanarayana, I., Braibanti, A., Sambasiva, R.R., Ramam, V.A., Sudarsa, D. and Rao, G.N. (2008) Neural Networks in Fisheries Research Science Direct. 92, 115-139.

[10] Manimannan, G., Arulkumar, C. and Lakshmi Priya, R. (2016) Classification of agricultural productivity index of Cauvery delta zone using artificial neural network. Agric. Sci. Digest. 36(4), 261-266.

[11] Hyun, K., Song, M.Y., Kim, S. and Chon, T.S. (2005) Using an artificial neural network to paternize long-term fisheries data from South Korea. Aquat. Sci. 67, 382–389.

[12] Benzer, R. and Benzer, S. (2015) Application of artificial neural network into the freshwater fish caught in Turkey. International Journal of Fisheries and Aquatic Studies. 2(5), 341-346

[13] Morimoto E., Taira Y. and Nakamura M. (2009) Identification of Fish Species using Neural Networks. J of National Fisheries University. 58(1), 65-71.

[14] Sun, L., Xiao, H., Yang, D. and Li, S. (2009) Forecasting Fish Stock Recruitment by Using Neural Network. Global Congress on Intelligent Systems. 96-100.

[15] Huang, C.F., Huang, A.C., Pai, T.Y., Ni, R.X., Chu, F.J., Wan, T.J. and Shi, D.H. (2017) Prediction and diagnosis of extraordinary situations for wastewater treatment systems using neural network approach. Fresen. Environ. Bull. 26, 3293-3299.

[16] Nikoo, M., Razavi, S.A. and Hadzima-Nyarko, M. (2018) Artificial Neural Network Combined with Imperialist Competitive Algorithm for Determination of River Sediments. Fresen. Environ. Bull. 27, 4658-4667.

[17] Ben-Tuvia, A. (1966) Red Sea fishes recently found in the Mediterranean. Copeia. 2, 254-275.

[18] Gücü, A.C., Bingel, F., Avşar, D. and Uysal, N. (1994) Distribution and occurrence of Red Sea fish at the Turkish Mediterranean coast northern Cilician basin. Acta Adriatica. 34, 103-113.

[19] Ismen, A. (2003) Maturity and fecundity of Lizardfish (Saurida undosquamis Richardson, 1848) in Iskenderun Bay (Eastern Mediterranean). Turkish Journal of Zoology. 27, 231-238.

[20] Manaşırlı M., Avşar D. and Yeldan, H. (2011) Population dynamical parameters of brush tooth lizard fish Saurida undosquamis (Richardson, 1848) from the Northeastern Mediterranean Coast of Turkey. Ege Journal of Fisheries and Aquatic Sciences. 28(4), 111-115.

[21] Gokce, G., Sangün, L., Özbilgin, H. and Bilecenoğlu, M. (2007) Growth and mortality of the brushtooth lizardfish (Saurida undosquamis) in Iskenderun Bay (eastern Mediterranean Sea) using length frequency analysis, Journal of Applied Icthyology. 23(2007), 697-699.

[22] Ghaedi, A.M. and Vafaei, A. (2016) Principal Component Analysis-Artificial Neural Network and Multiple Linear Regression for The Removal of Basic Blue Dye by Alumina Nanoparticle Loaded on Activated Carbon Prepared from Palm Kernel. Fresen. Environ. Bull. 25, 6215-6217.

[23] Lei, T., Sun, X., Xianghong Guo, X. and Ma, J. (2017) Analysis of The Importance of The Factors That Influence Urea Hydrolysis Through an Artificial Neural Network. Fresen. Environ. Bull. 26, 618-6190.

[24] Yüksek, A.G., Bircan, H., Zontul, M. and Kaynar, O. (2007) An Application on Forming Air Quality Model with Artificial Neural Networks in. Cumhuriyet Üniversitesi İktisadi ve İdari Bilimler Dergisi. 8(1), 97-112.
[25] Jayalakshmi, T. and Santhakumaran, A. (2011) Statistical Normalization and Back Propagation for Classification. International Journal of Computer Theory and Engineering. 3(1), 89-93.
[26] Bugday, E. (2018) Application of Artificial Neural Network System Based on ANFIS Using GIS For Predicting Forest Road Network Suitability Mapping. Fresen. Environ. Bull. 27, 1656-1668.
[27] Yavuz, S. and Deveci, M. (2013) The Effect of Statistical Normalization Techniques on the Performance of Artificial Neural Network. Erciyes Üniv. İktisadi ve İdari Bilimler Fakültesi Dergisi. 40, 167-187
[28] Mohagheghian, M., Ghaedi, A.M. and Vafaei, A. (2016) Application of Genetic Algorithm-Adaptive Neuro-Fuzzy Inference System and Genetic Algorithm-Multiple Linear Regression for Simultaneous Determination of Glycyrrhizic Acid and Liquiritin in Licorice Root. Fresen. Environ. Bull. 25, 6218-6223.
[29] Öztemel, E. (2003) Artificial neural networks. Papatya Yayınları. 44.

Received: **06.08.2018**
Accepted: **28.02.2019**

CORRESPONDING AUTHOR

Levent Sangun
University of Cukurova,
Vocational School of Adana,
P.O. Box 01160,
Çukurova, Adana – Turkey

e-mail: leventsangun@gmail.com

© by PSP Volume 28 – No. 4/2019 pages 2848-2854 Fresenius Environmental Bulletin

SINTERING CHARACTERISTICS OF CERAMSITE OBTAINED FROM LAKE SEDIMENTS, CLAY, AND LIRIODENDRON

Zhulai Wang[1,2,*], Zuhui Fan[2], Zizeng Lin[2], Yali Liu[2]

[1]Ministry of Education Key Laboratory of Integrated Regulation and Resource Development on Shallow Lakes, Hohai University, Nanjing 210098, PR China
[2]School of Civil Engineering, Nanjing Forestry University, Nanjing, Jiangsu Province 210037, PR China

ABSTRACT

In order to evaluate the feasibility that the three raw materials of lake sediment, clay, liriodendron were mixed for producing ceramsite and examine their sintering characteristics, the specific surface area, pore size distribution, bulk and apparent density were chosen as the study object. The results showed that at the lower preheating and sintering temperatures and duration, many small pores were formed in the inner of the ceramsites, while at the higher preheating and sintering temperatures and duration, small pores started melting to form larger pores resulting in the decline of the specific surface area and the increase of the bulk and apparent density. As the lake sediments decreased, the specific surface area of the ceramsites also declined and the bulk and apparent density increased, while as the amount of the liriodendron rose, the specific surface area would also increase and the bulk and apparent density decrease. In addition, the influence for the increase of the organic matters was greater than the influence for the decline of the preheating and sintering temperatures and duration.

KEYWORDS:
Ceramsite, Lake sediment, Clay, Liriodendron, Sintering characteristics

INTRODUCTION

Booming economy and rapid modernization have resulted in the gradual growth of solid waste in the world, especially in the developing countries [1]. The harm of solid waste to the environment is becoming more and more serious. In China, solid waste was divided into industrial waste, hazardous waste, and municipal waste [2]. Lake sediment is one of municipal wastes, and its harm to environment is also very serious. How to utilize the sediment in lakes is one of the hotspots in the current research. Previously, the raw materials for producing ceramsite are these matters, such as clay, shale, and so on, which are the non-renewable resources. In recent years, the amount of solid wastes such as sewage sludge [3], coal ash [4], sediment [5-7], and so on, as the raw materials for producing ceramsite gradually increased. Lake sediment as the raw material for producing ceramsite both solves the environment harm of lake sediment and provides the new approaches for the choice of the raw material of ceramsite.

The objective of this paper is the evaluation of the feasibility that the three raw materials of lake sediment, clay, liriodendron were mixed for producing ceramsite and examine their sintering characteristics. The lake sediment is the main raw material, while the clay and liriodendron are the additives, which provide the viscosity and the organic matter, respectively. The effect of the process parameters on the specific surface area, pore size distribution, bulk and apparent density of these ceramsites manufactured above was examined. The process parameters included the mass ratios of the three raw materials, preheating temperatures and duration, and sintering temperatures and duration. This research provides the theoretical basis for the actual production of ceramsite.

MATERIALS AND METHODS

Materials. Lake sediment, clay, and liriodendron were the three raw materials of producing ceramsite in this study. Lake sediment was obtained from Xuanwu Lake in Nanjing, China and dewatered through a filter press. Both clay and liriodendron came from Nanjing Forestry University, Nanjing, China, and clay was in the work site while liriodendron was the leaves dropped from the trees. The plasticity index of clay was greater than 17.

The chemical compositions of lake sediment and clay mentioned above are shown in Table 1.

TABLE 1
Chemical compositions of raw materials analyses

Chemical compositions	SiO_2	CaO	MgO	Al_2O_3	K_2O	Fe_2O_3	Na_2O	MnO_2	TiO_2	Ignition loss rate
Lake sediment (wt-%)	52.63	3.21	2.84	16.56	1.83	7.69	1.52			13.72
Clay (wt-%)	84.62	0.82	1.03	7.33	1.86	4.09	0.03	0.05	0.62	

TABLE 2
Sample contents and ratios

Type of ceramsite	Lake sediment (wt-%)	Clay (wt-%)	Liriodendron (wt-%)
TLA	95	5	0
TLB	90	10	0
TLC	85	15	0
TLD	90	5	5
TLE	80	10	10
TLF	70	15	15

TABLE 3
Preheating and sintering temperatures and duration of ceramsite

Number	Preheating temperature and duration Sintering temperature and duration
1	300 °C, 10 min 750 °C, 10 min
2	300 °C, 20 min 750 °C, 20 min
3	400 °C, 10 min 850 °C, 10 min
4	400 °C, 20 min 850 °C 20 min
5	500 °C, 10 min 950 °C, 10 min
6	500 °C, 20 min 950 °C, 20 min

The chemical composition of liriodendron is mainly the organic matter including cellulose, polysaccharide, protein, and so on. The three raw materials were dried at 105 °C for 2h in a drying oven and then ground with a TYSP-200 high-speed pulverizer (Zhejiang Yongkang red sun electromechanical Co., Ltd., China) at sizes below 100 meshes to be ensure well thorough mixing. The dry weight ratios of lake sediments : clay : liriodendron were examined in this study and given in Table 2. The ratios were identified as TLA, TLB, TLC,TLD,TLE, and TLF.

Methods. Preparation of ceramsite. In view of the sample contents and ratios above in Table 2, the raw materials were mixed and added some proper water (with the formation of ceramsite just as the basis), and then the ceramsite was manufactured at the particle sizes of 6-8 mm by hand. The ceramsite made above was left in a room at a temperature of about 20 °C for 2 days.

Preheating and sintering of ceramsite. After the preparation of ceramsite, the next step was the preheating and sintering of the ceramsite. The crack would appear on the surface of the ceramsite if the ceramsite had not been preheated. The preheating temperatures and duration and the sintering temperatures and duration were given in Table 3 as follows. The ceramsite was heated in a chamber electric furnace (SX2-12-10, Shanghai experimental electric furnace factory，China) at a 10 °C/min every preheating and sintering temperature. In accordance with the preheating temperatures and duration and the sintering temperatures and duration, the numbers of the ceramsite were identified as 1, 2, 3, 4, 5, and 6.

Detection methods. The specific surface area and pore size distribution of the ceramsite were conducted by specific surface area and pore size analyzer (V-Sorb 2800, Beijing golden APP Technology Co., Ltd., China). The chemical compositions of lake sediment and clay were determined by electron energy disperse spectroscopy (INCA 250 EDS, UK). The detection method for the bulk density of the ceramsite was that a certain volume of ceramsite was put in a measuring cylinder and the volume was read out, while the weight of the ceramsite was weighed by electronic analytical balance. The testing method for the apparent density of the ceramsite was that on the basis of the vol-

ume of the ceramsite above, some water was added in the measuring cylinder to ensure these water submerged just and the volume that the volume of the bulk density subtracted the water volume was the volume of the apparent density of the ceramsite. The calculation formulas of the bulk and apparent density were as follows.

$$\text{Bulk density} = \frac{\text{mass of ceramsite bodies}}{\text{bulk volume of ceramsite bodies}} \text{kg.m}^{-3} \quad (1)$$

$$\text{Apparent density} = \frac{\text{mass of ceramsite bodies}}{\text{volume of ceramsite bodies}} \text{kg.m}^{-3} \quad (2)$$

RESULTS AND DISCUSSION

Effect of process parameters on specific surface area of ceramsite. Effect of preheating and sintering parameters on specific surface area. In order to examine the effect of the preheating and sintering temperatures and duration on the specific surface area of the ceramsite, the experiment was conducted in view of Table 3. The results are shown in Fig. 1 as follows.

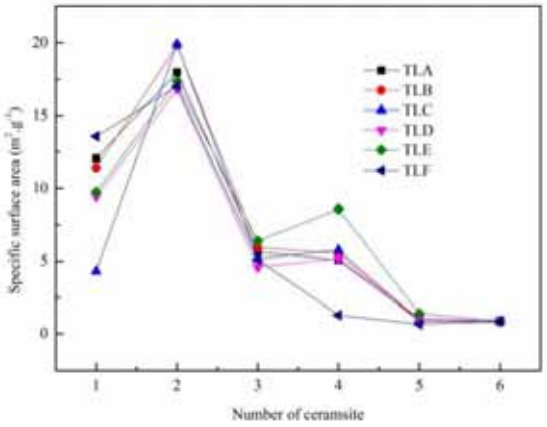

FIGURE 1
Effect of preheating and sintering parameters on specific surface area

It can be seen from Fig. 1 that at the same preheating and sintering temperatures, as the preheating and sintering duration varied from 10 min to 20 min, the specific surface areas of the ceramsites gradually increased, and especially as the preheating and sintering temperatures were 300 ºCand 750 ºC, respectively, the variation of the specific surface area of the ceramsite was the most evident and the data of this specific surface area was the maximum as the duration of 20 min. Meanwhile, the variation of the specific surface area of the ceramsite was the the minimum as the preheating and sintering temperatures were 500 ºC and 950 ºC, respectively. In general, as the preheating and sintering temperatures varied 300-500 ºC and 750-950 ºC, respectively, the specific surface area of the ceramsites increased first and then decreased up to the minimal. The explanation of the phenomenon above was that at a certain preheating and sintering temperature and duration, the organic matters started decomposing to form CO_2, CO, and C and Fe_2O_3 reacted to produce CO_2, CO, too. These gases volatilized from the interior of the ceramsite to form pore structures. At 300 ºC, 20 min, and 750 ºC ,20 min, these pore structures mainly were small pores, which resulted in the specific surface area was the maximum, while at 500 ºC, 20 min, and 950 ºC ,20 min, there were some small pores started melting to form larger pores resulting in the appearing of the minimal specific surface area.

Effect of mass ratios of the raw materials on specific surface area. To examine the effect of the mass ratios of the raw materials on the specific surface areas of the ceramsites, the experiment was also conducted in view of Table 3. The results are shown in Fig. 2 as follows.

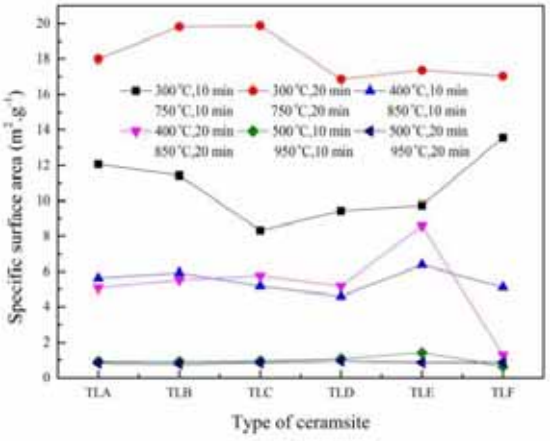

FIGURE 2
Effect of mass ratios of the raw materials on specific surface area

It can be seen from Fig. 2 that at the lower preheating and sintering temperatures and duration, as the ratio of the lake sediment decreased and the ratios of the clay and the liriodendron increased, the specific surface areas of the ceramsites declined first and then started rising. Meanwhile, at the higher preheating and sintering temperatures and duration, as the types of the ceramsites varied from TLA to TLF, the specific surface areas of the ceramsites had no evident difference. This phenomenon can be explained as a result of at the lower preheating and sintering temperatures and duration, the influence for the decrease of the lake sediment was greater than the increase of the clay and the liriodendron and the organic matters of the lake sediment were more than the clay and the liriodendron. In addition, at the lower preheating and sintering temperatures

and duration, the influence for the increase of the liriodendron was over than the decrease of the lake sediment, and the amount for the organic matters of the liriodendron was more than the organic matters of the lake sediment. In contrast, at the higher preheating and sintering temperatures and duration, the influence for the variation of this temperatures and duration was over than the mass ratios of the raw materials.

Effect of process parameters on pore size distribution of ceramsite. Effect of preheating and sintering parameters on pore size distribution. In order to evaluate the effect of the preheating and sintering parameters on the pore size distribution, the sample of TLD was chosen as the study object. The preheating and sintering temperatures and duration were given in Table 3. The results are shown in Fig. 3-4 as follows.

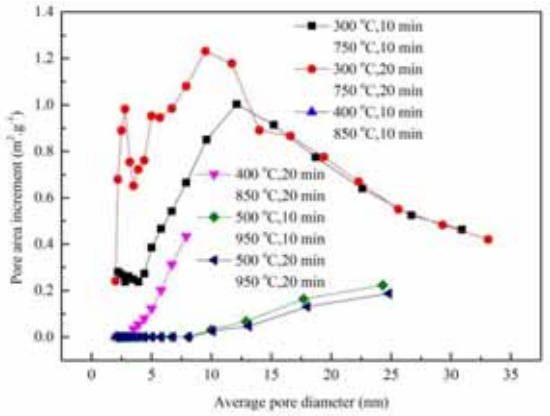

FIGURE 3
Effect of preheating and sintering parameters on pore area increment

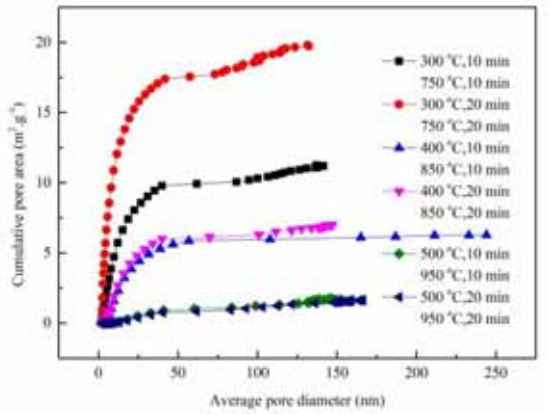

FIGURE 4
Effect of preheating and sintering parameters on cumulative pore area

The difference of the pore area increment between the lower and higher preheating and sintering temperatures and duration can be seen from Fig. 3. At the lower preheating and sintering temperatures and duration, the average pore diameter mainly was in the 5-15 nm range, and as the temperatures and duration increased, the larger pores appeared, whose quantity was relatively less. In contrast, at the higher preheating and sintering temperatures and duration, the pore diameters in 5-15 nm were not many, and as the increase of the temperatures and duration, the quantity of the larger pores started rising. It can be seen from Fig. 4 that the preheating and sintering temperatures and duration varied from 300 °C,10 min and 750 °C,10 min to 300 °C,20 min and 750 °C,20 min, the cumulative pore area was larger and finally, at the latter preheating and sintering temperatures and duration, the cumulative pore area was the most in all temperatures and duration. Meanwhile, at the lower pore diameter, the increment of the cumulative pore area was very evident. The explanation of the phenomenon above was that at 300 °C,10 min and 750 °C,10 min, the small pores formed not completely, while at 300 °C,20 min and 750 °C,20 min, owing to the evaporation of the water and the decomposition of the organic matters, the small pores formed completely and their quantities reached the most. As the temperatures and duration increased, these small pores appeared before started melting to form the larger pores and the complex crystalline phases.

Effect of mass ratios of the raw materials on pore size distribution. In order to examine the mass ratios of the raw materials on the pore size distribution of the ceramsite, the samples of TLA, TLB, TLC, TLD, TLE, and TLF were chosen as the study objects. The preheating and sintering temperatures and duration were 300 °C,10 min and 750 °C,10 min. The results are shown in Fig. 5-6 as follows.

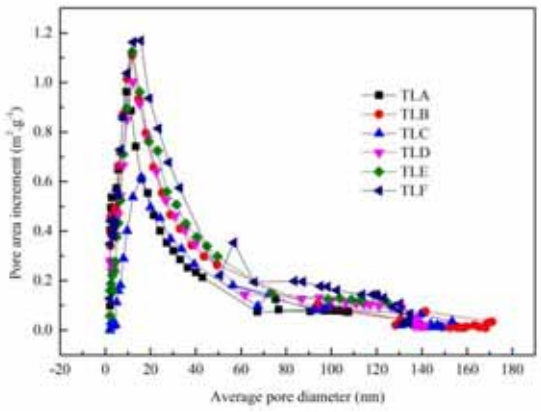

FIGURE 5
Effect of mass ratios of the raw materials on pore area increment

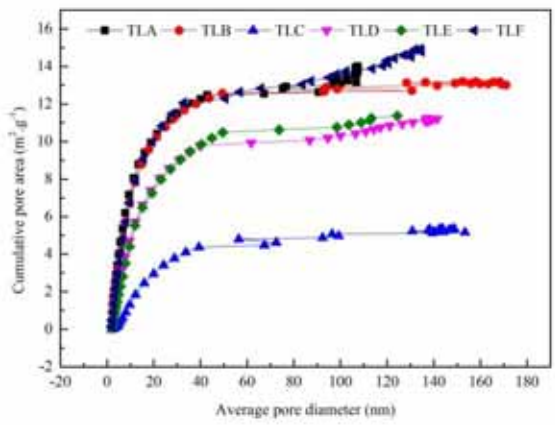

FIGURE 6
Effect of mass ratios of the raw materials on cumulative pore area

The difference of the pore area increment can be seen from Fig. 5 as the types of the samples varied from TLA to TLF. The pore area increment for the samples of TLA, TLB, TLC was less than the samples of TLD, TLE, TLF in a 10-30 nm range. As the average pore diameters were over than 50 nm, the pore area increment was smaller and no evident difference in all types of the samples. It can be seen from Fig. 6 that the cumulative pore areas were the largest as the samples were TLA, TLB, and TLF, while the cumulative pore area of the sample of TLC was the smallest. As the average pore diameters varied from 0 to 30 nm, the all cumulative pore areas increased significantly, while over than 30 nm, the increment of the cumulative pore areas was not evident. The phenomenon above can be explained as a result of that as the types of the samples varied from TLA, TLB, TLC to TLD, TLE, TLF, the mass of the lake sediment was the decrease while in contrast, the content of the liriodendron was the increase. The results showed that the influence of the increase of the liriodendron exceeded the influence of the decrease of the lake sediment and it further proved the organic matter content of the liriodendron was more than the content of the lake sediment. The contribution of the small pores to the specific surface area was more than the large pores because of the more amount of the small pores.

Effect of process parameters on bulk and apparent density of ceramsite. Effect of preheating and sintering parameters bulk and apparent density. To evaluate the preheating and sintering parameters on the bulk and apparent density of the ceramsite, the sample of TLA was chosen as the study object. The preheating and sintering temperatures and duration were given in Table 3. The results are shown in Fig. 7 as follows.

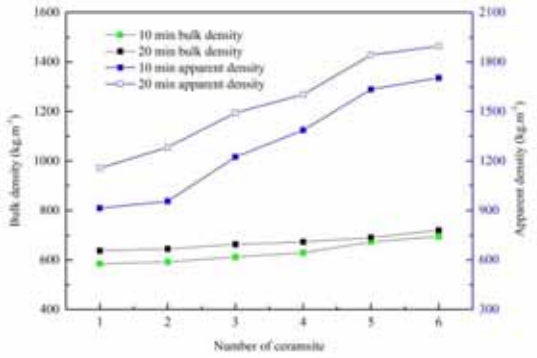

FIGURE 7
Effect of preheating and sintering parameters on bulk and apparent density

It can be seen from Fig. 7 that as the preheating and sintering temperatures and duration increased, no matter 10 min or 20 min, the bulk density of the ceramsite had no evident difference, while the apparent density rose sharply. As the preheating and sintering duration varied from 10 to 20 min, both the bulk density and the apparent density of 20 min were more than 10 min. The explanation of the phenomenon above was that the rising of the preheating and sintering temperatures had no evident influence on the bulk density and this was because the rising of the temperatures resulted in only the melting of the inner pores, while the diameter of the ceramsite in outer surface had no change. Meanwhile, as the temperatures increased, owing to the melting of the inner pores, the amount of the pores connected with the outer surface of the ceramsite rose, which resulted in the decline for the volume of the ceramsite bodies, and finally, the apparent density of the ceramsites gradually became greater than before. In addition, as the preheating and sintering duration prolonged, the reason for the increase of the bulk and apparent density was still the melting for the inner pores of the ceramsite.

Effect of mass ratios of the raw materials on bulk and apparent density. In order to examine the effect of mass ratios of the raw materials on the bulk and apparent density of the ceramsites, the samples of TLA, TLB, TLC, TLD, TLE, and TLF were as chosen as the study objects. The preheating and sintering temperatures and duration were 300 °C, 10 min and 750 °C, 10 min, and 300 °C, 20 min and 750 °C, 20 min. The results are shown in Fig. 8 as follows.

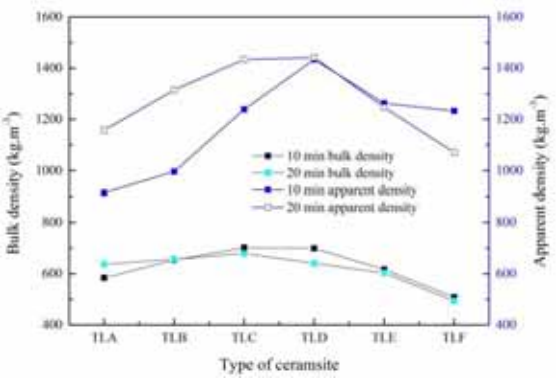

FIGURE 8
Effect of mass ratios of the raw materials on bulk and apparent density

As the samples varied from TLA to TLF, the bulk density of 10 min was over than 20 min except from TLA to TLB, and but the difference of the bulk density between 10 and 20 min was not evident. Meanwhile, as the samples varied from TLA to TLD, the apparent density of 20 min was greater than 10 min while it was contrary from TLD to TLF, and the difference of the apparent density between 10 and 20 min was larger than the bulk density except from TLD to TLE. The phenomenon above can be explained as a result of the difference of the preheating and sintering duration and the difference of the mass ratios of the raw materials. As the samples varied from TLA to TLC, owing to the decrease of the lake sediment, the decline of the organic matter resulted in the bulk density increase, while as the samples varied from TLC to TLF, the increase of the liriodendron was the reason of the decline of the bulk density. The influence of the increase of the organic matter was over than the variation of the duration from 10 to 20 min. The reason of the change of the apparent density was similar with the bulk density.

CONCLUSIONS

Based on the results obtained in this study, the conclusions are drawn as follows:

(1) At the lower preheating and sintering temperatures and duration, many small pores were form -ed in the inner of the ceramsites, while at the higher preheating and sintering temperatures and duration, small pores started melting to form larger pores resulting in the decline of the specific surface area and the increase of the bulk and apparent density.

(2) As the lake sediments decreased, the specific surface area of the ceramsites also declined and the bulk and apparent density increased, while as the amount of the liriodendron rose, the specific surface area would also increase and the bulk and apparent density decrease. In addition, the influence for the increase of the organic matters was greater than the influence for the decline of the preheating and sintering temperatures and duration.

ACKNOWLEDGEMENTS

The study was supported by the Fundamental Research Funds for the Central Universities (No. 2017B20514) and PAPD.

REFERENCES

[1] Song, Q., Li, J., Zeng, X. (2015) Minimizing the increasing solid waste through zero waste strategy. Journal of Cleaner Production. 104, 199-210.

[2] He, C., Yu, R., Chen, Z., Sun, H. (2016) Research on unattended hoisting in solid waste disposal. International journal of hydrogen energy. 41, 15817-15820.

[3] Li, J., Yu, G., Xie, S., Pan, L., Li, C., You, F., Wang, Y. (2018) Immobilization of heavy metals in ceramsite produced from sewage sludge biochar. Science of the Total Environment. 628-629, 131-140.

[4] Qin, J., Cui, C., Cui, X.Y., Hussain, A., Yang, C.M. (2015) Preparation and characterization of ceramsite from lime mud and coal fly ash. Construction and Building Materials. 95, 10-17.

[5] Qi, Y., Dai, B., He, S., Wu, S., Huang, J., Xi, F., Ma, Y., Meng, M. (2016) Effect of chemical constituents of oxytetracycline mycelia residue and dredged sediments on characteristics of ultra-lightweight ceramsite. Journal of the Taiwan Institute of Chemical Engineers. 65, 225-232.

[6] Yue, D., Yue, Q., Gao, B., He, H., Yu, H., Sun, S., Lı, Q., Wang, Y., Zhao, Y. (2014) Preparation and bloating mechanism of porous ultra-lightweight ceramsite by dehydrated sewage sludge and Yellow river sediments. 12, 1029-1035.

[7] Li, T., Sun, T., Li, D. (2018) Preparation, sintering behavior, and expansion performance of ceramsite filter media from dewatered sewage sludge, coal fly ash, and river sediment. J Mater Cycles Waste Manag. 20, 71-79.

Received: **11.08.2018**
Accepted: **01.03.2019**

CORRESPONDING AUTHOR

Zhulai Wang
Ministry of Education
Key Laboratory of Integrated Regulation and
Resource Development on Shallow Lakes,
Hohai University,
Nanjing 210098 – P.R. China

e-mail: wangzhulai@126.com

© by PSP Volume 28 – No. 4/2019 pages 2855-2863 Fresenius Environmental Bulletin

THE EFFECT OF SOME ROOTSTOCKS ON THE PHYSICAL AND CHEMICAL PROPERTIES OF FRUIT GROWING PROCESS IN ANNA APPLE CULTIVAR

Ali Ikinci*, Ibrahim Bolat

Harran University, Faculty of Agriculture, Department of Horticulture, 63300 Sanliurfa, Turkey

ABSTRACT

The apple tree that grows in temperate, especially cold-temperate climatic regions between the latitudes of 30° - 50° in the world is also successfully being grown in subtropical climate conditions by using the cultivars with low chilling needs. In this study, phenological, pomological and some chemical features of 'Anna' apple cultivar on different rootstocks were determined in the conditions of Sanliurfa, which shows a semiarid climate characteristic, between 2014 and 2015. In the research, fruit diameter measurements of the fruits were made at 5-day intervals from fruit set to fruit harvest. According to the results obtained, it was determined that the growth of fruit diameter on three different rootstocks in Anna apple cultivar showed a growth that would form a single sigmoid curve. It was determined that Anna apple cultivar is grafted on different rootstocks reached to the earliest full blooming stage (18th March) and the earliest harvest date (5th July) on M9 rootstock. The biggest fruits (221.42 g) were obtained from the trees on MM 111 rootstocks, the smallest fruits (179.76 g) were obtained from the trees on seedling rootstocks, minimum Brix degree (14.8%) was obtained from the trees on seedling rootstocks, and minimum titratable acidity (0.61%) was obtained from the trees on MM 111 rootstocks. In Anna trees, the period from full flowering to harvest varied between 109 days (for M9) and 115 days (for seedling rootstocks). The highest fruit set rate was obtained from the trees on the seedling rootstock with 22.6%.

KEYWORDS:
Apple rootstocks, fruit growth, fruit drop ratio, fruit set ratio, flower drop, M9

INTRODUCTION

Being a temperate climate and particularly a cool temperate climate fruit, apple is grown between 30°- 50° north and south latitudes [1]. During winter the trunk and main branches of apple trees stand temperatures of -35, -40 °C and old branches stand temperatures up to -20 °C. Blossoms can stand temperatures of -2.2, -3.3 °C and small fruits (about in diameter of 1 cm) can stand temperatures of -1.1, -2.2 °C. Apple trees blossom in late period so they are damaged less by late spring frosts. Types of apples show differences in terms of resistance to low temperatures. Undoubtedly, resistance to cold changes depending on the type, rootstocks and applied cultivation systems [2, 3].

It is confirmed that the temperature within the interval of 30-40 days following the blossoming of commercial apples has significant impact on the ripening period of the fruit to reach optimum size, firmness of fruit flesh at harvest, cell size and specific weight [4]. One of the most important environmental factors affecting growth and yield of the plants is temperature. The changes in seasonal temperatures year by year affect the yield of apple trees but temperature is not the only factor in this respect [5]. Warrington et al. [4] have determined that growth of apples is largely affected by the temperature during the early ripening period following blossoming and the fruits are less sensitive to temperature in medium and late periods.

The fruit load expressed as the number of fruits per tree is affected by many environmental factors such as light, temperature, and photosynthesis and by product management applications. The most important fruit orchard management applications that affect fruit load and quality of fruits are rootstock and blossom and fruit thinning applications [6, 7]. While dwarf and semi-dwarf rootstocks breeding and the use of obtaining rootstocks in apple tree growing has been started to be used effectively in the world a century ago, use of clonal rootstocks with different characteristics for apple tree farming has only been started in the years of 1968 and 1970 in our country. In comparison to the other fruit species, apple is the most common and successful fruit type for intensive breeding.

Rootstocks have important effects on the performance of the apple cultivar; early fruit maturing, the crown shape and size, the rate of photosynthesis; growth rate and duration, resistance against various soil conditions, cold weather, drought, disease and pests and also the intake of nutrients from the soil, bud breaking time and various fruit features [1, 8-10]. Fruit size is one of the most important determinants of price [9, 10]. Fruit varieties,

rootstock, tree age, crop load, alternate bearing, position of flower on spur, etc. such as genetic factors, pruning, disease and pest control, thinning, nutrition, irrigation, external hormone applications such as cultural factors and environmental factors such as soil, humidity, light, temperature, wind and gases affect fruit size on the tree [4, 9, 11-15]. Many of the studies on the influence of rootstocks on the scion variety did not show consistency from site to site and varied over time. Rootstocks affect the fruit quality characteristics such as ripening, storability, mineral composition [16], size and fruit firmness [9, 17] of the scion cultivar.

Fruit; they expand at unequal proportions from fruit set to maturity. In most fruits, development forms are defined as single or double sigmoid curves. The development of fresh weight or fruit diameter after flowering creates a sigmoid growth curve pattern. Fruits with single sigmoid growth curves exhibit slow growth at the beginning and at the end stages of growth, while growths are much faster at the mid-development stage. Apples, avocados, bananas, oranges, pears, pineapples, strawberries, melons and tomatoes are examples of fruits that have this development model. On the other hand, the fruit with a double sigmoid growth curve pattern exhibits two rapid growth rate periods separated by a relatively slow growth period. This type of fruit includes peaches, apricots, plums, sweet cherries, sour cherries, figs, blackcurrants, blueberries, raspberries, grapes and olives [11, 18].

While fruit growth and development of an apple tree grafted on a particular rootstock may be good, the performance of another type on the same rootstock may not be good. In other words, while fruit efficiency and development of an apple variety on a rootstock are quite good, the performance of the same variety may not be good on another rootstock. Therefore, because of the effect of rootstock on fruit efficiency and fruit size, selection of suitable scion/rootstocks components is one of the most important considerations for the garden setting.

In order to popularize apple farming in Sanliurfa and in the territory, it is necessary to identify scion/rootstocks components that are suitable for the ecological conditions of the region and to repeat these studies with the current apple cultivars. Because of the varieties and rootstocks developed every year, apples are grown in rather different ecologies than other species of fruits. Due to breeding works, these newly developed and preferred in foreign trade should be tested in different ecologies [19]. On the other hand, as apple fruit has variety and rootstock riches suitable for different ecologies and soil structures, these varieties and rootstocks should also be tested in varying ecologies without losing time.

This study was carried out with the aim of determining the performance of early ripening 'Anna' apple cultivar, which ripens in July on 3 different rootstocks under the conditions of Sanliurfa.

MATERIALS

The research was carried out on 9-year-old Anna apple trees that were grafted on seedling rootstock, M9 and MM 111 rootstocks in Research and Application Garden (37º10' N and 38º59' E; altitude: 535 m) of Horticulture Department of the Faculty of Agriculture in Harran University between the years of 2014 and 2015. The planting distances of the trees that were grafted on seedling rootstocks and MM 111 rootstocks were 5 x 5 m, and the planting distances of the trees that were grafted on M9 rootstocks were 5 x 2.5 m. The irrigation in the garden where the research was carried out was through the drip irrigation system. The trees were subjected to a central leader pruning and training system. Technical and cultural processes such as fertilization, disease, and pest control were carried out regularly in accordance with the standards, and fruit thinning was not applied.

TABLE 1
Climate data from the weather station in the experimental orchard (2014 - 2015)

Months	Temperature			Average relative humidity (%)	Amount of precipitation (mm)
	Minimum temperature (°C)	Average temperature (ºC)	Maximum temperature (ºC)		
January	-4.7	4.5	17.5	62.3	51.8
February	-4.0	7.9	20.0	70.3	54.9
March	1.8	12.2	23.6	61.8	28.9
April	4.0	17.8	28.5	55.5	40.4
May	11.0	23.8	39.1	39.8	16.7
June	17.8	30.8	44.0	25.5	2.7
July	20.3	32.2	43.7	26.8	0.8
August	20.0	33.4	45.2	29.8	0.0
September	12.0	27.2	42.0	33.3	16.9
October	9.8	21.0	34.2	42.0	35.6
November	2.2	11.4	26.8	55.3	33.4
December	-4.3	6.8	18.5	57.3	33.6

Climatic features. According to the meteorological data obtained during the study from the meteorological station that was established in the research and application garden where the research was carried out (Table 1), the average temperature was 19.1 ºC, the highest temperature was 45.2 ºC, the lowest temperature was -4.7 ºC, and the total precipitation was 389 mm. The average relative humidity was 49.10%. Relative humidity increases to the highest level (70.3%) in February and decreases to the lowest level (25.5%) in June.

Soil properties. The soil (0-40 cm) of the garden where the study was carried out was medium textured, fertile and contained 40% of clay, 33.2% of silt, 21.4% of sand and varying amounts of organic material between the rates of 0.48 and 1.16%. The soil pH was between 8.20 and 8.45, and $CaCO_3$ content varied between 19% and 25% (w/w). N and P values of organic matter in the garden soil were low, and the K value was high.

METHODS

Determination of phenological characteristics. As for phenological characteristics; bud swell, bud break, first blooming, full bloom, post-bloom and harvest date of the fruit trees were separately determined according to rootstock differences. Bud break, the beginning of blooming, full bloom, post-bloom, and harvest dates were observed. The dates were determined as follows: The beginning of blooming; as 5% of the flowers were bloomed, full bloom; as 70% of the flowers were bloomed and post-bloom; as 95% of the petals of the flowers were dropped [19, 20].

Pomological characteristics. For the examined Anna apple cultivar, pomological characteristics such as fruit width (mm), fruit height (mm), fruit weight (g), fruit volume (cm^3), fruit flesh hardness [measured by 11.1 mm probes of the penetrometer], total ºBrix (%) and titratable acidity (%) were examined on 20 fruits picked from each scion/rootstock combination in a way that to represent the general characteristics of the cultivar [19, 20].

Flower and fruit drop rate and periods. From Anna apple trees on each rootstock, 5 similar trees were identified, and at least 500 flowers were counted on the selected branches and in different directions of these trees, and these figures were recorded. Shedding of flowers and fruits on the branches, which were marked and flower counts made, were determined from the starting date of full bloom until fruit maturity. Determination of shedding of flowers and fruits was made at 7-day intervals until the 30th day after full blooming and later at 10-day intervals [21, 22].

Fruit diameter development. Fruit diameter measurements were made on the fruits on grafted trees on 3 different rootstocks of Anna apple cultivar at 7-day intervals for the first 50 days after the full blooming date, and at 10-day intervals after that date. By the calculations on the results of diameter measurement made by a digital caliper, the daily diameter development rates of fruits were determined [22].

Statistical analysis. The research was based on a randomized block trial design with 3 repetitions and with 2 trees for each repetition. JMP 8.0 package software was used to compare the results obtained from the experiment. LSD Test ($p \leq 0.05$) was used to compare the differences between the averages.

RESULTS AND DISCUSSION

Phenological characteristics. The results of the phenological observations made on Anna cultivar apple trees that were grafted on seedling rootstock, M9 and MM 111 rootstocks in Sanliurfa conditions are given in Table 2.

According to the observations, the earliest and latest bud swellings occurred on the trees grafted on MM 111 (1st March) and seedling rootstocks (8th March) in the years of 2014 and 2015, respectively. The earliest (6th March) and latest (12th March) bud break and the earliest (12th March) and the latest (19th March) first blooming occurred on the trees grafted on M9 and seedling rootstocks, respectively. While the trees grafted on M9 rootstocks were in full bloom period on March 18, the trees grafted on seedling rootstocks reached the full bloom period on March 27 at the latest. Blooming on the rootstocks ended between the dates of March 26 (M9) and April 4 (seedling rootstock), and the fruits reached the earliest harvesting maturity on the trees grafted on M9 rootstock (5th July) and the latest on the trees grafted on seedling rootstock (20th July).

It was determined that Anna apple cultivar grafted on seedling rootstocks, M9 and MM 111 reached the earliest blooming and the earliest fruit maturity on M9 rootstocks and the latest blooming and the latest fruit maturity on seedling rootstocks.

Atay et al. [14] reported that Jersey Mac, Galaxy Gala and Braeburn cultivars grafted on MM 106 rootstocks were on blooming stage in 20th, 22nd and 20th April in 2006, respectively, and they reached the blooming stage in the conditions of Egirdir on 28th April, 1st May and 28th April in 2007, respectively. Researchers stated that Jersey Mac, Galaxy Gala and Braeburn varieties reached the harvesting stage on 30th July – 03rd August, 27th August – 31st August and 31st August – 22nd October in 2007, respectively.

TABLE 2
Some phenological observation results of Anna apple cultivar grafted on different rootstocks (average of the years 2014-2015).

Rootstocks	Years	B.S.	B. B.	B. F.	F. B.	E. F.	H. D.	DNFFBH
Seedling	2014	05. Mar.	11. Mar.	16. Mar.	25. Mar.	01. Apr.	14. Jul.	111
	2015	08. Mar.	12. Mar.	19. Mar.	27. Mar.	04. Apr.	20. Jul.	115
M9	2014	03. Mar.	06. Mar.	12. Mar.	18. Mar.	26. Mar.	05. Jul.	109
	2015	04.Mar.	08. Mar.	16. Mar.	23. Mar.	30. Mar.	11. Jul.	110
MM 111	2014	01.Mar.	07. Mar.	14. Mar.	20. Mar.	28. Mar.	08. Jul.	110
	2015	05.Mar.	09. Mar.	18. Mar.	25. Mar.	31. Mar.	14. Jul.	111

B.S.: Bud swell, B.B.: Bud break, B.F.: Beginning of flowering, F.B.: Full bloom, E.F.: End of flowering, H.D.: Harvest date, DNFFBH: Number of days from full bloom to harvest

In a study carried out in Nigde-Sazlica, according to the results of two years observation on apple cultivars grafted on M9 and MM 106 rootstocks, the dates of bud swell, bud break, first blooming, full blooming, post blooming and harvesting dates were determined as March 22nd (Galaxy Gala / M9), April 14th (Fuji / M9), March 29th (Galaxy Gala / M9, Mondial Gala / M9) - April 21st (Fuji / M9), April 14th (Galaxy Gala / M9) - May 5th (Fuji / M9), April 19th (Mondial Gala / M9) - May 10th (Fuji / M9), April 25th (Galaxy Gala / M9) - May 17th (Fuji / M9) and August 20th (Galaxy Gala / M9) - October 17th (Granny Smith / M9), respectively [23].

The performance of 10 apple cultivars grafted on MM 106 rootstocks was examined during the Apple Cultivars Adaptation Experiment conducted in the Directorate of Fruit Research Station of Egirdir between the years of 2003 and 2009. In examined cultivars, bud swell occurred between 21st and 25th March, bud break occurred between 29th March and 1st April, first blooming occurred between 19th and 25th April, full blooming occurred between 24th and 27th April, post-blooming occurred in 1st and 5th May and harvesting maturity occurred in 23rd August (for Rubinstein), 14th November (for Cripps Pink (Pink Lady™), respectively [19].

In an investigation carried out in the conditions of Sanliurfa between 2008 and 2012, bud swelling, bud breaking, first blooming, full blooming, post-blooming and harvesting dates of Anna apple cultivar grafted on M9 rootstock were on 6th March, 11th March, 20th March, 25th March, 2nd April and 13th July, respectively, and the same phenological characteristics occurred 1-2 days later for Anna cultivar apple trees grafted on MM 106 rootstocks [24].

According to the results of phenological observations made on Mondial Gala apple variety grafted on M9, M26, MM 106 and MM 111 rootstocks between the years of 2003 and 2009, the date of bud swell was determined as between 20th-25th March, bud break as between 29th March and 5th April, first blooming as between 17th and 21st April, full blooming as between 1st and 7th May, and harvesting dates as between 25st August and 1st September [25].

In a study carried out in Nigde between 2006 and 2007, number of the days from full blooming to harvest were found as 122 days (Galaxy Gala / M9 and Mondial Gala / M9) and 168 days (Granny Smith / M9) for 14 old apple tree cultivars grafted on M9 and MM 106 rootstocks, respectively [23].

Phenological observations made on apple cultivars in our country and in foreign countries have obtained different results. This means that blooming of apple varieties differ depending on the ecological conditions of the farming region. The fact that climatic factors vary from year to year in the region of fruit orchard is also one of the most important reasons why blooming dates and blooming duration of fruit trees differ. Blooming time and duration (full blooming) in fruit garden can differ depending on cultivar, rootstock, ecology, and applied cultural processes, and high weather temperatures during the blooming period will shorten the blooming time [26]. The latitude and longitude, altitude, warm and cold winds of the place where the production is being made, rootstocks and cultural practices significantly influence the flowering process.

Pomological characteristics. The fruit characteristics of Anna apple trees grafted on seedling rootstocks, M9 and MM 111 rootstocks are given in Table 3. The average fruit weights of Anna apple cultivar trees grafted on seedling rootstocks, M9 and MM 111 rootstocks vary between 179.76 (for seedling rootstock) - 221.42 g (for MM 111), fruit width varies between 71.80 (for seedling rootstock) - 75.65 mm (for MM 111), fruit height varies between 72.39 (for seedling rootstock) - 77.30 mm (for MM 111), fruit volume varies between 189.87 (for seedling rootstock) - 238.71 cm³ (for MM 111), fruit flesh hardness varies between 16.4 (for seedling rootstock) - 18.6 lb/cm² (for MM 111), ºBrix varies between 14.8 (for seedling rootstock) - 15.4% (for MM 111) and titratable acidity content varies between 0.61 (for MM 111) - 0.77% (for M9) (Table 3).

According to the results obtained based on the averages of two years, it is determined that weight, volume, size, firmness and TSS content of fruits of clonal rootstocks are higher than those of seedling rootstocks.

TABLE 3
Fruit quality characteristics of Anna apple cultivar grafted on different rootstocks (average of the years 2014-2015)

Rootstocks	Fruit width (mm)	Fruit length (mm)	Fruit weight (g)	Fruit volume (cm^3)	Fruit flesh firmness (lb/cm^2)	TSS (%)	Titratable acidity (%)
Seedling	71.80 b	72.39 b	179.76 b	189.87 c	16.4 b	14.8 c	0.75 ab
M9	72.54 b	76.59 ab	209.09 ab	214.58 b	17.2 ab	15.1 b	0.77 a
MM 111	75.65 a	77.30 a	221.42 a	238.71 a	18.6 a	15.4 a	0.61 b

Within columns, means followed by different letters are significantly different according to the LSD test ($P \leq 0.05$).

Atay et al. [14] determined fruit weights of Galaxy Gala and Jerseymac apple cultivars grafted on MM 106 rootstocks in the conditions of Eğirdir as 150.14 g and 135.71 g, fruit flesh firmness as 13.25 lb/cm² and 19.62 lb/cm², ºBrix as 13.19% and 12.36%, pH level as 3.41 and 3.09, and titratable acidity level as 0.38% and 0.55%, respectively.

Bozbuğa and Pırlak [23] determined the average fruit weight of apple cultivars grafted on M9 and MM 106 rootstocks in the conditions of Nigde as between 144.6 g (for Galaxy Gala / M9) - 216.3 g (for Fuji / M9), fruit diameter as between 70.1 (for Galaxy Gala / M9) – 81.7 mm (for Fuji / M9), fruit height as between 57.6 (for Mondial Gala / M9) – 70.3 mm (for Granny Smith / M9), brix degree as between 12.2 (for Granny Smith / M9) - 16.5% (for Fuji / M9) and fruit flesh firmness as between 11.90 (for Early Red One / MM 106) – 18.96 lb/cm² (for Granny Smith / M9), respectively.

In the conditions of Egirdir (Isparta), in a kind of adaptation trial where 10 apple cultivars grafted on MM 106 rootstocks were involved; fruit weight of the cultivars was determined as between 162 (for Rubinstein) - 287 g (for Crown Gold), fruit width as between 69 (for Early Red One)- 84 mm (for Novaja), fruit length as between 57 (for Gala Selecta) – 77 mm (for Topred), fruit flesh firmness as between 5.30 (for Crown Gold) – 21.05 lb/cm² (for Cripps Pink (Pink Lady™)), pH as between 2.48 (for Cripps Pink (Pink Lady™)) - 4.14 (for Topred), titratable acidity as between 0.31 (for Topred) - 1.12% (for Cripps Pink (Pink Lady™)) and brix degree as between 12.20 (for Scarlet spur) - 16.40% (for Cripps Pink (Pink Lady™)), respectively [19].

For Gala apple cultivar grafted on M9 rootstocks in Čelarevo (Serbia), average fruit weight (g), fruit width (mm), brix degree (%) and titratable acidity level were determined as 174.4 g, 75.0 mm, 12.4% and 0.16%, respectively [27].

In a study conducted by Ikinci and Bolat [24] in Sanliurfa between 2008 and 2012, for Anna apple cultivar grafted on M9 rootstocks, fruit weight was determined as 93.42 g, fruit diameter as 71.14 mm, fruit height as 81.98 mm, fruit volume as 234.58 cm³, fruit flesh firmness as 18.58 lb/cm², brix degree as 14.40% and titratable acidity as 0.45%. The findings obtained in our study on Anna fruit characteristics had similarities with the findings of Ikinci and Bolat [24].

In fruit growing, the fruit dimensions and the chemical structure of the fruit are significantly affected by the ecologies where they grow. Rootstocks, cultural practices (such as fertilization, irrigation etc.) and differences in fruit set rates also have very important effects on fruit quality characteristics. In particular, it has been reported that the rootstocks the cultivars are grafted on affecting the size of the fruit, acidity and brix degree content of the fruit and fruit skin color. The studies conducted on different fruit species have reported that the brix degree varies depending on the strength of the rootstocks.

Fruit growth rate and daily increment of fruit diameter. The fruit diameters of Anna apple cultivar grafted on seedling rootstocks, M9, and MM 111 rootstocks were determined as 14.61, 15.28 and 16.86 mm, respectively, 14 days after full blooming, and daily diameter growth rate in that period was determined as 0.83, 0.80 and 0.99 mm/day, respectively (Figure 1). The fruit diameters after 28 days of full blooming according to fruit samples taken from Anna trees grafted on the same rootstocks reached to 34.50 mm, 31.99 mm and 34.52 mm, respectively, and daily diameter growth rates in the fruits of the same period reached the highest levels of 1.91 mm, 1.30 mm and 1.37 mm, respectively. After this date, the diameter growth of the fruits started to slow down, and 60 days after full blooming, diameters of the fruits reached 53.89 mm, 60.38 mm and 51.56 mm, respectively, 60 days after full blooming, the daily diameter growth rate of Anna fruits decreased to 0.62, 0.90 and 0.68 mm/day, respectively (Figure 1). Golden Delicious and Granny Smith apple cultivars were grown in Zubin Potok (Kosovo) conditions were found to have average fruit growth of 14.3-14.9 mm 25 days after petal fall [21].

Janković et al. [21], Golden Delicious and Granny Smith cultivars grafted on M9 rootstock were determined that the daily fruit growth rate in apple cultivars is in two stages. In the first stage, when the fruit size was 5 mm, they reported that the daily fruit growth varied between 0.1-0.5 mm. The researchers found that in the second stage when the fruit size was above 5 mm, the daily fruit growth varied between 0.5-1.7 mm.

While the fruits on the trees grafted on seedling rootstocks reached the harvest stage 115 days after the full blooming, the fruit diameter deter-

mined as 71.8 mm, and diameter growth rate was determined as 0.14 mm/day in that period. The fruits on the trees grafted on M9 rootstocks reached the harvest stage 110 days after the full blooming (Figure 1). Average fruit diameter on Anna trees grafted on M9 rootstocks reached 75.65 mm during the harvesting period, and the daily diameter increase was 0.13 mm/day in this period. While the fruits of Anna trees grafted on MM 111 rootstocks were reaching harvest maturity 110 days after the full blooming, such as the ones on the trees grafted on M9, their diameters decreased to 72.54 mm and daily diameter rate has decreased to 0.27 mm/day on average in this stage.

Average fruit diameters of 'Red Delicious', 'Granny Smith' and 'Gala Smith' apple cultivars grafted on seedling rootstocks, MM 106 and M.7a rootstocks in Arizona's arid climate conditions in 1990-1991 were varying between 56 mm (for Granny Smith / seedling rootstock) and 73.8 mm (for Red Delicious / M.7a). It was determined that while 'Red Delicious' and 'Granny Smith' cultivars grafted on MM 106 and M.7a were producing bigger fruits than the ones grafted on seedling rootstocks, there was no significant effect on fruit diameter of all 'Gala' cultivar rootstocks [28]. In the ecological conditions of Wisconsin (USA), it was determined that there was no significant effect of M 26, Ottawa -3, M9 Pajam -1 and Vineland-605-1 rootstocks in terms of fruit diameter growth, fruit weight and efficiency effect of Gala apple cultivar [9].

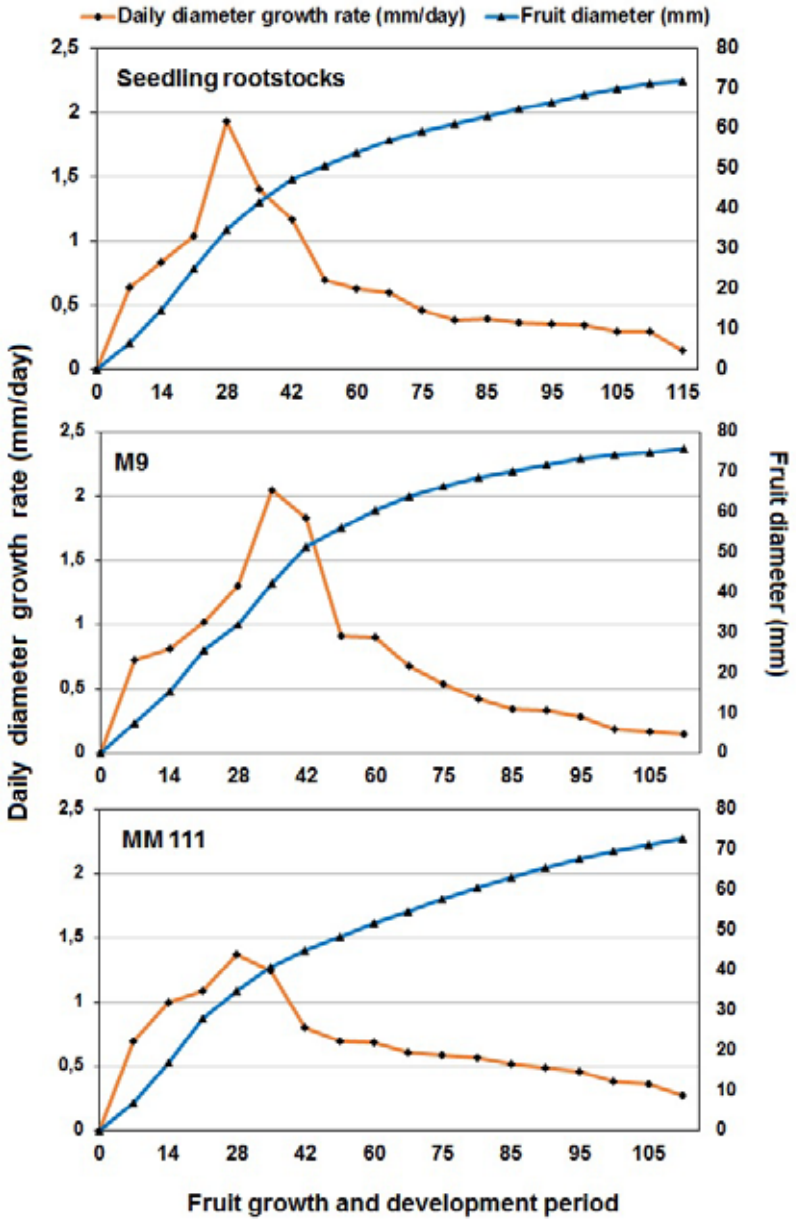

FIGURE 1

Diameter growth (mm) and daily diameter growth rate (mm/day) of the fruits of Anna apple trees grafted on seedling rootstock, M9 and MM 111 rootstocks from the date of full blooming to harvest

In a two-year study in the United States (Arizona), the daily average fruit diameter growth rates of 'Red Delicious', 'Granny Smith' and 'Gala' apple cultivars grafted on seedling rootstocks, MM 106 and M.7a were determined as between 0.33 mm (for Granny Smith / seedling rootstocks) and 0.49 mm (for Red Delicious / M.7a) [28]. In our research that we carried out in the conditions of Sanliurfa, the average daily fruit diameter growth rate of Anna apple cultivar grafted on seedling rootstocks, M9, and MM 111 rootstocks was determined as 0.62, 0.70 and 0.65 mm, respectively, from full blooming to harvest period. The daily diameter growth rate determined in our study was about two times more than the ones determined in arid conditions of Arizona state of US.

Yuri et al. [29] reported that absolute daily growth rate of the fruits of Ultra Red Gala apple cultivar grafted on MM 111 rootstocks continuously increased to 2.5 g/day from full blooming to the 90th day, and their growth rate have slowed down after the 90th day, and the absolute growth rate of the fruit slowed down to 1.75 g/day 130 days after full blooming. Similarly, Bastias et al. [30] determined that while absolute growth rate of 3-years-old 'Fuji' apple grown in pots under blue, red, gray and white shade (control) covers in Bologna (Italy) was 0.75-1.0 g/day 50 days after the full blooming of the fruits, the absolute growth rate of the fruit reached 2.1 - 2.2 g/day 103 days after the full blooming.

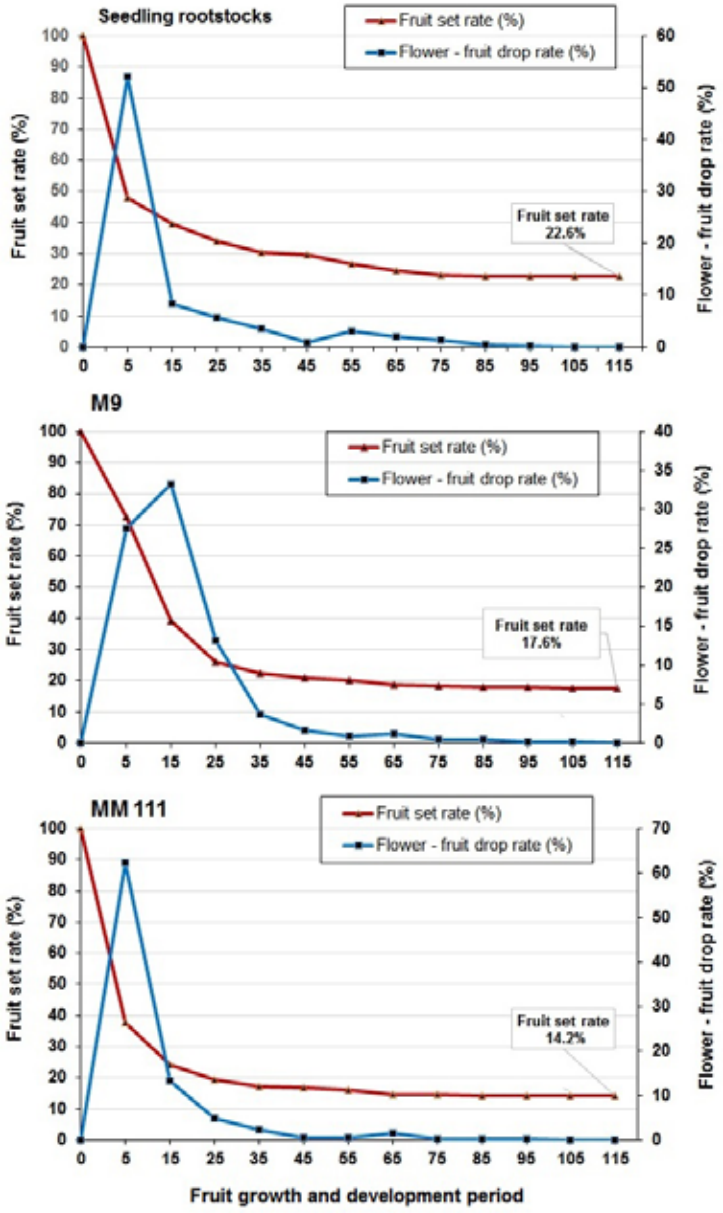

FIGURE 2
The ratio of the flower-fruit drop rate (%) and fruit set rates (%) of Anna apple trees grafted on seedling, M9 and MM 111 rootstocks

Flower - fruit drop rate and fruit set rate (%). While the shedding rates of flowers and fruits have reached the level of 52% 5 days after the full blooming of Anna apple trees grafted on seedling rootstocks, flower and fruit shedding sharply decreased to the rate of 8.4% 15 days after the full blooming (Figure 2). While the flower and fruit shedding rate decreased to 0.8% after 45 days of full blooming, it increased slightly to 3% again 55 days after the full blooming. After this period which is called June drop, the fruit shedding rate slowed down incrementally, and there was no fruit shedding between 105th and 115th days after the full blooming (Figure 2).

The fruit set rate (%), which was accepted as 100% initially, decreased to 48% 5 days after the full blooming (Figure 2). While the fruit set rate was at 26.6% 55 days after the full blooming, the fruit set rate decreased to 22.6% in the harvesting period (115 days after the full blooming).

While flower-fruit shedding rate was 27.6% 5 days after the full blooming of Anna apple cultivar grafted on M9 rootstocks, the flower-fruit shedding rate increased to 33.2% 15 days after the full blooming (Figure 2). For the trees grafted on MM 111 rootstocks, while the flower-fruit shedding rate was 62.4% 5 days after the full blooming, it decreased to 13.4%, similar to the trees grafted on seedling rootstocks, 15 days after the full blooming. While the fruit set rate was 72.4% 5 days after the full blooming of Anna trees on M9 rootstocks, the fruit set rate of the trees grafted on MM 111 was determined as 37.6%.

65 days after full blooming on Anna cultivars grafted on M9 and MM 111 clonal rootstocks, a very small increase in fruit shedding was determined, which could be named as June drop. During the harvest period (115 days after the full bloom), on Anna trees grafted on M9 and MM 111 rootstocks, fruit set rates were determined at the levels of 17.6% and 14.2% respectively.

CONCLUSION

The highest fruit set rate at 22.6% was determined on the trees grafted on seedling rootstocks in Anna apple cultivar grafted on different rootstocks. Although fruit set rates of the trees grafted on seedling rootstocks were higher, fruit dimensions and fruit sizes fell behind the other rootstocks. As Anna trees grafted on seedling rootstocks were observed in terms of phenological characteristics, it was determined that they were delayed 3-4 days in comparison with the ones grafted on M9 and MM 111 rootstocks, and on the other hand, fruit maturity also occurred with a one-week delay. The fruits with bigger fruit size, harder fruit flesh, higher brix degree, and bigger average daily diameter growth rate were the fruits of the trees that were grafted on clonal rootstocks. According to the results obtained from the research, for intensive apple growing, it is determined that the performance of Anna cultivar grafted on M9 and MM 111 rootstocks is better when the soil is suitable for apple growing and where irrigation is possible in Sanliurfa and in the region.

ACKNOWLEDGEMENTS

The authors declare that no conflict of interest exists.

REFERENCES

[1] Soylu, A. (2003) Apple. Temperate climate fruits-II, Pome fruits. Uludağ University Faculty of Agriculture Lecture Notes. No: 72, Bursa, 1-75 (in Turkish).

[2] Özbek, S. (1978) Apple growing. Special fruit cultivation (Deciduous fruit trees). Cukurova University Faculty of Agriculture Publications, Publication No: 128, Textbooks: 11., Adana, 15-94.

[3] Özçağıran, R., Ünal, A., Özeker, E. and İsfendiyaroğlu, M. (2005) Apple. Temperate climate fruit species -II, Pome fruit trees. Volume: II. Ege University Faculty of Agriculture Publications. No: 556, Bornova, İzmir, 3-72.

[4] Warrington, I.J., Fulton, T.A., Halligan, E.A. and de Silva, H.N. (1999) Apple fruit growth and maturity are affected by early season temperatures. J. Amer. Soc. Hort. Sci. 124(5), 468–477.

[5] Calderon-Zavala, G., Lakso, A.N. and Piccinini, R.M. (2004) Temperature effects on fruit and shoot growth in the apple (Malus domestica) early in the season. Acta Hort. 636, 447–453.

[6] Palmer, J.W., Giuliani, R. and Adams, H.M. (1997) Effects on crop load on fruit and leaf photosynthesis of 'Braeburn'/M26 apple trees. Tree Physiology. 17, 741–746.

[7] Meland, M. (2009) Effects of different crop loads and thinning times on yield, fruit quality, and return bloom in Malus x domestica Borkh. 'Elstar'. Journal of Horticultural Science and Biotechnology. ISAFRUIT Special Issue. 117–121.

[8] Öz, F., Burak, M., Büyükyılmaz, M., Özelkök, S. and Ergun, M.E. (1994) Apple frequent planting experiment. Bahçe. 23(1-2), 93-103 (in Turkish).

[9] Al-Hinai, Y.K. and Roper, T.R. (2004) Rootstock effects on growth and quality of 'Gala' apples. HortScience. 39(6), 1231-1233.

[10] Gjamovski, V. and Kiprijanovski, M. (2011) Influence of nine dwarfing apple rootstocks on vigour and productivity of apple cultivar 'Granny Smith'. Scientia Horticulturae. 129, 742–746.
[11] Westwood, M.N. (1995) Temperate-Zone Pomology, Physiology and Culture (Third Edition). Timber Press, Portland, Oregon. 523p.
[12] Rom, C.R. (1996) Environmental factors regulating growth: light, temperature, water, nutrition. In: Maib, K.M., Andrews, P.K., Lang, G.A., Mullinix, K. (Eds.) Tree Fruit Physiology: Growth and Development. Good Fruit Grower, Washington.
[13] Stern, A. and Flaishman, M.A. (2004) Synthetic cytokinins increase fruit size of Royal Gala (*Malus domestica*) apple in Israel. Acta Horticulturae. 636, 557-563.
[14] Atay, E., Pırlak, L. and Atay A.N. (2010) Determination of fruit growth in some apple varieties. Journal of Agricultural Sciences. 16, 1-8.
[15] Senyigit, U., Kadayifci, A. and Uysal, F.O. (2018) Response of 'Jersey Mac' apple trees grafted on M9 rootstock to deficit irrigation under transition zone in west Anatolia. Fresen. Environ. Bull. 27, 2567-2573.
[16] Drake, S.R., Larsen, F.E., Fellman, J.K. and Higgins, S.S. (1988) Maturity, storage quality, carbohydrate, and mineral content of 'Goldspur' apples as influenced by rootstock. J. Amer. Soc. Hort. Sci. 113, 949-952.
[17] Marini, R.P, Barden, J.A., Cline, J.A., Perry, R.L. and Robinson, T. (2002) Effect of apple rootstocks on average 'Gala' fruit weight at four locations after adjusting for crop load. J. Amer. Soc. Hort. Sci. 127, 749-753.
[18] Ezura, H. and Hiwasa-Tanase, K. (2010). Fruit development. In: Pua, E.C., Davey, M.R. (eds.) Plant Developmental Biology - Biotechnological Perspectives. Springer, Berlin Heidelberg New York, 301-318.
[19] Özongun, Ş., Dolunay, E.M., Öztürk, G. and Pektaş, M. (2014). Performance of some apple varieties in Eğirdir (Isparta) conditions. Fruit Science. 1(2), 21-29.
[20] Ünüvar, G. and Pırlak, L. (2016) Determination of phenological and pomological characters of some apple cultivars grafted on M9 rootstock at Karaman ecological conditions. Nevsehir Journal of Sciences and Technology TARGID Special Issue. 96-106 (in Turkish).
[21] Jankovic, D., Jankovic, J. and Blagojevic, R. (2009) Growth rate of apple fruit as a method of predicting their abscission. Acta Agriculturae Serbica. 14(28), 23-30.
[22] Greene, D.W., Lakso, A.N. and Schwallier, P. (2013) Development of a fruitlet growth model to predict thinner response on apples. HortScience. 48(5), 215–216.
[23] Bozbuğa, F. and Pırlak, L. (2012) Determination of phenological and pomological characteristics of some apple cultivars in Niğde-Turkey ecological conditions. The Journal of Animal and Plant Sciences. 22(1), 183-187.
[24] Ikinci, A. and Bolat, I. (2016) Determination of phenological, pomological and yield characteristics of low chilling apple cultivars budded on M9 and MM 106 rootstocks." VIII International Scientific Agricultural Symposium "Agrosym 2016", Jahorina, Bosnia and Herzegovina, October 06-09, 2016. Book of Proceedings. 2016, 627-636.
[25] Özongun, S., Dolunay, E.M., Pektas, M., Öztürk, G., Çalhan, O. and Atay, E. (2016) Yield and quality alterations of some apple cultivars on different rootstock. Journal of Agriculture Faculty of Ege University. 53(1), 35-42.
[26] Jackson, J.E. (2003) Biology of apples and pears. Cambridge University Press. Cambridge, UK., 488p.
[27] Radivojević, D.D., Milivojević, J.M., Oparnica, C., Vulić, T.B., Djordjević, B.S. and Ercişli, S. (2014) Impact of early cropping on vegetative development, productivity and fruit quality of Gala and Braeburn apple trees. Turk J. Agric For. 38, 773-780.
[28] Hussein, I.A. and Slack, D.C. (1994) Fruit diameter and daily fruit growth rate of three apple cultivars on rootstock-scion combinations. HortScience. 29(2), 79-81.
[29] Yuri, J.A., González Talice, J., Verdugo, J. and Del Pozo, A. (2011) Responses of fruit growth, quality, and productivity to crop load in apple cv. Ultra Red Gala/MM111. Scientia Horticulturae. 127, 305-312.
[30] Bastías, R.M., Manfrini, L. and Grappadelli, L.C. (2012) Exploring the potential use of photo-selective nets for fruit growth regulation in apple. Chilean Journal of Agricultural Research. 72(2), 224-231.

Received: **11.09.2018**
Accepted: **27.02.2019**

CORRESPONDING AUTHOR

Ali Ikinci
Department of Horticulture, Faculty of Agriculture, Harran University, Şanlıurfa – Turkey

e-mail: aliikinci61@hotmail.com

© by PSP Volume 28 – No. 4/2019 pages 2864-2875 Fresenius Environmental Bulletin

RESPONSES OF CHLOROPLASTIC ANTIOXIDANT DEFENSE AND PHOTOSYNTHESIS CHARACTERISTICS OF *HEDYSARUM SCOPARIUM* AND *ATRAPHAXIS BRACTEATA* UNDER DROUGHT STRESS

Xiaoxi Zhang[1,2], Hui Liu[1], Gang Han[3,*]

[1]College of Life Sciences, Yan'an University, Yan'an 716000, China
[2]Institute of Soil and Water Conservation, Northwest A&F University, Yangling 712100, Shaanxi, China
[3]College of Forestry, Northwest A&F University, Yangling 712100, China

ABSTRACT

A water-controlled pot-culture experiment was conducted to clarify the mechanism of the photosystem adaptability of *Hedysarum scoparium* and *Atraphaxis bracteata* to drought stress, with the responses of the chloroplastic antioxidant defense system and characteristic parameters of the light/CO_2 response curves of these shrubs detected. The results indicated that (1) for *H. scoparium*, its chloroplastic SOD and DHAR activities significantly increased by 233% and 52% in light drought (LD) soil, its SOD and DHAR activities and AsA and GSH contents increased by 209%, 37%, 96% and 100% in moderate drought (MD) soil, and its SOD, GR and DHAR activities and AsA, GSH and Car contents significantly increased by 57%, 51%, 37%, 42%, 63% and 179%, but the accumulation of H_2O_2 and MDA (54.9% and 146.5%) was also observed in the serious drought (SD) soil. For *A. bracteata*, its chloroplastic GR and DHAR activities and AsA content significantly decreased by 20%, 57% and 19% in LD soil with the accumulation of MDA (214%) simultaneously observed. In the MD and SD soils, the SOD activity and AsA, GSH and Car contents significantly increased by 63%, 40%, 32% and 135%, while the accumulation of H_2O_2 and MDA was also observed (194% and 145-245%). (2) The P_{nmax}, *AQY* and *TPU* of *H. scoparium* significantly decreased by 22%, 19% and 13% in MD soil, while the P_{nmax}, *AQY*, V_{cmax}, J_{max}, *TPU* and R_l significantly decreased by 52%, 19%, 31%, 21%, 26% and 16% in SD soil. However, G_m significantly increased by 130% in SD soil. For *A. bracteata*, its P_{nmax}, *AQY* and *LSP* significantly decreased by 50%, 19% and 35-41% in all types of drought soil. In conclusion, in the revegetation of desert regions, *H. scoparium* can be planted in LD and MD conditions, while *A. bracteata* can only be planted in LD conditions.

KEYWORDS:
Chloroplastic antioxidases and antioxidants, desert shrubs, drought stress, light/CO_2 utilization

INTRODUCTION

Hedysarum scoparium Fisch. et Mey. (Papilionaceae) and *Atraphaxis bracteata* A. Los. (Polygonaceae) are the common psammophytes of Northwest China and are distributed widely in arid drifting sand dunes or inter-dune areas of desert regions in Inner Mongolia, Gansu, Ningxia and Xinjiang Provinces. They not only are the key species in the desert ecosystem but also play important roles in the artificial revegetation of arid regions. However, the survival and retention rates of these species during artificial afforestation are still low, and the growth of their seedlings is slow as well. Furthermore, as the global climate changes, the effects of drought stress are more likely to increase gradually [1, 2]. As photosynthesis is important for the survival and biomass accumulation of plants, while it is strongly affected by drought [3, 4], it is necessary to investigate the responses of the photosystem to increasing drought stress and thus provide targeted scientific management strategies for these psammophytes [5].

Under drought conditions, the water deficit causes the relative excess of light energy, and the balance of electron production and consumption is disturbed [6]. Hence, the contents of reactive oxygen species (ROS) in chloroplasts, the primary sites of photosynthesis, increase sharply [6-8], which will cause the inactivation of enzymes, degradation of proteins [9], and especially damage to the thylakoid membrane structure. Consequently, the chloroplast is quite sensitive to ROS accumulation caused by drought [7]. As the main photosynthetic apparatus, if the chloroplast is injured and its functions are lost, the photosynthetic activity of mesophyll cells will decrease sharply, and the normal metabolism of the whole plant will also be hindered. Fortunately, plants have developed a self-contained antioxidant system to maintain the balance of the production and removal of ROS, thus avoiding oxidation injuries [10]. Relative to studying the plant- or tissue-level antioxidant response to drought stress [11, 12], investigating the response mechanism of the chloroplastic antioxidant system is more helpful to fundamentally

clarify the impacts of drought on photosynthesis. Few efforts have been made to investigate the responses of the chloroplastic antioxidant system to drought stress [13-15]; however, in consideration of the physiological differences among plant species, investigations of the specific antioxidant response of these 2 shrubs are still necessary.

In addition to the regulation of the chloroplastic antioxidant defense system, plants can also adjust gas exchange and metabolic activity to resist drought stress [16, 17]. For instance, *Cotinus coggygria* can increase the apparent quantum yield (*AQY*) and Rubisco activity in light drought conditions and decrease the stomatal conductance to maintain proper water content and water utilization efficiency [18]. In addition, plants can decrease mesophyll conductance to decrease photosynthetic metabolism and adapt to drought conditions [19-21]. Plants can also adjust the light/dark respiratory rates to dissipate the excess light energy to protect the photosynthetic apparatus from injury [22]. Certainly, serious drought will significantly decrease the photosynthetic efficiency of plants. As examples, previous studies demonstrated that drought will cause significant decreases in maximum net photosynthetic rate (P_{nmax}), maximum electron transfer rate (J_{max}), triose phosphate utilization rate (*TPU*), maximum carboxylation rate (V_{cmax})/J_{max} and *AQY* [3, 4, 23-26]. The determination of the abovementioned characteristic parameters of light/CO_2 response curves is helpful to estimate whether photosynthesis is functioning and to assess the ability of plants in drought conditions to utilize light and CO_2. Hence, simultaneously investigation of the alterations of the mentioned parameters and the chloroplastic antioxidant system can clarify the drought resistance mechanism of plants more comprehensively and is helpful for quantitatively measuring the drought resistance ability of plants.

Hence, in this study, the responses of the chloroplastic antioxidant defense system and characteristic parameters of the light/CO_2 response curves of *H. scoparium* and *A. bracteata* to light, moderate and severe drought stresses were detected. The goal was to (1) clarify the mechanism of the adaptability of the photosystem of these species to increasing drought stress and providing a scientific basis for choosing targeted scientific management strategies for these shrubs during revegetation in desert regions and (2) quantitatively assess their drought resistant ability, thus choosing suitable shrubs to be planted in regions with specific drought degrees. It was hypothesized that these 2 shrubs could resist increasing drought stress by (1) an effective chloroplastic antioxidant system, which might be observed as increases in both the chloroplastic antioxidase activities and the antioxidant contents, as well as low H_2O_2 and MDA contents; (2) the ability to maintain light and CO_2 utilization in drought, which might be observed as the changes in characteristic parameters of light/CO_2 response curves. The research approach is shown in Fig. 1.

MATERIALS AND METHODS

Study area. The pot cultivation experiment was carried out in the nurseries of Northwest A&F University, Yangling, China. The climate here is classified as a warm semi-humid continental monsoon climate, with an average annual sunshine duration of 2150 h, an average annual precipitation of 635 mm, an average annual humidity of 70%, an average annual temperature of 12.9°C, an annual effective accumulative temperature (over 10°C) of 4169.2°C, and a frost-free period of 221 d.

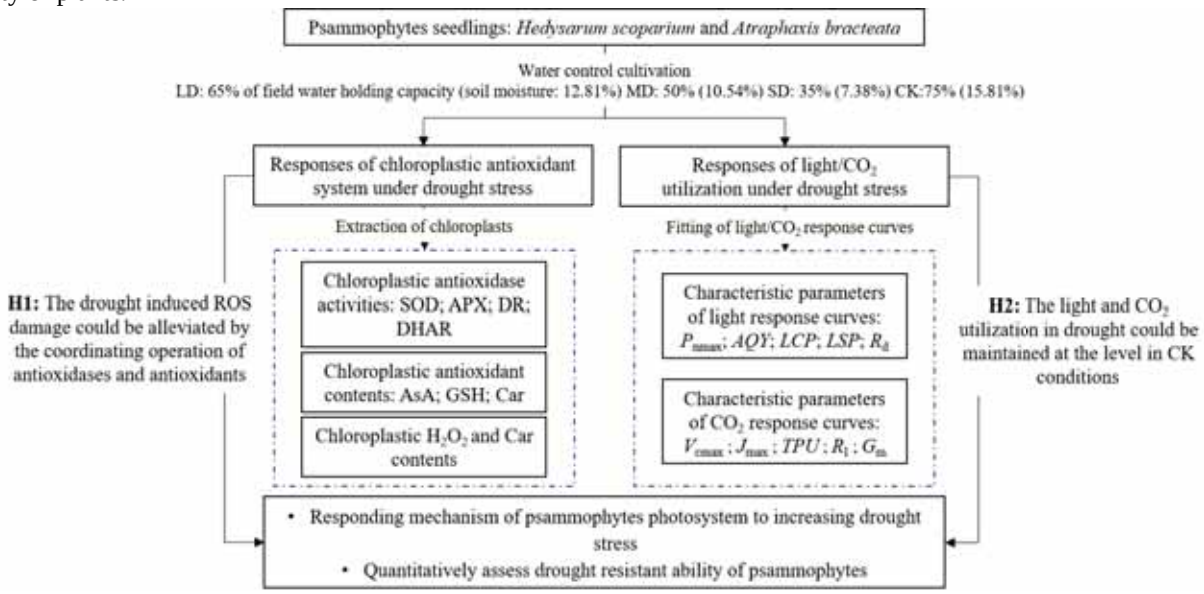

FIGURE 1
The study route.

TABLE 1
Initial properties of the soil sample.

Field water holding capacity (%)	Content of organic matter (g kg^{-1})	Contents of available nutrients (mg kg^{-1})			pH (soil w: water v=1: 2.5)
		N	P	K	
21.08	5.93	4.90	4.89	20.65	8.00

Materials. The one-year-old seedlings of *H. scoparium* and *A. bracteata* used for experiments were purchased from Yanchi County, Ningxia Province, China. The sandy soil used for experiments was collected from Yangling, China and uniformly mixed. The defects in the samples were removed, and then the field water holding capacity and other basic characteristics were measured (Table 1).

Experimental design. In this study, an outdoor pot-culture experiment was conducted. In late February 2012, 18 kg of the prepared soil sample was placed in plastic barrels (which are 29 cm in upper diameter, 25 cm in bottom diameter and 35 cm in height), and a total of 60 barrels of soil samples were prepared. Well-grown *H. scoparium* seedlings were planted in 30 barrels, and the *A. bracteata* seedlings were planted in the remaining 30 barrels. A total of 3 seedlings were planted in the same barrel. After planting, the soil was sufficiently watered to maintain the survival and growth of the seedlings.

On the 15th of July, the seedlings were moved to a removable canopy, and the water-controlled experiment was conducted. According to previous studies, 3 types of drought conditions were designed: light drought (LD, 65% of field water holding capacity, soil moisture of 12.81%), moderate drought (MD, 50% of field water holding capacity, soil moisture of 10.54%) and serious drought (SD, 35% of field water holding capacity, soil moisture of 7.38%). The soil with suitable water moisture (75% of field water holding capacity, soil moisture of 15.81%) was used as a control (CK). The water control was conducted by weighing the cultural barrels. To eliminate the error caused by seedling weight, for each shrub species, the 3 seedlings in one pot were pulled up and weighed to adjust the standard weight. When controlling the soil moisture, the barrels were not watered until the soil moisture decreased to the designed values. Subsequently, plastic film was covered on the barrels to prevent excessive evaporation. The barrels were weighed at 6:00 p.m. every day and watered by reserved rigid plastic pipes, which were buried in the soil (depth: 20 cm and diameter: 2 cm) according to the weight loss, to maintain the soil moisture consistency. When the soil moisture reached the designed level, seedlings in one barrel of each treatment (each species × each type of drought soil) were pulled up and weighed to adjust the standard weight on the 15th and 28th days. Within a week after the 30th day, on sunny, cloudless days, three seedlings were chosen as replicates for the following determinations (each seedling was randomly chosen from one barrel, and a total of 3 barrels were randomly chosen from the barrels sharing the same treatment).

Determination of the chloroplastic antioxidant indices. The upper fresh mature leaves of seedlings were collected at 9:00 a.m.-10:00 a.m. for the determination of chloroplastic antioxidant indices. The methods for obtaining chloroplasts were suggested by Kao [27] and modified. Specifically, 10 g of leaves was frozen in liquid nitrogen, ground and extracted with 50 mL of cold buffer solution (pH 7.8) containing 0.05 mol L^{-1} of Tris, 0.4 mol L^{-1} of sucrose and 0.002 mol L^{-1} of EDTA. Homogenates were filtered through four layers of cheesecloth. The filtrate was centrifuged first at 500xg at 4°C for 5 min. The supernatant was centrifuged again at 2000xg for 15 min with Percoll reagent. The deposits were rinsed with the extracting buffer and centrifuged again. The obtained chloroplasts (deposits) were stored in a -50°C freezer, and a portion of them was suspended and used for the following determinations. Each 0.5 mL of the suspension was mixed with (1) 3 mL of 0.05 mol L^{-1} of phosphate buffer (PBS, pH 7.8) containing 0.015 mol L^{-1} of methionine, 65 μmol L^{-1} of nitroblue tetrazolium (NBT), 0.1 mmol EDTA, 2.0 μmol L^{-1} of riboflavin. The reaction was conducted in 4000 lux of light for 15 min and terminated in dark, and the absorbance was immediately detected at 560 nm. The superoxide dismutase (SOD, EC 1.15.1.1) activity unit was performed as the amount of enzyme required causing a 50% inhibition in the rate of *p*-nitro blue tetrazolium chloride reduction [28]. (2) Additionally, the sample was mixed with 3 mL of 0.025 mol L^{-1} of PBS (pH 7.0) containing 0.1 mmol L^{-1} of EDTA, 5 mmol L^{-1} of AsA and 0.02 mol L^{-1} of H_2O_2, and the absorbance alteration over 1 min was detected at 290 nm (extinction coefficient=2.88 mmol L^{-1} cm^{-1}). The ascorbate peroxidase (APX, EC 1.11.1.11) activity unit was measured as the amount of enzyme required to consume AsA at 1 μmol min^{-1} [29]. (3) Then, the sample was mixed with 3 mL of 0.05 mol L^{-1} of PBS (pH 7.8) containing 2.4 mmol L^{-1} of NADPH, 10 mmol L^{-1} of oxidized glutathione, and the absorbance alteration over 3 min was detected at 340 nm (extinction coefficient=6.22 mmol L^{-1} cm^{-1}) for calculating the glutathione reductase (GR, EC 1.6.4.2) activity [30]. (4) Then, 0.5 mL of the suspension was mixed with 0.025 mol L^{-1} of PBS (pH 7.0) containing 8 mmol L^{-1} of DHA, 70 mmol L^{-1} of reduced glutathione

(GSH) and 0.1 mmol L^{-1} of EDTA, and the absorbance alteration over 3 min was detected at 265 nm (extinction coefficient=14.6 mmol L^{-1} cm^{-1}) to calculate the dehydroascorbate reductase (DHAR, EC 1.8.5.1) activity [31]. All enzymatic units were expressed as specific activity, with the protein content determined using the Bradford [32] method.

For the determinations of ASA, GSH, H_2O_2 and MDA, the chloroplasts were obtained according to the abovementioned method, mixed with 20 mL of trichloroacetic acid (TCA), and centrifuged at 3000×g; the suspension was used for the following determinations: (1) 0.1 mL of the suspension was mixed with 1.5 mL of 0.5% TCA, 1 mL of ethyl alcohol, 0.5 mL of 0.4% phosphoric acid-ethyl alcohol solution, 1 mL of 0.5% 2'-bipyridyl-ethyl alcohol solution and 0.5 mL of 0.03% $FeCl_3$ -ethyl alcohol solution; the mixture was stored at 30□ for 60 min and the absorbance was determined at 534 nm. The AsA content was calculated according to Tanaka et al. [33] as μg mg^{-1} chloroplasts (chl for short); (2) 1 mL of the suspension was mixed with 0.5 mL of Na_2PO_4-NaOH buffer and 0.5 mL of 4 mmol L^{-1} 5,5'-dithiobis-2-nitrobenzoic acid (DTNB). The mixture was diluted to 5 mL and stored at 25°C for 5 min, and the absorbance was determined at 412 nm. The GSH content was calculated according to Ellman [34] as μg mg^{-1} chl; (3) 1 mL of the suspension was mixed with 0.1 mL of 20% titanium tetrachloride in concentrated HCl and 0.2 mL of ammonium hydroxide. The mixture was centrifuged at 3000×g. The precipitate was washed five times with ice-cold acetone and solubilized with 3 mL of 1 mol L^{-1} H_2SO_4, and the absorbance was determined at 410 nm. The H_2O_2 content was determined as titanium-peroxide complex yield: mmol mg^{-1} chl [35]; (4) 2 mL of the suspension was mixed with 2 mL of 0.67% thiobarbituric acid (TBA), the mixture was heated in boiling water for 25 min and quickly cooled in an ice bath, and the absorbance of the mixture was determined at 532 and 600 nm. The amount of MDA was calculated based on an extinction coefficient of 155 mmol L^{-1} cm^{-1}, and its content was calculated according to Chen and Wang [31] as nmol mg^{-1} chl. For the determination of Car content, the chloroplasts were extracted in 80% acetone in the dark at -30°C, the extracts were filtered through a 0.45 mm membrane, and the absorbance was determined at 470, 645 and 662 nm. The Car content was calculated according to Chen and Wang [31] as μg mg^{-1} chl.

Determination of the characteristic parameters of light/CO_2 response curves. Measurements of the light response were taken on the same leaves as above but were exposed to full sunlight. Three leaves were chosen as replicates (n=3) and came from the three seedlings selected as replicates previously. At 8:00 a.m.-11:00 a.m., a Li-6400 portable gas exchange system (Li-Cor Inc., Lincoln, NE, USA) and Li-6400 illuminant (Li-6400-02B) was used to provide photosynthetically active radiation (PAR) with different light intensities: 2000, 1600, 1200, 1000, 800, 600, 400, 300, 200, 150, 100, 50, 20 and 0 μmol m^{-2} s^{-1}. The net photosynthetic rate corresponding to different light intensities was determined. During the determination, the air flow velocity was maintained at 500 ml min^{-1}, the temperature was 30°C, the CO_2 concentration was 380 μmol mol^{-1} and the relative environmental moisture was 40-60%.

Subsequently, the light response curve (photosynthetic rate- PAR) was simulated by the non-rectangle hyperbola model suggested by Farquhar et al. [36] (Eq. 1), and the maximum net photosynthetic rate (P_{nmax}, μmol CO_2 m^{-2} s^{-1}), light compensation point (*LCP*, μmol m^{-2} s^{-1}), light saturation point (*LSP*, μmol m^{-2} s^{-1}) and dark respiratory rate (R_d, μmol·m^{-2}·s^{-1}) were calculated according to the methods suggested by Farquhar et al. [36]. In addition, the light response curve within a weak light scope (*PAR* ≤ 200 μmol m^{-2} s^{-1}) was analyzed by linear regression, and the apparent quantum yield (*AQY*, μmol μmol^{-1}) was calculated.

$$P_n = \frac{AQY \cdot PAR + P_{nmax} - \sqrt{(AQY \cdot PAR + P_{nmax})^2 - 4AQY \cdot PAR \cdot K \cdot P_{nmax}}}{2K} - R_d \quad (1)$$

in which P_n is the net photosynthetic rate and K is the curvature factor of the light response curve.

Measurements of CO_2 response were conducted in terms of light response, including leaf choice, determination time and equipment. A CO_2 mixing system of Li-6400 was used as the gas source for providing different CO_2 concentrations: 2000, 1800, 1600, 1400, 1200, 1000, 800, 600, 400, 300, 200, 150, 120, 90, 60, and 30 μmol·m^{-2}·s^{-1}, and the net photosynthetic rate corresponding to different intercellular CO_2 concentrations (C_i, μmol·mol^{-1}) was determined. During the determination, the air flow velocity was maintained at 500 ml min^{-1}, the temperature was 30°C, the light intensity was 1400 μmol mol^{-1} (saturated light intensity) and the relative environmental moisture was 40-60%.

A modified photosynthetic biochemical model [37] was used for the simulation of the CO_2 response curve (photosynthetic rate- C_i). The model was divided into 3 parts:

(1) in low C_i conditions (< 200 mol mol^{-1}), as P_n was limited by Rubisco, the model is presented as Eq. 2:

$$P_n = V_{cmax}\left[\frac{C_i - \Gamma^*}{C_i + K_c(1 + O/K_o)}\right] - R_l \quad (2)$$

(2) along with the increase in C_i (> 300 mmol mol^{-1}), as P_n was limited by the reproduction of RuBP, the model is presented as Eq. 3:

$$P_n = J\left[\frac{C_i - \Gamma^*}{4C_i + 8\Gamma^*}\right] - R_l \quad (3)$$

(3) along with the continuous increase in C_i, as P_n was limited by *TPU*, the model is presented as Eq. 4:

$$P_n = 3TPU - R_l \quad (4)$$

where P_n is the net photosynthetic rate, V_{cmax} is the maximum carboxylation rate, C_i is the intercellular CO_2 concentration, G_m is the mesophyll conductance, Γ^* is the photosynthetic compensation point (the dark respiration under light was not included), K_c and K_o are the Michaelis-Menten constants of Rubisco to CO_2 and O_2, O is the CO_2 concentration in the chloroplast (210 mmol mol^{-1}), R_l is the dark respiratory rate under light, J is the electron transport rate, J_{max} is the maximum electron transport rate and *TPU* is the triose phosphates utilization rate.

Based on the abovementioned analyses, the V_{cmax}, J_{max}, *TPU* and R_l were calculated using the methods suggested by Sharkey et al. [37] and Long and Bernacchi [38], while the G_m was calculated using the method suggested by Sharkey et al. [37].

Statistical analyses. Statistical analysis was conducted using SPSS 19.0 for Windows. Data were subjected to one-way analysis of variance (ANOVA) and Duncan's multiple range test ($P < 0.05$). The normality assumption was tested with the Kolmogorov and Smirnov test and the equal variance assumption with the method of Bartlett. SigmaPlot 12.5 software was used for drawing.

RESULTS

Responses of the antioxidant defense system in the chloroplasts of the shrubs under different soil moistures. Increasing drought stress caused different responses to the antioxidant defense system in the chloroplasts of the 2 types of shrub species (Fig. 2-4). For *H. scoparium*, in general, its chloroplastic SOD activity exhibited an increase-decrease with increasing drought degrees, while its GR and DHAR activities and antioxidant contents exhibited an obvious increasing tendency. Specifically, in LD soils, only the chloroplastic SOD and DHAR activities significantly increased by 233% and 52% ($P < 0.05$). In MD soil, the activities of SOD and DHAR significantly increased by 209% and 37% again ($P < 0.05$), and the contents of AsA and GSH started to exhibit significant increases relative to the CK levels (96% and 100% increased, $P < 0.05$). In SD soil, the SOD activity sharply decreased by 75% (though it was still significantly higher than that in CK, $P < 0.05$), whereas the GR activity and Car content started to exhibit significant increases relative to the CK levels (51% and 179%, $P < 0.05$), and the DHAR activity and AsA and GSH contents were significantly higher than those in MD soil (51%, 42% and 63% increased, $P < 0.05$). However, the H_2O_2 and MDA contents in the chloroplasts significantly increased by 54.9% and 146.5% in SD soils relative to CK, respectively ($P < 0.05$).

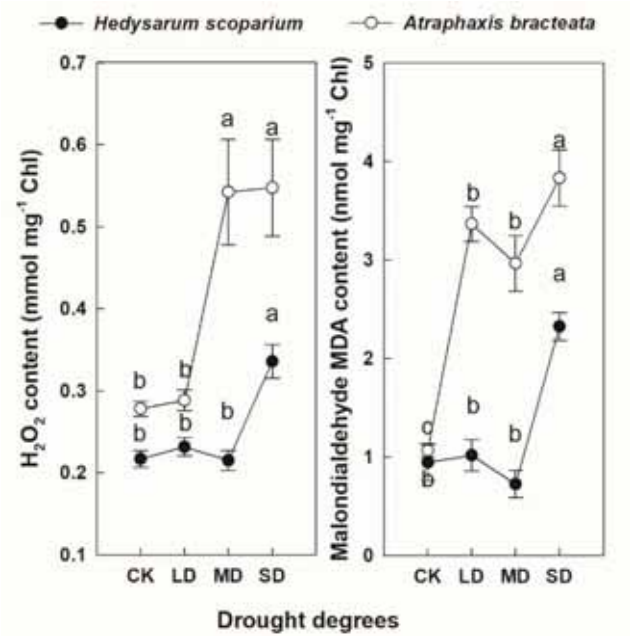

FIGURE 2

The activities of antioxidant enzymes in the chloroplasts of *H. scoparium* and *A. bracteata* in different soil moistures.

The SOD activity unit was performed as the amount of enzyme required to cause a 50% inhibition in the rate of p-nitro blue tetrazolium chloride reduction, and the activity of other enzymes was measured as the consumption rate of substrates in one minute by one mg of protein, with the protein content determined using the Bradford [32] method. CK: control, LD/MD/SD: light/ moderate /severe drought. The different letters above the same circles indicate significant differences at the 0.05 level. This information also applies to the legends below.

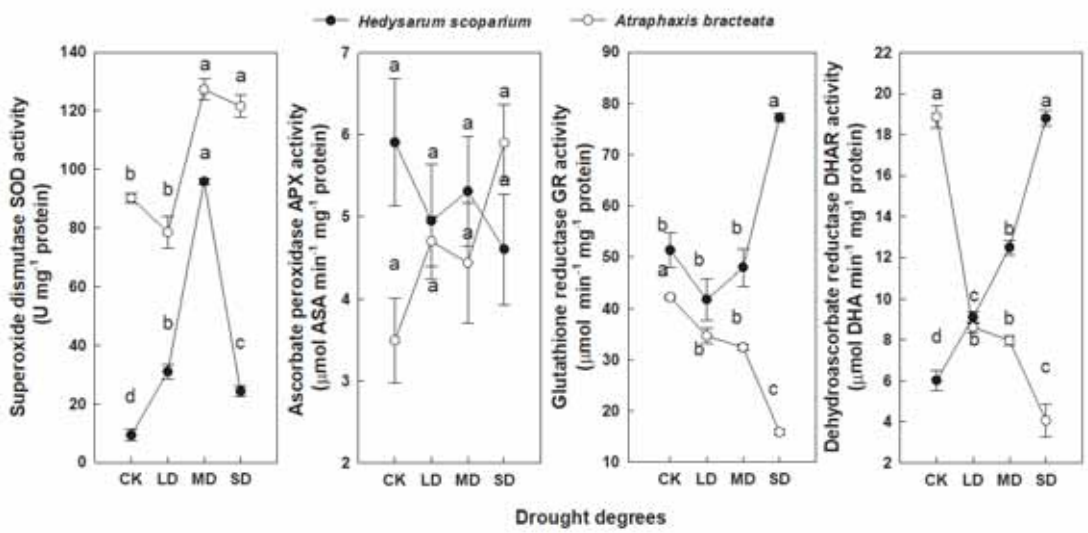

FIGURE 3

The content of antioxidants in the chloroplasts of *H. scoparium* and *A. bracteata* in different soil moistures.
All contents were performed as μg in one mg FW of chloroplasts (chl for short).

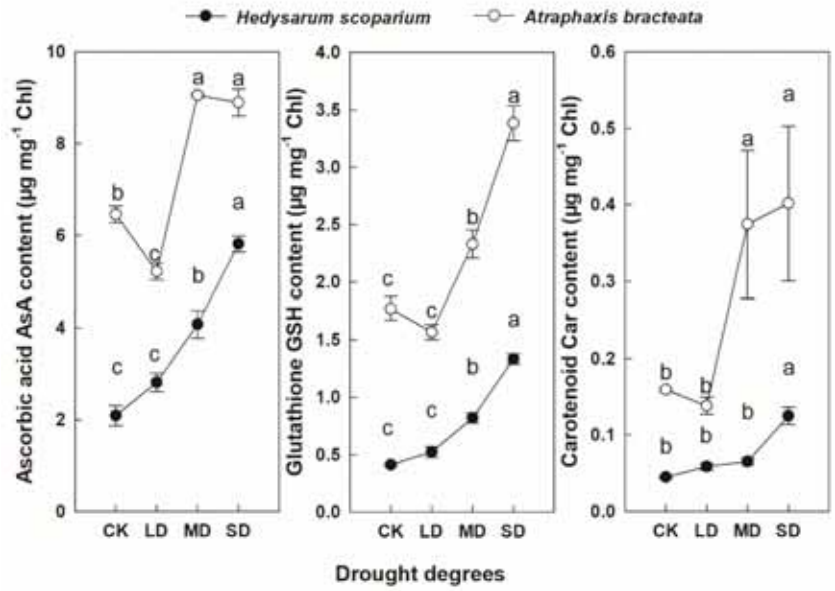

FIGURE 4

The content of H_2O_2 and MDA in the chloroplasts of *H. scoparium* and *A. bracteata* in different soil moistures.

For *A. bracteata*, in general, its chloroplastic GR and DHAR activities decreased with increasing drought stress, while the SOD activity and antioxidant contents exhibited an obvious increasing tendency. Specifically, in LD soils, the GR and DHAR activities and AsA contents exhibited significant decreases relative to CK (20%, 53% and 19%, $P < 0.05$), while the MDA content significantly increased by 214% ($P < 0.05$). In MD soil, the SOD activity significantly increased by 63%, while the activities of GR and DHAR were maintained at the levels found in LD soil ($P < 0.05$). Simultaneously, significantly higher AsA, GSH and Car contents than those in CK were observed (40%, 32% and 135% higher, $P < 0.05$). In addition, although a significant increase in the H_2O_2 content was observed (194.4% of the CK level, $P < 0.05$), the MDA content did not significantly increase ($P < 0.05$). In SD soil, the SOD activity and AsA and Car contents were maintained at levels similar to those in MD soil, while the activities of GR and DHAR decreased by 51% and 49%, respectively ($P < 0.05$). In contrast, the GSH content exhibited a significant increase relative to the MD level (45% increased, $P < 0.05$). In addition, the H_2O_2 content remained at a high level in MD conditions, while the MDA content exhibited a further significant increase (29%, $P < 0.05$).

Responses of characteristic parameters of light/CO_2 response curves of the shrubs under different soil moisture levels. In general, for both shrub species, drought stress caused significant

decreases in the photosynthetic response characteristic parameters (Fig. 5). Under LD conditions, the characteristic parameters of the light/CO_2 response curves of *H. scoparium* did not exhibit significant alterations. Under MD conditions, the P_{nmax}, *AQY* and *TPU* exhibited significant decreases (22%, 19% and 13%, $P < 0.05$). Under SD conditions, the P_{nmax} and *TPU* exhibited a further significant decrease (52% and 26% decreased again, $P < 0.05$), *AQY* maintained a level similar to that under MD conditions, and V_{cmax}, J_{max} and R_l started to exhibit a significant decrease relative to the CK condition (31%, 21% and 16% decreased, $P < 0.05$); however, G_m significantly increased by 130% ($P < 0.05$).

Under LD conditions, P_{nmax}, *AQY* and *LSP* of *A. bracteata* significantly decreased by 50%, 19% and 35% ($P < 0.05$, Fig. 5). Under MD and SD conditions, P_{nmax} and *LSP* were maintained at low levels similar to those under LD conditions, while *AQY* exhibited a continuous significant decrease (13% and 17% decreased, $P < 0.05$).

DISCUSSIONS AND CONCLUSIONS

On the responses of the chloroplastic antioxidant defense system to drought stress. Consistent with hypothesis (1), it was confirmed that *H. scoparium* could resist increasing drought stress by simultaneously increasing the chloroplastic antioxidant activities and antioxidant contents. As observed, its SOD and DHAR activities increased in LD conditions, which is similar to the investigation of Yang et al. [39], who found that the activities of SOD in *Populus kangdingensis* and *P. cathayana* significantly increased by 1.5% and 3.5% in drought conditions (the soil moisture was 50% of the field water holding capacity), indicating that $O_2^{\cdot-}$ and H_2O_2 could be scavenged solely by enzymatic reactions in LD conditions. Along with the increasing drought degree, as was assumed (hypothesis 1), *H. scoparium* relied on increases in both the antioxidase activities and the antioxidant contents to protect its chloroplasts: the chloroplastic SOD and DHAR activities increased in MD conditions, and SOD, DHAR and GR activities increased in SD conditions, while the chloroplastic AsA and GSH contents increased in MD conditions, and the AsA, GSH and Car contents increased in SD conditions. The results were contrary to the findings of Yao et al. [15], in which the chloroplastic SOD of *Malus micromalus* and *M. hupehensis* significantly increased by 20-57%, while the AsA and GSH contents significantly decreased by 50-60% and 36-62% under 0-15% polyethylene glycol treatments, indicating that the function of the chloroplastic antioxidant system of *H. scoparium* could be more effectively activated than in *Malus* plants, and the coordinating operation of antioxidases and antioxidants could start highly effective AsA-GSH cycling to remove excess ROS, at least in MD conditions [8, 40]. This might be because drought-induced increases in ROS production induced the expression of drought resistance genes, thus activating the components of the antioxidant system and maintaining ROS injury at a controllable level [8]. However, in contrast to hypothesis (1), the antioxidant system of *H. scoparium* could not completely protect its chloroplasts from ROS damage under SD conditions. Similar to the previous findings of Yao et al. [15], in which 400-600% and 6.2-94% increases in the chloroplastic H_2O_2 and MDA of *M. micromalus* and *M. hupehensis* were found under 25% polyethylene glycol treatment, 54.9% and 146.5% increases in H_2O_2 and MDA accumulation were observed in the chloroplasts of *H. scoparium* under SD conditions (Fig. 4). This might be attributed to the fact that the molecular structure of SOD in *H. scoparium* chloroplasts might have been destroyed by ROS [5], leading to a decrease or loss of its enzyme activities—in SD conditions, the SOD activity decreased by 75% relative to in MD conditions, which was similar to the findings of Yao et al. [15], who observed 50-57% decreases in the chloroplastic SOD activities of *M. micromalus* and *M. hupehensis* under the 15-25% treatments of polyethylene glycol. Consequently, although the antioxidant contents and other antioxidase activities in the chloroplasts are maintained at relatively high levels, the discordant in the antioxidant system still cause ROS accumulation and peroxidation of the cytomembrane.

However, in contrast with hypothesis (1), it was not possible for *A. bracteata* to increase both the chloroplastic antioxidase activities and antioxidant contents under increasing drought stress, although the SOD activity and AsA, GSH and Car contents increased with increasing drought stress, and the activities of GR and DHAR immediately exhibited continuous decreases. As observed, the chloroplastic GR and DHAR were inhibited (or destroyed) even in LD conditions, which was contrary to the findings of Yao et al. [15], who found 25% increases in the chloroplastic GR activity of *M. micromalus* and *M. hupehensis* under weak drought stress, indicating that the adaptability of the enzymatic antioxidant ability of *A. bracteate* to increasing drought stress was very limited. The possible reasons might be the inhibitory effects on gene expression and protein modification caused by drought [41]. Hence, the efficiency of AsA-GSH cycling decreases due to the decrease in enzyme activities [42, 43]. It is noteworthy that under LD conditions, although no significant increase in H_2O_2 content was observed, the peroxidation of the cytomembrane was noticed. This might be caused by the unvaried SOD activity in chloroplasts leading to a weak ability to catalyze the dismutation of superoxide radicals ($O_2^{\cdot-}$) into H_2O_2 and O_2. Thus, excess $O_2^{\cdot-}$ may cause cytomembrane injury but does not lead to H_2O_2 accumulation. In MD

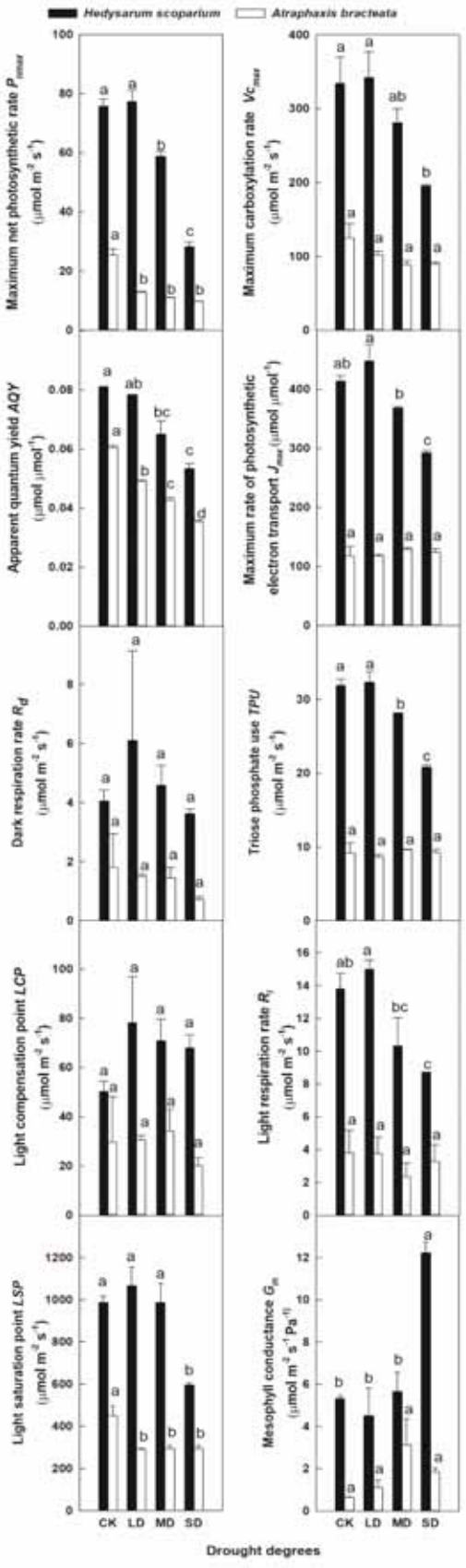

FIGURE 5
Characteristic parameters of light/CO_2 response curves of *H. scoparium* and *A. bracteata* in different soil moistures.

conditions, in contrast, the increased SOD activity accelerated the dismutation of $O_2^{\cdot-}$, thus leading to the accumulation of H_2O_2. However, because the increase in the antioxidant contents and the injury caused by $O_2^{\cdot-}$ is weakened, the peroxidation of the cytomembrane is not aggravated. Under SD conditions, similar to that in the chloroplasts of *H. scoparium*, the strong suppression of the antioxidant enzymes (especially on GR and DHAR) under drought causes quite low efficiency of AsA-GSH cycling; thus, the peroxidation of the cytomembrane aggravated again.

Notably, it was found that the chloroplast antioxidant system of the 2 shrubs exhibited diverse responses to increasing drought stress; that is, *H. scoparium* tended to intensify the synthesis of antioxidases and antioxidants, while *A. bracteate* tended to increase the synthesis of antioxidants. The abovementioned results are similar to the results of Reddy et al. [6], which demonstrated that there are obvious interspecific differences in antioxidant regulating mechanisms. These might be caused by the following reasons: (1) because of the differences in the biological and physiological properties, such as the water absorption and stomatal conductance adjustment abilities of the 2 shrubs, their relative water contents (or leaf water potential) could be quite different in the same drought condition, leading to different antioxidative responses; (2) as reviewed by Zhang [44], even having the same relative water contents, the possibility could not be ruled out that the sensitivity of the related genes or antioxidants to drought of the 2 shrubs were dissimilar, thus causing differences in their responses to increasing drought stress. Certainly, as the related indices were not detected in the present study, further investigations are still needed to clarify the actual mechanism.

On the responses of characteristic parameters of light/CO_2 response curves to drought stress. In contrast to hypothesis (2), *H. scoparium* and *A. bracteata* could not maintain highly effective light and CO_2 utilization in drought stress, at least in MD and SD conditions: our results demonstrated that under MD conditions, not only the net photosynthetic capacity (P_{nmax}) and the abilities of utilizing weak light (*AQY*) were inhibited but the efficiency of utilizing TP to combine other organic matters (*TPU*) of *H. scoparium* was also lowered. This reduction might be caused by the hydrolyzation of starch and the accumulation of saccharides in leaves, which hindered the output of photosynthetic production. These results were also supported by the findings of Wu et al. [24], Wang et al. [26] and Xia et al. [25], in which 12-21% decreases in P_{nmax} of *Sophora davidii* were observed under 20-40% water field capacity conditions, while 39-59% decreases in P_{nmax} and 40% decreases in *AQY* of *Periploca sepium* were observed under 30-45% water field capacity conditions. Under SD conditions, the ability to utilize high

light of *H. scoparium* was inhibited further, but it can still maintain the ability to utilize weak light to some extent to maintain photosynthesis. However, the decreases in V_{cmax} and J_{max} demonstrated that the potential of CO_2 utilization and electron transport efficiency of *H. scoparium* are greatly decreased, which was in line with the findings of Martin-StPaul et al. [3], who found that the V_{cmax} and J_{max} of *Quercus ilex* decrease by 13% and 10%, respectively, along with increasing drought stress. These decreases might have resulted from the photosynthetic apparatus being destroyed or degraded under drought stress [8, 45], leading to decreases in Rubisco activity, the combination of ATP and NADPH and the reproduction of RuBP [46-48]. In the present study, we observed obvious accumulation of H_2O_2 and membrane lipid peroxidation injury in *H. scoparium* chloroplasts (Fig. 4), which might be the dominant reasons for the abovementioned structural damage and loss of function of the photosynthetic apparatus. In addition, under drought conditions, the lack of water results in an insufficient electron donor, thus affecting the J_{max}. Notably, *H. scoparium* could adjust the R_l to reduce the consumption of photosynthetic production and consequently maintain the balance of carbon payments to adapt to drought stress, which was supported by the finding of Li et al. [18]. In addition, unlike other plants that decrease their mesophyll conductance and reduce the diffusion of CO_2 to chloroplasts to reduce metabolism for adapting drought [19-21], the mesophyll conductance of *H. scoparium* even exhibited a significant increase, which is in line with the findings of Sperlich et al. [49], demonstrating that *H. scoparium* could partially maintain its photosynthesis ability by adjusting CO_2 diffusion within leaves in severe drought stress [49]. It was speculated that *H. scoparium* could adjust the expression or activity of water channel proteins to regulate leaf mesophyll conductance [50, 51]. Certainly, it would be expected that mesophyll conductance decreases as the water deficit increases to a critical degree [20, 21], further studies are still needed to clarify the potential mechanisms.

Relative to *H. scoparium*, the P_{nmax}, *AQY* and *LSP* of *A. bracteata* significantly decrease even in LD stress (Fig. 5), which was similar to the results reported by Wang et al. [26] and Xia et al. [25], indicating that the maximum photosynthetic capacity and the ability to absorb/transfer the light energy (both of high and weak light) of *A. bracteata* were significantly decreased and its light ecological amplitude was narrowed [26]. These phenomena might be caused by the decreases in the Rubisco activities and electron transport rate of PSII [52] and the injury to photosynthetic pigments [42, 53, 54], which is also supported by our abovementioned results observing the membrane injury of *A. bracteata* chloroplasts in LD conditions (Fig. 4). Under MD and SD conditions, the P_{nmax} and *LSP* of *A. bracteata* were maintained at the level observed in LD conditions, while *AQY* exhibited a continuous decrease, which was in line with the findings of Wu et al. [24], Wang et al. [26] and Xia et al. [25]. These results suggest that in MD and SD, *A. bracteata* could maintain only a weak ability to utilize high light to some extent; however, its ability to utilize weak light exhibited a further sharp decrease, leading to decreases in the transformation efficiency of light energy.

Similar to the responses of the chloroplastic antioxidant system, there are also obvious differences in the mechanism of the response of photosynthetic metabolism to drought stress, demonstrating that the self-adjustment of photosynthesis to drought is directly associated with the plant species [55], resulting from the long-term evolution process. *H. scoparium* is not affected under LD conditions; however, under MD conditions, its ability to utilize high and weak light decrease, while under SD conditions, although its abilities of utilizing high light and CO_2 decrease sharply, *H. scoparium* can still maintain its ability to utilize weak light to some extent and can adapt to drought stress by adjusting respiration metabolism and gas diffusion. For *A. bracteata*, it mainly maintains the ability to utilize high light to some extent under drought conditions, especially under MD and SD conditions. In addition, its ability to utilize CO_2, respiration and mesophyll conductance is not affected at all times. Comparatively, the self-adjustment and adaptation of *H. scoparium* under different drought conditions are more effective and flexible. In addition, all characteristic parameters of *H. scoparium* are much higher than those of *A. bracteata*; hence, *H. scoparium* exhibits higher levels of photosynthetic metabolism and drought resistance, and it might be more suitable to be used in the revegetation of desert regions that are subject to droughts.

In conclusion, the responses of chloroplastic antioxidant defense and the photosynthesis characteristics (biological properties) of the 2 shrub species to drought stress highly matched their habitat conditions in the revegetation of desert regions; *H. scoparium*, which exhibits anti-drought abilities, can be planted in drifting sand dunes with relative poor soil water conditions (MD and SD), while *A. bracteata* can only be planted in inter-dune areas with favorable water conditions (LD). Of course, for the revegetation in these regions, proper drought-resisting methods, such as utilization of water-retaining agents and ROS scavengers, genetic engineering approaches [56], and mycorrhizal inoculation [57], should be used simultaneously with afforestation to avoid drought stress and enhance drought-resisting abilities based on the chloroplastic antioxidant defense system.

ACKNOWLEDGEMENTS

This research was supported by the by the Natural Science Basic Research Plan in Shaanxi Province of China (2018JQ4047), the Young Talent fund of University Association for Science and Technology in Shaanxi, China (20170704), and the Specialized Research Fund for the Doctoral Program of Yan'an University (YDBK2017-26).

REFERENCES

[1] Dai, A. (2013) Increasing drought under global warming in observations and models. Nat. Clim. Change. 3, 52-58.

[2] Williams, A.P., Allen, C.D., Macalady, A.K., Griffin, D., Woodhouse, C.A., Meko, D.M., Swetnam, T.W., Rauscher, S.A., Seager, R. and Grissinomayer, H.D. (2013) Temperature as a potent driver of regional forest drought stress and tree mortality. Nat. Clim. Change. 3, 292-297.

[3] Martin-StPaul, N.K., Limousin, J.-M., Rodríguez-Calcerrada, J., Ruffault, J., Rambal, S., Letts, M.G. and Misson, L. (2012) Photosynthetic sensitivity to drought varies among populations of *Quercus ilex* along a rainfall gradient. Funct. Plant Biol. 39, 25-37.

[4] Keenan, T., Sabate, S. and Gracia, C. (2010) Soil water stress and coupled photosynthesis-conductance models: bridging the gap between conflicting reports on the relative roles of stomatal, mesophyll conductance and biochemical limitations to photosynthesis. Agric. For. Metorol. 150, 443-453.

[5] Huseynova, I.M. (2012) Photosynthetic characteristics and enzymatic antioxidant capacity of leaves from wheat cultivars exposed to drought. Biochim. Biophys. Acta. 1817, 1516-1523.

[6] Reddy, A.R., Chaitanya, K.V. and Vivekanandan, M. (2004) Drought-induced responses of photosynthesis and antioxidant metabolism in higher plants. J. Plant Physiol. 161, 1189-1202.

[7] Gill, S.S. and Tuteja, N. (2010) Reactive oxygen species and antioxidant machinery in abiotic stress tolerance in crop plants. Plant Physiol. Biochem. 48, 909-930.

[8] Zlatev, Z. and Lidon, F.C. (2012) An overview on drought induced changes in plant growth, water relations and photosynthesis. Emi. J. Food Agric. 24, 57-72.

[9] Foyer, C.H. and Noctor, G. (2005) Redox homeostasis and antioxidant signaling: a metabolic interface between stress perception and physiological responses. Plant Cell. 17, 1866-1875.

[10] Lubovská, Z., Dobrá, J., Štorchová, H., Wilhelmová, N. and Vanková, R. (2014) Cytokinin oxidase/dehydrogenase overexpression modifies antioxidant defense against heat, drought and their combination in *Nicotiana tabacum* plants. J. Plant Physiol. 171, 1625-1633.

[11] Li, W., Zhao, Y., Zhou, Z., Sun, G.-y. and Liu, T. (2012) Effects of drought stress and rehydration on chlorophyll fluorescence characteristics and antioxidant enzyme activities in leaves of *Taxus cuspidata*. J. Desert Res. 32, 112-116.

[12] Das, A., Mukhopadhyay, M., Sarkar, B., Saha, D. and Mondal, T.K. (2015) Influence of drought stress on cellular ultrastructure and antioxidant system in tea cultivars with different drought sensitivities. J. Environ. Biol. 364, 875-882.

[13] Cruz de Carvalho, M.H. (2008) Drought stress and reactive oxygen species: production, scavenging and signaling. Plant Signal Behav. 3, 156-165.

[14] Osakabe, Y., Osakabe, K., Shinozaki, K. and Tran, L.-S.P. (2014) Response of plants to water stress. Front. Plant Sci. 5, e86.

[15] Yao, Y., Zhang, D., Wang, Y. and Gao, X. (2000) Antioxidant metabolism of the chloroplast in apple seedling under water stress. J. Fruit Sci. 17, 1-6.

[16] Lawlor, D.W. and Tezara, W. (2009) Causes of decreased photosynthetic rate and metabolic capacity in water-deficient leaf cells: a critical evaluation of mechanisms and integration of processes. Ann. Bot. 103, 561-579.

[17] Pinheiro, C. and Chaves, M. (2010) Photosynthesis and drought: can we make metabolic connections from available data? J. Exp. Bot. 62, 869-882.

[18] Li, J., Qi, X., Xu, C., Wang, C., Liu, H. and Sun, P. (2015) Short-term responses of leaf gas exchange characteristics to drought stress of *Cotinus coggygria* seedlings. Sci. Silvae Sin. 51, 29-41.

[19] Lopez, D., Venisse, J.S., Fumanal, B., Chaumont, F., Guillot, E., Daniels, M.J., Cochard, H., Julien, J.L. and Gousset-Dupont, A. (2013) Aquaporins and leaf hydraulics: poplar sheds new light. Plant Cell Physiol. 54, 1963-1975.

[20] Perez-Martin, A., Michelazzo, C., Torres-Ruiz, J.M., Flexas, J., Fernández, J.E., Sebastiani, L. and Diaz-Espejo, A. (2014) Regulation of photosynthesis and stomatal and mesophyll conductance under water stress and recovery in olive trees: correlation with gene expression of carbonic anhydrase and aquaporins. J. Exp. Bot. 65, 3143-3156.

[21] Tomás, M., Flexas, J., Copolovici, L., Galmés, J., Hallik, L., Medrano, H., Ribas-Carbó, M., Tosens, T., Vislap V. and Niinemets, Ü. (2013) Importance of leaf anatomy in determining mesophyll diffusion conductance to CO_2 across species: quantitative limitations and scaling up by models. J. Exp. Bot. 64, 2269-2281.

[22] Wang, H., Han, L., Xu, Y. and Niu, J. (2014) Photosynthetic responses of the heteromorphic leaves in *Populus euphratica* to light intensity and CO_2 concentration. Chin J Plant Ecol. 38, 1099-1109.

[23] Galmés, J., Flexas, J., Savé, R. and Medrano, H. (2007) Water relations and stomatal characteristics of Mediterranean plants with different growth forms and leaf habits: responses to water stress and recovery. Plant Soil. 290, 139-155.

[24] Wu, F., Bao, W., Li, F. and Wu, N. (2008) Effects of water stress and nitrogen supply on leaf gas exchange and fluorescence parameters of *Sophora davidii* seedlings. Photosynthetica. 46, 40-48.

[25] Xia, J.-b., Zhang, S.-Y., Zhang, G.-C., Xie, W.-J. and Lu, Z.-H. (2011) Critical responses of photosynthetic efficiency in *Campsis radicans* (L.) Seem to soil water and light intensities. Afr. J. Biotech. 10, 17748-17754.

[26] Wang, R., Xia, J., Yang, J., Zhao, Y., Liu, J. and Sun, J. (2013) Comparison of light response models of photosynthesis in leaves of *Periploca sepium* under drought stress in sand habitat formed from seashells. Chin. J. Plant Ecol. 37, 111-121.

[27] Kao, C.H. (2006) Plant Physiology Laboratory Manual. Wunan Publishing Co.

[28] Beyer, W.F. and Fridovich, I. (1987) Assaying for superoxide dismutase activity: some large consequences of minor changes in conditions. Anal. Biochem. 161, 559-566.

[29] Saruyama, H. and Tanida, M. (1995) Effect of chilling on activated oxygen-scavenging enzymes in low temperature-sensitive and-tolerant cultivars of rice (*Oryza sativa* L.). Plant Sci. 109, 105-113.

[30] Ding, H., Zhu, W., Yang, S. and Yang, X. (2005) Dynamic changes in antioxidative systems in roots of tomato (*Lycopersicom esculentum* Mill.) seeding under zinc stress and recovery. Chin. J. Appl. Environ. Biol. 11, 531-535.

[31] Chen, J. and Wang, X. (2006) Plant physiology experimental guide. In Higher Education Press, Beijing.

[32] Bradford, M.M. (1976) A rapid and sensitive method for the quantitation of microgram quantities of protein utilizing the principle of protein-dye binding. Anal. Biochem. 72, 248-254.

[33] Tanaka, K., Suda, Y. and Kondo, N. (1985) Ozone tolerance and the ascorbater-dependent hydrogen peroxide decomposing system in chloroplasts. Plant Cell Physiol. 26, 1425-1431.

[34] Ellman, G.L. (1959) Tissue sulfhydryl groups. Arch. Biochem. Biophys. 82, 70-77.

[35] Mukherjes, S. and Choudhuri, M. (1983) Implication of water stress induced change in the lever of endogenous ascorbic acid under hydrogen peroxide in *Vigna* seedings. Physiol. Plant. 58, 166-170.

[36] Farquhar, G.D. and Berry, J.v.C.S. (2001) Models of photosynthesis. Plant Physiol. 125, 42-45.

[37] Sharkey, T.D., Bernacchi, C.J., Farquhar, G.D. and Singsaas, E.L. (2007) Fitting photosynthetic carbon dioxide response curves for C3 leaves. Plant Cell Environ. 30, 1035-1040.

[38] Long, S. and Bernacchi, C. (2003) Gas exchange measurements, what can they tell us about the underlying limitations to photosynthesis? Procedures and sources of error. J. Exp. Bot. 54, 2393-2401.

[39] Yang, F., Xu, X., Xiao, X. and Li, C. (2009) Responses to drought stress in two poplar species originating from different altitudes. Biol. Plant. 53, 511-516.

[40] Nogués, I., Llusià, J., Ogaya, R., Munné-Bosch, S., Sardans, J., Peñuelas, J. and Loreto, F. (2014) Physiological and antioxidant responses of *Quercus ilex* to drought in two different seasons. Plant Biosyst. 148, 268-278.

[41] Ishikawa, T., Takahara, K., Hirabayashi, T., Matsumura, H., Fujisawa, S., Terauchi, R., Uchimiya, H. and Kawai-Yamada, M. (2009) Metabolome analysis of response to oxidative stress in rice suspension cells overexpressing cell death suppressor Bax inhibitor-1. Plant Cell Physiol. 51, 9-20.

[42] Anjum, S.A., Xie, X.-Y., Wang, L.-C., Saleem, M.F., Man, C. and Lei, W. (2011) Morphological, physiological and biochemical responses of plants to drought stress. Afr. J. Agric. Res. 6, 2026-2032.

[43] Kannan, N. and Kul, G. (2011) Drought induced changes in physiological, biochemical and phytochemical properties of *Withania somnifera* Dun. J. Med. Plant Res. 5, 3929-3935.

[44] Zhang, Y. (2015) Effects of drought stress on physiological and characteristics of jinsha pomelo. Jiangxi Agricultural University.

[45] Vassileva, V., Demirevska, K., Simova-Stoilova, L., Petrova, T., Tsenov, N. and Feller, U. (2012) Long-term field drought affects leaf protein pattern and chloroplast ultrastructure of winter wheat in a cultivar-specific manner. J. Agro. Crop Sci. 198, 104–117.

[46] Carmo-Silva, A.E., Gore, M.A., Andrade-Sanchez, P., French, A.N., Hunsaker, D.J. and Salvucci, M.E. (2012) Decreased CO_2 availability and inactivation of Rubisco limit photosynthesis in cotton plants under heat and drought stress in the field. Environ. Exp. Bot. 83, 1-11.

[47] Mishra, K.B., Iannacone, R., Petrozza, A., Mishra, A., Armentano, N., Vecchia, G.L., Trtílek, M., Cellini, F. and Nedbal, L. (2012) Engineered drought tolerance in tomato plants is reflected in chlorophyll fluorescence emission. Plant Sci. 182, 79-86.
[48] Li, R.-H., Guo, P., Michael, B., Stefania, G. and Salvatore, C. (2006) Evaluation of chlorophyll content and fluorescence parameters as indicators of drought tolerance in barley. J. Integrative Agric. 5, 751-757.
[49] Sperlich, D., Barbeta, A., Ogaya, R., Sabaté, S. and Peñuelas, J. (2016) Balance between carbon gain and loss under long-term drought: impacts on foliar respiration and photosynthesis in *Quercus ilex* L. J. Exp. Bot. 67, 821-833.
[50] Guo, S., Kaldenhoff, R., Uehlein, N., Sattelmacher, B. and Brueck, H. (2007) Relationship between water and nitrogen uptake in nitrate- and ammonium-supplied *Phaseolus vulgaris* L. plants. J. Plant Nutr. Soil Sci. 170, 73-80.
[51] Miyazawa, S.I., Yoshimura, S., Shinzaki, Y., Maeshima, M. and Miyake, C. (2008) Deactivation of aquaporins decreases internal conductance to CO_2 diffusion in tobacco leaves grown under long-term drought. Funct. Plant Biol. 35, 553-564.
[52] Ashraf, M. and Harris, P.J.C. (2013) Photosynthesis under stressful environments: An overview. Photosynthetica. 51, 163-190.
[53] Zhang, L.T., Zhang, Z.S., Gao, H.Y., Xue, Z.C., Yang, C., Meng, X.L. and Meng, Q.W. (2011) Mitochondrial alternative oxidase pathway protects plants against photoinhibition by alleviating inhibition of the repair of photodamaged PSII through preventing formation of reactive oxygen species in Rumex K-1 leaves. Physiol. Plant. 143, 396-407.
[54] Bijanzadeh, E. and Emam, Y. (2010) Effect of defoliation and drought stress on yield components and chlorophyll content of wheat. Pak. J. Biol. Sci. 13, 699-705.
[55] Chaves, M.M., Flexas, J. and Pinheiro, C. (2009) Photosynthesis under drought and salt stress: regulation mechanisms from whole plant to cell. Ann. Bot. 103, 551-560.
[56] Logan, B.A., Kornyeyev, D., Hardison, J. and Holaday, A.S. (2006) The role of antioxidant enzymes in photoprotection. Photosynthesis Res. 88, 119-132.
[57] Benhiba, L., Fouad, M.O., Essahibi, A., Ghoulam, C. and Qaddoury, A. (2015) Arbuscular mycorrhizal symbiosis enhanced growth and antioxidant metabolism in date palm subjected to long-term drought. Trees. 29, 1725-1733.

Received: **07.10.2018**
Accepted: **28.02.2019**

CORRESPONDING AUTHOR

Gang Han
College of Forestry,
Northwest A&F University,
Yangling 712100 – China

e-mail: zxphg@nwsuaf.edu.cn

© by PSP Volume 28 – No. 4/2019 pages 2876-2879 Fresenius Environmental Bulletin

ASSESSMENT OF THE WHEATGRASS EFFECTS ON ANTIOXIDANT CAPACITY AND DNA DAMAGE IN RATS WITH EXPERIMENTAL RENAL FAILURE

Leyla Mis[1,*], Bahat Comba[2], Yildiray Basbugan[3], Semih Yasar[4], Arzu Comba[2]

[1]Department of Physiology, Faculty of Veterinary Medicine, Yuzuncu Yil University, TR-65090 Van, Turkey
[2]Alaca Avni Celik Vocational High School, Hitit Universty, Corum, Turkey
[3] Department of Internal Medicine, Faculty of Veterinary Medicine, Yuzuncu Yil University, TR-65090 Van, Turkey
[4]Ozalp Vocational High School Yuzuncu Yil University, TR-65090 Van, Turkey

ABSTRACT

In this study, it was aimed to evaluate the effect of wheatgrass on antioxidant capacity and DNA damage in rats with renal failure. In the study, 200-300 g 24 healthy Wistar -Albino male rats obtained from YYU Experimental Animal Unit were used. The rats were randomly divided into 4 groups and each group was formed with 6 rats. Groups were allocated as; 1. Control Group, 2. Renal Failure Group (Genta Group) 3. Renal Failure + Wheatgrass Group (Genta +Wheatgrass) 4. Wheatgrass Group. Gentamicin sulfate was given intraperitoneal at a dose of 50 mg/kg for 1 week and once a day to the groups with renal failure (Groups 2 and 3). Wheat grass extract (10 ml/kg) was added to the drinking water of the wheatgrass group rats (3rd and 4th groups) once a day. This practice lasted for 4 weeks. Total oxidant, antioxidant quantities, DNA damage were evaluated at the end of 4 weeks. The result that wheatgrass could be useful in renal failure was reached.

KEYWORDS:
Rat, TAS, TOS, Wheatgrass, Renal failure

INTRODUCTION

Wheatgrass contains many vitamins, SOD, mucopolysaccharide, cytochrome oxidase. Thus, the cellular activity is increased by the abundant amount of enzymes contained therein. With some important enzymes such as SOD, some pathological changes that can occur can be prevented. Wheatgrass can reduce the burden of digestive system and kidneys by clearing blood circulation and help in the treatment of kidney inflammation [1].

In stress or disease states, as the quantity of oxidizing agents that occur with organs and tissue disorders increases, fulfilling physiological functions for cells, tissues and organs become difficult. Antioxidants are molecules that can prevent these negative effects of oxidant molecules. Therefore, we need antioxidants to prevent the excessive stress occurred as a result of today's living conditions. Wheatgrass is a product with a high antioxidant effect used in recent years. For this reason, wheatgrass is rapidly taking its place among the foods to be consumed in our daily life.

The formation of free radicals, which are initiators of some vital chronic diseases that cause various damage to the organism, as the result of oxidation during the metabolism process, have increased the importance of antioxidant compounds while fighting them [2]. Cytotoxic aldehydes such as malondialdehyde, which is the result of lipid peroxidation, cause damage by binding to proteins and DNA [3].

Gentamicin is a group of aminoglycoside antibiotics that have nephrotoxic effects and are used in urinary tract infections. Clinical symptoms are occurred as a result of nephrotoxicity when gentamicin is used over 2 mg/kg daily and over 5 days. Serum creatinine concentration is elevated in creatinine clearance after administration of gentamicin, which is used in healthy animals at a dose of 10 mg/kg for one week at 8-hours intervals. Urine volume increased slightly due to increased tubule secretion and decreased reabsorption, whereas in urine sediment; tubular epithelial cells, dense cell debris, cellular and granular particles were observed [4].

This study aimed to determine the effect of wheatgrass on oxidative stress and DNA damage in the case of renal failure.

MATERIALS AND METHODS

In this study, 200-300 g Wistar arAlbino 24 healthy male rats were used. The rats were randomly assigned to 6 groups and fed adducts with standard pellet feed and water for 7 days to ensure adaptations. After adaptation of the rats, the cages were grouped as follows.

Group 1 (Control Group): The rats in the control group were fed with adlibitum pellet feed and water.

Group 2 (Genta group with Renal Failure): gentamicin sulfate with a dose of 50 mg / kg was given intraperitoneally for 1 week and once a day.

Group 3 (Genta + Wheatgrass group): In this group, rats were given intraperitoneal injection of gentamicin sulfate at a dose of 50 mg / kg for 1 week and once a day. Wheat grass extract was added to drinking water at a dose of 10 ml / kg every day for 4 weeks.

Group 4: (Wheatgrass Group): Wheatgrass extract of wheatgrass was added to drinking water of wheatgrass group for 4 weeks.

At the end of the study, blood samples were taken from all groups under ketalar anesthesia [5]. Urea, creatinine, TAS, TOS, 8OHdG values were measured from the obtained serum samples. Colorimetric kits (Rel Assay Diagnostics) were used to measure TAS TOS values [6, 7]. The 8OHdG value was reacted with the Elisa kit (Enzo).

RESULT

Serum TAS (mmol Trolox Equiv/L), TOS (µmol Equiv/L), OSI (Arbitrary Unit), 8OHdG (ng/ml), urea (mg/dl) and creatinine (mg/dl) values of all groups were given at Table 1.

Rats in the Genta group had serum urea, creatinine, TOS, $p < 0.05$; OSI was found to be higher than the other groups with $p < 0.01$ significance, but these values were similiar to the control group in the rats in the Genta + Wheatgrass group. However, TAS values were significantly higher in the wheatgrass group than in the other groups. Serum 8OHdG level was higher in the Genta group than in the other groups but not statistically significant (Table1).

DISCUSSION

Karadağ and his colleagues [8], investigated the effects of wheatgrass on CML cells. In this study, they showed that apoptosis is decreased in wheatgrass applied cells and this decrease was caused by decrease of ROS. They found that wheatgrass increased SOD and CAT antioxidant enzymes. AYDOS et al. [9] studied the antiproliferative, apoptotic and antioxidant activities of the wheatgrass (Triticum aestivum L.) extract in the KML (K562) cell line, and they found that the highest observed apoptotic and antiproliferative effect was seen in the cell series ($P < 0.001$) treated at the extract of wheatgrass in the water at the 48th hour and that the MDA level, CAT and SOD activities were elevated. The wheatgrass extract has antioxidant activity, indicating that it inhibits the proliferation of leukemia cells and induces apoptosis.

It has been reported that wheatgrass may inhibit hematological disorders associated with chemotherapy in patients with breast cancer [10]. It has been proved that wheatgrass is useful under various conditions such as anemia, diabetes, cancer, eczema, constipation, kidney diseases and colds [11].

Gentamicin is known to accumulate in proximal renal tubules, leading to renal toxicity through lysosomes, mitochondria, or membrane damage [12]. Some antioxidants have a protective effect on this toxicity, suggesting that these damages may be related to radical metabolism [13].

In this study, the serum urea and creatinine values of the rats in the gentamicin group were measured as the highest, and the values in the wheatgrass+ gentamicin and gentamicin groups were close to the control group values.

The damage of free radicals in the tissues is thought to be the main cause of heart disease and vascular stiffness. At the same time, free radicals also affect the nucleic acids of cells. Excessive cell death leads to early aging and on the other hand, cells undergo changes to form cell lines that support cancer and other similar diseases. Antioxidants neutralize free radicals and prevent cells from being damaged [14]. Increased free radicals can lead to loss of membrane integrity and genetic mutations [15]. Reactive oxygen species such as hydroxyl, superoxide anion, and oxygen radicals are believed to cause carcinogenesis, mutagenesis, aging, and arteriosclerosis. Endogenous antioxidants have been found to protect the body against reactive oxygen, but there is an interesting increase in the protective functions of natural antioxidants found in plants [16].

TABLE 1
TAS-TOS-OSI 8OHdG, urea and creatine values of all groups

Parameters	Control Mean±SD	Wheatgrass Mean±SD	Genta Mean±SD	Wheatgrass+Genta Mean±SD	P
8OHdG	12.54±4.78	16,13±5.74	19.35±4,56	17.57±6,25	≥0,5
TAS	0.63±0,25^{b}	0,92±0,34^{a}	0.41±0,13^{b}	0.56±0,21^{b}	≤0,5
TOS	6.38±1,52^{b}	5,25±1,44^{b}	10,13±2,34^{a}	7.4±1,76^{b}	≤0,5
OSİ	1,01±0,59^{b}	0,57±0,57^{c}	2,47±1,8^{a}	1,32±0,84^{b}	≤0,01
Ürea	33,45±4,58^{c}	35.65±5,36^{c}	61,25±7,58^{a}	43,45±3,78^{b}	≤0,5
Creatinine	0,51±0,04^{b}	0,52±0,03^{b}	0,69±0,06^{a}	0,55±0,05^{b}	≤0,5

a, b, c: The difference between the mean group with different letters in the same line are statistically significant

The balance between antioxidant defense and free radicals' production in organism is very important for health. If there are too few free radicals or few antioxidants, this can lead to permanent or chronic damage. Although the measurement of the oxidant or antioxidant components can be performed separately, this process is time consuming and costly. Thus, Total Antioxidant Status (TAS), Total Oxidative Status (TOS) and Oxidative Stress Index (OSI) measurements reflect this situation and they are more economical [17, 18]. In a study, fucoidan supplementation was reported to be effective against oxidative stress in rats with renal failure [19].

In this study, the serum TOS value of rats in the gentamicin group was at $p < 0.05$; OSI was found to be significantly higher with $p < 0.001$ significance. These values were close to the control group for the rats in the Gentamicin + wheatgrass group. Serum 8OHDG levels were higher in the gentamicin group than in the other groups but it was not statistically significant. However, TAS values were significantly higher in the rats in the wheatgrass group than in the other groups with $p < 0.05$ significance. Other studies findings [8, 9] showed that wheatgrass extract has antioxidant activity, are consistent with the findings of this study.

Kidneys are very important for sustaining metebolism [20]. In assessing the nephrotoxicity mechanism of gentamicin, oxidative stress can be shown as the main focal point [21]. In this case, the reactive oxygen species (ROS) activity may increase and the activity of the antioxidant enzymes may decrease [21, 22]. Some antioxidants have a protective effect on this toxicity, suggesting that these damages may be related to radical metabolism [13].

CONCLUSION

Worldwide, phytotherapy methods acquire great importance and studies in this field are increasing their importance in each day. Wheatgrass has been proven to be extremely effective in the treatment and prevention of deadly diseases such as cancer, and the antioxidant effect has been proven in recent years. In conclusion, we believe that antioxidants in wheatgrass extract may be effective in alleviating the function loss and oxidative damage in renal tissue that intensive dose of gentamicin sulfate created. For this reason, we can say that the use of wheatgrass extract may be beneficial in reducing oxidative stress in renal failure at appropriate doses.

REFERENCES

[1] Ernst, E. (2001) A primer of complementary and alternative medicine commonly used by cancer patients. Medical J Aust. 174, 88-92.

[2] Wei, Y., Pang, C. (2005) The Role of Mitocondria in human aging process. Biotech International. 17, 8-13.

[3] Simic, M. (1994) DNA Markers of oxidative processes in vivo: relevance to carcinogenesis and anticarcinogenesis. Carcinogenesis. 54, 1918-1923.

[4] Sahin, T., Çamkerten, İ. (2003) Use of antibiotics in kidney diseases of cats and dogs. Van Vet Journal. 14(1) 82-86.

[5] Ragbetli, M.Ç., Kara, M., Çolçimen, N., Koyun, N., Çakmak, G., Akyol, V., Deniz, Ö.M., Yurt, K. (2018) Prenatal exposure to low-dose diclofenac sodium does not affect total neuron numbers in spinal segment T13 in rats. Journal of Chemical Neuroanatomy. 87, 49–53.

[6] Erel, O. (2004) A novel automated method to measure total antioxidant response against potent free radical reactions. J Clin Biochem. 37, 112-9.

[7] Erel, O. (2005) A new automated colorimetric method for measuring total oxidant status. J Clin Biochem. 47, 119-129.

[8] Karadag, A., Ozkan, T., Altinok, B., Aydos, S. and Sunguroglu, A. (2007) Antiproliferative and apoptotic effects of wheatgrass extracts on chronic myeloid leukemia (CML) cell line. Planta Med. 73, 991-3.

[9] Aydos, S., Avcı, A., Özkan T., Karadağ, A., Gürleyik, E., Altınouk, B. and Sunguroğlu, A. (2011) Antiproliferative, apoptotic and antioxidant activities of wheatgrass (Triticum aestivum L.) extract on CML (K562) cell line. Turk J Med Sci. 41(4) 657-663.

[10] Artamonova, E., Demidov, L., Kharkevitch, G., Manziuk, L., Pirogova N (2008) Adjuvant fermented Wheatgrass extract (Avemar) nutraceutical improves survival of high-risk skin melanoma patients: a randomized, pilot, phase II clinical study with a 7-year follow-up. Cancer Biotherapy Radiopharmaceuticals. 23(4), 669.

[11] Satyavati R., Jaspreet, K., Vandana, G. (2011) Functional Foods in Health and Diseas. 11, 444-456.

[12] Comba, B., Mis, L., Uslu, S. and Comba, A. (2017) The effect of barley grass on antioxidant capacity and DNA damage in rat with renal failure. Fresen. Environ. Bull. 26, 6135-6140.

[13] Kavutcu, M., Canbolat, O., Oztürk, S., Olcay, E., Ulutepe, S., Ekinci, C., Gökhun, I.H., Durak, I. (1996) Reduced enzymatic anti-oxidant defense mechanism in kidney tissues from gentamicin-treated guinea pigs, effects of vitamins E and C. Nephron. 72, 269-74.

[14] Floyd, R. (1990) Role of oxygen free radicals in carcinogenesis and brain ischemia. FASEB Free Radicals in Diagnostic Medicine, D. Armstrong, Plenum Press, New York, 1-15.
[15] Vincent, M., Russell, W., Low, P. and Feldman, E. (2004) Oxidative Stress in the Pathogenesis of Diabetic Neuropathy. Endocrine. Reviews. 25, 612-628.
[16] Osawa, T., Yoshida, A., Kawakishi, S., Yamashita, K. and Ochi, H. (1995) Oxidative stress, antioxidants, aging and disease. In: Cutler. R.G., Packer, L., Bertram, J. and Mori, A. (eds.) Oxidative Stress and Aging. Birkhauser Verlag, Basel, Switzerland, 367-377.
[17] Ozcan, E.A. (2004) A novel automated method to measure total antioxidant response against potent free radical reactions. J Clin Biochem. 37, 112-119.
[18] Ozcan, E.A. (2005) A new automated colorimetric method for measuring total oxidant status. J Clin Biochem. 38,1103-1111.
[19] Yılmaz, M., Mert, H., Irak, K., Ertan, R. and Mert, N. (2018) The effect of fucoidan on the gentamicin induced nephrotoxicity in rats. Fresen. Environ. Bull. 27, 2235-2241.
[20] Kargun, K. (2018) Investigation of role of casr gene polymorphism in the pathogenesis of patients with chronic renal failure. Fresen. Environ. Bull. 27, 6356-6361.
[21] Cuzzocrea, S., Mazzon, E., Dugo, L., Serraino, I., Di Paola, R., Britti, D., De Sarro, A., Pierpaoli, S., Caputi, A., Masini, E. and Salvemini, D. (2002) A role for superoxide in gentamicin-mediated nephropathy in rats. Eur. J. Pharmacol. 450, 67-76.
[22] Maldonado, P.D., Barrera, D., Medina-Campos, O.N., Hernández-Pando, R., Ibarra-Rubio, M.E. and Pedraza-Chaverri, J. (2003) Aged garlic extract attenuates gentamicin induced renal damage and oxidative stress in rats. Life Sci. 73, 2543-2556.

Received: **09.10.2018**
Accepted: **06.03.2019**

CORRESPONDING AUTHOR

Leyla Mis
Department of Physiology,
Faculty of Veterinary Medicine,
Yuzuncu Yil University,
TR-65090 Van – Turkey

e-mail: leylaaslan23@hotmail.com

© by PSP Volume 28 – No. 4/2019 pages 2880-2888 Fresenius Environmental Bulletin

A STATISTICAL INVESTIGATION OF THE RELATIONSHIP BETWEEN SPECIES AND ENVIRONMENTAL VARIABLES OF MALACOFAUNA IN FEEDING STREAMS OF SAPANCA LAKE (TURKEY)

Serap Kosal Sahin[1,*], Esra Albayrak[2]

[1]Istanbul University, Department of Inland Water Resources and Management, Ordu Street No: 200, 34134 Laleli, Istanbul, Turkey
[2]Istanbul University, Institute of Science, Department of Basic Sciences, 34452, Beyazit, Istanbul, Turkey

ABSTRACT

To understand the relationship between water quality and species composition of streams and to evaluate the effects of water pollution and climate change, mollusks are widely used in ecology. In this study, we investigated the malacofauna in feeding streams of Sapanca Lake, and the relationship between species and environmental variables. This study was conducted at Maşukiye, Yanık, Kurtköy, Mahmudiye and Istanbul streams that are feeds of Sapanca Lake between January 2015 - September 2015. A total of 7 taxa which is including one taxon from Prosobranchia (*Valvata naticina*) and six taxa from Pulmonata (*Ancylus fluviatilis*, *Physella acuta*, *Radix labiata*, *Radix ovata, Planorbis planorbis* and *Planorbarius corneus*) were reported. All of them were reported from the area for the first time. Also, some physicochemical parameters (water temperature, dissolved oxygen, electrical conductivity, pH, nitrite, nitrate, phosphate, total phosphorus, flow rate, depth, and width) were analyzed. According to CCA results, electrical conductivity is the most important environmental parameter affecting the distribution of the determined species. Alpha and beta diversity indices showed that the richest and poorest streams were Mahmudiye Stream and Istanbul Stream, respectively. Obtained results from the relationship between species and environmental variables showed that the investigated streams are no dangerous dimension in terms of water pollution but there is a possibility of pollution on the streams. For this reason, it is necessary to take precautions for these streams.

KEYWORDS:
Malacofauna, Diversity, CCA, Sapanca Lake, Turkey

INTRODUCTION

The available freshwater resources in the world are rather limited. Therefore, the sustainable use of existing water resources must be ensured and protected. Various policies are being developed both in Turkey and in other world states to ensure the proper use and preservation of natural resources. The Water Framework Directive, one of the most up-to-date directives of the European Union, is one of them. In the framework of harmonization studies in the Water Framework Directive in Turkey, some regulations have been issued. One of these is the Water Quality Regulation on Surface Water prepared by T.C Forestry and Water Affairs Ministry. The aim of this regulation is to protect the quality of water resources in the framework of ecosystem principles and to improve the quality of water in line with the needs of the country and the quality classification of drinking water and surface waters have been done. [1]. In line with the objectives of this regulation, it is necessary to determine the quality classes of freshwater resources and take the necessary precautions. There are various biological resources and physicochemical parameters used for determination of water quality but benthic macroinvertebrates are the most important water source effective in determining water quality. In this context, studies on mollusks and their ecology, which constitute a large part of indicator species that are important in determining water quality, are particularly valuable. There are few studies on mollusks and their ecology in the inland waters of Turkey. [2-3], [4], [5], [6-7], [8-9], [10-11], [12-15]. This is a major deficiency in water quality assessment approaches. Although there are studies on the benthic macroinvertebrate fauna of Sapanca Lake [16]. there is no such study about the feeding streams of Sapanca Lake. For this reason, five streams (Maşukiye, Yanık, Kurtköy, Mahmudiye, and Istanbul) which feed Lake Sapanca have been chosen as a study area and the distributions, diversity and ecological preferences of the mollusks species were determined seasonally.

This study was aimed to determine the relationship between species and environmental variables of malacofauna in feeding streams of Sapanca Lake.

MATERIALS AND METHODS

Study Area. Istanbul, Kurtköy, Keçi, Mahmudiye, Yanık, Karaçay, Balıkhane, Çifteçınar, Tuzla, Karlıtarla, Eşme, Kuru, Maden, Çatalölü, Altıkuruş, Harmanlar, Aygır, Cehennem ve Arifiye streams are the feeds of Sapanca Lake. These streams, which are usually fed by the snow of the Samanlı Mountains and seasonal rains, play an important role in the water level of the lake. Five of the active streams (Maşukiye, Yanık, Kurtköy, Mahmudiye and Istanbul) feeding the Sapanca Lake has been selected and a total of ten stations were sampled between January 2015 and September 2015 seasonally. Coordinates were recorded with a geographical positioning system (GPS-Garmin brand) unit (Figure1).

Sampling Procedures and Measurements. In the sampling, a hand grab made of Müller materials with an opening of 0.25 mm was used and an area of 1 m^2 in which water vegetation was concentrated was selected and the area was scanned reversely to the bottom sediment flow direction. Scanned bottom sediment was transferred to plastic jars and fixed with 70% alcohol. The identification of the Mollusc specimens extracted from this sediment was made according to [17-19]. Crusts of species are housed in Istanbul University Faculty of Aquatic Sciences inland water biology laboratory. Four major water variables (water temperature (°C), dissolved oxygen (DO/mg/l), electrical conductivity EC (µS/cm) and pH) were measured in situ. Nitrite NO_2-N (mg/L), nitrate NO_3N (mg/L), phosphate PO_4-P (mg/L) and total phosphorus (TP) analyzed in the laboratory using the ion chromatography. Flow rate was measured by using a flow-meter. The maximum, minimum and average values of some physicochemical parameters are shown in Table 1.

Statistical Analyses. To understand the relationships between the obtained species and the environmental variables, and also to compare the streams in terms of species diversity, some statistical analyzes were performed. In these analyzes, which are based on the species composition and abundance, species included at least three times and more in the five streams that make up our study area participated in the calculation.

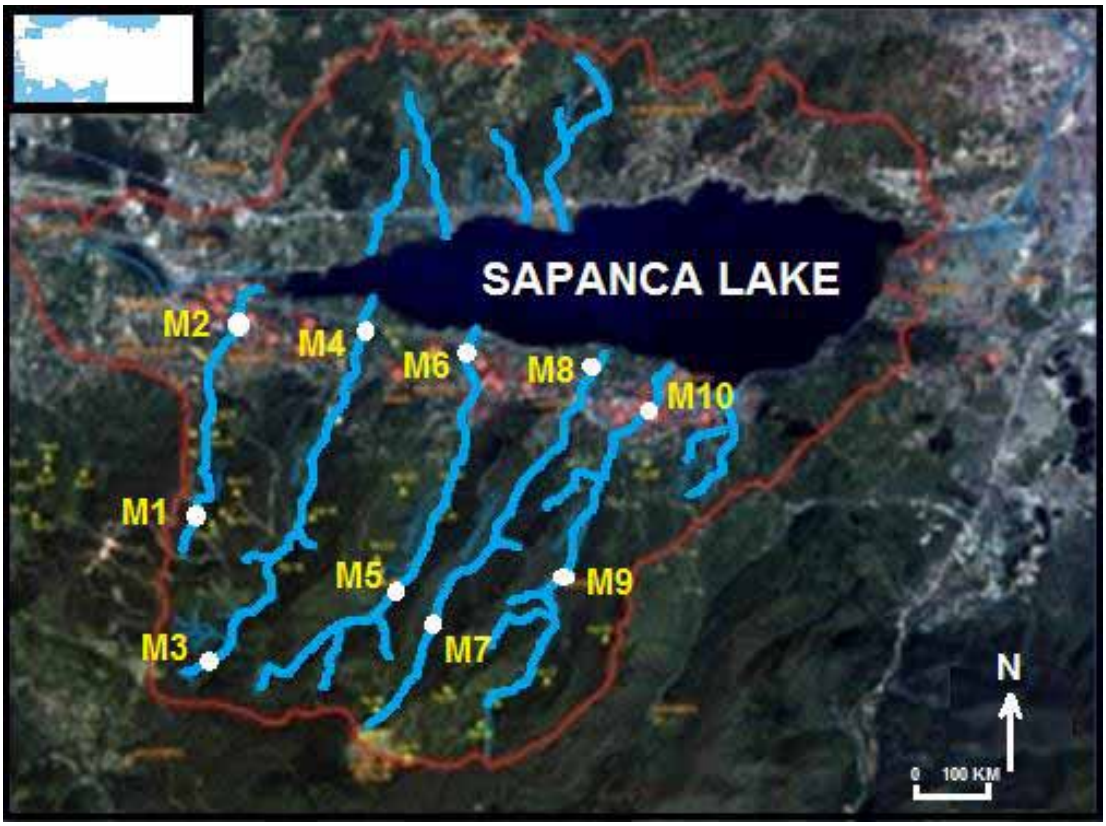

FIGURE 1
Study area and sampling stations. (M 1: Upper Maşukiye Stream, M 2: Down Maşukiye Stream, M 3: Upper Yanık Stream , M 4: Down Yanık Stream, M 5: Upper Kurtköy Stream, M 6: Down Kurtköy Stream, M 7: Upper Mahmudiye Stream, M 8: Down Mahmudiye Stream, M 9: Upper Istanbul Stream , M 10: Down Istanbul Stream).

TABLE 1

The highest and lowest and average values of the measured physiochemical parameters from 10 different stations. [Wt: Temperature (^{0}C), DO: dissolved oxygen (mg/L), pH, NO_2-N (nitrite nitrogen mg/L), NO_3—N (nitrate nitrogen mg/L), PO_4: phosphate (mg/L), EC: electrical conductivity (µS/cm), TP: total phosporus (mg/L), Flow rate (m/s), Depth (cm), Width(cm)].

Stations		Temperature (°C)	pH	EC (µS/cm)	DO (mg/L)	Flow Rate (m/s)	Depth (cm)	Width (cm)	NO_2-N (mg/L)	NO_3-N (mg/L)	PO_4 (mg/L)	TP (mg/L)
M1	MİN.	8.7	7.35	244	6.03	0.33	6	245	0.01	0.0243	0.0007	0.0055
	AVG.	12.1	7.545	287	8.98	0.66	18.35	397.5	0.01575	0.0787	0.00315	0.01015
	MAX.	15.5	7.74	330	11.93	0.99	30.7	550	0.0215	0.1331	0.0056	0.0148
M2	MİN.	8.8	6.95	257	2.35	0	9	98	0.0139	0.0101	0.0003	0.0046
	AVG.	14.85	7.4	315.5	5.76	0.47	16.05	299	0.0392	0.0611	0.00675	0.01065
	MAX.	20.9	7.85	374	9.17	0.94	23.1	500	0.0645	0.1121	0.0132	0.0167
M3	MİN.	7.6	6.72	122	6.25	0.2	0.89	310	0.0068	0.0141	0.004	0.0046
	AVG.	13.5	7.375	246	9.785	1.4	13.695	415	0.01545	0.04045	0.00755	0.0143
	MAX.	19.4	8.03	370	13.32	2.6	26.5	520	0.0241	0.0668	0.0111	0.024
M4	MİN.	7.7	6.83	227	6.09	0	6	370	0.0017	0.0141	0.0014	0.0037
	AVG.	12.1	7.085	306.5	8.43	0.68	25.2	440	0.0092	0.05685	0.0027	0.02135
	MAX.	16.5	7.34	386	10.77	1.36	44.4	510	0.0167	0.0996	0.004	0.0392
M5	MİN.	8.3	7.14	146	6.18	0.63	6.1	101	0.0049	0.0088	0.0003	0.0051
	AVG.	13.05	7.395	213	9.34	0.9125	20.7	548	0.01045	0.03145	0.00985	0.00625
	MAX.	17.8	7.65	280	12.5	1.195	35.3	995	0.016	0.0541	0.0194	0.0074
M6	MİN.	9.07	7.22	165	6.24	0.44	6.6	530	0.0206	0.0214	0.0057	0.0047
	AVG.	14.085	7.735	220.5	9.115	0.66	33.85	737.5	0.03885	0.46635	0.006	0.01365
	MAX.	19.1	8.25	276	11.99	0.88	61.1	945	0.0571	0.9113	0.0063	0.0226
M7	MİN.	6.2	6.62	105	6.06	0.5	12	512	0.003	0.0111	0.0025	0.0015
	AVG.	11.1	7.07	152	9.28	0.773	16.65	721	0.00575	0.04195	0.0044	0.0116
	MAX.	16	7.52	199	12.5	1.046	21.3	930	0.0085	0.0728	0.0063	0.0217
M8	MİN.	8.3	6.67	135	6.17	0.54	7.4	290	0.0077	0.0208	0.0022	0.0097
	AVG.	15.5	7.17	190	8.38	0.963	19.85	394	0.03605	0.0395	0.0095	0.0203
	MAX.	22.7	7.67	245	10.59	1.386	32.3	498	0.0644	0.0582	0.0168	0.0309
M9	MİN.	7.7	6.88	170	6.32	0.37	10	530	0.006	0.0158	0.0006	0.0057
	AVG.	13.4	7.365	241.5	9.76	0.69	24.6	628	0.00975	0.036	0.0039	0.01295
	MAX.	19.1	7.85	313	13.2	1.01	39.2	726	0.0135	0.0562	0.0072	0.0202
M10	MİN.	7.7	7.14	190	6.05	0	3.75	250	0.0051	0.0089	0.0024	0.0049
	AVG.	16.1	7.465	243.5	7.57	64	20.775	445	0.0257	0.0561	0.02595	0.0206
	MAX.	24.5	7.79	297	9.09	1.28	37.8	640	0.0463	0.1033	0.0495	0.0363

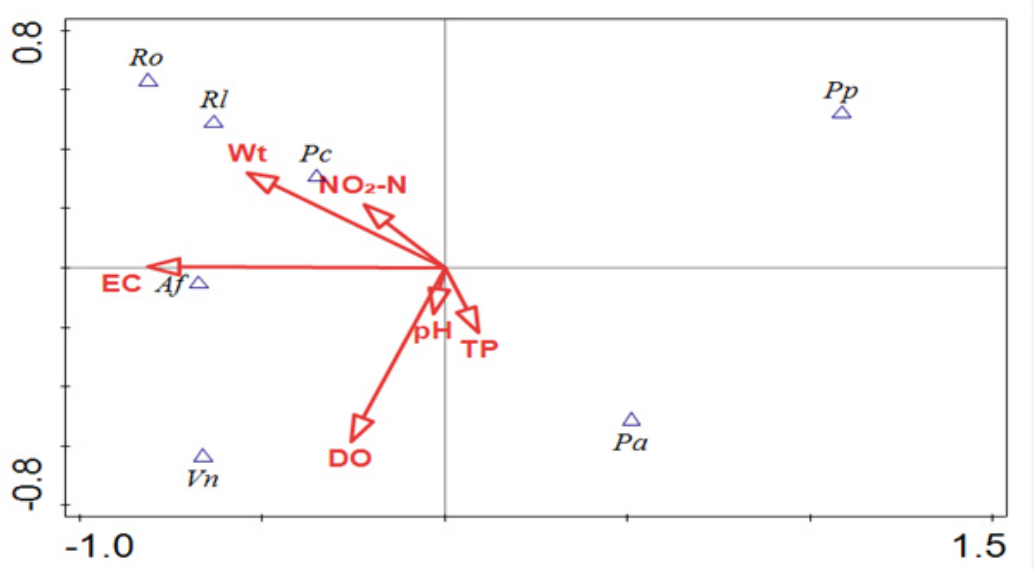

FIGURE 2

CCA diagram of six environmental variables (arrows) and seven species (triangle) found more than three times during the study.

TABLE 2
Distribution of 7 species determined by seasons (Vn: *Valvata naticina*, Af: *Ancylus fluviatilis,* Pa:*Physella acuta,* Rl: *Radix labiata,* Ro: *Radix ovata,* Pp: *Planorbis planorbis*, Pc: *Planorbarius corneus*).

		Pa	Rl	Ro	Af	Vn	Pc	Pp	TOTAL
Winter 2015	**1**	1			3	1			5
	2	2	1			2	2	1	8
	3	1							1
	4	4							4
	5								
	6	1							1
	7							1	1
	8	1							1
	9								
	10						1	1	2
Spring 2015	**1**	1							1
	2	23	8	17	48	21	7	27	151
	3							1	1
	4							1	1
	5	1						2	3
	6	2						3	5
	7	1						4	5
	8	1							1
	9	2							2
	10	2						1	3
Summer 2015	**1**	7							7
	2	16	12	8	3	6	2	5	52
	3								
	4	128	30	20	9	36	18	3	244
	5							1	1
	6	32	10	7	5	10	6	11	81
	7								
	8		1						1
	9							1	1
	10	2							2
Autumn 2015	**1**	1				2			3
	2						1	3	4
	3				1				1
	4	1							1
	5					2			2
	6	6	3	3	6	5	6	1	30
	7	1							1
	8	5	7	3	7	16	9	3	50
	9	2							2
	10	6						1	7
		250	72	58	82	101	52	71	**686**

The Canonical Correspondence Analysis (CCA) [20]. was conducted with the Monte Carlo test (499 permutations) after Detrended Correspondance Analysis (DCA), explains to the suitability of data for CCA, using the CANOCO version 5 program to understand the effect of environmental factors on species. In order to minimize the arc effect, it was selected that seven species and the six most influential environmental variables for CCA (Figure 2, Table 3).

In order to determine the similarities/ differences between the species diversity in the studied areas, the streams have been examined in terms of species diversity within themselves (alpha diversity) and among them (beta diversity). The calculations were made utilizing various indices [Shannon-Wiener (H'), Margalef (D), Brillouin (D), Simpson (D and 1/D) and Berger-Parker Dominance (d) indices for Alpha diversity (Table 4); Whittaker index for Beta diversity (Table 5)] and according to the "Species Diversity and Richness, version 4 program [21]. Also Randomization Test was conducted using a Shannon Wiener index with 10000 random partitions [22] for a significant difference in diversity between two samples.

RESULTS AND DISCUSSION

A total of 7 taxa and 686 individuals were encountered between January 2015- September 2015. One species belongs to Prosobranchia [*Valvata naticina,* Menke, 1845] and six species belong to Pulmonata [*Ancylus fluviatilis,* O.F. Müller, 1774; *Physella acuta* Draparnaud, 1805; *Radix labiata,* Rossmässler, 1835; *Radix ovata* (Draparnaud, 1805); *Planorbis planorbis* (Linnaeus, 1758) and *Planorbarius corneus* (Linnaeus, 1758)] were reported. These taxa are the first record for the region. Distribution of species by stations and seasonal density of gastropod taxa in the streams are shown in Table 2, Figure 3 respectively.

The highest number of individuals was found at station 4 while the lowest individuals were determined at station 3. In our study, *Physella acuta* was found to be the most common species with 250 individuals. The physicochemical parameters of water are quite effective in the distribution of species. When we investigate our study area and its seasonal characteristics, the highest dissolved oxygen level was found at station 3 (13.32 mg/L) at the autum season in upper Yanık Stream. The lowest nitrite nitrogen level was seen at station 4 (0.0017 mg/L) in down Yanık Stream and the lowest nitrate nitrogen (0.0088 mg/L) and phosphate (0.0003 mg/L) values were determined at station 5.

The amount of dissolved oxygen is one of the most important indicators of water quality and is the regulator of metabolic events in the environment [23]. Low concentrations of oxygen are expected in areas under intensive pollution pressure due to environmental pollutants. The minimum average oxygen level in our study was measured as 5.76 mg / L. This value was detected at the station 2 in the down Maşukiye Stream.

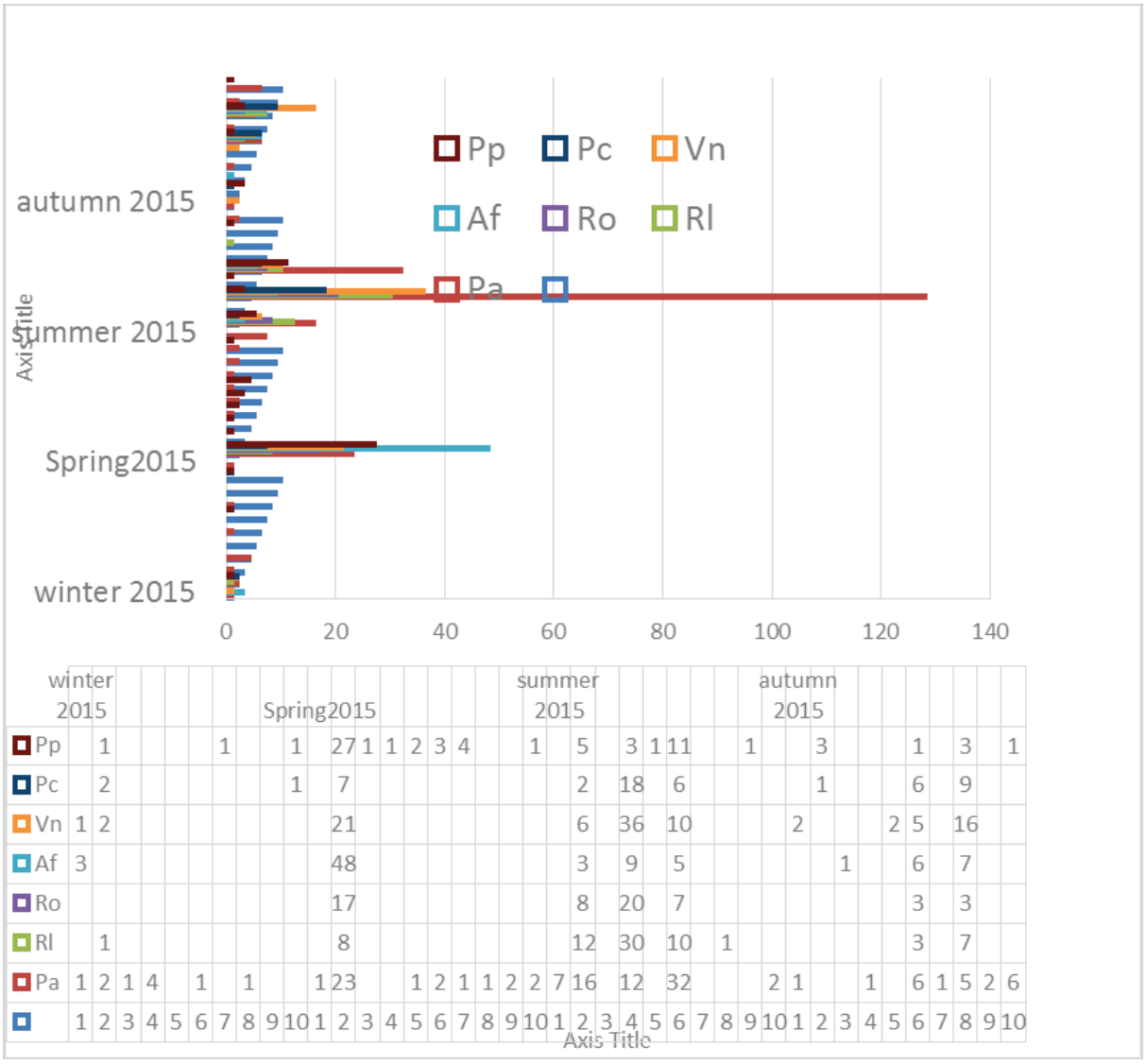

FIGURE 3
The seasonal density of gastropod taxa in the streams.

TABLE 3
The summary table of permutation test results of CCA with six environmental variables and seven species (Test of significance of all canonical axes; F-ratio= 1.676, P-value= 0.022).

	Axis 1	*Axis 2*	*Axis 3*	*Axis 4*
Eigenvalues	0.1772	0.0556	0.0243	0.0181
Explained variation (cumulative)	18.67	24.52	27.08	28.98
Pseudo-canonical correlation	0.7407	0.4974	0.4159	0.5023
Explained fitted variation (cumulative)	63.20	83.03	91.69	98.13

TABLE 4
Results of alpha diversity indices values along with variance (Var. H) and expecte(Exp. H) values for five different streams.

Stream Name	Shannon Wiener H'	Margalef D	Brillouin D	Simpson D	Simpson 1/D	Berger Parker Dominance d	Variance H'	Exp H'	Species No.
Maşukiye	1.849	1.102	1.786	6.027	0.16592	0.2338	0.0007945	6.354	7
Yanık	1.461	1.084	1.407	3.073	0.3254149	0.5296	0.003537	4.309	7
Kurtköy	1.806	1.247	1.702	5.382	0.1858045	0.3415	0.002712	6.087	7
Mahmudiye	1.859	1.465	1.68	6.507	0.15368065	0.2667	0.003471	6.42	7
İstanbul	0.708	0.6792	0.5774	1.763	0.5672149	0.7368	0.03092	2.03	3
All Sample Index	**1.78**	**0.9187**	**1.754**	**4.945**	**0.20222447**	**0.3644**			**7**
Jackknife Std Error	**0.1265**	**0.0521**	**0.1258**	**1.276**	**0.78369906**	**0.1102**			**0**

Nitrite nitrogen is either absent or at trace level in clean waters [24]. High concentrations can be reached in the water where organic pollution is present [25]. According to [26] nitrite nitrogen has a toxic effect on aquatic organisms and persistent in the water may be harmful to aquatic organisms. There is no major risk in our study since it is between 0.0001 and 0.0645 mg / L but because of the 8. the station at the bottom of Mahmudiye is an organic input, the rate has increased and requires measures. During the summer and autumn seasons, the nitrite nitrogen values at the station 8 were found relatively high. (0.0644, 0.0626).

The amount of orthophosphate in the wastewater pollution is a suitable indicator and the amount of orthophosphate in the uncontaminated waters does not exceed 0.1 mg / L and is usually 0.03 mg /L. When the upper limit of 0.1 mg / L is exceeded, pollution can be mentioned [27]. No values exceeding 0.1 mg / L were detected in our study. [28] the pH value is a decisive factor for mollusk species. It has also been reported that low pH (<6) may prevent or even kill mollusks. In our study, the pH value is measured at the range of 6.62-8.25 so there is no limiting effect.

On the other hand, the CCA results have provided a possible correlation of approximately 50% between species and environmental variables (Table 3). Accordingly, electrical conductivity (EC, $p = 0.002$, $F = 4.1$) is the most statistically significant variable on species ($p < 0.01$) (Fig.2).

According to the environmental variables which are measured, the streams can be considered in the 1st and 2nd quality water classes [1]. However, when the streams are investigated in terms of the obtained species, it is seen that a total of 6 of 7 species belong to the Pulmonata group, which live in habitats that generally have eutrophic conditions [29]. Also, it is known that when there is deterioration in an environment or eutrophic conditions occur, susceptible species living there are affected, while persistent species remain in the environment. In other words, the fact that the ratio of non-cosmopolitans (sensitive) to cosmopolitan species in an environment is lower than 1 indicates the presence of a degradation / low water quality in this environment [30]. Therefore, this situation can be explained as a sign of pollution in the streams. These species have been seen in particular at points where human influences were observed in our study area. Also, these species were detected more intensely at the stations near the Sapanca Lake.

TABLE 5
Results of beta diversity indices for five different streams

Index	Beta Diversity
Whittaker Bw	0.129
Cody Bc	2
Routledge Br	0
Routledge Bi	0.07581
Routledge Be	1.079
Wilson & Shmida Bt	0.3226
Harrison 1	3.226
Harrison 2	0

When analyzed the streams for alpha diversity (Table 4), according to this, Shannon-Wiener (H') which is one of the most frequently used indices, and the other values, it was seen that the richest stream is the down Mahmudiye Stream (H'=1.859). This was followed by Maşukiye (H'=1.849) and Kurtköy (H'= 1.806) streams with close values. In addition to this, randomization test, which is based on the Shannon Wiener index, results showed that these approximate values among the H' values of Mahmudiye, Maşukiye, and Kurtköy streams are non-critical, and can refer to the same diversity. However, the similarity between Mahmudiye and Maşukiye streams is higher than Kurtköy, and estimated probability diversities are almost equal and the difference between indices is low (Delta= 0.010) ($p< 0.05$). While the other alpha indices values, Margalef's and Simpon's indices (D), supported to the Shannon index results, the Brillouin index has lower values. This situation can be explained by [31] as "Both the Shannon and Brillouin indices give similar and often correlated estimates of diversity. However, when two indices are used to measure the diversity of a particular data set, the Brillouin index will always produce the lower value. This is because the Brillouin index describes a known collection about which there is no uncertainty. The Shannon index, by contrast, must estimate the diversity of the unsampled as well as the sampled portion of the community." Also, probably that Mahmudiye, Maşukiye, and Kurtköy streams have similar species produced the insignificant differences in the other indices results. The poorest stream was found to be the Istanbul Stream represented by the lowest H' value (H'= 0.708). It is supported by Margalef (D), Brillouin (D), Simpson (D) indices. In addition to this, it is known that a decrease in the value of the diversity index is associated with a reduction in diversity and an increase in dominance. Therefore, Istanbul Stream seems to have the highest values in terms of dominance. High values of Berger-Parker (d) and Simpson (1/D) indices, generally representing occurrences of predominant species, show particularly high predominance in the Istanbul Stream. In the last instance, when this diversity index results were reviewed on the basis of the Shannon Wiener index, it is seen that the H' values, which often fall between 1.5 and 3.5 [31] are low generally for all the studied streams and this situation is related that there is no variance in the species identity of individual [32] When viewed from this aspect to the results of beta diversity indices (Table 5), it is seen that representing similar species almost in all the streams caused the beta value to be low.

CONCLUSION

This study is the first study to determine the relationship between malacofauna and species and environmental variable of Maşukiye, Yanık, Kurtköy, Mahmudiye and Istanbul streams. *Valvata naticina, Ancylus fluviatilis*, *Physella acuta*, *Radix labiata, Radix ovata*, *Planorbis planorbis* and *Planorbarius corneus* were the first to record for the Maşukiye, Yanık, Kurtköy, Mahmudiye and Istanbul streams. All of these streams are a possibility of contamination according to the parameters measured and the species composition determined. For these reasons, measures must be taken for the following processes. From this point of view, during the study period, due to the six of seven species were obtained from streams are pulmonary gastropods which can be defined as "cosmoecious species" [33] with wide ecological tolerance levels and cosmopolitan characters feature and only one species (*Valvata naticina*) that can be defined, is another sign of a deterioration/pollution in the streams.

ACKNOWLEDGEMENTS

This research has been supported by the Unit of Scientific Research Projects, Istanbul University (Project No: 2384). We are grateful Elif Gökkır and Derya Akdemir for contribution in this study.

REFERENCES

[1] YSKYY. (2016) Regulation on Management of Surface Water Quality. Official Gazette Numbered 29797 (in Turkish).

[2] Bilgin, F.H. (1967) Systematic and ecological studies on gastropods living in freshwater vicinity in Izmir. Ege University. Science Faculty. Scientific Reports Series. 36, 1-54 (in Turkish).

[3] Bilgin, F.H. (1980) Systematic and distribution of mollusca species collected from some important freshwater in Western Anatolia. Dicle University. Journal of Medicine Faculty. 8, 1-64 (in Turkish).

[4] Geldiay, R. and Bilgin, F.H. (1969) Some of the documents that have been detected from Turkey about freshwater mollusk. Ege University. Science Faculty. Scientific Reports Series. 90, 1-34 (in Turkish).

[5] Kubilay, A. and Timur, G. (1995) Identification of mollusk species in benthic fauna of Egridir Lake, distribution by seasons and zones. Turkish Journal of Zoology. 19, 241-243 (in Turkish).

[6] Schütt, H. (1988) The Danubian character of the mollusc fauna of the Sapanca Lake (Marmara Region, Turkey). Zoology in the Middle East. 2, 79-85.
[7] Schütt, H. (1993) Pseudamnicola species and other freshwater gastropods (Mollusca, Gastropoda) from East Anatolia (Turkey), the Ukraine and the Lebanon, Basteria. 57, 161-171.
[8] Soylu, E. (1990) The Mollusc fauna of Lake Sapanca. Istanbul University. Journal of Fisheries Faculty. 4, 73-89 (in Turkish).
[9] Soylu, E. (1996) Mollusks of Lake Terkos. Anadolu University. Journal of Science Faculty. 2, 5-17 (in Turkish).
[10] Şeşen, R., and Bilgin, F.H. (1988) Taxonomy of mollusca species detected in some freshwater of Hatay Province and studies on distribution. X. National Biology Congress. Sivas. 2, 97-110 (in Turkish).
[11] Şeşen, R. and Yıldırım, M.Z. (1993) A preliminary research about parasitological importance of freshwater snail in Turkey. T. Journal of Parasitological. 17, 137-147 (in Turkish).
[12] Yıldırım, M.Z., Küçük, F., Gülyavuz, H. and İkiz, R. (1995) A research on the species of gastropoda founded in Side (Antalya) coasts. II Ecology and Environment Congress. September. Ankara, 11-13 (in Turkish).
[13] Yıldırım, M.Z. and Morkoyunlu, A. (1997) A new Sadleriana subspecies from the Burdur Lake Basin Sadleriana byzanthina demirsoyi ssp. some scological characteristics of the subspecies. SDÜ Journal of Science Faculty. 5, 41-43 (in Turkish).
[14] Yıldırım, M.Z. (1999) Prosobranchia in Turkey (Gastropoda: Mollusca) species and zoogeographic distributions. Turkish Journal of Zoology. Additional number (3), 895-896 (in Turkish).
[15] Yıldırım, M.Z. and Karaşahin, S. (2000) The gastropoda species that distributed in freshwater collected from Antalya vicinity. SDÜ Journal of Institute Science. 4, 199-207(in Turkish).
[16] Koşal Şahin, S. (2002) Qualitative and quantitative seasonal change of the benthic fauna of Sapanca Lake. Master's thesis. Istanbul University. Institute of Science. Istanbul, Turkey (in Turkish).
[17] Glöer, P. (2002) Mollusca freshwater gastropods of Northern and Central Europa, identifacition keys, life sweise, distribution. Conch Books. 73. section, 327 pp.(in German).
[18] Macan, T.T. (1977) A Key to the British Fresh anda Brackish Water Gastropods. Freshwater Biology. Association Scientific Publication. No: 13.
[19] Zhadin, V.I. (1965) Mollusks of Fresh and Brackish waters of the U.S.S.R. Ed. Pavlovski, E.N. No:46, Israel Program for Scientific Translations Ltd. Jerusalem, 368p.
[20] Ter Braak, C.J.F. (1986) Canonical correspondence analysis: a new eigenvector technique for multivariate direct gradient analysis. Ecology. 67(5), 1167–1179.
[21] Seaby, R.M. and Henderson, P.A. (2006) Species Diversity and Richness Version 4. Pisces Conservation Ltd., Lymington, England.
[22] Solow, A.R. (1993) A simple test for change in community structure. Journal of Animal Ecology. 62, 191-193.
[23] Tanyolaç, J. (2004) Limnology. 3rd edition. Ankara: Hatipoğlu Press. (in Turkish).
[24] Girgin, S. and Kazancı, N. (1994) Researches on Inland Waters of Turkey I. Evaluation of Water Quality of Ankara Stream Using Physico - Chemical and Biological Parameters. Ankara: Özyurt Press, 184p. (in Turkish).
[25] Egemen, Ö. and Sunlu, U. (1996) Water Quality. Second Edition. Ege University Press, İzmir, Turkey, 14, 153p. (in Turkish).
[26] Stevens, R.J., Laughlin, R.J. (1994) Determining nitrogen - 15 in nitrite or nitrate by producing nitrous oxide. Soil Science Society of America Journal. 58,1108 -1116.
[27] Höll, K. (1979) Water (investigation, evaluation, processing, chemistry, bacteriology, virology, biology) (6. edition) Berlin: de Gruyter, 586 p. (in German).
[28] Gallordo, A., Prenda, J. and Pujente, A. (1994) Influence of quality of some environmental factors on the freshwater macroinvertebrates distribution in two adjacent river basins under Mediterranean climate II. Molluscs. Arch. Hydrobiol. 131, 449-463.
[29] Yıldırım, M.Z. (2004) The Gastropods of Lake Eğirdir. Turkish Journal of Zoology. 99, 97-102.
[30] Külköylüoğlu, O. (2004) On the usage of ostracoda (Crustacea) as bioindicator species in the different aquatic habitats in the Bolu region, Turkey. Ecological Indicators. 4,139-147.
[31] Magurran, A.E. (2003) Measuring biological diversity. Blackwell Publishing Company, Oxford.
[32] Legendre, P.D., Borcard, P. and Peres-Neto, R. (2005) Analyzing beta diversity: partitioning the spatial variation of community composition data. Ecological Monographs. 75, 435–450.
[33] Külköylüoğlu, O. (2013) Diversity, Distribution and Ecology of Non-marine Ostracoda (Crustacea) in Turkey: Application of Pseudorichness and Cosmoecious Species Concepts. Recent Research Development in Ecology. 4, 1- 18.

Received: **15.10.2018**
Accepted: **07.03.2019**

CORRESPONDING AUTHOR

Serap Kosal Sahin
Istanbul University,
Department of Inland Water Resources
and Management,
Ordu Street No: 200,
34134 Laleli, Istanbul – Turkey

e-mail: serap@istanbul.edu.tr

© by PSP Volume 28 – No. 4/2019 pages 2889-2896 Fresenius Environmental Bulleti

AEROSOL BLACK CARBON IN THE NORTHEASTERN QINGHAI-TIBET PLATEAU: DISTRIBUTION, HEALTH RISKS, AND CORRELATION WITH SOIL BLACK CARBON

Xiuyun Min[1,2,3], Jun Wu[1,2,3,*], Jian Lu[3,4], Ronggao Qin[5], Chunliang Gao[1,2], Leiming Li[1,2,3], Xiaoying Guo[1, 2]

[1]Key Laboratory of Comprehensive and Highly Efficient Utilization of Salt Lake Resources, Qinghai Institute of Salt Lakes, Chinese Academy of Sciences, Xining, Qinghai 810008, China
[2]Qinghai Provincial Key Laboratory of Geology and Environment of Salt Lakes, Xining, Qinghai 810008, China
[3]University of Chinese Academy of Sciences, Beijing 100049, China
[4]Key Laboratory of Coastal Environmental Processes and Ecological Remediation, Yantai Institute of Coastal Zone Research, Chinese Academy of Sciences, Yantai, Shandong 264003, China
[5]Faculty of Land Resource Engineering, Kunming University of Science and Technology, Kunming, Yunnan 650093, China

ABSTRACT

The aerosol black carbon (BC) plays an important role in climate change. This study investigated the distribution of aerosol BC in the northeastern Qinghai-Tibet Plateau. The concentrations of aerosol BC in the study area ranged from 0.184 to 4.920 μg m^{-3} with average value of 1.135 μg m^{-3}. No significant correlations existed between soil BC and aerosol BC. Four different health endpoints including low birth weight (LBW), percentage lung function decrement of school-aged children (PLFD), cardiovascular mortality (CM), and lung cancer (LC) were used to evaluate the potential health risks posed by aerosol BC. The highest health risks of LBW, PLFD, CM, and LC reached 14.922, 39.580, 14.475, and 6.821 numbers of equivalent passively smoked cigarettes (PSC), respectively. The highest concentration and health risk of aerosol BC occurred in the industrial area. The concentrations and health risks of aerosol BC in the study area were at a middle level among global regions.

KEYWORDS:
Aerosol black carbon, The Qinghai-Tibet Plateau, Anthropogenic influences, Health risk

INTRODUCTION

Black carbon (BC), generally produced from the imcomplete combustion of fossil fuels or biomass [1], exists ubiquitously in various environmental matrices such as air, soil, sediment, snow, and glacier [2]. BC possesses unique physic-chemical characteristics such as large specific surface area, feature with 3-dimentional structure, variable particle size, and optical properties [3]. BC has been identified as the second contributor to regional atmospheric warming [4]. Aerosol BC can strongly absorb solar radiation from the visible to the infrared wavebands to affect atmospheric visibility and surface albedo so as to make the atmosphere warm [1]. Previous studies have also illustrated that aerosol BC can change regional atmospheric stability and movement to significantly influence hydrologic cycle and regional climate [5, 6]. Aerosol BC is also reported to have strong influences on human health due to its potential of inducing cardiovascular and respiratory diseases as well as increasing blood pressure [7].

Aerosol BC can be transported into soils via dry or wet deposition [8]. BC captured from the atmosphere is generally stored in soils for a long term to subsequently contribute to global carbon sequestration and reduction of greenhouse effect to some extent [9]. More than 90% of BC produced from the imcomplete combustion was reported to be remained in terrestrial ecosystems [10] while BC sequestered in soils could accordingly increase the content of aerosol BC if it was released [11]. Furthermore, wind erosion is another factor capable of transporting a huge amount of soil BC into the atmosphere [12]. Therefore, relationship between soil BC and aerosol BC might exist due to the potential interaction of them.

Known as “the third Pole”, the Qinghai-Tibet Plateau has attracted global interests due to its unique features including high elevation, harsh natural conditions, fragile ecosystem, and relatively weak anthropogenic disturbance [13]. However, unexpected soil/air pollution has occurred in this plateau to exert the potential risks to the ecosystem and humans [13-16]. The Qinghai-Tibet Plateau is one of the most climate-change sensitive regions in

the world to attract wide attention [17], with annual increase in temperature of 0.03 °C during the past three decades [18]. Moreover, the northeastern Qinghai-Tibet Plateau was reported to exhibit the most significant effects of climate change [19]. Some studies have shown that BC has significant impacts on the climate change as well as the fate and transport of contaminants during soil-air exchange process [20, 21]. However, studies on health risks of aerosol BC and relationship between aerosol BC and soil BC around the northeastern Qinghai-Tibet Plateau are still limited although some research work on aerosol BC around the Qinghai-Tibet Plateau has been performed [22-24].

Therefore, this study performed field work, analysis, and evaluation to investigate the distribution and health risks of aerosol BC as well as relationship between aerosol BC and soil BC around the Qinghai-Tibet Plateau. The final aim of this study is to provide comprehensive information on aerosol BC for the similar high-elevation areas.

MATERIALS AND METHODS

Study area. The northeastern Qinghai-Tibet Plateau area is selected as the study area (Figure 1) because it is disturbed by more anthropogenic activities than other regions of this plateau [14]. The average elevation, annual precipitation, the annual temperature, and the annual evaporation of the study area are >3100 m, <100-300 mm, approximately -5 °C, and 1200 mm, respectively [25, 26]. The study area covered the background area, salt-lake area, urban area agricultural and pastoral area, mining area, and industrial area. The background area covered the regions with the least anthropogenic disturbance, mainly including Gyaring Lake, Har Lake, and Ngoring Lake. The agricultural and pastoral area mainly covered the agricultural fields and pastures. The industrial area included regions with the chemical and petrochemical factories. The mining area mainly covered coal and iron mining regions. The salt-lake area included the main salt lakes in the northeastern Qinghai-Tibet Plateau. The urban area mainly covered Delingha City and Golmud City.

Determination of soil BC and aerosol BC. The field work was performed during June 14th to June 29th of 2017. Total 147 topsoil (0-20 cm) samples were collected. Contents of BC in soils determined by the chemo-thermal oxidation (CTO-375) [27] and dichromate oxidation ($K_2Cr_2O_7/H_2SO_4$) [28] were marked as BCT and BCD, respectively. The concentrations of aerosol BC were in situ monitored by a microAeth AE51 real-time monitor (Aethlab Inc., San Francisco, CA, USA) using the 880-nm optical absorption. The flow rate was set at 100 mL min^{-1} for all monitoring experiments. The time interval of AE51 measurements was set as 1 min. The concentration of aerosol BC at each monitoring site that was the same sampling site for each soil sample was continuously monitored for 30 min. The average 1-min concentration of aerosol BC was used to represent the aerosol BC concentration at each site. A total of 147 data on concentration of aerosol BC were obtained (Figure 1).

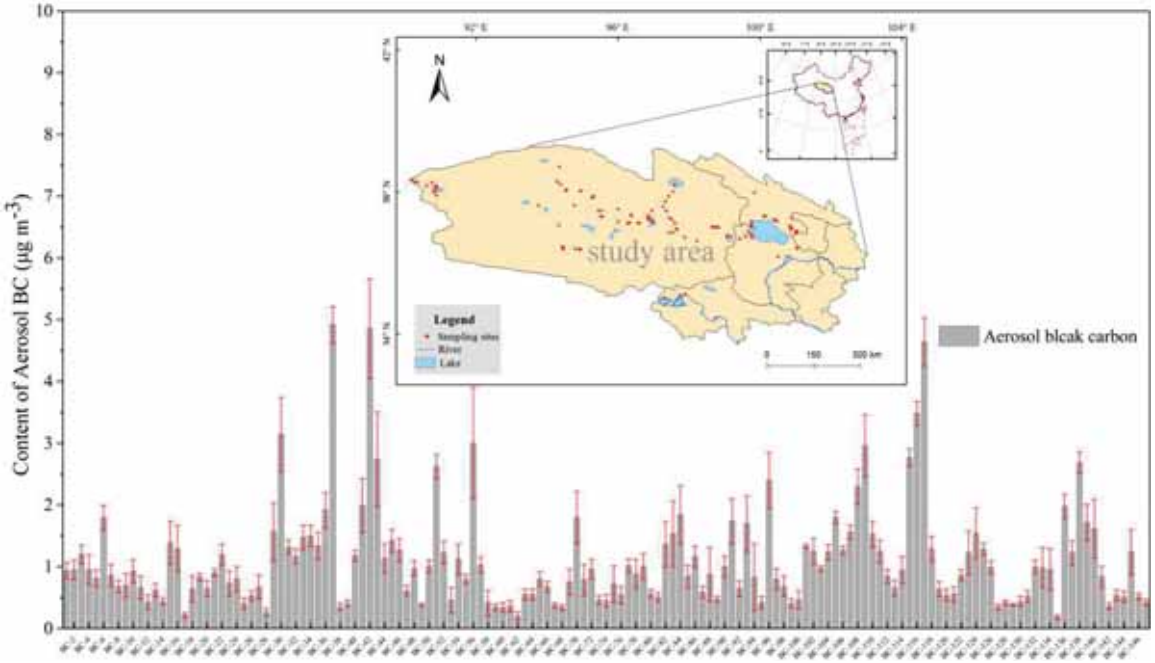

FIGURE 1

Concentrations of aerosol black carbon in the northeastern Qinghai-Tibet Plateau.

Health risk assessment. Health risks posed by aerosol BC was evaluated by the previously reported method [13, 29]. Health risks were assessed using four health endpoints including low birth weight (LBW) that described a birth weight < 2.5 kg after 37-week gestation, lung cancer (LC), cardiovascular mortality (CM), and percentage lung function decrement of school aged children (PLFD). The detailed information on calculation of LBW, LC, CM, and PLFD referred to the references [29]. The numbers of passively smoked cigarettes (PSC) was used to show the potential health risks [29]. The lowest concentration of aerosol BC in site Eboliang of this study (0.184 μg m^{-3}) was chosen as background BC concentration.

RESULTS AND DISCUSSION

Distribution of Aerosol BC. The concentrations of aerosol BC drastically varied at different monitoring sites of the study area (Figure 1). The concentrations of aerosol BC ranged from 0.184 to 4.920 μg m^{-3} with an average value of 1.135 μg m^{-3}. The maximal concentration of aerosol BC in this study area, occurring at Chaka town, was consistent with week-averaged concentration of aerosol BC in one monitoring site of Xining [13]. The minimal concentration of aerosol BC occurred at a Yardang landform park in Eboliang. The concentrations of aerosol BC in this study area were similar with the average daily concentrations of BC in Lulang that was in southeastern Qinghai-Tibet Plateau [30]. The concentration of aerosol BC at the Qinghai Lake (0.219 μg m^{-3}) was relatively low, even lower than that previously reported (0.36 μg m^{-3}) [24]. The average concentration of aerosol BC in this study area (1.135 μg m^{-3}) was consistent with the average daily concentration of BC (1.331 μg m^{-3}) in Mt. Muztagh Ata of the Western Qinghai-Tibet Plateau [31] and the mean concentration of BC (1.391 μg m^{-3}) in Ranwu of the southeastern Qinghai-Tibet Plateau [12], but higher than that of Western Trans-Himalayas (0.75 μg m^{-3}) [32] and that of Linzhi in the southeast of Tibetan Plateau (0.76 μg m^{-3}) [33]. The relatively high concentrations aerosol BC might reveal that the impact of anthropogenic activities in the northeastern Qinghai-Tibet Plateau was greater than that in other regions of this plateau. The average concentration of aerosol BC in the northeastern Qinghai-Tibet Plateau was significantly lower than the mean value of BC at Maitri (8.25 μg m^{-3}) and Larsemann Hills (6.03 μg m^{-3}) of Indian Antarctic stations [34]. Moreover, some studies have showed that the distribution of aerosol BC was significantly affected by different factors including altitude and meteorological conditions [35]. The aerosol BC in this study area might be caused by the incomplete combustion due to "plateau effects" such as relatively low pressure and oxygen content. Combustion of fossil fuels and biofuels such as yak dung and crop residues contributes to aerosol BC with certain percentage in the northeastern Qinghai-Tibet Plateau [36]. In addition, the northeastern Qinghai-Tibet Plateau offered ideal conditions including scarce vegetation, windy weather, and little precipitation for transport of aerosol BC.

Impact of anthropogenic activities on distribution of aerosol BC. The statistical summary on concentrations of aerosol BC in 6 different functional areas was shown in Figure 2. The concentrations of aerosol BC of the background area ranged from 0.460 to 1.539 μg m^{-3} with an average value of 0.913 μg m^{-3}. The concentrations of aerosol BC in background area were comparable with those at Tengchong monitoring station of the southeastern Qinghai-Tibet Plateau [37], but higher than those at Waliguan meteorological station [38] and Nam Co [39]. The average concentration of aerosol BC in salt-lake area was 0.981 μg m^{-3}, higher than that in Salt Lake City [40]. Production activities for utilization of salt-lake resources might be an important factor influencing distribution of aerosol BC in this area. The average concentration of aerosol BC in the urban area reached 1.302 μg m^{-3}, lower than that in Xiamen [41], Shenzhen [42], and Beijing [43]. Less frequent industrial activities and low population density might contribute to relatively low concentration of BC in urban areas when compared with big cities. The concentrations of aerosol BC in agricultural and pastoral area ranged from 0.201 to 3.145 μg m^{-3} with an average value of 0.887 μg m^{-3}, possibly influenced by combustion of yak dung in this area. The concentrations of aerosol BC in the industrial area ranged from 0.219 to 4.856 μg m^{-3} with an average value of 1.641 μg m^{-3} while those in mining area ranged from 0.184 to 3.003 μg m^{-3} with an average value of 0.981 μg m^{-3}. The concentrations of aerosol BC in the industrial area were lower than those in an industrial city of southern Taiwan during summer [44] and an industrial city (Kanpur) of northern India [45]. The results of this study indicated that the average concentration of aerosol BC in industrial area was the highest and that in agricultural and pastoral area was the lowest. The average concentration of BC in salt-lake area was similar with that in mining area, lower than that in urban area, and higher than that in background area. Industrial activities, mining, traffic, combustion of biomass, and tourism might contribute to the distribution of aerosol BC in the study area to different extents, which was also proved by previous studies [46].

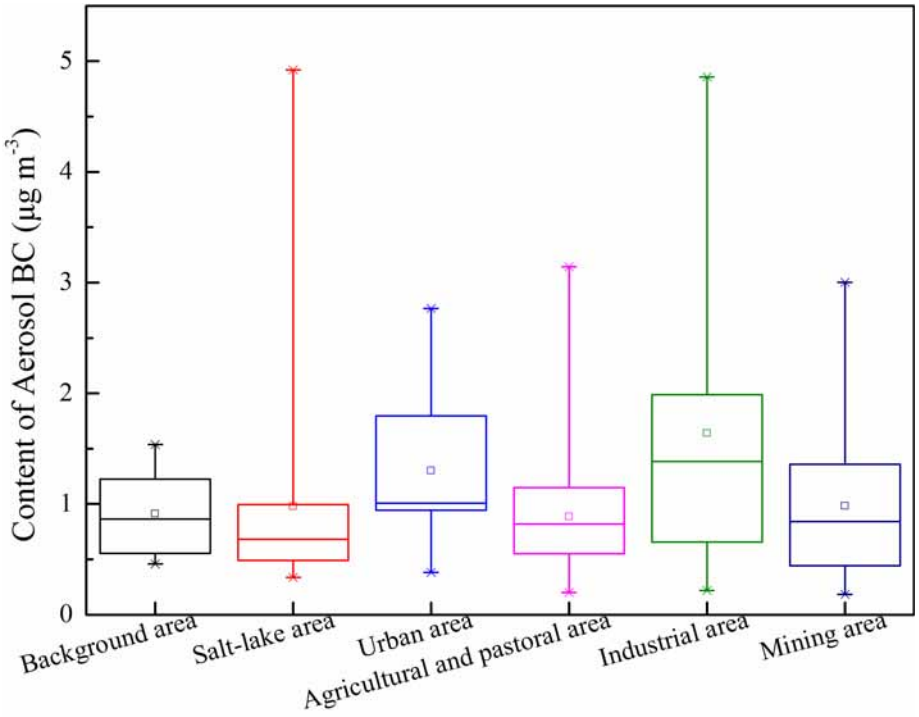

FIGURE 2

Concentration box plot of aerosol black carbon in different functional areas of the northeastern Qinghai-Tibet Plateau. In each box, the bottom and top of the box illustrate the 25th and 75th percentiles; the mid-line of the box means the median value; the small square represents the average value; the bottom and top of the whiskers refer to the minimal and the maximal values.

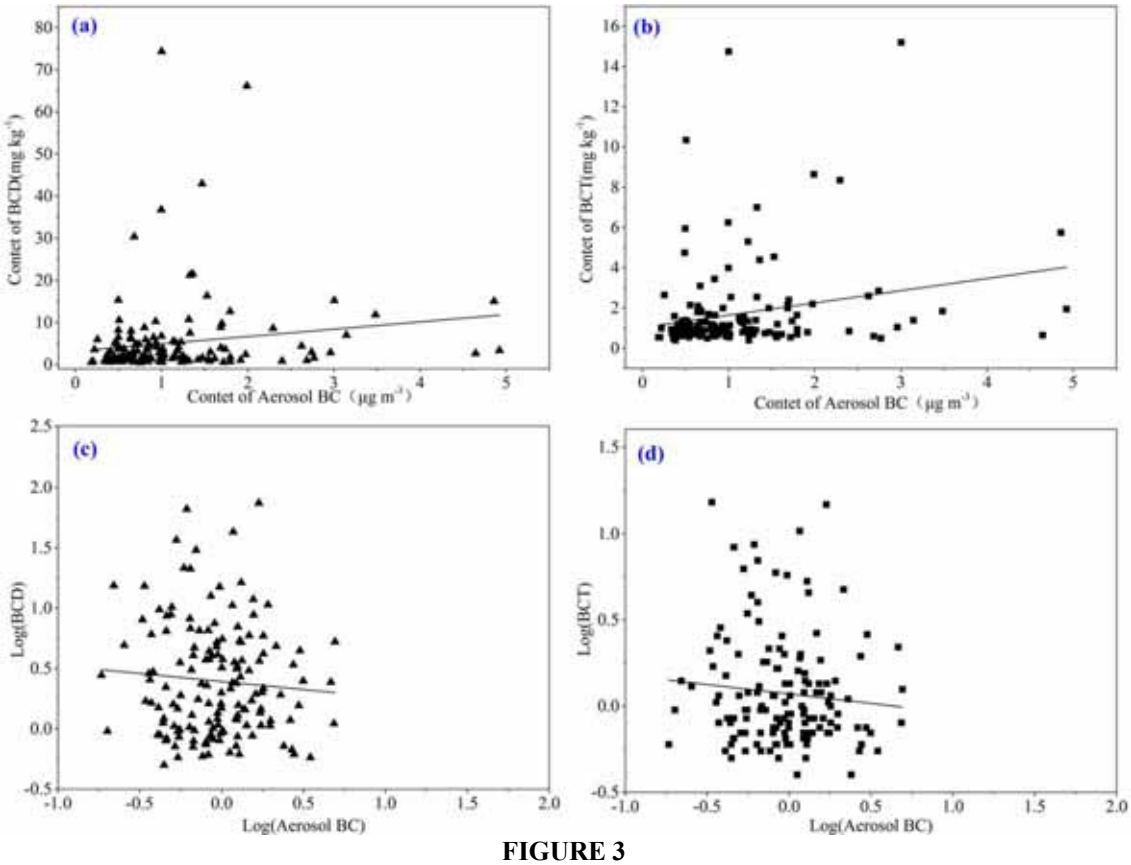

FIGURE 3

Correlation between aerosol BC and soil BC of the northeastern Qinghai-Tibet Plateau. BCD and BCT refer to total soil BC and soot soil BC, respectively.

The correlation between soil BC and aerosol BC. The contents of total BC (BCD) and soot BC (BCT) in soils were in the ranges of 0.504-74.381 and 0.400-15.200 g kg^{-1} with an average value of 5.152 and 1.719 g kg^{-1}, respectively. The contents of soil BC in agricultural and pastoral areas, industrial areas, and mining areas were significantly higher than those in other functional areas.

No significant correlations existed between concentrations of soil BC and aerosol BC (Figure 3). Some studies showed that rainfall, snowfall, and wind could influence the aerosol BC [47]. Moreover, photochemical decomposition and microbial degradation also contributed to aerosol BC [24]. Soil BC was affected by multiple factors such as soil physic-chemical properties and organic matter [48]. Therefore, more complex intern relationships between aerosol BC and soil BC needs to be further explored although interaction between soil BC and aerosol BC exists.

Health risks posed by aerosol BC in the study area. Four endpoints including were used to evaluate the potential health risks caused by aerosol BC. The results indicated that potential health risks caused by aerosol BC at different sites drastically varied (Figure 4). The distribution pattern of health risks posed by aerosol BC was identical with that of aerosol BC concentration in this study area. Health risks of LBW, PLFD, CM, and LC were in the ranges of 0.001-14.922, 0.002-39.580, 0.001-14.475, and 0.000-6.821 equivalent numbers of PSC, respectively. The average health risk of LBW, PLFD, CM, and LC was 2.903, 7.700, 2.816 and 1.327 equivalent numbers of PSC, respectively. Compared with other three health endpoints, the health risks of PLFD possessed the highest values. The health risks of four health endpoints followed the order of PLFD>LBW>CM>LC. The highest health risk posed by aerosol BC occurred at Chaka town while the lowest health risk occurred at the Yardang landform Park of Eboliang. The average potential health risk posed by aerosol BC in the study area was lower than that in Xining [13].

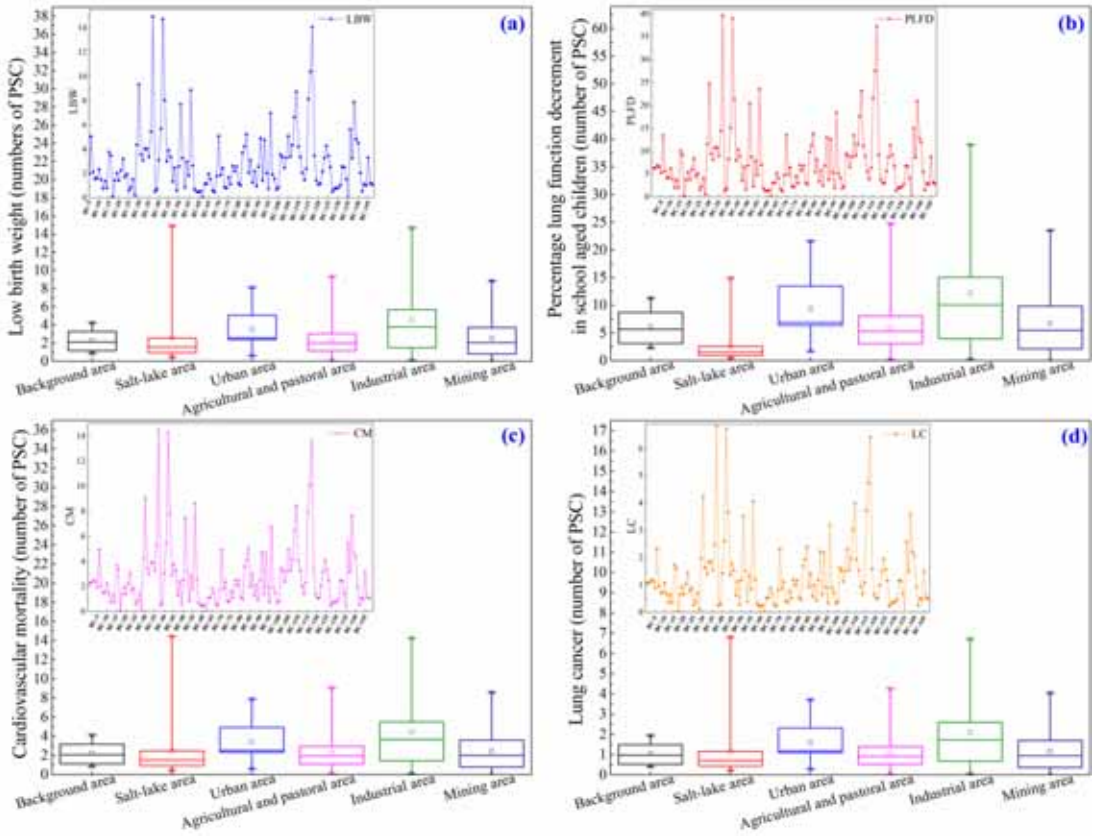

FIGURE 4

Box plots of health risks including low birth weight, percentage lung function decrement of school aged children, cardiovascular mortality, and lung cancer in different functional areas. In each box, the bottom and top of the box illustrate the 25th and 75th percentiles; the mid-line of the box means the median value; the small square represents the average value; the bottom and top of the whiskers refer to the minimal and the maximal values, PSC means passively smoked cigarettes.

The health risks of LBW, PLFD, CM, and LC in different function areas were shown in Figure 4. Health risks of LBW, PLFD, CM, and LC in background area were in the ranges of 0.870-4.269, 2.308-11.324, 0.844-4.141 and 0.398-1.952 numbers of PSC with average values of 2.296, 6.089, 2.227 and 1.049 numbers of PSC, respectively. Health risks of LBW, PLFD, CM, and LC in salt-lake area were in the ranges of 0.483-14.922, 1.281-39.580, 0.469-14.475 and 0.221-6.821 numbers of PSC with average values of 2.510, 6.659, 2.435 and 1.148 equivalent number of PSC, respectively. The average risk of LBW, PLFD, CM, and LC in urban area reached 3.523, 9.346, 3.418 and 1.611 equivalent number of PSC while that of LBW, PLFD, CM, and LC in agricultural and pastoral area reached 2.215, 5.875, 2.149, and 1.013 equivalent number of PSC, respectively. Health risks of LBW, PLFD, CM, and LC in industrial area were in the ranges of 0.111-14.721, 0.294-39.048, 0.107-14.281 and 0.051-6.730 equivalent number of PSC with the average values of 4.591, 12.176, 4.453 and 2.098 equivalent number of PSC, respectively. Health risks of LBW, PLFD, CM, and LC in industrial area were in the ranges of 0.001-8.881, 0.002-23.558, 0.001-8.615 and 0.000-4.060 equivalent number of PSC with average values of 2.511, 6.659, 2.435 and 1.148 equivalent number of PSC, respectively. The distribution pattern of health risks posed by aerosol BC in different function areas was similar with that of aerosol BC concentration. Compared with global cities/regions, the health risks of aerosol BC in the northeastern Qinghai-Tibet Plateau were at the middle level [13].

CONCLUSIONS

The contents of aerosol BC in the study area was in the range of 0.184-4.920 μg m^{-3} with a mean value of 1.134 μg m^{-3}. No significant correlations existed between soil BC and aerosol BC. The health risk posed by aerosol BC were evaluated using LBW, PLFD, CM, and LC with the highest values of 14.922, 39.580, 14.475, and 6.821 equivalent numbers of PSC, respectively. The health risks of aerosol BC showed the same pattern with concentrations of aerosol BC in study area. The highest concentration of aerosol BC and health risk occurred in the industrial area, while the lowest occurred in the agricultural and pastoral area. Compared with global regions, the concentrations and health risks of aerosol BC in the northeastern Qinghai-Tibet Plateau were at the middle level.

ACKNOWLEDGEMENTS

This work was financially supported by One Hundred Talents Program of Chinese Academy of Sciences (Y610061033 and Y629041021), National Natural Science Foundation of China (41671319 and 41867031), Thousand Talents Plan of Qinghai Province (Y740171071), and Two Hundred Talents Program of Yantai (Y739011021). The authors would like to thank the editor and reviewers for their valuable suggestions and comments on the manuscript.

REFERENCES

[1] Zhang, H. and Wang, Z. (2011) Advances in the Study of Black Carbon Effects on Climate. Adv. Climate Change Res. 2, 23-30.
[2] Kuhlbusch, T.A.J. (1998) Black carbon and the carbon cycle. Science. 280, 1903-1904.
[3] Koelmans, A.A., Jonker, M.T.O., Cornelissenc, G., Bucheli T.D. and Gustafsson, Ö. (2006) Black carbon: The reverse of its dark side. Chemosphere. 63, 365-377.
[4] Jacobson, M.Z. (2001) Strong radiative heating due to the mixing state of black carbon in atmospheric aerosols. Nature. 409, 695-697.
[5] Menon, S., Hansen, J., Nazarenko, L. and Luo, Y. (2002) Climate effects of black carbon aerosols in China and India. Science. 297, 2250-2253.
[6] Ramanathan, V. and Carmichael, G. (2008) Global and regional climate changes due to black carbon. Nat. Geosci. 1, 221-227.
[7] Louwies, T., Nawrot, T., Bianca C., Dons, E., Penders, J., Provost, E., Panis, L.I. and De Boever, P. (2015) Blood pressure changes in association with black carbon exposure in a panel of healthy adults are independent of retinal microcirculation. Environ. Int. 75, 81-86.
[8] Ji, Z., Kang, S., Cong, Z., Zhang, Q. and Yao, T. (2015) Simulation of carbonaceous aerosols over the Third Pole and adjacent regions: distribution, transportation, deposition, and climatic effects. Cli. Dynam. 45, 2831-2846.
[9] Lehmann, J., Gaunt, J. and Rondon, M. (2006) Bio-char sequestration in terrestrial ecosystems - a review. Mitig. Adapt. Strat. Gl. 11, 403-427.
[10] Kuhlbusch, T.A.J., Andreae, M.O., Cachier, H., Goldammer, J.G., Lacaux, J.P., Shea, R. and Crutzen, P.J. (1996) Black carbon formation by savanna fires: Measurements and implications for the global carbon cycle. J. Geophys. Res. 101, 23651-23665.

[11] Yang, M., Nelson, F.E., Shiklomanov, N.I., Guo, D. and Wan, G. (2010) Permafrost degradation and its environmental effects on the Tibetan Plateau: A review of recent research. Earth-Sci. Rev. 103, 31-44.

[12] Wang, M., Xu, B., Wang, N., Cao, J., Tie, X., Wang, H., Zhu, C. and Yang, W. (2016) Two distinct patterns of seasonal variation of airborne black carbon over Tibetan Plateau. Sci. Total Environ. 573, 1041-1052.

[13] Wu, J., Lu, J., Min, X. and Zhang, Z. (2018) Distribution and health risks of aerosol black carbon in a representative city of the Qinghai-Tibet Plateau. Environ. Sci. Pollut. R. 25, 1-10.

[14] Wu, J., Lu, J., Li, L., Min, X. and Luo, Y. (2018) Pollution, ecological-health risks, and sources of heavy metals in soil of the northeastern Qinghai-Tibet Plateau. Chemosphere. 201, 234-242.

[15] Wu, J., Lu, J., Luo, Y., Duan, D., Zhang, Z., Wen, X., Min, X., Guo, X. and Boman, B.J. (2016) An overview on the organic pollution around the Qinghai-Tibet plateau: The thought-provoking situation. Environ. Int. 97, 264-272.

[16] Wu, J., Duan, D., Lu, J., Luo, Y., Wen, X., Guo, X. and Boman, B.J. (2016) Inorganic pollution around the Qinghai-Tibet Plateau: An overview of the current observations. Sci. Total Environ. 550, 628-636.

[17] Liu, X. and Chen, B. (2000) Climatic warming in the Tibetan Plateau during recent decades. Int. J. Climatol. 20, 1729-1742.

[18] Xu, B., Cao, J., Hansen, J., Yao, T., Joswia, D. R. Wang, N., Wu, G., Wang, M., Zhao, H., Yang, W., Liu, X. and He, J. (2009) Black soot and the survival of Tibetan glaciers. P. Natl. Acad. Sci.USA. 106, 22114-22118.

[19] Zhao, L., Ping, C.L., Yang, D.Q., Cheng, G.D., Ding, Y.J. and Liu, S.Y. (2004) Changes of climate and seasonally frozen ground over the past 30 years in Qinghai-Xizang (Tibetan) Plateau, China. Global Planet. Change. 43, 19-31.

[20] Bajwa, A., Ali, U., Mahmood, A., Chaudhry, M. J. I., Syed, J.H., Li, J., Zhang, G., Jones, K.C. and Malik, R.N. (2016) Organochlorine pesticides (OCPs) in the Indus River catchment area, Pakistan: Status, soil–air exchange and black carbon mediated distribution. Chemosphere. 152, 292-300.

[21] Ali, U., Sweetman, A.J., Jones, K.C. and Malik, R.N. (2018) Higher atmospheric levels and contribution of black carbon in soil-air partitioning of organochlorines in Lesser Himalaya. Chemosphere. 191, 787-798.

[22] Babu, S.S., Chaubey, J.P., Krishna, M.K., Gogoi, M.M., Kompalli, S.K., Sreekanth, V., Bagare, S.P., Bhatt, B.C., Gaur, V.K., Prabhu, T.P. and Singh, N.S. (2011) High altitude (~ 4520 m amsl) measurements of black carbon aerosols over western trans-Himalayas: Seasonal heterogeneity and source apportionment. J. Geophys. Res. 116, 1-15.

[23] Zhao, S., Zhao, S., Ming, Ji., Xiao, C., Sun, W. and Qin, X. (2012) A preliminary study on measurements of black carbon in the atmosphere of northwest Qilian Shan. J. Environ. Sci. 24, 152-159.

[24] Wang, Q., Wang, Q., Schwarz, J.P., Cao, Ju., Gao, R., Fahey, D.W., Hu, T., Huang, R.J. Han, Y. and Shen, Z. (2014) Black carbon aerosol characterization in a remote area of Qinghai-Tibetan Plateau, western China. Sci. Total Environ. 479, 151-158.

[25] Chen, S., Liu, W., Ye, B., Yang, G., Yi, S., Wang, F., Qin, X., Ren, J. and Qin, D. (2011) Species diversity of the vegetation in relation to biomass and environmental factors in the upper area of Shule River. Acta Prataculturae Sin. 20, 70-83. (in Chinese).

[26] Xie, X., Yang, G. J., Wang, Z.R. and Wang, J. (2010) Landscape pattern change in mountainous areas along an altitude gradient in the upper reaches of Shule River. Chinese J. Ecol. 29, 1420-1426. (in Chinese).

[27] Agarwal, T. and Bucheli, T.D. (2011) Adaptation, validation and application of the chemo-thermal oxidation method to quantify black carbon in soils. Environ. Pollut. 159, 532-538.

[28] Song, J., Peng, P. and Huang, W. (2002) Black Carbon and Kerogen in Soils and Sediments. 1. Quantification and Characterization. Environ. Sci. Technol. 36, 3960-3967.

[29] van der Zee, S.C., Fischer, P.H., Hoek, G. (2016) Air pollution in perspective: Health risks of air pollution expressed in equivalent numbers of passively smoked cigarettes. Environ. Res. 148, 475-483.

[30] Zhao, Z.Z., Wang, Q.Y., Xu, B.Q., Shen, Z.X., Huang, R.J., Zhu, C.S., Su, X.L., Zhao, S.Y., Long, X., Liu, S.X. and Cao, J.J. (2017) Black carbon aerosol and its radiative impact at a high-altitude remote site on the southeastern Tibet Plateau. J. Geophys. Res. 122, 5515-5530.

[31] Zhu, C.-S., Cao, J., Xu, B. Q., Huang, R.J., Wang, P., Ho, K.F., Shen, Z.X., Liu, S.X., Han, Y.M., Tie, X.X., Zhao, Z.Z. and Chen Antony, L.W. (2016) Black Carbon Aerosols at Mt. Muztagh Ata, a High-Altitude Location in the Western Tibetan Plateau. Aerosol Air Qual. Res. 16, 752-763.

[32] Kompalli, S.K., Krishna Moorthy, K., Suresh Babu, S. and Manoj, M.R. (2014) Aerosol mass size distribution and black carbon over a high altitude location in Western Trans-Himalayas: Impact of a dust episode. Aeolian Res. 15, 161-168.
[33] Cao, J., Tie, X., Xu, B., Zhao, Z., Zhu, C., Li, G. and Liu, S. (2010) Measuring and modeling black carbon (BC) contamination in the SE Tibetan Plateau. J. Atmos. Chem. 67, 45–60.
[34] Chaubey, J.P., Moorthy, K.K., Babu, S.S. and Nair, V.S. (2011) The optical and physical properties of atmospheric aerosols over the Indian Antarctic stations during southern hemispheric summer of the International Polar Year 2007–2008. Ann. Geophys. 29, 109-121.
[35] Mao, Y.H. and Liao, H. (2016) Impacts of meteorological parameters and emissions on decadal, interannual, and seasonal variations of atmospheric black carbon in the Tibetan Plateau. Adv. Clim. Change Res. 7, 123-131.
[36] Xiao, Q., Saikawa, E., Yokelson, R. J., Chen, P., Li, C. and Kang, S. (2015) Indoor air pollution from burning yak dung as a household fuel in Tibet. Atmo. Environ. 102, 406-412.
[37] Engling, G., Zhang, Y.N., Chan, C.Y., Sang, X.F., Lin, M., Ho, K.F., Li, Y.S., Lin, C.Y. and Lee, J.J. (2011) Characterization and sources of aerosol particles over the southeastern Tibetan Plateau during the Southeast Asia biomass-burning season. Tellus B. 63, 117-128.
[38] Ma, J. (2003) Size distributions of ionic aerosols measured at Waliguan Observatory: Implication for nitrate gas-to-particle transfer processes in the free troposphere. J. Geophys. Res. 108, 1-12.
[39] Ming, J., Xiao, C., Sun, J., Kang, S. and Bonasoni, P. (2010) Carbonaceous particles in the atmosphere and precipitation of the Nam Co region, central Tibet. J. Environ. Sci. 22, 1748-1756.
[40] Mouteva, G.O., Randerson, J.T., Fahrni, S.M., Bush, S.E., Ehleringer, J.R., Xu, X.M., Santos, G.M., Kuprov, R., Schichtel, B.A. and Czimczik, C.I. (2017) Using radiocarbon to constrain black and organic carbon aerosol sources in Salt Lake City. J. Geophys. Res. 122, 9843-9857.
[41] Wang, Q., Huang, R., Zhao, Z., Zhang, N., Wang, Y., Ni, H., Tie, X., Han, Y., Zhuang, M., Wang, M., Zhang, J., Zhang, X., Dusek, U. and Cao, J. (2016) Size distribution and mixing state of refractory black carbon aerosol from a coastal city in South China. Atmos. Res. 181, 163-171.
[42] Huang, X.F., Sun, T.L., Zeng, L.W., Yu, G.H. and Luan, S.J. (2012) Black carbon aerosol characterization in a coastal city in South China using a single particle soot photometer. Atmos. Environ. 51, 21-28.
[43] Ji, D., Li, L., Pang, B., Xue, P., Wang, L., Wu, Y., Zhang, H. and Wang, Y. (2017) Characterization of black carbon in an urban-rural fringe area of Beijing. Environ. Pollut. 223, 524-534.
[44] Cheng, M.D. (2014) Geolocating Russian sources for Arctic black carbon. Atmos. Environ. 92, 398-410.
[45] Tripathi, S.N., Dey, S., Tare, V. and Satheesh, S.K. (2005) Aerosol black carbon radiative forcing at an industrial city in northern India. Geophys. Res. Lett. 32, 1-4.
[46] Jaffe, D., Putz, J., Hof, G., Hof, G., Hee, J., Lommers-Johnson, D.A., Gabela, F., Fry, J., Ayres, B., Kelp, M. and Minsk, M. (2015) Diesel particulate matter and coal dust from trains in the Columbia River Gorge, Washington State, USA. Atmo. Pollut. Res. 6, 946-952.
[47] Li, C., Bosch, C., Kang, S., Andersson, A., Chen, P., Zhang, Q., Cong, Z., Chen, B., Qin, D. and Gustafsson, Ö. (2016) Sources of black carbon to the Himalayan–Tibetan Plateau glaciers. Nat. Commun. 7, 1-7.
[48] Zong, Y., Xiao, Q. and Lu, S. (2016) Black carbon (BC) of urban topsoil of steel industrial city (Anshan), Northeastern China: Concentration, source identification and environmental implication. Sci. Total Environ. 569-570, 990-996.

Received: **28.10.2018**
Accepted: **24.02.2019**

CORRESPONDING AUTHOR

Jun Wu
Key Laboratory of Comprehensive and
Highly Efficient Utilization of Salt Lake Resources,
Qinghai Institute of Salt Lakes,
Chinese Academy of Sciences,
Xining, Qinghai 810008 – China

e-mail: junwu@isl.ac.cn

© by PSP Volume 28 – No. 4/2019 pages 2897-2907 Fresenius Environmental Bulletin

RESEARCH ON SOURCES APPOINTMENT OF ABNORMAL CO IN UNDERGROUND MINE

Xinran Hou[1,2], Liwen Guo[1,2], Fusheng Wang[1,2,*], Yunyun Xu[3], Xianwei Dong[1,2], Dong Gao[1], Yiming Sun[1]

[1]North China University of Science and Technology, College of Mining Engineering, Hebei, Tangshan,063210, China
[2]Mining Development and Safety Technology Key Lab of Hebei Province, Hebei, Tangshan,063210, China
[3]Tangshan University, Civil Engineering College, Hebei, Tangshan,063000, China

ABSTRACT

Coal spontaneous combustion is a major disaster in underground mine. CO as a common indicator gas due to its good correlation with coal self-heating temperature. However, abnormal high concentration of CO was detected without coal fire during production process of some underground mines that not only impact production but also threat the safety of miners. To investigate the sources appointment of abnormal CO without coal spontaneous combustion, quantitative analysis of primordial and oxidation product were conducted with self-designed vacuum desorption and coal/gas interaction testing apparatus. The results indicated that CO as a gaseous product generated from coal oxidation under ambient temperature (18-22℃) was the main source in underground mine. Coal oxidation ability under ambient temperature was too partial to completely demonstrate coal spontaneous combustion propensity. Infrared spectra and ESR indicated the mechanism of coal oxidation under ambient temperature. It showed that oxygen-containing functional groups were prone to oxidation under ambient temperature. The results of the research could be improve the accuracy of early detection with CO for coal spontaneous combustion.

KEYWORDS:
Carbon monoxide, primordial gas, ambient temperature oxidation, coal spontaneous combustion

INTRODUCTION

Coal spontaneous combustion continues to be a serious problem around the world such as China, USA, Australia and India [1-5]. Coal spontaneous combustion events are quite common in underground mining, coal stockpiles, transport. All the time, researchers pay attention to the problem due to its threats to human health and life, safety production, the environment. Coal fires are response for the increase in greenhouse gases, and doubles the risk of lung cancer who expose to smoke from coal fires [6]. In addition, some coal fires are difficult to extinguish and some coal fields can burn for even centuries (e.g., Changji, Xinjiang, Liuhuanggou coal field:1874-2003). In China, coal supplies more than 60% of its energy consumption, but there are more than 56% of coal mines are prone to spontaneous combustion [7].

Spontaneous combustion of coal is a complex physicochemical reaction in natural [8]. Coal oxidation reaction exothermic then the heat from the reaction may accumulate under given conditions and lead to coal spontaneous combustion, and mine fire may occur ultimately if the state continues. Early detection is critical to successfully prevention coal mine fire. In order to prevent coal spontaneous combustion and assess its risk many methods were proposed. Many kinds of gases released to mine atmosphere accompanied by the oxidation of coal processes. The most important indicator gases to determine the stages of coal oxidation include: carbon monoxide, ethylene, propylene, acetylene [9]. This method has been widely used all over the world because of its practicability and reliability which by observing the concentration of gases generated from coal self-heating process. Carbon monoxide as a main indicator gas especially for early detection due to the linear relation between its concentration and coal temperature at the early stage of coal spontaneous combustion [10, 11]. However, a strange phenomenon appeared frequently during production process in some Chinese mines. The phenomenon is that carbon monoxide concentration is very high at normal temperature, such as Lin Nangcang, Xun Yao and Ping Zhuang the concentration of CO were more hundred times compared to the permissible maximum concentration of "Safety Regulations of Coal Mine", but without coal spontaneous combustion [12, 13]. In the light of the above, coal spontaneous combustion isn't the unique source of CO in coal mine. Therefore, early prediction and forecast of mine fire were affected, and lots of unnecessary control measures were still adopted. In addition, carbon monoxide is a poisonous gas, which threatens human health and life. To find out sources for unusual high concentration of carbon monoxide and improve the accuracy of mine fire prediction and forecast, a few studies have been reported.

It is a well-established fact in coal mining that carbon monoxide occurs naturally in coal beds. Zwak [14] detected carbon monoxide gas in underground mines without coal spontaneous combustion. Crushing experiments and dissolution experiments of coals were carried out by Charles E. Melton et al. under high-vacuum mass spectrometry. High concentration carbon monoxide was detected under these conditions and primordial CO in coal seams was the source of it [15]. During the transformation of plant into coal, gases naturally accumulated in coal seams. This can lead to gases detected in underground mine may be derived from the natural gases [16]. Natural gases as free gases accumulated in coal macro-pores, fractures and fissures, and they can be adsorbed in the coal structure [17,18]. The gases detected in underground mines, the high concentration gases may be caused by desorption of gases naturally accumulated in coal seams. Similar conclusions were draw in the work presented by Qi et al [19]. Three sources of carbon monoxide emitted from coal in the grinding process were examined by B·Taraba, include: (1) desorption; (2) oxidation; (3) mechanically activated decarbonylation of coal [20].

Carbon monoxide, as well as carbon dioxide and water, are the main products of coal oxidation, being evolved already under ambient temperature. The reaction of coal oxidation begins as soon as coal contacts with oxygen in air. Coal weathering and coal self-heating occur simultaneously during the process, in coal stockpiles, transported coal and coal preparation processes [21]. Figure 1 shows self-heating of coal stockpile under ambient temperature. Air transported oxygen into coal stockpile for the oxidation of coal. The heat released from the reaction of coal and oxygen accumulates whilst away from the stockpile. Water vapour is transported either into the stockpile or away from the stockpile depending on the relative humidity of the atmosphere and the equilibrium relative humidity within the coal for a given coal water content [22]. There is a slow process taking days to several months, and these differences are depend on the characteristics of coal. Unlike other combustions, released H_2O, CH_4, CO between 20 to 100℃ without a visible flame [23-26]. Tang [27] studied the low-temperature from 25℃ to 100℃ with characteristics tester and gas chromatograph. Low rank coals were more easily oxidized under ambient temperature and resealed a certain CO. The oxidation of coal under ambient temperature was closely related to coal spontaneous combustion propensity.

Previous studies indicate that CO as a primordi al gas accumulates in coal seam and as a combustio n product generated from coal oxidation at low tem perature. Therefore, the values of gas detected in pr actice can't reflect states of coal spontaneous comb ustion objectively because of the existence of primo rdial carbon monoxide. Based on above theories, th e aim of this research is to improve the prediction a nd foresting of coal spontaneous combustion accura cy. Primordial CO accumulated in coal and CO fro m the oxidation of coal under ambient temperature were considered. A self-design testing equipment (v acuum-desorption) was conducted to determine pri mordial CO accumulated in coal. The amount of C O emitted during the oxidation of coal under ambie nt temperature was investigated by the coal/gas inte raction testing equipment designed by ourselves. Th at can improve the accuracy of early detection and b etter reflect the real condition of coal spontaneous c ombustion. Most of the previous studies paid attenti on to gases generated due to coal spontaneous comb ustion. In the study, mechanism of unusual high con centration of carbon monoxide under ambient temp erature without coal spontaneous combustion were analyzed with FTIR and ESR.

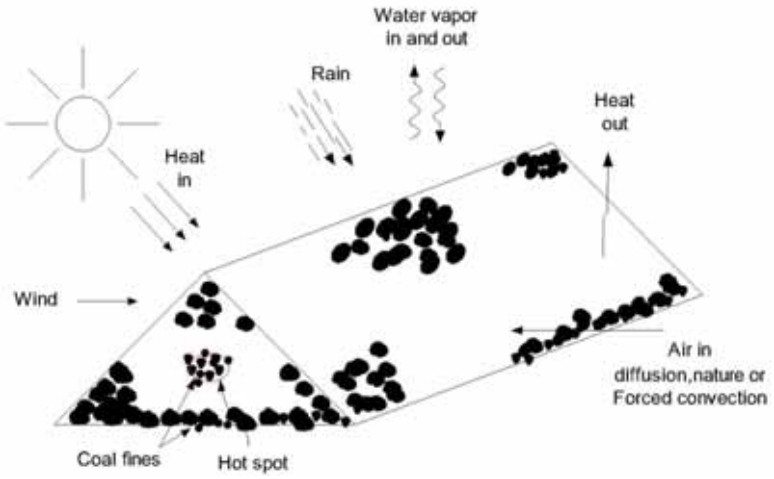

FIGURE 1
Schematic diagram of a coal stockpile

EXPERIMENTAL

Samples. For the purpose of the experiments, four coal samples were selected from LNC coal mine of Kailuan (group) Co., Ltd., China which has been obsessed by high concentration CO. two coal samples were collected from 11# coal seam (samples denoted 1 and 2), others were collected from 12# coal seam (samples denoted 3 and 4).

In order to eliminate particularities of each coal sample, coal samples at three points were selected every two meters and mixed adequately. Coal samples were directly extracted from the coal wall, and stripped of the oxide layer on the surface of coal seam. The coal samples were crushed in a cylinder crusher in order to separate particle size 60~80 and below 200 meshes, then were dried in a drying oven with 40℃ and vacuum for 2h. The samples were prepared according to the standard GB-474-2008. Four representative coal samples were obtained from each sample with the method.

Vacuum Desorption. In order to measure primordial CO accumulated in coal, a vacuum desorption experimental device was designed. Figure 2 is the structure of the device which include: vacuum pump, coal sample chamber, crush and grind system. Four coal samples were grinded in a vacuum after that N_2 was filled into the coal sample chamber to keep one atmosphere. The gas of coal sample chamber was siphoned and detected every other day until the CO concentration was kept constant with time. Primordial CO in coal can be calculated by the equation as follow:

$$X = \frac{(V_1 - V_2 - V_3)}{M} \times C \qquad (1)$$

Where X is the amounts of primordial carbon monoxide; ml/g, V_1 is the volume of coal sample chamber; cm^3, V_2 is the volume of coal sample in coal sample chamber; cm^3, V_3 is the volume of the grinding media; cm^3, M is the quality of coal sample; g, C is the volume percent; %.

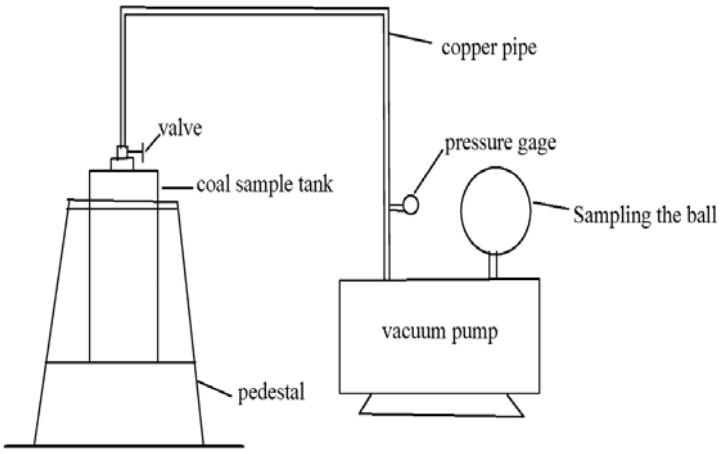

FIGURE 2
Schematic of vacuum desorption experimental device

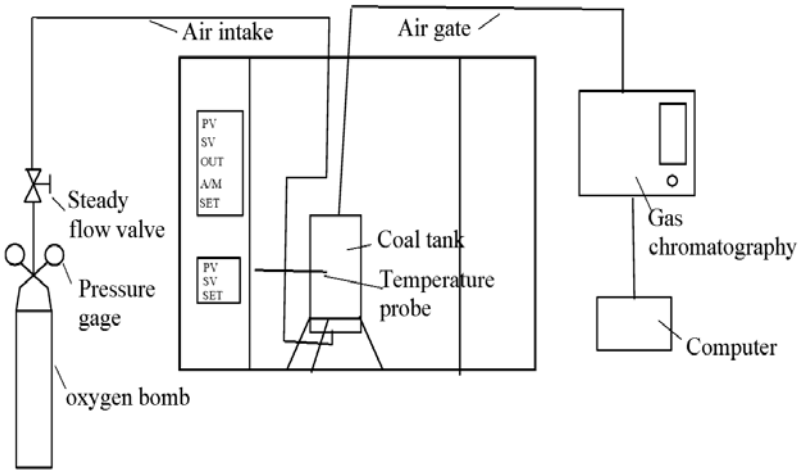

FIGURE 3
Schematic of the device

Oxidation under Ambient Temperature. The oxidation of the selected coals at ambient temperature were investigated by self-design testing equipment. The structure of the coal/gas interaction testing equipment is shown in Figure 3. The basics of the research were the two devices: reaction chamber under controlled temperature and gas chromatography. In order to conduct the experiment, four coal samples of grain size 60-80 mesh and 80g in turn were placed in the reaction chamber which was under ambient temperature (18-22℃). The temperature of coal samples were controlled under ambient temperature (error ±1℃) and continued for 32 days in air atmosphere. The concentration of CO from coal samples oxidation at ambient temperature was detected every 1h until it sustained steadily for 24+h.

Oxidation at Low Temperature. CO concentration generated from coal oxidation at low-temperature was investigated by the coal/gas interaction testing experiment as shown in Figure 3. Dry air flowed into coal sample chamber with the rate of 100 ml/min, the temperature enclosure was set to increase from 20°C to 280 °C at a programmed rate of 0.3 °C/min. During the process of coal oxidation, the CO gases emitted from the outlet were analyzed by gas chromatography.

Infrared Spectrum. Coal samples with particle sizes of 200 meshes were selected for infrared spectrum. A KBr powder background was collected prior to sample analysis as a baseline reference. Prepared coal samples and KBr were dried in vacuum drying oven under ambient temperature. Coal and KBr were mixed, grinded and pressed with mass ratio1:150. Experimental wavenumber range was 400 to 4000 cm^{-1} and samples were scanned for 30 times.

ESR Spectra. The ESR spectra were obtained with high attenuation, microwave frequency of 9035 MHz, and microwave power of 1 mW to avoid signal saturation. Additionally, the central magnetic field was 322.054 mT, while the scanning width was 5 mT. The modulation width was 0.2 mT, and the time constant was 0.03 s. The scanning time was 30 s, whereas a magnification of 20 was used.

RESULTS AND DISCUSSION

Sample Characterization. The results of the proximate and ultimate analyses of examined samples are given in Table 1. The selected coal samples differ in terms of chemical and physical properties which enabled the assessment of the effects of CO generation on coal oxidation under ambient temperature. Coal sample 1 contains the lowest carbon content and the highest ash content compared to the remaining coal samples selected. The volatiles content of the four selected coal samples are all between 10% w/w to 37% w/w. The coal samples are all bituminous coals based on Chinese National Standards of Chinese classification of coals (GB/T5751-2009).

Primordial CO. Vacuum desorption experiments were conducted on coal samples. Coal reaction chamber is a standard cylinder with 9.6cm diameter and 5.8cm height. The coal samples density is 1.3 g/cm^3. Primordial CO can be calculated by equation (1), the results are shown in Table 2.

TABLE 1
Characteristics of the samples

parameter	unit	Coal samples no.			
		1	2	3	4
Carbon, *C*	% w/w	50.68	57.49	59.97	62.31
Hydrogen, *H*	% w/w	3.71	4.227	3.992	4.027
Oxygen, *O*	% w/w	8.833	15.437	3.083	12.434
Nitrogen, *N*	% w/w	0.77	0.81	0.78	0.85
Sulfur, *S*	% w/w	0.307	0.456	0.275	0.449
Moisture, *M*	% w/w	2.42	2.44	1.62	2.33
Ash, *A*	% w/w	33.28	19.14	30.28	17.60
Volatiles, *V*	% w/w	28.72	35.12	27.82	34.78
Fixed Carbon, FCad	% w/w	35.58	43.3	40.28	45.29

TABLE 2
Primordial CO accumulated in coal samples

Sample	M/g	V_1/cm^3	V_2/cm^3	V_3/cm^3	C/%	primordial CO X/mL.g^{-1}
1	919.03	1866.52	706.95	60	0.0025	2.99×10^{-5}
2	726.80	1866.52	559.08	60	0.0256	4.46×10^{-4}
3	835.36	1866.52	642.58	60	0.0013	1.84×10^{-5}
4	705.20	1866.52	542.46	60	0.0006	1.08×10^{-5}

The selected coal samples are all contain primordial CO, and coal sample 2 has the most and coal sample 4 has the least, but there is no significant difference among the four coal samples. Carbon monoxide naturally accumulated in coal macropores, fractures and fissures during the transformation of plant material into coal which as a result of bio-geo-chemical process.

CO production under ambient temperature. CO generated from four coal samples oxidation under ambient temperature was determined by self-designed coal/gas interaction testing experiment. The detected values of CO of the four coal samples include coal oxidation products and gases accumulated in coal. The values of CO are given in Table 3. The results show that all the coal samples have been oxidized to yield CO under ambient temperature. CO release form coal under ambient temperature is several and dozens times compare to primordial coal (sample 1:45 times, sample 4:10 times). The results of the comparison are shown in Figure 4.

TABLE 3
The amounts of CO/mL.g^{-1}

Sample	primordial CO	The release CO	Oxidized products
1	2.99×10^{-5}	1.36×10^{-3}	1.33×10^{-3}
2	4.46×10^{-4}	1.07×10^{-3}	6.24×10^{-4}
3	1.84×10^{-5}	1.92×10^{-4}	1.74×10^{-4}
4	1.08×10^{-5}	4.5×10^{-5}	3.42×10^{-5}

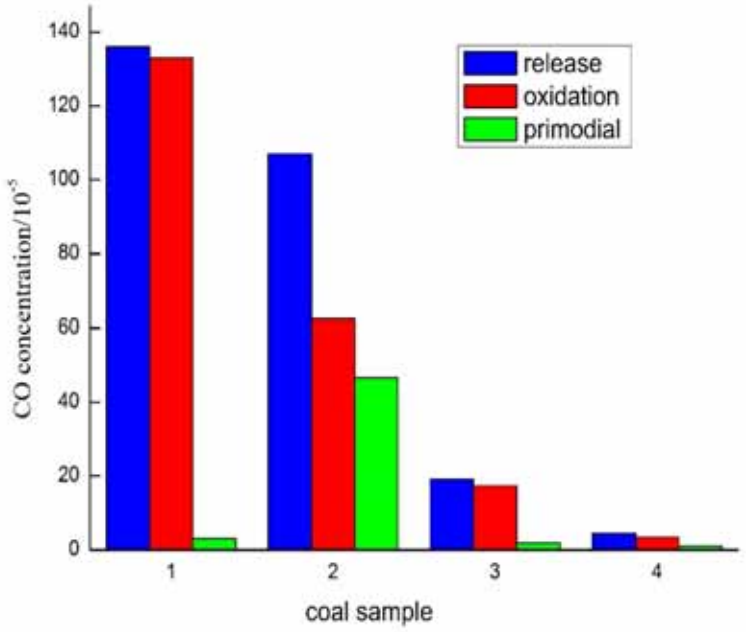

FIGURE 4
The CO release/ oxidation / primordial from Per gram coal under ambient temperature

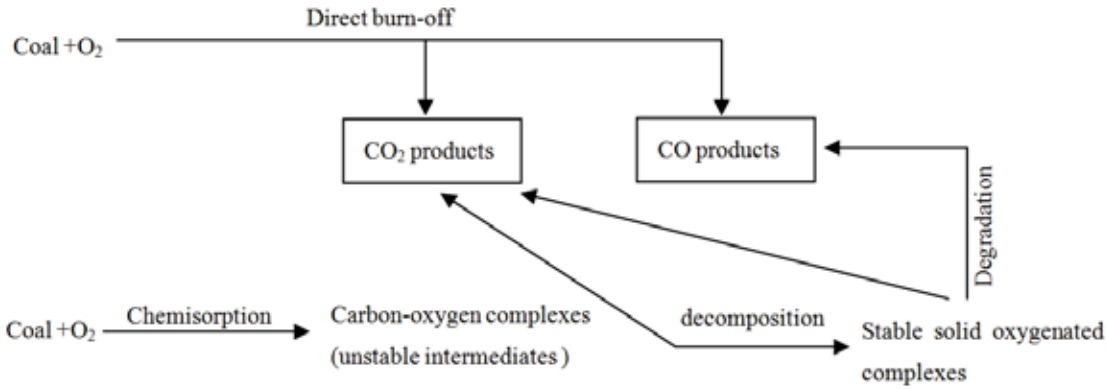

FIGURE 5
Two process of low-temperature interaction of coal with oxygen

This phenomenon indicates that ambient temperature oxidation was reacted between coal and oxygen. CO of oxidized product as the primary source of its release detected. They ranked in the following order staring with the most to the least under ambient temperature:

sample 1 > sample 2 >sample 3> sample 4

Under ambient temperature, coal sample1 with the lowest carbon content is the most prone to oxidation. CO production generated from coal sample 1 oxidation is significantly higher than coal sample 4 that with highest carbon content. CO of oxidation products tend to decrease with the increase of carbon content in coal. Coal surface was oxidized into unstable carbon-oxygen compounds that decomposed into CO under ambient temperature. The oxidation reaction can continue, with the surface of coal increased as the decomposition of carbon-oxygen compounds and the release of CO. Two pathways of CO production during coal oxidation were proposed by Haihui Wang: (1) the direct burnoff reaction (2) the decomposition of the stable oxygenated complexes containing -C＝O groups (Figure 5) [28].

It has already been verified that low rank coal with high volatile, and is more susceptible to spontaneous combustion. The volatile matter contents of selected coal samples were ranked in the following order staring with the most content to the least content:

sample 2 > sample 4 >sample 1> sample 3

For the purpose of comparison, coal sample 2 contains the most volatile matter that is more subject to spontaneous combustion than other samples. But CO generated from coal sample 1 oxidation under ambient temperature is the most. It is evident that oxidant capacity of coal under ambient temperature can't prove high capacity of spontaneous combustion. This result is consistent with the status in coal mines where high concentration of CO without coal spontaneous combustion. Based on the analysis of the experiment, it demonstrated that the values of detected CO for early prediction and forecasting of mine fire may be overstated, relatively.

CO production under a temperature-programmed system. Figure 6 shows the CO concentration of coal oxidation under low-temperature. CO concentration of four coal samples oxidation are all relatively low and CO from coal sample 4 is the lowest below 80℃. But CO concentration of coal sample 4 oxidation rapidly increased with the temperature, compared to other coal samples above 80℃. The CO concentration of coal sample 4 oxidation is obviously higher than that of other coal samples after 100℃. It is evidence that oxidization ability of coal under ambient temperature can't represent which in the whole oxidation process under low-temperature. CO detected under ambient temperature for early prediction and forecasting of mine fire may be overstated or understated.

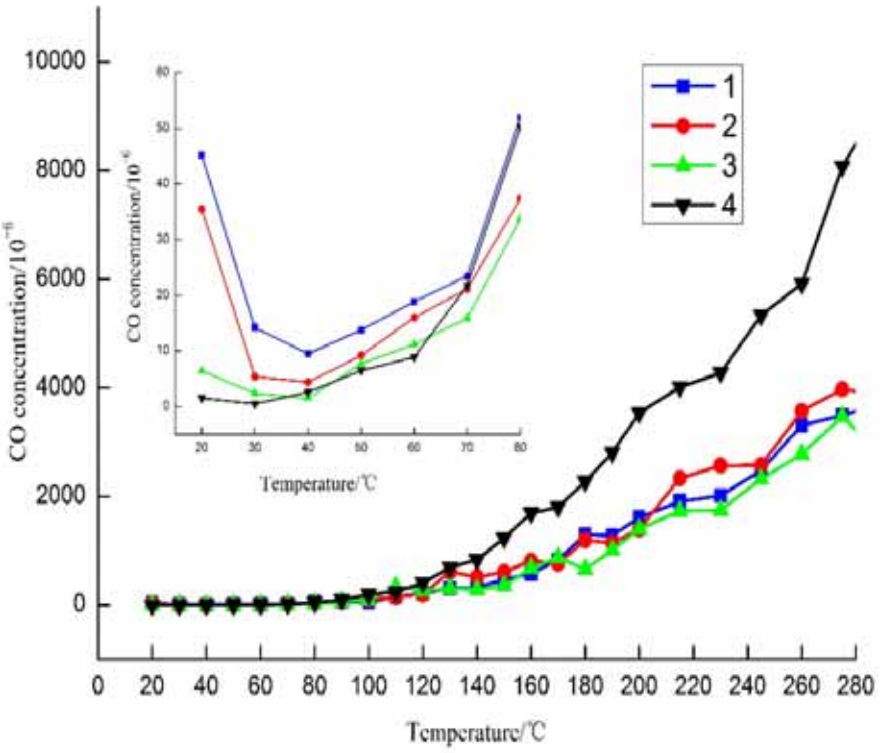

FIGURE 6
CO emissions from sample 1, 2, 3, 4 under 20℃-280℃

To prove LNC coal samples can produce CO with the increased temperature especially under ambient temperature, three coal samples from QJY, TS and LJT of Kailuan (group) Co., Ltd. China which were without high CO concentration during mining process were selected. Particle sizes of 60-80 meshes, 80g of the each coal sample was prepared for temperature-programmed system. CO emission from coal samples was detected during the temperature rise from 20 ℃ to 280 ℃, and was recorded to study the production of CO during the oxidation of coal samples. As shown in Figure 7, the concentration of CO increased with the increase in temperature during the oxidation of coal samples. The CO concentration of LNC was the highest among all the coal samples. CO emission from LNC begin with 20℃, form other coal samples begin with 60℃. It is indicate that there is no primordial CO accumulated in QJY, TS and LJT coal samples, and they can't appear oxidation under ambient temperature. However, there are evidences to prove that primordial CO may accumulate in LNC and more importantly LNC coal sample may be oxidized under ambient temperature. CO concentration from LNC was higher than that from other coal samples during the whole oxidation process (20℃ to 280℃). The growth rate of CO generated from the four coal samples increased with temperature, which from LNC grew more rapidly than other coal samples especially above 70℃ that is the critical temperature of LNC.

The process of coal spontaneous combustion can be divided into three stages by critical temperature and crack temperature. Before critical temperature is called low oxidation reaction stage, from critical temperature to crack temperature is called rapid oxidation reaction stage, above crack temperature is called drastic oxidation reaction stage. The critical temperature is the transition point from low to rapid oxidation. The first point of acceleration in the CO concentration curve of coal-oxygen reaction is the critical temperature. Furthermore, the intersection between the tangent of the critical temperature and maximum tangent of the CO production rate is the cracking temperature [29]. The characteristic temperatures of selected coal samples were shown in Table 4. Critical temperature and crack temperature of LNC were significantly less than those of other coal samples. It is obvious from the above that LNC coal sample was more prone to oxidation than other three coal samples which may be related to coal molecular structure.

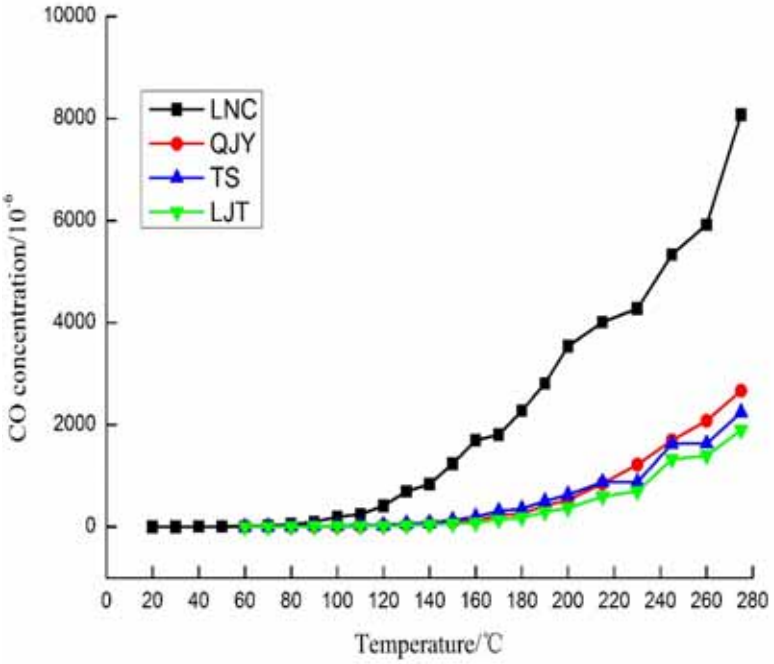

FIGURE 7
CO emission from the oxidation of four different coal samples

TABLE 4
Characteristic temperatures of coal samples

Coal sample	Critical temperature (℃)	Crack temperature (℃)
LNC	70-80	145-155
QJY	90-100	200-210
TS	80-90	210-220
LJT	90-100	220-230

Mechanism. From coal macromolecular structure, aromatic structures are the basic structure units of coal macromolecules. The basic structure units are connected by bridges whose side chains connect active functional groups in coal surface including alkyl, aryl, carbonyl, carboxyl and hydroxyl moieties. These active functional groups are subjected to attack by oxygen or energy from sunlight or thermal radiation, and so on. The type and qualitative analysis of functional groups in coal can be determined by infrared spectrum experiment. To discuss the mechanism of CO production from the oxidation of LNC coal sample under ambient temperature, QJY, TS and LJT coal samples were prepared for infrared spectrum and ESR experiments. Function groups in coal molecule of the each coal sample under ambient temperature were scanned, with the results shown in Figure 8. The data collected by FTIR demonstrate that the content of oxygen-containing functional groups in LNC coal sample were obviously higher than these in other coal samples. These oxygen-containing functional groups include: associate hydroxyl groups (wavenumber: 3684-3697 cm^{-1}, stretching vibration and bending vibration), free hydroxyl groups (3684-3697 cm^{-1}, stretching vibration and bending vibration of alcohols or phenol free groups), carbonyl groups (wavenumber: 1740-1800cm^{-1}, stretching vibration), carbon-oxygen single bond (wavenumber: 1120-1080cm^{-1}, stretching vibration). Because of the active chemical property of these oxygen-containing functional groups, they were oxidized as coal exposed in air atmosphere, then the chemical bonds were ruptured, and functional groups became unstable oxides which decomposed into carbon monoxide and other functional groups.

Figure 9 shows the changes in concentrations of free radicals of LNC, QJY, TS and LJT coal samples with temperature. It is obviously free radicals concentration of LNC were higher than those of QJY, TS and LJT start with 20℃. It is illustrated the reasons of oxidation of LNC coal sample under ambient temperature and high concentration of CO was detected underground LNC coal mine during the production process. The free radical concentration of LNC sharply increased with a fast rate above 70℃, which is correspond with CO emission characteristics. Because of high concentration in LNC coal molecular from 20℃ to 180℃, LNC coal sample was more vulnerable to oxidation than QJY, TS and LJT. Considering these investigated experiments, it was believed that the oxidation of the oxygen-containing functional groups under ambient temperature was the major source of CO. Equation (5)-(7) showed the reactions of these oxygen-containing functional groups in LNC coal sample.

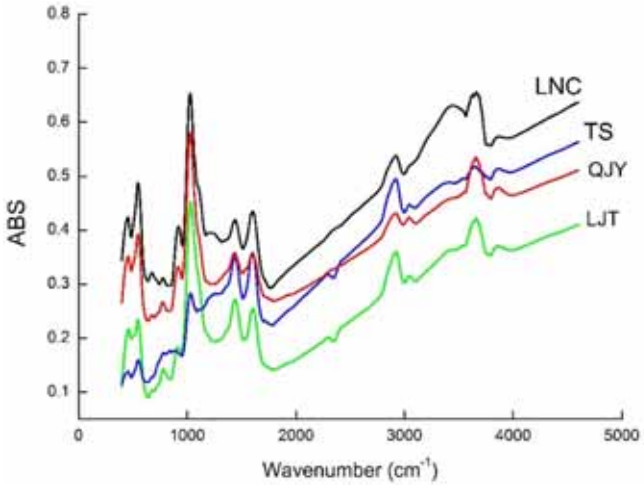

FIGURE 8
IR spectra of experimental coal samples

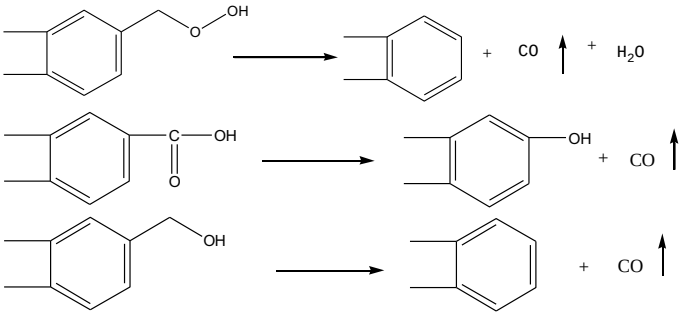

(5)

(6)

(7)

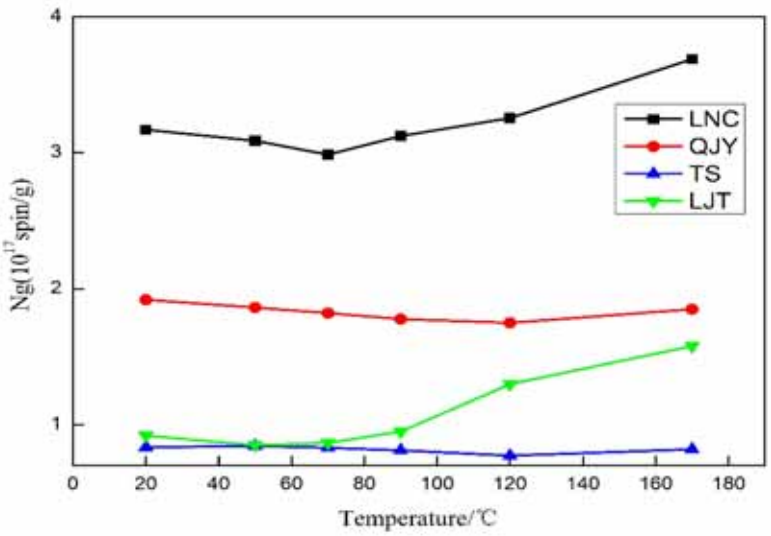

FIGURE 9
Concentration of free radicals

CONCLUSIONS

The sources of abnormal CO without coal spontaneous combustion were investigated by experiments with self-designed experimental facilities and the main conclusions are as follows:

(1) Conventionally, people thought that the coal spontaneous combustion is the only reason caused CO emission in underground mine. However, the experimental studies of vacuum desorption and oxidation of coal samples under ambient temperature proved that two other sources of carbon monoxide in coal mine under ambient temperature. One source is desorption of adsorbed primordial CO, the other source is oxidation products of coal under ambient temperature. The two sources of CO may be the main causes of the high concentration CO underground mine.

(2) The value of fire indices calculated on the basis of the concentration of gases with primary and oxidation products under ambient temperature may be incorrect. Carbon monoxide detected underground mine may be overstated respectively as the result of primordial CO and oxidation products.

(3) The oxidation of coal samples experiments under low-temperature temperature proved that oxidation ability of coal is different in the course of the oxidation process. It is evidence that coal with weaker capacity in the initial stage of oxidation process may become stronger than other coals with coal oxidation spontaneous combustion.

(4) Associate hydroxyl groups, free hydroxyl groups, carbonyl groups and carbon-oxygen single bond are prone to oxidation to release carbon monoxide under ambient temperature that is the source of CO during coal oxidation under ambient temperature.

Finally, carbon monoxide as an indicator gas consistently for prediction of coal spontaneous combustion. It is possible that other unclear source(s) of CO that influences the effect of forecast and predict. In order to predict coal spontaneous combustion accurately, various sources of CO should be considered.

ACKNOWLEDGEMENTS

The work presented in this paper was supported by National Natural Science Foundation of China (51474086 and 50974050), Graduate Student Innovation Fund of North China University of Science and Technology (2017B16), College Students Innovation and Entrepreneurship Training Program of North China University of Science and Technology (x2018243).

In addition, thanks are due to related people at the LNC, QJY, TS and LJT coal mines in China. It is because of their support, that the works described in this paper could be successfully completed.

REFERENCES

[1] Smith, M.A., Glasser, D. (2005) Spontaneous combustion of carbonaceous stockpiles. Part I: the relative importance of various intrinsic coal properties and properties of the reaction system. Fuel. 84, 1161–1170.

[2] Carras, J.N., Day, S.J., Saghafi, A., Williams, D.J. (2009) Greenhouse gas emissions from low-temperature oxidation and spontaneous combustion at open-cut coal mines in Australia. Int. J. Coal Geol. 78, 161–168.

[3] Song, Z., Kuenzer, C. (2014) Coal fires in China over the last decade: a comprehensive review. Int. J. Coal Geol. 133, 72–99.

[4] Taraba, B., Pavelek, Z. (2014) Investigation of the spontaneous combustion susceptibility of coal using the pulse flow calorimetric method: 25 years of experience. Fuel. 125, 101–105.
[5] Nimaje, D.S., Tripathy, D.P. (2016) Characterization of some Indian coals to assess their liability to spontaneous combustion. Fuel. 163, 139–147.
[6] Zhang, L.L., Qin, B.T. (2014) Development of a New Material for Mine Fire Control, Combustion Science and Technology. 186, 928-942.
[7] Xu, Y.L., Wang, L.Y., Tian, N., Zhang, J.P., Yu, M.G., Delichatsios, M.A. (2017) Spontaneous combustion coal parameters for the Crossing-Point Temperature (CPT) method in a Temperature–Programmed System (TPS). Fire Safety Journal. 91, 147–154.
[8] Deng, J., Lei, C.K., Xiao, Y., Cao, K., Ma, L., Wang, W.F., Laiwang, B. (2018) Determination and prediction on "three zones" of coal spontaneous combustion in a gob of fully mechanized caving face. Fuel. 211, 458–470.
[9] Dudzińska, A., Cygankiewicz, J., Włodarek, M. (2017) Natural content of gases: Carbon monoxide, carbon dioxide, hydrogen and unsaturated hydrocarbons of ethylene, propylene and acetylene in selected bituminous coal seams. Int. J. Coal Geol. 178, 110–121.
[10] Zhang, W.Q., Jiang, S.G., Wang, K., Wang, L.Y., Xu, Y.L., Wu, Z.Y., Shao, H., Wang, Y.H., Miao, M.L. (2015) Thermogravimetric dynamics and FTIR analysis on oxidation properties of low-rank coal at low and moderate temperatures. Int. J. Coal Prep. Util. 35, 39–50.
[11] Zhang, Y.L., Wang, J.F., Wu, J.M., Xue, S., Li, Z.F., Chang, L.P. (2015) Modes and kinetics of CO_2 and CO production from low-temperature oxidation of coal. Int. J. Coal Geol. 140, 1–8.
[12] Liu, H.W., Wang, F. (2015) Application status and development tendency of fire prevention and extinguishing technology with water mist in underground mine. Coal Science and Technology. 43, 86-92.
[13] Deng, J., Jiang, Z.G., Xiao, L. (2008) Analysis on produce mechanism and influence factor of CO gas on the coal exploitation working face. Journal of coal science and engineering. 14, 432-435.
[14] Zwak, J., Selcl, P. (1988) Occurrence of carbon monoxide in the drainage atmosphere. Proceedings of the Conference on 30 Years of the Mine Drainage. DT Ostrava.
[15] Melton, C.E., Giardini, A.A. (1975) Composition and volume of gas released by crushing coal from West Virginia, Kentucky and Alabama. Fuel. 54, 162-164.
[16] Zapušek, A., Marsel, J. (1998) Measurement of the composition of gas desorbed from coal by gas chromatography. Chromatographia. 48, 154–155.
[17] Kim, A.G., Douglas, L.J. (1973) Gases desorbed from five coals of low gas content. Bureau of Mines Report of Investigations.
[18] Diamond, W.P., Schatzel, S.J. (1988) Measuring the gas content of coal: a review. Int. J. Coal Geol. 35, 311–331.
[19] Qi, X., Wang, D., Zhong, X., Xu, Y., Milke, J.A. (2011) A Chemical Reaction Model of the Self-Heating of Coal. Asia-Pacific and Power and Energy Engineering Conference. 55, 1-5.
[20] Taraba, B. (1994) Disintegration of coal as a non- oxidative source of carbon monoxide. Mining Engineer. 154, 55-56.
[21] Huggins, F.E., Huffman, G.P. (1989) Coal weathering and oxidation: the early stages. Chemistry of coal weathering. 14, 33–60.
[22] Carras, J.N., Young, B.C. (1994) Self-heating of coal and related materials: models, application and test methods. Prog. Energy Combust. Sci. 20, 1-15.
[23] Pisupati, S., Scaroni, A. (1993) Natural weathering and laboratory oxidation of bitu-minous coals: organic and inorganic structural changes. Fuel. 72, 531–542.
[24] Fierro, V., Miranda, J., Romero, C., Andrés, J., Arriaga, A., Schmal, D., Visser, G.H. (1999) Prevention of spontaneous combustion in coal stockpiles: experimental results in coal storage yard. Fuel. Process Technology. 59, 23–34.
[25] Wang, H., Dlugogorski, B., Kennedy, E. (2002) Examination of CO_2, CO and H_2O formation during low-temperature oxidation of a bituminous coal. Energy. Fuel. 16, 586–592.
[26] Wang, H., Dlugogorski, B., Kennedy, E. (2003) Coal oxidation at low temperatures: oxygen consumption, oxidation products, reaction mechanism and kinetic modelling. Prog Energy Combust Science. 29, 487–513.
[27] Tang, Y.B. (2015) Sources of underground CO: Crushing and ambient temperature oxidation of coal. Journal of Loss Prevention in the Process Industries. 38, 50-57.
[28] Wang, H.H., Dlugogorski, B.Z., Kennedy, E.M. (2003) Pathways for Production of CO_2 and CO in Low-Temperature Oxidation of Coal. Energy Fuels. 17, 150-158.
[29] Deng, J., Zhao, J.Y., Zhang, Y.N., Huang, A.C., Liu, X.R., Zhai, X.W., Wang, C.P. (2016) Thermal analysis of spontaneous combustion behavior of partially oxidized coal. Process Safety and Environmental Protection. 104, 218–224.

Received: **06.11.2018**
Accepted: **17.02.2019**

CORRESPONDING AUTHOR

Fusheng Wang
North China University of Science and Technology,
College of Mining Engineering,
Hebei, Tangshan,063210 – China

e-mail: fswang3418@163.com

© by PSP Volume 28 – No. 4/2019 pages 2908-2915 Fresenius Environmental Bulletin

ADSORPTION ABILITY OF AIR POLLUTANTS BY INDIGENOUS TREE SPECIES IN TA-PIEH MOUNTAINS

Hui Wang[1], Yao-qing Sun[1], Miao Zhang[1], Wen-jing Liu [1], Le Yang[1], Xing-wen Zhou[2,*]

[1]Xinyang College of Agriculture and Forestry, Henan Xinyang 464000
[2]College of Biology and Pharmacy, Yulin Normal University, Guangxi Zhuang Autonomous Region Yulin, China, 537000

ABSTRACT

To enhance the ability of indigenous tree species in Ta-pieh Mountains to decontaminate toxic gases, Euonymus japonicus, Salix babylonica and Morus alba are surveyed by means of fumigation experiments for sensitivity to SO_2 and HF. Response surface methodology is applied to adsorption and purgation ability of indigenous tree species on SO_2 and HF. The results show that trees can absorb and accumulate the contaminants in the atmosphere through the leaves, and the amount of adsorption and accumulation is large. The tree species have adsorption and purgation ability to air pollutants, and have differences according to the type of pollutant gas. After treating them in fumigation chamber, the weakest one, Morus alba, contains 9.5 mg/kg of sulfur while the strongest one, Euonymus japonicus, contains 478.9 mg/kg. The weakest one, Salix babylonica, contains 6.9 mg/kg of fluorine while the strongest one, Euonymus japonicus, contains 401.5 mg/kg.

KEYWORDS:
Indigenous tree species, artificial fumigation method, absorbency, SO_2 , HF

INTRODUCTION

The issue of emission reduction of industrial air pollutants is a major environmental concern of most developing countries due primarily to the air pollution at both the national and the global level.

Hydrogen fluoride (HF) is the principal source of fluorine for the synthesis of many important compounds including pharmaceuticals and polymers, thus is widely used in very large quantities in industries such as the semiconductor and petroleum industries [1]. As well known, HF is a very hazardous reagent because of its low boiling point and high toxicity [2,3]. However, in the practical production and employ processes, the excess of HF used is difficult to avoid the smuggling of small portion of HF gases completely. On the other hand, HF and/or other fluoride gases can generate in the application of fluoride compounds, such as SF6 as electrical insulator [4,5], as well as coal combustion [6]. Moreover, HF gas in humidity will corrode the metal and insulation materials, and then break down the life of electric apparatus. Then again, the HF gas would yield in the running of pulse chemical laser based on the discharge of SF6 and hydrocarbons, which would sharply decrease the performance of the laser [7]. Additionally, HF is the target analyte liberated in the hydrolysis of fluorinated G-type chemical warfare agents [8]. Therefore, to avoid the health threat and environmental pollution as well as to preserve the life of industrial equipment, it is very important and necessary to find an efficient method for detecting and eliminating HF gas [9].

Since the Industrial Revolution, coal and other fossil fuels are widely used everywhere in the world. Meanwhile, due to high contents of S-contained compounds in fossil fuels, million tons of SO_2 are emitted into air per year by burning for energy, causing serious air pollution. The most effective way to control the emission of SO_2 from flue gas by combustion of fossil fuels is flue-gas desulphurization (FGD). Up to now, many absorbents, such as limestone, magnesium oxide, ammonia water and seawater, are used to capture SO_2 and all of them can decrease the pollution of SO_2. However, SO_2 is also a useful resource in the chemical industry. Most of the processes and absorbents only pay attention to the control of air pollution caused by SO_2 and ignore the recycle of SO_2, because the absorbents are very difficult to regenerate and recover SO_2. The adsorption processes are irreversible and can result in secondary pollution. Although organic amines can be used to reversibly absorb SO_2 from flue gas, the process suffers from solvent loss. Therefore, it is urgent to explore new absorbents for the reversible, efficient, and environmentally-friendly capture of SO_2.

Plants not only have a certain degree of resistance to atmospheric pollutants in a certain concentration range, but also have a considerable ability to absorb harmful gases. Through the pores on the leaves and the lenticels on the branches, the plants absorb atmospheric pollutants into the body, neutralize them in the body through redox processes to form non-toxic substances, or excrete

them through roots, or accumulate and store them in an organ. Inside. The adsorption, degradation, accumulation and discharge of air pollutants by plants actually play a role in purifying air pollution [10-15].

In order to find the native tree species with high adsorption and purification ability, this paper studies and discusses the adsorption and purification ability of some native tree species in the Dabie Mountains to the main atmospheric pollutants through artificial simulation of the fumigation method, thus providing a theoretical basis for the scientific selection of soil-sucking native tree species. This paper studies the field of environmental protection and air pollutants can be effectively removed by indigenous tree species.

EXPERIMENTAL

Fumigations with SO_2 or HF were performed using the chamber system. This consisted of a single pair of 0.7 m^3 Perspex chambers, located in a glasshouse and ventilated with charcoalfiltered air at a rate of four changes per minute. The pollutant gases were added continuously to one chamber to provide a constant concentration and monitored throughout the experimental periods by sampling the air within both chambers through chemistry for the gas under study. In addition, checks were carried out periodically using a continuous SO_2 monitor and HF. The glasshouse in which the system was installed received supplementary heating and lighting as required.

RESULTS AND DISCUSSION

Surface plot of sulphur adsorption (mg/kg) vs ambient temperature, humidity is shown in Fig.1. The high concentration of SO_2 gas will greatly exceed the plant's ability to withstand, causing the plants to fall off the leaves in a short period of time (1 to 2 days or a few hours), and the growth and development are severely blocked until they die. Due to the long-term pollution of SO_2 in plants, plants gradually produce some symptoms that are not easily noticed by people, causing plants to grow to varying degrees. Plants have not shown any symptoms under the influence of low concentration of SO_2 for a long time, but the physiological activities inside the plant have been invaded and growth and development are hindered. The strong light and high temperature, the more sensitive the plant is to sulfur dioxide, the more susceptible it is to damage. It is seen that sulphur adsorption increases when ambient temperature and light time increases.

Surface plot of sulphur adsorption (mg/kg) vs humidity and smoke time is shown in Fig.2. It is seen that sulphur adsorption increases when smoke time and humidity increases. Sulfur dioxide enters from the pores and gradually spreads to the sponge tissue and the palisade tissue cells. The damage of sulfur dioxide to plants begins at the cell membrane and changes the permeability of the membrane. The initial damage is the cell membrane of the most active palisade tissue cells of photosynthesis, and then the cell membrane of the sponge tissue is damaged. Chloroplasts and chlorophyll are successively destroyed. At the same time, the cytoplasm is separated, the tissue is dehydrated, withered, and dead, and finally the surface of the leaf is damaged, forming many faded spots.

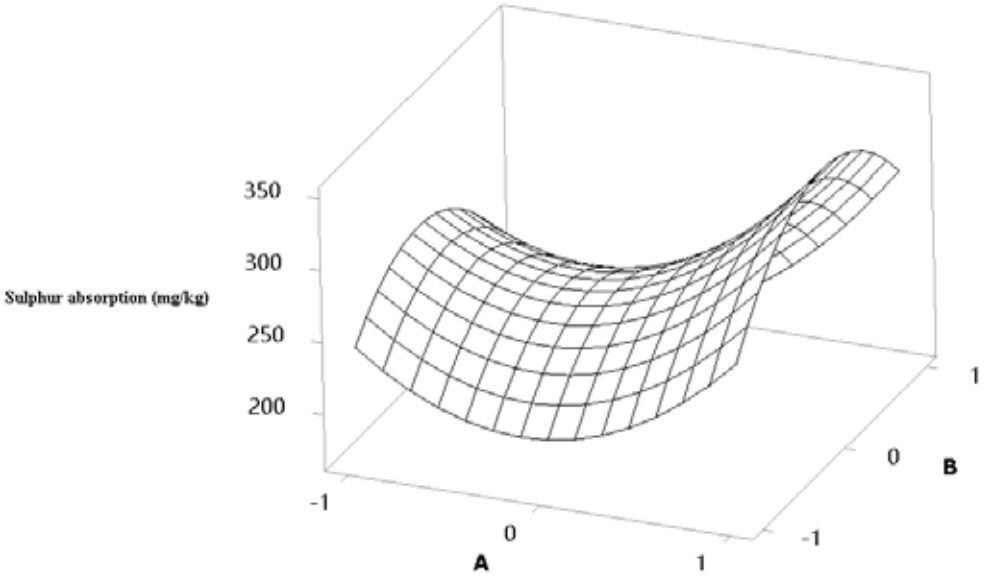

FIGURE 1
Surface Plot of Sulphur adsorption (mg/kg) vs B, A

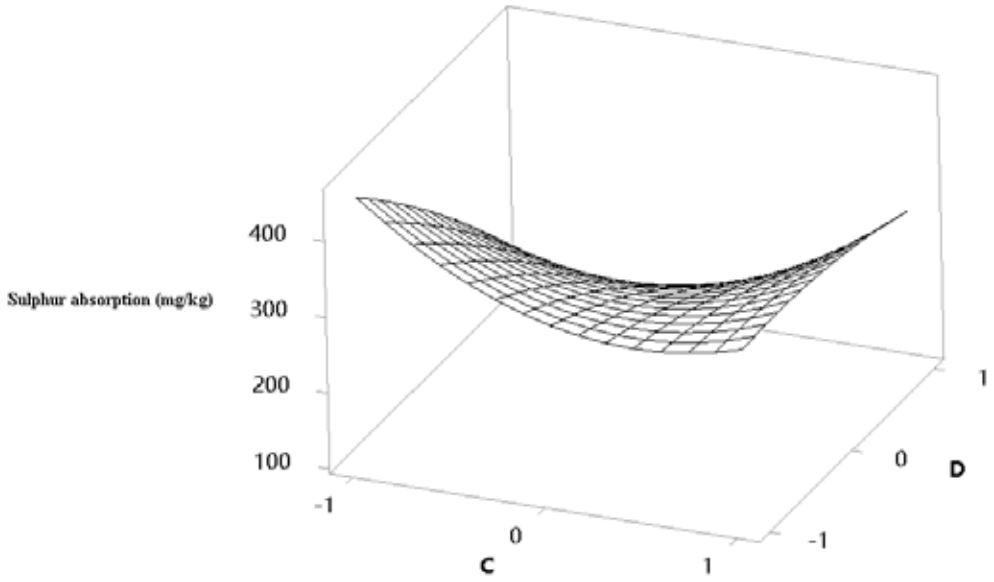

FIGURE 2
Surface Plot of Sulphur adsorption (mg/kg) vs D, C

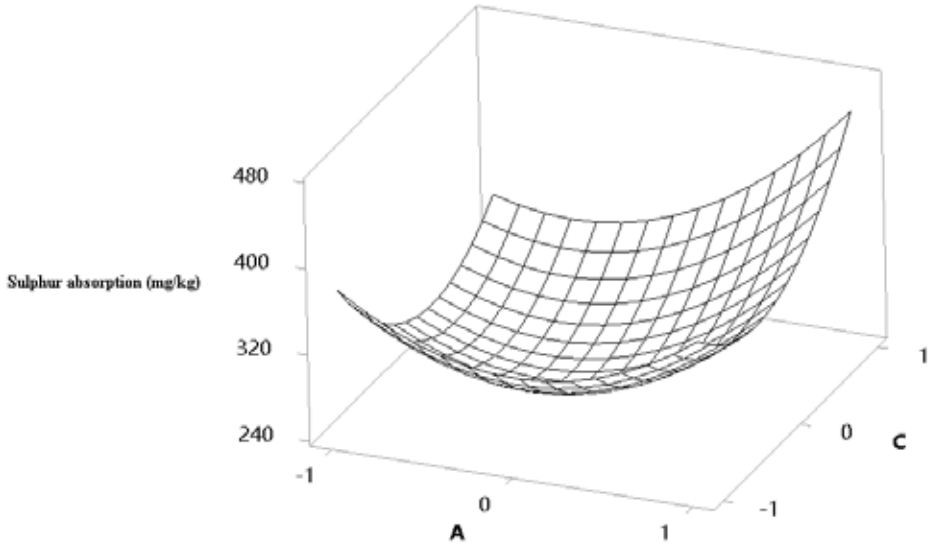

FIGURE 3
Surface Plot of Sulphur adsorption (mg/kg) vs C, A

Surface plot of sulphur adsorption (mg/kg) vs ambient temperature, humidity is shown in Fig.3. It is shown that symptoms mainly occur between the veins. Generally, dots and block-like lesions of different sizes and without regular distribution are present, and the boundary between them and normal tissues is obvious. There are also a few lesions distributed on the edge of the leaves, or the whole leaves are chlorotic and yellow, but the young leaves are not easily damaged. The color of the lesions is mostly yellow or reddish brown, but the shape, distribution and color of the lesions vary depending on the plant species and the conditions of the damage. For example, monocotyledonous lesions are often stripped along parallel veins and distributed at the tip or leaf ridge.

Surface plot of sulphur adsorption (mg/kg) vs light time, smoke time is shown in Fig.4.

Fig.5 shows that there is interaction between humidity and light time. Increased range of humidity on sulphur adsorption is not very obvious. Within a certain concentration of sulfur dioxide, the damage of the leaves is related to leaf age. The order of its damage is mature leaves, old leaves, and young leaves. This is because the young leaves are the most resistant, the mature leaves are the most sensitive, and the old leaves are somewhere in between.

Fig.6 shows that there is interaction between ambient temperature and smoke time. Increased range of smoke time on sulphur adsorption is not very obvious.

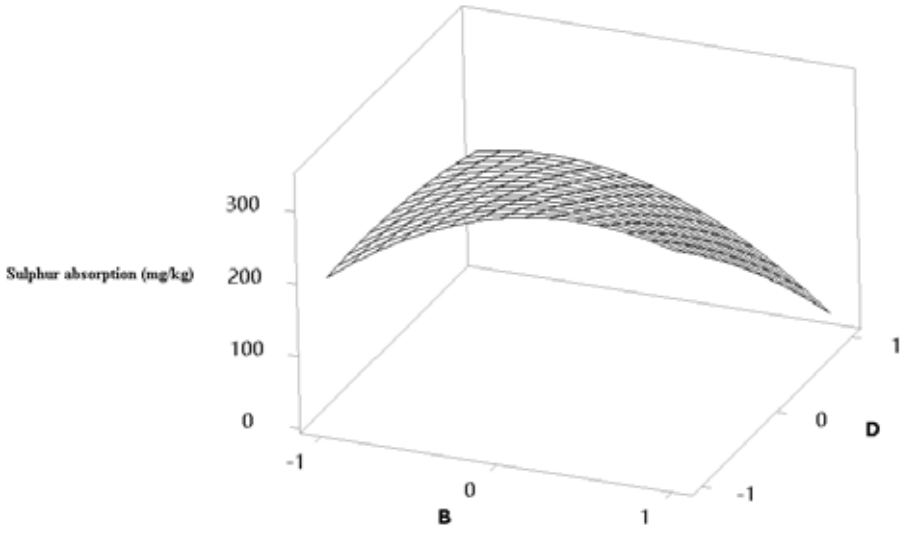

FIGURE 4
Surface Plot of Sulphur adsorption (mg/kg) vs D, B

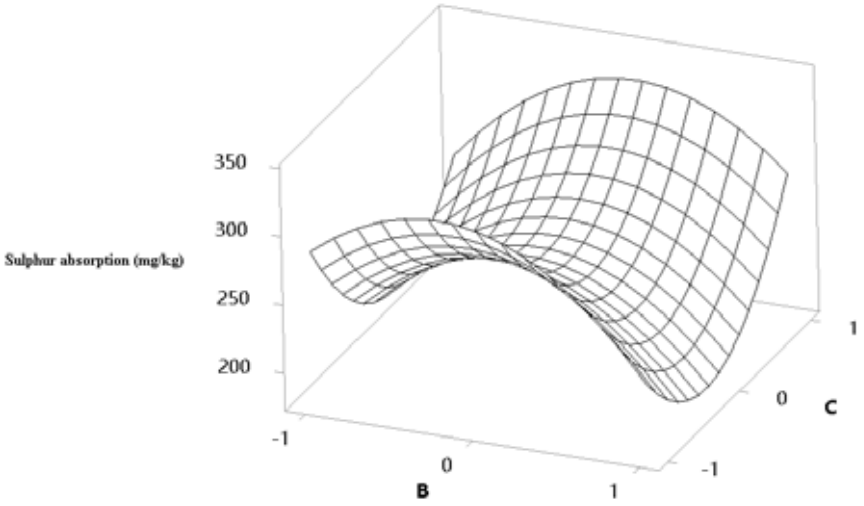

FIGURE 5
Surface Plot of Sulphur adsorption (mg/kg) vs C, B

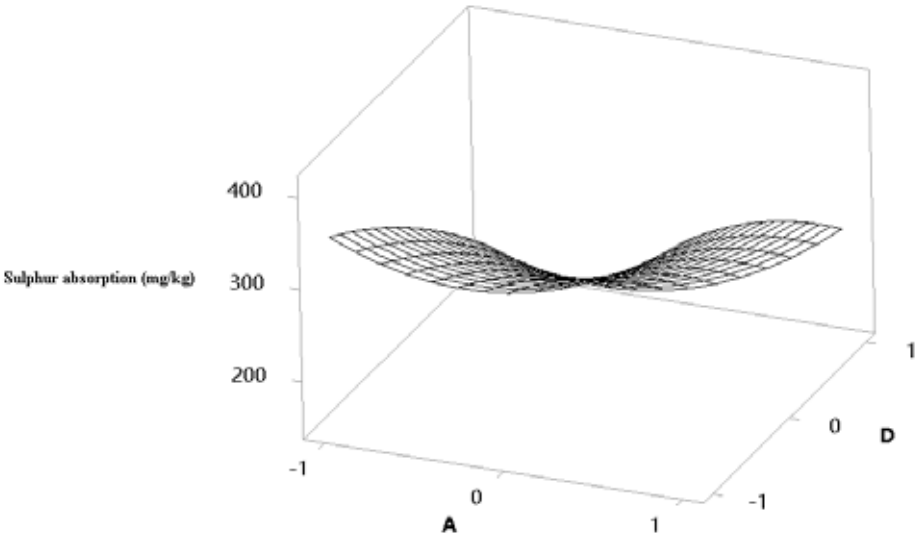

FIGURE 6
Surface Plot of Sulphur adsorption (mg/kg) vs D, A

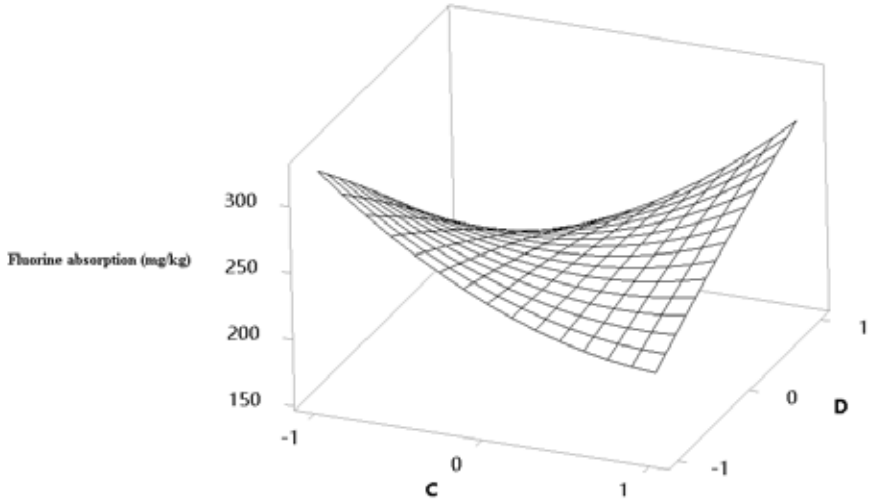

FIGURE 7
Surface Plot of Fluorine adsorption (mg/kg) vs D, C

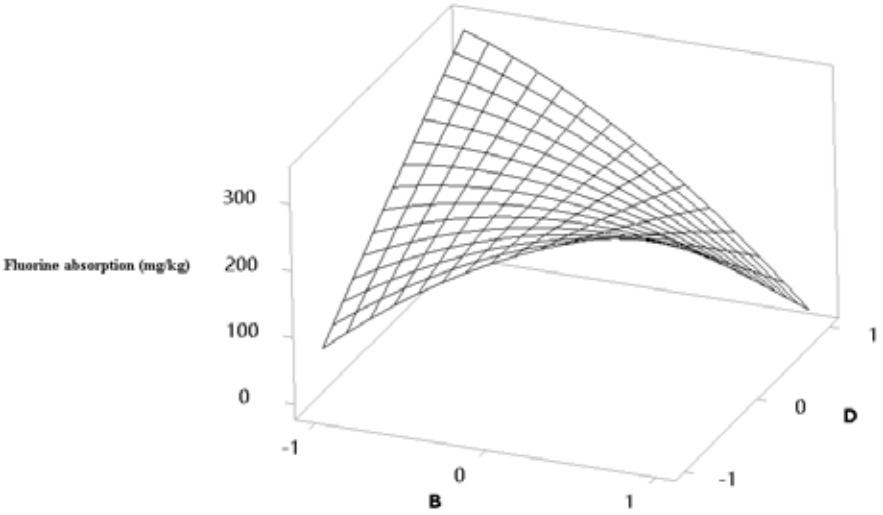

FIGURE 8
Surface Plot of Fluorine adsorption (mg/kg) vs D, B

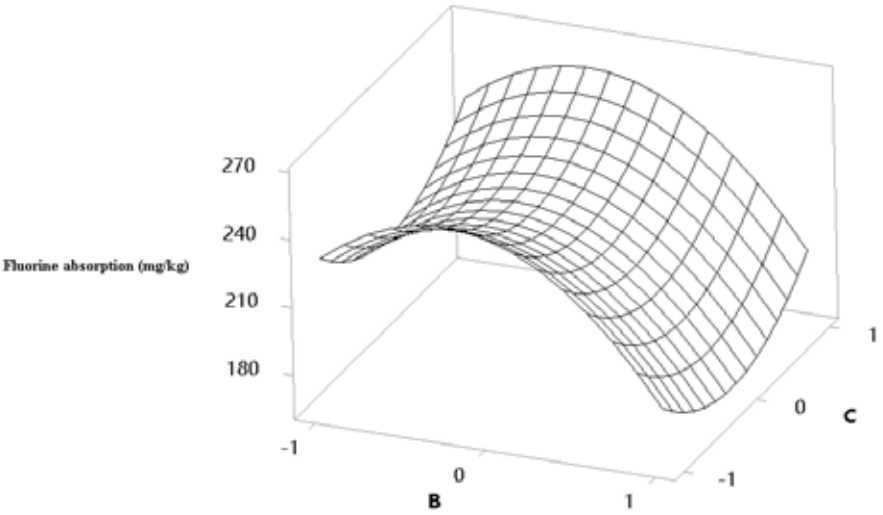

FIGURE 9
Surface Plot of Fluorine adsorption (mg/kg) vs C, B

Fig.7-9 shows effect of humidity, smoke time and light time on fluorine adsorption. For HF, most of the lesions are distributed on the tip and leaf margin. There is a clear dark red line between the damaged lesion and the normal tissue. A few are inter-pulse lesions and young leaves are vulnerable. In addition, the distribution of the lesions has a certain relationship with the thickness of the leaves, the thickness and the direction of the veins. Usually, the lateral veins are not obvious, and the lesions of the weak leaves are connected into a whole block, and the position is not fixed. The obvious lesions of the lateral veins are scattered. Between the veins; the damaged parts of the parallel veins are often at the tip of the leaf or the bulge of the leaves; the thick and hard spots of the leaf are often distributed on the ridges or leaf margins on both sides of the main vein; the large and thin lesions of the leaves are mostly distributed at the edges, often Connected into a large piece.

Fig.10-12 shows that after treating them in fumigation chamber, the weakest one, Morus alba, contains 9.5 mg/kg of sulfur while the strongest one, Euonymus japonicus, contains 478.9 mg/kg. The weakest one, Salix babylonica, contains 6.9 mg/kg of fluorine while the strongest one, Euonymus japonicus, contains 401.5 mg/kg.

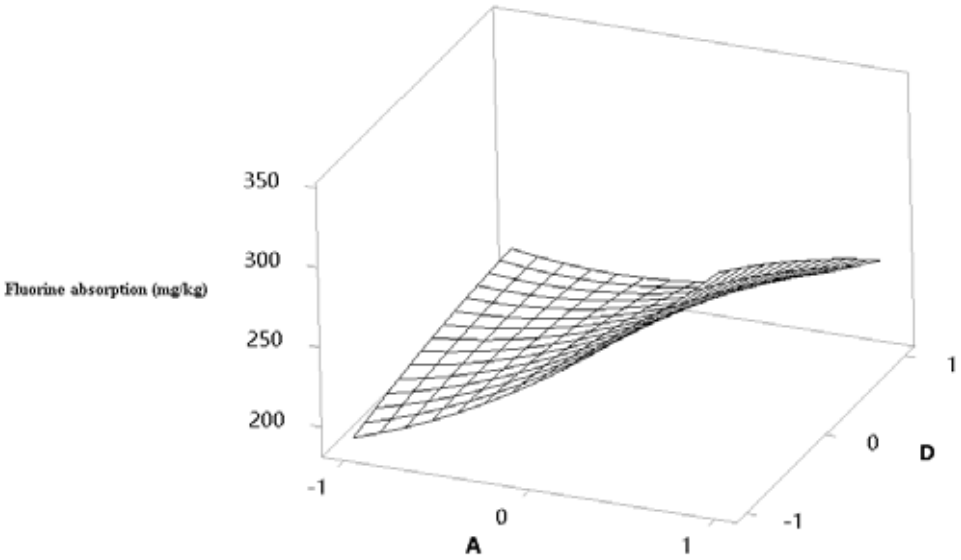

FIGURE 10
Surface Plot of Fluorine adsorption (mg/kg) vs D, A

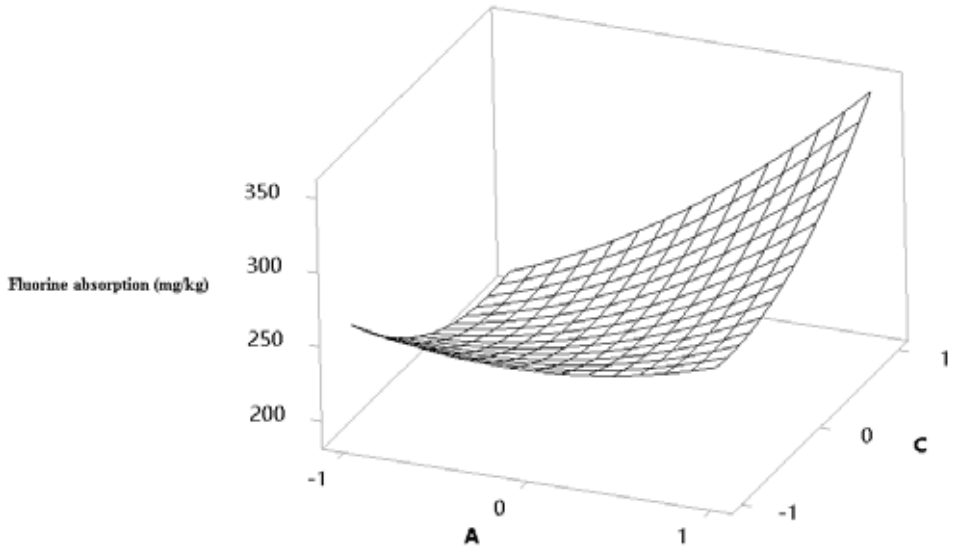

FIGURE 11
Surface Plot of Fluorine adsorption (mg/kg) vs C, A

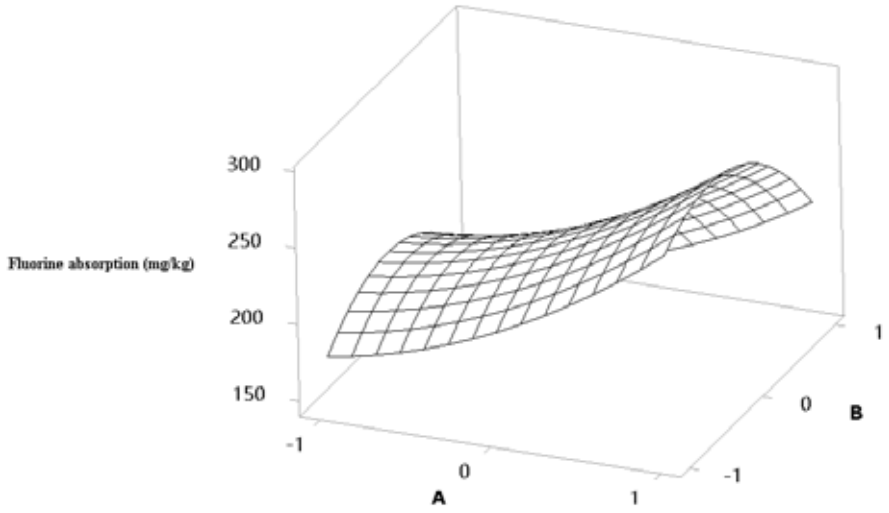

FIGURE 12
Surface Plot of Fluorine adsorption (mg/kg) vs B, A

CONCLUSION

Response surface methodology is applied to adsorption and purgation ability of indigenous tree species on SO_2 and HF. The results show that trees can absorb and accumulate the contaminants in the atmosphere through the leaves, and the amount of adsorption and accumulation is large. The tree species have adsorption and purgation ability to air pollutants, and have differences according to the type of pollutant gas. After treating them in fumigation chamber, the weakest one, Morus alba, contains 9.5 mg/kg of sulfur while the strongest one, Euonymus japonicus, contains 478.9 mg/kg. The weakest one, Salix babylonica, contains 6.9 mg/kg of fluorine while the strongest one, Euonymus japonicus, contains 401.5 mg/kg.

ACKNOWLEDGEMENT

This paper is supported by Key scientific research projects for colleges and Universities of Henan Province (No.17B220002) and National Natural Science Foundation of China (No. 31360197).

REFERENCES

[1] Huang, T.M., Yang, S., Pang, Z.H. (2017) Hydrogeochemistry evolution and fluoride accumulation in an arid piedmont alluvial-proluvial plain. Fresen Environ Bull. 26, 3569-3576.

[2] Alkan, S., Turgut, U., Irende, I., Kul, A.R. (2018) Thermodynamic study of activated carbon from pear shell and acacia tortilis reactions with immobilized lipases. Fresen Environ Bull. 27, 4343-4348.

[3] Uzunosmanoglu, O., Uyanik, A., Engin, M.S. (2011) The removal of cadmium (ii), copper (ii) and lead (ii) from aqueous solutions by olive tree pruning waste. Fresen Environ Bull. 20, 3135-3140.

[4] Sedgwick, D.M., Hammond, G.B. (2018) The history and future challenges associated with the hydrogenation of vinyl fluorides. Journal of Fluorine Chemistry. 207, 45-58.

[5] Gromov, O.B. (2014) System Researches "Fluorides of Alkaline Metals – Hydrogen Fluoride" Procedia Chemistry. 11, 30-34.

[6] Afzal, S., Rahimi, A., Ehsani, M.R., Tavakoli, H. (2010) Experimental study of hydrogen fluoride adsorption on sodium fluoride. Journal of Industrial and Engineering Chemistry. 16, 147-151.

[7] Li, Z., Hammond, G.B., Xu, B. (2016) Quantification of hydrogen fluoride-based reagents using a bifunctional NMR internal standard. Journal of Fluorine Chemistry. 184, 72-74.

[8] Langerman, N. (2016) Hydrogen fluoride & alkylation. Journal of Chemical Health and Safety. 23, 53-55.

[9] Chaban, V. (2015) Hydrogen fluoride capture by imidazolium acetate ionic liquid. Chemical Physics Letters. 625, 110-115.

[10] Ren, S.H., Hou, Y.C., Zhang, K., Wu, W.Z. (2018) Ionic liquids: Functionalization and adsorption of SO_2. Green Energy & Environment. 3, 179-190.

[11] Xu, L., Xu, S.H., Zhi, L.Q., He, X.D., Zhang, C.H., Cai, Y.Q. (2017) Methylsiloxanes release from one landfill through yearly cycle and their removal mechanisms (especially hydroxylation) in leachates. Environ Sci Technol. 51, 12337-12346.

[12] Li, X.F., Deng, D.S. (2018) Physicochemical property and solubility of SO_2 in glycerin derivatives. Journal of Molecular Liquids. 264, 66-71.
[13] Ma, H.C., Du, C.W., Liu, Z.Y., Li, X.G. (2018) Effect of SO_2 content on SCC behavior of E690 high-strength steel in SO_2-polluted marine atmosphere. Ocean Engineering. 164, 256-262.
[14] Wang, S.G., Chen, B. (2016) Accounting of SO_2 Emissions from Combustion in Industrial Boilers. Energy Procedia. 88, 325-329.
[15] Zhang, Q., Tao, Q., He, H.P., Liu, H.M., Komarneni, S. (2017) An efficient SO_2-adsorbent from calcination of natural magnesite. Ceramics International. 43, 12557-12562.

Received: **11.10.2018**
Accepted: **09.02.2019**

CORRESPONDING AUTHOR

Xing-wen Zhou
College of Biology and Pharmacy, Yulin Normal University, Guangxi Zhuang Autonomous Region Yulin, China, 537000

e-mail: 1870828433@qq.com

© by PSP Volume 28 – No. 4/2019 pages 2916-2922 Fresenius Environmental Bulletin

STUDY OF INSECTICIDAL AND BEHAVIORAL EFFECTS AND SOME CHARACTERISTIC OF NATIVE DIATOMACEOUS EARTH AGAINST THE BEAN WEEVIL, *ACANTHOSCELIDES OBTECTUS* (COLEOPTERA: CHRYSOMELIDAE)

Mustafa Alkan[1,*], Sait Erturk[1], Tugba Akdeniz Firat[1], Emin Ciftci[2]

[1]Plant Protection Central Research Institute, Deparment of Entomology, Ankara, Turkey
[2]İstanbul Technical University, Faculty of Mines Department of Geological Engineering, İstanbul, Turkey

ABSTRACT

In this study, efficacy and some characteristics of the local diatomaceous earth (DE) were investigated against been weevils [*Acanthoscelides obtectus* (Say) (Col.: Bruchidae)] on chickpeas (*Cicer arientum* L.) under laboratory conditions. In the experiments, Turco000, Turco004, and Turco020 derived from native sources (Ankara, Turkey), and Protector®, a commercial product, were used. The bioassays were carried out at 25±1°C temperature, 65±1% r.h. with six concentrations of DEs (100, 200, 400, 600, 800 and 1000 ppm) at the Plant Protection Central Research Institute, Entomology Laboratory in Ankara in 2016. The mortality of adults was evaluated after the 4th, 7th and 14th days of treatments. In order to determine progeny production (F1), the treated chickpeas were further incubated at the same conditions for the 55-days. Turco000 gave 100% mortality to *A. obtectus* adults at 1000 ppm after 4th day as Protector® at 600 ppm concentration did. The lowest mortality rate was observed at Turco020 at a dose of 100 ppm 7 days after treatment. When the effects of diatomaceous earth formulation on the fertility of F1 were investigated, it was determined that all diatomaceous earth formulation had an effect on different rates. There was no progeny production with Turco000 at 200 ppm concentration at the end of 55-day incubation period and this was followed by Turco004 and Turco020, respectively. Results showed that the protective residual effect of Turco000 continued throughout the experiments. In conclusion, Turco000 can be used as a valuable tool for *A. obtectus* in stored product pest management programs.

KEYWORDS:
The bean weevil, Local Diatomaceous earth, Effectiveness, Progeny production

INTRODUCTION

The bean weevil *Acanthoscelides obtectus* (Say) (Coleoptera: Chrysomelidae) is a major pest of beans and other legumes from the Fabaceae family. The primary host of this weevil is the common bean (*Phaseolus vulgaris*). The weevil also attacks chickpeas (*Cicer arietinum*) and other stored legumes [1]. The consequence of the insect damage to the products causes qualitative and quantitative losses to both nutritional properties and the market value of the stored legumes. The storage period of the legumes, which have an important place in human nutrition, must be carried out under suitable conditions and protected with minimum loss. In stored products, direct or indirect losses from biotic and abiotic factors such as relative humidity, temperature, grain size, and insect species occur during storage. Harmful organisms such as microorganisms, mites, rodents, and insects are among the biotic factors that cause this loss. Stored legumes are particularly damaged by Bruchidae (Coleoptera) family members in the field and/or post-harvest period. These organisms degrade the quality of the product due to the body residues such as exuvia, seta and the substances they release on the product. It has been observed that alternative efforts to the chemical control have recently gained a significant increase in order to reduce this damage rate. Bean weevil, which has a wide spreading area and adapts to environmental conditions, has high tolerances against various insecticides [2]. For this reason, many research and efforts have been made to find effective means of ensuring long-term storage of legumes. The use of natural enemies, plant extracts, volatile oils, and inert dust have been accepted as promising strategies for the control of *A. obtectus* until now [3, 4, 5, 6, 7]. In stored products, various control methods have been applied to insect pests. These methods include; physio-mechanical methods (modified atmosphere, cooling, drying, high temperature, radio waves etc.), biotechnical control methods, cultural control methods and use of synthetic chemicals intensively. Fumigation is the most

common chemical control method in the world. Fumigation is preferred because of its rapid penetration, ease of use and low cost in control of storage pests. Methyl bromide, one of the fumigants used intensively, has been banned except in limited applications, under the Montreal Protocol. The residue of some insecticides applied directly to the product to protect stored legumes from insect pests may cause acute or chronic toxicity to the consumer at significant levels. On the other hand, the development of resistance in the pests also causes problems in practice. It has been known that resistance to some important stored product pests against many effective substances such as malathion, chlorpyrifos-methyl, fenitrothion, pirimiphos-methyl, etrimfos and the like which are being used in storage [8]. One of the physical control treatment is diatomaceous earth applications.

Diatoms, either solitary or colonial, microscopic are photosynthesizing algae that have a siliceous skeleton, called frustule and are found in almost every aquatic environment ranging from freshwaters to marine waters. In fact, they are found virtually anywhere moist enough. They have both benthic and planktonic forms that both are restricted to the photic zone, since they are all strictly autotrophic (water depths down to about 200 m depending on the water clarity). Diatoms have a variety of different diameter or length such as 20-200 microns, some even reach up to 2 millimeters in length. They are recorded in geological records since Cretaceous. Diatoms may occur in such large amounts and be well preserved enough to form sediments composed almost entirely of diatom frustules, then called diatomites or partly of frustules, then called diatomaceous earth, in both cases, it becomes economic deposits and may be used in a number of applications including filters, agriculture, paints, toothpaste, and many others.

Elements such as iron, calcium, aluminum, and thorium are present in the form of oxides in the components of the diatomaceous earth, which are basically amorphous silica. In insects, cuticle acts as an exoskeleton and provides protection and support for internal organs. The main barrier to prevent water loss from an insect is the epicuticular lipids. In insect morphology, epicuticular lipids act as a platform for the semiochemicals. Also plays an important role like retention of water in the body, protection from the body external corrosive and toxic substances [9]. Diatomaceous earth absorbs the cuticular lipids and it also abrades the cuticles of insects and causing death by desiccation [10, 11]. Diatomaceous earth can be successfully incorporated into the IPM program as they have proven to be very effective against insect pest species with low mammalian toxicity, long-lasting efficacy and being natural insecticides.

In this study, we intend to determine the effectiveness of native diatomaceous earth obtained from central Anatolia around Ankara region as stored-legume protectants against *Acanthoscelides obtectus*. Also, the present study was designed to assess the effect of particle size and behavioral effect of the tested diatomaceous earth on the insects under laboratory conditions.

MATERIALS AND METHODS

Insect mass-rearing. *Acanthoscelides obtectus* adults were reared in sterile 1-L glass jars on chickpeas in incubators (Nüve ID 501, Ankara, Turkey) maintained at about 25±1°C and 65±1% relative humidity. For the prevention of possible contamination, chickpeas were kept in the deep freezer at -18 ºC at least 7 days. The clean chickpea

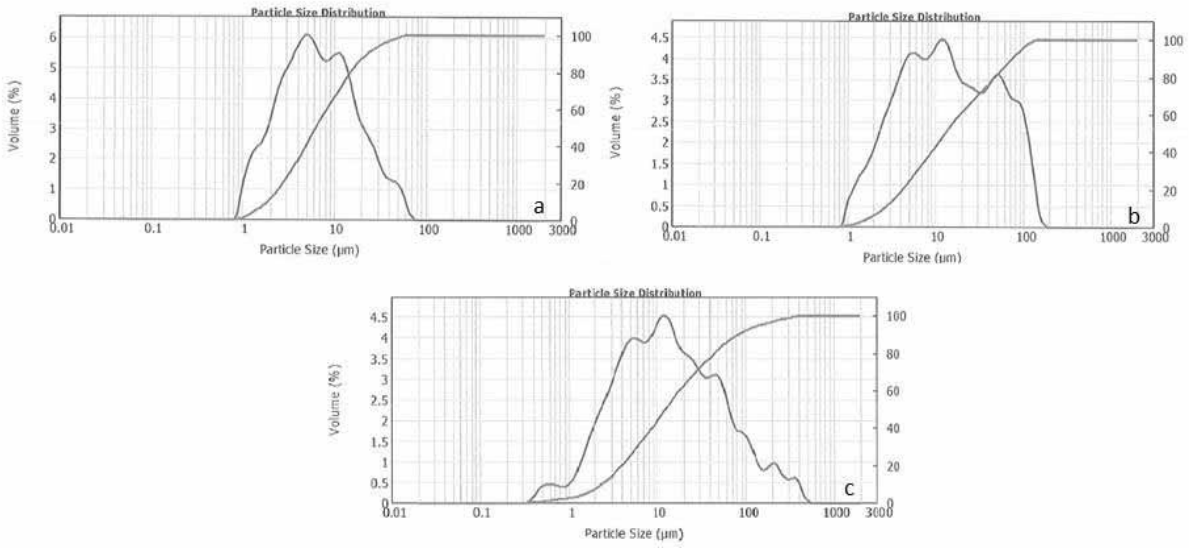

FIGURE 1
Grain size distribution of native DE's (a: Turco000 b: Turco004 c: Turco020).

used as both food source and oviposition area was filled to half of the jar. Approximately, 450-500 mixed-sex adult individuals were transferred in the glass jar. In order to ventilation, the lids of the glass jar were drilled, each lid has eight holes with a diameter of 1mm. The adults on the chickpeas were vacuumed after 24 hours later. Thus, we have obtained 0-24 hours old eggs. The newly emergence adults were observed about 30-33 days after. In the trials, 1-3 days old mixed-sex adults were used.

Diatomaceaus earth characterization. DE's used in this study were acquired from a local commercial company operating in Ankara-Kazan and Beypazarı counties (Beg-tuğ Mineral). Physico-chemical tests and analysis of the DE's (e.g. grain size, chemical content, and morphology) were carried out at General Directorate of Mineral Research and Exploration (MTA) labs in Ankara, Turkey. Grain size distribution and SEM images of the DE's are presented in Figure 1 and 2, respectively. The chemical composition of the DE's is given in Table 1.

Representative splits from each DE were put on glass slides then coated using a gold sputter coater at MTA Labs for the SEM study. Photomicrographs were taken to show diatom varieties in the samples (Figure 2). Based on the SEM observations, each split contained varying amount of diatoms of pinnate type. Centric types were not observed.

About 10 g splits from each sample were pulverized to <450 micron using a Retsch vibratory disk mill (RS 200) and then X-rayed using a Bruker D8 Advance XRD integrated with a dedicated LynEye detector for 0-70º 2Θ with 0.019º/sn step speed using 40 KV and 40 mA Cu Kα radiation source at room temperature. Ni filter was used (ITU-JAL labs, Istanbul). Diffraction data were then evaluated using the MDI Jade software to determine crystalline mineralogical contents of the samples and presented in Figure 3).

Mineral contents of the DE are represented by the common soil phases such as feldspars, calcite, quartz, mica and common clay varieties along with some secondary oxides and zeolites. Based on the abundance of the frustules, opal-CT may be detected by XRD.

Insecticidal activity assays. A Turkish chickpea variety, *Cicer arietinum*, Koçbaşı, with 11 % moisture content was used for bioassays. Local diatomaceous earth and Protector® were used at the concentration of 100, 200, 400, 600, 800 and 1000 ppm. Untreated chickpea (control group) was used as the control for the diatomaceous earth samples. For each concentration, 280 g chickpea was used in 1-liter volume PVC bags. Chickpeas and DT were put into plastic bags and then sealed and shaken for 5 minutes to provide a good mixture. To ensure even distribution of DE the bags left for 10 minutes for dust settlement. Each vial (volume of 225ml, 3wx8h cm) was fitted with a plastic lid prepared as for the rearing jars. The vials were then filled with 70 g of DE treated chickpea and with 10 mixed sex adults weevils each. Test vials were placed in an incubator (Nüve ID 501) adjusted at 25±1°C and %65±1 r.h. Assessment of the mortality of the treated live and dead individuals was recorded after 4, 7 and 14 days respectively.

TABLE 1
Chemical contents of three native diatomaceous earth

Treatment	SiO_2 (%)	CaO (%)	Al_2O_3 (%)	Fe_2O_3 (%)
Turco000 (1-10µ)	95.00	0.83	1.42	1.77
Turco004 (10-30µ)	83.26	3.49	6.25	4.91
Turco020 (43-65µ)	83.90	2.74	6.25	3.71
Protector <9.46µ	69.70	0.41	5.80	1.05

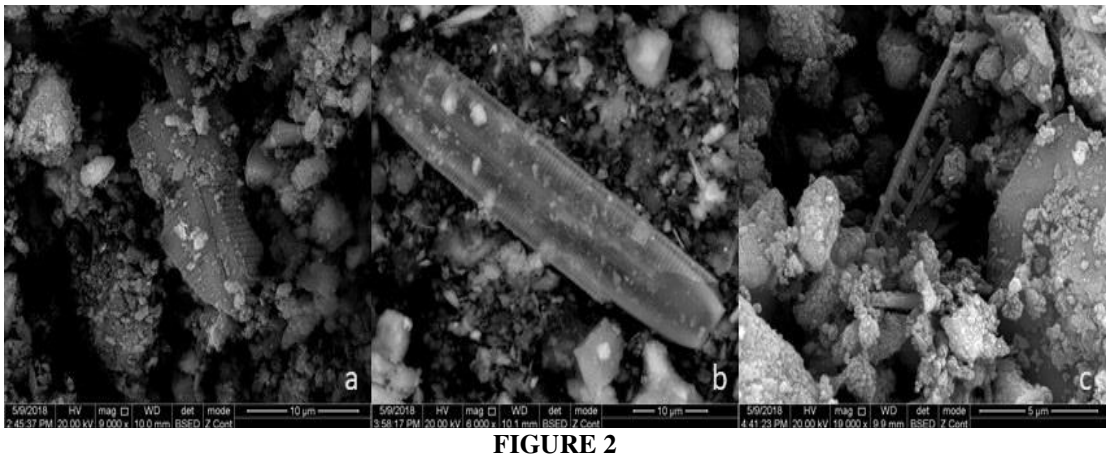

FIGURE 2
SEM images of Turco 000 (a), Turco 004 (b) and Turco 020 (c) showing general size and shape varieties of diatoms.

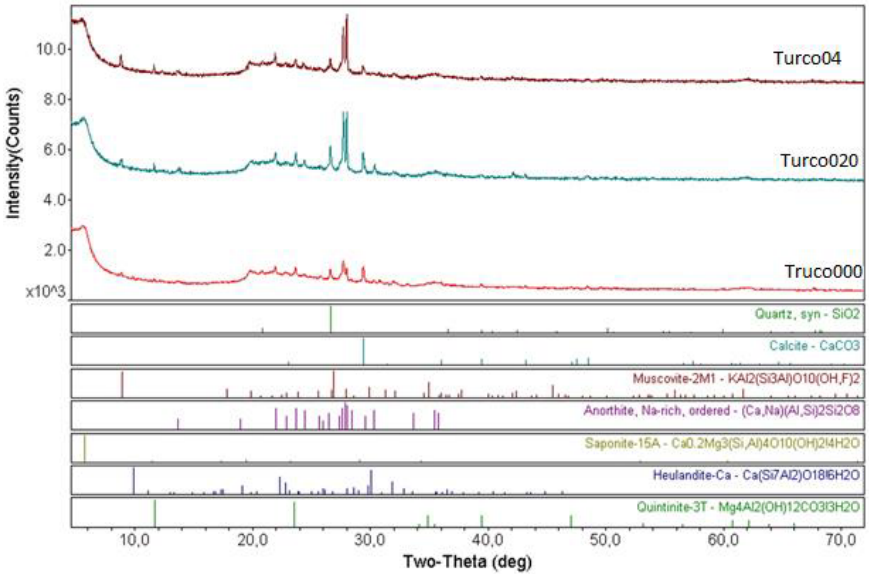

FIGURE 3
Collage of X-ray diffractograms of the subject samples.

TABLE 2
Toxicity of different doses of Turco000 diatomaceous earth against *Acanthoscelides obtectus* adults

Treatment	Mortality (%)±StDev		
	4 DAT	7 DAT	14 DAT
Control	2.57±3.41b*	5.71±2.57c	5.71±2.57c
100ppm	7.47±3.81b	14.64±0.67b	67.82±1.11b
200ppm	90.56±4.71a	100.00±0.00a	100.00±0.00a
400ppm	96.19±5.38a	-	-
600ppm	99.35±2.57a	-	-
800ppm	99.35±2.57a	-	-
1000ppm	100.00±0.00a	-	-
Protector©	100.00±0.00a	-	-

*Different letters in the same column indicate statistically different from each other (Anova P<0,05, Tukey test). DAT: Day After Treatment

Effect of Diatomaceous earth on F1 progeny. After 14 days from the contact toxicity test, dead and live insects were removed from the treated chickpea. The same jars were kept at 25±1°C and 65±1% relative humidity condition until the first adult was seen and then newly emerged adult insects were counted.

Inhibition rate was calculated according to the formula below.

IR = (Cn – Tn) / Cn * 100

IR% : Inhibition rate
*C*n : Number of newly emerged insects in the untreated (control) jar
*T*n : Number of newly emerged insects in the treated jar.

Statistical analysis. Contact toxicity screening test results were firstly converted into percent mortality and then were subjected to arcsine ($n' = \arcsin\sqrt{n}$) transformation and ANOVA. Variance analysis was carried out with transformed data, and additionally, the differences among treatments were analyzed by means of Tukey multiple comparison tests ($p<0.05$). All statistical analyses were conducted with MINITAB® Release 16 package program.

RESULTS

When the insecticidal activity of Turco000, with the lowest particle diameter, on *A. obtectus* was examined, it was determined that all insects applied at the dose of 1000 ppm on the fourth day were died (Table 2). After the four days application, Turco000 was included in the same statistical group with the control group the only dose of 100 ppm. In other doses, Turco000 was in the same statistical group as the positive control group ($F_{(df=7,24)}=48,03$; $p<0,05$). Insecticidal activity was found to be greater than 90% at application doses of 200 to 800 ppm, but 100% mortality was seen at 1000 ppm. Seven days after treatment, mortality rates were determine as 100% at doses of 200 ppm and above

($F_{(df=7,24)}$=332,34; p<0,05). While all dose applications were in the same statistical group with the positive control group, the only dose of 100 ppm was in the different statistical group.

The effectiveness of Turco 020 was similar to Turco 000 (Table 3). In the evaluation made after four days of treatment, 97% or above mortality rates were determined in all doses except from a dose of 100 ppm ($F_{(df=7,24)}$=147,58; p<0,05). At doses of 400 ppm and above, 100% mortality rate was reached at both the seventh day ($F_{(df=7,24)}$=132,99; p<0,05) and the 14th day ($F_{(df=7,24)}$=187,79; p<0,05) applications. In all three intervals, at doses of 200 ppm and above, all treatments were in the same statistical group as the positive control.

Turco020 has a different effect than other diatomaceous earth used in this study, by terms of mortality rates and particle sizes. At the end of the fourth day, Turco020 did not gave 100% mortality at not any application dose and the highest mortality rate was determined as 97.43% at 1000 ppm dose and only this treatment had taken place in the same statistical group as the positive control ($F_{(df=7,24)}$=76,76; p<0,05) (Table 4). After the seventh day application, mortality rates of all doses were higher than fourth days treatment and it was determined that at the dose of 1000 ppm gave %100 mortality rates ($F_{(df=7,24)}$=116,00; p<0,05). At the dose of 200 ppm gave 90% and above mortality rates after the 14th day after treatment. Application doses of 400 ppm and above were in the same statistical group as a positive control ($F_{(df=7,24)}$=77,17; p<0,05).

It was determined that having different particle sizes and application doses, showed different suppression effects on the progeny production of *A. obtectus*. After the long storage period (55 days), it was seen that Turco000 and Turco004 showed minimum dose and maximum inhibition effect. In the progeny production, made 55 days after the application, the highest inhibitory effect with the lowest dose was found in Turco000 and Turco004. Besides, Turco020 showed lower activity in terms of suppression of F1 production (Table 5).

TABLE 3
Toxicity of different doses of Turco004 diatomaceous earth against *Acanthoscelides obtectus* adults

Treatment	Mortality (%)±StDev		
	4 DAT	7 DAT	14 DAT
Control	0.65±2.57b*	10.00±0.00b	12.23±0.50b
100ppm	2.57±3.41b	21.83±1.49b	99.35±2.57a
200ppm	97.43±3.41a	98.66±5.28a	100.00±0.00a
400ppm	100.00±0.00a	100.00±0.00a	-
600ppm	100.00±0.00a	-	-
800ppm	100.00±0.00a	-	-
1000ppm	100.00±0.00a	-	-
Protector©	100.00±0.00a	-	-

*Different letters in the same column indicate statistically different from each other (Anova P<0,05, Tukey test). DAT: Day After Treatment

TABLE 4
Toxicity of different doses of Turco020 diatomaceous earth against *Acanthoscelides obtectus* adults

Treatment	Mortality (%)±StDev		
	24 DAT	48 DAT	72 DAT
Control	0.00±0.00e*	0,65±2.57e	10,00±0.00d
100ppm	0.00±0.00e	12,23±0.50d	70,25±0.81c
200ppm	2.57±3.41de	21,61±2.23cd	90,56±4.71b
400ppm	14.64±0.67d	42,48±0.25c	99,35±2.57ab
600ppm	57.52±0.25c	85,81±1.65b	100,00±0.00a
800ppm	85.08±9.03bc	99,35±2.57a	-
1000ppm	97.43±3.41ab	100,00±0.00a	-
Protector©	100.00±0.00a	100,00±0.00a	-

*Different letters in the same column indicate statistically different from each other (Anova P<0,05, Tukey test). DAT: Day After Treatment.

TABLE 5
The effects of diatomaceous earth on the growth of *Acanthoscelides obtectus*

Treatment	IR (%)					
	100ppm	200ppm	400ppm	600ppm	800ppm	1000ppm
Turco 000	12,68	100,00	100,00	100,00	100,00	100,00
Turco 004	93,25	98,77	99,39	100,00	100,00	100,00
Turco 020	16,06	59,59	100,00	98,96	100,00	100,00
Protector®	96,96	100,00	100,00	100,00	100,00	100,00

Based on the geochemical and mineralogical analyses, the DE that used in this research contained varying amounts of diatoms. The DE's also contained common soil phases. Pinnate-type diatoms form was prevalent.

DISCUSSION AND CONCLUSIONS

Diatomaceous earth is very important as the only natural bio-rational pesticide of mineral origin in the world. Damage occurs to the insects' protective wax coat on the cuticle, mostly by sorption and to a lesser degree by abrasion, or both. The result is the loss of water from the insect's body through desiccation resulting in death [10]. The aim of this study was to investigate the effect of particle size on the insecticidal and behavioral efficiency of the native diatomaceous earth for controlling of adults of *A. obtectus*. When the results of the study were examined, it was determined that the diatomaceous earth having the lowest particle size had a high mortality effect on the studied insect. Because of the reduction of the particle size, it is thought that the applied DE may be caused by the greater attachment of the insect body due to the widening of the surface area. [12], reported that the particle size distributions of diatomaceous earth particles also play an important role in the insecticidal activity of diatomaceous earth. Similarly, [13] showed that the particle size of the diatomaceous earth on the insecticidal efficacy is not an important parameter but strongly effective on the mortality. In another study conducted with inert powders such as zeolite and diatomaceous earth, contact activity of particle size against pests was investigated. In terms of zeolite, there was no significant correlation between particle size and mortality, while the same was found to be significant for DE. In this bioassay, the differences between particle size and particle size distribution in terms of insect mortality was clearly seen in the same diatomaceous earth. The inert dust, which are the subjects of economic entomology studies, have the potential to be the promising plant protection product especially against the stored product pests. Morphological differences between species are another factor affecting the activity of DE. According to [14], some insects have greater sensitivity to DE because of their anatomy and physiology. Generally, insects with a large surface area in relation to the volume of their body are more sensitive in that they lose relatively greater amounts of water from their body. Insects with a rough or hairy body surface collect more particles per unit of the area causing greater cuticle damage. Therefore, such insects are more sensitive to DE than others. Similarly, the number and location of the setae in the unit area varies in the body of the test insect in this study. Due to these morphological changes, differences were found in the mortality, especially in terms of particle size. Varying DE doses are used for the control of different insect species. These include the volume of the surface area, the state of hair growth in the body, the thickness of the cuticle layer, the biological period of the insect and insect behavior [15, 16, 17]. Turco020 is thought to be retained by bristles before it reaches the cuticle because the particle size in Turco 020 is relatively large compared to the other two formulations. As a result, the turco 020 is not able to fulfill its abrasive effect on the insect cuticle and it is thought to cause slowdown in insect death.

The effect of physiological age on the mortality of insects is important. [18] stated that, when conducting studies on the efficacy of diatomaceous earth on the insects, researchers should standardize the age of the insect in terms of reducing variability. [19] revealed that adult lifespan of the bean weevil adults 7-14 days. For this purpose, age limitation was used to obtain safety data in diatomaceous earth studies so that mixed sex adults were chosen randomly to avoid possible differences between genders.

The results of this study suggest that diatomaceous earth obtained from local sources can be used in the storage of bean weevil in storage conditions.

ACKNOWLEDGEMENTS

Author(s) would like to thank Beg-Tuğ Mineral for providing financial support and the diatomaceous earth. We also like to knowledge Dr. Ebru KAVUKÇU, MTA Mineralogy and Petrography division director for SEM and geochemical analyses.

REFERENCES

[1] Milanovic, D., Aleksic, I., Tucic, N. (1991) Nonrandom association between host choice and fitness in bean weevil (*Acanthoscelides obtectus*). Zool Syst Evolut-forsch. 29, 108-114.

[2] Alvarez, N., Hossaert-McKey, M., Rasplus, J.Y., McKey, D., Mercier, L., Soldati, L., Aebi, A., Shani, T., Benrey, B. (2005) Sibling species of bean bruchids: a morphological and phylogenetic study of *Acanthoscelides obtectus* Say and *Acanthoscelides obvelatus* Bridwell. Journal of Zoological Systematics and Evolutionary Research. 43, 29–37.

[3] Stathers, T.E., Denniff, M., Golob, P. (2004) The efficacy and persistence of diatomaceous earths admixed with commodity against four tropical stored product beetle pests. Journal of Stored Products Research. 40, 113-123.

[4] Jovanovic, Z., Kostic, M., Popovic, Z. (2007) Grain-protective properties of herbal extracts against the bean weevil *Acanthoscelides obtectus* Say. Industrial Crops and Products. 26, 100–104.
[5] Jumbo, L.O.V., Faroni, L.R., Oliveira, E.E., Pimentel, M.A., Silva, G.N. (2014) Potential use of clove and cinnamon essential oils to control the bean weevil, *Acanthoscelides obtectus* Say, in small storage units. Industrial Crops and Products. 56, 27-34.
[6] Berger, A., Degenkol, T., Vilcinskas, A., Schöller, M. (2017) Evaluating the combination of a parasitoid and a predator for biological control of seed beetles (Chrysomelidae: Bruchinae) in stored beans. Journal of Stored Products Research. 74, 22-26.
[7] Adarkwah, C., Obeng-Ofori, D., Ulrichs, C., Schöller, M. (2017) Insecticidal efficacy of botanical food by-products against selected stored-grain beetles by the combined action with modified diatomaceous earth. Journal of Plant Diseases and Protection. 124, 255-267.
[8] Arthur, F.H. (1996) Grain protectants: current status and prospects for the future. Journal of Stored Products Research. 32(4), 293-302.
[9] Howard, R.W., Blomquist, G.J. (2005) Ecological, behavioral, and biochemical aspects of insect hydrocarbons. Annual Review Entomology. 50, 371-393.
[10] Ebeling, W. (1971) Sorptive dust for pest control. Annual Review of Entomology. 16, 123-158.
[11] Rigaux, M., Haubruge, E., Fields, P.G. (2001) Mechanisms for tolerance to diatomaceous earth between strains of *Tribolium castaneum*. Entomologia Experimentalis Applicata. 101, 33–39.
[12] Korunic, Z. (1997) Rapid assessment of the insecticidal value of diatomaceous earths without conducting bioassays. Journal of Stored Products Research. 33, 219-229
[13] Vayias, B.J., Athanassiou, C.G., Korunic, Z., Rozman, V. (2009) Evaluation of natural diatomaceous earth deposits from south-eastern Europe for stored-grain protection: the effect of particle size. Pest Management. Science. 65, 1118-1123.
[14] Carlson S.D., Ball, H.J. (1962) Mode of action and insecticidal value of a diatomaceous earth as a grain protectant. Journal of Economic Entomology. 55, 964-970.
[15] Bartlett, B.R. (1951) The action of certain inert dust materials on parasitic Hymenoptera. Journal of Economic Entomology. 44, 891–896.
[16] Subramanyam, B., Madamanchi, N., Norwood, S. (1998) Effectiveness of Insecto applied to shelled maize against stored-product insect larvae. Journal of Economic Entomology. 91, 280–286.
[17] Mewis, I., Reichmuth, C. (1999) Diatomaceous earths against the Coleoptera granary weevil *Sitophilus granarius* (Curculionidae), the confused flour beetle *Tribolium confusum* (Tenebrionidae) and the mealworm *Tenebrio molitor* (Tenebrionidae). In: Zuxun, J., Quan, L., Yongsheng, L., Xianchang, T., Lianghua, G. (Eds.) Stored Product Protection. Proceedings of the Seventh International Working Conference on Stored Product Protection. Beijing, Vol. 1, 1998. Sichuan Publishing House of Science and Technology, Sichuan Province, P.R. China, 765–780.
[18] De Paula, M.C.Z., Flinn, P.M., Subramanyam, B.H., Lazzari, S.M.N. (2002) Effects of age and sex on mortality of *Tribolium castaneum* (Herbst) (Coleoptera: Tenebrionidae) exposed to Insecto-treated wheat. Journal of the Kansas Entomological Society. 75, 158-162.
[19] Sönmez, E., Güvenç, D., Gülel, A. (2016) The changes in the types and amounts of fatty acids of adult *Acanthoscelides obtectus* (Coleoptera: Bruchidae) in terms of age and sex. International Journal of Fauna and Biological Studies. 3(4), 90-96.

Received: **04.12.2018**
Accepted: **20.02.2019**

CORRESPONDING AUTHOR

Mustafa Alkan
Plant Protection Central Research Institute,
Deparment of Entomology,
Ankara – Turkey

e-mail: alkan0101@gmail.com

© by PSP Volume 28 – No. 4/2019 pages 2923-2926 Fresenius Environmental Bulletin

LEACHING OF SOIL SALINITY BY DRIP IRRIGATION METHOD IN GREENHOUSE CONDITIONS

Abdullah Sayici, Harun Kaman*

Akdeniz University, Faculty of Agriculture, Department of Agricultural Structures and Irrigation, 07058 Campus, Antalya, Turkey

ABSTRACT

In the study, the leaching activity of saline soils was investigated at 4 different levels. The mean values of initial soil salinity were: T1 (2 dS/m), T2 (3 dS/m), T3 (3.8 dS/m) and T4 (6 dS/m). At the end of the research, it was aimed to decrease the soil salinity to 0.7 dS/m. Leaching water was applied by the drip irrigation method. In order to demonstrate an effective leach-salinity relationship, the leaching was not done in one application. Leaching water was applied in equal amounts every day for 15 times. In order to determine the soil salinity values at each leaching, soil samples were taken from three replicates of different depths. After the soil samples taken for salinity measurement became air-dried, filters were leached from the mud extracts prepared in the laboratory conditions by a routine method. During the leaching process, leaching water was applied in different amounts to each treatment. According to the results obtained, the salt accumulation in T1, T2, T3 and T4 was generally reduced to the target salinity level (0.7 dS/m) at the end of the research. At the end of production season, it could be suggested in the light of the obtained data that the salt accumulation, which occurs in the soil, could be effectively leached by the drip irrigation method.

KEYWORDS:
Drainage, irrigation, salinity, leaching

INTRODUCTION

When the amount of soluble salts in the soil exceeds the limit value of growth and development of plants in agriculture, problems arise. As the salt content in the soil increases, the water intake of the plant is also limited accordingly. When the salt concentration is sufficient to reduce the usable water potential, the plant gets stressed, which is named as salt stress in agriculture [1]. Some applications can be used to reduce the harmful effects of salinity in vegetable production. These applications mainly consist of the use of high-quality water, energy and careful soil management components. In this case, an effective soil leaching program becomes very important. As a result, leaching becomes a mandatory practice for a sustainable irrigated agriculture to prevent the accumulation of soluble salts in the plant root zone. However, in most areas, irrigation can be at undesirable levels resulting from inadequate irrigation practices. Leaching the salt from the plant root zone means increasing the salinity of the drainage water. For this reason, decreasing the leaching amount and increasing the irrigation efficiency means decreasing the salinity in the drainage water [2], even though it means an increase in the salt concentration in the lower parts of the plant root zone.

As known, irrigation water contains slightly soluble/dissolved materials. On the other hand, plant root zones also contain soluble substances from fertilizers used as plant nutrients. In general, as the temperature increases, the number of irrigation applications and the amount of irrigation water used also increase. As a result, although the quality of soil and irrigation water at the beginning of the season is good, salt accumulation takes place in the plant root zone at the end of the production season. This is one of the most important problems for agricultural producers. Producers are trying to solve this problem in two ways. The first one is to change the soil in the greenhouse. However, this is not a sustainable and economical solution. The second one is to carry out the leaching process for improvement purposes. There is an unconscious and excessive use of water in the improvement process of the soil. In this study, it is aimed to investigate the possibilities for the improvement of the greenhouse soil with different salinity levels by leaching with the use of drip irrigation method.

MATERIALS AND METHODS

This research was carried out at the Research and Application Land of the Faculty of Agriculture at Akdeniz University in Antalya. The soil layer in the study is about 45-50 cm deep. The soil type in the research area is in the Gölbaşı series. The Gölbaşı series, which developed on massive travertines, were included in the Entisol group due to their lack of profile development. All the profiles of this series of soils with AC horizon possess clay-tin textures. They are located in almost flat and nearly

flat topography [3]. Leaching water was supplied from the pumping system in the Research and Application Area. Leaching applications were done by drip irrigation method. Leaching water was applied with the drip irrigation system. The study was conducted on the values of the initial salinity of the leach which are T1 (2 dS/m), T2 (3 dS/m), T3 (3.8 dS/m) and T4 (6 dS/m). This study was carried out in 3 replicates in 12 parcels. The area of each parcel was 11 m^2. Solarisation nylon cover was used to cover the parcels. Thus, the surfaces of the leached parcels were closed to prevent the evaporation in the soil surface. The leaching water requirement for each treatment (T1, T2, T3 and T4) investigated in the study was calculated by the following equation proposed by Ayyıldız [4].

$$\frac{Dys}{Dt} = \frac{1}{\frac{5\times(ECe)s}{(ECe)\delta}} + 0.15$$

In the equation, Dys is the required leaching water (m); Dt is the soil depth to be leached (m); (ECe) is the electrical conductivity value (dS/m) of the saturate melt in the soil profile before leaching; and (ECe)s is the electrical conductivity value (dS/m) of the desired saturation melt in the soil profile after leaching.

It was aimed to decrease the salinity value of greenhouse soil to 0.7 dS/m at the end of the leaching application in the research. The calculated amount of leaching water was applied in 15 times. Thus, the relationship between the amount of leaching water in different quantities and the salinity reduction in the soil was revealed.

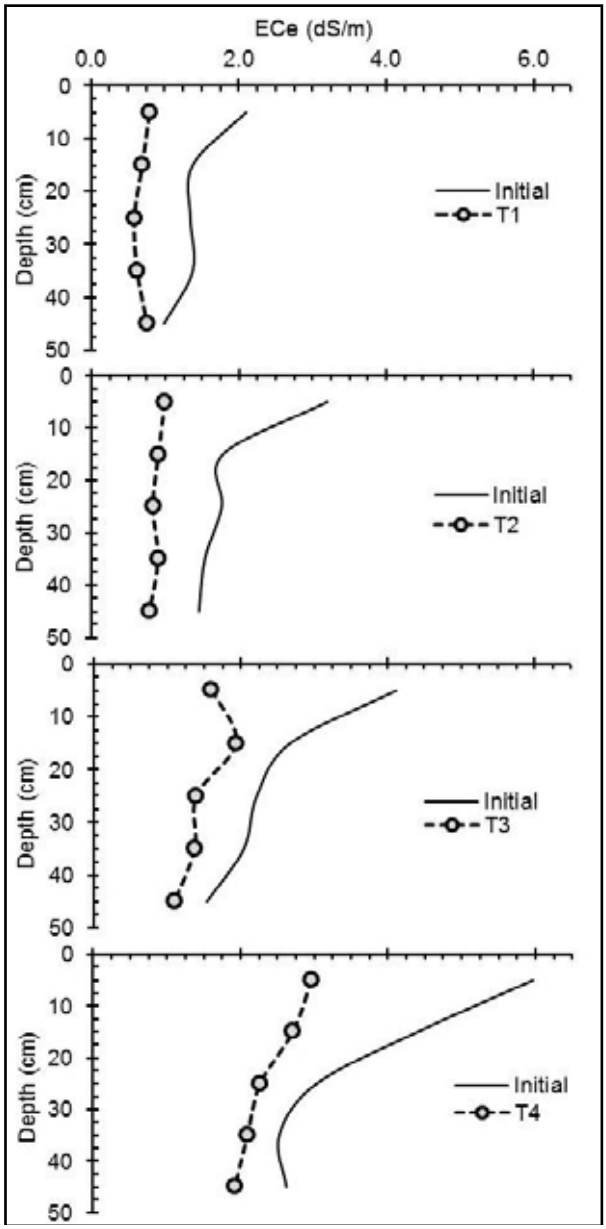

FIGURE 1
Soil salinity change in T1, T2, T3 and T4 after the first-day leaching.

RESULTS AND DISCUSSION

In the study, the leaching curves were made separately for fifteen days. As it will cover a lot of space, only the first and second leach curves are given in the paper. The change in the salinity at the end of the first leach of the T1, T2, T3 and T4 treatments is shown in Figure 1. The salinity changes in the T1, T2, T3 and T4 treatments at the end of the second leach is shown in Figure 2.

The soil salinity in T2 was 0.99 dS/m in the range of 0-10 cm, 0.90 dS/m in the range of 10-20 cm, 0.83 dS/m in the range of 20-30 cm, 0.89 dS/m in the range of 30-40 cm and 40-50 cm is 0.78 dS/m. Soil salinity in T3 was 1.93 dS/m in the range of 0-10 cm, 1.93 dS/m in the range of 10-20 cm, 1.39 dS/m in the range of 20-30 cm, 1.37 dS/m in the range of 30-40 cm and 1.10 dS/m in the range of 40-50 cm. The soil salinity of T4 was 2.71 dS/m in the range of 0-10 cm, 2.71 dS/m in the range of 10-20 cm, 2.26 dS/m in the range of 20-30 cm, 2.10 dS/m in the range of 30-40 cm and 1.92 dS/m in the range of 40-50 cm.

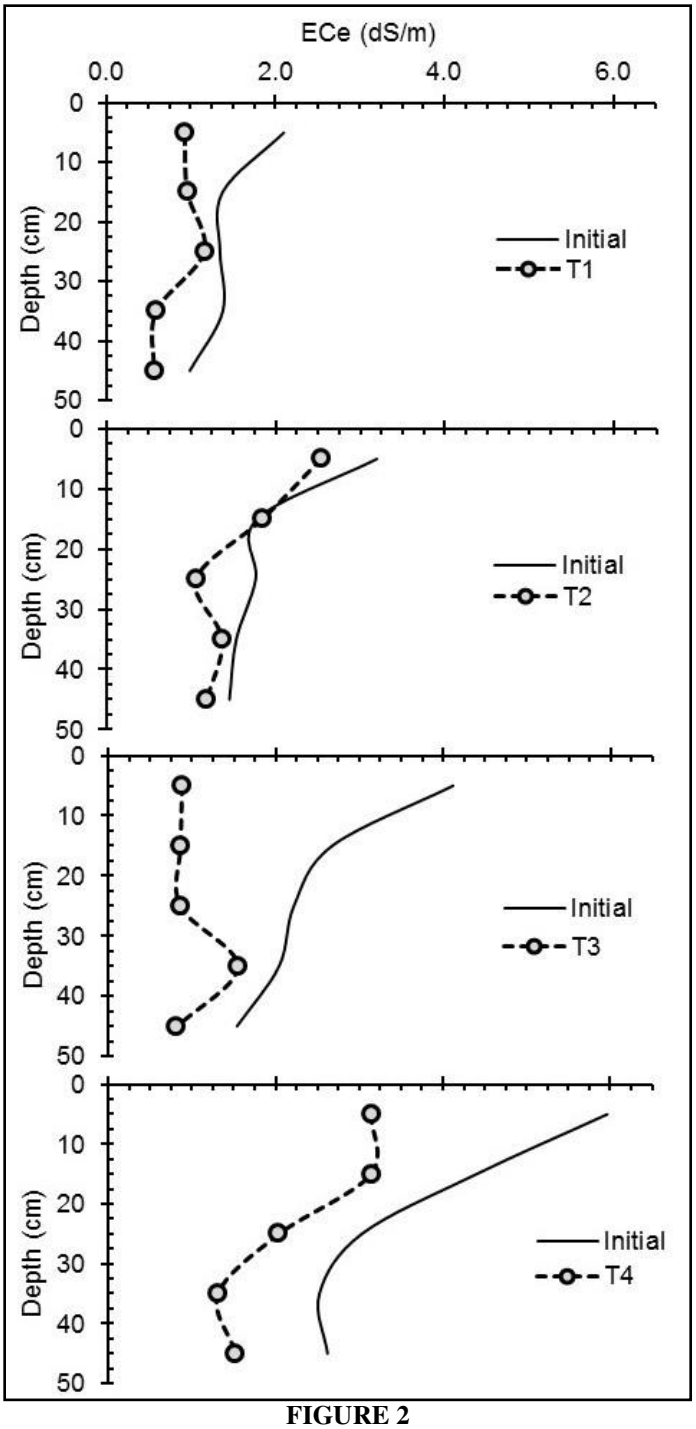

FIGURE 2
Soil salinity change in T1, T2, T3 and T4 after the leaching on the second day.

The soil salinity of T2 was 2.54 dS/m in the range of 0-10 cm, 1.85 dS/m in the range of 10-20 cm, 1.05 dS/m in the range of 20-30 cm, 1.36 dS/m in the range of 30-40 cm and 40-50 cm and 1.18 dS/m, respectively. Soil salinity in T3 was 0.88 dS/m at 0-10 cm, 0.86 dS/m at 10-20 cm, 0.85 dS/m at 20-30 cm, 1.54 dS/m at 30-40 cm and 0.82 dS/m at 40-50 cm. The soil salinity of T4 was 3.14 dS/m in the range of 0-10 cm, 3.14 dS/m in the range of 10-20 cm, 2.04 dS/m in the range of 20-30 cm, 1.30 dS/m in the range of 30-40 cm and 1.52 dS/m in the range of 40-50 cm. The leaching operations from the third day to the fifteenth day were similar to the first and second-day leachings.

Miyamoto et al. [5] conducted a study and found out that the quality of irrigation water is not a factor in salinity formation and the salinity problem takes place over time. In the study, salt accumulation in the soil was different as expected in the greenhouse soil salted with irrigation water at different salinity level. The importance of leaching is made clear in our study as Miyamoto et al. [5] did. According to Kovda [6], it is emphasized that seasonal saltiness coming from irrigation waters will cause salinity in the soil and soil leaching must be applied. Like Kovda [6], we have once again demonstrated the importance of leaching at the end of the season with this study. In addition, we carried out the leaching operation by drip irrigation method and investigated the leaching efficiency by drip irrigation method. Looking at the results obtained at the end of the season without any need for another system, plants should be leached in the field, and drip irrigation should be used with the amount of calculated water.

CONCLUSION

In this study, it was aimed to leach salt minerals in the soil with four different salinity levels by leaching the soil. It was aimed to determine the most effective leaching facilities with the least amount of leaching water in the study. Besides, it was also aimed to determine the usability of the drip irrigation system in the leaching process without extra cost at the end of the production season. Producers will be able to prevent the salinization problem in the greenhouse soil if they apply the method we have investigated in this study. Thus, leaching the salt in the soil will be possible with the use of a small amount of leaching water. As a result, with this study, it is suggested that the drip irrigation method could be used effectively in leaching soil salinity in greenhouse conditions.

ACKNOWLEDGEMENTS

This study was supported by the Research Fund of Akdeniz University. Project Number: FYL-2016-1816.

REFERENCES

[1] Levitt, J. (1980) Responses of plants to envirmental stres induced responses in cucumber plants. J.Plant Physiol. 150, 206-211.
[2] Oster, J.D. and Rhoades, J.D. (1978) Calculated drainage water compositions and salt burdens resulting from irrigation with river waters in the Western United States. J. of Environmental Quality. 4, 73-79.
[3] Sarı, M., Aksoy, T., Köseoğlu, T., Kaplan, M., Kılıç, Ş. and Pilanalı, N. (1993) Detailed soil survey of the settlement area of Akdeniz University and ideal land use planning. Akdeniz University Publications, Antalya, 145p. (in Turkish).
[4] Ayyıldız, M. (1983) Irrigation water quality and salinity problems in irrigation. AU Faculty of Agriculture Publications. No.879, Ankara. (in Turkish).
[5] Miyamoto, S., Riley, T., Gobran, G. and Petticrew, J. (1986) Effect of saline water ırrigation on soil salinity, pecan tree growth and nut production. Irrigation Science. 7, 83-95.
[6] Kovda, V.A. (1978) Arid land irrigation and soil fertility. Problems of salinity, alkalinity, compaction. In arid land ırrigation in developing countries environmental problems and effects. Edited By E. B. Worthington, Pergamon Pres, Oxford, England.

Received: **07.12.2018**
Accepted: **28.02.2019**

CORRESPONDING AUTHOR

Harun Kaman
Akdeniz University,
Faculty of Agriculture,
Department of Agricultural Structures and Irrigation,
07058 Campus, Antalya – Turkey

e-mail: hkaman@akdeniz.edu.tr

© by PSP Volume 28 – No. 4/2019 pages 2927-2936 Fresenius Environmental Bulletin

GENETIC DIVERSITY IN PAKISTANI SOYBEAN GENOTYPES AND NORTH AMERICAN ANCESTRAL LINES USING AGROMORPHOLOGICAL AND RAPD MARKERS

Masood Jan[1], Mohammad Nisar[2], Mohammad Ihsan[2], Farhatullah[1], Gul Jan[3], Fatih Hanci[4,*]

[1]Department of Plant Breeding and Genetics, Khyber Pakhtunkhwa Agricultural University Peshawa, Pakistan
[2]Department of Botany, University of Malakand, KPK Pakistan
[3]Departmentt of Botany, Abdul Wali Khan University Mardan, Pakistan
[4]Faculty of Agriculture, Erciyes University, Kayseri, Turkey

ABSTRACT

In this study, 47 landraces, 16 genotypes from NARC collection and 18 ancestral lines of US germplasm, in total 81 Soybean [*Glycine max* (L.) Merr] genotypes were assessed, to molecular and morphological characterization. The genetic diversity was evaluated with 20 Random Amplified Polymorphic DNA (RAPD) markers and 7 morphological characters. Chi-square test for homogeneity showed significant variability for all investigated characters. Only six RAPD primers were polymorphic that showed polymorphism in 29 out of 81 genotypes. The remaining primers were excluded from the molecular study. Pair-wise dissimilarity matrix for each primer followed by an average was calculated using bivariate data set generated from all loci of the primers. A total of 474 loci were detected with an average of 79 loci for each primer and 16.32 loci were amplified genotype. Cluster analysis showed that genetic diversity exists among all three groups (land races, collection from NARC and US ancestral). High level of genetic polymorphism was observed based on the six RAPD markers. A dendrogram was constructed using Unweighted Pair Groups of Arithmetic Means, which distinguished the genotypes into four major groups. Group-IA comprised eleven land races, two US genotypes and four NARC genotypes. Group IB comprised of eight US genotypes. Group-IIA comprised of one US genotypes and one land races genotype. Group-IIB comprised of one US genotype and one NARC genotype. Based on molecular study soybean genotypes code 8-7 (land races) and U14 (US genotype; Ralsoy) showed maximum genetic distance. This information can be utilized for genetic analysis, genotype identification from different sources and development of improved germplasm.

KEYWORDS:
Genetic diversity, Soybean, Morphology, RAPD.

INTRODUCTION

Soybean [*Glycine max* (L.) Merr] is one of the major sources of edible vegetable oils and of high protein feed supplements for livestock in the world. A native of Asia, the soybean was introduced to the rest of the world where it became a major crop in countries like USA [1]. Relatively, a few countries produce soybean thus giving them significant economic power in the world oilseed trade. Soybean oil accounts for 20 to 25% of total world fats and oil production. Soybean meal is a major protein component in livestock feed [2]. In Pakistan, improved lines of soybean were introduced from the USA in the early 1960s and its commercial cultivation was reported in early 70s. Since then its cultivation had been very unstable and fluctuating in the country. Soybean cultivation went as high as 6613 hectares in 1994-95 and declined to 373 hectares in 2005-06. Its cultivation never attained a peak of ten thousand hectares [3]. In the Oilseeds Development Strategy [4] a very intensive and extensive study has been conducted by foreign and local scientists. It was revealed that soybean becomes somewhat popular in Khyber Pakhtunkhwa, but never picked up appreciable area in Panjab, Sindh, and Baluchistan. According to MINFAL (2008-2009), soybean was grown on an area of 51 hectares with the total production of 31 tons in Pakistan.

Genetic variation among traits is important for breeding and in selecting desirable types. Knowledge of diversity patterns allows breeders to understand the evolutionary relationships in a better way among accessions and to sample germplasm in a more systematic fashion for the development of improved strategies for incorporation of useful diversity in their breeding programs [5]. Various methods such as morphological traits, total seeds protein, and molecular markers are used for the assessment of genetic variation in crops. Molecular markers are used from the last several years to make genetic maps, assessment of genetic variation and the location of interest genes in significant crops for the wanted characters [6]. Randomly amplified polymorphic DNA sequences or RAPD

markers are based on the amplification of unknown DNA sequences using single, short and random oligonucleotide primers [7]. RAPD markers have often been used for studying genetic diversity within plant genotype collections. These markers have been proposed by several groups as efficient tools for identification of DNA markers associated with agronomically important traits. A number of molecular markers including Restriction Fragment Length Polymorphism (RFLP), Randomly Amplified Polymorphic DNA (RAPD), Amplified Fragment Length Polymorphism (AFLP) and Simple Sequence Repeat (SSR) have been developed for this purpose [8]. In this study, we used 20 different RAPD markers along with seven morphological traits for the analysis of genetic diversity in soybean germplasm.

MATERIALS AND METHODS

The present study was carried out on three groups of soybeans. The research material comprised of 47 land races, 16 improved lines and 18 imported ancestral lines of US germplasm. The land races were collected from different locations of Khyber Pakhtunkhwa (Marghuz, Mizrina and Tindo) of District Sadda, central Kurram Agency. The improved lines were provided by gene bank of Plant Genetic Resource Institute (PGRI) of National Agricultural Research Center (NARC) Islamabad. The US ancestral lines were imported from the USDA (United States Department of Agriculture). These lines are the parental lines of US soybean germplasm. Information regarding all the genotypes are given in Table 1-3. After germination young seedlings were transferred to pots and were kept at green house Institute of Biotechnology and Genetic Engineering (IBGE) KP Agricultural University Peshawar in 2009 and were used for morphological and molecular characterization. Two types of experiments were conducted, in the first experiment we studied the qualitative characterization of soybean e.g. Seed shape, seed color, leaf color, leaf structure, flower color, flower position and plant structure. In the second experiment, these lines were used for molecular diagnosis through molecular markers using RAPD primers. For statistical analysis, data regarding morphological markers were analyzed to check out homogeneity. Chi-square test was applied to know whether two or more sample came from the same population or different population [9].

TABLE 1
List of Soybean genotypes collected from various sources/ locations of Khyber Pakhtunkhwa.

S. No	Genotype Code	Area of collection	S. No	Genotype Code	Area of collection
1	1-1	Tindo*	25	8-7	Marghuz
2	1-2	Tindo	26	8-8	Marghuz
3	3	Tindo	27	8-9	Marghuz
4	4-1	Tindo	28	8-10	Marghuz
5	4-2	Tindo	29	8-12	Marghuz
6	5-1	Tindo	30	8-15	Marghuz
7	6-2	Tindo	31	8-16	Marghuz
8	6-3	Tindo	32	8-17	Marghuz
9	6-4	Tindo	33	8-19	Marghuz
10	6-5	Tindo	34	13	Mizrina
11	6-6	Tindo	35	13-3	Mizrina
12	6-7	Tindo	36	15-1	Mizrina
13	6-8	Tindo	37	15-2	Mizrina
14	6-9	Tindo	38	16-1	Mizrina
15	6-10	Tindo	39	16-2	Mizrina
16	6-11	Tindo	40	16-3	Mizrina
17	6-12	Tindo	41	17	Tindo
18	6-13	Tindo	42	17-1	Tindo
19	6-14	Tindo	43	17-2	Tindo
20	7	Mizrina*	44	18-1	Tindo
21	8-3	Mizrina	45	F (3-1)	Tindo
22	8-4	Mizrina	46	F (4-1)	Tindo
23	8-5	Marghuz*	47	F (8-4)	Tindo
24	8-6	Marghuz			

* District Sadda, central Kurram Agency of Khyber Pakhtunkhwa

TABLE 2
List of US ancestral lines provided by USDA (United States Department of Agriculture)

S. No	Genotype Code	Name	S. No	Genotype Code	Name
1	U1	AK Harrow	10	U10	Mandarin
2	U2	Arksoy	11	U11	Mukden
3	U3	Capital	12	U12	Ogden
4	U4	Dunfield	13	U13	Perry
5	U5	Haberlandt	14	U14	Ralsoy
6	U6	Illini	15	U15	Richland
7	U7	Jackson	16	U16	S 100
8	U8	Korean	17	U17	CNS
9	U9	Lincoln	18	U18	Roanoke

TABLE 3
List of germplasm provided by gene bank of Plant Genetic Resource Institute (PGRI) of National Agricultural Research Center (NARC) Islamabad

S. No	Genotype Code	S. No	Genotype Code
1	003303	9	003772
2	003755	10	003773
3	003757	11	003774
4	003763	12	003778
5	003765	13	003780
6	003766	14	003781
7	003767	15	003782
8	003768	16	017452

TABLE 4
The sequence information and amplification conditions of the RAPD primers (10 bp) used to characterize soybean genotypes

S. #	Primer	Sequence	Molecular Weight (MW)	Melting temperature	% GC
1	GL* Decamer D-16	GGGGTGACGA	3133	33.60C	60
2	GL Decamer D-18	GGCCTGAGTA	3135	33.60C	60
3	GL Decamer D-20	GTTGCGATCC	3229	29.50C	60
4	GL Decamer D-21	GCTGTGAGGC	3289	29.50C	60
5	GL Decamer D-25	GTTACGAACC	3198	29.50C	60
6	GL Decamer D-28	GGCCGTGTGA	3198	33.60C	60
7	GL Decamer D-31	GGGATTATCC	3135	29.50C	60
8	GL Decamer C-08	GAGGACACTC	3039	29.50C	60
9	GL Decamer C-09	GAACGGACTC	3037	29.50C	60
10	GL Decamer C-10	GAATTAGGTC	3031	29.50C	60
11	GL Decamer C-13	GAACGGACTC	3321	29.50C	60
12	GL Decamer G-02	AGCGTCGATG	3318	29.50C	60
13	GL Decamer G-03	AGCGTGTCTG	3059	29.50C	60
14	GL Decamer G-05	TCGGATCCAC	2856	29.5	70
15	GL Decamer G-08	AGCCCGACTG	3021	29.50C	50
16	GL Decamer G-09	TCACGTCCAC	2942	29.5	70
17	GL Decamer G-17	TGGCGTCCAC	2952	29.5	70
18	GL Decamer G-20	CTCTCCGCCA	2924	33.60C	70
19	GL Decamer G-22	AGGGCCGCCA	2942	33.60C	60
20	GL Decamer G-27	ATCGGCGCGA	2949	33.60C	60

*GL= Genelink Technology USA

DNA Extraction and Polymerase Chain Reaction (PCR). Genomic DNA was extracted from plants according to the method of Weining and Langridge (19919 [10]. The PCR was carried out in a 25 µL volume of a master mixture according to the method of Devos and Gale (1992) [11]. PCR amplification was performed with initial denaturation at 94ºC for 4 min, followed by 40 cycles each consisting of a denaturation at 94ºC for 1 min, annealing step of 1 min at 30ºC and extension at 72ºC for 1 min. Last cycle was followed by 10 min extension at 72ºC. All reactions were performed with Gene Amp PCR system 2700 (Applied Biosystem) programmable thermocycler. The amplification products were then electrophoresed on 1% agarose/TBE (Tris Borate EDTA) gel and visualized by staining with ethidium bromide under ultraviolet (uv) light and photographed using gel documentation system "Uvitee". Twenty RAPD primers were used for molecular evaluation. The sequences information of the primers is shown in Table 4.

Statistical analysis. For statistical analysis, every scorable band was considered as a single locus/allele. The loci were scored as present (1) or absent (0). Bi-variate 1-0 matrix was generated. Genetic distances were calculated using "Unweighted Pair Group of Arithmetic Means" (UPGMA) procedure as described by [12]. The following formula was used for genetic distance determination.

GD=1-dxy/dx+dy-dxy. Where GD= Genetic distance between two genotypes.
dxy = total number of common loci (bands) in two genotypes.
dx = total number of loci (bands) in genotype 1.
dy = total numbers of loci (bands) in genotypes 2.

RESULTS AND DISCUSSION

The data obtained at the end of the morphological characterization, were subjected to Chi-square test for homogeneity. Chi-square test showed 3.84 ($P \leq 0.05$) and 6.63 ($P \leq 0.01$) level of probability at 1 degree of freedom and 5.99 ($P \leq 0.05$) and 9.21 ($P \leq 0.01$) level of probability at 2 degree of freedom. Among the studied traits, seed shape was less variable compared to others. 45 (95.74%) of the genotypes had round shape seeds while only 2 (4.26%) of them were wrinkled seed. Our results are supported by the finding of Chowdhury et al. (2002), who reported 48 soybean genotypes, seed shape of 41 (85.42%) was round and 4 (8.33%) were wrinkled [13]. They further concluded that the soybean germplasm was less variable in seed shape. The tabulated X^2_S for three groups (Landraces, US and Improved) is 3.84 and 6.63 at 5% and 1% levels of probability respectively, which is smaller than the corresponding calculated X^2_S value (39.34) at both 5% and 1% levels of probability. These results indicated that seed shape (round or wrinkled) is not equally distributed in among these groups. Different types of seed color were observed in the studied germplasm. A high genetic variability was noted in genotypes that had yellow, green and black seeds, 42 (51.85%), 16 (19.75%), 23 (28.39%) respectively, as shown in Table 5. Among the different collections, all the improved lines collected from NARC and most of the US ancestral lines had yellow seeds. Only one soybean genotype from the US ancestral lines was identified that had green seeds. However, high genetic variability was found in the genotypes collected from Khyber Pakhtunkhwa. Unlike the Collection from NARC and US ancestral lines, genotypes with black seeds were the most dominant in the land races collection. These results indicate that seed color (yellow, green and black) is equally distributed in land races but not equally distributed in US ancestral lines. Among the different collections, higher genetic variability was noted in the land races genotypes and Collection from NARC in which 31 and 9 genotypes had yellow leaves and xyz genotypes had green leaves. On the other hand, US ancestral lines had more genotypes with yellow than green leaves. Our observations are in agreement with the findings of Mehetre et al., (1994), who reported 42 soybean genotypes, among them xyz were yellow and had green leaves and they also reported that the soybean germplasm are more variable in leaf color [15]. The tabulated X^2_S for three groups (Landraces, US and Improved) is 3.84 and 6.63 at 5% and 1% levels of probability respectively, which is smaller than corresponding calculated X^2_S value (13.03) at both 5% and 1% levels of probability. These results showed that leaf color (yellow green and green) is not equally distributed in land races at 5% level of probability but equally distributed at 1% level of probability. In improved lines there were equal distribution of flower color at 5% and 1% levels of probability. Twelve genotypes from Khyber Pakhtunkhwa and two from US ancestral lines had broad leaves. Our results are supported by the finding of Dong et al., (2001) who studied 6,172 accessions of annual wild soybean collected from 25 provinces in China and reported that leaf shape had the highest variation among the eight qualitative traits [16]. The tabulated X^2_S for three groups (Landraces, US and Improved) is 3.84 and 6.63 at 5% and 1% levels of probability respectively, which is smaller than corresponding calculated X^2_S value (22.37) at both 5% and 1% levels of probability. These results indicated that leaf shape narrow and broad is not equally distributed in land races and US ancestral lines, but equally distributed in improved lines. The US ancestral lines on the other hand, had more genotypes with white (12; 66.66%) than purple flower. Our results are supported by the finding of Faisal et al., (2011), who reported high genetic variability in 92 soybean genotypes with two types of flower color white and purple [14]. The tabulated X^2_S for three groups (Landraces, US and Improved) is 3.84 and 6.63 at 5% and 1% levels of probability respectively, which is smaller than corresponding calculated X^2_S value (22.44) at both 5% and 1% levels of probability. These results showed that flower color (White and Purple) is not equally distributed in land races, but equally distributed in US ancestral and improved lines. Two types of flower position were noted in the different genotypes; terminal and axillary, as shown in Table 9. Terminal was the dominant flower position found in 55 genotypes (67.90%) whereas 26 genotypes (32.10%) had flower on axillary position. Among the different collections, higher genetic variability was noted in the land races genotypes and Collection from NARC in which 32 and 10 genotypes (68.08% and 62.50%) had terminal position and 15 and 6 genotypes (31.91% and 37.50%) had axillary position respectively. Our results are supported by the find-

ing of Karad et al. (2005), who studied 123 accessions of annual wild soybean and reported that flower position is more variable in soybean in the studied genotypes [17]. Dense genotypes were dominant in the collected from Khyber Pakhtunkhwa (29; 61.70%) and less dense genotypes were dominant in the US ancestral lines (16; 88.88%). Eighteen genotypes from Khyber Pakhtunkhwa (38.29%) had less dense and two from US ancestral lines (11.11%) had dense plant structure. Our result are in agreement with the findings of Faisal et al., (2011), who reported high genetic variability in 92 soybean genotypes with plant shape, among them 60 (65.22%) was erect, 13 (14.13%) was semi erect and 19 (20.65%) was spreading [14]. The tabulated X^2s for three groups (Landraces, US and Improved) is 3.84 and 6.63 at 5% and 1% levels of probability respectively, which is smaller than corresponding calculated X^2s value (14.79) at both 5% and 1% levels of probability. These results indicated that plant structure (less dense and dense) is equally distributed in land races and improved lines

Based on molecular data a dendrogram was constructed by using Molecular Evolutionary Genetics Analysis (MEGA-4) (Figure 1) which distinguished the genotypes into four major groups. Group-A, B, C and D. Group-A is comprised of 40 genotypes, having 17 land races genotypes 16 Group-B is comprised of four genotypes, one land races (16-10) and three from NARC (3303, 3755 and 3763). Group-C is comprised of six genotypes having two land races (6-4 and 17-2) and four from NARC (3773, 3774, 3782 and 17452). Polymerase chain reaction-based assays have been used to study the genetic polymorphism in various plant species such as rice, wheat, soybean. In recent time molecular markers are widely used to asses and evaluate genetic diversity of different crops [18]. A total of 20 RAPD primers (Table 4) were used but only six primers (Table 10) showed genetic polymorphism among 29 out of 81 soybean genotypes at the level of their genome (Table 11, 12 and 13). The remaining primers and *genotypes* were excluded from the study. The RAPD primers, obtained from Gene Link USA, were arbitrarily selected. Only scorable bands were included in the analysis. A total of 474 loci were detected by six RAPD primers, thus amplifying an average of 79 loci for each primer. Thus an average of 16.32 loci were amplified per genotype using six RAPD primers. The RAPD profiles were analyzed visually and finger prints were obtained which were reproducible within the particular genotype under similar conditions. The maximum numbers of 10 loci were amplified by the primer G-03 and C-09 and the minimum numbers of 3 loci were amplified by the primer D-16. None of the loci was monomorphic, while maximum polymorphism of 100% was observed in all genotype.

TABLE 5
Test of homogeneity table for seed color of 81 soybean genotypes.

	Yellow	Green	Black	Total	X2 cal
Land races	9 (19.14%)	15 (31.91%)	23 (48.93%)	47	1.54
US	17 (94.44%)	1 (5.55%)	0 (0%)	18	14.22
Improved	16 (100%)	0 (0%)	0 (0%)	16	--
Total	42 (51.85%)	16 (19.75%)	23 (28.39%)	81	31.4
X2S					15.76

X2tab values are 5.99 and 9.21 at 5% and 1% levels of probability respectively at 2 df.
X2tab values are 3.84 and 6.63 at 5% and 1% levels of probability respectively at 1 df.

TABLE 6
Test of homogeneity table for leaves color of 81 soybean genotypes.

	Yellow green	Green	Total	X2 cal
Land races	31 (65.95%)	16 (34.04%)	47	4.78
US	15 (83.33%)	3 (16.66%)	18	8.00
Improved	9 (56.25%)	7 (43.75%)	16	0.25
Total	55 (67.90%)	26 (32.10%)	81	10.38
X2S				13.03

X2tab values are 3.84 and 6.63 at 5% and 1% levels of probability respectively at 1 df.

TABLE 7
Chi-square table for leaf structure of 81 soybean genotypes.

	Narrow	Broad	Total	X2 cal
Land races	35 (74.46%)	12 (25.53%)	47	11.24
US	16 (88.88%)	2 (11.11%)	18	10.88
Improved	9 (56.25%)	7 (43.75%)	16	0.25
Total	60 (74.07%)	21 (25.92%)	81	18.78
X2S				22.37

X2tab values are 3.84 and 6.63 at 5% and 1% levels of probability respectively at 1 df.

TABLE 8
Test of homogeneity table for flower color of 81 soybean genotypes.

	White	Purple	Total	X2 cal
Land races	39 (82.98%)	8 (17.02%)	47	20.44
US	12 (66.66%)	6 (33.33%)	18	2.00
Improved	8 (50%)	8 (50%)	16	0
Total	59 (72.84%)	22 (27.16%)	81	9.79
X2S				22.44

X2tab values are 3.84 and 6.63 at 5% and 1% levels of probability respectively at 1 df.

TABLE 9
Test of homogeneity table for flower position of 81 soybean genotypes.

Flower position	Terminal	Axillary	Total	X2 cal
Land races	32 (68.08%)	15 (31.91%)	47	6.14
US	13 (72.22%)	5 (27.77%)	18	3.54
Improved	10 (62.50%)	6 (37.50%)	16	1.00
Total	55 (67.90%)	26 (32.10%)	81	10.38
X2S				10.68

X2tab values are 3.84 and 6.63 at 5% and 1% levels of probability respectively at 1 df.

TABLE 10
List of RAPD primers with number and size of the amplified alleles and polymorphism used in the PCR analysis

S. No	Primer name	Total Alleles	Size of allele	Percent polymorphism
1	GL Decamer D-20	9	250~3500	100
2	GL Decamer C-09	10	250~4000	100
3	GL Decamer G-09	7	250~2500	100
4	GL Decamer G-20	9	250~4000	100
5	GL Decamer D-16	3	1300~3000	100
6	GL Decamer G-03	10	250~4000	100

TABLE 11
12 land races soybean genotypes collected from different locations of Khyber Pakhtunkhwa (Marghuz, Mizrina and Tindo) for molecular analysis

S. No	Genotype code	Area of collection	S. No	Genotype code	Area of collection
1	6-4	Tindo*	7	7	Mizrina*
2	6-5	Tindo	8	8-7	Marghaz*
3	6-6	Tindo	9	8-12	Marghaz
4	6-8	Tindo	10	8-19	Marghaz
5	6-9	Tindo	11	18-1	Tindo
6	6-14	Tindo	12	F(8-4)	Mizrina

* District Sadda, central Kurram Agency of Khyber Pakhtunkhwa

TABLE 12
US ancestral lines provided by USDA (United States Department of Agriculture)

S. No	Genotype code	Name	S. No	Genotype code	Name
1	U1	AK Harrow	7	U10	Mandarin
2	U2	Arksoy	8	U13	Perry
3	U4	Dunfield	9	U14	Ralsoy
4	U6	Haberlandt	10	U15	Richland
5	U7	Jackson	11	U17	CNS
6	U8	Korean	12	U18	Roanoke

TABLE 13
Germplasm provided by gene bank of Plant Genetic Resource Institute (PGRI) of National Agricultural Research Center (NARC) Islamabad

S. No	Genotype code	S. No	Genotype code
1	003757	4	003782
2	003773	5	017452
3	003780		

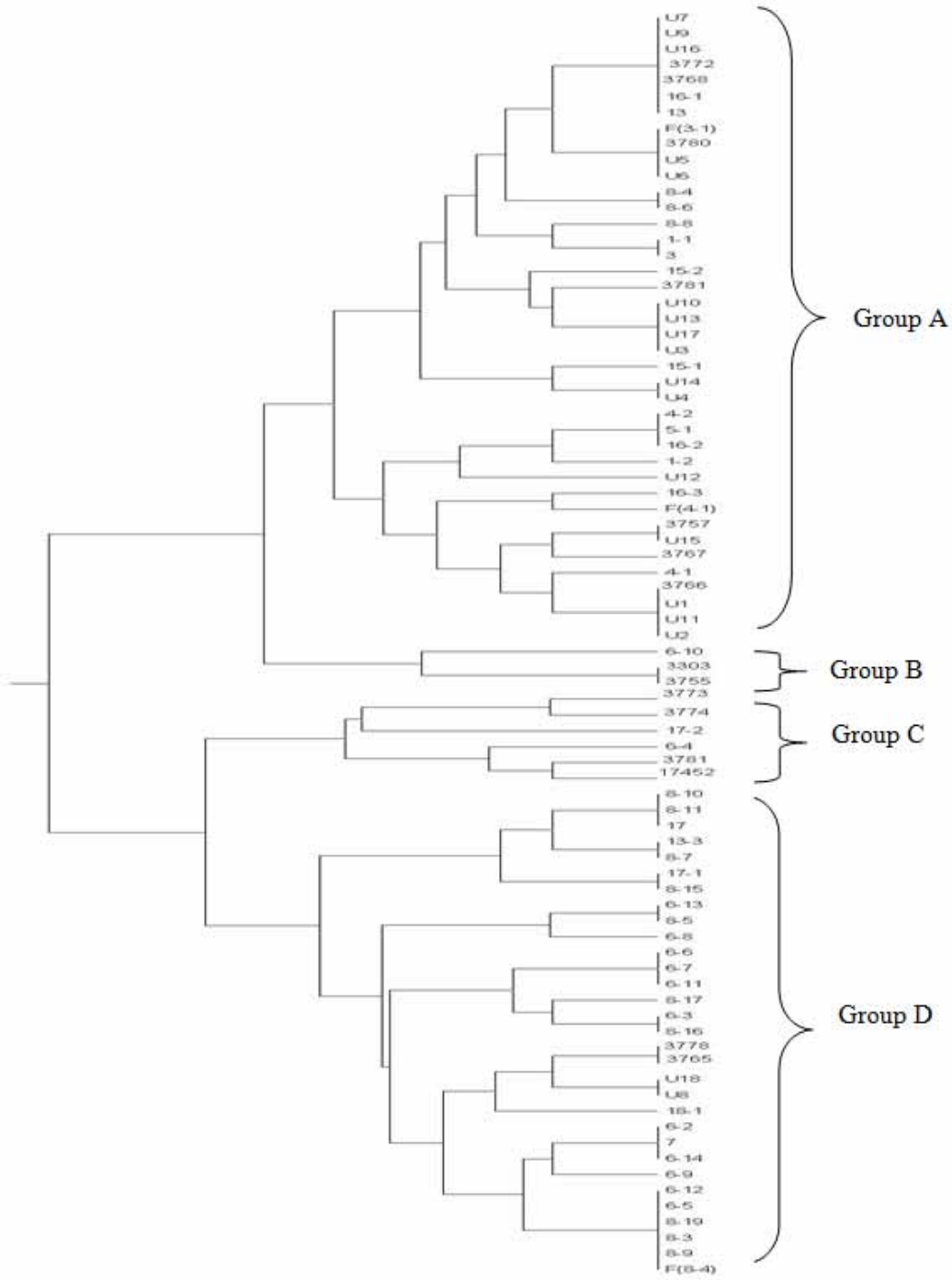

FIGURE 1
Dendrogram of all Soybean genotypes generated for qualitative characteristic using Molecular Evolutionary Genetics Analysis (MEGA-4)

In hordeum species these markers have made possible the characterization of different cultivars, the understanding of phylogenetic relationships, and genetic mapping [19, 20, 21, 22]. Both botanical and agronomic traits have limitations in the discrimination of soybean lines, and it is generally difficult to identify soybean cultivars on the basis of seed morphology [19]. Other markers such as isozymes, proteins and hordeins have been used successfully in the analysis and identification of lines [23, 24, 25]. Though isozymes are fast and easy to use but their relatively low number and level of variability limit their use in genetic diversity studies [26]. Furthermore molecular markers, such as RFLP, AFLP, STS and microsatellites, present the most powerful way to access genetic diversity, to undertake genetic mapping and to identify different lines [27]. It has been shown that different markers reveal different classes of variation [28]. RAPD which is a PCR based marker has the advantages of being readily used, requiring very small amount of genomic DNA. It does not need blotting and radio-

active detection [29]. DNA finger prints can be generated with Random Amplified polymorphic DNA (RAPD) by using short nucleotides of arbitrary sequence as primers [8].

Molecular analysis of the soybean genotypes using RAPD showed various levels of genetic polymorphism for the loci as detected by using all six primers. A total of 474 loci were detected by six RAPD primers, thus amplifying an average of 79 loci for each primer. Similarly, 16.32 loci were amplified per genotype using six RAPD primers. The RAPD profiles were analyzed visually, and finger prints were obtained which were reproducible within a particular genotype under similar conditions. The maximum numbers of 10 loci were amplified by the primer G-03 and C-09 and the minimum numbers of 3 loci were amplified by the primer D-16 (result reference). None of the loci was monomorphic. While maximum polymorphism of 100% was observed in all genotype. Genetic distance estimated for all the possible combinations ranged from 0 to 1. Maximum genetics distance (0.950) was observed in land races genotypes code 8-7 (Marghuz) and US genotypes name U14 (Ralsoy), followed by land races genotype (result reference) code 6-5 (Tindo) and 18-1 (Tindo), 6-8 (Tindo) and 8-19 (Marghuz) and 8-7 (Marghuz) and US genotypes U13 (Perry) (94.30%). Minimum genetic distance (0.186) was noted between one US genotypes name U1 (AK Harrow) and one NARC genotypes code 03773.

CONCLUSION

As one of the most important legume crops, a total of 81 soybean lines of Soybean was evaluated. There was a significant genetic diversity exists among all three groups (land races, collection from NARC and US ancestral). High level of genetic polymorphism was observed based on the six RAPD markers. UPGMA analysis distinguished the genotypes into four major groups. Group-IA comprised eleven land races, two US genotypes and four NARC genotypes. Group IB comprised of eight US genotypes. Group-IIA comprised of one US genotypes and one land races genotype. Group-IIB comprised of one US genotype and one NARC genotype. Based on molecular study soybean genotypes code 8-7 (land races) and U14 (US genotype; Ralsoy) showed maximum genetic distances. These studies are useful for genetic analysis, genotype identification and development of improved germplasm.

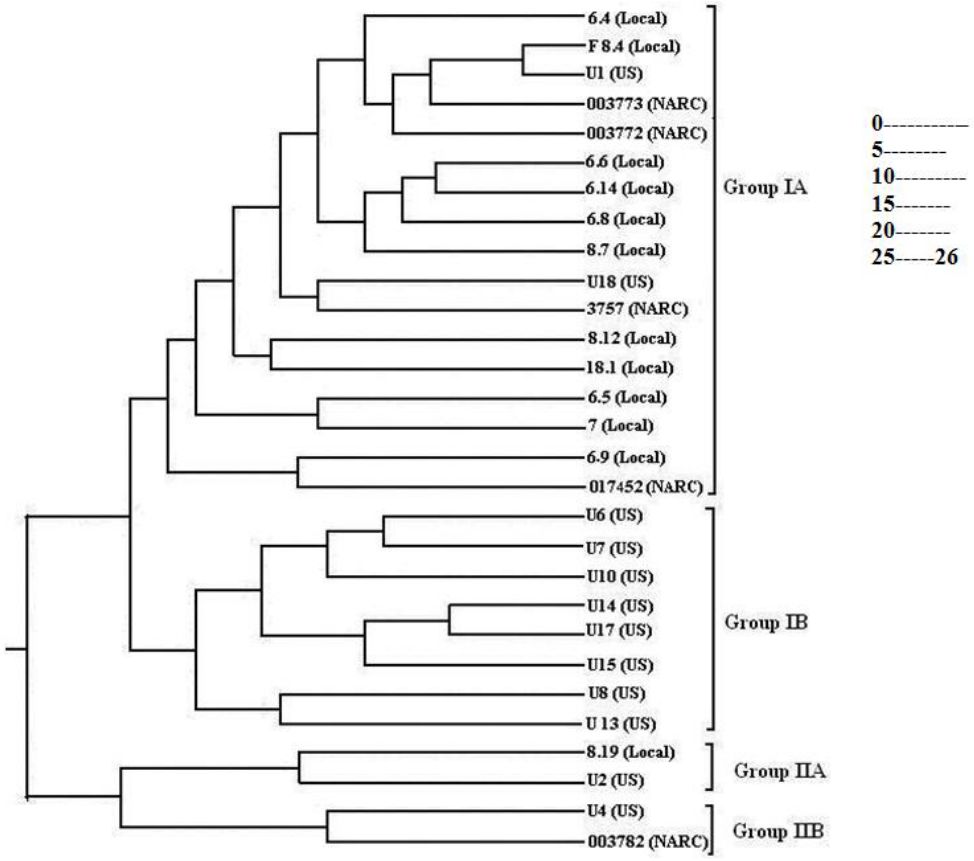

FIGURE 2
Dendrogram of all 29 Soybean genotypes, generated for polymorphic loci through six RAPD primers using unweighted pair group of arithmetic means (UPGMA).

REFERENCES

[1] Blackman, S.A., Obendorf, R.L and Leopold, A.C. (1992) Maturation Proteins and Sugars in Desiccation Tolerance of Developing Soybean Seeds. Plant Physiol. 100(1), 225–230.

[2] Sacks, F.M., Lichtenstein, A. and Winston, M. (2006) Soy protein, isoflavones, and cardiovascular health: an American Heart Association Science Advisory for professionals from the Nutrition Committee. Circulation. 113(7), 1034–44.

[3] MINFAL. (2006) Ministry of Food, Agriculture and Livestock, Government of Pakistan.

[4] MINFAL. (1995) Ministry of Food, Agriculture and Livestock, Government of Pakistan.

[5] Bretting, P.K., Widrlechner, M.P. (1995) Genetic markers and plant genetic resource management. Plant Breeding Reviews. 13, 11-87.

[6] Garcia, G.M., Stalker, H.T., Schroeder, E., Lyerly, J.H., Kochert, G. (2005) A RAPD-based linkage map of peanut based on a backcross population between the two diploid species Arachissteno sperma and A. cardenasii. Peanut Sci. 32, 1-8.

[7] Ovesna. J., Polakova, K. and Leisova, L. (2002) DNA Analyses and their Applications in Plant Breeding. Plant Breed. 1, 29-40.

[8] Williams, J.G.K., Kubelik, A.R., Livak, K.J., Rafalski, J.A., and Tingey, S.V. (1990) DNA polymorphisms amplified by arbitrary primers are useful as genetic markers. Nucleic Acids Res. 18, 6531-6535.

[9] Gomez, K.A. and Gomez, A.A. (1983) Chi-Squire test: In statistical procedure for Agricultural Research. 2nd Ed. A Wiley-Intersciences Publication, John Wiley and sons, New York. 464p.

[10] Weining, S. and Langrindge, P. (1991) Identification and mapping of polymorphism in cereals based on polymerase chain reaction. Theoretical and Applied Genetics. 82, 537-544.

[11] Devos, K. and Gale, M.D. (1992) The use of randomly amplified marker in wheat. Theor. Appl. Genet. 101, 107-118.

[12] Nei, M. and Li, W.H. (1979) Mathematical model for studying genetic variation in terms of restriction endonucleases. Proc. Natl. Acad. Sci. USA. 76, 5269-5273.

[13] Chowdhury, A.K., Srinives, P., Tongpamnak, P., Saksoong, P. and Chatwachirawong, P. (2002) Genetic Relationship among Exotic Soybean Introductions in Thailand: Consequence for Varietal Registration. Science Asia. 28, 227-239.

[14] Faisal, A.M., Ashraf, M., Qurashi, A. and Khan, M.R. (2011) Investigation and comparison of some morphological traits of the soybean populations using cluster analysis. Pak. J. Bot. 43(2), 1249-1255.

[15] Mehetre, S.S., Mahajan, C.R., Patil, P.A. and Hajare, D.N. (1994) Genetic divergence in soybean (*Glycine max* (L.) Merrill.). Indian J. Gen. Plant Breed. 54(1), 83-88.

[16] Dong, Y.S., Zhuang, B.C. and Zhao, L.M. (2001) The genetic diversity of annual wild soybeans grown in China. Theor Appl Genet. 103, 98–103.

[17] Karad, S.R., Harer, P.N., Kadam, D.D., Shinde, R.B. (2005) Genotypic and phenotypic variability in soybean (Glycine max (L.) Merrill). J. Maharashtra Agric. Univ. 30(3), 365-367.

[18] Baloch, F.S., Alsaleh, A., Saenz de Miera, L.S., Hatipoglu, R., Çiftçi, V., KarakVoy, T., Yıldız, M., Ozkan, H. (2015) DNA based iPBS-retrotransposon markers forinvestigating the population structure of pea (*Pisum sativum*) germplasm from Turkey. Biochem. Syst. Ecol. 61, 244e252.

[19] Hoffman, D.L. and Bregitzer, P. (1996) Identification of reproducible PCR-RAPD markers that enable the identification of closely related six-rowed malting barley (*Hordeum vulgare* L.) cultivars. Journal of American Society of Breeding Chemistry. 54, 172–176.

[20] Marillia, E.F., Scoles, G.J. (1996) The use of RAPD markers in *Hordeum* phylogeny Genome. 39, 646–654.

[21] Dahleen, L.S., Hoffman, D.L., Dohrmann, J., Gruber, R. and Franckowiak, J. (1997) Use of a subset of doubled-haploid lines for RAPD interval mapping in barley. Genome. 40, 626–632.

[22] Ordon, F., Schiemann, A., Friedt, W. (1997) Assessment of the genetic relatedness of barley accessions (*Hordeum vulgare* s.l.) resistant to soil-borne mosaic-inducing viruses (BaMMV, BaYMV, BaYMV-2) using RAPDs. Theor Appl Genet. 94, 325–330.

[23] Hoffman, D.L. and Goates, B.J. (1990) Polymorphism and genetic basis of -N-acetylglucosaminidase, hexokinase, and -D-galactosidase in barley (*Hordeum* spp.). Biochemical Genetics. 28, 487–493.

[24] Konishi, T. and Matsuura, S. (1991) Geographic differentiation in isozyme genotypes of Himalayan barley (*Hordeum vulgare*). Genome. 34, 704–709.

[25] Bernardo, A., Luque, A., Cuadrado, A., Negro, A., Jouve, N. and Soler, C. (1997) The assessment of genetic variation in Spanish primitive cultivars of barley, *Hordeum vulgare* L. by a combination of isozymes and hordeins. Genetic Research and Crop Evolution. 44, 217–226.

[26] Le Gouis, J., Erdogan, M., Friedt, W. and Ordon, F. (1995) Potential and limitations of isozymes for chromosomal localization of resistance genes against barley mild mosaic virus (BaMMV). Euphytica. 82, 25–30.

[27] Graner, A., Jahoor, A., Schondelmaier, J., Siedler, H., Pillen, K. and Fischbeck, G. (1991) Construction of an RFLP map of soybean. Theoretical and Applied Genetics. 83, 250-56.
[28] Russell, J.R., Fuller, J.D., Macaulay, M., Hatz, B.G., Jahoor, A., Powell, W., Waugh, R. (1997) Direct comparison of levels of genetic variation among barley accessions detected by RFLPs, AFLPs, SSRs and RAPDs. Theoretical and Applied Genetics. Genetika. 44(8),1084-1088.
[29] Cipriani, G., Dibella, R. and Testolin, R. (1996) Screening of RAPD primers for molecular taxonomy and cultivar finger printing in the genus, *Actinidia*. Euphytica. 90, 169-167.

Received: **14.12.2018**
Accepted: **21.02.2019**

CORRESPONDING AUTHOR

Fatih Hanci
Faculty of Agriculture, Erciyes University, Kayseri, Turkey

e-mail: fatihhanci@erciyes.edu.tr>

© by PSP Volume 28 – No. 4/2019 pages 2937-2941 Fresenius Environmental Bulletin

TRAPPING GENDERS OF *CERATITIS CAPITATA* (DIPTERA: TEPHRITIDAE) AND OTHER DIPTERAN WITH VARIOUS ATTRACTANTS ON POMEGRANATE FRUITS IN TURKEY

Nihat Demirel*

Hatay Mustafa Kemal University, Faculty of Agriculture, Department of Plant Protection, 31034 Hatay, Turkey

ABSTRACT

The Mediterranean fruit fly, *Ceratitis capitata* (Wiedemann) (Diptera: Tephritidae), is a serious pest on pomegranate fruits in Turkey. The study was conducted in 2013-2014 to catch genders of *Ceratitis capitata* (Diptera: Tephritidae) and other Dipteran with attractants on pomegranate fruits in Hatay province of Turkey. In both years, the transparent 500 ml polyethylene bottles with four holes were used as traps. After two-year of the study, the trapping male, female of *C. capitata* and other Dipteran with various attractants varied in each of the sampling year. In 2013, traps baited with the combination of ammonium acetate + ammonium carbonate had the highest mean of catches male, female and male + female on the 'Katırbaşı' pomegranate. In 2014, two studies were conducted at 'Hicaz' and 'Katırbaşı' pomegranate orchards. At the'Hicaz', traps baited with the combination of ammonium acetate + ammonium bicarbonate had the highest mean of male, while ammonium acetate + ammonium carbonate had the highest mean of female. In addition, traps baited with the combination of ammonium acetate + ammonium carbonate and ammonium acetate + ammonium bicarbonate had the highest mean of male + female. At the 'Katırbaşı', traps baited with a single of the diammonium phosphate and the combination of ammonium acetate + ammonium bicarbonate had the highest mean of male, female and male + female. Traps baited with the combination of ammonium acetate + yeast powder in 2013 and a single of ammonium bicarbonate in 2014 had the highest mean of other Dipteran species.

KEYWORDS:
Mediterranean fruit fly, attractants, pomegranate, Turkey

INTRODUCTION

Pomegranate, *Punica granatum* L. (Punicaceae: Myrtiflorae), is an important tropical and subtropical tree [1], widespread in Turkey where it comprises approximately 30.530 ha with a total produce of 465.200 tons of fruit per annum, and Hatay province's share is 1.288 ha and 20.430 tons [2]. The Mediterranean fruit fly (Medfly), *Ceratitis capitata* (Wiedemann) (Diptera: Tephritidae), is one of the most important fruit pests throughout the world [3, 4, 5, 6, 7, 8, 9, 10]. The Medfly is a polyphagous tropical fruit fly, which attacks more than three hundred and fifty botanical species [11]. The females puncture the fruits and lay eggs below the skin of the host fruits, which are destroyed by larval feeding [10, 12, 13, 14]. This pest caused significant damages on pomegranate fruits in Turkey [7, 10, 15]. Insecticidal protection from *C. capitata* is possible by using a cover spray or a bait spray [16]. Protein bait sprays mixed with organophosphates or low toxicity insecticides are successfully used as area-wide integrated pest management techniques to control *C. capitata* populations [17, 18]. The traps baited with trimedlure and attractants are important tools for detection, monitoring and controlling of the *C. capitata* on different host plants [5, 7, 10, 19, 20, 21, 22, 23]. Traps baited with lures are also continuously used to monitor and control population size and spread [10, 21, 22, 23, 24]. The purpose of the current study was to catch genders of the Mediterranean fruit fly, *C. capitata* (Wiedemann) and other Dipteran with various attractants on pomegranate fruits in Hatay province of Turkey.

MATERIALS AND METHODS

The study was conducted in 2013-2014 to catch genders of *C. capitata* and other Dipteran with various attractants on pomegranate fruits in Hatay province of Turkey. In the first year, the study was conducted in 'Katırbaşı' pomegranate from 24 October to 29 November 2013, and in the second year, 'Hicaz' and 'Katırbaşı' pomegranate orchards from 23 October to 27 November 2014. In the first year, a single and the combinations of two and three lures; ammonium acetate, ammonium carbonate, yeast powder (*Saccharomyces cerevisiae*, Dr. Oetker), were used as synthetic food-based lures (Table 1). The study was conducted as randomized complete block design with 6 treatments and 5 replications. In the second year, a single and the combinations of two and three lures;

ammonium acetate, ammonium carbonate, trimethylamine, ammonium bicarbonate, di-ammonium phosphate and cadaverine, were used as synthetic food-based lures (Table 1). The study was conducted as randomized complete block design with 7 treatments and 5 replications. In both years, the transparent 500 ml polyethylene bottles containing a 3-mm diameter four holes were used as traps. Each of the traps consisted of 300 ml one or mixed the lures, 2 ml of 10% propylene glycol to decrease water evaporation and 2 ml of 2% dichlorvos (DDVP), were hanged 1-1,30 m above ground on the pomegranate branches (1 trap per three tree). Traps were removed and brought to the laboratory and captured female and male of *C. capitata* and other Dipteran were counted. All data were analyzed by analysis of variance (ANOVA) with using the SAS software and means were separated by using the Least Significant Difference (LSD) Multiple Comparison Tests ($P < 0.05$) [25].

TABLE 1
Traps baited with attractants used at 'Katırbaşı' and 'Hicaz'pomegranate orchards in Antakya district of Hatay province in 2013-2014.

Treatments (attractants)	2013	2014
	Lures (gr)/trap[z]	Lures (gr)/trap[z]
Ammonium acetate	0.3	0.3
Ammonium carbonate	0.3	0.3
Ammonium bicarbonate	----	0.3
Diammonium phosphate	----	0.3
Ammonium acetate+ammonium carbonate	0.3+0.3	0.3+0.3
Ammonium acetate +ammonium bicarbonate	----	0.3+0.3
Ammonium acetate +yeast powder	0.3+0.6	----
Ammonium carbonate+yeast powder	0.3+0.6	----
Ammonium acetate+ammonium carbonate +yeast powder	0.3+0.3+0.6	----
Ammonium acetate+ trimethylamine +cadaverine	----	0.3+0.3+0.2

[z]Cadaverine used as (mg) and rest of the treatments used as (gr).

TABLE 2
Capture of the genders of *C. capitata* and other Dipteran, traps baited with attractants at 'Katırbaşı' pomegranate orchard in Antakya district of Hatay province in 2013.

Treatments (attractants)	Means of catches insects per five traps[z]			
	C. capitata (♂)	*C. capitata* (♀)	*C. capitata* (♂,♀)	Dipteran
Ammonium acetate	45.80b	59.40bc	105.20b	28.20c
Ammonium carbonate	57.20ab	74.40ab	131.60ab	29.80c
Ammonium acetate+ammonium carbonate	81.80a	111.20a	193.00a	46.20c
Ammonium acetate +yeast powder	10.80c	15.20d	26.00c	288.40a
Ammonium carbonate +yeast powder	27.60bc	42.20bcd	69.80bc	237.20ab
Ammonium acetate + ammonium carbonate + yeast powder	10.80c	21.40cd	32.20c	141.40bc

[z] Numbers within a column not followed by the same letter are significantly different ($P<0.05$) by LSD.

TABLE 3
Capture of the genders of *C. capitata* and other Dipteran, traps baited with attractants at 'Hicaz' pomegranate orchard in Antakya district of Hatay province in 2014.

Treatments (attractants)	Means of catches insects per five traps[z]			
	C. capitata (♂)	*C. capitata* (♀)	*C. capitata* (♂,♀)	Dipteran
Ammonium acetate	84.40ab	143.20bc	227.60b	53.00ab
Ammonium bicarbonate	98.00ab	189.00ab	287.00ab	81.60a
Ammonium carbonate	39.80c	85.20cd	125.00c	15.80b
Diammonium phosphate	80.60b	179.20ab	259.80ab	60.00ab
Ammonium acetate+ammonium carbonate	76.60b	233.40a	310.00a	45.60ab
Ammonium acetate +ammonium bicarbonate	108.80a	200.80ab	309.60a	23.80ab
Ammonium acetate+ trimethylamine +cadaverine	15.00c	23.40d	38.40d	3.60b

[z] Numbers within a column not followed by the same letter are significantly different ($P<0.05$) by LSD.

TABLE 4
Capture of the genders of *C. capitata* and other Dipteran, traps baited with attractants at 'Katırbaşı' pomegranate orchard in Antakya district of Hatay province in 2014.

Treatments (attractants)	Means of catches insects per five traps[z]			
	C. capitata (♂)	*C. capitata* (♀)	*C. capitata* (♂,♀)	Dipteran
Ammonium acetate	5.60c	16.20d	21.80d	14.60ab
Ammonium bicarbonate	41.20ab	89.80ab	131.00ab	40.40a
Ammonium carbonate	27.20bc	58.00bc	85.20bc	27.20ab
Diammonium phosphate	51.20a	111.80a	163.00a	7.20b
Ammonium acetate+ammonium carbonate	21.80bc	50.80bcd	72.60cd	12.20b
Ammonium acetate +ammonium bicarbonate	57.80a	105.00a	162.80a	13.60ab
Ammonium acetate+ trimethylamine +cadaverine	8.20c	21.20cd	29.40cd	3.40b

[z] Numbers within a column not followed by the same letter are significantly different (P<0.05) by LSD.

RESULTS AND DISCUSSION

The trapping the genders of *C. capitata* and other Dipteran with various attractants varied in each of the sampling year. In the first year, a total of 2,789 *C. capitata* adults (1619♀, 1170♂) and 3856 other Dipteran adults were caught by attractant traps at the 'Katırbaşı' pomegranate orchard (Table 2). The highest mean of male, female and male + female of *C. capitata* were caught by the combination of ammonium acetate + ammonium carbonate attractant traps (F=4,11, P= 0,0041; F=4,88, P= 0,0015; F=4,77, P= 0,0018, respectively). The highest mean of other Dipteran were caught by the combination of ammonium acetate + yeast powder attractant traps (F=3,62, P= 0,0080).

In the second year, two studies were conducted on 'Hicaz' and 'Katırbaşı' pomegranate. A total of 7,787 *C. capitata* adults (5271♀, 2516♂) and 1417 other Dipteran adults were caught by attractant traps at the 'Hicaz' pomegranate orchard (Table 3). The highest mean of male *C. capitata* was caught by the combination of ammonium acetate + ammonium bicarbonate attractant traps (F=7,66, P= 0,0001), while the female was caught by the combination of ammonium acetate + ammonium carbonate attractant traps (F=7,15, P= 0,0001). In addition, the highest mean of male + female were caught by the combination of ammonium acetate + ammonium carbonate and ammonium acetate + ammonium bicarbonate attractant traps (F=9,13, P= 0,0001). The highest mean of other Dipteran was caught by a single of ammonium bicarbonate attractant traps (F=1,47, P= 0,2095).

A total of 3,329 *C. capitata* adults (2264♀, 1065♂) and 593 other Dipteran adults were caught by attractant traps at the 'Katırbaşı' pomegranate orchard (Table 4). The highest mean of male, female and male + female of *C. capitata* were caught by a single of the di-ammonium phosphate and the combination of ammonium acetate + ammonium bicarbonate attractant traps (F=4,82, P= 0,0008; F=5,79, P= 0,0002; F=6,53, P= 0,0001, respectively). The highest mean of other Dipteran was caught by a single of the ammonium bicarbonate attractant traps (F=3,62, P= 0,0080).

The traps baited with protein-based baits and lures are used for the capture of male and female *C. capitata* [5, 20, 21, 26, 27]. Several commercial formulations of ammonia have been produced for use as lures in fruit fly traps including ammonium acetate (BioLure), ammonium bicarbonate (AgriSense Lure) and ammonium carbonate (ISCA technologies) [5]. In addition, several studies have been conducted to evaluate various attractants; a single of ammonium carbonate for female [28], the combination of ammonium acetate + putrescine [29]; ammonium acetate + trimethylamine + putrescine [24, 26, 30, 31, 32], ammonium acetate + trimethylamine + cadaverine; ammonium acetate + trimethylamine + cadaverine [21] were used for *C. capitata*. Moreover, the food-based baits of diammonium phosphate caught significant number of *C. capitata* [15, 33] and the high number of nontarget insects [15, 22]. Çalıklı [15] reported that the highest catch of Medfly was by the combination of the ammonium acetate + ammonium carbonate attractants with a ratio of 66.5% and the highest catch of other Diptera species was by the combination of the ammonium acetate + yeast powder with the ratio of 50.70 % on satsuma mandarin.

CONCLUSIONS

The present study was conducted to evaluate trapping of the genders of *C. capitata* and other Dipteran with various attractants on two different varieties of pomegranate in Hatay province of Turkey. As a result of two years of investigations, the trapping of the genders of *C. capitata* and other Dipteran varied in each of the sampling year. In 2013, the highest mean of male, female and male+female *C. capitata* on the 'Katırbaşı' pomegranate were observed with the combination of ammonium acetate + ammonium carbonate attractant traps. In 2014, the highest mean of male *C. capitata* on the 'Hicaz' pomegranate were observed with the combination of ammonium acetate + ammonium bicarbonate, while the female *C. capitata* were observed by the combination of ammonium acetate + ammonium carbonate attractant traps. In

addition, the highest mean of male + female *C. capitata* were observed with the combination of ammonium acetate + ammonium carbonate and ammonium acetate + ammonium bicarbonate attractant traps. The highest mean of male, female and male+female *C. capitata* on the 'Katırbaşı' pomegranate were observed with di-ammonium phosphate and ammonium acetate + ammonium bicarbonate attractant traps. The combination of ammonium acetate + yeast powder in 2013 and a single of ammonium bicarbonate in 2014 had the highest mean of other Dipteran species.

ACKNOWLEDGEMENTS

This project was supported by University of Mustafa Kemal of Scientific Research Projects (BAP). (The project number is 11965).

REFERENCES

[1] Morton (1987) Pomegranate. In: Morton, J.F. (ed.) Fruits of warm climates. Miami, Florida (USA). 352–355.

[2] Anonymous (2016). Turkish Statistical Institute.https://biruni.tuik.gov.tr/bitkiselapp/bitkisel.zul18.01.2019.

[3] White, I.M. and Elson-Harris, M. (1992) Fruit flies of economic importance: their identification and bionomics. CAB international, Wallingford, U.K. 601p.

[4] Demirel, N. (2007) Behavior paradigms in the Mediterranean fruit fly, Ceratitis capitata (Weidemann). Journal of Entomology. 4(2), 129-135.

[5] Shelly, T.E., Epsky, N., Jang, E.B., Reyes-Flores, J., and Vargas, R.I. (2014) Trapping and the Detection, Control, and Regulation of Tephritid Fruit Flies. Lures, Area-Wide Programs, and Trade Implications. 643p.

[6] Cocuzza, G.E.M., Mazzeo, G., Russo, A., Giudice, V.L., and Bella, S. (2016) Pomegranate arthropod pests and their management in the Mediterranean area. Phytoparasitica. 44, 393-409.

[7] Demirel, N. (2016) Population density and damage ratios of Mediterranean fruit fly, *Ceratitis capitata* (Wiedemann) (Diptera: Tephritidae) on pomegranate orchards in Turkey. Entomol. Appl. Sci. Letters. 3(5), 1-7.

[8] Demirel, N. and Akyol, E. (2017) Evaluation of mass trapping for control of Mediterranean fruit fly, Ceratitis capitata (Wiedemann) (Diptera: Tephritidae) in Satsuma mandarin in Hatay province of Turkey. International Journal of Environmental Agriculture Research. 3(12), 32-37.

[9] Kılıç, G., and Demirel, N. (2018) A population fluctuation and damage rates of Ceratitis capitata (Wiedemann) (Diptera: Tephritidae) on persimmon fruits in Turkey. Fresen. Environ. Bull. 27, 5072-5077.

[10] Demirel, N., Yıldırım, A.E., and Kılıç, G. (2018) Effectiveness of various attractants for Mediterranean Fruit Fly, Ceratitis capitata (Wiedemann) (Diptera: Tephritidae) on pomegranate fruits in Turkey. Fresen. Environ. Bull. 27, 3191-3198.

[11] Liquido, N.J, Shinoda, L.A., and Cunningham, R.T. (1991) Host Plants of the Mediterranean Fruit Fly (Diptera Tephritidae): An Annotated World Review. Entomological Society of America. Miscellaneous Publications, No. 77.

[12] Christenson, L.D., Foote, R.H. (1960) Biology of fruit flies. Ann. Review of Entomol. 5, 171-192.

[13] Thomas, M.C., Heppner, J.B., Woodruff, R.E., Weems, H.V., Steck, G.J., and Fasulo, T.R. (2010) Mediterranean Fruit Fly, *Ceratitis capitata* (Wiedemann) (Insecta: Diptera: Tephritidae). University of Florida, IFAS Extension. EENY-214.

[14] Braham, M. (2015) Insect larvae associated with dropped pomegranate fruits in an organic orchard in Tunisia. J. Entomol. and Nematol. 7, 5–10.

[15] Calikli, S. (2015) Use of various attractants for control of the Mediterranean Fruit Fly, *Ceratitis capitata* (Wiedemann) (Diptera: Tephritidae). Mustafa Kemal University, M.Sc. Thesis. 65p.

[16] Roessler, Y. and Chen, C. (1994) The Mediterranean fruit fly, *Ceratitis capitata*, a major pest of citrus in Israel, its regulation and control. Bulletin OEPP/EPPO Bulletin. 24, 813-816.

[17] Vargas, R.I., Peck, S.L., McQuate, G.T., Jackson, C.G., Stark, J.D., and Armstrong, J.W. (2001) Potential for areawide integrated management of Mediterranean fruit fly (Diptera: Tephritidae) with a braconid parasitoid and a novel bait spray. J. Econ. Entomol. 94, 817-825.

[18] Urbaneja, A., Chueca, P., Monton, H., Pascual-Ruiz, S., Dembilio, O., Vanaclocha, P., Abad-Moyano, R., Pina, T., and Castanera, P. (2009) Chemical alternatives to malathion for controlling *Ceratitis capitata* (Diptera: Tephritidae), and their side effects on natural enemies in Spanish citrus orchards. J. Econ. Entomol. 102, 144-151.

[19] Gilbert, J., and Bingham, R.R. (1999) Insect Trapping Guide. California Department of Food and Agriculture. MF 1–9.

[20] IAEA (International Atomic Energy Agency) (2003) Trapping guidelines for area-wide fruit fly programmes. Insect Pest Control Section, International Atomic Energy Agency, Vienna, Austria.
[21] Navarro, V., Alfaro, F., Dominguez, J., Sanchis, J. and Primo, J. (2008) Evaluation of traps and lures for mass trapping of Mediterranean fruit fly in citrus groves. J. Econ. Entomol. 101, 126–131.
[22] Boulahia Kheder, S., Jerraya, A., Fezzani, M. and Jrad, F. (2010). First results in Tunisia on the mass trapping an alternative way to control the Mediterranean fruit fly Ceratitis capitata (Diptera,Tephritidae). Annals of INRAT, Vol. 82, 168-180.
[23] Boulahia-Kheder, S., Salleh, W., Awadi, N., Fezzani, M. and Jrad, F. (2011) Efficiency of different traps and lures used in mass-trapping of the Mediterranean fruit fly *Ceratitis capitata* Wied. (Diptera: Tephritidae). Integrated control in Citrus fruit crops. IOBC/wprs Bulletin. 62, 215-219.
[24] Epsky, N.D., Hendrichs, J., Katsoyannos, B.I., Vasquez, L.A., Ros, J.P., Zumreoglu, A., Pereira, R., Bakri, A., Seewooruthun, S.I., and Heath, R.R. (1999) Field evaluation of female targeted trapping systems for Ceratitis capitata (Diptera: Tephritidae) in seven countries. J. Econ. Entomol. 92(1), 156–164.
[25] SAS Institute, (1998) User's Guide, version 6. SAS Institute, Cary, NC, USA.
[26] Heath, R.R., Epsky, N.D., Dueben, B.D., Rizzo, J. and Jeronimo, F. (1997) Adding methyl-substituted ammonia derivatives to food-based synthetic attractants on capture of the Mediterranean and Mexican fruit flies (Diptera: Tephritidae). J. Econ. Entomol. 90, 1584–1589.
[27] Gazit, Y., Rössler, Y., Epsky, N.D. and Heath, R.R. (1998) Trapping females of the Mediterranean fruit fly (Diptera: Tephritidae) in Israel: comparison of lures and trap type. J. Econ. Entomol. 91(6), 1355-1359.
[28] Reynolds, A.H. and Prokopy, R.J. (1997) Evaluation of odor lures for use with red sticky spheres to trap apple maggot (Diptera: Tephritidae). J. Econ. Entomol. 90, 1655-1660.
[29] Heath, R.R., Epsky, N.D., Guzmán, A., Dueben, B.D., Manukian, A., and Meyer, W.L. (1995) Development of a dry plastic insect trap with food-based synthetic attractant for the Mediterranean fruit fly and Mexican fruit fly (Diptera: Tephritidae). J. Econ. Entomol. 88, 1307-1315.
[30] Katsoyannos, B.I., Heat, R.R., Papadopoulus, N.T., Epsky, N.D. and Hendrichs, J. (1999) Field evaluation of Mediterranean fruit fly (Diptera: Tephritidae) female selective attractants for use in monitoring programs. J. Econ. Entomol. 92, 583–589.
[31] Miranda, M.A., Alonso, R. and Alemany, A. (2001) Field evaluation of Medfly (Dipt., Tephritidae) female attractants in a Mediterranean agrosystem (Balearic Islands, Spain). J. Appl. Entomol. 125, 333- 339.
[32] Alemany, A., Alonso, D., and Miranda, M.A. (2004) Evaluation of improved Mediterranean fruit fly attractants and retention systems in the Balearic Islands (Spain). In: Proceedings of the 6th International Symposium on Fruit Flies of Economic Importance. Ed. by Barnes, B.N. Isteg Scientific Publications, Centurion. 355–359.
[33] Boulahia-Kheder, S., Loussaïef, F., Ben Hmidène, A., Trabelsi, I., Jrad, F., Akkari, Y., and Fezzani, M. (2012) Evaluation of two IPM programs based on mass-trapping against the Mediterranean fruit fly *Ceratitis capitata* on citrus orchards. Tunisian J. Plant Protec. 7, 53-66.

Received: **27.01.2019**
Accepted: **28.02.2019**

CORRESPONDING AUTHOR

Nihat Demirel
Mustafa Kemal University,
Faculty of Agriculture,
Department of Plant Protection,
31034, Hatay – Turkey

e-mail: ndemirel@mku.edu.tr

© by PSP Volume 28 – No. 4/2019 pages 2942-2948 Fresenius Environmental Bulletin

EFFECTS OF SALINITY STRESS ON THE GROWTH CHARACTERISTICS OF FOUR TURFGRASS SPECIES

Ramazan Keyikoglu, Elcin Aksu, Mehmet Arslan*

Akdeniz University, Faculty of Agriculture, Department of Field Crops, 07059 Antalya, Turkey

ABSTRACT

Salinity stress is one of the main problems in turfgrass management. This study was carried out to determine the salinity tolerance of various cool-season turfgrass cultivars (*Lolium perenne* "Belida", *Festuca rubra commutata* "Casanova", *Poa protensis* "Evora" and *Festuca rubra trichophylla* "Smyrna") by using irrigation waters with different salinity levels. The study was conducted under greenhouse conditions, planting cultivars in plastic pots filled with a mixture of soil, sand, and peat (4:1:1 by volume) as a growing substrate. Then, 6 different irrigation water sources with gradually increased salinity levels [0.54 (T_0, control; well water EC value), 25 mM (T_1), 50 mM (T_2), 100 mM (T_3), 150 mM (T_4) and 200 mM (T_5)] were applied to the turfgrass cultivars. During the experiment, observations and measurements were made on turfgrass quality, clipping yield, chlorophyll content, shoot and root dry weights. As a result, it was determined that Belida (*Lolium perenne* L.) and Smyrna (*Festuca rubra trichophylla*) varieties were highly tolerant to salinity stress.

KEYWORDS:
Turfgrass quality, Saltwater irrigation, Salinity tolerance

INTRODUCTION

Salinity is one of the important factors that adversely affects and limits plant growth and development worldwide. According to some researchers, approximately 10% of the total area on the earth's surface is composed of soils facing the problem of salinity, and approximately half of the irrigation areas are affected by salinity [1-2]. The salinity and alkalinity problem in Turkey is seen in about 1.5 million ha areas. This rate corresponds to approximately 30% of the field suitable for irrigation [3-4].

Due to the effects of climate change, surface water is decreasing, increasing the usage pressure on groundwater and water quality problems are experienced. This event negatively affects the grass areas, especially the golf courses in the coastal area. In time, the seawater may infiltrate into the groundwater by seepage in coastal areas, and salinization of these waters may occur [5]. As is known, in recent years, there has been a rapid increase in the grass industry worldwide and growth in irrigated turfgrass leads to increased pressure on limited freshwater resources [6]. Further, there is a critical water shortage in the rapidly growing urban areas as a result of the irrigation of the golf course and football fields and other landscaping areas with potable water [2].

Karagüzel and Ortaçesme [7] reported that there is a high salinity problem due to sea water mixing in salty sea winds and groundwater in turfgrass areas especially in coastal part of the Mediterranean Region. In addition, it is emphasized that it is useful to determine the salinity levels of the cool-climate grass species and varieties that are used extensively in turfgrass management in the region. The use of turfgrass species in the Mediterranean Region has further increased with the number of tourism areas and urban settlements and, consequently, the amount of urban turfgrass, in particularly golf courses, that have increased in recent years.

Considering that the coastline of Antalya is one of the major tourism region, different novelties are needed both visually and functionally in the maintenance of turfgrass species used in green areas, especially in golf courses [8]. Because, the golf is played on the turfgrass fields, it is necessary to have a healthy homogeneous grass cover on the field. Otherwise, the areas where the turfgrass cover is not good do not satisfy even nonprofessional golf players [9].

Developments in the turf industry in coastal areas are triggering the reduction of clean water used in irrigation. The blight on the leaves of the turfgrass exposed to high salinity irrigation waters and the decrease in root and shoot development are very closely related to the salt tolerance of the varieties of turfgrass [10]. The difference between the turfgrass species is evaluated by the increase in turfgrass quality and leaf blight with increased salinity and the shoot/root growth not falling below 50%. The use of salt-tolerant plants in the treatment of salty areas can be considered as a good measure. To increase the use of salinity tolerant plants, agronomic studies related to plant breeding are needed [11]. It is important to create a turfgrass field that is long-lasting, suitable for purpose, low maintenance,

superior in color and quality, does not require too much shape, has a high coating speed and ratio, and minimally affected by adverse conditions [12].

Due to the climatic characteristics of the Mediterranean Region, warm climate turfgrass species have problems due to dormancy in winter. Therefore, in this region, overseeding in winter is very important, especially in fields such as golf courses where turfgrass quality is vital [13-14]. Although breeding studies attempt to overcome these problems, they cannot solve these issues completely [15].

In all turfgrass areas located on the coastline of Antalya, warm-season turfgrass species such as bermudagrass (*Cynodon dactylon*) are used. The winter period yellowing (dormancy) in these areas is solved using the overseeding method with cool-season of turfgrass, such as *Lolium perenne, Poa proatensis* and *Festuca rubra* [16]. The turfgrass species used in greenfields are more important than the establishment and maintenance functions in performing the many known positive functions suitable for their ecology [17] because, stress factors such as temperature, drought, salinity and high humidity are important factors limiting the development and growing of turfgrass [18].

In the future, the irrigation water used in turfgrass areas is expected to be more saltier than in the past. In many countries, considering the plant and soil structure, the possibilities of using salt water in irrigation are investigated [19]. Because Turkey is in arid and semiarid climate, irrigation is important factor for plant development in these regions. Therefore, recovery and re-use of wastewater are becoming more and more important in order to meet the water requirements, which are constantly increasing despite limited water resources, while salinity-tolerant cultivation efforts are continuing [5-20].

The aim of this study is to determine the effects of salt water irrigation in turfgrass areas on turfgrass quality and chlorophyll content in the coastline of Antalya, which is mainly located in the Mediterranean Region with many turf sports fields and mainly urban green areas with golf courses. For this purpose, irrigation waters with different levels of salinity were applied to several cool season turfgrass species and varieties determined by considering the results of scientific studies performed in similar regions' climate conditions.

MATERIAL AND METHODS

This research was conducted to determine the reactions and tolerances of the most preferred cool-season turfgrass species and varieties under salinity stress conditions in a greenhouse in Antalya. In the experiment, *Lolium perenne* "Belida", *Festuca rubra commutata* "Casanova", *Poa protensis* "Evora" ve *Festuca rubra trichophylla* "Smyrna" were used as plant material. The desing was a level factorial desing with repilicates, with divided parcels consisting of 4 turfgrass varieties and 6 salinity levels forming the main parcels of varieties of turfgrass and the sub-parcels of the salt levels. A total 72 plastic pots (4x6x3) were used in this study. Turfgrass seeds were sown at a rate 30 g^{-2} in plastic pots on 11.10.2017 and covered with a thin layer of peat and irrigated daily or every 2 days with well waters. The turfgrass varieties were not irrigated with salinity water until their germination and development was completed. After reaching an appropriate plant height, plants were clipped to 4 cm once every 2 weeks. All of the plastic pots were fertilized with NPK (15:15:15) fertilizer once every 2 weeks until the end of the experiment at a rate of 5 g/m^{-2}/month. The garden soil used in the experiment was sieved and mixed in a 4:1:1 ratio (garden soil + washed river sand + peat) with a volumetric mixture. The mixture was filled into 22 cm diameter x 20 cm deep plastic pots. In addition, physical and chemical properties of soil samples were analyzed. The chemical and physical properties of the soil and sand mixture are presented in Table 1. The chemical properties of the irrigation water are presented in Table 2. The temperature and humidity values recorded for each day during the trial are presented in Table 3.

TABLE 1
The chemical and physical properties of soil and sand mixture used in the plastic pots

Characteristics	Determined amount	Evaluation
pH	7.7	Light alkali
Lime, %	27.5	Too limy
Organic material, %	0.64	Very low
Total nitrogen, %	0.080	Low
Phosphorus, kg P_2O_5/da	2.25	Low
Potassium, kg K_2O/da	20.9	Low
Calcium, kg CaO/da	1428.4	Lot
Magnessium, kg MgO/da	84.2	Enough
Iron, ppm	2.21	Low
Manganese, ppm	4.01	Enough
Zinc, ppm	0.38	Low
Copper, ppm	0.73	Enough

TABLE 2
The chemical properties of the irrigation water used with the plastic pots

Characteristics	Determined amount
pH	7.2
EC, dS m^{-1}	0.76
K+, me L^{-1}	0.06
Ca^{2+}, me L^{-1}	5.61
Mg^{2+}, me L^{-1}	1.33
Na^{+}, me L^{-1}	0.92
Cl^{-}, me L^{-1}	1.45
Sodyum Adsorpsiyon Oranı, SAR, $(me\ L^{-1})^{1/2}$	0.487

TABLE 3
The temperature and humidity for each day during the trial

Day/Date	Temperature, ^{O}C		Humidity, %		Day/Date	Temperature, ^{O}C		Humidity, %	
	Max.	Min.	Max.	Min.		Max.	Min.	Max.	Min.
2.6.2018	34,7	4,9	69	12	3.1.2018	38,1	11,4	70	10
2.7.2018	30,8	9,9	67	24	3.2.2018	37,9	9,8	56	10
2.8.2018	34,1	13,8	71	21	3.3.2018	36,3	12,4	64	12
2.9.2018	33,7	12,9	72	22	3.4.2018	34,8	15	68	21
2.10.2018	35	11,8	65	16	3.5.2018	36,4	23,2	51	15
2.11.2018	36	12,1	66	14	3.6.2018	36,2	23,2	55	16
2.12.2018	36,3	10,9	66	11	3.7.2018	35,8	22,6	53	13
2.13.2018	35	11,3	63	12	3.8.2018	37,2	14	72	12
2.14.2018	34,3	12,1	65	12	3.9.2018	37	13,6	69	11
2.15.2018	33	9,9	65	19	3.10.2018	41,4	13,9	51	10
2.16.2018	34	10,5	60	13	3.11.2018	41,4	11,6	61	10
2.17.2018	32	11	62	12	3.12.2018	41,4	11,6	63	10
2.18.2018	32	12,3	55	10	3.13.2018	41	11,8	63	11
2.19.2018	28	15	76	42	3.14.2018	42,2	12,1	67	10
2.20.2018	23,8	14,4	67	40	3.15.2018	41	12,2	72	10
2.21.2018	32,1	13,4	70	23	3.16.2018	37,2	12,1	67	11
2.22.2018	30,9	12,1	71	24	3.17.2018	34,3	11,4	61	11
2.23.2018	26,6	20,5	47	32	3.18.2018	35,4	13,3	64	16
2.24.2018	32	9,6	48	10	3.19.2018	36,2	12,1	63	15
2.25.2018	36,4	8,5	73	16	3.20.2018	35,8	11,8	63	14
2.26.2018	33,6	8,6	75	18	3.21.2018	37,2	12,3	62	13
2.27.2018	30,9	8,4	73	22	3.22.2018	36,8	12,2	62	12
2.28.2018	37,8	11,1	67	11	3.23.2018	37,4	12,6	62	11
					3.24.2018	36,2	13	66	13

Saltwater Irrigation Applications. In this study, 6 different irrigation water sources with gradually increased salinity levels [0.54 (T_0, control; well water EC value), 25 mM (T_1), 50 mM (T_2), 100 mM (T_3), 150 mM (T_4) and 200 mM (T_5)] were applied to turfgrass cultivars. NaCl was used in the preparation of salt water. Considering the Sodium Adsorption Rate (SAR) of the well water used, the electrical conductivity (EC) values of the water in all saline subjects were adjusted by EC-meter in the laboratory. The desired salt concentration was gradually reached due to the fact that high salt doses can have a sudden toxic effect. When watering is reduced to 50% of the field capacity of the pots, the amount of water is increased to 75% of the field capacity [21]. Saltwater irrigation applications were started on 2.6.2018.

Observations and Measurements. Turfgrass quality. Turfgrass quality was assessed visually using a 1-9 scoring scale. The value of 1 is completely yellowed and brown, dead grass, 6 is the minimum acceptable turfgrass quality, and the value of 9 refers to ideal quality with ideal shoot density, texture, color and homogeneity [22]. In order to determine the turfgrass quality, 2 observations were recorded 1 week after the application of saline (2.15.2018) and at the end of the study (3.28.2018).

Clipping yield. After the salt water application was started, the products obtained by clipping the shoots from 4 cm were collected and dried at 72 ° C for 48 hours and their dry weights were determined. (1. clipping harvested on 20.02.2018; 2. clipping harvested on 08.03.2018).

Chlorophyll content. To determine the green leaf density in the experiment, a Minolta SPAD-502 device (SPAD meter) was used to make 2 readings from 5 leaves from each plant in a plastic pot and the values were recorded as SPAD values (Rodriguez and Miller, 2000). Further, to determine

chlorophyll concentrations, 0.25 g of the samples were taken from the leaves, and CaCO3 was added to the tip of the spatula on top of it and then placed a top of the homogenizer. The resulting solution was added to 50 ml of acetone. The drained solution was added to the spectrophotometer and read at 663 nm for chlorophyll A and spectrophotometer at 645 nm for chlorophyll B. Then, the measured values were multiplied by 20.2 constant, and chlorophyll A and chlorophyll B values were calculated as mg/g. The total chlorophyll content was obtained as mg/g using the the addition of chlorophyll A and chlorophyll B values. All operations during the analysis were made under half-shade condition [23]. Examples of measurement and analysis of chlorophyll concentrations were taken twice on 2.6.2018 and 2.15.2018.

Shoot and root dry weight. When the experiment was finished (3.28.2018), the plants were carefully removed from the pot, and all shoots and roots were harvested from the root crown that brought them together. The shoots and roots were carefully washed away from the soil and immediately dried in paper envelopes at 72 °C for 48 hours to determine their dry weight [24].

ANOVA and Duncan's multiple range test for comparisons were determined by SAS 9.3 [25].

RESULTS

Saltwater irrigation significantly affected the growth, development and quality characteristics of the turfgrass varieties during the 1. Screening Period (1SP) and during the 2. Screening Period (2SP). However, there was no significant difference between salinity stress levels in the 1SP except for turfgrass quality, but there were significant differences between the SPAD values and the total root dry weight at the 2SP. The variety x salinity interaction was important for some characteristics (Table 4).

When the leaf width and length characteristics of the turfgrass varieties exposed to saltwater irrigation were examined, the width of the leaf of the Belida was highest with the values of 1.06 mm and 1.59 mm during the 1SP and 2SP. Leaf lengths of 15.35 cm (1SP) and 8.72 cm (2SP) were obtained from the Belida. In terms of the clipping yield values, the Belida had the highest values (3.65 g at 1SP and 11.63 at 2SP). As saltwater irrigation continued, leaf width and length and clipping yield values decreased. When turf quality values were examined, values of 6.77, 7.16, 7.72, and 6.77 were obtained for the Belida, Evora, Smyrna and Casanova in the 1SP, while values of 4.88, 1.77, 5.88, and 3.50 values were obtained during the 2SP, respectively. While Evora was the most affected by the saltwater irrigation applications, Smyrna was the least affected variety. Further, when the SPAD readings used in the estimation of the plants' chlorophyll content were examined, the values of the Belida, Evora, Smyrna and Casanova in the 1SP were 30.32, 39.42, 52.74, and 74.73, respectively. In the 2SP, 32.41, 32.84, 49.29 and 38.71 values were obtained (Table 5). Although the Casanova had the highest SPAD value during the 1SP, the SPAD value was the most decreasing variety with the highest effect from the saltwater irrigation applications.

When the total chlorophyll content of the turfgrass varieties were evaluated, the total chlorophyll content of the Belida, Evora, Smyrna and Casanova were determined as 38.05, 41.23, 30.16, and 29.37 mg/g, respectively. In the 2SP, values of 32.29, 35.46, 25.93, and 29.89 were obtained. While saltwater irrigation applications resulted in a decrease in the total chlorophyll content of other turfgrass varieties, there was no significant difference in the Casanova. At the end of the experiment, the total shoot dry weight values obtained from the plants were removed from the pots were measured as 11.60, 7.86, 6.55, and 4.91 g for the Belida, Evora, Smyrna and Casanova, respectively. Total root dry weight values were determined as 15.22, 12.80, 6.37, and 6.40, respectively. It was shown that the Belida had a higher shoot and root weight than other turfgrass varieties.

TABLE 4
Results of variance of some characteristics under salinity stress.

Source	Leaf width (mm)	Leaf length (cm)	Clipping yield (g)	Turf quality	SPAD	Totall Chlorophyll	Totall shoot dry weight (g)	Totall root dry weight (g)
First Screening								
Cultivar (C)	**	**	**	**	**	**	-	-
Salinity (S)	ns	**	ns	**	ns	ns	-	-
C x S	ns	ns	ns	**	ns	*	-	-
Second Screening								
C	**	**	**	**	**	**	**	**
S	**	**	**	**	ns	**	**	ns
C x S	*	ns	**	**	ns	**	**	**

*,**, ns: Significant at p=0.05 and 0.01, and nonsignificant (p>0.05), respectively.

TABLE 5
Mean comparison of main effects of turfgrass cultivars for salinity.

Cultivars	Leaf width (mm)	Leaf length (cm)	Clipping yield(g)	Turf quality	SPAD	Totall Chlorophyll	Total shoot dry weight (g)	Total root dry weight (g)
	First Screening							
Belida	1,06a*	15,35a	3,65a	6,77b	30,32d	38,05a	-	-
Evora	1,06a	11,59b	2,03b	7,16a	39,42c	41,23a	-	-
Smyrna	0,69b	9,78c	1,46b	7,72b	52,74b	30,16b	-	-
Casanova	0,33c	9,51c	1,62b	6,77b	74,73a	29,37b	-	-
	Second Screening							
Belida	1,59a	8,72a	11,63a	4,88b	32,41b	32,29a	11,60a	15,22a
Evora	1,07b	7,52ab	7,86b	1,77d	32,84b	35,46a	7,86b	12,80b
Smyrna	0,50c	7,67a	6,54b	5,88a	49,29a	25,93b	6,55b	6,37c
Casanova	0,42c	6,21b	4,91c	3,50c	38,71b	29,89ab	4,91c	6,40c

*: Means with different letter(s) in each trait is significantly different at 5% probability level according to Duncan's multiple range test.

TABLE 6
Mean comparison of main effects of salinity stress levels.

Salinity (NaCI) level (mM)¶	Leaf width (mm)	Leaf length (cm)	Clipping yield (g)	Turf quality	SPAD value	Totall Chlorophyll mg/g	Totall Yaprak (g)	Totall Root weight(g)
1SP								
0	0.74a*	10,72b	2,07a	7,0a	47,27a	32,25a	-	-
25	0.80a	11,87ab	2,47a	6,91a	50,72a	34,79a	-	-
50	0.70a	12,91a	2,00a	6,91a	49,18a	33,53a	-	-
100	0.79a	11,77ab	2,16a	7,16a	48,79a	34,00a	-	-
150	0.79a	11,34ab	2,16a	7,58a	51,39a	34,86a	-	-
200	0.88a	10,75b	2,29a	7,08a	48,45a	38,80a	-	-
2SP								
0	1,05ab	7,34ab	6,62b	6,25a	39,06a	33,86a	6,62b	10,92a
25	1,13a	8,41a	11,15a	6,08a	39,44a	31,05ab	11,19a	10,14a
50	0,86bc	8,93a	8,06b	6,00a	41,70a	33,56a	8,06b	10,96a
100	0,84bc	7,86ab	6,42b	3,66b	35,54a	30,73ab	6,41b	10,35a
150	0,75c	6,41b	6,75b	1,41c	35,61a	30,83ab	6,69b	9,08a
200	0,75c	6,23b	7,41b	0,66c	38,54a	25,31b	7,41b	9,75a

*: Means with different letter(s) in each trait is significantly different at 5% probability level according to Duncan's multiple range test.

Table 6 shows the effects of the different salinity levels of irrigation water on the development and quality characteristics of the turfgrass varieties. Before, the leaf width, leaf length, and clipping yield increased significantly with T1 application and then continued to decrease with higher doses of salt applications. As the salt doses increased, the grass quality, SPAD values, and total chlorophyll content values decreased inversely with the salt density. The T1 and T2 salt applications resulted in a slight increase in total shoot and total root dry weight values, while decreasing the denser salt doses. When Table 5 and Table 6 were evaluated together, saltwater irrigation applications significantly reduced the development and turf qualities of the cool-season turfgrass varieties. This the decrease was highest in the Evora (*Poa protensis*). The Belida (*Lolium perenne*) had the highest leaf width, leaf length, clipping yield, and total root and shoot dry weight values. But the least affected variety by salinity was the Smyrna (*Festuca rubra trichophylla*) while in the Casanova (*Festuca rubra commutata*), the foreground with thin leaf texture was moderately affected by the salinity.

DISCUSSION

According to the results of numerous studies using different types of turfgrass species, it is stated that turfgrass quality generally decreases in relation to increased salinity [11-22-26-27]. The development of shoot growing in turfgrass is an indicator of plant viability under stress according to the control conditions, and is an indicator of commonly used salinity tolerance [28]. The variance in the dry weight of the shoot due to the salt dose and the application time are widely used as salt tolerance indicators [29].

In their study, Marcum and Pessarakli [28] used 35 new varieties of *Lolium perenne* to determine the salinity tolerance, the root and shoot development of the salt, and significantly reduces the clipping yield. Researchers point out that there is a large variation and genetic potential in this population. Harivandi et al. [30] reported that, due to the limited availability of renewable drinking water resources, some governments impose restrictions on water use and many must use saline irrigation water

in the field, thus reporting that salinity-tolerant grass plants are needed.

Sever Mutlu et al. [31] reported that, *Lolium perenne* L. "Blackcat" and *Festuca arundinaceae* Schreb. "Barlexas" turfgrasses' response to salinity, salt stress, clipping yield, shoot growth, and the turfgrass quality features of both types was reduced. However, the 24-epibrassinolide (EBL) applications of salinity on the negative effects of enriching the quality of turfgrass is reported.

Dai et al. [20] conducted research to compare *Poa annua* L. and some cool-season turfgrasses (*Poa pratensis, Aprostis stolonifera* ve *Lolium perenne*) with regard to salinity. As a result, *Lolium perenne* was more resistant to salinity than *Poa pratensis* and *Poa annua* was also found to be resistant to moderate salinity. Pessarakli and Kopec [32] studied, ryegrass varieties, and the effects of salinity stress, root and shoot lengths and weights and clippping yield values have been found to decrease in proportion to the increasing salt doses. Researchers have found that root length is more affected by shoot length and ryegrass varieties show high salinity tolerance.

CONCLUSION

The results of this study, in which the effects of saline irrigation water stress on the developmental characteristics and quality of cool-season turfgrasses, are examined, and the literature results are consistent. As a result, it was determined that the Belida (*Lolium perenne* L.) and Smyrna (*Festuca rubra trichophylla*) varieties were highly tolerant to salinity stress.

ACKNOWLEDGEMENT

We would like to express our appreciation to the Akdeniz University Scientific Research Project Commission, which supported this study (FYL-2018-3133).

REFERENCES

[1] Carrow, R.N. and Duncan, R.R. (1998) Salt affected turfgrass sites: Assessment and management. Ann Arbor Press, Chelsea.

[2] Marcum, K.B. (2006) Use of Saline and Non-Potable Water in the Turfgrass Industry: Constraints and Developments. Agricultural Water Management. 80,132–146.

[3] Ekmekçi, E., Apan, M. ve Kara, T. (2005) The Effects of Salinity on Plant Growth. J.of Fac. Of Agric., OMU, 20 (3), 118-125.

[4] Kanber, R., Çullu M.A., Kendirli, B., Antepli, S. ve Yılmaz, N. (2005) Irrigation, Drainage and Salinity. Turkey Agriculture Engineering VI, Technical Congress. 213-251, Ankara.

[5] Sarıca, N. (2014) Determination of Salinity Tolerance in Some Warm Season Turfgrass Cultivars and Assesment of The Results for Landscaping Practice. MSc Thesis in Landscape Architecture, Akdeniz University. 71 p. Antalya.

[6] Pessarakli, M. (2008) Handbook of Turfgrass Management and Physiology. Crc Press. p.p.389-406, Arizona.

[7] Karagüzel, O. ve Ortaçeşme, V. (1997) The Effects of Sea Winds on the Ornamental Plants Used in the Mediterranean Coastal Area Landscape Plantations. Turkey Seaside '97: Seaside and Sea Areas of Turkey: I. National Congress Abstract Book, p. 431-439, Seaside Areas Management Committe Publish. METU, Ankara.

[8] Baysal, O.H. and Karagüzel, O. (2005) Effects of Paclobutrazol on Growth Characteristics of *Lolium perenne* 'Ovation' and *Cynodon dactylon* x *Cynodon transvaalensis* 'Tifway'. Mediterranean Agricultural Sciences. 18(3), 355-363.

[9] Quast, D.H., and Qtto, W. (2004) Golf Course Turf Management: Tools and Techniques, New York: McGraw-Hill, 520 p.

[10] Yılmaz, E., Tuna, A.L. ve Bürün, B. (2011) Tolerance Strategies Developed by Plants To the Effects of Salt Stress. C.B.U. Journal of Science. 7(1), 47-66.

[11] Uddin, K., Juraimi, A,S., Ismail, M.R., Othman, R. and Rahim, A.A. (2009) Growth Response of Eight Tropical Turfgrass Species to Salinity. African Journal of Biotechnology. 8(21), 5799-5806.

[12] Kusvuran, A., Tansi, V. (2009) Determining the best suitable turf grass species, mixtures and turf performance for Cukurova conditions. Cukurova University Fac. of Agriculture, Dept. of Field Crops. (Ph. D. Thesis).

[13] Vengris, J. and Torello, W.A. (1982) Lawns, Basic Factors, Contruction and Maintenance of Fine Turf Areas. Thomson Publications, California, USA. 195 p.

[14] Skerman, P.J. and Riveros, F. (1989) Tropical Grasses. FAO, Roma. 758 p.

[15] Arslan, M. and Citak, S. (2016) Farmyard Manure Usage Mitigates the Harmful Effect of NaCl on Germination and Seedling Growth of Silage Maize (Zea mays L.). Fresen. Environ. Bull. 25, 1543-1548.

[16] Arslan, M. and Cakmakci, S. (2004) Determination of adaptation ability and performances of different grass species and cultivars in coastal conditions of Antalya province. Akdeniz University, Journal of the Faculty of Agriculture. 17(1),31- 42.
[17] Avcıoğlu, R., Salman, A., Demiroğlu, G. ve Erekul, O. (1998) Problems and Solutions for Turfgrass Areas in Aegean Region. Aegean Region, I. Agriculture Congress, 265-271, 7-11 September 1998, Aydın.
[18] Jiang, Y and Huang, B. (2001) Drought and Heat Stress Injury to Two Cool-Season Turfgrasses in Relation to Antioxidant Metabolism and Lipid Peroxidation. Crop Sci. 41, 436–442.
[19] Arslan, M. (2018) An Analitical Approach to Salinity Problems of Coastal Turfgrass Areas. International Symposium Ecology 2018. 19-23 June 2018 Kastamonu, Turkey.
[20] Dai, J., Huff, D.R. and Schlossberg, M.J. (2009) Salinity Effects on Seed Germination and Vegetative Growth of Greens-Type *Poa annua* Relative to Other Cool-Season Turfgrass Species. Crop Science. 49,1-8.
[21] Kurunc, A., Unlukara, A. and Cemek, B. (2011) Salinity and drought affect yield response of bell pepper similarly. Acta Agriculturae Scandinavica, Section B-Soil & Plant Science. 61 (6), 514-522.
[22] Alshammary, S.F., Qian, Y.L. and Wallner, S.J. (2004) Growth response of four turfgrass species to salinity. Agricultural Water Management. 66, 97–111.
[23] Williams, S. (1984). Official Methods of Analysis of the Association of Official Analytical Chemist. Published by the Association of Official Analytical Chemist. Inc.Wircinia 22 209, USA. 140 pp.59-60.
[24] Bıçakcı, T., Aksu, E. and Arslan, M. (2018) Effect of Seed Cotaing on Germination, Emergence and Early Seedling Growth in Alfalfa (Medicago sativa L.) under Salinity Conditions. Fresen. Environ. Bull. 27, 6978-6984.
[25] SAS Institute (2011) SAS/STAT software 9.3, SAS Institute, Cary, NC.
[26] Qian, Y.L. Fu, J.M. Wilhelm, S.J. Christensen, D. and Koski, A.J. (2007) Relative Salinity Tolerance of Turf-type Saltgrass Selections. Hortscience. 42(2),205–209.
[27] Marcum, K.B. and Murdoch, C.L. (1994) Salinity Tolerance Mechanisms of six C4 Turfgrasses. J.Amer. Soc. Hort. Sci. 119,779–784.
[28] Marcum, K.B., Pessarakli, M. (2010) Salinity Tolerance of Ryegrass Turf Cultivars. HortScience. 45(12), 1882-1884.
[29] Uddin, M.K. and Juraimi, A.S. (2013) Salinity Tolerance Turfgrass: History and Prospects. The Scientific World Journal. 2013, Article ID: 409413.
[30] Harivandi, M.A., Marcum, K.B., and Qian, Y. (2008) Recycled, gray, and saline water irrigation, p. 243–258. In: Beard, J.B. and M.P. Kenna (eds.). Water quality and quantity issues for turfgrasses in urban landscapes: Special Pub. 27. Council for Agricultural Science and Tech- nology, Ames, IA.
[31] Sever Mutlu, S., Atesoglu, H., Selim, C, Tokgöz, S. (2017) Effects of 24-epibrassinolide application on cool-season turfgrass growth and quality under salt stress. Grassland Science. 63, 61-65.
[32] Pessarakli, M., Kopec, D.M. (2009) Screening various ryegrass cultivars for salt stress tolerance. Journal of Food, Agriculture & Environment. 7 (3&4), 739-743.

Received: **31.01.2019**
Accepted: **28.02.2019**

CORRESPONDING AUTHOR

Mehmet Arslan
Akdeniz University,
Faculty of Agriculture,
Department of Field Crops,
07059 Antalya, Turkey

e-mail: mehmetarslan@akdeniz.edu.tr

© by PSP Volume 28 – No. 4/2019 pages 2949-2956 Fresenius Environmental Bulletin

ACUTE AND CHRONIC EFFECTS OF PRESSURE ON DYNAMIC THIOL-DISULPHIDE HOMOEOSTASIS IN DIVERS

Ali Erdal Gunes[1,*], Hakim Celik[2], Ozgur Yilmaz[3], Celal Erbas[3], Evren Gumus[4]

[1]Harran University, School of Medicine, Department of Underwater and Hyperbaric Medicine, Sanliurfa, Turkey
[2]Harran University, School of Medicine, Department of Medical Physiology, Sanliurfa, Turkey
[3]Cukurova University, Department of Motor Vehicles and Transport Technologies, Underwater Technology Programme, Adana, Turkey
[4]Harran University, School of Medicine, Department of Medical Genetics, Sanliurfa, Turkey

ABSTRACT

During scuba diving, difficult physical activity, oxidative stress caused by hyperoxia and cold exposure affects the health status of divers. Dynamic thiol-disulphide homoeostasis has never been investigated before on compressed air diving in a hyperbaric chamber. We aimed to evaluate acute effect of diving on thiol/disulphide homeostasis in divers and compare the chronic effects of dives with healthy individuals.

Seventeen of the underwater technology students were admitted to the dive pressure chamber for a 5-minute deep-air dive at 40 meters. Pre-post diving samples were taken to investigate the acute stress of diving. In order to investigate chronic stress, we compared the results of 17 medical school students.

Demographic data of the students of both universities were similar. Increase in Dynamic Thiol-Disulphide Homoeostasis for acute effect were statistically significant ((403.5±5.4vs.420.2±2.5, p=0.012; 18.6±2.7vs.25±1, p=0.040; 5.1±0.7vs.6.8±0.3, p=0.042; 4.5±0.6vs.5.9±0.2, p=0.051; 91.1±1.2vs.88.1±0.4, p=0.042). Increase in native thiol values between serum before and after diving are not statistically significant (366.4±1.5 vs.370.2±2.1 p=0.14).

Difference in Dynamic Thiol-Disulphide Homoeostasis for chronic effect were not statistically significant (403.5±5.4vs.408.5±4.8, p=0.491; 18.6±2.7vs.17.2±2.2, p=0.685; 5.1±0.7vs4.6±0.6, p=0.663; 4.5±0.6vs.4.13±0.5, p=0.626; 91.1±1.2vs.91.7±1, p=0.663). Difference in native thiol values between serum study and control groups were statistically significant (366.4±1.5vs.374.2±3.3; p=0.045).

The stress during the air dives creates acute oxidative stress to the diver and disrupts the dynamic thiol/disulphide balance, but there were no changes observed to disrupt the homeostasis of thiol/disulphide chronically.

KEYWORDS:
Thiol-Disulphide Oxidoreductase, Thiol, Disulphides, Underwater Medicine, Homeostasis

INTRODUCTION

In the last few years, diving with an underwater breathing apparatus (scuba diving) has become a popular sporting entertainment all over the world [1]. Sport and recreational scuba diving mean that using nitrox (which does not exceed 40% oxygen) or compressed air as a dive breathing gas, and the diver can directly access to the surface without decompression stops and dive depth of no more than 40 meters. Unlike sportive dives and limits, dives for professional purposes are more complicated, usually requiring decompression stops when coming to the surface. Besides, in these dives, we use various gas mixtures, such as trimix, heliox or hydrox [2].

There is homeostasis between free radical production and antioxidant defence mechanisms in our bodies. If deterioration of homeostasis, it means oxidative stress. Adverse effects of oxidative stress involved in the pathophysiology of many illnesses and cell ageing [3]. In addition to pressure and temperature changes in an underwater environment, oxygen inhalation in high-pressure exposure causes oxidative stress [4]. Add to this, develops intravascular bubble formation with endothelial dysfunction is the most important load on dive stress [5]. Furthermore, hyperoxia due to the hyperbaric environment during diving and oxygen inhalation at high pressure can cause oxidative stress [6].

'Thiol' is the name of the organic compound, containing the sulfhydryl group. (SH) [7]. Albumin and total protein thiols are the main thiol sources in plasma. Other sources that contribute to the plasma thiol content include cysteine, cysteinylglycine, glutathione, homocysteine and c-glutamylcysteine as low-molecular-weight thiols [8]. Thiols react with free radicals to protect the human body against tissue and cell damage caused by reactive oxygen products (ROS) [9]. Thiols enter the oxidation reaction with oxidant molecules in order to create disul-

phide bonds [10]. As long as appropriate circumstances persist, this disuphide (oxidised status) bonds could be converted to thiol groups again. Therefore, we can talk about the thiol-disulphide homeostasis in our body [11]. Dynamic thiol/disulphide homeostasis is involved in the antioxidant system, the activity of some enzymes and cell signal transduction [12]. Recently, the new, simple method for measuring thiol/disulphide homeostasis has been developed by Erel et al. [13].

Although oxidative stress that divers have been exposed to pressure whilst air breathing in a hyperbaric chamber. Oxidative stress in diving previously investigated in different studies, dynamic thiol-disulphide homoeostasis has never been investigated before on compressed air exposure in a hyperbaric chamber. The goal of this study is evaluate the thiol/disulphide homeostasis before-after air diving and compare these divers pre-dive stress to healthy subjects for investigating chronic effect of air diving oxidative stress.

METHODS

Study Design. The experimental protocol received the approval of Harran University local ethical committee (No:18/09/06) and adhered to the basic principles of the Declaration of Helsinki. The present study was a controlled experimental design, with pre-post measures. The before planned dive and after, serum samples will be collected and the acute air dive effects will be examined. The serums were taken from medical students who are in the similar demographic parameters with professional diver students and will be examined with the chronic effects compared with the diver serum taken before the dive (Figure 1).

Subject. We recruited 17 professional diver students (16 male, 1 female) and 18 volunteers' medical students (18 male) as a control group and after obtaining consent, approved them (Figure 1). All were nonsmokers and non-alcohol-drug addict. They have no history of orthopedic, cardiovascular, renal or metabolic disorders. All participants stated that they did not have any medications and did not fly within 48 hours before study day. Five days before to ensure that all the drivers knew the protocol and they never did a dive for 5 days. The dive students had experience of diving for 150 hours including self-contained scuba apparatus, 184 hours surface supplied breathing apparatus and 20 hours of pressure room. Diver students' lifestyles were organized. Divers were instructed to refrain from heavy physical activity and alcohol-smoke consumption and getting regular personal sleep time in the five days preceding the diving.

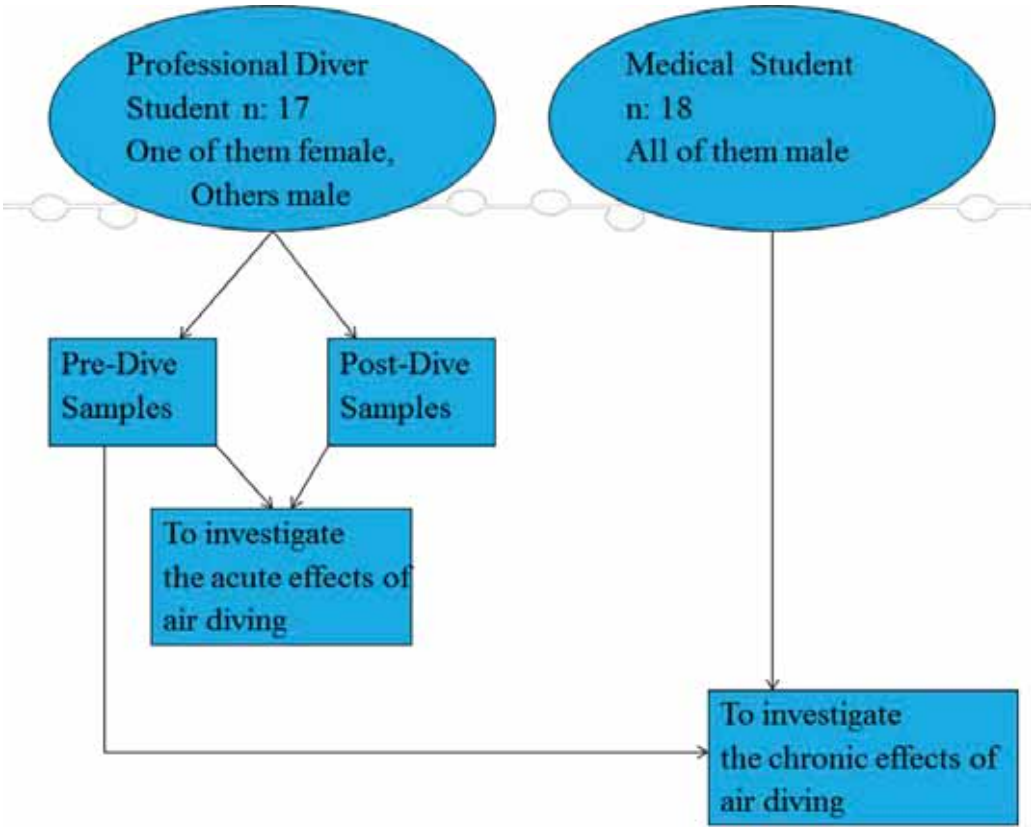

FIGURE 1
The schema shows that the working plan and the status of the groups.

Diving Session and Sample Collections. Before dive samples, blood were taken at 10: 45 before the dive. The dive depth plan was set at 132 feet sea water (fsw) and 5 minutes bottom time, without deco time according to US Navy Air decompression table. The descent rate was set at 70 feet/minute, ascent rate was set at 25 meters/minute, with a decompression stop at 5 meters for three minutes. The session was performed in the hyperbaric chamber (Barotech MULTI DK 1700, Istanbul, TURKEY). The session was performed in triplet groups. The session was ended for 14 minutes. During the dive, the ambient temperature was kept constant 25 °C with air conditioning and divers were able to receive air from the special mask. After dive samples, blood samples were collected at 11.30. Control group blood sample were collected after all divers examinations. An antecubital vein was selected for blood samples. Samples were collected in tubes for the serum to discrete the serum and centrifuged 15,000 rpm for 10 minutes and stored at –80 ºC for three months stored until analysis.

Thiol/Disulphide Biochemical Analysis. The biochemical analyses were performed at the Harran University Physiology Lab. Serum total and native thiol analyses were evaluated using a commercial kit (Rel Assay, Gaziantep, TURKEY) developed by Erel [13]. Erel and Neselioglu used modified Ellman's method to measure the total thiol content. The amount of disulphide bonds was calculated as (total thiol – native thiol)/2. After total measurement other ratios were calculated from these measured parameters.

Statistical Analysis. All statistical values were evaluated with the Statistical Package for the Social Sciences for Windows software (SPSS ver. 21.0, IBM Inc., Chicago, IL). The values are expressed as the mean and standard deviation. The data obtained from the laboratory were assessed whether or not normally distributed by the Shapiro Wilk test. Since regularly distributed data, Paired t-test was used to evaluate the values obtained before and after diving. Study and control groups are independent and normally distributed groups. Therefore, Independent t-test was used to evaluate the values obtained before the dive and control group. The statistical results were accepted to be significant when the *p*-value was less than 0.05.

RESULTS

Demographic characteristics of all individuals are presented in Table 1. The all study conducted with 35 subjects, including male medical student and dive students. The study group mean age 20.6±0.8 and body mass index (BMI) 22.8±1.6; control group mean age 19.4±0.3, BMI 23.7±2.2. There were no statistically significant differences between the two groups concerning age, gender and BMI (p>0.05).

TABLE 1
Demographic characteristics of the study groups.

Parameters	Study Group (Diver Students) (n= 17)	Control Group (Medical Students) (n= 18)	p-Values
Age (years)	20.6±0.8	19.4±0.3	= *0.081*
Sex (female/male)	1/16	0/18	= *0.057*
BMI (kg/m2)	22.8±1.6	23.7±2.2	= *0.066*

*BMI: Body Mass Index; Values are presented as mean±SD
*p< 0.05 is statistically significance

TABLE 2
The mean values of total thiol, disulphide, (%) disulphide-to-native thiol, (%) disulphide-to-total thiol, and (%) native thiol-to-total thiol in study group after-before dive to investigation of acute air dive effect.

Parameters	Study Group (Diver Students) (n=17) Before dive	Study Group (Diver Students) (n=17) After Dive	p-Values
Native thiol (µmol/l)	366.4±1.5	370.2±2.1	*0.140*
Total thiol (µmol/l)	403.5±5.4	420.2±2.5	***0.012***
Disulphide (µmol/l)	18.6±2.7	25±1	***0.040***
Disulphide/native thiol (%)	5.1±0.7	6.8±0.3	***0.042***
Disulphide/total thiol (%)	4.5±0.6	5.9±0.2	***0.051***
Native thiol/total thiol (%)	91.1±1.2	88.1±0.4	***0.042***

* Values are presented as mean±SD
*p< 0.05 as a statistically significance

Changes in serum total thiol, disulphide, disulphide/native thiol, disulphide/total thiol and native thiol/total thiol between before and after diving serum were statistically significant (403.5±5.4vs.420.2±2.5, p=0.012; 18.6±2.7vs.25±1, p=0.040; 5.1±0.7vs.6.8±0.3, p=0.042; 4.5±0.6vs.5.9±0.2, p=0.051; 91.1±1.2vs.88.1±0.4, p=0.042, respectively, Table 2). Changes in native thiol values between serum before and after diving are not statistically significant (366.4±1.5 vs.370.2±2.1 p=0.14, Table 2, Figure 2).

Changes in serum total thiol, disulphide, disulphide/native thiol, disulphide/total thiol and native thiol/total thiol between study group (Dive students) and control group (Medical students) were not statistically significant (403.5±5.4vs.408.5±4.8, p=0.491; 18.6±2.7vs.17.2±2.2, p=0.685; 5.1±0.7vs4.6±0.6, p=0.663; 4.5±0.6vs.4.13±0.5, p=0.626; 91.1±1.2vs.91.7±1, p=0.663, respectively, Table 3). Changes in native thiol values between serum study and control groups were statistically significant (366.4±1.5vs.374.2±3.3; p=0.045, Table 3, Figure 3).

TABLE 3
The mean values of total thiol, disulphide, (%) disulphide-to-native thiol, (%) disulphide-to-total thiol, and (%) native thiol-to-total thiol in study group and control group to investigation of chronic air dive effect.

Parameters	Study Group (Diver Students) (n= 17) Before Dive	Control Group (Medical Students) (n= 18)	p-Values
Native thiol (µmol/l)	366.4±1.5	374.2±3.3	***0.045***
Total thiol (µmol/l)	403.5±5.4	408.5±4.8	*0.491*
Disulphide (µmol/l)	18.6±2.7	17.2±2.2	*0.685*
Disulphide/native thiol (%)	5.1±0.7	4.6±0.6	*0.663*
Disulphide/total thiol (%)	4.5±0.6	4.13±0.5	*0.626*
Native thiol/total thiol (%)	91.1±1.2	91.7±1	*0.663*

* Values are presented as mean±SD
*p< 0.05 as a statistically significance

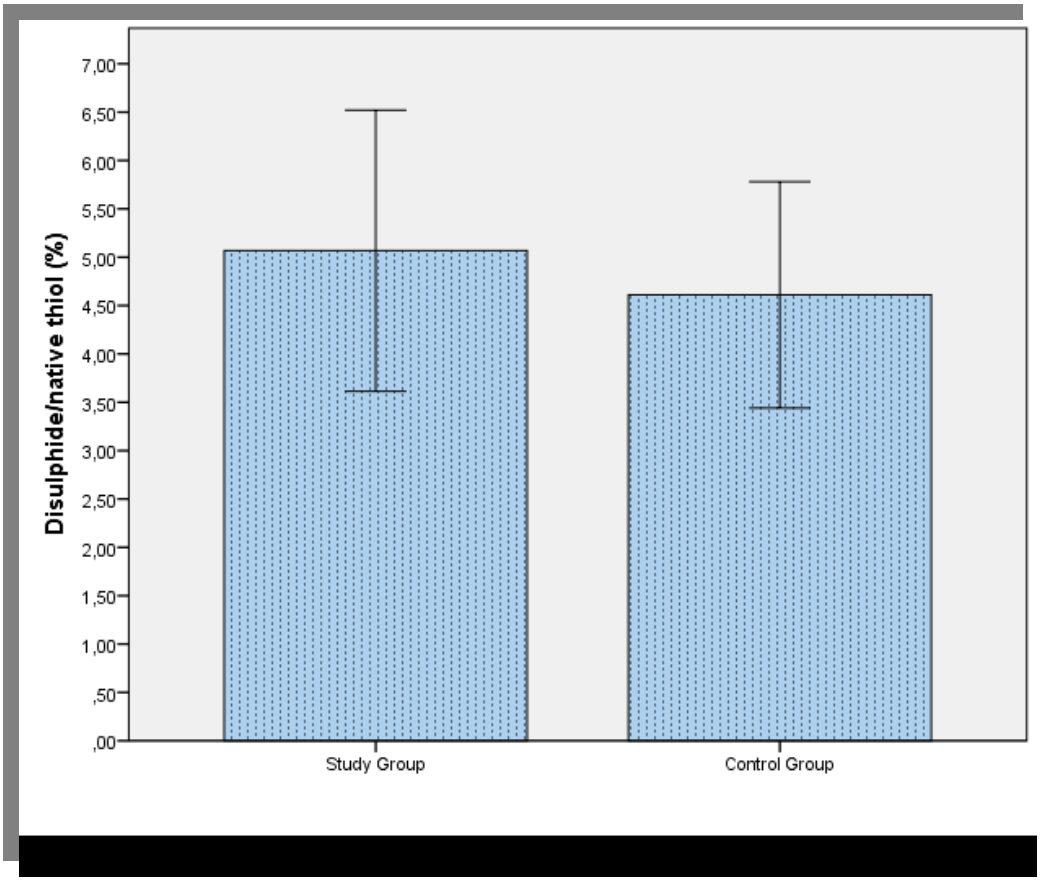

FIGURE 2
The statistical significance chart of the disulphide/native thiol ratio before and after diving.

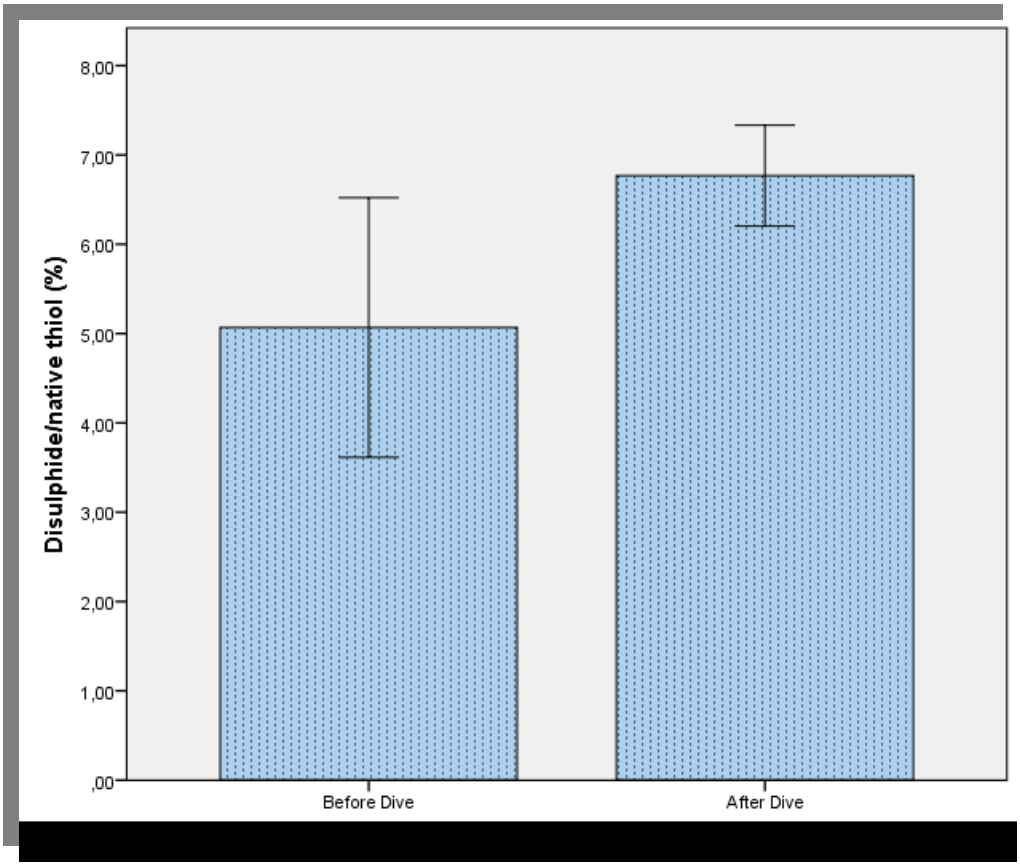

FIGURE 3

The non-statistical significance chart of the disulphide/native thiol ratio before and after diving.

DISCUSSION

Diving is defined by changes in environmental conditions, such as exposure to the hyperbaric environment, inhalation of compressed air, the effect of exposure to water, and exposure to warm-cold temperatures. Also, dive equipment creates a challenging physical activity due to its heavy weight and increased resistance to underwater movement, and it creates psychological stress because the underwater human ability is physiologically limited [1, 3] The most important source of oxidative stress during diving is the increase in oxygen pressure due to the increase in environmental pressure. The increase in dissolved oxygen causes oxidative stress [6].

In the present study, we performed 132 fsw dives to compensate the partial pressure of the oxygen in the inhaled air is equal to 1 atmosphere absolute. 132 fsw is the upper limit of sportive or recreational diving and is a severe depth for professional diving. With this selection, we have made sure that our assessment is valid for not only sportive/recreational diving but also professional diving.

The present study, laboratory values showed that significant increase in disulphide/total thiol, disulphide/native thiol and disulphide/total thiol ratios, and a significant reduction in native thiol/total thiol ratio. In our study, we have shown that deep-air diving acutely dissolves thiol/disulphide homeostasis. However, due to the anti-oxidation system against oxidative stress in the body, it has been shown that air diving does not cause chronic oxidative stress. Differences other than native thiol are statistically insignificant. When the laboratory parameters of chronic effects are examined, the differences other than thiol are statistically insignificant.

Dynamic thiol disulphide homeostasis has a critical role in the individual's antioxidant protection, body detoxification, programmed cell death, the balance of enzyme activity, and intercellular signal transduction [14]. Thiols is an important antioxidant that ROS with non-enzymatic method [15]. In the last decade, a large number of information has been collected over the past decade. Thiols enter the oxidation reaction with ROS to form disulphide bonds. Disulphide bonds are reversible linkages between serum total thiols and they are formed by oxidation of cystine remnant under oxidative stress. The disulphide bonds could be reduced back to the thiol groups. Thus, the balance of thiol-disulphide homeostasis is ensured throughout life [16]. Total thiols include that reduced to free glutathione forms and linked protein forms in intracellular and extracellular areas. Native thiol expression that only reduced bonds, while total thiol expression that both reduced and oxidized bonds [17].

In compressed air dives, the diver breathes the air throughout the dive. As the pressure increases, the partial pressures of oxygen and inert gases increase. Human blood and tissue are saturated with inert gases parallel to the partial pressure of dissolved gases from respiration. Once the divers have started the ascent to the water surface, the pressure gradient is reversed, and they create bubbles from the tissues to the bloodstream [18]. ROS induces vascular smooth cell proliferation by oxidising LDL structure, stimulating macrophages and endothelial activation [19]. A previous study reported that sequential dives cause endothelial dysfunction in large vessels and increase ROS load. [20]. Besides, prolonged and cumulative oxidative stress causes endothelial dysfunction after dive.[20] In the published study, the depth of the dive varies between 180-262 fsw and the depth of the dive is very high than our study. Also, six consecutive dives were performed in the study, and cumulative oxidative stress was evaluated [20]. In this study, we found that oxidative stress occurred in parallel with this study and observed the rate of disulphide/native thiol acutely decreased significantly. However, in our study, we also found that air diving does not cause chronic oxidative stress. In the study mentioned above, vasoconstriction due to hyperoxia was considered, and additionally, endothelial activation was reported due to activation of adhesion molecules [20]. In the previous study of the same researcher, they planned 98 fsw air dives to produce oxidative stress [21]. According to this study, our plan of the 132 fsw depth descended is sufficient to stress.

In medical hypothesis study evaluated air and oxygen dives and observed endothelial dysfunction due to oxidative stress only in air diving. In this study, it was reported that hyperbaric oxygen therapy inhibits neutrophil adhesion, does not create enough stress to create endothelial dysfunction alone, and it is necessary for the formation of nitrogen bubble to stress [22]. The previous study showed that the activated endothelium releases endothelial microparticles which cause dysfunction of the endothelium in the distal regions [23]. Endothelial microparticles have a size of several microns and pass through the lung to the arterial system. In the study performed by diving with air in the pressure chamber, it has been reported that the release of vascular cell adhesion molecule-1 (VCAM-1) and has increased endothelial microparticles [24]. VCAM-1 is known as a proinflammatory marker for the endothelium. In the same study, they did not see this change in hyperbaric oxygen therapy in contrast to air diving. In another study, although endoglin positive microparticles were released in air diving, these microparticles were not seen in hyperbaric oxygen therapy [25].

In recent years, studies on scuba dive reported that physical activity during diving increases oxidative stress [1, 26]. Sureda et al. stated that stress caused by dry pressure chamber diving is less than scuba diving. Because scuba diving has stress factors such as immersion, exercise and temperature changes [26], in our study on thiol/disulphide homeostasis, it could be done temperature changes and exercise for divers in the pressure chamber to observe a more severe deterioration in homeostasis. However, this may be stated as the limits of our study.

Some studies have shown that physical exercise has an effect on resistance to oxidative stress [3, 6, 26] Diving at 132 fsw needs very good health and physical status [26]. The training status of the divers will provide a better tolerance for stress because it has been increased the basal antioxidant condition in regular training athletes [26]. Antioxidant effects of the exercise during diving were shown in another study [6]. In another study, there was an increase in plasma malondialdehyde in 3 hours after a single dive with 164 fsw [27]. Based on these studies, the dive can activate the antioxidant system and does not cause chronic oxidative stress. The human body reduces oxidative stress by activating the anti-oxidant system in response to this stress. In the present study, we have already demonstrated that the thiol/disulphide balance is not impaired in chronic effects of stress and the results are compatible with the mentioned studies.

Our study showed that even a single deep dive disrupts serum thiol disulphide homeostasis. These results suggest that previous studies did not indicate the change of total amount of thiol and disulphide homeostasis of body. We think that this fully automated system ensures better monitoring physiological stress. Before this assay method, in the study, it was shown that only the thiol levels which are the only aspect one side of this homeostasis are determined [28]. However, the levels of the thiol-disulphide homeostasis are measured bi-side wholly new and easy methods [13].

CONCLUSION

In this study, it was found that air dives cause acute oxidative stress, but there is no chronic side to this effect. Studies that investigate the effects of air diving are relatively minimal, and there are often study of the oxidative effects of hyperbaric oxygen therapy. This article important regarding it is the only article in the literature that examines the acute and chronic effects of air diving on dynamic thiol-disulphide Homeostasis. The duration of the effect or the tendency to return to normal values should be investigated with further studies planned with large populations.

ACKNOWLEDGEMENTS

We would like thank to Harran University Physiology Laboratory Researcher Assistant Seyda Nur Dagli for conducting biochemical procedures.

This article, has been accept as the verbal presentation at the 11 TH International Symposium On Underwater Research. 15 November, Antalya, Turkey.

AEG conducted the study, performed air dive applications, prepare serum samples and submitted the article to this journal as a writer. OY and CE performed all diving procedures. HC has performed biochemical assessments and made a statistical evaluation. AEG and EG designed the method and drafted the article. All authors checked and approved the paper.

Authors declare that no conflict interest in this article.

The authors proclaimed that this study had received no financial support.

REFERENCES

[1] Perovic, A., Unic, A., Dumic, J. (2014) Recreational scuba diving: negative or positive effects of oxidative and cardiovascular stress? Biochem Medica. 24(2), 235-247.

[2] CMAS International Diver Training Standards and Procedures Manual. (2012) http://www.cmas.org/document?sessionId=&fileId=2212&language=1. Accessed December 12, 2018.

[3] Gomes, E.C., Silva, A.N., Oliveira, M.R.De. (2012) Oxidants, antioxidants, and the beneficial roles of exercise-induced production of reactive species. Oxid Med Cell Longev. 2102, 12p.

[4] Doubt, T.J. (1996) Cardiovascular and thermal responses to SCUBA diving. Med Sci Sports Exerc. 28(5), 581-586.

[5] Wang, Q., Mazur, A., Guerrero, F. Lambrechts, K., Buzzacott, P., Belhomme, M., Theron, M. (2015) Antioxidants, endothelial dysfunction, and DCS: in vitro and in vivo study. Appl Physiol. 119(12), 1355-1362.

[6] Ferrer, M.D., Sureda, A., Batle, J.M., Tauler, P., Tur, J.A., Pons, A. (2007) Scuba diving enhances endogenous antioxidant defenses in lymphocytes and neutrophils. Free Radic Res. 41(3), 274-281.

[7] Sen, C.K., Packer, L. (2000) Thiol homeostasis and supplements in physical exercise. Am J Clin Nutr. 72(2Suppl). 653S-69S.

[8] Turell, L., Radi, R., Alvarez, B. (2013) The thiol pool in human plasma: the central contribution of albumin to redox processes. Free Radic Biol Med. 65, 244-253.

[9] Chen, A.F., Chen, D.-D., Daiber, A., Faraci, FM., Li, H., Rembold, C.M., Laher, I. (2012) Free radical biology of the cardiovascular system. Clin Sci (Lond). 123(2), 73-91.

[10] Cremers, C.M., Jakob, U. (2013) Oxidant Sensing by Reversible Disulfide Bond Formation. Biol Chem. 288(37), 26489-26496.

[11] Jones, D.P., Liang, Y. (2009) Measuring the poise of thiol/disulfide couples in vivo. Free Radic Biol Med. 47(10), 1329-1338.

[12] Circu, M.L., Aw, T.Y. (2010) Reactive oxygen species, cellular redox systems, and apoptosis. Free Radic Biol Med. 48(6), 749-762.

[13] Erel, O., Neselioglu, S. (2014) A novel and automated assay for thiol/disulphide homeostasis. Clin Biochem. 47(18), 326-332.

[14] Biswas, S., Chida, A.S., Rahman, I. (2006) Redox modifications of protein–thiols: Emerging roles in cell signaling. Biochem Pharmacol. 71(5), 551-564.

[15] Elmas, B., Karacan, M., Dervişoğlu, P., Kösecik, M., İşgüven, Ş.P., Bal, C. (2017) Dynamic thiol/disulphide homeostasis as a novel indicator of oxidative stress in obese children and its relationship with inflamma-tory-cardiovascular markers. Anatol J Cardiol. 18(5), 361-369.

[16] Burke, V. (2006) Obesity In Childhood And Cardiovascular Risk. Clin Exp Pharmacol Physiol. 3(9), 831-837.

[17] Codoñer-Franch P, Valls-Bellés, V., Arilla-Codoñer, A., Alonso-Iglesias, E. (2011) Oxidant mechanisms in childhood obesity: the link between inflammation and oxidative stress. Transl Res. 158(6), 369-384.

[18] Papadopoulou, V., Eckersley, R.J., Balestra, C., Karapantsios, T.D., Tang, M-X. (2013) A critical review of physiological bubble formation in hyperbaric decompression. Adv Colloid Interface Sci. 191-192, 22-30.

[19] Tavakoli. S., Asmis, R. (2012) Reactive Oxygen Species and Thiol Redox Signaling in the Macrophage Biology of Atherosclerosis. Antioxid Redox Signal. 17(12), 1785-1795.

[20] Obad, A., Marinovic, J., Ljubkovic, M., Breskovic, T., Modun, D., Boban, M., Dujic Z. (2010) Successive deep dives impair endothelial function and enhance oxidative stress in man. Clin Physiol Funct Imaging. 30(6), 432-438.

[21] Obad, A., Valic, Z., Palada, I., Brubakk, A.O., Modun, D., Dujić Z. (2007) Antioxidant pretreatment and reduced arterial endothelial dysfunction after diving. Aviat Space Environ Med. 78(12), 1114-1120.

[22] Madden, L.A., Laden, G. (2009) Gas bubbles may not be the underlying cause of decompression illness – The at-depth endothelial dysfunction hypothesis. Med Hypotheses. 72(4), 389-392.

[23] Brodsky, S.V., Malinowski, K., Golightly, M., Jesty, J., Goligorsky, M.S. (2002) Plasminogen activator inhibitor-1 promotes formation of endothelial microparticles with procoagulant potential. Circulation. 106(18), 2372-2378.
[24] Vince, R.V., McNaughton, L.R., Taylor, L., Midgley, A.W., Laden, G., Madden, L.A. (2009) Release of VCAM-1 associated endothelial microparticles following simulated SCUBA dives. Eur J Appl Physiol. 105(4), 507-513.
[25] Madden, L.A., Chrismas, B.C., Mellor, D., Vince, R.V., Midgley, AW., McNaughton, L.R., Atkin, S.L., Laden G. (2010) Endothelial function and stress response after simulated dives to 18 msw breathing air or oxygen. Aviat Space Environ Med. 81(1), 41-45.
[26] Sureda, A., Ferrer, M.D., Batle, J.M., Tauler, P., Tur, J.A., Pons, A. (2009) Scuba diving increases erythrocyte and plasma antioxidant defenses and spares NO without oxidative damage. Med Sci Sports Exerc. 41(6), 1271-1276.
[27] Sureda, A., Batle, J.M., Ferrer, M.D., Mestre-Alfaro, A., Tur, J.A., Pons, A. (2012) Scuba diving activates vascular antioxidant system. Int J Sports Med. 33(7), 531-536.
[28] Aleisa, A.M., Al-Rejaie, S.S., Abuohashish, H.M., Ola, M.S., Parmar, M.Y., Ahmed, M.M. (2014) Pretreatment of Gymnema sylvestre revealed the protection against acetic acid-induced ulcerative colitis in rats. BMC Complement Altern Med. 14(1), 49.

Received: **05.02.2019**
Accepted: **28.02.2019**

CORRESPONDING AUTHOR

Ali Erdal Gunes
Harran University, School of Medicine,
Department of Underwater and
Hyperbaric Medicine, Osmanbey Campus,
Research and Application Hospital,
63300 Sanliurfa – Turkey

e-mail: aerdalg@gmail.com

© by PSP Volume 28 – No. 4/2019 pages 2957-2967 Fresenius Environmental Bulletin

EVALUATION OF PLANT GROWTH REGULATORS AND CASEIN HYDROLYSATE ADDITION ON SECONDARY PRODUCTS PRODUCTION IN CULTURES OF DATE PALM

Abdullatif A Al-Khateeb[1], Mohei El-Din Solliman[1,2], Hossam S El-Beltagi[1,3*], Heba Allah A Mohasseb[1,2], Solliman A Al-Khateeb[1]

[1]Agricultural Biotechnology Department, College of Agricultural and Food Sciences, King Faisal University, P.O. Box 420, Alhassa 31982, Kingdom of Saudi Arabia
[2]Plant Biotechnology Department, National Research Centre, Dokki – Egypt, 12622, Cairo, Egypt
[3]Biochemistry Department, Faculty of Agriculture, Cairo University, Giza, Cairo, Egypt

ABSTRACT

The present study was designed to evaluate the effect of some plant growth regulators and precursors on the secondary metabolites synthesis and development from Khalas and Sukari varieties of date palm (*Phoenix dactylifera* L.) through tissue culture technique, where date palm accumulating broad range of different chemicals in their tissues. Steroids, phenolics and glycosides compounds were specified by gas chromatography/mass spectroscopy (GC-MS) analysis. Cholesterol is an important steroid applied in many growth and development processes and all metabolites has been assigned to having health benefit and nutritional value in the human diet. It is one of ideal animal stores has recently been discoverd among plants and It should be noticed that the obtain chromatograms represent not only the steroids but also all the compounds in the extracts. Offshoots were taken from adult of khalas and sukari were cultured on culture media were included different concentrations of 2,4-D,2ip and BA where the highest percentages of callus production 22.5, 21.23, 20.25, and 19.55 were registered with shoot tip, and primordial leaf explants with 3 mg/l 2,4-D 3 mg/l 2iP and 5 mg/l BA with shoot tip. The primeval leaf of Khalas and Sukari of date palm cultivars appeared the best organ tissue for callus production, while the maximum cell number was 5.13 with 1.0 mg/l 2,4-D +1.0 mg/l 2iP + 3 mg/l NAA. Meantime, the steroid formation was answered differently to the various IBA concentration (0.0, 0.2 and 0.4) utilized in this study where steroid formation reaching its maximum value with 0.4 mg/l IBA concentrations which motivated steroid formation compared with the control 0 mg/l IBA. Furthermore, different concentrations of casein hydrolysate (0,1,2,3 and 4g/l) were studied for achievement and accumulation of total steroid, phenolic and other compounds in cell cultures of shoot tips and primeval leaves of Khalas and Sukari date palm cultivars where the maximum values of total phenolic compound 3.4 (mg/g F.W) were registered with 2g/l casein hydrolysate. likewise, dry, fresh weights (g/flask), and dry matter content (%) as an indicator for cell growth parameters were registered. The best results of dry weight 0.74 (g/ flask); fresh weight 5.05 (g/ flask) and dry matter content 8.5 (%) from shoot tip explants and Khalas date palm cultivar presented the best results compared with Sukari cultivar.

KEYWORDS:
Date palm, phytochemical analysis, tissue culture, plant growth regulators, precursors, steroids and phenolics.

INTRODUCTION

Date palm (*Phoenix dactylifera* L.) a widely distributed plant in Saudi Arabia, West Asia and North Africa, is extensively planted in the Arab countries and grown to some extent, in Southern Europe. It is used for nutritive and therapeutic purposes. Its pollen grains are utilized as antisterility agent [1]. Plant tissue culture is regarded as a source of commercially important steroids, alkaloids, and terpenes for pharmaceutical industry [2-4]. These compounds, known collectively as secondary products, are mostly obtained from plants grown under tropical conditions.

The objective of biotechnology is to use its tools to help convert a country's diverse biological resources into useful products and processes that are accessible to its people for economic development and employment generation [5, 6]. Bioreactors have several advantages for the mass cultivation of plant cells: better control in scaling up cell suspension cultures under defined parameters for the production of bioactive compounds; various stages of bioreactor operation have constant regulation of conditions; efficient and easy handling of culture such as inoculation or harvest; enhanced nutrient uptake by submerged culture conditions, which stimulate the multiplication rate and a higher yield of bioactive compound and large numbers of plantlets are easily produced and can be scaled-up [7, 8].

Plants possess solar-powered biochemical factors, which manufacture both primary and secondary

metabolites from air, water, minerals, and energy from sunlight. Many species of higher plants biosynthesize and accumulate extractable organic substances in quantities sufficient to be economically useful as chemical feed-stocks or as raw materials for various scientific, technological, and commercial applications. Natural substances are employed, either directly or indirectly, by a large number of industries as the pharmaceuticals, cosmetics, foods, agrochemicals, chemurgical industries, industrial oils, flavors and fragrances, resins (e.g. rosin and tall oil), gums, natural rubber, waxes, saponins and other surfactants, pesticides e.g., insecticides and rodenticides), and many special products [9].

Plants and some animal products are used in folklore medicine for treatment of several diseases, e.g. Hypertension, cardiac diseases, kidney disjunction and Diabetes etc. However, nothing could be traced concerning drugs, which are used in the treatment of sterility except date palm pollen grains. The pollen grains from date palm have been known by the Arabs to be nutritive and used as antisterility agent. Cholesterol and coprostanol are the animal sterols, while ß-sitosterol, campestral, stigmasterol, ergosterol and brassicasterol are the principal plant sterols, [10]. Cholesterol, one approved to be the typical animal sterol, has recently been found to be rather widely distributed among plants. So far, cholesterol has been identified in the pollen of many plants, including the date palm and in oil palm [11, 12].

Phenolics are mediates of phenylpro-panoid metabolism [13] and precursors of lignin [14] and phenylpropanoid phytoalexins [15]. Their precipitation in cell walls is an important defense-mechanism response to pathogen infection [16]. Plant cells cultivated in vitro synthesize phenolic compounds, however, in some cases changes in the quality and quantity of the substances are recommended [17]. This is probably due to the specificity of tissue culture as an artificial biological system in which the basic function of phenols is to interfere with cell proliferation [18]. A substitution pattern of phenols was affected, according to the rate of IAA degradation [19]. Also, he reported that phenols were found to react with hydrogen peroxide produced during IAA degradation, thereby protecting cellular constituents from their toxic effect.

The difficulties of getting the origin plants led to the view that a lot of convenient and ultimately cheaper sources of secondary products would be to grow tissue cultures of the plant origins on a large scale, and then extract the accumulated calli cultures biomass and spent medium for the product.

The present investigations were planned to evaluate the effect of adding some precursors as plant growth regulators and casein hydrolysate on the growth, development and secondary metabolite synthesis (phenols, steroids and glycosides) from date palm (*Phoenix dactylifera* L.).

MATERIALS AND METHODS

Date palm material . The study was conducted on adult date palm plants of the cultivar Khalas and Sukari.

Culture media and multiplication stages. Offshoots were taken from adult date palm (*Phoenix dactylifera* L.) of cultivar *Khalas and Sukari* variety was used as plant material.

Nutrient media. Segments (explants) of sterilized shoot tip, as well as primordial leaves were cultured on solidified Ms-nutrient medium (MS) supplemented with 1.7 g/1 phytagel and 30 g/l sucrose. The MS-nutrient medium was conditioned by addition of 170 mg/1 NaH Po .2H O + 200 mg/l H PO + I mg/l thiamine HCI and 3 g/l activated charcoal. Various phytohormones i.e., 5 mg/l of 6-benzyladenine (BA) and 3 mg/l of 2-isopentenyl adenine (2iP) as a cytokinin were added to MS medium in a combination with 2,4-dichlorophenoxy acetic acid (2,4-D) as an auxin at different concentrations as follow:
Mdate 1= MS medium free growth regulators
Mdate 2= MS +0 mg/l 2,4-D + 3 mg/l 2iP + 5 mg/l BA
Mdate 3= MS +1 mg/l 2,4-D + 3 mg/l 2iP + 5 mg/l BA
Mdate 4= MS + 3 mg/l 2,4-D + 3 mg/l 2iP + 5 mg/l BA
Mdate 5= MS + 5 mg/l 2,4-D + 3 mg/l 2iP + 5 mg/l BA
Mdate 6= MS + 10 mg/l 2,4-D + 3 mg/l 2iP + 5 mg/l BA

The pH of the culture media was adjusted to 5.7 with 0.1 M NaOH or 0.1 M HCI before adding the phytagel. The culture media were then dispensed into small jars (150 ml), each one contained 40 ml and 15 cultures were employed per treatment. All cultures media were autoclaved at 121°C ± 1 for 20 min. Cultures were incubated in darkness in a growth chamber at a constant temperature of 28 °C ± 1 then incubated under light condition (1500 Lux) from cool white fluorescent lamps and sub-cultured after every six weeks.

Cell production. The obtained calli from different explants, shoot tip or primordial leaves were saved and re-suspended in an agitated liquid MS media as follow:
MDP1= MS medium free growth regulators
MDP2= MS +1 mg/l 2,4-D + 1mg/l 2iP + 0 mg/l NAA
MDP3= MS +1 mg/l 2,4-D + 1 mg/l 2iP + 1 mg/l NAA
MDP4= MS + 1 mg/l 2,4-D + 1mg/l 2iP + 3 mg/l NAA
MDP5= MS + 1 mg/l 2,4-D + 1 mg/l 2iP + 5 mg/l NAA

MDP6= MS + 1 mg/l 2,4-D + 1 mg/l 2iP + 10 mg/l NAA

Measurement of cell growth parameters. The cell numbers were counted as suggested by Neumann [20] and estimated during the growth period of cultivation as growth parameters. The fresh and dry weights and dry matter contents were also recorded.

Casein enzymatic hydrolysate treatment. As nitrogen source on enhancement and production of total phenolic compounds casein hydrolysate were added in concentrations of (0,1,2,3 and 4g/l) to modify MS medium containing 1 mg/l 2,4-D, 1mg/l 2iP and 2 mg/l NAA.

Determination of total phenolic compounds. In order to identify the phenolic compounds present in the samples, 100 mg of lyophilized cell suspension cultures (cell and liquid medium) of each date palm cultivars were soaked in 5 ml of 70% MeOH, sonicated for 30 min, and centrifuged twice at 10.000 rpm for 10 min. The supernatants were then subjected to total phenolic compound analysis using Folin-Denis method as described [21]. A calibration curve was established using chlorogenic acid (Sigma- Aldrich, USA) as standard.

Steroids biosynthesis in Date palm tissues. For steroid formation the different IBA concentration (0.0, 0.2and 0.4) used in this study. Steroid formation was of positive correlation responses with increasing IBA concentrations from 0.0 mg/l to 0.2 mg/l and the maximum value with 0.4 mg/l IBA concentrations which stimulated steroid formation.

Preparation of Date palm ethanol extracts. Callus was dried at 40˚C for 24 hrs in oven with vacuum, samples was grounded into powder using a mortar under steam of liquid nitrogen, then subjected to extraction. A quantity of 3.0 g of callus powder was extracted with 15 ml of ethanol (70%) at room temperature, protected from sunlight and mixed several times with a sterile glass rod, the mixture was then filtered through Wattman No.1 filter paper. The extracted liquid was subjected to rotary evaporation to dryness in order to remove the ethanol [22], then the extract was stored at 4ºC in refrigerator for future use.

Phytochemical screening. Phytochemical screenings were performed using standard procedures [23].

Tests for phenols. The extracts were taken in water and warmed. To this 2 mL of ferric chloride solution was added and observed for formation of green or blue colour.

Test for Flavonoids. Crude extracts were mixed with 2ml of 2% solution of NaOH. An intense yellow color was formed which turned colorless on addition of a few drops of dilute acid which indicated the presence of flavonoids.

Test for Tannin. To 0.5 ml of extract solution, 1 ml of water and 1-2 drops of ferric chloride solution were added. No color change was observed which indicates the absence of tannins.

Tests for steroids. Two milliliter of acetic anhydride was added to 0.5 g of extract and 2 mL of sulphuric acid was added by the sides of the test tube and observed the colour change from violet or blue-green

Tests for glycosides. About 0.5 mL of alcoholic extracts was taken and subjected to the following test, 1 mL of glacial acetic acid containing traces of ferric chloride and 1 mL of conc. Sulphuric acid was added to extract and observed for the formation of reddish brown color at the junction of two layers and the upper layer turned bluish green in the presence of glycosides.

Qualitative phytochemical analysis by GC-MS. The adapted samples were chosen on the basis of their total Date palm extract as well as those of high total biochemical active constituents in callus tissues, which considered as promising treatments and subjected to by GC-MS analysis after filtered with 0.22 µm pore size syringe filter. GC-MS analysis was carried out in College of Agricultural and Food Sciences, King Faisal University, Al-Hassa, Saudi Arabia, was performed using GC-MS apparatuses, instrument employing the following conditions: a HP-5MS capillary column (Agilent Technologies, Santa Clara, CA) operating at electron impact mode at 70 ev. Pure helium gas with built-in purifier was used at a constant flow rate of 1.0 ml/min employed with a splitless mode with injector temperature 250°C and ion source 280°C. The stepped temperature program was as follows: initial temperature oven was started at 220°C and hold for 5 minutes and followed by a ramp to 300°C at 5°C/min hold for another 15 minutes. A post-run of 5 minutes at 300°C was sufficient for the next sample injection.

Mass analyzer was used in full scan mode scanning from m/z 40-550 and mass spectra were taken at 70 eV. For the compound identification, manual spectral matching was ascertained by using the mass spectral library of National Institute Standard and Technology (NIST) version 2.0 and with the aid of Automated Mass Spectral Deconvolution and Identification (AMDIS) software version 2.70 by deconvoluting the chromatography peak at the corresponding retention time [24]. It should be noticed that the obtain chromatograms represent not only belong to saponifiable but also some bioactive compounds in

the unsaponifiable fraction in the Date palm extracts of each treatment.

RESULTS AND DISCUSSION

Biotechnology is a set of rapidly emerging and far-reaching new technologies with great promise in areas of sustainable food production, nutrition security, health care and environmental sustainability.

Callus production. The effects of modified MS medium with different concentrations 3 mg/l 2,4-D, 3 mg/l 2iP and 5 mg/l BA on percentage of callus formation from shoot tip, and primordial leaf explants of Khalas and Sukari date palm cultivars are shown in Figure (1). The highest percentages of callus production 22.5, 21.23, 20.25, and 19.55 were registered with shoot tip, and primeval leaf explants of Khalas and Sukari date palm cultivars, respectively. The significant obtained results of callus production were monitored with MS medium supplemented with 4 mg/l 2,4-D + 4 mg/l 2iP and 3 mg/l BA. In addition, supplementation of MS medium with 5 mg/l 2,4-D + 3 mg/l 2iP +5 mg/l BA showed the meddle effects of callus production. However, disarmament of growth regulators from MS-medium completely failed on callus production from the used different explants. The obtained results clearly showed that modified of MS medium with 3 mg/l 2,4-D + 3 mg/l 2iP + 5 mg/l BA gave the best results of callus production. Moreover Shoot tip, and primeval leaf of Khalas and Sukari of date palm cultivars appeared the best organ tissue for callus production, respectively.

From the above results, it is clear that calli were obtained from the two types of explants. However, shoot tip explants gave the highest value of callus formation compared with primordial leaves of the different date palm cultivars. This may be due to its meristematic tissues. In this respect, shoot tip explants of date palm has been successfully used for either embryonic calli induction or embryos formation by several authors [25-27]. In addition, from the obtained results, its clear that the combination of 2,4-D and 2iP with BA appeared to be the most suitable medium for callus production. In addition, the obtained results are in line with those reported by Mater [28] and Madhuri et al. [29].

Cell suspension production. Illustrated data in Fig. (2) show that the effect of supplementation of liquid MS- medium with 1 mg/l 2,4-D + 1 mg/l 2iP in a combination with different concentrations of NAA i.e., 1,3,5 and 10 (mg/l) on cell number (x 105) of the different cultures. The maximum cell number 5.13, 4.96, 3.11 and 1.22 were recorded with Khalas and Sukari cell lines of shoot tip and primordial leaf

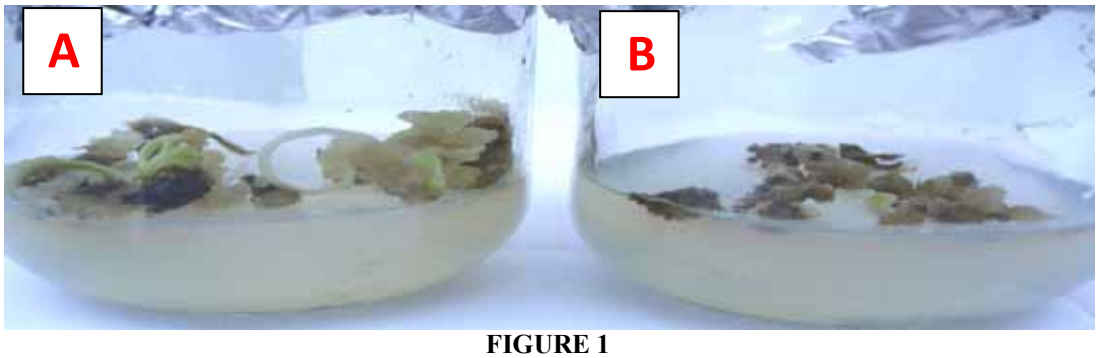

FIGURE 1
Callus formation from shoot tip explant of Khalas (A) and Sukari (B) date palm cultivars, cultured on MS medium supplemented with 4 mg/l 2,4-D and 4 mg/l 2iP and 3 mg/l BA and incubated under dark condition

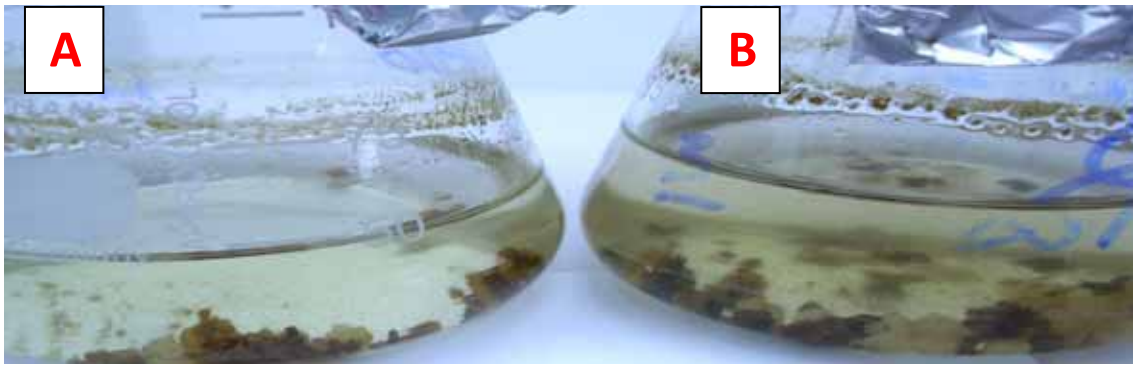

FIGURE 2
Suspension production from shoot tip calli of Khalas (A) and Sukari (B) date palm cultivar, cultured on MS medium supplemented with 1 mg/l 2,4-D and 1 mg/l 2iP and 3 mg/l NAA and incubated under dark condition at 26 ºC.

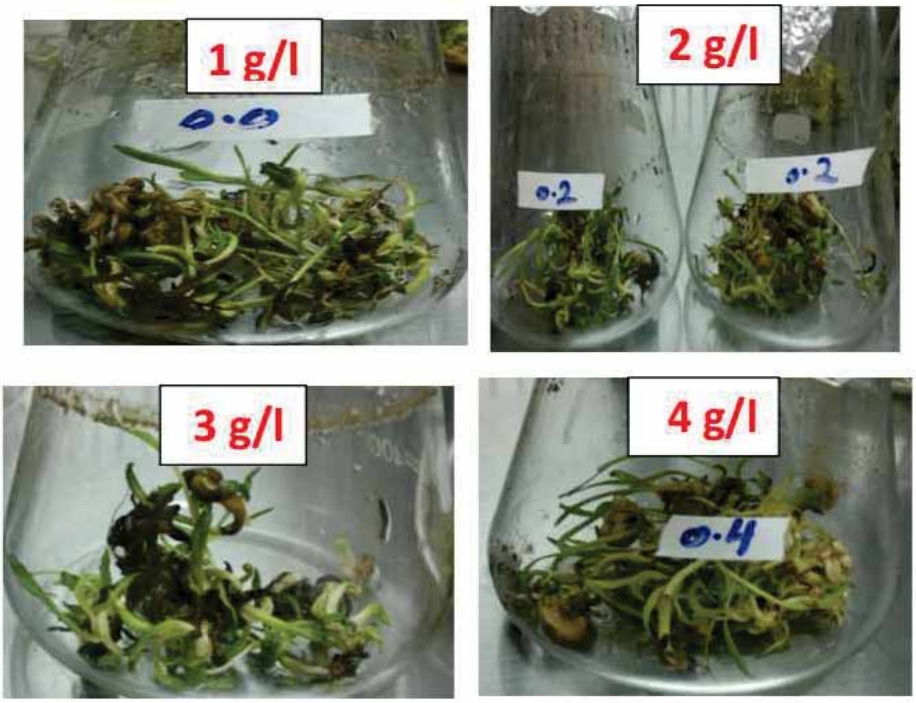

FIGURE 3
Shoots culture of Khalas date palm cultivar, cultured on MS medium supplemented with different concentrations of Casein hydrolysate (0, 1, 2, 3 and 4 g/l).

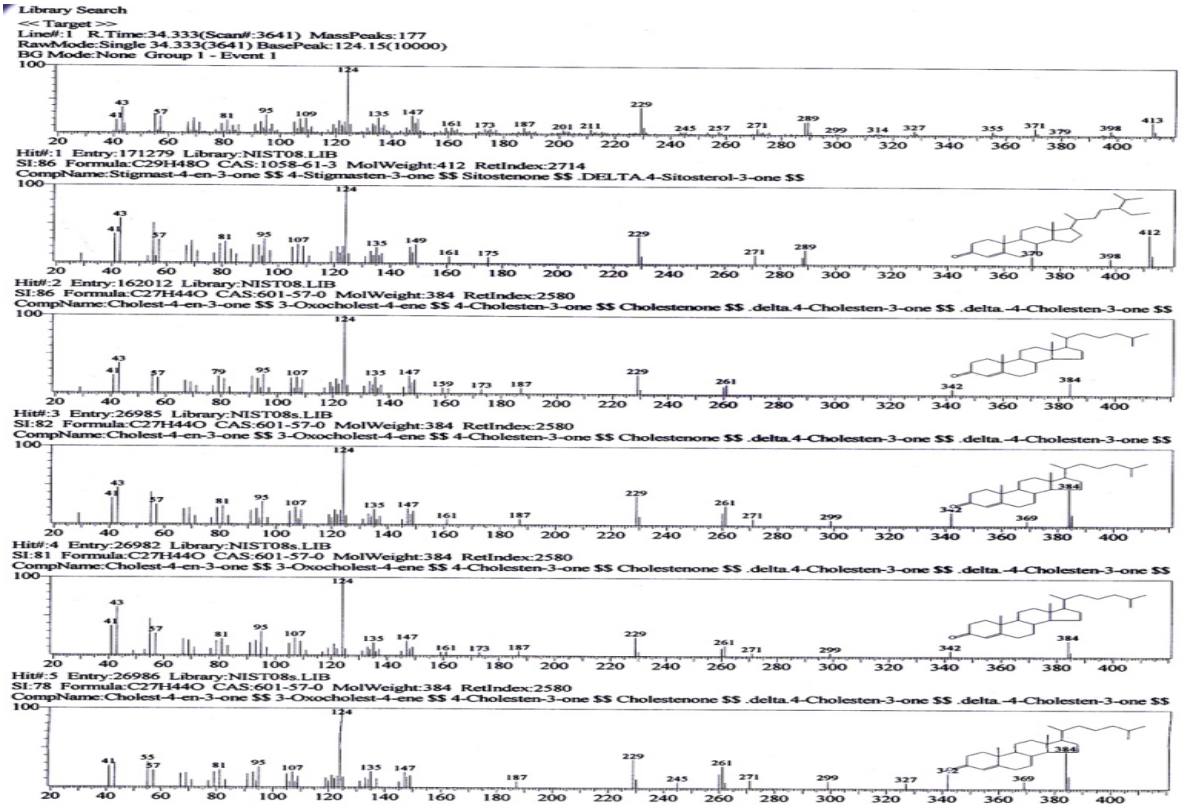

FIGURE 4a
Chromatogram obtained from the GC-MS with the extract of date palm steroid

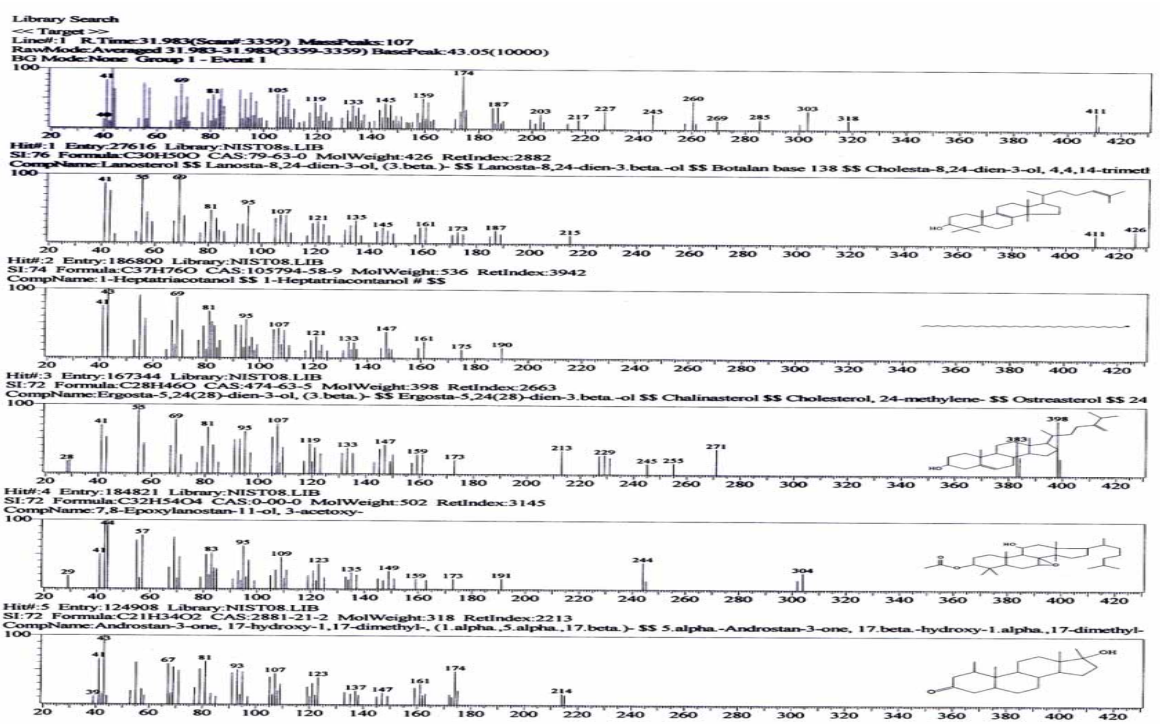

FIGURE 4b
Chromatogram obtained from the GC-MS with the extract of date palm steroid

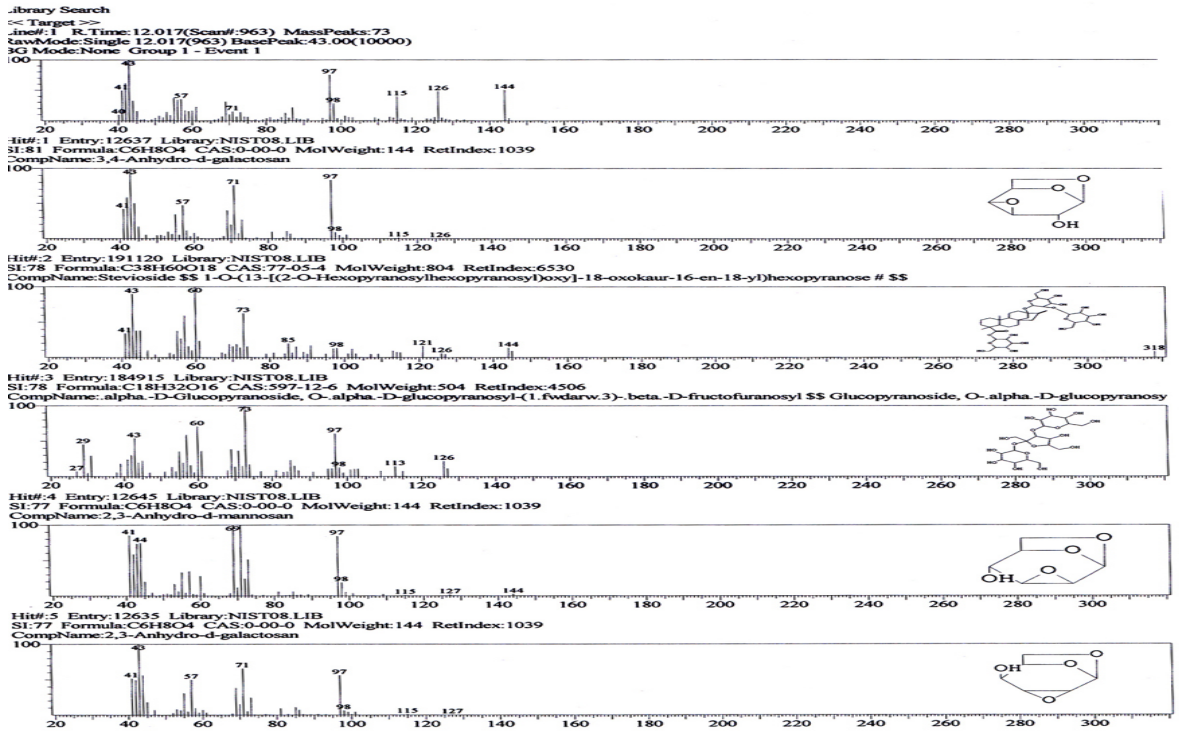

FIGURE 5
Chromatogram obtained from the GC-MS with the extract of date palm glycosides

explants, respectively. These records were estimated with MS medium augmented with 1mg/l 2,4-D + 1mg/l 2iP + 2 mg/l NAA compared with other NAA concentrations. Shoot tip explants of the different cultivars gave the best results compared with primordial leaf explants. Moreover, fresh and dry weights (g/flask), and dry matter content (%) of derived suspension cultures were determined as indictor for cell growth parameters. Concerning Khalas date palm cultivar, the best results of fresh weight 5.05 (g/ flask); dry weight 0.74 (g/ flask) and dry matter content 8.5 (%) were recorded with derived cells from

shoot tip explants compared with 7.15 (g/ flask), 0.63 (g/ flask) and 8.4 (%) for fresh, dry weights and dry matter contents of primordial leaf cell cultures. And the medium contained 1 mg/l 2,4-D + 1mg/l 2iP + 3 mg/l NAA gave the best results compared with others tested MS media. Similar results were obtained with Sukari date palm cultivar, However, Khalas date palm cultivar showed the best results compared with Sukari cultivar.

The above results clear that, supplementation of MS-medium with NAA as auxin and BA as cytokinin were more suitable for callus and subsequently suspension production from the used explants of Khalas and Sukari date palm cultivars. It was found that, addition of 3 mg/l of NAA to MS-medium gave the maximum nutmber of date palm cell cultures compared with the other NAA concentrations.

In this study, the obtained results are in close with Gamborg and Shyluk (1981) [30], they concluded that, callus initiation and production was depending on the presence of auxin and cytokinin, which stimulates cell division and cell elongation, respectively. Moreover, the obtained results by Nussbaumer et al. [31] they 5 reported that supplementation of B medium with 1 mg/l of each of NAA and BA gave the best results of growth value for *Datura,* and these results are in harmony with our obtained results.

Phytochemical screening. The qualitative analysis of ethanolic date palm tissue extracts showed the presence of phenolic substances, flavonoids, glycosides, tannins, steroids (Table 1). The presence of the bioactive constituents in date palm tissue extract after addition of casein hydrolysate (0,1,2,3 and 4g/l) to modified MS medium containing 1 mg/l 2,4-D+1mg/l 2iP + 2 mg/l NAA indicates how the treatments enhanced the production of the bioactive compounds and improved its potential use as an excellent source of food supplement.

TABLE 1
Bioactive constituents analysis of Khalas and Sukari tissue extract

Bioactive constituents	Khalas tissue extract	Sukari tissue extract
Phenols	+	+
Flavonoids	+	+
Glycosides	+	+
Tannins	+	+
Steroids	+	+

Phytochemical Analysis and GC-MS profiling in the Date Palm Tissue. Evaluation of date palm secondary metabolism, such as phenolics, Steroids, glycosides and other compounds. Higher plants such as date palm accumulate a wide range of different chemicals in their tissue. These can conveniently be divided into two types of compounds: products of primary plant metabolism, such as proteins, fats and carbohydrates, which guarantee the primary functions of growth and development; and products of secondary metabolism such as phenolics.

In this study different concentrations of Casein hydrolysate (0,1, 2, 3 and 4g/l) were added to modify MS medium containing 1 mg/l 2,4-D+1mg/l 2iP + 2 mg/l NAA to study their effects on enhancement and production of steroid, phenolic, glycosides and other compounds. Data illustrated in (Fig 4, 5 and 6) that the effect of fortified MS nutrient medium on achievement and accumulation rate of total steroid, phenolic, glycosides and other compounds in cell cultures of shoot tips and primeval leaves of Khalas and Sukari date palm cultivars. The maximum values of total phenolic compound 3.4, 2.5, 2.12 and 1.94 $(mg/g\ F.W)^{-1}$ were recorded with primordial leaves of Khalas and Sukari and shoot tips of Khalas and Sukari date palm cultivars, respectively. The optimum concentration of Casein hydrolysate added to nutrient MS medium to achievement of total phenolic compounds production was 2g/l compared with other concentrations of Casein hydrolysate (Fig. 6). The highest dynamic values of phenolic compound accumulation were recorded at the end of the 30 days of cultivation. Moreover, the accumulation rates were reduced at the 5^{th} week of cultivation with all used Casein hydrolysate concentrations. Concerning the highest values of steroids accumulation rate 6554, 5894, 5645 and 5334 U/g^{-1} fresh weight was recorded with derived cells from primordial leaves and shoot tips of Khalas and Sukari (Fig.4) date palm cultivars, respectively. For maximum peroxides accumulation, augmentation of MS nutrient medium with 2 g/l of Casein hydrolysate was favorable to 21 days of cultivation. However, the accumulation rates of peroxides were reduced after 21 days of cultivation with all derived date palm suspension and liquid cultures.

By nature of its prevalence in the mammalian body and its central position as a precursor of bile acids and steroid hormones, cholesterol is, biochemically, the most important steroid. Because of its wide distribution and its involvement in atherosclerotic heart disease and its sequelae, cholesterol has been the most widely studied of all biologically occurring steroids. The ensuing discussion will be concerned primarily with this sterol. It is clear from the data that steroid formation had responded differently to the different IBA concentration (0.0, 0.2 and 0.4) used in this study. Steroid formation was of positive correlation responses with increasing IBA concentrations from 0.0 mg/l to 0.2 mg/l in case of tissue only or 2.0 mg/l for cholesterol in case of liquid cultures, reaching its maximum value with 0.4 mg/l IBA concentrations which stimulated steroid formation compared with the control, followed by 0.2 mg/l cholesterol, respectively (Fig. 4).

Additionally, through the biosynthetic pathways to the flavonoids synthesis, among the not well elucidated condensation and polymerization phases, the condensed tannins or non-hydrolysable tannins

TABLE 2
Chemical compounds that produced in tissues and media of date palm.

Group name	Compound name	Retention time	Peak area	symbol
Steroid compounds	cholesterol	31.983	398	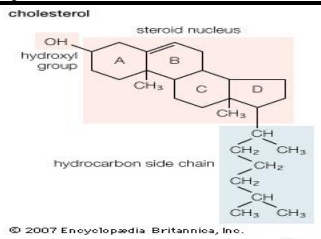
	sitosterol	34.33	412	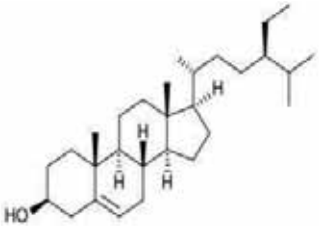
	stigmasten	34.33	412	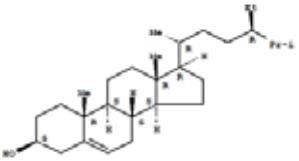
	cholesten	34.33	384	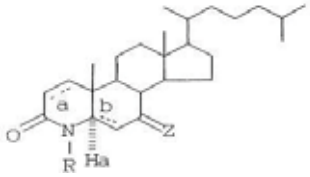
	cholesta	31.983	426	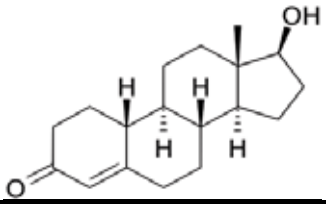
Glycoside compounds	galactosan	12.017	144	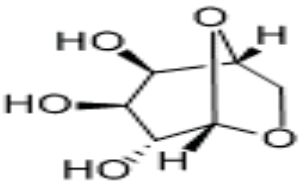
	glucopyranoside	12.017	504	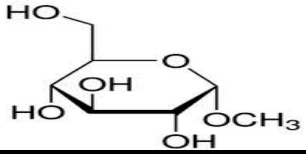
Phenolic compounds	benzaldehyde	12.808	228	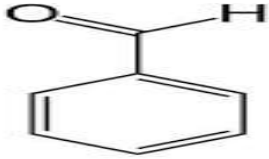
	Vanillic aldehyde	12.808	152	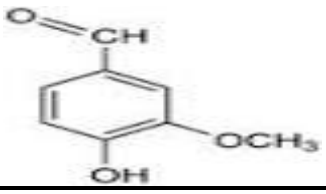

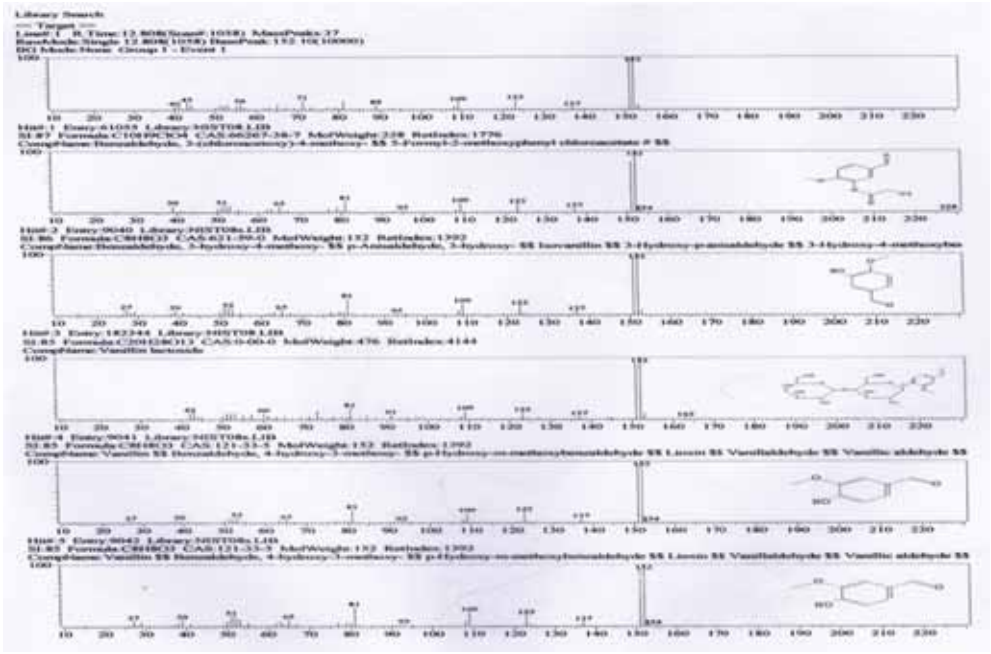

FIGURE 6
Chromatogram obtained from the GC-MS with the extract of date palm phenolics

and glycosides are formed (Fig. 5). Hydrolysable tannins are derivatives of gallic acid or hexahydroxydiphenic acid [32]. So the highest values of total phenolic compound accumulation 2.4, 2.1, 1.96 and 1.74 (mg/g^{-1}F.W) were recorded with primordial leaves of Khalas and Sukari and shoot tips of Khalas and Sukari date palm cultivars, respectively. In addition, the maximum value of total phenolic accumulation was recorded after three weeks of cultivation (Fig. 6). These obtained results are in agreement with those obtained by Del-Rio [33] who reported that the highest phenol levels were detected after 120 days in leaves, stems and roots of *Olea europaea* L. fruits. Moreover, these findings agree with observations made for the increased levels of phenolic compounds observed in the fruit of Brotomax olive varieties [34] and in different organs of other plant species [35-37].

The result of the present study further revealed that phenolic content increased quantitatively with the increase in age of suspension from main to the third week of cultivation. The percentage of browning and necrosis are also in conformity with increase in phenolic content in old culture. The increase in phenolic content is normally associated with increase in the enzymes that regulate the synthesis of phenolic compound, while the intensity of browning is related with the hyperactivity of oxidative enzymes [38-40]. An increase in production of phenolic compounds has been associated with a decrease in growth, a decline in protein synthesis.

It should be noticed that the obtained chromatograms represent not only the steroids but also all the compounds in the extracts of each treatment by Gas Chromatography-Mass Spectroscopy (GC-MS) analysis (Table 2).

ACKNOWLEDGEMENTS

The authors would like to thank Deanship of Scientific Research at King Faisal University, Saudi Arabia, for funding and supporting this research under Grant No.130068.

REFERENCES

[1] Taha, H.S., Abdel-El Kawy, A.M., Abd-El-Kareem, F.M., El-Shabrawi, H.M. (2010) Implement of DMSO for enhancement and production of phenolic and peroxides compounds in suspension cultures of Egyptian date palm (Zaghlool and Samany) cultivars. J. Biotech Biochem. 1(1), 1-10.

[2] Taha, H.S. (2002) Effect of biotic stress (*Aspergillus niger*) on production and accumulation of total alkaloids in suspension cultures of *Atropa belladonna* L. Ann. Agric. Sci. Ain Shams Univ. 47(1), 43-54.

[3] Taha, H.S. (2003) Effect of biotic stress (*Aspergillus niger*) on the production and accumulation of total alkaloids in *Atropa belladonna* l. *Via* tissue culture. Acta Hort. 597, 257-264.

[4] El-Beltagi, H.S., Ahmed, O.K., El-Desouky, W. (2011) Effect of low doses γ-irradiation on oxidative stress and secondary metabolites production of rosemary (*Rosmarinus officinalis* L.) callus culture. Radiat Phys Chem. 80(9), 968-976.

[5] Taha, H.S., Bekheet, S.A., El-Bahr, M.K. (2011) A new concept for production and scaling up of bioactive compounds from Egyptian date palm (Zaghlool) cultivar using bioreactor. The First scientific conference for the development of the date palm and dates sector in the arab world 4-7 December 2011, King Abdulaziz City for Scientific and Technology, Riyadh, Kingdom of Saudi Arabia.
[6] Jain, S.M., Al-Khayri, J.M., Johnson, D.V. (2011) Preface. In: Jain, S.M., Al-Khayri, J.M. and Johnson, D.V. (Eds.) Date Palm Biotechnology. Springer, Netherlands. pp. v-vii.
[7] Fulzele, D.P and Heble, M.R. (1994). Large-scale cultivation of *Catharanthus roseus* cells: production of ajmalicine in a 20-l airlift bioreactor. J. Biotechnol. 35(1), 1-7.
[8] Othmani, A., Mazid, R., Bayoudh, C., Trifi, M., Drira, N. (2011) Bioreactors and automation in date palm micropropagation. In: Jain, S.M., Al-Khayri, J.M., Johnson, D.V. (eds.) Date palm biotechnology. Dordrecht: Springer, 119-136.
[9] Balandrin, M.J., Klocke, J.A. (1988) Medicinal, aromatic and industrial materials from plants. In: Bajaj, Y.P.S. (ed.) Biotechnology in Agriculture and Forestry. Medicinal and Aromatic plant. 4, Springer-Verlag, Berlin, Heidelberg, 1-36.
[10] Bailey, A.E. (1964) Industrial oil and fat products. Interscience publishers, Inc., New York.
[11] Bennett, R.D., Ko, S.T., Heftmann, E. (1966) Isolation of estrone and cholesterol from the date palm. Phytochem. 5, 231.
[12] Solver, H.T., Thompson, R.H., Merola, G.V. (1983) Determination of tocpherols and sterols by Capillary gas chromatography. J Am Oil Chem Soc. 60, 1524.
[13] Cvikrová, M., Hrubcová, M., Eder, J., Binarova, P. (1996) Changes in the levels of endogenous phenolics aromatic monoamines phenylalanine ammonia-lyase peroxidase and auxin oxidase activities during initiation of alfalafa embryogenic and non-embryogenic calli. Plant Physiol. Biochem. 34(6), 853-861.
[14] Lewis, N.G., Yamamoto, E. (1990) Lignin: occurrence, biogenesis and Bio-degradation. Annu Rev Plant Physiol Plant Mol Biol. 41, 455-96.
[15] Kessmann, H., Choudhary, A., Dixon, R. (1990) Stress responses in alfaalfa. III. Induction of medicarpin and cytochrome P450 enzyme activities in elicitor-treated cell suspension cultures and protoplasts. Plant Cell Rep. 34(3), 38-41.
[16] Bolwell, G., Robins, M., Dixon, R. (1985) Metabolic changes in elicitor treated bean cells. Enzymic responses associated with rapid changes in wall components. Eur J Biochem. 148, 571-578.
[17] Zagoskina, N.V., Zaprometov, M.N. (1983) Effect of kinetin on formation of phenol compounds in the long-passaged tea plant tissue culture. Physiology and biochemistry of cultivated plants. 15(3), 250-253.
[18] Ozyigit, I.I., Kahraman, M.V., Ercan, O. (2007) Relation between explant age, total phenols and regeneration response in tissue cultured cotton (*Gossypium hirsutum* L.) Afr J. Biotechnol. 6(1), 3- 8.
[19] Winer, L., Riov, J., Goren, R. (1993) Catabolism of indole-3-acetic acid in citrus leaves: identification and characterization of indole-3-aldehyde oxidase. Physiologia Plantarum. 89(1), 220-226.
[20] Neumann, K.H. (1966) Root formation and nucleic acid content in phloem cultures of carrot root on synthetic nutrient medium of various hormone combinations. Les Phytohormones et I Oranogenese 38, 95-102. (In German)
[21] Jeong, G-T., Je-Chang, W., Don-Hee, P. (2007) Effect of plant growth regulators on growth and biosynthesis of phenolic compounds in genetically transformed hairy roots of *Panax ginseng* C.A. Biotechnol Bioprocess Eng. 12(2), 86-91.
[22] Akueshi, C.O., Kadiri, C.O., Akueshi, E.U., Agina, S.E., and Ngurukwem, B. (2002) Antimicrobial potentials of *Hyptis sauvedens* Poit (Lamiaccae). Nigeria. J Bot. 15, 37- 41.
[23] Sofowora, A. (1993) Medicinal plants and traditional medicine in Africa. Screening plants for bioactive agents. 2nd Ed. Spectrum Books Ltd, Sunshine House, Ibadan. Nigeria. 134-156.
[24] Cheong, B.E., Zakaria, N.A., Cheng, A.Y.F., Teoh, P.L. (2016) GC-MS analysis of *Strobilanthes crispus* plants and callus. Transactions on Science and Technology. 3(1-2), 155 – 161.
[25] Tisserat, B. (1979) Propagation of date palm (*Phoenix dactylifera* L.) in vitro. J Exp Bot. 30, 1275-1283.
[26] Zaid, A., Tisserat, B. (1983) Morphogenetic responses obtained from a variety of somatic explants tissues of date palm. Botanical Magazine. 96, 67-73.
[27] El-Kazzaz, A.A., El-Bahr, M.K. (2001) A method for *in vitro* propagation of the Egyptian date palm cultivar Samany. Arab J Biotech. 4(2), 285-292.
[28] Mater, A.A. (1986) In vitro propagation of (*Phonix dactylifera* L.). Date Palm J. 4(2), 137-152.
[29] Madhuri, S., Chandramati, S., Sharon, M., Shankar, C. (1999) Regeneration of date palm (*Phonix dactylifera* L.) through direct organogenesis. Indian J Plant Physiol. 4(4), 323-326.
[30] Gamborg, O.L., Shyluk, J.P. (1981) Nutrition, media and characteristics of plant cell and tissue cultures. In: Thorp, T.A. (ed.) Plant Tissue culture: Methods and Application in Agriculture. Academic Press, New York. 21-44.

[31] Nussbaumer, P., Kapetanidis, T., Christen, P. (1998) Hairy roots of *Datura candida* X *D.aurea*: Effect of culture medium composition on growth and alkaloid biosynthesis. Plant Cell Reports. 17(5), 405-409.
[32] Stafford, H.A. (1983) Enzymic regulation of procyanidin bisynthesis, lack of a flav-3-en-3-ol intermediate. Phytochem. 22, 2643 2646.
[33] Del Rýo, J.A., Baidez, A.G., Botia, J.M., Ortuno, A. (2003) Enhancement of phenolic compounds in olive plants (*Olea europaea* L.) and their influence on resistance against. *Phytophthora sp.* Food Chem. 83(1), 75-78.
[34] Del Rýo, J.A., Arcas, M.C., Botýa, J.M., Baidez, A., Fuster, M.D., Ortuno, A. (2000) Involvement of phenolic compounds in the antifungal defense mechanisms of *Olea europaea* L. and *Citrus sp*. Recent Research Developments in Agricultural and Food Chem. 4, 331-341.
[35] Fuster, M.D., Garcýa, D., Ortuno, A., Botýa, J.M., Sabater, F., Porras, I., Lidon, G.A., Del Rio, J.A. (1995) Selection of citrics highly productive in secondary metabolites of industrial interest. Modulation of synthesis and/or accumulation processes. In: Garcýa Viguera, C., Castaner, M., Gil, M.I., Ferreres, F., Tomás-Barberán, F.A. (Eds.) Current trends in fruit and vegetables phytochemistry. Madrid: Consejo Superior Invest. 81–85.
[36] Ortuno, A., Botýa, J.M., Fuster, M.D., Porras, I., Garcýa Lidon, A., Del Rýo, J.A. (1997) Effect of Scoparone (6,7-dimethoxycoumarin) biosynthesis on the resistance of tangelo Nova, *Citrus paradisi* and *Citrus aurantium* fruits against *Phytophthora parasitica*. J Agr Food Chem. 45, 2740-2743.
[37] Del Rýo, J.A., Gonzalez, A., Fuster, M.D., Botýa, J.M., Gomez, P., Frýas, V. Ortuno, A. (2001) Tylose formation and changes in phenolic compounds of grape roots infected with *Phaeomoniella chlamydospora* and *Phaeoacremonium species*. Phytopathologia. Mediterranea. 40, S394-S399.
[38] Cochrane, M.P. (1994) Observation on the germ aleurone of Barley. Phenol oxidase and peroxidase activity. Ann Bot. 73, 121-128.
[39] Afify, A.M.R., El-Beltagi, H.S., Abd El-Salam, S.M., Omran, A.A. (2012) Protein solubility, digestibility and fractionation after germination of sorghum varieties. PLoS ONE 7. e31154, 1-6.
[40] Youssef, S.A., Safwat, G., Shalaby, A.A., El-Beltagi, H.S. (2018) Effect of phytoplasma infection on plant hormones, enzymes and their role in infected sesame. Fresen. Environ. Bull. 27, 5727-5735.

Received: **06.02.2019**
Accepted: **22.02.2019**

CORRESPONDING AUTHOR

Hossam S El-Beltagi
Plant Biotechnology Department
College of Agricultural and Food Sciences,
King Faisal University, P.O. Box 420,
Alhassa 31982 – Kingdom of Saudi Arabia

e-mail: lbltg@yahoo.com

© by PSP Volume 28 – No. 4/2019 pages 2968-2977 Fresenius Environmental Bulletin

IDENTIFICATION AND EXPRESSION ANALYSIS OF ACID INVERTASES GENE FAMILY IN ROOTS OF METALLICOLOUS AND NON-METALLICOLOUS POPULATIONS OF *RUMEX JAPONICUS* UNDER COPPER STRESS

Yu-Qiao Cao[1], Zhuang-Zhuang Wei[1], Jia-Yang Xu[2], Hui-Fang Shao[1], Zi-Cheng Xu[1], Wu-Xing Huang[1,*]

[1]College of Tobacco Science, Henan Agricultural University, Zhengzhou, Henan, 450002, China
[2]College of Agronomy and Biotechnology, China Agricultural University, Beijing, 100193, China

ABSTRACT

Recent researches indicate that under heavy metal stress, metallicolous population (MP) of metallophyte display a higher activity of acid invertases enzymes, which are rate-limiting in sucrose catabolism, than non-metallicolous population (NMP). Because most of these metallophytes are non-model plants for which the background genomic information is limited, it is unclear whether the higher activities of acid invertases are the result of higher expression of individual or total acid invertases gene family members. Based on high throughput RNA sequencing, in present study we identified eight acid invertases genes, including six cell wall invertase genes (*RjcwINV1-6*) and two vacuolar invertase genes (*RjvINV1-2*), from MP and NMP of *Rumex japonicus*, and determined their expression patterns under Cu stress. The seedlings of *R. japonicus* were exposed to control or 20 μM Cu^{2+} for 48 hours under hydroponic conditions. The transcript levels of *RjcwINV2*, *RjcwINV5* and *RjvINV1* in MP were significantly higher than them in NMP, while *RjvINV2* only expressed in NMP. The results suggested that different members of the acid invertases gene family have varying expression patterns under Cu stress. Furthermore, the higher acid invertases activities of MP under Cu stress could be due in part to elevated expression of individual instead of total acid invertases genes.

KEYWORDS:
Rumex japonicas, Acid invertases, Gene family, Copper stress

INTRODUCTION

During the last few decades, many soils are detrimental to plant owing to elevated levels of heavy metal (HM), caused either by ore outcrop weathering processes or by the result of human activities such as mining, smelting, traffic emissions and the use of pesticides [1, 2]. A restricted number of plant species called metallophyte, however, have evolved HM tolerance and are able to survive and reproduce in these metalliferous sites [3]. It was first recognized by Prat who showed a Cu mine population of *Silene dioica* was able to grow in Cu contaminated soils [4]. Since this initial work, the biogeochemical, physiological, genetic and molecular aspects of heavy metal tolerance in toxic metals such as zinc, lead, copper, cadmium and nickel have received sustained attention [5, 6].

Root performance is crucial for plants to colonise in metalliferous soils, because roots among the organs are directly exposed and first subjected to HM stress. Roots depend on sucrose (Suc) imported from source leaves to sustain heterotrophic metabolism [7]. Suc cannot be used directly and must instead be cleaved into hexoses by invertase or Suc synthase. Plants possess three isoforms of invertase with different biochemical properties and subcellular locations. Neutral/alkaline invertase (N/A-Inv) are localized in the cytosol. Acid invertases are either bound to the cell wall (cell wall invertase, CW-Inv), involved in Suc partitioning, cell division and differentiation, or localized in the vacuole (vacuolar invertase, V-Inv), playing an important role in sugar storage, cell enlargement, and osmoregulation [8].

It is conceivable that for the roots of metallophytes to maintain HM tolerance and grow in metalliferous soils, they must gain sufficient hexoses supplied by efficient Suc metabolism. Consistent with this hypothesis, previous investigations revealed significantly higher activities of CW-Inv and V-Inv in the roots of plants from metallicolous population (MP) than in plants from non-metallicolous population (NMP) in *Kummerowia stipulacea* [9], *Rumex dentatus* [10], *Rumex japonicus* [11] and *Elsholtzia haichowensis* [12]. The activity of acid invertases is usually regulated at the transcriptional level by biotic or abiotic stresses. Recent studies suggest that the genes encoding acid invertases from higher plants constitute a multigene family [13, 14]. However, the

number of acid invertases gene family members in metallophyte and their expression under HM stress have received little attention. It is unclear whether the higher activities of acid invertases in roots of MP are the result of higher expression of individual or total acid invertases gene family members.

In recent years, high throughput RNA sequencing (RNA-seq) has been become a comprehensive and accurate tool for gene expression analyses [15]. RNA-seq has been used to elucidate the response of plants to various environmental stresses, such as cold, salt, drought and invasion by pathogens [16, 17]. *Rumex japonicus* is a perennial herb with fast growth and high biomass. Ke et al. reported that MP of *R. japonicus* had higher Cu tolerance and mineral nutrient deficiency tolerance than NMP [18]. Huang et al. reported that the roots of MP manifest a significantly higher activity of acid invertases enzymes than that of NMP [11]. In this study, in order to understand acid invertases gene family and their expression patterns in metallophyte under HM stress, acid invertases genes in roots of *R. japonicus* were first identified based on RNA-seq platform, and then the expression levels of these genes were estimated and further validated by quantitative real-time PCR (qRT-PCR). This knowledge is of considerable importance for understanding Suc metabolism, which may be crucial for plant root growth and HM tolerance maintenance that has evolved in metallophytes.

MATERIALS AND METHODS

Plant materials, Cu treatments and sampling. Two populations of *R. japonicus* were selected for study, one (MP) at an ancient waste heap of the Cu mine of Tonglushan hill in Hubei Province, China, the other (NMP) at the campus of Wuhan University. Background values of Cu concentration in the soils of the two sites (62.5 mg kg^{-1} Cu in NMP and 1044.5 mg kg^{-1} Cu in MP) were listed in our previous study [11]. In each population, large quantities of seeds were taken from more than 50 randomly selected plants, and the seeds were finally pooled.

Seeds from the two populations were sterilized and then germinated on wet filter paper in dark. The germinated seeds were evenly sown in round plastic pots filled with quartz sands and fertilized occasionally with Hoagland's solution depending on growth status. When the seedlings developed five leaves, healthy and uniform seedlings were selected and transplanted to solution culture pots. Each pot contained 1 L Hoagland's solution and was covered with a foam plastic plate. The plates each were drilled with 5 evenly arranged, 5-mm-diameter holes, one hole facing one plant. The roots were immersed in the solution. Cu tolerant individuals and sensitive individuals were screened by Wilkins tolerance index [19, 20]. Then, the treatment of these plants by Cu was conducted. According to preliminary tests, 20 μM Cu concentration was used. Solution Cu^{2+} was supplemented as $CuCl_2 \cdot 2H_2O$. Each treatment was replicated three times. 48 hours after treatment, two populations of R. *japonicus* were concurrently harvested to avoid interference from possible diurnal changes in expression of genes. Roots were washed with deionized water and immediately frozen in liquid nitrogen and stored at -80 °C for RNA extraction.

RNA extraction, library construction and sequencing. Frozen root samples were ground in liquid nitrogen to a fine power. Then the total RNA was extracted using TRIzol reagent (Invitrogen, Carlsbad, CA, USA) according to the manufacturer's instructions and was digested with DNase I (TaKaRa, Kyoto, Japan) to eliminate any traces of contaminating genomic DNA. Quality of the extracted RNA was checked by agarose gel electrophoresis and RNA concentration was measured using Qubit RNA Assay Kit in Qubit 2.0 Flurometer (Life Technologies, Carlsbad, CA, USA). Additionally, RNA integrity was assessed using the RNA Nano 6000 Assay Kit of the Bioanalyzer 2100 system (Agilent Technologies, Santa Clara, CA, USA).

Samples with RNA integrity number values above 8.5 were used for libraries construction. A total amount of 6 μg RNA per sample was used as input material for the RNA preparations. Sequencing libraries were generated using NEBNext® Ultra™ RNA Library Prep Kit for Illumina® (NEB, Cambridge, MA, USA) following manufacturer's recommendations and index codes were added to attribute sequences to each sample. PCR products were purified and library quality was assessed on the Agilent Bioanalyzer 2100 system. The clustering of the index-coded samples was performed on a cBot Cluster Generation System using TruSeq PE Cluster Kit v3-cBot-HS (Illumina) according to the manufacturer's instructions. After cluster generation, the library preparations were sequenced on an Illumina Hiseq 2500 platform and 125 bp paired-end reads were generated.

Data filtering, de novo assembly and annotation. The raw data of fastq format were firstly processed through in-house Perl scripts. Clean data were obtained by removing reads containing adapter, reads containing ploy-N and low quality reads from raw data. All the downstream analyses were based on clean data with high quality. The clean reads were assembled using Trinity software as described for *de novo* transcriptome assembly without a reference genome [21]. The unique assembled transcripts were further subjected to the process of sequence-splicing redundancy removal with sequence clustering software to acquire non-redundant transcripts called unigenes.

The assembled unigene sequences were aligned by BLASTx to the publicly available protein databases which included NCBI non redundant protein

(Nr), Gene Ontology (GO), Clusters of Orthologous Groups (COG), Swiss-Prot protein and the Kyoto Encyclopedia of Genes and Genomes, and aligned by BLASTn to nucleotide databases with an $E \leq 10^{-5}$. If the assembled unigene sequences could not be aligned to any database, the software ESTScan was used to predict the protein coding sequence and its sequence orientation. And then, GO annotation of the unigenes was performed based on the best hits from Nr annotation using BLAST2GO program, and the results of GO annotation were further used to conduct GO functional classification by WEGO software.

Identification of acid invertases gene family members. Gene sequences of six known acid invertases genes from Arabidopsis (GeneID:842563, 837777, 824426, 820590, 820591, 818191), three from potato (GeneID:102604560, 102604230, 102577489), and seven from tomato (GeneID: 778304, 543992, 107029797, 544241, 544175, 543713, 543502) were selected as queries to search the full set of acid invertases genes in *R. japonicus*. BLAST matches achieved similarity scores of >50 and probability scores of $<10^{-4}$ were collected as candidate sequences. These candidate sequences of acid invertases genes were further verified by their annotated database obtained in above describe. Furthermore, candidate acid invertases proteins were confirmed by searching for conserved domains of invertase.

Expression analysis of each acid invertases gene and verified by qRT-PCR. Expression level for each member of acid invertases gene family was calculated using the fragments per kilobase of exon per million mapped reads (FRKM) method. Expression pattern of each acid invertases gene were further validated using qRT-PCR. The qRT-PCR was performed with the SYBR® Premix ExTaq™ (TaKaRa, Dalian, China) on the ABI 7500 System (Applied Biosystems, Foster City, CA, USA). The glyceraldehyde-3-phosphate dehydrogenase (GAPDH) gene was used as a reference control. The specific primers were designed using Beacon Designer 7.0 software (Table 1). The reaction was performed using the following conditions: denaturation at 95 °C for 30 s, followed by 40 cycles of amplification (95 °C for 5 s, 60 °C for 30 s). Each plate was repeated three times in independent runs for all reference and selected genes. Gene expression was evaluated by the $2^{-\Delta\Delta Ct}$ method. For each sample, three technical replicates of the qRT-PCR assay were used with three biological replicates. Results were expressed as means ± standard deviation of the number of experiments. A Student's t-test for the values was performed at $P<0.05$.

TABLE 1
Sequences of primers used in this study.

Primers	Sequences (5' - 3')
RjcwINV1-F	GAGGACGAAAACGGGTGTTG
RjcwINV1-R	AATGGGTCAGTTGGGTCGTC
RjcwINV2-F	CCCTATCTTGTCTGGCACCG
RjcwINV2-R	GACTCCACGGTCTCCTACCT
RjcwINV3-F	CACATCAACGGACCTCGTCA
RjcwINV3-R	CCGGACCAACAACCGTTTTC
RjcwINV4-F	GGCATCACTTCTTCTCAGGCAGA
RjcwINV4-R	TCCGCCATTTTTATACGCCCCA
RjcwINV5-F	AGGGTTTATCCGGTCTTGGC
RjcwINV5-R	GCTCCATGCACTCAAACCTG
RjcwINV6-F	AACATAGCGTTTCCTGCCGA
RjcwINV6-R	GAGTTGATGTTTCCGCTCGC
RjvINV1-F	AACGGCCTCGACACTTCAAT
RjvINV1-R	TCTTTGGGACATCTGGCACC
RjvINV2-F	CGGGTCCAAGATCAACACCA
RjvINV2-R	GAACGGCGTGGAGTACATGA
GAPDH-F	TTGTTTCAACTGACTTTGTGGGT
GAPDH-R	CTGTATCCCATCTCATTGTCG

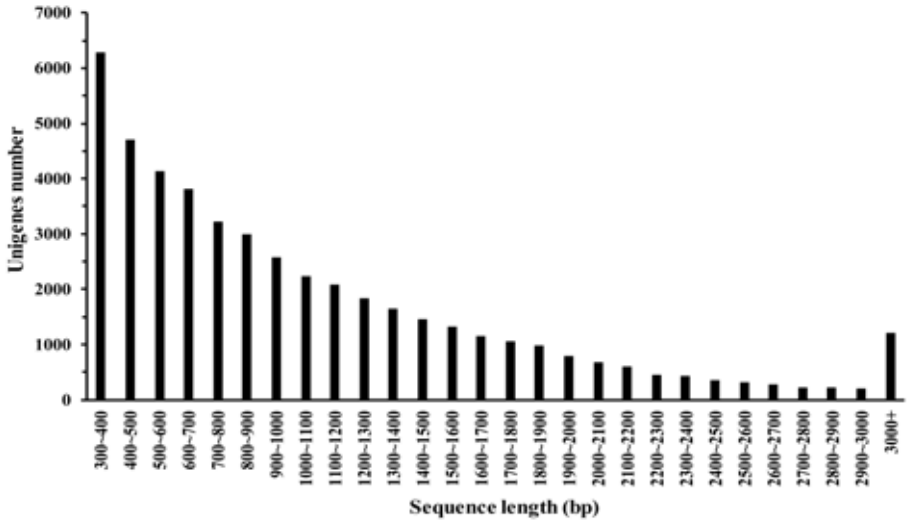

FIGURE 1
The length distribution of the assembled transcripts.

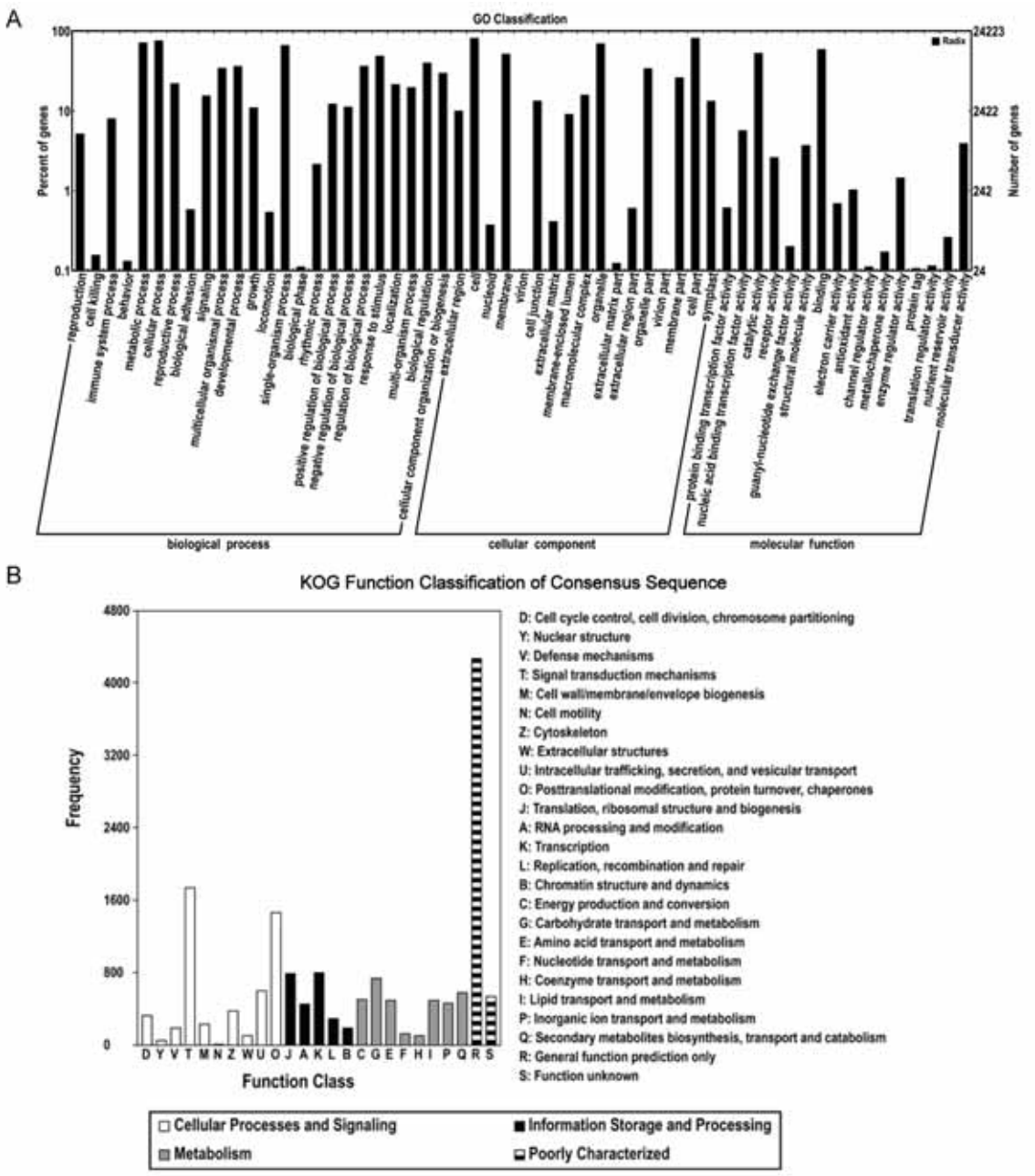

FIGURE 2
Gene ontology classification (A) and KOG function classification (B) of assembled unigenes.

RESULTS

Illumina sequencing and de novo transcriptome assembly. A large volume data was generated with the Illumina HiSeq 2500 sequencing the two *R. japonicus* cDNA libraries, NMP and MP. According to Illumina's RNA transcriptome sequencing, a sequence can generate 2×150 basepairs (bps) from each Paired-End of a cDNA fragment. After removing the low quality reads and trimming off the adapter sequences, 26,821,310 (NMP) and 28,772,909 (MP) high-quality, clean paired-end sequencing reads were obtained, respectively. Because no appropriate reference genome sequence was available for *R. japonicus*, a *de novo* assembly program Trinity was selected for *de novo* assembly of all the 55,594,219 clean reads. Finally, a total of 47,252 unigenes were obtained with the average size of 1,070.04 bp and N50 size of 1,382 bp in transcript length. The size distribution of the assembled transcripts is shown in Figure 1.

Function annotation and classification of the assembled unigenes. GO assignments were used to classify the functions of the predicted *R. japonicus* roots genes under Cu stress. Based on sequence homology, 24,223 unigenes (51.26% of all assembled unigenes) were assigned at least one GO term, including 57 functional groups at the second level

(Figure 2A). Among which, 'cell' (19,896 sequences, 42.11%), 'cell part' (19,870 sequences, 42.06%) and 'organelle' (16,962 sequences, 35.90%) terms were dominant in the cellular component, while 'cellular process' (18,463 sequences, 39.07%), 'metabolic process' (17,402 sequences, 36.83%) and 'single-organism process' (16,143 sequences, 34.16%) were the most highly represented under biological process, and 'binding' (14,327 sequences, 30.32%) and 'catalytic activity' (12,820 sequences, 27.13%) were the most abundant subcategories for the molecular function. Furthermore, only a few transcripts were clustered in terms of 'protein tag', 'channel regulator activity', 'biological phase', 'translation regulator activity', 'extracellular matrix part', and 'behavior'.

To further evaluate the completeness of the *de novo* assembly transcriptome and predict possible functions, all assembled unigenes were compared against the KOG database for the analysis of phylogenetically widespread domain families. The results revealed 14,364 unigenes with significant homology and assigned them into the appropriate KOG clusters. These KOG classifications were grouped into 25 functional categories (Figure 2B). The three largest categories were 'general function prediction only' (29.69%), 'signal transduction mechanisms' (12.10%), 'post translational modification, protein turnover, chaperones' (10.18%).

Identification of acid invertases genes. The exact number of acid invertase genes present in *R. japonicus* is unknown, because its genome has not yet been sequenced in its entirety. To identify putative acid invertases genes expressed in roots of *R. japonicus*, well-annotated acid invertase genes from *Arabidopsis*, potato, and tomato were used to search the family members from above transcriptome data, resulting in the discovery of twenty-four acid invertases-like ESTs. The SeqMan software was used in the assembly, and then, the Blastx and Blastn programs available on the NCBI web server were used to examine the integrity and the homology of these contigs. A total of eight acid invertase genes were identified, including six CW-Inv genes and two V-Inv genes. Multiple alignments (Figure 3 and 4) of them with acid invertases genes from some selected species showed that they all contained two well conserved regions of plant acid invertases, including a β-fructosidase motif (NDPN) and a catalytic domain (WECP/VD). The presence of a Val residue in the latter motif is characteristic of V-Inv, whereas in CW-Inv the Val residue is replaced by Pro.

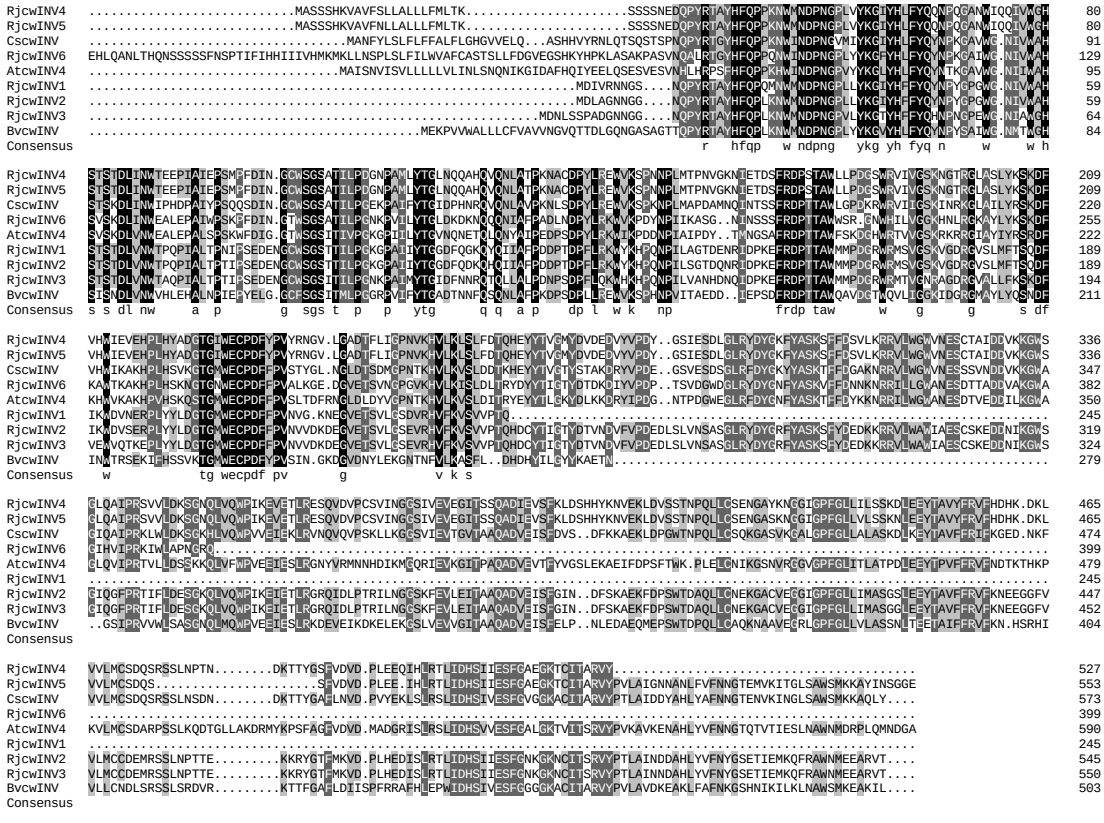

FIGURE 3

Alignment of the deduced CW-Inv amino acid sequences of *R. japonicas* (*RjcwINV1-6*) with CW-Inv genes from some selected plant species. GenBank accession numbers of the sequences are *CscwINV* (*Citrus sinensis*, XP006466029), *AtcwINV4* (*Arabidopsis thaliana*, NP565837), *BvcwINV* (*Beta vulgaris*, CAC81921). Consensus shows the identical amino acid residues.

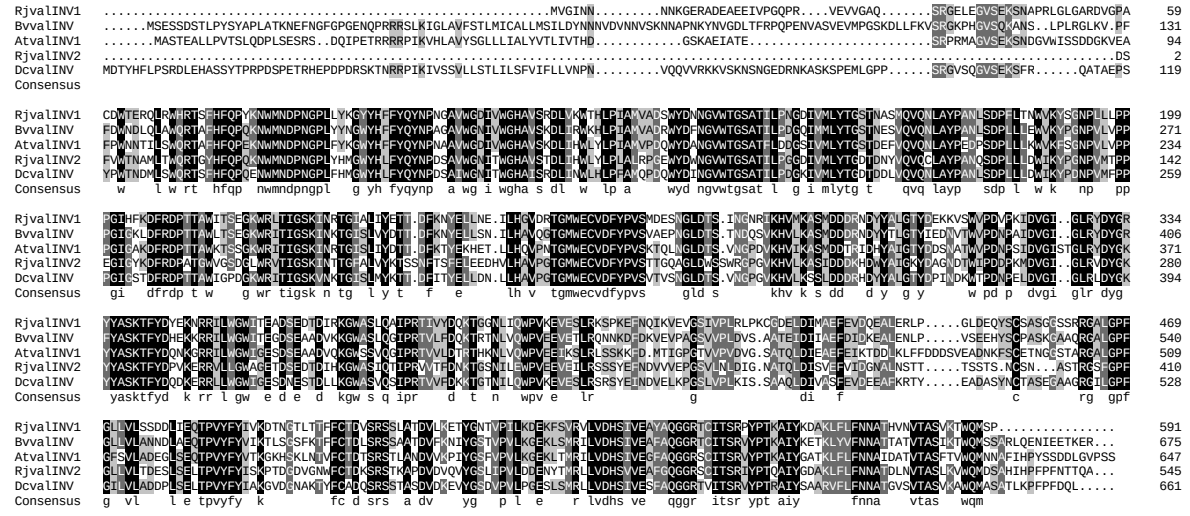

FIGURE 4

Alignment of the deduced V-Inv amino acid sequences of *R. japonicas* (*RjvINV1-2*) with V-Inv genes from some selected plant species. GenBank accession numbers of the sequences are *BvvINV* (*Beta vulgaris*, CAD19321), *AtvINV1* (*Arabidopsis thaliana*, NP564798), *DcvINV* (*Daucus carotas*, CAA53098). Consensus shows the identical amino acid residues.

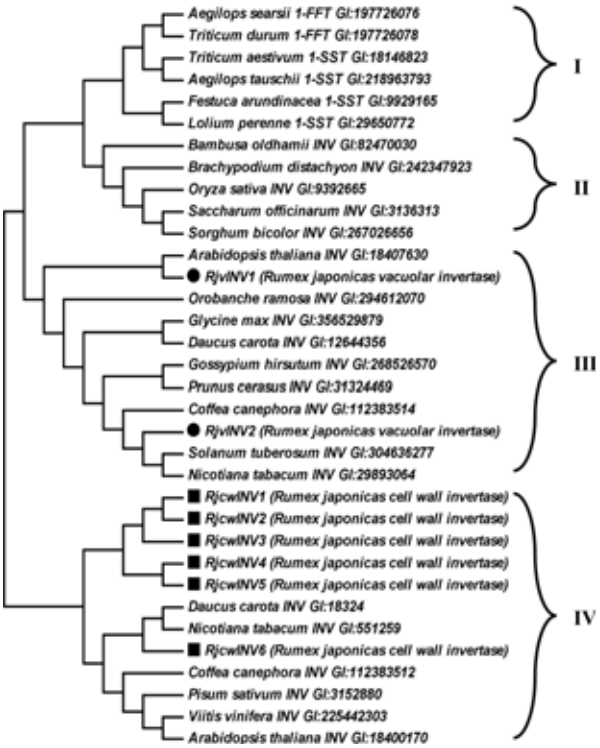

FIGURE 5

Unrooted phylogenetic tree of acid invertases and frucsyltransferase sequences. (I) fructosyltransferase of plants; (II) V-Inv of monocot plants; (III) V-Inv of dicot plants; (IV) CW-Inv of dicot plants.

On the basis of the deduced amino acid sequences, we constructed an unrooted phylogenetic tree from the sequences of plant acid invertase genes and fructosyltransferase genes, namely, RjcwINV1-6 and RjvINV1-2 (Figure 5). Four major groups were discerned: (I) fructosyltransferase of plants; (II) vacuolar invertase of monocot plants; (III) vacuolar invertase of dicot plants, including *RjvINV1* and *RjvINV2*; (IV) cell wall invertase of dicot plants, including *RjcwINV1*, *RjcwINV2*, *RjcwINV3*, *RjcwINV4*, *RjcwINV5*, and *RjcwINV6*.

Expression patterns of eight acid invertases genes under Cu stress. FPKM considers the effect of sequencing depth and gene length for the reads count at the same time, and is currently the most

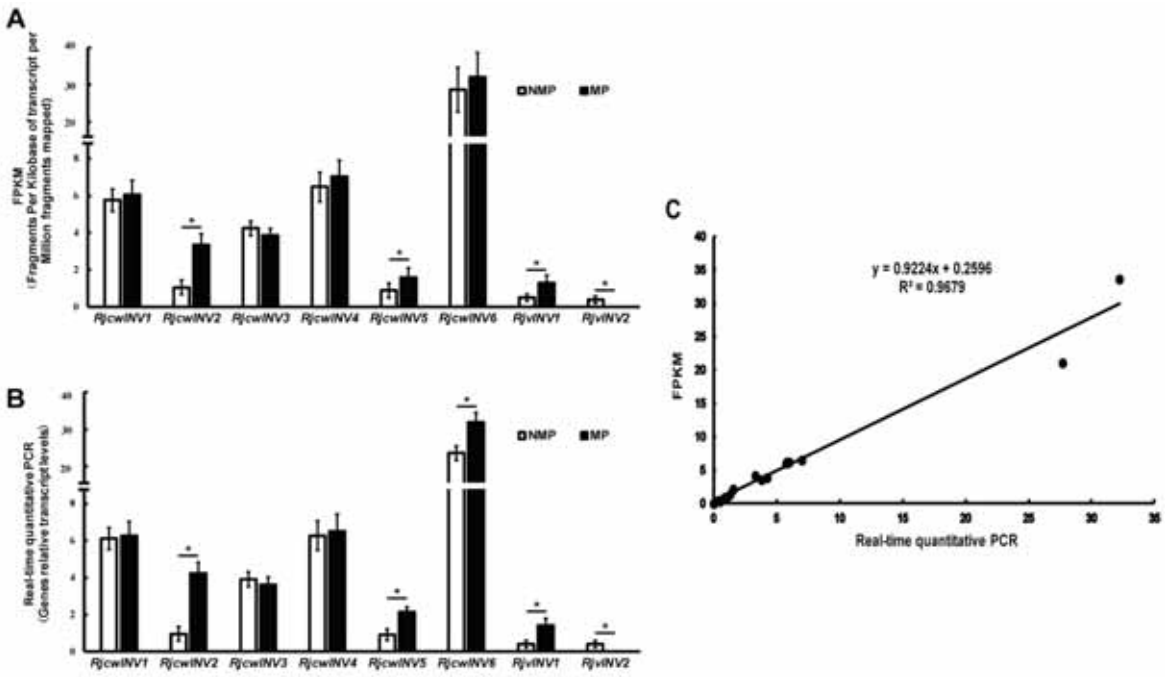

FIGURE 6

Validation of the RNA-Seq expression profiles of eight acid invertases genes by qRT-PCR. (A) FPKM of eight acid invertases genes. (B) qRT-PCR of eight acid invertases genes. (C) Correlation analysis of FPKM and qRT-PCR results.

commonly used method for estimating gene expression levels using transcriptome data. The differentially expressed acid invertases genes between NMP and MP were determined with a log-fold expression change greater than 2 or less than -2 using a greater statistically significant value ($P<0.005$) as well as false discovery rates ($FDR<0.001$). From that, the expression levels of *RjcwINV2*, *RjcwINV5* and *RjvINV1* in MP were significantly higher than them in NMP, while *RjvINV2* only expressed in NMP (Figure 6A). The RNA-Seq data was confirmed by subsequent qRT-PCR analysis (Figure 6B). We found similar expression patterns for the acid invertase genes in the qRT-PCR and RNA-seq data analyses, with a correlation coefficient (R^2) as high as 0.9679 (Figure 6C).

DISCUSSION

Rumex japonicus is a perennial herb with fast growth and high biomass. It also grows easily in wetland habitats. Interestingly, this species is also found in the old Cu mine heap at Tonglushan Hill, a famous copper mine in the Hubei Province of China. Huang et al. reported that the roots of MP manifest a significantly higher activity of acid invertases enzymes than that of NMP [11]. Because the genome sequence of the *R. japonicus* is still unavailable, very little is known about the reason why the higher acid invertase activities in MP, especially in genetic and molecular aspects. However, the arrival of RNA-Seq technologies allow investigators to simultaneously measure the changes and regulation at a genome-wide level under certain biological conditions for non-model plants for which the background genomic information is not available [22]. In this study, based on *de novo* transcriptome sequencing and assembly, a total of 47,252 unigenes were obtained from *R. japonicus* roots cDNA libraries of NMP and MP. Comparison of the assembled unigenes to gene catalogs of other species, 24,223 transcript sequences (51.26% of all assembled unigenes), including 57 functional groups based on GO databases (Figure 2A) and 25 functional categories based on KOG databases (Figure 2B), were annotated by BLAST analysis and functional bioinformatics analyses. Meanwhile, a considerable number of unannotated transcripts were generated, which may represent a specific gene pool for *R. japonicus* studies. The gene catalog provided a comprehensive understanding of the gene transcription profiles of *R. japonicus*, and laid a solid foundation for further investigation of HM stress mechanisms and identification of novel genes in metallophyte.

Available molecular data show that CW-Inv and V-Inv are represented by more than one gene in any given plant. In addition, the number of acid invertases gene family members in different species is not equal. For instance, there are two V-Inv genes and six CW-Inv genes in *Arabidopsis* [23], two V-Inv genes and nine CW-Inv genes in rice [24], two V-Inv genes and four CW-Inv genes in potato [25], three V-Inv genes and five CW-Inv genes in Populus [13], and six acid invertases genes in tea plant [14]. In this study, we identified eight acid invertases

genes, six CW-Inv, and two V-Inv, from the RNA-seq data of young roots of NMP and MP of *R. japonicus*. The deduced amino acid sequences of the eight genes showed high similarity to the acid invertases of other species (Figure 3 and Figure 4), all of which contain the highly conserved β-fructosidase motifs NDPNG/A and catalytic sites WECP/VD. According to hypothesis the presence of a Val residue in the latter motif is characteristic of V-Inv, whereas in CW-Inv the Val residue is replaced by Pro, the proteins deduced from the *RjvINV1-2* sequences belong to the V-Inv cluster, while proteins deduced from the *RjcwINV1-6* sequences belong to the CW-Inv cluster [26].

A phylogenetic tree we constructed based on available sequence data in combination with the cluster method revealed that V-Inv and fructosyltrans-ferase share high homology, whereas CW-Inv is distinctly divergent from them (Figure 5). These patterns lend credence to the hypothesis that an initial duplication was responsible for the genesis of V-Inv and CW-Inv before the divergence between dicot and monocot plants, and that the genes encoding plant fructan biosynthetic enzymes evolved from an ancestral V-Inv gene [27]. In other words, an ancestral gene was duplicated before the divergence of monocots and dicots, with one duplicate evolving into the V-Inv and various fructosyltransferase, and the other evolving into the CW-Inv. Our phylogenetic tree reconfirmed that the proteins deduced from the *RjvINV1-2* sequences belong to the V-Inv cluster, while proteins deduced from the *RjcwINV1-6* sequences belong to the CW-Inv cluster.

Compared with several differential screening techniques (e.g., differential display, subtraction libraries, and differential hybridization), RNA-Seq is known to have a wider dynamic range, higher technical reproducibility, and provide a better estimate of expression levels [22]. Based on FPKM, the expression levels of *RjcwINV2*, *RjcwINV5* and *RjvINV1* in MP were significantly higher than them in NMP, while *RjvINV2* only expressed in NMP in present study (Fig. 4A). And the RNA-Seq data was confirmed by qRT-PCR analysis (Fig. 4B). Firstly, these results suggest that under Cu stress, the expression of individual instead of total acid invertases genes in MP of *R. japonicas* differed from those in NMP. Different members of the acid invertases family have already been reported to have varying expression patterns under stress conditions. For example, the expression of three CW-Inv genes (*Incw1*, *Incw2*, and *Incw4)*, two V-Inv genes (*Ivr1* and *Ivr2*) was shown to be significantly suppressed in the ovaries under drought condition, however, a V-Inv gene (*Inv1*) was shown to be slightly induced in young leaves [28]. Secondly, these results suggest that the higher acid invertases activities of MP under Cu stress could be due in part to elevated expression of individual acid invertases genes. As acid invertases are key enzymes in Suc metabolism, and their substrates and hydrolytic products are both nutrients and signaling molecules, increasing evidence has shown that acid invertases play a pivotal role in defense responses to various abiotic and biotic stresses such as heat, cold, drought, wounding, hypoxia, salinity and pathogen infection [29,30]. Though we did not study the mechanisms adopted by MP of *R. japonicas* in this study, these mechanisms may include the following, as reported in the literature: cell wall binding, metal exclusion or efflux from roots, enhanced syringaldazine peroxidase activity, transporting cytosolic metal into the vacuole, and overexpression of phytochelatin, metallotionein and transporters genes [31-33]. To utilise these mechanisms, the roots of MP must spend extra carbon and energy. Because carbon and energy are supplied by hexoses that are cleaved from Suc, it is reasonable to consider that the activity of Suc-cleaving enzymes in roots of MP may accordingly be higher than those of the NMP. This is what was observed in the previous study by Huang et al. [11].

CONCLUSIONS

In conclusion, this study identified six CW-Inv genes and two V-Inv genes from roots of NMP and MP of *R. japonicas* by RNA-seq. Transcript levels analysis indicated that different members of the acid invertases gene family have varying expression patterns under Cu stress. These results suggested that the higher acid invertases activities of MP under Cu stress could be due in part to elevated expression of individual instead of total acid invertases genes. This knowledge is of considerable importance for understanding Suc metabolism, which may be crucial for plant root growth and the HM tolerance maintenance that has evolved in metallophyte.

ACKNOWLEDGEMENTS

This work was supported by the National Nature Science Foundation of China (Projects 31200393) and program of the Education Department of Henan Province (17A210020).

REFERENCES

[1] Singh, S., Parihar, P., Singh, R., Singh, V.P., Prasad, S.M. (2016) Heavy metal tolerance in plants: role of transcriptomics, proteomics, metabolomics, and ionomics. Frontiers in Plant Science. 6, 1143.

[2] Mustafa, G., Komatsu, S. (2016) Toxicity of heavy metals and metal-containing nanoparticles on plants. Biochimica et Biophysica Acta-Proteins and Proteomics. 1864, 932-944.

[3] Pollard, A.J., Reeves, R.D., Baker, A.J. (2014) Facultative hyperaccumulation of heavy metals and metalloids. Plant Science. 217-218(1), 8-17.
[4] Prat, S. (1934) The factor of resistance to copper. Journal of the German Botanical Society. 52, 65-78. (in German).
[5] Hall, J.L. (2012) Cellular mechanisms for heavy metal detoxification and tolerance. Journal of Experimental Botany. 53, 1-11.
[6] Lange, B., Antony, V.D.E., Baker, A.J.M., Echevarria, G., Mahy, G., Malaisse, F., Pourret, O., Verbruggen, N., Faucon, M.P. (2017) Copper and cobalt accumulation in plants: a critical assessment of the current state of knowledge. New Phytologist. 213(2), 537-551.
[7] Gibson, S.I. (2005) Control of plant development and gene expression by sugar signaling. Current Opinion in Plant Biology. 8(1), 93-102.
[8] Roitsch, T., Gonzalez, M.C. (2004) Function and regulation of plant invertases: sweet sensations. Trends Plant Science. 9, 606-613.
[9] Zhang, L., Pan, Y., Lv, W., Xiong, Z.T. (2014) Physiological responses of biomass allocation, root architecture, and invertase activity to copper stress in young seedlings from two populations of *Kummerowia stipulacea* (maxim.) Makino. Ecotoxcology and Environmental Safety. 104(2), 278-284.
[10] Cai, S.W., Huang, W.X., Xiong, Z.T., Ye, F.Y., Ren, C., Xu, Z.R., Liu, C., Deng, S.Q., Zhao, J. (2013) Comparative study of root growth and sucrose-cleaving enzymes in metallicolous and non-metallicolous populations of *Rumex dentatus* under copper stress. Ecotoxcology and Environmental Safety. 98(12), 95-102.
[11] Huang, W.X., Cao, Y., Huang, L.J., Ren, C., Xiong, Z.T. (2011) Differential expression of acid invertase genes in roots of metallicolous and non-metallicolous populations of *Rumex japonicus* under copper stress. Chemosphere. 84(10), 1432-1439.
[12] Cai, S., Xiong, Z.T., Li, L., Li, M., Zhang, L., Liu, C., Xu, Z.R. (2014) Differential responses of root growth, acid invertase activity and transcript level to copper stress in two contrasting populations of *Elsholtzia haichowensis*. Ecotoxicology. 23(1), 76-91.
[13] Chen, Z., Gao, K., Su, X., Rao, P., An, X. (2015) Genome-wide identification of the invertase gene family in *Populus.* PLoS One. 10(9), e0138540.
[14] Qian, W., Yue, C., Wang, Y., Cao, H., Li, N., Wang, L., Hao, X., Wang, X., Xiao, B., Yang, Y. (2016) Identification of the invertase gene family (*INVs*) in tea plant and their expression analysis under abiotic stress. Plant Cell Reports. 35(11), 2269-2283.
[15] Wang, W., Li, R., Zhu, Q., Tang, X., Zhao, Q. (2016) Transcriptomic and physiological analysis of common duckweed *Lemna minor* responses to NH_4^+ toxicity. BMC Plant Biology. 16, 92.
[16] Fan, X.D., Wang, J.Q., Yang, N., Dong, Y.Y., Liu, L., Wang, F.W., Wang, N., Chen, H., Liu, W.C., Sun, Y.P., Wu, J.Y., Li, H.Y. (2013) Gene expression profiling of soybean leaves and roots under salt, saline-alkali and drought stress by high-throughput Illumina sequencing. Gene. 512(2), 392-402.
[17] Liu, M.M., Xing, Y.M., Zhang, D.W., Guo, S.X. (2015) Transcriptome analysis of genes involved in defence response in *Polyporus umbellatus* with *Armillaria mellea* infection. Scientific Reports. 5, 16075.
[18] Ke, W., Xiong, Z.T., Chen, S., Chen, J. (2007) Effects of copper and mineral nutrition on growth, copper accumulation and mineral element uptake in two *Rumex japonicus* populations from a copper mine and an uncontaminated field sites. Environmental and Experimental Botany. 59(1), 59-67.
[19] Wilkins, D.A. (1957) A technique for the measurement of lead tolerance in plants. Nature. 180, 37-38.
[20] Wilkins, D.A. (1978) The measurement of tolerance to edaphic factors by means of root growth. New Phytologist. 80, 623-633.
[21] Grabherr, M.G., Haas, B.J., Yassour, M., Levin, J.Z., Thompson, D.A., Amit, I., Adiconis, X., Fan, L., Raychowdhury, R., Zeng, Q., Chen, Z., Mauceli, E., Hacohen, N., Gnirke, A., Rhind, N., di Palma, F., Birren, B.W., Nusbaum, C., Lindblad-Toh, K., Friedman, N., Regev, A. (2011) Full-length transcriptome assembly from RNA-Seq data without a reference genome. Nature Biotechnology. 29, 644-652.
[22] Perkins, J.R., Antunes-Martins, A., Calvo, M., Grist, J., Rust, W., Schmid, R., Hildebrandt, T., Kohl, M., Orengo, C., McMahon, S.B., Bennett, D.L. (2014) A comparison of RNA-seq and exon arrays for whole genome transcription profiling of the L5 spinal nerve transection model of neuropathic pain in the rat. Molecular Pain. 10, 7.
[23] Sherson, S.M., Alford, H.L., Forbes, S.M., Wallace, G., Smith, S.M. (2003) Roles of cell-wall invertases and monosaccharide transporters in the growth and development of *Arabidopsis.* Journal of Experimental Botany. 54, 525-531.
[24] Ji, X., Van den Ende, W., Van Laere, A., Cheng, S., Bennett, J. (2005) Structure, evolution, and expression of two invertase gene families of rice. Journal of Molecular Evolution. 60(5), 615-634.

[25] Liu, X., Zhang, C., Ou, Y., Lin, Y., Song, B., Xie, C., Liu, J., Li, X.Q. (2011) Systematic analysis of potato acid invertase genes reveals that a cold-responsive member, *StvacINV1*, regulates cold-induced sweetening of tubers. Molecular Genetics and Genomics. 286, 109-118.
[26] Goetz, M., Roitsch, T. (1999) The different pH optima and substrate specificities of extracellular and vacuolar invertases from plants are determined by a single amino-acid substitution. Plant Journal. 20(6), 707-711.
[27] Van den Ende, W., Lammens, W., Van Laere, A., Schroeven, L., Le Roy, K. (2009) Donor and acceptor substrate selectivity among plant glycoside hydrolase family 32 enzymes. FEBS Journal. 276(20), 5788-5798.
[28] Kakumanu, A., Ambavaram, M.M., Klumas, C., Krishnan, A., Batlang, U., Myers, E., Grene, R., Pereira, A. (2012) Effects of drought on gene expression in maize reproductive and leaf meristem tissue revealed by RNA-Seq. Plant Physiology. 160(2), 846-867.
[29] Ruan, Y.L., Jin, Y., Yang, Y.J., Li, G.J., Boyer, J.S. (2010) Sugar input, metabolism, and signaling mediated by invertase: roles in development, yield potential, and response to drought and heat. Molecular Plant. 3(6), 942-955.
[30] Ruan, Y.L. (2014) Sucrose metabolism: gateway to diverse carbon use and sugar signaling. Annual Review of Plant Biology. 65, 33-67.
[31] Llugany, M., Lombini, A., Poschenrieder, C., Dinelli, E., Barceló, J. (2003) Different mechanisms account for enhanced copper resistance in *Silene armeria* ecotypes from mine spoil and serpentine sites. Plant and Soil. 251(1), 55-63.
[32] Schwartz, M.S., Benci, J.L., Selote, D.S., Sharma, A.K., Chen, A.G., Dang, H., Fares, H., Vatamaniuk, O.K. (2010) Detoxification of multiple heavy metals by a half-molecule ABC transporter, HMT-1, and Coelomocytes of *Caenorhabditis elegans.* Plos One. 5(3), e9564.

Received: **21.08.2018**
Accepted: **23.02.2019**

CORRESPONDING AUTHOR

Wu-Xing Huang
College of Tobacco Science,
Henan Agricultural University,
Zhengzhou – China

e-mail: 555552001@sina.com

AUTHOR INDEX

A

Abbas, A. 2771
Adali, O. 2825
Ahmad, A. 2656
Ahmad, F. 2771
Akcetin, M. O. 2780
Aksu, E. 2942
Albayrak, E. 2880
Ali, A. 2530
Ali, S. 2688
Alkan, M. 2916
Al-Khateeb, A. A. 2957
Al-Khateeb, S. A. 2957
Altindag, F. 2407
Altinel, B. 2368
Altun, S. K. 2802
Annac, M. C. 2754
Annanurov, S. 2625
Antmen, Z. F. 2483
Arihan, O. 2407
Arshad, S. 2656
Arslan, M. 2942

B

Bajestan, M. S. 2390
Basbugan, Y. 2876
Bayram, M. 2787
Belal, E. 2771
Bensaid, M. 2390
Bickici, E. 2457
Biczak, R. 2469
Bolat, I. 2855

C

Cakir-Arica, S. 2545
Cankaya, F. 2754
Canoglu, M. C. 2816
Cao, F. 2523
Cao, Y.-Q. 2968
Celik, H. 2949
Celik, I. 2664
Cetin, H. 2375
Cetin, S. C. 2575
Chen, K. 2771
Chen, S. 2539
Ciftci, E. 2916
Cig, F. 2747
Colcimen, N. 2407
Comba, A. 2876
Comba, B. 2876

D

Daher, B. T. 2511
Dalgic, G. 2671
Deger, Y. 2407
Degirmencioglu, A. 2511
Demirata, B. 2413
Demirdoven, A. 2787
Demirel, N. 2937
Demirhan, B. 2599
Demirhan, B. E. 2599
Desbiez, C. 2442
Dikmen, U. 2575
Dong, X. 2807, 2897
Duzguner, V. 2697

E

Ege, T. 2825
Eken, M. 2457
El-Beltagi, H. S. 2957
Erbas, C. 2949
Erdem, A. 2780
Ersahin, S. 2575
Ertugrul, O. 2511
Ertunc, F. 2442
Erturk, S. 2916

F

Fan, Z. 2848
Farhatullah 2927
Firat, T. A. 2916

G

Gamli, O. F. 2703
Gao, C. 2889
Gao, D. 2897
Gao, Y. 2625
Ge, Z. 2608
Genc, S. 2617
Gencoglan, C. 2433
Gencoglan, S. 2433
Gul, S. 2656
Gulsoy, S. 2380
Gumus, E. 2949
Gunduz, M. N. 2679
Gunes, A. E. 2949
Gungor, C. 2397
Guo, L. 2897
Guo, N. 2506
Guo, T. 2523
Guo, X. 2889
Guo, Z. 2506
Gurbuz, S. 2802
Gurlek, O. G. 2679

H

Hamash, M. H. 2475
Hamayun, M. 2656, 2688
Han, D. 2835
Han, G. 2864
Hanci, F. 2927
Hou, J. 2608
Hou, W. 2450
Hou, X. 2897
Huang, H. 2625
Huang, M. 2539
Huang, W.-X. 2968
Hussain, A. 2656, 2688

I

Ihsan, M. 2927
Ikinci, A. 2855
Ipek, A. 2650
Iqbal, A. 2656, 2688
Istipliler, D. 2368

J

Jan, G. 2927
Jan, M. 2927
Jin, C. 2426

K

Kaman, H. 2923
Kamanbedast, A. A. 2390
Kang, H. 2835
Kang, R. 2771
Kara, H. E. S. 2599
Karadag, H. 2464
Keyikoglu, R. 2942
Khalaf, A. M. 2475
Khan, A. L. 2688
Khan, S. A. 2688
Khan, U. A. 2530
Kilinc, C. 2795
Koc, I. 2747
Kocabiyik, K. 2375
Kocyigit, U. M. 2739
Konuskan, O. 2795
Kurt, P. 2754

L

Li, F. 2495
Li, H. 2835
Li, J. 2539, 2561
Li, L. 2539, 2889
Liang, R. 2633
Lin, Z. 2848
Liu, H. 2539, 2864
Liu, M. 2506, 2725
Liu, W.-J. 2908
Liu, X. 2807
Liu, Y. 2848
Liu, Z. 2495
Lu, H. 2725
Lu, J. 2889
Lu, Y. 2835
Luo, C. 2539
Luo, F. 2539
Luo, M. 2450

M

Ma, X. 2450
Masjedi, A. 2390
Mazlum, Y. 2679
Mendes, M. 2747
Mert, A. 2380
Min, X. 2889
Mis, L. 2876
Mohasseb, H. A. A. 2957
Mohtar, R. H. 2511

N
Namli, A. 2747
Ni, Y. 2561
Nikpeyma, Y. 2433
Nisar, M. 2927
Nowak, G. 2469

O
Onaran, A. 2787
Onay, H. 2671
Oz, S. 2545
Ozdek, U. 2407
Ozgunaltay-Ertugrul, G. 2511
Ozkan, A. M. G. 2825
Ozkan, G. 2380
Ozkok, A. 2644, 2650
Ozsoy, A. N. 2582
Ozturk, H. H. 2397
Ozyurt, D. 2413

P
Park, J. 2807
Pazir, F. 2368
Pinar, S. M. 2747
Poblocki, J. 2469
Pu, X. 2633
Purmohammadi, M. H. 2390

Q
Qi, Y. 2523
Qin, R. 2889
Qiu, L. 2561

R
Rehman, G. 2656
Rezania, S. 2807
Rynkiewicz, M. 2469

S
Saban, M. 2754
Sahin, S. K. 2880
Sakin, E. 2553
Sangun, L. 2842
Sayici, A. 2923
Semiz, G. 2375
Sen, A. 2825
Senol, H. 2380
Shah, M. 2656, 2688
Shams, W. A. 2656
Shao, H.-F. 2968
Shen, J. 2807
Snieg, M. 2469
Solliman, M. E.-D. 2957
Sorkun, K. 2650
Soysal, M. I. 2617
Stanislawski, K. 2469
Sun, Y. 2897
Sun, Y.-Q. 2908
Sunal, S. 2575

T
Tang, H. 2450
Tao, Y. 2523
Tekin, A. B. 2716
Telesinski, A. 2469
Temel, S. 2421
Tokatli, K. 2787
Tong, S. 2426
Tonk, F. A. 2368
Topkaya, S. 2442
Tosun, M. 2368
Tufekcioglu, M. 2589

U
Ucak, A. B. 2433
Uzun, F. T. 2464

W
Wan, F. 2561, 2625
Wang, C. 2725
Wang, F. 2897
Wang, H. 2523, 2539, 2908
Wang, J. 2835
Wang, W. 2733
Wang, Y. 2495, 2835
Wang, Z. 2848
Wei, Z.-Z. 2968
Wrobel, J. 2469
Wu, J. 2889

X

Xiao, L. 2561
Xu, J.-Y. 2968
Xu, M. 2561
Xu, X. 2807
Xu, Y. 2897
Xu, Z.-C. 2968

Y

Yakan, S. 2697
Yanar, Y. 2787
Yang, L. 2908
Yanardag, I. H. 2553
Yang, K. 2835
Yardim, E. N. 2747
Yasar, S. 2876
Yavuz, M. 2589
Yayintas, O. T. 2413
Yazici, M. 2679
Yazici, N. 2664
Yilmaz, A. E. 2575
Yılmaz, O. 2949
Yilmaz, S. 2413
Yousaf, K. 2771
Yuceer, Y. K. 2413

Z

Zaman, K. 2656
Zeng, X. 2625
Zhang, C. 2523
Zhang, J. 2725
Zhang, M. 2908
Zhang, W. 2523
Zhang, X. 2771, 2864
Zhang, Y. 2450
Zhao, C. 2426
Zhao, G. 2633
Zhao, S. 2835
Zhao, Y. 2426
Zhao, Z. 2539
Zhong, Z. 2625
Zhou, X.-W. 2908

SUBJECT INDEX

A

abiotic stress 2530
absorbency 2908
ACC deaminase 2688
acetylcholinesterase 2739
Acid invertases 2968
Acrylamide 2599
Aerosol black carbon 2889
Aflatoxin M_1 2802
agricultural technologies 2511
Agro-ecosystems 2747
agronomic traits 2539
Al-bearing acid mine drainage 2633
aluminum speciation 2633
ambient temperature oxidation 2897
amorphous 2633
Anatomical studies 2650
Anthocyanin 2450
Anthropogenic influences 2889
antiepileptic potentials 2739
Antigenotoxicity 2545
anti-inflammatory 2656
antioxidant 2656
antioxidant capacity 2413
Apple rootstocks 2855
Aquifer recharging 2816
artificial fumigation method 2908
Artificial Neural Networks 2842
Aspect 2664
attractants 2937
Azinphos-methyl 2464

B

Bacillus coagulans 2426
Bacillus subtilis 2780
Bahla Aquifer 2816
basin 2664
Bed slope 2390
bile acids 2825
biochar 2553
biodegradation 2426
bioindication 2469
Biological activity 2787
Black sea 2671,
BP Neural Network 2725
breeding values 2617
Brushtooth lizardfish 2842

C

C emission 2553
Cadmium 2530
Canonical correlation 2582
Caralluma acutangular 2688
Carbon monoxide 2897
Carbon-dioxide Emissions 2608
carbonic anhydrase 2739
Cassia nemophila 2656
Catalase 2464
CCA 2880
Ceramsite 2848
Check dams 2390
chemical composition 2650
chemical compound 2644
Cherax quadricarinatus 2679
chick quality 2582
Chitosan 2787
Chloroplastic antioxidases and antioxidants 2864
Chlorothalonil 2426
Clay 2848
climate change 2511
CO_2 emission 2397
CO_2 emissions 2483
coal spontaneous combustion 2897
Coat protein 2442
Color 2450
colorimetry 2413
Comice Pear 2433
Cone 2380
Copper stress 2968
copper-contaminated sand 2807
Corn (*Zea mays*) 2795
Cost 2754
Crayfish 2679
Crop production 2511
Cucurbit viruses 2442
CYP450s 2825

D

Daily feeding 2671
dairy cow 2697
data analyses 2716
Date palm 2957
Dent corn inbred line 2368
desert shrubs 2864
diabetes 2656
digital divide 2716
Dimethoate 2464
Diplotaenia turcica 2407
Discharge 2390
Disinfection 2780
Distance 2390
distance from emitter 2469
Diversity 2880
dormancy release 2495
doxorubicin 2545
Drainage 2923
Drosophila melanogaster 2545
drought stress 2864
Drying mechanism 2523

E

Effectiveness 2916
egg quality 2582
electrical resistivity 2807
ELISA 2802
Embryo 2475
endocrine disruptors 2457
endogenous hormone 2495
energy and Chemical Industry Base 2835
Energy consumption 2483
energy use 2397
Environment capacity 2625
Environmental Justice 2816
Environmentally extended Input-output 2608
enzyme inhibition 2739
essential oil 2380
estimation 2842
Euphorbia (spurge) honey 2644
extra-cellular enzymes 2688

F

F_1 hybrids 2368
Flow depth 2390
flower drop 2855
fluoride 2469
forest 2664
Forest fires 2575
freshwater pollution 2457
fruit drop ratio 2855
fruit growth 2855
fruit set ratio 2855
fuel consumption 2397, 2511
fungal endophytes 2688

G

GC-MS 2413, 2650
Gelatinization 2771
Gene expression 2450
Gene family 2968
Genetic diversity 2927
genetic trend 2617
Geotechnical characterization 2816
Gonocytes 2475
grain yield 2795
gray system dynamic model (GM) 2835
growth 2679
growth and yield parameters 2747
growth stage 2421

H

Health risk 2889
heritability 2617
HF 2908
Holstein Friesian 2617
Homeostasis 2949
hoof trimming 2697
horse chestnut 2469
Hospital 2754
Hybridization 2368
hydrothermal 2771

I

ict adoption 2716
Idesia polycarpa Maxim 2495
image processing 2703
in vitro cultures 2530
Indigenous tree species 2908
indole acetic acid 2688
Infiltration characteristics 2816
Insecticide 2464
Ionic Zn 2561
irrigation 2923
Irrigation automation 2433
Iskenderun Bay 2457

J

juniper 2380

K
Kernel characteristics 2368

L
Lake sediment 2848
land use 2511
Land use pattern 2835
Larvicidal activity 2375
leaching 2923
Lead acetate 2475
leaf area index 2795
Lethal doses 2787
light/CO_2 utilization 2864
Liriodendron 2848
Liver cancer 2506
Local Diatomaceous earth 2916
low intensity fire 2575
low temperature treatments 2495

M
M9 2855
macro and micro mineral content 2421
Malacofauna 2880
management 2664
Meat analysis 2599
Medical Waste 2754
medicinal plants 2825
Mediterranean fruit fly 2937
melissopalynology 2644
meloxicam 2697
MgO nanoparticles 2561
Micro-bubble excitation 2523
Microplastic 2671
milk product 2802
Mineql+ model 2633
Molecular variability 2442
Morphology 2927
Mosses 2413
Mullus barbatus 2671
mutation 2545

N
Nanoprobe 2506
Natural compounds 2787
natural resources 2664
Near-infrared fluorescence 2506
nephropathy 2656
Noaea mucronata 2421
normalization 2842
nutshell 2747

O
oak honey 2650
o-coumaric acid 2825
olive leaves 2703
optimization 2771
Organophosphate 2464
Ovary 2407
Oxidative stress 2697

P
paclobutrazol 2539
Patient 2754
phenolic subtances 2703
Phenylurea 2739
phytochemical analysis 2957
Phytotoxicity 2561
Pinus brutia 2375
plant density 2795
plant growth regulators 2957
Plant pathogenic fungi 2787
PLC 2433
Polyethylene glycol 2530
pomegranate 2937
precursors 2957
primordial gas 2897
principal component analysis 2380
Progeny production 2916
Pseudostellaria heterophylla 2539

Q
quail 2582
quality 2539
Quantum dot 2599
Quercus frainetto Ten. 2650

R
RAPD 2927
Rat 2407, 2876
refined olive oil 2703
Renal failure 2876
response surface method 2771
rice quality 2771
Room temperature phosphorescence 2599
Rose 2450
Rumex japonicas 2968
Rural tourism 2733
rural vitalization 2733
RUSLE and GIS 2589

S
saffron 2545
salinity 2923
Salinity tolerance 2942
Saltwater irrigation 2942
Sapanca Lake 2880
SE Turkey 2553
Seasons feeding 2671
Seed essential oil 2375
seeding rate 2539
Seminiferous tubules 2475
Sensitivity 2506
sensory profile 2703
Sheet and rill erosion 2589
Sintering characteristics 2848
site factors 2380
slope 2664
Sludge drying 2523
SMART assay 2545
SO_2 2908
soil properties 2575
soil salinity 2553
Soybean 2927
soybean oil 2679
SPAD value 2795
Specificity 2506
spectrophotometry 2413
stabilization 2807
Staphylococcus aureus 2780
Stereology 2407
steroids and phenolics. 2957
Structural Decomposition Analysis 2608
Sugar beet cultivation 2397
sugar composition 2644
Sugar treatment 2450
Sugarcane callus 2530
survival 2679
Sweet corn inbred line 2368
Swiss mice 2475

T
Targeting 2506
TAS 2876
TDABC 2754
Testis 2475
Thaumetopoea wilkinsoni 2375
The bean weevil 2916
the germination rate 2495
The Qinghai-Tibet Plateau 2889
Thermogravimetric analysis 2523, 2633
Thiol; Disulphides 2949
Thiol-Disulphide Oxidoreductase 2949
Tillage 2483
Time Driven Activity Based Costing 2754
TiO_2 nanoparticles 2780
tissue culture 2957
TOS 2876
total 2644
traditional yoghurt 2802
Turfgrass quality 2942
Turkey 2375, 2802, 2880, 2937
turkish agriculture 2716

U
unconfined compressive strength 2807
Underwater Medicine 2949
Unused Capacity 2754
Urban lakes 2625

V
Value-Based Health Care 2754
variance components 2617
varieties 2795
Verbascum (mullein) honey 2644
Viscum album L. 2825
Visible light 2780

W
Wadi Keed Dam 2816
Water quality improvement 2625
water requirement 2511
Water Resource Forecast 2725
Water Resources Carrying Capacity 2725
weeds 2747
Western China 2733
wheat 2483, 2747
Wheatgrass 2876
wood vinegar 2747
WorldView-2 2589

X
X-ray diffraction 2633

Y
yield 2539

Z
ZnO 2561
Zucchini yellow mosaic virus 2442

1, 2,…9, 0.
17 alpha-ethinylestradiol (EE2) 2457

FEB – GUIDE FOR AUTHORS

General

FEB accepts original papers, review articles, short communications, research abstracts from the entire sphere of environmental-chemistry,-biology,-microbiology,- technology, -biotechnology and-management, furthermore, about residue analysis/ and ecotoxicology of contaminants.

Acceptance or no acceptance of a contribution will be decided, as in the case of other scientific journals, by a board of reviewers. Papers are processed with the understanding that they have not been published before (except in form of an abstract or as a part of a published lecture, review or thesis);that they are not under consideration for publication elsewhere; that their publication has been approved by all co-authors, if any, as well as-tacitly or explicitly- by the responsible authorities at the institute where the work has been carried out and that, if accepted, it will not be published elsewhere in the same form, in either the same or another language, without the consent of the copyright holders.

Language

Papers must be written in English. Spelling may either follow American (Webster) or British (Oxford) usage but must be consistent. Authors who are less familiar with the English language should seek assistance from proficient colleagues in order to produce manuscripts that are grammatically and linguistically correct.

Size of manuscript

Review articles should not exceed 30 typewritten pages. In addition up to 5 figures may be included.

Original papers must not exceed 14 typewritten pages. In addition up to 5 figures may be included.

Short-Communications should be limited to 4 typewritten pages plus not more than 1 illustration.

Short descriptions of the authors, presentation of their groups and their research activities (with photo) should together not exceed I typewritten page. Short research abstracts should report in a few brief sentences (one-fourth to one page) particularly significant findings. Short articles by relative newcomers to the chemical innovation arena highlight the key elements of their Master and PhD-works in about I page.

Book Reviews are normally written in-house, but suggestions for books to review are welcome.

Preparation of manuscript

Dear authors,

FEB is available both as printed journal and as online journal on the web. You can now e-mail your manuscripts with an attached file. Save both time and money. To avoid any problems handling your text please follow the instructions given below:

When preparing your manuscripts have the formula K/SS (Keep It Simple and Stupid) in mind. Most word processing programs such as MS-Word offer a lot of features. Some of them can do serious harm to our layout. So please do not insert hyperlinks and/or automatic cross-references, tables of contents, references, footnotes, etc.

1. Please use the standard format features of your word processor (such as standard.dot for MS Word).
2. Please do not insert automatisms or secret link-ups between your text and your figures or tables. These features will drive our graphic department sometimes mad.
3. Please only use two fonts for text or tables "Times New Roman" and for graphical presentations "Arial".
4. Stylesheets, text, tables and graphics in shade of grey
5. Turn on the automatic language detection in English (American or British)
6. Please - check your files for viruses before you send them to us!!

Manuscripts should send to:parlar@wzw.tum.de
or:parlar@prt-parlar.de

Thank you very much!

STRUCTURE OF THE MANUSCRIPT

Title page: The first page of the manuscript should contain the following items in the sequence given: A concise title of the paper (no abbreviations). The names of all authors with at least one first name spelled out for every author. The names of Universities with Faculty, City and Country of all authors.

Abstracts: The second page of the manuscript should start with an abstract that summarizes briefly the contents of the paper (except short communications). Its length should not exceed 150-200 words. The abstract should be as informative as possible. An extended repetition of the paper's title is not considered to be an abstract.

Keywords: Below the Summary up to 6 key words have to be provided which will assist indexers in cross-indexing your article.

Introduction: This should define the problem and, if possible, the frame of existing knowledge. Please ensure that people not working in that particular field will be able to understand the intention. The word length of the introduction should be 150 to 300 words.

Materials and methods:
Please be as precise as possible to enable other scientists to repeat the work.

Results: Only material pertinent to the subject must be included. Data must not be repeated in figures and tables.

Acknowledgements: Acknowledgements of financial support, advice or other kind of assistance should be given at the end of the text under the heading "Acknowledgements". The names of funding organisations should be written in full.

References: Responsibility for the accuracy of references rests with the authors. References are to be limited in number to those absolutely necessary. References should appear in numerical order in brackets and in order of their citation in the text. They should be grouped at the end of the paper in numerical order of appearance. Abbreviated titles of periodicals are to be used according to Chemical or Biological Abstracts, but names of lesser known journals should be typed in full. References should be styled and punctuated according to the following examples:

ORIGINALPAPERS:
l. Author, N.N. and Author, N.N. (Year) Full title of the article. Journal and Volume, first and last page.
BOOK OR PROCEEDING:
2. Author, N.N. and Author, N.N. (Year) Title of the contribution. In: Title of the book or proceeding. Volume (Edition of klitor-s, ed-s) Publisher, City, first and last page

DOCTORAL THESIS:
3. Author, N.N. (Year) Title of the thesis, University and Faculty, City

UNPUBLISHED WORK:
Papers that are unpublished but have been submitted to a journal may be cited with the journal's name followed by "in press". However, this practice is acceptable only if the author has at least received galley proofs of his paper. In all other cases reference must be made to “unpublished work" or "personal communication".

Discussion and Conclusion: This part should interpret the results in reference to the problem outlined in the introduction and of related observations by the author/s or others. Implications for further studies or application may be discussed. A conclusion should be added if results and discussion are combined.

Corresponding author: The name of the corresponding author with complete postal address

Reprints:
1 - 4 pp.: 200,- EURO + postage/handling
5 - 8 pp.: 250,- EURO + postage/ handling
More than 8pp: 350,- EURO +postage/ handling.
The prices are based upon the number of pages in our journal layout (not on the page numbers of the submitted manuscript).
Postage/ Handling: The current freight rate is Germany 10 €, Europe 18 €, International 30 €.
VAT: In certain circumstances (if no VAT registration number exists) we may be obliged to charge 7% VAT on sales to other EU member countries.MESAEP and SECOTOX members get a further discountof 20% (postage/ handling full).